सत्यमेव जयते

INDIAN AGRICULTURAL
RESEARCH INSTITUTE, NEW DELHI.

I. A. R. I. 6.
MGIPC—S1—6 AR/54—7-7-54—10,000.

Journal of

POLYMER SCIENCE

VOLUME V • 1950

Editorial Board: **W. T. ASTBURY · P. M. DOTY · H. MARK**

Advisory Board:

P. D. BARTLETT
Cambridge, Mass.

C. C. DAVIS
Lexington, Mass.

P. DEBYE
Ithaca, N. Y.

A. DOBRY
Paris

J. DUCLAUX
Paris

M. G. EVANS
Manchester

E. H. FARMER
Welwyn Garden City

P. J. FLORY
Ithaca, N. Y.

R. M. FUOSS
New Haven, Conn.

K. FREUDENBERG
Heidelberg

A. FREY-WYSSLING
Zürich

C. S. FULLER
Summit, N. J.

MILTON HARRIS
Washington, D. C.

P. H. HERMANS
Utrecht

R. HOUWINK
Delft

M. L. HUGGINS
Rochester, N. Y.

W. KUHN
Basel

O. KRATKY
Graz

M. MATHIEU
Paris

H. W. MELVILLE
Birmingham

K. H. MEYER
Geneva

G. NATTA
Milan

C. C. PRICE
Notre Dame, Ind.

P. PUTZEYS
Louvain

E. K. RIDEAL
London

CH. SADRON
Strasbourg

G. SMETS
Louvain

H. M. SPURLIN
Wilmington, Del.

THE SVEDBERG
Uppsala

J. C. SWALLOW
Welwyn Garden City

G. S. WHITBY
Akron, Ohio

54364

INTERSCIENCE PUBLISHERS, INC.

Copyright, 1950, by Interscience Publishers, Inc.

CONTENTS

Vol. V, Nos. 1–6, 1950

Journal of Polymer Science

NUMBER 1, FEBRUARY

NOLLE, A. W.: Dynamic Mechanical Properties of Rubberlike Materials 1

HART, R., et SMETS, G.: Vitesse de Polymérisation et de Copolymérisation de l'Acétate d'Isopropényle 55

SIPS, R.: Mechanical Behavior of Viscoelastic Substances 69

MOORE, W. R.: Nitrocellulose–Solvent Interaction 91

SIEGEL, B. M., JOHNSON, D. H., and MARK, H.: Molecular Weight Investigations of High Polymers with the Electron Microscope 111

BILLMEYER, F. W., JR., and STOCKMAYER, W. H.: Method of Measuring Molecular Weight Distribution 121

BOYER, R. F.: Concentration Dependence of Diffusion of Chloroform in Polystyrene (Letter to the Editors) 139

CRANK, J., and PARK, G. S.: (Letter to the Editors) 140

ROTHMAN, S., SIMHA, R., and WEISSBERG, S. G.: Viscosities of Very Dilute Polymer Solutions (Letter to the Editors) 141

REVIEW 143

SUMMARIES OF ARTICLES RECEIVED S1

NUMBER 2, APRIL

SCHAUENSTEIN, E., and TREIBER, E.: Ultraviolet Absorption Spectra of Actomyosin. I 145

BOLDUAN, O. E. A., and BEAR, R. S.: Unidirectional Nature of the Large Periodic Structure of Collagen Fibrils 159

SMITH, E. F., and WANGSGARD, A. P.: Photoelastic Strain Analyzer 169

JIRGENSONS, B.: Denaturation of Plant Proteins. III. Optical Rotation, Viscosity, and Reducing Capacity of Denatured Proteins 179

CARR, C. W., KOLTHOFF, I. M., MEEHAN, E. J., and STENBERG, R. J.: Studies on the Rate of the Emulsion Polymerization of Butadiene-Styrene (75:25) as a Function of the Amount and Kind of Emulsifier Used. I. Polymerizations with Commercial and Pure Soaps 191

CARR, C. W., KOLTHOFF, I. M., MEEHAN, E. J., and WILLIAMS, D. E.: Studies on the Rate of the Emulsion Polymerization of Butadiene-Styrene (75:25) as a Function of the Amount and Kind of Emulsifier Used. II. Polymerizations with Fatty Acid Soaps, Rosin Soaps, and Various Synthetic Emulsifiers 201

HERZFELD, S. H., ROGINSKY, A., CORRIN, M. L., and HARKINS, W. D.: Monomer–Polymer Ratio in Emulsion Polymerization of Styrene 207
HARKINS, W. D.: General Theory of Mechanism of Emulsion Polymerization. II.......................... 217
DE WILDE, M. C., et SMETS, G.: Copolymérisation de l'Anhydride Maléique avec Différents Monomères Vinyliques............. 253
FINEMAN, M., and ROSS, S. D.: Linear Method for Determining Monomer Reactivity Ratios in Copolymerization (Letter to the Editors).. 259
POWERS, P. O.: "Bound" Water in Phenol-Formaldehyde Condensates (Letter to the Editors)............................ 262
JELLINEK, H. H. G.: Degradation of High Polymers (Letter to the Editors).. 264
REVIEW.. 266
FINKELSTEIN, P., and MCLAREN, A. D.: Photochemistry of Proteins. VI. *p*H Dependence of Quantum Yield and Ultraviolet Absorption Spectrum of Chymotrypsin. (Errata, article in *J. Polymer Sci.*, 4, 573–582, 1949)........................ 267
FLORY, P. J., and LEUTNER, F. S.: Occurrence of Head-to-Head Arrangements of Structural Units in Polyvinyl Alcohol. (Errata, article in *J. Polymer Sci.*, 3, 880 1948). 267
SUMMARIES OF ARTICLES RECEIVED.... .... S17

NUMBER 3, JUNE

HERMANS, P. H., and WEIDINGER, A.: Quantitative Investigation of X-Ray Diffraction by "Amorphous" Polymers and Some Other Noncrystalline Substances................................ 269
KATCHALSKY, A., KÜNZLE, O., and KUHN, W.: Behavior of Polyvalent Polymeric Ions in Solution.......................... 283
KOLTHOFF, I. M., and DALE, W. J.: Potassium Ferricyanide–Diazothio Ether–Mercaptan Recipe for Emulsion Polymerization of Butadiene and Styrene. II. Effect of Some Chemical Variables 301
VAN AMERONGEN, G. J.: Influence of Structure of Elastomers on Their Permeability to Gases................................ 307
MÜNSTER, A.: Die Löslichkeit hochpolymerer Fadenmoleküle...... 333
CONN, W. R., and NEHER, H. T.: Inhibiting Effect of Acrylonitrile on Polymerization of Vinyl Acetate........................ 355
FOSTER, F. C.: Friedel-Crafts Copolymerization of Chloroprene–Styrene.. 369
SHEPPARD, E., MCLAREN, A. D., and JOHNSON, P.: Ultracentrifuge Studies on the Crystalline Compound of Trypsin and of Soybean Trypsin Inhibitor (Letter to the Editors).................. 375
BOYER, R. F., and SPENCER, R. S.: Critical Concentration Effects in Dilute High Polymer Solutions (Letter to the Editors)........ 375
ATHERTON, E.: Pyrolysis of Polystyrene (Letter to the Editors).... 378

McLaren, A. D., and Lewis, C.: Concerning the Inactivation-Denaturation of Pepsin (Letter to the Editors) 379
Doty, P. M., and Steiner, R. F.: Note on the Distribution of Polymer Molecules in Dilute Solution (Letter to the Editors) 383
Reviews 387
Polymer News 390
Summaries of Articles Received S21

Number 4, August

Kolthoff, I. M., and Medalia, A. I.: Redox Recipes. II. Redox Recipes in Alkaline Medium Initiated by the System Cumene Hydroperoxide–Iron–Sugar at 30° 391
Maschka, A., und Mendl, A.: Untersuchung einer katalysierten Leinölstandölkochung unter Heranziehung der Ultraviolettspektrographie (Vergleich mit nichtkatalysierten Prozessen) 429
Campbell, H., and Johnson, P.: Aging of Solutions of Cellulose Nitrate 443
Brown, C. J.: Some Polymeric Derivatives of Phosphonitrile Chloride 465
Peterlin, A.: Viscosity and Sedimentation of Linear Macromolecules Exhibiting Partial Solvent Immobilization 473
Wiley, R. H., and Hobson, P. H.: Polymerization of *m*- and *p*-Formylstyrenes 483
Bovey, F. A., and Kolthoff, I. M.: Mechanism of Emulsion Polymerizations. IV. Kinetics of Polymerization of Styrene in Water and Detergent Solutions 487
Krigbaum, W. R., and Wall, F. T.: Viscosities of Binary Polymeric Mixtures 505
Simha, R.: Degradation of High Polymers (Letter to the Editors) .. 515
Haas, H. C.: Catalysis of the Dechlorination by Zinc (Letter to the Editors) 515
Reviews 517
Hermans, P. H., and Weidinger, A.: Quantitative Investigation of X-Ray Diffraction by "Amorphous" Polymers and Some Other Noncrystalline Substances. (Errata, Article in *J. Polymer Sci.* **5**, 269, 1950) 518

Number 5, October

Kuhn, H., and Kuhn, W.: Effects of Hampered Draining of Solvent on the Translatory and Rotatory Motion of Statistically Coiled Long-Chain Molecules in Solution. Part I. Translation Resistance; Rate of Diffusion and Sedimentation 519
Stuart, H. A., und Peterlin, A.: Optische Anisotropie und Form von Fadenmolekülen. I. Depolarisationsgrad der Lichtzerstreuung von Lösungen mit Fadenmolekülen 543
Stuart, H. A., und Peterlin, A.: Optische Anisotropie und Form von Fadenmolekülen. II. Künstliche Doppelbrechung 551
Hermans, P. H., and Weidinger, A.: Crystallinity of Precipitated Cellulose 565

BOVEY, F. A., and KOLTHOFF, I. M.: Studies of Retarders and Inhibitors in the Emulsion Polymerization of Styrene. II. Inhibitors 569
MERZ, E. H., and RAETZ, R. W.: Influence of Molecular Weight on the Properties of Polystyrene. II. Fractionation of the Polymer 587
SPENCER, R. S.: Flow of Linear Amorphous Polymers 591
WILEY, R. H., BRAUER, G. M., and BENNETT, A. R.: Refractometric Determination of Second-Order Transition Temperatures in Polymers. V. Determination of the Refractive Indices of Elastomers at Temperatures from 25 to −120 °C 609
SIMHA, R., WALL, L. A., and BLATZ, P. J.: Depolymerization as a Chain Reaction 615
RISEMAN, J., and EIRICH, F. R.: Intrinsic Viscosity of Macromolecules (Letter to the Editors) 633
HAWARD, R. N.: Degradation of Ethyl Cellulose in Solution (Letter to the Editors) 635
REVIEWS 636
SUMMARIES OF ARTICLES RECEIVED S27

NUMBER 6, DECEMBER

VAN AMERONGEN, G. J., KONINGSBERGER, C., and SALOMON, G.: Chlorination of Natural Rubber. I. Preparation and Properties of Chlorinated Rubber 639
VAN AMERONGEN, G. J., and KONINGSBERGER, C.: Chlorination of Natural Rubber. II. Preparation and Properties of Rubber Dichloride 653
KOLTHOFF, I. M., DALE, W. J., and MILLER, I. K.: Potassium Ferricyanide–Diazothio Ether–Mercaptan Recipe for Emulsion Polymerization of Butadiene and Styrene. III. Determination of *p*-Methoxyphenyl Diazothio-(2-naphthyl)-ether 667
O'HARA, J. B., and PRUTTON, C. F.: Heterogeneous System for Polymerization of Vinyl Chloride 673
GOLDSTEIN, GILBERT, and STERN, KURT G.: Experiments on the Sonic, Thermal, and Enzymic Depolymerization of Desoxyribosenucleic Acid 687
CRAIG, DAVID, JUVE, A. E., and DAVIDSON, W. L.: Tetramethylthiuram Disulfide Vulcanization of Extracted Rubber. I. Introduction and Compounding 709
ALFREY, TURNER, JR., BOHRER, JOHN, HAAS, HOWARD, and LEWIS, CHARLES: Experimental Study of Copolymerization. IV 719
HERRENT, P., and JNOFF, G.: Titration Potentiométrique de la Viscose. III 727
PALS, D. T. F., and HERMANS, J. J.: New Method for Deriving the Intrinsic Viscosity of Polyelectrolytes (Letter to the Editors) 733
HERMANS, P. H., and VERMAAS, D.: Note on Density Determination of Cellulose Fibers by the Flotation Method in Carbon Tetrachloride (Letter to the Editors) 734

Basu, Sadhan: Molecular Weight of Nylon by End-Group Titration (Letter to the Editors) 735
Arnett, L. M., Meibohm, F. P. H., and Smith, A. F.: New Observations on the Small-Angle X-Ray Diffraction of Synthetic Fibers (Letter to the Editors) 737
Wales, M.: Transport of Uncharged Polymer Molecules by an Inhomogeneous Electric Field (Letter to the Editors) 739
Powers, P. O.: Mechanism of the Heat Bodying of Linseed Oil (Letter to the Editors) 741
Gaylord, N. G., and Eirich, F. R.: Peroxide-Catalyzed Polymerization of Isopropenyl Acetate (Letter to the Editors) 743
Flory, Paul J., and Fox, Thomas G, Jr.: Molecular Configuration and Thermodynamic Parameters from Intrinsic Viscosities (Letter to the Editors) 745
Review 748
Bovey, F. A., and Kolthoff, I. M.: Mechanism of Emulsion Polymerizations. IV. Kinetics of Polymerization of Styrene in Water and Detergent Solutions (Errata, article in *J. Polymer Sci.*, 5, S22–3, 487–504, 1950) 748
Author Index 749
Subject Index 753

JOURNAL OF POLYMER SCIENCE VOL. V, NO. 1, PAGES 1-54

Dynamic Mechanical Properties of Rubberlike Materials*

A. W. NOLLE,† *Acoustics Laboratory, Massachusetts Institute of Technology, Cambridge, Massachusetts*

I. INTRODUCTION

THE PURPOSE of this paper is to present data concerning the dynamic mechanical behavior of rubberlike materials and to interpret these data insofar as possible. The data were obtained by five experimental methods which have been described in another paper.[1] For convenience of discussion the experimental techniques will be referred to by the short titles which are listed below, together with the frequency ranges of the experimental methods:

The rocking-beam oscillator (0.1 to 25 cps.)
The vibrating reed (10 to 500 cps.)
Longitudinal-wave resonance (below 300 cps.)
Longitudinal-wave transmission (1 to 40 kc.) (strip transmission)
The magnetostriction method (12 to 120 kc.)

In addition certain data are obtained at a frequency of 15 megacycles by measuring the velocity and attenuation of bulk waves in rubber. The various experiments are conducted at temperatures in the range from −60° to 100°C. Each experimental method is useful throughout some temperature interval within this range. The exact limits of these intervals are dependent upon the nature of the particular rubber under study.

The quantities which are found from the experimental methods are the real and imaginary parts E_1 and E_2 of the complex dynamic Young's modulus E^*, where

$$E^* = E_1 - iE_2 \tag{1}$$

The quantity E_1 is the ordinary Young's modulus, in the case of a material which has no viscous losses, and is therefore a measure of the magnitude of the elastic force, which is in phase with displacement. The quantity E_2 is a measure of the magnitude of the viscous force which is out of phase with the displacement by $\pi/2$ radians. It is easily shown that:

---

* Submitted in partial fulfillment of the requirements for the degree of Doctor of Philosophy at the Massachusetts Institute of Technology. This work was supported in part under Contract NObs-25391, Task No. 1, with the Bureau of Ships.

† Now at the Department of Physics, University of Texas, Austin, Texas.

[1] A. W. Nolle, *J. Applied Phys.* **19,** 753–774 (1948). This paper contains references to previous work, most of which has dealt with dynamic rubberlike elasticity at frequencies not exceeding several hundred cycles per second and is therefore not directly connected with the results given in the present paper.

$$E_2 = \gamma\omega \tag{2}$$

where γ is the extensional viscosity coefficient and ω is frequency in radians per second. Both E_1 and E_2 will always be given the dimensions of dynes per square centimeter. It will usually be most convenient to give experimental results in terms of the real part of the modulus, E_1, and the dimensionless *loss factor*, E_2/E_1. The loss factor E_2/E_1 is equal to the cotangent of the mechanical impedance phase angle for a rigidly supported rubber sample which is small compared to an acoustic wave length, and is therefore a convenient measure of the "lossiness" of the sample.

Because the complex dynamic modulus of rubberlike materials varies with frequency, significant values for the real and imaginary parts of the modulus can be given only by experiments in which sinusoidal displacements are employed. All the experimental methods considered here are sinusoidal. Moreover, the strain amplitudes imposed on the rubber samples are always sufficiently small that nonlinear effects are avoided. In all experiments, except the vibrating reed, a static strain much larger than the dynamic strain is imposed on the sample. The dynamic modulus measured under this condition may be termed the *differential dynamic modulus*.

A more detailed discussion of the experimental quantities, together with mathematical relations by which the experimental quantities may be calculated from the results of each experiment, is contained in the previous paper in which the experimental methods are treated.[1]

II. DESCRIPTIVE DISCUSSION OF DYNAMIC MECHANICAL PROPERTIES OF RUBBERS

Summary of Results

Before a detailed discussion of the behavior of the complex dynamic modulus as a function of temperature and frequency is presented, it is appropriate to describe in more compact form the general nature of the dispersion effects as indicated by the experimental data. For this purpose, sketches of surfaces representative of the frequency-temperature behavior of the real modulus E_1 and of the loss factor E_2/E_1 are shown in Figure 1. These sketches are a semiquantitative representation of the experimentally observed behavior of the buna-N compound B-5, but the results have been extrapolated out of the observed range of frequency and temperature in some directions, in accordance with the best conclusions that can be reached from the experimental data. (Actual experimental results have been obtained throughout most of the frequency range shown below 10^5 cps. The complex bulk-wave modulus has been measured at 15 megacycles, and from this it has been possible to find upper limits to the values of the real and imaginary parts of the complex Young's modulus at 15 mc.)

The real part of the modulus, E_1, always increases with increasing frequency. In the room-temperature range a significant variation of this

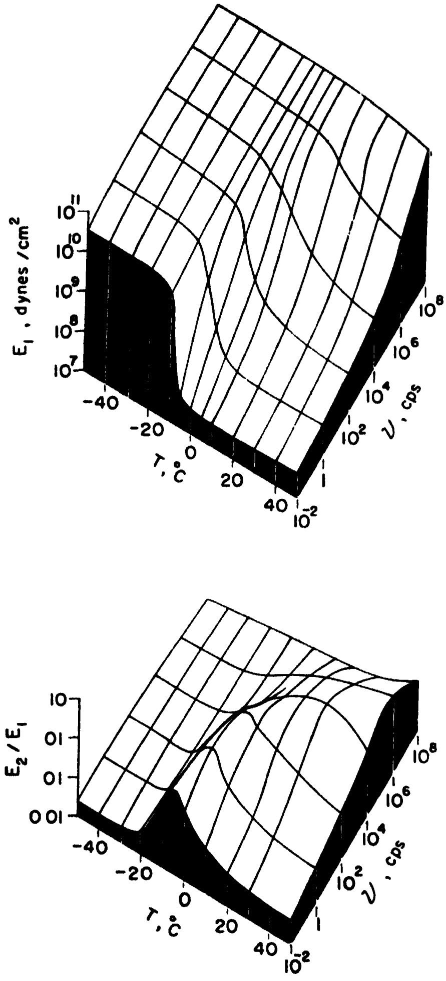

Fig. 1. Sketches showing approximate behavior of real part of dynamic Young's modulus (above) and of loss factor E_2/E_1 (below) over a wide range of frequency and temperature. The sketches are based on experimental data for buna-N compound B-5 (carbon filled), but are extrapolated according to the general conclusions reached in Part II of this paper.

quantity with frequency is shown experimentally to occur over at least six decades of frequency. The quantity E_1 also increases with decreasing temperature, except that in the region of the higher temperatures and very low frequencies E_1 is proportional to the absolute temperature. At low frequencies there exists a temperature range in which the increase of the real modulus with decreasing temperature is so rapid as to resemble a freezing phenomenon, but the manifestation of this "freezing" effect is dependent upon the rate of force application; thus at the higher temperatures the "freezing" occurs much less abruptly with decreasing temperature. The real modulus E_1 appears to approach limiting values at low temperatures or at high frequencies. At sufficiently low temperature the modulus is large for all observable frequencies and the dispersion is small.

At a given frequency the loss factor E_2/E_1 has a maximum with respect to temperature, which lies approximately in the temperature range where E_1 is increasing most rapidly with decreasing temperature. At the higher frequencies the maximum occurs at higher temperatures. For sufficiently low temperature or for sufficiently high frequency the loss factor becomes small.

Comparison with Dispersion in Polar Dielectrics

The experimental results reveal a high degree of similarity between the viscoelastic behavior of rubber and the dielectric behavior of polar materials. This similarity is best displayed when the rubber data are presented in terms of compliance (the reciprocal of modulus), but inasmuch as the concept of modulus is generally more familiar and more useful in work with rubbers, the dynamic modulus results will be discussed as such in the following paragraphs. The tabulation on p. 5 compares the results for the dynamic modulus of rubber which are either experimentally confirmed or strongly suggested by the data with those which have been found by other investigators for polar dielectrics.

For a more nearly complete discussion of simple polar dielectrics one may consult the work of Debye,[2] while for a discussion of the more complicated dielectrics one may consult the work of Kauzmann.[3]

For all rubbers investigated the range of dispersion is very broad in terms of frequency; significant variation of the modulus is often observed over at least six decades of frequency. The dielectric analogue is therefore not the simple Debye polar liquid or gas, in which dispersion occurs over one decade of frequency, but the more complicated dielectrics such as high polymers and in particular the rubbers themselves. (It does not follow that the reciprocal dynamic modulus and the dynamic dielectric constant for a given sample show identical frequency dependence, however.) The wide dispersion range may be described by the statement that the material has a wide distribution of relaxation times, in contrast to the Debye material, which has one relaxation time. The relaxation spectrum of rubber will be discussed in Part III of this paper. The significance of a wide relaxation spectrum from the dielectric point of view is illustrated in Figures 2 and 3.

---

[2] P. Debye, *Polar Molecules*. Chemical Catalog Co., Inc., New York, 1929.

[3] W. Kauzmann, *Rev. Modern Phys.*, **14**, 12 (1942).

	Rubber	*Dielectric*
(1)	Real part of the modulus always increases or remains constant with increasing frequency.	Real part of the dielectric constant always decreases or remains constant with increasing frequency.
(2)	Imaginary part of the modulus has a maximum with respect to temperature at constant frequency, and vice versa.	Imaginary part of the dielectric constant has a maximum with respect to temperature at constant frequency, and vice versa.
(3)	Loss factor E_2/E_1 has a maximum with respect to temperature at constant frequency, and vice versa.	Loss factor has a maximum with respect to temperature at constant frequency, and vice versa.
(4)	Imaginary part of the modulus approaches zero at zero frequency and probably approaches progressively smaller values at high frequencies past the peak.	Imaginary part of the dielectric constant approaches zero at zero frequency and at very high frequencies.
(5)	Imaginary part of the modulus is large where the real part changes rapidly with logarithm of frequency or with temperature.	Imaginary part of the dielectric constant is largest where the real part changes most rapidly with logarithm of frequency or with temperature.
(6)	Real part of the dynamic modulus approaches limiting high value at low temperatures.	Real part of the dynamic dielectric constant approaches limiting low value at low temperature.
(7)	Real part of the modulus has limiting values at high and low frequencies.	Real part of the dielectric constant has limiting values at high and low frequencies.
(8)	An increase of frequency is qualitatively equivalent to a decrease of temperature in effect upon the dynamic modulus.	An increase of frequency is qualitatively equivalent to a decrease of temperature in effect upon the dynamic dielectric constant.
(9)	Real part of the modulus decreases with increasing temperature in regions of appreciable dispersion, but increases with increasing temperature at low frequencies.	Real part of the dielectric constant increases with increasing temperature in regions of appreciable dispersion, but decreases with increasing temperature at low frequencies.

Figure 2 illustrates the theoretical behavior of a Debye dielectric as plotted by Cole and Cole.[4] This behavior, corresponding to one relaxation time, is approached by various practical liquid and gaseous dielectrics. Figure 3 shows dielectric data for natural rubber as plotted by Kauzmann[3] from the work of Scott, McPherson, and Curtis.[5] Because of the wide relaxation spectrum of natural rubber, the dielectric dispersion curve for this material extends over nearly three decades of frequency as compared to one decade for the Debye material.

Actual experimental data from the present series of measurements will be cited in the following paragraphs to substantiate the aspects of rubberlike elasticity which are included in the foregoing tabulation. It will be found that the temperature effects mentioned above are more completely described by the experimental data than are the frequency effects, because at the higher temperatures there exist important relaxation effects at frequencies above the present upper frequency limit of about 10^5 cps. for direct Young's modulus measurements.

[4] K. S. Cole and R. H. Cole, *J. Chem. Phys.*, **9**, 341 (1941).

[5] A. H. Scott, A. T. McPherson, and H. L. Curtis, *Bur. Standards J. Research*, **11**, 173 (1933).

1. Increase of Real Modulus With Increasing Frequency. Figure 4 presents experimental dynamic modulus data for compound B-5, a carbon-filled buna-N cement, from 10 cps. to 18 kc. The data below 1000 cps. were obtained as shear modulus by G. W. McClure of the M. I. T. Acoustics Laboratory, who measured the low-frequency mechanical impedance of the material with an electromechanical vibrator in which the material was deformed in shear between a moving plate and a fixed plate. These data have been multiplied by 3 to give Young's modulus. The data above 1000 cps. were obtained by the longitudinal-wave transmission method, in which the quantities measured directly are the wave length and the attenuation for longitudinal waves in a thin strip. The continuous upward trend of the real part of the modulus over these several decades of frequency is evident. Qualitatively similar data have been obtained for butyl, GR-S, neoprene, and natural rubbers. Usually the low-frequency modulus has been measured by the vibrating-reed method rather than by the shear vibrator method mentioned above; in such a case fewer different low frequencies are represented, but similar results are obtained.

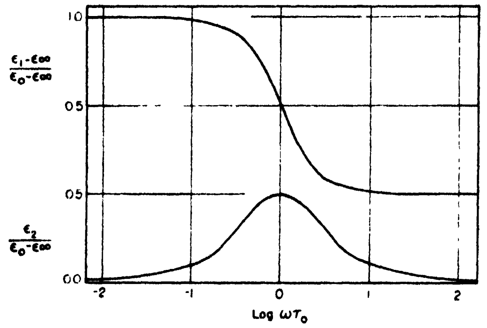

Fig. 2. Real part (ϵ_1) and imaginary part (ϵ_2) of dielectric constant plotted against a generalized frequency parameter, for a simple Debye dielectric (after Cole and Cole[4]).

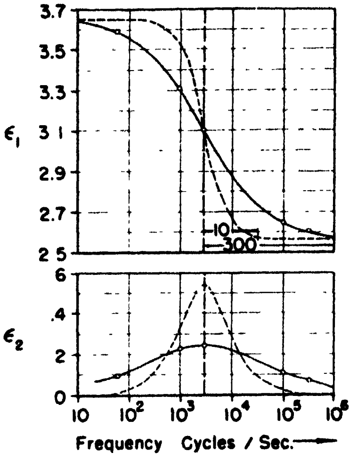

Fig. 3. Dielectric behavior at 0°C. of natural rubber vulcanized with 8% sulfur; dotted curves are closest approximation by Debye relations (taken from Kauzmann[3]; original data due to Scott, McPherson, and Curtis[5]).

Figure 5 shows the dynamic modulus of a natural rubber gum vulcanizate, compound N-1, for frequencies from 1 cps. to 6 kc. (The 1 cps. modulus is indistinguishable from the value[6] of the static modulus for this compound.) These data are obtained by the rocking-beam oscillator for frequencies up to 25 cps, by longitudinal-wave resonance in a thin strip for frequencies to 300 cps., and by the longitudinal-wave transmission method for the higher frequencies. Within these frequency limits only a gradual increase of the real modulus with increasing frequency is present, reflecting

---

[6] E. Guth, H. M. James, and H. Mark, in *Advances in Colloid Science,* Volume II, *Rubber,* pp. 253–298. Interscience, New York, 1946.

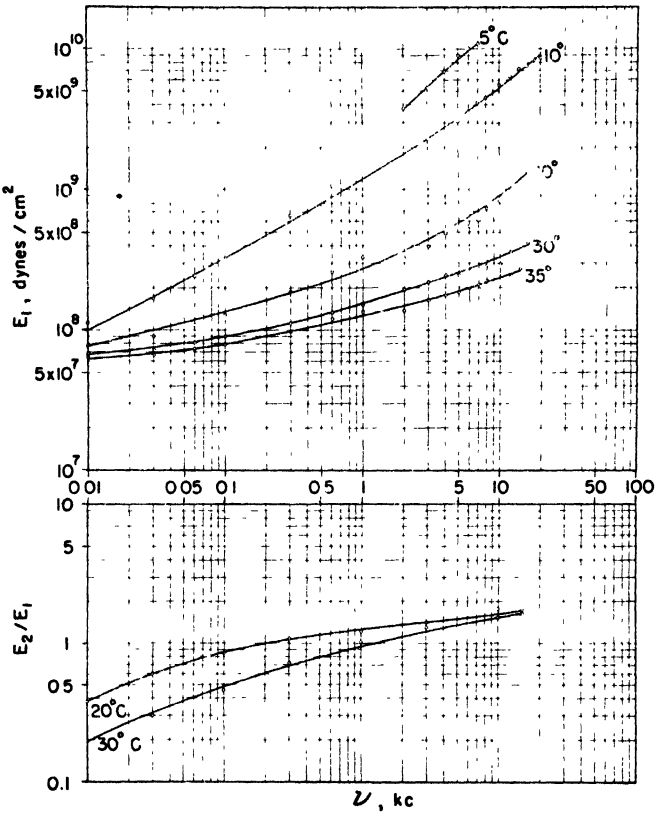

Fig. 4. Above, real part of dynamic Young's modulus as a function of frequency. Below, loss factor E_2/E_1 as a function of frequency. Buna-N compound B-5 (carbon-filled vulcanizate). 10% static elongation for data above 1 kc. (longitudinal-wave transmission experiment). Lower frequency data obtained by shear deformation with negligible static strain.

the faster relaxation spectrum of natural rubber as compared to the buna-N synthetics. No valid instance of a decrease of the real part of the modulus with increasing frequency has been found in any of the experimental data.

The validity of Assertion *1* may be established by a simple argument based on the definition of the real part of the modulus. The real part of the modulus, E_1, is easily shown to be equal to $Re(-i\omega Z_m)$, where Z_m is the mechanical impedance of a unit cube of the sample, other than the impedance which is due to the motion of the mass of the sample. Such an impedance will never include reactance having the sign associated with masslike impedance. Consequently the impedance can be represented by combinations of mechanical resistances and springs, or from the electrical point of view by combinations of resistances and capacitances (at least at frequencies where the ordinary laws of mechanics hold). For no such combination can $Re(-i\omega Z_m)$ decrease with increasing frequency.

2. *Maximum of Imaginary Part of Modulus.* The maximum of the imaginary part of the modulus, E_2, with respect to temperature is illustrated in Figure 6, which is a plot of dynamic modulus data for the buna-N vulcanizate B-100. The modulus quantities are plotted as a function of temperature, for frequencies of 12 and 70 kc. The data are obtained from the magnetostriction rod apparatus. The actual value of the maximum of E_2 is larger at the higher frequency in this particular range. Figure 7 shows data obtained at low frequencies for the compound B-5, which is also a buna-N vulcanizate but which contains carbon. These data are obtained by the vibrating-reed method. In this method, which depends upon finding the frequency and the band width for the forced-vibration resonance of a rubber reed, the frequency is proportional to the square root of the modulus. Therefore the result is not a true constant frequency curve. While E_1 and E_2/E_1 are plotted here instead of E_2, one may see by inspection that a maximum of E_2 exists within the temperature range of the plot.

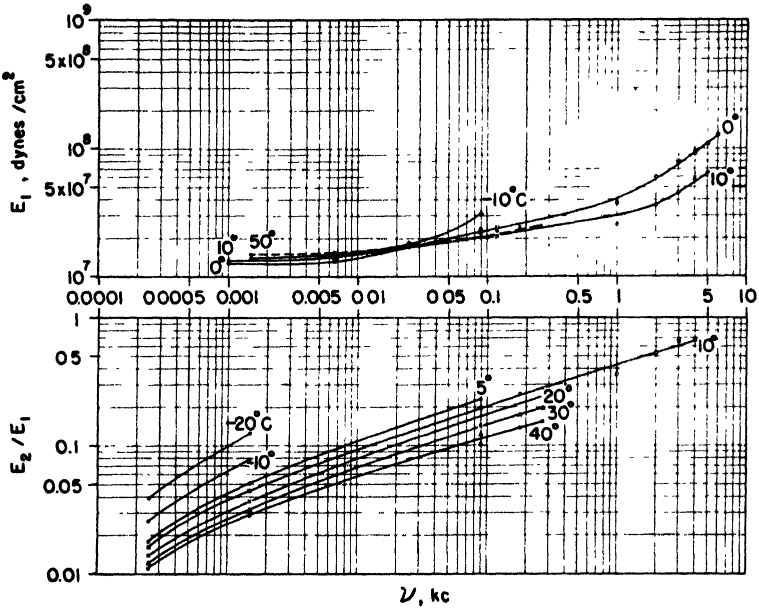

Fig. 5. Above, real part of dynamic Young's modulus as a function of frequency. Below, loss factor E_2/E_1 as a function of frequency. Natural rubber gum vulcanizate N-1. 10% static elongation.

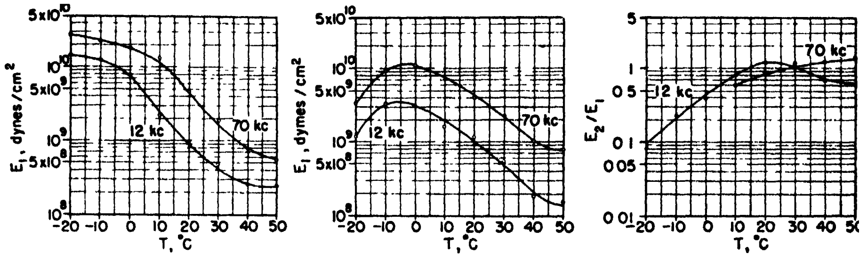

Fig. 6. Left, real part of dynamic Young's modulus as a function of temperature. Center, imaginary part of dynamic Young's modulus. Right, loss factor E_2/E_1. Buna-N gum vulcanizate B-100. Static deformation less than 1% compression.

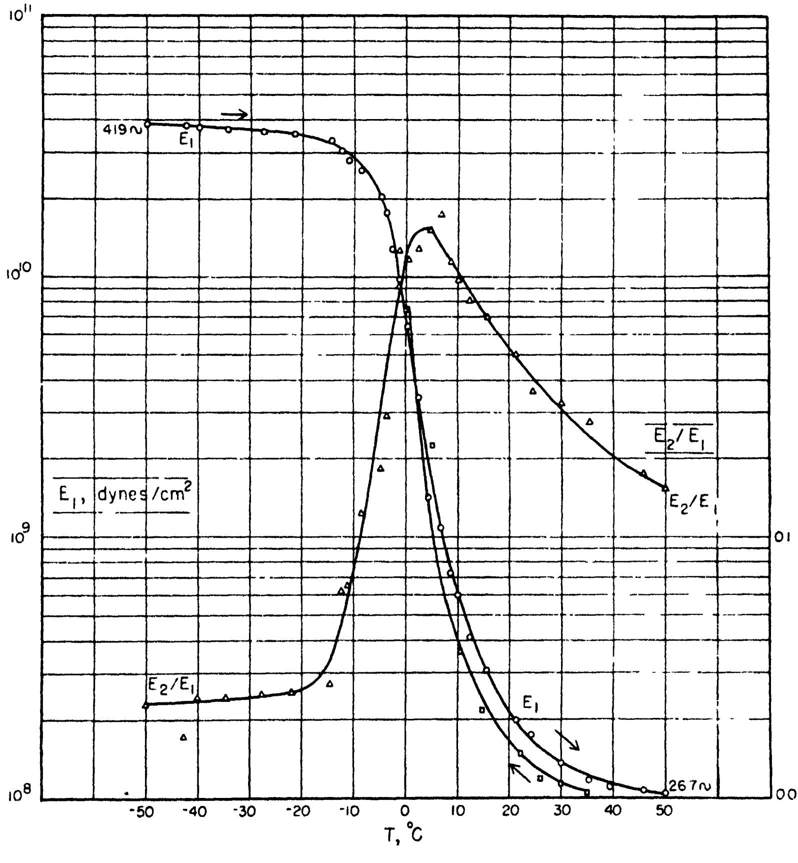

Fig. 7. Real part of dynamic Young's modulus and loss factor E_2/E_1 as functions of temperature. Buna-N carbon-filled vulcanizate B-5. No static deformation. Data from vibrating-reed experiment; frequency varies with modulus.

The other methods of measurement are not capable of giving results through the region of lower temperatures in which the imaginary part of the modulus for a given material has its maximum.

The maximum of the imaginary part of the modulus with respect to *frequency* is difficult to observe in the ordinary range of temperature in which true rubberlike elasticity is observed. This maximum is not observed with the method of longitudinal-wave transmission in thin strips, because excessive attenuation always prevents extending the frequency of measurement up to the value where the maximum might occur. The maximum certainly occurs at some frequency higher than 10 or 20 kc. at room temperature for all the rubbers which have been studied. The magnetostriction method provides information at higher frequencies, but since this method covers only one decade of frequency it cannot provide a reliable indication of a broad maximum. Insofar as the present measurements are concerned the existence of a maximum of the imaginary part of the modulus with respect to frequency rests upon the observed principle that an increase of frequency is qualitatively equivalent to a decrease in temperature. Hence it appears justifiable to assert that the maximum occurs with respect to frequency as well as with respect to temperature. This assertion is in agreement with the relaxation spectrum interpretation of the results, which will be discussed in a later section.

A maximum of E_2 with respect to frequency has been observed experimentally by Sack, Laub, and Work[7], who found a maximum of this quantity at about 2500 cps. for temperatures of $-20\,^{\circ}$C. and lower, in the case of a butadiene-styrene copolymer.

3. Maximum of the Loss Factor E_2/E_1. The maximum of E_2/E_1, which is equal to the cotangent of the mechanical impedance phase angle of the viscoelastic system, can be found as a function of temperature by any of the methods which indicate the maximum of E_2 alone as a function of temperature. This is illustrated in Figures 6 and 7, to which reference was made in the preceding paragraphs. All the experimental evidence shows that E_2/E_1 continues to decrease progressively as the temperature is lowered by any amount below that corresponding to the maximum.

Some scanty experimental data have been obtained with regard to the maximum of E_2/E_1 as a function of frequency. In Figure 6 it appears that for the higher temperatures E_2/E_1 increases from 12 to 70 kc., while for the lower temperatures the quantity decreases with increasing frequency over this range. Thus E_2/E_1 may increase or decrease with frequency according to the part of the frequency–temperature range investigated, from which the existence of a maximum with respect to frequency may be postulated. The postulate is strengthened by the observation that an increase of frequency is qualitatively equivalent to a decrease in temperature.

Figure 8 shows dynamic modulus data as a function of frequency at several different temperatures for the buna-N vulcanizate B-1. The curve for E_2/E_1 at 20°C. shows a peak within the observable frequency range, while the slopes of the other E_2/E_1 curves indicate that the peak must exist at higher or lower frequencies for higher or lower temperatures, respectively. These data were obtained by the longitudinal-wave transmission method.

---

[7] H. S. Sack, H. L. Laub, and R. N. Work, *J. Applied Phys.*, **18**, 450 (1947).

In principle one can observe a low-frequency peak by means of the vibrating-reed resonance method, but the observation would necessitate the use of many reeds of different lengths and the examination of resonances in the difficult temperature range in which the relative band width of the sample is very large.

Further evidence for the existence of a frequency maximum of the loss factor, in the case of the particular compound B-5, has been deduced from the results of 15 mc. bulk-wave transmission measurements (see Appendix I). It appears that the loss factor at room temperature for this compound is less than unity at 15 mc., whereas longitudinal-wave transmission measurements at 20 kc. give a value of about 2.

4. Vanishing of E_2 at Extreme Frequencies. That E_2 must approach zero at zero frequency is readily seen from the definition of the quantity, $E_2 = \gamma\omega$. E_2 must approach zero as ω approaches zero unless the viscosity γ becomes infinite under this condition. One may readily ascertain that the viscosity does not become large without limit at low frequency by observing that a sample of vulcanized material will reach an equilibrium elongation after a suitable time interval when a weight is attached to the sample. For all of the materials studied E_2 does indeed become progressively smaller with decreasing frequency. However, E_2 never becomes so small as to be undetectable at any frequency within the range of practicable laboratory procedure, because the viscosity γ is measurably large at all frequencies.

Experimental measurements at high frequencies have not been sufficiently numerous to demonstrate that E_2 can be made smaller than any preassigned value by increase of frequency. That E_2 does decrease with sufficiently high frequency is suggested by the same evidence which suggests that E_2 has a maximum value with respect to frequency. The experimental observation that E_2 becomes progressively smaller with considerable temperature reduction, together with the principle of equivalence between decrease of temperature and increase of frequency, is thus the main experimental basis for suggesting that the high-frequency trend of E_2 is toward progressively smaller values rather than toward some finite limiting value smaller than the maximum.

5. Imaginary Part of Modulus Is Large Where Real Part Changes Rapidly With Logarithm of Frequency or With Temperature. The vibrating-reed data of Figure 7 illustrate clearly how E_2/E_1 and E_2 become large at temperatures where E_1 is highly temperature-sensitive; the maximum value of E_2/E_1 as a function of temperature in fact coincides closely with the region of maximum slope for E_1. Similar behavior is observed for all the rubbers which are represented in this investigation.

The data of Figures 4 and 5 show that the imaginary part of the modulus becomes large relative to the real part—that is, E_2/E_1 becomes large, for those combinations of temperature-frequency in which the real part of the modulus is changing rapidly with the logarithm of frequency. By an extension of the Debye relaxation theory one would expect in addition that the *maximum* of E_2 with respect to frequency coincides closely with the *maximum* derivative of E_1 with respect to the logarithm of frequency. It is not possible to cite experimental measurements which confirm this expectation,

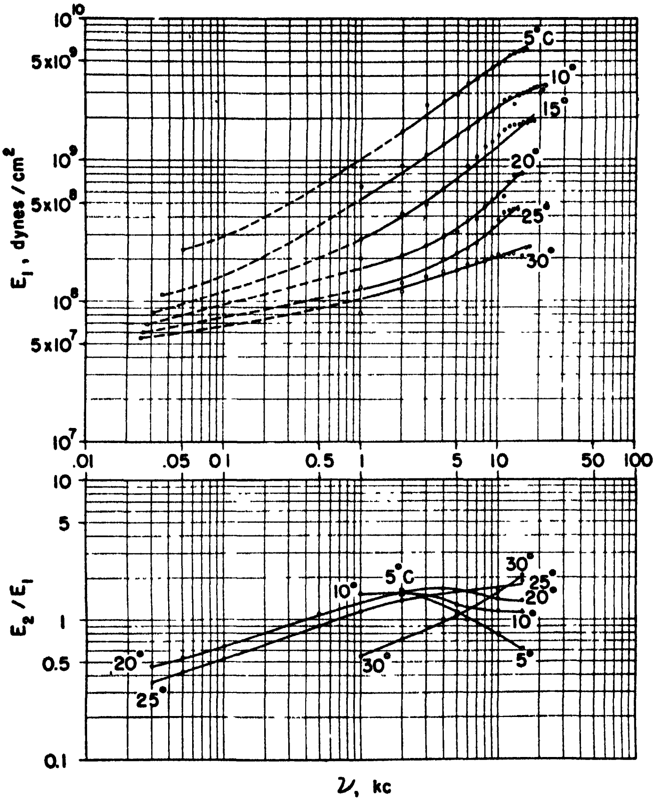

Fig. 8. Above, real part of dynamic Young's modulus as a function of frequency. Below, loss factor E_2/E_1 as a function of frequency. Buna-N gum vulcanizate B-1. Higher frequency data from longitudinal-wave transmission experiment (10% static elongation); low-frequency data from vibrating-reed experiment (no static deformation).

because as explained under section *2* above, the maximum of E_2 at ordinary temperatures lies in a frequency range in which measurements by the present techniques are difficult.

6. Real Part of Modulus Approaches Limiting High Value at Low Temperature. This conclusion is strongly suggested by the results of variable-temperature experiments with the vibrating-reed technique. Data comparable to those of Figure 7 are found for each rubberlike material. The sample stiffens rapidly with decreasing temperature through a certain temperature range. For lower temperatures little additional stiffening occurs with further reduction of temperature. *The low-temperature dynamic modulus which thus appears to approach a limiting value, is about* 2×10^{10} *dynes/cm.*^{2} *for all the gum rubbers investigated.* These include buna-N, butyl, GR-S, neoprene, and natural rubber. Carbon loading increases the figure somewhat. It must be understood that the above discussion of the low-temperature dynamic behavior of rubber is based on experimental results obtained at temperatures above 200° Kelvin. It appears probable that the important changes in the dynamic behavior in the temperature range between 200° and 300° K. are due to the effects of temperature upon the relaxation mechanisms. Thus it is possible that in the limit of zero temperature the complete suppression of thermal agitation might lead to another result.

7. Real Part of Modulus Has Limiting Values at Low and High Frequencies. The real part of the modulus obviously has a limiting low-frequency value only for vulcanized materials in which continuous plastic flow cannot occur under reasonable static forces. For these materials one can easily demonstrate the existence of a limiting low-frequency modulus, or static modulus, by attaching a weight to a sample and observing that the system eventually reaches an equilibrium configuration which does not vary significantly for days.

The supposition that there is a limiting high-frequency modulus is not directly verified by experimental data because of the difficulty of making measurements at sufficiently high frequencies. It appears that Young's modulus measurements for frequencies up to several megacycles would be necessary in order to examine the question for rubbers at room temperature. The notion that the real modulus approaches a limiting large value with increasing frequency is suggested by the observation that at no frequency up to 120 kc. does the real modulus exceed several times 10^{10} dynes/cm.^{2} with cooling to −20°C., even though the modulus at several hundred cycles reaches about this magnitude with cooling to a temperature of −10°C. or lower. (This observation was made on the buna-N compounds B-99 and B-100.) Thus the large limiting value of the modulus at low temperature seems also to represent a large limiting value with respect to frequency for these low temperatures. From the general equivalence between decreasing temperature and increasing frequency which is found at observable temperatures and frequencies, one may suppose that at higher temperatures the modulus also approaches a large limiting value with increasing frequency, but that the leveling of the curve occurs at frequencies well above the 120 kc. limit of the experimental measurements.

8. Equivalence of Frequency Increase With Temperature Decrease. The qualitative equivalence between an increase of frequency and a decrease in temperature may be seen in any of the plots of experimental data in which both frequency and temperature occur as parameters. For example, in

Figure 4 it is evident that a given increase of real modulus over that found at a particular frequency–temperature combination may be obtained either by going to a lower temperature or by going to a higher frequency. In Figure 6 it appears that an increase of frequency shifts the points on the modulus temperature curves in the same sense as a decrease of temperature. In particular one may notice that the temperature maximum of E_2/E_1 is shifted to a higher temperature by an increase of frequency.

It should not be inferred that such details of the modulus curves as the slope with respect to frequency or temperature are transferred through an increase of frequency which is followed by such an increase of temperature as maintains the modulus itself constant. This quantitative transfer of the curves is not found over any wide range of temperature or frequency. For example, it may be seen in Figure 6 (compound B-100) that the modulus increases much less rapidly with decreasing temperature at 12 kc. and 70 kc. than is the case in Figure 7 (compound B-5) for low frequencies. (The compounds to which the data of these two figures apply are sufficiently similar to make this particular comparison valid; consequently a separate figure for low-frequency data pertaining to compound B-100 is not included.) On a theoretical basis one would *not* in general expect the logarithmic frequency derivative of the real modulus to be the same on every point of an equal-modulus contour in the temperature–frequency plane, except in the case of a substance having a single relaxation time.

9. Real Modulus Increases With Decreasing Temperature in Dispersion Regions and Increases With Increasing Temperature at Low Frequencies. It has been found experimentally that the real dynamic modulus of natural rubber when measured at low frequencies increases with increasing temperature in essentially the manner predicted by the kinetic theory of rubberlike elasticity. As the frequency of measurement is increased the temperature effect gradually reverses, until above 100 cps. the real modulus decreases with increasing temperature. A similar phenomenon is observed for butyl rubber, but the change occurs at about one cycle per second for this rubber. It appears that equivalent results probably hold for all the synthetic rubbers, but that the change of temperature dependence for some of these rubbers occurs at a small fraction of one cycle per second. This topic is considered in detail in Part III.

Representation of Dynamic Modulus Data in the Complex Plane

Cole and Cole[4] have shown that the dielectric data for a large number of polar materials fall on circular arcs in the complex plane. The nature of the plot is shown in Figure 9. The horizontal and vertical scales represent, respectively, the real and imaginary parts ϵ_1 and ϵ_2 of the complex dielectric constant, ϵ^*. Each point along the arc corresponds to a different frequency. A different arc is found for each temperature. The left and right ends of the arc represent, respectively, the limiting values of the dielectric constant at infinite frequency and at zero frequency, ϵ_∞ and ϵ_0. The arc is determined by these two values and by the parameter α, whose geometric significance in terms of the arc is indicated in the figure. Values of α range from 0 to 1. The condition $\alpha = 0$ corresponds to a semicircular arc, which is found for a simple Debye dielectric with a single relaxation time. As shown by Cole and Cole, the Debye expression for the dielectric constant of a simple polar substance may be written:

$$u + v = \epsilon_0 - \epsilon_\infty \qquad (3)$$

where $u = \epsilon^* - \epsilon_\infty$, and where in this particular case $v = i\omega\tau_0(\epsilon^* - \epsilon_\infty)$. Thus the vectors u and v, illustrated in Figure 9, are perpendicular and have a constant resultant; the locus of their intersection is a circle. The relaxation time τ_0 is equal to a constant factor times the relaxation time used by Debye.

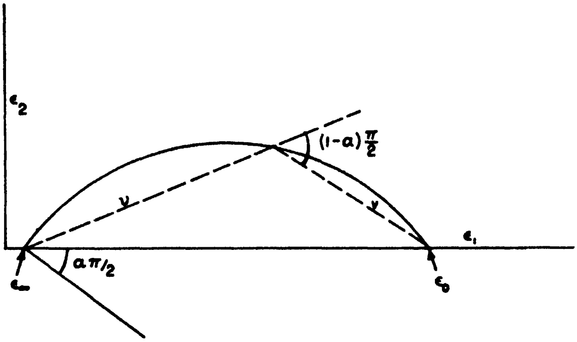

Fig. 9. Sketch of arc in complex plane as usedby Cole and Cole[4] for representation of dielectric data. Horizontal axis, real part of dielectric constant. Vertical axis, imaginary part of dielectric constant.

While the circular arc plot thus has theoretical justification for a Debye dielectric, the application of the same type of plot to more complicated dielectric data is justified only because the circular arc plot is found experimentally to be a satisfactory representation of the data. The more complicated materials, which do not have a single relaxation time, give rise to data which can be fitted on an arc which is less than a semicircle, that is, an arc for which $\alpha > 0$. Although no theory has been built from fundamental postulates to explain the behavior of such data, Cole and Cole give a consistency test which may be applied to the arc data. The general equation for the arc may be written:

$$\epsilon^* - \epsilon_\infty = (\epsilon_0 - \epsilon_\infty)/\left| 1 + i^{(1-\alpha)}f(\omega) \right| \qquad (4)$$

Cole and Cole argue that for a sinusoidal signal $e^{i\omega t}$ the quantity $i\omega$ behaves as a single entity in all linear circuit transformations. Consequently $f(\omega)$ must depend on ω as $\omega^{1-\alpha}$. Then (4) becomes:

$$\ln |v/u| = \ln |(\epsilon_0 - \epsilon^*)/(\epsilon^* - \epsilon_\infty)| = \text{constant} + (1 - \alpha) \ln \omega \qquad (5)$$

Thus $(1-\alpha)$ is the slope of the plot of $\ln |v/u|$ against $\ln \omega$. The value of α obtained from a plot of this nature should agree with the value obtained from the circular arc.

In order to investigate the suitability of the Cole arc as a representation of dynamic modulus data, it is desirable that the complex modulus data be transformed into complex compliance. The complex compliance S^* is defined as:

$$\begin{aligned} S^* &= S_1 + iS_2 = 1/E^* \\ S_1 &= E_1/(E_1^2 + E_2^2) \\ S_2 &= E_2/(E_1^2 + E_2^2) \end{aligned} \tag{6}$$

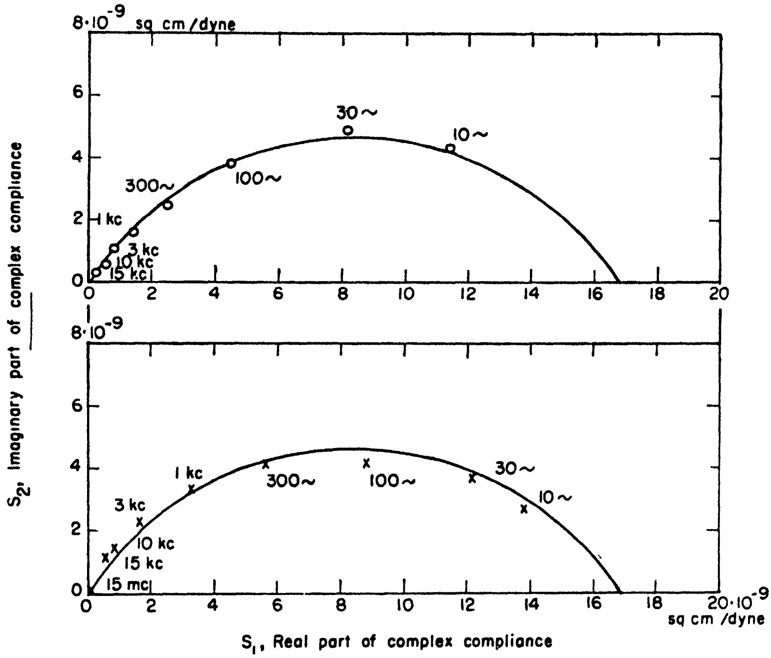

Fig. 10. Rubber compliance data plotted in the complex plane. Buna-N carbon-filled vulcanizate B-5. Above, 20°C. Below, 30°C. The same arc is used for both plots, but is chosen to fit the 20°C. data.

This transformation is desirable because compliance, which is the ratio of mechanical displacement to mechanical force, is analogous to the dielectric constant, which is the ratio of electric displacement to electromotive force.

The first illustration of the plotting of complex compliance is given in Figure 10; 20°C. and 30°C. data are shown for the carbon-loaded buna-N vulcanizate B-5. To facilitate comparison of the data for the two temperatures the same arc is drawn for each set of data, although the arc is chosen for an optimum fit to the 20° data and some readjustment would be required to secure the best fit at 30°. While the arc is a satisfactory representation of the data over the frequency range which is covered here, the data do not pass the consistency test of equation (5). The value of α from the 20° arc is 0.35, while the value obtained by plotting ln v/u against ln ω is 0.43 (this plot is not shown). Thus the progress of the compliance vector along the arc with frequency is that which would be associated with a larger value of α (that is, with a flatter arc or a wider relaxation spectrum) than that which is obtained by making the actual circular arc plot.

A second example is shown in Figure 11, which is a plot of complex compliance data for the buna-N gum vulcanizate B-1. The circular arc affords an approximate but by no means exact representation of these data.

Thus it appears that the Cole arc can serve as a useful means for compact presentation of complex compliance data for rubberlike materials. However, since the arc representation for present data does not pass the consistency test of equation (5), the Cole plot will not be taken as the basis for analysis of the experimental results, and the interpretation of the arc in terms of a relaxation spectrum will be omitted. The results of this interpretation, which leads to a relaxation spectrum having symmetry on a logarithmic scale, may be found in the paper by Cole and Cole.[4]

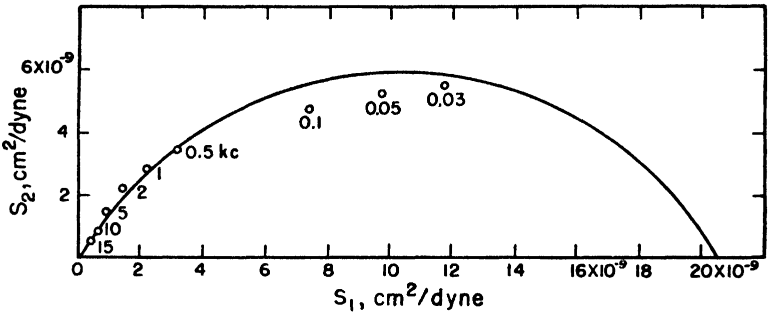

Fig. 11. Rubber compliance data plotted in the complex plane. Buna-N gum vulcanizate B-1, 20°C. Based on modulus data taken from Figure 8.

Complex modulus data, as well as complex compliance data, should fall on an arc which intersects the real axis at two points. Unfortunately the experimental measurements do not extend to frequencies high enough to encompass the maximum of E_2. For this reason the available modulus data, when plotted in the complex plane, simulate a curve segment which is only slightly bent and the result is not instructive.

Effect of Additional Parameters on Dynamic Modulus

To ascertain the importance of some of the variables of composition and of static deformation as possible sources of variation in the dynamic modulus some short investigations of their effects were undertaken. The results are described in the following paragraphs. A complete examination of any one of these topics would require an extended research program.

Static Deformation

In general, the static deformation of a sample influences both the magnitude and the phase angle of the dynamic modulus. The evidence on this point is summarized in the following two statements: (*a*) Static elongation up to 50% produces less than a two-to-one change in E_1 and in E_2/E_1 for both natural and synthetic rubbers, while for some compounds the effect is much smaller than this limit. (*b*) The effect cannot generally be described in terms of any simple systematic shift of the modulus–frequency curves or of the modulus–temperature curves.

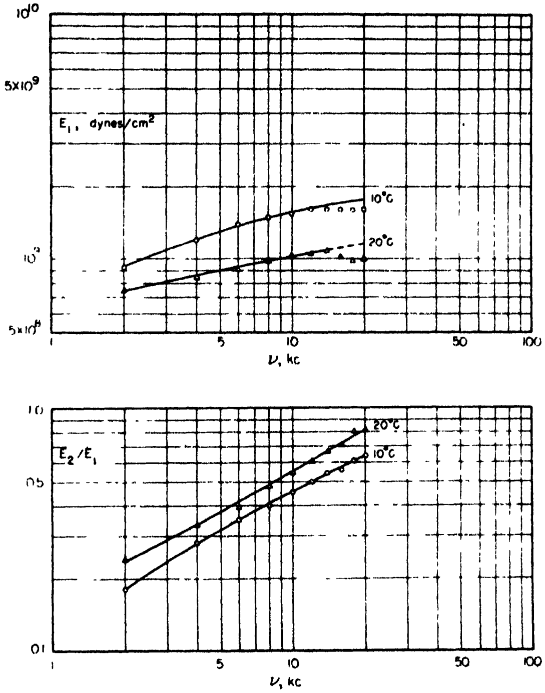

Fig. 12. Above, real part of dynamic Young's modulus as a function of frequency. Below, loss factor E_2/E_1 as a function of frequency. Neoprene vulcanizate CG-1. 10% static elongation.

If the real part of the differential dynamic modulus were equal to the slope of the static stress–strain curve, the real modulus would decrease systematically with increasing elongation, in the case of gum vulcanizates, up to the value of strain at which the well-known upward inflection of the stress–strain curve occurs. There is no reason to doubt that this effect is observable at very low frequencies. But this simple relation has not been observed at frequencies greater than one kilocycle, except that this behavior is approximated by natural rubber (latex film) at temperatures above 40 °C., even for frequencies as large as 5 kc. In general, the real dynamic modulus may either increase or decrease with increasing static elongation. Elongation greater than 50% has not been studied with the present techniques because the samples are not strongly enough held in the apparatus to support the stress corresponding to greater extensions.

An anomalous behavior with respect to static elongation is displayed by the neoprene compound CG-1. This compound shows a decrease in the real part of the modulus, and in addition a striking increase of 10 to 20 times in the loss factor E_2/E_1 when the static elongation is increased from 10 to 40%. Experimental data on this point, obtained with the longitudinal-wave transmission technique, are shown in Figures 12 and 13.

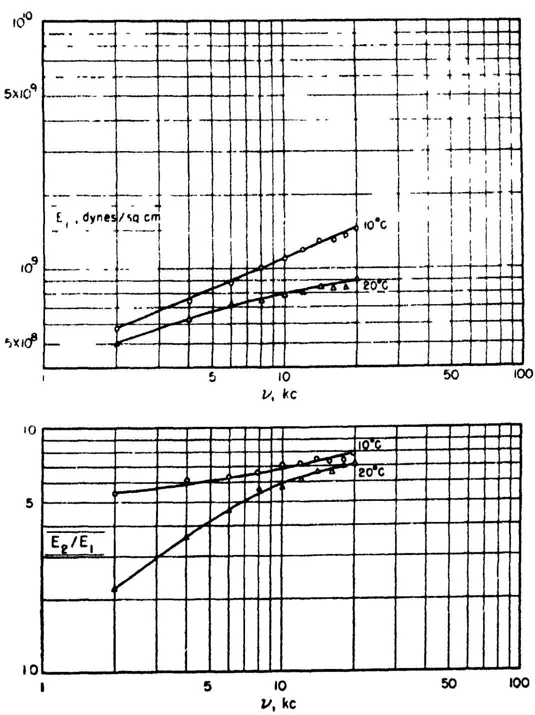

Fig. 13. Above, real part of dynamic Young's modulus as a function of frequency. Below, loss factor E_2/E_1 as a function of frequency. Neoprene vulcanizate CG-1. 35–40% static elongation.

The high sensitivity of this compound to static elongation is associated with a sudden yielding which is observed when a sample is strained to slightly more than 5% elongation in a static testing machine. The sample proceeds from just over 5% to nearly 100% elongation with negligible increase in stress. The effect is irreversible.

The central purpose of the investigation reported in this paper is to examine the dynamic modulus as a function of temperature and frequency.

The importance of the subsidiary investigation of the effect of static elongation is to indicate that static strain can be a significant parameter in dynamic modulus measurements, though in general of lesser importance than temperature and frequency. Consequently the static deformation should be reported for each measurement of dynamic modulus. The dynamic data given in this paper, except those of Figure 13, correspond to static elongation or compression not exceeding 10%.

Vulcanization

It is evident that a nonzero dynamic modulus at vanishingly low frequency can only be found in a vulcanized rubber, because in the absence of vulcanization rubber flows without a sharp limit under a static force. Thus

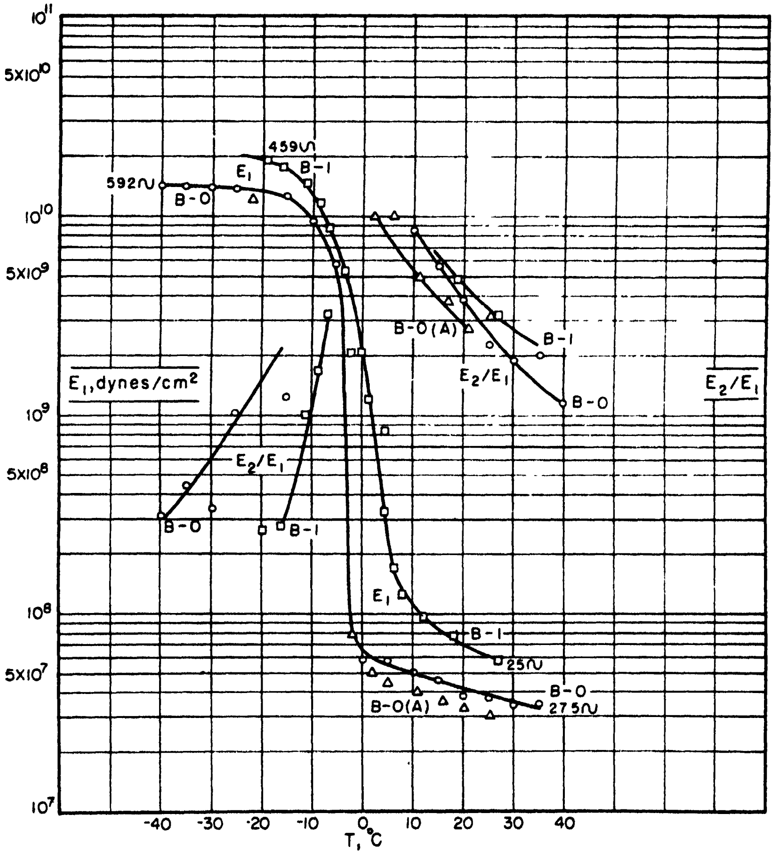

Fig. 14. Real part of dynamic Young's modulus and loss factor E_2/E_1 as functions of temperature. Buna-N unvulcanized gum B-0 and buna-N gum vulcanizate B-1. No static deformation. Data from vibrating-reed experiment; frequency varies with modulus. Points "B-0(A)" (triangles) are data for compound B-0 before evaporation of solvent.

vulcanization must have a first-order effect on the dynamic modulus at frequencies of a fraction of a cycle per second. On the other hand, the experimental data concerning the dynamic modulus suggest that the increase of the modulus above the static value, as frequency is increased or temperature is reduced, is due to a set of relaxation mechanisms (probably hindered intermolecular motion) which have little relation to the static elastic network. Hence at sufficiently high frequency the degree of vulcanization should not have a first-order effect on the dynamic modulus. In the case of buna-N rubber the relaxation effects are evident at relatively low frequencies; thus the modulus even at 20 or 30 cps. should not be highly dependent upon vulcanization.

This hypothesis has been investigated by comparing the dynamic modulus of a completely unvulcanized, unfilled buna-N gum sample (Hycar OR-15) with that of a gum vulcanizate of the same material. The unvulcanized and vulcanized materials are designated, respectively, B-0 and B-1. The two samples are milled and cast from solvent in the same way, except that curing agents are added to the sample B-1. Dynamic modulus data as a function of temperature for these two samples, as determined by the vibrating-reed experiment, appear in Figure 14. The frequencies used in the measurements lie in the range 25 to 600 cps. The real modulus for B-1 exceeds that for B-0 by a little more than 50% at room temperature, and by a little more than 40% at temperatures well below the stiffening range. The stiffening temperature for the unvulcanized material is about 5°C. lower than that for the vulcanizate. The curves for E_2/E_1 are separated in the same sense as the stiffening temperatures. Additional points are included for the case in which the unvulcanized material contains a large amount of solvent. The presence of the solvent reduces the real part of the modulus by almost 20% at 20°, but has much less effect at low temperatures. The ability of the unvulcanized material to flow without limit under steady stress was verified experimentally.

While the unvulcanized sample is difficult to manipulate in the longitudinal-wave transmission apparatus, some limited data were secured from this experiment as shown in Figure 15. Comparable data for the vulcanized sample B-1 appear in Figure 8. It may be seen that, in the higher frequency regions, where greater dispersion is found, the real modulus for B-1 is as much as three times larger than that for B-0 (for example, at 10 kc., 20°C.). The ratio is everywhere at least 1.5. The greater disparity between the two compounds in regions of large dispersion is evidently a consequence of a partial difference between the relaxation spectra. Another aspect of this effect appears in Figure 14, in which a large disparity in the real modulus is seen between the two materials at temperatures in the immediate neighborhood of 0°C., where the most rapid stiffening with decreasing temperature occurs.

These results on the influence of vulcanization upon dynamic modulus afford excellent support for the supposition that the relaxation effects found in the frequency range of the present study are related to hindered intermolecular motion. Apparently there exist hindrances to intermolecular motion such that, when a force is applied for an interval of time which is short compared to the relaxation times of any of the hindrances, the molecules behave as though bound into a coherent elastic network by actual primary chemical bonds through the process of vulcanization. There is no

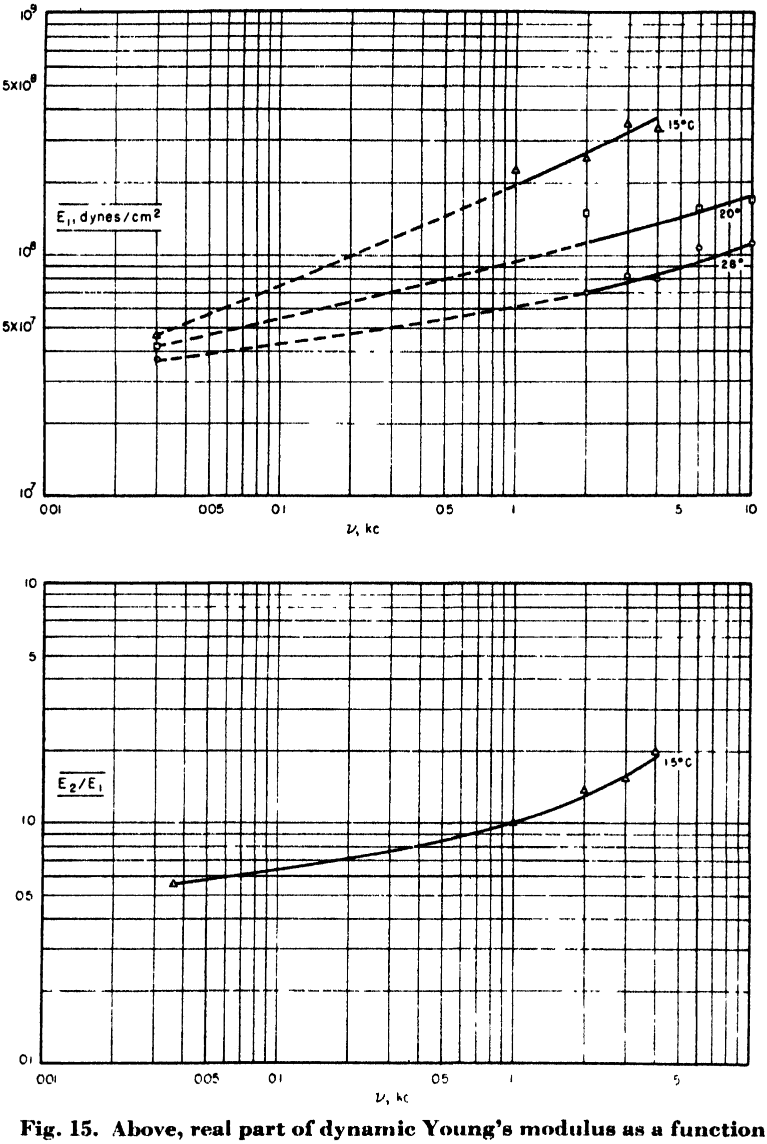

Fig. 15. Above, real part of dynamic Young's modulus as a function of frequency. Below, loss factor E_2/E_1 as a function of frequency. Buna-N unvulcanized gum B-0. Data from reed experiment and longitudinal-wave transmission experiment. Static deformation cannot be specified because the material flows under load.

reason to expect perfect correspondence of dynamic modulus between a vulcanized material and an unvulcanized material, because the vulcanization process inevitably forms linkages in and between a large number of molecules which do not actually become bound into the static elastic network. This effect would be expected to alter considerably the relaxation spectrum of the intermolecular hindrances which have been suggested above, even though the fraction of the molecules which is bound into the static elastic network is small for light vulcanization such as was considered here (1.5% sulfur).

Loading

While the present study is primarily restricted to the examination of rubberlike materials in the simple states, usually as gum vulcanizates, a large series of dynamic measurements has been carried out for one compound with carbon loading. This is the buna-N vulcanizate B-5, which contains 50 parts by weight of P33 black to 100 parts of Hycar OR-15.

Dynamic modulus data for the carbon-filled compound B-5 appear in Figures 4 and 7, while data for the corresponding unloaded compound B-1 appear in Figures 8 and 14. In the neighborhood of room temperature the loaded material has a modulus whose real part is from 50 to 100% larger than that for the gum material. Less temperature reduction is required to produce rapid stiffening in the case of the carbon-filled sample than in the case of the gum, with the result that the disparity in modulus becomes larger as the temperature is lowered into the neighborhood of 0°C. The loss factor E_2/E_1 is of the same order of magnitude for both compounds. Both of these effects of carbon loading—the increase of modulus and the increase of the stiffening temperature—are well known in rubber technology from experience with slower rates of deformation.[8,9]

Classification of Results by Compounds

Condensed Comparison of Compounds

Unfortunately there is no means for compact but clear graphic comparison of the over-all behavior of the complex modulus in the temperature–frequency plane for several different compounds. However, Table I affords a compact presentation of representative data for the various compounds whose dynamic modulus has been studied in this program. Both the real part of Young's modulus E_1 and the loss factor E_2/E_1 are given for temperatures of 10° and 30°C. at 5 kc. The derivative $\partial \ln E_1/\partial \ln \nu$, where ν denotes frequency in cycles per second, is given at each of these temperatures in order to indicate the relative amount of dispersion at 5 kc. All of the modulus data for materials under static elongation were obtained by the technique of longitudinal-wave transmission. The data for compound B-100, under 2% compression, were obtained by the magneto-

---

[8] E. Guth, *J. Applied Phys.*, **16**, 20 (1945).

[9] H. E. Greene and D. L. Loughborough, *ibid.*, **16**, 3 (1945).

TABLE I

SOME COMPARATIVE DYNAMIC MODULUS DATA VARIOUS COMPOUNDS

Compound designation	Description	Static deformation	E_1, dynes/cm.^{2} (real part Young's mod.), 5 kc.		E_2/E_1 (loss factor), 5 kc.		$\partial \ln E_1/\partial \ln \nu$, 5 kc.		Low-freq. stiffening temp., °C., about 100 cps.
			10°C.	30°C.	10°C.	30°C.	10°C.	30°C.	
N-1 (heat)	Natural rubber gum vulc.	10% elongation	6.6×10^7	$*4.0 \times 10^7$	0.68	*0.45	0.72	—	−47
B-0 (solvent)	Hycar OR-15 gum; not vulc.	? elongation (creeps)	$*1.0 \times 10^9$	—	—	—	—	—	− 3
B-1 (solvent)	Hycar OR-15 gum. vulc.	10% elongation	1.5×10^9	1.7×10^8	1.3	1.1	0.70	0.32	+ 1
B-5 (solvent)	Hycar OR-15 carb. load. vulc.	10% elongation	3.2×10^9	2.6×10^8	1.2	1.4	0.69	0.35	+ 3
B-99 (heat)	Hycar OR-15 gum vulc.	10% elongation	4.2×10^9	1.9×10^8	0.60	1.65	0.22	0.63	—
B-100 (heat)	Hycar OR-15 gum vulc.	2% compression	$*1.5 \times 10^9$	$*2.6 \times 10^8$	—	—	—	—	—
U-50 (heat)	GR-I (butyl) gum vulc.	5% elongation	4.0×10^8	$*8.0 \times 10^7$	1.3	*1.8	0.70	*0.55	−24
CG-1 (solvent)	CG neop. oxide-loaded vulc.	10% elongation	1.3×10^9	—	0.32	—	0.27	—	− 3
		35–40% elongation	8.3×10^8	—	6.2	—	0.40	—	—
GN-50 (heat)	GN neop. oxide-loaded vulc.	5% elongation	1.0×10^8	$*5.5 \times 10^7$	1.6	*0.7	0.32	*0.21	−18
S-50 (heat)	GR-S loaded vulc.	5% elongation	1.2×10^9	$*9.8 \times 10^7$	1.0	*0.65	0.1–0.2	0.1–0.2	−37†

* Indicates interpolated or extrapolated data. † Gum compound.

striction technique. The "low-frequency stiffening temperature" is the temperature at which the most rapid change in the real part of the modulus with respect to temperature is found with the vibrating-reed technique. "Heat" or "solvent" indicates the method of preparation of the sample (see Appendix III for the detailed composition of the samples).

The various rubbers fall into the listing, in the order of increasing values of the 5 kc. real modulus:

1. N-1 (natural rubber)
2. GN-50 (BN neoprene)
3. S-50 (GR-S)
4. U-50 (GR-I)
5. CG-1, 35-40% elongation (CG neoprene)
6. CG-1, 10% elongation (CG neoprene)
7. B samples (Hycar OR-15, buna-N rubber)

This listing in the order of increasing E_2/E_1 is probably the best single means for classifying rubbers according to their potentialities as practical absorbers of mechanical energy. Literally, the ratio E_2/E_1 is the measure of the damping of an oscillating system composed of a rigidly terminated rubber sample and a mass. The damping of such a system may be expressed by:

$$\ln (y_0/y_1) = E_2/E_1 \qquad (7)$$

where y_1/y_0 is the ratio of amplitude reduction in one cycle of free vibration. But while the quantity E_2/E_1 is perhaps the best single index of mechanical energy absorption capability, this quantity is not the only index of such capability and in some applications is not the most desirable one. For example, if one wishes to provide the greatest absorption of mechanical energy in a piece of damping material of a given size, in a system which has a *constant velocity* of vibration, it is necessary to search for the material which offers the largest value of effective resistance $\gamma = E_2/\omega$. On the other hand, the largest energy absorption for *constant force* applied to a sample of the damping material of given size is obtained for the material which has the largest value of the quantity $(E_2\omega)/(E_1^2 + E_2^2)$, that is, the material which has a large loss factor but a small absolute value of the complex modulus. A number of similar special cases exist.

Natural Rubber

The most significant data for natural rubber gum vulcanizates have been obtained at relatively low frequencies. Satisfactory measurements have not been achieved for frequencies greater than 6 kc. The difficulty in securing measurements at higher frequencies is largely attributable to the low sound velocity in natural rubber, which requires that unreasonably thin samples be prepared in order to maintain a sample thickness small compared to a wave length at the higher frequencies. Additional difficulties in the longitudinal-wave transmission experiment in particular are: the copious transmission of flexural waves as well as longitudinal waves in strips of convenient (0.1 cm.) thickness; the large attenuation per centimeter of longitudinal waves at the higher frequencies. (The attenuation per wave length is small because the loss factor E_2/E_1 is relatively small for natural rubber, but the spatial attenuation is large in consequence of the low wave velocity.)

The real modulus of natural rubber increases with increasing temperature for frequencies as high as 100 cps. (this result is discussed in Part III). Other rubbers (for example, buna-N and butyl rubber) fail to display this "kinetic theory" temperature dependence at frequencies above one cycle per second. Thus the existence of kinetic temperature behavior at low audiofrequencies for the case of natural rubber seems to indicate that the relaxation spectrum for natural rubber is characteristically faster than that for the synthetic rubbers. In agreement with this supposition, the experimental data show that natural rubber is characterized in the audiofrequency range by a smaller loss factor and a smaller real modulus than those synthetic rubbers which are considered in this paper.

Buna-N Rubber. Hycar OR-15

Hycar OR-15 is the rubber which has received most attention in this series of investigations. All of the experimental methods listed at the beginning of this paper, except the longitudinal-wave resonance method, are highly satisfactory for dynamic measurements of this rubber. Hycar OR-15 has been studied in the form of unvulcanized gum, vulcanized gum cast in solvent, vulcanized gum heat-cured under pressure, and vulcanized compound with light carbon loading. Data for this rubber will be used for the calculation of an approximate relaxation spectrum and for most of the calculations of activation energies in Part III.

The Hycar OR-15 compounds have a larger real dynamic modulus in the audiofrequency range than the other rubbers considered here, and a higher audiofrequency loss factor E_2/E_1 than the other rubbers except butyl (excluding the anomalous high loss displayed by CG neoprene after irreversible deformation). The large real modulus in the audiofrequency range appears to be the result of a weighting of the relaxation spectrum toward long relaxation times (that is, of dispersion effects which set in an unusually low frequencies), because the static modulus of lightly vulcanized Hycar OR-15 is several times 10^7, of the same order of magnitude as the static modulus for comparable preparations of the other rubbers. Moreover, the real part of the audiofrequency modulus is relatively large for an unvulcanized sample of Hycar OR-15, for which the static modulus is essentially zero. The preponderance of very large activation energies must be greater for Hycar OR-15 than for other rubbers, because the low-frequency stiffening temperature as determined by the vibrating-reed technique is near 0°C. for the Hycar OR-15 compounds. This is appreciably higher than the stiffening temperature of the other rubbers.

Butyl Rubber (GR-I)

Butyl rubber is especially well suited to the experimental techniques used in this program, but, since butyl samples became available only in the later stages of the program, less experimental work has been devoted to this rubber than to Hycar OR-15. Dynamic modulus data for the butyl compound U-50, obtained by the longitudinal-wave transmission technique between 1 and 20 kc., appear in Figure 16. The loss factor E_2/E_1 is somewhat greater than that for Hycar OR-15 (buna-N) preparations in the same frequency and temperature range. Butyl rubber appears to be a more satisfactory practical energy absorber in the audiofrequency range than Hycar OR-15, because, in addition to having the larger loss factor of the two rubbers in this range, butyl rubber is somewhat less sensitive to temperature changes in the temperature region above 0 °C. The low-frequency dynamic stiffening temperature for U-50 is approximately −18 °C. The low-frequency dynamic stiffening temperature for U-50 is approximately −18° as contrasted with 1° for a comparable Hycar OR-15 compound, B-1. Both figures refer to data obtained with the vibrating-reed technique; the data of this type for U-50 are not shown graphically.

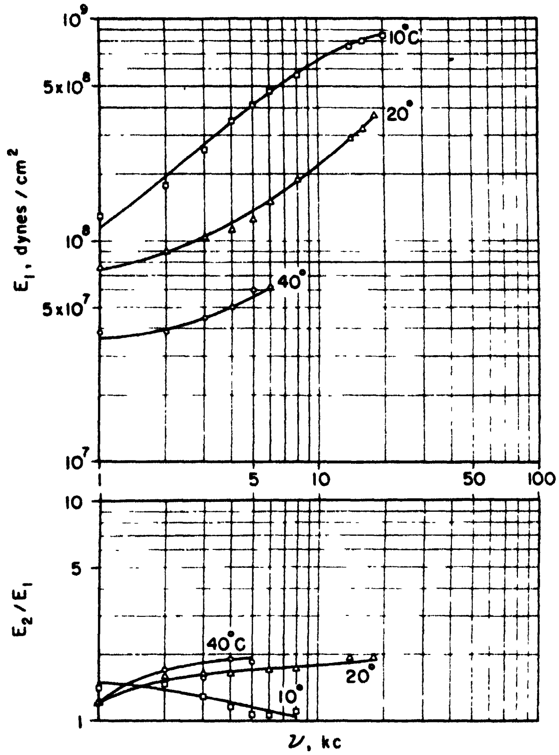

Fig. 16. Above, real part of dynamic Young's modulus as a function of frequency. Below, loss factor E_2/E_1 as a function of frequency. Butyl gum vulcanizate U-50. 5% static elongation.

Neoprene

The neoprenes, together with GR-S, form a class of relatively low-loss synthetic rubbers among the four synthetics which are considered here. *Limited studies have been made of the two commercial varieties of neoprene*, CG neoprene, and GN neoprene. Both of these rubbers were studied in the form of gum vulcanizates with a relatively large content of metallic oxides. The inclusion of these oxides in neoprene vulcanizates is standard practice in rubber technology.

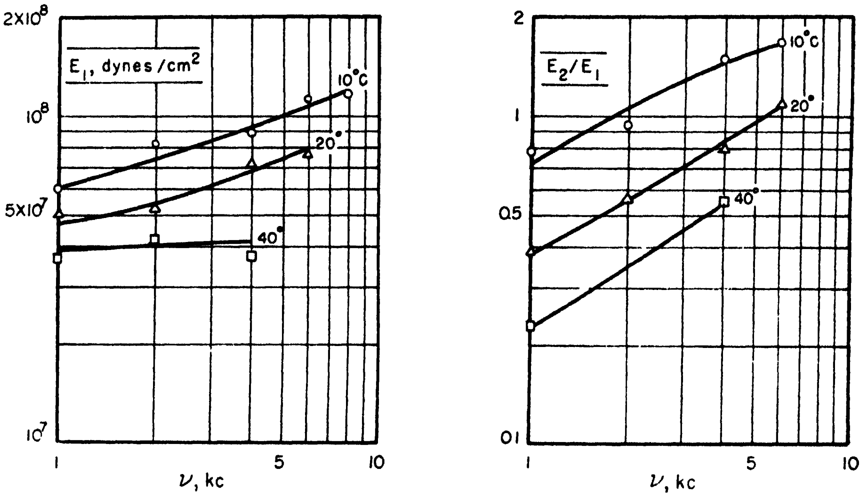

Fig. 17. Left, real part of dynamic Young's modulus as a function of frequency. Right, loss factor E_2/E_1 as a function of frequency. Neoprene vulcanizate GN-50. 5% static elongation.

Data for the GN neoprene compound GN-50 appear in Figures 17 and 18. Figure 17 contains the data obtained between 1 and 8 kc. by the longitudinal-wave transmission method. Figure 18 is a plot of E_1 and E_2/E_1 as functions of temperature; the data were obtained by the vibrating-reed technique. The low-frequency stiffening temperature as indicated by this figure is about −18°C. In the audiofrequency range, the real modulus of GN-50 is smaller than that for all the other rubbers except natural rubber, while the loss factor is greater than that for GR-S but less than that for buna-N (Hycar OR-15) rubber. As a result of the low velocity of longitudinal waves in GN-50, difficulties of much the same nature as those for natural rubber are encountered in performing longitudinal-wave transmission measurements for GN-50.

CG neoprene, as represented by the compound CG-1, has an audiofrequency loss factor smaller than that for natural rubber. The tremendous increase in the loss factor which occurs when this rubber is stretched in excess of 10% has been illustrated in Figures 12 and 13. The stressed and unstressed forms of the compound have also been studied by the vibrating-reed technique. The results (not shown) indicate that the difference at low frequency between the two forms disappears when the temperature is lowered to −5 °C. Thus it appears that the irreversible deformation effect is not directly connected with those mechanisms which contribute to the *increase of the modulus at low temperatures.*

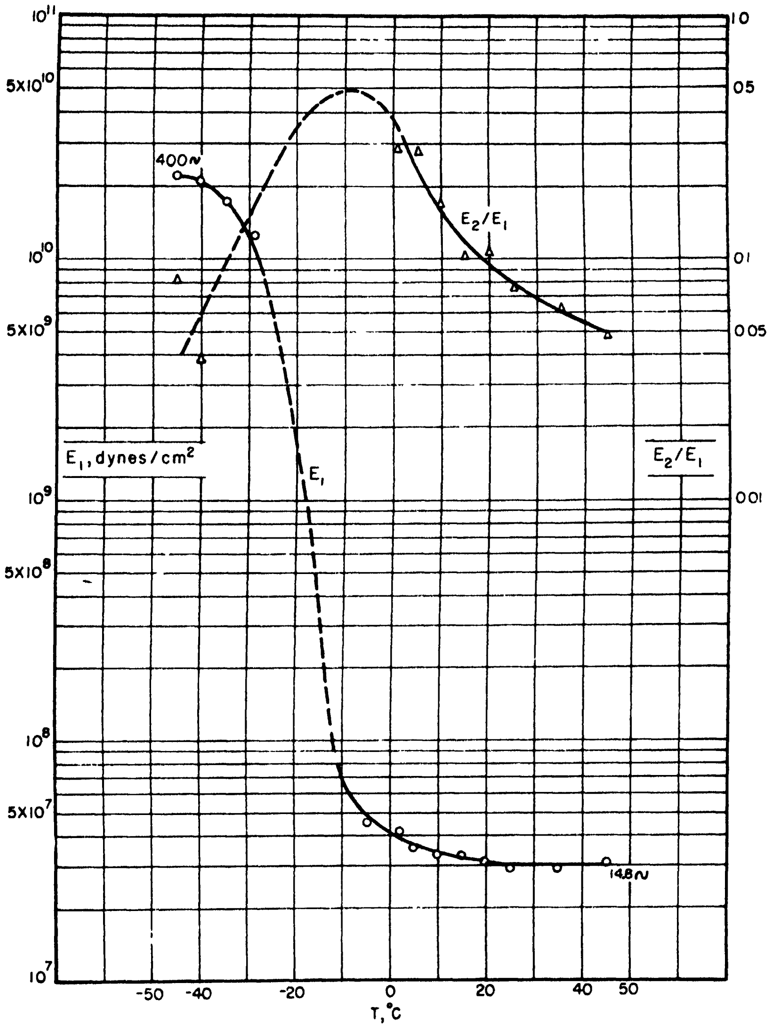

Fig. 18. Real part of dynamic Young's modulus and loss factor E_2/E_1 as functions of temperature. Neoprene vulcanizate GN-50. No static deformation. Data from vibrating-reed experiment; frequency varies with modulus.

GR-S Rubber

Little attention has been given to GR-S rubber in the present investigation. Longitudinal-wave transmission measurements for GR-S are more difficult than for buna-N and butyl rubbers. The difficulties attending longitudinal-wave transmission measurements in GR-S at frequencies above about 5 kc. are much the same as those found with natural rubber.

Some longitudinal-wave transmission data for the GR-S compound S-50 are plotted in Figure 19. E_1 and E_2/E_1 are shown as functions of frequency from 1 to 6 kc. The audiofrequency real dynamic modulus is greater than that for GN neoprene and less than that for butyl rubber, while the loss factor is greater than that for natural rubber but less than that for GN neoprene. GR-S may reasonably be classed with the neoprenes as a low-loss synthetic rubber insofar as the audiofrequency results are concerned.

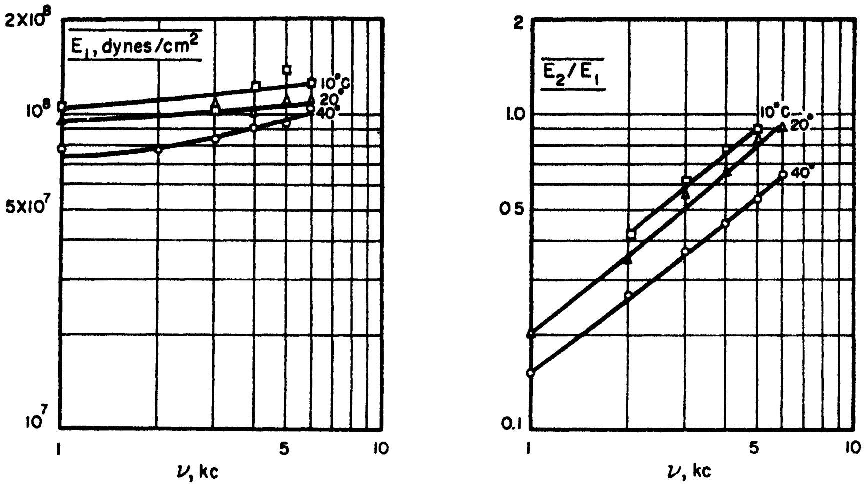

Fig. 19. Left, real part of dynamic Young's modulus as a function of frequency. Right, loss factor E_2/E_1 as a function of frequency. GR-S carbon-filled vulcanizate S-50. 5% static elongation.

III. THEORETICAL DISCUSSION OF THE RESULTS.

Temperature Dependence of Dynamic Modulus in Relation to Predictions of Kinetic Theory

The kinetic theory of rubberlike elasticity, as exemplified by the work of James, Guth, and Mark,[6,10,11] leads to the following stress–strain relation for rubber:

$$KT\left[L_z - \frac{1 + \alpha(T - T_0)}{L_z^2}\right] \tag{8}$$

In this equation Z is the stress in dynes applied to a sample which is a unit cube at the temperature T_0 (Kelvin) in the absence of stress, K is a constant

---

[10] H. M. James and E. Guth, *J. Chem. Phys.*, **11**, 455 (1943).

[11] H. M. James and E. Guth, *J. Applied Phys.*, **15**, 294 (1944).

best evaluated experimentally, T is Kelvin temperature, α is the volume coefficient of thermal expansion, and L_z is the relative length of the sample along the stress axis z. (In the absence of stress, at temperature T_0, L_z is unity.) By differentiating (8) one obtains the following expression for the differential modulus $\partial Z/\partial L_z$:

$$\partial Z/\partial L_z = KT\left[1 + 2\,\frac{1 + \alpha(T - T_0)}{L_z^3}\right] \tag{9}$$

This result indicates that the differential modulus at any particular static elongation should be very closely proportional to the absolute temperature. The thermoelastic inversion effects associated with the total stress–strain function (one of these effects is a reversal of the stress–temperature coefficient as a function of elongation) do not enter into the behavior of the differential modulus.

In contrast to these predictions of the kinetic theory of rubberlike elasticity, it is found experimentally for both natural and synthetic rubbers that the real part of the dynamic modulus as given by audiofrequency measurements decreases with increasing temperature. Yet one may demonstrate with ordinary "static" testers that the slope of the quasistatic stress–strain curve, for natural rubber at least, is proportional to the absolute temperature as required by the theory.

Two possible explanations for this apparent contradiction suggest themselves. One of these is that the temperature behavior of the modulus is a function of the strain amplitude. Static testing machines generally impose large strains on the sample, whereas the strains involved in measurements at frequencies of several kilocycles are necessarily small. The other possible explanation is that the temperature dependence of the modulus is a function of frequency. This latter possible explanation is the more promising of the two, because the so-called kinetic theory of rubberlike elasticity is in reality a theory of *equilibrium* strains, and does not take into account any *dynamic* hindrances which may give rise to relaxation effects and thereby make the modulus dependent upon frequency. The relaxation rates of molecular hindrances are known to be sensitive to temperature.[3] A variation of strain amplitude, on the other hand, would be expected primarily to produce a variation in nonlinearity.

Thus it appears that a logical experimental approach to the question of dynamic elastic temperature dependence is to make a series of measurements of the dynamic modulus of natural rubber as a function of temperature at various constant frequencies ranging from a fraction of a cycle per second to frequencies well in the audio range. Experimental data of this kind are shown in Figure 20. The compound is N-1, a 5% sulfur, accelerated natural rubber gum compound. Other investigators[12] have shown that the results of stress–strain curves for this compound, taken at rates up to 100% elongation per second, are in agreement with kinetic theory. In

[12] S. L. Dart, R. L. Anthony, and P. E. Wack, *Rev. Sci. Instruments*, 17, 106 (1946).

Figure 20, modulus–temperature curves (solid) are shown for frequencies from 0.22 to 280 cps. The data at 24.5 cps. and at the lower frequencies were obtained by the rocking-beam oscillator technique. The data at the higher frequencies were obtained by the longitudinal-wave resonance technique. The static elongation is 10%, while the dynamic strain amplitude does not exceed 1 to 2%. No evidence of nonlinearity was observable in the experiments. These results should be comparable to the predictions of the kinetic theory concerning the differential modulus.

The uncertainty of the data for a particular frequency is 1 to 2%. The uncertainty between data for different frequencies is somewhat greater, because it was necessary to place a fresh sample in the apparatus for each new frequency. The "constant frequency" nature of the curves is approximate, since the experimental methods depend upon small changes in the frequency of resonance of the apparatus to indicate changes in modulus. These frequency changes, amounting to a few per cent at most, are unimportant because the modulus is not highly sensitive to frequency in the low frequency range. In Figure 20 the data for each frequency have been multiplied by a suitable factor ranging from 0.83 to 1.25 to permit convenient presentation upon an expanded scale. In reality the curves seem to approach a common value at the high temperatures, and the actual modu-

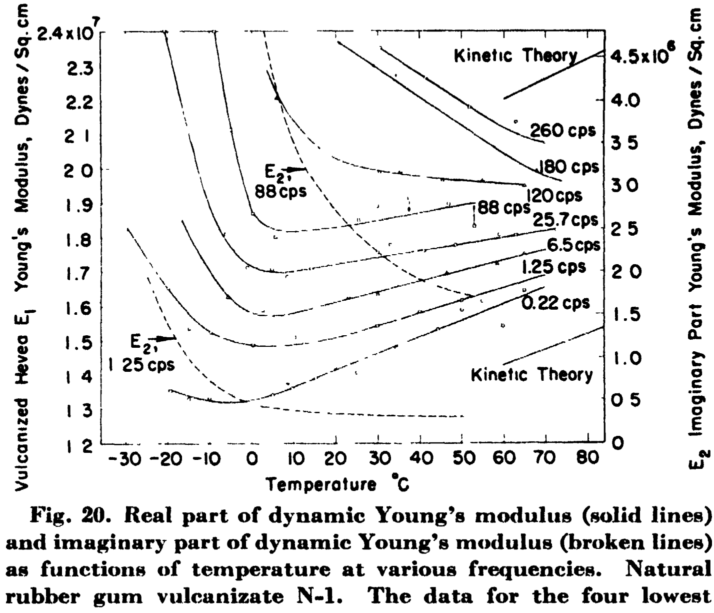

Fig. 20. Real part of dynamic Young's modulus (solid lines) and imaginary part of dynamic Young's modulus (broken lines) as functions of temperature at various frequencies. Natural rubber gum vulcanizate N-1. The data for the four lowest frequencies are from the rocking-beam oscillator experiment; data for the higher frequencies are from the longitudinal-wave resonance experiment. Absolute values have been multiplied by factors ranging from 0.83 to 1.25 to permit clear presentation on an expanded scale. Straight lines show temperature dependence required by kinetic theory.

lus values for the two lowest frequencies are almost indistinguishable. Some of the same data are shown on a frequency scale in Figure 5. Measurements were not attempted at temperatures above 80° C.; even at 70° the sample begins to take on a semipermanent set and ceases to be comparable to the original material.

At the very low frequencies the modulus increases substantially in proportion to the absolute temperature, in agreement with the kinetic theory, except that for sufficiently low temperatures the kinetic temperature dependence is not found for any of the frequencies which are considered. For successively higher frequencies the modulus increases less rapidly with increasing temperature. Between 88 and 120 cps. the proportional temperature effect disappears altogether; for the higher three frequencies the modulus decreases with increasing temperature over the entire temperature range of the study, and the magnitude of the temperature effect becomes progressively larger than that predicted by kinetic theory.

The experiments are free from crystallization effects. A well-vulcanized compound such as N-1 does not crystallize except at very large extensions.[13] Thus the stiffening of the sample at lower temperatures in violation of the kinetic theory, which is observed at each frequency, appears to be another instance of the manner in which a decrease of temperature can change the relation between the relaxation times of the material and the period of the applied force in the same sense as would an increase of frequency. An alternate description of the results in Figure 20 is the statement that with increasing frequency the low-temperature region, in which nonkinetic temperature dependence is found, gradually extends to higher temperatures until above 100 cps. this region covers the entire range of observed temperatures. Greene and Loughborough[9] have obtained results resembling those of Figure 20 but for finite deformations by applying force suddenly to a rubber sample and measuring the strain after a specified time interval. Variation of the time interval corresponds to variation of frequency in the present experiment.

The nonkinetic temperature effect appears in regions of appreciable dispersion. This finding is in keeping with the supposition that the dynamic behavior of the material is governed by a temperature-sensitive set of relaxation mechanisms. While Figure 20 is not intended to give a quantitative picture of frequency dependence, it is clear that the rate of increase of the modulus with the logarithm of the frequency becomes large in the low-temperature regions, and in the higher frequency regions, where the nonkinetic temperature effect is found. The behavior of the imaginary part of the modulus is also significant, because when dispersion occurs through the operation of a set of relaxation mechanisms there is an appreciable resistive loss factor associated with the regions of dispersion. The existence of this effect in the present data may be seen from the two dashed curves of Figure 20 which show E_2, the imaginary part of Young's modulus, as a function of temperature at 1.25 cps. and at 88 cps. E_2 becomes large where the nonkinetic temperature effect occurs—at low temperatures and at the higher frequencies.

---

[13] L. A. Wood, in *Advances in Colloid Science*, Volume II, *Rubber*, p. 57. Interscience, New York, 1946.

Similar experimental results have been found for butyl rubber. Figure 21 shows rocking-beam oscillator data giving the real part of the dynamic modulus as a function of temperature, at three different frequencies, for the butyl compound U-50. At 0.15 cps. the modulus increases with increasing temperature in the range above 10°C. At 5.2 cps. the modulus is substantially independent of temperature in the range. At 11 cps. the modulus decreases steadily with increasing temperature.

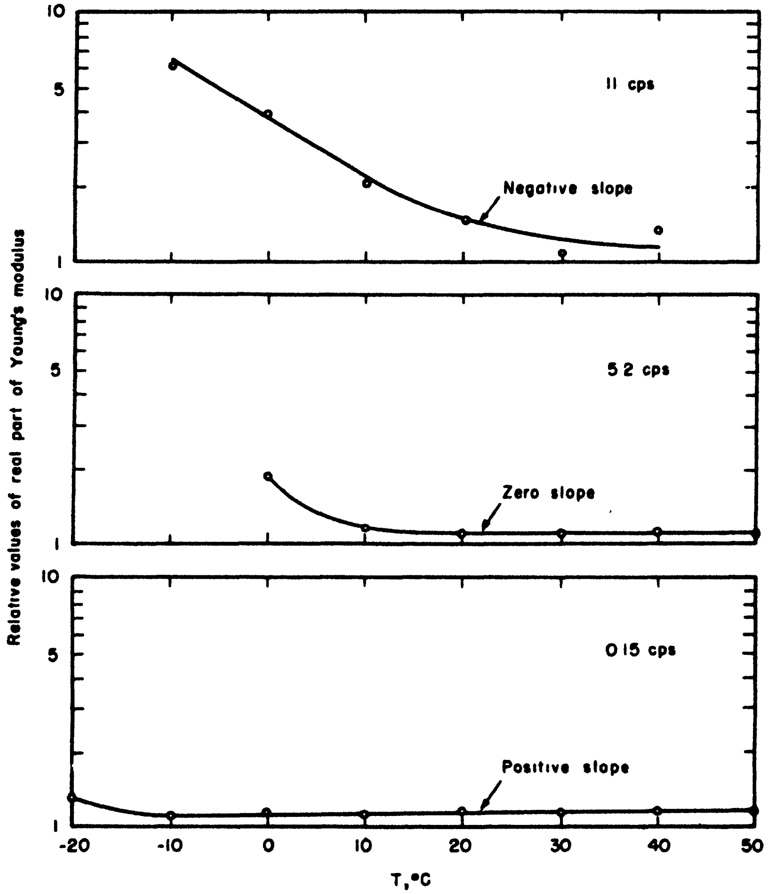

Fig. 21. Relative values of real part of dynamic Young's modulus, as a function of temperature, at three different frequencies. Butyl gum vulcanizate U-50. Rocking-beam oscillator experiment; 10% static elongation. Reversal of temperature coefficient of the modulus occurs at about 5 cps.

It has already been pointed out that buna-N rubber (as represented by Hycar OR-15) shows important relaxation effects at lower frequencies than the other rubbers considered here. It is therefore not surprising that at the lowest conveniently observable frequencies the dynamic modulus of this rubber fails to show kinetic temperature dependence. For example, Figure 22 shows rocking-beam oscillator data for the real modulus of the Hycar OR-15 compound B-100 at 0.16 cps.; the modulus decreases steadily with increasing temperature. It is doubtful whether a different result would be obtained from a stress-strain tester at ordinary rates of deformation. In order to ascertain whether the behavior of Hycar OR-15 follows the kinetic theory even under truly static conditions, another test has been devised. From equation (8) one may show that according to kinetic theory the thermal expansion coefficient of a rubber sample along the stress axis is, for constant stress:

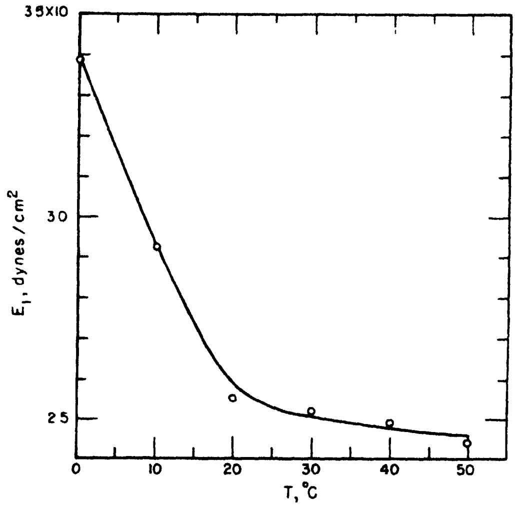

Fig. 22. Real part of dynamic Young's modulus as a function of temperature. Buna-N gum vulcanizate B-100. Rocking-beam oscillator data. 10% static elongation; 0.16 cps.

$$(1/L_z)(\partial L_z/\partial T)_Z = [1 + \alpha(2T - T_0) - L_z^3]/[L_z^3 + 2\alpha(T - T_0) + 2]T \quad (10)$$

According to this equation the stress-axis thermal expansion coefficient should change from positive sign to negative sign with increasing elongation L_z, and when $T = T_0$ should pass through zero at approximately:

$$L_z = 1 + \alpha T/3 \quad (11)$$

The thermal expansion coefficient of a strip of the Hycar OR-15 compound B-100 was measured under various static loads with the result shown in Figure 23. A reversal of the coefficient, as required by kinetic theory, occurs at about 7% elongation. The existence in the *static* behavior of B-100 of this element of agreement with kinetic theory makes it reasonable to suppose that the *dynamic* behavior must in the limit of very low frequency approach that of the kinetic theory, even though the agreement is not found at readily observable frequencies.

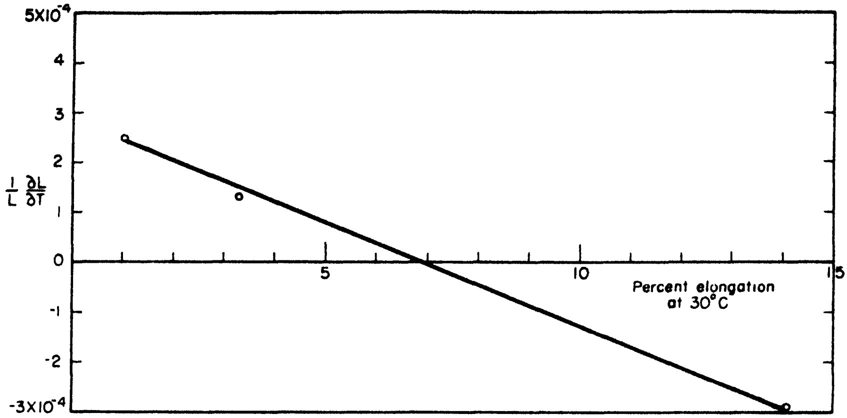

Fig. 23. Thermal expansion coefficient along stress axis as a function of static strain. Buna-N gum vulcanizate B-100. Thermoelastic inversion occurs as required by kinetic theory.

The experimental results cited above constitute a strong case for the point of view that the kinetic theory represents the limiting differential dynamic behavior of any rubberlike material at very low frequency, and that the departures from kinetic theory observed at higher frequencies can be explained on the basis of frequency effects alone.

"Second-Order Transition" and the Dynamic Modulus

Figure 7 shows a relatively sudden increase of the low-frequency real dynamic modulus for a buna-N compound as the temperature is lowered through the range just below 0°C. The other synthetic rubbers show corresponding behavior, though the critical temperature range is lower for the other synthetics. Figure 24 shows low-frequency data for the 2% sulfur, natural rubber compound N-2. The modulus of this natural rubber compound also increases rapidly when the temperature is lowered through a certain region, but the effect for natural ruber is found at about −50°C.

This effect is one manifestation of what has often been regarded as a second-order transition. Boyer and Spencer[14] in their review paper mention the following several properties of a rubber or high polymer which exhibit sudden changes at the temperature of this "transition":

1. The volume-temperature curve
2. Heat capacity
3. Compressibility
4. Thermal conductivity
5. Elastic modulus
6. Refractive index
7. Dielectric properties

---

[14] R. F. Boyer and R. S. Spencer, in *Advances in Colloid Science*, Volume II, *Rubber*, pp. 1–55. Interscience, New York, 1946.

The "transition" temperature is generally somewhat lower than the "brittle point" temperature of a given compound, which is sometimes defined as the temperature below which a sample will break as a result of a sudden sharp bend.

The results of the present experiments indicate that the term "second-order transition" must be applied with caution in the case of the dynamic modulus of rubbers. A second-order transition should represent a thermodynamic singularity—for instance, the disappearance of some form of ordering as the temperature increases above a critical value. A transition in this sense does not appear to describe the increase with decreasing temperature of the dynamic modulus as measured at the higher frequencies. For example, according to Figure 6 the real dynamic modulus of an unloaded buna-N cement, measured at 12 kc. or at 70 kc., increases gradually with

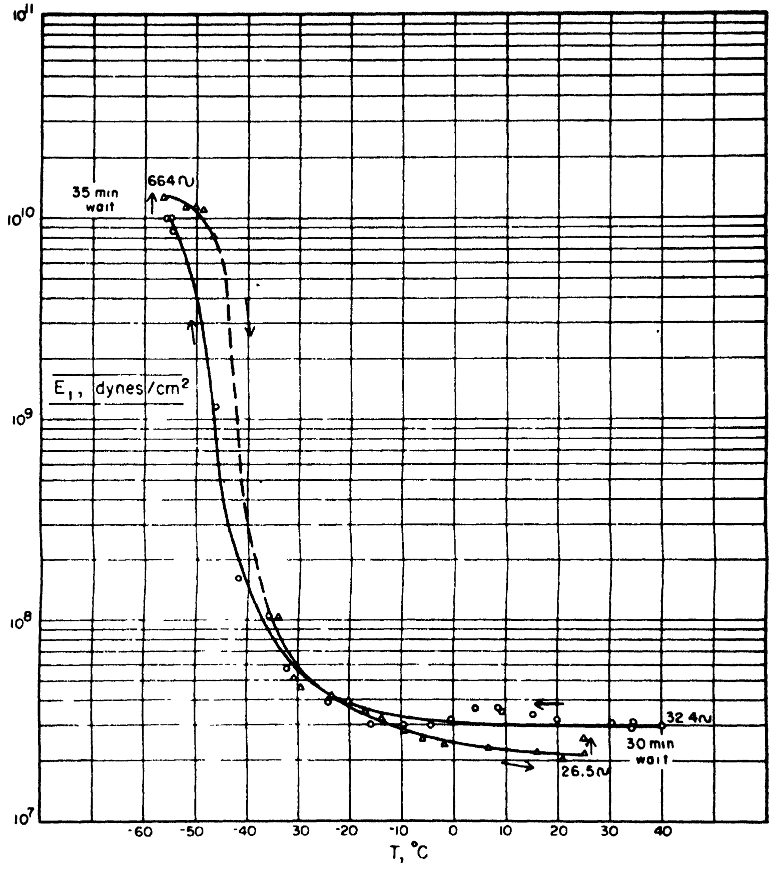

Fig. 24. Real part of dynamic Young's modulus as a function of temperature for down and up temperature cycles. Natural rubber gum vulcanizate N-2. No static deformation. Data from vibrating-reed experiment: frequency varies with modulus.

decreasing temperature in the range between 0° and 40°C. The steepest part of the modulus-temperature curve is shifted to higher temperature as the frequency is increased. This result contrasts sharply with the low-frequency data of Figure 14, according to which the same compound displays an abrupt increase in its real dynamic modulus, measured between 25 and 600 cps., as the temperature is reduced through a narrow range about 0°C.

Apparently the increase in the real modulus with decreasing temperature, observed at high frequencies, is simply a special aspect of the relaxation behavior of the rubber. Reduction of temperature alters the characteristic relaxation times until, when these begin to be longer than the period of force alternation, the amount of strain which occurs in response to unit force is reduced and the value of the dynamic modulus increases. Since increasing the characteristic relaxation times has the same qualitative effect as increasing the frequency—namely, to make the relaxation times long compared to the period of force application— it follows that an increase of frequency should affect the dynamic modulus in qualitatively the same manner as a decrease of temperature, in agreement with the results shown in Figure 1.

On the other hand, at low frequencies the real part of the dynamic modulus increases very rapidly with decreasing temperature in a narrow temperature range, as shown in Figure 14, while the position of the stiffening range on the temperature scale becomes less sensitive to frequency, measured in logarithmic units, as shown in Figure 1. These observations suggest that reduction of temperature, aside from increasing the characteristic mechanical relaxation times, introduces an additional stiffening phenomenon akin to freezing. The temperature at which this "freezing" effect occurs is nearly independent of frequency; thus the "freezing" effect, whether or not it actually constitutes a second-order transition, is not a simple continuation of the relaxation stiffening found at higher frequencies. When dynamic modulus measurements are performed at high frequencies, the relaxation stiffening occurs at higher temperatures than the freezing phenomenon and the latter is masked; when similar measurements are performed at very low frequencies, the freezing effect sets in at a temperature higher than that at which the relaxation stiffening would be expected, and the relatively sharp freezing phenomenon is observed.

In the literature there are other instances of phenomena resembling second-order transitions which, as in the case of the high-frequency mechanical behavior of rubbers, are actually relaxation rate effects. Boyer and Spencer[14] mention a number of investigations in which the observed "transition" temperature has been found to depend upon the rate of heating or cooling. This is undoubtedly a relaxation rate effect, which in a particular instance may or may not accompany the occurrence of a true second-order transition. The effective "static" relaxation time for rubber becomes extremely long at low temperatures. The attainment of equilibrium conditions within the material requires periods which may amount to many hours at sufficiently low temperature, and a variety of differing experimental results may be observed by making measurements before equilibrium is established. In the present dynamic modulus experiments a small increase of the real modulus and a very large decrease in the loss factor can be observed over a period of at least half an hour after the sample is brought to a temperature somewhat below the "transition." Spencer and Boyer[15] in 1946 published an investigation of the volume–temperature curve of polystyrene which shows that the discontinuity observed at ordinary rates of heating and cooling is completely absent if the experimental measurements are made after the attainment of equilibrium. They conclude that the "second-order transition" is in this case a relaxation rate effect. Frenkel[16] reaches a similar conclusion for amorphous bodies in general, on the basis of the work of Kobeko. Nevertheless the present experiments, as discussed above, indicate that a simple relaxation rate concept may not be sufficient to explain the temperature behavior of the dynamic modulus of rubbers over the entire frequency range.

The foregoing discussion is not meant to imply that the sudden change in the dynamic modulus of rubber in a certain range of temperature is a fictitious effect due to the rate of cooling. The fact that relaxation rates decrease vastly in a certain temperature range requires that the *dynamic* modulus increase rapidly in this range, because the dynamic modulus is by definition the modulus determined from a sinusoidal deformation with a fixed frequency and has no necessary direct connection with static equilibrium. It is the *static* modulus which might be expected to display a variety of values in the "transition" region according to the rapidity of the temperature change. The real part of the dynamic modulus for temperatures below the "transition" has been found to vary only slightly between the period following rapid cooling and the period when equilibrium is established; for example, while the dynamic modulus of compound N-2 as found by the vibrating-reed technique increases by a factor of 300 between room temperature and −55 °C., the further increase when the sample remains for half an hour at −55° is only 20%. The quantity E_2'/E_1, however, decreases by a factor of 3 or 4 during this period.

An additional question of interest is the relation between the brittle temperature and the dynamic stiffening temperature. The brittle-point determination is a specialized test which does not necessarily give the same result in terms of temperature as do other methods for examining the "transition." The brittle-point temperature is the temperature at which long-range elasticity disappears completely so that the material will rupture with a relatively small deformation. (In practice, the result depends upon the rate of deformation.[17]) It is found that the dynamic modulus *vs.* temperature curves obtained in the present investigation show no special features at the brittle temperature. The real dynamic modulus shows a steady increase with decreasing temperature, beginning with temperatures above the brittle point and continuing through temperatures below the brittle point. Koch[18] noticed that the "static" modulus is most sensitive to temperature in the range above the brittle point; consequently he introduced the concept of a "stiffening temperature," which is higher than the brittle-point temperature.

---

[15] R. S. Spencer and R. F. Boyer, *J. Applied Phys.*, 17, 398 (1946).

[16] J. Frenkel, *Kinetic Theory of Liquids*, p. 214. Oxford Univ. Press, London, 1946.

[17] A. R. Kemp, F. S. Malm, and G. G. Winspear, *Ind. Eng. Chem.*, 35, 488 (1943).

Table II illustrates the lack of agreement between the temperature of most rapid dynamic modulus stiffening, as found in the present investigation by the vibrating-reed technique, and brittle-point determinations given by other investigators.

TABLE II

COMPARISON OF BRITTLE AND DYNAMIC STIFFENING TEMPERATURES

Material	Dynamic modulus stiffening, °C.	Source	Brittle point, °C.	Source
Natural rubber, 2% S	−44	Fig. 24	−57*	19
Hycar OR-15	+ 1	Fig. 14 (compound B-1)	−19	20
GN neoprene	−20	Fig. 18	−40	20

* This figure is for raw smoked sheet. A figure for smoked sheet cured in the same fashion as N-2, the compound to which Figure 24 applies, was not found in the literature.

Interpretation of Results in Terms of a Relaxation Spectrum

The foregoing discussions of experimental results have made it clear that dispersion in the dynamic modulus of rubberlike materials occurs over a frequency range much wider than that which corresponds to a single relaxation time. One possible means for describing this extreme dispersion is to reduce the results to a relaxation spectrum, which in the most general case is a population of elementary relaxation times. In special cases the distribution need not be continuous.

This artifice has been much used as a means for describing the behavior of dispersive dielectrics (see, for example, Kauzmann[3] or Cole and Cole[4]) and of viscoelastic materials (see, for example, Alfrey and Doty[21]). Whether or not the representation of dispersion phenomena in terms of a relaxation spectrum is particularly advantageous depends upon whether or not the distribution of relaxation times can be explained in terms of fundamental principles from the structure of the material. Such basic theoretical explanations have not as yet been established for the continuous relaxation spectrum of rubber. Thus a continuous relaxation spectrum is not preferable to other methods for describing dispersion phenomena in rubber insofar as any fundamental significance of the description is concerned.

For present purposes a relaxation element may be defined as a spring and a dashpot connected together. If the spring and the dashpot are mechanically in series, the element is a Maxwell element; if the spring and the dashpot are mechanically in parallel, the element is a Voigt element. Any observed dispersion characteristic may be represented by an unlimited parallel set of Maxwell (series) elements or by an unlimited series set of Voigt (parallel) elements. Here a set of Maxwell elements will be used, because the additive impedance property of these elements is useful for describing modulus. The impedance of the Voight elements would have to be added as reciprocals to give the reciprocal of modulus. The writer does not mean to imply, however, that any greater "fundamental significance" attaches to the Maxwell representation than to the Voigt representation; the actual intermolecular connections may well represent a combination of the two types. A set of Maxwell elements and the analogous set of electrical elements are shown in Figure 25. One may ascertain by inspection of the network that the complex modulus for the set of relaxation elements follows qualitatively the behavior described in Part II with respect to frequency and temperature, if the resistance elements have a viscous temperature dependence.

---

[18] E. A. Koch, *Kautschuk*, **16**, 151 (1940); *Rubber Chem. Tech.*, **14**, 799 (1941).

[19] G. T. Kohman and R. L. Peek, *Ind. Eng. Chem.*, **20**, 81 (1928).

[20] G. E. King, *ibid.*, **35**, 949 (1943).

[21] T. Alfrey and P. Doty, *J. Applied Phys.*, **16**, 700 (1945)

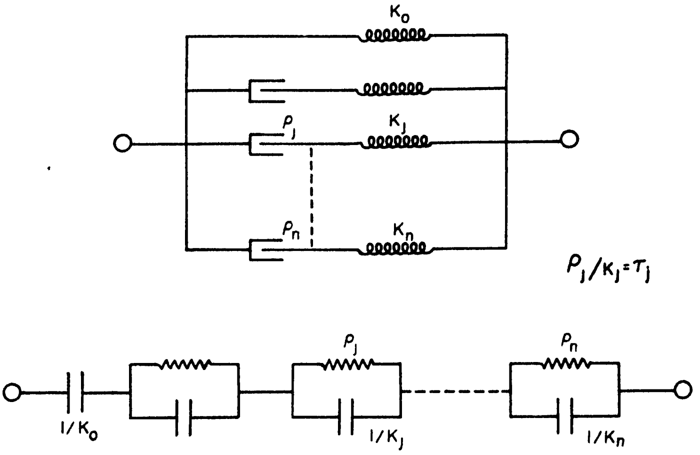

Fig. 25. Above, set of Maxwell mechanical elements. Below, equivalent set of electrical elements.

It may be shown[1] that the complex modulus is related to the viscoelastic mechanical impedance Z_m of a unit cube sample by:

$$E^* = -i\omega Z_m \tag{12}$$

Since the elementary impedances are additive in the set of elements of Figure 25, it is only necessary to find the impedance function for an element in order to express the complex modulus of the set as a sum. According to simple circuit theory the impedance of the jth element is:

$$Z_{mj} = \rho_j \frac{1 + i\tau_j\omega}{1 + \tau^2_j\omega^2} \tag{13}$$

Thus the contributions to the real and imaginary parts of the modulus from this jth element are:

$$E_{1j} = K_j/(1 + 1/\tau_j^2\omega^2) \tag{14a}$$

$$E_{2j} = K_j\tau_j\omega/(1 + \tau_j^2\omega^2) \tag{14b}$$

The total real and imaginary parts of the modulus, due to the entire set of relaxation mechanisms, are:

$$E_1 = \sum_0^n (E_{1j}) \tag{15a}$$

$$E_2 = \sum_0^n (E_{2j}) \tag{15b}$$

Each of the individual mechanisms displays dispersion comparable to that of a simple Debye dielectric. A particular mechanism other than K_0 contributes nothing to the modulus for zero frequency, and contributes K_j to the modulus at infinite frequency. For $\omega = 1/\tau_j$ the contribution to the modulus is $K_j/2$; therefore this frequency may be regarded as the critical frequency for the jth element. The modulus contribution of the element changes from $0.018K_j$ to $0.91K_j$ over the decade of frequency which has the critical frequency at its logarithmic center. Thus the important dispersion effects occur over about one decade of frequency, and the modulus contribution of the element is only slightly influenced by frequency variations outside of this critical decade. The imaginary part of the modulus, E_{2j}, has the value $K_j/2$ at the critical frequency of the jth element, $\omega = 1/\tau_j$. The value is reduced to $0.29K_j$ at either end of the critical frequency decade.

For the case of the dynamic behavior of rubber, dispersion is continuously observable over at least six to eight decades of frequency. A continuous relaxation spectrum is therefore convenient for expressing the dynamic behavior of rubber. A continuous spectrum requires that the summations of (15b) be replaced by integrals. Thus the real and imaginary parts of the modulus are:

$$E_1(\omega) = \int_0^\infty \frac{W(\tau)}{1 + 1/(\tau\omega)^2}\, d\tau \tag{16a}$$

$$E_2(\omega) = \omega \int_0^\infty \frac{W(\tau)}{1 + (\tau\omega)^2}\, \tau d\tau \tag{16b}$$

The function $W(\tau)$ is defined as the *strength of the relaxation spectrum.* In other words:

$$W(\tau) = K(\tau)n(\tau) \tag{17}$$

where $K(\tau)$ is the stiffness associated with those relaxation mechanisms having a relaxation time τ, and $n(\tau)\,d\tau$ is the number of mechanisms having a relaxation times between τ and $\tau + d\tau$.

The process of finding a relaxation spectrum from experimental modulus data by means of the integral equations (16a) and (16b) would be very cumbersome. Therefore an approximate method for making this calculation will be derived. The basic simplification for the approximate method is obtained by replacing the function (14a) by a step function. Thus, instead of (14a) the following relations will be used:

$$\begin{aligned} E_{1j} &= 0, & \omega &< 1/\tau_j \\ E_{1j} &= K_j, & \omega &> 1/\tau_j \end{aligned} \tag{18}$$

With this simplification (16a) is replaced by:

$$E_1(\omega) = \int_{1/\omega}^{\infty} W(\tau)\,d\tau \tag{19}$$

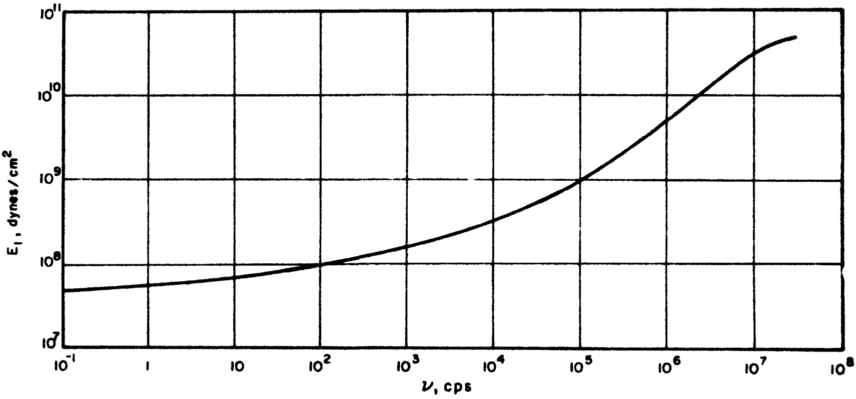

Fig. 26. Approximate behavior of real part of dynamic Young's modulus over wide frequency range at 30°C. Buna-N carbon-filled vulcanizate B-5. Experimental data for the middle of this frequency range have been extrapolated to reach static modulus at very low frequency and to reach value indicated by ultrasonic bulk wave velocity at 15 mc.

By computing the derivative $dE_1/d\omega$ from (19) one finds that $W(1/\omega)$ is given by the expression:

$$W(1/\omega) = \omega^2 dE_1/d\omega \tag{20}$$

The relation (20) provides a simple means for calculating the approximate strength of the relaxation spectrum under the assumption that the dispersion range is quite wide in comparison to one decade of frequency. Roughly speaking, the approximation leads to a relaxation spectrum which is about one decade greater in extent than the spectrum which would be found from the exact equations (16a) and (16b). This discrepancy will not seriously influence the appearance of the wide relaxation spectra which may be expected for rubbers. The approximation which has been used here is similar to that which has been used by Alfrey and Doty[21] in deriving the relaxation spectrum from a creep curve.

A specific calculation of the relaxation spectrum for the buna-N compound B-5 will now be considered. The relaxation spectrum will be calculated from the data of Figure 26, which is an approximate plot of the real part of the dynamic modulus for the compound B-5 at 30°C., between 10^{-1} and 10^8 cps. The data for the range 10 cps. to 16 kc. are taken directly from Figure 5. The curve is extrapolated to lower frequencies in such fashion as to approach the static modulus in the decade below 1 cps. The curve is extended to higher frequencies by joining segments of curves taken at lower temperatures. Finally, at 15 mc. the curve approaches the value for Young's modulus which is consistent with the 15 mc. compressional-wave measurement described in Appendix I. The construction of the curve of Figure 26 makes use of the principle that an increase in frequency is equivalent to a decrease in temperature. It was shown in Part II that this equivalence does not extend exactly to the slope of the logarithmic modulus curves. Thus the portion between 10^5 and 10^7 cps. of the curve in Figure 26 is only a rough approximation which must serve the present purpose in the absence of direct Young's modulus measurements at higher frequencies.

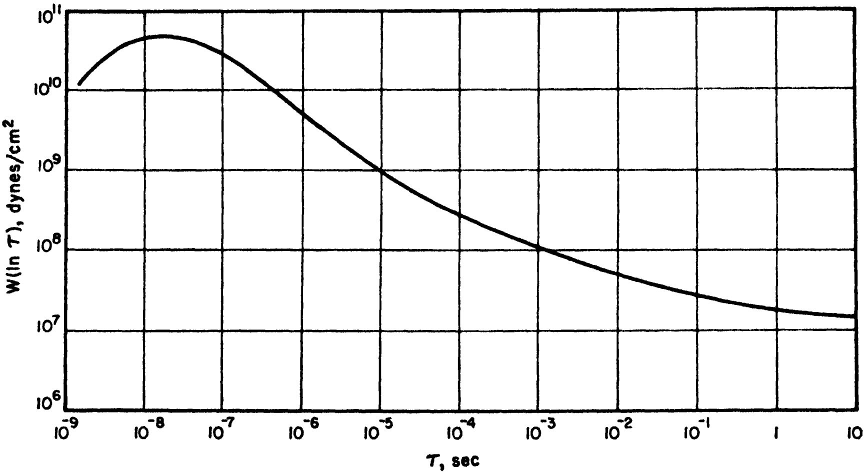

Fig. 27. Approximate strength of the relaxation spectrum, $W(\ln \tau)$, for buna-N carbon filled vulcanizate B-5. Calculated from modulus data of Figure 26.

The relaxation spectrum derived from the curve of Figure 26 by means of equation (20) appears in Figure 27. The quantity plotted here is $W(\ln \tau)$, which is the strength of the relaxation spectrum between $\ln \tau$ and $(\ln \tau + d \ln \tau)$.. Evidently $W(\ln \tau) = \tau W(\tau)$. The actual form of (20) which was used to derive this function is:

$$W(\ln \tau) = E_1 d(\ln E_1)/d(\ln \nu) \qquad (\tau = 1/2\pi\nu) \qquad (21)$$

The great width of the spectrum is not surprising in view of the large dispersion range of the dynamic modulus. The peak of the spectrum corresponds to the leveling off of the real modulus versus frequency function at high frequencies. In view of the approximate nature of Figure 26, the frequency (or relaxation time) corresponding to this leveling is known only by a rough inference. Information is not available from which to determine the downward course of the relaxation spectrum on the short-time side of the peak.

Kuhn[22] has evaluated for natural rubber a function equivalent to $W(\tau)$ by performing mathematical operations on an *ad hoc* function which represents the observed relaxation of stress as a function of time. The result is that $W(\tau)$ is proportional to $1/\tau$. But if this result is correct the real part of the dynamic modulus at frequency ω must be approximately:

$$E_1(\omega) = \text{constant} \int_{1/\omega}^{\infty} d\tau/\tau.$$

Thus the real modulus for any finite frequency is infinite. For this reason no credence can be placed in Kuhn's result as a wide-range relaxation spectrum, although according to Figure 27 Kuhn's result is qualitatively correct in the region of the longer relaxation times.

Interpretation of Results in Terms of Activation Energies

The diffusion rate theory of Frenkel[22a] and the closely related chemical rate theory of Eyring reach the common conclusion that the rate of flow for molecular entities, which progress along some coordinate by overcoming potential energy barriers, is proportional to $\exp(-\Delta U/kT)$, where k is Boltzmann's constant and ΔU is the height of one of the energy barriers. The quantity ΔU is called an activation energy.

According to these theories the rate of a simple chemical reaction should be proportional to $\exp(-\Delta U/kT)$, or the viscosity of a simple liquid should be proportional to $\exp(\Delta U/kT)$. A number of instances have been reported in which the observed temperature dependence of a chemical reaction rate or of a viscosity is in agreement with this conclusion. Accordingly various investigators have sought to describe other more complicated flow processes in terms of reaction rate or diffusion rate theory and to assign activation energies for the processes. An example of one of these attempts, closely related to the present topic of relaxation phenomena in rubbers, is the comprehensive examination of dielectric data in terms of chemical rate processes which has been published by Kauzmann.[3] The Kauzmann paper represents an adaption of the chemical rate theory of Eyring to relaxation problems.

While Kauzmann computed activation energies from the variation with temperature of the frequency of maximum dielectric loss, it will be necessary to use a different method of calculation to obtain activation energies from dynamic modulus data thus far obtained. Little dynamic modulus information has been obtained at the frequency of maximum loss because of experimental limitations. For the purpose of computing activation energies from dynamic modulus data obtained in the present experiments, the following approximate relations have been derived:

---

[22] W. Kuhn, O. Kunzle, and A. Preissman, *Helv. Chim. Acta*, 30, 307 (1947).

[22a] J. Frenkel, *Kinetic Theory of Liquids*. Oxford Univ. Press, London, 1946.

$$\Delta U = -RT^2(\partial E^*/\partial T)(\nu\partial E^*/\partial\nu) = -RT(\partial E^*/\partial \ln T)/(\partial E^*/\partial \ln \nu) = RT(d \ln \nu/d \ln T)E^* = \text{constant} \quad (22)$$

Here ΔU is the activation energy in kilocalories per mole, R is the gas constant (0.00198 kcal./mole), ν is frequency in cycles/sec., and T is Kelvin temperature.

By application of suitable forms of (22) to the dynamic modulus data presented in Figures 5 and 8 for compounds B-1 (Hycar OR-15, unloaded) and B-5 (Hycar OR-15, loaded), activation energies in the neighborhood of 30 kcal./mole are obtained. For the natural rubber compound N-1, activation energies of the order of 10 kcal./mole are found.

The striking feature of the activation energy data is the large value of the energies. Mark[23] gives a figure for the cohesive energy of a 5 Å. length of a molecular chain, surrounded by four neighboring chains, of 1.1 kcal./mole in the case of polybutadiene, and 1.3 kcal./mole in the case of natural rubber. The length of one monomer unit is of the order of 5 Å. The observed values of the activation energy therefore suggest that the concerted motion of at least 25 monomer units may be involved in the prevailing type of molecular diffusion in the case of Hycar OR-15. In this connection it is noteworthy that Eyring and Kauzmann[24] have suggested from a study of activation energy data for the viscous flow of the higher paraffins that the motion of these large molecules occurs in segments of about 20 carbon units. It is likewise significant that large activation energies have been reported for the dielectric behavior of rubbers. Kauzmann[3] found an activation energy of 25 kcal./mole for natural rubber vulcanized with 2% sulfur.

The relaxation effects which give rise to the large activation energies found from dynamic modulus data are apparently not due to hindrances opposing simple rotation about C—C bonds. Guth, James, and Mark[6] cite evidence to the effect that the rotational hindrance is of the order of 1 kcal./mole. It is not surprising that the activation energy data for frequencies in the audio range do not correspond to the value for the C—C rotational hindrance, if Frenkel is correct in calculating the time for reordering of a rubber molecular chain, through rotational bond rearrangement, as 10^{-7} sec. (See section 5 of the next discussion.)

It would be expected that, at a given temperature, those relaxation mechanisms which give rise to dispersion at the higher frequencies, having the shorter relaxation times, would be characterized by activation energies smaller than those of the mechanisms contributing to dispersion at the lower frequencies. The methods which have been necessarily used to obtain activation energies from present dynamic modulus data are not considered sufficiently precise to test for the presence of this effect.

---

[23] H. Mark, in *Advancing Fronts in Chemistry*, pp. 7-13. Reinhold, New York, 1945.

[24] C. F. Eyring and W. Kauzmann, *J. Am. Chem. Soc.*, **62**, 3113 (1940).

Indications Toward a Dynamic Modulus Theory

This concluding section will be devoted to a summary of those findings, indicated or strongly suggested by the experimental results detailed in this paper, which may afford a partial basis for future attempts to construct a theory of the dynamic modulus.

1. The Effective Chain Length between Hindrances Becomes Shorter at High Frequencies or at Low Temperatures. According to the kinetic theory of rubberlike elasticity,[6,10,11] the Young's modulus of a chain molecule is inversely proportional to the mean squared length of the chain. As rubber is vulcanized, the average effective chain length between hindrances is reduced as cross-links between adjacent chains and in the same chain are formed. The static modulus of rubberlike materials, which is of the order of 10^7 dynes/cm.^{2} for light vulcanization, increases to several times 10^{10} as vulcanization is made extreme. The large modulus of highly vulcanized, or "hard" rubber, is undoubtedly the result both of a reduction in the effective chain length and of the incorporation of a greater fraction of the molecules into the coherent static elastic network. James and Guth[10] have estimated that in natural rubber with 5 to 8% sulfur content, only about 25% of the molecular constituents are bound into the coherent elastic network, but they suggest that this fraction varies with the degree of vulcanization.

The dynamic modulus of rubberlike materials appears to approach a value of several times 10^{10} dynes/cm.^{2}, with increasing frequency or with decreasing temperature, just as the static modulus approaches a similar value with increasing vulcanization. This suggests the view that there are many points within the material at which adjacent chain segments are bound by van der Waals forces, and that when a deforming force is applied to the material for a period which is short compared to the relaxation time of the hindrances offered by the van der Waals forces, these hindrances are effectively points of chain fixation in the same sense as are vulcanization points. Thus the effective chain length is shorter at higher frequencies. Low temperatures produce the same state of affairs by making the various relaxation times long in comparison to any ordinary periods of sinusoidal force application.

In support of this point of view there is the evidence cited in Part II to the effect that the presence or absence of moderate vulcanization has a relatively small effect upon the dynamic modulus at sufficiently high frequency. The static modulus is of course very small in the absence of vulcanization.

2. A Larger Fraction of the Molecular Chains Contributes to the Modulus at Higher Frequencies or at Lower Temperatures. The discussion of this point is largely covered by the remarks concerning item *1.* If one accepts the postulate that effective inter- and intramolecular hindrances, comparable in their results to the linkages of vulcanization, are introduced as the frequency of measurement is increased, items *1* and *2* both follow by essentially the same arguments.

3. The Observed Activation Energies Indicate the Frequent Occurrence of Concerted Jumps by Segments Comprising Several Monomer Units. This conclusion is supported by the large values of activation energy reported in the preceding section, where this topic is more fully discussed.

4. Relaxation Spectra Having a Width of at Least Six Decades Are Found in Rubberlike Materials. This conclusion is indicated by the relaxation spectrum analysis which has been presented. The width of the relaxation may indeed extend to relaxation times many decades smaller or larger than those which have been examined with the present techniques, although it appears that the present measurements cover most of the frequency range of appreciable dispersion and therefore most of the population of relaxation elements. It is possible that by studying the imaginary part of the modulus one could demonstrate an extension of the relaxation spectrum to very long relaxation times, even though the variation with frequency of the real part of the modulus becomes difficult of measurement at the very low frequencies.

5. The Relaxation Times for Recording of the Individual Molecular Chains about C—C Bonds Do Not Explain the Observed Relaxation Spectrum. It seems fairly certain that the inherent reordering time of a chain which is free of large cumulative hindering potentials along appreciable portions of its length cannot be identified with the observed relaxation times. The hindrances to rotational rearrangement about carbon bonds are thought to be as small as 0.5 kcal./mole.[6] In this event the "jump time" for an indidividual bond rotation is of the order of 10^{-13} sec. Frenkel[25] shows that the reordering time for a chain of 1000 monomer units, in solution, is of the order of 10^{-7} sec. The chain in solution would not be subject to cumulative coherent potential hindrances along its length. The relaxation times which are found experimentally in solid rubber must therefore be explained in terms of the hindrances to which the molecule is subjected in the environment rather than in terms of the statistics of the individual molecule. Part of this environmental effect must be due to the presence of those cumulative potential hindrances which account for the large observed activation energies. One cannot assert on the basis of the present data that relaxation effects due to the time required for reordering of individual "free" chain segments are unimportant at frequencies of many megacycles. In this connection it is interesting to note that Alpert,[26] in a nuclear magnetic resonance experiment, has recently found evidence of molecular rotation in natural rubber at frequencies exceeding 3×10^7 cps.

6. The Temperature and Frequency Dependence of the Reciprocal Modulus is Similar to That of the Dielectric Constant for a Polar Material. This point has been elaborated in Part II.

The author is pleased to acknowledge the invaluable guidance of Prof. R. H. Bolt and helpful consultations with Prof. L. Tisza and Prof. W. H. Stockmayer of the Massachusetts Institute of Technology.

---

[25] J. Frenkel, *Kinetic Theory of Liquids*, p. 469. Oxford Univ. Press, London, 1946.

[26] N. L. Alpert, *Phys. Rev.*, **72**, 637 (1947).

APPENDIX I. INVESTIGATION OF DYNAMIC MODULUS BY ULTRASONIC BULK-WAVE TRANSMISSION MEASUREMENTS

It is possible to deduce an approximate upper limit for the Young's modulus loss factor E_2/E_1 and an approximate value for the real dynamic Young's modulus from measurements of the velocity and attenuation of plane bulk waves in a rubber sample. In the present investigation such measurements have been performed in the range from 10 to 30 megacycles. A detailed description of the experimental method and of the results is the subject of another publication.[27]

In a viscoelastic medium the velocity of bulk ("compressional") waves is approximately:

$$c = [k + 4\mu_e/3)/\rho]^{1/2} \tag{23}$$

where k is the bulk modulus, μ_e is the shear modulus, and ρ is the density of the medium. The attenuation in decibels per centimeter is approximately:

$$L = 5.791\mu\omega^2/\rho c^3 \tag{24}$$

where μ is the shear viscosity coefficient. These relations are nearly correct when the attenuation per wave length is small compared to 54.5 decibels.

Thus it is possible, from a knowledge of the velocity and attenuation for bulk waves at a specified frequency, to calculate values for the quantities $(k + 4\mu_e/3)$ and μ. It should be remarked that the above relations are derived on the basis of the classical assumption of Stokes that there is no viscous loss associated with an all-sided compression. The general validity of Stokes' assumption has almost certainly been disproved by the results of modern investigations of the attenuation of sound in liquids. Therefore it is best to assume that the value of μ as given above is only an upper limit for the value of the shear viscosity, since the experimentally observed wave attenuation could be due in part to the "forbidden" compressional viscosity. The "Young's modulus viscosity" (γ) is somewhere between 2 and 3 times μ. The ratio would be 3 if Poisson's ratio were 1/2, but in view of the large dynamic Young's modulus (*ca.* 10^{10} dynes/cm.^{2}) which is found at very high frequencies, one must assume that Poisson's ratio is somewhat less than 1/2 for the present purpose. Similarly the real Young's modulus lies between 2 and 3 times μ_e.

The following bulk-wave data were obtained for the buna-N compound B-5:

Density: 1.18 g./cm.^{3} Temperature: About 25 °C.
Frequency: 15 mc. ($\omega = 9.43 \times 10^7$) L: 194 db./cm. c: 2.03×10^5 cm./sec.
Effective stiffness: $(k + 4\mu_e/3) = 4.8 \times 10^{10}$ dynes/cm.^{2}
Shear viscosity on Stokes' assumption: $\mu = 73$ poises

An independent measurement of Young's modulus or of Poisson's ratio would be required to complete the above data. In the absence of such a

---

[27] A. W. Nolle and S. C. Mowry, *J. Acoustical Soc. Am.*, **20**, 432 (1948).

measurement, one may derive an upper limit for E_2/E_1 by making reasonable assumptions which are introduced below. Suppose that the "Young's modulus viscosity," γ, is equal to 2.5μ, or at most 180 dyne-sec./cm.^{2} Then $E_2 = \gamma\omega$ is at most 1.7×10^{10} dynes per square centimeter. But E_1 at 15 mc. must be at least 2×10^{10} dynes/cm.^{2} This conclusion is reached by extrapolating lower frequency data according to the principle that a decrease in temperature is approximately equivalent to an increase in frequency (Part II); the modulus actually becomes larger than 10^{10} at audiofrequencies at 0°C., and by joining segments of the isothermal modulus-frequency curves, one may infer that the modulus should be at least 2×10^{10} at 15 mc., 25°C. Alternatively, one may suppose in regard to the experimentally determined value of $(k + 4\mu_e/3)$ that k is equal to the bulk modulus for water, 2.3×10^{10} dynes/cm.^{2} (That this is essentially correct may be deduced from the well-known approximate equality of the characteristic acoustic bulk-wave impedance ρc of rubber to that of water, which obtains even at temperatures and frequencies for which the shear modulus is very small compared to the bulk modulus.) Then μ_e is 1.9×10^{10} dynes/cm.^{2} and E_1 is about $2.5\mu_e$, or 1.7×10^{10}. In either event the Young's modulus loss factor, E_2/E_1, is less than unity at 15 mc., 25°C. But according to Figure 4, E_2/E_1 at 10 kc., 25°C. for the compound B-5 is about 1.5 and is increasing with increasing frequency. The results of the ultrasonic compressional-wave measurement therefore suggest that the loss factor E_2/E_1, for constant temperature, has a maximum with respect to frequency.

APPENDIX II. SYMBOLS

The convention that a sinusoidal variation with time is represented by the real part of $e^{-i\omega t}$ has been followed consistently, except where it is necessary to cite the work of other authors who have used the positive sign convention. Thus $-i$ as used here is comparable to the j of electrical engineering.

Symbol	Definition
c	Acoustic phase velocity, cm./sec.
$E^* = E_1 - iE_2$	Complex Young's modulus, dynes/cm.^{2}
k	Bulk elastic modulus, dynes/cm.^{2}; Boltzmann's constant
L	Acoustic attenuation, db./cm.
L_z	Length of unit cube rubber sample along stress axis, value unity for zero stress
R	Gas constant, kcal./mole/°C.
$S^* = S_1 + iS_2$	Complex compliance, cm.^{2}/dyne
t	Time, sec.
T	Temperature, centigrade, or centigrade absolute
ΔU	Activation energy
$W(\tau)$	Strength of relaxation spectrum between τ and $\tau + d\tau$, dynes/cm.^{2}
Z_m	Mechanical impedance, dynes-sec./cm.
Z	Stress, dynes/cm.^{2}

α	Volume coefficient of thermal expansion; dimensionless parameter of Cole arc
γ	Extensional viscosity coefficient (also known as "normal" or "Young's modulus" viscosity coefficient), dynes-sec./cm.^{2}
$\epsilon^* = \epsilon_1 + i\epsilon_2$	Complex dielectric constant
μ	Shear viscosity coefficient, dynes-sec./cm.^{2}
μ_e	Shear elastic modulus, dynes/cm.^{2}
ν	Frequency, cps.
ρ	Density, g./cm.^{3}
ω	Frequency, radians/sec.

APPENDIX III. INDEX OF RUBBER COMPOUNDS DISCUSSED IN THE TEXT

All the following formulas are given in parts by weight. Except in the case of the latex formula, for which the ingredients are mixed in liquid dispersion, the essential solid ingredients are mixed in the milling process. The milling time is given with some of the formulas.

Solvent-cast samples are prepared by dissolving the milled material in the indicated amount of solvent and pouring a thin layer of the solution into a flat glass dish. The evaporation of the solvent and the curing (vulcanization) of the sample occur gradually at room temperature over a period of several days.

Molded samples are placed under pressure in a mold of suitable dimensions and are cured at an elevated temperature for a period which generally does not exceed one hour. For these samples a curing time and a curing temperature are given.

Samples N-1 and N-2 were supplied by Notre Dame Polymer Physics Research Laboratory. The other samples were compounded by Mr. Joseph Zallen of the M. I. T. Acoustics Laboratory.

I. Natural rubber

N-1:	sp.gr. 0.975	Crepe rubber	100
		ZnO	3
		S	5
		Diphenylguanidine	1
		30 minutes at 147°C.	
N-2:	sp. gr. 0.953	Smoked sheet	100
		ZnO	5
		S	2
		Captax	1.5
		Bardol B	5
		50 minutes at 120°C.	
Latex:	sp.gr. 0.975	Crepe rubber	100
		ZnO	3 (as 60% paste)
		S	5 (as 40% paste)
		Piperidine pentamethylene dithiocarbamate	2
		Cast as liquid and cold-cured.	

II. Hycar OR-15 (buna-N rubber: copolymer butadiene, acrylonitrile)

B-0:	sp.gr. 1.02	Hycar OR-15. 20 minutes milling. Cast as 20% solution in methyl ethyl ketone. Unvulcanized.

B-1:	sp.gr. 1.06	Hycar OR-15	100
		ZnO	5
		S	1.5
		Butyl 8 (a dithiocarbamate)	10 ml.
		Methyl ethyl ketone	480
		20 minutes milling. Solvent-cast.	
B-5:	sp.gr. 1.18	Hycar OR-15	100
		ZnO	5
		S	2
		Butyl 8	10 ml.
		P 33 black (soft thermal black)	50
		Methyl ethyl ketone	480
		Benzoic acid (gel inhibitor)	2
		15 minutes milling. Solvent-cast.	
B-99:	sp.gr. 1.05	Hycar OR-15	100
		ZnO	5
		S	2
		Mercaptobenzothiazole	2
		30 minutes at 149 °C.	
B-100:	sp.gr. 1.05	Hycar OR-15	100
		ZnO	5
		S	1.5
		Benzothiazyl disulfide	1.3
		60 minutes at 143° C.	

III. Butyl rubber or GR-I (copolymer isobutylene, isoprene)

U-50	sp.gr. 0.91	GR-I 70	100
		ZnO	5
		S	2
		Stearic acid	1.5
		Thiuram M (tetraethylthiuram disulfide)	1
		Mercaptobenzothiazole	0.5
		40 minutes at 153 °C.	

IV. Neoprene (polychloroprene)

GN-50:	sp.gr. 1.32	Neoprene GN	100
		ZnO	5
		MgO	7
		10 minutes at 153 °C.	
CG-1:	sp.gr. 1.45	Neoprene CG	100
		PbO	20
		Neozone A	2
		Silene EF (calcium silicate)	2
		Toluene	320
		Accelerator 833	3
		10 minutes milling. Solvent cast.	

V. GR-S (Copolymer butadiene, styrene)

S-50:	sp.gr. 1.14	GR-S	100
		SRF (semireinforcing black)	50
		ZnO	5
		S	2
		Stearic acid	1.5
		Mercaptobenzothiazole	1.5
		50 minutes at 143 °C.	

Résumé

Les résultats expérimentaux sont rapportés pour le module dynamique complexe de Young des substances élastomères, pour des fréquences de 10^{-1} à 10^{-6} cycles par seconde, et à une température variant, au maximum de $-60°$ à $+100$ °C. La part réelle du module varie, de façon significative, avec la fréquence au moins sur six décades, et

s'accroît avec une augmentation de fréquence ou une diminution de température. La part imaginaire du module est grande dans les parties des diagrammes température-fréquence où la part réelle présente un gradient important; pour certains composés elle atteint des valeurs plus grandes que la part reélle. Le comportement du module inverse, ou la "compliance," en fonction de la température et de la fréquence est qualitativement le même que celui de la constante diélectrique des diélectriques polaires, présentant une grande dispersion. Les mesures les plus importantes, qui supportent ces conclusions, ont été faites sur les vulcanisats Buna-N. Aux très faible fréquences, la part réelle du module dynamique est proportionelle à la température absolue, comme requis par la théorie cinétique de l'élasticité du caoutchouc. A une fréquence plus élevée, représentant le début de la dispersion, l'effet inverse de la température débute. La fréquence de transition est de l'ordre de 100 cps pour le caoutchouc naturel, et un cps pour le caoutchouc butylique. Le durcissement du caoutchouc avec une diminution de température, parfois considéré comme une évidence d'une transition de second ordre, devient progressivement moins abrupte avec des fréquences croissantes. Il semble de ce fait, que la "transition" de second ordre, telle qu'observée aux fréquences élevées, est actuellement un effet de vitesse de relaxation. Aux très faibles fréquences, il existe une transition thermique du module, dont la forme est d'ordinaire indépendante de la fréquence, et qui n'est pas nécessairement la continuation du durcissement par relaxation aux fréquences élevées. L'arc de Cole dans le diagramme complexe constitue une représentation approximative des résultats de "compliance" dynamique. La déformation statique de l'échantillon jusqu'à 50% d'élongation influence le module dynamique par un facteur inférieur à deux dans la plupart des cas, mais l'effet est rarement négligeable. La présence ou l'absence de vulcanisation n'affecte pas, de façon critique, le module dynamique à haute fréquence; l'accroissement du module réel avec une augmentation de fréquence doit être dû, de ce fait, en partie à des empêchements de relaxation intermoléculaire, qui sont équivalents aux liaisons, dues à la vulcanisation, aux fréquences élevées. La comparaison est faite entre les résultats obtenus pour le buna-N, le caoutchouc-butylique, le GR-S, le néoprène et le caoutchouc naturel. Dans le domaine des fréquences auditives, le caoutchouc présente l'angle de perte le plus faible, tandis que le buna-N et les caoutchoucs butyliques présentent les pertes les plus considérables. Comme autre expression de ces résultats, une méthode approximative est utilisée pour trouver un spectre de relaxation pour les vulcanisats de buna-N. Le spectre s'étend sur, au moins, six décades, mais les extrémités ne peuvent être tracées avec les résultats actuels. Les énergies d'activation pour les processus d'écoulement moléculaire, figurant dans la déformation dynamique, sont calculées par une méthode approximative au départ des résultats pour le buna-N et les caoutchoucs naturels. Des valeurs d'environ 30 et 10 Kcal/mole ont été trouvées respectivement. Ces importantes énergies d'activation suggèrent que les effets importants de la relaxation observés de les domaines de fréquence du présent travail proviennent d'empêchements aux mouvements des segments moléculaires, constitués de plusieurs unités monomériques, plutôt que d'une rotation restreinte autour des liaisons C-C.

Zusammenfassung

Es werden experimentelle Resultate für den komplexen dynamischen Young Modul von kautschukähnlichem Material in dem Frequenzbereich 10^{-1} bis 10^{-5} Hertz pro Sekunde und in einem Temperaturbereich, dessen äusserste Grenzen −60° und +100°C. sind, angegeben. Der reelle Teil des Moduls variiert bezeichnenderweise mit der Frequenz über mindestens 6 Dekaden, und nimmt zu mit zunehmender Frequenz oder mit abnehmender Temperatur. Der imaginäre Teil des Moduls ist gross in den Teilen der Temperatur-Frequenz-Ebene, wo der reelle Teil einen grossen Gradienten hat, und erreicht in einigen Verbindungen grössere Werte als der reelle Teil. Das Verhalten des reziproken Moduls, oder Fügigkeit, in Anbetracht zu Temperatur und Frequenz ist qualitativ das gleiche wie das der dielektrischen Konstante von polaren Dielektrika, die

ein grosses Dispersionsbereich haten. Die ausführlichsten Messungen zur Unterstützung dieser Schlüsse wurden mit Buna-N-Vulkanisaten ausgeführt. Bei sehr geringen Frequenzen ist der reele Teil des dynamischen Moduls proportional der absoluten Temperatur, wie es die kinetische Theorie kautschukähnlicher Elastizität verlangt. Bei einer höheren Frequenz, die das Beginnen der Dispersion darstellt, tritt der gegenseitig Temperatureffekt ein. Die Frequenz des Übergangs ist in der Grössenordnung von 100 Hertz pro Sekunde für natürlichen Kautschuk und 1 Hertz pro Sekunde für Butylkautschuk. Das Steifwerden von Kautschuk mit abnehmender Temperatur, welches manchmal als Anzeichen eines Übergangs 2. Ordnung angesehen wird, wird mit steigender Frequenz progressiv weniger ausgesprochen. Es scheint deshalb, dass der Übergang "zweiter Ordnung," wie er bei höheren Frequenzen beobachtet wird, in Wirklichkeit ein Effekt der Relaxationsgeschwindigkeit ist. Bei sehr niedrigen Frequenzen besteht ein Temperaturübergang des Moduls, dessen Form fast unabhängig von der Frequenz ist und der nicht unbedingt eine Fortsetzung des durch Relaxation hervorgerufenen Steifwerdens ist, welches bei höherer Temperatur gefunden wurde. Es wurde gefunden, dass der Cole-Bogen in der Komplexebene eine ungefähre Representation der dynamischen Fügigkeitsdaten ist. Eine statische Deformation der Probe bis 50% Elongation beeinflusst den dynamischen Modul mittels eines Faktors, der in den meisten Fällen kleiner als 2 ist, aber seine Wirkung ist selten zu vernachlässigen. Die Gegenwart oder Abwesenheit von Vulkanisation beeinflusst den dynamischen Hochfrequenz-Modul nicht kritisch; also muss die Zunahme des reellen Moduls mit zunehmender Frequenz teilweise durch intermolekulare Relaxations hinderungen bedingt sein, welche bei genügend hoher Frequenz Vulkanisationsbindungen gleichwertig sind. Daten für Buna-N, Butyl, GR-S, Neopren und natürlichen Kautschuk werden verglichen. Im hörbaren Frequenzbereich hat natürlicher Kautschuk den kleinsten Verlustwinkel, während Buna-N und Butylkautschuk die grössten Verlustwinkel haben. Als anderer Ausdruck der Resultate wird eine annähernde Methode zum Auffinden eines Relaxationsspektrum für Buna-N-Vulkanisate benutzt. Das Spektrum dehnt sich über mindestens 10 Dekaden aus, aber seine Extreme können mit den vorliegenden Daten nicht umrissen werden. Aktivierungsenergien für Molekül-Fliess-Prozesse, die in dynamischen Deformationen enthalten sind, werden mittels einer annähernden Methode aus Daten für Buna-N und natürlichen Kautschuk berechnet. Werte von ungefähr 30 beziehungsweise 10 kcal/mole wurden gefunden. Diese grossen Aktivierungsenergien lassen vermuten, dass die bedeutenden Relaxationseffekte im Frequenzbereich der vorliegenden Arbeit vielmehr durch Hinderungen bewirkt werden, die der Bewegung von aus mehreren monomeren Einheiten zusammengesetzten Molekülsegmenten entgegentreten, als aus einer verhinderten Rotation um C-C Bindungen.

Received March 1, 1918.

JOURNAL OF POLYMER SCIENCE VOL. V, NO. 1, PAGES 55–67

Vitesse de Polymérisation et de Copolymérisation de l'Acétate d'Isopropényle

R. HART et G. SMETS, *Laboratoire de Chimie Macromoléculaire, Université de Louvain, Belgium*

L'acétate d'isopropényle, qui fait l'objet de cette étude peut être considéré structurellement, comme l'homologue supérieur de l'acétate de vinyle, par substitution par un groupe méthyle, de l'hydrogène fixé au carbone porteur du groupe acétoxylé.

Du point de vue de la polarité de la double soudure, cette substitution doit entraîner un caractère négatif plus prononcé de la liaison éthylénique; les essais de copolymérisation ont permis de vérifier cette influence. Par cette substitution également, ce monomère acquiert une structure allylique; celle-ci fait supposer des propriétés semblables à celles de l'acétate d'allyle, dont ce monomère nouveau ne diffère que par la position différente du groupe acétoxylé. Ce comportement a été retrouvé par des essais de polymérisation.

L'acétate d'isopropényle s'obtient, soit par addition d'acide acétique au propine en présence de fluorure de bore, soit par action du cétène sur l'acétone en présence d'acide sulfurique.

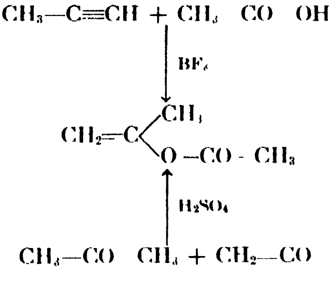

A. VITESSE DE POLYMÉRISATION DE L'ACÉTATE D'ISOPROPÉNYLE

La polymérisation de ce monomère présente une analogie remarquable avec la polymérisation de l'acétate d'allyle, et se différencie très considérablement de celle de l'acétate de vinyle.

Ainsi, sous l'action de la lumière ultra-violette, durant vingt-cinq à cent heures, il se forme, après entraînement à la vapeur de l'excès de monomère, un produit liquide, très visqueux; les rendements sont très faibles. En présence d'halogénures métalliques ($SnCl_4$, BF_3, $AlCl_3$) il ne se manifeste aucune polymérisation.

Par chauffage prolongé à 100° en présence de 0.25% de peroxyde de benzoyle, ce monomère ne polymérise qu'avec des rendements minimes (environ 1%). Pour obtenir des rendements plus élevés, il est nécessaire d'utiliser des quantités importantes d'initiateur, par exemple 2 à 10%. Dans de telles conditions, les poids moléculaires moyens des polymères obtenus sont faibles; ainsi, en présence de 5% de peroxyde de benzoyle, par chauffage durant 30 heures à 100°C., on obtient un poids moléculaire de 1068, soit un décamère. Dans des conditions semblables, Bartlett et Altschul[1] ont obtenu dans le cas de l'acétate d'allyle un poids moléculaire de 1300.

De même que ces auteurs, nous avons suivi la vitesse de disparition du peroxyde de benzoyle et de l'acétate d'isopropényle au cours de la polymérisation. Les résultats sont renseignés dans le tableau I.

La décomposition du peroxyde de benzoyle est du premier ordre par rapport à sa concentration; la constante de vitesse k_1 est de 1.025×10^{-4}/ sec.$^{-1}$ (fig. 1).

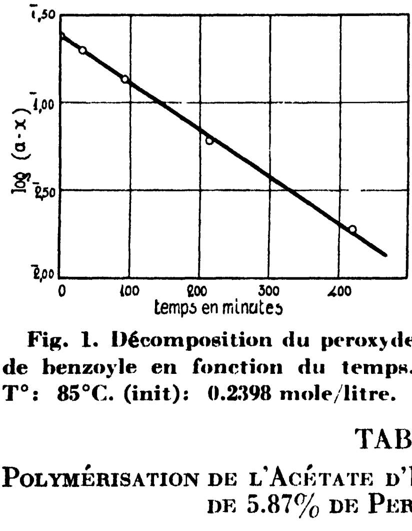

Fig. 1. Décomposition du peroxyde de benzoyle en fonction du temps. T°: 85°C. (init): 0.2398 mole/litre.

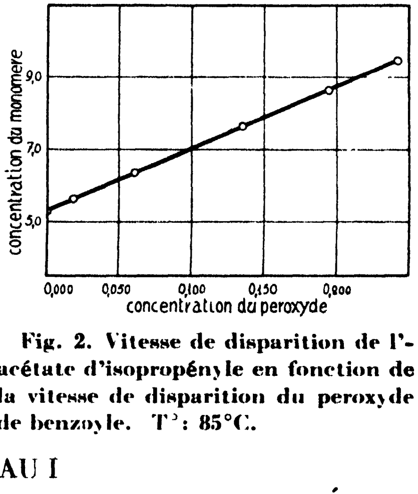

Fig. 2. Vitesse de disparition de l'acétate d'isopropényle en fonction de la vitesse de disparition du peroxyde de benzoyle. T°: 85°C.

TABLEAU I

POLYMÉRISATION DE L'ACÉTATE D'ISOPROPÉNYLE Á 85° C. EN PRÉSENCE DE 5.87% DE PEROXYDE DE BENZOYLE

Durée, min	(Init)[a]	(M)[b]	% polym.
0	0.2398	9 408	0
30	0 1952	8 602	8 6
91	0 1345	7 611	19 1
211	0.0611	6.372	32 3
420	0 0186	5 628	40 2
24 heures	0 000	5.310	43 6

[a] (Init), concentration molaire en peroxyde de benzoyle.
[b] (M), concentration molaire en monomère.

D'autre part, en établissant le diagramme des variations de la concentration en monomère en fonction de la variation de la concentration en peroxyde de benzoyle au cours d'une polymérisation, on constate une relation linéaire; il y a donc un rapport constant (fig. 2):

$$\Delta(\mathrm{M})/\Delta(\mathrm{init}) = 17.0$$

La polymérisation de ce dérivé allylique peut être schématisée par les étapes suivantes:

(*a*) activation:

$$\mathrm{init} \xrightarrow{k_1} 2\mathrm{R}^* \tag{1}$$

(*b*) propagation:

$$\mathrm{R}^* + \mathrm{M} \longrightarrow \mathrm{R{-}M}^*$$

$$\mathrm{R{-}M}^* + \mathrm{M} \xrightarrow{k_2} \mathrm{R{-}M{-}M}^* \tag{2}$$

(*c*) transfert de chaîne:

$$\mathrm{R}^* + \mathrm{M} \xrightarrow{k_3} \mathrm{R{-}H} + r^* \tag{3}$$

$$r^* + \mathrm{M} \xrightleftharpoons{k_4} r{-}\mathrm{M}^* \tag{4}$$

(*d*) rupture:

$$\mathrm{R}^* + \mathrm{R}^* \xrightarrow{k_5} \text{addition ou disproportionation} \tag{5}$$

$$\mathrm{R}^* + r^* \xrightarrow{k_6} \ldots \tag{6}$$

$$r^* + r^* \xrightarrow{k_7} \ldots \tag{7}$$

Les réactions d'activation et de propagation de chaîne sont les réactions habituelles à toutes les polymérisations. La réaction (5) est exclue; elle entraînerait une vitesse de disparition du monomère proportionnelle à la racine carrée de la concentration en monomère, ce qui est contradictoire avec le rapport constant trouvé.

Les deux autres processus de rupture sont également possibles, toutefois le processus (7) semble le plus probable. Ce sont les processus de transfert de chaîne qui sont particulièrement intenses dans le cas des dérivés allyliques. Par collision d'une chaîne en croissance avec une molécule de monomère, celui-ci donne très aisément lieu à un transfert de chaîne par suite de la mobilité de l'hydrogène en alpha de ce dérivé, suivant la réaction:

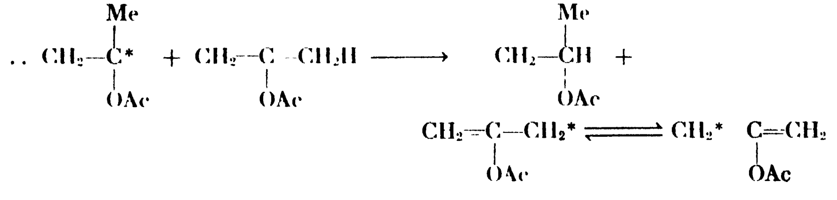

$$\cdots\ \mathrm{CH_2{-}\underset{OAc}{\overset{Me}{C^*}}} + \mathrm{CH_2{-}\underset{OAc}{C}{-}CH_2H} \longrightarrow \mathrm{CH_2{-}\underset{OAc}{\overset{Me}{CH}}} + \mathrm{CH_2{=}\underset{OAc}{C}{-}CH_2^*} \rightleftharpoons \mathrm{CH_2^*\ \underset{OAc}{C}{=}CH_2} \tag{3}$$

Le radical r^* ne réagit toutefois pas avec une nouvelle molécule de monomère, par suite de l'équilibre (1). Le produit d'addition éventuellement formé se redécompose en radical r^* et en monomère, laissant ainsi le milieu inchangé. Les radicaux r^*, qui se forment très aisément suivant la réaction (3), s'éliminent du milieu de réaction exclusivement par l'un des deux phénomènes de rupture (6) ou (7).

Ce phénomène a été désigné par Bartlett et Altschul[1] "degradative chain transfer," rupture de chaîne désactivante. La réaction (4) ne se passe toutefois pas par suite d'un manque de réactivité du radical r^*, mais par suite de la réversibilité du processus lui-même; les essais de copolymérisation décrits ci-dessous, entre l'acétate d'isopropényle et l'acétate de vinyle en sont la preuve. Dès que le radical r^* se trouve en présence d'un autre monomère vinylique, qui n'est plus de nature allylique, il s'y additionne aisément, même si la réactivité de ce dernier monomère est du même ordre que celle de l'acétate d'isopropényle (voir chlorure et acétate de vinyle: plus loin).

Cette interprétation du comportement allylique diffère nettement de celle indiquée antérieurement par Bartlett et Altschul; elle conduit toutefois à la même équation finale:

$$\Delta(\mathrm{M})/\Delta(\mathrm{init}) = (k_2 + k_4)/k_7$$

En vue de vérifier simultanément cette interprétation du comportement allylique et du schéma de polymérisation, il nous a paru particulièrement intéressant d'examiner les réactions de copolymérisation de ce même monomère en présence d'autres monomères vinyliques ordinaires; à ce titre nous avons essayé les copolymérisations avec l'acétate de vinyle, le chlorure de vinyle, le méthacrylate de méthyle et le styrène.

B. VITESSES DE COPOLYMÉRISATION

(a) Copolymérisation de l'acétate d'isopropényle avec l'acétate de vinyle

Dans le tableau II et les tableaux suivants, nous avons indiqué les résultats des essais de copolymérisation effectués; l'indice 2 désigne toujours l'acétate d'isopropényle.

TABLEAU II

M_2	Analyse	m_2	Durée, min.	% polym
0.100	11.43	0.108	23	8.1
0.200	11.30	0.180	40	9.0
0.400	10.94	0.388	102	9.2
0.500	10.75	0.502	140	8.0
0.600	10.61	0.590	240	8.4
0.715	10.42	0.712	400	7.2
0.800	10.28	0.806	820	9.0
0.900	10.12	0.917	33 heures	9.5

La copolymérisation a été effectuée en solution benzénique à une concentration totale des monomères de 8 mole/litre, en présence de 7.2×10^{-3} moles/litre de peroxyde de benzoyle, comme initiateur; la température a été maintenue à 75°C. Les fractions molaires M_2 indiquent la teneur molaire en acétate d'isopropényle dans le mélange initial des monomères; les fractions molaires m_2 indiquent la fraction molaire en acétate d'isopropényle dans le copolymère.

Les copolymères obtenus ont donc pratiquement la même composition moléculaire que les mélanges de monomères dont on est parti. Dans la figure 3, ces résultats s'échelonnent sur la diagonale du diagramme de copolymérisation; une telle copolymérisation est dite "azéotropique."

En utilisant l'équation habituelle de la copolymérisation,[2] on trouve comme valeurs des rapports des constantes de propagation:

$$r_1 = r_2 = 1$$

Les deux monomères présentent donc une réactivité sensiblement égale vis-à-vis d'un même radical.

(b) Copolymérisation du chlorure de vinyle et de l'acétate d'isopropényle (tableau III)

TABLEAU III

M_2	% Cl_2	m_2	Durée, Min.	Rendement, %
0 107	52 68	0 017	135	12
0 208	47 65	0 107	220	11
0 295	43 35	0 162	530	15
0 395	38 62	0 227	870	13
0 604	30 19	0 350	1300	9.1
0 768	21 25	0 511	98 heures	5 3

Ces copolymérisations ont été effectuées à 65°C., en présence de 0.20% de peroxyde de benzoyle, comme initiateur. La courbe de copolymérisation est également contenue dans la figure 3 (Courbe III); les valeurs donnant la meilleure concordance avec les résultats expérimentaux sont les suivantes:*

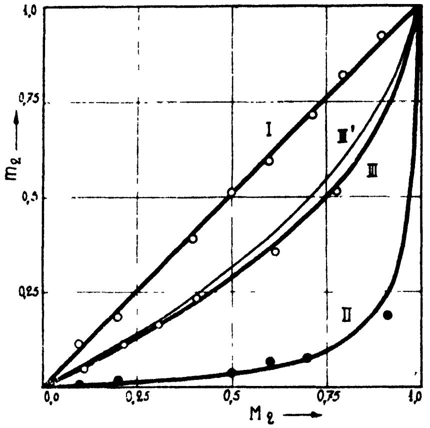

Fig. 3. Courbes de copolymérisation de l'acétate d'isopropényle (2) avec l'acétate de vinyle (I), le chlorure de vinyle (III), et le méthacrylate de méthyle (II). La courbe III' se rapporte au système chlorure de vinyle-acétate de vinyle.

$$r_1 = 2.2 \qquad r_2 = 0.25$$

Dans les deux cas, le chlorure de vinyle est plus réactionnel que l'acétate d'isopropényle.

En comparant ces résultats avec ceux obtenus dans le cas de la copolymérisation du chlorure de vinyle (m_1) avec l'acétate de vinyle (m_2) où

$$r_1 = 2.1 \text{ et } r_2 = 0.3 \text{ (figure 3, courbe III')}$$

on constate également que ces valeurs sont très proches de celles déterminées avec l'acétate d'isopropényle.[3] Ces données de copolymérisation confirment donc entièrement la similitude de réactivité des deux acétates, comme le supposait la copolymérisation azéotropique précédente.

---

* Dans le diagramme, les valeurs de M_2 ont été corrigées en tenant compt des quantités de monomères consommés.

(c) Copolymérisation du méthacrylate de méthyle et de l'acétate d'isopropényle (tableau IV)

TABLEAU IV

M_2	Analyse[a]	m_2	Durée min	% polym.
0.100	0.06	0.006	20	6.1
0.200	0.15	0.015	20	5.5
0.500	0.34	0.034	40	6.7
0.600	0.60	0.060	40	5.4
0.700	0.72	0.072	60	6.0
0.900	1.95	0.195	120	4.8

[a] Les résultats d'analyse experiment le nombre de millimoles depotasse caustique nécessaires pour saponifier Igr. de copolymère.

Ces copolymérisations ont été effectuées en solution benzénique à une concentration totale en monomères de 8 moles/litre, en présence de 8.2×10^{-3} moles/litre de peroxyde de benzoyle comme initiateur; la température a été maintenue à 75°C. La courbe, qui est également renseignée dans la figure 3 (courbe II), s'interprète le mieux par les valeurs des rapports des constantes de vitesses de propagation:

$$r_1 = 30 \text{ et } r_2 = 0.017$$

Ces résultats indiquent que le méthacrylate de méthyle entre trente à cinquante fois plus vite dans le copolymère que l'acétate d'isopropényle; comme prévu, le méthacrylate de méthyle est donc beaucoup plus réactionnel.

(d) Interprétation de ces résultats: Réactivité relative des monomères et polarité de la liaison éthylénique

Par application du calcul semi-quantitatif, indiqué par Alfrey et Price,[4] nous nous sommes efforcés de caractériser l'acétate d'isopropényle à l'égard des autres monomères quant à la polarité de sa double soudure et sa réactivité générale.

Les trois monomères de référence, que nous avons utilisés, sont caractérisés par les valeurs relatives suivantes:[5]

chlorure de vinyle: $Q = 0.028$ $e = -0.19$
acétate de vinyle: $Q = 0.018$ $e = -0.61$
méthacrylate de méthyle: $Q = 0.64$ $e = 0.0$

TABLEAU V

Système	r_1	r_2	Q	e
Chlorure de vinyle-acétate d'isopropényle	2.2	0.25	0.015	−0.97
Acétate de vinyle-acétate d'isopropényle	1.0	1.0	0.018	−0.61
Méthacrylate de méthyle-acétate d'isopropényle	30	0.017	0.021	−0.82

En appliquant ces valeurs aux copolymérisations de ces monomères avec l'acétate d'isopropényle, on trouve (Tableau V):

Ces valeurs sont suffisament concordantes, et amènent à des valeurs moyennes de $Q = 0.018$ et $e = -0.80$.

En utilisant des valeurs de $e = -0.8$ et de $Q = 1.0$ pour le styrène, comme monomère de référence, on trouve pour l'acétate d'isopropényle les valeurs $e = -0.97$ et $Q = 0.023$ (calculées par rapport au chlorure de vinyle).[6]

En comparant ces valeurs à celles de l'acétate de vinyle, indiquées plus haut, on constate que la réactivité de ces deux monomères sont sensiblement du même ordre de grandeur; d'autre part, la présence du groupe méthyle à l'endroit de la double soudure entraîne un caractère légèrement plus négativé de la soudure éthylénique.

Une réactivité semblable de ces deux monomères était imprévisible en se basant uniquement sur les essais de polymérisation de ces monomères, pris isolément; par copolymérisation, il a été ainsi possible de justifier le schéma de polymérisation présenté au début de cette étude.

C. DEGRÉS DE POLYMÉRISATION ET TRANSFERT DE CHAÎNE AU COURS DE LA COPOLYMÉRISATION

(a) Méthacrylate de méthyle–acétate d'isopropényle

Des mélanges de composition identique de méthacrylate de méthyle et d'acétate d'isopropényle ont été copolymérisés en présence de quantités variables de peroxyde de benzoyle. Les degrés de polymérisation des polymères ont été déterminés par mesure osmotique (microméthode de Zimm). Le tableau VI indique les résultats obtenus à une température de réaction de 75°C.; la série A se rapporte à des essais effectués sur des mélanges de monomères dont le rapport molaire méthacrylate de méthyle/acétate d'isopropényle est égal à 2.41. Dans la série B le rapport molaire utilisé correspondant s'élève à 0.141.

TABLEAU VI

Peroxyde, moles/litre $\times 10^{-3}$	Durée, min.	% polym.	Vitesse, mole/litre min^{-1}	P
		SÉRIE A		
4.40	40	7.17	1.7×10^{-2}	2400
11.34	24	6.97	2.7	1950
21.30	17	6.56	3.6	1630
		SÉRIE B		
2.15	112	6.40	0.5	1370
10.91	48	5.87	1.14	910
21.24	34	5.61	1.5	850

En établissant un diagramme, exprimant le logarithme de la vitesse brute de polymérisation en fonction du logarithme de la concentration initiale en peroxyde, on obtient dans les deux séries A et B une droite dont le coefficient angulaire est égal à 0.47. La vitesse de polymérisation est donc proportionnelle à la racine carrée de la concentration en peroxyde de benzoyle; au cours de ces copolymérisations, il n'y a donc pas de transfert de chaîne désactivant (réaction 4). Les radicaux r^*, issues d'un transfert de chaîne au départ d'une chaîne en croissance et d'une molécule d'acétate d'isopropényle, donnent naissance à une nouvelle chaîne par addition d'une molécule de méthacrylate de méthyle. Le processus normal de rupture de chaîne suivant le mécanisme (5), se rétablit, entraînant la loi habituelle de la racine carrée de la concentration en initiateur.

Si, par contre, on établit la relation unissant le logarithme du degré de polymérisation moyen au logarithme de la concentration en peroxyde, on obtient:

$$\begin{array}{ll} \text{série A} & \log \bar{P} = -0.24 \log (\text{init}) \\ \text{série B} & \log \bar{P} = -0.21 \log (\text{init}) \end{array}$$

Le degré de polymérisation moyen, contrairement à la vitesse de polymérisation, ne varie donc pas proportionnelement à la racine carrée de la concentration en initiateur. Ce comportement s'explique par un important transfert de chaîne, dû principalement à l'acétate d'isopropényle (mobilité de l'hydrogène alpha allylique).

On sait que le degré de polymérisation est égal au rapport de la vitesse de propagation à la somme des vitesses de rupture et de transfert de chaîne (respectivement v_p, v_r, et v_t). Au cas ou il n'y a pas de transfert de chaîne, le degré de polymérisation est égal à la longueur de chaîne cinétique ν, c.a.d.

$$\bar{P} = v_p/(v_r + v_t) \qquad \nu = v_p/v_r$$

Il en résulte:

$$1/\bar{P} = (1/\nu) + K_t \tag{8}$$

où K_t est égal au rapport des constantes de vitesses de transfert de chaîne et de propagation. Si la concentration en monomère est maintenue constante (séries A et B), cette dernière relation peut se mettre sous la forme suivante:

$$1/\bar{P} = \text{Const. (init)}^{0.5} + K_t \tag{9}$$

La constante K_t est donc l'ordonnée à l'origine de la droite exprimant $1/\bar{P}$ en fonction de la racine carrée de la concentration en peroxyde. Par application de cette relation aux deux séries A et B relatées ci-dessus, on obtient:

$$\begin{array}{ll} \text{série A} & K_t = 2.6 \times 10^{-4} \\ \text{série B} & K_t = 5.2 \times 10^{-4} \end{array}$$

La constante de transfert est d'autant plus élevée qu'il y a plus d'acétate d'isopropényle dans le milieu de réaction. Dans le cas, où ce dérivé est seul présent, le transfert de chaîne joue le rôle principal dans le phénomène de rupture (équation 4) et le degré de polymérisation est pratiquement constant.

(b) Chlorure de vinyle–acétate d'isopropényle

Des phénomènes de transfert de chaîne semblables ont pu être mis en évidence en présence de chlorure de vinyle. Ici également la vitesse est proportionnelle à la racine carrée de la concentration en peroxyde de benzoyle. Les résultats sont indiqués dans tableau VII.

TABLEAU VII

Peroxyde, % en poids de la masse totale des monomères	Durée, min.	Rendt., %	Vitesse, % polym./min.	[η], acétone 20°
0.050	720	13.3	1.85×10^{-2}	0.188 (44,000)
0.096	680	17.2	2.54	0.183
0.192	375	16.3	4.34	0.172
0.789	300	23.1	7.70	0.157 (33,000)

La température de réaction était maintenue à 65°; le rapport molaire acétate d'isopropényle/chlorure de vinyle: 0.394. Ici également les viscosités intrinsèques des copolymères ne varient que dans un rapport de 1 à 1.2 (au lieu de 1 à 4) alors que les concentrations en initiateur varient dans un rapport de 1 à 16. Les poids moléculaires de 44,000 et 33,000 ont été déterminés par la méthode osmotique, en utilisant le dioxane comme solvant.

(c) Polymérisation du styrène en présence d'acétate d'isopropényle

Dans le but de déterminer une éventuelle copolymérisation du styrène et de l'acétate d'isopropényle, des quantités variables de ces deux monomères ont été polymérisées à 75° en présence de peroxyde de benzoyle (9.48×10^{-3} mole/litre). Les résultats analytiques des dosages de carbone varient de 92.25 à 92.85%; pour le polystyrène pur cette teneur est égale à 92.31%. Le styrène et l'acétate d'isopropényle ne copolymérisent donc pas, ou ne copolymérisent que dans une très faible proportion. Ce comportement est analogue à celui de l'acétate de vinyle à l'égard du styrène.[7] D'autre part les variations de vitesse et de poids moléculaire sont proportionnelles à la concentration molaire du styrène, si on garde une concentration constante en initiateur. A l'égard du styrène, l'acétate d'isopropényle agit comme un simple solvant.

En vue de vérifier cette hypothèse, des mesures comparatives ont été effectuées en polymérisant du styrène en solution dans le benzène (tableau VIII) et dans l'acétate d'isopropényle (tableau IX), à une même température, avec des concentrations variables en initiateur. Les vitesses initiales de polymérisation, ainsi que les viscosités intrinsèques des polymères formés, ont été mesurées. Les tableaux suivants indiquent les résultats obtenus. Les vitesses expriment la variation de concentration molaire par minute. Les viscosités intrinsèques ont été déterminées en solution toluénique.

TABLEAU VIII

POLYMÉRISATION DU STYRÈNE EN SOLUTION BENZÉNIQUE

T°, 75 °C.; [Styrène], 6.51 Moles/Litre

Peroxyde, %	Durée, min.	% polym.	Vitesse	[η]
0.095	63	3.41	3.55×10^{-3}	0.74
	105	5.64		
0.226	47	4.18	5.66×10^{-3}	0.51
	79	6.95		
0.530	32	3.88	8.40×10^{-3}	0.39
	59	7.38		

TABLEAU IX

POLYMÉRISATION DU STYRÈNE EN SOLUTION DANS L'ACÉTATE D'ISOPROPÉNYLE

T°, 75 °C.; [Styrène], 7.09 Moles/Litre

Peroxyde, %	Durée, min.	% polym.	Vitesse	[η]
0.062	84	3.65	3.08×10^{-3}	0.88
	106	4.70		
	122	5.30		
0.124	59	3.65	4.32×10^{-3}	0.68
	77	4.57		
	92	5.76		
0.312	35	3.21	6.63×10^{-3}	0.48
	78	7.34		
0.622	41	5.63	9.43×10^{-3}	0.37
	60	8.13		
	91	12.21		

En établissant les diagrammes, exprimant les logarithmes des vitesses en fonction des logarithmes de la concentration en peroxyde, on obtient une droite dont la tangente est égale à 0.51 et 0.48, pour a polymérisation en solution benzénique et en solution dans l'acétate d'isopropényle respectivement. La loi habituelle de la racine carrée de la concentration en initiateur se trouve vérifiée (fig. 4).

En tenant compte par ailleurs, que la viscosité intrinsèque du polystyrène, préparé à 75°C., est liée au degré de polymérisation par la relation:

$$[\eta] = KP^a \text{ c.a.d. } \log [\eta]/a = K' + \log P$$

où la constante $a = 0.72$,[8] on peut tracer les diagrammes des $(\log [\eta])/a$ en fonction du logarithme de la concentration en peroxyde. Au cas où il n'y a pas de transfert de chaîne appréciable, l'équation (9) citée plus haut, permet de prévoir une fonction linéaire (fig. 4).

En effet, les coefficients angulaires des droites obtenues sont respectivement égaux à −0.52 en solution benzénique et −0.48 pour la solution dans l'acétate d'isopropényle. Le degré de polymérisation du polystyrène, de même que la vitesse de polymérisation, varient en fonction de la racine carrée de la concentration en peroxyde de benzoyle; le transfert de chaîne

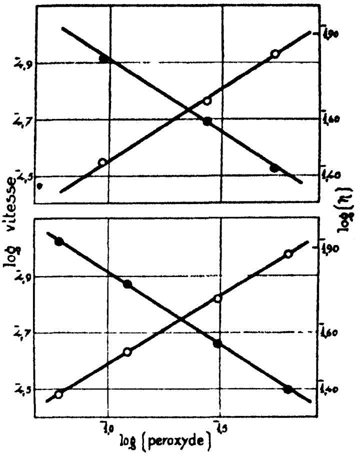

Fig. 4. Variations de la vitesse de polymérisation et du degré de polymérisation en fonction de la concentration en initiateur. Diagramme supérieur: en solution benzénique; diagramme inférieur: en solution dans l'acétate d'isopropényle. T°: 75°C.

sur solvant est donc négligeable. Ces phénomènes sont liés à la stabilité des radicaux styréniques terminant une chaîne en croissance, et à la réactivité des molécules de styrène monomère.

PARTIE EXPERIMENTALE

1. Préparation de l'acétate d'isopropényle

L'acétate d'isopropényle a été préparé par deux méthodes différentes. Dans le premier procédé[9] il résulte de la condensation de l'acide acétique et du propine. Le propine a été obtenu par la méthode de Lebeau-Picon: l'iodure ou le sulfate de méthyle, réagit à −60°C. sur une solution d'acétylène monosodé dans l'ammoniaque liquide.[10,11] L'appareillage utilisé est celui décrit par Tchao Yin Lai.[12]

L'addition du propine à l'acide acétique s'effectue en présence de 1% d'oxyde mercurique et de 5% de complexe acétique du fluorure de bore. Le rendement de cette méthode est faible, environ 20%.

La seconde méthode consiste dans l'action du cétène sur l'acétone en présence d'acide sulfurique[13]; elle permet d'obtenir rapidement des quantités importantes de monomère avec un rendement meilleur. Le cétène est condensé avec l'acétone en présence de 1.2% d'acide sulfurique[14]; la solution est maintenue vers 55–56°C. Le contact cétène-acétone est assuré en introduisant le cétène par un agitateur creux, muni d'un double joint à mercure. Le produit obtenu est soumis à la distillation; celle-ci fournit rapidement un produit pur avec un rendement de 55% environ.

Les constantes physiques de l'acétate d'isopropényle sont:

Eb. 97°2–97°4 C sous 757 mm. RM_D (calc.): 26.47
$D_4^{20} = 0.9212_3$ n_D^{20}: 1.4010 RM_D (trouvé): 26.39

ANALYSES: *calc.* 59.96% C, 8.06% H; *trouvé* 59.87% C, 8.36% H.

2. Polymérisation de l'acétate d'isopropényle

Le monomère est purifié, avant son emploi, par distillation dans une atmosphère d'azote; les ampoules de polymérisation sont également scellées sous atmosphère d'azote. La vitesse de polymérisation a été déterminée par différence; le monomère, qui n'a pas réagi, est entraîné à la vapeur, et est dosé par saponification alcaline dans le distillat. Cette méthode de dosage est parfaitement reproductible, même en présence de polymère et d'initiateur. La vitesse de disparition du peroxyde de benzoyle est suivie par titrage iodométrique en solution *neutre*, après addition d'iodure de potassium. En effectuant le titrage en solution neutre, la méthode est parfaitement reproductible; en milieu acide, par contre, les réactions secondaires de l'acétate d'isopropényle empèchent son emploi, et la rendent inutilisable. Le mode opératoire est le suivant.

Diluer le contenu des ampoules par de l'acétone et additionner un excès d'iodure de potassium à 50%. Agiter cinq minutes, ajouter 20 cc. de benzène pour éviter la précipitation du polymère au moment de la dilution, et titrer l'iode libéré par le thiosulfate sodique $N/20$. Les polymères destinés à la cryoscopie ont été dissous dans l'acétone, et précipités par un mélange méthanol-eau. Le gel qui précipite est redissous dans l'acétone; celle-ci est évaporée sous vide à une température inférieure à 35 °C.

3. Copolymérisations

Les copolymères, obtenus au départ de chlorure de vinyle et d'acétate d'isopropényle, sont précipités par addition de méthanol. Ils sont redissous dans l'acétone et reprécipités à l'état poudreux dans le méthanol. Les dosages de chlore ont été effectués microanalytiquement par la méthode de Carius.

Les copolymères d'acétate de vinyle et d'acétate d'isopropényle sont isolés en déversant le contenu des ampoules dans l'éther de pétrole (Eb. 50–70°C.). Le précipité visqueux est redissous dans l'acétone et séché sous vide à une température inférieure à 35°C. Leur composition à été déterminée par saponification alcaline, par ébullition en présence de KOH N durant trois heures et titrage en retour.

Les copolymères à base de méthacrylate de méthyle et d'acétate d'isopropényle ont été également précipités par l'éther de pétrole. Les copolymères sont redissous dans l'acétone et précipités par un mélange de méthanol-eau. On les sèche à poids constant. Leur analyse a été également faite par saponification alcaline en présence de potasse alcoolique. Dans ces conditions les chaînons méthacrylate de méthyle ne sont pas saponifiables, contrairement à ceux de l'acétate d'isopropényle. 1 g. de copolymère est dissous dans 30 cc. d'acétone, et additionné de 10 cc. KOH alcoolique. Après ébullition de trois heures, et addition de 25 cc. de benzène on titre l'excès de KOH; un essai témoin donne par différence la quantité utilisée.

Les polystyrènes, obtenus soit en solution benzénique, soit en solution dans l'acétate d'isopropényle, sont précipités à l'alcool méthylique, redissous dans la butanone et reprécipités par le méthanol. Les déterminations osmométriques ont été réalisées dans des microosmomètres de Zimm[16]; les mesures ont été effectuées en solution acétonique ou en solution dans le dioxane à 25°C.

Remercîments: Les auteurs remercient l'Institut pour l'Encouragement de la Recherche dans l'Industrie et l'Agriculture (I.R.S.I.A.) de l'aide qu'il accordée à l'un d'eux.

References

1. Bartlett et Altschul, *J. Am. Chem. Soc.*, **67,** 812–16 (1945).
2. Mayo et Lewis, *J. Am. Chem. Soc.*, **66,** 1594 (1944). Alfrey et Goldfinger, *J. Chem. Phys.*, **12,** 205 (1944).
3. Agron, Alfrey, Bohrer, Haas et Wechsler, *J. Polymer Sci.*, **3,** 157 (1948).
4. Alfrey et Price, *J. Polymer Sci.*, **2,** 101 (1947).
5. Fordyce, Chapin, et Ham, *J. Am. Chem. Soc.*, **70,** 2049 (1948).
6. Price, *J. Polymer Sci.*, **3,** 772 (1948).
7. Michalek et Clark, *Ind. Eng. Chem.*, **22,** 1559 (1944).
8. H. Mark dans A. Weissberger, éd., *Physical Methods of Organic Chemistry*, Part I. Interscience, New York, 1949, p. 351.
9. Hennion et Nieuwland, *J. Am. Chem. Soc.*, **56,** 1802 (1934).
10. Lebeau et Picon, *Compt. rend.*, **1913,** 1077.
11. Meinert et Hurd, *J. Am. Chem. Soc.*, **52,** 4544 (1930).
12. Tchao Yin Lai, *Bull. soc. chim. Belg.*, IV, **53,** 687 (1933).
13. Gwynn et Degering, *J. Am. Chem. Soc.*, **64,** 2216 (1942).
14. Si on utilise, comme agent condensant, le complexe acétique du fluorure de bore au lieu d'acide sulfurique, on obtient avec de bons rendements, l'acide β-méthylcrotonique au lieu d'acétate d'isopropényle. R. Hart, *Bull. Soc. Chim. Belges*, **58,** 255 (1949).
15. Zimm et Meyerson, *J. Am. Chem. Soc.*, **68,** 911 (1946).

Résumé

En présence de peroxyde de benzoyle, l'acétate d'isopropényle polymérise de la même façon que l'acétate d'allyle. Son comportement lors de la copolymérisation avec l'acétate de vinyle, le chlorure de vinyle et le méthacrylate de méthyle montre que ce monomère possède une réactivité générale semblable à celle de l'acétate de vinyle. Le caractère négatif de la double soudure est plus prononcé (−0.8). Ces copolymérisations sont caractérisées par un important transfert de chaîne, dû à la présence de l'acétate d'isopropényle. A l'égard du styrène, l'acétate d'isopropényle se comporte comme un solvant; il n'y a ni copolymérisation, ni transfert de chaîne.

Zusammenfassung

In Gegenwart von Benzoyl-peroxyd polymerisiert Isopropenylazetat wie Allylazetat. Sein Verhalten während der Copolymerisation mit Vinylazetat, Vinylchlorid und Methyl-methacrylat zeigt, dass dieses Monomere ungefähr die gleiche allgemeine Reaktionsfähigkeit wie Vinylazetat besitzt: der negative Charakter der Doppelbindung ist stärker ausgesprochen (−0.8). Eine erhebliche Kettenübertragung, die durch die Gegenwart von Isopropenylazetat bedingt ist, findet im Laufe dieser Copolymerisationen statt. Auf Styrol wirkt Isopropenylazetat als Lösungsmittel; in diesem Falle findet weder Copolymerisation noch Kettenübertragung statt.

Reçu February 20, 1949

JOURNAL OF POLYMER SCIENCE VOL. V, NO. 1, PAGES 69-89

Mechanical Behavior of Viscoelastic Substances*

ROBERT SIPS,† *Princeton University, Princeton, New Jersey*

I. INTRODUCTION

In order to explain the properties of viscoelastic substances, the mechanical behavior of these substances is usually represented by mechanical models which are generally made up of more or less complicated assemblages of deformable units. These units, in turn, result of the formation of a spring, which represents the elastic properties of the element, and a dashpot, which represents schematically the viscous properties of the element. The two constituents (spring and dashpot) can be assembled either in series or in parallel.

The viscoelastic properties of the material under study can then be compared accurately with those of a system of deformable units of the type just described, assembled in series, in parallel, or in a combination of the two ways.[1]

In particular, two of these combinations have been studied. In the first, called the Voigt model, all the deformable units are placed in series. If one then applies a force to the two extremities of the chain of elements, each element obviously sustains the same force.

If, on the contrary, all the elements are connected in parallel, one obtains a Maxwell model. If this model is given an arbitrary deformation, each element will sustain individually the same deformation.

The Voigt model is generally used to represent the phenomenon of creep, and the Maxwell model is particularly well adapted to the representation of relaxation phenomena.

In the following, we have attempted to describe the behavior of linear samples of viscoelastic substances under the influence of a variable axial force, using a Maxwell model as a fundamental model. We obtain a linear integral-differential equation which expresses in the most general way the relation between force and deformation and which depends only on the relaxation function.[2,3]

Considered from the purely macroscopic point of view, this fundamental equation is merely the general expression of the principle of linear superposition, and could accordingly be obtained without the use of any model whatever.

---

* Contribution from Frick Chemical Laboratory, Princeton University, Princeton, N.J.

† Visiting Fellow at Princeton University, 1947-1948. Present address: 361 Rue de Mérode, Brussels, Belgium.

By a simple integration by parts the fundamental equation can now be transformed into a linear integral equation (of the Volterra type) with variable upper limit, where the unknown function is the relative elongation. In order to solve this integral equation, we have to introduce a resolvant function and this turns out to be the ordinary creep function. In this way we obtain a relation between the creep and relaxation functions which can be put in a remarkably symmetrical form.

We then show how all the other properties of the viscoelastic substances, like recovery or extension under constant rate, can be calculated, still using the relaxation as the only necessary experimental datum. It thus appears that, as far as small deformations are concerned, that is, deformations for which the principle of linear deformation applies, the relaxation function provides a complete description of all the mechanical properties of viscoelastic substances. We have even shown, going back to the Maxwell model, that the mean values of the elasticity and friction coefficients of the spring-dashpot elements can be calculated when the relaxation function is known.

It is quite evident that the creep function could have been used just as well, but, as has been shown in this laboratory, the relaxation function can be measured with a much higher degree of accuracy and should therefore be used preferentially.

The second part of the present paper is mainly concerned with practical methods for solving the integral equation. The last section gives a comparison between the calculated and experimentally measured values of the creep function for a sample of polyisobutylene whose relaxation function was known. It should be especially emphasized that the calculation of the creep function does not involve the use of a single adjustable constant and is therefore a particularly stringent test of the validity of the whole theory.

II. GENERAL EQUATIONS

Let us consider first a simple deformable unit consisting of a spring and dashpot in series. For each unit, the relation between the length l and the force f will have the form:

$$dl/dt = (1/\alpha) \times (df/dt) + (1/\eta)f \tag{1}$$

where α is a coefficient of elasticity and η a coefficient of viscosity.

Now suppose l is a function of time $l = l(t)$. The differential equation, being a linear equation of the first order, can be integrated immediately, giving:

$$f(t) = \alpha\int_0^t e^{-k(t-\tau)}l'(\tau)\,d\tau + f_0e^{-kt} \tag{2}$$

with $k = \alpha/\eta$. The constant f_0 is the value of $f(t)$ for $t = 0$.

If at the beginning of the experiment the spring of the deformable element is free of tension, we shall have $f_0 = f(0) = 0$, giving the simpler equation:

$$f(t) = \alpha\int_0^t e^{-k(t-\tau)}l'(\tau)\,d\tau \tag{3}$$

Let us now pass to the most general model, made up of an infinity of different elements, all in parallel and each defined by a pair of constants α and k. To describe the model completely, we must introduce a distribution function $N_1(\alpha,k)$, such that:

$$N_1(\alpha,k)\, d\alpha\, dk \tag{4}$$

is the number of elements with viscoelastic constants between α and $\alpha + d\alpha$, and k and $k + dk$. The total number of elements will then be given by:

$$N = \int_0^\infty \int_0^\infty N_1(\alpha,k)\, d\alpha\, dk \tag{5}$$

The quantity $l(t)$ having by definition the same value for all the elements, we see immediately that the total force acting on the material will have the value:

$$F(t) = \int_0^\infty \int_0^\infty \left[N_1(\alpha_1 k)\alpha \int_0^t e^{\,k(t-\tau)} l'(\tau)\, d\tau\right] d\alpha\, dk \tag{6}$$

Let us now introduce an auxiliary function $N(k)$, defined by:

$$\int_0^\infty \alpha N_1(\alpha,k)\, d\alpha = N(k) \tag{7}$$

Equation (6) then becomes:

$$F(t) = \int_0^t l'(\tau)\, d\tau \int_0^\infty N(k) e^{-k(t-\tau)}\, dk \tag{8}$$

III. RELAXATION

We shall now examine what our general equation becomes when it is applied to the study of relaxation phenomena.

The usual experimental technique consists in taking a sample of the material under study, completely free of tensions, and extending it as rapidly as possible so that the length goes from the initial value L_0 to the value $L_0 + \Delta L_0$ in a very small time Δt. The sample is then kept at constant length $L_0 + \Delta L_0$, and the decrease of tension is measured.

We can always assume that during the short period of stretching the instantaneous length is a linear function of the time, so that between $t = 0$ and $t = \Delta t$ we can put:

$$l'(t) = \Delta L_0 / \Delta t \tag{9}$$

For values of t greater than Δt, since the length is constant, $l'(t) = 0$. Equation (8) then becomes:

$$F(t) = \int_0^{\Delta t} (\Delta L_0 / \Delta t)\, d\tau \int_0^\infty N(k) e^{-k(t-\tau)}\, dk \tag{10}$$

The interval Δt being by hypothesis extremely small, we can let Δt tend to zero in this formula, giving:

$$F(t) = \Delta L_0 \int_0^\infty N(k) e^{-kt}\, dk \tag{11}$$

If the deformation between $t = 0$ and $t = \Delta t$ is very rapid, it will be purely elastic, and we shall have also, in the conventional notation of elasticity theory:

$$\Delta L_0 = L_0 F(0)/\sigma E \tag{12}$$

and consequently: $F(0) = \Delta L_0 \sigma (E/L_0) = \Delta L_0 \int_0^\infty N(k)\,dk$

It then results that: $$\int_0^\infty N(k)\,dk = \sigma E/L_0 \tag{13}$$

In the present work, we assume at all times that the deformations are sufficiently small so that the changes in cross-sectional area are negligible.

From the preceding, it results finally that the relaxation of stress will be given by:

$$F(t) = \sigma E\,\frac{\Delta L_0}{L_0}\,\frac{\int_0^\infty N(k)e^{-kt}\,dk}{\int_0^\infty N(k)\,dk} = \sigma E\,\frac{\Delta L_0}{L_0}\,[1 - \psi(t)] \tag{14}$$

where $\psi(t)$ is the usual relaxation function. Consequently, therefore:

$$\psi(t) = \frac{\int_0^\infty N(k)[1 - e^{-kt}]\,dk}{\int_0^\infty N(k)\,dk} \tag{15}$$

Let us suppose now that at time $t = t_1$, we give a new extension ΔL_1 to our material, letting the length increase from $L_0 + \Delta L_0$ to $L_0 + \Delta L_0 + \Delta L_1$ in a very short time Δt. During this interval we shall have as above:

$$l'(t) = \Delta L_1/\Delta t$$

We shall therefore have to use the following values for $l'(t)$ in equation (8):

$$\begin{array}{ll} l'(t) = \Delta L_0/\Delta t & 0 < t < \Delta t \\ l'(t) = 0 & \Delta t < t < t_1 \\ l'(t) = \Delta L_1/\Delta t & t_1 < t < t_1 + \Delta t \\ l'(t) = 0 & t_1 + \Delta t < t \end{array}$$

and, if we subsequently let $\Delta t \to 0$, we finally get, for $t > t_1$:

$$\begin{aligned} F(t) &= E\,\Delta L_0 \int_0^\infty N(k)e^{-kt}\,dk + E\,\Delta L_1 \int_0^\infty N(k)e^{-k(t-t_1)}\,dk \\ &= \sigma E\left[\frac{\Delta L_0}{L_0}\,\frac{\int_0^\infty N(k)e^{-kt}\,dk}{\int_0^\infty N(k)\,dk} + \frac{\Delta L_1}{L_0}\,\frac{\int_0^\infty N(k)e^{-k(t-t_1)}\,dk}{\int_0^\infty N(k)\,dk}\right] \\ &= \sigma E\left[\frac{\Delta L_0}{L_0}\,(1 - \psi(t)) + \frac{\Delta L_1}{L_0}\,(1 - \psi(t - t_1))\right] \end{aligned} \tag{16}$$

This is confirmed by experiment.

The same reasoning can be repeated for a third deformation taking place at time t_2, and so on. We shall therefore have, in general, for values of t following the nth extension:

$$F(t) = \sigma E \sum_{p=0}^{p=n} \frac{\Delta L_p}{L_0}\,[1 - \psi(t - t_p)] \tag{17}$$

Let us return now to the general equation (8). Making use of (14), we see that it can be written in the following form:

$$F(t) = (\sigma E/L_0)\int_0^t l'(\tau)[1 - \psi(t - \tau)]\,d\tau \tag{18}$$

In a more general way, if we allow the length of the sample to vary in a discontinuous way, we can write formula (18) as a Stieltjes integral in the following manner:

$$F(t) = (\sigma E/L_0)\int_0^t [1 - \psi(t - \tau)]\,dl(\tau) \tag{18'}$$

We obtain in this way, supposing the relaxation function $\psi(t)$ to be known, the most general relation between the force acting on a linear sample and its length.

If the principle of the linear superposition of stresses, expressed by formula (16), is accepted as an experimental fact, the general relation (18) can immediately be obtained by passing to the limit, by considering the continuous deformation as the result of a large number of extremely small successive deformations, and by replacing the sum by an integral.

IV. CREEP

By applying to equation (18′) the general formula for integration by parts of a Stieltjes integral, it becomes:

$$F(t) = \sigma E[\lambda(t) - \int_0^t \lambda(\tau)\psi'(t - \tau)\,d\tau] \tag{19}$$

where $\lambda(t)$ is the relative elongation, defined by:

$$\lambda(t) = [l(t) - L_0]/L_0$$

In this equation the integral is an ordinary integral, but the functions $\lambda(t)$ and $F(t)$ can be discontinuous. Equation (19), which can be written as:

$$\lambda(t) - \int_0^t \lambda(\tau)\psi'(t - \tau)\,d\tau = F(t)/\sigma E \tag{20}$$

is an integral equation with variable limits of the Volterra type. The solution of such an equation is given by:

$$\lambda(t) = \frac{1}{\sigma E}\left[F(t) + \int_0^t F(\tau)\varphi'(t - \tau)\,d\tau\right] \tag{21}$$

where the function $\varphi'(t - \tau)$ is the resolvant function.

There exists the following relation between the functions ψ' and φ', which results immediately from the general theory:

$$\varphi'(t - \tau) = \psi'(t - \tau) + \int_0^t \psi'(t - \xi)\varphi'(\xi - \tau)\,d\xi \tag{22}$$

Equation (21), being completely equivalent to (19), can be used just as well as this latter equation for the description of the mechanical properties of viscoelastic substances. We shall apply it particularly in the following to the phenomenon of creep.

We shall, however, first make a final modification of equation (21), transforming it into a Stieltjes integral by means of an integration by parts. This gives us:

$$\lambda(t) = (1/\sigma E) \int_0^t [1 + \varphi(t - \tau)]\, dF(\tau) \tag{23}$$

which is completely equivalent to (18′). In this equation, the function φ is defined in such a manner as to have $\varphi(0) = 0$.

Let us now pass to the study of creep. In a typical experiment of this sort, a constant force F is suddenly applied to a linear sample of the viscoelastic substance. The initial length L_0 undergoes first an instantaneous elastic extension, followed by a separate progressive extension.

In the Stieltjes integral $dF(t)$ will be zero everywhere, except, however, for $t = 0$, where $dF(t)$ will be equal to F. Consequently:

$$\lambda(t) = (F/\sigma E)\, [1 + \varphi(t)] \tag{24}$$

which shows that $\varphi(t)$, which was introduced simply as a resolving function, is actually the familiar creep function, which can be obtained experimentally without difficulty.

It therefore follows from (23) that the creep function can be used equally as well as the relaxation function to describe the properties of viscoelastic bodies.

The important question, therefore, is to find the relation which exists between the creep and relaxation functions $\psi(t)$ and $\varphi(t)$. This relation is evidently given by equation (22). Putting $\tau = 0$ in the latter, we obtain:

$$\varphi'(t) - \int_0^t \psi'(t - \tau)\varphi'(\tau)\, d\tau = \psi'(t) \tag{25}$$

which shows that the function φ' is itself a solution of a Volterra equation. But it is easily seen that this relation can equally well be written:

$$\psi'(t) + \int_0^t \varphi'(t - \tau)\psi'(\tau)\, d\tau = \varphi'(t) \tag{26}$$

which shows that $\varphi(t)$ being known, $\psi(t)$ can in turn be determined by solving a Volterra integral equation.

The preceding discussion shows the remarkable symmetry which exists between the properties of the relaxation and creep functions.

We shall return later in detail to the actual calculation of the creep function when the relaxation function is known.

V. RECOVERY (RETRACTION)

Let us suppose that the sample, after having undergone a sudden elongation bringing the initial length L_0 to $L_0 + \Delta L_0$, and after having been maintained thereafter until a time T at the same length is suddenly released. At time T, the tension will suddenly change from $F(T)$ to zero. The length of the sample will undergo a sudden elastic decrease, followed by a slow change. We shall call the length immediately after the release of the external tension $L_0 + \Delta L_T$, so that at time T the length will change in an infinitely short time from $L + \Delta L_0$ to $L + \Delta L_T$.

The general equation (18′) will become in the present case, for values of $t > T$:

$$0 = \Delta L_0[1 - \psi(t)] - (\Delta L_0 - \Delta L_T)[1 - \psi(t - T)] + \int_T^t l'(\tau)[1 - \psi(t - \tau)]\, d\tau \quad (27)$$

In this equation, let us set $t = T$. It then becomes:

$$\Delta L_0[1 - \psi(T)] = \Delta L_0 - \Delta L_T \quad (28)$$

or, more simply,

$$\Delta L_T = \Delta L_0 \psi(T) \quad (29)$$

If, therefore, one quickly stretches the sample and immediately releases it, we shall have $T = 0$ in the preceding equation, and as a result $\Delta L_T = 0$; *i.e.*, there is no permanent deformation produced. If, on the contrary, one maintains the sample in the deformed state for a very long time, corresponding to $T = \infty$, there will be produced a permanent deformation equal to:

$$\Delta L_\infty = \Delta L_0 \psi(\infty) \quad (30)$$

If the material can relax completely, $\psi(\infty) = 1$, and $\Delta L = \Delta L_0$. After release the material will thus retain completely the deformation originally applied to it.

The variation of the length of the sample as a function of time following the initial instantaneous elastic retraction is obtained by solving the following integral equation, which is obtained by integrating (27) by parts, and putting, as above,

$$\frac{l(t) - L_0}{L_0} = \lambda(t)$$

$$\lambda(t) - \int_T^t \lambda(\tau)\psi'(t - \tau)\, d\tau = (\Delta L_0/L_0)[\psi(t) - \psi(t - T)] \quad (31)$$

The determination of the function $\lambda(t)$ reduces therefore to the solution of a Volterra integral equation of the same type as that considered previously, but with the difference, however, that the lower limit of the integral is no longer zero.

This equation may be solved in the following way. Let us put:

$$t = T + t_1 \qquad \tau = T + \tau_1$$

which amounts to choosing a new origin for time, corresponding to the instant when the retraction begins. The integral equation then becomes:

$$\lambda(T + t_1) - \int_0^{t_1} \lambda(T + \tau_1)\psi'(t_1 - \tau_1)\, d\tau_1 = (\Delta L_0/L_0)[\psi(T + t_1) - \psi(t_1)] \quad (32)$$

The equation now being reduced to the form (20) studied above, we can write directly the solution in the form corresponding to equation (21):

$$\lambda(T + t_1) = (\Delta L_0/L_0)[\psi(T + t_1) - \psi(t_1)] + (\Delta L_0/L_0) \int_0^{t_1} [\psi(T + \tau_1) - \psi(\tau_1)]\varphi'(t_1 - \tau_1)\, d\tau_1 \quad (33)$$

and returning to the variables t and τ:

$$\lambda(t) = (\Delta L_0/L_0)[\psi(t) - \psi(t - T) + \int_T^t [\psi(\tau) - \psi(\tau - T)]\varphi'(t - \tau)\, d\tau] \quad (34)$$

We obtain in this way an explicit form for the value of $\lambda(t)$. One can determine in a completely analogous manner, by using (23) in place of (18′) the retraction which takes place when a creep experiment is suddenly interrupted by removal of the applied load.

VI. EXTENSION AT CONSTANT RATE

Another case of interest is the type of experiment in which the length of the sample increases at a constant rate. In this case, the elongation is proportional to time, and consequently:

$$l'(t) = v = \text{constant} \quad (35)$$

v therefore being the rate of extension.

In the present case, equation (18) becomes:

$$F(t) = (\sigma E/L_0)v \int_0^t [1 - \psi(t - \tau)]\, d\tau = (\sigma Ev/L_0)[t - \int_0^t \psi(\tau)\, d\tau] \quad (36)$$

which, on differentiation, gives

$$F'(t) = (\sigma Ev/L_0)[1 - \psi(t)] \quad (37)$$

The time derivative of the tension at any given time value, in an experiment in which the sample is extended at constant speed, is therefore proportional to the tension measured in a relaxation experiment, at the same time value.

VII. EXPLICIT SOLUTION OF THE INTEGRAL EQUATION (25)

It is seen from the preceding sections that once the relaxation function is known, and limiting ourselves to the domain of deformations in which force and deformation are strictly proportional, we can deduce by simple calculation the majority of the other mechanical properties of viscoelastic substances which are of particular interest.

The other mechanical property of most interest here is creep. Many authors have sought a relation between creep and relaxation, but it appears that up to the present time there has never been published a deduction of the creep function from an experimental relaxation curve which has been given experimental verification.

As we have seen above, the derivation of the creep function from the relaxation function requires the solution of the following integral equation [denoted previously as (25)]:

$$\varphi'(t) - \int_0^t \psi'(t - \tau)\varphi'(\tau)\, d\tau = \psi'(t) \tag{38}$$

It is possible to obtain a completely general solution of this equation, either in the form of an infinite series, or in the form of a definite integral.

Since the integral equation is of the type studied by Volterra, it can always be solved by successive approximations in the following form:

$$\varphi'(t) = \psi'(t) + \int_0^t \psi'(t - \tau)\psi'(\tau)\, d\tau + \int_0^t \psi'(t - \tau) \int_0^\tau \psi'(\tau - \tau_1)\psi'(\tau_1)\, d\tau_1\, d\tau + \ldots \tag{39}$$

the series so formed being always convergent for finite values of t.

Another form of the general solution is obtained by applying the Laplace transformation to both sides of the equation. If we put:

$$L(f) = \int_0^\infty e^{-st}f(s)\, ds \tag{40}$$

it is seen that (38) can be written in the following form:

$$L(\varphi') - L(\psi')L(\varphi') = L(\psi') \tag{41}$$

from whence:

$$L(\varphi') = L(\psi')/(1 - L(\psi')) \tag{42}$$

and the problem reduces to the inversion of a Laplace transform to obtain φ' from $L(\varphi')$.

For practical purposes, however, the two preceding methods can be used only for certain very special forms of the function $\psi'(t)$.

Let us note, here, that if $\psi'(t)$ is the function corresponding to $\varphi'(t)$, equation (38) indicates that the function corresponding to $e^{-\lambda t}\varphi'(t)$ will be $e^{-\lambda t}\psi'(t)$.

Let us now pass on to the general forms of $\psi(t)$ which can be used to represent the experimental values of the relaxation function in all cases.

The function $\psi(t)$ being equal to zero for $t = 0$, and tending asymptotically to a well-defined limit $\psi(\infty)$ for $t \to \infty$, it is always possible to represent $\psi(t)$, to an adequate approximation, by a series of the form:

$$\psi(t) = A_1(1 - e^{-\lambda_1 t}) + A_2(1 - e^{-\lambda_2 t}) + \ldots + A_n(1 - e^{-\lambda_n t}) \tag{43}$$

where the A's and the λ's are positive constants.

It then follows that:

$$\psi(\infty) = A_1 + A_2 + \ldots + A_n \tag{44}$$

If the substance can relax completely, we shall evidently have:

$$\psi(\infty) = A_1 + A_2 + \ldots + A_n = 1 \tag{45}$$

The corresponding form of ψ' is:

$$\psi'(t) = A_1\lambda_1 e^{-\lambda_1 t} + \ldots + A_n\lambda_n e^{-\lambda_n t} \tag{46}$$

By applying the Laplace transformation, we obtain:

$$L(\psi') = \frac{A_1\lambda_1}{t+\lambda_1} + \ldots + \frac{A_n\lambda_n}{t+\lambda_n} \tag{47}$$

and consequently, substituting (47) in equation (42):

$$L(\varphi') = \left[\frac{A_1\lambda_1}{t+\lambda_1} + \ldots + \frac{A_n\lambda_n}{t+\lambda_n}\right] \Big/ \left[1 - \frac{A_1\lambda_1}{t+\lambda_1} - \ldots - \frac{A_n\lambda_n}{t+\lambda_n}\right] \tag{48}$$

If we multiply the numerator and denominator of this fraction by the product

$$(t+\lambda_1)\ldots(t+\lambda_n)$$

$L(\varphi')$ becomes = the quotient of a polynomial of degree $(n-1)$ in t divided by a polynomial of degree n, so that we can write it in the following form:

$$L(\varphi') = \frac{B_1}{t+\mu_1} + \ldots + \frac{B_n}{t+\mu_n} \tag{49}$$

where the B's and the μ's are new constants. The constants μ, being the roots of the denominator, are determined by the identity:

$$\left(1 - \frac{A_1\lambda_1}{t+\lambda_1} - \ldots - \frac{A_n\lambda_n}{t+\lambda_n}\right)(t+\lambda_1)\ldots(t+\lambda_n) = (t+\mu_1)\ldots(t+\mu_n) \tag{50}$$

i.e., the algebraic equation of degree n:

$$\left(1 - \frac{A_1\lambda_1}{t+\lambda_1} - \ldots - \frac{A_n\lambda_n}{t+\lambda_n}\right)(t+\lambda_1)\ldots(t+\lambda_n) = 0 \tag{51}$$

possesses n roots equal to

$$-\mu_1, -\mu_2, \ldots, -\mu_n$$

Let us now consider the expression:

$$\Phi(t) = \frac{A_1\lambda_1}{t+\lambda_1} + \ldots + \frac{A_n\lambda_n}{t+\lambda_n} \tag{52}$$

When t varies from $-\infty$ to $+\infty$, $\Phi(t)$ passes n times from $-\infty$ to $+\infty$, since we suppose the A's to be positive. The curve $y = \Phi(t)$ possesses n vertical asymptotes, and between two successive asymptotes y varies from $-\infty$ to $+\infty$. For

$$t > -\lambda_n$$

y decreases from $+\infty$ to 0. The straight line $y = 1$ therefore intersects the curve in n real points; consequently the algebraic equation (51) will have all n of its roots real and positive. In addition, we see that:

$$\mu_1 < \lambda_1 < \mu_2 < \lambda_2 < \ldots < \mu_n < \lambda_n$$

Once the μ's are known, the B's can be obtained in the following manner: We have identically, equating the two expressions for $L(\varphi')$ and multiplying both sides by $(t + \mu_1)$:

$$\left[\left(\frac{A_1\lambda_1}{t+\lambda_1} + \ldots + \frac{A_n\lambda_n}{t+\lambda_n}\right)(t+\mu_1)\right] \Big/ 1 - \frac{A_1\lambda_1}{t+\lambda_1} - \ldots - \frac{A_n\lambda_n}{t+\lambda_n} = \left(\frac{B_1}{t+\mu_1} + \ldots + \frac{B_n}{t+\mu_n}\right)(t+\mu_1)$$

Let $t \to -\mu_1$ in the two sides of this equation. The left side will tend toward the limit.

$$\left[\frac{A_1\lambda_1}{\lambda_1-\mu_1} + \ldots + \frac{A_n\lambda_n}{\lambda_n-\mu_1}\right] \Big/ \frac{A_1\lambda_1}{(\lambda_1-\mu_1)^2} + \ldots + \frac{A_n\lambda_n}{(\lambda_n-\mu_1)^2} = 1 \Big/ \left[\frac{A_1\lambda_1}{(\lambda_1-\mu_1)^2} + \ldots + \frac{A_n\lambda_n}{(\lambda_n-\mu_1)^2}\right]$$

and consequently,

$$B_1 = 1 \Big/ \left[\frac{A_1\lambda_1}{(\lambda_1-\mu_1)^2} + \ldots + \frac{A_n\lambda_n}{(\lambda_n-\mu_1)^2}\right] \tag{53}$$

The values of B_2, B_3, ... B_n can be obtained in the same manner and it is easy to see, in addition, that the B's will all be positive.

The value of $L(\varphi')$ once obtained, we shall immediately deduce that:

$$\varphi' = B_1e^{-\mu_1 t} + \ldots + B_ne^{-\mu_n t} \tag{54}$$

and then the creep function φ is obtained by integration.

$$\varphi(t) = (B_1/\mu_1)(1 - e^{-\mu_1 t}) + \ldots + (B_n/\mu_n)(1 - e^{-\mu_n t}) \tag{55}$$

The problem is therefore completely solved.

One particular case is interesting. Let us suppose that the viscoelastic substance used is capable of relaxing completely, which is expressed by the relation:

$$\psi(\infty) = A_1 + A_2 + \ldots + A_n = 1 \tag{56}$$

One sees from this that, in this case, equation (51) possesses a zero root, *i.e.*, $\mu_1 = 0$. The first term of $\varphi'(t)$ will therefore be a constant B_1, and the expression for φ will contain a linear term B_1t. The function φ therefore increases indefinitely; that is to say, under the influence of a constant force the material will stretch indefinitely.

This clearly applies only to the domain of deformations sufficiently small for the principle of linear superposition to apply. Outside of this domain, the sample undergoes a contraction in cross-sectional area which is not negligible and will finally break in any actual experiment.

The most difficult part of the problem of predicting the creep function will be, in general, the construction of a function of the form (43) which represents with sufficient precision the experimental relaxation function. If this can be achieved the remainder of the work required presents only minor difficulties. An approximate value of the quantities μ can be obtained in the following manner:

In the immediate neighborhood of $t = -\lambda_k$ the predominant part of $\Phi(t)$ is clearly $(A_k\lambda_k)/(t + \lambda_k)$. It then results that for $-\lambda_{k+1} < t < \lambda_k$ $\Phi(t)$ will be very closely equal to:

$$\frac{A_{k+1}\lambda_{k+1}}{t + \lambda_{k+1}} + \frac{A_k\lambda_k}{t + \lambda_k}$$

and consequently, an approximate value for $-\mu_{k+1}$ will be the root of the second degree equation, corresponding to $\Phi(t) = 1$,

$$(t + \lambda_{k+1})(t + \lambda_k) - A_{k+1}\lambda_{k+1}(t + \lambda_k) - A_k\lambda_k(t + \lambda_{k+1}) = 0 \quad (57)$$

lying between $-\lambda_k$ and $-\lambda_{k+1}$. Once this approximate value is known, the exact value can be obtained without difficulty using Newton's method. An approximate value for the final root μ_1 may be obtained simply by setting:

$$(A_1\lambda_1)/(t + \lambda_1) = 1 \quad (58)$$

As we have said above, the principal difficulty in using the preceding method is the representation for $0 \leqq t \leqq \infty$ of the function $\psi'(t)$ by a Dirichlet series:

$$\psi'(t) = \sum A_n\lambda_n e^{-\lambda_n t} \quad (59)$$

There exists no practical method for the solution of this problem. Consequently, we are going to consider some other methods of solution of the integral equation (25). Let us note at the outset that it is not absolutely necessary to find an empirical expression for $\psi(t)$ which represents this function for *all* values of t. The integral equation shows, actually, that if we can devise an empirical representation of the relaxation function $\psi(t)$ valid for example for $0 \leqq t \leqq T$, and for which it is possible to solve this integral equation, the solution obtained will represent the function $\varphi(t)$ in the same domain, $0 \leqq t \leqq T$, of values of t.

Under these conditions the simplest method of representation which suggests itself is to utilize a polynomial in t. It will always be possible, for values of t between certain limits, to determine constants C such that:

$$\psi(t) = C_1t + C_2t^2 + \dots + C_nt^n \quad (60)$$

In this case, the definite integral contained in equation (25) reduces to a sum of terms of the form:

$$\int_0^t (t - \tau)^k \varphi(\tau)\, d\tau$$

But it is known that:

$$(d^{k+1}/dt^{k+1}) \int_0^t (t - \tau)^k \varphi(\tau)\, d\tau = \Gamma(k + 1)\varphi(t) \quad (61)$$

so that, by differentiating the integral equation $n + 1$ times, we obtain a linear differential equation of $(n + 1)$th order, with constant coefficients. Putting $t = 0$ in the integral equation and its first n derivatives, we obtain a system of $n + 1$ linear equations which will give us the values of φ and its first n derivatives for $t = 0$.

The problem will thus be reduced to the solution of a linear differential equation of order $n + 1$ with constant coefficients, knowing the initial values of the function and of its first n derivatives.

We can, however, obtain the solution in a more elegant way, by using the Laplace transformation again. We have, in the case under consideration:

$$\psi(t) = C_1 t + C_2 t^2 + \dots + C_n t^n \tag{62}$$

$$\psi'(t) = C_1 + 2C_2 t + \dots nC_n t^{n-1} \tag{63}$$

$$L(\varphi') = \frac{C_1\Gamma(2)}{t} + \frac{C_2\Gamma(3)}{t^2} + \dots + \frac{C_n\Gamma(n+1)}{t^n} \tag{64}$$

Therefore, substituting in (42):

$$L(\varphi') =$$

$$\left[\frac{C_2\Gamma(2)}{t} + \dots + \frac{C_n\Gamma(n+1)}{t^n}\right] \Big/ 1 - \frac{C_2\Gamma(2)}{t} - \dots - \frac{C_n\Gamma(n+1)}{t^n} \tag{65}$$

$L(\varphi)$ is the quotient of a polynomial in t of degree $(n - 1)$, by a polynomial in t of degree n. We can therefore determine constants $D_1, \dots D_n, \alpha_1, \alpha_n$, in such a way as to have identically:

$$L(\varphi') = \frac{D_1}{t + \alpha_1} + \dots + \frac{D_n}{t + \alpha_n} \tag{66}$$

The α's will be the roots of the equation:

$$t^n - C_1 t^{n-1} - 2C_2 t^{n-2} - \dots - n!C_n = 0 \tag{67}$$

with their signs changed.

There is no reason, *a priori*, that the roots should be positive, or even real.

Once the quantities α are known, we can deduce from this the following value for D_1:

$$D_1 = 1 \Big/ \left[\frac{C_1\Gamma(3)}{(-\alpha_1)^2} + \dots + \frac{C_n\Gamma(n+2)}{(-\alpha_1)^{n+1}}\right] \tag{68}$$

and the corresponding values for $D_2, \dots D_n$.

If $L(\varphi')$ is put in the form (66), it obviously results that:

$$\varphi' = D_1 e^{-\alpha_1 t} + \dots + D_n e^{-\alpha_n t} \tag{69}$$

$$\varphi = \frac{D_1}{\alpha_1}(1 - e^{-\alpha_1 t}) + \dots + \frac{D_n}{\alpha_n}(1 - e^{-\alpha_n t}) \tag{70}$$

With the present method, the determination of the constants $C_1, \ldots C_n$ offers hardly any difficulty. The most exacting numerical operation will be the solution of an algebraic equation of nth degree, and once the quantities α are known, the calculation of the quantities $D_1, \ldots D_n$, and then of $\varphi(t)$ itself, may be effected immediately.

Our second method is therefore more simple to use, but will not in general be applicable for all values of t.

The problem can equally well be solved in a nearly analogous way, in the case where the function $\psi(t)$ can be put in the following form:

$$\psi(t) = Ae^{-\lambda_1 t}(\alpha_0 + \alpha_1 t + \ldots + \alpha_n t^n) + Be^{-\lambda_2 t}(\beta_0 + \beta_1 t + \ldots + \beta_n t^n) + \ldots \quad (71)$$

which is, in a way, a generalization and a combination of the two forms of representation used above. It is, in addition, easy to see that the possibility of solution of the integral equation (25) in the three preceding cases, results simply from the fact that this integral equation can be reduced to a linear differential equation with constant coefficients.

We shall now, in conclusion, consider a different case in which the problem will no longer reduce to a differential equation. Let us suppose, first, that for $0 \leqq t \leqq T$, we have:

$$\psi(t) = At^m \quad (72)$$

where m is any positive number. The integral equation can be solved by successive approximations, and we find:

$$\varphi'(t) = mAt^{m-1} + \frac{m^2A^2\Gamma^2(m)}{\Gamma(2m)}t^{2m-1} + \ldots \quad (73)$$

and in turn:

$$\varphi(t) = At^m + \frac{A^2\Gamma^2(m+1)}{\Gamma(2m+1)}t^{2m} + \frac{A^3\Gamma^3(m+1)}{\Gamma(3m+1)}t^{3m} + \ldots \quad (74)$$

which can be written, substituting $x = A\Gamma(m+1)t^m$:

$$\varphi(t) = E_m(x) - 1 \quad (75)$$

where:

$$E_m(x) = 1 + \frac{x}{\Gamma(m+1)} + \frac{x^2}{\Gamma(2m+1)} + \ldots \quad (76)$$

is the Mittag-Leffler function.

We can obtain the solution of the integral equation with equal ease in the case where $\psi(t)$ has the following form:

$$\psi(t) = k_1 t^m + k_2 t^{2m} + \ldots + k_n t^{nm} \quad (77)$$

Let us consider first the case where:

$$\psi = At^m \tag{78}$$

Then:

$$L(\psi') = mA\,\frac{\Gamma(m)}{t^m} \tag{79}$$

and:

$$L(\varphi') = \left[\frac{mA\Gamma(m)}{t^m}\right] \Big/ \left[1 - \frac{mA\Gamma(m)}{t^m}\right] \tag{80}$$

From this it follows that if we introduce a new constant $\gamma = A\Gamma(m + 1)$:

$$L[mt^{m-1}E'_m(\gamma t^m)] = 1/(t^m - \gamma) \tag{81}$$

Now let us return to the general case (77). Here:

$$\psi' = mk_1t^{m-1} + \ldots + nmk_nt^{nm-1} \tag{82}$$

and:

$$L(\psi') = mk_1\,\frac{\Gamma(m)}{t^m} + \ldots + nmk_n\,\frac{\Gamma(nm)}{t^{nm}} \tag{83}$$

Consequently:

$$L(\varphi') = \left[mk_1\,\frac{\Gamma(m)}{t^m} + \ldots + nmk_n\,\frac{\Gamma(nm)}{t^{nm}}\right] \Big/ 1 - \frac{mk_1\Gamma(m)}{t^m} - \ldots - \frac{nmk_n\Gamma(nm)}{t^{nm}} \tag{84}$$

$L(\varphi')$ is therefore equal to the quotient of a polynomial of degree $n - 1$ in t^m, by a polynomial of degree n in t^m. We can therefore, proceeding in exactly the same way as previously, write $L(\varphi')$ in the form:

$$L(\varphi') = \frac{K_1}{t^m - \gamma_1} + \ldots + \frac{K_n}{t^m - \gamma_n} \tag{85}$$

from which, as a result of (81):

$$\varphi'(t) = K_1mt^{m-1}E'_m(\gamma_1t^m) + \ldots + K_nmt^{m-1}E'_m(\gamma_nt^m) \tag{86}$$

And finally, by integration:

$$\varphi(t) = K_1[E^m(\gamma_1t^m) - 1] + \ldots + K_n[E^m(\gamma_nt^m) - 1] \tag{87}$$

In the case where $m = 1$, one obviously obtains the results obtained previously.

In conclusion, we note that the methods used above can equally well be applied to find the relaxation function, if the creep function is known.

VIII. MEAN VALUES OF α AND η

We have seen above that all the mechanical properties of viscoelastic solids can be interpreted by considering the material as a collection of Maxwell elements each characterized by two constants α and η, or α and k.

It is therefore of interest to calculate the mean values of these two quantities, which are probably the physical constants characteristic of the substance studied.

The mean values will be defined in the following manner.

$$\alpha_m = \frac{\int_0^\infty \int_0^\infty \alpha N_1(k,\alpha)\, dk\, d\alpha}{\int_0^\infty \int_0^\infty N_1(k,\alpha)\, dk\, d\alpha} = \frac{\int_0^\infty \int_0^\infty \alpha N_1(k,\alpha)\, dk\, d\alpha}{N}$$

$$\eta_m = \frac{\int_0^\infty \int_0^\infty (\alpha/k) N_1(k,\alpha)\, dk\, d\alpha}{N}$$

In the two cases, the integration with respect to α can be carried out immediately, and one obtains:

$$N\alpha_m = \int_0^\infty N(k)\, dk \qquad N\eta_m = \int_0^\infty \frac{N(k)}{k}\, dk$$

We have seen previously that:

$$\int_0^\infty N(k)\, dk = \sigma E/L_0$$

and consequently:

$$\alpha_m = \sigma E/NL_0$$

To calculate η_m, let us note that:

$$1 - \psi(t) = (1/N\alpha_m)\int_0^\infty N(k)e^{-kt}\, dk$$

so that:

$$\int_0^\infty [1 - \psi(t)]\, dt = \frac{1}{N\alpha_m}\int_0^\infty \frac{N(k)}{k}\, dk = \frac{\eta_m}{\alpha_m}$$

Knowledge of the relaxation function therefore permits the easy calculation of the value of the mean friction coefficient η_m.

The coefficient η_m can be obtained equally well experimentally in the following manner. Let us consider again the Maxwell model and suppose that it is subjected to the action of a constant force, as in the case of creep experiments. If the model does not contain a spring without a dashpot, and therefore if the substance is capable of complete relaxation, after a sufficiently long time all the springs will have acquired a constant deformation, and consequently a constant tension, and the deformation of the system will be determined uniquely by the viscous friction of the dashpots.

For each element, one will therefore have:

$$\frac{dl}{dt} = \frac{1}{\eta} f \qquad f = \eta \frac{dl}{dt} = \frac{\alpha}{k} \frac{dl}{dt}$$

By multiplying by $N_1(\alpha_1 k)\, d\alpha\, dk$ and integrating as before, this becomes:

$$F = \frac{dl}{dt}\int_0^\infty \int_c^\infty \frac{\alpha}{k} N_1(\alpha,k)\, d\alpha\, dk = \frac{dl}{dt}\int_0^\infty \frac{N(k)}{k}\, dk$$

which can be written:

$$F = N\eta_m \frac{dl}{dt} \qquad \text{or} \qquad \eta_m = \frac{F}{N(dl/dt)}$$

Since the quantities F and dl/dt can be obtained experimentally, it is seen that one must always have:

$$\frac{F}{dl/dt} = N\eta_m = \frac{\sigma E}{L}\int_0^\infty [1 - \psi(t)]\, dt$$

This relation can be obtained in still another way. We have seen that when the relaxation function $\psi(t)$ can be put in the form:

$$\psi(t) = A_1(1 - e^{-\lambda_1 t}) + \ldots + A_n(1 - e^{-\lambda_n t})$$

and that:

$$\psi(\infty) = A_1 + \ldots + A_n = 1$$

one of the roots μ is zero, and the creep function contains a linear term, so that:

$$\varphi(t) = B_1 t + B_2(1 - e^{-\mu_2 t}) + \ldots$$

All the constants μ_n are positive, so that after a sufficiently long time,

$$\varphi(t) = B_1 t + (B_2 + \ldots + B_n)$$

The coefficient B_1 is easily calculated. In fact, according to (53), one has (with $\mu_1 = 0$):

$$B_1 = \frac{1}{\dfrac{A_1}{\lambda_1} + \ldots + \dfrac{A_n}{\lambda_n}} = \frac{1}{\int_0^\infty [1 - \psi(t)]\, dt}$$

The creep function reduces, therefore, after a sufficiently long time, to a linear function whose angular coefficient can be calculated when the relaxation function is known. This could be verified experimentally.

The length of the sample, in the case of a creep experiment, after a sufficiently long time, and in the case of a material capable of complete relaxation, will therefore have the following form:

$$(l - L_0)/L_0 = (F/E\sigma)(A + B_1 t)$$

where the coefficient B_1 has the value given above, and A is a constant.

It is unfortunately not possible, for the practical (effective) calculation of B_1 to use the empirical formula:

$$1 - \psi(t) = A \log [(t + a)/(t + b)]$$

which gives an infinite integral between 0 and ∞. The calculation of the integral will probably have to be done numerically.

It is easily verified from the preceding that when the substance cannot relax completely, the coefficient η_m is infinite. This evidently arises from the fact that the integral:

$$\int_0^\infty [N(k)/k]dk$$

is infinite if $N(0)$, and therefore also $N_1(\alpha, 0)$ is not zero.

IX. EXPERIMENTAL VERIFICATION

To conclude the present work, we shall now apply the theory given above to an actual experimental case, *i.e.*, the relaxation of stress and creep of polyisobutylene.

The relaxation and creep data which are used here are some preliminary data obtained by R. D. Andrews and N. Hofmann-Bang in this laboratory on a sample of polyisobutylene of viscosity-average molecular weight (M_v) 1,480,000. Relaxation of stress was measured using a flat ring sample on a beam balance type relaxation apparatus; the method has been described in the literature.[4] Creep was measured on strips of polymer (approximate dimensions: $^5/_{16}$ in. wide, 0.090 in. thick, 5 in. long) cut from the same sheet as the relaxation sample. The strips were held at the ends by bar clamps. Suitable weights were suspended from the lower clamps and the change of length followed with a cathetometer.

The experimental relaxation data for this polymer can be fitted over the complete time interval of the experiment by the following empirical equation (t in hours):

$$F(t) = 9.19 \log \left(\frac{t + 7.42}{t + 0.00061}\right)$$

This corresponds to the relaxation function:

$$\psi(t) = 1 - 0.256 \log \left(\frac{t + 7.42}{t + 0.00061}\right)$$

The accuracy of fit is seen from Figure 1, which shows experimental stress values as circles and a solid curve corresponding to the above empirical equation.

Unfortunately, it does not seem possible to solve the integral equation (24) exactly for this form of $\psi(t)$. For the time range:

$$0.003 \text{ hour} \leqslant t \leqslant 1 \text{ hour}$$

however, we can write with small error (less than 4%):

$$\psi(t) = 0.765t^{0.167}$$

corresponding to equation (72).

Using this latter empirical expression for $\psi(t)$ and substituting $A = 0.765$ and $m = 0.167$ in equation (74), the following values are obtained for the creep function $\varphi(t)$.

t	$\varphi(t)$	t	$\varphi(t)$
0	0	0.200	1.346
0.025	0.688	0.500	1.955
0.050	0.842	1.000	2.804
0.100	1.052		

These values are represented in Figure 2.

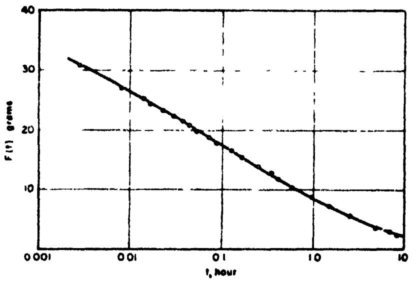

Figure 1

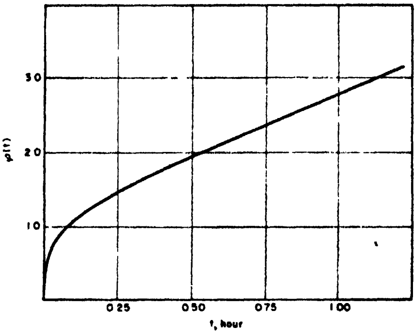

Figure 2

We have compared the values formed in this way with those obtained directly, at the same temperature, on a sample of the same polymer. If $l(t)$ is the length of the sample subjected to the action of a constant force, we shall have, as we have seen before:

$$\frac{l(t)}{l(0)} - 1 = \frac{F}{E\sigma}[1 + \varphi(t)]$$

In a particular experiment, the weight suspended to the sample was 20.56 g., while the sample itself weighed 2.48 g. Consequently, we have a value of F equal to:

$$20.56 + {}^1/_2\, 2.48 = 21.80 \text{ g.}$$

The factor $^1/_2$ results from the fact, which can be proved easily, that the total extension of a linear sample due to its own weight is equal to that caused by a concentrated weight, equal to half the total weight of the sample, applied to its free end.

To obtain the value of the constant $F/E\sigma$, we have used the experimental point $\varphi(t) = 0.568$ for $t = 1$ hour, from which:

$$F/E\sigma = 0.0568/3.804 = 0.0149$$

The results of the calculation are as follows:

t, hours	$\left(\frac{l(t)}{l(0)} - 1\right)_{exptl.}$	$0.0149[1 + \varphi(t)]$
0.036	0.0256	$0.0149 \times 1.760 = 0.0262$
0.069	0.0296	$1.940 = 0.0289$
0.138	0.0320	$2.190 = 0.0326$
0.202	0.0336	$2.340 = 0.0350$
0.254	0.0352	$2.46 = 0.0366$
0.347	0.0400	$2.66 = 0.0396$
0.460	0.0432	$2.88 = 0.0432$
0.634	0.0480	$3.19 = 0.0475$
0.807	0.0528	$3.48 = 0.0519$
1.000	0.0568	$3.801 = 0.0568$
1.270	0.0632	$4.24 = 0.0632$

In this table, the values of $\varphi(t)$ were obtained by interpolation from Figure 2. It is immediately apparent that the agreement between theory and experiment is remarkably satisfactory. The maximum error hardly exceeds 1%, which is of the order of magnitude of the error involved in using the approximate empirical formula (72) in place of the exact value.

We have, in addition, compared with the theoretical values the results of other creep experiments carried out on samples of the same form and the same material at the same temperature, but with different applied weights. The results are shown in Figure 3. Curves I, II, III are theoretical curves corresponding to weights of 20.56 g. (weight of the sample itself is 2.48 g.), 10.88 g. (sample weight is 2.56 g.) and 10.32 g. (sample weight is 2.54 g.). Curves I, II, III represent, respectively, the equations:

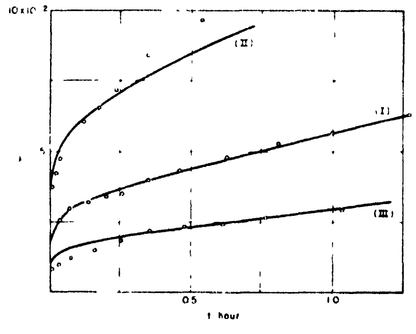

Figure 3

$$\begin{array}{ll} \text{I} & 0.0119[1 + \varphi(t)] \\ \text{II} & 0.0079[1 + \varphi(t)] \\ \text{III} & 0.0288[1 + \varphi(t)] \end{array}$$

The numerical coefficients in these equations were determined in the following manner:

$$0.0079 = 0.0119 \times \frac{10.32 + 0.5 \times 2.54}{20.56 + 0.5 \times 2.48}$$

$$0.0288 = 0.0149 \times \frac{40.88 + 0.5 \times 2.56}{20.56 + 0.5 \times 2.48}$$

On the same graph we have also shown the experimental points. The agreement is generally very good, except for the very small deformations, where experimental error is significant.

On the other hand, it can be seen also that as soon as the relative elongation exceeds about 6%, the deformations are no longer proportional to the applied loads, and the preceding theory ceases to be applicable.

The author is grateful to Professor A. V. Tobolsky for suggesting the present problem and for many helpful discussions, and also to Dr. R. D. Andrews for allowing us unrestricted use of unpublished experimental data, as well as for helping to edit the manuscript.

References

1. These theories are reviewed by T. Alfrey, Jr., in *Mechanical Behavior of High Polymers*, Interscience, New York, 1948. References to recent work in this field by Simha, Leaderman, and others are collected there
2. B. Gross, *J. Applied Phys.*, **18**, 212 (1947).
3. B. Gross, *ibid.*, **19**, 257 (1948).
4. R. D. Andrews, N. Hoffman-Bang, and A. V. Tobolsky, *J. Polymer Sci.*, **5**, 669 (1948).

Résumé

En utilisant un modèle generalisé de Maxwell, ou, sinon, le principe de Boltzmann de superposition linéaire, l'auteur obtient une relation générale entre la force et la déformation pour un échantillon d'une substance visco-élastique. Cette relation contient, comme seule donnée expérimentale, la fonction de relaxation. Utilisant cette fonction, il est possible de prédire toutes les propriétés usuelles, et particulièrement l'étirement et la contraction. La relation entre l'étirement et la relaxation peut être exprimée par une équation intégrale linéaire du type Volterra. De nombreuses méthodes de résolution de cette équation sont indiquées, et l'une d'elles a été appliquée dans un cas expérimental, celui du polyisobutylène. Les valeurs calculées et observées sont en accord remarquable.

Zusammenfassung

Mit Hilfe des generalisierten Maxwell'schen Modells oder des Boltzmann'schen Prinzipes linearer Superposition wird die Beziehung zwischen einer Kraft und der Verformung einer linearen Probe eines viskoelastischen Stoffes abgeleitet. Diese Beziehung enthält als die einzigen experimentellen Daten die Erschlaffungsfunktion. Durch Anwendung dieser Beziehung wird es gezeigt, die alle gewöhnlichen Eigenschaften, -besonders das Kriechen und Rückfederungsvermögen vorausgesagt werden können. Die Beziehung zwischen dem Kriechen und der Erschlaffungsfunktion kann als eine lineare Integralgleichung des Volterra Types ausgedrückt werden. Einige Lösungsmethoden dieser Gleichung werden angeführt, und eine von ihnen wird an einem Versuche an Polyisobutylen angewandt. Die berechneten und beobachteten Werte der Kriechungsfunktion,stimmen bemerkenswert gut überein.

Received January 7, 1949

JOURNAL OF POLYMER SCIENCE VOL. V, NO. 1, PAGES 91-109

Nitrocellulose–Solvent Interaction

W. R. MOORE, *Physical Chemistry Laboratory, Department of Chemistry and Dyeing, Technical College, Bradford, England*

INTRODUCTION

Estimation of nitrocellulose–solvent interaction, by swelling in binary mixtures, by precipitation from solution, and from the viscosities of dilute solutions, suggests that, within a limited range of liquids, interaction is related to the cohesive energy density of the solvent.[1] Such a relationship is of some interest since it suggests that Gee's cohesive energy density method[2] may be used to give an account of the interaction of nitrocellulose and solvent or swelling liquids. Gee's method, however, applies only to cases of endothermic solution or swelling, while solutions of nitrocellulose are formed exothermally. Further, swelling and solution involve solvation,[3–6] molecules of solvent or swelling liquid being attached to specific points on the polymer chains. Such a process must be included in any general account of the interaction of nitrocellulose and solvents. In this paper, the methods of estimation given above are applied to a wider range of solvents in homologous series. The absorption of solvent by nitrocellulose from solvent–hexane mixtures has also been examined as a means of estimating the concentration of solvent in swollen polymer and in the liquid in equilibrium with it.

EXPERIMENTAL

1. Materials Used

A fibrous nitrocellulose was used, from cotton linters, with a mean N content of 12.55%. Such nitrocellulose is not a homogeneous polymer but it is likely that the influence of chain length on swelling and solubility will be small compared with that of N content.[7] The nitrocellulose was dried for at least 3 hours at 100° and for 7 days over sulfuric acid at room temperature. Swelling was studied in binary mixtures of solvents and hexane containing varying concentrations of solvent up to that at which solution occurred. Homologous series of alkyl methyl ketones, alkyl formates, acetates, butyrates, and dialkyl phthalates were used as solvents, all being dried over potassium carbonate and redistilled before use. Hexane, boiling range 67–69°, density 0.669 20°C/20°, aromatic hydrocarbons less than 5%, was used as nonsolvent as it is known to be absorbed only slightly by nitrocellulose.[8] Preliminary experiments showed it to have no measurable swelling action. Other so-called nonsolvents, such as alcohols or aromatic hydrocarbons, may have solvent or swelling action under certain conditions and cannot be regarded as complete nonsolvents.[9–11]

2. Estimation of Swelling

0.2 g. of nitrocellulose was weighed into graduated well-stoppered glass tubes and 10 g. binary mixture added. The tubes were well shaken and thermostated at 25°, being occasionally shaken during the next two hours and the fibers allowed to settle until a constant bulk volume was obtained. Preliminary experiments showed that equilibrium was attained during this period, attainment apparently occurring almost immediately in mixtures involving smaller solvents. The final bulk volume was noted and the greater part of the supernatant liquid decanted and reserved. The fibers were shaken with the remaining liquid and examined microscopically – shape and mean diameter being noted. Excess hexane was added to 2 cc. of the previously reserved liquid, turbidity or a precipitate indicating dissolved nitrocellulose.

3. Estimation of Composition of Liquid and Absorption of Solvent by Nitrocellulose

The composition of the remaining liquid was estimated by a method depending on variation of dielectric constant with composition. A diagram of the apparatus is given in Figure 1. It consists of a valve oscillator incorporating a quartz crystal in the grid circuit. Measurements of capacity were made in a small test condenser C_2, in which the mixture formed the dielectric, in parallel with a variable condenser C_1. As the capacity of C_1 is increased the anode current falls to a minimum and then, as the point of resonance is passed, rises sharply. The sharp rise provided a reference point against which measurements of capacity change of C_2 could be made, these being obtained as difference readings on the dial of C_1. The coil L was 35 turns 26 gauge D.C.C. copper wire on a 1 inch former. V was a P.X.4 tube. The values of the other components were: C_1 20 $\mu\mu$F, C_3 0.1 μF, R

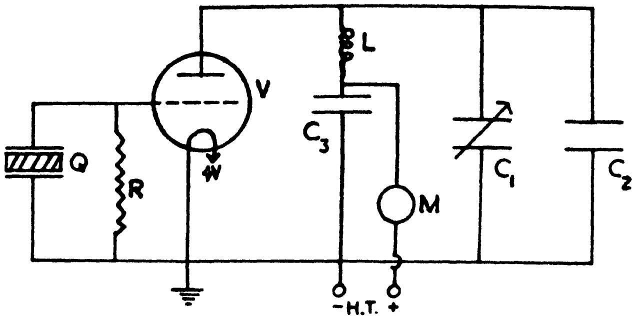

Fig. 1. Dielectric method for estimating composition of liquid phase.

TABLE I

SWELLING AND ABSORPTION IN SOLVENT–HEXANE MIXTURES

Compound	Initial mole fraction	Mole fraction at equilibrium	Bulk volume, cc	Addition of hexane to liquid	N_2	Fiber diam., mm.	Comments
Hexane only			0.9			0.016	
Acetone	0.1	0.0963	1.9	No ppt.	0.398	0.025	Swelling only radial
	0.2	0.1924	1.1	No ppt.	0.614	0.036	Axial contraction
	0.3	0.2904	1.55	No ppt.	0.702	0.052	
	0.4	0.3902	1.8	No ppt.	0.748		Very swollen masses
	0.5	0.4895	2.0	Very slight ppt.	0.792		
	0.6	--	2.0	Ppt.			
	0.7	Dissolved					
Ethyl methyl ketone	0.1	0.0966	1.55	No ppt.	0.379	0.025	Swelling only radial
	0.2	0.1947	2.2	No ppt.	0.522	0.036	Axial contraction
	0.3	0.2928	1.55	No ppt.	0.619	0.052	
	0.4	0.3901	2.3	Very slight ppt.	0.726		Very swollen masses
	0.5	—	2.55	Ppt.			
	0.6	Dissolved					
Methyl *n*-propyl ketone	0.1	0.0973	1.45	No ppt.	0.341	0.024	Swelling only radial
	0.2	0.1950	1.9	No ppt.	0.436	0.036	Axial contraction
	0.3	0.2963	1.65	No ppt.	0.584	0.052	
	0.4	0.3908	2.5	Very slight ppt.	0.705		Very swollen masses
	0.5	---	6.6	Heavy ppt.			
	0.6	Dissolved					
n-Amyl methyl ketone	0.1	0.0978	1.2	No ppt.	0.270	0.023	Radial swelling only
	0.2	0.1963	1.3	No ppt.	0.400	0.026	
	0.3	0.2946	2.5	Very slight ppt.	0.515		Very swollen masses
	0.4	Partially dissolved					
n-Hexyl methyl ketone	0.1	0.0985	1.1	No ppt.	0.196	0.023	Radial swelling only
	0.2	0.1970	1.2	No ppt.	0.342	0.025	
	0.3	0.2955	1.9	Very slight ppt.	0.436	0.031	Axial contraction, breaking
	0.4	Partially dissolved					
Methyl nonyl ketone	0.1	0.0987	0.95	No ppt.	0.161	0.017	Some a little swollen radially
	0.2	0.1976	1.0	No ppt.	0.285		
	0.3	0.2964	1.05	No ppt.	0.404		
	0.4	0.3947	1.1	Very slight ppt.	0.495		Some a little swollen radially, others broken
	0.5	0.4930	1.3	Slight ppt.	0.592		
	0.6	Partially dissolved					

5000 ohms. C_2 was made of two concentric thin glass tubes, sealed together at one end. The inner tube, 10 mm. diameter, contained mercury to serve as one electrode. The outer tube was of 15 mm. diameter and 2 cc. of binary mixture was placed in the space between the tubes. This liquid could be easily poured out and the space rinsed with hexane and dried between determinations. The two concentric tubes were centrally placed in a wider tube containing mercury which served as the other electrode. The whole apparatus was screened. For a series of binary mixtures involving a particular solvent a calibration curve was first obtained by plotting readings of C_1 against concentration of solvent. This curve was used to estimate changes in composition following absorption of solvent by nitrocellulose. Readings were quite reproducible and changes in composition representing 0.001 mole fraction of solvent easily detected. The method is rapid compared with chemical methods of estimation. Volatilization of components does not occur during the time required for determination, as may be the case in methods involving change of refractive index. Further, the method is applicable to mixtures in which the refractive indices of components differ only slightly. The absorption of solvent by nitrocellulose was calculated from the change in composition of mixture, assuming no absorption of hexane. Results are means of at least three determinations.

4. Precipitation with Hexane

The volume of hexane required to precipitate nitrocellulose from solution in different solvents was found by adding hexane to 5 cc. of 1% solution at 25° until turbidity, not removed by shaking, just appeared. In some cases the end point was not very precise but consistent differences between different solvents were obtained. The appearance of the solutions was also noted.

5. Viscosity Determinations

Viscosities, relative to the solvent, of solutions containing 0.05, 0.1, and 0.2 g. nitrocellulose in 100 cc. of solvent were determined in Ostwald viscometers at 25°, kinetic energy corrections being applied where applicable. In the case of phthalate solutions, rates of shear were such as to eliminate anomalous viscosity effects. With aliphatic solvents, rates of shear with solutions involving the least viscous liquids were such as to possibly lead to somewhat lower viscosities than would be obtained with very low rates of shear. Because of the known initial fairly rapid decrease of viscosity with time[12,13] all solutions were allowed to stand for 2 weeks before viscosities were determined. The ratio of specific viscosity and concentration, η_{sp}/c, was plotted against concentration for each solvent and the plots extrapolated to zero concentration to obtain the intrinsic viscosity $[\eta]$.

RESULTS AND DISCUSSION

Swelling and absorption results are given in Tables I–V, absorption of solvent being denoted by A_2, the molar concentration of solvent in the

TABLE II

SWELLING AND ABSORPTION IN FORMATE–HEXANE MIXTURES

Formate	Initial mole fraction	Mole fraction at equilibrium	Bulk volume, cc.	Addition of hexane to liquid	N_2	Fiber diam., mm.	Comments
Methyl	0.1	0.0970	1.2	No ppt.	0.347	0.022	Swelling only radial
	0.2	0.1933	1.6	No ppt.	0.572	0.025	
	0.3	0.2912	2.3	No ppt.	0.678	0.032	Axial contraction
	0.4	0.3898	1.4	No ppt.	0.757	0.037	
	0.5	0.4894	1.5	No ppt.	0.785		Very swollen masses
	0.6	0.5891	1.8	Very slight ppt.	0.857		
	0.7	0.6897	1.5	Slight ppt.	0.887		Aggregated in clumps
	0.8	Dissolved					
Ethyl	0.1	0.0975	1.2	No ppt.	0.325	0.022	Swelling only radial
	0.2	0.1944	1.35	No ppt.	0.520	0.024	
	0.3	0.2920	1.9	No ppt.	0.656	0.030	Axial contraction
	0.4	0.3900	1.7	Very slight ppt.	0.734	0.046	
	0.5	0.4884	1.95	Slight ppt.	0.779		Very swollen masses
	0.6	—	2.5	Ppt.			
	0.7	Dissolved					
n-Propyl	0.1	0.0971	1.2	No ppt.	0.323	0.022	Swelling only radial
	0.2	0.1955	1.3	No ppt.	0.463	0.024	
	0.3	0.2923	1.6	No ppt.	0.623	0.029	Axial contraction
	0.4	0.3903	2.8	Slight ppt.	0.676	0.036	
	0.5	Partially dissolved					
n-Butyl	0.1	0.098	1.15	No ppt.	0.249	0.022	Swelling only radial
	0.2	0.1951	1.2	No ppt.	0.468	0.023	
	0.3	0.2937	1.3	No ppt.	0.581	0.025	
	0.4	0.3914	4.1	Slight ppt.	0.670	0.037	Axial contraction, some breaking
	0.5	Dissolved					
n-Amyl	0.1	0.098	1.15	No ppt.	0.253	0.022	Swelling only radial
	0.2	0.196	1.2	No ppt.	0.428	0.023	
	0.3	0.2942	1.3	No ppt.	0.562	0.025	
	0.4	—	1.8	Heavy ppt.	—	0.030	Axial contraction, some breaking
	0.5	Dissolved					

polymer phase. N_2 is based on the group C_6 and is defined by

$$N_2 = N_s/(N_s + N_c)$$

where N_s is the number of molecules of solvent absorbed by a number N_c of C_6 groups. Concentrations in the liquid phase are given in mole fractions of solvent. Plots of N_2 against the equilibrium mole fraction of solvent in the liquid phase are given in Figures 2–6 for each homologous series of solvents. With the smaller solvents the plots suggest a tendency

TABLE III

SWELLING AND ABSORPTION IN ACETATE-HEXANE MIXTURES

Acetate	Initial mole fraction	Mole fraction at equilibrium	Bulk volume, cc.	Addition of hexane to liquid	N_2	Fiber diam., mm.	Comments
Methyl	0.1	0.0964	1.65	No ppt.	0.392	0.023	Swelling only radial
	0.2	0.1945	2.75	No ppt.	0.532	0.028	
	0.3	0.2910	1.55	No ppt.	0.688	0.032	Axial contraction
	0.4	0.3903	1.5	Very slight ppt.	0.727		Very swollen masses, aggregated in clumps
	0.5	0.4895	0.9	Slight ppt.	0.779		
	0.6	--	1.1	Ppt.			
	0.7	Dissolved					
Ethyl	0.1	0.0970	1.15	No ppt.	0.316	0.023	Swelling only radial
	0.2	0.1944	1.25	No ppt.	0.526	0.025	
	0.3	0.2912	1.2	No ppt.	0.649	0.030	Axial contraction
	0.4	0.3900	2.7	Very slight ppt.	0.714	0.050	
	0.5		5.8	Heavy ppt.			Very swollen masses
	0.6	Dissolved					
n-Propyl	0.1	0.0974	1.1	No ppt.	0.292	0.020	Swelling only radial
	0.2	0.1931	1.25	No ppt.	0.519	0.024	
	0.3	0.2919	2.6	Very slight ppt.	0.637	0.053	Axial contraction
	0.4		1.7	Heavy ppt.			Very swollen masses
	0.5	Dissolved					
n-Butyl	0.1	0.098	1.1	No ppt.	0.226	0.020	Swelling only radial
	0.2	0.1913	1.15	No ppt.	0.510	0.023	
	0.3	0.2923	2.25	Slight ppt.	0.614	0.029	Swelling at points along fiber, breaking
	0.4	Partially dissolved					
n-Amyl	0.1	0.098	1.0	No ppt.	0.238	0.020	Swelling only radial
	0.2	0.1954	1.05	No ppt.	0.449	0.023	
	0.3	0.2934	1.65	Slight ppt.	0.565	0.026	Swelling radial, some breaking
	0.4	--	12.2	Heavy ppt.			Very swollen masses, breaking
	0.5	Dissolved					

to a limiting value of absorption. Mixtures of such solvents and hexane, however, are likely to exhibit deviations from ideal behavior. At the higher solvent concentrations the rate of change of activity with concentration will probably be less than that for an ideal solution Absorption will depend on activity rather than concentration and the apparent tendency to a limiting value may be due to only small changes in activity at higher concentrations. As the size of the solvent is increased and its internal

TABLE IV

Swelling and Absorption in n-Butyrate–Hexane Mixtures

n-Butyrate	Initial mole fraction	Mole fraction at equilibrium	Bulk volume, cc.	Addition of hexane to liquid	N_2	Fiber diam., mm.	Comments
Methyl	0.1	0.0972	1.15	No ppt.	0.292	0.022	Swelling only radial
	0.2	0.1936	1.3	No ppt.	0.537	0.024	
	0.3	0.2908	1.55	Slight ppt.	0.660	0.028	
	0.4	0.3899	2.8	Ppt.	0.710	0.037	Axial contraction
	0.5	Partially dissolved					
	0.6	Dissolved					
Ethyl	0.1	0.0978	1.1	No ppt.	0.260	0.021	Swelling only radial
	0.2	0.1940	1.3	No ppt.	0.498	0.023	
	0.3	0.2915	1.45	Slight ppt.	0.632	0.026	
	0.4	—	2.2	Heavy ppt.		0.031	Axial contraction
	0.5	Dissolved					
n-Propyl	0.1	0.0978	1.1	No ppt.	0.244	0.021	Swelling only radial
	0.2	0.1948	1.2	No ppt.	0.473	0.022	
	0.3	0.2919	1.3	No ppt.	0.613	0.024	Radial swelling, some breaking
	0.4	0.3900	1.75	Ppt.	0.682	0.026	
	0.5	Partially dissolved					
	0.6	Dissolved					
n-Butyl	0.1	0.098	1.1	No ppt.	0.264	0.020	Swelling only radial
	0.2	0.1959	1.15	No ppt.	0.408	0.021	
	0.3	0.2937	1.2	No ppt.	0.535	0.022	
	0.4	0.3924	1.3	Slight ppt.	0.599	0.023	
	0.5	—	1.55	Ppt.	—	0.025	Swelling radial, breaking
	0.6	Dissolved					
n-Amyl	0.1	0.098	1.0	No ppt.	0.264	0.019	Swelling only radial
	0.2	0.1965	1.1	No ppt.	0.372	0.020	
	0.3	0.2952	1.15	No ppt.	0.449	0.021	
	0.4	0.3939	1.2	No ppt.	0.543	0.022	
	0.5	0.4913	1.4	Slight ppt.	0.643	0.024	Swelling radial, breaking
	0.6	—	2.35	Heavy ppt.	—	0.026	
	0.7	Partially dissolved					
	0.8	Dissolved					

pressure becomes closer to that of hexane, deviations from ideal behavior should become less and the plots exhibit less curvature. This is seen to be generally true. If sorption is carried out from the vapor phase plots of molecular absorption against activity of small solvents are not far removed from those anticipated for ideal solutions.[14]

Figures 2–6 also show a steric effect. For a given concentration of solvent in the liquid phase absorption decreases, in each series of solvents, with increasing size of solvent. The effect is particularly marked with phthalates. Diethyl is readily absorbed, di-n-propyl and di-n-butyl progressively less so, while di-n-amyl and di-n-hexyl are not absorbed in

TABLE V

SWELLING AND ABSORPTION IN PHTHALATE-HEXANE MIXTURES

Phthalate	Initial mole fraction	Mole fraction at equilibrium	Bulk volume, cc.	Addition of hexane to liquid	N_2	Fiber diam., mm.	Comments
Diethyl	0.05	0.013	2.3	No ppt.	0.513	0.030	Axial contraction
	0.1	0.087	2.3	No ppt.	0.688	0.040	
	0.15	0.130	2.5	No ppt.	0.746	0.056	
	0.2	0.171	2.55	No ppt.	0.767		Very swollen masses
	0.25	0.2205	2.4	Very slight ppt.	0.811		
	0.3	0.267	2.0	Slight ppt.	0.827		Very swollen masses, aggregated in clumps
	0.35	—	2.35	Ppt.			Very swollen and broken
	0.4	Partially dissolved					
	0.45	Dissolved					
Di-*n*-propyl	0.05	0.0485	1.1	No ppt.	0.196	0.018	Swelling only radial
	0.1	0.095	2.8	No ppt.	0.429	0.031	Axial contraction
	0.15	0.141	3.2	Very slight ppt.	0.559	0.051	
	0.2	—	3.6	Ppt.			Very swollen masses, breaking
	0.25	Partially dissolved					
	0.3	Dissolved					
Di-*n*-butyl	0.05	0.0493	1.0	No ppt.	0.105	0.018	Swelling only radial
	0.1	0.0975	2.2	Very slight ppt.	0.266	0.030	
	0.15	—	2.45	Ppt.			Some slightly swollen, others broken
	0.2	Partially dissolved					
	0.25	Dissolved					
Di-*n*-amyl	0.05	0.05	1.0	No ppt.	Nil	0.018	
	0.1	0.1	1.1	No ppt.	Nil		Some fibers perhaps a little swollen, others broken
	0.15	0.15	1.2	Very slight ppt.	Nil		
	0.2	0.2	1.35	Slight ppt.	Nil		
	0.25	—	1.6	Ppt.			
	0.3	—	1.9	Heavy ppt.			
	0.35	Dissolved					
Di-*n*-hexyl	0.05	0.05	1.0	No ppt.	Nil		Fibers not swollen; breaking, increasing with concentration of phthalate
	0.1	0.1	1.05	No ppt.	Nil		
	0.15	0.15	1.1	No ppt.	Nil		
	0.2	0.2	1.1	Very slight ppt.	Nil		
	0.25	0.25	1.15	Very slight ppt.	Nil		
	0.3	0.3	1.15	Very slight ppt.	Nil		
	0.35	0.35	1.3	Slight ppt.	Nil		
	0.4	—	1.35	Ppt.			
	0.45	Partially dissolved					

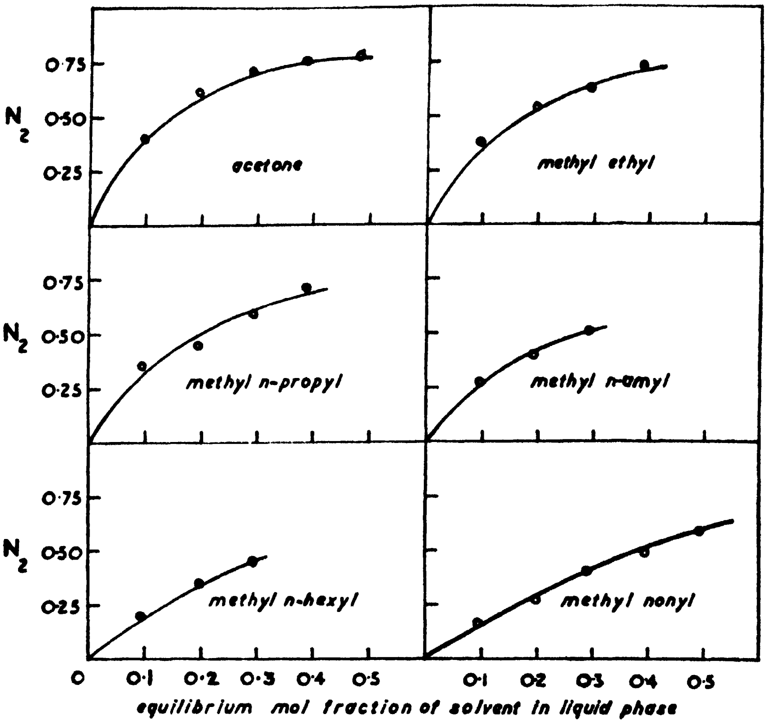

Fig. 2. Absorption of ketones from ketone–hexane mixtures.

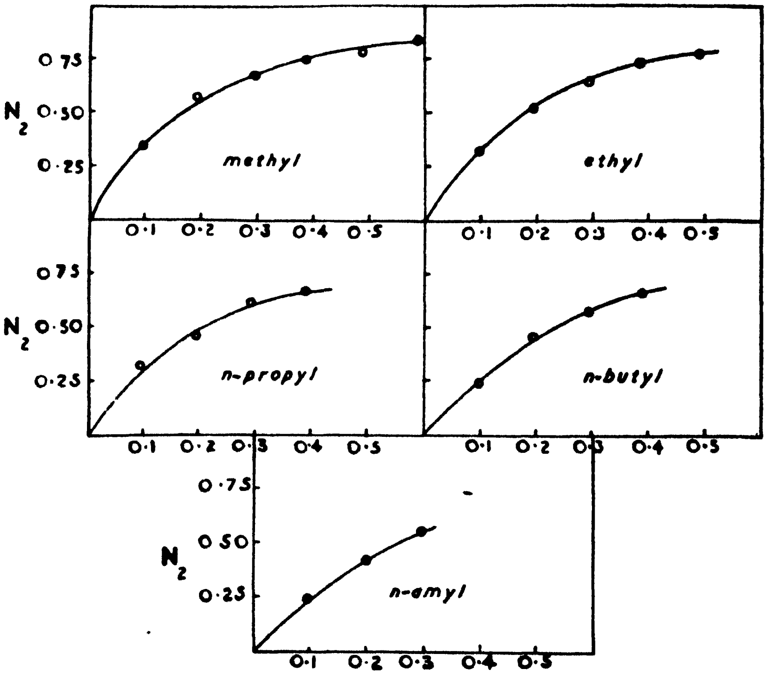

Fig. 3. Absorption of formates from formate–hexane mixtures.

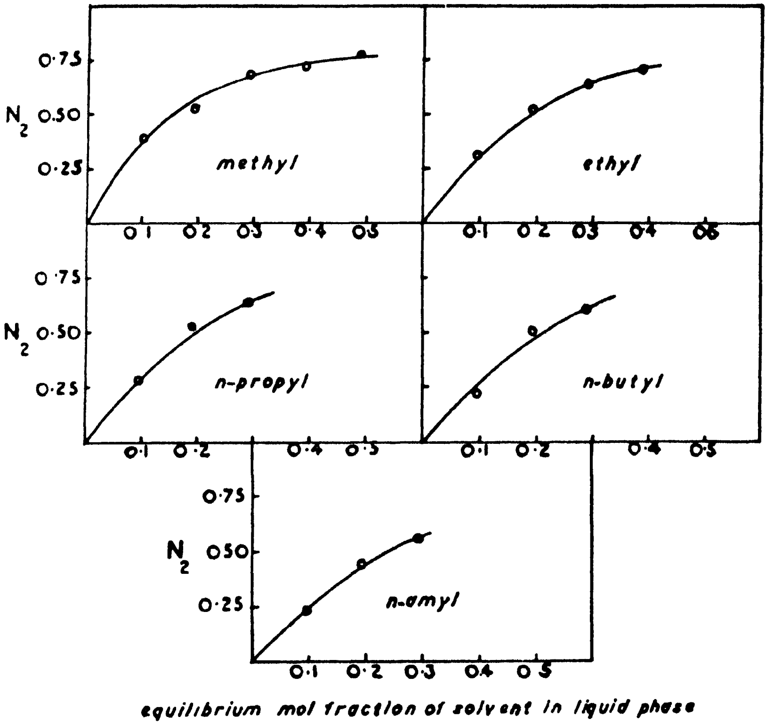

Fig. 4. Absorption of acetates from acetate–hexane mixtures.

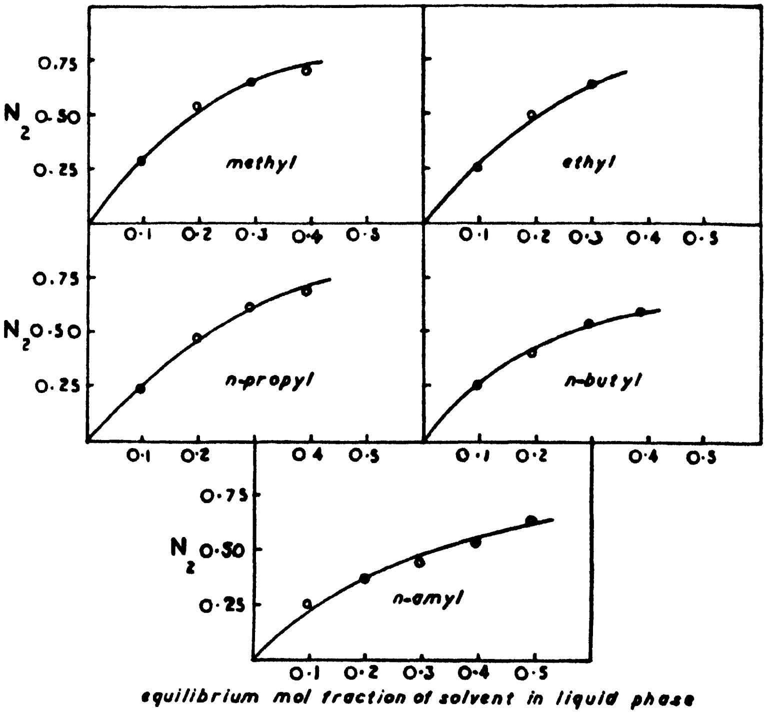

Fig. 5. Absorption of *n*-butyrates from butyrate–hexane mixtures.

measurable amounts. This steric effect may be ascribed to increasing difficulty in penetration into the fibers as the size of the solvent increases. Similar effects have been reported by Mathieu and Petitpas[14] and Desmaroux[15] has shown that camphor, dissolved in hexane, is not absorbed below a certain critical concentration. It should be noted, however, that size of solvent is not the only factor determining entry into the fibers. The relatively large absorption values for diethyl and di-*n*-propyl phthalates, both fairly large solvents, suggest that some other factor is operative.

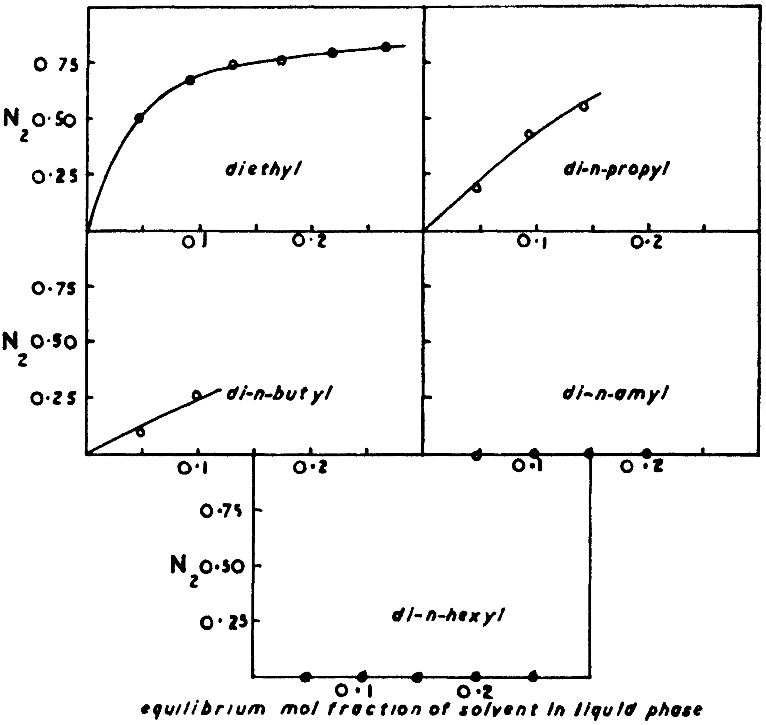

Fig. 6. Absorption of phthalates from phthalate–hexane mixtures.

The steric effect is paralleled in a general way by swelling. With smaller solvents of a series and low solvent concentrations swelling is only radial. Increasing concentration leads to axially contracted, radially swollen fibers. The packing of such fibers is closer than where radial swelling only occurs and this leads to a decrease in the bulk volume although the swelling of individual fibers is greater. At the highest solvent concentrations before solution occurs the fibers swell to almost spherical masses and the bulk volume may increase though a tendency for highly swollen fibers to aggregate together in clumps may lead to a further decrease. Presumably the molecules of the smaller solvents enter both amorphous and crystalline regions of the fibers.[14] With larger solvents the axially contracted form is not observed and at higher solvent concentrations the fibers tend to break

TABLE VI

(A) Action of Mixtures Containing 0.5 Mole Fraction Aliphatic Solvent

Solvent	Bulk volume, cc.	$(E/V)^{1/2}$(cal./cc.)$^{1/2}$
Methyl formate	1.5	10.2
Acetone	2.0	9.8
Methyl acetate	0.9	9.55
Ethyl formate	1.95	9.4
Ethyl methyl ketone	2.55	9.2
Ethyl acetate	5.8	9.05
n-Propyl formate	Partially dissolved	8.95
n-Propyl methyl ketone	6.6	8.9
Methyl-*n*-butyrate	Partially dissolved	8.85
n-Propyl acetate	Dissolved	8.75
n-Butyl formate	Dissolved	8.7
n-Amyl methyl ketone	Dissolved	8.55
Ethyl *n*-butyrate	Dissolved	8.55
n-Amyl formate	Dissolved	8.5
n-Butyl acetate	Dissolved	8.5
n-Hexyl methyl ketone	Dissolved	8.45
n-Amyl acetate	Dissolved	8.3
n-Propyl *n*-butyrate	Partially dissolved	8.3
n-Butyl *n*-butyrate	1.55	8.1
Methyl nonyl ketone	1.3	7.8
n-Amyl *n*-butyrate	1.4	7.8

(B) Action of Mixtures Containing 0.2 Mole Fraction Phthalate

Phthalate	Bulk volume, cc.	$(E/V)^{1/2}$(cal./cc.)$^{1/2}$
Diethyl	2.55	9.4
Di-*n*-propyl	3.6	8.8
Di-*n*-butyl	Partially dissolved	8.4
Di-*n*-amyl	1.35	8.2
Di-*n*-hexyl	1.1	8.0

up into elongated fragments. In such cases, the values of swelling and absorption preceding solution are considerably less than those observed with smaller solvents. The larger solvents probably enter chiefly the amorphous regions. The breaking into elongated fragments, also observed by Mangenot and Raison[16] with nitrated cotton and ramie fibers in cyclopentanone and diethyleneglycol dinitrate, may be accompanied by swelling of some fibers. This does not occur with the largest solvents and in mixtures involving di-*n*-amyl and di-*n*-hexyl phthalates breaking occurs without swelling even at lower solvent concentrations.

Solution of fibers does not appear to depend on the attainment of particular values of swelling or absorption. With smaller solvents solution is preceded, at solvent concentrations less than that causing solution, by high degrees of swelling and absorption. With larger solvents smaller swelling and absorption values precede solution and with the largest solvents solution appears to occur without measurable swelling or absorption at lower concentrations. It may be noted that two modes of solution are possible, as suggested by Mathieu and Petitpas.[14] With small solvents, entering both amorphous and crystalline regions of the fiber, dispersion of chains may lead to a "molecular" solution. Such dispersion of chains should be preceded, at lower solvent concentrations, by high degrees of swelling and absorption. With larger solvents, where entry is restricted to amorphous regions, a dispersion of crystalline regions, initially little affected by solvent, may occur. Further action of the solvent may lead to progressive removal of chains from the dispersed crystalline regions and ultimately to the "molecular" type of solution. Such a dispersion should be preceded, at solvent concentrations less than that causing the dispersion, by smaller degrees of swelling and absorption. The breaking of fibers into elongated fragments may be due to break-up of the fibers at points in the amorphous regions where packing of chains is most open and the forces between them weakest, this break-up being followed by dispersion of the fragments. Where solution occurs without swelling and absorption at lower solvent concentrations, as in the cases of di-*n*-amyl and di-*n*-hexyl phthalates, presumably the solvent molecules are too large to enter other than a few relatively large spaces in the fibers where packing of chains is sufficiently open to permit entry.

At low concentrations, the smaller solvents appear to be the best swelling agents, possibly because of the greater amount of solvent absorbed. This is not, however, the case at higher concentrations. Comparison of the swelling or solvent power of mixtures initially containing equal mole fractions of different solvents suggests a relation between the action of such mixtures and the cohesive energy density of the solvent. The cohesive energy density is E/V, where E equals $L_e - RT$, L_e being the molar latent heat of vaporization and V the molar volume of the solvent, both at the temperature T. The relationship is seen in Table VI, where bulk volumes in mixtures initially containing 0.5 mole fraction aliphatic solvents and 0.2 mole fraction phthalates are given with the solvent $(E/V)^{1/2}$ values at 25°. The latter are taken from published data,[2,17,18] from vapor pressure data, by estimation from values for homologous compounds or from the Hildebrand rule.[19] In the two last cases, values are only approximate. While bulk volume, for reasons previously given, is only an approximate measure of swelling power, the action of the mixtures appears to vary with $(E/V)^{1/2}$ in a manner similar to that observed with nonpolar polymers. The mole fraction of solvent in the mixtures in equilibrium with swollen fibers will not be that initially present but reference to Tables I–V indicates that with aliphatic solvents the change in mole fraction following absorption is not large. With such solvents swelling is seen to increase as the value of $(E/V)^{1/2}$ decreases from 10.2 to 8.9, a range involving the smaller solvents. Between 8.9 and 8.3 partial or complete solution occurs. At values lower than 8.3, involving larger solvents, only slight swelling occurs, probably because entry is restricted to amorphous regions. Similar results are seen with phthalates, although here solution occurs at lower solvent concentrations and the changes in mole fraction are larger for mixtures involving diethyl and di-*n*-propyl phthalates, suggesting that solvent type is an additional factor affecting swelling or solution. The relationship between cohesive energy density of solvent and action of mixtures is shown in Figure 7, where bulk volumes in the mixtures involving aliphatic solvents given in Table VI are plotted against solvent $(E/V)^{1/2}$. Partial or com-

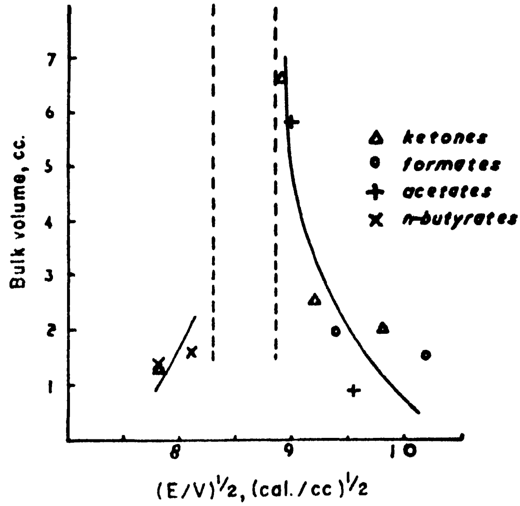

Fig. 7. Action of mixtures containing 0.5 mole fraction solvent as function of $(E/V)^{1/2}$.

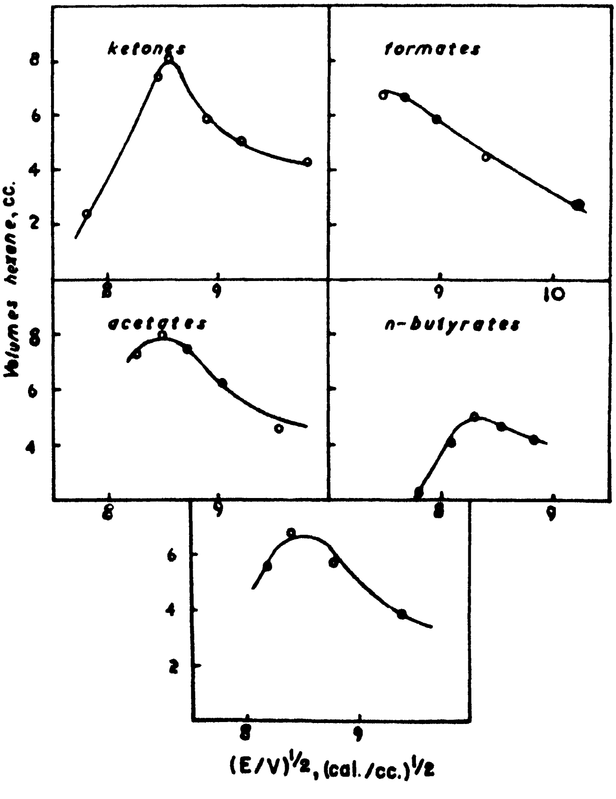

Fig. 8. Volumes of hexane for precipitation as a function of $(E/V)^{1/2}$.

TABLE VII

Volumes of Hexane Required to Cause Precipitation from 5 cc. 1% Solution

Solvent	Volume hexane, cc.	Appearance of solution
Acetone	4.3	Clear
Methyl ethyl ketone	5.05	Clear
Methyl *n*-propyl ketone	5.9	Clear
Methyl *n*-amyl ketone	7.85	Clear
Methyl *n*-hexyl ketone	7.5	Clear
Methyl *n*-nonyl ketone	2.45	Deposited specks of gel
Methyl formate	2.7	Very slightly cloudy
Ethyl formate	4.5	Very slightly cloudy
n-Propyl formate	5.9	Clear
n-Butyl formate	6.7	Clear
n-Amyl formate	6.75	Clear
Methyl acetate	4.75	Clear
Ethyl acetate	6.3	Clear
n-Propyl acetate	7.55	Clear
n-Butyl acetate	8.05	Clear
n-Amyl acetate	7.4	Clear
Methyl *n*-butyrate	4.2	Very slightly cloudy
Ethyl *n*-butyrate	4.7	Clear
n-Propyl *n*-butyrate	5.05	Clear
n-Butyl *n*-butyrate	4.1	Slightly cloudy
n-Amyl *n*-butyrate	2.35	Slightly cloudy, deposited specks
Diethyl phthalate	3.9	Clear
Di-*n*-propyl phthalate	5.7	Clear
Di-*n*-butyl phthalate	6.8	Clear
Di-*n*-amyl phthalate	5.6	Clear
Di-*n*-hexyl phthalate	Not completely dissolved	

TABLE VIII

Intrinsic Viscosities and Initial Slopes of η_{sp}/c vs. c Curves

Solvent	$[\eta]$	Initial slope
Acetone	2.42	0.66
Methyl ethyl ketone	2.47	2.0
Methyl *n*-propyl ketone	2.64	2.4
Methyl *n*-amyl ketone	3.10	4.0
Methyl *n*-hexyl ketone	3.02	3.0
Methyl formate	3.02	1.5
Ethyl formate	3.10	1.5
n-Propyl formate	3.18	3.2
n-Butyl formate	3.47	4.8
n-Amyl formate	3.81	5.7
Methyl acetate	2.80	0.2
Ethyl acetate	3.10	2.8
n-Propyl acetate	3.36	3.6
n-Butyl acetate	3.60	4.8
n-Amyl acetate	3.52	4.2
Methyl *n*-butyrate	3.57	4.4
Ethyl *n*-butyrate	3.69	5.5
n-Propyl *n*-butyrate	3.77	6.6
n-Butyl *n*-butyrate	3.60	6.5
Dimethyl phthalate	3.65	4.0
Diethyl phthalate	4.17	6.1
Di-*n*-propyl phthalate	4.40	6.3
Di-*n*-butyl phthalate	4.90	7.0
Di-*n*-amyl phthalate	4.55	6.9

plete solution occurs between the limits indicated by the broken vertical lines.

The volumes of hexane required for precipitation are given in Table VII. They agree generally with the proportions of hexane in the mixtures which just cause solution. In each homologous series the volumes vary with solvent $(E/V)^{1/2}$, in a similar way to swelling or solvent action of mixtures, and as shown in Figure 8. The plots suggest that, for a particular series, the largest volume of hexane is required when the solvent $(E/V)^{1/2}$ value is about 8.5. The differences in the volumes of hexane required for solvents of different series but of approximately the same $(E/V)^{1/2}$ suggests again that solvent type is important.

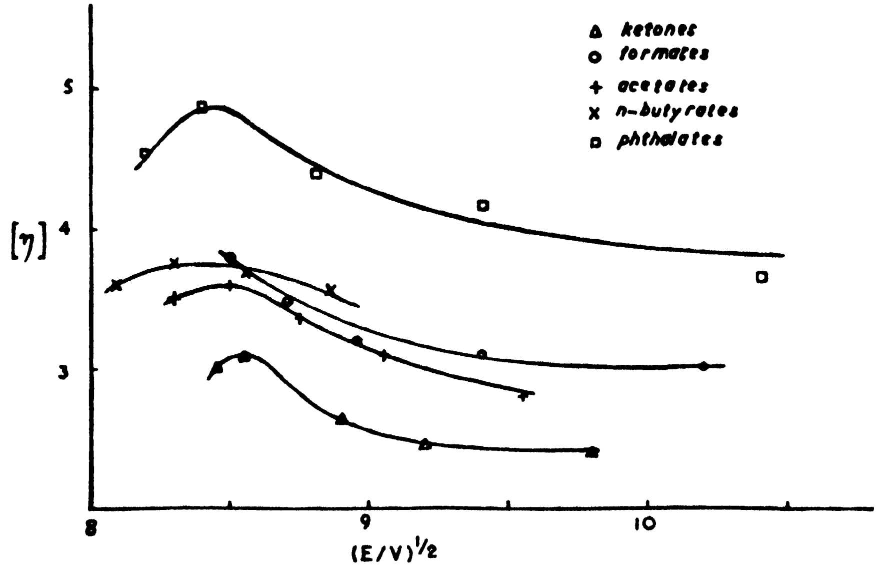

Fig. 9. Intrinsic viscosity as a function of $(E/V)^{1/2}$.

Intrinsic viscosities for each series of solvents are given in Figure 9. Results from *n*-amyl *n*-butyrate, and *n*-nonyl methyl ketone are not included as their solutions deposited gelatinous specks in the viscometer. Solutions of *n*-butyl *n*-butyrate exhibited the same property to a smaller degree. For each series, the intrinsic viscosities vary with solvent $(E/V)^{1/2}$ in a similar way to that observed for precipitation and as illustrated in Figure 9. The initial slopes of the specific viscosity concentration plots were also found to vary with solvent $(E/V)^{1/2}$. Values are given in Table VIII. Solvent type again appears to be important.

Interaction of nitrocellulose and solvent for each series appears to be related to the cohesive energy density of the solvent. Theories developed to account, in at least a semi-quantitative way, for the interaction of nonpolar polymers and liquids relate swelling, the volume of nonsolvent required for precipitation and viscosity to heat of dilution effects and hence, following Hildebrand[19] and Gee,[2] to the cohesive energy density of liquid. Gee, considering that all solvents will produce about the same increase in entropy when imbibed by a polymer to the same extent, has shown that for rubber the degree of swelling is a function of $V_0^{1/2}[(E_0/V_0)^{1/2} - (E_r/V_r)^{1/2}]$ where the subscripts 0 and r refer to solvent and rubber, respectively, V_0 being the molar volume of solvent. Swelling, or other measure of interaction, will be a maximum when this expression is zero, *i.e.*, when E_0/V_0 and E_r/V_r are equal. This correlation of cohesive energy density and interaction applies only when heat is absorbed in mixing. Swelling and solution of nitrocellulose, however, occur exothermally. A tentative explanation, which includes the process of solvation, may be advanced.[20] Consideration of the heat changes involved in swelling or solution of nitrocellulose[21,22] indicate that the first stage in interaction is solvation, occurring with evolution of heat. Solvated chains are then separated or dispersed with the absorption of a smaller amount of heat. Separation of solvated chains may well depend on the same forces as are involved in swelling or dispersion of nonpolar polymers and similar theories should apply. The relationship observed will then be one between cohesive energy density of solvent and interaction of solvated polymer and solvent. The $(E/V)^{1/2}$ value at which interaction is a maximum will, presumably, be that of the solvated polymer. A similar suggestion has recently been made by Spurlin.[23]

At first sight, interaction in solvent-hexane mixtures might be expected to be related to the cohesive energy density of the mixture rather than that of the solvent. Taking the average number of NO_2 groups per C_6 unit as 2.43 for a 12.55% N nitrocellulose, absorption of solvent corresponding to one solvent molecule per NO_2 group leads to a value of 0.709 for N_2. This value is seen to be exceeded at higher concentrations of small solvents, suggesting that solvent molecules are absorbed in excess of those required for solvation. Solvated chains will thus be surrounded by solvent molecules and their separation or dispersion should depend on their interaction with solvent. With larger solvents, where entry is mainly restricted to amorphous regions, similar conditions may exist. Assuming the number of C_6 groups in the amorphous regions to be approximately half the total number,[14] absorption values at the higher solvent concentrations also suggest an excess of solvent molecules over those required for solvation.

The relationship between interaction and cohesive energy density of solvent may thus be tentatively interpreted in terms of interaction between solvent and solvated polymer. Such an interpretation, while certainly a simplification, does explain observed results and links the more recent theories of polymer-solvent interaction with solvation. It also provides an explanation for the well-known variation in solvent power, determined by the precipitant method, as a homologous series of solvents is ascended.[4,24] At this stage, no explanation is offered for the variations in interaction due to solvent type. Similar variations have been reported by Richards[25] for polythene, by Boyer and Spencer[26] for styrene-divinylbenzene gels, and discussed by Gee in the case of rubber.

Entropy effects have not been considered although they must play some part in interaction. Solvation will result in a decrease in entropy of solvent and in swelling this will vary with the extent to which entry into crystalline and amorphous regions of the fiber is permitted. Swelling or dispersion of chains will, however, involve an increase in entropy. The properties of the system acetone-nitrocellulose over the concentration range 0.1–70% nitrocellulose have been discussed by Schulz.[27,28] In the concentration range 20–70% nitrocellulose the entropy term is relatively small compared with the heat term. Recent work[29] suggests that entropy effects are much less in solutions of cellulose derivatives than in solutions of polymers with flexible chains such as rubber and other hydrocarbons. It is hoped to consider these effects and the effects of varying solvent type and nitrogen content of nitrocellulose in a further paper.

The author is indebted to Dr. G. Gee for suggesting the method of estimating the composition of the liquid mixtures, and wishes to thank Dr. R. L. Elliott for stimulating discussion during the course of this work.

References

1. Moore, *Trans. Faraday Soc.*, **43**, 543 (1947).
2. Gee, *Trans. Inst. Rubber Ind.*, **18**, 226 (1943).
3. Kargin and Papkov, *J. Phys. Chem. U. S. S. R.*, **7**, 483 (1936).
4. Doolittle, *Ind. Eng. Chem.*, **36**, 239 (1944).
5. Doolittle, *ibid.*, **38**, 535 (1946).
6. Doolittle, *J. Polymer Sci.*, **2**, 121 (1947).
7. Wadano, *Kolloid Z.*, **93**, 324 (1940).
8. McBain, *Sorption of Gases by Solids*, 1932, p. 371.
9. Samec, in *Colloid Chemistry*. Alexander, ed., Vol. IV, Reinhold, New York, 1932, p. 48.
10. Mason, *Trans. Faraday Soc.*, **16**, 95 (1920).
11. Mardles, in *Colloid Chemistry*. Alexander, ed., Vol. IV, p. 94.
12. Morozov and Panfilov, *J. Gen. Chem. U. S. S. R.*, **9**, 759 (1939).
13. Spurlin, in E. Ott, ed., *Cellulose and Cellulose Derivatives*. Interscience, New York, 1943, p. 886.
14. Mathieu and Petitpas, *Trans. Faraday Soc.*, **B42**, 17 (1946).
15. Desmaroux, *Mém. services poudres*, **1928**, 23.
16. Mangenot and Raison, *Summ. Brit. Cotton Research Assn.*, **20**, 273 (1940).
17. Gee, *Trans. Faraday Soc.*, **40**, 466 (1944).
18. Frith, *ibid.*, **41**, 90 (1945).
19. Hildebrand, *Solubility of Non-electrolytes*. Reinhold, New York, 1936.
20. Moore, *Trans. Faraday Soc.*, **43**, 824 (1947).
21. Nakashima and Saito, *J. Soc. Chem. Ind. Japan*, **38**, 252 (1935).
22. Clement, *Ann. chim.* (12), **2**, 240 (1947).
23. Spurlin, *J. Polymer Sci.*, **3**, 714 (1948).
24. Davidson and Reid, *Ind. Eng. Chem.*, **19**, 977 (1927).
25. Richards, *Trans. Faraday Soc.*, **42**, 20 (1946).
26. Boyer and Spencer, *J. Polymer Sci.*, **3**, 97 (1948).
27. Schulz, *Z. physik. Chem.*, **A184**, 1 (1939).
28. Schulz, *ibid.*, **B52**, 253 (1943).
29. Morey and Tamblyn, *J. Phys. and Colloid Chem.*, **51**, 721 (1947).

Résumé

L'interaction de la nitrocellulose fibreuse avec certains solvants a été étudiée au moyen de l'absorption du solvant dans un mélange de solvant et d'hexane, par l'étude du gonflement et de la dissolution dans de tels mélanges, par la précipitation de la solution par addition d'hexane, ainsi que par des mesures viscosimétriques. Les phénomènes d'absorption et de gonflement font supposer que la pénétration dans les régions amorphes ou cristallines de la fibre est conditionnée par la grandeur des molécules de solvant. Les résultats des mesures de gonflement, de viscosité et de précipitation indiquent une relation entre l'interaction et la densité d'energie de cohésion du solvant. Les théories habituelles des interactions polymère-solvant, applicables aux cas où il y a absorption de chaleur par mélange, peuvent également être appliquées aux interactions entre la nitrocellulose solvatée et le solvant.

Zusammenfassung

Die Wirkung von Faser-Nitrocellulose und Lösungsmittel aufeinander wurde durch Absorption des Lösungsmittels aus Lösungsmittel-Hexan Gemischen, durch Quellung und Lösen in solchen Gemischen, durch Ausfällen aus der Lösung mit Hexan und durch Viskositätsmessungen untersucht. Absorptions- und Quellungsresultate lassen annehmen, dass die Grösse der Lösungsmittelmolekeln von Wichtigkeit ist, indem sie den Eintritt in amorphe oder kristalline Bereiche der Faser bestimmt. Die Resultate von Quellung, Viskosität und Fällung zeigen, dass zwischen der gegenseitigen Einwirkung und der kohäsiven Energiedichte des Lösungsmittels eine Beziehung besteht. Es wird angenommen, dass die bekannten Theorien der Wirkung von Polymer und Lösungsmittel aufeinander, die gültig sind, wenn beim Mischen Wärme absorbiert wird, auch auf die Wirkung von gelöster Nitrocellulose und Lösungsmittel aufeinander angewendet werden können.

Received February 21, 1949

JOURNAL OF POLYMER SCIENCE VOL. V, NO. 1, PAGES 111-120

Molecular Weight Investigations of High Polymers with the Electron Microscope*

BENJAMIN M. SIEGEL,† *Chaim Weizmann Institute of Science, Rehovot, Israel*, and DWIGHT H. JOHNSON‡ and H. MARK, *Institute of Polymer Research, Polytechnic Institute of Brooklyn*

INTRODUCTION

The weight of macromolecules can be determined by the measurement of the osmotic pressure, the scattering of light, and the diffusion and sedimentation rate in the ultracentrifuge. High polymers of molecular weights below 1×10^6 can be adequately characterized with any of the above methods, but definite limitations are encountered with higher molecular weights, except in the case of the ultracentrifuge. The osmotic pressure decreases with increasing molecular weight and the method reaches a practical limit at about 1×10^6. Light scattering also fails to yield accurate results in the high molecular weight range because of the dissymmetry of the scattering.[1] The ultracentrifuge is at present the only method for determining very high molecular weights with any accuracy. However, the method is complicated and time consuming. Thus, another method for measuring molecular weights of very large molecules would be useful if only as a check on the results from the sedimentation-diffusion data obtained with the ultracentrifuge.

The electron microscope offers a possibility for directly measuring the size of molecules if one succeeds in depositing them individually on a screen and if their density can be estimated. The basic problems involved are to make a dispersion of the sample into single molecules and to enhance the low contrast which this type of specimen produces in a normal electron microscope diagram.

The accuracy to which particle diameters of 100 A. can be measured with the electron microscope is small but increases rapidly with the size, and above a molecular weight of approximately 1.5×10^6 is within a useful limit.

Husemann and Ruska were the first to report a comprehensive study of molecular weight measurements from electron micrographs. They used glycogen and iodine substituted glycogen as specimens[2,3] and obtained good agreement with the osmotic molecular weights of 1.5 × 10^6 and 6 × 10^6, respectively.

---

* Portion of thesis submitted by D. H. Johnson to the Polytechnic Institute of Brooklyn, 1948, in partial fulfillment for the degree of Doctor of Philosophy.

† Present address: Cornell University, Ithaca, N. Y.

‡ Present address: Princeton University, Princeton, N. J.

A very interesting study of synthetic polymers with the electron microscope was carried out by Boyer and Heidenreich.[4] Using very dilute solutions (0.1 to 10 p.p.m.) of polychlorostyrene in benzene they precipitated the polymers with propanol and deposited a drop of the suspension on silica membranes. The electron micrographs showed nebular formations with peripheral dispersions of small individual particles of almost circular cross section. They are considered to be single molecules and the molecular weights are calculated assuming that the molecular weight is a function of the square of the diameter of the particle. Postulating even such loosely coiled chains in the precipitated macromolecules, molecular weights were obtained which are four to five times larger than those obtained from light scattering measurements.

It seemed worth while, therefore, to explore whether another method of specimen deposition would furnish better dispersions and whether the recent techniques developed in electron microscopy might not tend to a closer agreement with other methods. Foremost of the advances for this particular problem is the technique of "shadow-casting" developed by Wyckoff and Williams.[5,6] In shadow-casting a thin layer of heavy metal is obliquely evaporated on the specimen and it is the metal layer that produces an image of high contrast which is a topographical representation of the specimen. Thus the electron microscope method no longer need be limited to molecules with heavy atoms and the increased contrast available for all specimens makes it a much more promising technique. Shadow-casting does introduce a limitation, since it prevents the full utilization of the resolving power of the electron microscope, which under ideal conditions has been reported as low as 8.5 10 Å.[7] The best resolution which can be expected after a specimen has been shadow cast is apparently 25 to 30 Å.

EXPERIMENTAL

All electron micrographs were taken with an RCA type EMU electron microscope. The objective pole piece of the instrument was corrected according to the procedure of Hillier and Ramberg,[8] and a self-biased gun was used as the electron source.

The fractions used in this investigation were portions of two polystyrene samples.[9,10] The first was polymerized in emulsion at 63°C. using a persulfate catalyst, whereas the second was polymerized in bulk at 95°C. without catalyst. The two polystyrenes were then fractionated by preferential evaporation of solvent from a solution of the polymers in a solvent-nonsolvent mixture.[11] Table I indicates the solution characteristics of the samples chosen after fractionation.

The basic problem involved in making the electron microscope a useful tool for molecular weight determinations is to obtain a dispersion of the polymeric material into single molecules completely separated from each

TABLE I

Fraction	Osmotic molecular weight	[η] at 30°C
J-3	4.8×10^5	1.46 in toluene
		0.80 in MEK
J-2	1.1×10^6	2.07 in toluene
		1.09 in MEK
J-1	1.8×10^6	3.23 in toluene
		1.37 in MEK
S-1	—	2.03 in MEK (at 28.5°C.)[a]

[a] Molecular weight estimated to be 2.5×10^6.

other. Long-chain polymer molecules in a "good" solvent are stretched out into loose, random coils and as the solvent becomes progressively "poorer" the molecules curl up more and more tightly. The procedure developed here is based on the following consideration: a dilute solution of a polymer in a poor solvent when dispersed into a fine mist will contain but few tightly coiled molecules in each droplet. The probability of aggregation will be small as a result of the very small concentration.

The polystyrene samples were therefore dissolved in the "poor" solvent cyclohexane, which had been triply distilled,* and the solutions were then sprayed onto the collodion film or glass slide using a DeVilbiss #40 Nebulizer.† Most of the droplets have radii ranging between 0.3 and 2 microns.[12] Estimates on the droplet size indicated that the majority of them were about 2 microns in radius, and in determining the optimum dilution, a value was chosen which would allow for an average of between 25 and 50 molecules in each droplet of this size. This number seems to be a satisfactory compromise for obtaining wide dispersion and yet enough particles to observe.

Table II shows the average number of molecules present in droplets 2 microns in radius for a polymer concentration of 1 part per million.

TABLE II

M.W. of fraction	Concn., p.p.m. by wt.	No. molecules per droplet
0.5×10^6	1.0	32
1.0	1.0	16
2.5	1.0	6

From Table II it can be seen that a concentration of 1 p.p.m. would be satisfactory for molecular weights up to 1×10^6, while for the 2.5×10^6 sample about 10 p.p.m. should be used.

---

* In making the initial solutions of fractions J-1 and S-1 it was necessary to use approximately 3% by volume of CCl_4 with the cyclohexane to ensure the solution of the complete fraction.

† It should be noted that the #40 Nebulizer is similar in effect to the technique used by Cravath and co-workers (footnote 13).

A qualitative check on the amount of specimen deposited was performed in the following manner. A glass microscope slide was coated with a thin layer of carbon black by passing through a luminous flame, and an amount of specimen nebulized onto its surface. By an examination of the slide with a superimposed 200-mesh specimen screen under a low-power optical microscope, the number of droplets per square could be counted and then an estimate made of the volume of solution required to adequately cover the specimen screen.

RESULTS AND DISCUSSION

The first specimens were prepared by nebulizing dilute polymer solutions in cyclohexane directly onto collodion substrates and shadowing with uranium.

A blank specimen was prepared to check that the solvent had no observable effect on the membrane and left no insoluble and visible residue. The substrate was shadowed with 3 A. of uranium at an angle of 1:5 to reveal the fine structure. Figure 1 shows a micrograph of a cast collodion substrate upon which the triply distilled cyclohexane solvent has been nebulized. Identical results were obtained when a collodion membrane was shadowed without treating with cyclohexane.

Figure 2 represents a micrograph obtained when fraction J-3 (M.W. = 1.8×10^5) was nebulized onto a collodion substrate using a 1 p.p.m. solution; 3 A. of uranium was employed for shadowing. The particles observed were estimated to be prolate spheroids from a consideration of their cross sections and shadows. The major and minor axes of all particles contained in an area of approximately 4 square microns were measured. A millimeter rule was used in conjunction with a 10 × microscope for measurement of the particles; the measurements were made to the nearest 0.25 mm. (corresponding to 30 A. in the specimen). The diffuseness of the particle edges made a more precise measurement impossible.

The volumes of the particles were then calculated by use of the equation:

$$V = {}^1/_3\pi ab^2$$

where a and b are the major and minor axes, respectively. In the case of Figure 2, the ratios of a/b were approximately 1. Undoubtedly, this resulted from the difficulty of discerning the particles' boundaries with sufficient precision.

A smoothed distribution curve was obtained by graphical differentiation of the cumulative number versus particle volume plot. Figure 6 shows the result for fraction J-3 and Table III gives the particle count and molecular weight calculated from the average volume. The bulk density value of polystyrene (1.06 g./cc.) was assumed for this calculation.

It can be seen that the agreement between the osmotic and electron microscope values is within the experimental error of both methods.

The number of particles counted is too small for a statistical treatment of the data and no special emphasis should be placed on the size distribution for this and the following fractions.

Figure 3 shows a micrograph of fraction J-2 (M.W. = 1.1×10^6) prepared by direct deposition from a 1 p.p.m. solution and shadowed with 3 Å. of uranium. Table IV shows the observed particle count and average molecular weight. A greater eccentricity was obtained than with fraction J-3. Figure 7 gives the number distribution of particle volumes and was obtained in the manner described for the preceding fraction. Again, reasonable agreement is obtained between the two methods.

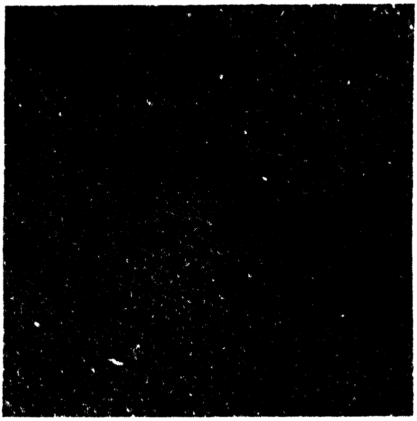

Fig. 1. Blank: collodion film with nebulized cyclohexane solvent. Shadowed with 3 Å. of uranium.

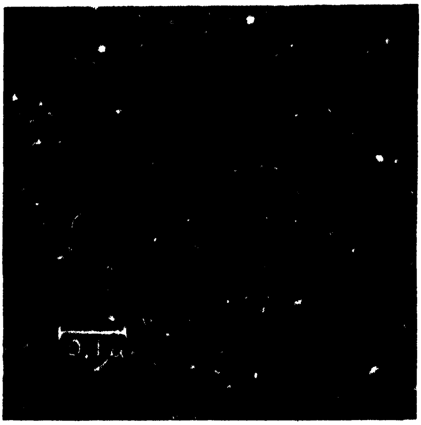

Fig. 2. Molecular dispersion of fraction J-3.

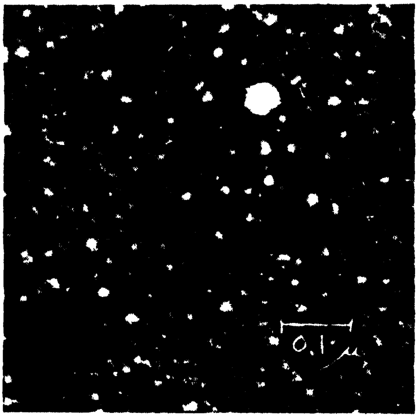

Fig. 3. Molecular dispersion of fraction J-2.

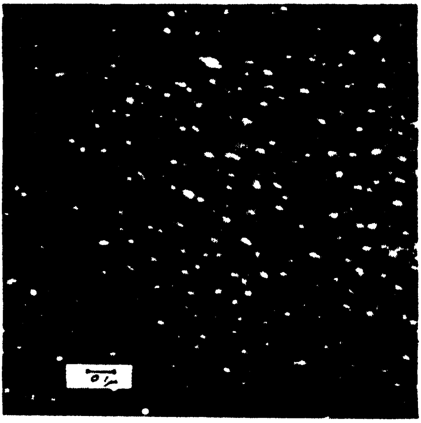

Fig. 4. Molecular dispersion of fraction S-1; preshadowed replica.

Figure 5 shows a micrograph of fraction J-1 (M.W. 1.8×10^6). Only a few molecules have been observed in this particular area of the field, but it

TABLE III

OBSERVED PARTICLE COUNT FOR POLYMER FRACTION J-3

Volume, Å^3 × 10^{-5}	Number of particles counted
30.6	4
22.0	10
14.2	14
9.1	70
3.8	31
Total	*129*

Average volume = 9.3×10^5
Average M.W. = 6.0×10^5
Osmotic pressure M.W. = 1.8×10^5

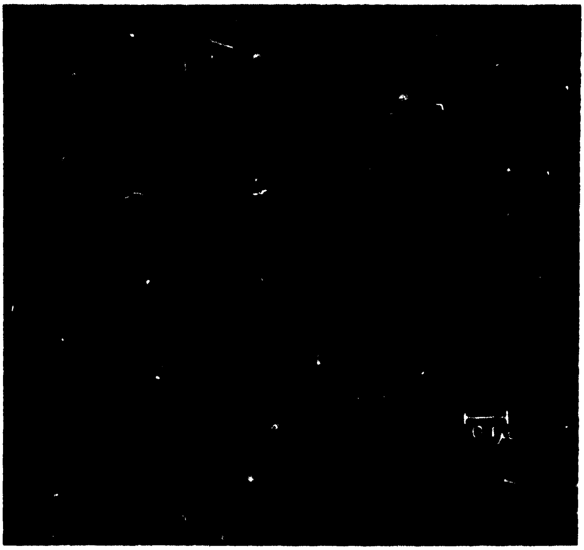

Fig. 5. Molecular dispersion of fraction J-1.

TABLE IV

OBSERVED PARTICLE COUNT FOR FRACTION J-2

Volume, Å^3 × 10^{-5}	Number of particles counted
52.0	4
30.0	21
14.5	83
9.1	41
4.2	16
Total	*165*

Average volume = 15×10^5
Average M.W. = 9.9×10^5
Osmotic pressure M.W. = 1.1×10^6

was found that even on a small count of only 27 particles the slope of the smoothed cumulative number curve gave what may be fortuitously close agreement. Table V gives the measurements on these particles; their size distribution is shown in Figure 8.

TABLE V

OBSERVED PARTICLE COUNT FOR FRACTION J-1

Volume, $Å^3 \times 10^{-6}$	Number of particles counted
1 0	3
1 8	4
2 2	5
3 0	10
5 8	3
7 0	2

Average volume = $3\ 0 \times 10^6$ Å.^{3}
Average M.W. = $1\ 9 \times 10^6$
Osmotic pressure M.W. = $1\ 8 \times 10^6$

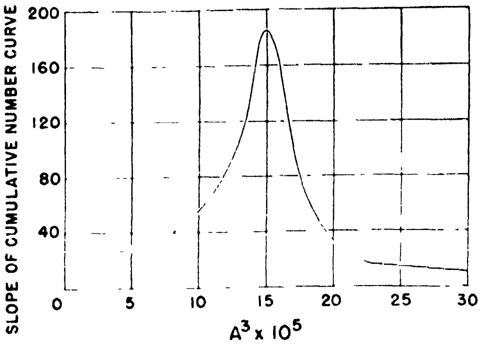

Fig. 6. Observed number distribution of particle volumes for fraction J-3.

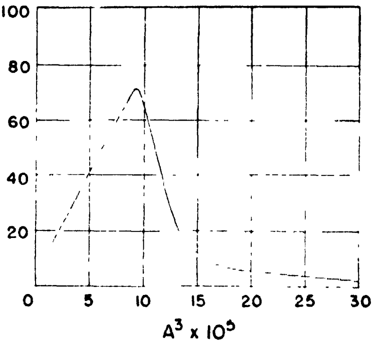

Fig. 7. Observed number distribution of particle volumes for fraction J-2.

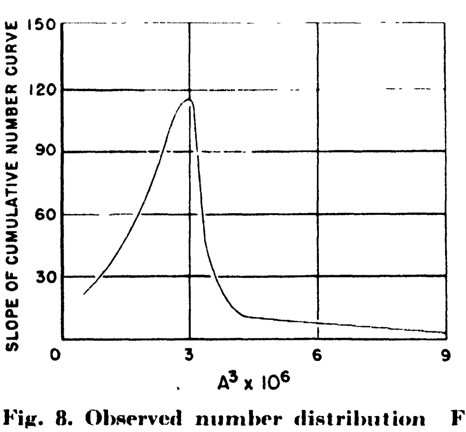

Fig. 8. Observed number distribution of particle volumes for fraction J-1.

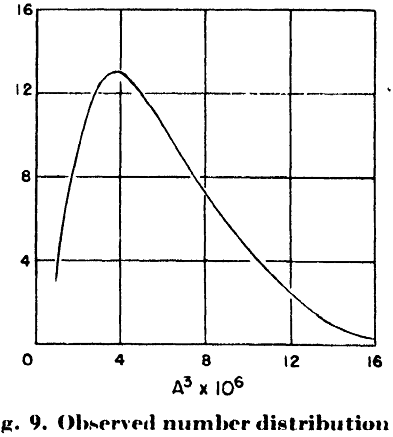

Fig. 9. Observed number distribution of particle volumes for fraction S-1.

Figure 4 is a micrograph of fraction S-1 for which there is only an approximate molecular weight of 2.5 × 10^6 estimated from viscosity measurements. The specimen was nebulized from a 10 p.p.m. solution in cyclohexane. However, in this case, the sample was deposited on a glass slide and pre-shadowed with 5 A. of gold and a collodion replica prepared following the usual procedure.[5,6] In obtaining this micrograph the zero bias gun was used to minimize the granulating of the gold and within the resolution obtained in this image none can be discerned. Table VI gives the observed volume particle count and the molecular weight obtained from the slope of a smoothed cumulative number curve, again assuming bulk density for the particles. The eccentricity observed in these particles is very marked and the ratios of a/b vary from about 1.2 to 2. The particle volume distribution is shown in Figure 9.

TABLE VI

Observed Particle Count for Fraction S-1

Range of volume, $Å^3 \times 10^{-6}$	Number of particles counted	Range of volume, $Å^3 \times 10^{-6}$	Number of particles counted
16.0–17.0	1	7.0–8.0	18
15.0–16.0	0	6.0–7.0	12
14.0–15.0	4	5.0–6.0	11
13.0–14.0	7	4.0–5.0	17
12.0–13.0	2	3.0–4.0	19
11.0–12.0	5	2.0–3.0	12
10.0–11.0	13	1.0–2.0	2
9.0–10.0	11	1.0	1
8.0–9.0	14		

Mean volume = 3.9 × 10^6 $Å^3$
Number-average M.W. = 2.5 × 10^6
M.W. estimated from intrinsic viscosity = 2.5 × 10^6

The background obtained with the directly shadowed collodion substrate is so rough as to seriously limit the measurement of molecules whose weight is less than 5 × 10^5, as can be readily seen in Figures 2, 3, and 5. The pre-shadowed replica technique of Wyckoff and Williams[5,6] as illustrated in Figure 4 unfortunately has serious limitations. When gold is used it reticulates when exposed to the electron beam and cannot be expected to give reliable results. A completely satisfactory metal has yet to be found whose stripping properties and stability to the electron beam would be suitable for use in this technique.

CONCLUSIONS

Molecular dispersions of high polymers can be obtained from very dilute solutions of the polymer in a poor solvent by nebulizing the solution into minute droplets of the order of 2 microns radius. The electron micrographs obtained with these shadow-cast specimens show the molecules to be deposited as prolate spheroids and the agreement of the particle sizes obtained with the molecular weights determined by other methods shows that the bulk density of the polymer can be used in reasonable approximation for the molecules deposited in a virtually "dry" state.

The measurement of molecular weights of polymers by this method is limited at present by two factors, the resolution possible with the electron microscope using the shadow-casting technique, and the structure of the substrate which obscures the smaller particles. Since the diameter of the particles can be measured only to within 25 A., a serious limitation is placed on the accuracy of the measurements, particularly of the smaller molecules and, therefore, reducing the roughness of the substrate would not appreciably improve the method. The method may be said to have a useful lower limit of 0.5×10^6 at present. However, since the accuracy increases rapidly with molecular weight, the region above 1×10^6 can be studied with the electron microscope and a direct method is provided which should be adaptable to a simple procedure for measuring the molecular weight of very high weight fractions of polymers. The improvement in techniques of preparing pre-shadowed replicas, which would not push down the lower limit of usefulness of this method, would at least enable one to observe the presence of the smaller particles and give a better indication of the distribution of molecular weights present.

The authors wish to thank Drs. A. Goldberg and E. Merz who very kindly provided samples of the fractionated polystyrene used in this investigation.

References

1. H. Mark, in *Chemical Architecture* (*Frontiers in Chemistry*, Vol. V). Interscience, New York, 1948, pp. 121–171.
2. E. Husemann and H. Ruska, *Naturwissenschaften*, **28**, 531 (1940).
3. E. Husemann and H. Ruska, *J. prakt. Chem.*, **156**, 1 (1940).
4. R. F. Boyer and R. D. Heidenreich, *J. Applied Phys.*, **16**, 621 (1945).
5. R. C. Williams and R. W. G. Wyckoff, *J. Applied Phys.*, **15**, 712 (1944).
6. R. W. G. Wyckoff and R. C. Williams, *ibid.*, **17**, 23 (1945).
7. J. Hillier, *J. Applied Phys.*, **17**, 307 (1946).
8. J. Hillier and E. G. Ramberg, *J. Applied Phys.*, **18**, 48 (1947).
9. A. Goldberg, *Doctoral Thesis*. Polytechnic Institute of Brooklyn, 1947.
10. E. Mertz, *Doctoral Thesis*. Polytechnic Institute of Brooklyn, 1947.
11. W. J. Badgley, *Doctoral Thesis*. Polytechnic Institute of Brooklyn, 1945.
12. H. A. Abramson, *Ann. Allergy*, **4**, 140 (1946).
13. A. M. Cravath, A. E. Smith, and J. R. Vinograd, *J. Applied Phys.*, **17**, 309 (1946).

Résumé

Le microscope électronique a été utilisé pour estimer le poids moléculaire de quatre fractions de polystyrène, dont les poids moléculaires, determinées par la méthode osmotique et viscosimétriques, s'élevaient à 4.8×10^5, 1.1×10^6, 1.8×10^6, et 2.5×10^6. Leurs solutions diluées (environ un pour mille) dans le cyclohexane ont été déposées en fines gouttelettes, de rayon approximatif de deux microns, sur des substrats de collodion. Par procédé de contraste avec de l'uranium, il a été possible d'observer la dispersion de ces particules sphéroidales élémentaires, obtenues par cetter méthode de dépot. En supposant que chaque particule est constituée d'une molécule, et que leur densité peut être, en première approximation, considérée égale à la densité du polystyrène en bloc, on trouvé des poids moléculaires de 6.0×10^5, 9.9×10^5, 1.9×10^6, et 2.5×10^6, ce qui

concorde dans les limites d'erreur admissibles avec les valeurs obtenues de las pression osmotique et de la viscosité. Le microscope électronique constituerait donc ainsi une méthode utilisable à la caractérisation des macromolecules, dont le poids moléculaire dépasse un million.

Zusammenfassung

Ein Elektronenmikroskop wurde zur Schaetzung der Molekulargewichte von vier Polystyrolfraktionen (die vorher durch osmotische Druckmessungen und Viskositaetsmessungen die Werte 1.8×10^5, 1.1×10^6, 1.8×10^6, und 2.5×10^6 ergaben) angewandt. Verduennte Loesungen (0.0001%) in Cyclohexan wurden in winzigen Troepfchen (von 1 Mikron Durchmesser) auf Kolloidummembranen gebracht. Schattenbeleuchtung mit 3 Å. Uranium ergab den notwendigen Kontrast fuer Beobachtungen der einzelnen, kugelfoermigen Teilchen, die durch diese Bereitungsmethode erhalten wurden. Wenn man annimmt, dass die Teilchen einzelen Molekuele darstellen, und dass ihre Dichte als der Polystyrolmasse gleich bewertet werden kann, ergeben sich Molekulargewichte von 6.0×10^5, 9.9×10^5, 1.9×10^6, und 2.5×10^6, was im Berreich des Versuchsirrtums mit den durch osmotischen Drucke und Viskositaeten erhaltenen Ergebnisse gut übereinstimmt. Das Elektronenmikroskop duerfte deshalb fuer die Bewertung von Makromolekuelen, mit Molekulargewichten, die hoeher als eine Million sind, von Nutzen sein.

Received December 1, 1948

JOURNAL OF POLYMER SCIENCE VOL. V, NO. 1, PAGES 121-137

Method of Measuring Molecular Weight Distribution*

F. W. BILLMEYER, JR., *E. I. du Pont de Nemours & Company, Polychemicals Department, Arlington, New Jersey,* and W. H. STOCKMAYER, *Department of Chemistry, Massachusetts Institute of Technology, Cambridge, Massachusetts*

I. INTRODUCTION

In a recent note, Spencer[1] has emphasized the need for a relatively rapid and inexpensive method of studying molecular weight distributions of polymers and has suggested a simple precipitation method offering this possibility. Briefly, the suggested experimental procedure consists of a series of small-scale, single-step fractional precipitations, in which increasing percentages of the total polymer are precipitated. The masses and average molecular weights of all the precipitates are measured, and from these data the integral or differential distribution curves may in principle be derived.[1,2]

In this paper we describe experimental results obtained with a number of polymethyl methacrylates and also present a brief theoretical discussion of the method. From both experimental and theoretical viewpoints, we have concluded that in practice this method cannot yield a very detailed description of the molecular weight distribution of a polymer; but that a single parameter characterizing breadth of distribution can in fact be obtained with fair precision, both rapidly and inexpensively.

II. THEORY

A. General Considerations

As pointed out by Spencer, any convenient method for determining molecular weight may be used to characterize the precipitates. In this discussion, it will be assumed that weight-average molecular weights are measured.

Let $w(M)$ be the normalized differential weight distribution of the whole polymer; that is, let $w(M)\,dM$ be the weight fraction of polymer with molecular weight in the range M to $M + dM$. Consider now that the polymer is partly precipitated from solution, under such conditions that a fraction $f(M)$ of the polymer of molecular weight M is precipitated. Thus if the whole polymer sample weighs one gram, the precipitate contains $f(M)w(M)\,dM$ grams of molecular weight in the range M to $M + dM$, and the total weight of precipitate is:

---

* Presented at the meeting of the Division of High Polymer Physics, American Physical Society, January 26-29, 1949.

$$x = \int_0^\infty f(M)w(M)\,dM \tag{1}$$

The weight-average molecular weight M_x of this precipitate is given by the relation:

$$xM_x = \int_0^\infty Mf(M)w(M)\,dM \tag{2}$$

As described above, the experiments yield values of x and M_x for a series of precipitates. We have found it convenient to express the results in terms of a new dimensionless quantity z, defined by the equation

$$z = x(M_x - M_w)/M_w = (1/M_w)\int_0^\infty (M - M_w)f(M)w(M)\,dM \tag{3}$$

in which M_w is the weight-average molecular weight of the whole polymer, given by:

$$M_w = \int_0^\infty Mw(M)\,dM \tag{4}$$

In an infinitely sharp fraction, z is always zero, while for a heterogeneous polymer z has a finite value (except for zeros at $x = 0$ and $x = 1$) measuring the breadth of the distribution. Since $f(M)$ is always an increasing function of M, z is always positive. The experiments described later are reported in the form of graphs of z against x.

Now, if the function $f(M)$ were precisely known for the experimental conditions attending every precipitation in the series, solution of the simultaneous linear integral equations (1) and (2) or (3) would yield the differential distribution function $w(M)$. Needless to say, detailed knowledge of $f(M)$ is not readily obtainable, although theoretical considerations[3,4] or experiments with fractions are helpful. In any case, we gain no further understanding of the method as long as $f(M)$ is regarded as an arbitrary function.

Greatest simplicity of interpretation is achieved if an extreme assumption respecting $f(M)$ is adopted[1]; namely, that all polymer molecules of molecular weight exceeding some value M_s are in the precipitate while all smaller molecules remain dissolved. For this special case, which corresponds to precipitation of polymer from infinitely dilute solution,[3,4] equations (1), (2) and (3) become:

$$x^* = \int_{M_s}^\infty w(M)\,dM \tag{5}$$

$$x^*M_x^* = \int_{M_s}^\infty Mw(M)\,dM \tag{6}$$

$$z^* = \int_{M_s}^\infty [(M/M_w) - 1]w(M) \qquad dM \tag{7}$$

where the asterisks (*), as used throughout this paper, denote quantities calculated with this limiting assumption for $f(M)$. When a series of such idealized precipitations is considered, differentiation of equations (5), (6), and (7) yields:[1]

$$M_s = d(x^*M_x^*)/dx^* = M_w[1 + (dz^*/dx^*)] \qquad (8)$$

Thus, a plot of $(1 - x^*)$ against corresponding values of M_s gives the integral weight distribution, and its slope is the differential distribution function $w(M)$.

Whether or not the special relations of equations (5) to (8) are valid, the experimental data we have obtained do not permit accurate evaluation of the distribution function. In fact, a statistical analysis of some of our experiments has shown that the plots of z against x are fitted as well by a parabola as by any other simple function. According to equation (8), the corresponding differential distribution curve is a rectangular box, which has little appeal as a means of expressing the experimental results. Although some improvements over the reproducibility and precision of our work are doubtless attainable, we do not believe they would be sufficiently great to overcome this difficulty, which is fundamentally due to the fact that $w(M)$ is derivable only as the solution of an integral equation.

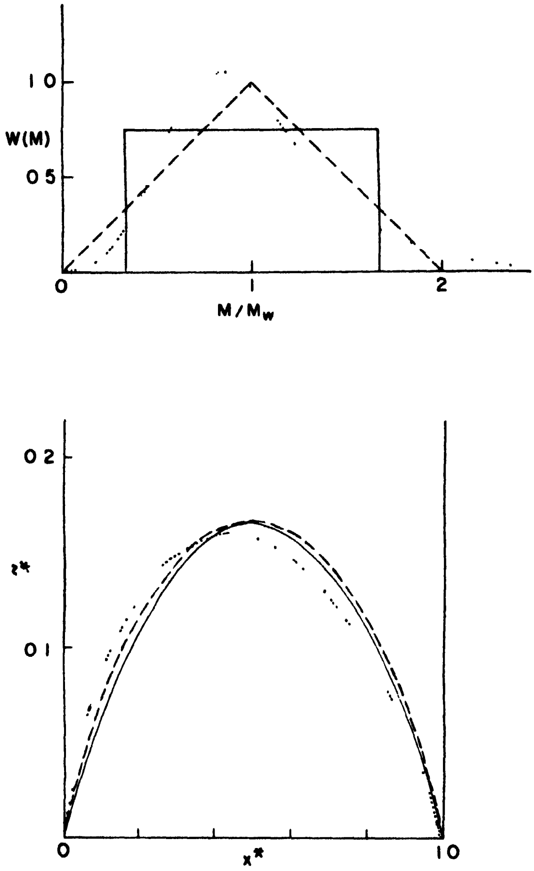

Fig. 1. Some molecular weight distributions and their $z^*(x^*)$ curves.

This means in practice that $z(x)$ would have to be known with virtually analytical precision in order to obtain a well-defined approximation to $w(M)$. Similar situations in other physical problems are well known.[5] To emphasize this point further, Figure 1 shows several differential distribution functions $w(M)$ and their corresponding $z^*(x^*)$ curves, as calculated from equations (5) and (7). Since the examples chosen are obviously somewhat extreme, it is clear that the method cannot be expected to disclose any fine details of the distribution.

Faced with this restriction to more limited results, we can proceed in several possible ways.

(*a*) We can abandon attempts to express the function $w(M)$, and rest content with the $z(x)$ curve itself, gradually acquiring, through sufficient experience, familiarity with this as a measure of distribution. Or perhaps we can translate the principal features of the $z(x)$ curve into more familiar characteristics of a distribution, such as several of its moments, without attempting to construct the complete distribution.

(*b*) Alternatively, we can assume that $w(M)$ follows a definite analytic form involving a small number of disposable parameters. When these parameters are chosen to fit the observed values of $z(x)$, the distribution curve is obtained. The success of this method clearly depends on choosing a function to represent $w(M)$ that is both sufficiently flexible to resemble any likely distributions and sufficiently tractable analytically to permit easy evaluation of $z(x)$ from equations (1) and (3). Procedures of this kind for evaluating molecular weight distributions have often been employed, for example by Lansing and Kraemer,[6] Jullander,[7] Boyer,[8] and Zimm.[9]

In the present work, both methods of attack have been utilized. In the discussion following, the idealized assumption for $f(M)$ is first employed, and the errors caused by this assumption are examined later.

B. A Single Convenient Measure of Breadth of Distribution

The experimental $z(x)$ curves (see Figures 7 to 12) are most definitely characterized by the maximum value of z, hereafter called H. It is possible that sufficiently refined experimental technique would justify the investigation of one or two more parameters, which might well be the half-width of the curve and the value of x at the maximum. However, for the present we deem it best to confine our attention to the parameter H. With the ideal assumption for $f(M)$, equation (8) shows at once that z^* has its maximum when $M_s = M_w$. Thus, from equation (7):

$$H^* = \int_{M_w}^{\infty} [(M/M_w) - 1]w(M)\,dM \tag{9}$$

It is seen that H^* is an incomplete first moment of the distribution about the point M_w, restricted to values of M greater than M_w. By use of equation (4), the above relation can also be written:

$$H^* = \int_0^{M_w} [1 - (M/M_w)]w(M)\,dM \tag{10}$$

which is now the incomplete first moment about M_w restricted to values of

M *less* than M_w. Clearly, H^* is a well-defined, if perhaps unfamiliar, measure of the breadth of a distribution. The experimentally observable quantity H is of course only an approximation to H^*, but, as will be seen later, a fairly satisfactory estimate of H^* can be made.

More familiar expressions of distribution breadth in polymers are the ratios M_w/M_n and M_z/M_w involving the number-, weight-, and z-average molecular weights. Unfortunately, knowledge of H^* does not uniquely fix M_w/M_n or M_z/M_w, and *vice versa*, so that to establish a relationship we must resort to the use of special forms for $w(M)$.

C. Special Distributions

Since the experimental data can be considered to yield only one parameter (H) with accuracy, an analytical expression chosen to represent $w(M)$ must similarly contain just one disposable constant. The function best combining tractability and plausibility is the familiar exponential form:[8–10]

$$w(M)\,dM = \frac{p^n e^{-p}\,dp}{\Gamma(n+1)} \qquad p = (n+1)M/M_w \qquad n > 0 \quad (11)$$

Distributions of this type have frequently been derived theoretically. Thus, for $n = 1$ the above distribution is that predicted for linear condensation polymers[11] and for addition polymers[12] made at low conversion (or under constant environment conditions) with chain termination by radical disproportionation or by chain transfer.[13] The case $n = 2$ corresponds to low-conversion addition polymers with termination by radical combination.[13] Higher values of n are predicted for certain special types of branched polymers[10,14] and also serve to describe fractions.[9]

Values of z^* and x^* are readily found by substitution of equation (11) into equations (5) and (7). Curves of $z^*(x^*)$ for $n = 1$, 2, and 5 are shown in Figure 2. Analytical expressions for H^* and for the molecular weight ratios M_w/M_n and M_z/M_w are given in Table I. From these expressions a plot of H^* against M_w/M_n has been constructed, as shown in Figure 3. Many of the polymers experimentally studied gave H values corresponding to distributions with n near 1 or 2, as expected from their origin. However, the largest value of H^* permitted for this type of distribution is $1/e = 0.368$ (for $n = 0$), while higher values of H are sometimes observed (see Table II). Thus, equation (11) is not sufficient to deal with all polymers, and other forms must sometimes be used.

The other distributions we have treated are listed in Table I. The logarithmic normal form of Lansing and Kraemer:[6]

$$w(M) = Ke^{-y^2} \qquad y = (1/\beta)\ln(M/M_0) \qquad (12)$$

$$1/K = \beta M_0(\pi)^{1/2}e^{\beta^2/4}$$

gives a much larger range of H^* values (up to unity), and a rather different relation of H^* to M_w/M_n. This distribution provides for fewer very small molecules than would be expected in any unfractionated synthetic polymer.

However, it might be used to describe high-conversion polymers that have been reprecipitated repeatedly to remove the fractions of lowest molecular weights.

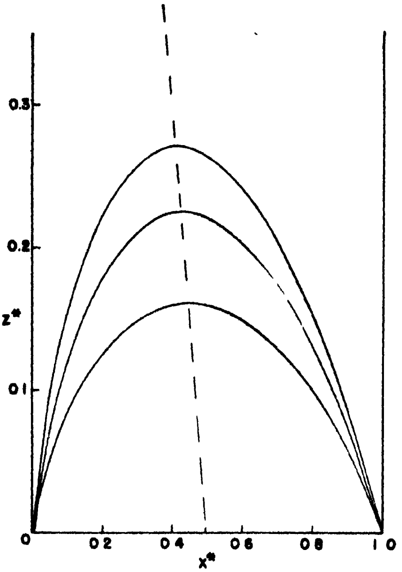

Fig. 2. $z^*(x^*)$ curves for the exponential distribution. Starting from top, curves for $n = 1$, 2, and 5. Broken line is the locus of possible values of H^*.

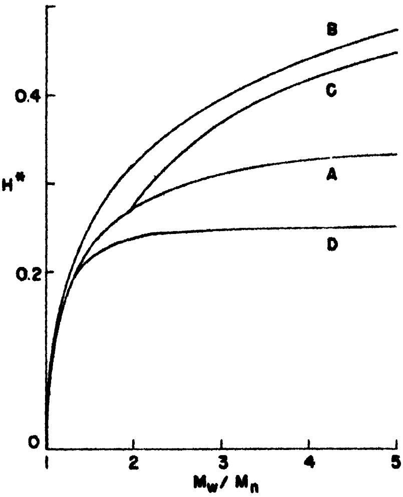

Fig. 3. The relation between H^* and M_w/M_n for various distributions: A, exponential; B, Lansing-Kraemer; C, two-component exponential; D, rectangular.

TABLE I

CHARACTERISTICS OF VARIOUS DISTRIBUTION FUNCTIONS

Distribution	M_w/M_n	M_z/M_w	H^*
A. Exponential, equation 11	$\frac{n+1}{n}$	$\frac{n+2}{n+1}$	$\left(\frac{n+1}{e}\right)^{n+1}/\Gamma(n+2)$
B. Lansing-Kraemer, equation 12	$e^{0.5\beta^2}$	$e^{0.5\beta^2}$	$\frac{2}{(\pi)^{1/2}}\int_0^{\beta/4} e^{-x^2}\,dx$
C. Two-component exponential, equation 13	$\frac{(1+\alpha)^2}{2\alpha}$	$\frac{3(\alpha^2+1)}{(1+\alpha)^2}$	$\frac{1}{2e}\left[\frac{\alpha+3}{\alpha+1}e^{-\alpha}+\frac{1+3\alpha}{1+\alpha}e^{-1/\alpha}\right]$
D. Rectangular, equation 14	$\frac{1}{2a}\ln\left(\frac{1+a}{1-a}\right)$	$1+\frac{a^2}{3}$	$\frac{a}{4}$

A distribution of possible merit in dealing with high-conversion addition polymers is a two-component exponential form:

$$w(M) = {}^1/_2\lambda^2 M(e^{-\lambda M} + \alpha^2 e^{-\alpha\lambda M}) \tag{13}$$

corresponding to equal parts by weight of two simple exponential distributions, each with $n = 1$. Many objections can easily be raised to this somewhat artificial expression, but it remains a relatively simple form with just one disposable parameter α. It should be noted that this distribution possesses but a single maximum, whatever the value of α.

The final distribution considered is the highly artificial rectangular box:

$$\begin{aligned} w(M) &= 1/(2aM_w) \text{ for } M_w\,(1-a) \leqq M \leqq M_w\,(1+a) \qquad (14) \\ &\equiv 0, \text{ elsewhere} \end{aligned}$$

This case is included only to examine further the sensitivity of H^* to the form of the distribution curve for a given value of M_w/M_n. As seen in Figure 3, this sensitivity is small when the distribution is narrow. Thus, for $M_w/M_n < 1.5$ there is very little difference between the exponential and box distributions, and even the Lansing-Kraemer curve is not markedly different up to this point. The exponential distribution is of course the most plausible because of its theoretical background, and we have preferred to use it for all polymers yielding H^* values of 0.27 (corresponding to $n = 1$) or less. For broader distributions, the several functions differ considerably, and there is less theoretical support for any one function. Further discussion of these cases is deferred until the experimental results are considered.

D. Fractionation Errors

As earlier stated, an exact treatment of the experimental data would require complete knowledge of the fractionation-factor $f(M)$, which describes the partition of each polymeric species between precipitate and solution. For our purpose, it is sufficient to consider the difference between the maximum value H^* of the idealized function $z^*(x^*)$ and the maximum value H of the experimental $z(x)$ curve. Fortunately, it is necessary to make only one very general assumption respecting $f(M)$ in order to achieve a satisfactory estimate of this difference.

Current theories of polymer solutions[3,4] indicate that the equilibrium distribution ratio of a polymer species between two phases is an exponential function of molecular weight within a homologous series of polymers; that is:

$$\ln (c'/c) = \alpha M \qquad (15)$$

where c' and c denote volume concentrations, in precipitate and solution respectively, of the polymer species of molecular weight M. The coefficient α depends in a complicated way on temperature and on the concentrations of all species in each phase, but this dependence need not be considered here. The justification of equation (15) is not based exclusively on theoretical considerations; it can be deduced by means of the Gibbs-Duhem equation from the experimental principle that osmotic pressures of polymer solutions depend on molecular weight only through the ideal van't Hoff term RTc/M. This principle, though not exact, receives general experimental support except for very high polymers, for which deviations are also expected on theoretical grounds.[15] In any case these deviations would only reduce the dependence on molecular weight to an effective power somewhat less than the first. Thus, while no very direct evidence exists for equation (15), it may be used with some confidence.

If now the actual volumes of precipitate and solution are V' and V, respectively, the function $f(M)$ is seen to be:[3,4]

$$f(M) = c'V'/(cV + c'V') = re^{\alpha M}/(1 + re^{\alpha M}) \qquad (16)$$

with $r = V'/V$. The unknown factor α can be eliminated by expressing it in terms of the molecular weight M_c of that polymer species which is just half precipitated. By setting $f(M_c) = 1/2$, one obtains:

$$\alpha M_c = \ln (1/r) \qquad (17)$$

Thus, for precipitation from very dilute solutions α would approach zero, $f(M)$ would approach the step-function previously used, and M_c would become identical with M_s.

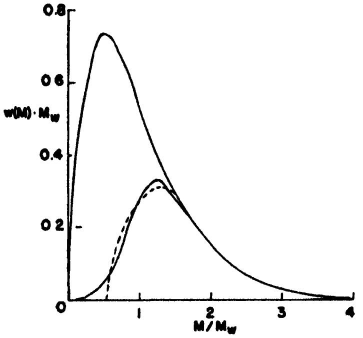

Fig. 4. Fractionation on precipitation. Solid lines: upper, whole polymer; lower, precipitate (equation 16). Broken line, precipitate (equation 18).

With equations (16) and (17) and a chosen value of r, calculations of $z(x)$ can be made by means of equations (1) and (3) for any chosen distribution-function $w(M)$. However, the form of equation (16) is not such as to yield simple analytical expressions for z and x. Consequently, we have made more use of the linear form:

$$\begin{aligned} f(M) &= 0 && \text{for } M < M_c(1 - b) \\ &= 1/2 + (M - M_c)/2bM_c && \text{for } M_c(1 - b) \leqq M \leqq M_c(1 + b) \qquad (18) \\ &= 1 && \text{for } M > M_c(1 + b) \end{aligned}$$

This approximation gives adequate resemblance to the predictions of equation (16) if the parameter b is properly chosen. We have arbitrarily required the two functions to give identical values for $f(M) = 0.1$ and 0.9, and thus obtained the relation:

$$b = (\log 9)/0.8 \log (1/r) = 1.2/\log (1/r) \qquad (19)$$

In our experiments, the dilution is such as to maintain the value of r at 0.01 or less. Consequently, an estimated value of $b = 0.5$ appears reasonable.

In Figure 4, these concepts are illustrated for a precipitation from an exponentially distributed polymer ($n = 1$), with $M_c = M_w$. The upper full curve shows the distribution-function $w(M)$ of the whole polymer, and the two lower curves give the distribution in the precipitate, $f(M)w(M)$. Of these, the full curve was calculated from equations (16) and (17) with $\alpha M_c/2.3 = 2.4$, and the broken line curve from equation (18) with $b = 0.5$. The two curves are related through the condition of equation (19). It is seen that except for very low polymer species the error made in using equation (18) is not large. This has been confirmed by several calculations of z and x.

Independent justification for the choice $b = 0.5$ is furnished by the observation that in the above example the precipitate distribution $f(M)w(M)$ can be closely approximated by an exponential distribution with $n = 5$. Exactly this distribution was recently chosen by Zimm[9] as descriptive of a singly precipitated and large polymer fraction.

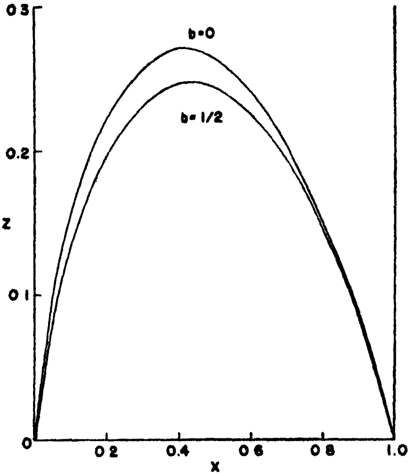

Fig. 5. $z(x)$ for the exponential distribution ($n = 1$) and several values of b.

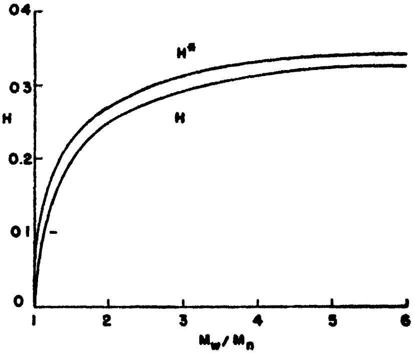

Fig. 6. H and H^* versus M_w/M_n for the exponential distribution.

For the exponential distributions of equations (11), a number of calculations with equations (1) and (3) have been made. Working first with the familiar case $n = 1$, we found that H could be evaluated with negligible error by setting M_c equal to M_w, at least for all values of b up to unity. For $n = 1$, the complete $z(x)$ curve with $b = 0.5$ is shown in Figure 5 compared to $z^*(x^*)$. It is seen that H is about 0.25, as compared to $H^* = 0.27$ for this distribution. For arbitrary values of n, H was calculated approximately by expanding in series and neglecting powers of b beyond the third. The simple result is

$$\frac{H^* - H}{H^*} = \frac{(n+1)b^2}{6} \cdots \qquad (20)$$

which gives excellent agreement with the more complete calculations for the case $n = 1$.

Equation (20) permits the translation of observed values of H in values of H^*, provided b is known. As stated earlier, we estimate $b = 0.5$ for our experiments, and this figure receives some support from the data, as will be seen. In Figure 6, a curve of H as a function of M_w/M_n for the exponential distributions is shown, for $b = 0.5$. It is seen that the difference between H and H^* is greatest for the sharper distributions, but amounts to only 0.02 or less for unfractionated polymers.

Again to investigate dependence on the detailed form of $w(M)$, calculations for the box distribution and for one example of equation (13) were also made. As might be expected, the magnitude of $(H^* - H)$ depends noticeably only on the values of b and H^* and not on any further detail. For values of H above 0.25, a uniform correction (to the nearest hundredth) of 0.02 is obtained.

It is to be noted from equation (20) that the correction to H is proportional to b^2. Thus, for the present method no less than for more complete fractionations, work with dilute solutions is imperative.

E. Other Molecular Weight Methods

The foregoing discussions are based on the supposition that weight-average molecular weights of the whole polymer and the separate precipitates are measured. If number averages are determined, the analysis need not be repeated. It is only necessary to replace $w(M)$ by the number- or mole-fraction distribution $N(M)$, M_w by M_n, and M_z by M_w, wherever these occur. Correspondingly, the weight of the precipitate is given by the quantity xM_x, the precipitate containing x moles of polymer and having a number-average molecular weight M_x. It should be pointed out, however, that the low-molecular weight "tail" of the precipitate,[4] as seen for example in Figure 4, causes much larger differences between H^* and H if number-average rather than weight-average molecular weights are measured.

III. EXPERIMENTAL

A. *Preparation of polymers*

Three sets of methyl methacrylate polymers were used in the distribution experiments. One series was dispersion polymerized, with benzoyl peroxide as catalyst, at nearly constant temperatures in the neighborhood of 100°C. This method of polymerization, in which the methyl methacrylate monomer is dispersed in the form of small droplets in water, has been described and discussed from a kinetic standpoint by Trommsdorff.[18] These polymers are designated A–D, H, K, O, and P. Polymer Y also was made in this way but had been dissolved in acetone and precipitated with methanol before being used; the others had no preliminary treatment. Polymer M was a fraction from polymer H. The fractionation was carried out some time ago in this laboratory* by precipitation of the polymer from acetone solution by the addition of hexane. The sample was separated into twelve primary fractions, of which M was one. It contained some fourteen per cent of the total material.

Two other sets of polymers were made by a bulk photopolymerization technique similar to that used by Cohen.[17] Polymers T and W were precipitated from the partially polymerized monomer at conversions of about fifteen per cent by the addition of methanol. Polymers E, X, and Z were prepared by allowing similar polymerizations to go to completion. Unpublished work done in this laboratory has indicated that these photopolymerizations follow the kinetics described by Trommsdorff,[16] Schulz and Harborth,[18] and Tong and Kenyon[19] for thermally initiated reactions. These polymerizations were not isothermal.

Two other polymers, L and B–C, have been included in the discussion (despite the fact that details of their preparation are not at hand) because of the availability of measurements of molecular weight made upon them.

B. Reagents

Acetone and methanol were Mallinckrodt's Analytical Reagent grade. Hexane (normal) was obtained from the American Mineral Spirits Company and was distilled through a Vigreux column before being used. Molecular weight measurements made at this laboratory were run in reagent-grade ethylene dichloride obtained from Paragon Testing Laboratories (now Paragon Division of The Matheson Company, Inc.).

C. Viscosity Measurements

(Viscosity and light-scattering measurements were made in this laboratory by A. M. Trzcinski.) These were carried out in ethylene dichloride solution in modified Ostwald viscometers at 25°C. Corrections for kinetic energy and shear rate were found to be insignificant; efflux times for the solvent were over 200 seconds. At first, intrinsic viscosities were estimated from measurements at several concentrations and extrapolation of the functions η_{sp}/c or $\ln \eta_{rel}/c$ to zero concentration; later the functions described[20] by one of us to estimate intrinsic viscosity were used.

D. Measurements of Light Scattering

The viscosity–molecular weight relationship for polymethyl methacrylates in ethylene dichloride has been investigated in this laboratory using light-scattering equipment developed by one of us (F. W. B.). It is hoped to publish the details of this work later. The resulting equation, $M = 3.8 \times 10^5[\eta]^{1.8}$, was used to convert viscosities to molecular weights. For polymers whose molecular weight was not determined directly by light scattering, the viscosity-average molecular weights from this formula have been converted to weight-average molecular weights by computations based upon the distributions of equation (11) (for $M_w/M_n < 2$) or equation (13) (for $M_w/M_n > 2$), using the value of M_w/M_n estimated from H^*.

---

* "This laboratory" denotes the Chemical Division Laboratory of the Polychemicals Department, E. I. du Pont de Nemours & Company, at Arlington, New Jersey.

E. Measurements of Osmotic Pressure

Some measurements of osmotic pressure were carried out by H. C. Lauterbach and D. L. Cleveland of the Massachusetts Institute of Technology, Plastics Research Laboratory; others by J. B. Nichols at the Chemical Department, Experimental Station, E. I. du Pont de Nemours & Company. Each group made measurements on benzene solutions of the polymers in small osmometers similar to those described by Zimm and Myerson[21] (at M. I. T.) and by Schulz[22] and Ewart[23] (at du Pont).

F. Fractionation Procedure

The experiments were run with the polymer dissolved in acetone and with hexane as the precipitant. It is quite possible that other solvent-precipitant systems (notably benzene-cyclohexane) might be more suitable. No effort was made to explore these possibilities.

The polymer solutions were made up to approximately 4 grams per 100 cc., except for polymers of very high molecular weight, which were used in more dilute solutions. The exact concentration was determined by evaporating portions to dryness. These solutions were further diluted 1:4 (if less than half of the total polymer was to be precipitated) or 1:8 (if more than half) with the additional acetone added in whole or in part to the hexane. The size of the sample was dictated by the requirement that sufficient polymer be precipitated for the subsequent viscosity measurement.

A few runs, for example on polymers A–D, E, and H, were carried out over the whole range of precipitation from $x = 0$ to $x = 1$. Later, when it was found desirable to obtain H instead of the whole curve, only a few experiments designed to fall between $x = 0.25$ and $x = 0.65$ were run. With experience it was possible to predict the proper amount of hexane to use; otherwise some preliminary experiments were performed.

The stock solutions and acetone–hexane mixtures were warmed to about 40°C. and mixed. The efficiency of the separation and the accuracy of the experiments are without doubt dependent upon the manner in which the precipitation is carried out. Every effort was made to mix the solution slowly and evenly and to avoid agglomeration of the precipitate. Working in dilute solutions and at a temperature above the final one, and diluting the precipitant with acetone, were all steps in this direction. The actual precipitation was carried out by adding the precipitant dropwise from a buret into the violently agitated solution.

The flasks then stood 24 hours at 25°C., after which the supernatant liquid was removed, and the polymer dissolved in a small amount of acetone and reprecipitated in a finely divided form by adding ten volumes of methanol. It was dried overnight in tared porous porcelain crucibles in a vacuum oven at 80°C. and weighed. Samples were then removed for the viscosity determination.

A polymer sample of four to six grams was used. The total elapsed time for one sample was three working days, but a number of samples could be run simultaneously, particularly by starting them on subsequent days.

IV. RESULTS

The experimental results for fourteen polymethyl methacrylates are summarized in Table II and in Figures 7 to 12. The table gives the weight-average molecular weight of the sample (by light scattering when available; otherwise by viscosity); the value of H from the distribution experiments; the value of H^* estimated from H through Figure 6, and using a uniform correction of 0.02 for all high values of H; the corresponding value of M_w/M_n derived from Figure 6 (which assumes the exponential distribution) for all H^* below 0.27 or from curve C of Figure 3 (which assumes the two-component exponential distribution) for all greater values of H^*; the osmotic molecular weight M_n when available; and in these cases the

TABLE II

MOLECULAR WEIGHT DISTRIBUTION DATA FOR POLYMETHYL METHACRYLATES

Polymer	M_w	H	H^*	M_w/M_n from H^*	M_n	M_w/M_n
A. FRACTIONATION						
M[a]	153,000	0.12	0.16	1.2	126,000	1.2
H	220,000	0.31	0.33	2.6	—	—
B. DISPERSION POLYMERS						
Y[b,c]	185,000	0.24	0.26	1.9	(71,000)	(2.6)
O	163,000	0.26	0.28	2.1	—	—
P	192,000	0.27	0.29	2.2	-	—
K	186,000	0.29	0.31	2.3	—	—
A-D	150,000	0.35	0.37	3.0	—	—
C. PHOTOPOLYMERS, LOW CONVERSION						
T	156,000	0.24	0.26	1.9	73,000	2.1
W[d]	178,000	0.25	0.27	2.0	98,000	1.8
D. PHOTOPOLYMERS HIGH CONVERSION						
X	2,050,000	0.35	0.37	3.0	—	—
Z	1,440,000	0.45	0.47	6.0	174,000	8.3
E	715,000	0.48	0.50	10.0	—	—
E. MISCELLANEOUS POLYMERS						
L	130,000	0.25	0.27	2.0	64,000	2.0
B-C	125,000	0.23	0.25	1.8	64,500	1.9

[a] Viscosity was measured in benzene at M. I. T. The molecular weight was calculated by an equation derived at M. I. T. from osmotic pressure work on a fractionated polymer.

[b] This polymer had been dissolved and reprecipitated before being used.

[c] The values in parentheses are considered doubtful.

[d] These osmotic measurements were carried out at du Pont; the others at M. I. T.

ratio M_w/M_n calculated from the osmotic and light-scattering measurements. In the figures the solid lines represent smooth curves through the experimental points, and the broken line represents the theoretical curve for the exponential distribution with $n = 1$ and $b = 0.5$, for purposes of comparison.

A. Fractionation

The experiments on the parent polymer, H, and its fraction, M, show clearly that the method gives results which are qualitatively correct. M has a distribution just about as wide as might have been expected from its origin, and there is good agreement between the value of M_w/M_n from direct measurement and that derived from H^* assuming the exponential-type distribution function.

B. Dispersion Polymers

The distribution breadths of these polymers are not unreasonable in view of the kinetics reported for this type of reaction.[16,18,19] Polymer Y has a distribution somewhat narrower than those of the others, reflecting the preliminary solution and methanol precipitation it had received; other work in this laboratory has shown that a considerable fraction of the polymer with molecular weight below 30,000 to 50,000 is left in acetone solution on the addition of methanol. The points for Polymer A-D represent two sets of experiments within each of which the exact methods of precipitation were varied somewhat in an effort to find the optimum conditions. We believe that this accounts in part for the spread in the experimental points.

C. Low-Conversion Photopolymers

These polymers are of particular interest because of the possibility of predicting in advance the values of M_w/M_n to be expected. If, as Wales *et al.*[24] suggest, the chain termination takes place by radical disproportionation, one would expect polymer formed initially to have $M_w/M_n = 2$; and this value should increase slowly up to the point where the explosive increase in reaction velocity occurs. Thus, these photopolymers which were taken from the reaction mixture at low conversions might be expected to have M_w/M_n near 2. Both measurements of H and direct measurements of M_w and M_n bear out this expectation.

D. High-Conversion Photopolymers

The tremendous increase in distribution breadth accompanying the explosive reaction described by Schulz[18] and Trommsdorff[16] is well exemplified by these polymers.

We believe that the peculiar double-peaked distributions for this type of polymer Trommsdorff has reported are probably not real.

The concept that these polymers are made up, broadly speaking, of two exponential-type distributions arising from the polymer formed before and

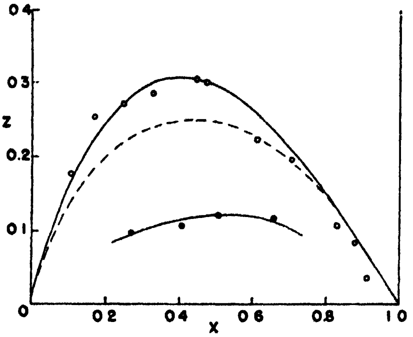

Fig. 7. Experimental $z(x)$ curves for a fraction, *M* (●), and its parent polymer, H (○).

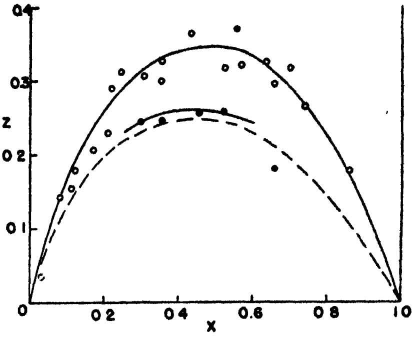

Fig. 8. Experimental $z(x)$ curves for some dispersion polymers. ○, polymer A–D; ●, polymer O.

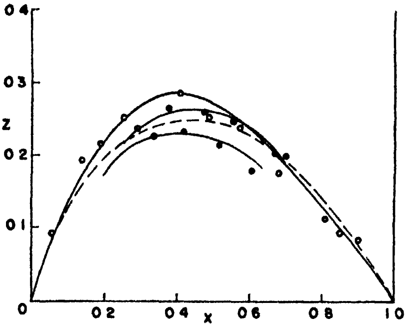

Fig. 9. Experimental $z(x)$ curves for some dispersion polymers. ○, polymer K; ◒, polymer P; ●, polymer Y.

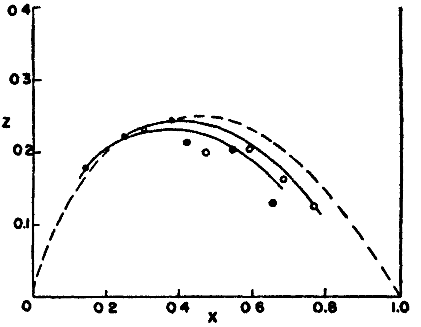

Fig. 10. Experimental $z(x)$ curves for some low-conversion photopolymers. ○, polymer W; ●, polymer T.

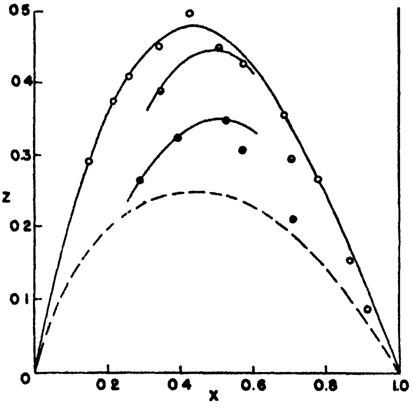

Fig. 11. Experimental $z(x)$ curves for some high-conversion photopolymers. ○, polymer E; ◒, polymer Z; ●, polymer X.

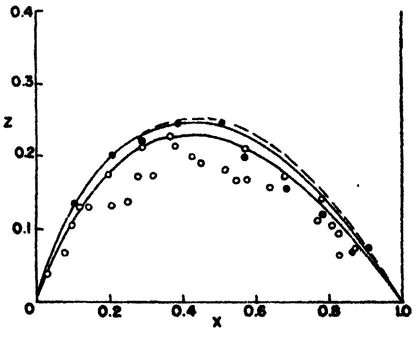

Fig. 12. Experimental $z(x)$ curves for some miscellaneous polymers. ○, polymer B–C; ●, polymer L.

after the explosive increase in reaction rate gives some theoretical justification to the use of the two-component exponential distribution (equation 13) in computing M_w/M_n from H^* for these polymers. And the fact that for Polymer Z this value of M_w/M_n is in good agreement with that obtained from the weight- and number-average molecular weights is in line with this reasoning. A further piece of evidence on this point is the observation of Lauterbach,[25] based upon fractionation experiments, that M_w/M_n for a thermally initiated (peroxide-catalyzed) high-conversion polymethyl methacrylate is between 7 and 8.

We wish to thank R. S. Spencer for communicating to us privately the contents of his note[1] concerning this method, and we wish to thank for their assistance in making the measurements of osmotic pressure and light scattering the following: Miss A. M. Trzcinski of the Polychemicals Dept. and Miss B. L. Price and J. B. Nichols of the Chemical Department of the du Pont Company, and Mrs. D. L. Cleveland and H. C. Lauterbach of the Plastics Research Laboratory, Massachusetts Institute of Technology.

References

1. R. S. Spencer, *J. Polymer Sci.*, **4**, 606 (1948).
2. F. T. Wall, *J. Am. Chem. Soc.*, **67**, 1929 (1945).
3. P. J. Flory, *J. Chem. Phys.*, **12**, 425 (1944).
4. R. L. Scott, *ibid.*, **13**, 178 (1945).
5. For two examples, see S. C. Collins and F. G. Keyes, *J. Phys. Chem.*, **43**, 5 (1939), and S. H. Bauer, *J. Chem. Phys.*, **7**, 1097 (1939).
6. W. D. Lansing and E. O. Kraemer, *J. Am. Chem. Soc.*, **57**, 1369 (1935).
7. I. Jullander, *J. Polymer Sci.*, **2**, 329 (1947).
8. R. F. Boyer, *Ind. Eng. Chem., Anal. Ed.*, **18**, 342 (1946)
9. B. H. Zimm, *J. Chem. Phys.*, **16**, 1099 (1948).
10. G. V. Schulz, *Z. physik. Chem.*, **B44**, 227 (1939).
11. P. J. Flory, *J. Am. Chem. Soc.*, **58**, 1877 (1936).
12. G. V. Schulz, *Z. physik. Chem.*, **B43**, 25 (1939).
13. E. F. G. Herington and A. Robertson, *Trans. Faraday Soc.*, **38**, 490 (1942).
14. J. R. Schaefgen and P. J. Flory, *J. Am. Chem. Soc.*, **70**, 2709 (1948).
15. B. H. Zimm, *J. Chem. Phys.*, **14**, 164 (1946).
16. E. Trommsdorff, H. Kohle, and P. Lagally, *Die makromol. Chem.*, **1**, 169 (1948).
17. S. G. Cohen, B. E. Ostberg, D. B. Sparrow, and E. R. Blout, *J. Polymer Sci.*, **3**, 264 (1948).
18. G. V. Schulz and G. Harborth, *Die makromol. Chem.*, **1**, 106 (1947).
19. L. K. J. Tong and W. O. Kenyon, *J. Am. Chem. Soc.*, **67**, 1278 (1945).
20. F. W. Billmeyer, Jr., *J. Polymer Sci.*, **4**, 83 (1949).
21. B. H. Zimm and I. Myerson, *J. Am. Chem. Soc.*, **68**, 911 (1946).
22. G. V. Schulz, *Z. physik. Chem.*, **A176**, 317 (1936).
23. D. M. French and R. H. Ewart, *Anal. Chem.*, **19**, 165 (1947).
24. M. Wales, J. W. Williams, J. O. Thompson, and R. H. Ewart, *J. Phys. & Colloid Chem.*, **52**, 983 (1948).
25. H. G. Lauterbach, unpublished work at the M. I. T. Plastics Research Laboratory.

Résumé

En se basant sur une suggestion de Spencer, une méthode d'estimation de la largeur de la distribution des poids moléculaires d'un haut polymère a été élaborée. Une solution de polymère est divisée en parties aliquotes, et une partie du polymère est précipitée dans chaque aliquote par addition d'un non-solvant, de telle sorte que toute la gamme est couverte depuis la solution complète jusqu'à la précipitation totale. Le poids et le

poids moléculaire moyen en poids de chaque précipité sont déterminés. De ces résultats, la largeur de la distribution est estimée en fonction d'un paramètre *H*, représentant l'écart de la distribution de celle d'une espèce moléculaire simple. Dans la partie théorique, *H* est rapportée à d'autres paramètres de la largeur de la distribution, tels que le rapport M_w/M_n, pour quelques fonctions de distributions, analytiquement bien connues. Une série d'expériences avec le polyméthacrylate de méthyle est décrite et les résultats sont discutés en rapport avec la cinétique de polymérisation. Des déterminations de pression osmotique et de la diffusion de la lumière ont été effectuées pour l'évaluation directe de M_w/M_n. Ces valeurs se rapprochent des valeurs M_w/M_n obtenues au départ de *H*. Les erreurs possibles, tant du point de vue théorique que du point de vue expérimental sont discutées.

Zusammenfassung

Auf den Vorschlag von Spencer gestützt, wurde eine Methode zur Abschätzung der Breite der Molekulargewichtsverteilung eines Hochpolymeren angegeben. Eine Polymerlösung wird in gleiche Portionen geteilt und das Polymer in jeder Portion durch Zugabe von Nichtlösungsmitteln teilweise ausgefällt, sodass der Bereich von völliger Lösung bis zu völliger Fällung ausgefüllt ist. Die Menge und das mittlere Molekulargewicht (weight average) wurde von jedem Niederschlag gemessen. Aus diesen Daten wird die Verteilungsbreite abgeschätzt, ausgedrückt durch einen Parameter *H*, der die Abweichung dieser Verteilung von der einer einheitlich molekularen Art darstellt. Im theoretischen Teil wird *H* zu anderen Parametern der Verteilungsbreite in Verbindung gebracht, z.B. M_w/M_n, für einige wohlbekannte analytische Verteilungsfunktionen. Eine Reihe von Versuchen mit Polymethyl-methacrylaten ist beschrieben, und die Resultate werden mit Bezugnahme auf die Polymerisationskinetik diskutiert. Bestimmungen des osmotischen Drucks und der Lichtstreuung wurden ausgeführt, um M_w/M_n direkt zu bestimmen. Diese Werte sind gut mit aus *H* geschätzten M_w/M_n Werten vergleichbar. Fehlerquellen in der theoretischen als auch in der praktischen Behandlung werden diskutiert.

Received April 1, 1949

JOURNAL OF POLYMER SCIENCE VOL. V, NO. 1, PAGES 139–142

LETTERS TO THE EDITORS

Concentration Dependence of Diffusion of Chloroform in Polystyrene

Crank and Park[1] have recently calculated the diffusion coefficient for chloroform in polystyrene from the rate of sorption and desorption. As is typical in diffusion experiments, the concentration varied from point to point in the specimen so that the diffusion constant calculated is an average value. By mathematical analysis of their data, however, they were able to calculate to a reasonably good approximation the actual concentration dependence of the diffusion constant.

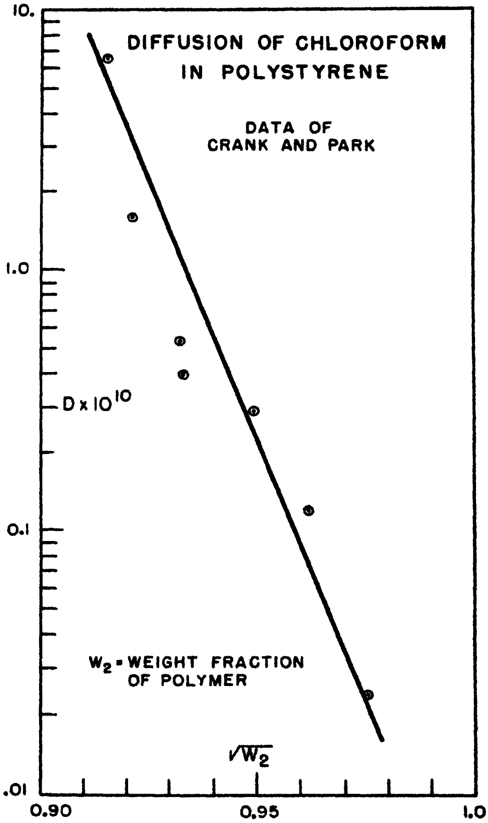

Fig. 1. Diffusion of chloroform in polystyrene (data of Crank and Park).

We were recently concerned with this same problem in connection with the diffusion of plasticizers in polyvinyl chloride.[2] By assuming that the diffusing molecule encountered a local viscous resistance, which varied as the melt viscosity of the polymer–solvent mixture, we obtained the relation:

$$\log D = A - B(\omega_2)^{1/2} \qquad (1)$$

where D is the diffusion constant at a given concentration, ω_2 is the weight fraction of polymer, and A and B are constants. Figure 1 shows the application of this equation to the calculated data of Crank and Park. The fit of the points is not as good as would be desired, but on the whole describes the behavior fairly well. A plot of log D versus weight fraction of polymer is somewhat poorer. As Crank and Park show in the accompanying letter, log D is linear in the volume fraction of plasticizer, and this is mathematically equivalent to equation (1) at low concentrations of plasticizer.[3] The fact that equation (1) has now been shown to apply to two sets of data suggests that it merits further attention for describing the functional dependence between diffusion and concentration. Moreover, this equation emphasizes how strongly the diffusion constant does increase with solvent concentration, and, hence, the necessity of allowing for this variation in treating experimental data.

References

1. J. Crank and G. S. Park, *Trans. Faraday Soc.*, **45**, 240 (1949).
2. R. F. Boyer, *J. Applied Phys.*, **20**, No. 6, 540 (1949).
3. R. F. Boyer and R. S. Spencer, *J. Polymer Sci.*, **2**, 157 (1949).

Received September 12, 1949

R. F. Boyer

The Dow Chemical Company
Midland, Michigan

We are indebted to R. F. Boyer for allowing us to see his letter on "Concentration Dependence of Diffusion of Chloroform in Polystyrene" prior to publication and we take this opportunity to mention the results of some further work carried out by one of us (G. S. P.).

Using the same experimental technique but graphically better methods of analysis, diffusion coefficient–concentration curves have been obtained for methylene chloride, chloroform, carbon tetrachloride, methylene bromide, bromoform, and methyl iodide in polystyrene. These results have all been shown to fit the expression:

$$\log D = \alpha + \beta v_1$$

where α and β are parameters, D is the diffusion coefficient and v_1 is the volume fraction of the diffusing molecule. This expression and the expression:

$$\log D = A + B\omega_2^{1/2}$$

given by Boyer can be shown with a fair degree of approximation to be mathematically equivalent forms over the range of concentrations considered. This means in effect that the general behavior of all our diffusion coefficients so far obtained is consistent with the prediction based on the Flory expression for melt viscosity, though as yet the agreement has not been examined quantitatively.

A full account of this work will be published elsewhere.

Received September 12, 1949

J. Crank
G. S. Park

Courtaulds Limited,
Research Laboratory
Maidenhead, Berks,
England

Viscosities of Very Dilute Polymer Solutions

In determinations of intrinsic viscosities, extrapolations are often made from a concentration range in which hydrodynamic interaction is pronounced since the average intermolecular distances are comparable with the molecular dimensions. In connection with the theory of the concentration dependence,[1] there is interest in the behavior at extreme dilution. A concave downward trend in the plot of η_{sp}/c *vs.* c at low concentration has been reported.[2,3] This suggests careful examination of the viscosity of solutions at concentrations well below the limit of 0.1% ordinarily used for polymers of molecular weight 10^5 to 10^6.

With this in view, we report a few results obtained with toluene solutions of a polystyrene fraction with molecular weight $\bar{M}_n = 500{,}000$ in the concentration range from 0.017 g./dl. upward. (The molecular weight was determined osmotically by G. A. Hanks.)

The viscometers used were of the Ubbelohde suspended level type, modified by expanding the reservoir to permit successive dilutions in the viscometer.[4] The two viscometers used for the lowest concentration (J_1 and J_2, see Fig. 1) were fitted with a filtering and dispensing unit,[5] eliminating artifacts which might otherwise arise from occlusion of the capillary by foreign particles. Because of the long flow times for toluene in viscometers J_1 and J_2 (467.8 and 369.8 sec., respectively), kinetic energy corrections were unnecessary. The other viscometers were calibrated and kinetic energy corrections applied. The maximum velocity gradients in the J_1 and J_2 viscometers were less than 1800 sec.$^{-1}$; in the R, S, and G, less than 1250 sec.$^{-1}$; and in the U_2, less than 435 sec.$^{-1}$.

The results of the viscosity measurements are shown in Figure 1 as a plot of η_{sp}/c *vs.* c. It might be of interest that the curve can be adequately represented up to $c = 3$ by a Baker type of equation:

$$\eta_r = \left(1 + \frac{[\eta]c}{2.9}\right)^{2.9}$$

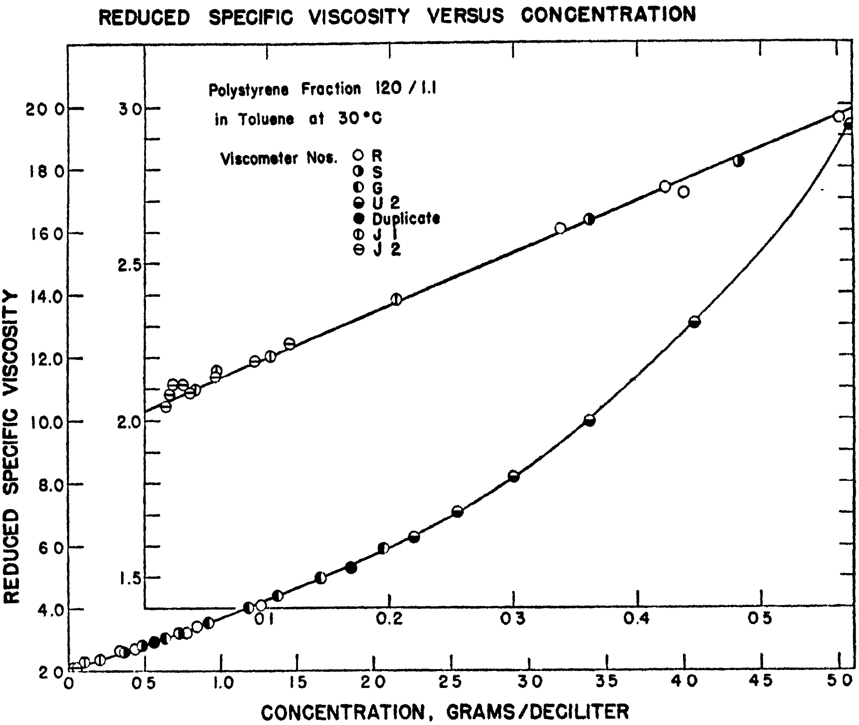

Figure 1

The insert exhibits a magnified portion of the low concentration region. The linear portion is based on a least squares calculation involving only the points for $0.1 < c < 1.0$ g./dl. The points for concentrations below 0.1 fit onto the line so drawn with no apparent systematic deviation and certainly show no downward trend. At the low velocity gradients employed in the critical concentration range (1800 sec.$^{-1}$), orientation effects are negligible for this polymer sample. The assessment of any deviations from linearity at these and higher dilutions requires more precise viscometry.

References

1. R. Simha, *J. Res. Natl. Bur. Stand.*, **42**, 409 (1949).
2. H. Staudinger, *Die hochmolekularen organischen Verbindungen.* Springer, Berlin, 1932, p. 201.
3. F. Howlett, E. Minshall, and A. R. Urquhart, *Shirley Inst. Mem.*, **18**, 251 (1943).
4. W. E. Davis and J. H. Elliot, *J. Colloïd Sci.*, **4**, 313 (1949).
5. S. Rothman, *Anal. Chem.*, in press.

S. Rothman
R. Simha
S. G. Weissberg

National Bureau of Standards
Washington, D. C.

Received December 13, 1949

REVIEW

The Colloid Chemistry of the Silicate Minerals. C. E. MARSHALL. Academic Press, New York, 1949. 195 pp. Price $5.80.

This volume is the first in a series of monographs prepared under the auspices of the American Society of Agronomy. It is also the first book in recent years devoted to this special field. The "Table of Contents" immediately makes the reader aware of the different aspect with which the general subject of clay and silicate minerals has been treated. The first chapters develop the concepts of the structure of the silicates and bring a short survey of the relation between the colloidal properties and the structure. The discussion then turns to such phenomena as adsorption, clay acids, ionic exchange reactions, and electrokinetic properties of clays; again the structures of the silicate minerals are used as basis for the explanation of these reactions. Chemical analysis of the minerals is considered critically and in the light of their structural configuration. Its usefulness along those lines is demonstrated. The chapter on size and shape of clay particles is of interest because of its discussion of the electron micrographs obtained from the major representatives of the silicate mineral groups.

In general, the text is clear and comprehensive and will serve well to introduce the reader to the intricacies of this subject. The book is well written and shows perspective. It should awaken the reader's interest for further study. Some of the subjects, such as, for example, electrochemical properties of clay films, adsorption, and exchange of organic ions could have profited by greater elaboration. The subject of thixotropy lacks in many references. The reproductions of several of the very elaborate clay models are not always clear enough to permit the detailed study of the structure. Possibly a different kind of reproduction would have been more easily understandable.

Dr. Marshall's book is recommended to the polymer chemist. It will supply the fundamental principles of the repetitive structure of silicate minerals and be useful for any further work on combinations of the latter with organic polymers. In addition, the logical grouping of the subject and the clear style of writing make for enjoyable reading.

D. S. le Beau

JOURNAL OF POLYMER SCIENCE VOL. V, NO. 2, PAGES 145-158

Ultraviolet Absorption Spectra of Actomyosin. I

E. SCHAUENSTEIN AND E. TREIBER, *Institute for Theoretical and Physical Chemistry, The University of Graz, Austria*

INTRODUCTION

The application of ultraviolet absorption spectrophotometry to high-molecular fibrous proteins seems tempting in many ways: first, because it offers the possibility of a quantitative analysis of absorbing amino acids like tyrosine, tryptophan, histidine, or phenylalanine, etc. as an important control of chemical methods; second, because it seems possible that the absorption spectrum opens new insights regarding the influence of swelling, stretching, or contraction on the chromophore systems of proteins. The method of absorption spectrophotometry may therefore be placed between the physical and the chemical investigating methods with regard to the results to be expected from its application to fibrous proteins.

The first material chosen was actomyosin, the fibrous protein of cross-striated muscles. No quantitative absorption measurements of exactly defined preparations of actomyosin could be found in the available literature, except two short abstracts in *Chemisches Zentralblatt*,[1,2] unfortunately without any numerical data.

DEFINITION OF MEASURED PARAMETERS AND MEASURING TECHNIQUE

According to proposals in the recent literature:[3] if Φ_i = intensity of incident light and Φ_e = intensity of excident light, then $\log \Phi_i/\Phi_e$ is the extinction E; if related to unit thickness of irradiated matter (1 cm.), we call it the modulus of extinction m. If the concentration of an absorbing solution is identified as c (if measured in moles per liter) or c' (if measured in grams per 100 cc.), then we define the molar and the specific extinction coefficient as $\epsilon = m/c$ and $\epsilon' = m/c'$, respectively. We generally employed the double spectrum method with rotating sector blinds.[4] By this means it was possible to eliminate the Schwarzschild and the intermittence effect. The extinction of the rotating blinds is given exactly as $E = \log (360°/\alpha°)$.

ABSORPTION SPECTRA OF ACTOMYOSIN IN AQUEOUS SOLUTION

Figure 1 shows the absorption spectrum of actomyosin in phosphate buffer, containing the necessary quantity of KCl to make the pH 6.3. The maximum at 3600 mm.$^{-1}$ appears rather smeared out, but is in good agreement with the previously cited papers.[1,2] Compared with the spectra of tyrosine and tryptophan, shown in Figures 2 and 3, Figure 1 permits the conclusion that these amino acids are chiefly responsible for the absorption of actomyosin in the ultraviolet, which agrees with the results of chemical analysis.[5] Figure 1 also shows differences between the spectra of actomyosin of rabbit and guinea pig, indicating various contents of tyrosine and tryptophan. (Similar phenomena could be obtained with actomyosin prepared from muscles of shells.) Such differences had been observed by means of chemical methods between the composition of dog and rabbit actomyosin.[6]

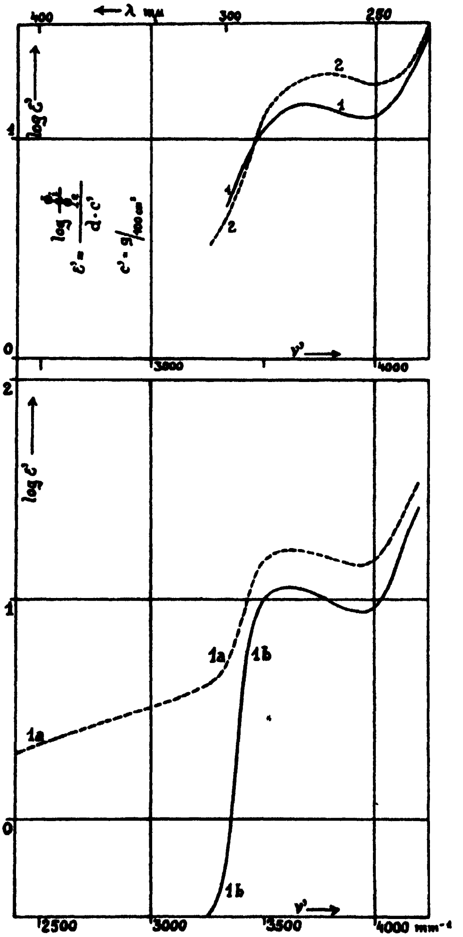

Fig. 1. Rabbit (curve *1*) and guinea pig (curve *2*) corrected for Tyndall effect; rabbit, without any correction (curve *1a*); rabbit, exactly corrected including wave dependence (curve *1b*).

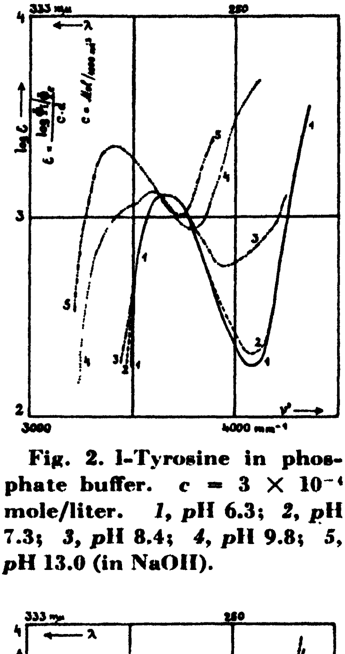

Fig. 2. l-Tyrosine in phosphate buffer. $c = 3 \times 10^{-4}$ mole/liter. *1*, pH 6.3; *2*, pH 7.3; *3*, pH 8.4; *4*, pH 9.8; *5*, pH 13.0 (in NaOH).

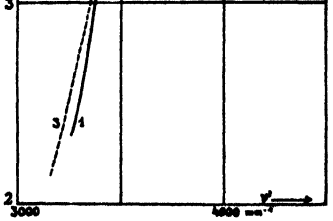

Fig. 3. Tryptophane in phosphate buffer. $c = 2 \times 10^{-4}$ mole/liter. *1*, pH 6.3, 7.3; *2*, pH 8.4, *3*, pH 13.0.

QUANTITATIVE SPECTROGRAPHIC ANALYSIS OF ACTOMYOSIN (Content of Tyrosine and Tryptophan)

The analysis was carried out following the directions of Holiday,[7] who determined quantitatively the tyrosine and tryptophan content of different proteins by means of absorption spectrum. The method is based on the difference in *p*H functions of the absorption spectra of both amino acids. For the calculation, the absorption spectra of pure tyrosine and tryptophan (Figs. 2, curve *5*, Fig. 3, curve *3*) and of actomyosin (Fig. 4, curve *4*) were used, all substances being dissolved in 0.1 *N* NaOH. We found that our actomyosin (rabbit) contained 8.0% tyrosine and 1.3% tryptophan; it had been prepared according to the directions of Weber[8] and Szent-Györgyi[9] which, according to the latter author, yield relative concentrations of actin and myosin ranging from 1:5 to 2:5. The maximal error of our analysis is ±10% including the errors of the only approximate correction for the ultraviolet Tyndall effect (*cf.* Experimental section).

The following table gives a compilation of the data obtained by chemical analysis for comparison:

Author	% tyrosine	% tryptophan	Remarks
Bailey[6]	3.4	0.8...0.85	Rabbit, actin content below 1...2%
Weber[10]	Not given	1.3	Rabbit, actomyosin 1:5..2:5
Jordan (Astbury)[11]	*ca.* 5.5	*ca.* 1.4	Probably actomyosin[a]
Present authors	8.0	1.3	—

[a] Calculated from the number of amino acid residues.

The tryptophan value of Weber is exactly identical with ours, whereas Bailey finds a rather smaller content with a practically actin-free preparation of myosin, from which we may infer that actin contains much more tyrosine and tryptophan than myosin.

Our results can be checked by comparison with the absorption spectrum of a model solution containing tyrosine and tryptophan in the concentration found. Since phenylalanine (which is absorbent at the frequencies considered here) has also been identified in myosin, it was added to the model solution, too, in a concentration that has been found in myosin by Bailey.[11a] Figure 5, curve *1*, shows this model spectrum taken in phosphate buffer solution at *p*H 6.3. We recognize perfect agreement of the maxima in wave length and a satisfying coincidence of the values log ϵ' ($\Delta = 0.07$), realizing that the error due to the Tyndall effect is essentially greater in the *p*H region below 9 than in the more alkaline region where the actomyosin particle breaks up into 4 or 5 smaller units,[9,22] which causes a decrease in actual error (Fig. 4, curve *4*, and Fig. 5, curve *4*).

Figure 5, curve *1*, however, indicates a considerable difference in the region between 3700–4200 mm.$^{-1}$ which might be explained first by the presence of an additional absorbing amino acid, second by the influence of certain systems of chemical bonds on the absorption of tyrosine and tryptophan, and third by the assumption that inside the particles of the dissolved protein the *p*H is more alkaline than that of the buffer solution,[3,6] (*cf.* Dubuisson[12]).

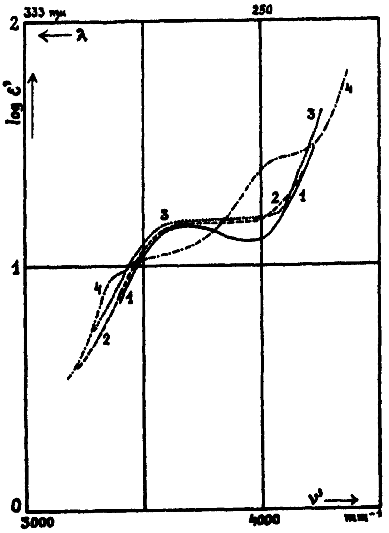

Fig. 4. Actomyosin in phosphate buffer. $c' = 0.08$ g./100 cc. *1*, *p*H 6.3, 7.3; *2*, *p*H 8.4; *3*, *p*H 9.0; *4*, in 0.1 *M* NaOH.

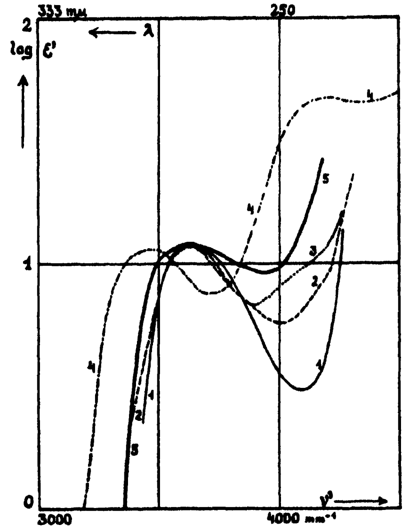

Fig. 5. Model solutions. *1*, *p*H 6.3 (phosphate buffer); *2*, *p*H 8.4 (phosphate buffer); *3*, *p*H 9.0 (phosphate buffer); *4*, *p*H 12.2 (in NaOH); *5*, actomyosin, *p*H 6.3, exactly corrected for Tyndall effect.

The curves *2* and *3* (Fig. 5) show that an increase in *p*H flattens the curve but cannot make it coincide in wave length with the experimental myosin curve.

Experiments of Bürgermeister[12a] exclude the possibility of another absorbing acid being present but show that the difference can be explained by the assumption of an additional absorbing system of chemical bonds together with the above named third possibility of increased internal *p*H. As these experiments have not yet been carried to completion, we are unable to give any more details, but a comparison of curve *4*, Figure 4, and curve *4*, Figure 5, already shows that this additional absorption has a rather characteristic *p*H function that indicates the possibility of mesomeric enol forms. Since the maximum of this additional absorption is situated at about 4000 mm.$^{-1}$, it seems very unlikely that it could be due to the peptide link itself. According to data of Anslow and Nassar,[18] the —CO—NH— system ought to show a range of absorption about 3570 mm.$^{-1}$, which we could not confirm for actomyosin.

pH FUNCTION OF THE ACTOMYOSIN SPECTROGRAM

Figure 4 presents the influence of variations of the *p*H on the absorption of actomyosin. It would seem most reasonable to make the *p*H variability of the spectrograms of pure tyrosine and tryptophan responsible for the observed effects. These absorption curves and their *p*H functions had already been measured by Holiday,[7] Kober,[14] Florence, Enselme and Pozzi[15] and Ross.[16] Since the published data did not coincide—probably caused by different degrees of purity—we preferred to repeat the measurements. The characteristic *p*H function (shift toward the red end and increase of extinction) of the L-tyrosine absorption band is undoubtedly due to the ionization of the phenolic hydroxyl group, indicating a "merichinoic" effect like:

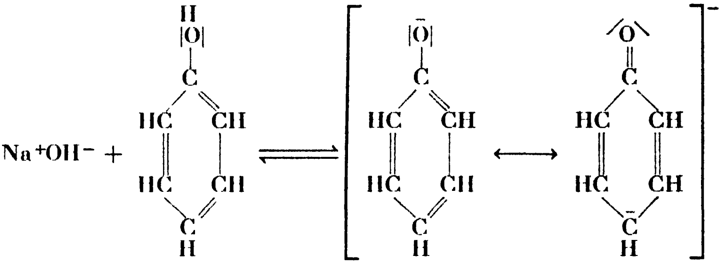

which has been observed in aliphatic systems (L-ascorbic acid[17]) as well as in aromatic systems, *e.g.*, phenol[18] or *o*- and *p*-dihydroxybenzene.[19]

In the case of a "true" equilibrium of dissociation (A $\rightleftharpoons$ B), the equation of Michaelis:[20]

$$\alpha = \frac{K}{K + 10^{-pH}}$$

(α = degree of dissociation; K = constant of dissociation = 1.5×10^{-10}) permits the calculation of the ratio of both components at any desired *p*H, thus offering the possibility of calculating the corresponding absorption curves on the basis of the measured absorption of the pure components (Fig. 2). It appeared now that the *p*H function of the actomyosin spectrum can only partially be interpreted by the *p*H function of the tyrosine band.

Figure 6 shows first that an increase in *p*H from 6.3 to 7.3 will not cause any remarkable change in the actomyosin band. The increase in log ϵ' at *p*H 8.4 could also be explained by the increased rate of phenolate form, amounting to more than 5% at this *p*H. But the identity of the spectra at *p*H 8.4 and 9.0 indicates (Figs. 4 and 6) that in this range of *p*H the *p*H-function of the above-named additional absorption begins to work, causing the typical superposition character of the now flattening curve. Therefore the dissociation function of the phenolic hydroxyl group within this range of *p*H cannot be given exactly. Similarly, in the actomyosin spectrum, taken in 0.1 N NaOH, only the wave length of the ascending branch and the very flat maximum at *ca.* 3400 mm.$^{-1}$ can be interpreted quantitatively by the tyrosine + tryptophan band.

Summarizing, we may state that the actomyosin spectrum in the ultraviolet represents a superposition of the absorption of tyrosine, tryptophan, and phenylalanine, with an additional absorption which is very unlikely to be due to the simple peptide link.

A quantitative discussion of the spectrogram is complicated, since that additional absorption shows a specific pH function, superposing with that of tyrosine at pH values greater than 9.

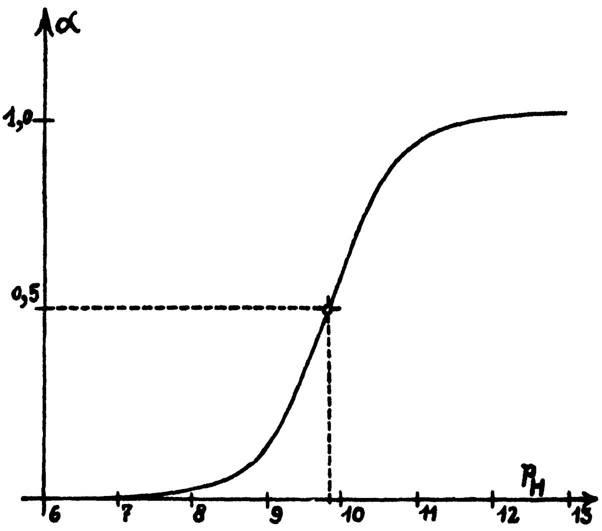

Fig. 6. Dissociation function of phenolic hydroxyl group of L-tyrosine.

Regarding the dissociation of phenolic OH groups of L-tyrosine between pH 8.4 and 9.0, no definite statements can be made as long as the additional chromophore itself and its pH function have not been measured for themselves.

Anticipating some results of experiments that are not finished at present, we would assume that the additional absorption can be ascribed to an influence of intermolecular H bonds.

Experimental details will be given later.

ABSORPTION SPECTRA OF ACTOMYOSIN FILMS

Since it seems very interesting to obtain spectrograms of solid preparations of actomyosin, a method had to be developed for preparing limpid films with as little orientation as possible. (*cf.* Experimental section). Films are required because the very thin "myosin-threads" of Weber did not appear very suitable for spectrographic measurements, especially because they show a considerable *a priori* orientation. Our films were—as expected[9]—exceedingly hygroscopic and did not show any visible orientation between crossed nicols. An x-ray fiber diagram gave the same result. They were practically insoluble even in concentrated solutions of KCl, which has already been explained by Szent-Györgyi,[9] by the assumption of intermolecular forces. The films show a considerable swelling in distilled water at room temperature. According to experiments of Fixl,[21] their thickness increases *ca.* 2.85 times, their breadth about 1.1, and their length about 1.05 times.

Dry Films, Unstretched

The spectrogram of Figure 7a agrees materially with the actomyosin spectrum in solution at *p*H 6–7. With the value of ~1.19 for the density,

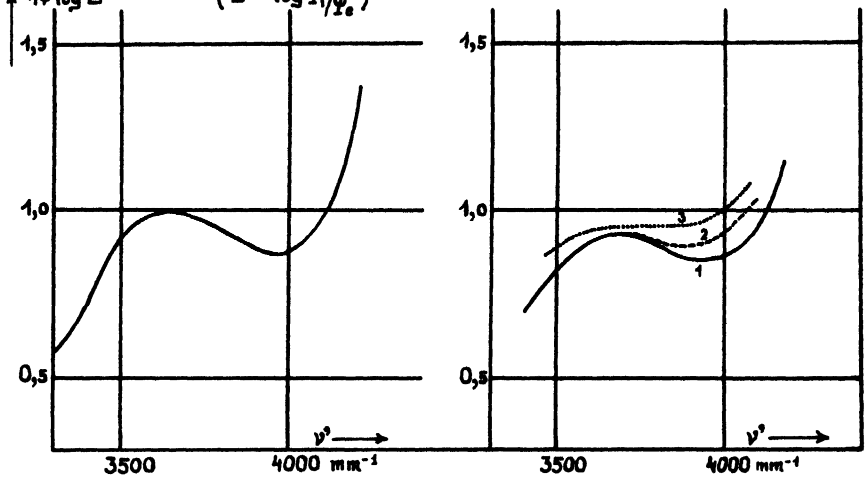

(a) (b)

Fig. 7. Absorption spectra of actomyosin films: a, dry; b, swollen in water; unexpanded (curve *1*); expanded about 2% (curve *2*); expanded 5–400% (curve *3*).

measured by floating the films in a solution of $(NH_4)_2SO_4$ we obtain a maximal specific extinction coefficient of $\log \epsilon' = 1.09$. This value agrees satisfactorily well with the $\log \epsilon'$ value of the dissolved actomyosin at *p*H 6–7, regarding the possible error in density measurement and quantitative analysis. Thus the precipitation of the colloid-dissolved protein into a solid and elastic gel has no influence on the chromophore systems.

Swollen, Unstretched, and Stretched Films

The spectrum of unstretched films swollen in water (Fig. 7b, curve *1*) shows no essential difference as compared with Figure 7a. Figure 7b, curves *2* and *3*, shows that the curve already flattens when the film has been stretched by as little as about 2%. The flattening is complete after about 5% extension.[22] From this point on, the curve will change no more, even if the film is stretched by 400%. Comparing Figure 7b, curve *3*, with Figure 4, curves 2 and *3*, it is recognized that a rather slight stretching induces an "alkalization" of the protein. If we ascribe to the actomyosin an intrinsic *p*H of at least 7 (as has been found in muscles by Dubuisson[12]), the spectrum of stretched films suggests a shift of the dissociation equilibria decisive of the absorption corresponding to a *p*H shift of about 1.5 units toward the alkaline region. This striking effect could be confirmed convincingly by means of measurements[21a] of the isoelectric point of actomyosin films which show a shifting of about 1.5 *p*H units toward the alkaline range of *p*H when the films are stretched for more than 5%.

The next interesting question was whether the observed effect might be due to an inter- or intramolecular reaction. To this end the volume of swollen actomyosin films was measured[21] in the extension. The upper curve of Figure 8 shows the observed result representing the reduced volume v/v_0 as a function of the extension percentage. The curve below gives, as a measure for the flattening of the absorption curve, the values (log $\epsilon'_{max.}$ — log $\epsilon'_{min.}$), also as a function of the extension percentage. We recognize immediately that the "alkalization" corresponds directly to an extraordinary defect in volume (v/v_0). Experiments of Fixl[21] showed that the defect in v/v_0 is essentially due to an almost instantaneous decrease of film thickness within the first 10% of stretching; furthermore, with dried films, the decrease in medium particle distance is expressed more in the direction perpendicular to the plane of the film than within it. Hence the probability of intermolecular bonds being formed will doubtlessly be much greater in the direction perpendicular to the plane than within it. Furthermore we observed that the flattening effect of the curve diminishes considerably when the films are redried:

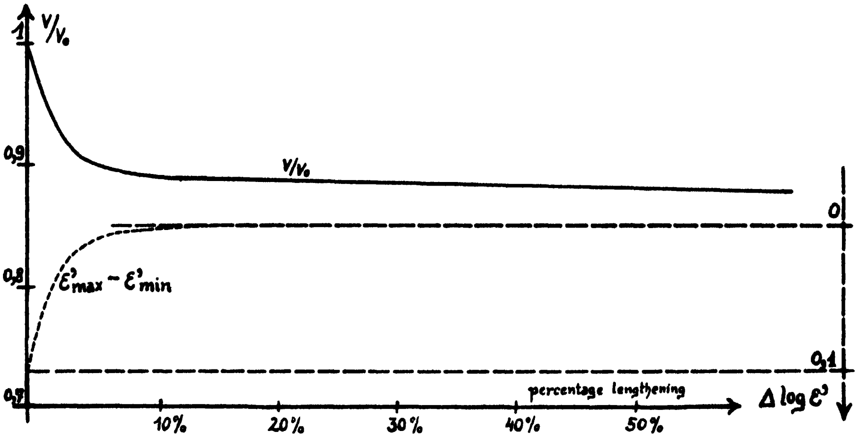

Figure 8

Actomyosin films	$\log \epsilon'_{max.} - \log \epsilon'_{min.}$
Unswollen, unstretched	0.12
Swollen, unstretched	~0.09
Swollen, stretched ≧ 10%	0.00
Stretched (to 60%), dried	~0.09

From the above it follows that the observed "alkali-effect" might be ascribed to an intermolecular reaction correlated to a closer packing of the particles. Although, the complexity of the *p*H function of the spectrogram still renders impossible the detailed discussion of the observed effect, the assumption may be made that it is caused by an approach of polar groups and the formation of hydrogen bonds between —CO— and —NH— groups as shown by Figure 9.

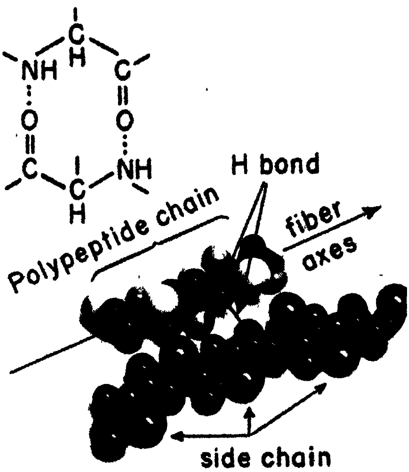

Figure 9

Conductivity measurements performed in collaboration with Treiber[21] proved that the resistance of water-swollen films decreased rapidly during the first 10% stretch and kept the attained low value (5% below unstretched resistance) during further extension. This seems to indicate the formation of an energy-conducting system as suggested by Wirtz,[23] and it appears indeed reasonable that such a conducting system across the peptide chains should be formed by the enolization of CO groups in connection with the formation of H bonds, once the chains have approached to a minimum distance. The following two points should be noted.

(*a*) The considerable size of the effect (about 1.5 *p*H units), which exceeds by far the hitherto observed changes of *p*H (0.02) in muscles, as published by Dubuisson.[12]

(*b*) The appearance of the effect at very low degrees of extension (about 5%), which reveals an energetically extraordinarily favored state causing a specific position of the particles relative to one another. Mere precipitation and swelling is not sufficient for the appearance of this state; on the other hand, it seems to be the *conditio sine qua non* of further expansibility in general.

EXPERIMENTAL

Preparation of Actomyosin (Solutions and Films)

Immediately after skinning and disemboweling the animal, a solution (I) was injected into the aorta so as to remove the blood from the muscles. The muscles were cooled in ice, rapidly minced, washed with solution I, pressed out and frozen in liquid air, as described by Deuticke.[21]

Solution I(*p*H ~ 5.6)
5 cc. 0.15 M Na_2HPO_4
95 cc. 0.15 M KH_2PO_4
300 cc. water
2 cc. 3.6 M KCl (*p*H ÷ 5.6)

The solid mass was powdered, washed again with solution I to remove the other proteins and myochrome, pressed out, and put in the icebox for 24 hrs. with 3 volumes of solution II. For spectrographic analysis at *p*H 7.3, 8.4, and 9.0, the ratio of the phosphate salts was changed as necessary; for *p*H 9 an additional small quantity of 1 M NaOH was added. The *p*H was measured with a glass electrode and an "Ultra-Jonograph" (supplied by Lautenschläger, Munich) with a maximal error of ±0.05 unit.

Solution II (*p*H ~ 6.3)
75 cc. 0.15 M Na_2HPO_4
125 cc. 0.15 M KH_2PO_4
50 cc. 3.6 M KCl
50 cc. water

After 24 hours the dissolved actomyosin was separated from the remainder by pressing out, filtering, and centrifuging the solution, which was then diluted with 10 volumes of distilled water. The precipitated actomyosin was separated with the centrifuge, immediately redissolved in solution II, taking as much of solution II as necessary to obtain a sufficiently limpid solution which was again centrifuged, and filtered once more immediately before measuring.

For preparing films, the first precipitation of actomyosin was dissolved in a modified solution II containing the double quantity of KCl. The highly viscous fluid was pressed slowly through a flat glass nozzle (width of slit 0.1 mm.) into a 0.05 M solution of NaCl and disposed onto a paraffin-coated glass or Plexiglas* plate. After 1 hour the NaCl solution was cautiously removed by means of a siphon and replaced by distilled water which was changed from time to time to wash out the included salts. After drying in open air at normal temperature we obtained perfectly limpid films of a thickness of 0.02 to 0.005 mm. depending on the concentration of the solution and its velocity when pressed out of the nozzle. The concentration of the spectrographically measured solution was analyzed according to the directions of Hermans.[25]

---

* According to the kind advice of Prof. F. Seelich, Med.-Chem. Institute, University Graz, for which we should like to express our indebtedness.

Approximate Tyndall Correction

Despite most careful purification, all solutions of actomyosin show a considerable Tyndall light scattering which is due to the size of the particles and must be taken into account generally with spectrographic measurements.[26] Since an exact correction under consideration of the frequency dependency is certainly rather complicated, we used one simplified, general method irrespective of wave length. We thought this admissible, having estimated the maximal error at about 20% in ϵ units[27] and recollecting that Holiday[7] also found other corrections to be unnecessary, by comparison with chemical analysis. Our method consisted in extending the time of exposure for the scattering object as compared with that for the system in itself taken for comparison until we obtained the same intensity at 1945 mm.$^{-1}$, where in no case any measurable absorption was to be expected.

Our method of approximate correction was tested by the application of an exact correction to actomyosin spectrograms taken at *p*H 6.3 as follows:

The values of ϵ' between 1760 and 3200 mm.$^{-1}$ (measured by photoelectric comparison of the double spectra) allow the estimation of the wave length exponent *n* in Rayleigh's law:

$$\epsilon'(\text{Tyndall}) = K\nu'^{n}$$

Thus *n* has been estimated as 2.25, *cf.* references 28 and 29.

Following the experiments of Schramm and Dannenberg[30] we may conclude that the above equation is also valid within the region of true aromatic absorption (*i.e.*, 3500 down to 4200 mm.$^{-1}$).

Therefore it seems permissible to correct for Tyndall scattering within this range of absorption by subtracting the intensity of Tyndall light estimated as described from the experimental curve.

Figure 1 shows the result: comparing the curves *1*, *1a*, and *1b*, one recognizes that the flat character of the actomyosin band is not essentially altered by this correction.

Figure 5 shows that the exactly corrected protein curve coincides quantitatively with the model spectrum as concerns the region of the absorption maximum, which confirms our spectrographic estimation of tyrosine and tryptophan content in actomyosin. It is clear, however, that the divergence at about 4000 mm.$^{-1}$ cannot be ascribed to an ultraviolet Tyndall effect.

In more alkaline solutions we found a decrease in Tyndall intensity, as found, for example, by Holwerda,[31] so that the difference between corrected and uncorrected absorption curves (3500–4200 mm.$^{-1}$) within that range of pH is negligibly small.

It should be noted that comparisons were made only between absorption curves corrected by the same methods.

Summary

(*1*) The ultraviolet absorption spectrogram of rabbit actomyosin may partially be interpreted as due to tyrosine, tryptophan, and phenylalanine and thus permits a quantitative spectrographic analysis of the tyrosine and tryptophan content with the following result (±10%): 8.0% tyrosine; 1.3% tryptophan.

(*2*) A correspondingly concentrated model solution shows identity of the maxima in wave length and coincidence in log ϵ'_{max}. Between 3600 and 4000 mm.$^{-1}$ there appears a considerable additional absorption of the actomyosin, indicating the presence of a certain system of chemical bonds not contained in the model solution.

(*3*) Presently, no further details regarding this system are available; the frequency of its absorption maximum, however, makes it very unlikely that it should be the common peptide link.

(*4*) The observed pH function of the spectrum shows that this additional absorbing system has a characteristic pH function of its own. Therefore, the pH function of the actomyosin spectrogram can only partially be interpreted by the pH function of the present aromatic amino acids.

(*5*) The transition from the colloidal solution to the precipitated protein films has no characteristic influence on the absorption. At very small degrees of extension (about 2%), however, a specific change in the curve begins to appear, which may be interpreted as an "alkalization" of the protein due to intermolecular reactions taking place as the packing of the particles becomes closer.

(*6*) Referring to measurements of the volume of stretched films, the assumption may be made that the observed effect is induced by the occurrence of an energetically extraordinarily favored quasi-native state (formation of hydrogen bonds between —CO— and —NH—), which represents the preliminary condition for stretching in general.

The experiments are continued in view of a complete identification of the additional absorbing system and the effects that occur in connection with the quasi-native state and with contractions.

We should like to express our indebtedness to Prof. Dr. O. Kratky, who suggested these investigations, for valuable discussions and generous aid in many ways.

We are also grateful to Prof. Dr. H. Lieb, director of the Med.-Chem. Institute, University of Graz, for kindly supporting us with chemical materials, and literature which rendered possible the performance of some of our experiments.

References

1. M. N. Ljubimowa and N. S. Schipalow, *Chem. Zentr.*, **1941**, II, 49.
2. K. Kondo, T. Jamada, and S. Shinano, *Chem. Zentr.*, **1938** I, 1587.
3. A. Thiel and F. Weidert, *Elektrotech. Z.*, **1937**, 5. Sonderdruck.

4. H. v. Halban, G. Kortüm, and B. Szigetti, *Z. Elektrochem.*, **42,** 212 (1936). G. Kortüm, *Kolorimetrie und Spektralphotometrie*, Berlin, 1942. G. M. Pool, *Z. Phys,.* **29,** 311 (1924).
5. K. Bailey, *Biochem. J.*, **31,** 1406 (1937). James Garden Sharp, *Biochem. J.*, **33,** 679 (1939). Tetsutaro Tadokoro, *Chem. Zentr.*, **1935, I,** 3951. P. Jordan, *Eiweissmolekule*, Stuttgart, 1947.
6. K. Bailey, *Biochem. J.*, **31,** 1406 (1937).
7. E. R. Holiday, *ibid.*, **30,** 1803 (1936).
8. H. H. Weber, *Naturwissenschaften*, **27,** 33 (1939).
9. A. Szent-Györgyi, *Chemistry of Muscular Contraction.* Academic Press, New York, 1947.
10. H. H. Weber, *Ber. Physiol.*, **61,** 382 (1931).
11. P. Jordan, *Eiweissmolekule.* Stuttgart, 1947.
11*a*. K. Bailey, *private communication*, for which we should like to express our gratitude.
12. M. Dubuisson, *Bull. soc. philomath. Paris*, **124,** 181 (1943).
12*a*. E. Bürgermeister and E. Schauenstein, brief communication in *Monatsh.*, **80,** 310 (1949).
13. G. A. Anslow and S. C. Nassar, *J. Optical Soc. Am.*, **31,** 118 (1941).
14. Kober, *J. Biol. Chem.*, **22,** 441.
15. G. Florence, J. Enselme, and M. Pozzi, *Bull. soc. chim. biol.*, **17,** 283 (1939).
16. W. F. Ross, *J. Biol. Chem.*, **104,** 531 (1934).
17. E. Schauenstein, *Monatsh.*, **78,** 415 (1948).
18. M. Pestemer and H. Flaschka, *ibid.*, **71,** 325 (1938).
19. A. Saint-Maxen and E. Dareuil, *Compt. rend.*, **197,** 1411 (1933).
20. L. Michaelis, *Die Wasserstoffionenkonzentration.* Springer, Berlin, 1922.
21. J. Fixl, *Doctoral Thesis*, University of Graz, 1949.
21*a*. D. Boerner and H. Lipp, Institute for Histology and Embryology, University Graz, *private communication.*
21*b*. E. Schauenstein and E. Treiber, *J. makromol. Chem.*, 4, 91 (1949); with a supplement, *ibid.*
22. O. Kratky, E. Schauenstein, and E. Treiber, *Monatsh.*, **78,** 174 (1948).
23 K. Wirtz, *Z. Naturforsch.*, **2*b*,** 91 (1947).
24 J H. Deuticke, *Z. physiol. Chem.*, **224,** 216 (1934).
25. P. H. Hermans, *Contribution to the Physics of Cellulose Fibres.* Elsevier, New York-Amsterdam, 1946.
26. W. Ostwald, *Handbuch Kolloidwiss.*, **1,** 113 (1924). See also: W. Ostwald, *Z. Elektrochem.*, **47,** 27, 65 (1941); E. Mayer-Pietsch and H. Troger, *ibid.*, **47,** 60 (1941); G. Schramm and H. Dannenberg, *Ber.*, **77,** 53 (1944); E. Treiber and E. Schauenstein, *Z. naturforsch.*, **4b,** (1949), *in press.*
27. E. Treiber, *Doctoral Thesis*, University of Graz, 1948.
28. W. Heller, H. B. Klevens, and H. Oppenheimer, *J. Chem. Phys.*, **14,** 566 (1946)
29 W. Heller and E. Vassy, *ibid.*, **14,** 565 (1946).
30. G. Schramm and H. Dannenberg, *Ber.*, **77,** 53 (1944).
31. B. Holverda, *Rec. trav. chim.*, **50,** 601 (1931).

English Synopsis, see Summaries, page S2, Vol. V, 1950.

Résumé

La méthode de spectrographie ultra-violette a été appliquée aux protéines fibreuses de poids moléculaire élevé. Par mesures dans des conditions variables (gonflement, *p*H variable, étirement, ètc.) les spectres permettent, indépendamment d'une analyse quantitative des acides aromatiques aminés, des conclusions nouvelles concernant la structure et les propriétés physico-chimiques et biologiques des protéines.

Zusammenfassung

Die Methode der ültravioletten Absorptionsspektrographie wird auf hochpolymere Faserproteine angewendet. Das Spektrogramm erlaubt, bei Messungen unter verschiedenen Bedingungen (Quellen, *p*H Änderung, Strecken u.s.w.) –abgesehen von einer quantitativen Analyse der aromatischen Aminosäuren—neue Schlüsse bezüglich der Struktur, sowie der physikalisch-chemischen und biologischen Eigenschaften der Proteine.

Received January 4, 1949

JOURNAL OF POLYMER SCIENCE VOL. V, NO. 2, PAGES 159-168

Unidirectional Nature of the Large Periodic Structure of Collagen Fibrils*

ORVIL E. A. BOLDUAN† and RICHARD S. BEAR, *Department of Biology, Massachusetts Institute of Technology, Cambridge 39, Massachusetts*

INTRODUCTION

It has been amply demonstrated, by means of both small-angle x-ray diffraction[1-3] and electron microscopy,[4-7] that the colloidal elements of the fibrous proteins of the collagen class are fibrils possessing a longitudinal macroperiod averaging normally 615 to 680 A., depending on the source and condition of the sample. No evidence has been obtained for transverse structure of a periodic sort in these fibrils.

It is desirable that the demonstration of the unidirectional nature of the collagen fibril's large periodic structure should not depend alone on negative evidence, which might result from lack of contrast or improper viewing aspect in electron microscope studies, or from a possible failure of intensity in pertinent diffractions. The present paper supplies positive indications that collagen fibrils lack, in their long-range structure, the full complement of three-dimensional order typical of normal crystals. The theory applied for this purpose is based on a recent summary of criteria useful in recognizing the diffraction phenomena characteristic of order-deficient systems.[8]

EXPERIMENTAL

Methods

The experimental work was performed with Ni-filtered CuK_α radiation (λ = 1.54 A.), using small-angle diffraction cameras described elsewhere[9] and Eastman Type K film. In particular the present evidence was obtained with a pinhole camera capable of resolving diffraction orders of 1200 A. spacings in both the meridional and equatorial directions on the film, with another able to resolve 800 A. meridionally and 400 A. equatorially, and with a slit camera whose meridional resolution was 1400 A. These figures for spacing resolution are conservative, and in practice one is able to resolve consecutive orders of spacings up to about twice these values.

---

[*] This paper represents a partial report on research sponsored by The Office of the Quartermaster General, Research and Development Branch, under Project No. 130-46 on "Determination of the Nature and Properties of Skin Structure" under direction of the Leather Subcommittee of the National Research Council Committee on Quartermaster Problems.

[†] Present address: PC Division, Physics Branch, Camp Detrick, Frederick, Md.

The 1200 A. pinhole camera has the merit of indicating collagen diffraction line shapes with a good degree of fidelity, since the maximum spacings to be resolved are those of moistened collagen specimens, about 675 A. This camera has, however, the disadvantage of slowness, requiring two-week exposures to register the strongest features. For this reason, supplementary evidence is obtained with the 800 A. camera, which serves quite well for the first dozen layer lines in several days. Since the exposure problem becomes even more severe when specimens are to be examined under tilt in the incident beam, it is necessary to employ the slit camera for this purpose. With the greater speed of slit cameras exposures may be still kept within a few days in spite of high meridional resolution.

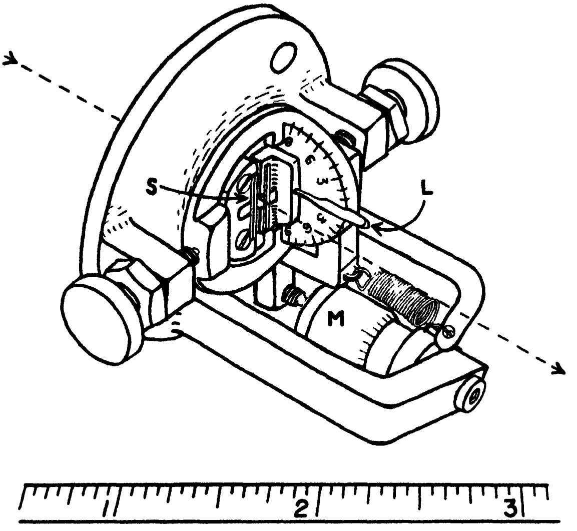

Fig. 1. Apparatus used to compare diffraction by tilted and untilted specimens simultaneously. This specimen holder is inserted in a vacuum camera relative to the axis of a ribbon beam (broken line) as shown. Of the two specimens at S, the left one remains fixed perpendicular to the beam, while the other may be tilted in increments of 10° by the lever L, intermediate positions being secured by adjusting the micrometer screw, M. The rule, marked in inches, indicates the size.

Figure 1 shows a specimen-tilting mechanism used in connection with the slit camera to study layer-line displacements as a function of accurately controlled tilting of the specimen from the usual normal relation to the incident beam. In use, the ribbonlike beam furnished by the camera slits is so wide that two narrow specimens placed side by side, with adequate distance between them to permit separation of their diffraction effects at the film, may be photographed simultaneously, one serving as an untilted control, the other being the experimentally varied sample.

The use of a control in this manner is helpful because small line displacements exhibited between tilted and untilted halves of the same fiber become unmistakable when registered side by side. Also, in this way allowance may be made for minor alterations in measured spacings, resulting from film shrinkage, etc., or from exposure to the vacuum of the camera and other aging phenomena, which become noticeable over an extended series of exposures. Such precautions are particularly necessary in studying colloidal structures. Collagen fibers possess spacings which are by no means constant and reproducible physical constants like those encountered with simpler inorganic and organic solids.

In the original description of collagen diffraction effects at small-angles,[1] the values given for the large spacings of dry collagen samples were those normally met with in specimens examined in simple cameras in which the samples remained roughly equilibrated with air. It was clear, even in the early experiments, that alterations in moisture content and other variables can alter the spacing more or less continuously over a wide range, from 680 to 615 A. normally, with special cases reaching as low as 550 A. As experience has increased, it has been found that the spacing observed with a given specimen may change spontaneously, particularly when exposed to the x-ray beam under the exhausting action of a vacuum camera. For example, a certain specimen whose slow alterations were followed over a period of a little more than a year, showed the following history: Originally as an air-dried, phosphotungstate-stained, kangaroo tendon strip (see below) its fiber period was 643 A., which decreased to 627 A. during almost constant use in an evacuated camera over a time of two months. After storage in a vial for a year it was again examined for another two months, during which its period decreased from 622 to 617 A. A few months later this had dropped to 607 A., where it seemed fairly stable, having attained a value about as low as has been observed with all but exceptionally treated specimens.

From these observations it is clear that spacing comparisons should be carried out with care, either by comparing results immediately after preparation of the specimens, or eliminating time drifts by means of a similarly drifting control.

The present and subsequent papers will detail several aspects of collagen small-angle diffraction. In all of this work, in order to have the basic material be reasonably reproducible and conveniently available in fair amounts, a single large supply of kangaroo tail tendon (actually from the smaller wallaby), supplied to us by Johnson and Johnson Co., was employed as a standard source. It may be assumed herein that the collagen referred to is that of the kangaroo tendon.

The diffraction effects of samples subjected to a variety of treatments have been studied. In general one may observe most of the essential characteristics in the following two preparations: (*1*) Samples of chemically untreated tendon as originally received; and (*2*) specimens subjected to phosphotungstic acid at a prescribed concentration and *p*H designed to introduce about 1.5% of the phosphotungstate.

As will be described more fully eventually, the use of the second type of specimen resulted from observations carried out in collaboration with Dr. T. P. Salo. In a series of specimens with variable amounts of phosphotungstate, it was observed that at the phosphotungstate content of about 1.5% the diffraction orders of the dry specimens with indices 4 to 9 and 11 became of nearly equal intensity on slit patterns, which is not normally the case.[1] Patterns of this material are particularly valuable in investigations involving line shapes or intensity persistence with tilt, since difficulties of comparing diffractions with very different intensity levels are largely eliminated.

The method of preparing this sample is as follows: The kangaroo tendon strips are soaked in water and introduced for 24 hours into an excess of solution containing 0.2% of the solid $H_3PO_4 \cdot 12WO_3 \cdot 15H_2O$, adjusted to a final *p*H of 7.0 with sodium hydroxide. After several washings to remove excess electrolyte the sample is ready for use. Hereinafter this sample will be designated PTA-stained collagen, other concentrations of "stain" being specified on subsequent occasions.

The untreated and PTA-stained samples have been examined dry, or remoistened with water. Maintenance of parallel alignment of the constituent ultramicroscopic fibrils of a massive specimen (usually about 1.0 mm. in thickness) is an important requisite when pinhole pattern line shapes or slit pattern intensity variations and line displacements with tilt are to be studied. This is accomplished by preconditioning the dry original specimens by immersion in water, followed by drying in air in clamps with application of tension near to the maximum the fiber is able to withstand. The specimen may then be used directly as an air-dried sample, though it is advisable to dry it further in an oven at 100 °C. over P_2O_5 in order to reduce the spacing drifts mentioned above. During exposure in the vacuum camera a tray of desiccant is also added to protect the specimen, which is exposed directly to the small air pressure of the camera, maintained there by leaks in spite of constant pumping.

When wet samples are to be photographed the stretched, air-dried samples described above are inserted into thin-walled Pyrex tubes and then water is added to moisten them, the ends of the tube being finally sealed. In this way damage to orientation accompanying insertion of a wet pliable fiber is minimized. When wet or dry samples are imperfectly oriented, this becomes readily apparent in arcing of the diffraction lines, which should be straight lines normal to the meridian of the pattern if good orientation has been achieved.

With wet specimens the results of pinhole camera study are relatively reproducible in important features, except for some difficulties in always obtaining perfect orientation. With dry materials, however, the pinhole patterns possess a certain amount of essential variability, as will be described in greater detail subsequently. These variations are, however, in a sense, ones of degree rather than of kind, so that the general description given here is satisfactory for present purposes. More specifically, the descriptions apply to the samples whose peculiar line shape properties depart minimally from those expected of "smooth," cylindrical fibrils.

Results

Figure 2 shows pinhole patterns of wet and dry specimens as obtained with the 800 A. camera. The corresponding patterns of the 1200 A. camera are similar but more difficult to reproduce. The following paragraphs list the important features of these pinhole patterns.

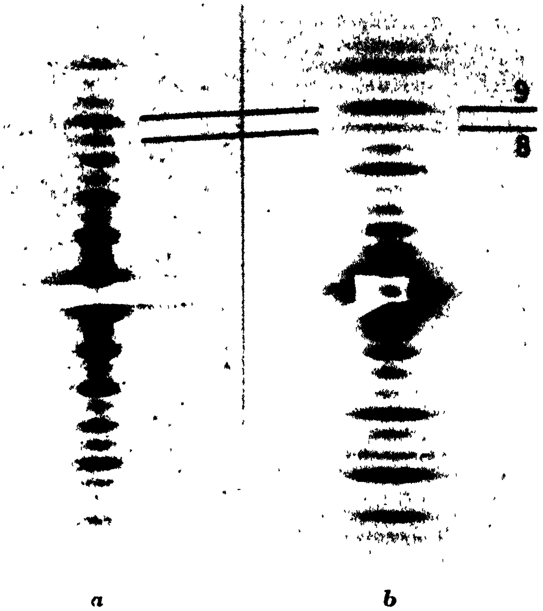

Fig. 2. Pinhole patterns of moist (2a) and dry (2b) kangaroo tail tendon (plain) obtained from a camera with a vertical (meridional) resolution of 800 A. and a horizontal (equatorial) resolution of 400 A. The original specimen-to-film distance was 150 mm.; the fundamental spacing on the left is 665 A., and on the right 629 A. Important layer lines are indicated.

(*1*) On patterns obtained from either wet or dry specimens, the layer lines show no indication of row-line structure, and have maximum intensities directly on the pattern meridian. Sharp equatorial diffractions at small angles are not present, though there is diffuse scatter streaking out from the central beam.

(2) Layer lines are remarkably straight, particularly with dry specimens. A small amount of arcing is sometimes encountered with wet specimens, as becomes most readily apparent at high orders. This disorientation arcing, while not great and hard to avoid completely with wet samples, is readily recognizable. The dry samples, however, when properly prepared seem to be almost totally devoid of disorientation.

(*3*) Layer lines are essentially as sharp in the meridional direction as the central beam. Indeed Kaesberg, Ritland, and Beeman,[10] using a double-crystal spectrometer, showed that the natural line width of collagen specimens is of the order of 20 seconds or less, which is small compared to the divergence of a few minutes allowed by the present collimating systems. On the other hand, the extensions of the layer lines normal to the pattern meridian (line lengths) are appreciably greater than the comparable lateral dimension of the undiffracted beam. The significance of line length is difficult to assess in patterns of wet samples because of the small amount of residual disorientation mentioned above. For dry specimens, however, the observed line lengths are often much greater, and must be treated as entirely significant because of the perfection of orientation.

(*4*) On patterns of wet samples, making rough allowance for the disorientation arcing, it would appear that all line lengths are approximately equal. This is not the case, however, for dry specimens, which may be said to show two major variations in line length: (*a*) a general increase in line length as the index of the layer line increases; and (*b*) pronounced departures from this general rule, which occur from one line to the next so that the general change is sometimes concealed. This latter phenomenon is seen, for example, in comparing the eighth and ninth lines of untreated tendon, the former being less intense over-all than the latter but streaking out to greater length. More striking still in PTA-stained dry specimens is a pronounced alteration in line lengths, with even orders long and odd orders apparently shorter out through the ninth layer line, the regularity breaking down beyond. This effect is reminiscent of the similar phenomenon reported before[1] for the intensities of wet collagen specimens, whose odd orders are strong, even ones weak, over a similar range of index. As far as can be seen, however, wet-specimen line lengths are comparable for both odd and even orders, remaining at all indices never more than equal in length to, usually shorter than, corresponding lines of dry specimens.

Because of "crossfire" in the direction on the film projecting parallel to line lengths, slit patterns may be registered in shorter times without damage to precision of measurement of line positions. Furthermore, since pinhole patterns essentially show sections through reciprocal space "disks"[8] representing the layer lines, it follows that patterns of tilted specimens should show greatest persistence in intensity for those lines whose pinhole-pattern line lengths are greatest. Consequently, the slit-tilt patterns are capable of demonstrating phenomena analogous to those described above from pinhole-pattern line shapes. Figure 3 shows slit-tilt patterns for dry plain and PTA-stained specimens, representative of the photographs from which the following data were obtained.

(*1*) As tilt increases all layer lines of dry specimens move toward higher diffraction angles in such a way as to retain equidistant separation, so that the patterns contain diffraction orders of an *apparent* fundamental period, $d = k\lambda/\xi_k$, where $\xi_k = r_k/s$, the ratio of the diffraction radius of the kth layer line, r_k, to the specimen-to-film distance, s. Accordingly, a single figure, representing the apparent fundamental period as the average of its determination at all observed layer lines, can be derived from one pattern at a given tilt. This is the source of the apparent spacings given in Table I. According to equation (1) of reference 8, division of the apparent spacing by cos θ in each instance should result in a constant value, which is the true fiber period b_0. That this is the case is shown in the last column of the table, whose values are constant within the error allowed by a one- or two-degree uncertainty as to precise setting for zero tilt.

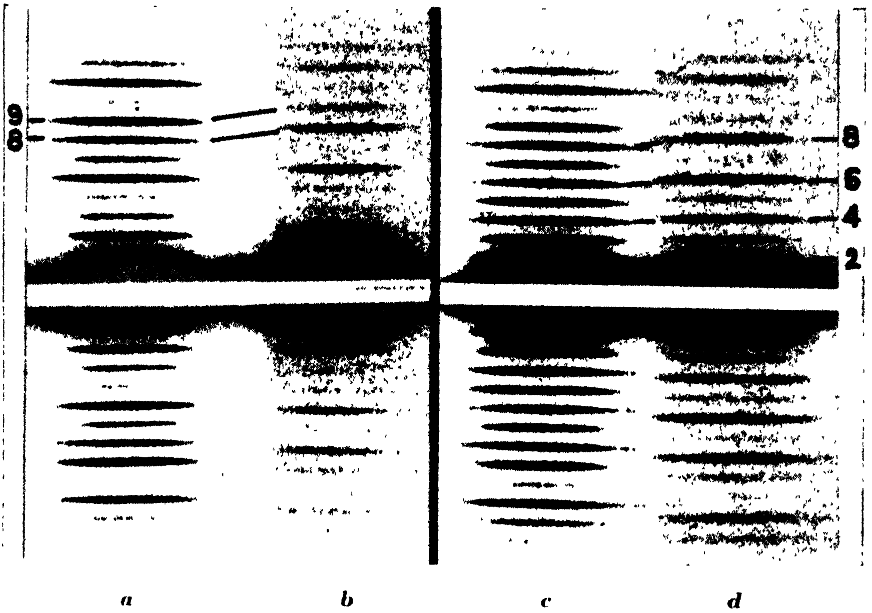

Fig. 3. Slit-tilt comparison photographs of collagen specimens. *3a* and *3b* show the simultaneously registered diffractions yielded by plain dry kangaroo tendon, at 0° and 20° tilt, respectively; *3c* and *3d* present a similar comparison of PTA-stained material. The connecting lines relate corresponding diffractions whose indices are marked in the margins. Note the widening of diffraction diameters after tilting, and the reversal in 8th and 9th order intensities in the comparison on the left and the greater persistence with tilt of even orders in the pair of patterns on the right. The original specimen-to-film distance was 150 mm.; see Table I for spacings.

(2) Corresponding to the short line lengths of wet specimens on pinhole patterns, tilting causes rapid loss in intensity before an angle of tilt whose cosine is sufficiently different from unity can be attained. In those wet specimens for which intensity persists over appreciable tilts the diffraction lines nevertheless do not become appreciably displaced, showing that disorientation is responsible for the persistence, as it was also in producing the arcing on pinhole photographs.

(3) Those lines of dry-specimen patterns that are longest on pinhole photographs persist at greater tilts with the slit camera. Figure 3 illus-

trates this point, showing, in addition to line displacements, the persistence of the eight order relative to the ninth for untreated tendon, as well as the predominance of the even orders of PTA-stained material after tilting. The fact that the higher orders remain at all after tilting of this magnitude is evidence for the generally large extension of their reciprocal-space disks.

Conclusions

The observations described above regarding general line shapes of collagen diffractions on pinhole photographs, and the displacements in position and the persistence with tilt of these in slit patterns, may now be considered in the light of the criteria for degree of order developed earlier.[8]

(*1*) The high resolution pinhole photographs fail to disclose other than the single set of meridional diffractions. This in itself suggests that regular order exists only along the axes of the collagen fibrils, and that order of large size is lacking or of a less perfect character transverse to fibril axes. The resolution of the cameras for small angles is so great that it seems inconceivable that transverse structure could exist and not have been resolved in these patterns. Transverse spacings larger than the cameras could detect would mean structure of the order of size or larger than the diameters of the fibrillar units seen in electron micrographs.[4] The present pinhole photographs disclose no reason to alter previous statements[1] that the collagen small-angle patterns consist solely of a single set of meridional diffractions, and that the largest transverse spacing is the equatorial one observed at wide angles, measuring 11 to 15 A. as a function of water content (Astbury's "side-chain" spacing).

(*2*) The fact that the collagen layer lines have appreciably greater lengths than the central beam's cross section is in line with the conception that the diffracting elements (fibrils) possess less than three-dimensional order. To be sure, if the fibrils are so thin that possible transverse periods could not be repeated many times, then diffraction effects would not be sharp laterally. Tendon fibril diameters are of the order of hundreds, perhaps a few thousands of A. as seen in electron micrographs,[4] giving room for fairly sharp diffractions for transverse spacings of moderate size (up to say 100 A.). Much larger spacings would scarcely be repeated enough times to be said to adopt a regular pattern across the fibril, so that one arrives at a similar conclusion, namely, that transverse regularity must be poor or nonexistent. However, the absence of even rudimentary row-line structure in the pinhole diagrams would seem to rule out the possibility of the existence of a large transverse regularity rapidly terminated by fibril boundaries.

(*3*) The diffraction displacements with tilt, observed in dry collagen specimens, furnish further evidence that the collagen diffractors possess less than the full complement of three-dimensional order. Since the diffraction maxima occur on the meridian, the full range of displacement becomes significant. Over this range the displacements follow the theory as expressed in equation (1) of reference 8. This excludes the possibility that the observed appreciable pinhole line lengths could be due to fibrillar disorientation, as is also indicated by the straightness of the layer lines on pinhole patterns. The observations of consecutive lines with different lengths on pinhole patterns and of equivalent differences in persistence of intensity on slit-tilt diagrams also indicate the reality of the line-length phenomena.

(*4*) Wet samples, like dry ones, show only one set of meridional diffractions, but the wet specimens do not yield clear evidence for diffraction displacements with tilt. In these cases line lengths are short and there is practically no persistence with tilt. This combination of observations can be most simply interpreted as indicating that the moistened collagen fibril is an object with unidirectional order, lacking transverse regularity but possessing sufficient diameter to cause reciprocal-space disk diameters to be small. Apparently the hydration extends the general cross-sectional area of the fibril from which coherent diffractions can occur.

One may conclude from the present results that the ultramicroscopic fibrils responsible for collagen small-angle diffraction possess a regularly repeated structure solely along their axes. Transversely there is no structure of large size apparent. The fibrils are of appreciable diameter but are limited in cross-sectional area which diffracts coherently, this area being greater for wet fibrils than for dry ones. The transverse structure has no marked structural features until one examines details as small as 11 to 15 A. or less.

While to a first approximation the fibrils are cylinders with axial periodicity of structure only, it is clear that in general they are not simple cylinders with invariable diffracting diameter. This is particularly apparent in the changes in line length accompanying drying and wetting, and even more peculiarly in the variable line lengths and degrees of persistence with tilt exhibited by different layer lines of dry specimens. Further examination of these anomalies will be a major task of subsequent papers.

TABLE I

VARIATION OF COLLAGEN DIFFRACTION POSITIONS WITH SPECIMEN TILT

Tilt, θ°	Apparent spacing, d, A.	True fiber period, $b_0 = d/\cos\theta$, A.
PTA-STAINED KANGAROO TENDON (DRY)		
0	626	626
10	615	625
15	604	625
20	589	626
25	573	629
30	550	635
PLAIN KANGAROO TENDON (DRY)		
0	611	611
10	604	613
20	578	615

References

1. R. S. Bear, *J. Am. Chem. Soc.*, **64,** 727 (1942); *ibid.*, **66,** 1297 (1944).
2. O. Kratky and A. Sekora, *J. makromol. Chem.*, **1,** 113 (1943). Kratky, *Monatsh.* **77,** 224 (1946); *J. Polymer Sci.*, **3,** 195 (1948).
3. M. H. Marks, R. S. Bear, and C. H. Blake, *J. Exptl. Biol.*, **111,** 55 (1949).
4. F. O. Schmitt, C. E. Hall, and M. A. Jakus, *J. Cellular Comp. Physiol.*, **20,** 11 (1942); *J. Am. Chem. Soc.*, **64,** 1234 (1942).
5. C. Wolpers, *Klin. Wochschr.*, **22,** 624 (1943); *ibid.*, **23,** 169 (1944); *Arch. path. Anat. Physiol.* (*Virchow's*), **312,** 292 (1944); *J. makromol. Chem.*, **2,** 37 (1948); *Biochem. Z.*, **318,** 373 (1948).
6. G. C. Nutting and R. Borasky, *J. Am. Leather Chemists' Assoc.*, **43,** 96 (1948).
7. F. O. Schmitt and J. Gross, *ibid.*, **43,** 658 (1948). Gross and Schmitt, *J. Exptl. Med.*, **88,** 555 (1948).
8. R. S. Bear and O. E. A. Bolduan, *Acta Cryst.*, *in press* (1950).
9. O. E. A. Bolduan and R. S. Bear, *J. Applied Phys.*, **20,** 983 (1949).
10. P. Kaesberg, H. N. Ritland, and W. W. Beeman, *Phys. Rev.*, **74,** 71 (1948).

English Synopsis, see Summaries, page S6, Vol. V, 1950.

Résumé

Des diagrammes de diffraction aux rayons X sous des angles petits ont été obtenus au départ d'échantillons de collagène (tendon de queue de kangourou) avec des cameras à fine ouverture et à fente, présentant un pouvoir de résolution des distances grandes (800 à 1400 A.). Les effets de diffraction ont été examinés quant aux formes des lignes et aux déplacements des positions des lignes et à la persistance des intensités de diffraction quand les fibres sont inclinées par rapport à l'incidence normale des rayons. A cet égard, les échantillons secs montrent un comportement à la diffraction, caractéristique des systèmes dont la structure périodique est moindre que tridimensionelle. Comme une seule série de diffractions méridionales a seulement pu être observée, on admet que les fibrilles de collagène sec possèdent une structure périodique unidimensionelle seulement (longitudinale), et qu'un ordre régulier transversal est absent. On a obtenu des résultats analogues avec les fibrilles humides, à l'exception toutefois que ceux-ci diffractent de façon cohérente sur une surface transversale beaucoup plus large. De quelques observations particulières indiquent qualitativement que les fibrilles secs ne diffractent pas de façon cohérente sur les mêmes parties de leurs sections transversales par rapport à toutes les lignes des couches de diffraction.

Zusammenfassung

Es wurden Kleinwinkel-Röntgendiagramme von Kollagen Präparaten (Schwanzsehne des Känguruhs) mit Loch- und Schlitzkameras für den Bereich grösser gitterabstande (800–1400 A.) erhalten. Die Beugungseffekte wurden untersucht in Bezug auf die Schichtlinien-Formen (Längen) und bezüglich der Verlagerung der Linien und die Persistenz der Beugungsintensitäten beim Neigen der Fasern aus der gewöhnlichen senkrechten Einfallsrichtung des Strahles. Trockene Präparate zeigten hierbei ein Beugungsverhalten, welches für Systeme mit weniger als dreidimensionaler Periodenstruktur charakteristisch ist. Da nur eine einzige Reihe von meridionalen Beugungen beobachtet werden konnte, wurde gefolgert, dass trockene Kollagenfasern eine periodische Struktur in einer Richtung (longitudinal) besitzen und dass ihnen eine regelmässige Anordnung in der Querrichtung fehlt. Dass gleiche wurde auch bei feuchten Fasern gefunden, mit der Ausnahme, dass diese über eine bedeutend grössere Querschnittfläche zusammenhängend beugen. Mehrere eigenartige Beobachtungen wiesen qualitativ darauf hin, dass die trocknen Fasern nicht zusammenhängend über die gleichen effektiven Teile ihrer Querschnitte auf alle Beugungsschichtlinien abbeugen.

Received April 18, 1949

JOURNAL OF POLYMER SCIENCE VOL. V, NO. 2, PAGES 169-178

Photoelastic Strain Analyzer

E. F. SMITH and A. P. WANGSGARD, *Development Laboratories, Bakelite Division, Union Carbide and Carbon Corp., Bound Brook, New Jersey*

I. INTRODUCTION

This paper describes the principles and apparatus necessary to measure photoelectrically "frozen in" strains when the material has such a low strain optical coefficient* that, at 100% strain and 0.01 inch thickness, less than 1/2 fringe is produced. The usual method of making photoelastic stress analysis is to observe the number of fringes formed in a polariscope or determine the retardation with a Babinet or similar compensator. Methods and equipment for making such analyses are well described in the literature. The photoelectric method was developed because of its suitability for use in the control laboratory. After the equipment has been adjusted for a given material the operation consists of reading a meter and determining the thickness. A nomograph is given for computing the strain from these two measurements.

"Vinylite" plastic planished rigid sheeting, before planishing, is formed by a calendering process which leaves residual or "frozen in" strains in excess of 100% as measured by shrinkage in hot oil. The surface is put on the calendered sheets by placing them between metal plates having the desired finish and then applying heat and pressure. This planishing process also anneals the sheets, thus relieving the "frozen in" strains. The amount of strain remaining after planishing is a measure of the effectiveness of the planishing cycle. The time, temperature, and pressure relations are adjusted to make the sheet as strain-free as possible. Because many of the applications for "Vinylite" rigid sheeting demand a low strain content it is important that strain be measured as a means of quality control. Cutting selected sheets into small squares and immersing them in hot oil is an indirect statistical method of quality control, it is time consuming and expensive, hence, the development of a nondestructive direct photoelastic control test.

---

* The reason for using strain optical coefficient is that optical retardation is more nearly linear with strain than stress for organic polymers. See H. Kilsky and A. C. Shearman, "Photoelastic Investigations of Structural Changes in Plastic Materials," *Proc. Physical Soc.*, 55, 383-395 (1943).

II. THEORETICAL

"Vinylite" resins are birefringement when strained. Examination of large sheets (20 in. × 50 in.) in polarized light showed that the strains present gave rise to retardations of less than π radians at any point. (Later measurements yielded very low strain optical coefficient.) This fact made it possible to devise a very successful method of measuring the strain photoelectrically.

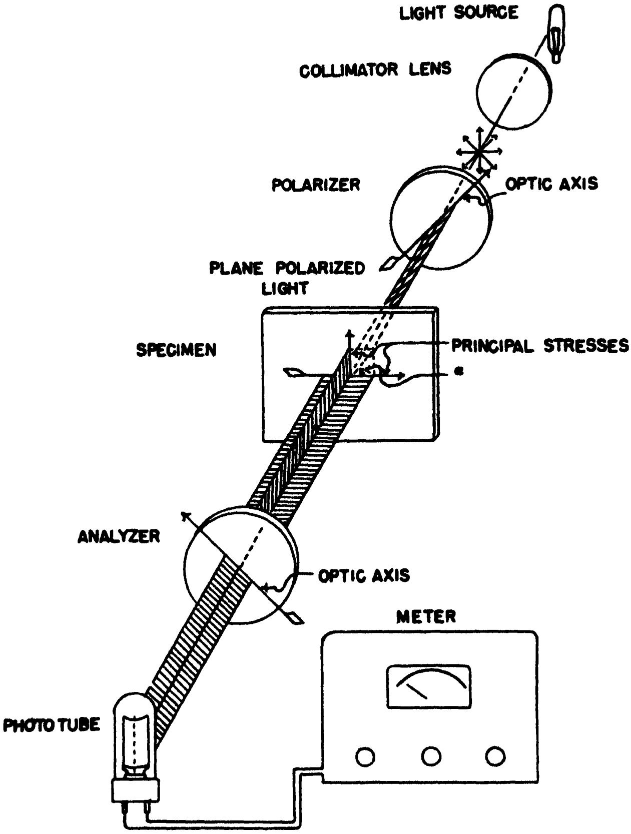

Fig. 1. Schematic representation of the photoelastic strain analyzer.

Let us suppose an arrangement such as indicated in Figure 1, *i.e.*, light source, polarizer, sheet specimen, analyzer, and phototube.

If the thickness of the specimen is d, and X and Y are the principal components of the "frozen in" strain, then δ, the phase difference (or optical retardation) between the ordinary and extraordinary rays, will be:[1]

$$\delta = c(X - Y)d \qquad (1)$$

where c is the strain optical coefficient. If the principle axis (X) of the sheet specimen makes an angle α with plane of polarization of the incident light, then the intensity of the light, I_c, transmitted by a crossed analyzer will be:

$$I_c = I_0 \sin^2 2\alpha \sin^2 \delta/2 \tag{2}$$

With the polarizer and analyzer parallel, the intensity is:

$$I_p = I_0(1 - \sin^2 2\alpha \sin^2 \delta/2) \tag{3}$$

If now, with the parallel position, the specimen is oriented by trial so as to make I_p a maximum, then clearly $\alpha = 0$, or $\pi/2$ and:

$$I_p(\text{max.}) = I_0 \tag{4}$$

whereas, if with the polaroids crossed and the same experiment is performed, then I_c is a maximum when α is $\pi/4$ or $3\pi/4$, etc., hence:

$$I_c(\text{max.}) = I_0 \sin^2 \delta/2 \tag{5}$$

from equations (4) and (5):

$$\delta = 2 \sin^{-1} [I_c(\text{max.})/I_p(\text{max.})]^{1/2} \tag{6}$$

Thus, from light intensity measurements, δ may be calculated, which (if c, the strain optical coefficient, is known) may be used in equation (1) to calculate the strain $X - Y$.

III. Apparatus

Initially, simple apparatus for testing was set up on an optical bench. Tests were performed on small specimens which later were annealed in oil. Having shown that reliable shrinkage values could be predicted from optical data, the machine to be described below was designed and constructed.

The method described above requires that the specimen be rotated relative to the optical system. In testing a 20 in. × 50 in. sheet, this obviously would be inconvenient. Hence, the machine designed achieved the same relation by rotation of two Polaroids in angular coincidence with the sheet remaining stationary. Figures 2 and 3 are photographs of the "Photoelastic Strain Analyzer." In Figure 2 the working parts are shown. At the left is the light source, at the right the photoelectric tube, and in between are two hollow shafts which contain the collimating lens, the Polaroid disk, and three fixed diaphrams. The hollow shafts are mounted on separate uprights so that there is approximately a 12 in. throat, which allows ample space to make observations at any point on a 20 in. sheet. Underneath are a motor, which by means of gears, turns the hollow shafts at the rate of 1 r.p.m., and a constant voltage transformer for the light source. The hollow shaft at the right is connected to its driving gear by means of a spring detent mechanism that seats every 90°. Thus, by grasping the disk, which is attached to the hollow shaft and which projects through the dust cover, the analyzer may be moved easily and quickly to either the "crossed" or "parallel" position. The hollow shaft at the left is keyed to its drive gear by means of a set screw which permits the Polaroid at the left (the polarizer) to be properly oriented with respect to the one at the right.

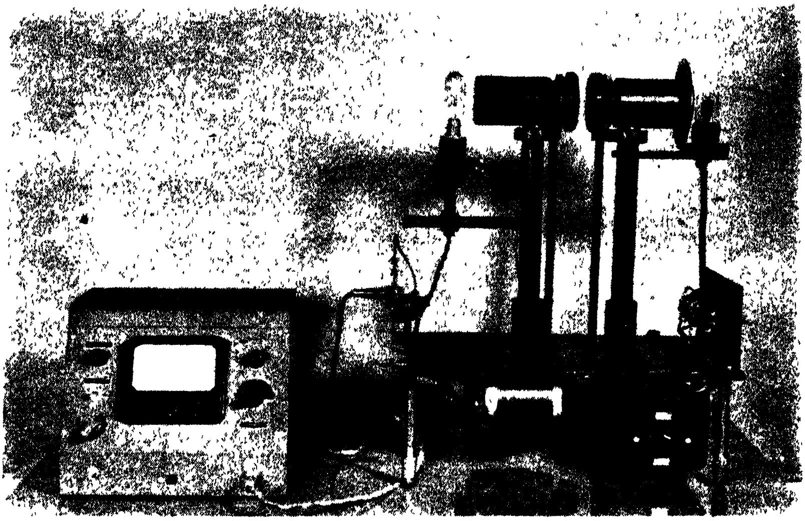

Fig. 2. Strain analyzer with light and dust covers removed

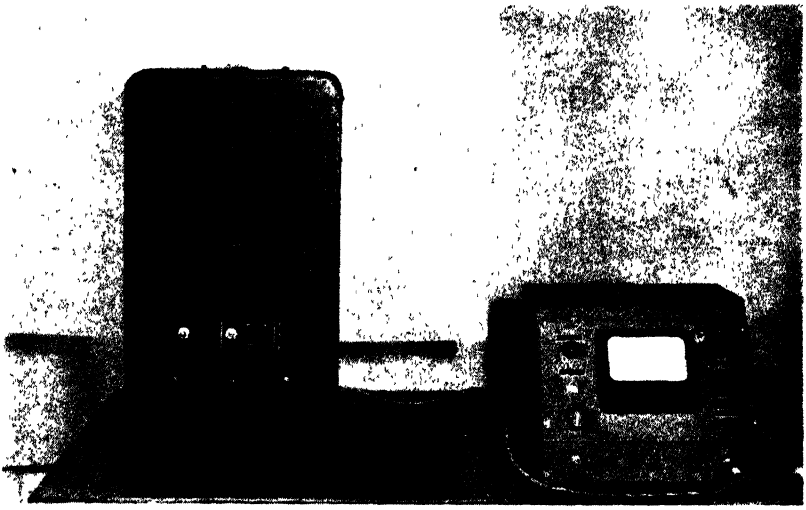

Fig. 3. Strain analyzer testing a matte sheet.

On the panels, front and rear, are located power plug, fuse, light switch, motor switch, phototube connections, etc.

Figure 3 is a photograph of the machine with covers in place and a 20 in. mat sheet in the slit between the Polaroids.

Figure 4 is a circuit diagram of the photocurrent meter. This circuit is standard except for one feature. This is the addition of a 9 volt negative power supply, a potentiometer (P4) and a 100 megohm resistor which make it possible to correct the meter reading to zero when there is phototube dark current and residual light through the crossed Polaroids.

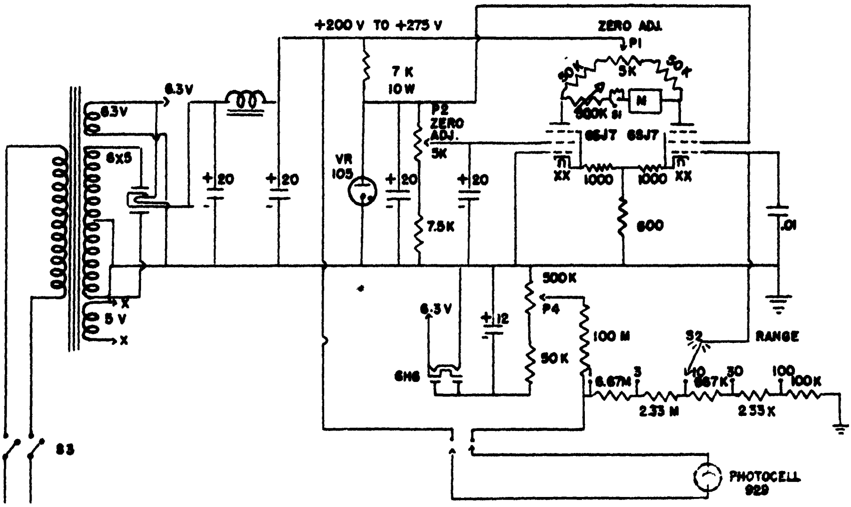

Fig. 4. Photoelectric meter circuit.

Switch S_1 shunts a resistor of 500K which is used in conjunction with a variable resistance of 500K to adjust the sensitivity so that I_0 is made equal to 100 (see Procedure).

IV. TESTING PROCEDURE

With the phototube disconnected, the photoelectric current meter is adjusted and balanced to zero. It is now connected and, with the Polaroids crossed (light source on), the grid bias (P4) is adjusted so that the meter again reads zero on the most sensitive scale. This corrects for phototube dark current and residual light through the crossed Polaroids. Next, with the test sheet in place and the Polaroids parallel, the optical system is rotated until a maximum photocurrent reading is reached. The meter sensitivity control is adjusted so that the meter reading is 100 (*i.e.*, $I_p(max.) = I_0 = 100$). The Polaroids are then crossed and the optical system rotated 45°, which makes I_c a maximum. This reading is taken.

V. CALCULATIONS AND RESULTS

From equation (1):

$$\delta/d = c(X - Y) = c[(L_1 - L_0)/L_0 - (W_1 - W_0)/W_0] \qquad (7)$$

where L_0 is annealed or unstrained length, L_1 is length before shrinkage, W_0 is annealed width, and W_1 is width before shrinkage.

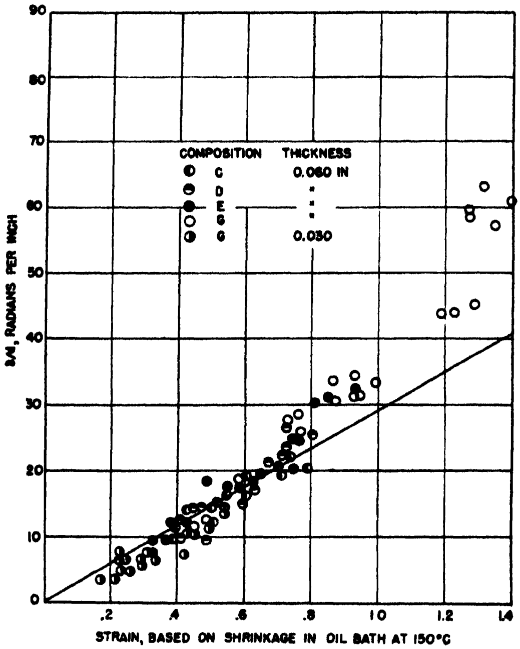

Fig. 5. Correlation tests on compounds differing slightly in formulation.

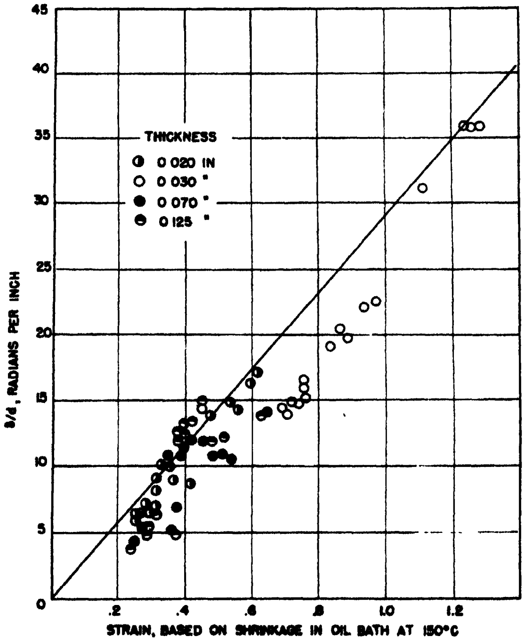

Fig. 6. Correlation tests on sheets of different thicknesses.

From equation (6) and given $I_0 = 100$,

$$\delta/d = (2/d)\sin^{-1}(I_c(max.)/100)^{1/2} \tag{8}$$

hence the following relation exists:

$$c\left[\frac{L_1 - L_0}{L_0} - \frac{W_1 - W_0}{W_0}\right] = \frac{2}{d}\sin^{-1}\left[\frac{I_c\,(max.)}{100}\right]^{1/2} \tag{9}$$

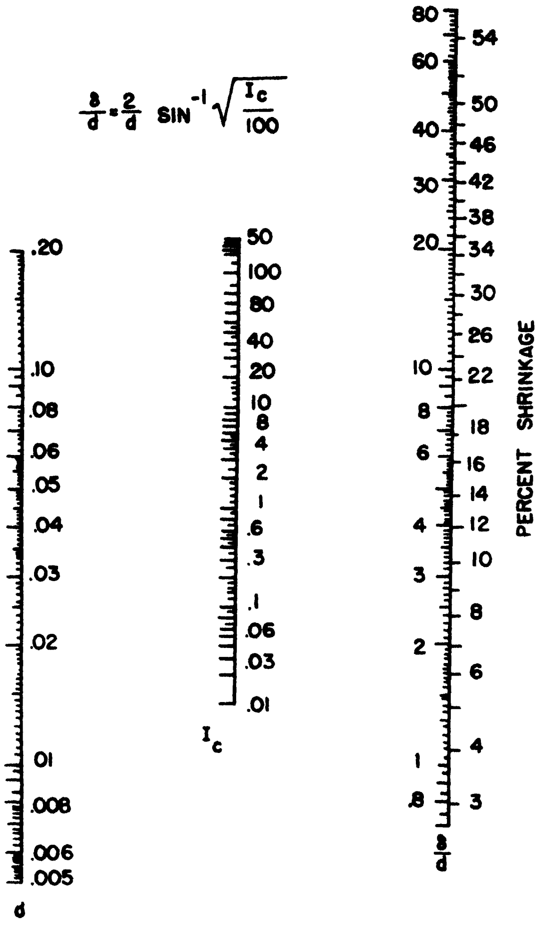

Fig. 7. Nomograph for computing per cent shrinkage.

Figures 5 and 6 are graphs of δ/d as calculated from equation (8) versus experimentally determined strain for specimens of various degrees of strain and various thicknesses. It will be observed that a reasonably straight line exists, as predicted by equation (9). The inverse slope of this line is the strain optical constant, c.

In practice, this graph is regarded as a calibration of the instrument and used to determine shrinkage from the optically measured values. It is now seen that the success of this method depends on the fact that the strain-optical coefficient, c, is of such low magnitude that δ does not become greater than 180° for sheets of commercial thicknesses and the usually encountered degree of strain. Otherwise, it would be necessary to determine the fringe order.

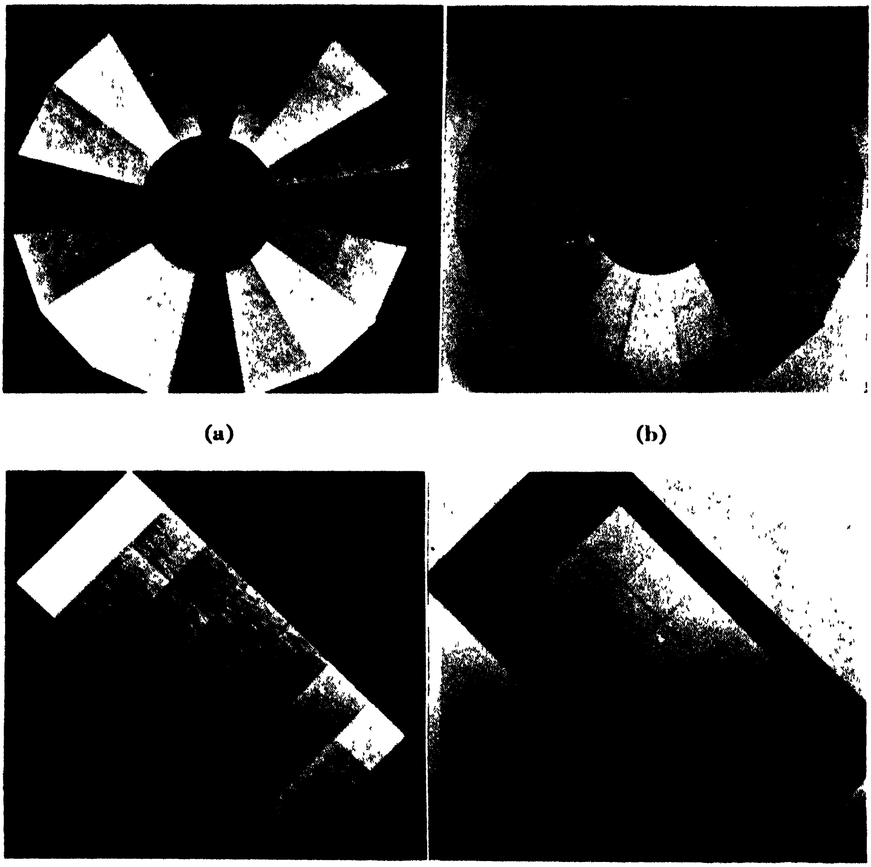

(a) (b)

(c) (d)

Fig. 8. Illustrative photographs.

Figure 7 is a nomograph supplied production inspectors so that they may immediately convert optical data to shrinkage values. Shrinkage as normally used here is the percent change in length of *unannealed* specimen when it is placed in the hot oil. This term has been in constant usage over a period of years and, in addition, is meaningful. It is therefore, retained. Shrinkage is defined as follows:

$$\text{Shrinkage} = S = \frac{L_1 - L_0}{L_1} \times 100 \tag{10}$$

For the material in question, it has been found that when specimens are placed in hot oil, the length (calender directions) decreases while the width increases. To a close approximation:

$$\frac{L_1 - L_0}{L_0} = -K \frac{W_1 - W_0}{W_0}$$

Hence, in equations (7) and (10) the shrinkage is expressible directly in terms of δ/d. This relation becomes part of the nomograph (Fig. 6).

Photographs have been taken which show rather strikingly the significance of equations (2) and (3). Figures 8a and 8b show the effect of varying α (or orientation of specimen) for the case of the crossed and parallel Polaroids, respectively. Similarly, Figures 8c and 8d illustrate the effect of varying δ (or strain level) for both cases when $\alpha = 45°$. The specimens of Figures 8a and 8b are small isosceles triangles cut from a fairly uniformly strained sheet such that the altitude of each triangle is perpendicular to the calendering direction. The specimens of Figures 8c and 8d are small squares cut so as to preserve their relative positions and orientation in a large sheet which purposely was poorly planished. The section near the center is relatively strain free. Strain, it is seen, increases radially from the center. These photos were taken by illuminating the assembled pieces through a large Polaroid sheet and photographing through a Polaroid filter.

The instrument described above has been in use now over a period of more than two years and has proved to be a useful adjunct in the production of strain-free Vinylite plastic rigid sheets. While primarily applicable to polished clear sheets, it has also been used with some success on certain semitransparent materials having either mat surfaces or which are pigmented.

The work of Mr. H. A. Swallow and Mr. J. P. Shook in designing the instrument is gratefully acknowledged.

Reference

1. See M. M. Frocht, *Photoelasticity*, Vol. I, Wiley, New York, 1941, page 136; or R. A. Houston, *A Treatise on Light*, Longmans, Green, New York, 1930, page 228.

English Synopsis, see Summaries, page S8, Vol. V, 1950.

Résumé

La théorie et l'instrumentation pour la détermination photoélectrique des niveaux "gelés" d'étirement sont décrites, lorsque l'épaisseur et les constantes optiques de la tension sont de telle grandeur que le retard optique est inférieur à π radians. La méthode est adaptée à l'usage dans un laboratoire industriel, et a été appliqué au contrôle du calandrage dans la production de feuilles plastiques de Vinylite transparente.

Zusammenfassung

Es wird die Theorie und Apparatur für die photoelektrische Bestimmung von "eingefrorenen" Spannungsniveaus beschrieben für den Fall dass die Dicke und optischen

Spannungskonstanten von einer solchen Grössenordnung sind, dass die optische Verzögerung auf Radianten π beschränkt ist. Diese Methode ist für Industrielaboratorien anwendbar und ist für die Betrichskontrolle von Glättungszyklen bei der Fabrikation von durchsichtigen Vinylitplatten benutzt worden.

Received May 3, 1949

JOURNAL OF POLYMER SCIENCE VOL. V, NO. 2, PAGES 179-189

Denaturation of Plant Proteins. III. Optical Rotation, Viscosity, and Reducing Capacity of Denatured Proteins

B. JIRGENSONS, *Victoria University of Manchester, Department of Chemistry, Manchester, England**

INTRODUCTION

In the previously published articles[1,2] it was stated that denaturation of plant proteins, as estimated by titration of the reducing groups, is mainly associated with an increase of viscosity. However, there are some cases when a protein with a high reducing capacity has a low viscosity (legumelin[1]), and also some opposite instances when a protein has high viscosity but a very low reducing power; an instance of such behavior is legumin in 30-40% propyl alcohol containing salt.[2] Is legumin in this case denatured or not? Whether a change in properties of a protein is called denaturation depends on the definition of denaturation. According to Neurath and co-workers[3] any nonproteolytic change of the unique structure of the native protein, giving rise to definite changes in chemical, physical, or biological properties, should be called denaturation. The usually investigated properties are solubility, size and shape of the molecules, and the reducing capacity. However, there is a very important property of proteins that has been too little investigated in order to estimate denaturation—the optical rotation of proteins. The changes in configuration of the protein molecule must be associated with noticeable changes in rotatory power.

The purpose of this work was to investigate the changes of optical rotation upon some treatment of plant proteins that usually cause denaturation. The changes in rotatory power are then compared with those of reducing capacity, viscosity, and solubility.

The optical rotation of typical proteins hitherto has been investigated mainly by Pauli,[4] Greenberg,[5] and Barker.[6] Since the optical activity of proteins, like that of the amino acids,[7] depends on solvent or pH, it was realized long ago that single data about the optical rotation of a protein are of little value. Much more important is the dependence of the rotation on hydrogen ion concentration or admixed quantity of acid. Almquist and Greenberg[5] investigated the variation of optical rotation with pH; the resulting curves for ovalbumin, serum albumin, and livetin are very similar.

---

* **Present address:** Texas Lutheran College, Seguin, Texas.

These observations naturally raise the question of how denatured proteins behave under similar conditions. The extensive results of Pauli and co-workers,[4] who denatured ovalbumin, edestin, and some other proteins mainly with urea and sodium salicylate, are very complicated. Some of the reagents (*e.g.*, sodium salicylate) increase the negative rotation angle. Barker[6] investigated alkaline heat-denatured albumin and found that the negative rotation increases upon denaturation. The negative angle increases also with decreasing *p*H, but measurements have been made only down to *p*H 6.5.

In the work presented in the following pages the dependence of specific rotation on *p*H for the proteins has been determined whenever possible, especially in the cases of solutions in dilute alkali, sodium dodecylbenzenesulfonate, and sodium salicylate.

EXPERIMENTAL

Methods and Substances

In the present series of experiments the following proteins were used: (*a*) globulin of green peas or vetches and (*b*) globulin of potato. The globulin of green peas was obtained as described previously.[2] Two fractions of the globulin were used: a twice-reprecipitated fraction obtained by 50% saturation with ammonium sulfate and a twice-reprecipitated fraction separated by 66% saturation. The solutions before final precipitation by dialysis were extracted with ether and petroleum ether in order to extract the lipids. Legumin was obtained from vetch meal in a similar way; before the extraction with sodium chloride the vetch meal was defatted by petroleum ether. The purification was carried out either as described previously or by reprecipitation by acetone on cooling with ice water. The precipitate was dissolved in 10% NaCl, dialyzed, and the globulin, which precipitates in the dialyzator, again dissolved and reprecipitated. Obviously, acetone does not denature legumin under such conditions, for the solubility did not change after such treatment; the reducing capacity and viscosity, too, is the same as for the legumin of pea; only the optical rotation is somewhat higher.

Tuberin (the globulin of potato) was obtained from potato juice. 4 kg. potatoes were washed, ground, and the juice pressed off. During the grinding $NaHSO_3$ was admixed (0.6%) to prevent the formation of dark-colored melanins. The juice was clarified in a Sharples supercentrifuge and tuberin precipitated by 50% saturation with saturated ammonium sulfate. The sediment was removed, dissolved in water, and dialyzed until no sulfate ions in the water were detected. The precipitate of globulin was then thoroughly washed with methyl alcohol and ether and dried in a vacuum desiccator at room temperature.

The optical rotation was determined with sodium light at 17–18°C. in a 10 cm. or 5 cm. tube. The angles quoted are the mean of usually 4 or 5 measurements. The experimental error is about $[\alpha]_D \pm 0.5°$.

Titrations with iodine were carried out with 0.002 *N* iodine in presence of 0.2 *N* KI and starch at 15°. Under these circumstances mainly the SH groups are oxidized when *p*H is kept below 6. The addition of iodine was stopped when color appeared and remained 15 seconds. In acid solutions at *p*H 3–5 the color does not fade; in neutral and slightly alkaline solutions at *p*H 6–8 the color fades, since other reducing groups are attacked and iodination occurs.[8]

The viscosity was determined as described previously. The intrinsic viscosity was determined by graphic extrapolation to zero concentration.

Influence of Heat on Legumin

Solutions of legumin in 10% NaCl or 4 *M* KBr or 2 *M* $CaCl_2$ do not become turbid when heated in a water bath up to 70°C. and kept at this temperature one hour or even more. There is also no change in reducing capacity and optical rotation of these solutions, when they, after the heating, are cooled and investigated.

Heating up to 80–90° for 30 minutes causes no change in reducing capacity or optical rotation; only some samples of legumin became a little turbid and the viscosity number η_{sp}/c increased from 0.005 to 0.009. The solutions of vetch legumin did not grow turbid even upon boiling for some minutes.

Heating of dry legumin 3 hours at 100–105° causes only a slight denaturation. Thus denatured legumin only partly dissolves in 4 *M* KBr. The viscosity of these solutions is the same as for the unheated globulin, and there is almost no change in the reducing capacity.

Heating of dry legumin 3 hours at 115° causes a deep denaturation: the substance did not dissolve in 4 *M* KBr or 10% NaCl but only in 0.1 *N* alkali.

Influence of Propyl Alcohol on Legumin

As it was found some time ago[2] the viscosity of legumin in solutions containing 30–40 volume per cent propyl alcohol and salt is very high, but the reducing capacity as low as for native globulin. Now it was found that the rotatory power of these solutions is about 25% higher than for the corresponding salt solution without alcohol; however, this increase is only transitory and in some hours the rotation angle decreases down to the usual values of native legumin.

Denaturation by Acetic Acid

Several samples of pure legumin have been dissolved in 50 volume per cent acetic acid and the viscosity, reducing capacity, and optical rotation of these solutions have been determined. The viscosity numbers η_{sp}/c are very high (Table I), but they do not increase in time. The reducing capacity is surprisingly low: for several samples it varied between 0.45–0.70 cc., 0.002 *N* iodine for 0.1 g. protein, *i.e.*, as for the solutions containing propyl alcohol (see also Table VII). The rotation angles of the solutions containing acetic acid are much higher than those for native legumin and the rotation does not change in time.

TABLE I

VISCOSITY NUMBERS OF PEA LEGUMIN (PRECIPITATED AT 66% SATURATION) IN 50 VOLUME PER CENT ACETIC ACID

c (g. per liter)	η_{sp}/c
20	0.0562
10	0.0535
5	0.0518
2.5	0.0492
1.25	0.0465
0 625	0.0448
$c \to 0$	0.043

A strong influence on the viscosity and rotatory power of these solutions have salts with multivalent cations. The results obtained with 40 volume per cent acetic acid and lanthanum nitrate are presented in Table II. Just after admixing of the salt the viscosity decreases, but then rises considerably in time; the rotatory power also increases in time. Under the influence of barium bromide, 0.4 mole per liter of the mixture, the viscosity numbers at the beginning are diminished to 0.02, but rise in 7 days to 0.08. Copper sulfate (0.4 mole per liter) decreases the viscosity at the start to 0.02, and in 7 days it rises to 0.087. The influence of KBr or KH_2PO_4 is much smaller.

TABLE II

PEA LEGUMIN[a] (0.8%) IN 40 VOLUME PER CENT ACETIC ACID, WITH LANTHANUM NITRATE: 0.04 MOLE PER LITER[b]

Time	η_{sp}/c	$[\alpha]_D$
Initial value	0 0257	−50.2
After 1 day	0.0437	−54.8
After 3 days	0.0727	−56.9
After 6 days	0.1012	−56.5

[a] Same as in Table I.

[b] Without salt, η_{sp}/c = 0.0490, and does not change with time.

The transitory decrease of the viscosity under the influence of salt must be considered as the inhibition of the electroviscosity effect. In time, however, the viscosity of the solutions containing salt increases, whereas the viscosity of the salt-free solutions in acetic acid remains constant. This increase of viscosity must be considered as being gelation.[9]

Denaturation by Alkali

1 g. of pea legumin was dissolved in 20 cc. 0.1 N NaOH, the excess of alkali neutralized with 0.1 N sulfuric acid to pH 5.8, and the precipitate

suspended in water and dialyzed until free from electrolytes; the pure legumin was then filtered and dried in a vacuum desiccator at room temperature. It was found that legumin reprecipitated in this manner cannot be dissolved in 10% NaCl, and thus it is strongly denatured.

If, however, legumin is dissolved in very dilute alkali, only a very slight denaturation occurs. It was found that the minimum of alkali required to dissolve 1 g. legumin, completely, is 35 cc. 0.01 *N* NaOH. Solutions obtained in this way have a *p*H of 7.4–8.2 and a $[\alpha]_D$ of −52 to −56°. After precipitation of legumin dissolved in this manner with dilute acid, the legumin can be dissolved in 10% NaCl, and these solutions have then the usual viscosity and optical rotatory power of native legumin.

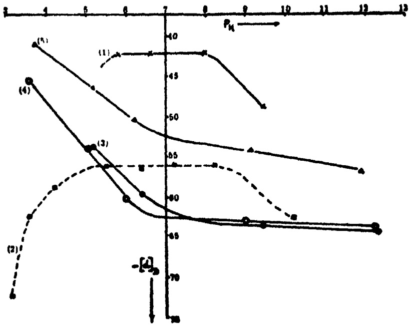

Fig. 1. *Curve 1:* native pea legumin in potassium bromide solution; *curve 2:* pea legumin in very dilute alkali (*p*H decreased with dilute acetic acid); *curve 3:* pea legumin denatured with sodium salicylate; *curve 4:* pea legumin denatured with detergent (sodium dodecylbenzenesulfonate); *curve 5:* tuberin denatured with detergent.

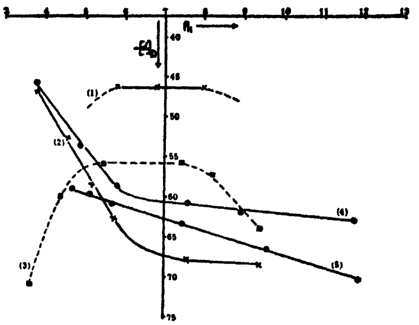

Fig. 2. *Curve 1:* vetch legumin with acetone reprecipitated, dissolved in 10% NaCl; *curve 2:* the same vetch legumin in 1% detergent; *curve 3:* deaminated vetch legumin in very dilute alkali (1 g. in 38 cc. 0.01 *N* NaOH and diluted to 1% of protein); *curve 4:* deaminolegumin-B, 1% solution in 1% detergent; *curve 5:* deaminolegumin-A, 1% solution in 1% detergent.

The viscosity numbers (η_{sp}/c) of such solutions in very dilute alkali are about 0.006–0.009 and can be diminished by addition of salt to the normal values of 0.004. The reducing capacities of these solutions have the values of native legumin, or they are only slightly higher (about 0.6 cc. 0.002 *N* iodine for 0.1 g. protein). These determinations, however, are possible only at *p*H below 7.5 since in alkaline solutions some other reactions with iodine occur and the titration values are then very high.

The optical rotation of these solutions in very dilute alkali is constant in the limits of *p*H 5.2–8.0. Around *p*H 5 it is impossible to determine the optical rotation, since legumin precipitates. In acid as well as more alkaline solutions the negative rotation angle increases (Fig. 1). It is interesting that almost the same data of rotation have been obtained for solutions of legumin in 1 *N* acetic acid when *p*H was varied by addition of alkali.

Denaturation by Salicylate and Detergent

The data concerning the changes of rotatory power as dependent on *p*H for the globulins denatured by sodium salicylate or sodium dodecylbenzenesulfonate are presented in Tables III–VI and in Figures 1 and 2. The solutions containing detergent or salicylate did not grow turbid after adding small quantities of acid, so that it was possible to obtain rather complete rotation curves. Similar results have been obtained with some other samples of legumin and the results are well reproducible. The rotation angles for the first fractions of legumin (precipitated by 48–55% saturation) are always lower than those for the last fractions of legumin (precipitated by 60–75% saturation). The shape of the rotation curves is the same for all kinds of pea and vetch legumin and also for tuberin. As it was found in preliminary experiments, similar curves are obtainable also with edestin, casein, and ovalbumin when they are dissolved in a solution of detergent.

TABLE III

1% PEA LEGUMIN (PRECIPITATED BY 50% SATURATION), DENATURED WITH 1% SODIUM DODECYLBENZENESULFONATE

*p*H	$[\alpha]_D$	0.002 *N* iodine for 0.1 g. protein, cc.	η_{sp}/c
6.2	−51.8	1.05	0.0102
5.0	−45.0	0.88	0 0085
3.8	−39.9	0.72	0 0066
9.0	−55.6		
11.8	−60 2		
13	−62.2		

TABLE IV

OPTICAL ROTATION OF PEA LEGUMIN (PRECIPITATED BY 66% SATURATION)

Stock solution: 1 g. legumin in 50 cc. 2% sodium dodecylbenzenesulfonate

Solution			
2% legumin, cc.	Other component	*p*H	$[\alpha]_D$
5	5 cc. water	6.0	−60 6
5	5 cc. 0.01 *N* H_2SO_4	5.1	−54.2
5	5 cc. 0.02 *N* acid	3 6	−45.8
5	5 cc. 0.01 *N* NaOH	9.0	−62.5
5	5 cc. 0.02 *N* NaOH	12 2	−64.0

TABLE V

OPTICAL ROTATION OF PEA LEGUMIN (PRECIPITATED BY 66% SATURATION)

Stock solution: 1 g. legumin in 100 cc. 3 *M* sodium salicylate

Solution			
1% legumin, cc.	Other component	*p*H	$[\alpha]_D$
5	5 cc. water	6.4	−59.5
5	5 cc. 0.01 *N* H_2SO_4	5.2	−54.1
5	5 cc. 0.01 *N* NaOH	9.4	−63.3
5	5 cc. 0.02 *N* NaOH	12.3	−64.4

TABLE VI

Optical Rotation of Tuberin, Denatured with Detergent

Stock solution: 0.8 g. globulin in 40 cc. 2% sodium dodecylbenzenesulfonate

pH	$[\alpha]_D$	0.002 N iodine for 0.1 g. protein, cc.	η_{sp}/c
6.2	−50.2	1.81	0.0108
5.2	−46.5	1.12	0.0082
3.7	−41.0	0.80	0.0070
9.1	−54.8		
11.9	−56.8		

Deaminated Legumin

The deamination was carried out in two ways: either by heating for two hours at 40–45°, or upon cooling of the slightly acid solution containing nitrite with ice water (2–4°) for 40 minutes.

(A) 2.5 g vetch legumin (precipitated at 66% saturation with ammonium sulfate) was dissolved in 100 cc. 10% NaCl, 2.5 g. sodium nitrite was admixed, and 0.1 N acetic acid was added until nitrogen bubbles appeared. The mixture was kept 1 hour at room temperature and then warmed 2 hours at 40–45°. The solution was then dialyzed, precipitating the deaminated legumin; it was filtered off, washed, and dried in a vacuum desiccator at room temperature; yield 2.2 g.

(B) 2 g. vetch legumin [the same as in (A)] was dissolved in 100 cc. 10% NaCl, 7 g. $NaNO_2$ was added, cooled with ice water, and dilute acetic acid added until pH 4.9 was reached. The mixture was kept for 40 minutes in ice water, then dialyzed in cold water; the deaminolegumin was obtained pure as described in (A).

Like legumin, both deaminated products dissolve in 10% NaCl or 0.01 N alkali. The rotatory power and viscosity of these solutions is almost the same as for legumin. Also, the dependence of rotation on pH is the same. The reducing capacity is somewhat smaller than the reducing capacity for legumin[2] because the SH groups are oxidized by deamination. However, there is some difference when the rotations of solutions of legumin and deaminated legumin in detergent are compared. There is a small difference in the dependence of $[\alpha]_D$ on pH in the case of deaminolegumin-B and legumin, but the difference is rather large in the case of deaminolegumin-A, as shown in Figure 2.

Optical Rotation, Reducing Capacity, and Viscosity of Native and Denatured Legumin

The most important results are summarized in Table VII. Osborne and Harries[10] obtained for the purest samples of their legumin (in 10% NaCl) the specific rotation of −41 to −44°. The author of this article found a value of −42° for a twice-reprecipitated fraction of pea legumin in 2 M KBr. This value did not change in the pH limits of 5.8–8 (Fig. 1). For the sample of vetch legumin that was reprecipitated by acetone, this author found −46° (in 10% NaCl), and this value also did not change in the pH limits of 5.6–7.6 (Fig. 2). It is difficult to decide whether this somewhat higher rotatory power is due to a very slight denaturation; the nitrogen content of this sample was the same as for the other products (about 17.4% for dry ash-free protein).

TABLE VII

OPTICAL ROTATION, REDUCING CAPACITY, AND INTRINSIC VISCOSITY OF NATIVE AND DENATURED LEGUMIN (PRECIPITATED AT 66% SATURATION)

Sample	pH	$[\alpha]_D$	Iodine for 0.1 g. protein, cc.	η_{sp}/c $(c \rightarrow 0)$
Native legumin of pea in 2 *M* KBr	5.8	−42.3	0.3	0.003
Native pea legumin in 10% NaCl	5.8	−42.0	0.3	0.003
Native pea legumin in 0.5 *M* $CaCl_2$	5.7	−47.5	0.4	0.003
Vetch legumin in 10% NaCl	5.8	−46.2	0.5	0.003
Vetch legumin in dilute NaOH	8.2	−56.0	3.9	0.007
Pea legumin in dilute CH_3COOH	3.9	−75.1	0.25	0.005
Pea legumin in 50% CH_3COOH	2.0	−60.2	0.5	0.043
Pea legumin with 40% propyl alcohol and $CaCl_2$ (final values)	5.7	−49.5	0.4	0.021
Pea legumin with sodium salicylate	6.4	−59.5	1.2	0.032
Vetch legumin with detergent	6.0	−60.2	1.1	0.010
Pea legumin with detergent	5.9	−58.4	1.1	0.009
Deaminated vetch legumin in dilute alkali	7.4	−55.6	0.5	0.008
Deaminated vetch legumin-A in detergent solution	5.7	−58.0	0.6	0.011

DISCUSSION AND CONCLUSIONS

Consideration of the results shows that the reagents that usually cause denaturation produce an increase in rotatory power and viscosity. But there are some exceptions when the reducing capacity does not rise upon denaturation. In the cases of propyl alcohol and acetic acid the reducing capacity is low, although the viscosity is high; the optical rotation is also high, at least for the solutions containing acetic acid. For solutions containing propyl alcohol the rise in rotatory power is only transitory. The intrinsic viscosity of legumin in solutions containing propyl alcohol or acetic acid is about 0.02, whereas in 10% NaCl it is about 0.003. The change is considerable, but not so great that a rather complete unfolding of the globular molecules of the native globulin should be assumed. The following fact can also be mentioned as a proof that there are not very long or loosely branched molecules. The minimum concentration of the protein necessary to produce jellies is very high for these solutions. In the cases of legumin denatured with acetic acid or propyl alcohol, loose jellies are formed only with 2–4% protein, whereas for true linear proteins (*e.g.*, gelatin) a much smaller concentration (about 0.5%) is needed. The increase of viscosity with time indicates that the rise in viscosity might also be due to the development of structure in the system as a whole. This increase with time is surely not due to a progressive uncoiling, since there is no reason to assume that it must occur. In any case, if some uncoiling occurs, it seems to be not very complete, *i.e.*, the denaturation not very deep, and in the case of acetic acid the denaturation is deeper than in the case of propyl alcohol. It is also quite clear that these results confirm the opinion that there are several degrees of denaturation.

The denaturation by salicylate or detergent is evident in all previously investigated properties. The most important observation is that not only the optical rotation of the protein but also the dependence of the rotatory power on *p*H is changed by these denaturing agents. Pauli and Kölbl[4] observed a similar behavior of ovalbumin that was denatured by heating of a solution containing urea.

At *p*H = 3 the solutions of the globulins in detergent solutions grow slightly turbid—the globulin coagulates. Tables III and VI show that, in such solutions, the decrease of the rotation angle with decreasing *p*H is accompanied by a decrease of reducing ability and viscosity. This behavior is easy to understand with the assumption that, under the influence of hydrogen ions, the unfolded assymmetric molecules of the protein–detergent complex are transformed upon coagulation into more compact and isometric particles. It is quite clear that, with such a change, the reducing groups will be less accessible, and that the reducing capacity and viscosity must thereby decrease.

It is noteworthy that deaminated legumin shows almost the same rotatory power as untreated legumin, and even the same dependence of rotation on *p*H as legumin itself. Obviously, the rotation is not very dependent on the free amino groups, *i.e.*, positive ionogene groups on the surface of the protein molecule

The fact that deaminated legumin dissolves easily in a detergent solution indicates that the free amino groups in the protein molecule are not very significant for the complex formation with detergent.[11] The optical rotatory power of these solutions also differs very little from that of legumin. Somewhat greater is the difference in the dependence of rotation upon *p*H for legumin and deaminated legumin (Fig. 2). This might be regarded as a proof that the amino groups, *i.e.*, positive ions in the surface of protein molecules, might have some influence on the configuration of the protein–detergent complex, although these groups are not essential for formation of the complex. The large lipophilic part of the detergent ion probably combines with the lipophilic part of the protein molecule, causing not only an increase of solubility, but also denaturation, with the resulting increase in viscosity, reducing capability, and optical rotation.

The optical rotatory power seems to be one of the surest means of estimating denaturation. The results show that it is possible to change the configuration of protein molecule to a certain extent in different ways with different reagents; the dependence of specific rotation upon *p*H is thereby very characteristic.

The author is grateful to Imperial Chemical Industries Ltd. and to Professor E. R. H. Jones, Director of the Chemistry Department, for facilities to perform this research.

References

1. B. Jirgensons, *J. Polymer Sci.*, **3,** 635 (1948).
2. B. Jirgensons, *ibid.*, **4,** 545 (1949).
3. H. Neurath, J. P. Greenstein, F. W. Putnam, and J. A. Erickson, *Chem. Revs.*, **34,** 157 (1944).
4. W. Pauli and R. Weiss, *Biochem. Z.*, **233,** 381 (1931). W. Pauli and W. Kölbl, *Kolloid-Beihefte*, **41,** 418 (1935). W. Pauli and L. Hofmann, *ibid.*, **42,** 34 (1935).
5. H. J. Almquist and D. M. Greenberg, *J. Biol. Chem.*, **93,** 167 (1931); **105** 519 (1934). D. M. Greenberg, in C. L. A. Schmidt, ed., *Chemistry of the Amino Acids and Proteins*, 2nd ed., Thomas, Springfield, 1943, p. 585, and literature cited therein.
6. H. Barker, *J. Biol. Chem.*, **103,** 1 (1933).
7. O. Lutz and B. Jirgensons, *Ber.*, **63,** 448 (1930); **64,** 1221 (1931).
8. H. S. Olcott and H. Fraenkel-Conrat, *Chem. Revs.*, **41,** 182 (1947).
9. W. G. Myers and W. G. France, *J. Phys. Chem.*, **44,** 1113 (1940). J. D. Ferry, *Advances in Protein Chem.*, **4,** 1 (1948).
10. B. Osborne and J. F. Harries, *J. Am. Chem. Soc.*, **25,** 842 (1903).
11. F. W. Putnam, *Advances in Protein Chem.*, **4,** 80 (1948). H. P. Lundgren, D. W. Elam, and R. A. O'Connell, *J. Biol. Chem.*, **149,** 183 (1943).

English Synopsis, see Summaries, page S3, Vol. V, 1950.

Résumé

La rotation optique de la légumine native et de la légumine dénaturée par la chaleur, par l'acide acétique, par les alcalis, par l'alcool propylique, par le salicylate sodique et dodécyl-benzène-sulfonate sodique, a été étudiée. Tous ces agents, sauf la chaleur, causent une augmentation du pouvoir rotatoire de la légumine. L'angle de rotation de la légumine native est constant dans des limites de *p*H de 5,2 à 8,0, mais s'accroît en solution acide et alcaline. Sous l'influence de concentration plus élevée en alcali, la légumine est fortement dénaturée, et après nautralisation et dialyse, elle devient insoluble dans une solution de NaCl 10%. Les variations de pouvoir rotatoire de la légumine ont été comparées aux variations correspondantes du pouvoir réducteur, déterminées iodométriquement, et comparées aux vicosités. Il n'y a pas de changement de pouvoir réducteur par chauffage de solutions neutres jusqu'à 90°, ou par traitement à l'alcool propylique ou à l'acide acétique 40–50%. Toutefois, la viscosité de la légumine traitée dans tous ces cas mentionnés ci-dessus est quelque peu plus élevée que la viscosité de la légumine native. Le chauffage de la légumine sèche durant trois heures à 100–105° cause seulement une dénaturation légère; après chauffage durant trois heures à 115°, la légumine devient toutefois insoluble dans une solution de chlorure de sodium 10%. Les solutions de légumine dans des mélanges alcool propylique-eau-sel ne manifestent qu'un accroissement passager de la rotation. L'angle de rotation de la légumine, en solution dans l'acide acétique à 40% volume et en présence de sel à cation polyvalent, s'accroît en fonction du temps; immédiatement après ajoute du sel, les viscosités de ce solutions diminuent puis, progressivement une gélatinisation s'opère, entrainant un accrossement de viscosité, qui dépasse considérablement la valeur initiale. La dépendance en fonction du *p*H de la rotation optique de la légumine et de la tubérine, qui ont été dénaturée par le dodécyl-benzène-sulfonate sodique ou de salicylate sodique, a été également étudiée. En solution acide, l'angle de rotation négatif décroît avec un accroissement de la concentration en ion hydrogène; en solution alcaline, l'angle de rotation ne s'accroît que faiblement par une augmentation de *p*H. La légumine, désaminée par un agent doux, présente généralement la même dépendance de la rotation spécifigue en fonction du *p*H que la légumine elle-même. La légumine désaminée se dissout dans une solution de détergent, et la rotation spécifique de ces solutions présente une dépendance

légérement différente du pH de celle que présentent les solutions correspondantes de légumine.

Zusammenfassung

Die optische Drehung von nativem Legumin und von Legumin, welches durch Erhitzen, Essigsäure, Alkalien, Propylalkohol, Natriumsalicylat und Natrium-dodecyl-benzol-sulfonat denaturiert war, wurden untersucht. Es wurde festgestellt, dass alle erwähnten Mittel, mit Ausnahme von Erhitzen, eine Erhöhung der optischen Drehung von Legumin bewirken. Der Drehwinkel von nativem Legumin ist in einem pH Bereich von 5.2–8.0 konstant, aber steigt in saurer und alkalischer Lösung an. Unter Einfluss einer grösseren Alkalikonzentration wird Legumin stark denaturiert, und nach Neutralisieren und Dialyse wird es in 10%igem NaCl unlöslich. Die Änderungen der optischen Drehung von Legumin sind mit den entsprechenden Änderungen des durch Jodtitration erhaltenen Reduktionsvermögens und der Viskosität verglichen worden. Beim Erhitzen von nahezu neutralen Lösungen bis 90° tritt keine Änderung des Reduktionsvermögens ein, ebensowenig bei Behandlung mit Propylalkohol oder 40–50%iger Essigsäure. In allen Fällen ist die Viskosität von so behandeltem Legumin jedoch etwas höher als die Viskosität von nativem Legumin. Erhitzen von trockenem Legumin während 3 Stunden auf 100–105° verursacht nur eine leichte Denaturierung, aber nach dreistündigem Erhitzen auf 115° wird Legumin in 10%iger NaCl unlöslich. Die Lösungen von Legumin in Propylalkohol-Wasser–Salz Gemischen zeigen nur eine vorübergehende Zunahme der Drehung. In Lösungen, die 40 Vol.% Essigsäure und ein Salz mit polyvalentem Kation enthalten, nimmt der Drehwert nach einigen Stunden Allmählich zu; sofort nach Zugabe von dem Salz nimmt die Viskosität dieser Lösungen ab, aber nach und nach tritt Gelatinierung ein, und die Viskosität steigt weit über ihren anfänglichen Wert an. Die Abhängigkeit der optischen Drehung vom pH für Legumin und Tuberin, die durch Natrium-dodecyl-benzol-sulfonat oder Natriumsalicylat denaturiert worden waren, ist untersucht worden. Es wurde gefunden, dass in saurer Lösung der negative Drehwert mit zunehmender Wasserstoffionenkonzentration abnimmt. In alkalischer Lösung nimmt der Drehwert mit steigendem pH nur wenig zu. Leicht desaminiertes Legumin besitzt fast die gleiche Abhängigkeit der specifischen Drehung vom pH wie Legumin selbst. Desaminiertes Legumin löst sich in Detergentienlösung und die specifische Drehung solcher Lösungen besitzt eine etwas verschiedene pH Abhängigkeit als die entsprechenden Leguminlösungen.

Received January 4, 1949

JOURNAL OF POLYMER SCIENCE VOL. V, NO. 2, PAGES 191–200

Studies on the Rate of the Emulsion Polymerization of Butadiene-Styrene (75:25) as a Function of the Amount and Kind of Emulsifier Used. I. Polymerizations with Commercial and Pure Soaps*

C. W. CARR, I. M. KOLTHOFF, E. J. MEEHAN, and R. J. STENBERG, *School of Chemistry, University of Minnesota, Minneapolis, Minnesota*

INTRODUCTION

From a practical and theoretical point of view it is of importance to study the effect on the rate of polymerization of the kind and amount of emulsifier used in the polymerization of butadiene (75) and styrene (25). This general problem was studied in several of the laboratories which cooperated in the government program of research on synthetic rubber. The following series of reports summarize the work done on the problem in this laboratory. Also included in this series are the results of work done on the closely allied problems of the effect of the amount of polymer formed in the latex, the size of the polymer particles, and the presence of added electrolyte on the rate of polymerization.

This first paper presents the time–conversion curves obtained with the use of the GR-S recipe in which commercial and pure soaps are compared. Early in the synthetic rubber program it was known that the degree of purity of the fats and oils used in manufacturing the commercial soaps has a significant effect on the rate of polymerization. Thus the purpose of this investigation was to find the difference between commercial soaps and soaps prepared from purified fatty acids on the rate of polymerization, and to determine which substances in the commercial soaps are responsible for the difference. This resulted in a large number of commercial soaps being compared with pure soaps and mixtures of pure soaps for their ability to promote the emulsion polymerization of butadiene (75) and styrene (25).

EXPERIMENTAL PROCEDURE

Polymerizations were carried out according to the GR-S recipe: butadiene, 75; styrene, 25; emulsifier, 5.0; *n*-dodecyl mercaptan, 0.5; potas-

---

* This investigation was carried out under the sponsorship of the Office of Rubber Reserve, Reconstruction Finance Corporation, in connection with the U. S. Government Synthetic Rubber Program.

sium persulfate, 0.3; water, 180 (all parts by weight). The materials for each run consisted of 50 g. of monomer and proportionate amounts of the other substances. The butadiene was 98.5% pure or better, and the styrene was free of inhibitors. A commercial mixture of primary mercaptans (principally *n*-dodecyl mercaptan) was used as modifier, and the potassium persulfate was of analytical reagent grade. The source and purity of the emulsifiers used will be given in the description of the various experiments.

Each charge was placed in an 8-ounce screw-cap bottle, and the bottles were kept at 0°C. At the start of the polymerization the bottles were placed in a thermostat at 50°C. and rotated end-over-end for various periods of time. The rate of polymerization was determined by taking weighed samples of latex from the bottles at the various times by use of the stopcock method.[1] A small amount of hydroquinone was added to the latex to stop further polymerization, and then the latex was evaporated to dryness in a weighed dish. The percent conversion was then calculated from the weight of latex sample taken and the weight of the dried residue, taking into account the weight of the solids initially present (soap, persulfate, and mercaptan).

INHIBITORS OR RETARDERS OF POLYMERIZATION IN COMMERCIAL SOAPS

Soon after this work was started, it was found that linoleic and linolenic acids present in commercial soaps act as retarders in the GR-S recipe. The hourly rate of conversion was decreased in direct proportion to the amount of these two substances present. On the other hand, such impurities in commercial soaps as tocopherols and lecithin have no appreciable effect on the rate of conversion even when added in relatively large quantities.

Wilson and Pfau[2] have reported in considerable detail their work on this problem. Our results are in complete agreement with theirs and will therefore be summarized only briefly.

Dr. W. C. Ault of the Eastern Regional Research Laboratories at Philadelphia kindly supplied us with samples of the purest fatty acids available. The following information on the fatty acids was given by Dr. Ault.

Stearic acid: melting point 69–70°C., acid number 198.7, and iodine number 0.

Palmitic acid: melting point 57.3–60.0°C., acid number 219, and iodine number 0.25.

Oleic acid: This material was prepared by a low temperature crystallization and fractional distillation procedure. Contains 98.3% oleic acid and 1.7% saturates.

Linoleic acid: It was prepared by the bromination of corn oil fatty acids. The tetrabromostearic acid was recrystallized and then the fatty acid obtained by reduction with zinc. The iodine number of this material was given as 182.3 (theory 181.0) and the acid number as 196.8 (theory 200). According to Dr. Ault, it is possible that there is a trace of ester present to account for the low acid number, but the product should be better than 98% linoleic acid.

Solutions of the potassium soaps were prepared from stearic and palmitic acids and of the sodium soaps from oleic and linoleic acids. This was done with standard potassium and sodium hydroxide solutions, respectively. An excess of 2% of fatty acid was present in the soap solutions. Twelve-hour polymerizations were carried out with potassium palmitate, potassium stearate, and sodium oleate. Various portions of sodium linoleate or water were substituted for equal portions of potassium palmitate and the mixtures were also used in twelve-hour polymerizations.

According to the data in Table I the pure soaps, potassium palmitate, potassium stearate, and sodium oleate, all gave the same conversion after 12 hours at 50°C. The conversions were practically identical with those obtained with the control soap. Mixtures of palmitate and oleate gave the same conversions as the unmixed soaps, showing that the iodine value is of no consequence in regard to the rate of polymerization.

TABLE I

TWELVE-HOUR POLYMERIZATIONS WITH SOAPS OF PURE FATTY ACIDS AND MIXTURES OF PURE SOAPS

Soap or soap mixture	Conversion %
Potassium palmitate[a]	78
Potassium stearate	78
Sodium oleate	78
95 parts potassium palmitate + 5 parts sodium oleate	78
50 parts potassium palmitate + 50 parts sodium oleate	79
95 parts potassium palmitate + 5 parts sodium linoleate	72
90 parts potassium palmitate + 10 parts sodium linoleate	66
Commercial soap, Procter & Gamble, Rubber Reserve quality (control)	78

[a] Equivalent amounts of soap were used; 5% sodium soaps and 5.25% potassium soaps on the basis of the monomers.

Substitution of 5% of palmitate by linoleate resulted in a decrease of 6% of the conversion or of 1.2% per 1% linoleate present in the palmitate. Substitution of 10% of palmitate by linoleate resulted in a decrease of 12% of the conversion or again 1.2% per 1% linoleate present in the palmitate. This figure is in close agreement with that given by Wilson and Pfau.[2] These authors also give figures which show that the retarding effect of linolenate is greater than that of linoleate.

It was of interest to know whether the linoleate acts as a "retarder" or as an "inhibitor" in the GR-S polymerization. For this reason the time–conversion curves with pure palmitate solutions and a mixture of palmitate and linoleate are presented in Figure 1. If the linoleate would act as an inhibitor, an induction period should be found. The results show conclusively, however, that linoleate is a retarder and not an inhibitor, *i.e.*, there is no induction period, and the hourly rate of conversion is decreased throughout the entire course of the polymerization. Again this is in agreement with the results of Wilson and Pfau.[2]

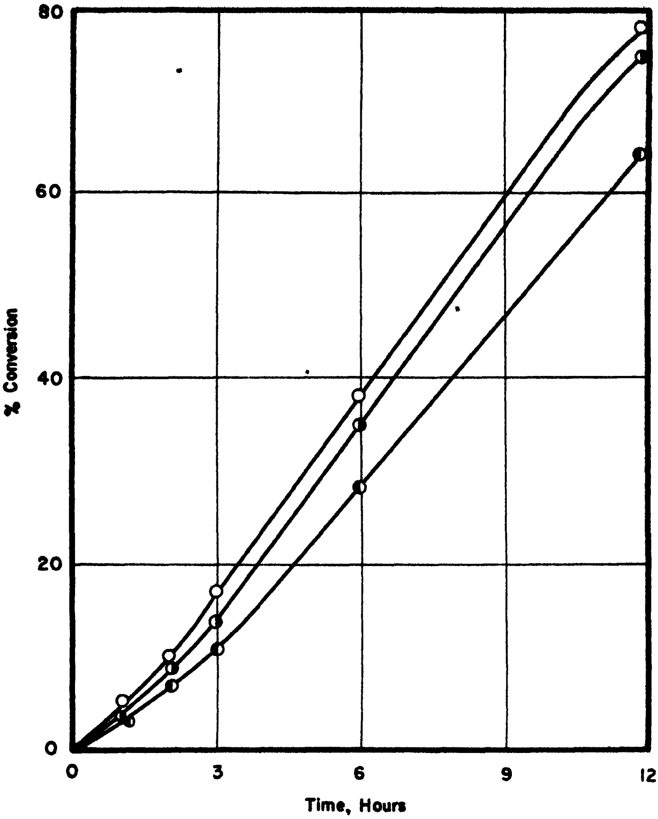

Fig. 1. Effect of linoleate on conversion in GR-S recipe. ○ potassium palmitate; ◑ 90 parts potassium palmitate + 10 parts water; ◐ 91.3 parts potassium palmitate + 8.7 parts sodium linoleate.

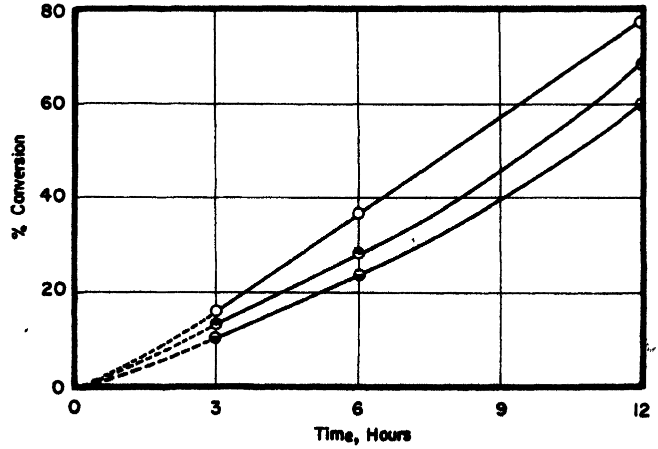

Fig. 2. Effect of linoleate on conversion in GR-S recipe (sulfole B-8 modifier). ○ 100 S. F. flakes; ⊖ 95 S. F. flakes + 5 linoleate; ◒ 90 S. F. flakes + 10 linoleate.

One experiment was carried out to determine whether or not linoleate exerts a retarding effect when tertiary mercaptans instead of the primary mercaptans are used as modifier. A commercial mixture of tertiary mercaptans (approximately C_{12}-, supplied by the Phillips Petroleum Company under the trade name Sulfole B-8) was used with the standard soap and with mixtures of this soap with linoleate. The results are shown in Figure 2. It is seen that linoleate exerts a retarding effect when the tertiary mercaptan mixture is used as a modifier. 1% of linoleate in the soap causes a retardation of about 1.2% in the conversion after 12 hours of polymerization at 50°C., in agreement with the retardation found with *n*-dodecyl mercaptan as a modifier.

Lecithin and tocopherol are two impurities likely to be found in commercial soaps. Accordingly, polymerizations were carried out to test the effect of these substances on the rate of reaction.

Tocopherol and lecithin samples were received from Dr. W. C. Ault. The tocopherol concentrates (α, β, and γ) contained 34.0% tocopherols, the lecithin was a commercial soybean product and probably a mixture of the phospholipids and neutral fat containing 50 to 60% phospholipids. The concentrations reported below are expressed in terms of the actual amounts for the tocopherol and in terms of the concentrate for the lecithin. Dr. Ault states that the tocopherol content of tallows would rarely, if ever, exceed a few thousandths or at most a few hundredths of one per cent. On the other hand, lecithin-like materials might occur to an appreciable extent. Therefore, it seems probable that tests covering the range up to 0.2% should be sufficient.

In the following experiments known amounts of the lecithin and tocopherol samples were added to solutions of standard soap, and the amounts used are expressed in parts added per 100 parts of soap. The results of the polymerization experiments are given in Table II.

TABLE II

EFFECT OF THE ADDITION OF LECITHIN AND TOCOPHEROLS TO THE RECIPE IN GR-S POLYMERIZATIONS

Addition to commercial soap, Rubber Reserve quality	Percent conversion after: 3 hrs.	6 hrs.	12 hrs.
0	16	37	78
0 2% lecithin	15	36	77
0.4% lecithin	16	37	78
0.01% tocopherol	15	35	77
0.1% tocopherol	10	32	72

It is seen that lecithin and tocopherols in amounts in which they may occur in commercial tallow soaps do not affect the rate of conversion. Even excessive amounts of lecithin do not affect the conversion. On the other hand excessive amounts of tocopherols decrease the conversion. Such amounts cause an induction period. As may be seen from the table, the rate of conversion is normal after the induction period. Thus, tocopherol does not act as a retarder, but as an inhibitor. Apparently it is destroyed during the induction period.

TESTING OF COMMERCIAL SOAPS IN THE GR-S POLYMERIZATION

In the previous section it was shown that linoleate (and linolenate) are the only substances that act as retarders in soaps. When fatty acids containing linoleate and linolenate are partially hydrogenated until all linoleate has disappeared, the soap prepared from such fats should give a rate of conversion comparable to that obtained with soaps prepared from pure fatty acids. Further experiments have fully substantiated this conclusion.

Two one-pound samples of soaps made from hydrogenated marine oil were received from Procter & Gamble with the information that marine oils contain anywhere from 15 to 20% C-20 and higher fatty acids.

Twelve-hour polymerizations at 50°C. were run, using these soaps in charges made according to the GR-S recipe. The percent conversion, the iodine values and thiocyanogen values of the soaps used in the polymerizations are given in Table III. The latter two values were supplied by Procter & Gamble. Polymerizations with these soaps resulted in satisfactory conversions, for the percent conversions were the same as with the control.

TABLE III

CONVERSION AFTER TWELVE HOURS AT 50°C. WITH SOAPS MADE FROM HYDROGENATED MARINE OILS

Soap sample	Percent conversion	Iodine value	Thiocyanogen value	Difference
HF-1	77	72.3	69.7	2.6
HF-2	77	49 7	47.5	2 2
Control	77	—	—	—

TABLE IV

CONVERSION AFTER TWELVE HOURS AT 50°C. WITH LEVER BROTHERS HYDROGENATED SOAPS

Soap sample	Percent conversion	Iodine value	Thiocyanogen value	Difference
R2RB	72	51.5	46.8	4 7
R2RB-H1	76	41.1	38.4	2 7
R2RB-H2	77	32.6	30.9	1.7
R2RB-H3	78	20.8	19.2	1.6
R5RB	67	59 1	50.9	8.2
R5RB-H1	76	39.7	37.2	2.5
R5RB-H2	77	31.0	29.4	1.6
R5RB-H3	78	22.2	20.7	1.5
Control	77	—	—	—

Further polymerizations with soaps of varying degrees of hydrogenation were carried out. The soaps were prepared by Lever Brothers from tallows R2RB and R5RB which had been hydrogenated at 150°C. with nickel catalyst. Each tallow was hydrogenated to 3 different degrees of unsaturation indicated by H_1, H_2, and H_3 in the soap number. The percent conversion, the iodine value, and thiocyanogen values of the fatty acids are shown in Table IV. The fatty acid analyses were supplied by Lever Brothers.

Apparently hydrogenation to an iodine value of approximately 40 is sufficient to give a conversion comparable to that of the control. Selective hydrogenation of linoleate and linolenate in the fats occurs. Once these substances are eliminated, no further hydrogenation is necessary, and the fats yield soaps with which normal rates of conversion are obtained.

Polymerizations have been carried out to test the effect of purity (distillation) and composition of fatty acids from which the soap is prepared. Most of the samples were received from Procter & Gamble, and they varied greatly in composition. Some of them were pressed and some were distilled. A few samples of Emery stearic acid were also investigated.

The Procter & Gamble soap samples are described as follows (letter from Victor Mills of Procter & Gamble):

> "1. Sodium soap of the free fatty acids from partially hydrogenated and distilled red oil. 2. Sodium soap of the free fatty acids from partially hydrogenated red oil (not distilled). 3. Sodium soap of single pressed stearic acid. 4. Potassium soap of single pressed stearic acid. 5. Sodium soap of single pressed stearic acid distilled as such. 6. Potassium soap of single pressed stearic acid distilled as such."

As communicated by Mr. Mills, the red oil was hydrogenated to an iodine value of 44. The amount of hydrogenation given was ample to eliminate all polyunsaturated acids. He states further that both the red oil and the stearic acid were derived from the same lot of tallow which was hydrolyzed to fatty acids; the fatty acids were separated into red oil (most oleic acid) and stearic acid by the usual pressing operations.

Sodium and potassium soaps were prepared in this laboratory from Emery single pressed stearic acid. In a letter from W. H. Shields of Emery Industries, Inc., the following information was supplied:

> "Liquid Kontakt and Kontakt D.P. Acid are used as fat splitting reagents. In the distillation of the fatty acids these reagents are left behind in the still residue. When the fatty acids are separated without distillation. the reagents are left in the fatty acids, the major portion being found in the oleic acid after the pressing. The two samples of single pressed stearic acid are approximately the same in titre, iodine value and composition excepting one has been pressed from distilled fatty acids and the other from undistilled fatty acids."

In Table V are given the results obtained with the soap samples as obtained from Procter & Gamble. In the experiments reported in Table VI the soaps were prepared in solution by neutralizing the various fatty acids with sodium or potassium hydroxide.

Considering the fact that none of the soaps used for the experiments in Table V had been made completely water-free by drying, the agreement between the results in Table V and Table VI is satisfactory. The same rates of conversion were found with the soaps of distilled and of undistilled single pressed stearic acid using both samples from Procter & Gamble and from Emery Industries. Therefore, when the soaps are free of linoleate and linolenate, a purification of fatty acids by distillation does not result in increased conversion.

TABLE V

POLYMERIZATIONS WITH DIFFERENT SOAP SAMPLES FROM PROCTER & GAMBLE

Soap sample	Percent conversion after: 3 hrs.	6 hrs.	9 hrs.	12 hrs.
Sodium soap of partially hydrogenated and distilled oleic acid	18	—	—	79
Sodium soap of partially hydrogenated oleic acid (not distilled)	17	—	—	77
Sodium soap of single pressed stearic acid	17	37	—	80
Potassium soap of single pressed stearic acid[a]	15	34	—	78
Sodium soap of single pressed stearic acid (distilled)	18	40	60	77
Potassium soap of single pressed stearic acid (distilled)[a]	18	40	60	77
Control	18	38	58	77

[a] Equivalent amounts of soap were used; 5% sodium soaps and 5.25% potassium soaps on basis of monomers.

TABLE VI

POLYMERIZATIONS WITH SOAPS PREPARED IN THIS LABORATORY FROM EMERY INDUSTRIES AND PROCTER & GAMBLE FATTY-ACIDS

Source of fatty acid	Type of soap	Percent conversion after: 3 hrs.	6 hrs.	9 hrs.	12 hrs.
Procter & Gamble	Sodium soap of hydrogenated and distilled oleic acid	20	42	64	81
	Sodium soap of hydrogenated oleic acid (not distilled)	18	38	61	78
	Sodium soap of single pressed stearic acid	20	42	63	81
	Potassium soap of single pressed stearic acid[a]	20	38	63	79
	Sodium soap of single pressed stearic acid (distilled)	19	42	63	81
Emery Industries	Sodium soap of single pressed stearic acid (distilled)	21	42	65	81
	Potassium soap of single pressed stearic acid (distilled)[a]	19	39	63	78
	Sodium soap of single pressed stearic acid (not distilled)	17	42	63	80
Control		16	38	58	78

[a] Equivalent amounts of soap were used; 5% sodium soaps and 5.25% potassium soaps on basis of monomers.

POLYMERIZATIONS WITH POLYMER SOAPS

At the request of Dr. O. W. Burke, Jr., of Rubber Reserve Company, the use of a number of polymer soaps as emulsifiers in GR-S polymerizations was investigated. Werner G. Smith Company sent us samples of the following sodium soaps.

From soya bean oils: Polysoy; Polysoy-dimers; Polysoy-dimers, partially hydrogenated.

From marine oils: Celesterol acids; Polymar-tetramers; Polymar-tetramers, partially hydrogenated.

From linseed oils: Polylin; Polylin-trimers; Polylin-trimers, partially hydrogenated (sample 1); Polylin-trimers, partially hydrogenated (sample 2).

In Table VII are data for the fatty acids from which the soaps were prepared as supplied by Dr. F. C. Haas of Werner G. Smith Company.

TABLE VII

ANALYSIS OF FATTY ACIDS FROM WHICH POLYMER SOAPS WERE PREPARED

Fatty acid	Free fatty acids (as oleic), %	Iodine value	Saponification value	Acid number	Polymerization, in percent after 12 hrs.
Polysoy	100	91.8	202.0	198.8	44
Polysoy-dimers	95.8	100.5	195.5	190.4	43
Polysoy-dimers, partially hydrogenated	—	—	—	—	43
Celesterol acids	96.2	119.8	198.0	191.2	39
Polymar-tetramers	87.1	146.0	186.0	173.3	25
Polymar-tetramers, partially hydrogenated	—	—	—	—	33
Polylin	—	—	—	—	35
Polylin-trimers	92.5	118.0	191.0	183.8	35
Polylin-trimers, partially hydrogenated (sample 1)	—	—	—	—	45
Polylin-trimers, partially hydrogenated (sample 2)	—	—	—	—	31
Control	—	—	—	—	78

According to Dr. Haas, each of the oils was subjected to selective polymerization until the desired viscosity was obtained. The monomer fraction of those designated as dimers, trimers, and tetramers was then removed by distillation. The oils were then converted into fatty acids and saponified. In a letter the following is stated by Dr. Haas:

"No one is quite certain of the exact composition of these acids. However, we can state that as long as the iodine value is above 85, there must be a linoleate portion present equivalent to 1.1 times the iodine value above 85. In other words, if the iodine value is 110, there will be approximately 27% of linoleate portion. We doubt very much whether there will be any linolenate or higher unsaturated portions present, due to the fact that the higher unsaturated acids will be the first to polymerize.

"Following are the approximate compositions of the various acids:

Polysoy Dimers: Monomers none, Dimers 65%, Trimers and higher Poly acids 35%.

Polylin Trimers: Monomers none, Dimers 45%, Trimers and higher Poly acids 55%.

Polymar Tetramers: Monomers none, Dimers 30%, Trimers 30%, Tetramers and higher Poly acids 40%.

"We have determined the molecular weight to be approximately as follows: Dimer acids 680, Trimers 840, Tetramers 1050."

The percent conversion after 12 hours obtained by using these soaps as emulsifiers in the GR-S recipe is shown in Table VII; it is seen that these soaps all give a small rate of conversion. The polysoy and polylin-trimers (partially hydrogenated, sample 1) gave the highest conversion which are only of the order of 43–45% after 12 hours as compared with 78% obtained with the control. Since these soaps gave faster polymerizations than the other samples, conversions with these two products were determined after a longer time. These two soaps gave 72 to 74% conversion after 18 hours at 50°C.

It was thought that the rate of conversion could be increased considerably by taking 10 parts of soap instead of 5 parts (GR-S recipe). However, even with these large amounts of soap, only 58% conversion was obtained after 12 hours. Thus, it seems apparent that these polymer soaps, which are of somewhat indefinite composition, are not as suitable for general use in the GR-S recipe as the ordinary fatty acid soaps.

References

1. A. I. Medalia, *J. Polymer Sci.*, **1**, 245 (1946).
2. J. W. Wilson and E. S. Pfau, *Ind. Eng. Chem.*, **40**, 530 (1948).

English Synopsis, see Summaries, page S4, Vol. V, 1950.

Résumé

Les savons alcalins des acides gras, stéarique, palmitique et oléique, produisent tous la même vitesse de conversion dans la préparation du GR-S, où ils sont utilisés comme émulsifiants. La présence de linoléate dans le savon cause une diminution de vitesse appréciable. Tous les savons commerciaux, purs de linoléate, donnent la même vitesse de conversion, que les savons purs. Le tocopherol et la lécithine n'exercent aucun effet sur la vitesse de polymérisation, du moins si leur concentration ne dépassent pas les quantités qui sont normalement présentes dans les savons commerciaux. En cas de concentration plus élevée, le tocophérol agit comme inhibiteur, occasionnant une période d'induction typique. Les rendements sont indiqués en présence de savons de polymère au lieu de savons d'acides gras.

Zusammenfassung

Die Alkaliseifen der Fettsäuren, Stearin-, Palmitin-, und Oleinsäure, zeigen alle die gleiche Umsatzgeschwindigkeit, wenn sie als Emulsionsmittel in der GR-S Vorschrift benutzt werden. Linoleat in der Seife verursacht eine ziemlich starke Verzögerung. Alle Handelsseifen, die kein Linoleat enthalten, gaben die gleiche Umsatzgeschwindigkeit wie reine Seifen. Tokopherol und Lecithin in Mengen, wie sie in Handelsseifen gefunden werden, haben keine Wirkung auf die Polymerisationsgeschwindigkeit. In grösseren Konzentrationen wirkt Tokopherol als Inhibitor, indem es eine typische Induktionsperiode hervorruft. Umsatzgeschwindigkeiten unter Benutzung von polymeren Seifen an Stelle von Fettsäureseifen sind angegeben.

Received March 28, 1949

JOURNAL OF POLYMER SCIENCE VOL. V, NO. 2, PAGES 201-206

Studies on the Rate of the Emulsion Polymerization of Butadiene-Styrene (75:25) as a Function of the Amount and Kind of Emulsifier Used. II. Polymerizations with Fatty Acid Soaps, Rosin Soaps, and Various Synthetic Emulsifiers*

C. W. CARR, I. M. KOLTHOFF, E. J. MEEHAN, and D. E. WILLIAMS, *School of Chemistry, University of Minnesota, Minneapolis, Minnesota*

INTRODUCTION

The first paper of this series[1] was concerned with the comparison of commercial and pure soaps in the emulsion polymerization of butadiene-styrene (75:25) according to the GR-S recipe. It was shown that certain unsaturated soaps, such as linoleate, which are present as impurities in commercial soaps, act as retarders for the polymerization, and that other impurities (lecithin and tocopherols) have no appreciable effect on the rate of the polymerization. As a continuation of this general problem of the effect of the emulsifier in the GR-S recipe, we report in this paper more data on the rate of conversion when different types of emulsifiers are used. These emulsifiers include sodium or potassium soaps of stearic, palmitic, myristic, lauric, and capric acids, several "rosin" soaps, and a number of synthetic detergents.

The experimental procedure was the same as that described in the previous paper.[1] Time-conversion curves at 50°C. were obtained for the GR-S recipe in which these various emulsifiers were substituted for the standard soap; 5 parts of the emulsifier per 100 parts of monomers being used in all experiments.

POLYMERIZATIONS WITH FATTY ACID SOAPS

The commercial soap used in the GR-S polymerization contains principally the fatty acids of 16 and 18 carbon atoms. Although not of direct practical interest, it was of theoretical interest to determine the rate of conversion when fatty acid soaps of shorter chain lengths were used. Sodium or potassium soaps were prepared from capric, lauric, myristic, palmitic,

---

* This investigation was carried out under the sponsorship of the Office of Rubber Reserve, Reconstruction Finance Corporation, in connection with the U. S. Government Synthetic Rubber Program.

and stearic acids. The C_{10}, C_{12}, and C_{14} acids were Eastman products; the palmitic and stearic acids were obtained from Dr. W. C. Ault of the Eastern Regional Laboratories. The time–conversion curves for polymerizations using these soaps are shown in Figure 1.

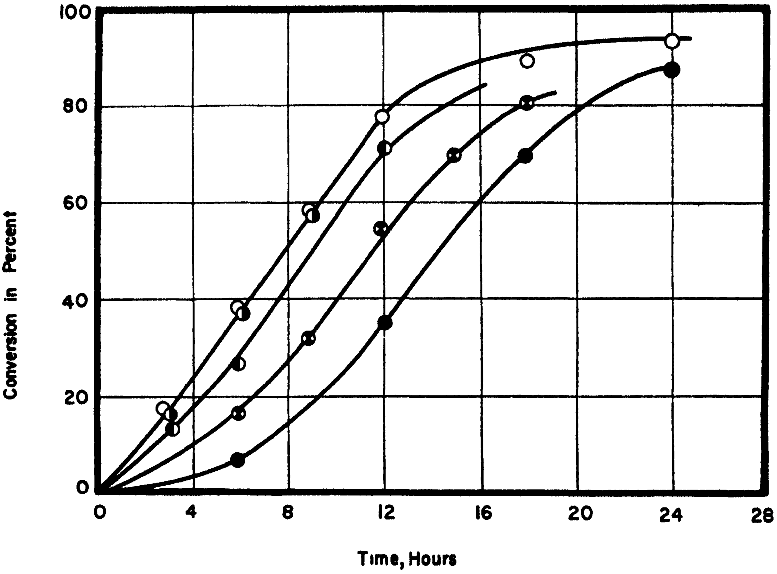

Fig. 1. GR-S polymerizations with fatty acid soaps of varying chain length. ○ C_{18}; ◑ C_{16}; ◐ C_{14}; ⊗ C_{12}; ● C_{10}.

As shown in the previous report, there is no detectable difference between the C_{16} and C_{18} soaps. On the other hand, with myristate, laurate, and caprate the initial rate of polymerization becomes progressively lower. After about 20% conversion, however, the rate has increased to such an extent that the further rate of polymerization approaches that of the C_{16} and C_{18} soaps.

POLYMERIZATIONS WITH SOME SYNTHETIC EMULSIFIERS

The following work was carried out with the use of a number of synthetic emulsifiers which are now commercially available instead of fatty acid soaps. These emulsifiers are as follows.

(*1*) Aerosol-18 (American Cyanamid Co.) Disodium salt of sulfonated mono-n-octadecyl succinamide. (*2*) Aerosol-AY (American Cyanamid Co.) Sodium salt of sulfonated diamylsuccinate. (*3*) Daxad-11 (Dewey and Almey Chemical Co.) Polyalkylaryl sulfonate. (*4*) Duponol (Dupont) Aryl sulfate. (*5*) Aquarex D (Naugatuck Chemical Co.) Sodium lauryl sulfonate. (*6*) Emulphor-O (General Dyestuff Corp.) Condensation product of oleyl alcohol and ethylene oxide. (*7*) Triton R-100 (Rohm & Haas Co.) Neutral sodium salt of a complex organic acid.

Many polymerizations were also carried out with sodium carbonate or borax added to the recipe to serve as buffers. The results of the experiments are summarized in Table I and indicate that none of the emulsifiers tested promotes the GR-S polymerization to the same extent as soap. The highest conversions obtained were less than 60% after 12 hours.

TABLE I

POLYMERIZATIONS WITH VARIOUS SYNTHETIC EMULSIFIERS (50 °C.)

Emulsifier	Further addition	Percent conversion after: 6 hrs.	12 hrs.
Aerosol-18. . . .	No addition	5	30
	0.05 *M* Na_2CO_3	12	35
	0 05 *M* borax	11	39
Aerosol MA . .	No addition	13	42
Aerosol-AY . .	No addition	5	17
	0 05 *M* borax	—	28
Daxad-11	No addition	3	19
	0 05 *M* Na_2CO_3	7	20
Dupanol	No addition	20	57
	0 05 *M* borax	23	56
Aquarex D	No addition	16	55
	0 05 *M* Na_2CO_3	17	44
	0.05 *M* borax	18	59
Emulphor O . .	No addition	21	41
	0 05 *M* Na_2CO_3	18	32
	0 05 *M* borax	16	28
Triton R-100	No addition	5	19
	0 05 *M* Na_2CO_3	—	15
	0 05 *M* borax	—	21
Soap (control)		38	78

POLYMERIZATIONS WITH DISPROPORTIONATED ROSIN SOAPS

The use of disproportionated (dehydrogenated) rosin soap in the GR-S recipe was introduced by Fryling.[2a] In a purified form it was soon found to be an adequate substitute for the fatty acid soaps. Other investigators

TABLE II

DESCRIPTION OF DISPROPORTIONATED ROSIN SAMPLES

Sample	Source	Acid No.
X-3518-92	Paul G. Carpenter, Hercules Powder Co.	184
Hercules 731	H. M. Spurlin, Hercules Powder Co.	165.1
K-wood	H. M. Spurlin, Hercules Powder Co.	155.4
X-wood	I. E. Knapp, Southern Regional Labs., Naval Stores Research Division	169
X-gum	I. E. Knapp, Southern Regional Labs., Naval Stores Research Division	162
N-wood	I. E. Knapp, Southern Regional Labs., Naval Stores Research Division	164
N-gum	I. E. Knapp, Southern Regional Labs., Naval Stores Research Division	167
Scrape gum	I. E. Knapp, Southern Regional Labs., Naval Stores Research Division	172

have confirmed these results.[3] As a part of the program for the development of the use of the rosin soaps, GR-S polymerizations with various rosin soaps were carried in this laboratory. Samples of rosins were received from other laboratories which were concerned with the problems of their preparation and further purification. Our work consisted primarily of testing these samples for their effect on the rate of polymerization.

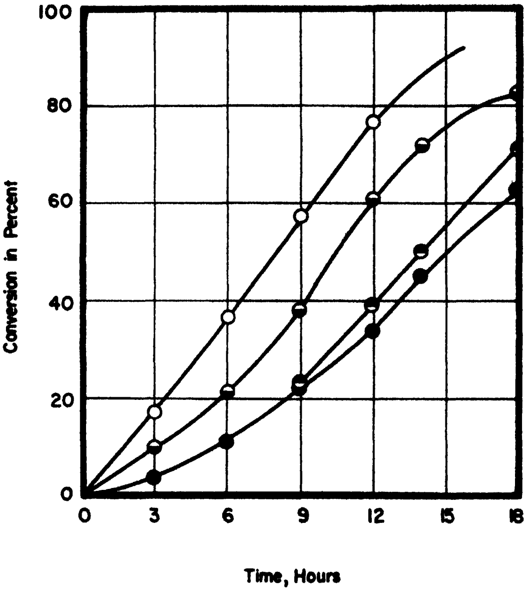

Fig. 2. GR-S polymerizations with various rosin soaps. ○ control, S. F. flakes; ◒ Rosin X-3518-92; ◓ Rosin 731; ● Scrape gum rosin.

The rosins used in these experiments are listed in Table II. The rosin acids were neutralized with sodium hydroxide solution, using 5 parts of sodium rosinate per 100 parts of monomers.

The conversions obtained with the sodium salts of the various rosin acids are given in Table III; in Figure 2 are shown the time–conversion curves

TABLE III

POLYMERIZATIONS WITH VARIOUS ROSIN SOAPS AT 50 °C.

	Polymerization time in hours					
Sample	3	6	9	12	14	18
	Conversions in per cent					
X-3518-92	10	21	38	61	72	83
Hercules 731	8	19	34	53	65	78
K-wood	6	14	26	43	55	74
X-wood	8	21	37	55	65	80
X-gum	7	16	32	52	62	77
N-wood	—	20	35	54	65	82
N-gum	—	13	24	39	50	68
Scrape gum	—	11	22	34	45	63

for rosins of 3 different activities as compared with that for fatty acid soap (SF flakes).

The per cent conversion for these samples in 14 hours at 50°C. varied between 45 and 72. The most active sample was X-3518-92. Samples giving conversions of 65% included Hercules 731, N-wood, and X-wood rosins. The other samples were of lower activity, the lowest being scrape gum rosin with a conversion of 45% in 14 hours.

Polymerizations were carried out also with the potassium salt of sample X-3518-92. The time-conversion curve was identical with that obtained with the sodium salt.

According to Dunbrook[2b] disproportionated wood rosin contains about 50% dehydroabietic acid, together with smaller amounts of dihydroabietic and tetrahydroabietic acids. In addition neutral bodies are present which act as diluents and are not inhibitors or retarders of polymerization. To determine the relative influence of the three acids, experiments were carried out with samples of dehydro-, dihydro-, and tetrahydroabietic acids. Pure samples of these three acids were obtained from Dr. D. A. Shepherd of the University of Illinois and were used in polymerizations with the GR-S recipe. The results of these investigations are given in Table IV. For comparison the rates of conversion obtained with the control fatty acid soap (SF flakes) and the 731 rosin are included in the table.

TABLE IV

POLYMERIZATIONS WITH DEHYDRO-, DIHYDRO-, AND TETRAHYDROABIETIC ACIDS IN THE GR-S RECIPE AT 50°C.

Emulsifier	Polymerization time in hours Conversions in per cent				
	3	6	9	12	14
Tetrahydroabietate	15	35	55	73	83
Dehydroabietate	12	31	49	66	78
Dihydroabietate	10	20	32	47	58
Rosin 731	9	20	34	53	65
Soap (control)	18	38	58	78	85

Of the pure products the dihydroabietate gives rise to slower polymerization in all stages of conversion than the other samples. The dihydroabietate gives the same rate of conversion as the 731 rosin for the first 9 hours' polymerization. However, at higher conversions the rate becomes slightly greater with the 731 rosin than with the dihydroabietate. The tetrahydroabietate gives the highest rate of conversion of the three pure components, reaching a value of 83% in 14 hours. During the first few hours of polymerization the rate obtained with this sample is slightly less than obtained with the control. From then on the rate becomes equal to that found with the GR-S recipe using fatty acid soap.

The results presented here indicate that the rate of the GR-S polymerization varies considerably with different kinds of emulsifiers. This variation of the rate is especially marked during the initial stages of the reaction. The way in which these data can be correlated with the present ideas concerning the polymerization mechanism will be presented in a subsequent paper, when also the effect of concentration of emulsifier will be discussed.

References

1. *J. Polymer Sci.* **5,** this issue.
2a. C. F. Fryling, *private communication.*
2b. R. F. Dunbrook, *India Rubber World,* **117,** 486 (1948).
3. J. T. Hayes, A. E. Drake, and Y. T. Pratt, *Ind. Eng. Chem.,* **39,** 1129 (1947). G. R. Cuthbertson, W. S. Coe, and J. L. Brady, *ibid.,* **38,** 975 (1946).

English Synopsis, see Summaries, page S4, Vol. V, 1950.

Résumé

Les savons d'acides gras, contenant 16 ou 18 atomes de carbone produisent la même vitesse de conversion dans la préparation du GR-S, où ils sont utilisés comme émulsifiants. En présence de myristate, laurate et caprate, la vitesse initiale de conversion devient progressivement plus faible. Après environ 20% de conversion, la vitesse ultérieure se rapproche de cele en présence de savons en C_{16} et C_{18}. Les rendements sont indiqués en présence de différents émulsifiants commerciaux, savons de colophane disproportionnés, composants purs de savons colophaniques y compris le tétrahydroabiétate sodique, le déhydroabiétate sodique et le dihydroabiétate sodique.

Zusammenfassung

Fettsäureseifen mit 16 oder 18 Kohlenstoffatomen bewirken die gleiche Umsatzgeschwindgkeit, wenn sie als Emulsionsmittel in der GR-S Vorschrift benutzt werden. Mit Myristat, Laurat, und Kaprat werden die anfänglichen Umsatzgeschwindigkeiten progressif geringer. Nach einem Umsatz von ungefähr 20% nähert sich die weitere Geschwindikeit derjenigen mit C_{16} und C_{18} Seifen. Umsatzdaten sind gegeben unter Benutzung von verschiedenen Handelsemulsionsmitteln, disproportionierten Harzseifen und reinen Komponenten von Harzseifen einschliesslich Natriumtetrahydroabietat, Natriumdehydroabietat und Natriumdihydroabietat.

Received March 28, 1949

JOURNAL OF POLYMER SCIENCE VOL. V, NO. 2, PAGES 207-215

Monomer–Polymer Ratio in Emulsion Polymerization of Styrene*

SIMON H. HERZFELD, ADELLE ROGINSKY, M. L. CORRIN, and WILLIAM D. HARKINS, *Department of Chemistry, University of Chicago, Chicago, Illinois*

INTRODUCTION

According to the theory of the mechanism of emulsion polymerization developed by Harkins[1] almost all the polymer is produced by reaction in the polymer particles. These, in turn, are initiated principally in the soap micelles present during the early stage of the polymerization process. It thus follows that, if this theory is correct, monomer must be present in the polymer particles. It is the purpose of this investigation to determine the amount of monomer associated with the polymer in the monomer-polymer or latex particle; this amount will be reported in terms of the monomer–polymer ratio M/P.

What is desired is the monomer–polymer ratio for the dynamic polymerization system. This is not an equilibrium value but a ratio determined by the relative rates of diffusion of monomer into the particle and of polymerization within the particle. This dynamic ratio cannot be determined directly; the values reported in this paper represent values found for systems in which an attempt has been made to so lower the rates of diffusion and polymerization that the dynamic values of the monomer–polymer ratio are but slightly altered before analysis. This attempt was probably successful with respect to the rate of polymerization; whether the diffusion rate was sufficiently reduced is uncertain. The monomer–polymer ratios reported in this paper are thus approximations to those occurring in the dynamic system.

Two different experimental methods were employed.

(*a*) *Gravimetric Method.* The total weight of the lower aqueous portion of the reaction system obtained by centrifuging the chilled reaction mixture was calculated on the basis of yield determination on both the aqueous portion and the whole mixture. The weight of monomer in the aqueous portion was then calculated by difference. Since this method involves a difference calculation it becomes increasingly inaccurate at low monomer conversions.

---

* This investigation was carried out under the sponsorship of the Reconstruction Finance Corporation, Office of Rubber Reserve, in connection with the Government's synthetic rubber program.

(*b*) *Spectrophotometric Method.*[2] The concentration and hence weight of monomer in the aqueous portion is determined spectrophotometrically in a benzene extract; the weight of polymer in this extract is also determined and the ratio calculated from these two experimental quantities. The accuracy of this method is essentially independent of the hydrocarbon conversion.

At low hydrocarbon conversions a considerable amount of monomer is dissolved in the soap solution. If the monomer–polymer ratio, as determined experimentally, is designated as M'/P then at low conversions, M'/P is greater than M/P, in which the unprimed M represents the monomer in the latex particles. At yields in excess of approximately 5%, the soap concentration is reduced to a point at which the solubilization of monomer is relatively small; hence at such yields M'/P and M/P are essentially equal.

EXPERIMENTAL

Polymerization Technic

All polymerizations were conducted on systems made up by the Mutual recipe but containing 100 parts of styrene and no butadiene. The concentration of soap, potassium laurate, was varied; the effect of this variation is discussed below. The reaction was carried out in a three-neck flask fitted with a mercury-sealed stirrer, inlet tube, and exit tube and maintained at constant temperature in a water bath. After the reaction mixture was placed in the flask the system was cooled to 0°C. and swept out with nitrogen. Samples were withdrawn as desired by applying nitrogen pressure to the inlet tube.

Gravimetric Method

The samples withdrawn were placed immediately in an ice bath and a small quantity of solid hydroquinone added. After ten minutes this sample was mixed thoroughly and the polymer in a weighed portion was precipitated by a large excess of methanol, washed and dried *in vacuo*. The total weight of polymer, P, and the per cent conversion were calculated from these data. Another portion of the sample was centrifuged for three minutes at 5000 g. and part of the lower aqueous portion removed by means of a needle hole in the plastic centrifuge tube. This process was carried out within ten minutes after withdrawal of the sample. The polymer in a weighed quantity of this aqueous portion was determined by the same means as described above. The weight of the aqueous portion was then calculated from the total weight of polymer, P, and the weight of polymer per unit weight of the aqueous portion. This weight of the aqueous portion, W_a, was plotted as a function of the yield (Fig. 1) and the values of the monomer–polymer ratio were calculated from smoothed values by W_a by means of the equation:

$$M/P = (W_a - W_r)/P$$

where W_r is the weight of all constituents in the aqueous phase (soap, water,

TABLE I

MONOMER–POLYMER RATIOS AT 35°C. FOR 5% OF SOAP BASED ON MONOMER, SPECTROPHOTOMETRIC METHOD

Expt. No.	Reaction time, hours	Per cent yield	Monomer-polymer ratio
3	0.2	0.55	3.96
2	0.33	1.16	3.19
1	0.5	1.41	3.09
2	0.67	3.74	2.66
3	0.6	4.00	2.48
1	1.0	6.25	2.59
2	1.0	6.68	2.57
3	1.0	8.23	2.49
2	1.25	8 65	2.51
2	1.5	11.95	2.51
3	1.5	13.95	2.40
2	1.75	14.94	2.41
2	2.0	17.52	2.38
2	2 25	20.22	2.28
3	2 0	21.00	2.32
2	2.5	22.15	2.21
2	2.75	22.86	2.21
1	2.5	23.44	2.06
1	3.0	29.21	1.88
3	2.5	29.60	1.86
1	3.5	34.18	1.62
1	4.0	39.07	1.38
1	4.5	40.52	1.36
1	5.0	40.97	1.30
3	3.5	45.48	1.05
3	4.5	59.11	0.59
3	6.0	74.66	0.26
3	7.5	82.16	0.16

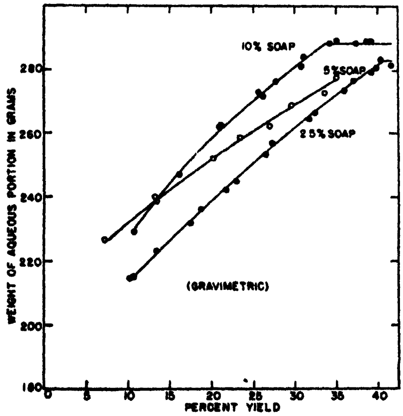

Fig. 1. Weight of aqueous portion as function of yield for emulsion polymerization of styrene at 40.7 °C. as determined by gravimetric method.

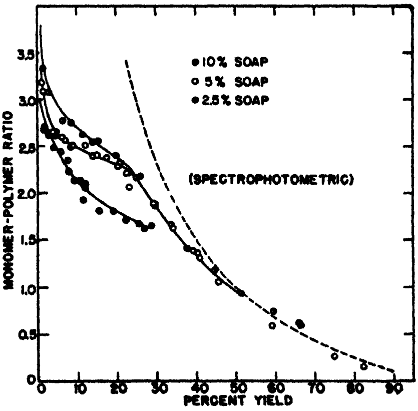

Fig. 2. Monomer–polymer ratio in emulsion polymerization of styrene at 35°C. as determined by spectrophotometric method.

etc.) with the exception of monomer. This method is based upon the experimental fact that essentially all the polymer produced in emulsion polymerization of styrene is found in the aqueous portion.

Spectrophotometric Method

Since hydroquinone interferes with the spectrophotometric determination of styrene, no hydroquinone was added to the samples withdrawn for analysis by this method. The samples were, however, swirled vigorously in air, since oxygen acts as a shortstop.[3] The per cent yield was determined by the technic described previously and the same centrifuging process was employed. Part of the aqueous portion was acidified with dilute sulfuric acid and extracted twice with benzene. The benzene extracts were combined, solutions made up in benzene–ethanol (85 parts by volume of benzene to 15 parts of ethanol) and analyzed for styrene in a Beckman spectrophotometer. Beer's law was shown to be valid for such systems at 2825 A. in the concentration range used in these measurements; the extinction coefficient expressed in grams of styrene per kilogram of solution is 7.26 ± 0.02 cm.^{-1} $(\text{g./kg.})^{-1}$. It has been shown by Meehan and Kolthoff[4] that substances other than styrene normally present in synthetic latices do not interfere with this determination. The polymer content of the benzene extract was determined after the addition of hydroquinone. Most of the solvent was removed at room temperature under reduced pressure and the polymer precipitated with methanol, washed, and dried. The monomer–polymer ratio was calculated from the two analyses.

RESULTS AND DISCUSSION

Values of the monomer–polymer ratio measured at 35 °C. by the spectrophotometric method are tabulated in Tables I–III and plotted against the yield in Figure 2. The curve in Figure 2 is obtained from the smooth

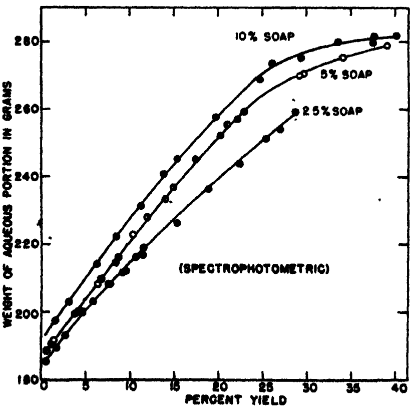

Fig. 3. Weight of aqueous portion as function of yield for emulsion polymerization of styrene at 35 °C., as determined by spectrophotometric method.

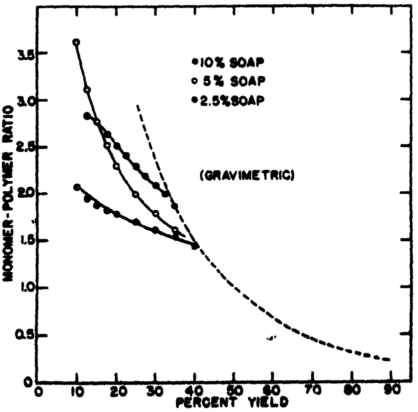

Fig. 4. Monomer–polymer ratio in emulsion polymerization of styrene at 40.7 °C. as determined by gravimetric method.

curve of the weight of the aqueous portion of the system versus the yield. The variation of the aqueous portion with yield is shown in Figure 3;

TABLE II

MONOMER–POLYMER RATIOS AT 35°C. FOR 2.5% SOAP BASED ON MONOMER, SPECTROPHOTOMETRIC METHOD

Expt. No.	Reaction time, hours	Per cent yield	Monomer–polymer ratio
2	0.33	0.47	3.28
1	0.5	1.66	2.67
2	0.68	1 69	2.69
2	0.84	2.64	2.62
1	1.0	4.55	2.62
2	1.08	4 59	2.65
2	1.33	5.80	2.44
2	1.68	7.54	2.35
1	1.5	7.69	2.23
2	1.84	9.06	2.14
2	2.08	9.38	2.06
2	2.33	10.55	2.13
1	2.0	11.39	1.92
2	2.68	11.52	2.09
1	2 5	15.32	1.80
1	3.0	18.94	1.79
1	3.5	22.37	1.70
1	4.0	25.40	1.67
1	4.5	26.98	1.62
1	5.0	28.67	1.65

TABLE III

MONOMER–POLYMER RATIOS AT 35°C. FOR 10% BASED ON MONOMER, SPECTROPHOTOMETRIC METHOD

Expt. No.	Reaction time, hours	Per cent yield	Monomer–polymer ratio
2	0.25	1.47	3.34
1	0.5	2.98	3.08
2	0.67	6.17	2.77
1	0.84	8.39	2.75
2	1.0	11.20	2.62
1	1.16	13.84	2.54
2	1.25	15.31	2.56
2	1.5	19.72	2.39
2	1 75	24.73	2.16
1	1.67	26.05	2.18
2	2.0	29.38	1.88
2	2.25	33.62	1.65
1	2.16	37.53	1.37
2	2.5	37.67	1.41
2	2.75	40.16	1.26
1	2.67	44.69	1.17
1	3.16	51.53	0.92
1	3.67	59.38	0.74
1	4.33	65.73	0.62
1	5.0	66.41	0.61

TABLE IV

MONOMER–POLYMER RATIOS AT 40.7°C. FOR 2.5% SOAP BASED ON MONOMER, GRAVIMETRIC METHOD

Expt. No.	Per cent yield	Weight of aq. portion	Monomer-polymer ratio[a]
—	10.0	214.0[b]	2.07
2	10.2	214.8	—
1	10.7	215.1	—
—	12.5	220.2[b]	1.95
2	13.6	223.4	—
—	15.0	260.4[b]	1.88
2	17.5	232.0	—
—	17.5	232.6[b]	1.82
1	18.6	236.2	—
—	20.0	238.7[b]	1.78
2	21.7	242.5	—
—	22.5	244.8[b]	1.69
1	22.9	244.9	—
—	25.0	250.6[b]	1.69
2	26.5	253.6	—
1	27.4	254.7	—
—	30.0	261.7[b]	1.60
1	31.8	264.5	—
2	32.6	266.8	—
—	35.0	272.0[b]	1.53
1	35.9	273.5	—
2	37.1	276.7	—
1	39.4	279.3	—
2	39.8	280.9	—
—	40.0	281.3[b]	1.45

[a] Calculated from smoothed curve of weight of aqueous portion versus yield.
[b] Read from smoothed curve of weight of aqueous portion versus yield.

TABLE V

MONOMER–POLYMER RATIOS AT 40.7°C. FOR 5% SOAP BASED ON MONOMER, GRAVIMETRIC METHOD

Expt. No.	Per cent, yield	Wt. of aq. portion	Monomer-polymer ratio[a]
1	7.1	226.6	—
—	10.0	232.0[b]	3.62
—	12.5	237.2[b]	3.11
1	13.2	240.1	—
—	15.0	242.2[b]	2.77
—	17.5	245.2[b]	2.52
—	20.0	251.6[b]	2.29
1	20.2	252.0	—
1	23.4	258.8	—
—	25.0	260.5[b]	1.98
1	27.0	262.5	—
1	29.6	269.0	—
—	30.0	269.1[b]	1.78
1	33.6	273.0	—
1	34.1	277.7	—
—	35.0	278.5[b]	1.61

[a] Calculated from smoothed curve of weight of aqueous portion versus yield.
[b] Read from smoothed curve of weight of aqueous portion versus yield.

different symbols are employed for different experiments. No distinction is made in Figure 2 between different experiments at the same soap concentration. Monomer–polymer ratios measured at 40.7°C. by the gravimetric method are tabulated in Tables IV–VI and plotted against the yield in Figure 4.

TABLE VI

MONOMER–POLYMER RATIOS AT 40.7°C. FOR 10% SOAP BASED ON MONOMER, GRAVIMETRIC METHOD

Expt. No.	Per cent yield	Wt. of aq. portion	Monomer–polymer ratio[a]
1	10.6	229.2	—
—	12.5	236.5[b]	2.84
2	13.4	238.7	—
—	15.0	244.6[b]	2.74
1	16.1	247.1	—
—	17.5	252.0[b]	2.63
—	20.0	258.8[b]	2.51
1	21.0	262.0	—
2	21.2	262.5	—
—	22.5	264.9[b]	2.40
—	25.0	270.5[b]	2.27
1	25.6	273.0	—
3	26.2	271.6	—
—	27.5	275.8[b]	2.18
2	27.8	276.5	—
—	30.0	281.0	2.08
1	30.8	281.0	—
3	31.1	284.1	—
—	32.5	285.8[b]	1.99
2	34.2	288.3	—
—	35.0	288.3[b]	1.86
1	35.2	289.0	—
3	37.4	288.3	—
—	37.5	288.3	1.65
2	38.6	289.1	—
1	39.3	288.9	—
—	40.0	288.3	—

[a] Calculated from smoothed curve of weight of aqueous portion versus yield.
[b] Read from smoothed curve of weight of aqueous portion versus yield.

The ratio between the amount of monomer and of polymer in the monomer–polymer or latex particle is equivalent to that measured in this paper only if the monomer in the aqueous portion is present almost entirely in the latex particle. This is true only if the micellar concentration of soap is relatively small. Values of the monomer–polymer ratio obtained at yields below approximately 5% measure solubilization of monomer in soap as well as solution in the latex particle and will not be considered further.

From the point of view of the Harkins theory the most significant feature of this work is that the latex particles undoubtedly contain a large amount of dissolved monomer. A second significant result is that the amount of monomer associated with the polymer in the latex particle, as expressed in terms of the monomer–polymer ratio, is not constant in the presence of a separate monomer phase. Whether the monomer–polymer ratios reported in this paper are a true measure of the dynamic values in the reacting system is a matter of conjecture; this uncertainty arises from a lack of knowledge concerning diffusion of the monomer into the latex particle after withdrawal of the sample and before removing the free monomer phase. If the monomer–polymer ratios reported represent true dynamic values they must be interpreted in terms of the rates of diffusion of the monomer into the latex particle and of polymerization within the particle. If the values reported are close to equilibrium values of the solubility of the monomer in the polymer, the solubility must vary with the yield.

Since the fugacity of the monomer must be constant in the presence of the free monomer phase this would indicate a pronounced change in the nature of the polymer with yield. The possibility that the monomer–polymer ratios reported in this paper may represent near-equilibrium values may be indicated by the fact that in different experiments at the same soap concentration and with varying reaction rates the measured monomer–polymer ratios fell upon the same curve. With 5 and 10% soap solutions at 35 °C. at yields in excess of 25%, monomer–polymer ratios as determined by the spectrophotometric method, are essentially equal. This, however, is not the case for the ratios measured at 40.7 °C. by the gravimetric method.

Values of the monomer–polymer ratio obtained by the spectrophotometric method at 35 °C. and the gravimetric method at 40.7 °C. are in agreement for soap concentrations of 5%. The values obtained by the gravimetric method at the higher temperature for 5% and 10% soap are somewhat higher than those determined for the same soap concentration by the spectrophotometric method at 35 °C.

TABLE VII

MONOMER–POLYMER RATIOS AT 35°C. FOR 10% SOAP BASED ON MONOMER WITH INTERMITTENT RETARDATION, SPECTROPHOTOMETRIC METHOD

Reaction time, hours	Per cent yield	Monomer–polymer ratio
0.33	0.07	37.98
0.53	1.23	3.54
0.73	2.75	3.09
0.93	4.82	2.87
1.13	5.82	2.81
1.35	8.07	2.79
1.57	9.56	2.79
1.78	10.44	2.81
2.00	12.00	2.78

It should be pointed out that in order to maintain a constant monomer–polymer ratio with increasing yield, the rate of diffusion of the monomer into the polymer particle must be large as compared to the rate of polymerization within the particle.

The values listed in Table VII represent monomer-polymer ratios for a system containing 10% soap and in which a small quantity of oxygen was admitted after each sample was withdrawn. The reaction rate was considerably slower than in the absence of oxygen. Insufficient data are at hand at the present time to warrant any conclusions as to the effect of reaction rate on the varition of the monomer–polymer ratio with yield.

References

1. W. D. Harkins, *J. Am. Chem. Soc.*, **69**, 1428 (1947).
2. R. S. Stearns and M. L. Corrin, *private communication*, 1944.
3. C. C. Price and C. E. Adams, *J. Am. Chem. Soc.*, **67**, 1674 (1945).
4. E. J. Meehan and I. M. Kolthoff, *private communication*, August, 1943.

English Synopsis, see Summaries, page S4, Vol. V, 1950.

Résumé

Les valeurs du rapport monomère-polymère sont données dans le cas de la polymérisation en émulsion du styrène à 35° et 40.7°C, et à différentes concentrations de savon. Deux méthodes expérimentales ont été utilisées, les techniques expérimentales sont décrites en détails. Les rapports monomère-polymère indiqués ne sont probablement pas les valeurs à l'équilibre, mais constituent un essai d'obtenir les valeurs dynamiques de ce rapport, ainsi qu'il se présente au cours de la polymérisation. Il n'est toutefois pas certain que ces valeurs, telles que rapportées, soient en accord raisonnable avec les valeurs dynamiques. Conformément à la théorie de la polymérisation en émulsion, présentée par Harkins, une quantité très appréciable de monomère est dissoute dans les particules monomère-polymère. En outre, le rapport monomère-polymère décroît avec un rendement croissant. Les résultats présentés ne permettent pas d'établir une corrélation entre la variation du rapport monomère-polymère d'une part, et le rendement et la concentration en savon, d'autre part.

Zusammenfassung

Werte des Monomer-Polymerisat-Verhältnisses in der Emulsionspolymerisation von Styrol bei 35° und 40.7°C. wurden für verschiedene Seifenkonzentrationen ermittelt. Zwei Versuchsmethoden wurden angewandt und werden beschrieben. Die angegebenen Verhältnisse von Monomer und Polymerisat sind wahrscheinlich nicht Gleichgewichtswerte, sondern stellen einen Versuch dar, dynamische Werte, wie sie währen der Polymerisation vorkommen, festzustellen. Ob die angegebenen Werte eine gute Annäherung an die dynamischen Werte darstellen, ist fraglich. In Ubereinstimmung mit der Emulsions polymerisations-Theorie, wie von Harkins dargestellt, wurde gefunden, dass eine grosse Menge des Monomers in den Monomer-Polymerisat-Teilchen gelöst ist. Es wird auch gezeigt, dass das Monomer-Polymerisat -Verhältnis mit steigender Ausbeute abnimmt. Die angegebenen Daten genügen nicht, zu einer Korrelation zwischen den Schwenkungen des Monomer-Polymerisat-Verhältnisses, der Ausbeute und der Seifenkonzentration.

Received March 31, 1949

JOURNAL OF POLYMER SCIENCE VOL. V, NO. 2, PAGES 217-251

General Theory of Mechanism of Emulsion Polymerization. II*

WILLIAM D. HARKINS, *George Herbert Jones Chemical Laboratory, University of Chicago, Chicago, Illinois*

I. INTRODUCTION: OUTLINE OF THE THEORY

The most fundamental relations of the theory of the mechanism of emulsion polymerization as presented in 1942–3[1] are as follows:

(*a*) In emulsion polymerization, with relatively insoluble monomers, nearly all of the polymer particle nuclei are initiated in the monomer solubilized in the interior of soap micelles.

(*b*) However, the micelles produce only an insignificant fraction of the polymer, which grows almost entirely in the polymer particles thus initiated. This occurs by polymerization of the monomer present in the swollen polymer particles. This monomer is supplied by diffusion from the monomer emulsion droplets through the aqueous phase and into the polymer particles, thus forming monomer–polymer particles. Monomer molecules are also captured by soap micelles as long as these are present and not saturated with monomer.

(*c*) A free radical mechanism was assumed.

A general outline of the theory[2] indicates in addition:

(*d*) Very little polymer forms in the monomer emulsion droplets, whose function is to act as a highly distributed reservoir of monomer.

(*e*) Extremely little polymer is produced in the aqueous phase. Later work gave an explanation of this fact. With relatively insoluble monomers, such as styrene, isoprene, or butadiene, free radicals are readily formed in the aqueous phase by the action of the catalyst on dissolved molecules of the monomer, or of a modifier (such as dodecyl mercaptan) if this is present. However, free radicals thus produced collide with other single molecules of this type much less frequently than with micelles when much soap is present.

When micelles are absent the relatively small number of collisions between a free radical and individual molecules of monomer in the aqueous phase produces only a very small number of polymer molecules. However, it is these few polymer molecules that capture monomer molecules diffusing through this phase, thus forming polymer particle nuclei. After a polymer

---

* This investigation was carried out under the sponsorship of the Reconstruction Finance Corporation, Office of Rubber Reserve, in connection with the Government's synthetic rubber program.

particle is once formed in the aqueous phase it exhibits no essential difference in behavior from a particle initiated in a soap micelle.

Thus the slow rate of polymerization in soap-free water as compared with that in micellar solutions is explained as due to the much smaller number of polymer–monomer particles present at any time in the soap-free system.

Even when soap is present the initial rate of polymerization is low in the absence of micelles.

II. PROPERTIES OF SOAP SOLUTIONS AS RELATED TO EMULSION POLYMERIZATION

There are two properties of soap solutions which are of fundamental importance in the mechanism of emulsion polymerization. Both of these are due to the fact that a long hydrocarbon chain, when immersed in water, possesses a very much higher free energy of the interfacial type than when it is surrounded by other hydrocarbon chains. This gives rise to two phenomena:

(*a*) The hydrocarbon chains of soap (also of acid, alcohol, amine, etc.) align themselves to form an adsorbed monolayer of ions (or molecules) at each interface between water and oil. The interfaces involved are those (*1*) between water and monomer emulsion droplets, of the order of 10,000 A. in diameter, and (2) between water and monomer–polymer or latex particles, commonly less than 1000 A. in diameter.

(*b*) Above a certain soap concentration known as the critical micelle concentration (cmc), the hydrocarbon chains, each with an ionic end, remove themselves from the water to form a small aggregate, usually of about 20 to 200 ions which form a double monolayer with the ionic ends oriented toward the water and the hydrocarbon chains inward. The thickness of this double ionic layer, which is designated as a micelle, is, in a solution of pure soap, very nearly twice the length of the soap molecule. By a process known as solubilization, monomer hydrocarbons are dissolved in the middle of the micelles, and, as shown by x-ray measurements, increase the thickness of the micelle. Long paraffin chain primary alcohol molecules align themselves between the soap molecules, with their polar groups toward the water. This is designated as solubility by film penetration.

Whenever a free radical grows in any individual micelle it continues to grow in the aqueous phase and thus forms a polymer particle. This absorbs monomer and becomes a monomer–polymer or latex particle.

Initially almost all of a relatively insoluble monomer is present in the emulsion as droplets which exhibit a distribution of sizes similar to that of hydrocarbon or other oils emulsified by soap, with a peak in the number distribution curve at about 1 *M* (10,000 A.).[3,4]

As shown later, both soap micelles and polymer particles inside the aqueous phase act as traps to capture monomer (and modifier) molecules in their diffusion through the solution and thus affect the rate of their diffusion.

Size of the Micelle

A new x-ray band discovered in this laboratory[5] is found to be related to the diameter of the micelle. When the Bragg spacings were calculated from this band, the values were found to be close to double the length of the soap molecule, which would correspond to a micelle two molecules in diameter. This band is designated as the micelle diameter or M-band.

It has been found by Corrin that if the maxima and minima of the M-band are determined in an entirely specific correct way, then the diameter of the micelle is given by multiplying the Bragg spacing for the maximum by 1.23 and that for the minimum by 1.71.

It is found that the radius of the micelle obtained in this way is 21.2 for potassium dodecanoate, 24.2 A. for the tetradecanoate. Also: (*a*) Independent of soap concentration in general to less than 0.3 A. (*b*) Increases with increasing number of carbon atoms when *n*-hydrocarbon chains are involved and is not very different from the length of the soap molecule.

Many tracings have been recorded from which a considerable number of micelle diameters may be calculated for pure soaps, and also when either nonpolar or polar–nonpolar solubilization is involved.

As examples of the values obtained the micelle of potassium dodecanoate is found to contain 61 molecules and of the tetradecanoate, 81 molecules.

With potassium tetradecanoate, ethylbenzene increases the number of soap molecules from 81 to about 124 and about 97 molecules of ethylbenzene are present at saturation.

It is outside the scope of this paper to review all of the work on the size of the micelle. By diffusion Hartley and Runnicles[6] obtained a value of 70 molecules of cetyl pyridinium chloride per micelle. Presumably this value is somewhat too large, since a salt was present. Debye and Anacker[7] by light scattering found that at its critical micelle concentration (cmc), dodecyl amine hydrochloride forms micelles, each of which contains 68 molecules.

Since increase of length of the hydrocarbon chain makes the decrease of free energy in the transfer of the hydrocarbon chain from the water to the micelle larger by about 1300 cal. per mole per CH_2 group, and since the repulsive energy of the ions is kept almost the same, the micelle must grow larger. Debye, Anacker, and Hagen[8] find the following values for the number (N) of molecules per micelle for the *n*-alkyl trimethyl ammonium bromides in water (Table I).

TABLE I

NUMBER OF MOLECULES PER MICELLE FOR *n*-ALKYL TRIMETHYL AMMONIUM BROMIDES

Number C atoms	N	cmc, *M*
C_{10}	36	0.0700
C_{12}	50	0.0151
C_{14}	75	0.00341

NUMBER OF SOAP MOLECULES PER MICELLE IN 0.0130 KBR

C_{10}	38	0.0672
C_{12}	56	0.0105
C_{14}	95	0.00176
C_{16}	170	

The most important aspect of the size of the micelle in emulsion polymerization is that of the number of monomer molecules present in a micelle. Some values are given in connection with the discussion concerning solubilization which follows.

Shape of the Micelle

Recently, as a basis for calculating the number of molecules in a micelle, Hartley's spherical model of the micelle has been adopted. This model seems to predict an extremely low density for the micelle.

Solubilization

In the polymerization of monomers which are hydrocarbons (*e. g.*, butadiene, styrene, isoprene) a most important property of the micelle is that not too large hydrocarbon molecules are dissolved inside the micelle between the ends of the hydrocarbon chains of the soap. This is known as solubilization. Since these molecules diffuse in and out of the micelle they do not remain altogether apart from the water. Nevertheless they keep mostly away from the polar-ionic edge of the micelle to avoid the higher free energy which this involves. A paper from this laboratory[10] exhibits the relations of solubilization most important for emulsion polymerization and gives references to other work.

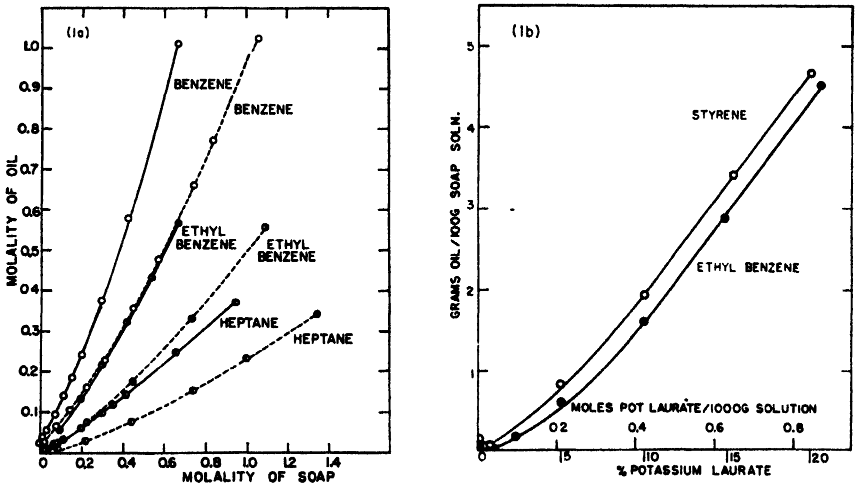

Fig. 1a. Solubility of oils, including styrene, in solutions of potassium dodecanoate (broken lines) and tetradecanoate (continuous lines). In b, potassium dodecanoate was used.

The increment in solubility per unit increase in the amount of soap, increases with soap concentration (Figs. 1a and 1b). It is found that the solubilization of a hydrocarbon increases the diameter of the micelle. In 0.4 molar potassium dodecanoate the diameter of the micelle was found to be 43.3 A. and when made 0.167 molar with respect to ethylbenzene, this became 55.5 or an increase (Δd_M) of 12.2 A. The micelle of the pure soap contained 61 molecules which increased to 93 molecules plus 37 of ethylbenzene when the solution was made 0.167 molar with respect to ethylbenzene. The importance of such relations to emulsion polymerization is pointed out later in connection with the function of the micelle in this connection.

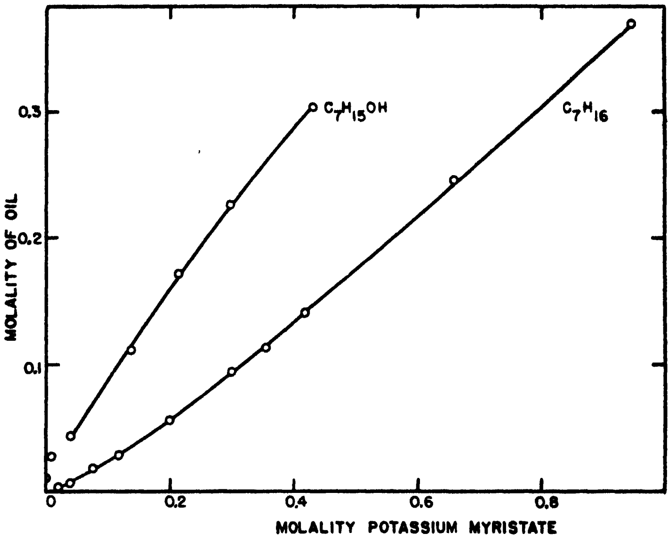

Fig. 2. The solubility of the alcohol by film penetration is much greater than that of the corresponding hydrocarbon, and the curvatures are different.

The diameter of the micelle as given by the M-band remains the same or becomes smaller when alcohols are solubilized. Long-chain alcohol molecules take positions between the soap ions with their polar groups toward the water, *i.e.*, their position and orientation are essentially the same as that of soap ions. The solubility relations are different and exhibit more complicated relations than are found in the ordinary solubilization of hydrocarbons which occurs in the hydrocarbon center of the micelle. On account of the great differences revealed by x-rays, mixed micelles of soap and alcohol (or other amphipathic molecules) are considered by the writer as a *new type of micelle*. As an example, Figure 2 shows that the 7 C-atom alcohol is more than twice as soluble as the corresponding hydrocarbon, and the curve is concave toward the soap concentration axis, whereas that for the hydrocarbon is convex.

Critical Micelle Concentration (cmc)

Since in emulsion polymerization nearly all of the polymer particles are initiated in the small number of monomer molecules dissolved in the micelle, it is evident that the existence or nonexistence of micelles and their number in a soap solution is of fundamental importance.

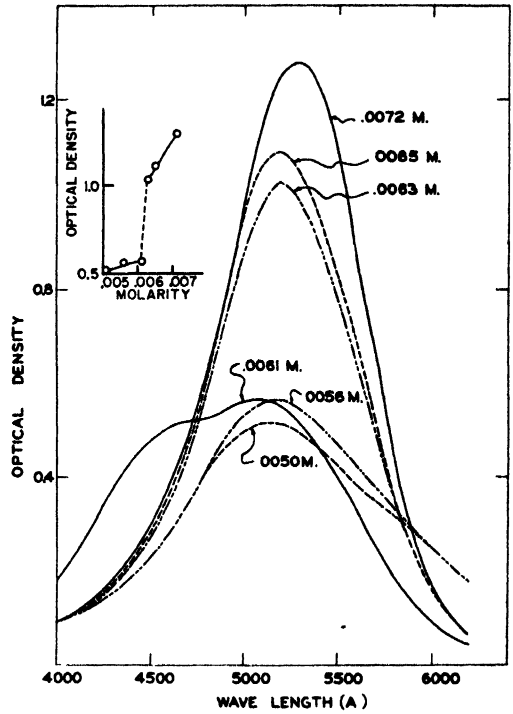

Fig. 3. Effect of the concentration of sodium dodecyl sulfate on the optical density of 5 × 10^{-5} molal neutral red; solutions aged for 18 hours. The sudden decrease in density between 0.0063 *M* and 0.0061 *M* occurs at the cmc.

What is known as the critical micelle concentration in aqueous solutions of potassium tetradecanoate is 0.0060 mole of the soap per 1000 g. of water. If a solution of a higher concentration is made 10^{-5} to 10^{-4} molar with respect to pinacyanol chloride (or certain other dyes) and titrated with water containing the same concentration of dye, a change of color occurs at this concentration, and this is almost as sharp as methyl orange in its change in a dilute solution between an acid and a base. With other dyes there is both a change of color and of fluorescence in ultraviolet light. For example the optical density of 5 × 10^{-5} molal neutral red in 1 × 10^{-4} sodium dodecyl sulfate, exhibits a remarkable shift at the critical micelle concentration. The optical density (Fig. 3) is almost doubled by an increase in the concentration of the soap from 0.0061 *M* to 0.0063 *M*. Not only these properties but almost all others change at this concentration. Now it would be extremely simple if below this concentration no micelles exist and above it they do exist.

However, it is not this simple, and Bury[11] has shown that the law of mass action governs the equilibrium between the unassociated long-chain ions and the aggregate. The equation as given by Corrin[12] is:

$$\frac{\gamma_a C_a}{(\gamma_d C_d)^m (\gamma_s C_s)^n} = K$$

in which γ_d, γ_s, and γ_a are the activity coefficients of the long-chain ion, the counter ion, and the aggregate, respectively; C represents concentration; m the number of paraffin ions and n of counter ions entering one micelle; and K is the equilibrium constant.

Nonapplicability of the Debye-Hückel Theory

Although the mass law is valid in the region of the cmc, the principle of ionic strength and the related Debye-Hückel theory are inapplicable, since the ionic micelle repels the counter ion to such a distance as to obscure any difference in effect between several separate counter ions and the same number of changes on a single ion. The best experimental evidence for the failure of this principle is to be found in the work of Corrin and Har-

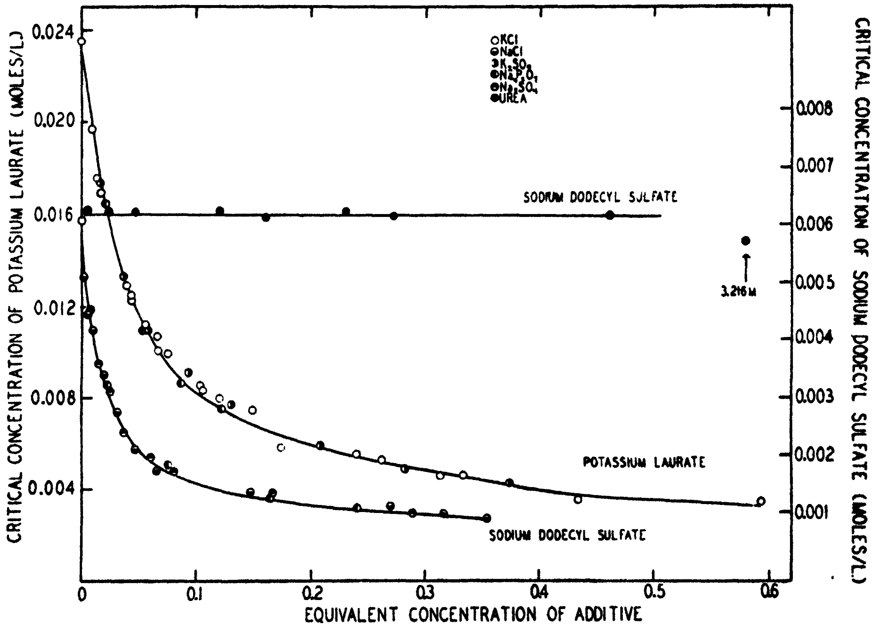

Fig. 4. Effects of salt on the cmc. The valence of the ion of the salt which has the same charge as the micelle is shown to have no effect.

kins[13] who found that the effect of ions of the ~~opposite sign of charge~~ from that of the micelle is independent of their charge when given in terms of the total equivalent concentration of the salt added (Fig. 4).

Grindley and Bury considered that the rapid increase in micelle concentration at the cmc is due to the large exponent with which the ion activities enter into the mass law expression. This explains the sharpness of the cmc when 14 or more C atoms are present in the chain, and its much wider range as a band for short chain soaps, such as those with 5 or 6 C atoms.

The critical micelle concentrations of the potassium soaps of *n*-long chain paraffin acids—found by Herzfeld, Corrin, and Harkins—are given in Table II. The values were obtained by titration using the color change in very dilute solutions (*ca.* 10^{-4} molar) or pinacyanol chloride.

TABLE II

CRITICAL MICELLE CONCENTRATIONS AT 25°C. OF SOAPS OF THE *n*-PARAFFIN ACIDS

(n = Number of C Atoms per Molecule)

n	cmc	*n*	cmc
14	0.006	9	0.200
13	0 013	8	0.401
12	0.024	7	0.780
11	0.049	6	1 49
10	0 097		

For soaps for $n = 10$ or below the cmc covers a considerable range; for example for $n = 8$, from *ca.* 0.15 to 0.4, as exhibited by the absorption spectrum. This range increases as n decreases.

TABLE III

EFFECT OF NATURE OF IONIC HEAD GROUP ON CRITICAL MICELLE CONCENTRATION OF COLLOIDAL ELECTROLYTES WITH TWELVE CARBON ATOMS IN THE NORMAL HYDROCARBON CHAIN AT 25°C.

Soap	cmc
Sodium dodecyl sulfate	0.0065
Sodium dodecyl sulfonate	0.010
Dodecyl ammonium chloride	0.013
Dodecyl trimethyl ammonium bromide	0 016
Potassium dodecylate	0 024

Each cmc *is multiplied by* 2 (*Fig.* 5) *for a decrease by* 1 *in the number of carbon atoms in the chain.* That the relation should be logarithmic was found by Stauff.

Below the cmc the soap solutions contain almost no micelles when the hydrocarbon chain is long, and are therefore ineffective in solubilization or penetration, and thus in initiating polymer particles.

In technical work soap mixtures are commonly used. If the cmc values of the separate soaps are not very different, then that for the mixture is not very different from the weighted mean value (Figs. 6a and 6b). How-

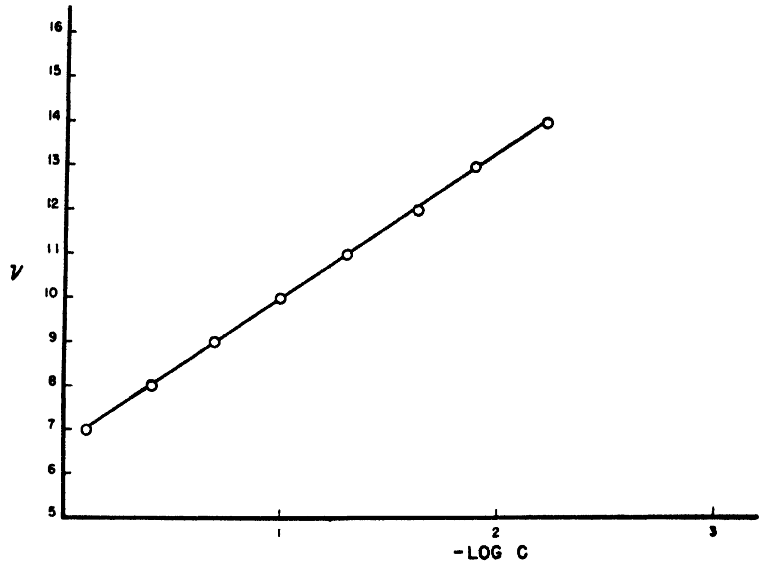

Fig. 5. Linear variation of the logarithm of the cmc with the number (γ) of carbon atoms in the soap molecule.

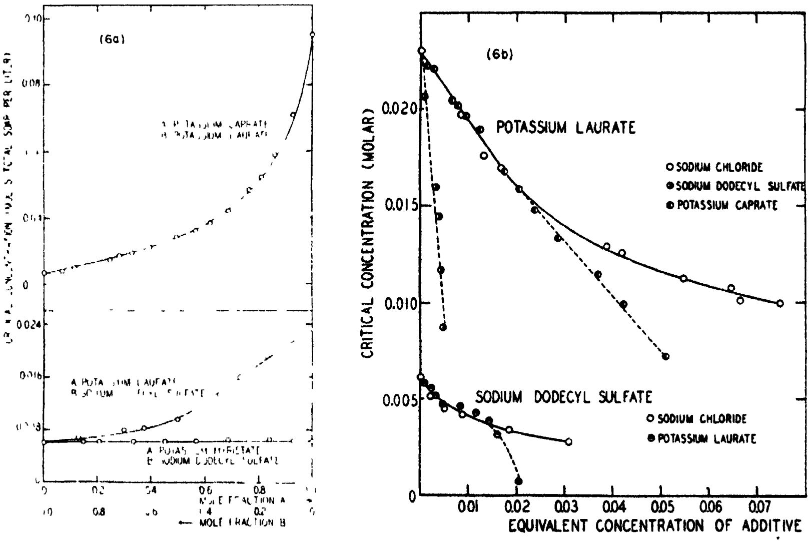

Fig. 6. Values of the cmc in mixtures of soaps. Short chain soaps act merely as salts. (a) Critical concentrations in mixtures of anionic soaps. (b) The effect of salts and other soaps on the critical concentration of potassium laurate and sodium dodecyl sulfate.

ever, if one soap has a much higher cmc than the others it acts as a salt to depress the cmc of the mixture.[14] These values are taken from the work of Tartar, of Ralston, and of Corrin and Harkins.

If a salt is added the effect of the charge of the ionic micelle is to attract more of the ions of opposite charge than corresponds to electrical neutrality, into the ionic atmosphere, thus giving a screening effect which reduces the repulsion between the ionic ends of the soap ions and the resulting work of approach. This both increases the size of the micelle and reduces the cmc.

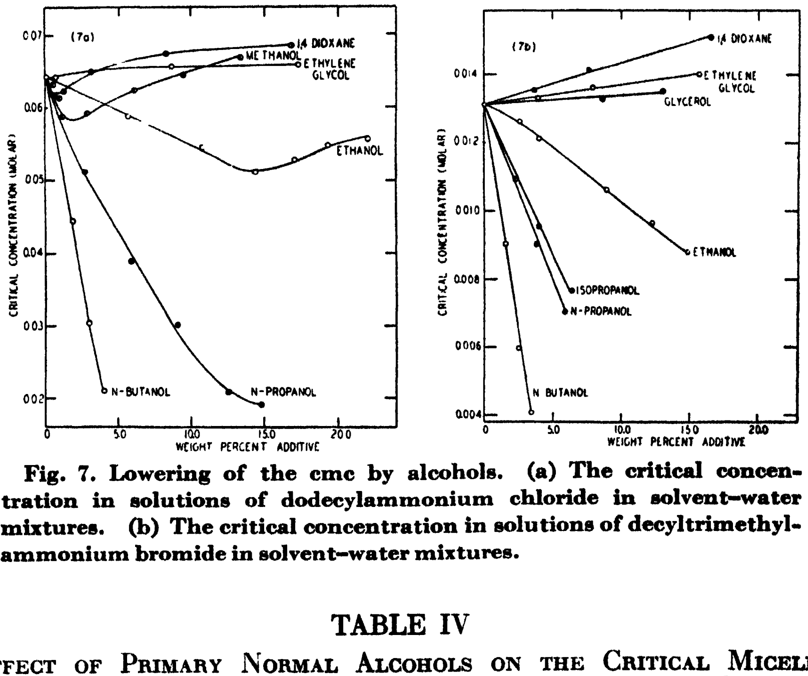

Fig. 7. Lowering of the cmc by alcohols. (a) The critical concentration in solutions of dodecylammonium chloride in solvent–water mixtures. (b) The critical concentration in solutions of decyltrimethylammonium bromide in solvent–water mixtures.

TABLE IV

EFFECT OF PRIMARY NORMAL ALCOHOLS ON THE CRITICAL MICELLE CONCENTRATION OF DODECYL AMMONIUM CHLORIDE AT 25 °C.

Number of C atoms in alcohol	Slope	Number of C atoms in alcohol	Slope
1	—	6	0.23[b]
2	−0.0012[a]	7	0.69[b]
3	−0.0052[a]	10	22.0[b]
4	0.19[a]	11	46.0[b]

[a] Determined Corrin.
[b] Determined Herzfeld.

The lowering of the cmc is given by *only* the ions of opposite sign of charge from that of the micelle. If m is the *total* concentration of the gegenion than for potassium dodecylate, log cmc = $-0.56969m - 2.6172$; and for decyl trimethyl ammonium chloride, log cmc = $-0.34287m - 1.5761$.

Lowering of the cmc by Alcohols. Since methanol is widely used in low temperature polymerization its effects are important.

Alcohols lower the cmc and the lowering increases very rapidly with the length of the hydrocarbon, as shown by Figures 7a and 7b and Table IV. With methanol and ethanol the decrease of cmc is followed by an increase as the concentration increases. With heptanol the lowering is very rapid: by about 50% when 1% is added.

One of the principal effects of the alcohols is to decrease the repulsion of the charged heads of the soap ions by increasing by penetration the distance between them. This lowers the cmc.

Diffusion of Monomers into Micellar Solutions. A process of importance in emulsion polymerization is the transfer of monomer and modifier from the emulsion droplets through the aqueous phase into micelles and into polymer–monomer particles, which serve as loci of polymerization. A question arose as to the distance to which molecules of oil can diffuse without being captured by the intervening micelles. This was investigated by a method used by Vinograd, Fong, and Sawyer.[15]

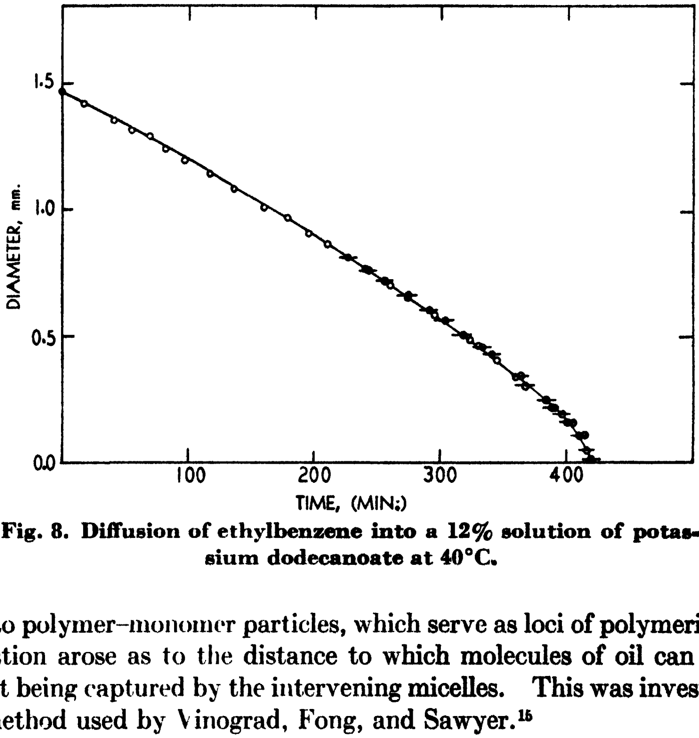

Fig. 8. Diffusion of ethylbenzene into a 12% solution of potassium dodecanoate at 40°C.

They measured by the use of a microscope the diameters of small drops of oil "submerged in soap solutions" and found that their diameters "decline *linearly* with time until 99% of the drop passes into the aqueous phase."

Stearns and Harkins[16] found a different relation: the rate of decrease of the diameter of the oil drop *increases with time* (Fig. 8), *i.e.*, as the drop grows smaller. The rate of decrease of diameter for a drop of ethyl benzene in 12.1% potassium dodecanoate solution at 40°C. was increased from −0.00260 mm. to −0.00430 mm. per minute by a decrease in the diameter from 1.4 mm. to 0.25 mm. The rate of diffusion is about twice as high as 40° as at 25°C.

In private communications to the writers, Professor P. Debye has developed a theory for the diffusion of molecules from an oil drop into a soap solution. From the relations developed by him the more rapid decrease of diameter for small than for large drops is to be expected. He introduces a quantity defined by the relation:

$$\Delta^2 = D/2$$

in which D is the diffusion constant for the oil (in the special case cited: ethyl benzene) and α is a constant such that $an\ dt$ is the number of molecules of the oil that are caught per cubic centimeter during the time dt by the soap at a place where the concentration of the oil is n. The quantity Δ is then representative for the characteristic thickness of the diffusion layer.

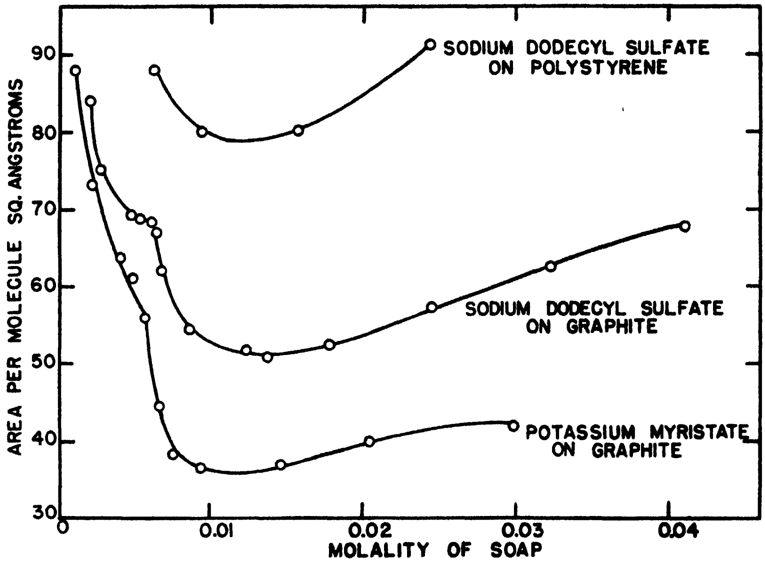

Fig. 9. Areas per soap molecule in adsorbed films on graphite.

The calculated value of Δ found by the use of the linear variation of the diameter d of the drop of ethylbenzene is *ca.* 50 A., while from a representative curve, similar to that of Figure 8 except that the concentration of the potassium dodecanoate was 10.6%, Debye calculated that Δ is about 0.06 mm. or 6×10^5 A.

Obviously, since this value is dependent upon the curvature it is only very approximate, but it is obvious that diffusion carries oil molecules, although they move very close to the micelles, past an extremely great number of them.

Thus the capture of oil molecules by micelles is in this sense a slow process i.e., even when unsaturated the micelle takes up only a small fraction of the oil molecules which approach it.

Area Occupied by Adsorbed Soap Molecules. Since in a not too dilute soap solution every monomer emulsion droplet and every monomer–polymer particle is surrounded by an adsorbed monolayer of soap, it is important to know the mean area occupied per soap molecule. In monolayers of *n*-long chain acids on water this mean area decreases to about 20 A.^{2} at a high film pressure. However, in a soap film there is a repulsion between the ionic heads which should increase this area.

The determination of the mean area per soap molecule for the emulsion is difficult, so graphite was chosen as having a nonpolar surface and determinations were made of the molecular area of the soap at the interface graphite soap solution.[17]

By nitrogen adsorption the surface area of the graphite was determined as 3.45 m^2/g. By dividing this area by the number of molecules adsorbed, the area per molecule was obtained. This gave the values shown in Figure 9. With sodium dodecyl sulfate the values decreased with increasing soap concentration until at the cmc, 0.006 *m*, the area per molecule became 68.3 A.^{2}, where a kink occurred in the m σ. With increase in *m* the value of σ (molecular area) fell to a minimum of 51.0 A.^{2} at about 0.01 *m*, and beyond that increased to 68 A.^{2} at 0.03 *m*. The curve for potassium tetradecanoate exhibits a similar shape but lower areas: 56 A.^{2} at the cmc, 36 A.^{2} at the minimum, and an increase to 42 A.^{2} at 3 *m*.

The uppermost curve for adsorption on polystyrene exhibits the same shape of curve beyond the cmc, but the molecular areas are meaningless since the sample is slightly porous.

In contrast, in solutions of sodium oleate, which has a much longer hydrocarbon chain, the molecular area at the cmc (0.0007–0.0012 *m*) is much lower (50 to 55 A.^{2}), and exhibits almost the minimum value. The cmc is poorly defined, presumably due to imperfect adlineation of the molecules as a result of the presence of the double bond in the middle of the hydrocarbon chain.

Nevertheless the molecular area increases with concentration beyond the minimum, as in the case of the other soaps. If the work of Hartley and of Tartar[18,19] is considered the increase of area beyond the minimum is not unexpected. However, that the lines which represent the area per molecule should be so highly curved as in the figure, is remarkable.

The molecular areas found for these soaps are larger than was expected, but Willson and collaborators[20] obtained values for the tetradecanoate and oleate which agree with the large areas obtained here within the experimental error of either the two widely diverse methods employed. In their work no molecular areas, other than that at the cmc, were obtained. The close agreement is remarkable since they adsorbed the soap on a butadiene: styrene (60:40) polymer, whereas as stated earlier, graphite was used in the work here. Also they determined the areas of the polymer by use of the electron microscope. Their values are valid at the cmc only. For potassium myristate the Goodrich value is 59 A.^{2}, the University of Chicago value 55 A.^{2}, for sodium oleate the values are 48.5 A. and about 50 to 55 A.^{2},

The value of the area is of importance:

(*a*) Since it determines the rate of disappearance of soap from the aqueous phase as the yield of polymer increases, and the amount of soap present determines the rate at which polymer latex particles are initiated.

(*b*) Soap titrations are employed widely as a means of calculating the interfacial area (sum for monomer–polymer particles and emulsion droplets) and from this, the mean size of the polymer–monomer particles. The values of the areas commonly used are undoubtedly too small, and this has introduced a large error in the values which have been obtained by this method.

III. INITIATION OF GROWTH OF POLYMER PARTICLE IN SOLUBILIZED MONOMER OF THE MICELLE

The theory of emulsion polymerization, as it was developed initially, indicated that in the emulsion polymerization of a relatively insoluble monomer (styrene, isoprene, butadiene) almost every polymer latex particle is initiated in its growth in the monomer solubilized inside the micelle.

To show what occurs several experiments of the type of the one cited here were carried out. A solution 0.39 molar with respect to potassium dodecanoate and 0.39 molar for the tetradecanoate was prepared. *This solution contained no monomer phase.* The x-ray M-band indicated a micelle diameter of 43 A. On saturating this with styrene this increased by 12 A. to 55 A. Potassium persulfate was added and on polymerization the diameter of the micelle as represented by the M-band returned to the initial thickness of 43 ± 1.0 A. This solution was again saturated with styrene. This gave an increase in diameter not far from the initial one of *ca.* 12 A. Obviously this process can be repeated over and over again, but the soap concentration decreases due to the adsorption of soap on the latex particles thus produced. These increase the turbidity of the solution.

A question now arises: if the monomer is polymerized while in the micelle, how does the weight of the molecule which is formed agree with the sum of the molecular weights of styrene in the micelle, *i.e.*, the so-called micelle molecular weight?

A 10% solution of potassium dodecanoate was prepared. When saturated with styrene at 25°C. this dissolved 1.9 g. styrene per 100 g. of solution. Such a solution was prepared with one-fourth and another with three-fourths of this amount of styrene, so all of the styrene present, except the very small amount in the water, was solubilized in the micelles. Potassium persulfate was added and the styrene polymerized at 50°C. Table V.

TABLE V

MOLECULAR WEIGHT OF STYRENE PER MICELLE IN UNDERSATURATED SOLUTIONS AND OF POLYMER PRODUCED IN A 10% SOLUTION OF POTASSIUM DODECANOATE

Degree of saturation, %	M.W. of monomer per micelle	M.W. of polymer (number average)[a]
77	3200	225,000
25	1000	4,400

[a] From viscosity and therefore not very accurate.

gives the sum of the molecular weights in the micelle (micelle M.W.) and the molecular weights of the polymer produced.

If the solubility of styrene in water at 50°C. is taken as 7×10^{-4} g. per gram of water, the number of molecules of styrene per cubic centimeter of aqueous phase is 4×10^{18}. The diffusion constant for styrene is about 10^{-5} cm.^{2}/sec. in the water. The growth of the polymer molecule, after it grows larger than the amount of styrene in the initial micelle, reduces the concentration of styrene out of the adjacent micelles. At a 10% concentration of potassium dodecanoate the number of micelles per cubic centimeter is about the same as the number of free styrene molecules, *i.e.*, those not solubilized in micelles. Thus the reduction in molecular weight of the polymer with increasing undersaturation of the micelles with styrene appears to be due to a lowering of the rate of diffusion in a direction out of micelles in which polymerization is not initiated.

Thus it is evident that in the absence of monomer emulsion droplets:

(*a*) The larger part of the polystyrene molecule is formed from styrene which was not present in the micelle in which the free radical has its initial growth. Most of the material of the polymer molecule comes from monomer molecules in the aqueous phase which diffuse out of other micelles. These are depleted in styrene in order to supply material to the free radical which has grown larger than corresponds to the amount of monomer in that micelle which was "stung" by the initial small free radical from the aqueous phase (or one inside which a primary free radical was formed by return of the catalyst) and in which the polymer molecule began its growth.

(*b*) As a result not only does the soap of the initial micelle change into adsorbed soap, but in addition a considerable number of other micelles lose their soap to the growing chain and thus disappear.

With 3% of potassium dodecanoate the number of micelles is of the order of 10^{18} per cubic centimeter. When 180 g. of water is used per 100 g. of monomer and the polymer particles reach their maximum size at a diameter of 800 A. the number of polymer particles formed is of the order of 1.5×10^{15} per cubic centimeter. In this case it takes only a little less than about 700 micelles to initiate one polymer particle, *i.e.*, the growth of a free radical occurs in only one out of nearly 700 of the micelles initially present. The material of the other micelles changes into adsorbed soap. It is not improbable that several polymer molecules may meet each other and form a small aggregate as the source of a single polymer particle. If this is true, it is obvious that the number of micelles present initially to give one polymer particle is smaller than the 700 listed here. It appears as if both micelles and polymer-monomer particles in water are extremely favorable loci for polymerization as compared with solutions of monomers in an oil phase. However, as pointed out above a great number of the initially existent micelles have no chance to give polymerization since they disappear very early to give adsorbed soap.

IV. STANDARD OR "MUTUAL" FORMULA FOR GR-S

The standard or mutual formula used for the production of GR-S is given in Table VI.

TABLE VI

Ingredient	Grams	Ingredient	Grams
Butadiene	75	Soap	5
Styrene	25	Potassium persulfate	0 3
Water	180	Lauryl mercaptan	0.5

Whenever in the work of this paper styrene or isoprene alone was used, 100 g. replaced the 75 g. of butadiene and 25 of styrene, and with an isoprene–styrene mixture the proportions were 75 g. of isoprene to 25 g. of styrene.

V. MONOMER-POLYMER RATIO (*M/P*) IN THE LATEX PARTICLE

According to the theory as initially presented by the writer, nearly all of the polymer produced in the emulsion polymerization of relatively insoluble monomers is formed in the monomer of monomer–polymer (latex) particles. The results of various types of experiments indicate that more than 99% of the polymer is produced in these particles. As long as emulsion droplets of monomer are present monomer diffuses from these, through the aqueous

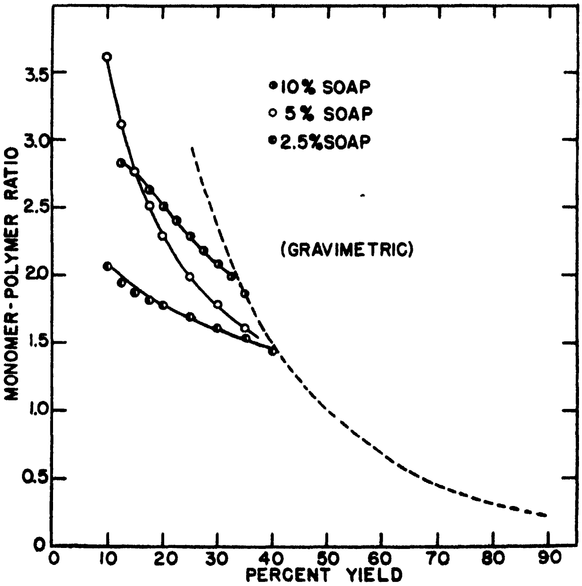

Fig. 10. The polymer–monomer (*M/P*) ratio by a gravimetric method. At higher yields than that at which the curves meet the line represented by dashes gives the *M/P* ratio.

phase and into the latex particles. Thus monomer is continually added by diffusion, but its amount in the particle is decreased by the polymerization which occurs inside it. Thus the value of M/P is changed at a rate which depends upon the rates of diffusion and of polymerization.

Experiments with isoprene indicate that the M/P ratios exhibit about the same values as with styrene.

The value of M/P at any given yield of polymer, smaller than that at which all of the monomer is in the polymer, is dependent upon the concentration of the soap, rates of diffusion and reaction, temperature, nature of the soap, length of the induction period, nature of the polymer, nature of the agitation, etc. Thus it may vary considerably. However the work of Herzfeld shows that good agreement between different experiments is obtained when these variables are kept nearly constant.

Since this ratio is considered in detail in a paper which follows, only a few of the more general relations are considered here as exhibited in Figure 10. This gives the values of the ratio above a 20% yield for 2.5, 5.0, and 10% as much soap as initial monomer or 1.37, 2.70, and 5.26% in the aqueous phase. At a 5% yield the values vary from $M/P = 2.5$ to 2.7.

The value of the ratio: (*a*) increases with soap concentration; and (*b*) decreases with yield; above a certain yield, the value of which changes with experimental conditions, all of the monomer is present in the monomer-polymer particles, so above that yield the value of the ratio is given by the equation:

$$M/P = (100 - y)/y$$

At lower yields the ratio is lower than that given by this equation, but higher than any ratio given in the region where this ratio is valid.

It is obvious from the values obtained that at low yields the monomer–polymer particle contains much more monomer than polymer. Thus (except for the monomer emulsion droplets, which act only as a storage reservoir and not as a seat of reaction) at yields above 5% essentially all of the monomer available for the reaction is associated with the polymer in the latex particles.

VI. DISAPPEARANCE OF SOAP WITH YIELD OF POLYMER

At low yields the monomer–polymer particles in the latex are very small. Consider, *e.g.*, that at 6% yield the electron microscope shows that the diameter of the polymer particles is 200 A., and the value of M/P is determined as 2.5, so the volume of the monomer-polymer particle is 3.5 times that of the polymer particle. If a monomer droplet 1 μ in diameter were to completely disappear and be converted into such monomer–polymer particles, the interfacial area would be increased by about 33 times.

Presumably, from what is known, the inference can be drawn that in the 2.78% solution of the mutual formula the micelles are not much larger than just above the critical micelle concentration, below which they disappear. In this region of the critical concentration, a region which is not always sharply defined, no polymer can be formed in micelles, since their number is not appreciable.

But the whole monomer particle does not disappear here. Now if half its area disappears, by conversion into monomer–polymer particles of the above size, then the area is increased by a factor of 23.

Under these conditions soap disappears rapidly from the solution by a change into adsorbed soap.

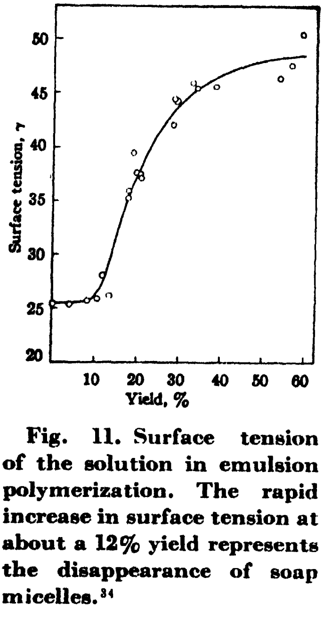

Fig. 11. Surface tension of the solution in emulsion polymerization. The rapid increase in surface tension at about a 12% yield represents the disappearance of soap micelles.[34]

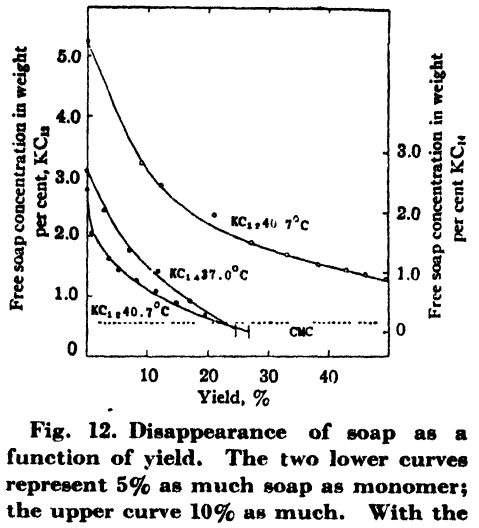

Fig. 12. Disappearance of soap as a function of yield. The two lower curves represent 5% as much soap as monomer; the upper curve 10% as much. With the higher amount of soap it has not disappeared at a 50% yield. The dye method used is not very accurate in the presence of latex but gives the general shape of the curves.[34]

Two methods have been used to determine the yield at which micellar soap disappears. In one of these the surface tension of the latex solution was determined as a function of yield (Fig. 11). A correct ring method was used. This involves the corrections of Harkins and Jordan.[21] The most essential feature of the work is to cream the emulsion without disturbing the equilibrium between the monolayer of soap on the emulsion droplets and the soap in the solution, but this can be done. It is also more difficult to obtain an accurate determination of the surface tension when polymer–monomer particles are present than in their absence. The surface tension begins to rise rapidly in the region of the critical micelle concentration, or in this case at a yield close to 15%.

This is a representative experiment, which when repeated half a dozen times at 50°C. with the same 75% of isoprene and 25 of styrene, gave about the same result.

Styrene gives somewhat larger particles, so the disappearance of micelles should occur at a higher yield. Figure 12 indicates that, with this monomer, micelles disappear at about a 20% yield when at 37°C. very slightly more than a 3% solution of potassium tetrandecanoate, or at 40.7°C. a 2.8% solution of the dodecanoate, is employed. In both of these experiments all of the monomer in the emulsion droplets had been transferred into the monomer–polymer particles.

With double the amount of soap (5.6%) all of the monomer had entered the monomer–polymer particles at a yield of 30%, but micelles remained at all yields.

These results were obtained by observing the disappearance of the fluorescence of Rhodamine 6 G and of two other dyes. In solutions of soaps alone these fluoresce when micelles are present or above the cmc, but not just below the cmc, since the single ions quench the fluorescence. In the presence of monomer–polymer particles this quenching is not so complete as in their absence. However the results indicate that with these two soaps the micelles disappeared at a yield of about 20%.

If half as much or 1.4% of soap is used the monomer–polymer particles are larger at the same yield, but since there is much less soap to be absorbed, its disappearance occurs at a much lower yield.

On account of the difficulties in the titration when latex particles are present, the curves which relate free soap concentration yield are inaccurate. However the rate of disappearance of soap is largest in the beginning and decreases with yield.

Although the following values are *highly variable* it may be said that with 2.8% of soap *ca.* 10^{18} micelles per cubic centimeter must disappear and the amount of soap contained in them be adsorbed, if polystyrene is involved, on *ca.* 1.5×10^{15} monomer–polymer particles at yields of 12 to 20%. The number of latex particles increases very little as the yield increases above these values. With less soap there are fewer micelles and a smaller number of latex particles.

The amount of polymer in a latex particle increases with time, so at the same yield the younger particles are smaller, in terms of polymer, than the older ones. The obvious inference is that if a latex were to be produced with a uniform particle size, then all of the particles should have the same age.

VII. RATE OF THE POLYMERIZATION REACTION

According to the writer's theory of the mechanism of emulsion polymerization almost all of the polymer is produced by the growth of free radicals in the monomer present in what had been considered by others as polymer particles, but are actually monomer–polymer particles. Since each of these particles constitutes a polymer reactor essentially independent of the other like particles, it is evident that the rate of reaction per unit volume of solution should be doubled by doubling the number of particles provided the size and monomer–polymer ratio could be kept the same, together with the same rate of addition to the particle of free radicals, and the supply of other reactants remains unmodified.

It had been found at work in the research laboratory of U. S. Rubber Company that in the polymerization of styrene the presence of atmospheric oxygen gave an induction period of several hours. On this account a high vacuum system of tubes was installed. The solids were evacuated at 10^{-5} mm. and the water and monomers distilled separately several times in another portion of the system where they were condensed by liquid nitrogen. Finally at low pressure the ice and solid monomers were allowed to melt and distil into a tube in liquid nitrogen which contained the soap and catalyst.

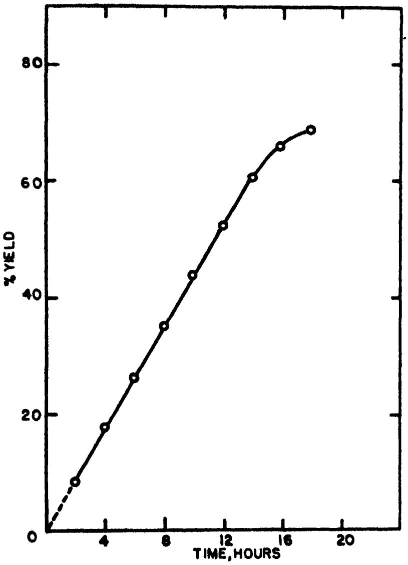

Fig. 13. Linear rate of polymerization of styrene-isoprene at 50°C. with no induction period.

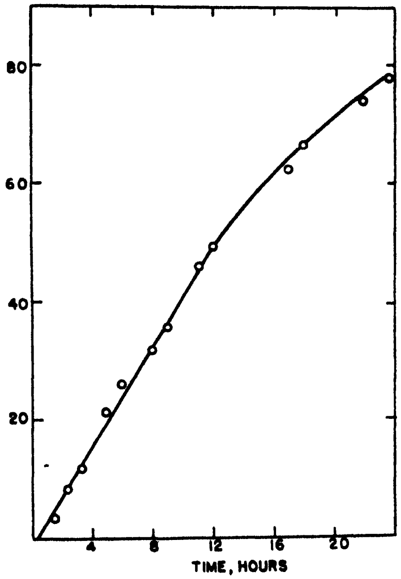

Fig. 14. Linear rate of polymerization with slight induction period.

The above treatment resulted in a linear rate of polymerization with no induction period at 50°C. as exhibited in Figure 13, with 75% isoprene and 25% styrene in the GR-S formula.

By the use of this technique 9 polymerizations with the same formula at 50°C. gave a linear rate to a yield of 50%, but an induction period of about 30 minutes (Fig. 14).

In two other experiments (Fig. 15) 5% as much air as liquid was introduced, but potassium ferricyanide was added to overcome the effects of the oxygen. With 0.2% there was no apparent induction period, and the remarkable result was obtained that the linear relation persisted up to a 75% yield.

In this experiment soap micelles are present up to a yield of about 15%, with very few micelles above a 10% yield. Thus above a 15% yield the number of polymer–monomer particles remains practically constant, and increases extremely little above 10%.

These experiments indicate that between a yield of 10 to 15% up to the upper limit of linearity the monomer–polymer particle produces polymer at a rate which is constant and independent of its size. The over-all rate varied only between 4.2 and 4.4% per hour in four sets of experiments.

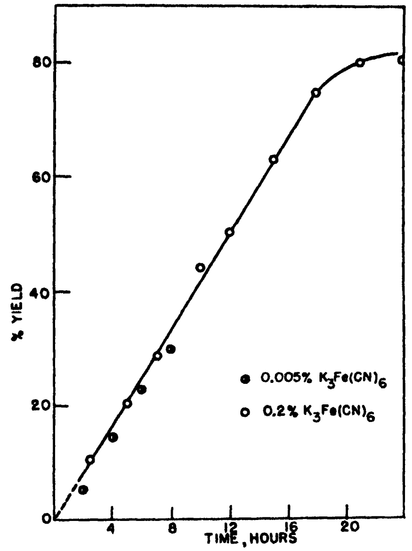

Fig. 15. Linear rate of polymerization of styrene-isoprene with potassium ferricyanide present. No induction period with 0.2% $K_3Fe(CN)_6$.

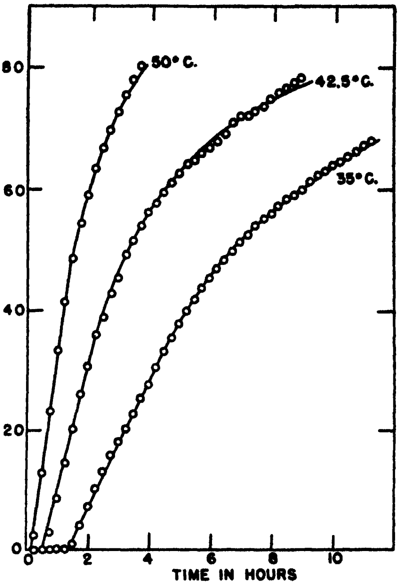

Fig. 16. Linear rate of polymerization of styrene at three different temperatures with decreasing induction period with increase in temperature.

The existence of this constant rate of polymerization as reported in 1943[22] has become the basis of two important extensions of the writer's theory. In one of these by Smith and Ewart, as discussed later, this is explained on the basis of the action of free radicals.

Another kinetic treatment by Corrin[23] made use of other experiments (Fig. 16 and Table VII) in which the linear relation was found in the polymerization of styrene at 35, 42.5, and 50°C. with 5% as much air as solution.

Thus the rate with styrene alone is, at 50°C., faster by a factor of 8.7, than when 75% is replaced by isoprene. At all of these temperatures the yield is a linear function of the time up to a high yield.

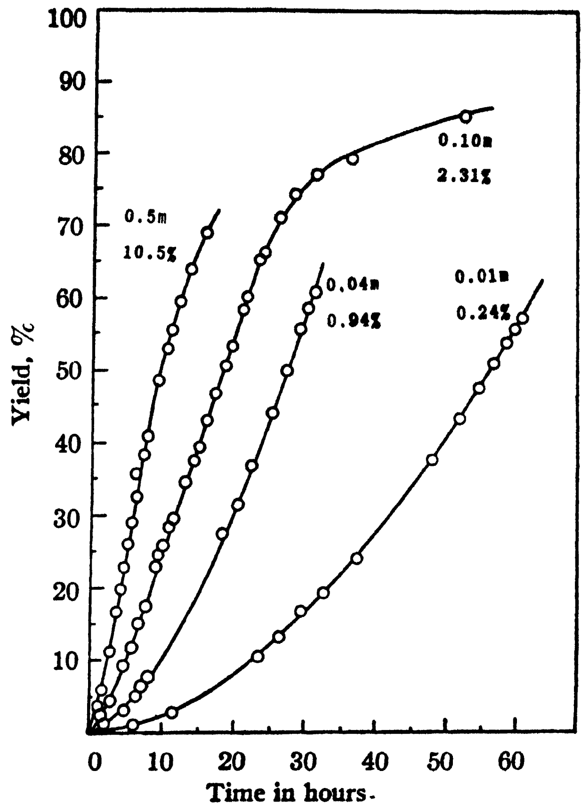

Fig. 17a. Yield of polystyrene as a function of soap concentration with the smallest concentration of potassium dodecanoate below the cmc.[14]

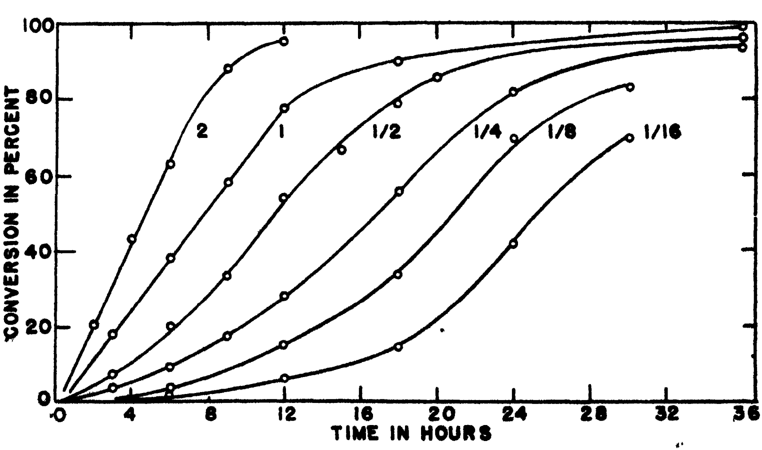

Fig. 17b. Effect of varying soap concentration in the mutual (GR-S) recipe (after Kolthoff). The numbers alongside the curves indicate the soap concentrations (C) with 1 equal to 5.0% of monomer, $^1/_2$ equal to 2.5%, $^1/_8$ equal to 0.625%, etc. The curves illustrate constant rate of reaction for 5 and 10% soaps.

TABLE VII

RATES AND INDUCTION PERIODS IN THE EMULSION POLYMERIZATION OF STYRENE (CORRIN)

(Mutual formula with styrene alone)

Temp., °C.	Rate, % per hour	Induction period, hours
35.0	10.0_6	1.27
42.5	17.2_3	0.35
50.0	37.4_1	0.16

The conclusion reached is that the reaction in the monomer–polymer particle is of a three-halves order with respect to monomer.

With no induction period the yield (y) is a linear function of the time (t) as expressed by the relation:

$$y = at$$

in which a is a constant. This becomes:

$$y = a(t - t_0)$$

when the induction period is t_0.

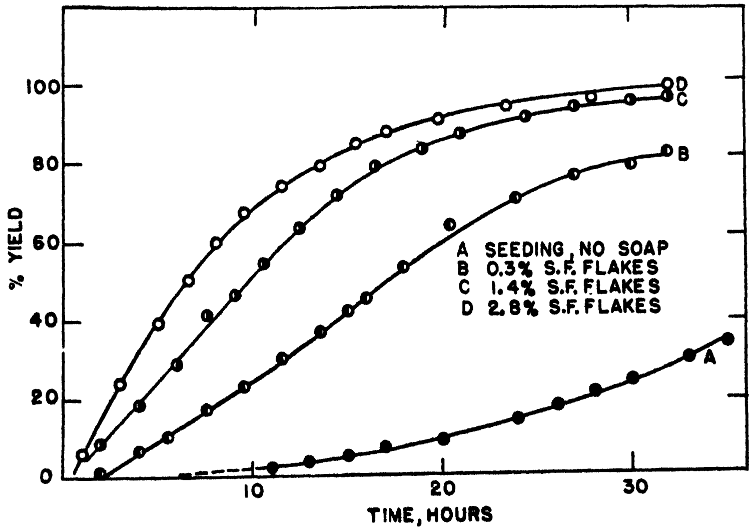

Fig. 18. Effect of soap concentration and seeding without soap upon the yield of polystyrene.

The effect of the concentration of potassium dodecanoate upon the rate for isoprene-styrene is exhibited in Fig. 17a and b, and of silica free (S. F.) flakes, a mixture of tallow soaps with a much higher mean molecular weight, in Figure 18 for isoprene alone. In the latter polymerization the rate is 85% higher with an initial soap concentration of 2.8% than with half this concentration.

According to the general theory presented here the overall rate of polymerization should be not very far from proportional to the number of monomer-polymer particles, and nearly every one of these has its origin in a soap molecule. Now if every soap micelle were to initiate a single polymer molecule, which becomes a monomer-polymer particle, then the yield of polymer should be nearly proportional to the initial amount of micellar soap. However, since, as shown earlier, relatively few of the micelles which exist initially produce polymer molecules, this does not need to be true. However it is to be expected that an increase in soap concentration should give an increased rate.

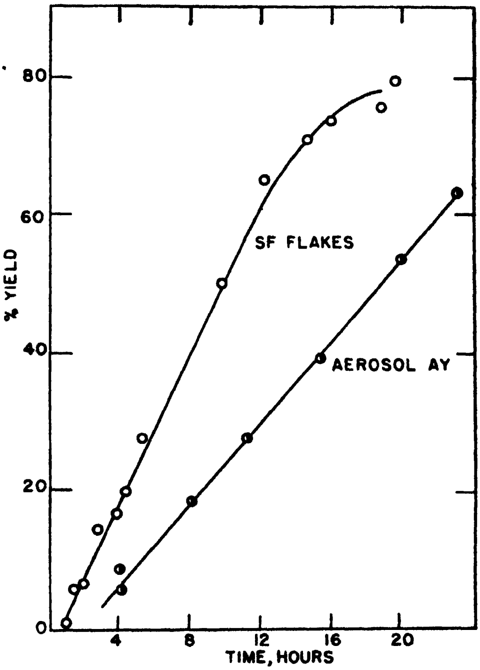

Fig. 19. Yield as a function of time for polystyrene with silica-free flakes and aerosol AY.

If the amount of soap is doubled, Smith and Ewart, on the basis of their theory,[24] find that for styrene the rate should be increased by 1.51. In this laboratory Stearns, with 75% isoprene and 25% styrene at 50°C. found the factor to be 1.85 between 2.5 and 5.0% as much soap as monomer by weight. For GR-S at 50°C., Kolthoff[25] obtained a ratio of 1.63 with S. F. flakes. In all of the cases cited above the yield was very nearly a linear function of time. With potassium myristate, Kolthoff found with GR-S the ratio 2.3 between 0.025 and 0.05 molar soap, and 2.1 between 0.05 and 0.1 molar soap. These high values were obtained from nonlinear curves as ratios of the yields at 6 hours. With butadiene alone the ratios from 0.024, 0.037, 0.95, and 0.19 molar soap were 1.77, 2.0, and 1.83, respectively, at 6 hours.

Figures 17 and 18 exhibit the effects of other concentrations of soap. The relation with lower concentrations is far from linear, exhibiting an inflection at a concentration which increases with decrease in soap concentration. Figure 19 shows the slower rate with aerosol AY, which has very small micelles.

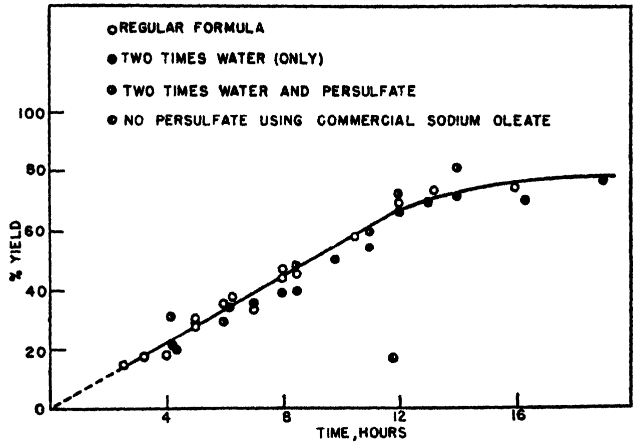

Fig. 20. Effect of the amount of water on the rate of polymerization of polystyrene.

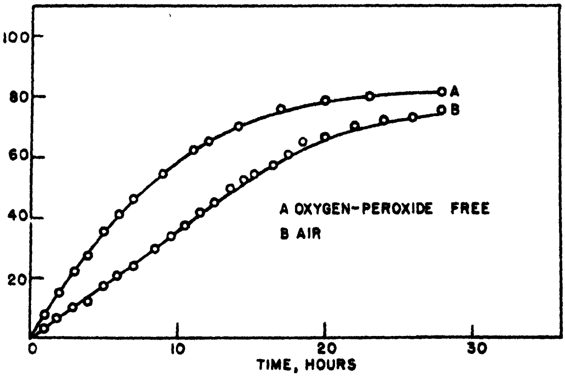

Fig. 21. Effect of oxygen in decreasing the rate of polymerization of polystyrene.

The effect on the rate of polymerization of the use of twice the weight of water (360 g. instead of 180 g.) is not very great, as shown in Figure 20 which represents 34 independent polymerizations. The rate seems to have been reduced slightly when the amount of persulfate was kept constant but its concentration reduced.

The rate was reduced greatly by the admission of a small amount of oxygen in the form of air (Fig. 21). Usually this gives an induction period, but in the case of curve *B* there is no apparent induction period. This is presumably due to the fact that only 5% as much air as solution was admitted.

It is shown in Figures 13 to 16 that under the best conditions the use of the mutual formula (5% as much soap as monomer) gives a linear relation between yield and time, *i.e.*, a constant total rate of reaction. With twice this amount of soap also the linear relation may persist, but with half (2.5%) or less than half the "mutual" amount, the over-all rate is much less at low than at higher yields, often attaining a maximum rate at about a 40% yield. The lower initial rate and the later increase seem to be related to the much smaller amount of polymer produced in the earlier stage of the reaction on account of the smaller number of micelles present.

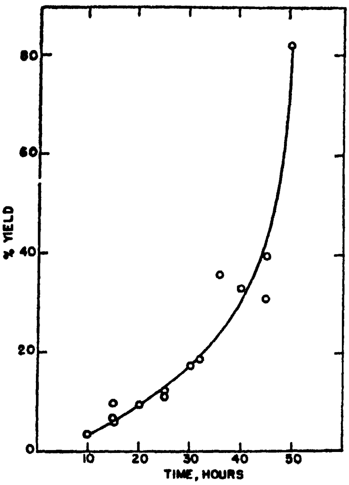

Fig. 22. Yield of polystyrene in water plus potassium persulfate at 50°C. as a function of time.

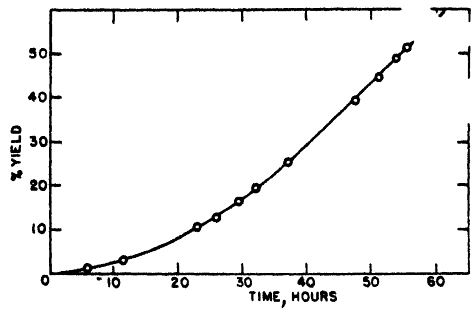

Fig. 23. Yield of styrene at 50°C. as a function of time in nonmicellar (0.006 *M*) potassium dodecanoate.

Thus it appears to be necessary to build up the amount of polymer above a low yield before a higher rate of polymerization can be attained (Figs. 17, 18, 22, 23). Insofar as data for these rates and the monomer-polymer ratio (M/P) are known the rates are in accord with the theory advanced by Corrin of this laboratory, according to which the rate is proportional to $(M/P)^{1/2}P$. Other factors probably enter and considerable work needs to be done to establish a more complete theory.

VIII. POLYMERIZATION IN WATER OR IN NONMICELLAR SOAP SOLUTIONS

See Figures 22 and 23.

Even when relatively insoluble monomers, such as styrene or isoprene are employed, polymerization occurs in water with only a catalyst present.

The rate of reaction is extremely slow at first, but becomes more rapid as it proceeds. Even at an extremely low yield of less than one per cent (0.75%) the diameters of polystyrene particles were found to be distributed irregularly from 400 A. up to very high values, some of these due to aggregation, since no soap is present to stabilize the suspension. At the same extremely low yield with potassium dodecanoate at 0.006 molar or one-fourth its cmc, the particles were already large with a peak in the number distribution curve at a diameter of 1850 A. (Fig. 24) with almost no particles below 1000 A. and with a small number between 3000 and 4700 A.

The very low initial rate of reaction is explained very simply. It should be slower with no soap than with nonmicellar soap, since almost no emulsion droplets are present and there is considerable aggregation of the latex particles. Thus though the diffusion coefficient is essentially unmodified, except at the oil–water interface where diffusion is slowed by the soap film, the diffusion path is greatly lengthened. The principal factor, which slows the rate of formation of moderately large polymer particle nuclei, is that nowhere does a diffusing free radical meet such high concentrations of monomer as in the micellar pockets of solubilized monomer present at higher concentrations of soap.

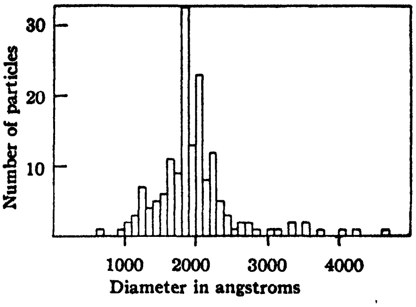

Fig. 24. Distribution of diameter of polystyrene with the rate represented in Figure 23.[34]

A remarkable feature of the reaction in water is that it changes from very slow to rapid with time. This seems to be due to the building up of a store of small polymer particles which increase the rate more than the single molecules.

An interesting case arises when a much more soluble monomer (acrylonitrile, methyl methacrylate, etc.) is completely dissolved and the rates of reaction determined with and without soap. This has been done in this laboratory with the former and in much more detail by Baxendale[26] with the latter. Both sets of experiments show that the rate of reaction is greatly increased by an increase in concentration of the detergent even when no micelles are present. Even as little as 10^{-5} cetyl trimethyl ammonium bromide doubled the rate of the latter. The cmc of this detergent is 8.5×10^{-4} mole per liter.

In either set of experiments the rate increases with increase in soap concentration, but at higher concentrations decreases. The increase in rate is not affected in any detectable way by the presence of micelles. The extremely rapid increase of rate with soap concentration is due to the emulsifying effect of soap on the monomer–polymer particles, *i.e.*, the soap prevents their aggregation and thus keeps their number high.

This is an example of a case in which the micelles are not needed to give polymerization with a water-soluble catalyst.

Baxendale used a "redox" (Fe^{++}-H_2O_2) polymerization, which at 25°C. gave a yield in 10 minutes of *ca.* 15% with no soap and 87.5% with 0.027 *M* cetyl trimethyl ammonium bromide. This is an extremely rapid polymerization which exhibits a very large increase of rate with very small increments of soap.

In this laboratory Lind used a 6.66% (0.495 *M*) solution of acrylonitrile at 35°C. with potassium persulfate as catalyst and obtained much lower rates of reaction, 5% per hour with 0.002 molal potassium lauryl sulfate (Baxendale's initial rate *ca.* 10% per minute with 0.001 *M* detergent) and 16% per hour at 0.012 molar.

The concentration of monomer in both these series of experiments is so high that a free radical which is formed in the water grows rapidly and thus gives a polymer molecule which serves as a nucleus for a monomer–polymer particle. This increases in size by the same mechanism as is involved when it is initiated in a micelle.

IX. NEGLIGIBLE FORMATION OF POLYMER IN THE MONOMER EMULSION DROPLETS

Experiments on isoprene or styrene were found, in a solution of soap and catalyst, to give at 50°C. only a negligible yield of polymer (Table VIII).

TABLE VIII

RATIO *P/M* OF POLYISOPRENE TO ISOPRENE IN THE ISOPRENE PHASE AT 46°C.

Per cent yield	*P/M*			
	Stearns	Simon	*M/P*	Remaining % monomer
5	0.001	—	2 0	85
5.3	—	0.005	—	—
9	—	0.01	—	—
25	0.005	—	1.75	31
29	—	0.015	—	—
40	0.01	—	—	—
45 (50°C.)	0.004	—	—	—

Polymerization mixtures of the composition 10 cc. of isoprene, 15 cc. of a solution of 1% potassium laurate and 0.05% potassium persulfate, and 0.01 cc. of lauryl mercaptan were carefully pipetted into bomb tubes. These tubes were shaken in a thermostat at 46°C. for various lengths of time. The tubes were then centrifuged, and the aqueous layer was frozen in liquid nitrogen. The monomer layer was decanted into tared flasks.

After flask plus monomer layer was weighed, the monomer was evaporated off in a vacuum desiccator. The flask with this remaining polymer was weighed, and the polymer–monomer ratio was computed. The polymer in the aqueous phase was precipitated and weighed after drying. From the total amount of polymer the percentage yield was calculated.

A second, less direct, method was used (Fig. 25). Drops of isoprene 0.42 and 0.52 mm. in diameter were allowed to hang at 50°C. in solutions which induce polymerization. The isoprene diffused into the aqueous phase until at a certain time the drop became distorted. It was then a monomer–polymer particle with a large enough amount of polymer to cause distortion and wrinkling when additional monomer diffuses out of the drop which has up to this time a smooth surface. The volume of the monomer–polymer particle is at this point about one-seventieth of the initial volume, but, since the amount of polymer present is unknown, this does not disagree with the lower values of P/M found by the more direct method.

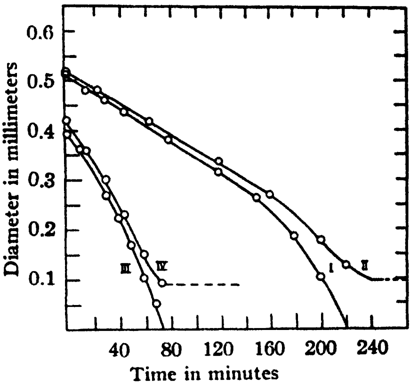

Fig. 25. Diffusion from a drop of isoprene into a 12% solution of potassium dodecanoate containing the standard amount of potassium persulfate at 50°C.[31]

X. EFFECT OF MODIFIER (REGULATOR)

Early in the current synthetic rubber program Ewart[27] found that mercaptans reduce the molecular weight of polystyrene produced in an emulsion, and that their effectiveness in improving the processing characteristics of GR-S is due to their effect in regulating the size of the molecules of polymer. It was found that the molecular weights of either polybutadiene or polyisoprene formed in the presence of a mercaptan is determined by the rate of reaction of the mercaptan. Also one molecule of polymer is produced per molecule of mercaptan consumed, and that this is true also holds in the formation of GR-S.[28–31]

Although the use of a mercaptan is not essential to the production of polystyrene, since it acts as a chain transfer agent, the copolymerization of styrene (25%) and butadiene (75%) when catalyzed with potassium persulfate proceeds with extreme slowness even at 50°C. when no mercaptan is present as a promoter. In the mutual formula 0.5 g. of dodecyl mercaptan is used with 100 g. of monomer. One of the earliest types of experiment carried out in this laboratory in 1943[82] is represented in Figure 26. This shows that the reaction rate at 50°C. is increased only slightly if the concentration of the mercaptan is multiplied by 4, and reduced only slightly if divided by 4, but is greatly lowered at one-twentieth the standard concentration (0.025 g. per 100 g. monomer).

According to the theory of the writer the mercaptan is stored largely in the monomer droplets, and from these diffuses out through the surrounding monolayer of soap into the aqueous phase, where it is more subject to a change to a free radical by oxidizing action of the catalyst than most monomers. This is specially true in the copolymerization of styrene and butadiene.

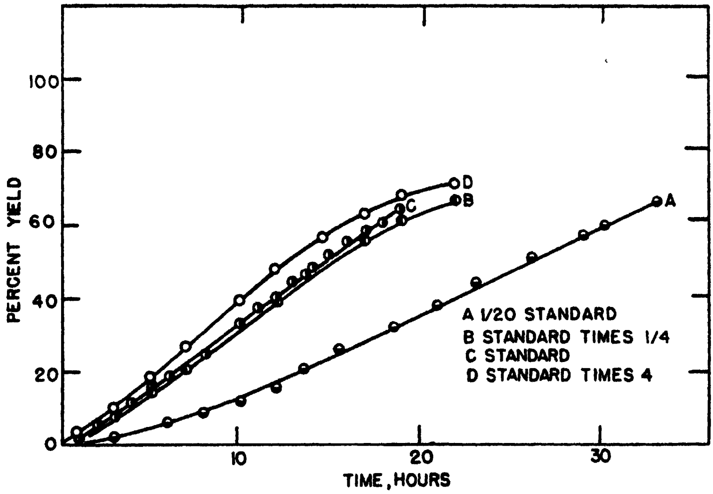

Fig. 26. Effect of the concentration of dodecyl mercaptan upon the rate of polymerization of styrene 25%, isoprene 75%.

It is obvious on this basis that the behavior of mercaptan as either the molecule or the free radical is highly dependent upon the rate of diffusion, which decreases with the length of the normal hydrocarbon chain and is increased by a branching of the chain. If the rate of diffusion is too high the mercaptan is used up too rapidly, if too low it does not get to the seat of the reaction quickly enough.

Dodecyl or other mercaptans act as promoters in GR-S polymerization, since the energy required for their change to free radicals is smaller than that of the monomers in the butadiene–styrene mixture. The mercaptan also acts as a chain transfer agent and decreases the amount of branching and cross linking. If too much mercaptan is used the molecular weight is low, so to prevent the necessity for the use of too large a quantity the polymerization is commonly stopped at a yield of about 70%, which is about 10 to 20% above the yield at which all monomer droplets have disappeared.

With the mercaptan as with the monomers their greatest effect is that in the polymer–monomer particle. They also influence the reaction in the oil solubilized in the micelle, although the number of molecules of mercaptan is relatively so small (one molecule to 700 of the initial monomer phase) that many micelles escape their influence; since if equilibrium were established relatively few of the micelles would contain even one molecule of mercaptan. Also, the mercaptan diffuses much more slowly than butadiene and more slowly than styrene, and the solubility in micelles is small. For example, only 0.0012 and 0.008 g. of *n*-dodecyl mercaptan dissolve in 100 g. of 0.3 molar solutions of potassium dodecanoate and tetradecanoate respectively at 25°C. and this is 3 times the initial concentration of soap in the mutual formula.

XI. REDOX SYSTEMS

Reduction oxidation systems which speed up copolymerization so that it can be carried out at 0°C. or even lower, have recently come into favor, since it is supposed that at the low temperature there is less branching and cross linking and thus longer chains can be built up. Ferrous ion, oxidized to ferric ion by benzoyl peroxide (Marvel) appears to function as a source of free radicals. Recently cumene hydroperoxide has come into favor. This presumably gives the free radical:

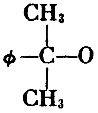

$$\phi\text{—}\overset{\displaystyle CH_3}{\underset{\displaystyle CH_3}{\overset{|}{\underset{|}{C}}}}\text{—}O$$

but it is not known whether this or smaller free radicals formed from it are responsible for its activity.

It is difficult to compare properly the rates of reaction at temperatures so different as those used with potassium persulfate and in redox systems, especially when it is considered that both the stability and catalytic activity, and also the relative solubilities of the monomers, are so different.

Redox systems give in general both a much more rapid polymerization and a much larger number of latex particles than when potassium persulfate is used. Thus it seems that redox systems are more efficient in initiating the growth of a free radical in the monomer inside a micelle.

A reducing agent, sodium sulfite, was found to give an increase of rate from 19.4% per hour to 30.2% per hour, at 42.5° when added initially to the mutual formula with potassium persulfate as catalyst.

Another, somewhat similar type of experiment, gave much more useful information. When the mutual formula is used at 35°C. all micelles disappear in general before the yield attains a value of 15%. The effect of the addition of ferrous sulfate at a 31.8% yield when no micelles are present is to *double* the rate of polymerization, as exhibited in Figure 27. The amount of ferrous sulfate added was 10% higher than that necessary to reduce completely the 0.17% of potassium persulfate present initially.

In this experiment the rate was double without the presence of micelles to initiate new polymer particles. Work of this type will be undertaken in an endeavor to determine if more than one free radical can grow simultaneously in a single latex particle.

All that is known at present is that when the very active redox catalyst is used initially more polymer nuclei are formed, which indicates that the micelles are used more efficiently, *i.e.*, initiation occurs in a greater function of the micelles present.

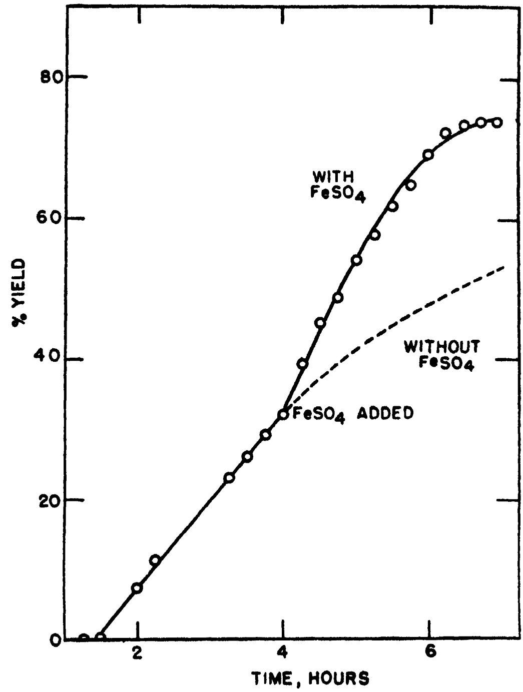

Fig. 27. Effect of adding ferrous sulfate at a 32% yield of polystyrene with potassium persulfate as the initial catalyst. The change to a redox polymerization doubles the rate.

Whether, however, in redox polymerization the number of latex particles is larger by a sufficient factor to explain the increased rate, is not known. There is a suggestion, in Figure 26, obtained in 1944,[33] that an increase in catalytic activity of the catalyst may increase the rate (by a factor of 2 in this case) without an increase in the number of monomer–polymer particles. The ferrous sulfate was added at a yield of 32.5% which is too high for the existence of micelles.

This seems to indicate an increase in the all-over rate, without an increase in the number of monomer–polymer particles, seemingly due to an increase in activity of the catalyst. Now that redox systems have come into use, other investigations of this type will be undertaken.

Summary

This paper develops further a general theory presented earlier. In emulsion polymerization the monomer emulsion droplets serve merely as a storehouse of monomer molecules. These diffuse into the water and are caught by: (*a*) soap micelles, and (*b*) polymer particles, giving polymer–monomer particles. With slightly soluble monomers (butadiene styrene, isoprene, etc.), nearly all of the polymer is produced by the growth of free radicals in the monomer present with the polymer in these polymer–monomer or latex particles. However, almost every latex particle is initiated by the growth of a polymer molecule which starts its growth in the monomer solubilized inside a micelle. The number of latex particles increases with yield until all of the micellar soap disappears by adsorption of a monolayer of soap upon them. The number of particles initiated inside the micelles increases with soap concentration and with the activity of the catalyst or catalysts, and with 5% as much soap as monomer and 2.8% as much as water, is of the general order of 1.5×10^{16} particles per cubic centimeters of water.

Soap is used for two purposes:

(*a*) To stabilize the emulsion of monomer and the polymer monomer particles by forming a monolayer of soap around each of them. This gives an electrical charge to all of the particles.

(*b*) An important function of a micelle is to solubilize a small core of monomer inside it and to provide a much larger target than a single monomer molecule with which a free radical of monomer or mercaptan may come in contact by diffusion. In it starts the growth of a polymer free radical which, under usual conditions, grows very much larger than corresponds to the amount of monomer in the micelle. The molecule thus formed absorbs monomer and thus starts the growth of a polymer–monomer particle. The number of micelles present initially, if the mutual formula is used with potassium dodecanoate or tetradecanoate is of the general order of 10^{18} per cubic centimeter of aqueous phase. Thus, several hundred micelles are present initially with the principal purpose of forming only one polymer particle. Thus, the greatest part of the soap is employed for a secondary purpose: to stabilize the colloidal particles (*ca.* 1.5×10^{15} per cubic centimeter of aqueous phase).

The monomer–polymer ratio (M/P) with a maximum value of 2.5 to 3.0 is discussed in its relationship to the theory, and many other relations, especially those concerned with diffusion and the structure of micelles are considered. It was found, for example, that with an amount of styrene in the micelle equivalent to a molecular weight of 3200, and no other styrene present except the very small amount dissolved in the water, the polymer exhibited a mean molecular weight of *ca.* 200,000. Thus, a polymer free radical initiated in a micelle grows until it not only includes all of the monomer in the micelle, but obtains most of its growth by uniting with monomer molecules in the water.

In connection with extensive x-ray investigations it was found that: (*a*) The long spacing band (I-band) known earlier gives no useful knowledge at present. (*b*) A new M-band was found giving the diameter of the soap micelle considered as a sphere. Apparent density (calculated from Wright and Tartar's densities) of the micelle is low. (*c*) Solubilization of hydrocarbons increases the diameter of the micelle: of an alcohol or amine, gives no increase, but with chain lengths of 5 to 7 carbon atoms reduces the diameter by as much as 10 A. A dye color or fluorescence titration shows that salts and alcohols greatly reduce the critical micelle concentration of soaps, and give results which prove that the Debye-Hückel theory is not applicable to micellar solutions.

Although the general outline of the theory was developed by the writer in 1942 in connection with work at the Research Laboratory of U. S. Rubber Company at Passaic, N. J., the paper as presented here is due to able collaboration of M. L. Corrin, S. H. Herzfeld, E. L. Lind, R. Mittelmann, R. W. Mattoon, H. Oppenheimer, A. Roginsky and R. S. Stearns.

References

1. W. D. Harkins, *three private communications*, to the Office of Rubber Reserve.
2. W. D. Harkins, *J. Chem. Phys.*, **13**, 381 (1945); *J. Am. Chem. Soc.*, **69**, 1428 (1947).
3. W. D. Harkins and N. Beeman, *Proc. Natl. Acad. Sci.*, **11**, 631 (1925); *J. Am. Chem. Soc.*, **51**, 1674 (1929).
4. E. K. Fischer and W. D. Harkins, *J. Phys. Chem.*, **36**, 98 (1932).
5. R. W. Mattoon, R. S. Stearns, and W. D. Harkins, *J. Chem. Phys.*, **15**, 209 (1947). W. D. Harkins, R. W. Mattoon, and R. Mittelmann, *ibid.*, **15**, 763 (1947).
6. G. S. Hartley and D. F. Runnicles, *Proc. Roy. Soc. London*, **A168**, 420 (1938).
7. P. Debye and E. W. Anacker, *private communication*, to the Office of Rubber Reserve.
8. P. Debye, E. W. Anacker, and R. M. Hagen, *private communication*, to the Office of Rubber Reserve.
9. K. A. Wright and H. V. Tartar, *J. Am. Chem. Soc.*, **61**, 544 (1939).
10. R. S. Stearns, H. Oppenheimer, E. Simon, and W. D. Harkins, *J. Chem. Phys.*, **15**, 496–507 (1947).
11. J. Grindley and C. R. Bury, *J. Chem. Soc.*, **1929**, 679.
12. M. L. Corrin, *J. Colloid Sci.*, **3**, 334 (1948).
13. M. L. Corrin and W. D. Harkins, *J. Am. Chem. Soc.*, **69**, 683 (1947).
14. M. L. Corrin and W. D. Harkins, *J. Colloid Sci.*, **1**, 469 (1946).
15. Vinograd, Fong, and Sawyer, Sept. 11–15, 1944, Meeting of the American Chemical Society.
16. R. S. Stearns and W. D. Harkins, *J. Chem. Phys.*, **14**, 214 (1946).
17. M. L. Corrin, S. C. Lind, and W. D. Harkins, *unpublished paper.*
18. R. C. Murray and G. S. Hartley, *Trans. Faraday Soc.*, **31**, 182 (1935).
19. K. A. Wright and H. V. Tartar, *J. Am. Chem. Soc.*, **61**, 544 (1939).
20. E. A. Willson, J. R. Miller and E. H. Rowe, B. F. Goodrich Co., *private communication*, to the Office of Rubber Reserve.
21. W. D. Harkins and H. F. Jordan, *J. Am. Chem. Soc.*, **52**, 1751 (1931).
22. W. D. Harkins, *private communication*, to the Office of Rubber Reserve.
23. M. L. Corrin, *J. Polymer Sci.*, **2**, 257 (1947).
24. W. V. Smith and R. H. Ewart, *J. Chem. Phys.*, **16**, 592 (1938).
25. I. Kolthoff, *private communication*, to the Office of Rubber Reserve.
26. J. H. Baxendale, M. G. Evans, and J. K. Kilham, *Trans. Faraday Soc.*, **42**, 674 (1946).
27. R. H. Ewart, *private communication.*

28. R. H. Ewart, W. V. Smith, and G. E. Hulse, *private communication.*
29. R. H. Snyder and F. T. Wall, *private communication.*
30. R. H. Snyder, J. N. Stewart, R. E. Allen, and R. J. Dearborn, *J. Am. Chem. Soc.*, 68, 1422 (1946).
31. F. T. Wall, F. W. Banes, and G. D. Sands, *ibid.*, 68, 1429 (1946).
32. *Unpublished work*, Sept. 4, 1943.
33. *Unpublished work*, Sept. 14–15, 1944.
34. W. D. Harkins, *J. Am. Chem. Soc.*, 69, 1428 (1947).

English Synopsis, see Summaries, page S5, Vol. V, 1950.

Résumé

Au cours de la polymérisation en émulsion, le système se présente initialement avec le monomère, dispersé en gouttelettes, entourées, elles-mêmes, d'une couche de savon. Le monomère diffuse à travers l'eau vers la partie hydrocarbonée interne de la micelle de savon, qui contient habituellement 40 à 100 molécules de savon. Si le catalyseur ou l'initiateur de chaîne est présent dans la phase aqueuse, il se forme das radicaux libres légers. Plusieurs de ceux-ci pénetrent dans les micelles, où ils s'accroissent avant d'être désactivés, en environ un millième de seconde. Une grande partie de cet accroissement se passe par extension des radicaux libres vers l'eau. Ce procédé continue jusqu'à ce que tout le savon micellaire ait disparu par adsorption du savon aux particules monomère-polymère, qui sont formées par diffusion du monomère vers les particules de polymères, ainsi constituées. La plus grande partie du polymère est produite par polymérisation du monomère dans des particules.

Zusammenfassung

In Emulsionspolymerisationen besteht das System anfangs aus Monomertröpfchen, die von einer monomolekularen Seifenschicht umgeben sind. Das Monomer diffundiert durdh das Wasser in den inneren Kohlenwasserstoffteil der Seifenmizellen, die gewöhnlich 40 bis 100 Seifenmolekuele enthalten. Wenn der Katalysator im Wasser ist, werden freie Radikale begildet. Viele von diesen dringen in die Mizellen ein, wo sie vor der Kettenbeendung ungefähr ein Tausendste einer Sekunde lang washsen. Viel von diesem Wachstum besteht in einer Verlängerung der freien Radikalen in das Wasser. Dieser Prozess geht vor sich, bis alle Seifenmizellen verschwinden durch die Adsorption der Seife an Monomer–Polymerisat-Teilchen die durch die Diffusion des Monomers in die so gebildeten Polymerisatsteilchen entstehen. Fast alles Polymerisat wird durch die Polymerisation des Monomers in diesen Teilchen gebildet.

Received July 15, 1948
Revised March 21, 1949

JOURNAL OF POLYMER SCIENCE VOL. V, NO. 2, PAGES 253-258

Copolymérisation de l'Anhydride Maléique avec Différents Monomères Vinyliques

M. C. DE WILDE ET G. SMETS, *Laboratoire de Chimie Macromoléculaire, Université de Louvain, Belgique*

L'étude de la copolymérisation de l'anhydride maléique avec plusieurs dérivés éthyléniques a été, jusqu'à présent, décrite dans quelques cas.[1] L'équation différentielle de la copolymérisation, utilisée généralement:[2]

$$\frac{m_1}{m_2} = \frac{dM_1}{dM_2} = \frac{M_1}{M_2}\frac{r_1M_1 + M_2}{r_2M_2 + M_1} \tag{A}$$

établit une relation entre la composition du copolymère (m_1/m_2) et le mélange de départ des monomères (M_1 et M_2) en fonction des rapports des constantes de vitesse de propagation:

$$r_1 = k_{11}/k_{12} \qquad \text{et} \qquad r_2 = k_{22}/k_{21}$$

Dans la copolymérisation de l'anhydride maléique avec différents monomères, la constante de vitesse k_{22} d'addition de cet anhydride à une chaîne en croissance se terminant par un radical anhydride maléique, est très faible; dans de nombreux cas, k_{22} et, donc, r_2 deviennent négligeables par rapport à r_1 dans l'équation précitée. Dans ce cas,

$$\frac{m_1}{m_2} = 1 + r_1\frac{M_1}{M_2} \tag{B}$$

c.a.d. que le rapport des monomères dans le copolymère est une fonction linéaire du rapport molaire des monomères dans le mélange initial, dont r_1 est la tangente.

Nous avons appliqué l'équation différentielle (A), ainsi que la méthode graphique de Mayo-Lewis,[2] pour déterminer les valeurs r_1 et r_2 dans la copolymérisation de l'anhydride maléique avec l'acrylate de méthyle, le méthacrylate de méthyle, le chlorure de vinyle, l'acétate de vinyle, et l'acétate d'isopropényle. Nous avons également appliqué l'équation simplifiée (B) dans le cas de l'acrylate et le méthacrylate de méthyle, où elle s'applique très bien; dans les autres cas, les valeurs de r_2 ne sont plus négligeables par rapport aux valeurs de r_1.

Dans le tableau ci-dessous, nous avons consigné les valeurs de r_1 et r_2 pour les différentes copolymérisations:

	r_1	r_2
Acétate d'allyle[3]	0.005 à 0.0075	0.018
Acétate d'isopropényle	0.032 ± 0.005	0.002
Styrène[4]	0.04 ± 0.006	—
Acétate de vinyle	0.055 ± 0.015	0.003
Chlorure de vinyle	0.296 ± 0.07	0.008
Acrylate de méthyle	2.8 ± 0.05	0.02
Méthacrylate de méthyle	6.7 ± 0.2	0.02

Si la valeur inverse du produit r_1r_2 mesure la sélectivité des différents systèmes envisagés, on voit que la tendance à alterner les monomères au sein des copolymères, est toujours très élevée pour tous les monomères à double soudure négativée.[5]

La formation de complexes hétéropolaires, stabilisés mésomériquement, par suite du passage d'un électron de la double soudure riche en électrons, à l'anhydride maléique, avide d'électrons, pourrait en être la cause; l'analogie avec les synthèses diéniques est considérable.[6–8]

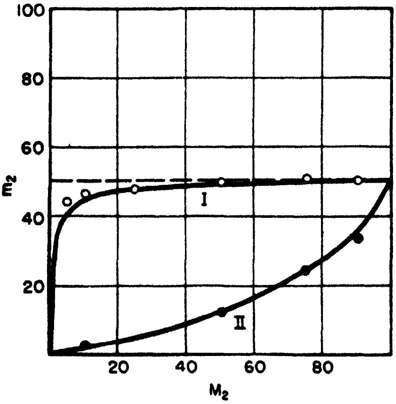

Fig. 1. Courbes de copolymérisation.

M_2: % molaire en anhydride maléique dans le mélange de départ; m_2: % molaire en anhydride maléique dans le copolymère. Courbe I: acétate d'isopropényle-anhydride maléique. Courbe II: méthacrylate de méthyle-anhydride maléique.

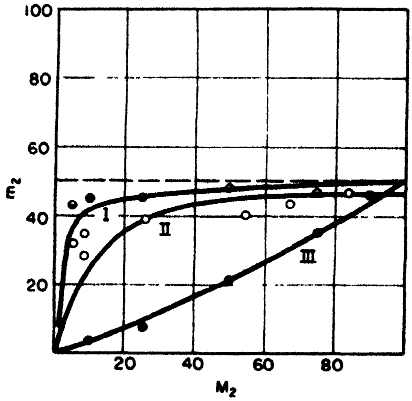

Fig. 2. Courbes de copolymérisation.

M_2: % molaire en anhydride maléique dans le mélange de départ; m_2: % molaire en anhydride maléique dans le copolymère. Courbe I: acétate de vinyle-anhydride maléique. Courbe II: chlorure de vinyle-anhydride maléique. Courbe III: acrylate de méthyle-anhydride maléique.

Les valeurs de r_2 sont toujours très faibles, et, de ce fait, difficiles à déterminer avec exactitude. Les valeurs de r_1 sont optimales dans chacun des cas envisagés; les courbes des figures 1–3 leur correspondent.

On remarquera qu'aux faibles concentrations en anhydride maléique dans le mélange de départ, les points expérimentaux sont toujours situés à des teneurs plus élevées en anhydride que la courbe tracée. Nous attribuons cet écart à la difficulté des dosages aux faibles teneurs en anhydride maléique, au fait que les rendements ne sont peut-être pas suffisament faibles pour obtenir la composition initiale du copolymère, et à la sélectivité particulièrement prononcée de toutes ces copolymérisations.

Pour les copolymères avec l'acrylate et le méthacrylate de méthyle, les points expérimentaux s'accordent remarquablement avec les valeurs de r_1 indiquées.

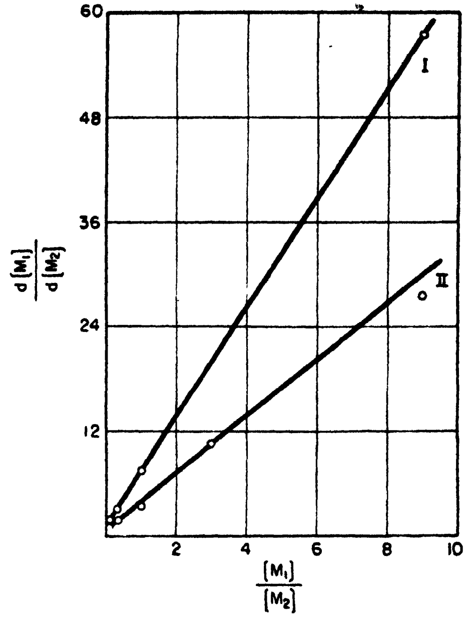

Fig. 3. Détermination de r_1: tangente des rapports molaires des monomères dans le mélange de départ $[M_1/M_2]$ par rapport aux rapports molaires dans le copolymère $d[M_1]/d[M_2]$. Droite I: méthacrylate de méthyle-anhydride maléique. Droite II: acrylate de méthyle-anhydride maléique.

Les valeurs de Q et de e, correspondant à l'anhydride maléique, suivant les équations de Alfrey et Price[9] sont fonctions des monomères de référence, que l'on utilise dans ce calcul:

$$r_1 = (Q_1/Q_2) \exp \{-e_1(e_1 - e_2)\}$$

$$r_2^{-1} = (Q_1/Q_2) \exp \{-e_2(e_1 - e_2)\}$$

Tenant compte des dernières valeurs attribuées au styrène (e: -0.8 et Q: 1), on trouve qu'à l'égard des monomères vinyliques, à double soudure négativée, les meilleures valeurs pour l'anhydride maléique sont:

$$Q\colon 0.18 \quad \text{et} \quad e\colon -2.65$$

Par contre, aux dépens des copolymérisations avec l'acrylate et le méthacrylate de méthyle, on trouve une valeur décroissante, s'élevant respectivement à 2.3 et 1.8 au maximum, pour la charge de la double soudure. Dans les cas de sélectivité accentuée, il semble que le schéma semiquantitatif d'Alfrey et Price est moins rigoureux.

PARTIE EXPERIMENTALE

L'anhydride maléique a été purifié par deux cristallisations successives dans le chloroforme, puis par distillation sous pression réduite. (Eb: 80–82°/14 mm.)

Le chlorure de vinyle (99.8%) a été purifié par barbottage successif dans la soude caustique, l'eau distillée, et par sèchage dans une colonne à chlorure calcique. Les autres monomères ont été distillés sous atmosphère d'azote, immédiatement avant leur emploi.

Toutes les copolymérisations ont été effectuées en solution dans du benzène déthiophéné, à une température de 75°; la concentration totale des monomères a été maintenue à deux-moles par litre de solution. Le peroxyde de benzoyle a été utilisé comme initiateur, à raison de 0.25 gr. pour 100 gr. de monomères. Les vitesses de copolymérisation des différents monomères avec l'anhydride maléique sont élevées, et fort voisines; elles n'ont pas fait l'objet d'une étude systématique; les copolymérisations ont toujours été arrêtées à des faibles rendements.

Les copolymères avec l'acrylate et le méthacrylate de méthyle sont solubles dans le benzène; au contraire, les autres précipitent gélifiés au cours de leur formation. Le contenu des ampoules est additionné d'éther de pétrole (Eb. 50–80°) en quantité telle que l'anhydride maléique reste dissous.

Les copolymères précipitent à l'état poudreux, sauf ceux de l'acrylate de méthyle aux faibles teneurs en anhydride maléique, qui précipitent à l'état gommeux. Les copolymères ainsi précipités sont lavés au benzène, additionné d'éther de pétrole, puis dissous dans l'acétone; par reprécipitation, ils sont isolés et séchés sous vide à poids constant à une température de 40–50°.

La détermination de la teneur en anhydride maléique des copolymères a été faite électrotitrimétriquement, après dissolution du copolymère dans l'acétone et addition ultérieure d'eau. L'inflexion de la courbe marque le point de neutralisation des fonctions maléiques; il est souvent possible de noter un premier point, correspondant à la formation des groupes maléates-acides. La soude utilisée était décinormale, sauf dans le cas de l'acétate d'isopropényle (*N*/50). Par suite de leur insolubilité dans l'eau, les copolymères au méthacrylate de méthyle, et ceux à l'acrylate de méthyle contenant peu d'anhydride maléique, ont été soumis à l'ébullition durant deux heures, en présence d'un excès de soude caustique; on titre en retour. Dans ces conditions les chaînons méthacrylate de méthyle ne sont pas saponifiés.

COPOLYMÉRISATION DE L'ACRYLATE DE MÉTHYLE ET DE L'ANHYDRIDE MALÉIQUE[a]

Monomères			Copolymères		
MA.	Acr. Me	Rendement	MA.	Acr. Me	Moles % MA. calc.
10	90	4.2	3.75	96.25	3.7
25	75	8.9	8.0	92.0	9.5
50	50	4.6	21.5	78.5	21
75	25	0.82	34.7	65.3	34.7
90	10	0.87	46.7	53.3	44

r_1: 2.8 ± 0.05 r_2: ≤ 0 02

[a] MA. désigne toujours l'anhydride maléique; le rapport r_2 lui correspond.

COPOLYMÉRISATION DU MÉTHACRYLATE DE MÉTHYLE ET DE L'ANHYDRIDE MALÉIQUE

Monomères			Copolymères		
MA.	Meth. Me	Rendement	MA.	Meth. Me	Moles % MA. calc.
10	90	(16)	(2.67)	(97.33)	1.7
50	50	5	12.08	87.92	11.85
75	25	5.9	24.35	75.65	24.2
90	10	2.34	32 78	67.22	35.8

r_1: 6.7 ± 0.2 r_2: ≤ 0.02

COPOLYMÉRISATION DU CHLORURE DE VINYLE AVEC L'ANHYDRIDE MALÉIQUE

Monomères			Copolymères		
MA.	Vin Cl	Rendement	MA.	Vin Cl	Moles % MA. calc.
5.38	94.62	1.65	31.7	68.3	16
8.33	91.67	3.16	29.4	70.6	22
25.9	74.1	5.4	38.5	61.5	38.5
54.8	45.2	3.24	39.3	60.7	44.2
67.1	32.9	1.54	43.2	56.8	45.2

r_1: 0.296 ± 0.07 r_2: 0.008

COPOLYMÉRISATION DE L'ACÉTATE DE VINYLE ET DE L'ANHYDRIDE MALÉIQUE

Monomères			Copolymères		
MA.	Vin Ac.	Rendement	MA.	Vin Ac.	Moles % MA. calc.
5	95	2.9	42.6	57.4	37
10	90	4.8	44.8	55.2	42
25	75	3.8	44.9	55.1	45.5
50	50	4.0	47.5	52.3	48.0
75	25	1.5	46.2	53.8	48.5

r_1: 0.055 ± 0.015 r_2: ~0.003

COPOLYMÉRISATION DE L'ACÉTATE D'ISOPROPÉNYLE ET DE L'ANHYDRIDE MALÉIQUE

Monomères			Copolymères		
MA.	Isopr. Ac.	Rendement	MA.	Isopr. Ac.	Moles % MA. calc.
5	95	0.88	44.2	55.8	39
10	90	1.1	46.17	53.83	44.1
25	75	1.8	47.74	52.26	47.74
50	50	1.7	49	51	49
75	25	1.4	50.25	49.75	49.7
90	10	1.6	49.99	50.01	50.5
		r_1: 0.032 ± 0.005		r_2: ± 0.002	

Références

1. Wagner-Jauregg, *Ber.*, **63,** 3213 (1930); Alfrey and Lavin, *J. Am. Chem. Soc.*, **67,** 2044 (1945); Bartlett and Nozaki, *ibid.*, **68,** 1495 (1946); Walling, Seymour, and Wolfstirn, *ibid.*, **70,** 1544 (1948).
2. Lewis and Mayo, *J. Am. Chem. Soc.*, **66,** 5941 (1944); Alfrey and Goldfinger, *J Chem. Phys.*, **12,** 204 (1944).
3. Bartlett and Nozaki, *loc. cit.*
4. Alfrey and Lavin, *loc. cit.*
5. Price, *J. Polymer Sci.*, **1,** 83 (1946).
6. Weiss, *J. Chem. Soc.*, **1942,** 245.
7. Woodward, *J. Am. Chem. Soc.*, **64,** 3058 (1948).
8. Walling, Seymour, and Wolfstirn, *loc. cit.*
9. Alfrey and Price, *J. Polymer Sci.*, **2,** 101 (1947).

English Synopsis, see Summaries, page S2, Vol. V, 1950.

Résumé

La copolymérisation de l'anhydride maléique avec différents dérivés vinyliques, tels le méthacrylate de méthyle, l'acrylate de méthyle, l'acétate de vinyle, l'acétate d'-isopropényle et le chlorure de vinyle, a été étudiée. Les rapports des constantes de vitesses r_1 et r_2 ont été déterminés dans chacun des cas. La sélectivité est particulièrement élevée avec les monomères caractérisés par une double soudure, riche en électrons; l'accord avec le schéma de Price et Alfrey est restreint dans ces cas.

Zusammenfassung

Die Mischpolymerisation von Maleinsaeure Anydrid mit verschiedenen Vinyl-Verbindungen wie Methakrylsaeure, Methylester, Vinylchlorid, Vinylazetat und Isopropenylazetat wurde untersucht. Die Verhaeltnisse der Geschwindigkeits-Konstanten r_1 und r_2 wurden fuer jeden dieser Faelle festgestellt. Die Mischpolymerisation mit Monomeren, die eine elektronreiche Doppelverbindung enthalten, zeichnet sich durch eine hohe Selektivitaet aus. In diesen Faellen koennen die Ergebnisse nicht gaenzlich durch das Alfrey-Price Schema erklaert werden.

Received January 3, 1949

JOURNAL OF POLYMER SCIENCE VOL. V, NO. 2, PAGES 259-265

LETTERS TO THE EDITORS

Linear Method for Determining Monomer Reactivity Ratios in Copolymerization

The copolymerization of two monomers M_1 and M_2 may be described schematically as follows:

$$M_1\cdot + M_1 \xrightarrow{k_{11}} M_1\cdot$$
$$M_1\cdot + M_2 \xrightarrow{k_{12}} M_2\cdot$$
$$M_2\cdot + M_2 \xrightarrow{k_{22}} M_2\cdot$$
$$M_2\cdot + M_1 \xrightarrow{k_{21}} M_1\cdot$$

The monomer reactivity ratios are given by $r_1 = k_{11}/k_{12}$ and $r_2 = k_{22}/k_{21}$, and the copolymer composition equation which relates the polymer composition to the monomer composition is given by:

$$\frac{dM_1}{dM_2} = \frac{M_1}{M_2}\,\frac{r_1M_1 + M_2}{r_2M_2 + M_1}\left(= \frac{m_1}{m_2} \text{ for low conversions}\right) \qquad (1)$$

where M_1 and M_2 refer to the monomer composition and m_1 and m_2 to the polymer composition.[1a–c]

The values of the monomer reactivity ratios, r_1 and r_2 in equation (1), have been determined by the elegant but laborious graphical method of Mayo and Lewis,[1b] using the integrated form of equation (1). A simpler method involves carrying out the copolymerizations to low conversions and using the approximate form of equation (1). The ratios r_1 and r_2 may then be obtained graphically from the initial and final slopes of the usual copolymerization curve in which the polymer composition is plotted against the monomer composition. This method may involve large uncertainties in the slopes and, consequently, in the r_1 and r_2 values, particularly in those cases where the slopes are steep or where experimental data at very low and very high concentration ratios are unavailable. The reliability of the determined values can be increased by the tedious method of calculating theoretical curves for pairs of values of r_1 and r_2 and fitting them to the experimental curves.

However, a simpler technique, which permits the use of data in the intermediate concentration regions and reduces the uncertainties in the r values, is possible. If $f = (m_1/m_2)$ and $F = (M_1/M_2)$, then equation (1) can be rewritten as:

$$f = F\frac{r_1F + 1}{r_2 + F} \tag{2}$$

By rearranging terms one obtains:

$$\frac{F}{f}(f - 1) = r_1\frac{F^2}{f} - r_2 \tag{3}$$

A plot of $(F/f)(f - 1)$ as ordinate and (F^2/f) as abscissa is a straight line whose slope is r_1 and whose intercept is minus r_2. Equation (2) can also be rearranged to:

$$\frac{f - 1}{F} = -r_2\frac{f}{F^2} + r_1 \tag{4}$$

In this case the slope is minus r_2 and the intercept r_1. In addition to simplifying the calculations, the use of equations (3) and (4) offers the considerable advantage that they permit the facile use of the method of least squares to get the best fit to the experimental data.

It is of interest to note that in the special case where $r_2 = 0$, equations (3) and (4) reduce to:

$$(f - 1) = r_1F \tag{5}$$

which is identical in form to one derived by Alfrey, Merz, and Mark.[2] Similarly, when $r_1 = 0$, the equations simplify to:

$$(1 - f) = r_2(f/F) \tag{6}$$

In Table I the values of r_1 and r_2 determined by using equations (3) and (4) are compared with those reported in the literature. The examples were chosen to include systems in which:

(a) $r_1 > 1;\quad r_2 < 1$
(b) $r_1 > 0;\quad r_2 = 0$
(c) $r_1 < 1;\quad r_2 < 1$

Excellent agreement was obtained between the reported values and those obtained by the use of either equation (3) or (4). The vinyl acetate–tetrachloroethylene* example gave a slightly negative value for r_2 when the best straight line was first drawn through the experimental points. Since neither r can be negative, the line was redrawn to make $r_2 = 0$ and this resulted in the second pair of values for r_1 and r_2 for this system reported in Table I.

As was to be expected, the values of r_1 and r_2 determined by plotting the terms of equations (3) and (4) agree very well. Having the two equations is, however, an advantage, since sometimes one of the two plots gives a better straight line through the points.

---

* The data for this system are relatively unsatisfactory. Only four experimental points were obtained, and, of these, two were for relatively high conversions, 30% and 22%.

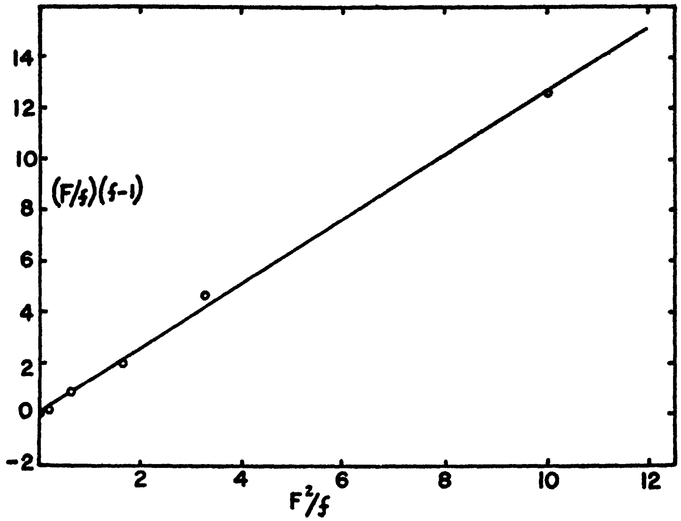

Fig. 1. Plot of $(F/f)(f-1)$ *vs.* F^2/f for styrene (M_1) pentachlorostyrene (M_2) copolymerization with least squares straight line.

The data for the styrene–pentachlorostyrene system have been treated by the method of least squares. This resulted in values of 1.26 and 0.064 for r_1 and r_2, respectively. Figure 1 shows the least squares straight line and the values of $(F/f)(f-1)$ *vs.* F^2/f from the experimental data.

TABLE I

COMPARISON OF r VALUES DETERMINED BY NEW METHOD WITH THOSE REPORTED IN LITERATURE

System	From plot of equation (3)		From plot of equation (4)		Reported		Ref. No.
	r_1	r_2	r_1	r_2	r_1	r_2	
Styrene (M_1)–pentachlorostyrene (M_2)	1.28	0.05	1.31	0.09	1.31	0.10	3
Methyl methacrylate (M_1)–pentachlorostyrene (M_2)	4.25	0.35	4.17	0.33	4.0	0.35	3
Vinyl acetate (M_1)–vinyl chloride (M_2)	0.29	1.85	0.25	1.81	0.3	2.1	4
Vinyl acetate (M_1)–tetrachloroethylene (M_2)	3.5	−0.17	3.55	−0.22	5.0	0.0	4
			Assume r_2 = 0.0				
	5.15	0.0	5.29	0.0			
Vinyl acetate (M_1)–*trans*-dichloroethylene (M_2)	0.86	0.0	0.87	0.015	0.85	0.0	5
Allyl chloride (M_1)–vinyl acetate (M_2)	0.58	0.65	0.66	0.69	0.67	0.7	4

References

1. (a) T. Alfrey, Jr., and G. Goldfinger, *J. Chem. Phys.*, **12**, 205 (1944). (b) F. R. Mayo and F. M. Lewis, *J. Am. Chem. Soc.*, **66**, 1594 (1944). (c) F. T. Wall, *ibid.*, **66**, 2050 (1944).

2. T. Alfrey, Jr., E. Merz, and H. Mark, *J. Polymer Sci.*, 1, 37 (1946).
3. T. Alfrey, Jr., and W. H. Ebelke, *J. Am. Chem. Soc.*, 71, 3235 (1949).
4. P. Agron, T. Alfrey, Jr., J. Bohrer, H. Haas, and H. Wechsler, *J. Polymer. Sci.*, 3, 157 (1948).
5. T. Alfrey, Jr., and S. Greenberg, *ibid.*, 3, 297 (1948).

MORTON FINEMAN
SIDNEY D. ROSS

Research Laboratories
Sprague Electric Company
North Adams, Massachusetts

Received December 8, 1949

"Bound" Water in Phenol-Formaldehyde Condensates

The paper by Bentz and Neville[1] in the December issue of this Journal is a valuable contribution to our understanding of the mechanism of the phenol formaldehyde reaction. The determination of free water by the Karl Fischer reagent is especially illuminatory. However, I feel that the authors' interpretation of "bound" water leaves something to be desired, since, in their discussion, they suggest it may be hydrogen bonded. It is hard to see why "free" water is not equally capable of forming hydrogen bonds.

We feel that the "bound" water is indeed chemically combined as methylol and dibenzyl ether groups, and that the authors' results can be interpreted in these terms.

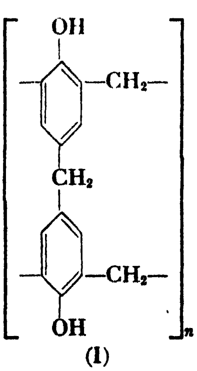

(1)

The authors have suggested that the power of adsorption is lost as polymerization proceeds. We feel this loss of adsorption is dependent only on loss of hydrophilic groups. The adsorbent capacity of ion-exchange resins certainly indicates that high polymers are not inherently devoid of this property.

In the following calculations, we have assumed that the residue in the authors' volatile determination contains only methylene groups and that no oxygen groups from formaldehyde remain in the residue. This appears to be the case, since the authors' figure of 59.3% volatile indicates an average segment weight of 114 as compared to 112 for an entirely cross-linked structure (I), this has been assumed throughout as the residue in the estimation of volatile matter.

The values in Table IV have been recalculated on the basis of the dry resin. It has been assumed that formaldehyde constitutes the only volatile material besides water. The authors have noted that formic acid is also present. The extraction method values have been used as the volatile content.

TABLE I

Sample No.	Per cent formaldehyde	Per cent bound water
1	10.5	14.3
2	9.6	10.9
3	9.2	10.3
4	6.7	10.0

It will be seen that the constancy of the value for bound water found by the authors disappears when the results are referred to the solid resin at various stages of drying.

The amount of bound water, here measured by the amount of water evolved from CH_2OH, and formaldehyde from CH_2OCH_2 groups which would be evolved in polymerization to Formula I has been calculated with the following results.

TABLE II

Reaction	Per cent formaldehyde	Per cent bound water
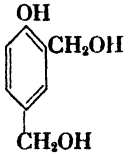 $\longrightarrow$ I	9.7	17.5
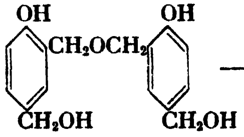 $\longrightarrow$ I	10.3	12.4
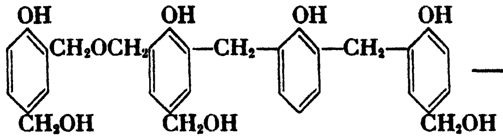 $\longrightarrow$ I	5.6	10.2

Since the authors start with 2.8 moles of formaldehyde to one of phenol and condense in an alkaline solution, it is probable[2] that dimethylol phenol is the principal product formed. However, the "bound" water available is more than obtained from Sample 1, indicating the condensation had proceeded beyond this point. Thus, the first sample of Table I may be a mixture of the two materials. It is not clear how much of the formaldehyde was combined in the resin and how much was obtained by evaporation of unreacted formaldehyde. Walker[3] has shown that formaldehyde tends to concentrate on vacuum distillation. It should be noted that the vapor pressures above that of water are due to the presence of methanol in the formaldehyde.

It will be noted that the content of formaldehyde and bound water decreases as concentration of the resin solution proceeds. This is an indication of further polymerization, and the last equation in Table II approaches the behavior of Sample 4. The formaldehyde value is somewhat less than found, but this value may be somewhat high since it includes free formaldehyde, formic acid, and all volatile materials other than water.

In conclusion, it is felt that the results are consistent with the assumption that "bound" water constitutes water other than that combined in the resin as methylol or dibenzyl ether groups. The heat stability of the latter groups is established[4] and is apparently greater where there is limited opportunity for formation of methylene bridges. The loss of water by formation of methylene linkages or dibenzyl ether groups, and the loss of the evolution of formaldehyde from dibenzyl ether groups and of water from methylol groups is believed to be the source of the "bound" water observed.

References

1. Bentz and Neville, *J. Polymer Sci.*, 4, 673 (1949).
2. Sprung, *J. Am. Chem. Soc.*, 63, 334 (1941).
3. Walker, *Ind. Eng. Chem.*, 32, 1016 (1940).
4. Euler, Adler, and Tingstam, *Arkiv. Kemi. Mineral Geol.*, A15, No. 10 (1941).

P. O. POWERS

Battelle Memorial Institute
Columbus 1, Ohio

Received January 12, 1950

Degradation of High Polymers

In a recent letter[1] Casassa gives an interesting derivation of the decrease of the number average molecular chain length with time. The calculation was carried out for a polymer of (infinitely) high molecular weight. It is interesting that the same expression as that found by Casassa is obtained for a homogeneous polymer sample of any finite molecular weight. The derivation is briefly as follows (different symbols are used here).

The number of links present initially in the system may be p_0, the initial chain length of the homogeneous polymer P_0. Let the number of chains initially present in the sample be a, then:

$$a(P_0 - 1) = p_0$$

After s links have been broken on the average in each original chain, the following relationship is valid:

$$p_0 = p + as \text{ or } s = (p_0 - p)/a$$

where p is the number of links in the system at time t. The number average chain length is as always given by:

$$P_n = P_0/(s + 1)$$

or:

$$P_n/P_0 = a/(p_0 - p + a)$$

finally,

$$p = a + p_0 - (aP_0/P_n)$$

If the rate of breaking bonds is given by:

$$-dp/dt = kp$$

then:

$$d\left(\frac{aP_0}{P_n} - p_0 - a\right)\bigg/dt = k\left(p_0 + a - \frac{aP_0}{P_n}\right)$$

or:

$$-P_n^{-2}aP_0\,\frac{dP_n}{dt} = k\left(p_0 + a - \frac{aP_0}{P_n}\right)$$

which yields finally:

$$-dP_n/dt = k(P_n^2 - P_n) \tag{1}$$

The integrated form of equation (1) is:

$$-\ln\left(1 - \frac{1}{P_n}\right) = kt - \ln\left(1 - \frac{1}{P_0}\right) \tag{1a}$$

Equations (1) and (1a) are valid for any type of degradation provided the rate of degradation is independent of chain length and location of the bond in the chain. Equation (1) is identical with Casassa's results.

Reference

1. Casassa, *J. Polymer Sci.*, **4**, 405 (1949).

H. H. G. Jellinek

11, Mount Park Crescent
London, W.5, England

Received December 23, 1949

REVIEW

The Adsorption of Gases on Solids (Cambridge Monographs on Physics). A. R. MILLER, Cambridge Univ. Press, Cambridge, 1949, 133 pp. Price $2.50.

In 1939 the late J. K. Roberts published a Cambridge Physical Tract entitled "Some Problems in Adsorption," in which he described both the experimental work he had done on the adsorption of gases on metals and the pertinent theoretical applications. The monograph by Miller is a revision and extension of Roberts' tract and represents a valuable addition to the adsorption literature. Statistical and kinetic models are used in developing equations for many types of adsorption, such as that leading to immobile or mobile films, and adsorption with and without interaction or with and without dissociation. Equations are developed for the variation of the heat of adsorption with surface covered, for the influence of dipole interactions, etc. Mathematical treatments are rather condensed and are not readily followed without reference to original papers. However, for a good review of the theoretical work in the field of monofilms on metals, one could do no better than to turn to this book.

It is rather astonishing that the book includes so few references to American authors, Langmuir excepted; thus the names of Brunauer, Emmett, Teller, Harkins, H. S. Taylor, Jura, McBain, etc. are not to be found. The subjects of multilayer adsorption and surface area determination are not treated in this highly specialized monograph.

The author of this review recalls the interesting visit and conversation he had with the late Dr. Roberts in the Cavendish Laboratory in 1933, and his admiration of the scientific energy and enthusiasm displayed by Dr. Roberts despite a serious disability suffered while fighting with the British forces in the first World War. It is good to see the work begun by him amplified and extended by so competent a scientist as A. R. Miller.

Malcolm Dole

JOURNAL OF POLYMER SCIENCE VOL. V, NO. 2, PAGES 267–268

ERRATA

Photochemistry of Proteins. VI. *p*H Dependence of Quantum Yield and Ultraviolet Absorption Spectrum of Chymotrypsin

(*J. Polymer Sci.*, 4, 573–582, 1949)

by PAUL FINKELSTEIN and A. DOUGLAS McLAREN

Institute of Polymer Research, Polytechnic Institute of Brooklyn, Brooklyn, New York

On pages 577 and 578, interchange the graphs for Figures 2 and 3 (the legend describing the present Figure 2 belongs to the graph for Figure 3, and *vice versa*).

Occurrence of Head-to-Head Arrangements of Structural Units in Polyvinyl Alcohol

(*J. Polymer Sci.*, 3, 880, 1948)

by P. J. FLORY and F. S. LEUTNER

The Goodyear Tire & Rubber Co., Research Laboratory, Akron, Ohio

We are indebted to Dr. A. M. Borders of the Institute of Paper Chemistry for pointing out an error in our numerical calculations of molecular weights from the intrinsic viscosities of degraded polyvinyl alcohols discussed in the paper of the above title. The molecular weights given in the previous Table VI for the degraded polymers are about 6.5% too low. The correct values as calculated from equation (2) are recorded in the third column of the revised table on page 268. Also included are the initial viscosity average molecular weights $\overline{M}_v^0$ (correct as previously given) and the values of Δ, the mole fraction of 1,2 units as calculated from $\overline{M}_v$ and $\overline{M}_v^0$ according to equation (6).

Sample	Initial mol. wt., $\bar{M}_v^0$	Mol. wt., $\bar{M}_v$ after degradation	$\Delta \times 100$; mole % of 1,2-glycol structure
1	165,000	6900	1.15
2	21,900	5060	1.26
3	25,600	5010	1.33
4	71,600	5060	1.52
5	70,500	4860	1.59
6	40,700	4030	1.86

The Δ values are 5 to 10% lower than those previously given. The relationship between Δ and the polymerization temperature consequently is altered slightly to:

$$\log \Delta = -1.00 - 283/T$$

in place of previous equation (8), or:

$$\Delta = 0.10 \exp(-1300/RT)$$

in place of (9).

JOURNAL OF POLYMER SCIENCE VOL. V, NO. 3, PAGES 269–281

Quantitative Investigation of X-Ray Diffraction by "Amorphous" Polymers and Some Other Noncrystalline Substances*

P. H. HERMANS and A. WEIDINGER, *Institute for Cellulose Research, AKU and Affiliated Companies, Utrecht, Netherlands*

INTRODUCTION

In previous papers[1] a method has been developed for the quantitative evaluation of monochromatic x-ray diffraction pictures of cellulose fibers, polythene, and a polyamide. This method involves the use of samples of randomized orientation, control of irradiated mass, and application of a technique indicated by J. M. Goppel for measurement of integrated primary beam intensity.

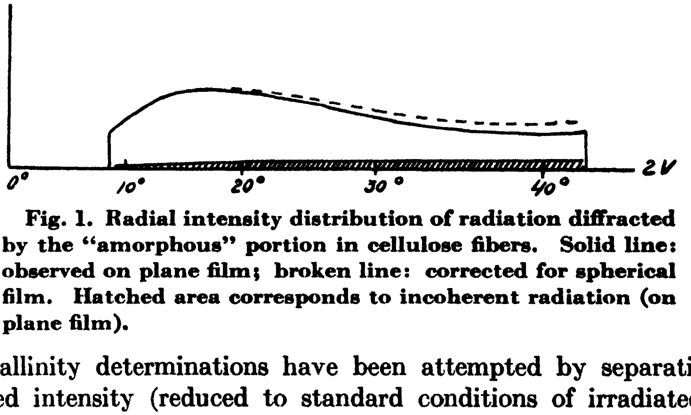

Fig. 1. Radial intensity distribution of radiation diffracted by the "amorphous" portion in cellulose fibers. Solid line: observed on plane film; broken line: corrected for spherical film. Hatched area corresponds to incoherent radiation (on plane film).

Crystallinity determinations have been attempted by separating the diffracted intensity (reduced to standard conditions of irradiated mass and total intensity) into the total intensity of the "crystalline peaks" and that of the "amorphous background." The latter, after correction for air scattering and incoherent radiation, was associated with the noncrystalline, so called amorphous, portion.

In cellulose fibers this background was found to yield between $2\vartheta = 7$–$42°$, a radial intensity distribution of the type reproduced in Figure 1. The curve given here is that found for an almost entirely amorphous cellulose powder. These curves have a flat maximum at about $2\vartheta = 16$–$18°$ and exhibit a marked intensity over the whole angular range included in the observation.

* Communication No. 61 from the Institute for Cellulose Research of the AKU and Affiliated Companies, Utrecht.

The broken line in Figure 1 gives the curve which one would have obtained when using a spherical film. It is found by multiplying the ordinates of the observed curve by cos 2ϑ. Since this correction does not essentially change the character of the curve and is irrelevant to the purpose of this paper, all other curves in this paper will be reproduced as those observed on the plane film.

The curve exhibits only one very broad and flat maximum. In the generalized Fourier analysis, after Zachariasen and Warren, the empirical diffraction curve of a liquid is being considered as a modulated classical diffraction curve. From the modulation the partition function of atomic distances relative to an arbitrarily selected center can be derived (if the atomic numbers of the atoms considered are near to each other).

Owing to the complicated structure of the cellulose molecule and its relative stiffness, the amorphous portion may be expected to exhibit such a multiple of different spacings that only very broad and flat maxima will occur.

It seemed of interest to compare the intensity distribution attributed to noncrystalline cellulose with that given by other noncrystalline substances. This can now be readily done, since our present technique[1,2] permits the reducing of all observations to directly comparable scale. This is achieved by using specimens with random orientation, reducing all observations to standard conditions of primary intensity and irradiated mass and applying reduction factors for atomic composition, computed as previously explained,[2] in order to reduce the coherent as well as the incoherent components of the diffracted radiation to a comparable scale. All curves appearing in this paper are thus standardized and refer to strictly monochromatized copper alpha radiation.

The reduction procedure used may be briefly recapitulated here. The intensity of coherent radiation observed on the photographs was divided by:

$$100\, I \frac{\rho d}{0.122} \frac{F}{F_c} \tag{1}$$

where I = the intensity of the comparison interference in the miniature camera after Goppel, ρd the density of the sample times its irradiated thickness, F the reduction factor for the atomic composition of the substance in question for coherent radiation, and F_c the corresponding reduction factor for cellulose (chosen as the standard substance); 0.122 is the standard value of ρd (which is equal to the value accepted in previous work on cellulose).[1] The value of ρd was calculated from a separate absorption measurement made on the same specimen and using the formula:

$$I = I_0 \exp\,(\mu_m \rho d) \tag{2}$$

where μ_m is the mass absorption coefficient.

The intensity of incoherent radiation was reduced using the same formula (1) after substituting F and F_c by f and f_c, the reduction factors calculated for incoherent radiation.[2] It should be remarked that all the curves reproduced in this paper are not corrected for scattering due to the air in the camera. Since this is only a small correction of almost equal amount for the different curves, it does not interfere with their comparability. It does not give rise to errors in the total integrated intensities appearing in Table I, which are corrected for air scattering.

TABLE I

Standardized Integrated Intensities of Coherent Radiation $I_{tot.}$ Diffracted between $2\vartheta = 7$ and 42° (in Arbitrary Units)

Specimen	$I_{tot.}$
Cellulose and derivatives	
Native ramie	3.5
Valonia cell wall	3.6
Wood pulp	3.8
Fiber G (du Pont)	3.6
Cellulose (1.14) acetate	3.7
Cellulose (1.2) methyl ether	3.8
Other carbohydrates	
Sucrose-glucose glass	3.7
Sugar, very finely ground	3.7
Soluble starch	3.7
Various substances	
Carbon black (Brownly)	3.6
Benzene soot	3.6
Spectrographite	3.5
Paraffin 20° (solid)	3.5
Paraffin 65° (molten)	3.6
Cetyl alcohol (molten)	3.7
Carbon tetrachloride	3.6
Dichloromethane	3.7
Water	3.6
Polymers	
Polythene 18° (solid)	3.6
Polythene 90° (solid)	3.5
Polythene 135° (molten)	3.6
Crêpe rubber 18°	3.6
Crêpe rubber 50°	3.6
Polystyrene	3.5
Polyvinyl acetate	3.7
Polymethyl methacrylate	3.8
Polyvinyl butyral	3.6
Bakelite resin	3.6
Polyhexamethylene sebacamide	3.8
Polyamide copolymer	3.6
Polyvinyl chloride	3.6
Polyvinylidene chloride	3.6
Rubber hydrochloride	3.7
Chlorinated polythene	3.6
Lignin from jute	3.6

CONSTANCY OF TOTAL DIFFRACTED RADIATION WITHIN THE ANGULAR RANGE OBSERVED

According to theory, the total radiation diffracted over all angles, if reduced according to the foregoing principles, should be equal for any substance.

We have found from numerous experiments with polymers and organic substances that also the integrated intensity within the restricted range between $2\vartheta = 7$ and 42° is practically equal for all substances investigated. This is demonstrated in Table I where the integrated intensities of coherent radiation found for a number of substances are listed. Since the experimental error is about ±5%, it is seen that the majority of the figures is constant within that limit. This is a material aid to our study. It means that the total surface under the standardized intensity curves is practically constant in all instances.

This indicates that even in the cryptocrystalline substances studied the degree of ordering giving rise to a modulation of the classical atomic diffraction curve is never very pronounced. In well crystallized substances large deviations may, of course, occur, since not all the diffraction lines will fall within this restricted angular range. As an extreme example we quote an experiment with a platelet cut from a diamond which gave no interferences at all in this range and where only incoherent radiation was observed.[1] On the other hand, a well crystallized graphite sample (spectrographite in Table I) fitted the general rule, indicating that the majority of its interferences fell within the relevant range.

The intensity *distribution* of the approximately constant amount of diffracted radiation over the angular range studied is, of course, different from substance to substance and depends upon its structure. Though, generally, an exact analysis of this dependence on a theoretical basis is, admittedly, extremely difficult in the case of noncrystalline substances, we have deemed it worth while to collect and compare experimental data for a number of representative cases. This subject has thus far been almost entirely neglected and was never approached on the basis of quantitative intensity measurements. In this paper such an approach is attempted.

ANGULAR RANGE INVESTIGATED

Some of the curves reproduced below were taken between $2\vartheta = 4$–$42°$ and others between $2\vartheta = 7$–$42°$. Small angle scattering effects corresponding to structural elements within the colloidal dimensions do not enter the picture. On the abscissa of all intensity distribution curves reproduced the diffraction angle 2ϑ as well as a scale in angstrom units is indicated. The latter corresponds to the value of d in the equation: $d = x/(4\pi \sin \vartheta/\lambda)$ calculated for the first maximum occurring in $(\sin x)/x$ and thus represents the locus of the first diffraction maximum that would occur in a gas consisting of diatomic molecules having an interatomic distance d. It will be allowed in first approximation to discuss the observed intensity distributions in terms of d as being the approximate inter-particle distances giving rise mainly to the observed intensity at the relevant locus. (The authors are aware of the fact that this is no more than a very rough procedure.)

LIQUID POLYTHENE AND MOLTEN PARAFFIN

In Figure 2 we reproduce the intensity distribution curves exhibited by a molten paraffin (m.p. 60°) taken at 65° and by molten polythene taken at 135°.* The molten paraffin curve is typical for low molecular liquids.

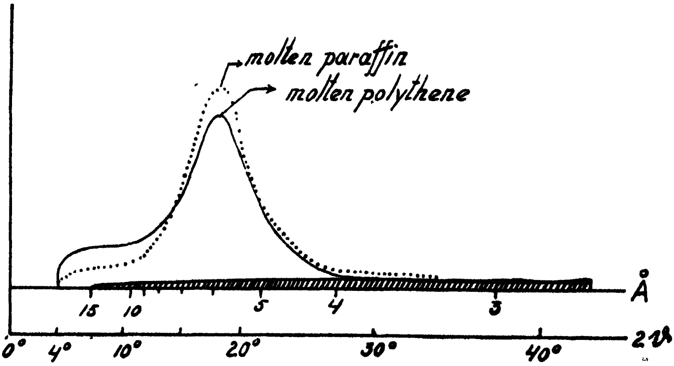

Fig. 2. Solid curve, liquid paraffin (at 65°); dotted curve, molten polythene (at 130°). The hatched areas correspond to incoherent radiation.

---

* These curves are reproduced from a previous paper.[2]

It has a broad maximum at $d \sim 5.8$ A. and a relative low intensity toward smaller and larger angles of diffraction. The pronounced maximum is indicative of the considerable amount of low distance order known to occur in liquids and which (for sufficiently small regions) is akin to the long range order present in the crystalline state. From this point of view ordinary liquids should hardly be designated as being "amorphous" in the sense of "completely disordered."

The liquid high molecular paraffin (polythene) shows a similar maximum at about the same locus. It is, however, less intense in that more radiation is diffracted at angles lower than that of the maximum ($2\vartheta < 10°$). At higher angles beyond $2\vartheta = 30°$ the paraffin and polythene curves practically coincide. This is clear since the d values of 4 A. and lower will mainly correspond to intramolecular periods which will be similar in both substances.

The higher intensity at lower angles in polythene may possible be due either to "low angle" diffraction effects corresponding to the structure factor of the cross section of the chains, or to frequently occurring intermolecular distances larger than 10 A. owing to the stiffness of the long chains which prevents them from fitting so well against each other as the molecules in liquid low molecular paraffin.

It would be of importance to investigate whether liquid polythene exhibits any scattering at very small angles, which is known to be absent in ordinary low molecular liquids, and also to measure its density as compared to low molecular paraffins at equal temperature. (The author is indebted to Prof. O. Kratky for a discussion on this subject.)

In previous work[2] it has been shown that the scattering within the range of $d \sim 10$ to 16 A., though continuously diminishing in intensity upon cooling and solidification of the polythene, persists also at room temperature, with about half the intensity of that exhibited by the molten polymer. It is probably proportional to the amount of the noncrystalline fraction in the polymer of which it is then to be regarded as an attribute.

In Figure 2 the contribution of coherent radiation to the background is indicated by the hatched area. It is seen that beyond the "liquid band," coherent radiation soon drops to negligible values and all the radiation diffracted at angles larger than 30° consists of the incoherent component. Comparing this with Figure 1 we see that the situation is quite different in amorphous cellulose in that a considerable amount of coherent radiation is diffracted beyond $2\vartheta = 30°$. We shall return to this point later.

NONCRYSTALLINE POLYMERS

In Figure 3 are collected the intensity distribution curves in some polymers reputed to be amorphous in nature. In Figure 3A, giving some vinyl polymers, it is seen that polystyrene, polyvinyl acetate, and polymethyl methacrylate yield two diffraction maxima having some similarity to "liquid bands." The maxima indicate that some spacings occur with a particular high frequency. There are more signs of a residual ordering in these polymers than in amorphous cellulose powder (*cf.* Fig. 3C). At higher angles of diffraction (beyond 30°) there is some more coherent scattering in the vinyl polymers than in either molten or solid polythene, and this is most pronounced in the methacrylate (which even has a second maximum at about 3.9 A.).

In Figure 3B isotropic Hevea smoked sheet heated to 50° (in order to melt the crystallites), polyvinyl butyral and a phenolformaldehyde resin are shown. It is striking that even in the Bakelite resin the character of the curve is still akin to that of a liquid substance. (The incoherent background in Figure 3B is drawn for rubber. For Bakelite the ordinates of this curve should be multiplied by 0.86.) One would have expected a higher degree of disorder.

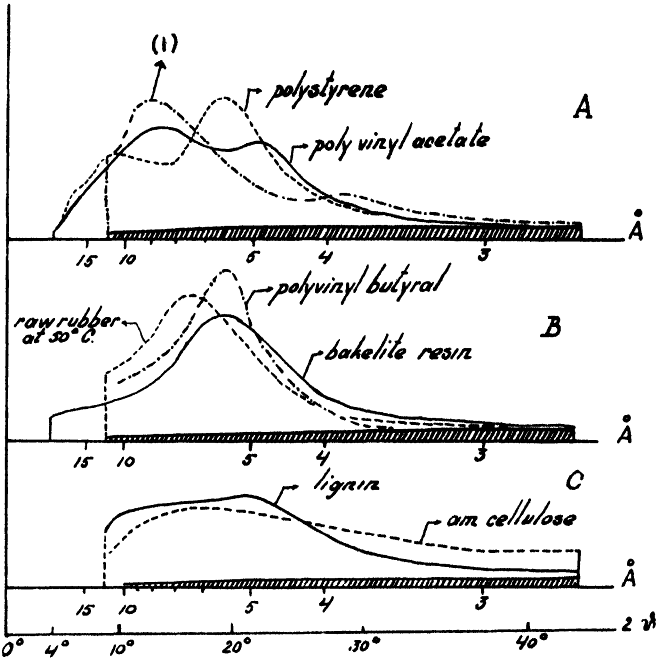

Fig. 3. Various polymers. In C the curve of amorphous cellulose from Figure 1 is repeated for comparison. Hatched area: incoherent radiation. Curve (1): polymethyl methacrylate.

In Figure 3C the curve obtained with lignin isolated from jute fiber is shown together with the amorphous cellulose curve from Figure 1. The lignin curve is almost as flat as the cellulose curve, indicating a very high degree of disorder. The extremely low degree of order in the amorphous portion of cellulose fibers as compared to that in other "amorphous" polymers may perhaps be associated with the stiffness of the cellulose chain and its complicated structure.

AMORPHOUS CARBOHYDRATES

In Figure 4A the curves of a commercial "soluble starch" and of glassy sugar are shown. (This preparation was obtained by melting together equal parts of glucose and cane sugar and rapidly cooling the melt. A plate was cut from the solidified melt and used for the x-ray experiment.)

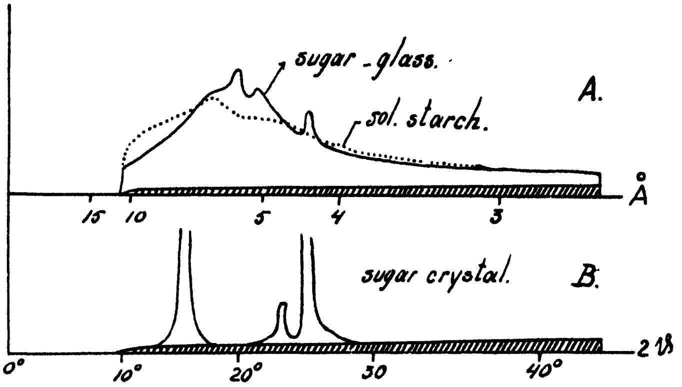

Fig. 4. (A) Dotted curve: soluble starch; solid curve: undercooled mixture of glucose and sucrose. Hatched area: incoherent scattering. (B) Single crystal of cane sugar.

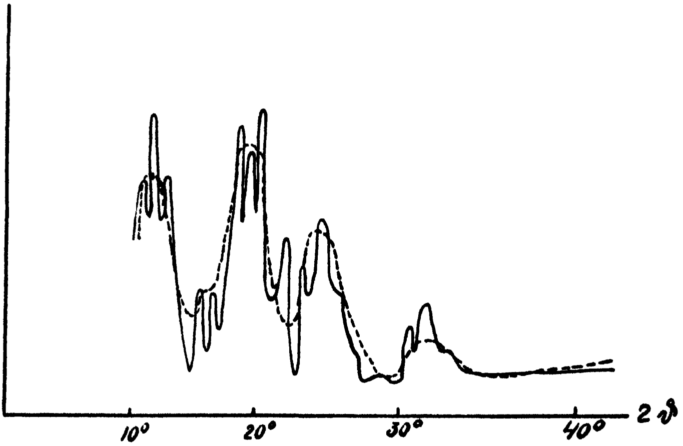

Fig. 5. Solid curve, sugar powdered by hand; broken curve, sugar powdered for 12 hours in the vibrating ball mill.

Apart from the fact that the sugar curve reveals a beginning recrystallization of the sugar, it is clearly demonstrated that the general character of the curves is akin to that given by amorphous cellulose. The considerable amount of coherent scattering at high diffraction angles is also present in these cases.

For comparison, the curve obtained from a single crystal of cane sugar is reproduced in Figure 4B. The entire coherent radiation consists of crystalline peaks. (Since the substance might be considered as being 100%

crystalline, it was assumed that the remaining background consists of incoherent radiation only. As a matter of fact, this background was used as a standard for the computation of the incoherent component in the other substances. More exactly, the sugar background also contains a component of scattering due to thermal vibrations. It has been assumed that this component is of the same order for the other substances investigated.)

We have also examined order in cane sugar crystals to determine the extent to which their order can be disturbed by mechanical disintegration.

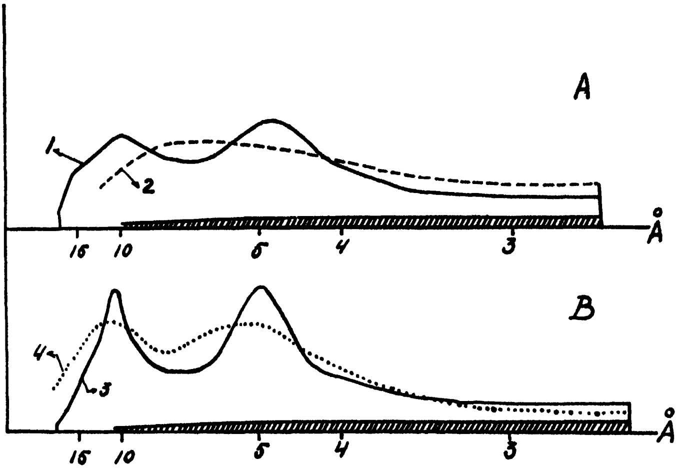

Fig. 6. *Curve 1*: a water-soluble cellulose acetate (1.14 acetyl groups per C_6); *curve 2*: amorphous cellulose; *curve 3*: water-soluble methyl cellulose (1.2 CH_3O per C_6); *curve 4*: cellulose acetate rayon.

To that end, we have subjected sugar suspended in dry carbon tetrachloride to the action of the vibrating ball mill.* In order to have a measure of the degree of dispersion reached, we have determined the heat of solution in water of the powder obtained. In a series of experiments under varied conditions the highest value reached was +11.0 cal./g. against −3.2 cal./g. for ordinary sugar crystals.

In Figure 5 the diffraction curve of sugar powdered by hand in a mortar and that of the optimal product from the vibrating ball mill are reproduced. (Compared to the other illustrations in this paper these curves are reproduced on a larger scale.) Though the numerous lines exhibited by the ordinary sugar powder have merged into three broader lines, the spectrum is still characteristic for a cryptocrystalline substance. The lines are of the same character as those met with in crystalline polymers like cellulose.

---

* In this mill the crystallinity of dry cellulose fibers can be almost completely destroyed; *cf.* P. H. Hermans and A. Weidinger, *J. Am. Chem. Soc.*, **68,** 2547 (1946).

NONCRYSTALLINE CELLULOSE DERIVATIVES

Some partially substituted cellulose esters and ethers are known to exist which are water soluble and exhibit no distinctly crystalline x-ray diagrams. The degree of substitution of such derivatives is about 1 per C_6. The water solubility is usually explained as being due to the irregular structure of the chains with the substituent not quite uniformly distributed over the 2.3 and 6 positions (or even along the chain). Hydrogen bonding between adjacent chains is thus sterically hindered, while the numerous remaining free OH groups are responsible for water solubility.

Figure 6A, curve 1, gives the intensity distribution curve of a water-soluble acetate with 1.14 acetyl groups per C_6.* For comparison the amorphous cellulose is repeated in curve 2. In Figure 6B, curve 3 refers to a water-soluble methyl cellulose (1.2 CH_3O per C_6), a commercial I.G. Farbenindustrie product, and curve 4 to an ordinary acetate rayon (degree of substitution about 2.5). The acetates exhibit only very diffuse maxima. The degree of order in these substances is but slightly better than that in amorphous cellulose powder. The methyl cellulose exhibits more pronounced, though still very diffuse, maxima.

It is seen that coherent scattering at high angles is still very pronounced in the water-soluble cellulose derivatives but markedly smaller in the acetate rayon.

DISCUSSION

According to the previous experimental data the occurrence of a diffuse coherent background of considerable intensity beyond diffraction angles of 35° is inherent to the carbohydrates in their noncrystalline state. It corresponds to interatomic interferences of atoms located at distances from each other of about 3.5 A. and less. Since the scattering power of oxygen is about 2.5 times higher than that of carbon, it seems likely that (mainly at least) interferences between oxygen atoms are involved.

The smallest intermolecular oxygen-to-oxygen distance occurring in the carbohydrates considered is that between the ring oxygen and the bridge oxygen, amounting to about 2 A. The O—O distances of the hydroxyls attached to the six-membered pyranose ring (which may also assume the flexible "tub-form"[3]) ranges from about 3.5 A., for adjacent transhydroxyls in their position of closest proximity, and upward for all other pairs. Furthermore, intra- and intermolecular hydrogen-bonded oxygens may occur,[8] corresponding to a O—O distance of about 2.7 A.

It does not seem likely that the 2 A. pairs from the configuration —O—C—O— play a significant part in relation to the background region under discussion, since polyvinyl butryral ($C_8H_{10}O_2$) which contains the same configuration in even higher concentration does not show any background in that region (see Fig. 3B). Neither do polyvinyl acetate and polymethylmethacrylate, which also have oxygen pairs at close proximity within the molecule (Fig. 3A). The relevant spacings of about 2 A. fall beyond the investigated region.

---

* The samples were obtained by courtesy of Dr. P. Clément, Paris.

It would seem, therefore, that the background under consideration is particularly associated with oxygen-to-oxygen distances in the order of 2.5–3.5 A. As such we may consider: (*a*) intramolecular hydrogen bonds (2.7 A.) (see ref. 1); (*b*) intermolecular hydrogen bonds (2.7 A.); (*c*) probably also other intermolecular O—O distances which may then range from 2.7 A. and upward. In ordinary cellulose acetate (Fig. 6B), where 2.5 of the 3 hydroxyl groups are shielded by substitution, the background at high angles is relatively low (amounting to roughly 20% of that present in amorphous cellulose powder). In the low substituted water-soluble cellulose derivatives (Fig. 6) it is considerably higher, suggesting that it is associated with intermolecular interaction of hydroxyl oxygen atoms.

Regardless of the relative contributions of the cases *a*, *b*, and *c*, it seems likely that true hydrogen bonding would materially contribute to scattering in the angular range considered.

If this view is correct, other polymers capable of hydrogen bond formation should also exhibit a background of this type whose intensity should stand in close relation to their noncrystalline fraction. Further work is necessary to investigate whether this rule is of general applicability, but we shall see in the next section that polyamides also do exhibit a similar background at high angles.

It should also be recalled that native cellulose fibers which contain half as much disordered substance as regenerated cellulose fibers also show a background at high angles of about half the intensity.

The interatomic spacings of the hydrogen atoms of adjacent molecules in solid polymers will, in part, also lie within the range under consideration. The scattered intensity by interferences between hydrogen atoms is, however, too small to be observable. However, if the hydrogens are substituted by heavier atoms, as for instance by chlorine, the picture will, of course, change and a background within the range considered due to intermolecular Cl—Cl spacings can again be expected. This is corroborated by experiments on chlorinated polymers (see later). Carbon tetrachloride and dichloromethane also exhibit a high background in this region (see later).

Detection of hydrogen bonding by background analysis will, therefore, not be possible in halogenated polymers. Further work would be necessary to know whether or not polymers very rich in oxygen but not capable of hydrogen bonding (if existent) will also show a background in the relevant region.

In conformity with the foregoing, water also exhibits considerable intensity at high angles (see later).

POLYHEXAMETHYLENE SEBACAMIDE

In a previous paper[2] different samples of this polymer with crystallinity ranging between about 50 and 70% have been described.

The observed intensity distribution curves beyond $2\vartheta = 30°$ of these samples are given in Fig. 7. (For the sake of clarity, this figure is drawn on an enlarged scale as compared to the other figures in this paper.) It is seen that all samples exhibit a detectable background intensity that runs antiparallel to the percentage of crystallinity. For comparison the amorphous cellulose curve has again been added. (See Discussion Section.)

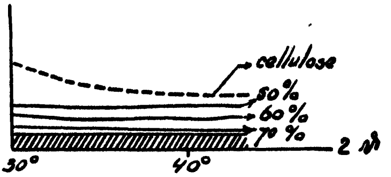

Fig. 7. Intensity distribution curves of hexamethylenesebacamide polymers of different crystallinity for diffraction angles beyond 30°. The cellulose background is given for comparison.

CHLORINATED POLYMERS

In Figure 8 the intensity distribution curves of polyvinylidene chloride (73% Cl), polyvinyl chloride (58.8% Cl) and of a chlorinated polythene

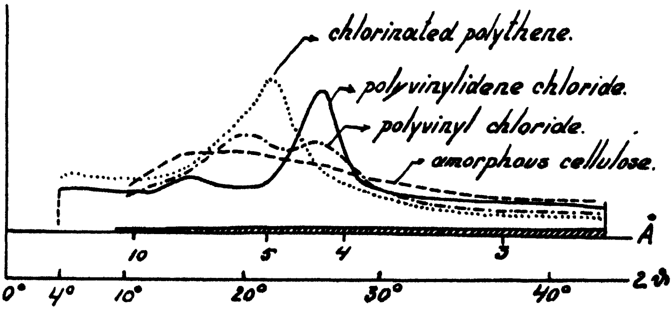

Fig. 8. Polymers containing chlorine compared with amorphous cellulose.

(40% Cl) are given. For comparison the amorphous cellulose curve has been added. It is seen that all the curves exhibit a significant background at high angles whose intensity increases with the chlorine content of the polymer. In polyvinylidene chloride this background almost reaches the level of that in amorphous cellulose.

A discussion of these facts is given earlier.

CCl$_4$ AND CH$_2$Cl$_2$

If our interpretation of the background at high angles in chlorinated polymers holds good, then liquid carbon tetrachloride and dichloromethane should also exhibit high intensity in the region under consideration.

The intramolecular Cl—Cl spacings range from 2.99 to 3.2 A. in these substances[4] and the intermolecular spacings between the chlorine atoms will be slightly higher and in same order as in the chlorinated polymers. The standardized intensity curves of these liquids are given in Figure 9

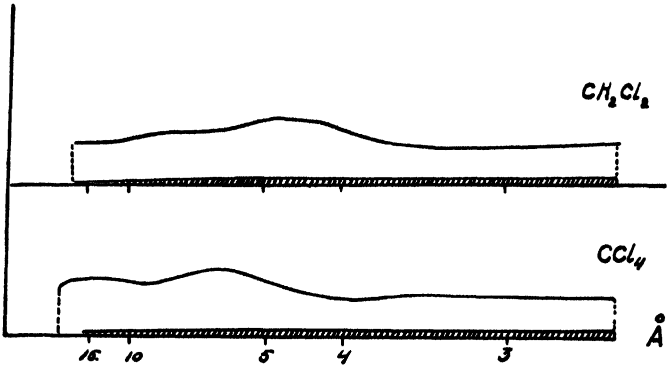

Fig. 9. CCl_4 and CH_2Cl_2.

and show that this is true. The liquids were exposed in a specially constructed cuvette with very thin mica windows. The scattering due to the mica was determined separately and subtracted.

WATER

Finally, Figure 10 shows the diagram of water. In this substance the scattered intensity must be almost entirely due to interferences between

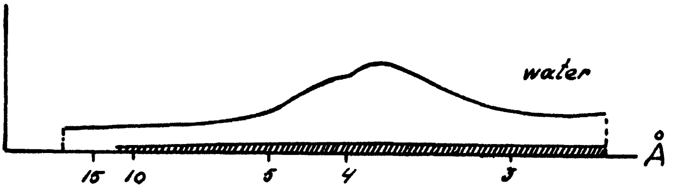

Fig. 10. Diagram of water.

oxygen atoms. It is seen that a considerable portion of the intensity is found in the high angle region considered. This is in conformity with the fact that water is a substance known to have abundant hydrogen bonding.

The authors are indebted to Professor H. Mark, Brooklyn, N. Y., to Dr. C. S. Fuller, Murray Hill, N. J., and to Dr. A. J. Staverman, Delft, for several polymer samples. The x-ray work was carried out by one of us (W.) in the Physical Institute of the Technical University, Delft.

References

1. P. H. Hermans and A. Weidinger, *J. Applied Phys.*, 19, 491 (1948); *Bull. soc. chim. Belge*, 57, 123 (1948); *J. Polymer Sci.*, 4, 709 (1949).
2. *J. Polymer Sci., in preparation.*
3. P. H. Hermans, J. de Booys, and C. J. Maan, *Kolloid Z.*, 102, 169 (1943).
4. H. A. Stuart, *Molekülstruktur*. Springer, Berlin, 1934, p. 72.

English Synopsis, see Summaries, page S5, Vol. V, 1950.

Résumé

Les courbes de distribution de l'intensité radiale, obtenues par exposition aux rayons-X monochromatiques de différents polymères non-cristallisés et partiellement cristallisés, sont quantitativement évalués, après correction pour une radiation incohérente, et réduite à des conditions standards d'intensité et de masse irradiée. On montre quelques courbes de distribution d'intensité, ainsi réduites, montrant une intensité intègrée constante dans les limites de l'erreur expérimentale, sans tenir compte de la composition atomique du polymère. La cellulose amorphe manifeste de loin le degré le plus élevé de désordre de tous les polymères examinés. On suggère, que, dans les polymères ne contenant que du C, H, O, et N, la présence d'un arrière-fond intense et cohérent dans les limites d'angles de diffraction de 35° à au delà constitue une indication des liaisons-hydrogène dans les parties non-cristallines. L'arrière-fond cohérent dans cette région est d'intensité nulle pour les polymères, qui ne contiennent pas de liaisons-hydrogène L'eau, substance riche en liaisons-hydrogène, montre une intensité considérable de la région relevée. Dans les polymères contenant de l'halogène, la détection de liaisons-hydrogène par cette méthode est impossible, due aux interférences intermoléculaires entre les atomes d'halogène des molécules adjacentes, qui causent une augmentation de l'intensité d'arrière-fond dans la même région angulaire.

Zusammenfassung

Verteilungskurven der radialen Intensität von isotropisch monochromatischen Röntgenaufnahmen von verschiedenen nicht-kristallinen und teilweise kristallinen Polymeren werden quantitativ bestimmt, für inkohärente Strahlung korrigiert und auf Standard-Bedingungen der Intensität und der bestrahlten Masse reduziert. Es wird gezeigt, dass die so reduzierten Intensitäts-Verteilungskurven tatsächlich eine konstante integrierte Intensität innerhalb der experimentellen Fehlergrenzen aufweisen, unabhängig von der atomaren Zusammensetztung des Polymers. Es wird angegeben, dass amorphe Cellulose bei weitem den höchsten Unordnungsgrad von allen untersuchten Polymeren zeigt. Es wird vorgeschlagen, dass in Polymeren, die aus keinen anderen Elementen als C, H, O, und N. bestehen, das Auftreten von einer kohärenten Hintergrundsintensität im Beriech von Beugungswinkeln von 35° und aufwärtz bezeichnend für Wasserstoffbindungen im nicht kristallinen Teil ist. Der kohärente Hintergrund hat in diesen Bereichen eine Intensität Null in Polymeren, wo keine Wasserstoffbindungen möglich sind. Wasser, eine Substanz, die reich an Wasserstoffbindungen ist, zeigt eine erhebliche Intensität im entsprechenden Bereich. In Halogen-haltigen Polymeren ist die Bestimmung von Wasserstoffbindungen auf diesem Wege unmöglich, da intermolekulare Interferenzen zwischen Halogenatomen von angrenzenden Molekülen bestehen, die eine Hintergrundsintensität in den gleichen Winkelbereichen entwickeln.

Received April 7, 1949

JOURNAL OF POLYMER SCIENCE VOL. V, NO. 3, PAGES 283-300

Behavior of Polyvalent Polymeric Ions in Solution

A. KATCHALSKY,* O. KÜNZLE, and W. KUHN, *University of Basel, Switzerland*

Polymeric molecules that carry a large number of ionizable groups exhibit interesting phenomena in aqueous solution that are not encountered in the solutions of polymeric substances in organic solvents. These phenomena may be attributed to the influence of the ionized groups on the shape of the molecules. The aim of the present paper is to deduce some of the properties of the solutions of polyvalent polymeric ions from a statistical consideration of the shape of the molecules under the influence of the electrostatic field due to the ionized groups.[1]

It is plausible to assume that, when a threadlike, coiled polymeric molecule is ionized, repulsive forces between the ionized groups become operative. Thus, for instance, if we add some alkali to a solution of polymethacrylic acid:

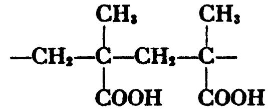

$$-CH_2-\overset{\displaystyle CH_3}{\underset{\displaystyle COOH}{C}}-CH_2-\overset{\displaystyle CH_3}{\underset{\displaystyle COOH}{C}}-$$

part of the carboxylic groups are ionized and the carboxylate ions repel each other electrostatically. Under the influence of the repulsive forces the coiled molecule opens and extends. With increase in the degree of ionization the repulsion overcomes the coiling tendency of the Brownian movement and finally the molecule is stretched to its full length. Thus, during the process of ionization or neutralization of the carboxylic groups, the molecule acquires all forms from a nearly spherical, highly coiled shape to an extended filament.

As is well known, many of the properties of polymer solutions (viscosity, streaming birefringence, and depolarization of scattered light) are largely determined by the shape of the solute molecules. In the case of the polymeric polyvalent ions we are able to change molecular shape—and subsequently viscosity, double refraction of flow, depolarization of scattered light, etc.—without correspondingly changing the molecular weight of the solute or the nature of the solvent. Therefore, these substances present a very remarkable case for the statistical investigation of polymers in general.

This paper deals only with very dilute solutions, for which we may safely assume that the free "opposite" ions, as, for instance, the alkali ions in the case of polymeric acids, are sufficiently far removed from the ionized groups of the polymer so that the simple picture of repulsion between charges of the same sign is not distorted.

---

* Present address: Chaim Weizmann Institute of Science, Rehovot, Israel.

I. SIMPLE PICTURE (FIRST APPROXIMATION)

In order to get an approximate idea of the magnitude of the forces operative in the ionized molecules, let us assume that the charges are concentrated around the molecular ends and let us neglect, for the time being, the charges distributed in the central portions of the molecule. As will be shown in section III, there exists a tendency for the charged groups to concentrate in the ends and to leave the mid-portions of the molecule at a lower degree of ionization, so that this first approximation is not entirely unjustifiable.

Let the distance between the molecular ends be h, the number of ionized groups ν, each group of charge ϵ. The dielectric constant of the solvent is designated by D. It is assumed that the dielectric constant in the molecule is practically equal to that of the solvent. With these designations the energy of electric repulsion will be given by:

$$E = (\nu^2\epsilon^2)/(4Dh) \tag{1}$$

Kuhn and Grün have shown[2] that the probability $W(h)\,dh$ of finding a molecule with its ends lying in the interval $h,h + dh$ will, in the case that the energy E of the system depends on h, be given by:

$$W(h)\,dh = \text{const} \times \exp\left\{(-3h^2/2NA^2) - (E/kT)\right\}h^2\,dh \tag{2}$$

where N is the number of statistical elements and A is the length of a statistical element.

Molecules of degree of polymerization Z can be divided for statistical reasons in a nonarbitrary way into "preferential statistical elements" each element showing statistical freedom of motion. If the number of monomeric units in a statistical element is equal to s and if the length of a monomeric unit, measured in the direction of the molecular chain, is b, the length of the preferential statistical chain element will be $A = sb$ and $N = Z/s$. The total hydrodynamic length of the chain is $L = Zb = NA$.

Introducing the value of the energy E into equation (2) we obtain:

$$W(h)\,dh = \text{const} \times \exp\left\{(-3h^2/2NA^2) - (\nu^2\epsilon^2/4DkTh)\right\}h^2\,dh \tag{3}$$

Equation (3) permits the evaluation of the mean square distance between the ends of a polyvalent polymeric ion carrying ν ionized groups according to the expression:

$$\overline{h^2} = \frac{\int_0^\infty h^2 W(h)\,dh}{\int_0^\infty W(h)\,dh}$$

and to compare this value with $\overline{h^2_{10}}$, *i.e.*, with the mean square distance between the ends of an *uncharged* molecule.

We can also deduce easily the most probable value of h (which we may designate by h_ν) by differentiating $W(h)$ and equating the differential to zero. This leads to the formula:

$$h_\nu^2 = \frac{\epsilon^2\nu^2}{4Dh_\nu kT}\,\frac{NA^2}{3} + \frac{2}{3}NA^2 \tag{4}$$

For *very low values of* ν, formula (4) reduces to the expression for the most probable value of an uncharged molecule:

$$h_\nu^2 \simeq {}^2/_3NA^2 = {}^2/_3h_{10}^2 \text{ (for low values of } \nu) \tag{5}$$

For *high values of* ν, the second term in equation (4) may be neglected, and we obtain:

$$h_\nu^3 = \frac{\epsilon^2\nu^2}{12DkT}NA^2 \qquad \text{or} \qquad h_\nu = \nu^{2/3}(NA^2)^{1/3}\left(\frac{\epsilon^2}{12DkT}\right)^{1/3}$$

$$\text{(for high values of } \nu) \tag{6}$$

The last expression gives an idea of the rate of increase of the molecular end-to-end distance with the degree of ionization and with the degree of polymerization.

Equation (6) can also be interpreted in another physical way: let us transcribe the equation as follows:

$$\frac{\nu^2\epsilon^2}{4Dh_\nu^2} = 3kT\frac{h_\nu}{NA^2} \tag{7}$$

The left-hand side of the equation is the negative value of the electrostatic repulsive force $\mathfrak{R}_e$ acting in the direction of h:

$$\mathfrak{R}_e = -\frac{\partial E}{\partial h} = -\frac{\nu^2\epsilon^2}{4Dh_\nu^2}$$

The right-hand side in (7) is the well-known expression (*Kolloid Z.*, 76, 258, 1936; *Exper.*, 1, 6, 1945) for the *elastic* retractive force, *i.e.*, the force that should be applied to the ends of a polymeric molecule in order to keep it at a distance h_ν against the coiling tendency of the Brownian movement.

Equation (7) thus demonstrates that the molecule will be extended by electrostatic repulsive forces until an equilibrium is attained between the electrical forces and the statistical restoring force, which are supposed to act at the molecular ends.

This result is not surprising when we remember that at the start of this approximation we assumed the electrical charges to act at the molecular ends. The result will be somewhat different if we take into account the charges distributed along the median parts of the molecule. These charges act at smaller distances apart and may be expected to contribute largely to the energy content of the molecule. A more detailed picture of the interaction between the charges situated on any part of the molecule will be given in section II.

It might be remarked that the use of equation (2) is justified in practice as long as h_ν is smaller than a third of the length of the fully stretched molecule, *i.e.*, as long as $h_\nu < NA/3$. For more fully stretched molecules, another formula[3] should be applied:

$$W(h)\,dh = \text{const} \times \exp\left\{-N\left[\ln \frac{\beta}{\sinh \beta} + \beta\mathfrak{L}(\beta)\right] - \frac{E}{kT}\right\} h^2\,dh \quad (8)$$

where $\mathfrak{L}$ is the Langevin function; and $\mathfrak{L}(\beta) = h/NA$; $\beta = \mathfrak{L}^*(h/NA)$; $\mathfrak{L}^*$ being the inverse Langevin function; thus:

$$\beta(h) = 3\frac{h}{NA} + \frac{9}{5}\left(\frac{h}{NA}\right)^3 + \frac{297}{175}\left(\frac{h}{NA}\right)^5 + \ldots$$

II. SECOND APPROXIMATION TO THE DETERMINATION OF THE ELECTROSTATIC ENERGY AS A FUNCTION OF h[4]

We now assume, contrary to our previous assumption, that the charge is *evenly distributed over the whole length of the molecular chain.* This distribution is assumed such that equal portions of the charge are situated at the junctions of consecutive statistical elements and at the ends of the molecule, *i.e.*, at $N + 1$ points; each charged point therefore carries:

$$n = \nu/(N + 1) \quad (9)$$

charges.

The contribution of two charges situated, respectively, at the ends of the i-th and $i + k$-th elements to the total potential energy will be:

$$\mu_{i,i+k} = \frac{\nu^2\epsilon^2}{(N + 1)^2 D}\overline{\left(\frac{1}{r_{i,i+k}}\right)} \quad (10)$$

where $\overline{(1/r_{i,i+k})}$ denotes the mean reciprocal distance between the points in question. If the values of all the $\overline{(1/r_{i,i+k})}$'s can be given explicitly, an integration over all $\mu_{i,i+k}$'s will give the total energy, E, due to electrostatic repulsion.

IIA. Distribution Function for the Distance between Two Statistical Chain Elements

From a consideration of the angle distribution of the statistical elements in a polymeric molecule whose ends are kept at a distance h it may be deduced[3] that the distance between the ends of two segments, k units apart, is independent of the position of the segments in the molecule and is determined *solely by the value of h and by the number of intervening elements k.* Thus the distance between the i-th and $i + k$-th segments is equal to the distance between the end of the chain and the k-th segment, or $r_{i,i+k} = r_{0,k}$. Hence, a calculation of the values of the distribution function $W(r_{0,k})$ also gives the distribution function for any other distance $r_{i,i+k}$ in the molecule.

Let us put a molecule of end-to-end distance h in a co-ordinate system so that one end falls into the origin of the system and h coincides with the z axis (Fig. 1).

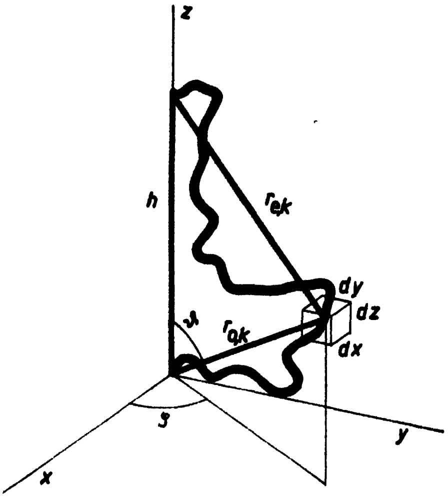

Figure 1

The probability that the k-th element is to be found in the volume element defined by x, $x + dx$; y, $y + dy$; and z, $z + dz$ is evidently given by the product of two probabilities:

(*1*) That the end of the thread of k elements, starting at the origin of coordinates, is found in the volume element $dx\,dy\,dz$, that is

$$W_1\,dx\,dy\,dz = \left(\frac{3}{2\pi kA^2}\right)^{3/2} \exp\,[-3r_{0,k}^2/2kA^2]\,dx\,dy\,dz \tag{11}$$

(2) That the end of the chain of $N - k$ elements, starting at the other end of the molecule, is found in the same volume element, that is,

$$W_2\,dx\,dy\,dz = \left(\frac{3}{2\pi(N-k)A^2}\right)^{3/2} \exp\left\{-3r_{e,k}/[2(N-k)A^2]\right\}\,dx\,dy\,dz \tag{12}$$

$r_{e,k}$ being the distance between $z = h$ and the volume element under consideration. The probability W_k of finding the k-th element in the volume $dx\,dy\,dz$ is thus given by:

$$W_k = CW_1W_2 \tag{13}$$

The proportionality constant C is given by the condition:

$$\int_0^\infty W_k\,dx\,dy\,dz = 1 \tag{14}$$

Integrating and introducing the value of C into equation (13), we obtain:

$$W_{\substack{k \\ x,x+dx \\ x,y+dy \\ z,z+dz}} = \left(\frac{3N}{2\pi A^2k(N-k)}\right)^{3/2} \exp\left\{-\frac{3}{2A^2k(N-k)}\right.$$
$$\left.\left[N(x^2+y^2+z^2) - 2khz + \frac{k^2h^2}{N}\right]\right\} \qquad (15)$$

Equation (15) may be readily transformed into a corresponding equation in polar coordinates. Introducing $x^2 + y^2 + z^2 = r_{0,k}^2$:

$$x = r_{0,k} \sin\vartheta \cos\varphi \qquad y = r_{0,k} \sin\vartheta \sin\varphi \qquad z = r_{0,k} \cos\vartheta$$

where ϑ is the angle between $r_{0,k}$ and the z axis, and φ the angle between the projection of $r_{0,k}$ on the x,y plane and the x axis, we obtain:

$$W_{\substack{k \\ r_{0,k},\, r_{0,k}+dr_{0,k} \\ \vartheta,\vartheta+d\vartheta \\ \varphi,\varphi+d\varphi}} = \left(\frac{3N}{2\pi A^2k(N-k)}\right)^{3/2} \exp$$
$$\left\{-\frac{3}{2}\,\frac{Nr_{0,k}^2 - 2hr_{0,k}\cos\vartheta}{A^2k(N-k)}\right\} \exp\left\{-\frac{3}{2}\,\frac{h^2k}{NA^2(N-k)}\right\} r_{0,k}^2 \sin\vartheta \qquad (16)$$

As we are not interested in the angle distribution but only in the probability of finding the k-th element at a distance $r_{0,k}$ to $r_{0,k} + dr_{0,k}$ we integrate equation (16) over all φ's from 0 to 2π and all ϑ's from 0 to π to obtain:

$$W(r_{0,k})dr_{0,k} = \left[\frac{3}{2\pi A^2(N-k)}\right]^{1/2} \left(\frac{N}{k}\right)^{3/2} \frac{r_{0,k}}{h} \times$$
$$\left[\exp\left\{-\frac{3N}{2A^2k(N-k)}\left(r_{0,k} - \frac{kh}{N}\right)^2\right\} - \right.$$
$$\left.\exp\left\{-\frac{3N}{2A^2k(N-k)}\left(r_{0,k} + \frac{kh}{N}\right)^2\right\}\right] dr_{0,k} \qquad (17)$$

The distribution function (17) leads to the mean value of $r_{0,k}^2$:

$$\overline{r_{0,k}^2} = h^2\left(\frac{k}{N}\right)^2 + A^2\,\frac{N-k}{N}\,k \qquad (18)$$

It may be remarked that for $k \ll N$, *i.e.*, near the origin of the molecule:

$$\overline{r_{0,k}^2} = kA^2$$

Thus the probability of finding the k-th element at a distance $r_{0,k}$ is for very small values of k independent of N and h and depends on k alone.

On the other hand, for $k = N$ we get $r_{0,k} = h$ as might be expected.

IIB. Mean Value of the Reciprocal Distance

Equation (17) permits the evaluation of the mean reciprocal distance $\overline{(1/r_{0,k})}$ which is needed for the final calculation of the energy:

$$\overline{\left(\frac{1}{r_{0,k}}\right)} = \frac{\int_0^\infty (1/r_{0,k})W(r_{0,k})\,dr_{0,k}}{\int_0^\infty W(r_{0,k})\,dr_{0,k}} \tag{19}$$

This equation leads[4] to the expression:

$$\overline{\left(\frac{1}{r_{0,k}}\right)} = \frac{N}{kh}\,\phi\left(\sqrt{\frac{3h^2}{2NA^2}\,\frac{k}{N-k}}\right) \tag{20}$$

where ϕ denotes the error integral:

$$\phi(x) = (2/\sqrt{\pi})\int_0^x e^{-w^2}dw$$

A short discusssion of equation (20) follows. For $k = N$:

$$\phi(\sqrt{\infty}) = \phi(\infty) = 1$$

$\overline{(1/r_{0,k})} = 1/h$ as should be expected. Even for small values of k, when statistics do not rigidly hold, equation (20) yields good approximate values. For very small values of x we have:

$$\phi(x) = \frac{2}{\sqrt{\pi}}\,x$$

hence for small values of k, or very small values of k/N:

$$\phi\left(\sqrt{\frac{3h^2}{2NA^2}\,\frac{k}{N-k}}\right) \simeq \frac{2}{\sqrt{\pi}}\sqrt{\frac{3h^2}{2NA^2}\,\frac{k}{N}} = \frac{h}{NA}\sqrt{\frac{6k}{\pi}}$$

or:

$$\overline{\left(\frac{1}{r_{0,k}}\right)} = \frac{N}{kh}\,\frac{h}{NA}\sqrt{\frac{6k}{\pi}} = \frac{1.38}{A\sqrt{k}} \tag{21}$$

for the case $k = 1$, *i.e.*, for a single statistical element:

$$\overline{(1/r_{0,k})} = 1.38/A$$

instead of the value $1/A$, which is as close an approximation as might be expected.

IIC. Calculation of the Total Energy of Electrostatic Repulsion

The knowledge of $\overline{(1/r_{0,k})}$ and the fact that the mean distance between the elements is dependent only on the number k of intervening elements, lead to a straightforward calculation of the electric repulsion energy.

As pointed out before, the energy contribution of two charges situated on the i-th and $i + k$-th elements and separated by the distance $r_{0,k}$ is:

$$\mu_{i,i+k} = \frac{\nu^2\epsilon^2}{(N+1)^2D}\overline{\left(\frac{1}{r_{0,k}}\right)} \tag{21}$$

Among N elements, there are $N - k + 1$ pairs of elements, k elements apart. The total contribution of these pairs is therefore:

$$(N - k + 1)\mu_{i,i+k} = \frac{N - k + 1}{(N + 1)^2} \frac{\nu^2\epsilon^2}{D} \overline{\left(\frac{1}{r_{0,k}}\right)} \tag{22}$$

The total energy of the electrical repulsion is now evidently obtained by summing over all values of k from 1 to N:

$$E = \frac{\nu^2\epsilon^2}{D} \sum_{k=1}^{N} \frac{N - k + 1}{(N + 1)^2} \frac{N}{kh} \phi \left(\sqrt{\frac{3h^2}{2NA^2} \frac{k}{N - k}}\right) \tag{23}$$

or as usually $N \gg 1$:

$$E = \frac{\nu^2\epsilon^2}{NDh} \sum_{k=1}^{N} \frac{N - k}{k} \phi \left(\sqrt{\frac{3h^2}{2NA^2} \frac{k}{N - k}}\right) \tag{24}$$

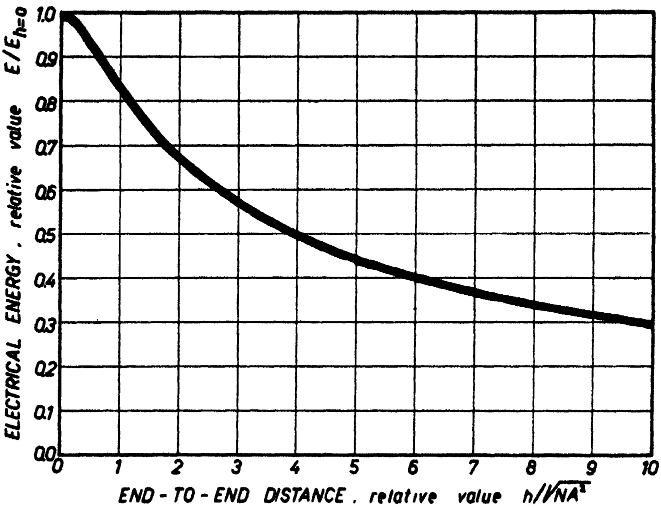

Fig. 2. Electrostatic energy E of an ionized chain molecule, having a given number of electric charges, as a function of the end-to-end distance h, according to equation (25). If $E_{h=0}$, is the electrostatic energy corresponding (for the degree of ionization considered), to an end-to-end distance $h = 0$, the relative energy $E/E_{h=0}$, is dependent on h/NA^2 only.

It may be shown,[5] that the first term of the sum does not largely contribute to the total energy of repulsion. It can also[5] be deduced from equation (23) that replacing the summation by integration and integrating from zero (instead of from one) as lower limit gives a negligible error. Hence we may safely replace the summation in equation (24) by integration:

$$E = \frac{\nu^2\epsilon^2}{NDh} \int_0^N \frac{N - k}{k} \phi \left(\sqrt{\frac{3h^2}{2NA^2} \frac{k}{N - k}}\right) dk \tag{25}$$

This expression cannot be solved analytically, but some approximations may be found to the curve at different values of ν. A numerical calculation of E gives the curve shown in Figure 2.

For higher values of h, *i.e.*, for fairly stretched molecules, a good approximation is:[6]

$$E = \frac{\nu^2\epsilon^2}{Dh_\nu}\ln\frac{3h_\nu^2}{2NA^2} \tag{26}$$

A comparison of formula (26) with the corresponding equation (1) of the first approximation shows at once that the energy calculated by the second approximation is much higher: the numerical coefficient has increased from $^1/_4$ to 2 and an additional positive factor:

$$\ln \sqrt{3}\, h_\nu/\sqrt{2} h_{10}$$

is operative. This increase in energy is evidently due to the contribution of the charges distributed over the median parts of the molecule.

IID. Distribution Function According to the Second Approximation

Introducing the value of E into equation (8) we obtain the probability distribution of the values of h for different degrees of ionization. Figure 3 gives a numerical evaluation of the distribution curves for $N = 100$, $A = 10^{-7}$ cm.

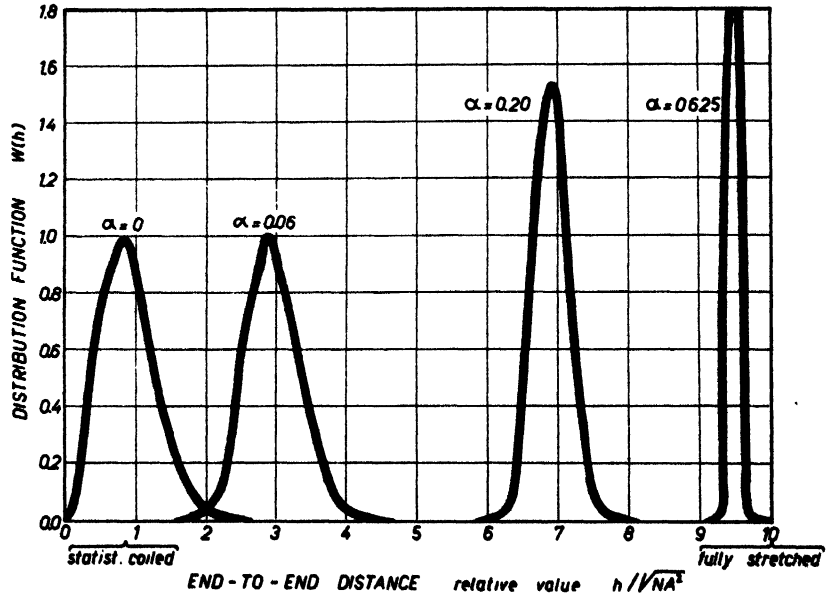

Fig. 3. Distribution function $W(h)$, according to equations (8) and (25) for values of $Z = 400$, $N = 100$, $A = 10^{-7}$ cm. at different values of the degree of dissociation α.

The mean degree of ionization $\alpha = \nu/Z$ increases from left to right. It may be observed that with increasing α, not only the mean and most probable values of h increase, but the form of the distribution curves changes. For higher degrees of ionization the curves are steeper and a larger percentage of the molecules have approximately the same dimensions as the most probable ones. Correspondingly, the difference between the most probable, the mean, and the square root of the mean square values of h, vanishes.

III. THIRD APPROXIMATION, CORRECTION FOR THE FORM OF THE ION DISTRIBUTION

Though the assumption that the charge is evenly distributed (second approximation) is plausible, there are good reasons to doubt its rigorousness. In order to get a clearer idea of the possible deviations from the homogeneous distribution, let us proceed as follows.

(*1*) We consider a coiled molecule having a constant degree of ionization α in all parts of the chain and we calculate the corresponding potential distribution at the different points of the chain (IIIA).

(*2*) Starting from this potential, we recalculate the distribution of the ionization according to the principle of Maxwell-Boltzmann (IIIB).

(*3*) This nonhomogeneous distribution of the degree of ionization α leads to a potential distribution along the chain, which differs from the first approximation mentioned.

The distribution of the ionization α and thus of the corresponding potential is then successively corrected in such a way that the α distribution assumed and the α distribution due to the corresponding potential function coincides as well as possible in all parts of the chain (IIIC).

IIIA. Distribution of the Potential Function of the Ionized Polymeric Molecule

In the first instance we assume the second approximation, *i.e.*, the constancy of the degree of ionization α over all parts of the chain to be true (Fig. 4a). We calculate the potential in the neighborhood of a given segment due to all other charged segments present in the filament.

The potential ψ_i in the *i*-th segment will be evidently given by the following expression:

$$\psi_i = \int_0^i \frac{\nu\epsilon}{ND} \overline{\left(\frac{1}{r_{0,k}}\right)}\, dk + \int_0^{N-i} \frac{\nu\epsilon}{ND} \overline{\left(\frac{1}{r_{0,k}}\right)}\, dk \tag{27}$$

Introducing the value of $(1/r_{0,k})$ from equation (20) we obtain:

$$\psi_i = \frac{\nu\epsilon}{ND}\left[\int_0^i \frac{N}{kh}\,\phi\left(\sqrt{\frac{3h^2}{2NA^2}\,\frac{k}{N-k}}\right) dk + \int_0^{N-i} \frac{N}{kh}\,\phi\left(\frac{3h^2}{2NA^2}\,\frac{k}{N-k}\right)^{1/2} dk\right]$$

Figure 4b shows a numerical evaluation of ψ_i over a chain molecule consisting of 1000 monomers, if the degree of ionization is

$$\alpha = \nu/Z = 0.5$$

(*i.e.*, if half of the carboxyl groups are ionized); and if the molecule is stretched to ten times its original end-to-end distance ($h_\nu/h_{10} = 10$).

It is seen at once that for homogeneous ionization the potential changes rather rapidly when we pass to the ends of the molecule ($i = 1$ and $i = N$). This run of the potential curve is incompatible with the assumption of constant α over the whole molecule as will be shown in the following paragraph.

IIIB. Dependence of the Degree of Ionization on the Potential and Vice Versa

For the sake of simplicity let us divide the large molecule into segments of different degrees of ionization α_i. Let each segment be enclosed in a semipermeable membrane, permeable only to hydrogen ions, in such a way that these can pass freely from one segment to another. In each segment an equilibrium will be established between the ionized and undissociated groups, so that:

$$\frac{\alpha_i a_H}{1 - \alpha_i} = K_i \tag{28}$$

where a_H is the hydrogen ion activity and K_i an equilibrium constant dependent on the nature of the ionizable group and on the potential in its neighborhood.

According to Bjerrum (*Z. phys. Chem.*, 1925)

$$K_i = K_0 e^{-\epsilon\psi_i/kT}$$

where K_0 is a specific constant and ψ_i the potential on the *i*-th segment:

$$\frac{\alpha_i}{1 - \alpha_i} = \frac{K_0}{a_H} e^{-\epsilon\psi_i/kT} \quad \text{or} \quad \alpha_i = \frac{1}{1 + (a_H/K_0)e^{\epsilon\psi_i/kT}} \tag{29}$$

It may be deduced that for approximately equal values of a_H and K_0, α_i will be strongly dependent on ψ_i, and different α_i's will result for different ψ_i's. Now, as shown in the previous paragraph, ψ_i varies with i, hence we should also expect α to change with the segment. Figure 4c shows the variation of the degree of ionization over the molecule assuming the potential distribution of Figure 4b. It is thus seen that the original assumption of the constancy of α is untenable.

IIIC. Form of the α_i Distribution

No simple analytical procedure is available to calculate in a direct way the distribution of the charged groups in the molecule. The procedure adopted by present authors was that of successive approximation: the degree

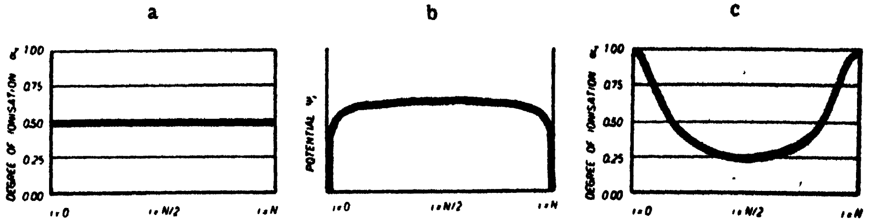

Figure 4

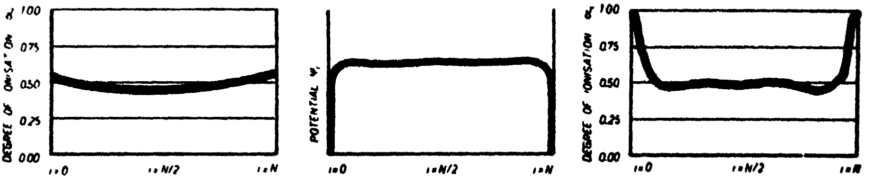

Figure 5

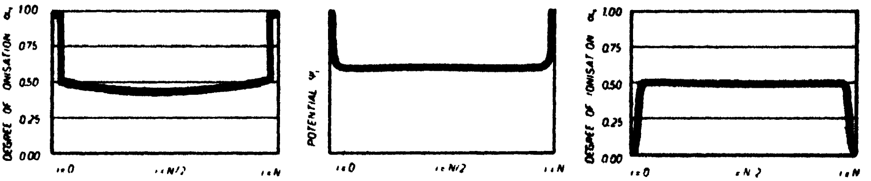

Figure 6

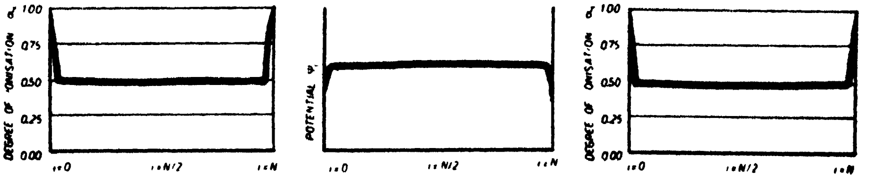

Figure 7

Figs. 4, 5, 6 and 7. (a) Assumed distribution of the electric charges along the filament. (b) Electrostatic potential along the filament, corresponding to charge distribution (a). (c) Distribution of the electric charges along the filament calculated according to the Maxwell-Boltzmann principle (Eq. 29) on the assumption of a potential distribution as shown in (b). Fig. 4a. Assumption of a uniform distribution of the charges over the filament, corresponding to the approximation used in section II. Fig. 5a. Assumption $\alpha_i = 0.478 + 0.180 [(i/N) - 0.5]^2 + 0.625 [(i/N) - 0.5]^4$. Fig. 6a. Assumption of a charge distribution, similar to 5a; 4% of the total charge accumulated at each end of the filament. Fig. 7a. Estimated actual charge distribution over the filament, intermediate between 5a and 6a. Fig. 7c. The charge distribution 7c calculated from the potential distribution 7b is identical with charge distribution 7a, which yields the potential 7b. (Self-consistent distribution of charge and potential.)

of ionization α_i was represented as a series of ascending powers of the form:*

$$\alpha_i = \alpha_0 + \alpha_2\left(\frac{i}{N} - 0.5\right)^2 + \alpha_4\left(\frac{i}{N} - 0.5\right)^4 + \dots \tag{30}$$

By means of equation (30) the potential was calculated from formula (27) suitably corrected for varying α:

$$\psi_i = \frac{\epsilon Z}{DN}\left[\int_0^i \alpha_{i-k}\overline{\left(\frac{1}{r_{0,k}}\right)}\,dk + \int_0^{N-i} \alpha_{i+k}\overline{\left(\frac{1}{r_{0,k}}\right)}\,dk\right] \tag{31}$$

and from the values of the potential thus obtained, α_i was again calculated from equation (29). Whenever the α_i's thus obtained were approximately equal to the original values, it was concluded that the coefficients of the sum (30) were of the right magnitude.

Figures 5 and 6 show the process of approximation. It will be observed that a small deviation from constancy in α_i produces a strong effect on ψ_i and correspondingly in the recalculated values of α_i. The true values of the α_i's obviously lie between the values of Figures 5a and 6a and approximately indicated in Figure 7. The general conclusion of these long calculations is that, in reality, there is a small tendency of the charges to accumulate near the molecular ends as was postulated in the first approximation; but this tendency is not sufficiently pronounced as to distort the picture developed in the second approximation.

Therefore, we believe that though a more rigorous calculation will tend to bring the formulas of part II somewhat near to the simpler formulas of part I, the true values will be much nearer to those obtained on the assumption of homogeneous distribution.

IV. COMPARISON WITH EXPERIMENTS. INFLUENCE OF THE DEGREE OF IONIZATION ON THE VISCOUS BEHAVIOR OF POLYMETHACRYLIC ACID

The results of the previous paragraphs permit the direct evaluation of several measurable quantities such as the viscosity, the double refraction of flow, the angle of orientation in flow, and the depolarization of scattered light in solutions of polyvalent polymeric ions.[4] The detailed experimental data will be presented in other papers. In this paragraph only the viscosity of aqueous solutions of polymethacrylic acid will be discussed.

IVa. Description of Experimental Behavior

Figure 8 represents a series of measurements of η_{sp}/c for a sample of polymethacrylic acid at different concentrations and at various degrees of neutralization with sodium hydroxide. The points corresponding to a given concentration, but to various degrees of ionization, are, for each concentration investigated, united to a curve. An inspection of the figure reveals that, contrary to the course of η_{sp}/c *vs.* c of polymer solutions in organic solvents, in our case η_{sp}/c *increases with decreasing concentration.* Another important fact is the increase of η_{sp}/c with increasing ionization α through addition of alkali. After about 80% neutralization the viscosity starts to decrease because of the influence of free electrolyte in the solution.

---

* This form was adopted for symmetry, reasons: the charge distribution around the center of the molecule ($i/N = 0.5$) must evidently be symmetrical.

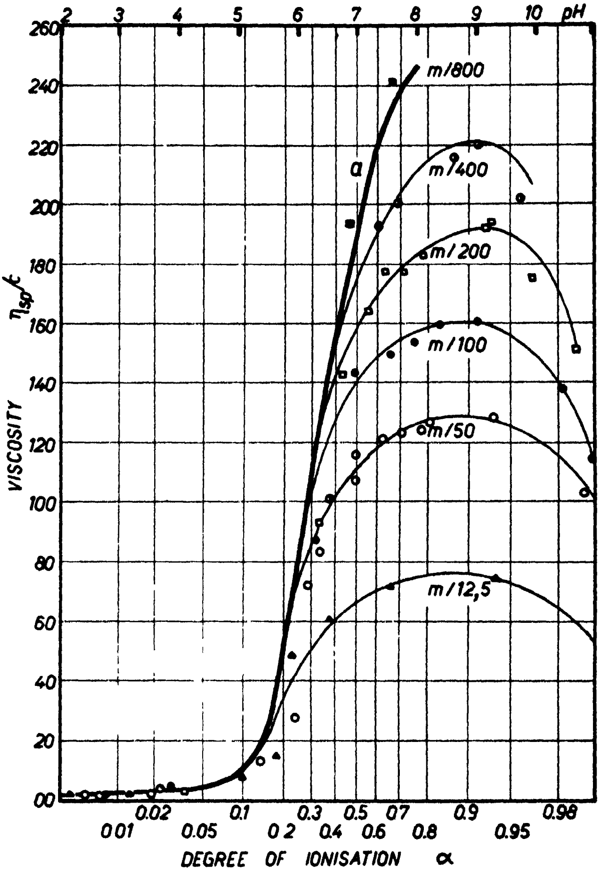

Fig. 8. Polymethacrylic acid in water. Experimental values of η_{sp}/c for different concentrations (mole methacrylic acid per liter), as a function of the degree of ionization α. With increasing dilution there is tendency, at each value of α, toward a limiting value, practically coinciding with curve *a*, calculated from equation (39).

But the most important fact for the further discussion is that at each degree of ionization the values of η_{sp}/c at decreasing concentration reach a limiting *upper* value, which may be identified with the intrinsic viscosity of the polymer at the corresponding degree of ionization. This upper limit is attained earlier by the lower degrees of ionization and only at very high dilutions by the solutions of higher α. We may assume that the limiting values of the intrinsic viscosities at extreme dilution are the values that the solution attains when the molecules display their full interference to hydrodynamic flow and exhibit the maximum degree of stretching, which is possible at the degree of ionization in question. At higher concentrations the influence of the surrounding opposite ions (gegenions) prevents the molecules from stretching to the maximal value possible at the pH in question, and hence the viscosity is lower. As the theoretical treatment presented in this paper is valid only for infinite dilutions, we shall discuss only the curve *a* of intrinsic viscosity in Figure 8.

IVB. Theoretical Formula for the Influence of α on the Intrinsic Viscosity

As shown by Kuhn and Kuhn, the intrinsic viscosity of a solution is given by the following expression:[7]

$$[\eta] = \frac{b\overline{h^2}}{48}\,\frac{N_L}{10^3}\,\frac{1}{-0.05 + 0.12\log_{10}\overline{h^2}/d_h bZ + 0.037\sqrt{(b^2Z^2)/h^2}} \tag{32}$$

where N_L is the Avogadro number, b the length of the monomeric unit projected on the molecular axis, $\overline{h^2}$ the quadratic mean of the end-to-end distance of the dissolved polymer, Z the degree of polymerization, and d_h the thickness of the chain. The last factor on the right-hand side of equation (32) takes account of the fact that, especially for high degrees of coiling, a part of the solvent is immobilized inside the coil.

The determination of the viscosity of an ionized polymer is thus largely equivalent to the determination of $\overline{h^2}$ at each degree of ionization. As shown above, the probability of finding a molecule of end-to-end distance h, which carries ν ionized groups, is given by equation (8), where E is the electrostatic energy discussed and determined in paragraphs II and III. According to the results obtained in section III, expression (25), corresponding to a uniform distribution of the electric charge over the filament, can be considered as a satisfactory approximation for all degrees of ionization. (For the actual evaluation, see Figure 2 and equation (26), the latter as an approximation for high values of h.)

Introducing these values for E in equation (8) it is easy to determine the mean square end-to-end distance from the equation:

$$\overline{h^2} = \frac{\int_0^\infty W(h)h^2\,dh}{\int_0^\infty W(h)\,dh} \tag{33}$$

For a considerable degree of ionization and correspondingly high values of h, the square of the most probable value of h can be used instead of $\overline{h^2}$; namely, we have shown above (see especially Figure 3) that the probability curve grows sharp with increasing ionization, an effect which reduces the difference between $\overline{h^2}$ and the square of the most probable value of h.

For fairly stretched molecules (for which this is true), we may at the same time use approximation (26). From equation (8) we obtain for the most probable value of h the following equation:

$$\frac{\partial \ln W(h)}{\partial h} = -\frac{\beta}{A} - \frac{1}{kT}\frac{\partial E}{\partial h} + \frac{2}{h} = 0 \tag{34}$$

The value of β is very well approximated by the formula:

$$\beta = \frac{3h}{NA}\left[1 + \frac{0.6(h/NA)^2}{1 - (h/NA)^2}\right] \tag{35}$$

which passes for $h \ll NA$ into the well-known expression $\beta = 3h/NA$. Introducing the value (26) for E, we obtain:

$$\frac{1}{kT}\frac{\partial E}{\partial h} = -\frac{\nu^2\epsilon^2}{DkTh^2}\left[\ln\frac{3h^2}{2NA^2} - 2\right] \tag{36}$$

We now introduce numerical values $\epsilon = 4.77 \times 10^{-10}$ e.s.u.; $D = 80$; $T = 293°$K., and $k = 1.38 \times 10^{-16}$ erg/degree. As h is fairly large, $2/h$ may be neglected in comparison with other terms of equation (34). Substituting αZ for ν (α is the degree of ionization and Z the degree of polymerization), we obtain from equations (34), (35), and (36):

$$\frac{3h}{NA^2}\left[1 + \frac{0.6(h/NA)^2}{1 - (h/NA)^2}\right] = \left\{7 \times 10^{-8}\text{ cm.}\right\}\frac{\alpha^2Z^2}{h^2}\left[\ln\frac{3h^2}{2NA^2} - 2\right] \tag{37}$$

Determining $\overline{h^2}$ from equation (33) or, for considerable values of α, the most probable value of h from equation (37) and introducing this value into the expression (32) for the intrinsic viscosity, we obtain the intrinsic viscosity as a function of the degree of ionization α. This curve is shown[8] together with an experimental curve. The close agreement between the theoretical and experimental curves is a strong support of the theory developed above.

A further simplification of the expressions is obtained if the last factor on the right-hand side of equation (32), which takes account of the partial immobilization of the solvent inside the coil, is substituted by a constant of value $3\pi/2$; this corresponds to neglecting the immobilization of the solvent inside the coil, a simplification that is justified in practice if the degree of polymerization is not too high or if the stretching of the coil by electrostatic action of the charges is considerable. In this case, equation (32) reduces to:

$$[\eta] = \frac{\pi b\overline{h^2}}{32}\frac{N_L}{10^3} \tag{38}$$

The intrinsic viscosity is in this case *exclusively* determined by $\overline{h^2}$.

Substituting for h in equation (37) the intrinsic viscosity from equation (38), denoting now by $[\eta]_\alpha$ the intrinsic viscosity at degree of ionization α and by

$$[\eta]_0 = (\pi bNA^2/32)(N_2/10^3)$$

that of the undissociated solution, and introducing the value $b = 2.5 \times 10^{-8}$ cm., corresponding to polymethacrylic acid, we obtain:

$$\frac{[\eta]_\alpha^{1/3}}{[\eta]_0} \cdot \frac{1 + \dfrac{0.6}{N}\dfrac{[\eta]_\alpha}{[\eta]_0}\dfrac{1}{1 - \dfrac{1}{N}\dfrac{[\eta]_\alpha}{[\eta]_0}}}{\ln \dfrac{3}{2}\dfrac{[\eta]_\alpha}{[\eta]_0} - 2} = 2.9 \times 10^{-2}\alpha^2 Z^2 \qquad (39)$$

By means of the last formula, using the experimental value $[\eta]_0 = 1.55$ and choosing appropriate values for Z and N (380 and 200, resp.), a simplified theoretical curve for the intrinsic viscosities was calculated and is drawn as the limiting curve *a* in Figure 8.

It is seen that this curve follows closely the experimental data. The agreement proves that even the simplified formula may be of use, at least as a rough approximation.

References

1. For a short exposition of some of these considerations see W. Kuhn, O. Künzle, and A. Katchalsky, "Dénouement de molécules en chaînes polyvalentes par des charges électriques en solution," paper read at the Colloque sur la chimie et la physique des très grosses molécules, Liège, April 7, 1948. *Bull. soc. chim. Belges*, **57**, 421 (1948). For similar considerations by J. J. Hermans and J. T. G. Overbeek (paper presented at the same symposium) see *Bull. soc. chim. Belges*, **57**, 154 (1948). For a more detailed representation of some of the main parts of the following consideration and the corresponding calculations see W. Kuhn, O. Künzle, and A. Katchalsky, *Helv. chim. acta*, **31**, 1994 (1948).
2. W. Kuhn and F. Grün, J. Polymer Sci., **1**, 183 (1946).
3. W. Kuhn and F. Grün, *Kolloid Z.*, **101**, 248 (1942); see also reference 4, page 2004.
4. W. Kuhn, O. Künzle, and A. Katchalsky, *Helv. chim. Acta*, **31**, 1994 (1948).
5. See reference 4, page 2007.
6. For a somewhat better, but not so simple, approximation see reference 4, page 2010.
7. W. Kuhn and H. Kuhn, *Helv. chim. acta*, **30**, 1233 (1947); **26**, 1394 (1943); **28**, 1533 (1945); **29**, 71 (1946). H. Kuhn, *Habilitation Thesis*, Basle, 1946; see also reference 4.
8. See reference 4, page 2024, Figure 6, curve 2.

English Synopsis, see Summaries, page S8, Vol. V, 1950.

Résumé

L'addition d'alcali à une solution diluée d'acide polyméthacrylique produit une forte augmentation de la viscosité intrinsèque, de cent trente fois par exemple, si 50% des groupes COOH— sont neutralisés (dans un échantillon particulier). Ce phénomène, de même que d'autres phénomènes connexes en biréfringence d'écoulement, peuvent s'interpréter comme un déroulement partiel ou complet du filament, produit par l'effet électrostatique qui accompagne le passage d'une molécule neutre à un ion polyvalent. En première approximation l'énergie électrostatique du filament a été considerée comme une fonction de la distance *h* des extrémités du filament et du degré d'ionisation *α*. En seconde approximation, on suppose une distribution uniforme des charges électriques le long de l'ion polyvalent. Une considération ultérieure montre que cette hypothèse est quelque peu inexacte, par suite d'une certaine concentration des charges au voisinage des extrémites des filaments; toutefois, cet effet laisse inchangé le résultat obtenu en seconde

approximation, concernant l'énergie du système. Par l'utilisation de cette détermination de l'énergie électrostatique, comme une fonction de *h* et de α, et par l'utilisation du principe de Maxwell-Boltzmann, la fonction de distribution (en ce qui concerne *h* et donc le déroulement partiel du filament) est déterminé en fonction du degré d'ionisation α. En introduisant la valeur moyenne de *h*, ainsi accessible, dans les formules qui expriment la viscosité intrinsèque en fonction de *h*, on obtient des expressions de la viscosité en fonction de α. Une approximation comparativement simple de cette fonction peut être développée. La dépendance de la viscosité intrinsèque en fonction de α concorde de façon satisfaisante avec les valeurs expérimentales des viscosités de l'acide polyméthacrylique, neutralisé par l'addition progressive de quantités d'alcali.

Zusammenfassung

Zugabe von Alkali zu einer verdünnten Lösung von Polymethacrylsäure bewirkt eine starke Zunahme der Grenzviskosität, z.B. um einem Faktor 130, wenn 50% der COOH Gruppen (eines bestimmten Produktes) neutralisiert werden. Dieses Phänomen, wie auch ähnliche Effekte bei der Strömungsdoppelbrechung können als teilweises oder vollständiges Aufrollen der Kette gedeutet werden. Die Aufvollung wird durch die elektrostatischen Kräfte hervorgerufen, welche auftreten wenn wir vom neutralen Molekül zum polyvalenten Ion übergehen. Um diese Entknäuelung zu beschreiben, wird zuerst in grober Näherung, dann in einer besseren zweiten Näherung, die elektrostatische Energie des auf dem Ionisationsgrade α befindlichen Fadens in Abhängigkeit vom Abstande *h*, in welchem sich die Fadenenden voneinander befinden, berechnet. Bei dieser zweiten Näherung wird eine gleichmässige Verteilung der elektrischen Ladungen über das polyvalente Ion vorausgesetzt. Eine zusätzliche Betrachtung zeigt, dass diese Voraussetzung nicht ganz exakt ist, in Folge einer gewissen Konzentrierung der Ladungen an den Kettenenden; es wird jedoch gezeigt, dass diese Tatsache die in der zweiten Näherung erhaltenen Resultate in Bezug auf die Energie des Systems praktisch unverändert lässt. Mittels dieser Bestimung der elektrostatischen Energie als Funktion von *h* und α und durch Benutzung des Maxwell-Boltzmann Prinzips wird die Verteilungsfunktion in Bezug auf *h* und dadurch das teilweise Aufrollen der Kette in Abhängigkeit vom Ionisierungsgrade α gefunden. Setzt man den so erhaltenen Mittelwert für *h* in die Formeln ein, welche die Grenzviskosität als Funktion von *h* angeben, so erhält man die Viskosität als Funktion von α. Eine rohe aber verhältnismässig einfache Näherung für diese Funktion kann angegeben werden. Die so erhaltene Abhängigkeit der Grenzviskosität von α steht in zufriedenstellender Ubereinstimmung mit den Viskositätswerten welche bei schrittweiser Neutralisation von Polymethacrylsäure mit Alkali beobachtet werden.

Received May 3, 1949

JOURNAL OF POLYMER SCIENCE VOL. V, NO. 3, PAGES 301-306

Potassium Ferricyanide–Diazothio Ether–Mercaptan Recipe for Emulsion Polymerization of Butadiene and Styrene. II. Effect of Some Chemical Variables*

I. M. KOLTHOFF and W. J. DALE, *School of Chemistry, University of Minnesota, Minneapolis, Minnesota*

In the first paper of this series,[1] suitable recipes have been given for polymerizations at 40° and at ice temperatures. In the present study, further observations on the effect of several chemical variables in the recipe are reported. A method of determination of MDN (*p*-methoxyphenyldiazothio (2-naphthyl) ether) in solution and in latex will be described in a subsequent paper.

EXPERIMENTAL

The reagents used and the methods of polymerization by the diazothio ether recipes have been described earlier.[1] Unless stated otherwise, the diazothio ether used was *p*-methoxyphenyldiazothio (2-naphthyl) ether (MDN).

Effect of MDN Added to Latices at Various Conversions

The time–conversion curve of the ferricyanide–MDN–mercaptan recipe has a peculiar shape; at 40° the conversion is 26% after one hour, 49% after 6 hours, and 81% after 10 hours. This is characteristic of practically all the MDN recipes, independent of the kind of mercaptan used and of the amount of soap present.

It seemed likely that most of the MDN disappears during the early stages of conversion. It was therefore of interest to see whether MDN would accelerate the conversion of a "neutral" ferricyanide recipe, when the polymerization was begun in the absence of MDN. The neutral ferricyanide recipe used employs 0.3% $K_3Fe(CN)_6$, 0.5% *n*-dodecyl mercaptan (*n*-DDM), 5.0% S. F. flakes, and 180% water (based on unit weight of monomers). *n*-Dodecyl mercaptan was used instead of the tertiary compound (Sulfole B8), because the latter gives a very poor rate of

---

* This investigation was carried out under the sponsorship of the Office of Rubber Reserve, Reconstruction Finance Corporation, in connection with the U. S. Government Synthetic Rubber Program.

polymerization with ferricyanide as activator in the absence of MDN. At conversions of 20 and 40%, 0.2% MDN in 0.2 ml. benzene was injected into the latices and the polymerizations were continued at 40°C. The data are shown in Table I.

TABLE I

EFFECT OF MDN ADDED TO THE NEUTRAL FERRICYANIDE–DDM RECIPE AT 20 AND 40% CONVERSION. $T = 40$°C.

Treatment	Total time, hrs.	Conversion, %
A. INJECTED AFTER 5 HOURS, CONVERSION = 20%		
Not injected (control)	5	20
	7	33
	9	38
Injected after 5 hours	7	76
	9	85
B. INJECTED AFTER 8 HOURS, CONVERSION = 39%		
Not injected (control)	8	39
	10	47
	12	57
Injected after 8 hours	10	79
	12	87

It is evident that at 20 and 40% conversion, the addition of MDN greatly increases the rate of conversion. At 40% conversion there are no free soap micelles in the latex; thus the accelerating effect of MDN in the various ferricyanide recipes occurs during the various stages of conversion independent of whether the soap micelles or the polymer particles are the loci of the polymerization.

Effect of Varying Amounts of Soap

It was found in this laboratory that the rate of polymerization in the mutual recipe (in which potassium persulfate is the activator) during the early stages of conversion is roughly proportional to the amount of soap used. Hence, it was of interest to investigate whether the initially rapid rate of conversion in the MDN recipes could be conveniently reduced by using less soap in the recipe. The data obtained with 1, $^1/_2$, and $^1/_4$ of the mututal recipe amount of soap are plotted in Figure 1. ("1" soap denotes 5 parts of soap per 100 parts of monomers.)

It is seen that the initial rate of polymerization decreases with decreasing amounts of soap. However, with the different amounts of soap used, there is a flat portion in the time–conversion curve after a faster initial rate. The flat portion may be caused by the autodecomposition of the MDN, possibly to thio β-naphthol, which is consumed slowly by the latex. After the decomposition products have disappeared, the rate increases considerably. This interpretation needs further investigation.

At 30°, the flat portion of the curve is much more pronounced. From

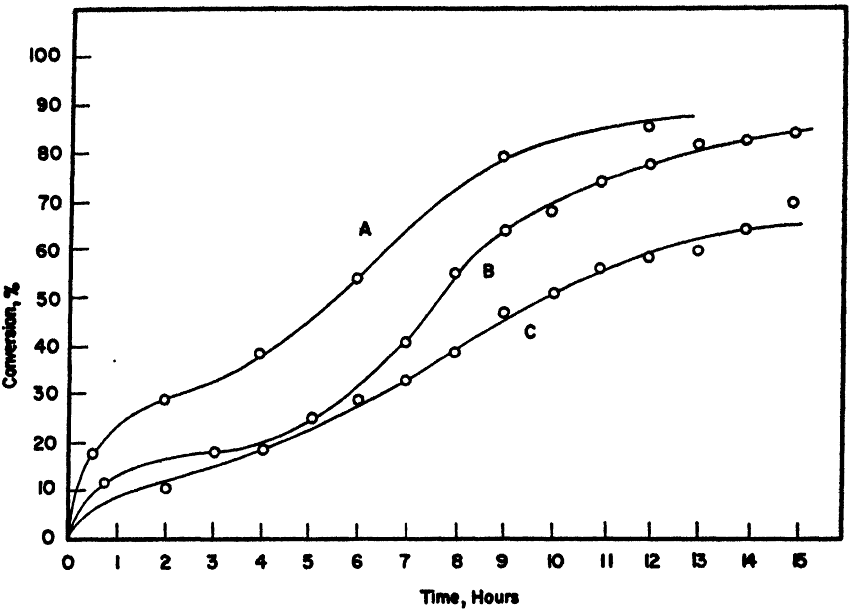

Fig. 1. Effect of varying amounts of soap on rate of conversion. A = 1; B = 1/2; C = 1/4 soap. (1 soap = 5 parts soap per 100 parts monomers.)

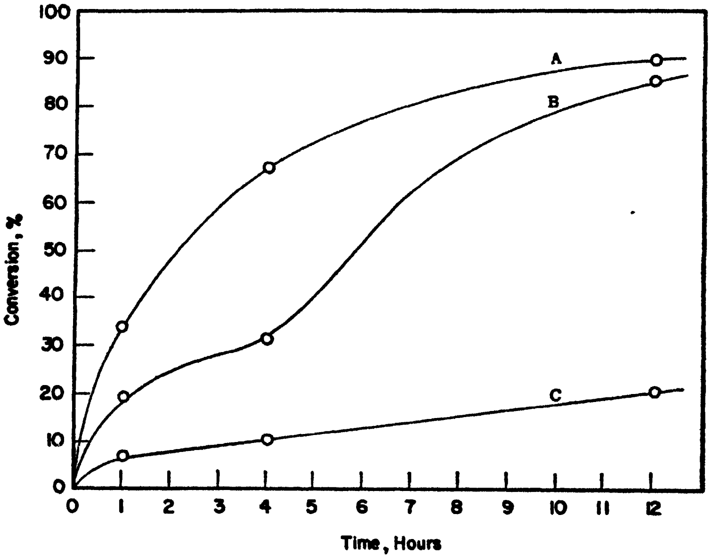

Fig. 2. Effect of *tert*-C_{12} mercaptan concentration in the ferricyanide-MDN-mercaptan recipe at 40 °C. A = 2 RSH; B = 1 RSH; C = 1/4 RSH. (1 RSH = 0.35%.)

a practical viewpoint, the use of less than five parts of soap in the ferricyanide-MDN-mercaptan recipes is undesirable because gel is formed at lower conversions with lesser amounts of soap.

Effect of Mercaptan Concentration

In the standard recipe for the preparation of GR-S with persulfate as the activator, the conversion rate is practically independent of the mercaptan concentration when the latter is varied between wide limits. In the present recipe, the rate increases greatly with the concentration of mercaptan as is evidenced from Figure 2. The rate of initiation of polymerization is probably proportional to the rate of production of mercapto radicals, which, it appears, depends on the rate of interaction of diazothio ether and mercaptan.

Experiments with Various Emulsifiers

Experiments were carried out in which various detergents, emulsifiers, and emulsion stabilizers other than S. F. flakes, were used. The results obtained with a few of these agents are shown in Figure 3. When an equal weight of Daxad 11 was substituted for the S. F. flakes in the ferricyanide–MDN–mercaptan recipe, the amount of conversion after 23 hours at 40° was only 1.5%. (Daxad 11 is the sodium salt of a condensed alkyl aryl sulfonic acid, Dewey and Almy Chemical Company.) In this recipe, the Daxad is apparently a stabilizer but not a solubilizer.

The rates of conversion obtained with 5.0 parts of Aerosol AY are given in Figure 3, and, for comparison, the curve obtained with 5.0 parts of S. F. flakes is also plotted.

A sample of sodium di-*tert*-butylnaphthalene sulfonate was obtained from the University of Illinois. The conversions obtained with 5 parts of this soap in the ferricyanide–MDN–mercaptan recipe are also shown in the figure. Reasonable conversions are obtained with both Aerosol AY and the naphthalene sulfonate, which do not have an alkaline reaction like the fatty acid soaps. It will be of interest to investigate the effect of varying *p*H by means of suitable buffers, using various alkyl and aryl sulfonates as emulsifiers.

Use of Other Diazothio Ethers in the Neutral Ferricyanide–Sulfole Recipe

A few experiments were carried out in which diazothio ethers other than MDN were used in the neutral ferricyanide–Sulfole recipe. The following were received from Prof. W. B. Reynolds: *p*-chlorophenyl diazothio-(2-naphthyl)-ether, *p*-methylphenyl diazothio-(2-naphthyl)-ether, and the coupling products of diazotized sulfanilic acid with thio *p*-cresol and thio *β*-naphthol. In each case the temperature was 40°, with S. F. flakes as the emulsifying agent and with 0.35% Sulfole B8 in the recipe. With each of the diazothio ethers used, a translucent latex was obtained similar to that described earlier.[1]

With 0.2 part of diazothio ether in each recipe, none gave as much conversion in 12 hours as did MDN. The conversions are plotted in Figure 4. It is of interest to note that a fluent curve without discontinuity was ob-

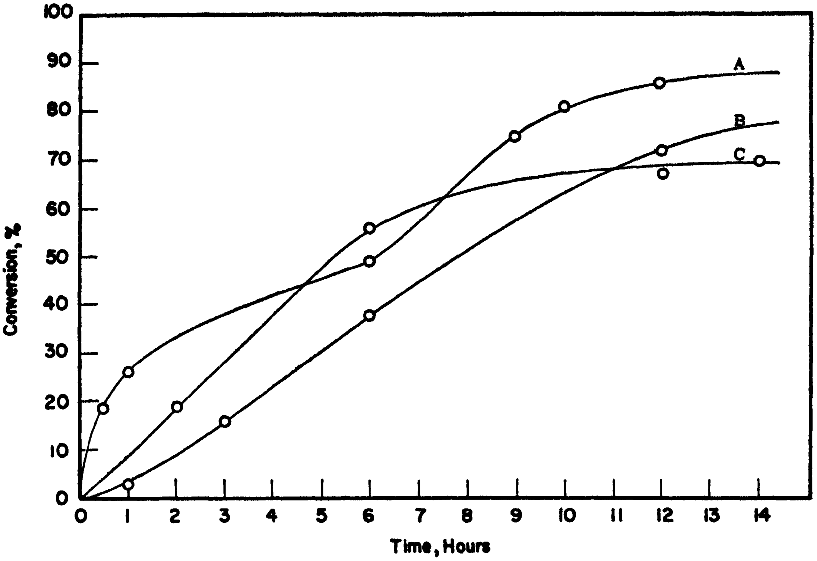

Fig. 3. Various detergents in the ferricyanide-MDN-mercaptan recipe at 40°C. A = S. F. flakes; B = aerosol AY; C = di-*tert*-butylnaphthalene sulfonate (Na salt).

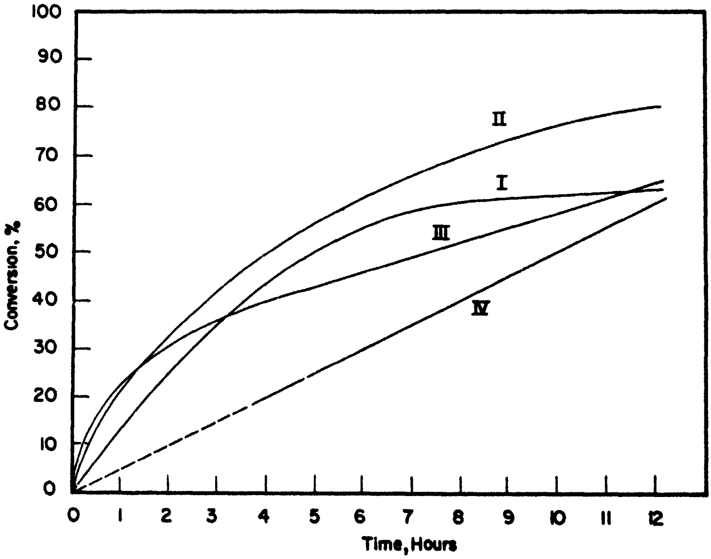

Fig. 4. Effect of various diazothio ethers at 40°C. Coupling products of diazotized: I, *p*-chloroaniline + thio β-naphthol; II, *p*-anisidine + thio β-naphthol; III, sulfanilic acid + thio *p*-cresol; IV, sulfanilic acid + thio β-naphthol.

served with the coupling product of *p*-anisidine and thio β-naphthol. (Compare curve II of Figure 4 with curve A in Figure 1.) From intrinsic viscosity data it was concluded that no matter which diazothio ether was used, the viscosities of the polymers were practically the same at any given conversion.

Other diazothio ethers should be investigated in this recipe. Professor Reynolds reports that the various types of diazothio ethers have distinctive properties when used in greater concentrations to promote and regulate the polymerization in the absence of other activators.[2]

References

1. I. M. Kolthoff and W. J. Dale, J. Polymer Sci., 3, 400 (1948).
2. W. B. Reynolds, private communication.

English Synopsis, see Summaries, page S6, Vol. V, issue 1.

Résumé

L'addition de MDN aux latex, présentant des conversions diverses, et préparés au moyen d'un recette ferricyanure-*n*-DDM, augmente la vitesse ultérieure de polymérisation. L'effet de différentes quantités de savons d'acides gras sur la courbe redement/temps au cours de la préparation au moyen du système MDN–ferricyanure–*t*-dodécylmercaptan est indiqué. La vitesse de conversion, trouvée avec le système MDN–ferricyanure, décroît considérablement avec des quantités décroissantes de mercaptan. L'emploi d'Aérosol AY et de di-*t*-butylnaphthalène sulfonate au lieu de savon d'acides gras entrainent des vitesses de conversions satisfaisantes. De nombreaux diazothioéthers ont été essayés en remplacement du MDN dans la préparation. Le *p*-méthyl-phényl-diazothio-(2-naphthyl)-éther donne des courbes conversion en fonction du temps très intéressantes.

Zusammenfassung

Zugabe von MDN zu Latex von verschiedenem Umsatz, hergestellt nach der Ferricyanid–*n*-DDM Vorschrift, erhöht stark die weitere Polymerisationsgeschwindigkeit. Die Wirkung von verschiedenen Mengen von Fettsäureseifen in der MDN–Ferricyanid–*t*-dodecyl-Merkaptan Vorschrift auf die Zeit–Umsatz-Kurve ist angegeben. Die mit der MDN–Ferricyanid Vorschrift gefundene Umsatzgeschwindigkeit nimmt mit abenhmenden Mengen von Merkaptan stark ab. Wenn man in der Vorschrift Aerosol AY, beziehungsweise di-*t*-Butylnaphthalinsulfonat anstatt Fettsäureseifen benutzt werden zufriedenstellende Umsatzgeschwindigkeiten fegunden. Verschiedene Diazo thioäther als Ersatz für MDN in der Vorschrift wurden untersucht. *p*-Methyl-phenyl-diazothio-(2-naphthyl)-äther ergibt eine hübsche Zeit–Umsatz-Kurve.

Received April 8, 1949

JOURNAL OF POLYMER SCIENCE VOL. V, NO. 3, PAGES 307-332

Influence of Structure of Elastomers on Their Permeability to Gases*

G. J. VAN AMERONGEN, *Rubber Foundation, Delft, The Netherlands*

INTRODUCTION

It is a known fact[1-6] that rubber membranes are permeable to gases and that the rate of permeation is a specific of a given gas and rubber. We may picture this permeation of gas through rubber as a process in which gas molecules dissolve on one side of the membrane, then diffuse through the rubber to the other side and there evaporate out of the membrane. Thus the process of permeation is divided into several independent processes, those of solution and evaporation being governed by Henry's law and that of diffusion by the diffusion equation (Fick's law).

The problem to be considered is why a given rubber should possess a given permeability to a given gas. It will at once be evident from what has just been stated that, while studying the problem, the process of solution (or evaporation) and that of diffusion must be dealt with separately. It was shown in earlier investigations[4,7] upon a series of rubber varieties and gases how the chemical structure of the rubber molecules affects the rate at which the gas passes through, and, notably, that the introduction of methyl and polar groups in the polymer molecules and crystallization reduce this rate of diffusion. It was also found that a gas diffuses more slowly as its molecules are larger. The solubility of the gas in the rubber is determined by its tendency to condense and the interaction between the rubber and the gas molecules.

These views will now be put to the test with reference to another series of rubbers and gases. We shall also see that knowledge of the necessary conditions for low permeability may help to evolve new kinds of rubber of low permeability.

PROCEDURE

The apparatus and methods employed for the determination of permeability, diffusivity, and solubility have already been described.[4]

The permeability is derived from the increased pressure in an evacuated space separated from a gas chamber by the membrane under test. The pressure increase is registered by a MacLeod pressure gage now set to a range up to 1.5 mm. Hg with an accuracy of 0.001 mm. Hg. This pressure gage ensures considerably greater relative accuracy of measurement than was formerly obtainable.

---

* Communication No. 99 from the Rubber Foundation, Delft, The Netherlands.

The permeation coefficient, or permeability Q, follows from:

$$q = QAt(p_1 - p_2)/d \tag{1}$$

where q = quantity of permeated gas, A = area of the membrane, p_1 and p_2 = pressures on both sides of the membrane, d = thickness of the membrane, and t = time. The quantity of permeated gas follows quite simply from the pressure increase, the volume, and the temperature of the space under vacuum. The p_1 pressure commonly amounted to approximately 1 atmosphere. The p_2 pressure, which was always less than 1.5 mm. Hg, can be disregarded with respect to p_1. The thickness of the membrane was determined with a Schopper thixometer to within an accuracy of 0.005 to 0.01 mm. As a rule, the determination of the thickness of the membrane is the least accurate part of the permeation test. Besides that, it is very difficult to make membranes of uniform thickness at every point.

The area of the membrane was assumed to be the same as that of the cross-section of the gas chamber, *i.e.*, 30.2 sq. cm. Some slight inaccuracy is here involved owing to edge effects and the presence of a supporting wire netting. For any measurements made at other than room temperature the dimensions of the membrane were corrected to allow for thermal expansion. The absolute determination of Q is accurate to within 5%, while the relative accuracy of measurements performed with one and the same membrane at different temperatures or with different gases is within 1%.

The diffusion coefficient, or diffusivity D, is derived from:

$$D = d^2/6\theta \tag{2}$$

where θ is the time lag of the permeation. This lag is related to the time required by the gas to establish a state of equilibrium in the degassed membrane. The time lag is found by extrapolating the pressure increase–time curve to the zero axis after the stationary state has been attained. It can be shown[4] that the stationary stage is reached after a period amounting to three times the time lag, so extrapolation to the zero axis should only be made from measurements taken after that time.

The absolute accuracy of the diffusion coefficient is, again, subject to the accuracy of the measurement of the thickness of the membrane; its relative accuracy is within 1%.

Finally, the solubility, S, follows from:

$$Q = DS \tag{3}$$

Previous investigations[4] have shown that the solubility found by the application of equation (3) is consistent with the values found by direct measurement.

In the following pages Q will be expressed as cubic centimeters of gas at 0°C. and 760 mm. pressure penetrating per second through a membrane with an area of 1 sq. cm. and a thickness of 1 cm. at 1 atm. pressure difference; *D* will be expressed in square centimeters per second and *S* in cubic centimeters of gas at 0 °C. and 760 mm. pressure which are dissolved in 1 cc. of material at a pressure of one atmosphere.

TABLE I

COMPOSITION OF THE MEMBRANES

Membranes	% N	Mixtures
Natural rubber	—	A
Methyl rubber, dimethylbutadiene bulk polymer	—	A
Polyisoprene, emulsion polymer	—	A
74% isoprene + 26% acrylonitrile emulsion copolymer	7.0	A
74% isoprene + 26% methacrylonitrile emulsion copolymer	5.3	B
Polybutadiene, emulsion polymer	—	A
Perbunan 18, 80% butadiene + 20% acrylonitrile copolymer	5.4	C
Perbunan (German), 73% butadiene + 27% acrylonitrile copolymer	7.2	A
Hycar OR 25, 68% butadiene + 32% acrylonitrile copolymer	8.4	C
Hycar OR 15, 61% butadiene + 39% acrylonitrile copolymer	10.2	C
Butyl rubber, 98% isobutene + 2% isoprene copolymer	—	D
Polymethylpentadiene, 85% 2-methyl- + 15% 4-methyl-1,3-pentadiene copolymer[8]	—	E
Vulcaprene A, polyesteramide-diisocyanate	—	F

Mixtures	A	B	C	D	E	F
Rubber	100	100	100	100	100	100
Zinc oxide	5	10	5	3	5	—
Sulfur	1.5	2	1.25	2	1.75	—
Stearic acid	2	1	1.5	1	1	1
Vulkakite AZ	1.8	—	—	—	—	—
Captax	—	—	—	0.5	—	—
Tuads	—	—	—	1	—	—
Altax	—	—	1.25	—	1	—
Vulcakite P	1.5	—	—	—	—	—
Phenyl-β-naphthylamine	1	1	1.5	—	—	—
Vulcafor VHM	—	—	—	—	—	5
Vulcafor VDC	—	—	—	—	—	0.75
Vulcanization temperature, °C.	142	110	152	155	145	125
Vulcanization time, min.	30	30	35	45	30	60

MEASUREMENTS

We used membranes of vulcanized rubber of the composition shown in Table I. The majority of the polymers mentioned in this table are commercial products, only polyisoprene, polybutadiene, and isoprene copolymers being specially made by emulsion polymerization* for the permeability test. The combined sulfur content of the vulcanized natural rubber was 1.4%. German Perbunan is the equivalent of American Perbunan

---

* Acknowledgments are due to Dr. W. Gaade and Dr. G. Salomon for their kindness in effecting these polymerizations for this purpose.

TABLE II. PERMEABILITY Q (IN 10^{-8} CM.^{2} SEC.$^{-1}$ ATM.$^{-1}$), DIFFUSIVITY D

No.	Rubber	Temp., °C.		H_2			N_2			O_2	
			Q	D	S	Q	D	S	Q	D	S
1	Natural rubber	25	37.4	10.2	0.037	6.12	1.10	0.055	17.7	1.58	0.112
		50	90.8	22.2	0.041	19.4	3.42	0.057	47.0	4.70	0.10
2	Methyl rubber	25	13	3.9	0.033	0.36	0.079	0.046	1.6	0.14	0.114
		50	38	10.5	0.036	2.2	0.41	0.054	7.1	0.61	0.116
3	Polyisoprene	25	37.9	10.03	0.038	5.37	0.94	0.057			
		50	89.0	—	—	17.0	2.53	0.067			
4	Isoprene-acrylonitrile copolymer	25	5.66	2.47	0.023	0.138	0.045	0.031	0.65	0.092	0.071
		50	18.5	6.50	0.029	0.99	0.30	0.033	3.43	0.45	0.076
5	Isoprene-methacrylonitrile copolymer	25	10.36	3.55	0.029	0.455	0.123	0.037	1.79	0.24	0.075
		50	30.0	8.74	0.034	2 43	0.56	0.043	7.52	0.83	0.091
6	Polybutadiene	25	32	9.6	0.033	4.9	1.1	0.045	14.5	1.5	0.097
		50	77	18	0.043	14.5	2.9	0.050	36	3.7	0.097
7	Perbunan 18	25	19.2	6.43	0.030	1.92	0.51	0.038	6.23	0.79	0.078
		50	49.1	14.5	0.034	7.00	1.55	0.045	19.1	2.30	0.083
8	Perbunan (German)	25	12.1	4.50	0.027	0.81	0.25	0.032	2.94	0.43	0.068
		50	33.7	11.1	0.030	3.58	0.98	0.037	10.5	1.44	0.073
9	Hycar OR 25	25	8.97	3.85	0.023	0.46	0.152	0.030	1.78	0.28	0.064
		50	26.3	9.60	0.027	2.30	0.70	0.033	7.08	1.08	0.066
10	Hycar OR 15	25	5.42	2.43	0.022	0.179	0.064	0.028	0.73	0.136	0.054
		50	17.0	6.56	0.026	1.08	0.34	0.032	3.50	0.565	0.062
11	Butyl rubber	25	5.50	1.52	0.036	0.247	0.045	0.055	0.99	0.081	0.122
		50	17.2	4.38	0.039	1.27	0.22	0.057	4.03	0.384	0.105
12	Polymethylpentadiene	25	32 4	—	—	2.09	0.30	0.070	7.62	0.55	0.138
		50	82.1	—	—	9.04	1 28	0.071	25.9	1.98	0.131
13	Vulcaprene A	25	4.78	2 60	0.018	0.373	0.145	0.026	1.15	0.24	0.048
		50	15.6	7.0	0.022	1.83	0.67	0.027	4.79	0.92	0.052

26. The thickness of the membranes varied from 0.2 to 2 mm., so for every diffusion process we were able to use a membrane giving a properly measurable time lag. This time lag should, by preference, be something between five and forty minutes. The gases used were commercial products taken from cylinders. (The helium gas came from Philips Co. and was generously placed at our disposal by the Kamerlingh Onnes Laboratory of Leyden.)

The experiments were first carried out at 25° and 50°C.; the results are given in Table II. The figures for butadiene rubber and methyl rubber had been estimated on a previous occasion[4] and have been given here for comparison only. Natural rubber and German Perbunan, which had also been studied before, were now retested under the more refined conditions. Generally speaking, the consistency between the present evidence and that coming from other sources is satisfactory.[2,5]

(IN 10^{-6} CM.^{2} SEC.$^{-1}$), AND SOLUBILITY S (IN CC. (N.T.P.) PER CC. AT 1 ATM.)

	CO_2			He			C_2H_2			Cyclopropane		
No.	*Q*	*D*	*S*	*Q*	*D*	*S*	*Q*	*D*	*S*	*Q*	*D*	*S*
1	99.6	1.10	0.90	23.7	21.6	0.011	75.5	0.467	1.62	192	0.180	10.7
	221	3.50	0.63	52.3	38.0	0.014	195	1.63	1.20	473	0.72	6.6
2	5.7	0.063	0.91	11								
	24	0.36	0.67	27								
4	3.3	0.031	1.07	5.93	8.01	0.0074						
	16.9	0.203	0.83	16.1	15.1	0.0107						
5	10.8	0.091	1.20									
	40.4	0.444	0.91									
6	105	1.05	1.00									
	200	2.8	0.72									
7	48.2	0.425	1.13	12.9	15.5	0.0083						
	120.8	1.42	0.85	31.2	26.6	0.0117						
8	23.5	0.190	1.24	9.32	11.7	0.0080	18.9	0.0764	2.48			
	67.9	0.77	0.88	23.4	23.0	0.0102	68.3	0.382	1.79	59.3	0.141	4.2
9	14.1	0.107	1.32	7.50	11.2	0.0067						
	45.9	0.515	0.89	19.6	22.1	0.0089						
10	5.67	0.038	1.49	5.20	7.92	0.0066						
	22.4	0.221	1.01	14.2	16.2	0.0088						
11	3.94	0.0578	0.68	6.40	5.93	0.011	1.28	0.0203	0.63			
	14.3	0.276	0.52	17.3	12.6	0.014	5.82	0.108	0.54	10.4	0.0224	4.7
12	34.2	—	—									
	100.8	1.48	0.68									
13	14.1	0.094	1.50									
	48.2	0.44	1.10									

The dependence of the various quantities upon the temperature will be discussed in the following pages, but we should note now the marked increase in diffusivity and permeability with rising temperature, whereas the solubility of He, H_2, and N_2 increases only slightly, and that of CO_2, C_2H_2, and C_3H_6 decreases with the temperature. The increase in solubility of H_2 and N_2 with the temperature is in agreement with Carpenter's findings.[9]

Permeability

Some hints as to the cause of varying permeability are already afforded by Table II. To obtain a complete picture, it is necessary to split up permeability into its constitutive quantities, *viz.*, diffusivity and solubility.

Butadiene-acrylonitrile polymers provide a clear example of how the nature of the polymer affects the permeability to various gases, as demonstrated in Figure 1. From it we see that acrylonitrile strongly reduces the permeability of butadiene copolymers to a given gas; in fact, with a sufficient acrylonitrile content the material reaches even the low permeability of butyl rubber. We hope to explain why the permeability is thus reduced by the presence of an increasing percentage of acrylonitrile when we discuss diffusivity and its dependence upon temperature. What we may say in advance, however, is that it is a general rule that the presence of polar groups in the polymer molecules produces low permeability. As nitrile groups have a very pronounced polar character, their effect in this sense is very great.

There is another general rule, *viz.*, that methyl groups in the polymer molecules bring about low permeability. Accordingly, polydimethylbutadiene, having one more methyl group per monomeric unit than natural rubber, has a low permeability. Butyl rubber likewise owes this quality to the many methyl groups with which it is enriched.

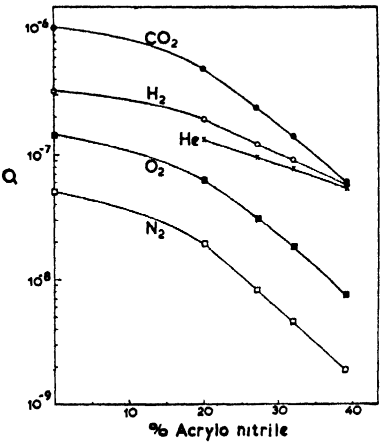

Fig. 1. Decreasing permeability of butadiene-acrylonitrile copolymers with increasing nitrile content at 25°C.

The permeability of polybutadiene, on the other hand, is little different from that of natural rubber, though the absence of methyl groups would have led one to expect a greater permeability. It is certain, however, that this polymer does not consist of pure 1,4-polybutadiene, but is polymerized in the 1,2 position to the extent of at least 20% and this makes comparison somewhat difficult. The fact that emulsion polyisoprene has virtually the same permeability as natural rubber goes to prove that this polyisoprene contains isoprene polymerized principally in the 1,4 position.

The realization that both nitrile and methyl groups tend to reduce permeability led to the production of the isoprene-acrylonitrile and isoprene-methacrylonitrile copolymers, which, taking the nitrile content into account, have exceptionally low permeability compared to the corresponding butadiene copolymers (*cf.* Table VI). With some gases the permeability of the isoprene-acrylonitrile copolymer is the same as that of butyl rubber; with others it is even appreciably lower.

For practical convenience we have collected in Table III the permeabilities of various polymers relative to natural rubber. The figures for air were obtained on the reasonable assumption that permeability is an additive property and that we may therefore approximately write:

TABLE III

PERMEABILITY OF ELASTOMERS AT 25°C. WITH REFERENCE TO NATURAL RUBBER (PURE GUM VULCANIZATES)

Rubber	H_2	N_2	O_2	CO_2	He	Air
Natural rubber	100	100	100	100	100	100
Polybutadiene	86	80	82	105	—	81
Buna S	81	78	73	94	74	76
Polymethylpentadiene	87	34	43	34	—	38
Perbunan 18	51	31	35	48	55	33
Perbunan (German)	32	13	17	24	39	15
Neoprene G	27	14	17	20	—	15
Isoprene-methacrylonitrile copolymer	28	7.4	10.1	10.8	—	8.5
Hycar OR 25	24	7.5	10	14	32	8.5
Polydimethylbutadiene	35	5.9	9.0	5.7	47	7.2
Vulcaprene A	13	6.1	6.5	14	—	6.3
Butyl rubber	15	4.0	5.6	4.0	27	4.8
Hycar OR 15	15	2.9	4.1	5.7	22	3.4
Isoprene-acrylonitrile copolymer	15	2.3	3.7	3.3	25	2.8
Thiokol B	3.2	—	1.2	2.4	—	—

$$Q_{air} = {}^4/_5 Q_{N_2} + {}^1/_5 Q_{O_2} \qquad (4)$$

To complete the picture we have also included in Table III the figures for Buna S (the equivalent of GR-S), Neoprene and Thiokol B, taken from the records of previous experiments.[4]

Diffusivity

The size of the gas molecules determines the rate at which various gases diffuse in a given rubber. Figure 2 shows in a few cases how the rate of diffusion diminishes as the diameter[10] of the gas molecules increases.

The effect of the nature of the rubber upon diffusivity is made apparent by Figure 3, instancing butadiene-acrylonitrile copolymers.

Comparing Figure 3 with Figure 1 we see that in this case the permeability and diffusivity run parallel; hence apparently solubility with respect to a certain gas is only slightly influenced by the chemical nature of the polymer. When we consider the question of the dependence of diffusivity upon the temperature we shall see why diffusivity decreases with increasing nitrile content of the polymer. As with permeability, however, the general rule applies that the presence of polar groups and of methyl groups in the polymer molecules brings about low diffusivity.

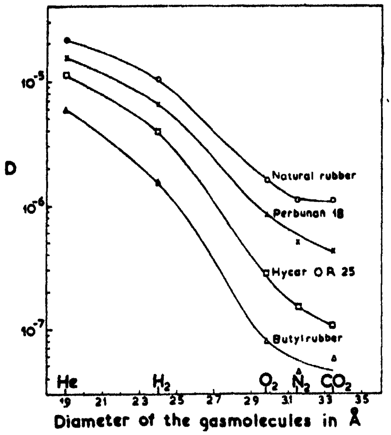

Fig. 2. Rate of diffusion as a function of diameter of gas molecules at 25°C.

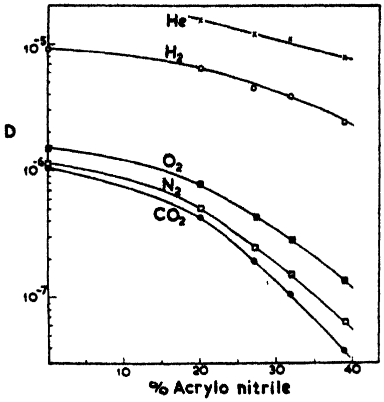

Fig. 3. Decreasing diffusivity of butadiene-acrylonitrile copolymers with increasing nitrile content at 25°C.

Solubility

It had been discovered in earlier experiments that the solubility of a gas is connected with its tendency to condense, of which the boiling point or the critical temperature is a measure.[4,6] It appears from Figure 4, which also incorporates data derived from another source,[4,6] that the logarithm

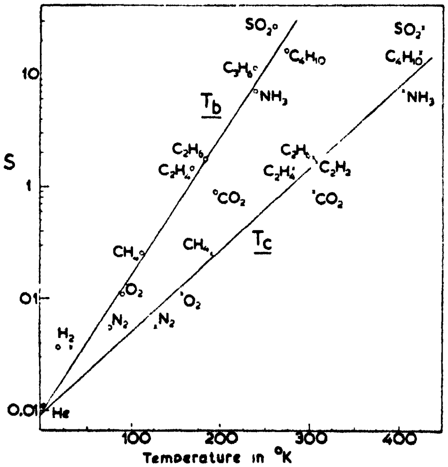

Fig. 4. Solubility of gases in vulcanized natural rubber at 25°C. as a function of critical temperature T_c and boiling point T_b.

of the solubility is a linear function of the critical temperature T_c or of the boiling point T_b, with the following equations applying:

$$\log S = -2.1 + 0.0074T_c$$

$$\log S = -2.1 + 0.0123T_b$$

These equations can be derived on the basis of the assumption that the process of solution of a gas is synonymous with its condensation followed by mixing with the rubber.[6,11] In that case we can relate the saturated vapor pressure of the gas to its solubility; for the rubber with the dissolved gas may be conceived of as a mixture of two liquids above which a vapor pressure of 1 atm. prevails. We can write for the free energy of dilution $\Delta\overline{F}_1$ of a rubber–liquid system:

$$\Delta\overline{F}_1 = RT \ln p_m/p_0 \tag{7}$$

where p_m = vapor pressure of the mixture and p_0 = vapor pressure of the solvent. The following equation holds for ideal liquid mixtures:

$$\Delta\overline{F}_1 = RT \ln N_1 \tag{8}$$

where N_1 is the molar fraction of component one in the mixture, R is the gas constant, and T is the temperature. When applying equations (7) and (8) to the system of rubber and liquefied gas, one can take 1 atm. for p_m and the saturated vapor pressure of the pure liquefied gas at the prevailing temperature for p_0. In so doing we find values for N_1 which show that in this case the rubber seems to behave like an ideal liquid of a molecular weight of approximately 300. A well-known fact that has emerged from investigations respecting swelling, however, is that equation (8) is not applicable to rubber. In its stead Huggins[12] found:

$$\Delta\overline{F}_1 = RT(\ln v_1 + v_2 + \mu v_2^2) \tag{9}$$

where v_1 and v_2 are volume fractions of liquid and polymer, respectively. μ is a constant connected with the heat of mixing and an effect of entropy, and related to the compatibility of the two components.

Assuming that with gas-rubber, p_m = 1 atm. and $v_2 = 1$, then combining (7) and (9), we obtain:

$$\ln 1/p_0 = \ln v_1 + 1 + \mu \tag{10}$$

The relation between v_1 and the solubility S is:

$$v_1 = SV_1/22{,}400 \tag{11}$$

where V_1 is the molar volume of the liquefied gas at the temperature of the experiment.

Table IV gives some results of μ calculated in this way. The pressure and the molecular volume of the liquefied gases at 25°C. were calculated from published data.[10,13] The pressure of gases which are above their critical point at 25°C. was found by extrapolating to above the critical point of the ln p_0: $1/T$ function.[14] At the boiling point the molecular volume of these gases is 30 to 40 cc., increasing with the temperature. The assumed value of 50 cc. is a rough estimate. It was supposed that the solubility of NH_3 and SO_2 in butyl rubber is approximately the same as the known solubility of these gases in polyisobutene.[4]

It is known that μ is below 0.5 for compatible systems, so the higher μ is, so much less compatible are the two components and the less satisfactorily does the gas dissolve. This can be stated more simply by saying that the solubility of a given gas in various rubbers is influenced by a specific interaction between the gas and the rubber. As a result, a nonpolar gas, like H_2 or O_2, dissolves rather more readily in a nonpolar rubber than in a polar one. Gases of a polar nature, on the contrary, such as CO_2 or NH_3, dissolve more readily if more polar groups are present in the rubber. Figure 5 illustrates this reciprocal influence of the nature of the polymer and the gas in a series of butadiene-acrylonitrile copolymers.

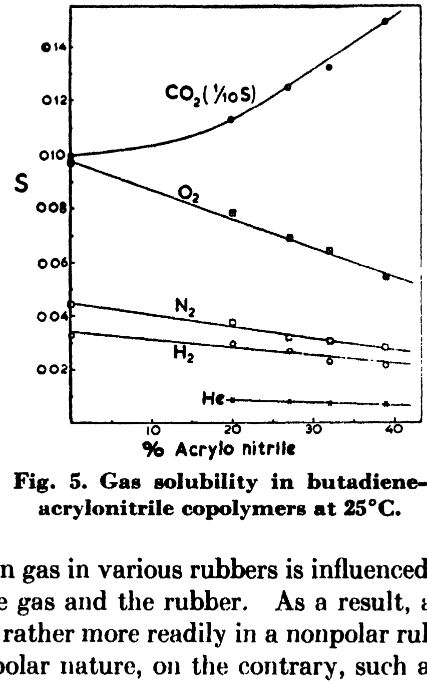

Fig. 5. Gas solubility in butadiene-acrylonitrile copolymers at 25°C.

TABLE IV

CALCULATION OF THE μ CONSTANT AT 25°C.

Gas	p_0, atm.	V_1, cc. at 25°C.	Natural rubber		German Perbunan		Butyl rubber	
			S	μ	S	μ	S	μ
N_2	1000	~50	0.055	~1.1	0.032	~1.6	0.055	~1.1
O_2	700	~50	0.112	~0.7	0.068	~1.2	0.122	~0.65
CH_4	370	~50	0.25	~0.55				
CO_2	63.5	63	0.90	0.8	1.24	0.5	0.68	1.1
C_2H_2	47	68	1.62	0.45	2.48	0.05	0.63	1.4
C_3H_8	9.5	89	6.5	0.4				
C_4H_{10}	2.6	101	16	0.65				
NH_3	9.9	28.4	6.9	1.45	13.5	0.75	~1.2	~3.2
SO_2	3.8	49	23.6	0.6	48	−0.1	~3.6	~2.5

DEPENDENCE OF PERMEABILITY AND DIFFUSIVITY UPON TEMPERATURE

On the evidence of former measurements,[1,4] when a linear connection was found between log Q or log D with $1/T$, we may write:

$$Q = Q_0e^{-W/RT} \tag{12}$$

$$D = D_0e^{-E/RT} \tag{13}$$

where Q_0 and D_0 are constants, W is the activation energy for the permeation, and E is the activation energy for the diffusion.

We shall see presently that the assumption of a linear connection of log Q or log D with $1/T$ is only tenable within a very limited range of temperature and that the activation energies depend upon the temperature. At a first approximation, equations (12) and (13) may be applied to the 25°C. range, up to which the measurements in Table II extend, and it is permissible to regard the energies as being constant. The various energies thus calculated are presented in Table V.

The energy of activation for the permeation is of little theoretical value and is used only for the calculation of the heat of solution.

ENERGY OF ACTIVATION FOR DIFFUSION

a. Relation to Energy of Cohesion

We may define the energy of activation for the diffusion as the energy necessary to push the rubber molecules far enough apart to form a hole for the infiltration of the gas molecules. Generally speaking, the greater the energy of activation for the diffusion is, the slower may diffusion be expected to be. We find that this actually is so if we compare Tables V and II.

Another prediction is that this energy of activation is in proportion to the necessary size of the hole. The energy has to be larger for the larger gas molecules and for the more powerful forces of cohesion. Figure 6 makes it plain that the energy of activation actually does increase with the diameter of the gas molecules.

It was pointed out elsewhere[4] that the cohesive forces of the rubber molecules per unit of length of the molecule are determining the energy of activation. Greater energy is needed if a larger number of polar and methyl groups is present in the polymer molecules. This effect of polar groups in the polymer upon the energy of activation is very clearly exemplified in the series of butadiene-acrylonitrile copolymers, for which see Figure 7.

From Figure 8 it can be deduced how methyl groups in the rubber increase the energy of activation. This increase runs entirely parallel with the energy of cohesion of a monomeric unit, as a measure of which the boiling point of the monomer was taken on the assumption that Trouton's rule applies. Thus methyl groups not only raise the boiling point and in-

TABLE V

ENERGIES OF ACTIVATION (CAL./MOLE) W AND E FOR PERMEATION AND DIFFUSION WITH THE CONSTANTS D_0 AT 25–50°C.

	H_2			N_2			O_2			CO_2			He			C_2H_2		
Compound	W	E	D_0	W	E	D_0	W	E	D_0	W	E	D_0	W	E	D_0	W	E	D_0
Natural rubber	6800	6000	0.26	8800	8700	2.6	7500	8300	1.94	6100	8900	3.7	6100	4300	0.031	7300	9500	4.3
Methyl rubber	8000	7500	1.3	13300	12400	105	11300	11100	20	11200	12800	160	6600					
Isoprene-acrylonitrile copolymer	9100	7400	0.67	15000	14500	1880	12700	12100	70	12500	14400	1150	7600	4900	0.031			
Isoprene-methacrylonitrile copolymer	8100	6900	0.41	12800	11600	39	11000	9600	2.6	10100	12200	81						
Polybutadiene	6600	5100	0.053	8200	7200	0.22	7100	6800	0.15	5200	7300	0.24						
Perbunan 18	7200	6200	0.23	9900	8500	0.88	8600	8100	0.69	7000	9200	2.4	6800	4200	0.019			
Perbunan (German)	7900	6900	0.52	11400	10400	10.7	9700	9200	2.4	8100	10700	13.5	7000	5200	0.077	9800	12300	82
Hycar OR 25	8200	7000	0.52	12300	11700	56	10500	10300	9.9	9000	12000	67	7400	5200	0.074			
Hycar OR 15	8800	7600	0.92	13800	12700	131	12000	10900	13.6	10500	13400	260	7700	5500	0.087			
Butyl rubber	8700	8100	1.36	12500	12100	34	10700	11900	43	9900	12000	36	7600	5800	0.105	11600	12800	50
Polymethylpentadiene	7100	—	—	11200	11100	42	9400	9800	8.5	8300	—	—						
Vulcaprene A	9000	7600	0.98	12200	11700	55	10900	10200	7.5	9400	11800	42						

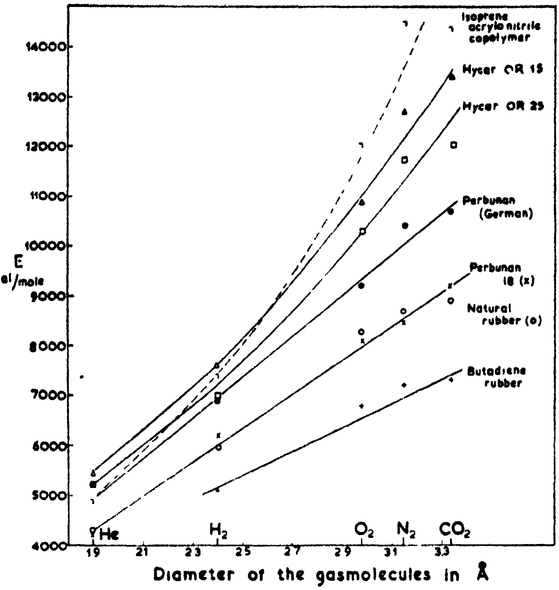

Fig. 6. Relationship between energy of activation and diameter of the gas molecules.

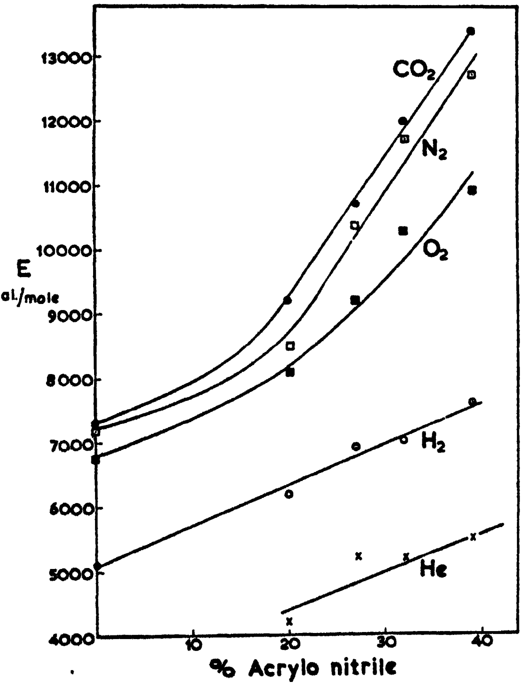

Fig. 7. Influence of the nitrile content upon the energy of activation for diffusion in the case of butadiene-acrylonitrile copolymers.

crease the energy of cohesion of the monomer, but also the energy of cohesion per unit of chain length and the energy of activation in the polymer.

It is necessary to stress at this point that the cohesive energy per unit of length of the macromolecule, which may be considered as determining the activation energy, is distinct from the cohesive energy density (C.E.D.) this latter giving the cohesive energy per cubic centimeter of material. It will be evident that there are far fewer monomeric units per cubic centimeter in methyl rubber than in butadiene rubber; quite possibly, therefore, there may be little difference between the C.E.D.'s of these two rubbers, even if there is considerable difference in the cohesive energy of a unit of length of the macromolecules. The discovery made by Barrer and Skirrow,[6] *viz.*, that, according to gas solubility measurements, the C.E.D. of a series of rubber-sulfur vulcanizates remains virtually unchanged with increasing sulfur content, does not necessarily imply that the cohesive energy per unit of length of the chain molecule remains unchanged. It is arguable that the introduction of combined sulfur causes a reduction in the total length of the chain per cubic centimeter of material, because the combined sulfur does not contribute to the length of the chain and the density of the rubber does not increase in proportion to the quantity of combined sulfur. Moreover, the binding of the sulfur is probably accompanied by considerable shortening of the chains through cyclization, which, with unchanged C.E.D., is responsible for further increase in the calculated cohesive energy per unit of chain length. In point of fact,[5] an increase in the combined sulfur content from 1.7% to 11.3% does go hand in hand with an increase in the activation energy for N_2 from 8000 to 11,000 cal. per mole.

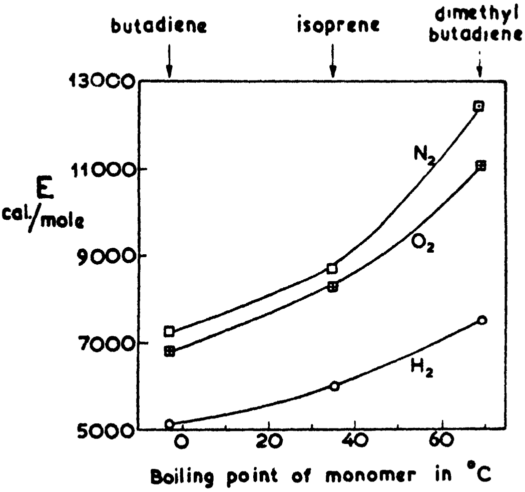

Fig. 8. Relation of boiling point of dienes to energy of activation for the diffusion in their polymers.

To obtain a rubber with a high activation energy and, with it, a low rate of diffusion and permeability, it seemed obvious that methyl groups should be combined with strongly polar groups. And the argument was vindicated by copolymers of isoprene with acrylonitrile and methacrylonitrile which combine rubberlike properties with an exceptionally marked activation energy together with very low permeability superior to most of the other varieties of rubber.

TABLE VI

ISOPRENE COPOLYMERS COMPARED WITH BUTADIENE COPOLYMERS AT 25°C.

Compound	% N	Q_{H_2}	Q_{N_2}	E_{H_2}	E_{N_2}
Isoprene-acrylonitrile	7 0	5 7	0.14	7400	14,500
Butadiene-acrylonitrile	7 0	12.5	0.85	6700	10,100
Isoprene-methacrylonitrile	5.3	10 4	0.46	6900	11,600
Butadiene-acrylonitrile	5.3	19	1.9	6200	8,500

Table VI shows how much lower is the permeability and greater the activation energy of isoprene copolymers than of butadiene copolymers of the same nitrile content. The values for the butadiene copolymers were estimated from Figures 1 and 7.

b. Relation to Brittle Point

The assumption that the permeability of the rubber largely depends upon the activation energy for the diffusion and, with it, upon the cohesive forces between the rubber chains connotes the supposition that the activation energy can be related to other physical properties, the viscosity of the rubber being the first to come to mind. It has been established by many investigations that the dependence of the viscosity upon the temperature can be formulated by equations of the following type:

$$\eta = Ae^{E_{visc.}/RT} \tag{14}$$

where η is the viscosity, $E_{visc.}$ the activation energy of the viscosity, and A a constant. Eyring[15] has placed this equation on a theoretical basis. He found that with a great many liquids $E_{visc.}$ is related to the heat of evaporation and, therefore, to the cohesive energy of those liquids. Thus this relation resembles the connection found between the energy of activation for diffusion and the cohesive energy per unit of length of the rubber molecule. The value of 8 to 10 kcal./mole was found for $E_{visc.}$ of natural rubber,[16,17] but as, unfortunately, measurements of the viscosity dependence of synthetic rubbers upon temperature are not yet available, no further comparison with the activation energy for diffusion is possible.

The brittle point[18] is another important quantity to which the activation energy for diffusion can be related. As a rubberlike material cools down, its rubberlike properties gradually disappear; it becomes harder and harder, until ultimately it will break or disintegrate under a sudden impact of force. The temperature at which such fracture occurs is known as the brittle point. This point serves as an index as to the utilizability of rubber at low temperatures. The brittle point test has to be performed under standardized conditions, because the position of the point depends to some extent upon the force to which the material is subjected. Fracture occurs the moment the material ceases, within the time allowed, to give way by deformation to the force applied.

The total deformation D of a viscoelastic material may consist of a high-elastic and a viscous-plastic component.[19]

$$D = D_{\text{h.e.}} + D_{visc.} \tag{15}$$

This can be reduced to:

$$D = D_{\text{h.e.}(\infty)}[1 - e^{-t/\tau}] + \sigma t/\eta \tag{16}$$

where D is the total deformation, $D_{\text{h.e.}(\infty)}$ is high elastic deformation after infinite time, σ is the stress, η is the viscosity coefficient, τ is the orientation time, and t is the time.

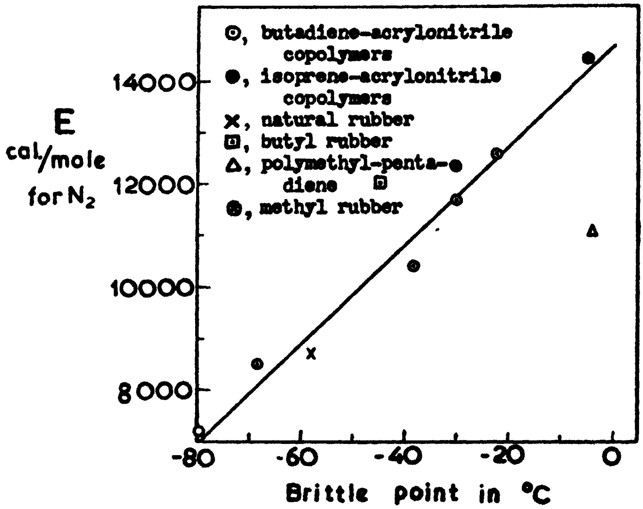

Fig. 9. Relationship between the activation energy for the diffusion of nitrogen and the brittle point in some elastomers.

Both the orientation time τ and the viscosity η can be related to an activation energy by equations such as (14), from which it follows that, the higher the activation energies, the higher are τ and η and the lower is the amount of deformation under a given force within a given time, this being manifested by increasing brittleness of the material. Since in the brittle point test the amount of deformation is kept constant while the temperature is varied, greater activation energy results in a higher brittle point temperature. The assumption that greater activation energy for diffusion is related to greater activation energy for the viscosity leads to the conclusion that rubber with a high activation energy for diffusion must possess a high brittle point; and that experiment has shown this to be so is apparent from Figure 9.

The brittle points cited have been borrowed from measurements performed by Salomon[20,21] and by Boonstra.[22] The correlation is clearly evident on the whole, the exceptions being that butyl rubber has greater activation energy than the position of the brittle point would lead one to expect, while on the other hand polymethyl pentadiene exhibits insufficient activation energy, possibly due to the very irregular buildup of this polymer.

HEAT OF SOLUTION

We can calculate the heat of solution of the gas in the elastomer from the dependency of the permeation and diffusion on the temperature by substitution of equations (12) and (13) in the basic equation $Q = DS$, which gives:

$$S = S_0e^{-\Delta H/RT} \tag{17}$$

and:

$$\Delta H = W - E \tag{18}$$

where $S_0 = Q_0/D_0$ is a constant and ΔH is the heat of solution. In a previous publication[4] the heat of solution was expressed somewhat differently as $H = \Delta H + RT$ cal./mole, where, therefore, the figures are +600 cal./mole higher.

Table VII sets out the heats of solution now found. These figures are accurate to within about 400 cal./mole. A fact to be noted is that the gases which do not readily condense generally exhibit heat absorption, which is compatible with the fact that the solubility of these gases increases a little with the temperature.

TABLE VII

HEATS OF SOLUTION OF GASES IN VARIOUS RUBBERS IN CAL./MOLE

Compound	He	H_2	N_2	O_2	CO_2	C_2H_2
Natural rubber	1800	800	100	− 800	−2800	−2200
Perbunan 18	2600	1000	1400	500	−2200	
Perbunan (German)	1800	1000	1000	500	−2600	−2500
Hycar OR 25	2200	1200	600	200	−3000	
Hycar OR 15	2200	1200	1100	1100	−2900	
Butyl rubber	1800	600	400	−1200	−2100	−1200
Isoprene-acrylonitrile copolymer	2700	1700	500	600	−1900	
Vulcaprene A		1400	500	700	−2400	

We may represent the process of solution of a gas as consisting in condensation of the gas combined with the mixing of that condensed gas with the rubber.[11] As a result, the heat of solution subdivides as follows:

$$\Delta H = \Delta H_{cond.} + \Delta\bar{H}_1 \tag{19}$$

where $\Delta H_{cond.}$ is the molar heat of condensation and $\Delta \bar{H}_1$, is the partial molar heat of mixing of the liquefied gas with the rubber.

The heat of condensation is very sensitive to temperature, decreasing by about five to twenty calories per degree of rising temperature, which often makes it difficult to establish it exactly for a gas at room temperature, certainly where the permanent gases are concerned. It is difficult to imagine any condensation of these gases above their critical point and in any event it does not readily lend itself to calculation of the heat of condensation. It can, however, be positively asserted that this "heat of condensation" of gases such as He, H_2, N_2, and O_2 is very low at room temperature, since the heat of evaporation at the boiling point of these gases is very low, *viz.*, 24, 216, 1360, and 1610 cal./mole, respectively. Furthermore, owing to the dependence upon temperature and the great temperature difference between the boiling point and room temperature, these figures should be a good deal lower still at room temperature. Therefore, so far as He and H_2 are concerned, there is no necessity to take considerable (negative) heat of condensation into account. In these cases the heat of solution is determined chiefly by the heat of mixing, which can be calculated by means of Hildebrand's equation[23]:

$$\Delta \bar{H}_1 = V_1[(E_1/V_1)^{1/2} - (E_2/V_2)^{1/2}]^2 v^2_2 \tag{20}$$

and also according to:[12]

$$\Delta \bar{H}_1 = (RT/v_2^2)[\mu - 1/z] \tag{21}$$

where V_1 and V_2 = molar volume of the liquefied gas and the rubber, respectively; E_1 and E_2 = energy of vaporization of the liquefied gas and the rubber, respectively; E_1/V_1 and E_2/V_2 = cohesion energy density (C.E.D.) of the liquefied gas and the rubber, respectively; v_2 = volume fraction of rubber ($\simeq 1$ in this case); z = coordination number (usually $z \simeq 6$ to 8); and μ = a constant given by equation (9).

If we apply these equations to the permanent gases, we are again faced with the difficulty that the cohesion energy density (C.E.D.) cannot be calculated for these gases at room temperature. At the boiling point of He, H_2, N_2, and O_2, however, $(E_1/V_1)^{1/2}$ amounts to 0.67, 2.5, 5.9, and 7.4, respectively, but it decreases in a marked degree with rising temperature, owing to decreasing E_1 and increasing V_1. If these excessive C.E.D.'s are used for the calculation of the heat of mixing with natural rubber $[(E_2/V_2)^{1/2} = 7.98]$,[24] the results are 1800, 900, 140, and 10 cal./mole, respectively, which may presumably be higher.

The heat of mixing can also be calculated with the aid of equation (21), using the value for μ given in Table IV. Here again the result is a positive value for the heat of mixing.

Heat absorption such as found with some permanent gases, therefore, is quite compatible with the hypothesis that the heat of condensation is low and that consequently the heat of mixing decides the heat of solution.

The C.E.D. of butadiene-acrylonitrile rubbers is greater than that of natural rubber. From this a higher heat of mixing can generally be calculated from equation (20) for gases with a C.E.D. lower than that of the rubber. Accordingly, the evidence of the experiment shows the heat of solution in these rubbers of He, H_2, N_2, and O_2 to be higher than in natural rubber.

Finally, the heat of solution of readily condensing gases, such as propane, butane, NH_3, and SO_2, is determined chiefly by the heat of condensation,[6,11] while the heat of mixing is of secondary importance.

DEPENDENCE OF ACTIVATION ENERGY ON TEMPERATURE

It has hitherto been assumed that the activation energies for permeation and diffusion are independent of the temperature and, within the experimental range of 25 to 50 °C. under consideration, this approximately meets the facts. There were grounds, however, for questioning the validity of this assumption as applied to a wider range of temperature and measure-

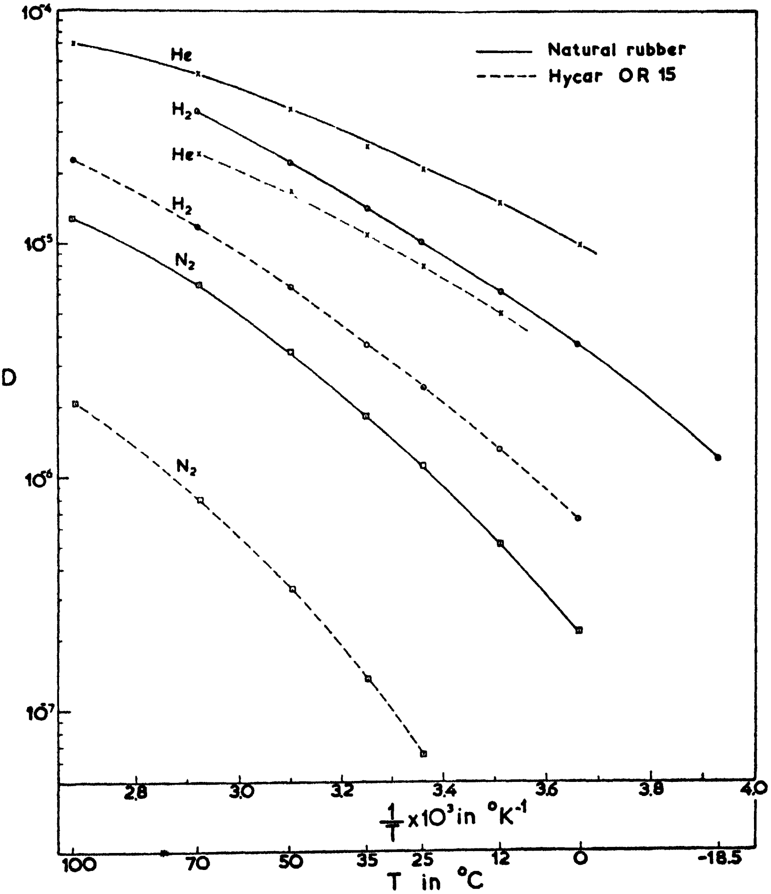

Fig. 10. Rate of diffusion as a function of temperature.

ments were therefore performed upon a few gases and rubbers at temperatures ranging from −18.5 to +100°C.

Figure 10 shows that the relation between log D and $1/T$ within a wider range of temperature is no longer linear, despite the first impression that it is. At the higher temperatures D is lower than it should be if the relation were truly linear. A similar curvature is obtained when log Q is plotted against $1/T$. Barrer and Skirrow[5] find a similar response of D and Q to the temperature in the majority of the cases they investigated.

The changing slope of the log D:$1/T$ and log Q:$1/T$ curves can be interpreted as a change in the activation energies for diffusion and permeation caused by changing temperature. The permeabilities, diffusivities, and activation energies within the measured temperature limits are set out in Table VIII.

Generally speaking, measurements within so wide a temperature range are less precise than at normal temperature. One difficulty is that the measurements at all these temperatures cannot be performed with a membrane of the same thickness. The reported values are often the result of two overlapping series of measurements. Above 100°C. the rubber begins to give off gas and this makes it impossible to take measurements. Since, as we have seen, the activation energies for permeation and diffusion depend very greatly upon the temperature, these energies can only be allowed to be approximately constant within a relatively narrow range of temperature. The heat of solution which can be calculated from E and W is as a rule fairly indifferent to temperature, the experimental error being the important factor here. Hence the dependence of the activation energy for permeation W upon the temperature is governed chiefly by the activation energy for diffusion E. The fact that E is dependent upon the temperature makes it clear that the equation $D = D_0 \exp. (-E/RT)$ is an oversimplification. A better empirical representation of the problem follows from:

$$\frac{d \ln D}{d(1/T)} = -\frac{E_0 + aT}{R} \tag{22}$$

or, when integrated:

$$D = CT^{a/R}e^{-E_0/RT} \tag{23}$$

where the initial assumption based on the experiment is that:

$$E = E_0 + aT \tag{24}$$

and:

$$a = dE/dT \tag{25}$$

This kind of dependence of activation energies upon temperature is a common phenomenon at rates of reaction for which similar equations can be written.[25] In the case of the activation energy for diffusion this dependence upon the temperature becomes comprehensible if one regards this quantity as the energy required to loosen up the molecular chain for a

TABLE VIII

PERMEABILITIES Q (IN 10^{-8} CM.^{2} SEC.$^{-1}$ ATM.$^{-1}$), DIFFUSIVITIES D (IN 10^{-6} CM.^{2} SEC.$^{-1}$) AND ENERGIES OF ACTIVATION W AND E (IN CAL./MOLE) IN DEPENDENCY ON TEMPERATURE

Compound	Temp., °C.	H_2 Q	H_2 D	H_2 W	H_2 E	N_2 Q	N_2 D	N_2 W	N_2 E	He Q	He D	He W	He E
Natural rubber	−18.5	3.8	1.3										
	0	11.9	3.7	8100	7100	1.14	0.22	—	—	8.5	10.0		
	12	21.5	6.2	7600	6700	2.80	0.52	11,100	10.700	14.6	15.0	6800	5100
	25	37.4	10.2	7100	6300	6.12	1.10	9,700	9,400	23.7	21.6	6300	4700
	35	55.0	14.2	6800	6000	10.2	1.82	8,900	8,800	33.3	27.7	6100	4400
	50	90.8	22.2	6400	5800	19.4	3.42	8,100	7,900	52.3	38.0	5900	4000
	70	157	37.1	5800	—	39.0	6.63	7,000	6,600	88.8	53.4	5700	3300
	100	298	—	—	—	80.3	13.0	—	—	170.5	72.1		
Perbunan (German)	12	6.35	2.53	—	—	0.31	0.105	—	—				
	25	12.1	4.50	8200	7400	0.81	0.25	12,200	11,200				
	35	18.7	6.70	7900	7000	1.56	0.46	11,500	10,600				
	50	33.7	11.1	7600	6300	3.58	0.98	10,500	9,300				
	70	64.8	18.9	7000	5000	8.79	2.1	9,500	—				
Hycar OR 15	0	1.22	0.665										
	12	2.63	1.32	9900	8600	—	—	—	—	2.81	5.00	—	—
	25	5.42	2.43	9200	8000	0.179	0.064	—	—	5.20	7.92	7900	5800
	35	8.90	3.74	8800	7700	0.400	0.138	13,900	13,100	8.00	10.7	7700	5500
	50	17.0	6.56	8300	7100	1.08	0.338	12,900	10,900	14.2	16.2	7400	5000
	70	34.7	11.9	7500	6200	3.40	0.805	11,600	9,000	27.4	24.2	—	—
	100	80.2	23.0	—	—	11.50	2.12						
Butyl rubber	0	1.26	0.41										
	12	2.77	0.80	9800	8700	—	—	—	—	3.6	3.7	—	—
	25	5.50	1.52	9000	8400	0.25	0.045	—	—	6.4	5.9	7600	6100
	35	9.00	2.41	8800	8200	0.50	0.090	12,600	12,200	9.8	8.3	7600	5800
	50	17.2	4.38	8600	7500	1.27	0.22	11,800	11,400	17.3	12.6	7500	5400
	70	37.0	8.24	8200	6800	3.53	0.59	11,100	10,000	33.7	20.0	—	—
	100	91.8	17.6	—	—	13.1	1.7	—	—				

given distance. This energy corresponds to the cohesive energy of the chain element concerned, which, like the heat of vaporization of every substance, must depend upon the temperature. It is known that the heat of vaporization as a function of the temperature can be described as follows:

$$\Delta H_v = \Delta H_0 + \int_0^T \Delta C_p \, dT \tag{26}$$

where ΔH_v is the heat of vaporization, ΔH_0 is a constant, and ΔC_p is change in specific heat on vaporization. Assuming ΔC_p to be a constant, we get an equation similar to (24) after integration.

Table IX gives the values for dE/dT obtained from the smoothed linear curve $E:T$.

TABLE IX

dE/dT VALUES FOR SOME DIFFUSIONS

Compound	H_2	N_2	He
Natural rubber	−28	− 68	−32
Perbunan (German)	−52	− 80	—
Hycar OR 15	−42	−114	−32
Butyl rubber	−33	− 66	−28

THEORETICAL DISCUSSION

It will be interesting to see whether dependence of E upon the temperature can be made to fit into the zone theory propounded by Barrer[26,27] and the transition state theory developed by Eyring[15] to account for the process of diffusion.

Certainly, the zone theory does require E to be a function of the temperature. According to this theory, diffusion answers the equation:

$$D = {}^1/_6 \nu d^2 e^{-E_0/RT} \sum_{f=1}^{n} \left(\frac{E_0}{RT}\right)^{f-1} \frac{1}{(f-1)!} \tag{27}$$

where ν is frequency, d is distance, E_0 is total energy of activation, and f is number of degrees of freedom for activation. If we suppose that the first term of the series is the decisive factor, it can be deduced[27] that:

$$E = E_0 - (f-1)RT \tag{28}$$

and:

$$dE/dT = -(f-1)R \tag{29}$$

Then, with the aid of equation (29), we can find directly from Table IX the number of degrees of freedom which, according to the zone theory, have to be reckoned with for the activation in the process of diffusion.

An alternative is to apply the transition theory[15] to diffusion. This theory starts from the assumption that diffusion is a reaction satisfying the following equation:

$$D = d^2k^1 \tag{30}$$

where *d* is the jump and distance k^1 is a rate constant.

The constant k^1 follows from:

$$k^1 = \kappa(kT/h)K^\ddagger \tag{31}$$

where *k* is the Boltzmann constant, *h* is the Planck constant, κ is the transmission coefficient (usually $\kappa \simeq 1$), and $K^\ddagger$ is the equilibrium constant for activated and initial states.

It is supposed here that diffusion takes place after an activated state has been reached which is in equilibrium with the initial state. The constant $K\ddagger$ stands in relation to the standard free energy of the process by means of the familiar thermodynamic equation:

$$\ln K^\ddagger = -\Delta F^\ddagger/RT \tag{32}$$

Also:

$$\Delta F^\ddagger = \Delta H^\ddagger - T\Delta S^\ddagger \tag{33}$$

where $\Delta F^\ddagger$, $\Delta H^\ddagger$, and $\Delta S^\ddagger$ are the standard free energy, heat, and entropy changes, respectively.

After substitution of (33) in (32) and thereafter of (32) in (31) and (30), we obtain:

$$D = \kappa(kT/h)d^2e^{\Delta S^\ddagger/R}e^{-\Delta H^\ddagger/RT} \tag{34}$$

This equation agrees with equation (13) found by experiment, where:

$$E = \Delta H^\ddagger + RT \tag{35}$$

and:

$$D_0 = \frac{\kappa kTd^2}{he} e^{\Delta S^\ddagger/R} \tag{36}$$

If $\Delta S^\ddagger$ is calculated according to equation (36), we find values of 10 to 26 entropy units per mole.[5]

If it be desired to apply equation (34) to a diffusion process, where the activation energy is dependent upon temperature, the proper course would seem to be to take the dependence of $\Delta S^\ddagger$ and $\Delta H^\ddagger$ upon the temperature also into account. For this we can write:

$$\Delta H^\ddagger = \Delta H_0^\ddagger + \int_0^T \Delta C_p^\ddagger\, dT \tag{37}$$

and:

$$\Delta S^\ddagger = \Delta S_0^\ddagger + \int_0^T (\Delta C_p^\ddagger/T)\, dT \tag{38}$$

where $\Delta H_0^\ddagger$ and $\Delta S_0^\ddagger$ are constants and $\Delta C_p^\ddagger$ is change in specific heat on activation. After substitution of (37) and (38) in (33) and (32) we obtain:

$$\ln K^{\ddagger} = -\frac{\Delta H_0^{\ddagger}}{RT} + \frac{S_0^{\ddagger}}{R} - \frac{1}{RT}\left\{\int_0^T \Delta C_p^{\ddagger}\,dT - T\int_0^T \frac{\Delta C_p^{\ddagger}}{T}\,dT\right\} \tag{39}$$

For $\Delta C_p^{\ddagger}$ we can write:

$$\Delta C_p^{\ddagger} = \alpha + \beta T + \gamma T^2 + \dots \tag{40}$$

Considering only the first two terms, we get from this:

$$\ln K^{\ddagger} = -\frac{\Delta H_0^{\ddagger}}{RT} + \frac{\Delta S_0^{\ddagger}}{R} - \frac{\alpha}{R} + \frac{\alpha \ln T}{R} + \frac{\beta T}{2R} \tag{41}$$

In (31) and (30) this gives:

$$D = \kappa \frac{kT}{h} e^{(\Delta S_0^{\ddagger} - \alpha + {}^1/_2\beta T)/R}\, T^{\alpha/R}\, e^{-\Delta H_0^{\ddagger}/RT} \tag{42}$$

The formal agreement between this equation and equation (23), which was found experimentally, is satisfactory.

From (13) and (42) one finds the following for the dependence of the energy of activation upon the temperature:

$$\frac{d \ln D}{d(1/T)} = -\frac{E}{R} = -\frac{\Delta H_0^{\ddagger}}{R} - \frac{\alpha T}{R} - \frac{\beta T^2}{2R} - T \tag{43}$$

or:

$$E = \Delta H_0 + (\alpha + R)T + {}^1/_2\,\beta T^2 \tag{44}$$

which, after disregarding the β term, is likewise the dependence on temperature found experimentally, where $dE/dT = \alpha + R$. It should be noted that the constants $\Delta H_0^{\ddagger}$ and $\Delta S_0^{\ddagger}$ are only of account insofar as they are used within the measuring range in equation (42), because only two terms of the progression of $\Delta C_p^{\ddagger}$ were used.

THE CONSTANT D_0

We see in Table V that the constant D_0 is larger in proportion to the greater energy of activation E. It has been shown before[4] how the two quantities stand in relation to each other, regardless of the diffusion process, approximately according to:

$$\log D_0 = E/2000 - 4.2 \tag{45}$$

A comparable functional relationship was found by Barrer and Skirrow,[5] who also suggest possible interpretations of the constant D_0 on the basis of the transition state theory[15] and the zone theory.[26]

It is obvious that there must be some close connection between this relationship and the fact that the activation energy E is a function of the temperature. And, in fact, D_0 is not constant for the diffusion of a given gas through rubber, but also depends upon the temperature, according to :

$$D_0 = C(Te)^{\alpha/R} \tag{46}$$

which equation can be derived from (23). A complete interpretation of D_0 should bring equation (45) into relation with equation (46).

In conclusion, I wish to express my sincere thanks to Miss W. Karssen for her able assistance in carrying out the experiments, to Dr. G. Salomon for his interest and discussions, and to the Rubber Foundation for permission to publish the results of the investigation.

References

1. R. M. Barrer, *Trans. Farad. Soc.*, **35**, 628 (1939).
2. T. P. Sager, *J. Research Natl. Bur. Standards*, **25**, 309 (1940).
3. G. J. van Amerongen, *Rev. gen. caoutchouc*, **21**, 50 (1944); *Rubber Chem. and Technol.*, **20**, 479 (1947).
4. G. J. van Amerongen, *J. Applied Phys.*, **17**, 972 (1946), *Rubber Chem. and Technol.*, **20**, 495 (1947).
5. R. M. Barrer and G. Skirrow, *J. Polymer Sci.*, **3**, 549 (1948).
6. R. M. Barrer and G. Skirrow, *J. Polymer Sci.*, **3**, 564 (1948).
7. G. J. van Amerongen, *J. Polymer Sci.*, **2**, 381 (1947).
8. F. M. McMillan, E. T. Bishop, K. E. Marple, and T. W. Evans, *India Rubber World*, **113**, 663 (1946).
9. A. S. Carpenter, *Trans. Faraday Soc.*, **43**, 529, 822 (1947).
10. C. D. Hodgman, *Handbook of Chemistry and Physics*, 29th Ed. Chem. Rubber Pub. Co., Cleveland, 1945.
11. G. Gee, *Quart. Revs. London*, **1**, 295 (1947), *Rubber Chem. and Technol.*, **21**, 591 (1948).
12. M. L. Huggins, *Ann. N. Y. Acad. Sci.*, **43**, 1 (1942); **44**, 431 (1943).
13. Landolt-Börnstein, *Physikalisch-Chemische Tabellen.* Springer, Berlin, 1923–1936.
14. J. H. Hildebrand, *Solubility.* Reinhold, New York, 1936, p. 30.
15. S. Glasstone, K. J. Laidler, and H. Eyring, *Theory of Rate Processes.* McGraw-Hill, New York, 1941, p. 516.
16. H. M. Smallwood, *J. Applied Phys.*, **8**, 505 (1937).
17. D. W. Saunders and L. R. G. Treloar, *Trans. Inst. Rubber Ind.*, **24**, 92 (1948).
18. R. F. Boyer and R. S. Spencer, in H. Mark and G. S. Whitby, eds., *Advances in Colloid Science*, Vol. II. Interscience, New York, 1946, p. 35.
19. R. F. Tuckett, *Trans. Faraday Soc.*, **39**, 158 (1943).
20. G. Salomon and C. Koningsberger, *J. Polymer Sci.*, **2**, 522 (1947).
21. G. Salomon, *J. Polymer Sci.*, **3**, 22 (1948).
22. B. Boonstra, unpublished measurements.
23. J. H. Hildebrand, *Solubility.* Reinhold, New York, 1936, p. 73.
24. G. Gee, in H. Mark and G. S. Whitby, eds., *Advances in Colloid Science*, Vol. II. Interscience. New York, p. 186.
25. E. A. Moelwyn-Hughes, *Reactions in Solution*, 2nd ed. Clarendon Press, Oxford, 1947, pp. 4, 53.
26. R. M. Barrer, *Trans. Faraday Soc.*, **38**, 322 (1942).
27. R. M. Barrer, *Trans. Faraday Soc.*, **39**, 237 (1943).

English Synopsis, see Summaries, page S7, Vol. V, 1950.

Résumé

Le sujet de cette étude était l'effet de la structure des polymères analogues au caoutchouc, sur la perméabilité, la diffusibilité et la solubilité d'une série des gaz. Les copolymères de butadiène-acrylonitrile perdent beaucoup de leur "diffusitivité" et de leur perméabilité suivant leur teneur croissante en acrylonitrile. La présence de groupes

méthyle dans le polymère diminue habituellement de façon semblable la "diffusitivité" et la perméabilité. Cette connaissance rend possible la synthèse d'un copolymère isoprène-acrylonitrile, dont la perméabilité aux gaz est petite, bien qu'il possède des propriétés analogues au caoutchouc. La relation entre la vitesse de diffusion et la température fournit l'énergie d'activation E de la diffusion. Une énergie d'activation plus élevée pour un gaz déterminé dans une série de caoutchoucs entraine toujours une vitesse de diffusion plus faible. La valeur de l'énergie d'activation E est d'autant plus grande que les forces de cohésion existant entre les molécules sont grandes, et que les dimensions des molécules gazeuses sont grandes également. Des mesures effectuées sur une large échelle de température (de $-18°$ à $+100°$) montrent clairement que l'énergie d'activation est fonction de la température, et une équation expérimentale tenant compte de ce phénomène est donnée. Cette dépendance de l'énergie d'activation en fonction de la température est compatible avec la théorie des zônes de Barrer, ainsi qu'avec la théorie de l'état de transition d'Eyring pour la diffusion. La constante μ pour plusieurs systèmes de gaz et caoutchouc est obtenue par calcul au départ de la solubilité du gaz. La chaleur de dissolution est obtenue au départ de la dépendance de la solubilité du gaz dans le caoutchouc en fonction de la température. Cette chaleur de dissolution consiste principalement en chaleur de mélange dans le cas des gaz, qui condensent difficilement, comparé à celle-ci, la chaleur de condensation du gaz en phase liquide est faible.

Zusammenfassung

Der Gegenstand dieser Arbeit war der Effekt der Struktur kautschukartiger Polymerer auf die Permeabilität, Diffusivität und Löslichkeit einer Reihe von Gasen. Es wurde gefunden, dass Butadien-Acrylnitril-Copolymere mit steigendem Nitrilgehalt viel von ihrer Diffusivität und Permeabilität verlieren. Die Gegenwart von Methylgruppen in der Polymermolekeln verringert im allgemeinen die Diffusivität und Permeabilität entsprechend. Diese Kenntnis ermöglichte es uns, ein Isopren-Acrylnitril-Copolymer zu synthetisieren, welches abgesehen davon, dass es kautschukartige Eigenschaften besitzt, nur sehr wenig Gas permeiern lässt. Die Beziehung zwischen Diffusionsgeschwindigkeit und Temperatur ergab die Aktivierungsenergie E für die Diffusion. Eine grössere Aktivierungsenergie für ein gegebenes Gas in einer Reihe von Kautschukpolymeren ergibt immer eine geringere Diffusionsgeschwindigkeit. Es wird gezeigt, dass die Aktivierungsenergie E umso grösser ist, je grösser die Kohäsionskräfte zwischen den Kautschukmolekülen und je grösser die Gasmolekeln sind. Messungen, die in einem grossen Temperaturbereich vorgenommen wurden (-18 bis 100° C.) zeigten deutlich, dass die Aktivierungsenergie eine Funktion der Temperatur ist, und eine experimentelle Gleichung wird hierfür gegeben. Die Abhängigkeit von E von der Temperatur ist nachweislich vereinbar mit Barrers Zonentheorie und mit Eyrings Transitionsstadiumstheorie für Diffusion. Die Konstante μ für verschiedene Systeme von Gas und Kautschuk wird durch Berechnung aus der Löslichkeit des Gases abgeleitet. Die Lösungswärme wird von der Temperaturabhängigkeit der Löslichkeit des Gases in Kautschuk abgeleitet. Diese Lösungswärme besteht im Falle von Gasen, die schwer kondensieren, hauptsächlich aus Mischungswärme. Die Kondensationswärme vom Gas zur flüssigen Phase ist im Vergleich damit klein.

Received April 25, 1949

JOURNAL OF POLYMER SCIENCE VOL. V, NO. 3, PAGES 333-353

Die Löslichkeit hochpolymerer Fadenmoleküle

ARNOLD MÜNSTER, *Forschungslaboratorium der Zellstofffabrik Waldhof, Wiesbaden-Kostheim*

Bei dem Problem der Löslichkeit hochpolymerer Fadenmoleküle handelt es sich in den meisten Fällen um Gleichgewichte zwischen zwei binären oder sogar ternären flüssigen Phasen. Die mathematische Behandlung derartiger Probleme führt auf grosse Schwierigkeiten, zumal wenn die Polydispersität der Fadenmoleküle berücksichtigt wird. Verschiedene Autoren[1-3] haben daher versucht, Ergebnisse, die bei der Behandlung einfacherer Systeme erhalten wurden, auf die komplizierten Fälle zu übertragen. Dieses Verfahren hat den Nachteil, dass man von vorneherein nicht sagen kann, wie weit eine derartige Näherung gerechtfertigt ist. Im folgenden werden wir für die wichtigsten Spezialfälle zunächst die exakte thermodynamische-statistische Theorie entwickeln und dann die Näherungsannahmen genau präzisieren, die jeweils gemacht werden müssen, um die Rechnung bis zu übersichtlichen Endformeln durchzuführen.

Die spezielle Grundlage unserer Rechnungen wird die statistische Theorie der polydispersen irregulären Lösung bilden, die kürzlich entwickelt wurde.[4] Dabei werden wir jedoch in der Entwicklung der Verdünnungswärme nach Potenzen des Molenbruches nur das erste (quadratische) Glied berücksichtigen, was für die meisten Fälle ausreicht. Ferner setzen wir voraus, dass die Fadenmoleküle nur wenig beweglich sind; dies trifft für die Cellulosederivate bei nicht zu hohem Polymerisationsgraden zu. Für den athermischen Anteil der Verdünnungsentropie werden wir in einigen Fällen die geschlossenen Ausdrücke von Flory,[5] Huggins,[6] oder Miller[7] verwenden.

In den folgenden Formeln bezeichnen die Indizes α und β die beiden im Gleichgewicht befindlichen Phasen, 1 die gelösten Fadenmoleküle, 2 das Lösungsmittel, 3 das Fällungsmittel, n Fadenmoleküle vom Polymerisationsgrad n.

VERTEILUNG ZWISCHEN ZWEI NICHT MISCHBAREN LÖSINGSMITTELN

Monodisperse Lösung

Das Verteilungsgleichgewicht der Fadenmoleküle zwischen zwei nicht mischbaren Lösungsmitteln ist von Schulz[1] als Ausgangspunkt für seine theoretischen Überlegungen über die Löslichkeit gewählt worden. Bezeichnen wir mit μ die chemischen Potentiale, so lautet die Gleichgewichtsbedingung:

$$\mu_{1\alpha} = \mu_{1\beta} \tag{1}$$

Wir wählen den reinen gelösten Stoff als Normalzustand und nehmen an, dass die Verdünnungswärme negativ ist. Dann gilt für verdünnte Lösungen.[8]

$$\Delta\mu_1 = RT\left\{\ln \mathrm{N}_1 - \ln z + \frac{z-2}{z} n^2 \mathrm{N}_1 - (z-2)\frac{n}{2}\frac{E}{RT} - \frac{z-2}{z} n^2[\exp(-E/RT) - 1]\mathrm{N}_1\right\} \tag{2}$$

Hier ist R die Gaskonstante, T die absolute Temperatur, z die Koordinationszahl, n der Polymerisationsgrad, E die Wechselwirkungsenergie zweier benachbarter Bausteine verschiedener Fadenmoleküle, normiert auf die unendlich verdünnte Lösung und:

$$\mathrm{N}_1 = n_1/(nn_1 + n_2) \tag{3}$$

wo n_1 und n_2 die Molzahlen bedeuten. Aus Gl. (1) und (2) folgt:

$$\frac{\mathrm{N}_{1\alpha}}{\mathrm{N}_{1\beta}} = \exp\left\{(z-2)\frac{n}{2}\frac{E_\alpha - E_\beta}{RT} - \frac{z-2}{z} n^2[(2 - e^{-E_\alpha/RT}]\mathrm{N}_{1\alpha} - (2 - e^{-E_\beta/RT})\mathrm{N}_{1\beta}]\right\} \tag{4}$$

Wir setzen zur Abkürzung:

$$\Delta E \equiv E_\alpha - E_\beta \tag{5}$$

und definieren im Anschluss an Schulz[9] das Trennungsverhältnis ϑ durch die Gleichung

$$\frac{\mathrm{N}_{1\alpha}}{\mathrm{N}_{1\beta}} = \frac{m_{1\alpha}}{m_{1\beta}}\frac{v_\beta}{v_\alpha} \equiv \vartheta\varphi \tag{6}$$

wo m_1 die Masse der Fadenmoleküle, v das Volumen einer Phase und $\varphi = v_\beta/v_\alpha$ ist. Dann wird für beliebig wachsende Verdünnung ($\mathrm{N}_1 \rightarrow 0$) aus Gl. (4):

$$\vartheta = \frac{1}{\varphi}\exp\left\{(z-2)\frac{n}{2}\frac{\Delta E}{RT}\right\} \tag{7}$$

Dies ist im Wesentlichen die von Schulz[9] abgeleitete Gleichung für die Verteilung der Fadenmoleküle zwischen zwei nicht mischbaren Lösungsmitteln. Sie stellt somit das exakte Grenzgesetz für unendliche Verdünnung dar. Für niedrige endliche Konzentration ergibt sich aus Gl. (4):

$$\vartheta = \frac{1}{\varphi} \exp \left\{ (z-2) \frac{n}{2} \frac{\Delta E}{RT} \right.$$

$$\left. \frac{z-2}{z} n \frac{V_2}{M_0} \frac{m_1}{v_\beta (1+\vartheta)} \left[\left(2 - e^{-E_\alpha/RT}\right) \varphi\vartheta - \left(2 - e^{-E_\beta/RT}\right) \right] \right\} \quad (8)$$

Hier ist V_2 das Molvolumen des Lösungsmittel, das im Sinne des Gittermodells der Statistik dem Molvolumen eines Bausteins der Fadenmoleküle (Grundmolvolumen) gleichgesetzt wird, M_0 das Molgewicht eines Bausteins (Grundmolgewicht) und m_1 die Gesamtmasse der Fadenmoleküle. Hier besteht somit ein wesentlich komplizierterer Zusammenhang zwischen ϑ und n als in Gl. (7).

Um die Verhältnisse bei beliebigen Konzentrationen zu überblicken, setzen wir mit Benutzung der Formel von Flory[5] und Huggins[6] für das chemische Potential der Fadenmoleküle:

$$\Delta\mu_1 = RT \left\{ \ln \mathrm{N}_1^* - (n-1)(1-\mathrm{N}_1^*) - (z-2) \frac{n}{2} \frac{E}{RT} - \right.$$

$$\left. \frac{z-2}{z} n \left[\exp(-E/RT) - 1\right] \mathrm{N}_1^* \right\} \quad (9)$$

wo $\mathrm{N}_1^* = n\mathrm{N}_1$ der Volumenbruch der Fadenmoleküle ist. Man sieht, dass dieser Ausdruck [abgesehen von einem hier unwichtigen Faktor $(z-2)/z$] wieder auf Gl. (4) und (8) führt. Gl. (2) stellt somit für die hier behandelten Probleme eine über den ganzen Konzentrations bereich brauchbare Formel dar. Von dieser Tatsache werden wir bei allen weiteren Rechnungen Gebrauch machen.

Polydisperse Lösung

Bei dem Verteilungsgleichgewicht einer polydispersen Lösung kann das totale Massenverhältnis der Fadenmoleküle in beiden Phasen nicht aus Gl. (8) unter Benutzung eines mittleren Polymerisationsgrades berechnet werden, denn dieser wird in beiden Phasen untereinander und von dem des Ausgangsproduktes verschieden sein. Man kann Gl. (8) aber auch nicht auf die Verteilung der Fadenmoleküle vom Polymerisationsgrad n anwenden, da diese von der Verteilung der Moleküle aller übrigen Polymerisationsgrade abhängt. Wir müssen daher die vollständige Theorie der polydispersen Lösung[4] zugrundelegen. Diese liefert für das chemische Potential der gelösten Fadenmoleküle vom Polymerisationsgrad n:

$$\Delta\mu_{1n} = RT \left\{ \ln \mathrm{N}_{1n} - \ln z + \frac{z-2}{z} n\bar{n}\mathrm{N}_1 - (z-2) \frac{n}{2} \frac{E}{RT} - \right.$$

$$\left. \frac{z-2}{z} n\bar{n} \left[\exp(-E/RT) - 1\right] \mathrm{N}_1 \right\} \quad (10)$$

Hier ist:

$$\mathrm{N}_{1n} = \frac{n_{1n}}{\sum n n_{1n} + n_2} \quad (11)$$

und $\bar{n}$ das Zahlenmittel der Polymerisationsgrade, wie es bei der osmotischen Molekulargewichtsbestimmung erhalten wird. N_1 ist durch die Gleichung:

$$\mathrm{N}_1 = \sum_n \frac{n_{1n}}{\sum n n_{1n} + n_2} \tag{12}$$

definiert. Dann gilt für das Gleichgewicht das Gleichungssystem:

$$\frac{\mathrm{N}_{1n\alpha}}{\mathrm{N}_{1n\beta}} = \exp\left\{(z-2)\frac{n}{2}\frac{\Delta E}{RT} - \frac{z-2}{z} n\left[\left(2 - e^{-E_\alpha/RT}\right)\bar{n}_\alpha \mathrm{N}_{1\alpha} - \left(2 - e^{-E_\beta/RT}\right)\bar{n}_\beta \mathrm{N}_{1\beta}\right]\right\} \tag{13}$$

Wir definieren die Verteilungsfunktion der Polymerisationsgrade $f(n)$ durch die Gleichung:

$$\mathrm{N}_{1n} = \mathrm{N}_1 f(n) \tag{14}$$

beziehungsweise:

$$n_{1n} = n_1 f(n) \tag{14a}$$

Es ist ferner, wenn wir die Masse der Fadenmoleküle vom Polymerisationsgrad n mit m_{1n}, ihr Teilungsverhältnis mit ϑ_n bezeichnen:

$$\mathrm{N}_{1\alpha} = \sum_n \mathrm{N}_{1n\alpha} = \sum_n \frac{V_2}{nM_0}\frac{m_{1n\alpha}}{v_\alpha} = \frac{V_2}{M_0 v_\alpha}\sum_n \frac{m_{1n}}{n}\frac{\vartheta_n}{1+\vartheta_n} \tag{15}$$

Ersetzen wir die Summierung näherungsweise durch eine Integration, so wird mit Gl. (14):

$$\mathrm{N}_{1\alpha} = \frac{V_2}{v_\alpha}\frac{m_1}{\bar{n}M_0}\int_0^\infty f(n)\frac{\vartheta_n}{1+\vartheta_n}\,dn \tag{16}$$

Aus. Gl. (6), (13), und (16) folgt für das Trennungsverhältnis der Fadenmoleküle vom Polymerisationsgrad n:

$$\vartheta_n = \frac{1}{\varphi}\exp\left\{(z-2)\frac{n}{2}\frac{\Delta E}{RT} - \frac{z-2}{z} n \frac{V_2}{M_0}\frac{m_1}{\bar{n}v_\beta}\int_0^\infty \frac{f(n)}{1+\vartheta_n}\left[\left(2 - e^{-E_\alpha/RT}\right)\bar{n}_\alpha \varphi\vartheta_n - \left(2 - e^{-E_\beta/RT}\right)\bar{n}_\beta\right] dn\right\} \tag{17}$$

Da das Integral nicht mehr von n abhängt, ist somit für die polydisperse Lösung bei beliebiger Konzentration, im Gegensatz zu Gl. (5), ln ϑ_n eine lineare Funktion von n wie es bereits Schulz[9] angenommen hat. Dieses Beispiel zeigt deutlich, dass die korrekte Berücksichtigung der Polydispersität von wesentlichem Einfluss auf die Ergebnisse ist. Auch die Abhängigkeit des Teilungsverhältnisses ϑ_n von φ, dem Volumenverhältnis der beiden Phasen, ist die gleiche wie in der Schulz'schen Formel, da nach (6) $\varphi\vartheta_n$ nicht von φ abhängt. Die betreffenden Zusammenhänge sind bereits von Schulz[9] an Hand einer graphischen Darstellung eingehend diskutiert worden. Da dieselbe auch in dem bekannten Buch von Ott[10] wiedergegeben ist, brauchen wir an dieser Stelle nicht darauf einzugehen. Es ist jedoch zu beachten, dass, wenn man die Schulz'sche Formel benutzt, der Exponent von der Verteilungsfunktion der Polymerisationsgrade $f(n)$ abhängt. Auch ist der Zusammenhang mit der Temperatur wesentlich komplizierter als in Gl. (7). Bemerkenswert ist in Gl. (8) und (17) das Auftreten der von Schulz nicht berücksichtigten Entropieterme.

ENTMISCHUNG BINÄRER LÖSUNGEN

Monodisperse Lösung

Wenn sich eine homogene binäre Lösung beim Abkühlen entmischt, haben wir ein Gleichgewicht zwischen zwei binären flüssigen Phasen, welche beide die gleichen Komponenten enthalten. Es ist daher hier noch eine weitere Gleichgewichtsbedingung für das Lösungsmittel zu berücksichtigen und wir haben:

$$\mu_{1\alpha} = \mu_{1\beta} \qquad \mu_{2\alpha} = \mu_{2\beta} \tag{18}$$

Wir müssen hier positive Verdünnungswärme annehmen, da nur unter dieser Bedingung Entmischung eintritt. Ferner stezen wir voraus $E \ll RT$ und entwickeln die Exponentialfunktionen bis zum linearen Glied. Dann wird:

$$\Delta\mu_1 = RT\left\{\ln \mathrm{N}_1 - \ln z + \frac{z-2}{z}\, n^2 \mathrm{N}_1 - (z-2)\frac{n}{2}\frac{E}{RT} + 3\,\frac{z-2}{z}\, n^2 \frac{E}{RT}\, \mathrm{N}_1\right\} \tag{19}$$

Für der das Lösungsmittel haben wir mit Benutzung der Miller'schen Formel[7] für die Verdünnungentropie einer athermischen Lösung:

$$\Delta\mu_2 = RT\left\{\ln(1 - \mathrm{N}_1^*) - \frac{z}{2}\ln\left[1 - \frac{2\mathrm{N}_1^*}{z}\left(1 - \frac{1}{n}\right)\right] - \frac{3}{2}\,\frac{z-2}{z}\,\frac{E}{RT}\,\mathrm{N}_1^{*2}\right\} \tag{20}$$

Mit Gl. (19) und (20) lauten die expliziten Gleichgewichtsbedingungen:

$$\ln \mathrm{N}_{1\alpha} + \frac{z-2}{z}\, n^2\left(1 + 3\,\frac{E}{RT}\right)\mathrm{N}_{1\alpha} = \ln \mathrm{N}_{1\beta} + \frac{z-2}{z}\, n^2\left(1 + 3\,\frac{E}{RT}\right)\mathrm{N}_{1\beta} \tag{21}$$

und:

$$\ln(1-N_{1\alpha}^{*})-\frac{z}{2}\ln\left[1-\frac{2N_{1\alpha}^{*}}{z}\left(1-\frac{1}{n}\right)\right]-\frac{3}{2}\frac{z-2}{z}\frac{E}{RT}N_{1\alpha}^{*2}=$$

$$\ln(1-N_{1\beta}^{*})-\frac{z}{2}\ln\left[1-\frac{2N_{1\beta}^{*}}{z}\left(1-\frac{1}{n}\right)\right]-\frac{3}{2}\frac{z-2}{z}\frac{E}{RT}N_{1\beta}^{*2}\qquad(22)$$

Der kritische Punkt der Entmischung berechnet sich aus den Gleichungen:

$$\partial\Delta\mu_2/\partial N_1^{*}=0\qquad\partial^2\Delta\mu_2/\partial N_1^{*2}=0\qquad(23)$$

Aus (20) und (23) folgt für den kritischen Volumenbruch (wenn höhere Potenzen von $1/n$ vernachlässigt werden):

$$N_{1k}^{*}=n^{-1/2}\,(2-8/z^2)^{-1/2}\qquad(24)$$

Durch Einsetzen dieses Wertes erhält man für die kritische Temperatur der Entmischung:

$$T_k=-3\,\frac{E}{R}\left[1-\frac{z}{z-2}\left(\frac{2-8/z^2}{n}\right)^{1/2}\right]\qquad(25)$$

Gl. (24) und (25) stimmen praktisch überein mit den Formeln, die Flory[5] aus seiner statistischen Theorie, Jenckel[12] aus der statistischen Theorie von Münster[13-15] abgeleitet hat. Letztere gibt die beiden ersten Glieder einer Reihenentwicklung der Miller'schen Funktion. Aus. Gl. (24) folgt, dass die kritische Konzentration bei sehr kleinen Volumenbrüchen (etwa von der Grössenordnung 10^{-1}–10^{-2}, entsprechend den Molenbrüchen 10^{-3}–10^{-6}) liegt. Die kritische Temperatur steigt nach Gl. (25) mit dem Polymerisationsgrad an. Beide Folgerungen sind von Jenckel[12] an den Systemen Polystyrol-Octadecylalkohol, Polyvinylacetat-Octadecylalkohol und Polyvinyloctadecyläther-Isoamylalkohol, die erstere auch von Brönsted und Volqvartz[16] an Lösungen von Polystyrol in verschiedenen aliphatischen Estern experimentell bestätigt worden.

Die vollständige Lösung der Gl. (21) und (22), welche die Entmischungskurve liefert, ist sehr umständlich. Wir wollen daher eine auch von Gee[17] benutzte Näherung einführen. Aus Gl. (24) folgt, dass in einiger Entfernung vom kritischen Punkt die verdünnte Phase praktisch nicht mehr vom reinen Lösungsmittel zu unterscheiden ist. Von Brönsted und Volqvartz[16] wurde dies auch direkt experimentell bestätigt. Wir werden daher nur einen geringen Fehler begehen, wenn wir in Gl. (22) für $\mu_{2\alpha}$ das chemische Potential des reinen Lösungsmittels setzen und demgemäss die Gleichgewichtsbedingung (21) vernachlässigen. Physikalisch bedeutet dies, dass wir die Bedingung für das Verschwinden des osmotischen Druckes aufsuchen. Auf diese Weise ergibt sich für die Entmischungstemperatur bei gegebenem Volumenbruch:

$$T_E=\frac{3}{2}\frac{z-2}{z}\frac{E}{R}N_1^{*2}\left\{\ln(1-N_1^{*})-\frac{z}{2}\ln\left[1-\frac{2N_1^{*}}{z}\left(1-\frac{1}{n}\right)\right]\right\}^{-1}\qquad(26)$$

Führen wir den Quellungsgrad der Gelphase:

$$Q = (1/N_1^*) - 1 \tag{27}$$

ein, so erhalten wir für die Quellung einer aus hochpolymeren Fadenmolekülen bestehenden Substanz durch ein Nichtlösungsmittel (wenn $1/n$ gegen 1 vernachlässigt wird):

$$\ln\left(1 + \frac{1}{Q}\right) + \frac{z}{2}\ln\left[1 - \frac{2/z}{(Q+1)}\right] + \frac{3}{2}\,\frac{z-2}{z}\,\frac{E/RT}{(Q+1)^2} = 0 \tag{28}$$

Für geringen Quellungsgrad folgt daraus der einfache Zusammenhang:

$$Q = \left(1 - \frac{2}{z}\right)^{z/2} \exp\left(\frac{3}{2}\,\frac{z-2}{z}\,\frac{E}{RT}\right) \qquad (Q \ll 1) \tag{28a}$$

Aus diesen Beziehungen ergebein sich einige bemerkenswerte Folgerungen. Gl. (26) zeigt zunächst, dass Entmischung nur eintreten kann, wenn $E < 0$, d.h. die Verdünnungswärme positiv ist, was wir zu Beginn schon angenommen hatten; bei negativer Verdünnungswärme hat man unbegrenzte Löslichkeit. Oberhalb der kritischen Temperatur gilt dies auch bei positiver Verdünnungswärme. Mit dem Erreichen der kritischen Temperatur sinkt nach Gl. (24) die Löslichkeit sprunghaft auf einen kleinen Wert und dann stetig auf praktisch Null. Damit erklärt sich die bekannte Tatsache, das hochpolymere Substanzen entweder unbegrenzt löslich oder praktisch unlöslich sind. Andererseits wirkt aber, wie sich aus Gl. (28) ergibt, auch jedes Nichtlösungsmittel mehr oder weniger stark quellend. Man kann also nicht aus der Tatsache der begrenzten Quellung auf durch Haupt- oder Nebenvalenzen gebildete stabile Netzstruktur schliessen, wie dies gelegentlich geschehen ist.[18] Es kann sich vielmehr um eine Erscheinung handln, die als solche von der molekularen Struktur unabhängig ist und sich in analoger Weise auch bei niedrig molekularen Systemen findet. Nur die enorme Viskosität der Gelphase und die Tatsache, dass die Gleichgewichtsflüssigkeit nahezu reines Lösungsmittel ist, sind durch die hochpolymere Struktur (aber nicht durch Vernetzung) bedingt. Zwar werden sich die Fadenmoleküle in der Gelphase dauernd an zahlreichen Stellen berühren; aber diese "Haftpunkte" wechseln statistisch wie die Bindungen in einem Flüssigkeitsgemisch. Aus Gl. (28) folgt schliesslich, dass die Zusammensetzung der Gelphase bzw. der Quellungsgrad praktisch unabhängig vom Polymerisationsgrad ist. Dieser Satz wurde bereits von Gee[19] ausgesprochen. Gl. (28) ist auch von praktischem Interesse, da sie die Resistenz eines hochpolymeren Stoffes gegen Quellung formuliert. Sie ist umso besser, je grösser $-E$ ist, dagegen unabhängig vom Polymerisationsgrad, sofern es sich überhaupt um einen hochpolymeren Stoff ($n \gg 1$) handelt.

In Abb. 1 ist die Entmischungstemperatur als Funktion des Volumenbruches nach Gl. (24), (25), und (26) dargestellt. Dabei ist zwischen $N_1^* = 0.2$ und N_{1k}^* bzw. $N_1^* = 0.3$ und N_{1k}^* interpoliert, da Gl. (26) naturgemäss in der Nähe des kritischen Punktes versagt. Abb. 2 zeigt ein experimentelles Beispiel aus den Messungen von Brönsted und Volqvartz.[16]

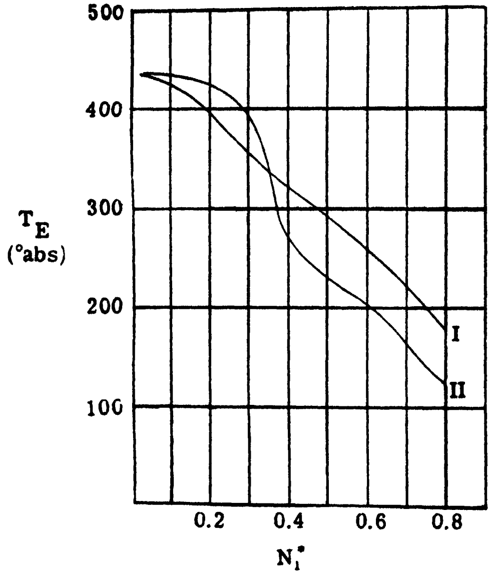

Abb. 1. Entmischungstemperaturen nach Gl. (24), (25), und (26). $E = -300$ cal., $n = 1000$. Kurve I: $z \to \infty$, $T_k = 435°$ abs., $N_{1k}^* = 0.0224$. Kurve II: $z = 4$, $T_k = 435°$ abs., $N_{1k}^* = 0.0258$.

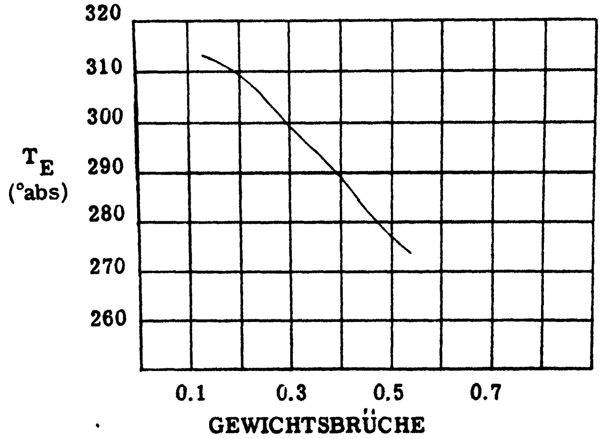

Abb. 2. Entmischungstemperaturen des Systems Polystyrol-*n*-Propyl-Laurat nach Messungen von Brönsted und Volqvartz.[16]

Man sieht, dass die für $z = 4$ berechnete Kurve einen wesentlich anderen Verlauf zeigt als die experimentell ermittelte. Dagegen gibt die nach der Flory'schen Näherung ($z \to \infty$) berechnete Kurve den allgemeinen Charakter, insbesondere die wechselnde Steigung der experimentellen Kurve gut wieder. Möglichkerweise hängt dies damit zusammen, dass in Flüssigkeiten über grössere Temperaturbereiche ein endlicher z-Wert nicht definiert werden kann. Auch der Absolutbetrag des Temperaturkoeffizienten der Löslichkeit liegt bei Abb. 1, Kurve I in der richtigen Grössenordnung. Es ist allerdings etwa 3–4 mal so gross wie in Abb. 2, doch haben sowohl Brönsted und Volqvartz[16] wie Jenckel[12] an anderen Systemen grössere Werte gemessen. Die Experimente über die Entmischung binärer Lösungen stellen daher eine neue eindrucksvolle Bestätigung der statistischen Theorie der hochmolekularen Lösungen dar.

Polydisperse Lösung

Die expliziten Gleichgewichtsbedingungen lauten hier:

$$\ln \mathrm{N}_{1n\alpha} + \frac{z-2}{z}\, n\bar{n}_\alpha \left(1 + 3\,\frac{E}{RT}\right) \mathrm{N}_{1\alpha} =$$

$$\ln \mathrm{N}_{1\beta} + \frac{z-2}{z}\, n\bar{n}_\beta \left(1 + 3\,\frac{E}{RT}\right) \mathrm{N}_{1\beta} \qquad (n \geq 1) \qquad (29)$$

und:

$$\ln\,(1 - \mathrm{N}^*_{1\alpha}) - \frac{z}{2} \ln \left[1 - \frac{2\mathrm{N}^*_{1\alpha}}{z}\left(1 - \frac{1}{\bar{n}_\alpha}\right)\right] - \frac{3}{2}\,\frac{z-2}{z}\,\frac{E}{RT}\,\mathrm{N}^{*2}_{1\alpha} =$$

$$\ln\,(1 - \mathrm{N}^*_{1\beta}) - \frac{z}{2} \ln \left[1 - \frac{2\mathrm{N}^*_{1\beta}}{z}\left(1 - \frac{1}{\bar{n}_\beta}\right)\right] - \frac{3}{2}\,\frac{z-2}{z}\,\frac{E}{RT}\,\mathrm{N}^{*2}_{1\beta} \qquad (30)$$

wo:

$$\mathrm{N}^*_{1\alpha} = \bar{n}_\alpha \mathrm{N}_{1\alpha} = \sum_n \frac{n n_{1n\alpha}}{\sum n n_{1n\alpha} + n_{2\alpha}} \qquad (31)$$

ist und $\bar{n}_\alpha$ das Zahlenmittel der Polymerisationsgrade in der α-Phase bedeutet. Da wir im vorhergehenden Abschnitt für unsere Überlegungen nur das chemische Potential des Lösungsmittels benutzt haben, folgt aus Gl. (30), dass unter der Voraussetzung $\mathrm{N}_{1\alpha} \rightarrow 0$ alle früheren Formeln ihre Gültigkeit behalten, wenn wir $\mathrm{N}^*_{1\alpha}$ durch Gl. (31) definieren und n durch $\bar{n}$ ersetzen. Das besagt, dass die betreffenden Eigenschaften unabhängig von der Verteilung der Polymerisationsgrade sind. Streng gilt dies allerdings nur für den kritischen Punkt selbst, für die Entmischungskurve nur insoweit, als die zu Gl. (26) führende Näherung brauchbar ist. Praktisch dürfte eine Abhängigkeit von der Polydispersität kaum in Betracht kommen.

ENTMISCHUNG TERNÄRER LÖSUNGEN

Monodisperse Lösung

Es sei E_{11} die Wechselwirkungsenergie zweier Bausteine verschiedener Fadenmoleküle, E_{33} die zweier Moleküle des Fällungsmittels und E_{13} die

Wechselwirkungsenergie eines Bausteins mit einem Molekül des Fällungsmittel. Alle diese Energien sind auf die in Bezug auf die Fadenmoleküle und das Fällungsmittel unendlich verdünnte Lösung normiert. Wir setzen für alle Energieparameter $E \ll RT$ voraus. Da wir uns hier auf isotherme Probleme beschränken, bedeutet dies lediglich eine Vereinfachung der Schreibweise. Die Ergebnisse werden davon nicht berührt. Die auf die Reinen Komponenten bezogenen chemischen Potentiale sind dann:

$$\Delta\mu_1 = RT\left\{\ln \mathrm{N}_1^* - \ln nz + \frac{z-2}{z} n\mathrm{N}_1^* - (z-2)\frac{n}{2}\frac{E_{11}}{RT} + \frac{z-2}{z} n\left(\frac{E_{11}}{RT}\mathrm{N}_1^* + \frac{1}{2}\frac{E_{13}}{RT}\mathrm{N}_3^*\right)\right\} \tag{32}$$

$$\Delta\mu_2 = RT\left\{\ln \mathrm{N}_2^* - \frac{z}{2}\ln\left[1 - \frac{2\mathrm{N}_1^*}{z}\left(1 - \frac{1}{n}\right)\right] + \frac{1}{2}\frac{z-2}{z}\left(\frac{E_{11}}{RT}\mathrm{N}_1^{*2} + \frac{E_{13}}{RT}\mathrm{N}_1^*\mathrm{N}_3^*\right) + \frac{z}{2}\frac{E_{33}}{RT}\mathrm{N}_3^{*2}\right\} \tag{33}$$

$$\Delta\mu_3 = RT\left\{\ln \mathrm{N}_3^* - \frac{z}{2}\ln\left[1 - \frac{2\mathrm{N}_1^*}{z}\left(1 - \frac{1}{n}\right)\right] - \frac{z}{2}\frac{E_{33}}{RT} + \frac{1}{2}\frac{z-2}{z}\frac{E_{13}}{RT}\mathrm{N}_1^* + z\frac{E_{33}}{RT}\mathrm{N}_3^*\right\} \tag{34}$$

Für ein Gleichgewicht zwischen zwei ternären Phasen lauten die Gleichgewichtsbedingungen:

$$\begin{aligned} \mu_{1\alpha} &= \mu_{1\beta} \\ \mu_{2\alpha} &= \mu_{2\beta} \\ \mu_{3\alpha} &= \mu_{3\beta} \end{aligned} \tag{35}$$

Das aus Gl. (32)–(35) folgende Gleichungssystem ist praktisch unlösbar. Versuche von Schulz und Jirgensons[1] sowie von Brönsted und Volqvartz haben nun gezeigt, dass auch bei ternären Systemen die eine Phase praktisch frei von Fadenmolekülen ist. Wir können daher auch hier eine analoge Näherung wie bei den binärem System anwenden und die erste der Gl. (35) unberücksichtigt lassen. Wir haben somit die expliziten Gleichgewichtsbedingungen (wenn der Index β die Gelphase bezeichnet):

$$\ln \mathrm{N}_{2\alpha}^* + \frac{z}{2}\frac{E_{33}}{RT}\mathrm{N}_{3\alpha}^{*2} = \ln \mathrm{N}_{2\beta}^* - \frac{z}{2}\ln\left[1 - \frac{2\mathrm{N}_{1\beta}^*}{z}\left(1 - \frac{1}{n}\right)\right] + \frac{1}{2}\frac{z-2}{z}\left(\frac{E_{11}}{RT}\mathrm{N}_{1\beta}^{*2} + \frac{E_{13}}{RT}\mathrm{N}_{1\beta}^*\mathrm{N}_{3\beta}^*\right) + \frac{z}{2}\frac{E_{33}}{RT}\mathrm{N}_{3\beta}^{*2} \tag{36}$$

und:

$$\ln N^*_{3\alpha} - \frac{z}{2}\frac{E_{33}}{RT} + z\frac{E_{33}}{RT}N^*_{3\alpha} = \ln N^*_{3\beta} - \frac{z}{2}\ln\left[1 - \frac{2N^*_{1\beta}}{z}\left(1 - \frac{1}{n}\right)\right] - \frac{z}{2}\frac{E_{33}}{RT} + \frac{1}{2}\frac{z-2}{z}\frac{E_{13}}{RT}N^*_{1\beta} + z\frac{E_{33}}{RT}N^*_{3\beta} \quad (37)$$

Wir wollen diese noch immer ziemlich komplizierten Gleichungen nur für den Spezialfall diskutieren, dass $E_{11} = E_{33} = 0$ ist. Physikalisch bedeutet diese Annahme, dass die Lösungen der Komponente 1 (Fadenmoleküle) bzw. 3 (Fällungsmittel) in 2 (Lösungsmittel) keine Verdünnungswärme zeigen. Subtrahiert man (37) von (36) und eliminiert in (37) $N^*_{3\alpha}$ so ergibt sich:

$$(1 - N^*_{1\beta} - N^*_{3\beta}) \exp\left[\frac{1}{2}\frac{z-2}{z}\frac{E_{13}}{RT}(N^*_{3\beta} - 1)N^*_{1\beta}\right] + N^*_{3\beta} = \left[1 - \frac{2N^*_{1\beta}}{z}\left(1 - \frac{1}{n}\right)\right]^{z/2} \exp\left[-\frac{1}{2}\frac{z-2}{z}\frac{E_{13}}{RT}N^*_{1\beta}\right] \quad (38)$$

Diese Gleichung gibt den Zusammenhang zwischen den Konzentrationen der Fadenmoleküle und des Fällungsmittels in der Gelphase. Die Zusammensetzung der α-Phase kann dann nach Gl. (37) berechnet werden.

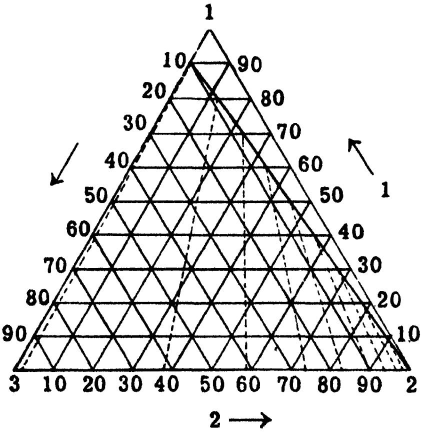

Abb. 3. Entmischung einer ternären Lösung nach Gl. (36) und (37) für $E_{11} = E_{33} = 0$, $E_{13} = 3000$ cal., $T = 298°$ abs., $n = 1000$, $z = 4$. Konzentrationen in Volumprozenten.

In Abb. 3 ist das Entmischungsdiagramm eines ternären Systems nach Gl. (36) und (37) für $E_{11} = E_{33} = 0$ dargestellt. In seinem allgemeinen Charakter entspricht es dem von Schulz und Jirgensons[1] sowie Brönsted und Volqvartz experimentell gefundenen Diagrammen. Insbesondere wird die von den genannten Autoren gefundene Tatsache, richtig wiedergegeben, dass das Fällungsmittel in der Solphase angereichert ist.* In Tabelle I ist dieser Effekt in Zahlen dargestellt.

TABELLE I

ANREICHERUNG DES FÄLLUNGSMITTELS IN DER SOLPHASE NACH GL. (37) UND (38)

$N^*_{1\beta}$	$N^*_{2\beta}/N^*_{3\beta}$	$N^*_{2\alpha}/N^*_{3\alpha}$
0.1	89.0	76.0
0.2	39.0	30.3
0.3	22.4	15.4
0.4	14.0	9.0
0.5	9.0	4.89
0.6	5.66	1.85
0.7	3.23	1.44
0.8	1.47	0.61
0.9	0.05	0.02

Auffallend ist in Abb. 3, dass sich das Gebiet der vollständigen Mischbarkeit in Richtung auf höhere Konzentrationen der Fadenmoleküle verbreitert. Ein derartiges Verhalten ist verhältnismässig selten, aber von Brönsted und Volqvartz an dem System Polystyrol-Propyllaurat-Äthyllaurat tatsächlich beobachtet worden. Dies ist umso bemerkenswerter, als zum mindesten die Voraussetzung $E_{33} = 0$ hier mit einiger Annäherung erfüllt ist. Aus Gl. (37) und (38) folgt schliesslich noch, dass für hinreichend grosse n der Verlauf der Entmischungskurve unabhängig vom Polymerisationsgrad ist. Auch dies ist von Brönsted und Volqvartz experimentell bestätigt worden.

Polydisperse Lösung. Fraktionierte Fällung

In analoger Weise wie bei binären Lösungen kann auch hier gezeigt werden, dass die Ableitungen des vorhergehenden Abschnittes mit hinreichender Genauigkeit für polydisperse Lösungen gelten. Es ist indessen nicht möglich, auf diesem Wege zu einer Theorie der fraktionierten Fällung zu gelangen, denn hier befindet sich über einen weiten Bereich eine verdünnte Lösung der Fadenmoleküle im Gleichgewicht mit der Gelphase. Dieser Widerspruch ist, wie schon Schulz und Jirgensons[1] bemerkt haben, wahrscheinlich dadurch zu erklären, dass der im vorhergehenden Abschnitt benutzte Ansatz ein Grenzgesetz für unendliche hohe Polymerisationsgrade darstellt. Brönsted und Volqvartz bemerken ausdrücklich, dass sie die kritischen Punkte mit der höchstmolekularen ihrer Polystyrolfraktionen bestimmt haben.

Für ein System aus zwei polydispersen ternären Phasen lauten die Gleichgewichtsbedingungen:

$$\begin{aligned} \mu_{1n\alpha} &= \mu_{1n\beta} \quad (n \geq 1) \\ \mu_{2\alpha} &= \mu_{2\beta} \\ \mu_{3\alpha} &= \mu_{3\beta} \end{aligned} \tag{39}$$

Eine vollständige Lösung dieses Gleichungssystems kommt hier naturgemäss noch weniger in Betracht als in den vorher behandelten Fällen. Es ist indessen möglich, lediglich aus den Gleichgewichtsbedingungen für die Fadenmoleküle einige bemerkenswerte Folgerungen abzuleiten.

Für das chemische Potential der Fadenmoleküle vom Polymerisationsgrad n gilt hier:

$$\Delta\mu_{1n} = RT\left\{\ln \mathrm{N}_{1n}^{*} - \ln nz + \frac{z-2}{z} n\mathrm{N}_{1}^{*} - (z-2)\frac{n}{2}\frac{E_{11}}{RT} + \frac{z-2}{z} n\left(\frac{E_{11}}{RT}\mathrm{N}_{1}^{*} + \frac{1}{2}\frac{E_{13}}{RT}\mathrm{N}_{3}^{*}\right)\right\} \tag{40}$$

Daraus folgt mit (39):

$$\frac{\mathrm{N}_{1n\alpha}}{\mathrm{N}_{1n\beta}} = \exp\left\{\frac{z-2}{z} n\left[\left(1+\frac{E_{11}}{RT}\right)\left(\mathrm{N}_{1\beta}^{*} - \mathrm{N}_{1\alpha}^{*}\right) - \frac{1}{2}\frac{E_{13}}{RT}\mathrm{N}_{3\alpha}^{*}\left(1 - \frac{\mathrm{N}_{3\beta}^{*}}{\mathrm{N}_{3\alpha}^{*}}\right)\right]\right\} \tag{41}$$

Auf Grund der Ergebnisse des vorhergehenden Abschnitts vernachlässigen wir $\mathrm{N}_{1\alpha}^{*}$ gegen $\mathrm{N}_{1\beta}^{*}$ und $\mathrm{N}_{3\beta}^{*}/\mathrm{N}_{3\alpha}^{*}$ gegen 1. Mit der Beziehung:

$$\frac{f(n)_{\beta}}{f(n)_{\alpha}} = \frac{n_{1\alpha} f(n)_{\beta}}{n_{1} f(n) - n_{1\beta} f(n)_{\beta}} \tag{42}$$

erhalten wir dann:

$$f(n)_{\beta} = \frac{\mathrm{N}_{1\alpha} n_{1} f(n)}{\mathrm{N}_{1\beta} n_{1\alpha} \exp\left\{\frac{z-2}{z} n\left[\left(1+\frac{E_{11}}{RT}\right)\mathrm{N}_{1\beta}^{*} - \frac{1}{2}\frac{E_{13}}{RT}\mathrm{N}_{3\alpha}^{*}\right]\right\} + \mathrm{N}_{1\alpha} n_{1\beta}} \tag{43}$$

Für das weitere setzen wir zur Abkürzung:

$$g \equiv \frac{z-2}{z}\left(1+\frac{E_{11}}{RT}\right) \qquad h \equiv \frac{1}{2}\frac{z-2}{z}\frac{E_{13}}{RT} \tag{44}$$

Wir multiplizieren jetzt Gl. (43) mit $n\,dn$ und integrieren über alle Polymerisationsgrade. Damit wird:

$$\mathrm{N}_{1\beta}^{*} = \frac{n_{1}}{n n_{1\alpha} + n_{2\alpha} + n_{3\alpha}} \int_{0}^{\infty} n f(n)\left[\exp\left\{n\left(g\mathrm{N}_{1\beta}^{*} - h\mathrm{N}_{3\alpha}^{*}\right)\right\} + \varphi\right]^{-1} dn \tag{45}$$

Für die meisten Fälle können wir das Volumen der Phase ohne grossen Fehler mit dem Gesamtvolumen identifizieren. Bezeichnen wir den gesamten Volumenbruch der Fadenmoleküle mit N_{1}^{*} so erhalten wir für den Volumenbruch der Fällung, die durch Zusatz einer dem Volumenbruch $\mathrm{N}_{3\alpha}^{*}$ entsprechenden Menge Fällungsmittel entsteht.

$$\mathrm{N}_{1\beta}^{*} = (\mathrm{N}_{1}^{*}/\bar{n}) \int_{0}^{\infty} n f(n)\left[\exp\left\{n\left(g\mathrm{N}_{1\beta}^{*} - h\mathrm{N}_{3\alpha}\right)\right\} + \varphi\right]^{-1} dn \tag{46}$$

Der Bruchteil der Gesamtmasse der Fadenmoleküle, der in die Fällung geht, sei:

$$\mu^*_{1\beta} \equiv m_{1\beta}/m_1 = (\mathrm{N}^*_{1\beta}/\mathrm{N}^*_1)\varphi \tag{47}$$

Aus Gl. (46) und (47) folgt:

$$\mu^*_{1\beta} = (\varphi/\bar{n}) \int_0^\infty nf(n)\left[\exp\left\{n(g\mathrm{N}^*_{1\beta} - h\mathrm{N}^*_{3\alpha})\right\} + \varphi\right]^{-1} dn \tag{48}$$

Aus dieser Beziehung ergibt sich, dass zwar ein Zusammenhang besteht zwischen dem gefällten Massenbruchteil der Fadenmoleküle und der Menge des zugesetzten Fällungsmittels, aber nicht zwischen $\mu^*_{1\beta}$ und dem Polymerisationsgrade n. Es ist daher prinzipiell unmöglich, ohne zusätzliche Annahmen aus Fällungsversuchen die Verteilungsfunktion der Polymerisationsgrade des Ausgangsproduktes exakt zu ermitteln. Die Frage, in welcher Weise durch zweckmässige Hilfsannahmen trotzdem eine angenäherte Bestimmung von $f(n)$ erreicht werden kann, wird in einer späteren Arbeit diskutiert werden.

Für die Verteilungsfunktion der Polymerisationsgrade in der Fällung folgt aus Gl. (43):

$$f(n)_\beta = \frac{f(n)\left[\exp\left\{n(g\mathrm{N}^*_{1\beta} - h\mathrm{N}_{3\alpha})\right\} + \varphi\right]^{-1}}{\int_0^\infty f(n)\left[\exp\left\{n(g\mathrm{N}^*_{1\beta} - h\mathrm{N}_{3\alpha})\right\} + \varphi\right]^{-1} dn} \tag{49}$$

Wir führen jetzt die Massenverteilungsfunktion:

$$\psi(n) = (n/\bar{n})f(n) \tag{50}$$

ein. Sie gibt die Gewichtsmenge von Fadenmolekülen des Polymerisationsgrades n die in 1 g. Substanz enthalten sind. Damit wird aus (49):

$$\psi(n)_\beta = \frac{\bar{n}}{\bar{n}_\beta} \frac{\psi(n)\left[\exp\left\{n(g\mathrm{N}^*_{1\beta} - h\mathrm{N}^*_{3\alpha})\right\} + \varphi\right]^{-1}}{\int_0^\infty (\bar{n}/\bar{n})\,\psi(n)\left[\exp\left\{n(g\mathrm{N}^*_{1\beta} - h\mathrm{N}^*_{3\alpha})\right\} + \varphi\right]^{-1} dn} \tag{51}$$

Wegen:

$$\bar{n}_\beta = \int_0^\infty nf(n)_\beta\, dn \tag{52}$$

folgt daraus mit Gl. (48) und (49) für die Massenverteilungsfunktion der Fällung:

$$\psi(n)_\beta = (\varphi/\mu^*_{1\beta})\psi(n)\left[\exp\left\{n(g\mathrm{N}^*_{1\beta} - h\mathrm{N}^*_{3\alpha})\right\} + \varphi\right]^{-1} \tag{53}$$

Diese Funktion bezieht sich auf 1 g. gefällte Substanz. Für Fraktionierungsprobleme ist es günstiger, die Funktion auf 1 g. Ausgangssubstanz zu beziehen. Bezeichnen wir die in dieser Weise normierte Massenverteilungsfunktion mit $\psi^*(n)$ und führen noch die Abkürzung ein:

$$\delta \equiv g\mathrm{N}^*_{1\beta} - h\mathrm{N}^*_{3\alpha} \tag{54}$$

so wird:

$$\psi^*(n) = \psi(n) \cdot 1/(\varphi^{-1}e^{\delta n} + 1) \tag{55}$$

Diese Gleichung bildet die Grundlage für die Theorie der fraktionierten Fällung. Die Grösse δ kann nach Gl. (54) sowohl positiv wie negativ sein. Aus Gl. (55) folgt indessen, dass eine Fraktionierung im üblichen Sinne, bei welcher die jeweils höchstmolekularen Anteile zuerst ausfallen, nur möglich ist, wenn $\delta < 0$ ist. Wenn dagegen $\delta > 0$ ist, so werden die niedrigmolekularen Anteile zuerst gefällt. Dieser Effekt ist von Morey und Tamblyn[3,21] an den Systemen Celluloseacetobutyrat-Aceton-Isopropyläther, Celluloseacetobutyrat-Pyridin-Isopropyläther, Celluloseacetobutyrat-Eisessig-Isopropyläther tatsächlich aufgefunden und als "reverse order precipitation" bezeichnet worden. Mark[22] hat ihn ebenfalls an Lösungen von Celluloseacetobutyraten beobachtet. Wir selbst haben den Effekt an dem System Cellulosetriacetat-Tetrachloräthan-Petroläther nachweisen können. Ob eine "reverse order precipitation" eintritt kann nur das Experiment entscheiden. Aus der Theorie lässt sich aber entnehmen, welche Umstände ihr Auftreten begünstigen. Berücksichtigen wir, dass (wie an anderer Stelle gezeigt wird) stets $E_{13} > 0$ und nach Gl. (46) $N_{1\beta}^*$ proportional der Ausgangskonzentration N_1^* ist, so folgt aus Gl. (44) und (54), dass umso eher $\delta > 0$ wird und damit "reverse order precipitation" eintritt, je höher die Konzentration der Ausgangslösung und je kleiner E_{13}, die "Fällungskraft" des Fällungsmittels ist. Indessen ist die "reverse order precipitation" nicht eine einfache Umkehrung der normalen Fällung, sondern ein ganz andersartiger Vorgang. Im letzteren Falle ist nämlich nach Gl. (55):

$$\text{für } n \longrightarrow \infty \ \psi^*(n)/\psi(n) \longrightarrow 1$$

$$\text{für } n \longrightarrow 0 \ \psi^*(n)/\psi(n) \longrightarrow \varphi/(1 + \varphi),$$

sodass die höchstmolekularen Anteile praktisch quantitativ ausfallen, während bei geeigneter Wahl von $\varphi (\varphi \ll 1)$ kaum niedrigmolekulare Anteile in der Fällung enthalten sind. Dagegen ist bei "reverse order precipitation":

$$n \longrightarrow 0 \ \psi^*(n)/\psi(n) \longrightarrow \varphi/(1 + \varphi)$$

sodass nur ein Bruchteil der niedrigmolekularen Anteile mit der ersten Fraktion ausfällt und diese auch in den folgenden Fraktionen in erheblicher Menge enthalten sind. Dies hat zur Folge, dass die ersten Fraktionen sich nur relativ wenig in ihrem mittleren Polymerisationsgrad unterscheiden und sehr stark polydispers sind. Da nach G. (44), (46), (54), und (55) für $N_1^* \rightarrow 0$ jedenfalls normale Fällung stattfindet und die Lösung sich im Laufe einer Fraktionierung zunehmend verdünnt, muss mit fortschreitender Fraktionierung ein Umschlag von "reverse order precipitation" zu normaler Fällung eintreten. Die Folge der mittleren Molekulargewichte der Fraktionen durchläuft also mindestens ein Maximum. Der Umschlag zu normaler Fällung kann sich durch einen Sprung in der

Folge der mittleren Molekulargewichte markieren, doch muss dies nicht unter allen Umständen zutreffen. Bereits vor dem Umschlag kann ein zweites Maximum auftreten wenn in diesem Gebiet $\partial\delta/\partial N^*_{3\alpha} > 0$ wird.

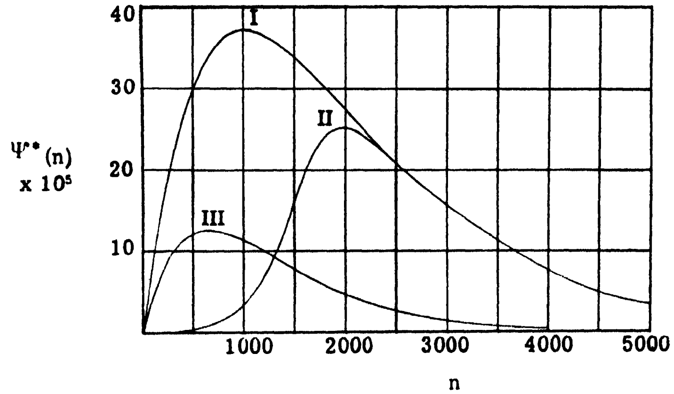

Abb. 4. Massenverteilungsfunktion einer Fraktion bei normaler Fällung und "reverse order precipitation." Ausgangsprodukt mit Kuhn'scher Verteilung. Kurve I: Ausgangsprodukt, $a = 10^{-3}$. Kurve II: Fraktion bei normaler Fällung, $\delta = -4.6 \times 10^{-3}$; $\varphi = 10^{-3}$. Kurve III: Fraktion bei "reverse order precipitation," $\delta = 8 \times 10^{-4}$; $\varphi = 1$.

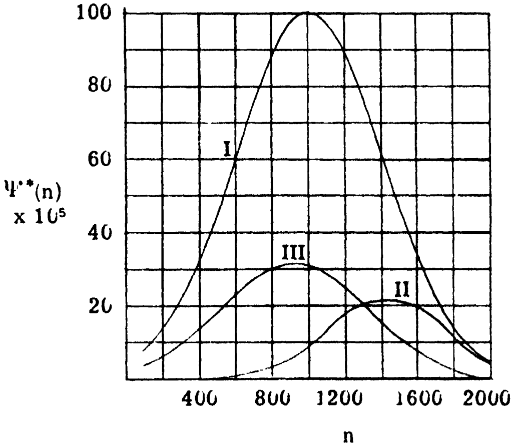

Abb. 5. Massenverteilungsfunktion einer Fraktion bei normaler Fällung und "reverse order precipitation." Ausgangsprodukt mit Gauss'scher Verteilung. Kurve I: Ausgangsprodukt, $k = 10^{-5}$; $n_{max.} = 10^3$. Kurve II: Fraktion bei normaler Fällung, $\delta = -4 \times 10^{-3}$; $\varphi = 10^{-3}$. Kurve III: Fraktion bei "reverse order precipitation," $\delta = 8 \times 10^{-4}$; $\varphi = 1$.

In Abb. 4 ist die erste Fraktion eines Ausgangsproduktes bei normaler Fällung und "reverse order precipitation" dargestellt. Dabei ist für das

Ausgangsprodukt die von Kuhn[23] berechnete Verteilungsfunktion abgebauter Fadenmoleküle:

$$\psi(n) = na^2(1 - a)^n \tag{56}$$

angenommen worden, wo a den Bruchteil der aufgespaltenen Bindungen bezeichnet. In Abb. 5 ist die gleiche Darstellung für ein Ausgangsprodukt mit Gauss'scher Verteilung:

$$\psi(n) = k \exp\left[-\pi k(n - n_{max})^2\right] \tag{57}$$

gegeben, wo n_{max} der dem Maximum von $\psi(n)$ entsprechende Wert von n und k eine Konstante ist. Der völlig verschiedene Charakter der Fraktionen bei normaler Fällung und "reverse order precipitation" ist aus den Kurven deutlich zu ersehen. Im letzteren Falle ist die Verteilung der Fraktion nahezu ein verkleinertes Abbild der Verteilung des Ausgangsproduktes. Abb. 6 zeigt den Verlauf einer Fraktionierung bei "reverse order precipitation." (Die letzten zwei Fraktionen sind der Übersichtlichkeit halber fortgelassen.) Man sieht daraus, wie stark die Fraktionen polydispers sind und sich gegenseitig überschneiden. In Tabelle II sind

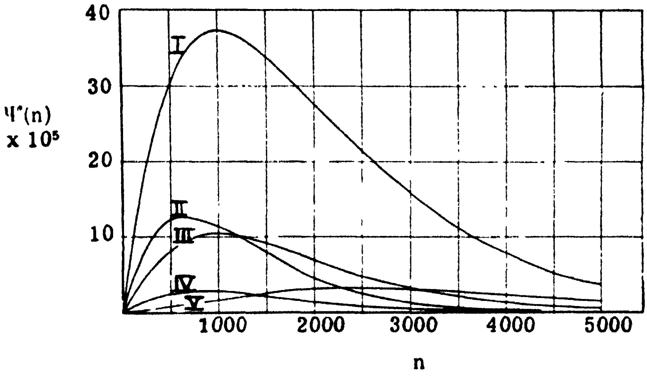

Abb. 6. Fraktionierung bei "reverse order precipitation." Kurve I: Ausgangsprodukt (Kuhn'sche Verteilung). Kurve II: 1. Fraktion. Kurve III: 2. Fraktion. Kurve IV: 3. Fraktion. Kurve V: 4. Fraktion, Parameterwerte siehe Tab. II.

TABELLE II

Fraktionierung bei "Reverse Order Precipitation"

	δ	φ	$\bar{n}$
Ausgangsprodukt	—	—	1073
Fraktion 1	$8\ 10^{-4}$	1	665
Fraktion 2	$4\ 10^{-4}$	1	945
Fraktion 3	8.10^{-4}	5×10^{-1}	779
Fraktion 4	-5.10^{-4}	1×10^{-1}	1760
Fraktion 5	-4.10^{-3}	1×10^{-2}	1890
Fraktion 6	—	—	560

die benutzten Parameterwerte und die mittleren Molekulargewichte der Fraktionen zusammengestellt.

Man sieht daraus, dass die ersten Fraktionen sich nur wenig in ihrem mittleren Polymerisationsgrad unterscheiden und dass die Folge der Molekulargewichte zwei Maxima durchläuft.

Die vorstehenden Folgerungen aus der Theorie werden durch die Experimente ausgezeichnet bestätigt. Dass bei hinreichender Verdünnung stets normale Fällung eintritt, haben Morey und Tamblyn[3] durch Versuche mit fraktionierten Produkten gezeigt. Ein geeignetes Mass für die "Fällungskraft" ist der Volumenbruchteil von Fällungsmittel, der bis zum Auftreten der ersten Trübung zugesetzt werden muss; er ist, wie an anderer Stelle gezeigt wird, proportional $1/E_{13}$. Während etwa eine, 0.5%ige Lösung von Nitrocellulose in Aceton sich schon bei Zusatz von *ca.* 10% Wasser trübt, muss man zu einer 1%igen Lösung von Cellulosetriacetat 45% Petroläther zusetzen, bis die erste Trübung auftritt. Der experimentelle Verlauf einer Fraktionierung bei "reverse order precipitation" besitzt ganz den Charakter, wie er sich aus Abb. 6 und Tabelle II ergibt. Wir zeigen dies zunächst in Tabelle III an einem Beispiel, dass der Arbeit von Morey und Tamblyn[3] entnommen ist.

TABELLE III

FRAKTIONIERUNG EINER 5%IGEN LÖSUNG VON CELLULOSEACETOBUTYRAT IN EISESSIG DURCH FÄLLEN MIT ISOPROPYLÄTHER NACH MOREY UND TAMBLYN[3]

Fraktion No.	$[\eta]_{c=0.25}$	Fraktion No.	$[\eta]_{c=0.25}$
1	1.63	8	1.93
2	1.78	9	1.71
3	1.58	10	1.34
4	1.48	11	1.17
5	2.06	12	0.95
6	2.67	13	0.69
7	2.21		

Die Autoren geben keine Polymerisationsgrade an, sondern nur Viskositäten. Tabelle IV zeigt unsere eigenen Ergebnisse an einem Linters-Triacetat vom viskosimetrischen Durchschnittspolymerisationsgrad DP = 446. Die Tabelle gibt viskosimetrische Durchschnittspolymerisationsgrade.

TABELLE IV

FRAKTIONIERUNG EINER 1%IGEN LÖSUNG VON LINTERS-TRIACETAT IN TETRACHLORÄTHAN DURCH FÄLLEN MIT PETROLÄTHER

Fraktion	DP	Fraktion	DP
A 417/4a	426	A 417/4d	412
A 417/4b	438	A 417/4e	425
A 417/4c	416	A 417/4f	403

Tabelle V enthält die entsprechenden Daten für ein Triacetat aus veredeltem Fichtenzellstoff vom viskosimetrischen Durchschnittspolymerisationsgrad DP = 568.

TABELLE V

FRAKTIONIERUNG EINER 1%IGEN LÖSUNG VON FICHTENZELLSTOFF-TRIACETAT IN TETRACHLORÄTHAN DURCH FALLEN MIT PETROLÄTHER

Fraktion	DP	Fraktion	DP
A 396/1a	353	A 396/1d	341
A 396/1b	397	A 396/1e	336
A 396/1c	390	A 396/1f	235

TABELLE VI

FRAKTIONIERUNG EINER 1%IGEN LOSUNG VON LINTERS-2$^1/_2$-ACETAT IN ACETON DURCH FÄLLEN MIT PETROLÄTHER

Fraktion	DP	Fraktion	DP
40/1a	654	40/1d	178
40/1b	622	40/1e	53
40/1c	390		

Bemerkenswert ist in diesem Zusammenhang, dass das System Cellulose-2$^1/_2$ Acetat-Aceton-Petroläther in 1%iger Lösung normale Fällung zeigt. Die betreffenden Daten sind in Tabelle VI zusammengestellt.

Aus den vorstehenden Untersuchungen ergibt sich, dass Systeme mit "reverse order precipitation" weder zur Gewinnung einheitlicher Fraktionen noch zur Ermittlung der Verteilung der Polymerisationsgrade im Ausgangsprodukt dienen können.

Morey und Tamblyn[3] haben zur Erklärung der reverse order precipitation einen besonderen Endgruppeneffekt angenommen. Diese Annahme erscheint von vorneherein sehr gekünstelt. Die obigen Rechnungen zeigen, dass sie auch überflüssig ist, denn das Auftreten der "reverse order precipiration" ist eine einfache Folgerung aus der thermodynamisch-statistischen Theorie der polydispersen ternären Systeme.

Literaturvercheichnis

1. G. V. Schulz und B. Jirgensons, *Z. physik. Chem.*, **B46**, 105 (1940).
2. M. Magat, *J. chim. phys.*, **44**, 14 (1947).
3. D. R. Morey und J. W. Tamblyn, *J. Phys. & Colloid Chem.*, **51**, 721 (1947).
4. A. Münster, *Z. Naturforsch.*, **3a**, 158 (1948).
5. P. J. Flory, *J. Chem. Phys.*, **10**, 51 (1942).
6. M. L. Huggins, *J. Phys. Chem.*, **46**, 151 (1942).
7. A. R. Miller, *Proc. Cambridge Phil. Soc.*, **39**, 54, 151 (1943).
8. A. Münster, *Z. Naturforsch.*, **2a**, 284 (1947).
9. G. V. Schulz, *Z. physik. Chem.*, **B46**, 137 (1940).
10. E. Ott, ed., *Cellulose and Cellulose Derivatives.* Interscience, New York, 1943, p. 880.
12. E. Jenckel, *Z. Naturforsch.*, **3a**, 290 (1948).
13. A. Münster, *Kolloid-Z.*, **105**, 1 (1943).

14. A. Münster, *Z. Naturforsch.*, **1**, 311 (1946).
15. A. Münster, *J. makromol. Chem.*, **2**, 227 (1948).
16. J. N. Brönsted, und K. Volqvartz, *Trans. Faraday Soc.*, **35**, 576 (1939).
17. G. Gee, *Quart. Rev. Chem. Soc.*, **1**, 265 (1947).
18. H. Staudinger, *Organische Kolloidchemie.* Braunschweig, 1941.
19. G. Gee, *Trans. Faraday Soc.*, **38**, 276 (1942).
21. D. R. Morey und J. W. Tamblyn, *J. Phys. Chem.*, **50**, 12 (1946).
22. *Nature of the Chemical Components of Wood*, TAPPI Monograph Series No. 6, New York, 1948, p. 87.
23. W. Kuhn, *Ber.*, **63**, 1503 (1930).

English Synopsis, see Summaries, page S8, Vol. V, 1950.

Zusammenfassung

Die Theorie der Löslichkeit hochpolymererFadenmoleküle wird auf der Grundlage der Thermodynamik und der statistischen Theorie der polydispersen Lösung entwickelt. Die Behandlung des Verteilungsgleichgewichtes zwischen zwei nicht mischbaren Lösungsmitteln ergibt für monodisperse Lösungen die von G. V. Schulz angegebene Formel als Grenzgesetz bei unendlicher Verdünnung, während bei endlichen Konzentrationen der Zusammenhang zwischen Teilungsverhältnis und Polymerisationsgrad komplizierter ist. Die Untersuchung der polydispersen Lösung zeigt überraschenderweise, dass hier der von G. V. Schulz postulierte Zusammenhang auch bei endlichen Konzentrationen gilt.

Für die Entmischung einer binären Lösung ergibtsich, dass die kritische Konzentration bei sehr niedrigen Konzentrationen der Fadenmoleküle liegt und dass die kritische Temperatur nur schwach mit dem Polymerisationsgrad ansteigt. Unter der Voraussetzung, dass die Solphase praktisch frei von Fadenmolekülen ist, wird die Entmischungskurve berechnet und eine Formel für den Quellungsgrad in Abhängigkeit von der Temperatur angegeben. Die Theorie erklärt die allgemeinen Löslichkeitseigenschaften hochpolymerer Substanzen und zeigt insbesondere, dass auch Nichtlösungsmittel stets quellend wirken. Eine derartige begrenzte Quellung ist daher nicht durch eine Netzstruktur bedingt. Für hochpolymere Produkte ist die Zusammensetzung der Gelphase bzw. der Quellungsgrad unabhängig vom Polymerisationsgrad. Der Vergleich der theoretischen Entmischungskurve mit den experimentellen Ergebnissen zeigt in allen wesentlichen Zügen eine gute Übereinstimmung. Die Ausdehnung der Untersuchung auf polydisperse Lösungen ergibt, dass die Entmischungskurve praktisch unabhängig von der Verteilung der Polymerisationsgrade ist.

Die Entmischung ternärer Systeme wird zunächst unter der Voraussetzung behandelt, dass die Solphase keine Fadenmoleküle enthält. Für einen Spezialfall wird ein vollständiges Entmischungs-Diagramm berechnet, das gute Übereinstimmung mit experimentellen Ergebnissen von Brönsted und Volqvartz zeigt und insbesondere die Anreicherung des Fällungsmittels in der Solphase wiedergibt. Auch diese Ergebnisse sind für polydisperse Lösungen unabhängig von der Verteilung der Polymerisationsgrade gültig.

Ausgehend von der Gleichgewichtsbedingung für die gelösten Fadenmoleküle wird eine Formel für die Massenverteilungsfunktion einer Fällung abgeleitet. Diese enthält einen Parameter δ, der sowohl positiv wie negativ sein kann. Für $\delta < 0$ beschreibt die Formel die übliche Fraktionierung. Für $\delta > 0$ tritt die von Morey und Tamblyn entdeckte "reverse order precipitation" auf, bei welcher die niedrigmolekularen Anteile zuerst ausfallen. Die Eigenschaften der "reverse order precipitation" werden aus der Theorie in Übereinstimmung mit den experimentellen Ergebnissen entwickelt. Es wird gezeigt, dass die Fraktionen in solchen Fällen sehr stark polydispers sind und sich überschneiden. Systeme mit "reverse order precipitation" sind daher zur Herstellung einheitlicher Fraktionen und zur Ermittlung der Verteilung der Polymerisationsgrade im Ausgangsprodukt unbrauchbar. Es wird über einen neuen Fall von "reverse order precipitation" bei dem System Cellulosetriacetat-Tetrachloräthan-Petroläther berichtet.

Résumé

La théorie de la solubilité des molécules polymères linéaires est développée en se basant sur la thermodynamique et la théorie statistique des solutions polydisperses. Quand on envisage l'équilibre de partage entre deux solvants non miscibles, on retrouve pour des solutions monodisperses la formule donnée par G. V. Schulz, comme formule limite aux dilutions infinies, tandis que pour les concentrations finales le rapport de partage et le degré de polymérisation est plus compliqué. L'examen de solutions polydispersées indique de façon très étonnante, que la relation de Schulz garde sa validité aussi pour les concentrations finales.

Dans le cas de la démixtion d'une solution binaire, la concentration critique est très basse pour les molécules linéaires, et la température critique ne croît que faiblement avec le degré de polymérisation. En supposant que la phase liquide est pratiquement exempte de polymère linéaire, on a calculé la courbe de démixtion et une formule est indiquée pour la dépendance thermique du degré de gonflement. La théorie explique les propriétés de solubilité générales des substances macromoléculaires et montre, en particulier, que des non-solvants agissent toujours comme gonflants.

Un gonflement limité de cette nature n'est pas dû à une structure en réseau. Pour les polymères la composition de la phase gélifiée ainsi que du degré de gonflement sont indépendants du degré de polymérisation. La comparaison de la courbe de démixtion théorique avec les résultats expérimentaux montre dans tous les cas une bonne correspondence. L'extension de cet examen aux solutions polydispersées montre que les courbes de démixtion sont pratiquement indépendants de la répartition des poids moléculaires. La démixtion de systèmes ternaires a été traitée en supposant que la phase-sol ne contient aucune molécule linéaire. Dans un cas particulier, on a calculé un diagramme complet de démixtion il se montre en bon accord avec les résultats expérimentaux de Brönstad et Volqvartz, et en particulier, il rend compte de l'enrichissement en précipitant dans la phase-sol. Ces résultats sont également applicables dans le cas de solutions polydipersées, indépendamment de la répartition des poids moléculaires.

Received May 15, 1949

JOURNAL OF POLYMER SCIENCE VOL. V, NO. 3, PAGES 355-367

Inhibiting Effect of Acrylonitrile on Polymerization of Vinyl Acetate

WILLIAM R. CONN and HARRY T. NEHER, *Rohm & Haas Co., Inc., Philadelphia, Pennsylvania*

In the course of an investigation of the copolymerization in emulsion of vinyl acetate and acrylonitrile, it was observed that mixtures of approximately equal weights of the two monomers polymerized readily, whereas, mixtures containing only 5-10% acrylonitrile failed to polymerize under similar conditions. It was of interest, therefore, to investigate in some detail the influence of various ratios of these two monomers on the course of their polymerization. The investigation showed not only that acrylonitrile retards the polymerization of the mixture, but that this retarding effect increases as the ratio of acrylonitrile to vinyl acetate decreases until, at about 1% concentration in the monomer mixture, acrylonitrile becomes an effective polymerization inhibitor. This effect of increasing inhibition with decreasing acrylonitrile concentration is contrary to the usual behavior of polymerization inhibitors. No satisfactory explanation of this anomalous behavior is apparent to the authors on the basis of the available data, but the effect is believed to be of sufficient general interest to deserve the attention of other workers in the field.

EXPERIMENTAL

Materials

The vinyl acetate was fractionated until it remained colorless on shaking for one minute with Fuchsin reagent. The acrylonitrile, ethyl methacrylate, and styrene were fractionated samples of commercial materials. The methacrylonitrile was fractionated until its refractive index at 20° was 1.4006-1.4008. The acrylic acid, acrylamide, and methacrylamide were prepared in high purity by known methods. The Triton 720, ammonium persulfate, benzoyl peroxide, and ethylene dichloride were of commercial quality; the same lots of each were used throughout this work. Distilled water was used in the emulsion polymerizations.

Apparatus

The emulsion polymerizations were carried out in a three-liter, three-necked flask equipped with a propeller-type agitator, thermometer, a sampling tube reaching near the bottom of the flask, and inlet and outlet tubes for nitrogen. Bubble counters were placed in the inlet and outlet lines. The sampling tube led downward through an eight inch condenser delivering into a 250 cc. Erlenmeyer flask. The flow of nitrogen was measured by a flow-meter containing two orifices, one to indicate the range 3–15 cc. per minute, the other 200–800 cc. per minute. The temperature was controlled by a water bath over a Bunsen burner.

The solution polymerizations were carried out in the same apparatus but with a stirrer consisting of a glass rod bent in a semicircle.

Emulsion Polymerization

The following were heated in a three liter flask: 825 cc. distilled water; 36 g. Triton 720; and 36 g. of a 25% solution of sodium α-hydroxyoctadecane sulfonate in water. This solution was freed from air by heating to 95° over a period of fifteen minutes, with nitrogen passing through at the rate of 450 cc. per minute and the agitator at 500 r.p.m. A cold bath was then applied, and the nitrogen flow increased to 800–900 cc. per minute in order to maintain a slow stream of nitrogen from the outlet. As soon as the cold bath was applied, a high flame was placed under it, so that in a few minutes the bath temperature was close to 50°. When the temperature of the solution reached 63°, there were added to it 3.0 g. ammonium persulfate and 600 g. monomer, the temperature dropping to 49–51°. The agitator speed was increased to 1200 r.p.m. for thirty seconds to emulsify the monomer thoroughly, then reduced to 500 r.p.m. for the remainder of the run. The flow of nitrogen was reduced to 5 cc. per minute. The emulsion was held at 50° ± 0.5°; the bath often had to be cooled to 46–47°. After forty-five minutes the removal of samples was begun. Samples were taken by increasing the flow of nitrogen and pinching closed the rubber tube leading from the outlet tube to the bubble counter at the end of the system; this forced emulsion up the sampling tube and down through the condenser into a weighed 250 cc. Erlenmeyer flask containing 2–3 mg. of hydroquinone. When sufficient sample was obtained, the flow of nitrogen was reduced to 5 cc. per minute. The samples were usually 30–80 g., weighed to the nearest 0.1 g.; the larger samples were taken in the early stages of conversion.

Isolation of the Polymer

After the sample was weighed, methanol was added until the polymer dissolved or coagulated. Steam was then passed through, removing the methanol and unchanged monomer, and leaving the polymer as a porous mass that could be cut into thin slices with scissors or as a powder that could be filtered. Occasionally some polymer redispersed during the steam distillation; this coagulated on addition of saturated sodium chloride solution. Excessive foaming during the steam distillation was prevented by the addition of a trace of Dow Corning Antifoam A. The polymer was separated from the water–soap mixture, broken or cut into small pieces, washed repeatedly with cold water, and dried overnight.

usually at 70°; when styrene was used, the samples were dried at 90°. The efficiency of this method of isolation was demonstrated by the following experiment. In a vinyl acetate:styrene (1:1) polymerization, the polymer samples were dried overnight at 90°. The least porous of these

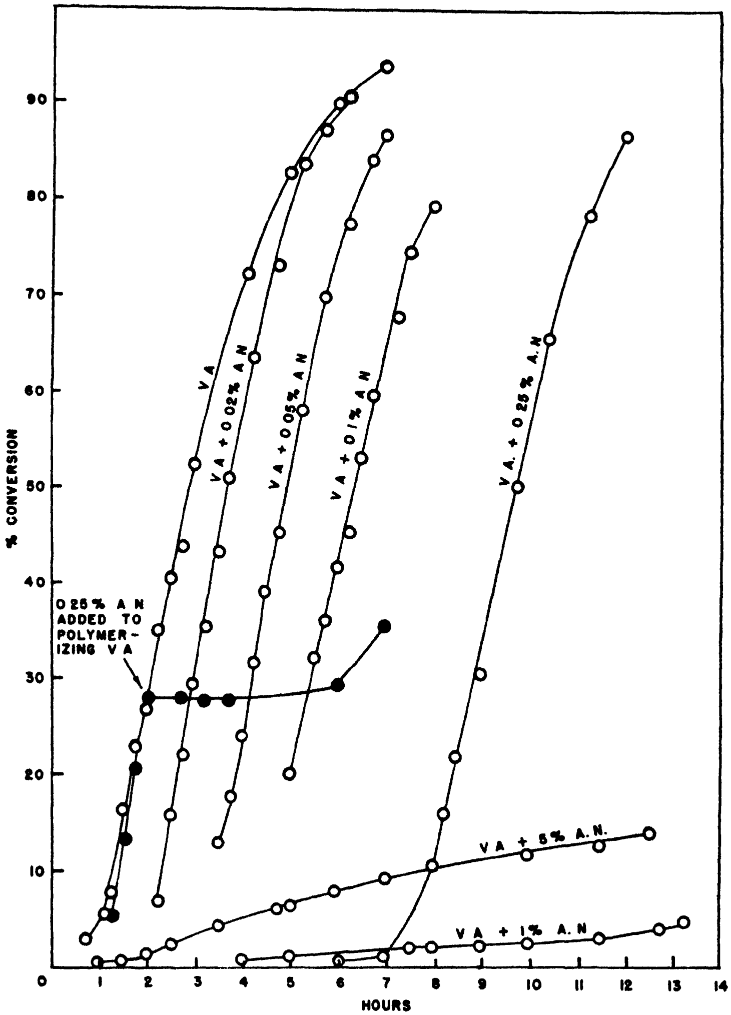

Fig. 1. The effect of small quantities of acrylonitrile on the polymerization of vinyl acetate in emulsion. Solid points obtained by adding 0.25% acrylonitrile to a polymerizing emulsion of vinyl acetate.

samples was broken into small pieces and a weighed sample heated at 150° for two hours, losing 1.3% by weight; this is within the limits of experimental error. A more porous sample lost only 0.6% by weight.

After drying, some of the polymer samples were analyzed for nitrogen (Kjeldahl).

Solution Polymerization

A mixture of 900 g. ethylene dichloride and 600 g. vinyl acetate was heated to refluxing with stirring, with nitrogen passing through at 7 cc. per minute. When the vapor reached the outlet tube, the temperature was lowered to 70°. Benzoyl peroxide (1.5 g.) was then added and the nitrogen flow set at 5 cc. per minute. Subsequent procedure was the same as for the emulsion polymerizations. In the absence of emulsifier, no Antifoam A was necessary in the steam distillations.

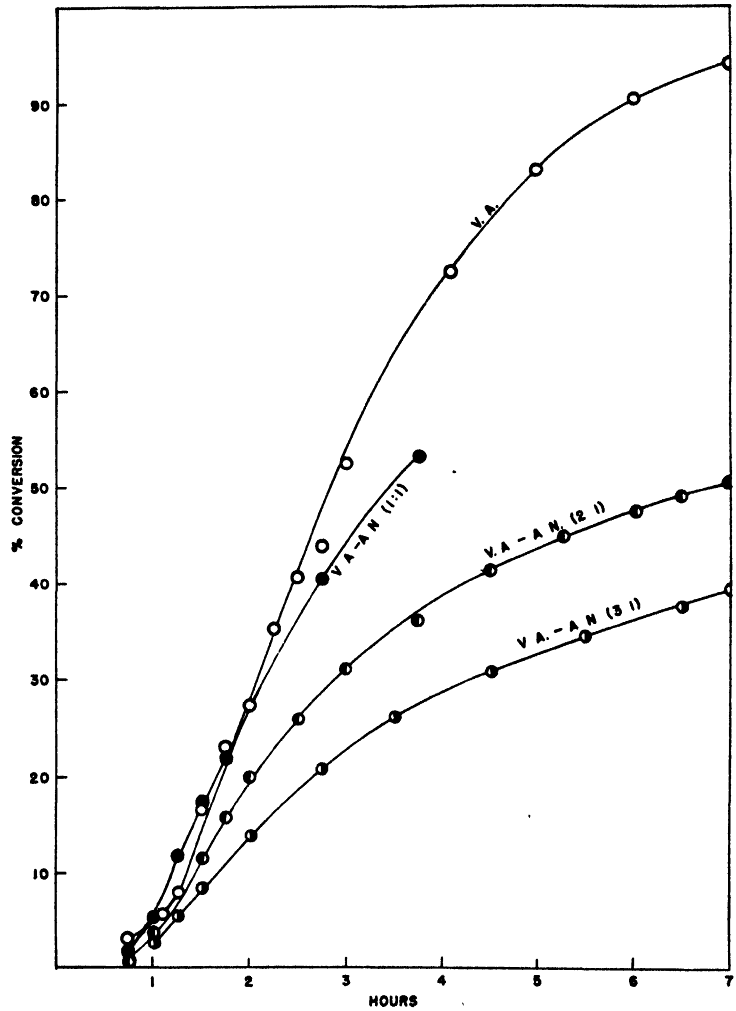

Fig. 2. The polymerization of vinyl acetate with larger amounts of acrylonitrile in emulsion.

All the polymerizations described were carried out under the above conditions, except where changes are noted in temperature or amount of catalyst.

RESULTS AND DISCUSSION

Copolymerization of Vinyl Acetate and Acrylonitrile in Emulsion

The inhibitory effect of small amounts of acrylonitrile on the polymerization of vinyl acetate is shown in Figure 1. Vinyl acetate polymerizes readily under the conditions of these experiments, after an induction period of approximately one hour. The addition of 0.02, 0.05, 0.1, and 0.25% (by weight) of acrylonitrile to the vinyl acetate increased the induction period to two, three, four, and seven hours, respectively. In each of these experiments, at the end of the induction period, the polymerization proceeded at a normal rate. In one run, 0.25% acrylonitrile

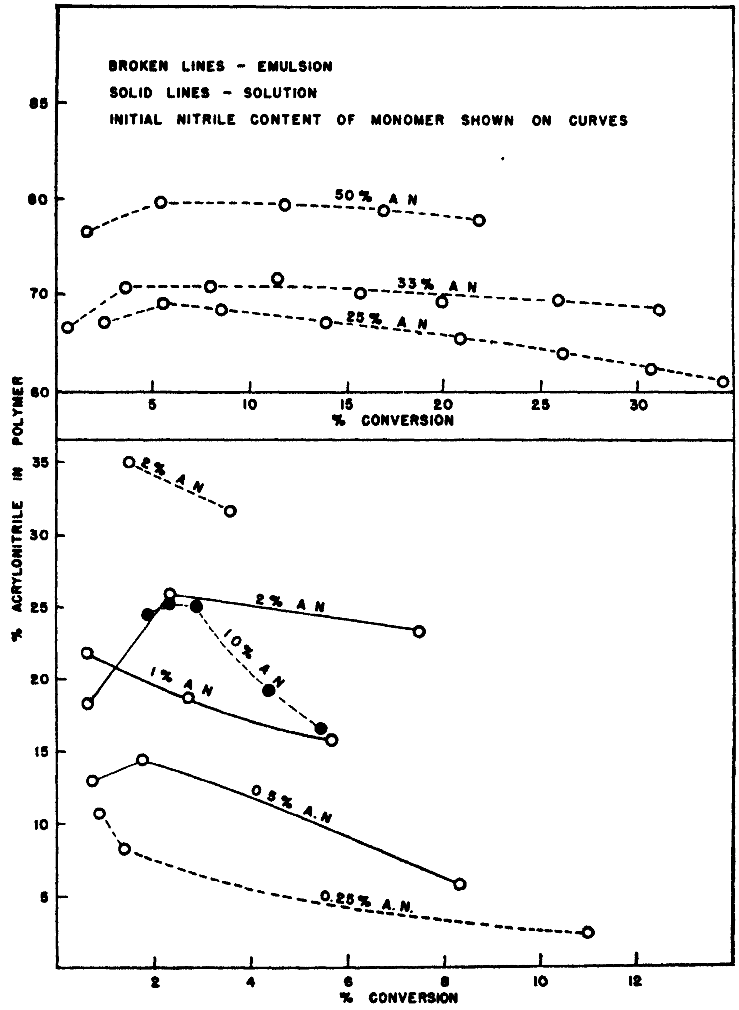

Fig. 3. Change in polymer composition with per cent conversion of vinyl acetate–acrylonitrile mixtures in emulsion and solution.

was added to a polymerizing emulsion of pure vinyl acetate at 28% conversion; the polymerization stopped immediately. With 1% acrylonitrile in the vinyl acetate, only 5% of the monomer polymerized during the first thirteen hours; possibly this period would have been followed by rapid polymerization if the experiment had been prolonged. Increasing the acrylonitrile content of the monomer to 5% increased the rate of polymerization considerably beyond that obtained during the long slow reaction period of the monomer containing 1% nitrile, although the conversion was still much slower than that of vinyl acetate alone. This trend was more pronounced when the nitrile content of the monomer was increased to 25–50% as shown in Figure 2. With increasing amounts of nitrile, the rate of conversion increased until, with 50% nitrile, the reaction was almost as rapid as that of vinyl acetate alone. With 50% nitrile, much of the polymer coagulated at 53% conversion. Using the terms "inhibitor" and "retarder" as defined by Kolthoff and Bovey, acrylonitrile acted as an inhibitor when present in amounts up to 0.25%, and as a retarder when over 1%. However, the retarding effect of the nitrile was inversely proportional to the amount present.

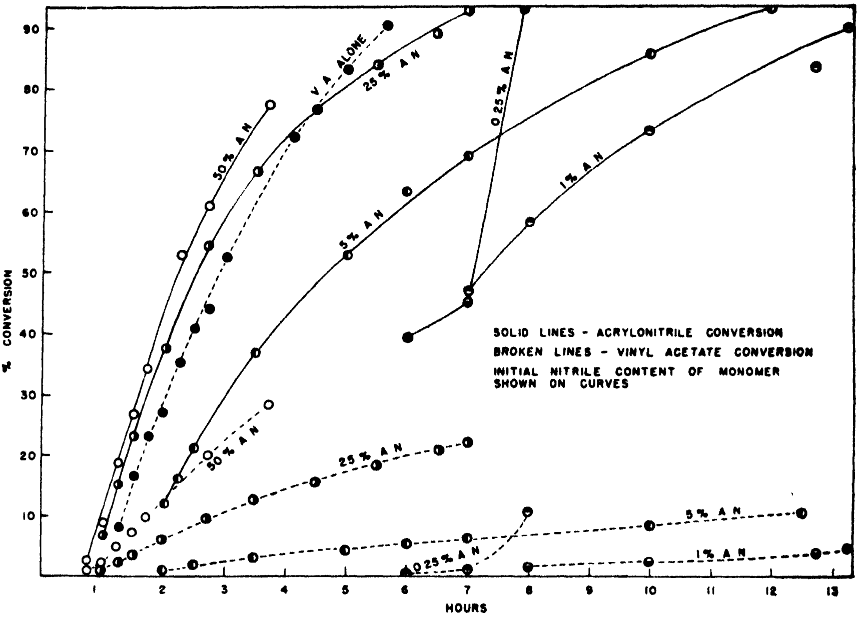

Fig. 4. The polymerization of the individual monomers in vinyl acetate-acrylonitrile mixtures in emulsion.

The presence of 1% acetonitrile had no effect on the polymerization of vinyl acetate.

The change of polymer composition with conversion of vinyl acetate:-acrylonitrile mixtures, in emulsion and in solution, is shown in Figure 3.

From these data were calculated the conversion–time curves of the individual monomers; these are shown in Figure 4 (emulsion) and Figure 7 (solution). In emulsion, the nitrile portion of the monomer mixture polymerized much more rapidly than did the vinyl acetate portion. With

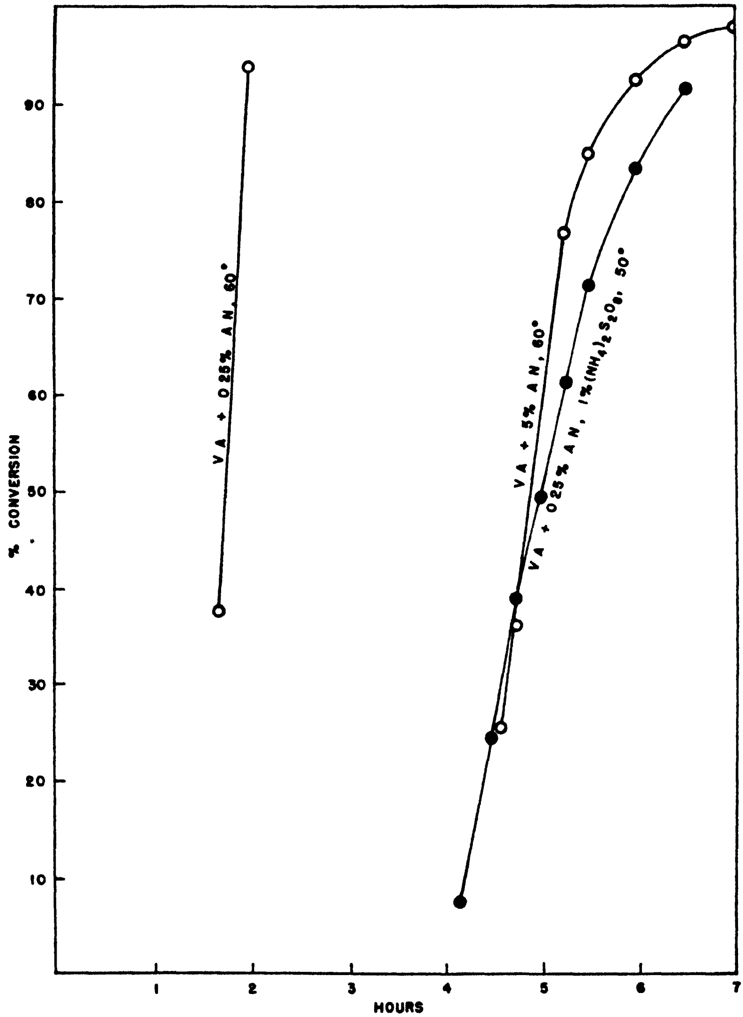

Fig. 5. The effect of increasing the temperature or catalyst on the polymerization of vinyl acetate containing small amounts of acrylonitrile in emulsion.

equal parts by weight of acrylonitrile and vinyl acetate, the nitrile polymerized more rapidly than did pure vinyl acetate by itself and the vinyl acetate also polymerized fairly rapidly. As the nitrile content of the monomer was decreased, the polymerization of both the nitrile and vinyl acetate became slower until, with 1% nitrile, the reaction was extremely slow. With 0.25% nitrile, however, after an induction period of seven hours, the nitrile polymerized very rapidly, and, when it had practically disappeared, the vinyl acetate started polymerizing. The polymerization of monomer mixtures containing 25–33% nitrile became very slow after the first few hours. During this time most of the nitrile had polymerized, leaving monomer mixtures low in nitrile; such mixtures would be expected

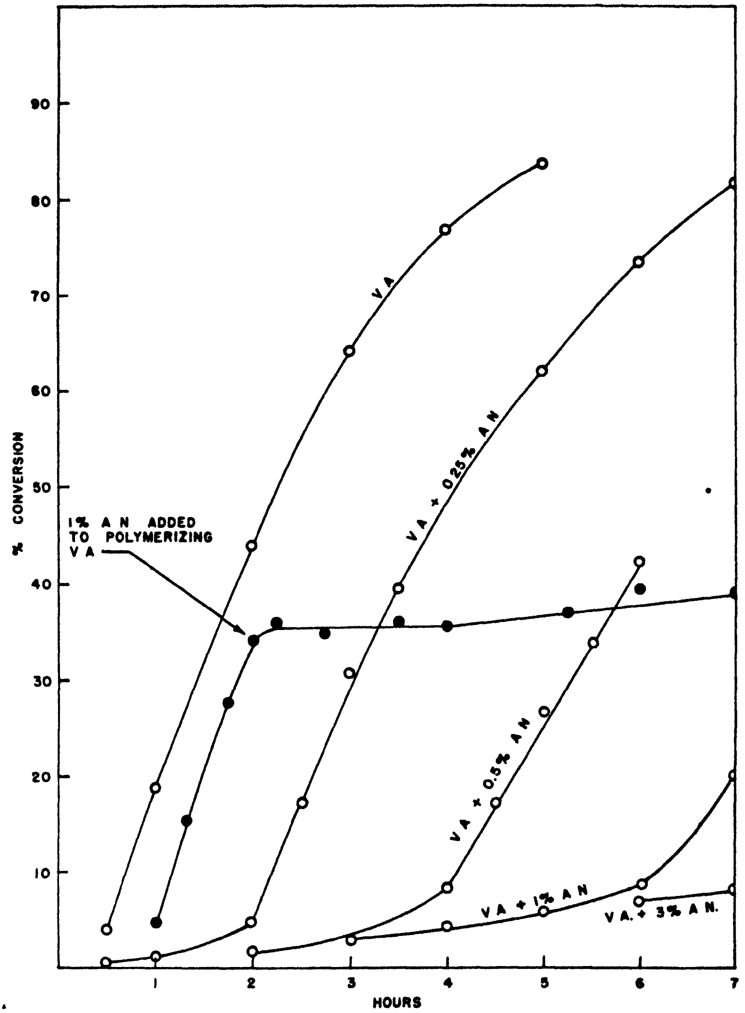

Fig. 6. The effect of small quantities of acrylonitrile on the polymerization of vinyl acetate in ethylene dichloride solution.

to polymerize slowly in view of the results obtained with small amounts of nitrile in the original monomer mixture.

Small amounts of acrylonitrile are strongly inhibitory to vinyl acetate at 60° as well as at 50°. This effect is seen in Figure 5. With 0.25% nitrile at 60°, there was an induction period of one and one-half hours, after which vigorous reaction occurred. With 5% nitrile at 60°, the induction period was four hours followed by rapid polymerization. Increasing the catalyst to double the standard amount at 50° with vinyl acetate containing 0.25% acrylonitrile reduced the induction period from seven hours to four hours.

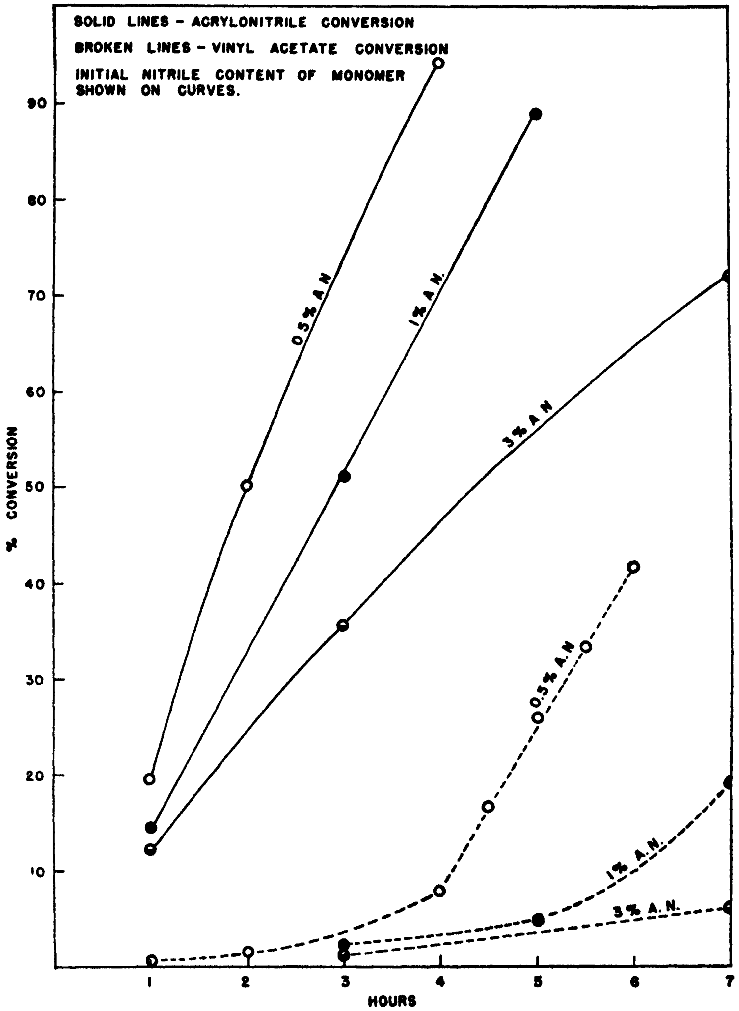

Fig. 7. The polymerization of the individual monomers in vinyl acetate-acrylonitrile mixtures in solution.

Copolymerization of Vinyl Acetate and Acrylonitrile in Ethylene Dichloride Solution

Small amounts of acrylonitrile inhibit the solution polymerization of vinyl acetate, as seen in Figure 6. With 0.25% nitrile, the induction period was increased from about twenty minutes (for pure vinyl acetate) to one and three-quarter hours. Increasing amounts of nitrile caused increasing inhibition until, with 3% nitrile in the monomer, only 8% conversion occurred in seven hours. The addition of 1% acrylonitrile to a

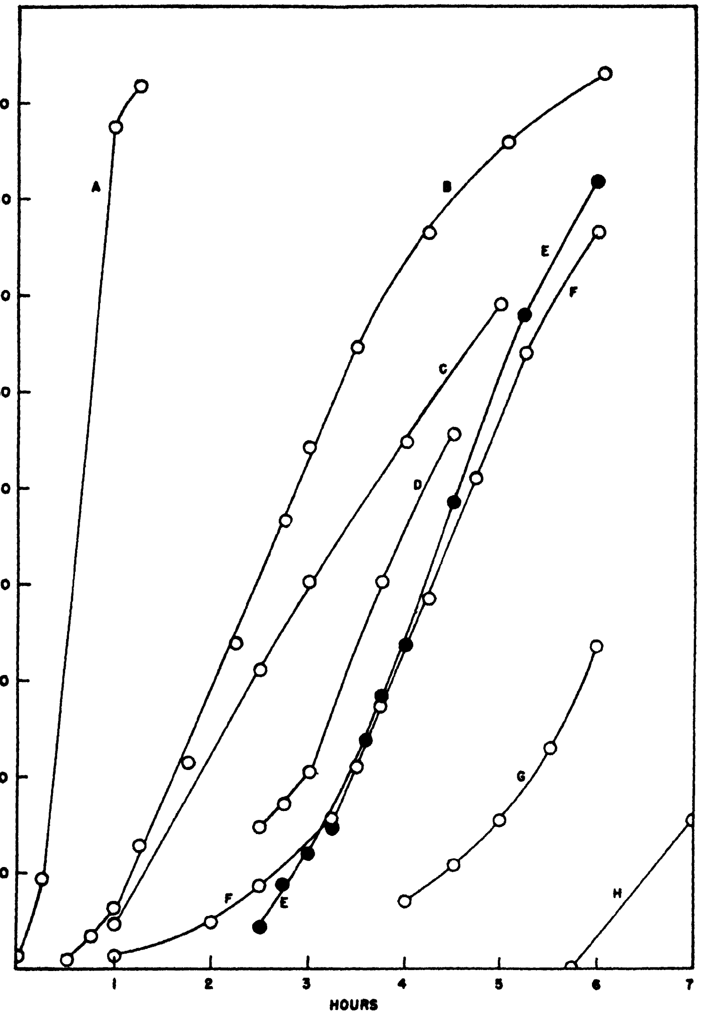

Fig. 8. The effect of small amounts of acrylamide, methacrylamide, and ethyl methacrylate on the polymerization of vinyl acetate in emulsion: B, vinyl acetate alone; C, plus 0.25% acrylamide; D, plus 2% acrylamide; E, plus 0.5% ethyl methacrylate; F, plus 1% ethyl methacrylate; G, plus 0.25% methacrylamide; H, plus 0.5% methacrylamide; and A, ethyl methacrylate alone.

polymerizing solution of pure vinyl acetate at 34% conversion stopped the reaction. When the monomer contained more than 3% nitrile the polymer which formed at low conversion was rich in nitrile and precipitated from the reaction mixture, making it impossible to obtain representative samples. For this reason higher acrylonitrile concentrations were not investigated.

The presence of 1% acetonitrile had no effect on the conversion of pure vinyl acetate in solution.

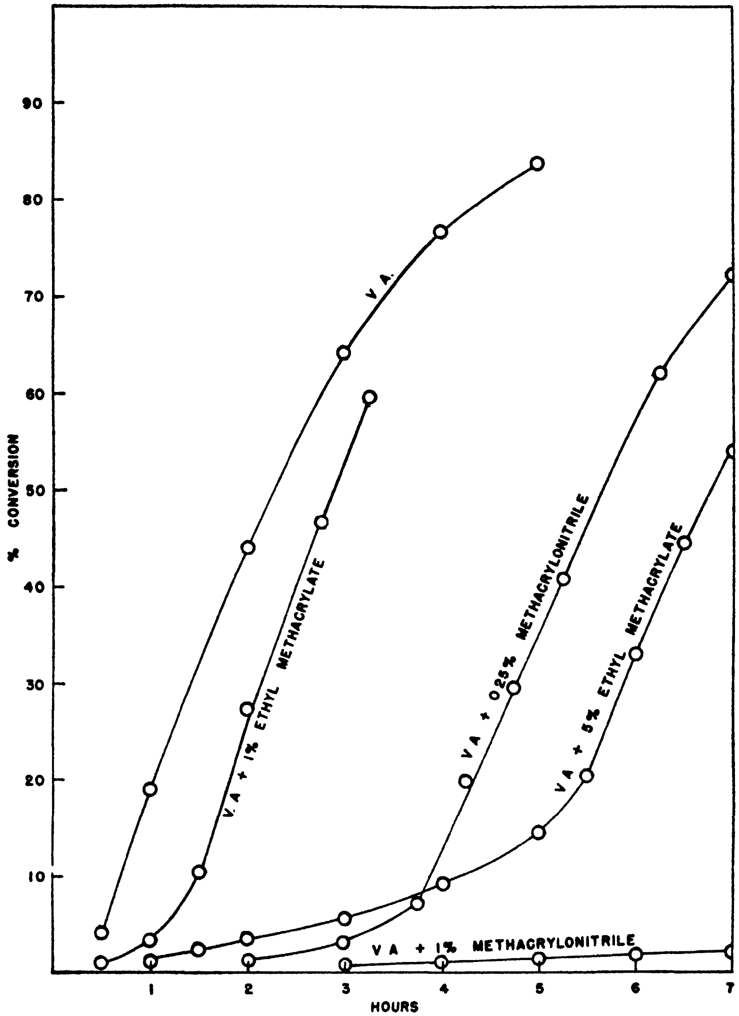

Fig. 9. The effect of small amounts of ethyl methacrylate and methacrylonitrile on the polymerization of vinyl acetate in ethylene dichloride solution.

The change of composition of the copolymers with increasing conversion in emulsion and solution is shown in Figure 3. In the polymerizations with 1% and 2% acrylonitrile in the monomer, copolymers formed at low conversions in emulsion are richer in nitrile than copolymers formed at corresponding conversions in solution. Possibly this is because the nitrile is more water-soluble than the vinyl acetate, the former thus being more concentrated at the site of polymerization in emulsion; this separation of monomers would not occur in solution. As in the emulsion polymerizations, the nitrile content passed through a maximum at low conversions in most of the runs.

The conversion–time curves of the individual monomers in vinyl acetate–acrylonitrile mixtures in solution are shown in Figure 7. As in emulsion, the nitrile polymerized more rapidly than did the vinyl acetate. The vinyl acetate did not start to polymerize rapidly until most of the nitrile had polymerized; in emulsion this sequence apparently occurred with small amounts of nitrile (0.02–0.25%) in the monomer (Fig. 1). There is one significant difference between emulsion and solution polymerization which can be seen in a comparison of Figures 4 and 7, *viz.*, in emulsion the rates, during the first seven hours, of both the acrylonitrile and vinyl acetate vary directly with the amount of nitrile present in the original mixture and in solution the rates of both monomers vary inversely with the nitrile content.

Inhibition of Vinyl Acetate by Monomers Other Than Acrylonitrile

In a search for other monomers which might exhibit the same type of inhibition as acrylonitrile toward vinyl acetate, the effects of small amounts of the following on the conversion of vinyl acetate in emulsion were determined: acrylamide, methacrylamide, ethyl methacrylate, methacrylonitrile, and styrene. The results obtained with the first three are shown in Figure 8 and the last two in Table I. All of these monomers inhibited the polymerization of vinyl acetate but, in all experiments in which different amounts gave different rates, the degree of inhibition or retardation was directly proportional to the amount present. However, as mentioned above, the rate of polymerization of vinyl acetate–acrylonitrile mixtures in emulsion was directly proportional to the amount of nitrile present. Acrylamide (0.25–2%) and ethyl methacrylate (0.5–1.0%) were mildly inhibitory, but methacrylamide greatly prolonged the induction period. Not shown in Figure 8 is the effect of 2% methacrylamide;

TABLE I

CONVERSION OF VINYL ACETATE CONTAINING VARYING AMOUNTS OF METHACRYLONITRILE OR STYRENE IN EMULSION, EXPRESSED AS PER CENT BY WEIGHT OF TOTAL MONOMER

Monomer composition	Temperature, °C.	Hours	Per cent conversion
1% Methacrylonitrile	50	7	0
5% Methacrylonitrile	50	7	0
1% Styrene	60	7	0
5% Styrene	60	7.5	0
0.25% Styrene	60	2	2.0
0.25% Styrene	60	3	15.1
0.25% Styrene	60	4.25	69 8

no polymerization occurred at 55° in eight hours. Small amounts of methacrylonitrile and of styrene also greatly inhibited the polymerization.

The inhibitory effect of small amounts of ethyl methacrylate and of methacrylonitrile on the polymerization of vinyl acetate in ethylene dichloride solution is shown in Figure 9. The methacrylate was mildly inhibitory, the methacrylonitrile strongly. With 1% methacrylonitrile in the monomer, the polymer formed after seven hours (2.1% conversion) contained 20.8% nitrile, indicating that both monomers were polymerizing during this early stage.

The authors gratefully acknowledge the assistance of Mr. Gerard A. Baldauf who carried out most of the polymerization reactions, including sampling and handling of the polymers.

English Synopsis, see Summaries, page S10, Vol. V, 1950.

Résumé

Une faible quantité d'acrylonitrile inhibe la polymérisation en émulsion de l'acétate de vinyle. Des quantités plus élevées retardent uniquement la réaction, et le retard est inversément proportionnel à la quantité de nitrile présent, de telle sorte qu'à une teneur de 40% environ en nitrile, le mélange polymérise à environ la même vitesse que l'acétate de vinyle soul. En cours des polymérisations en solution, le retard, occasionné par de faibles quantités d'acrylonitrile est directement proportionnel à la quantité présente. Avec des mélangès des deux monomères en émulsion, la copolymérisation de l'acrylonitrile et de l'acétate vinyle s'accélère avec une teneur croissante en nitrile; en solution, elle est plus faible avec une teneur croissante en nitrile. Le méthacrylonitrile la méthacrylamide et le styrène inhibent fortement la polymérisation de l'acétate de vinyle. Le méthacrylate d'éthyle et l'amide acrylique sont les inhibiteurs doux.

Zusammenfassung

Kleine Mengen von Acrylnitril inhibieren die Emulsionspolymerisation von Vinylacetat. Grössere Mengen verzogern bloss die Reaktion und die verzögernde Wirkung ist der vorhandenen Menge Nitril umgekehrt proportional, sodass bei ungefähr 40% Nitrilgehalt die Mischung ungefähr mit der selben Geschwindigkeit polymerisiert wie Vinylacetate allein. Bei Lösungspolymerisation ist die verzögernde Wirkung von kleinen Mengen Acrylnitril der vorhandenen Menge Acrylnitril umgekehrt proportional. Bei Gemischen der beiden Monomere in Emulsion wird die Polymerisation von sowohl Acrylnitril wie auch Vinylacetat mit steigendem Nitrilgehalt schneller; in Lösung wird die Polymerisation der beiden Monomere mit steigendem Nitrilgehalt langsamer. Methacrylnitril, Methacrylamid und Styrol inhibieren die Polymerisation von Vinylacetat stark. Äthylmethacrylat und Acrylamid sind milde Inhibitoren.

Received June 21, 1949

JOURNAL OF POLYMER SCIENCE VOL. V, NO. 3, PAGES 369-374

Friedel-Crafts Copolymerization of Chloroprene–Styrene

FREDERICK C. FOSTER, *Chemical and Physical Research Laboratories, The Firestone Tire & Rubber Company, Akron, Ohio*

INTRODUCTION

Although considerable experimental work has been done on the determination of monomer reactivity ratios in free radical copolymerizations, similar determinations for cationic catalyzed copolymerizations were first reported only recently.[1] The present paper presents experimental results on the determination of the monomer reactivity ratios for the copolymerization of chloroprene–styrene induced by a Friedel-Crafts type catalyst.

In the copolymerization of two monomers, M_1 and M_2, the respective monomer reactivity ratios, r_1 and r_2, have been defined by the following equations:[2]

$$\begin{aligned} &M_1\cdot + M_1 \xrightarrow{k_{11}} M_1\cdot \\ &M_1\cdot + M_2 \xrightarrow{k_{12}} M_2\cdot \qquad r_1 = k_{11}/k_{12} \\ &M_2\cdot + M_2 \xrightarrow{k_{22}} M_2\cdot \qquad r_2 = k_{22}/k_{21} \\ &M_2\cdot + M_1 \xrightarrow{k_{21}} M_1\cdot \end{aligned}$$

The differential equation for copolymerization then becomes:

$$\frac{d(M_1)}{d(M_2)} = \frac{(M_1)}{(M_2)}\,\frac{r_1(M_1) + (M_2)}{r_2(M_2) + (M_1)} \tag{1}$$

The corresponding integrated equation becomes:

$$r_2 = \frac{\log \dfrac{M_2^0}{M_2} - \dfrac{1}{p} \log \dfrac{1 - pM_1/M_2}{1 - p\,M_1^0/M_2^0}}{\log \dfrac{M_1^0}{M_1} + \log \dfrac{1 - pM_1/M_2}{1 - pM_1^0/M_2^0}} \tag{2}$$

where:

$$p = (1 - r_1)/(1 - r_2)$$

With the substitution of the growing complexes[3] [*e.g.*, $\bar{F}$-B(F_2)—CH_2—CH(C_6H_5)] for their respective free radicals, the above equations should be applicable to cationic catalyzed copolymerizations. The assumptions[4] necessary in developing the above equations should apply equally well to the cationic catalyzed copolymerizations.

EXPERIMENTAL

Styrene obtained from Koppers Company, Inc. was distilled under reduced pressure. The monomer was tested for the presence of polymer before use by adding a sample to methanol.

The chloroprene was obtained by fractionating Du Pont chloroprene solution (50% solution in xylene) and then distilling again just prior to use. A small amount of the monomer was added to methanol to test for the presence of polymer just before use.

The experiments were conducted by adding 50 cc. of cyclohexane and the amounts of the two monomers to a beverage bottle and then capping. The bottle was rotated in a constant temperature bath at −18°C. for at least an hour. It was then opened and 4 cc. of boron trifluoride–etherate added. The bottle was capped again and immersed in the constant temperature bath. The reaction was stopped by adding about 3 cc. of methanol and then the copolymer was coagulated by pouring the reaction mixture into several times its volume of methanol and stirring in a Waring Blendor. The copolymer was washed several times with methanol, the methanol decanted, and the copolymer was vacuum dried overnight. The copolymer was obtained as a granular powder.

As a test of copolymer purity, one of the copolymer samples was dissolved in acetone and reprecipitated by a large volume of methanol. After washing and drying in the usual manner, the copolymer gave the same analysis for chlorine, within experimental error, as it did before this treatment.

The chlorine analyses were performed by combustion of the sample in a Parr bomb followed by the Vollhard titration.

Initial monomer charges, M_1^0 and M_2^0, were determined by weighing the monomers. Monomer charge at time t, M_1 and M_2, was determined from data on per cent conversion and on copolymer composition by chlorine analysis. Per cent conversion was determined by recovering the total copolymer.

RESULTS

Table I lists the experimental values of monomer concentrations. M_1 and M_2 refer to chloroprene monomer and styrene monomer, respectively, on a mole basis.

Using equation (2), each set of values in Table I, M_1^0, M_2^0, M_1, M_2, yields a straight line plot of r_1 *vs.* r_2 in Figure 1. If there had been no errors in the determinations of monomer concentrations listed in Table I, the lines of Figure 1 should intersect in a common point characteristic of the true values of r_1 and r_2. The six experimental determinations are plotted in Figure 1. Values of 0.24 and 15.6 were selected for r_1 and r_2, respectively.

TABLE I

CHLOROPRENE (M_1)–STYRENE (M_2)

Expt No.	M_1^0	M_2^0	M_1	M_2
1	$0{\cdot}400_6$	$0{\cdot}173_8$	$0{\cdot}365_6$	$0{\cdot}065_8$
2	$0{\cdot}617_6$	$0{\cdot}122_4$	$0{\cdot}604_5$	$0{\cdot}101_6$
3	$0{\cdot}500_7$	$0{\cdot}198_9$	$0{\cdot}489_4$	$0{\cdot}155_7$
4	$0{\cdot}733_5$	$0{\cdot}220_5$	$0{\cdot}727_0$	$0{\cdot}199_6$
5	$0{\cdot}441_5$	$0{\cdot}194_9$	$0{\cdot}435_0$	$0{\cdot}165_9$
6	$0{\cdot}405_0$	$0{\cdot}340_7$	$0{\cdot}394_3$	$0{\cdot}241_2$

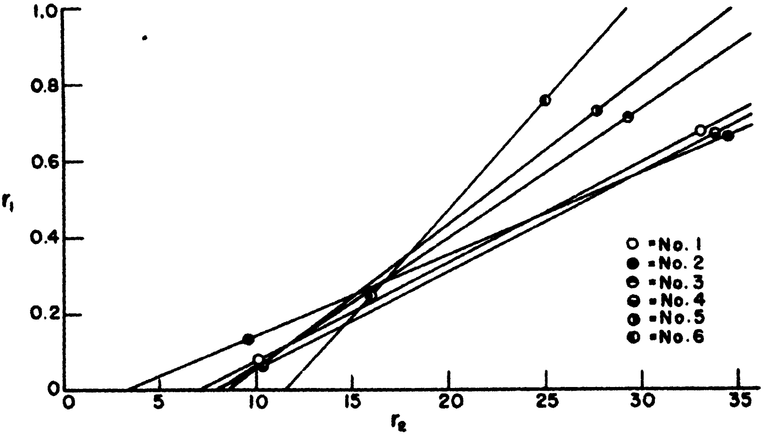

Fig. 1. Plot of r_1 vs. r_2 for the system chloroprene–styrene.

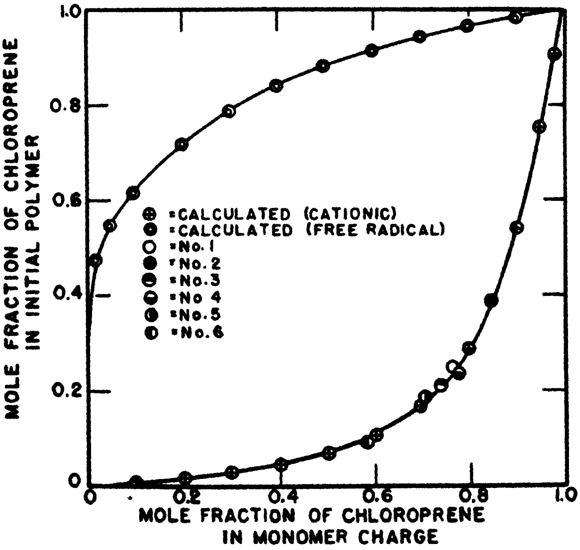

Fig. 2. Monomer–polymer composition curve chloroprene–styrene.

The calculated curve in Figure 2 was obtained by inserting the values of r_1 and r_2, mentioned above, in equation (1). The experimental points corresponding to each copolymerization are also plotted in Figure 2. The compositions of the copolymers are plotted against the interpolated average monomer concentrations. Since all of the reactions were stopped at relatively low conversions, this average monomer concentration is close to the average of the initial and final monomer concentrations. In cases where the conversion is high or the slope of the monomer–polymer curve is increasing rapidly, the chloroprene monomer concentration plotted should be somewhat more than the average of the initial and final concentrations.

Figures 1 and 2 illustrate that although a relatively large percentage of uncertainty exists in the determination of the values of r_1 and r_2, the selected values of r_1 and r_2 give a monomer–polymer composition curve that agrees with the experimental determinations within the precision of the chlorine analyses. In other words, relatively large percentage errors in r_1 and r_2 yield relatively small percentage errors in predicted copolymer composition.

The monomer–polymer composition curve for the free radical initiated copolymerization is also given in Figure 2. The values of r_1 and r_2 used in calculating this curve were taken from the published data of Wall.[5] Values used were 6.3 and 0.005 for r_1 and r_2, respectively. The value of 0.005 was used for r_2 instead of the listed value of 0, because it is assumed that styrene would homopolymerize under the conditions of the experiment and that the value of r_2 was merely indistinguishable from 0 over the range of their experiments.

DISCUSSION

The present data indicate a striking difference between the relative reactivity ratios in a free radical initiated copolymerization and the relative reactivity ratios in a cationically initiated copolymerization in the system chloroprene–styrene. In the free radical initiated copolymerization, both types of growing free radicals (those with a terminal chloroprene group or those with a terminal styrene group) exhibit a strong preference to react with chloroprene monomer rather than styrene monomer. In the cationically initiated copolymerization, both types of growing chains prefer to react with styrene monomer rather than chloroprene monomer.

Figure 2 illustrates the effect of the differences in reactivity ratios on the compositions of initial copolymers in the two systems. For example, a 50–50 mole per cent initial charge of chloroprene and styrene monomers will yield an initial copolymer with about 7 mole per cent chloroprene in a cationically catalyzed system but about 88 mole per cent chloroprene in a free radical catalyzed system.

This reversal of reactivities in the two types of catalyst systems is quite similar to the results of Alfrey on the copolymer system styrene-*p*-chlorostyrene.[1] The present data are consistent with Alfrey's suggestion that electron-donating groups increase reactivity and electron-withdrawing groups decrease reactivity in the carbonium ion systems. In the reactivity series proposed by Alfrey, chloroprene monomer would occupy a position of low reactivity, probably between 2,5-dichlorostyrene and methyl methacrylate.

The technique of adding the more reactive monomer in increments during the course of a copolymerization is often used to decrease the variation of chemical composition of copolymers with conversion. "Constant composition" copolymers are prepared by this method.

Figure 2 shows that in the free radical catalyzed system the above technique could be used only with great difficulty to prepare copolymers having average compositions between the range of 0–60 mole per cent chloroprene. Initial monomer loadings would have to be between 92–100 mole per cent styrene; and, over this range of monomer compositions, copolymer composition changes rapidly with conversion. In fact, if the true value of r_2 were 0 in the free radical system, as listed by Wall,[4] it would be impossible to prepare a copolymer containing more than 50 mole per cent styrene in this system.

However, it is over this same range of copolymer chemical compositions that "constant composition" copolymers could be prepared most readily in the cationically catalyzed copolymerization of chloroprene-styrene.

Consequently, in the preparation of copolymers containing narrow ranges of chemical compositions, the free radical catalyzed system and the cationically catalyzed system complement each other. Over the range of copolymer compositions from 0–60 mole per cent chloroprene the cationic catalyzed system would be preferable; over the range of copolymer composition from 60–100 mole per cent chloroprene the free radical catalyzed system would be preferable, other conditions being equal.

It should be pointed out that there were indications that the copolymers produced during the present experiments were low molecular weight copolymers. The intrinsic viscosity of the copolymer from experiment 5 was 0.06 in acetone. The same copolymer melted over the range of 75–85°C. with a low melt viscosity. Duplicate cryoscopic molecular weight determinations on sample 5, in ethylene bromide as solvent, gave values of 1930 and 1960.

The author wishes to express his appreciation to Drs. B. L. Johnson and F. W. Stavely for their continued interest in this work and also to The Firestone Tire & Rubber Company for permission to publish these results.

References

1. T. Alfrey, Jr., and H. Wechsler, *J. Am. Chem. Soc.*, **70,** 4266 (1948).
2. T. Alfrey, Jr., F. R. Mayo, and F. T. Wall, *J. Polymer Sci.*, **1,** 581 (1946).
3. C. C. Price, *Reactions at Carbon-Carbon Double Bonds*. Interscience, New York, 1946.
4. F. R. Mayo and F. M. Lewis, *J. Am. Chem. Soc.*, **66,** 1594 (1944). G. Goldfinger and T. Kane, *J. Polymer Sci.*, **3,** 462 (1948).
5. L. A. Wall, *ibid.*, **2,** 543 (1947).

English Synopsis, see Summaries, page S8, Vol. V, 1950.

Résumé

Les rapports des réactivités relatives ont été déterminées dans le cas de la copolymérisation de chloroprène–styrène à −18 °C., catalysé par le complexe éthéré du fluorure de bore. Conformément aux expériences antérieures d'Alfrey avec un système de monomères différents, il y a une inversion complète des réactivités relatives des deux monomères en passant d'un système initiateur par radicaux à un catalyseur Friedel-Crafts. Cette inversion des réactivités des monomères permet la production de copolymères de "composition constante" de chaque composition désirable, en choisissant un type de catalyseur approprié. Les copolymères obtenues dans ce travail en présence de catalyseurs cationiques ont toutefois des poids moléculaires peu élevés.

Zusammenfassung

Es wurden die relativen Reaktivitätsverhältnisse bestimmt für die Copolymerisation von Chloropren–Styrol bei −18 °C., mit Bortrifluorid-Ätherat als Katalisator. Ahnlich wir die früheren Befunde von Alfrey an einem anderen copolymeren System, wurde eine vollständige Umkehrung der relativen Reaktivität der beiden Monomeren festgestellt, wenn man das System vom Typ eines Freien-Radikal-Katalisators zu dem Typ eines Friedel-Crafts-Katalisators abändert. Diese Umkehrung der Reaktivitäten der Monomeren ermöglicht die Produktion von Copolymeren mit konstanter Zusammensetzung und von jeder erwünschten Zusammensetzung bei geeigneter Wahl des Katalisator Typs. Es bestehen Anzeichen dafür, dass die durch Kationen katalisierten Copolymeren, die in dieser Arbeit hergestellt wurden, niedermolekulare Copolymere sind.

Received May 9, 1949

LETTERS TO THE EDITORS

Ultracentrifuge Studies on the Crystalline Compound of Trypsin and of Soybean Trypsin Inhibitor

Recently Kunitz[1] has reported the isolation of a crystalline compound of trypsin and of soybean trypsin inhibitor which exhibits no residual proteolytic or inhibitory activity. We have found that the crystalline compound has a sedimentation constant, corrected to 20°C. in 0.1 *M* phosphate buffer, of 3.5–3.7 svedberg units in the *p*H range of 3.6–10.4. The values are nearly concentration independent in the range investigated (0.3–0.7% total protein). Below *p*H 2.9, the compound dissociates to give an apparent sedimentation constant of 2.4 svedberg units, a value corresponding closely to that of pure trypsin or inhibitor. Above *p*H 11, the compound is denatured.

Preliminary results of mixing equal weights of trypsin and inhibitor at *p*H 2.8 and 6.0 give values identical with the above. The results tend to support the hypothesis of Kunitz[1] that the compound formation involves salt linkages between amino and acid groups, since below *p*H 2.9 —COOH groups are unionized. A full account will be published later.

References

1. M. Kunitz, *J. Gen. Physiol.*, **30**, 311 (1947).

E. SHEPPARD
A. D. MCLAREN
P. JOHNSON*

Institute of Polymer Research
Polytechnic Institute of Brooklyn
Brooklyn, New York

Received February 17, 1950

Critical Concentration Effects in Dilute High Polymer Solutions

One of the older concepts relating to the physical chemistry of polymer solutions concerns the enormous volume requirements of such long chain molecules and the consequent necessity of working at extreme dilutions if such molecules are to be independent of each other in solution. As early as 1931, Eisenschitz and Rabinowitsch[1] expressed doubt about the validity of osmotic pressure and viscosity methods, because, at the concentrations normally used, the molecules do not move independently in solution. Similar thoughts have been expressed by other workers since that time, particularly with the idea of choosing a model based on the stretched out length of the molecule and calculating a "critical" concentration at which interference might be expected. Staudinger,[2] Signer and Gross,[3] Signer,[4] Campbell and Johnson,[5] Hulburt, Harman, Tobolsky, and Eyring,[6] have all made such calculations.

---

* Present address: Department of Colloid Science, Cambridge University, England.

The above deductions of critical concentrations were all based on a hypothetical model, whose dimensions were calculated from the molecular weight. Today, it is known from work on intrinsic viscosity and light scattering[7,8] that a polymer molecule such as polystyrene can be represented in dilute solution as a random coil whose dimensions can be ascertained physically as a function of molecular weight and solvent type.

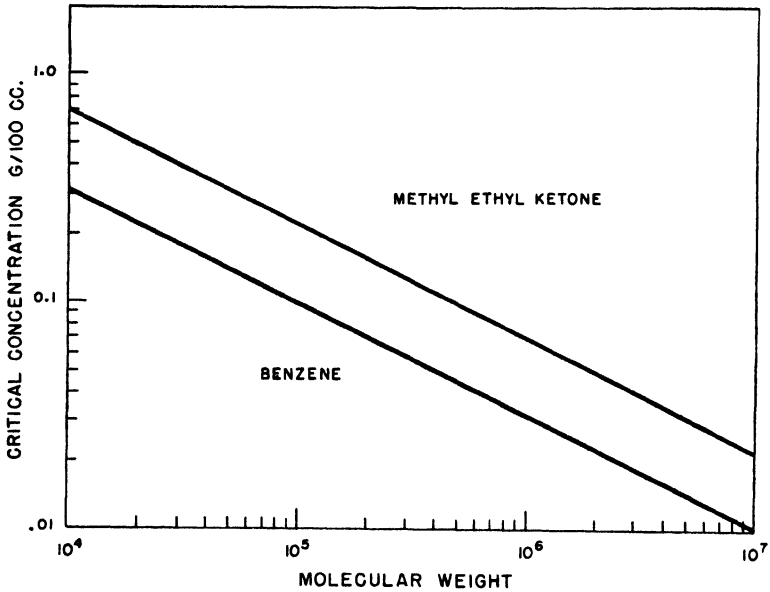

Fig. 1. Critical concentration for close packing of random coils in solution, based on data for polystyrene.

We propose, then, a new definition of critical concentration of polymer solutions as the concentration corresponding to the close packing of random coils having twice the measured diameter of actual molecules in actual solvents. The factor of two is arbitrarily introduced to allow for the fact that a random coil is not a smooth sphere. Based on experimental values[7-10] which indicate that polystyrene of molecular weight one million has a diameter $(\bar{R}^2)^{1/2}$ in benzene of about 1000 A. and in methyl ethyl ketone of about 750 A., it follows that:

$$c_{crit.}\ (g./100\ cc.) = 30.6\ M^{-1/2}\ \text{for benzene}$$

$$= 69.1\ M^{-1/2}\ \text{for methyl ethyl ketone}$$

where M is the molecular weight. Figure 1 is a plot of this equation for the two solvents, and might serve as a working guide. It is evident at once that many measurements currently made on polystyrene solutions for viscosity, osmosis, and light scattering are at concentrations above these limiting values.

The apparent success of the several linear plots for extrapolating to infinite dilution viscosity, osmotic pressure, and turbidity data, and the relatively good internal agreement among the various molecular weight measurement methods, especially when chemical end group methods, and a range of very good to very poor solvents are included, would seem to imply that the critical concentration concept is not of too great significance. There are, however, several instances in the literature when definite effects have been observed when working through or completely below the critical region. These are as follows:

(*1*) *Ultracentrifuge, sedimentation velocity.* Signer and Gross[11] found that high molecular weight polystyrene molecules were slowed down by presence of low molecular weight species above certain critical concentration regions which depended on molecular weight.

(*2*) *Osmotic pressure.* Jullander[12] found a very strong dependence of osmotic slope on molecular weight when all his measurements on a range of nitrocellulose samples were carried out below the usual concentration region, using the osmotic balance. Schulz and Dinglinger[13] found for polymethyl methacrylate in acetone that the reduced osmotic pressure plots π/c *vs.* c were concave up for high molecular weights, concave down for low molecular weights. In the latter case, this is equivalent to an increasing slope with decreasing molecular weight at quite low concentrations.

(*3*) *Viscosity.* Daněs found a break in the η_{sp}/c *vs.* c plot for polystyrene in benzene at c equal 0.3%, the slope being higher below this concentration.[14] Howlett, Minshall, and Urquart[15] found a similar break for secondary cellulose acetate in acetone in the region between 0.01 and 0.1%.

(*4*) *Streaming double refraction.* Signer and Gross[16] found that a quantity which might be called a reduced specific double refraction, $(N_1 - N_2)/\eta Gc$, is constant up to a certain concentration for polystyrene in cyclohexanone, and then decreases. This critical concentration decreases for increasing molecular weight, but the values are higher than would be indicated by Figure 1. In the above expression, the numerator is the refractive index difference, η is viscosity of the solution, and G is the velocity gradient, all at concentration c.

(5) *Electrophoretic mobility.* Signer and Brechbuhler[17] have recently cited a case where methyl cellulose at 0.4% concentration reduces the mobility of thymonucleic acid, sodium salt, whereas 0.062% methylcellulose has no such effect.

These few examples indicate that there are concentration effects in physical measurements on polymers which are possibly, but not necessarily, related to the critical concentration effects discussed in this letter. It might be expected that kinetic phenomena such as viscosity, sedimentation, velocity, *etc.* would be more strongly affected by space-filling effects than would equilibrium measurements such as osmotic pressure or optical turbidity. In any event, we believe it worth while to consider more carefully physical measurements on polymers at concentrations below those indicated by Figure 1, even if it involves the development of new testing techniques.

References

1. R. Eisenchitz and B. Rabinowitsch, *Ber.*, **64,** 2522 (1931).
2. H. Staudinger, *Die hochmolekularen organischen Verbindungen,* Springer, Berlin, 1932, p. 128 ff. See also J. Duclaux, *J. Polymer Sci.*, **2,** 626 (1947).
3. R. Signer and H. Gross, *Helv. Chim. Acta,* **17,** 59 (1934).
4. R. Signer, *Helv. Chim. Acta,* **18,** 701 (1935).
5. H. Campbell and P. Johnson, *Trans. Faraday Soc.*, **40,** 222 (1944).
6. H. M. Hulburt, R. A. Harman, A. V. Tobolsky, and H. Eyring, *Trans. N. Y. Acad. Sci.*, **44,** 418 (1943).
7. P. Debye and A. M. Bueche, *J. Chem. Phys.*, **16,** 573 (1948).
8. P. Debye, *J. Phys. Colloid Chem.*, **51,** 18 (1947).
9. P. M. Doty, W. A. Affens, and B. H. Zimm, *Trans. Faraday Soc.*, **B42,** 66 (1946).
10. B. H. Zimm, *J. Chem. Phys.*, **16,** 1099 (1948).
11. R. Signer and H. Gross, *Helv. Chim. Acta,* **17,** 726 (1934).
12. I. Jullander, Doctoral Dissertation, "Studies on Nitrocellulose Including the Construction of an Osmotic Balance," *Arkiv. Kemi, Mineral. Geol.*, **A21,** No. 8, 1 (1945).
13. G. V. Schulz and A. Dinglinger, *J. prakt. Chem.*, **158,** 130 (1941).
14. V. Z. Danĕs, *Kolloid Z.*, **68,** 110 (1934)
15. F. Howlett, E. Minshall, and A. R. Urquart, *Shirley Institute Memoirs,* **18,** 257 (1943). We are indebted to Dr. S. Weisberg of the National Bureau of Standards for this reference.
16. R. Signer and H. Gross, *Z. physik. Chem.*, **A165,** 161 (1933).
17. R. Signer and T. Brechbuhler, *Bull. soc. chim. Belg.*, 57, 163 (1948). We are indebted to Dr. R. Simha for this reference.

R. F. Boyer
R. S. Spencer

The Dow Chemical Company
Midland, Michigan

Received January 27, 1950

Pyrolysis of Polystyrene

The technique for measuring the rate of degradation of polystyrene, reported in this journal by Jellinek,[1] has been investigated with a view to its employment in a general study of polymer degradation.

Experiments were carried out with a small torsion balance in an evacuated glass envelope, using polystyrene fractions in order to check the agreement of the results obtained with this apparatus and those reported in the paper. The rate curves were very similar to Jellinek's and, assuming a zero order reaction, the activation energy calculated from the initial slopes is about 50 kcal., which is also in good agreement with his values.

It was observed, however, during the course of the reaction, that the torsion arm was subject to small erratic vibration. Closer examination showed that this effect was caused by the formation and bursting of bubbles of the liquid polymer, due presumably to the evolution of low molecular weight homologs in the body of the degrading polymer.

Small translucent globules, visible with the aid of a lens, were formed on the glass wall near the reaction vessel as the bubbles in the crucible burst. Repeated experiments left no doubt that a considerable fraction of the total weight lost by the polymer could be accounted for by this means.

On the basis of experiments it seems that great care must be exercised if one is not to be misled by the use of weight loss during pyrolysis as a measurement of monomer production.

Reference

1. H. H. G. Jellinek, *J. Polymer Sci.*, 4, 13 (1949).

E. Atherton

Imperial Chemical Industries Ltd.
Dyestuffs Division
Manchester 9, England

Received January 17, 1950

Concerning the Inactivation-Denaturation of Pepsin

It is a well-known fact that pepsin is unstable at *p*H above *ca.* 6[1–4]. It also exhibits a marked increase in quantum yields for inactivation by ultraviolet light at *ca.* *p*H 6 and higher.[5] It is the purpose of this discussion to point out semiquantitative reasons for the enhanced ultraviolet light sensitivity above *p*H 6 (which has been ascribed to a reduced intramolecular, Franck-Rabinowitch effect associated with the repulsion within the molecule brought about by increasing ionization with increasing *p*H above 5 to 6). To do this we choose a model:

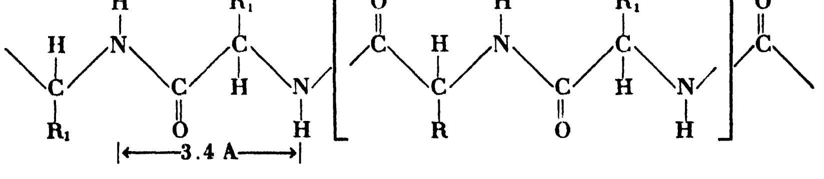

and make use of the composition formula of Brand:

$$\mathrm{Gly_{29}\text{-}Val_{21}Leu_{27}Ileu_{28}Pro_{15}Phe_{9}(CysH)_{2}(Cys)_{4}Met_{4}Try_{4}Arg_{2}His_{2}\text{-}Lys_{2}Asp_{2}Glu_{28}(Asp\text{-}NH_{2})_{32}Ser_{40}Thr_{28}Tyr_{16}(H_{2}PO_{3})(H_{2}O)_{2}}$$

for a molecular weight 34,400.[1,6] For this model we may either assume that all ionizing groups are distributed at random or with a definite periodicity similar to that prescribed by the Bergmann-Niemann hypothesis. This allows us to compute repulsion energies by integration. For our problem we could also use statistical summation which, for simplicity, would require a periodicity. In view of the large number of groups and the increased flexibility of integration methods, only integration methods are used in the following. In this model R_1 groups are ionized or potentially ionizable groups and R groups are nonionizable. The repeat distance is as in silk, 3.4 A. This model, a long rod, contains 302 amino acid residues and 30 acid residues, *i.e.*, every 10th residue bears a real or potential $-COO^-$. Only such acid groups need be taken into account in the pH region under consideration, basic groups having constant ionization charge.

Assuming a rod we have therefore a total length of 1027 A. It is also uniformly charged. We wish to calculate the electrostatic potential at the site of a possible break, induced by a quantum, in a rod of length l. Let σ be the linear charge density and a and b the length of the fragments, *i.e.*, $a + b = l$.

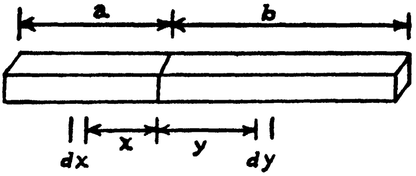

The potential on any two elements dx and dy will be dV where $dV = \sigma dx \sigma dy/\epsilon(x + y)$ and ϵ is the dielectric constant (taken as 80).

The total potential is:

$$V = \frac{\sigma^2}{\epsilon} \int_0^b \int_0^a \frac{1}{x + y}\, dx dy$$

$$= \frac{\sigma^2}{\epsilon} [l \ln l - a \ln a - (l - a)\ln(l - a)]$$

For our purposes an average repulsion energy is required, for the break may be at random. Clearly the potential will be zero if the break occurs at either end and will be a maximum at the center. The average repulsion energy, $\bar{V}$, is:

$$\bar{V} = \frac{\int_0^l V_{(a)} da}{\int_0^l da} = \frac{\sigma^2 l}{2\epsilon}$$

Our problem initially is to find how $\bar{V}$ varies with pH. This will depend on the pK's of the amino acid residues and on the pH. If our procedure is correct we should be able to calculate the isoionic point (isoelectric point in the absence of sorbed ions). For test purposes we consider chymotrypsinogen. Its composition for a molecular weight of 36,800 is, after Brand:[1,6]

$$\mathrm{Gly_{26}Val_{32}Leu_{29}Ileu_{16}Pro_{19}Phe_8(CysH)_4(Cys)_{10}Met_3Try_{10}\text{-}Arg_6His_3Lys_{20}Asp_{13}(Glu\text{-}NH_2)_{22}\text{-}}$$
$$\mathrm{(Asp\text{-}NH_2)_{18}Ser_{40}Thr_{35}Tyr_6(H_2O)_5}$$

For the data see Table I. Values of *p*K for the amino acids in proteins are from Cohn and Edsall[8] and Cannan.[9]

TABLE I

Ionization of Chymotrypsinogen

*p*K: *p*H	10 CysH_4	12.5 Arg_6	6.5 His_8	10 Lys_{20}	4.5 Asp_{13}	10 Tyr_6	Net total charge
8	0	6	0	20	−13	0	13
9	−0.4	6	0	18	−13	−0.6	10
9.5	−1	6	0	15	−13	−1.5	5.5
10	−2	6	0	10	−13	−3	−2
11	−3.6	6	0	1.8	−13	−5.4	−14

By this procedure the value found is 9.8. Anderson and Alberty give *p*H 9.5 for the isoelectric point.[10] This is excellent agreement, so we use the

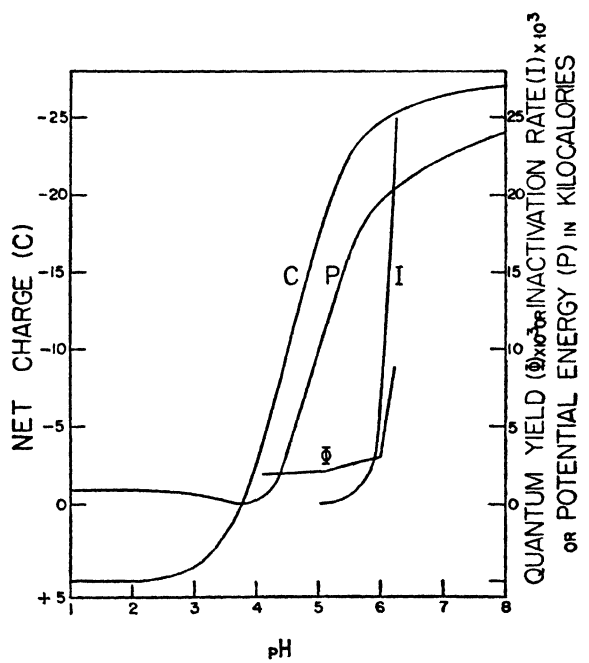

Fig. 1. Net charge (C), quantum yield (Φ), inactivation rate (I), or potential energy (P) in kilocalories versus *p*H for pepsin.

procedure for pepsin. The results are given in Figure 1, curve C. The isoionic point (net charge of zero) is at *ca.* 3.8. The fact that the known isoelectric point is considerably lower may be attributed to adsorption of anions.[1,11]

Now the model we have chosen does not conform to that of a globular protein because of its extreme length. As a first approximation we can fold the molecule end to end; this halves the length and doubles the charge density. By folding 4 times in this way and assuming that the length is always great compared to the cross section of the bundle (which of course becomes less true with each folding) we arrive at a length of 64 A. which is of the order of magnitude of the length of a globular protein of this molecular weight (*ca.* 42 A.). Of course our model is overtaxed by folding more than twice, but without a detailed knowledge of the charge distribution within a pepsin molecule our first approximations will suffice to reveal that internal, electrostatic repulsion potentials calculated as already indicated are of an appreciable magnitude.

As a sample calculation we consider the unfolded rigid rods of 1027 A. at pH 8.0 with an average net charge of -27. Taking the charge on the electron as 4.8×10^{-10} electrostatic units, the charge density σ, is 1.26×10^{-3} electrostatic units per centimeter. The average potential at the site of a possible break, $\overline{V}$, is:

$$\frac{(1.26)^2 \times 10^{-6} \times 1.03 \times 10^{-5}}{80 \times 2} = 1.02 \times 10^{-13} \text{ (e.s.u.)}^2/\text{cm.} = 1.02 \times 10^{-13} \text{ erg}$$

This is 1500 calories per mole. At pH 8 and a folding of four times we have 24,000 calories per mole of intramolecular repulsion. *Electrostatic potentials of this magnitude clearly cannot be ignored in any theory of protein denaturation.* Of course in thermal denaturation secondary bonds are broken but the repulsion potential at the break will exist. In Figure 1, curve P is a plot of potential energy in kilocalories/mole as a function of pH for our model folded four times, assuming that the cross section of the bundle is small compared to the length and as a first approximation that all molecules have the indicated (average) charge at a given pH, curve C.

It has been demonstrated that the sedimentation constant of pepsin decreases as the pH is increased from 7 to 10. Below 6 it is relatively constant[12] and if we assume no change of configurational entropy in a region of constant sedimentation constant then our calculated repulsion will be approximately the free energy change of the molecule due to ionization charges with change in pH (we are ignoring the free energy changes of ionization).

From Figure 1, curve Φ, we see how the quantum yield for inactivation takes a sudden rise at pH *ca.* 6*. From this we can say that at this pH the molecule is under such a strain as to undergo a more efficient light denaturation. The repulsion makes it much less probable that active free radicals will recombine and reaction with the solvent will be preferred.[13] Note also the rise in rate constant of thermal denaturation, curve I.

---

* A few factors have been ignored in the above considerations. It is recognized, for example, that only a small fraction, *ca.* 1%, of the molecules have the average charge at a given pH and for a given instant.[8] This does not alter the significant point that the intramolecular repulsion potential energy becomes high (about 20,000 calories per mole) for pepsin as the pH approaches 7. Also the influence of the ionic double layer on the repulsion of, *e.g.*, adjacent charges has been ignored: between pH 4 and 7 the ionic strength can be so low, however, that the double layer may be as large as the protein molecule and without influence on adjacent charges.

References

1. J. H. Northrop, M. Kunitz, and R. M. Herriott, *Crystalline Enzymes.* Columbia Univ. Press, New York, 1948.
2. J. Steinhardt, *Kgl. Danske Videnskab. Selskab. Mat. fys. Medd.*, **14,** 11 (1937).
3. J. B. Conn, D. C. Gregg, G. B. Kistiakowsky, and R. M. Roberts, *J. Am. Chem. Soc.*, **63,** 2080 (1941).
4. M. Bender and J. M. Sturtevant, *ibid.*, **69,** 607 (1947).
5. A. D. McLaren and S. Pearson, *J. Polymer Sci.*, **4,** 45 (1949).
6. E. Brand, *Abstracts of 111th Meeting A. C. S.*, Atlantic City, April, 1947.
7. E. Brand, *Abstracts of 112th Meeting A. C. S.*, New York, Sept., 1947.
8. E. J. Cohn and J. T. Edsall, *Protein, Amino Acids, and Peptides as Ions and Dipolar Ions.* Reinhold, New York, 1943.
9. R. K. Cannan, *Chem. Revs.*, **30,** 395 (1942).
10. E. A. Anderson and R. A. Alberty, *J. Phys. & Colloid Chem.*, **52,** 1345 (1948).
11. A. Tiselius, G. E. Henschen, and H. Svensson, *Biochem. J.*, **32,** 1814 (1938).
12. J. St. L. Philpot, *Biochem. J.*, **29,** 2458 (1935).
13. A. D. McLaren, in F. F. Nord, ed., *Advances in Enzymology.* Vol. IX, Interscience, New York, 1949, page 75.

Institute of Polymer Research
Polytechnic Institute of Brooklyn
Brooklyn, New York

A. D. McLaren
Charles Lewis

Received February 9, 1950

Note on the Distribution of Polymer Molecules in Dilute Solution

Current considerations of the possibility of critical concentration effects in dilute polymer solutions[1] and the related problem of the interpretation of the second virial coefficient[2] leads us to describe a very elementary point of view relevant to these matters. This concept, although quite approximate in nature, has the advantage of providing a consistent interpretation of several independently observable characteristics of dilute polymer solutions.

It is postulated that the average arrangement of polymer molecules in dilute solution is governed by the following considerations.

(*1*) The dissolved polymer molecule is represented statistically by a Gaussian distribution of the density of polymer segments in space. The statistical distribution of polymer molecules in solution is represented by a radial distribution function of their centers of gravity.

(*2*) The radial distribution function for polymer molecules at very low concentration in a good solvent resembles that for hard spheres except in that the ascent to the average value is much less abrupt. In poorer solvents the ascent is still more gentle and shifted closer to the origin. In the case of van't Hoff behavior the radial distribution is completely uniform at all distances of separation of the centers of polymer molecules.

(*3*) The midpoint in the ascent of the radial distribution curve corresponds to the interpenetration of two polymer molecules to the extent that the average density of polymer segments in the region of overlap has reached a value characteristic of the polymer–solvent system. An *effective diameter, D,* for the polymer molecules is defined by the spherical surfaces which come into contact when the characteristic value of segment density is reached.

(*4*) To the extent to which this behavior approaches that of hard spheres an excluded molecular volume may be defined which is four times the volume of a sphere of diameter D. The hard sphere model predicts that significant upward curvature will first occur in plots of reduced osmotic pressure, reciprocal reduced turbidity, or reciprocal dissymmetry coefficient against concentration at that concentration corresponding to filling volume of the solution with close-packed excluded-volume spheres. Inasmuch as the polymer molecules approximate soft spheres with less abrupt radial distribution functions it may be expected that the onset of significant upward curvature will be somewhat delayed. It is this concentration range which may be considered as the "critical concentration," for beyond this region the extent of interpenetration of polymer molecules will greatly increase with a consequent lowering of D.

The value of D relative to R will depend on the molecular weight, flexibility, and degree of branching of the polymer as well as the polymer–solvent interaction, and would not be simply related to the root mean separation of the ends of the chain, R.

The effective diameter can be estimated in two independent ways: one depends upon the interpretation of thermodynamic data and the other on first-order interference of scattered light. In the former method the polymer molecules are approximated as hard spheres, their diameter being identified with the effective diameter and approximately evaluated by use of the relation: $B = 2\pi D^3 N_0/3M^2$, where N_0 is Avogadro's number and M represents the molecular weight. Thus, D decreases as B decreases, becoming zero when van't Hoff behavior is attained. Consequently, resistance to interpenetration vanishes at $B = 0$, although the value of R has only diminished to about one-half its value in a good solvent.[3] It follows therefore, that the "critical concentration" is lowest when the value of B is greatest. Upon passing to increasingly poor solvents the critical concentration moves to higher concentration and ceases to exist when van't Hoff behavior is reached. It is just this behavior which has been shown to exist[4] in a recent study of the osmotic pressure of polystyrene in various solvents over a large concentration range. Here it was noted that large values of B were always associated with large values of the third virial coefficient, that is, curvature occurred at relatively low concentrations and became quite pronounced; when B was small curvature was not noticeable until high concentrations were reached and then it was only slight.

The alternative method of estimating D arises from a consideration of the scattering of light from a system of polymer molecules exhibiting an effective diameter. The intensity of light scattered at an angle θ from a polymer solution consistent with the foregoing postulates at concentrations less than the critical concentration can be shown to be given by an expression formally the same as that previously suggested for solutions of charged macromolecules:[5,6]

$$i_\theta = KcMP(\theta)\left[1 - \frac{\psi}{V}\Phi(ksD^*)\right]$$

The symbols are the same as used previously[4]; D^* is the effective diameter. (A factor of π^2 was accidentally omitted from the expression for K in reference 5.)

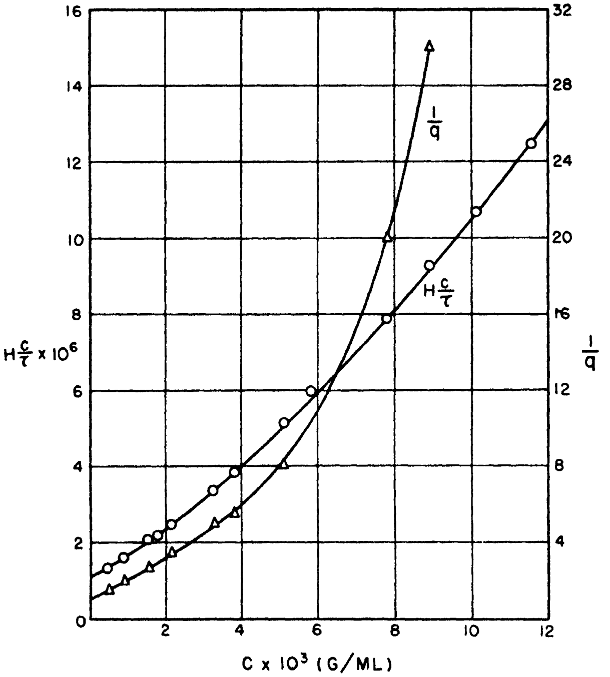

Fig. 1. Reciprocal reduced turbidity and reciprocal dissymmetry coefficient (45° and 135°) for a polystyrene fraction dissolved in toluene λ = 4360 A.

The data shown in Figure 1 of the customary turbidity and dissymmetry measurements for a toluene solution of a polystyrene fraction serve to illustrate the relations described. From the initial slope of the Hc/τ plot B is found to be 2.5×10^{-6}. Since from the intercept M is 900,000, D = 550 A. The dissymmetry data at low concentration can be fitted to the above equation with a value of D^* = 500 A., in good agreement with the estimate from B. Using this value of D^* for the radius of the excluded volume sphere, one finds that the total volume so occupied becomes equal to that of the solution at a concentration of about 0.30%. It can be seen in Figure 1 that the curvature in both the thermodynamic and diffraction data becomes significant at approximately this concentration. For the lower molecular weights or poorer solvents the effective diameter is, of course, found to be smaller and the curvature is first detected at higher concentrations and is much less abrupt.

It was previously estimated[1] that the effective diameter of a polymer molecule would be about $2R$, from which one would anticipate that the critical concentration would lie at such low values as to be experimentally inaccessible. However, in the above case it is seen that $D = 0.5R$ and in general for polystyrene in toluene it can be shown that $D/R = 0.075M^{1/6}$. The numerical factor will be different for different solvents. It seems unlikely that any solvent will provide a significantly higher numerical constant for polystyrene. Consequently, only by going to extremely high molecular weights will the critical concentration be shifted to extremely low concentrations: in this event only turbidity methods could be used. On the other hand, in solutions of polar polymers in solvating solvents as well as in low ionic strength solutions of charged polyelectrolytes D may be much larger than R with the result that for sufficiently high molecular weight polymers the region below the critical concentration will be inaccessible with present techniques: the molecular weight and the size of the molecule at infinite dilution could not be determined by equilibrium methods. This discussion does not, of course, apply to hydrodynamic methods, but it is not unlikely that a somewhat parallel situation exists there.

Finally, mention should be made that the viewpoint proposed here is probably capable of sufficient refinement to make a contribution to the general theory of polymer solutions. Though different in approach, it would not be incompatible with the current theories based on calculations of the configurational entropy of polymer chains because from both points of view it appears that it is the average density distribution of polymer segments that most simply characterizes the dilute polymer solution.

References

1. R. F. Boyer and R. S. Spencer, *J. Polymer Sci.*, **5**, 375 (1950).
2. P. J. Flory, *J. Chem. Phys.*, **17**, 1347 (1949).
3. P. Doty, W. A. Affens, and B. H. Zimm, *Trans. Faraday Soc.*, **B42**, 66 (1946). B. H. Zimm, *J. Chem. Phys.*, **16**, 1099 (1948).
4. M. Schick, P. Doty, and B. H. Zimm, *J. Am. Chem. Soc.*, **72**, 530 (1950).
5. P. Doty and R. F. Steiner, *J. Chem. Phys.*, **17**, 743 (1949).
6. G. Oster, *Rec. trav. chim.*, *in press.*

Gibbs Memorial Laboratory
Harvard University
Cambridge, Massachusetts

PAUL M. DOTY
ROBERT F. STEINER

Received March 17, 1950

JOURNAL OF POLYMER SCIENCE VOL. V, NO. 3, PAGES 387-389

REVIEWS

High-Polymer Physics—A Symposium. Howard A. Robinson, ed., Chemical Pub. Co., Brooklyn, 1948, 586 pp. Price $12.00.

This volume consists of the twenty-three papers delivered before the Annual Meeting of the High Polymer Division of the American Physical Society in January, 1946. As such it presents a definitive cross section of the research in the physics and physical chemistry of high polymers in progress at that time. The symposium was quite successful; the papers were well received, and viewed in the perspective of four years obviously represent a substantial contribution to the field.

The number of papers is too great to allow individual assessment here. Consequently, the only further purpose this review can serve is to question the propriety of publishing this group of papers collectively. It must be appreciated that there was no central theme to the Symposium, an unusually wide selection of topics was covered. Moreover, almost three years elapsed between their delivery and publication. By this time most of the contributions had appeared in various journals and their timeliness had waned. The attractiveness of the volume is further diminished by its exorbitant cost.

In conclusion, it is difficult to balance the convenience and interest of the book against the fact that it represents essentially a costly transfer of journal material to book form, a luxury an overburdened scientific literature can scarcely afford.

Paul M. Doty

The Physics of Rubber Elasticity. L. R. G. Treloar, Oxford Univ. Press, New York, 1949, 262 pp. Price $6.00.

This is a thoroughly excellent book. It covers the problem of rubber elasticity from both a theoretical and an experimental point of view. One outstanding feature of the book is the attention which is paid to behavior involving large strains. The major part of classical theory of elasticity is limited to the region of very small strains. In the case of rubber, strains of several hundred per cent are commonly encountered. The author provides a clear account of how these large strains can be handled theoretically, and what the experimental properties of rubber are in the large strain region.

One chapter is devoted to the photoelastic properties of rubber, and two to crystallization and its influence on the mechanical properties of rubber. The dynamic properties of rubbers are discussed briefly, as well as stress relaxation and flow. The kinetic theory of rubber elasticity is, of course, thoroughly treated.

This book is recommended to all who are interested in the mechanical behavior of high-polymeric substances.

Turner Alfrey, Jr.

Fundamentals of Synthetic Polymer Technology. R. Houwink, Elsevier, New York-Amsterdam, 1949, 270 pp. Price $3.75.

Dr. Houwink is well known for his numerous publications on synthetic and natural polymers. His book *Elasticity, Plasticity and Structure of Matter* published in 1937 found ready acceptance in this country and was an important factor in shaping thinking on the subject of polymers.

In the present book, the author has set himself the difficult task of presenting polymer fundamentals to the reader in the hope that he will thereby be enabled to "interpret the results of tests and the properties of the final products." Unfortunately, this aim is not very fully achieved. It is, however, a reassuring and heartening thought and one which is too often forgotten that polymer technology does in the end rest on determinable "basic principles" and concepts. The detailed explanation of polymer processes and properties in terms of fundamental factors is a much greater undertaking than the present volume. Nevertheless, by including in the same volume both the basic and the technological aspects, the author has facilitated and encouraged this type of approach to technology. This in itself is a step toward the larger goal.

Because the volume does cover both basic and technical aspects of polymers, the treatment is necessarily condensed. This condensed form (comprising almost an outline type of presentation in the first sections) provides an easily read and easily comprehended style which will be appreciated by those who are anxious to gain concepts rather than struggle with detail.

The book throughout adopts an elementary approach In the author's typical style, good use is made of illustrations, diagrams, graphs, and charts to assist the reader in a ready understanding of the topics under discussion. Both the theoretical and the practical worker in the polymer field will profit from the broad horizon this book provides, but it will be of chief interest to those who might be said to be engaged in the engineering applications of polymer products. The book is hardly suitable for a text, except perhaps under special circumstances.

The American reader will still find signs of European expression in the volume. These are, however, nowhere objectionable and do not harm the presentation or understanding of the text. One of the author's objects is to encourage understanding by presenting both the European and North American points of view, particularly in reference to testing. It is of questionable value to the American reader to learn that different countries employ different tests and specifications. The author has presented this material (Chapter IV) on a very elementary level, so that the arbitrary differences among different countries are fortunately minimized. Yet many will feel that the treatment is too elementary and general perhaps to be of value. In Chapter V, "Processing of Polymers," the different practices followed in different countries are not as evident and an integrated (again elementary) treatment is achieved.

The last sixty per cent of the volume is devoted to manufacturing processes and properties of most of the commercially known polymers including synthetic rubbers (Chapter VII). The author has succeeded in giving the reader a concise, easily-read account in this part, with well-selected topics and illustrations in each instance.

The theorist and the technical scientist both will differ with the author's statements in places. For example, many American rubber chemists will find it difficult to agree (p. 142) that it is any more "inadmissable" to compare normal sulfur vulcanizates in the aging tests of natural *versus* synthetic rubber than it is to compare the low-sulfur vulcanizates recommended by the author. The nature of the rubber compounding employed in any given application is determined by many factors in addition to the factor of aging. There are many instances where synthetic rubber is preferred to natural rubber because of its superior aging performance under service conditions. Also, in the recipe for GR-S (p. 128), "stabilizer" in the form of fish-oil soap is not added in American manufacture. More up-to-date information would be welcome also on some topics, for example, on the recent types of silicone, Thiokol, and neoprene synthetic rubbers, as well as some of the newer plastics. In spite of these deficiencies many will find in this volume the combination of basic and technical information they have been seeking. The author is to be commended on his selection of topics and the condensed and efficient style of this volume.

C. S. Fuller

Industrial Rheology and Rheological Structures. Henry Green, Wiley, New York, 1949, 323 pp. Price $5.50.

The scope of this book is not as broad as might be expected from the title. The primary emphasis is on two-phase, particle-vehicle systems, such as printing inks and paints, which were of particular rheological interest to the late Henry Green. Other types of materials are treated only rather superficially, and not in the way their industrial significance would seem to indicate. Realizing this at the outset, the book can then be evaluated in terms of what it accomplishes within its acknowledged limits.

The first seven chapters develop the foundations for Green's rheological "system." The general procedure is to start with a model of flow (deduced from microscopic observations), work out from that a logical design for a viscometer, and finally develop means of converting viscometric measurements into meaningful and usable numbers. The fundamental rheological quantities employed are the plastic viscosity and the yield value. To these may be added three coefficients of thixotropic breakdown, for materials which exhibit that phenomenon. The succeeding four chapters deal with laboratory applications of the system. Considerable space is devoted to a discussion of the rotational viscometer developed by Green and Weltmann, and its use. A few other viscometers are mentioned briefly, and the section closes with some comments on the use of rheological measurements in plant control.

The third section, comprising five chapters, emphasizes the important role of microscopy in the rheology of particle-vehicle systems. The techniques of fine-particle microscopy are outlined and some comments made on the problem of measuring average particle size. The last two chapters are concerned with the aggregation of particles to form rheological structures. These are divided into *loose structures*, as in Newtonian, pseudoplastic or dilatant materials, and *connected structures*, as in plastic, brittle, or thixotropic materials. Two-dimensional flocculates and structural artifacts are also discussed.

The book closes with a list of symbols, nine appendices, a rheological glossary of over eleven pages, and thirteen pages of index. Two of the appendices are particularly interesting. The first consists of several pages of advice to the industrial rheologist on dealing with management. The other endeavors to present the laboratory director with a simplified version of rheological fundamentals. Both are eloquent commentaries on Mr. Green's varied experience.

The style of the book is somewhat informal and very readable. This volume should be an invaluable practical and theoretical guide to the person investigating particle-vehicle systems. To others, it may be recommended as presenting varied and useful information in a pleasant manner. It must be regarded as a significant contribution in the far from overworked field of rheological literature.

R. S. Spencer

POLYMER NEWS

The Graduate School of Physics and The Institute of Polymer Rese of the Polytechnic Institute of Brooklyn announce the Seventh Annual Series of Summer Laboratory Courses. The courses offered in the 1950 series are:

June 12–23: *Industrial Applications of X-Ray Diffraction*
June 26–30: *Advanced X-Ray Diffraction*
June 26–30: *Methods in Physical Biochemistry*
July 17–21: *Weight and Shape of Polymers in Solution*
July 31–August 4: *Techniques of Polymerization and Copolymerization*

Inquiries should be addressed to Professor I. Fankuchen, Polytechnic Institute of Brooklyn, 85 Livingston Street, Brooklyn 2, New York.

The Society of Chemical Industry, Plastics and Polymer Group, has arranged a Symposium on *Polymer Chemistry as Applied to Plastics.* The Symposium will be held in Beveridge Hall, the University, London, on September 21, 22, and 23, 1950. It will be opened on the morning of September 21 by Prof. E. K. Rideal, M.B.E., M.A., D.Sc., F.R.S., and will include four subsequent sessions:

Sept. 21 (afternoon). Chairman, Prof. H. W. Melville, F.R.S. *The Tools of Polymer Research.* Osmometry, light scattering, infrared and x-ray spectroscopy, viscometry, organic chemistry.

Sept. 22 (morning). Chairman, Dr. J. C. Swallow. *The Relations between Structure and Properties of Polymers.* Effect of molecular size and shape, cross-linking etc. on electrical and physical properties, with particular reference to the crystalline, amorphous and rubbery states.

Sept. 22 (afternoon). Chairman, Dr. R. F. Hunter. *Polymerization and Polycondensation (Theory).* Kinetics of ionic and free radical reactions, redox systems, mechanism of polycondensation reactions, etc.

Sept. 23 (morning). Chairman, Dr. J. J. P. Staudinger. *Polymerization and Polycondensation (In Practice).* Continuous *vs.* batch polymerization, heat transfer problems, low temperature polymerization, high pressure reactions, practical aspects of continuous polycondensation reactions.

Each of the four sessions will involve the presentation of about six papers, which will be followed by general discussion. Shortened versions of the contributions will be preprinted and distributed to subscribing participants. The registration fee for the Symposium will be 10*s.* to members and £2 2*s.* to nonmembers of the Society of Chemical Industry. Communications relating to the Symposium should be addressed to Dr. N. J. L. Megson, Hon. Organizing Secretary, Ministry of Supply, Room 716, Shell Mex House, London, W.C.2, England.

JOURNAL OF POLYMER SCIENCE VOL. V, NO. 4, PAGES 391-427

Redox Recipes. II. Redox Recipes in Alkaline Medium Initiated by the System Cumene Hydroperoxide–Iron–Sugar at 30°*

M. KOLTHOFF and A. I. MEDALIA,† *School of Chemistry, University of Minnesota, Minneapolis, Minnesota*

As discussed in the previous paper of this series,[1] the combination in alkaline medium of an iron salt with a reducing sugar was found by German workers in the I. G.[2] to be highly effective in initiating polymerization in redox systems with benzoyl peroxide as oxidizing agent. Soon afterward we made use of this principle with cumene hydroperoxide (designated as CHP) as the oxidizing agent. The first experiments were very successful and since April 1946, a series of reports has been submitted to the Office of Rubber Reserve describing results which we have obtained with the CHP–iron–sugar system. The recipe developed is similar to that which has been published by Vandenberg and Hulse,[3] who used rosin soap as emulsifier. Although we have done some work with this emulsifier, most of our studies have been carried out with an emulsifier of higher purity. Many of the data given in this paper were obtained with pure potassium myristate as emulsifier. Marked differences have been found between the characteristics of time–conversion curves at 30°C. and at 0°C. (the two temperatures at which we have studied these systems). The present paper deals with data obtained at 30°; in a subsequent paper suitable recipes at 0° will be discussed.

EXPERIMENTAL

Reagents

Potassium myristate was prepared for use in the present work by neutralization of Eastman White Label myristic acid with potassium hydroxide in hot alcohol, followed by recrystallization from alcohol and vacuum-drying to constant weight. The active oxygen content of this potassium myristate, as determined by an iodometric procedure, was only 8 p.p.m. Potassium laurate and caprate were prepared similarly. The butadiene was Carbide and Carbon (99%), passed through ascarite to remove inhibi-

---

* This work was carried out under the sponsorship of the Office of Rubber Reserve, Reconstruction Finance Corporation, in connection with the Synthetic Rubber Program of the United States Government.

† Present address: Brookhaven National Laboratory, Upton, N. Y.

tor. The styrene was a Dow product, freshly distilled before use. Twice-distilled water was used throughout. The cumene hydroperoxide was a sample furnished by Hercules Powder Co., #X-3354-84, and was found by an iodometric procedure to contain 5.96% active oxygen, corresponding to 56.5% cumene hydroperoxide in the sample, the remainder being principally cumene and the decomposition products of CHP.[4] All amounts of CHP given are expressed in parts of this sample of 56.5% purity. The iron solutions were prepared by dilution of stock solutions which had been standardized by the usual methods. The stock solution of ferrous sulfate (Merck reagent grade $FeSO_4 \cdot 7H_2O$) was 0.2 *M* in ferrous iron and 0.01 *N* in sulfuric acid, the acid minimizing air oxidation. The stock solution in water of ferric nitrate (Merck reagent grade $Fe(NO_3)_3 \cdot 9H_2O$) was 0.2 *M*, solutions of this concentration having been shown to be stable.[5] A mixed tertiary mercaptan (Sulfole B-8) was obtained from Phillips Petroleum Company. Fructose was obtained from the Sugar Research Foundation of Massachusetts Institute of Technology; glucose was Mallinckrodt C.P.; and sodium pyrophosphate decahydrate was Mallinckrodt A.R.

Charging, Polymerization, and Sampling Procedures

With the exception of the iron salt, all water-soluble ingredients (sugar, soap, and pyrophosphate) were charged as aqueous solutions; the mercaptan and CHP were added as solutions in styrene; and the butadiene was added by weight, allowing a slight excess to boil off in order to remove air in the gas phase. The container was capped and shaken, and then the iron salt was injected through the sealant gasket[6] and the charge was placed on a rotor in a water bath at 30°. By adding ferrous salts in this way, air oxidation of ferrous iron, which is very rapid in alkaline pyrophosphate, was minimized; data illustrating this are given below. For the sake of uniformity, ferric salts were added in the same manner. The containers used were 4-oz. screw cap bottles, with molded Buna-N gaskets. Generally the total weight of the charge was approximately 50 g. Conversions were determined by the total solids method, with quinhydrone as inhibitor, using the "ejection" technique of sampling as described by Williams and Johnson.[7]

FUNDAMENTAL RECIPE

The recipe which has been studied in the present work is given on page 393.

The mechanism of activation by the peroxide–iron–sugar system has been discussed in the previous paper.[1] In brief, the proposed mechanism is that the sugar reduces the (complex) ferric iron to the (complex) ferrous state; the ferrous iron is oxidized by the peroxide, probably with the formation of organic free radicals, which initiate polymerization. The ferric iron is continually reduced by the sugar, so that polymerization continues to take place as long as there is sufficient peroxide, sugar, and monomer.

FUNDAMENTAL RECIPE:

Ingredient	Parts by weight
Butadiene	75
Styrene	25
Water	180
Potassium myristate	5.0
Sulfole mercaptan	0.35
$Na_4P_2O_7 \cdot 10H_2O$	1.0
Cumene hydroperoxide (56.5%)	Variable
$FeSO_4 \cdot 7H_2O$ or $Fe(NO_3)_3 \cdot 9H_2O$	Variable
Reducing sugar	Variable

Temperature: 30°C.

In a sense the iron salt may be regarded as a catalyst in the oxidation of the sugar by the peroxide; but since it is the reaction between the peroxide and the ferrous iron rather than that between the peroxide and the sugar which is chiefly responsible for initiation (see below), it seems preferable to state the mechanism in such a way as to focus attention on the peroxide–ferrous iron reaction.

RECIPE CONTAINING FERRIC IRON AND GLUCOSE

The use of ferric iron in the fundamental recipe gives slightly lower rates of polymerization than that of ferrous iron; on the other hand, the system with ferric iron is simpler and the results are more readily interpreted, and hence this type of recipe will be discussed first.

Variation of the Amount of Ferric Iron

Data showing the effect on the rate of conversion when the amount of ferric iron is varied while the amounts of pyrophosphate, CHP, and glucose are held constant are shown in Figure 1, which is plotted with a logarithmic abscissa. For convenience, a similar curve obtained with ferrous iron is plotted in this figure but is discussed in a later section. The amounts of CHP used in the polymerizations of Figure 1 are sufficient to keep the rate of conversion linear up to and beyond 1.5 hours (see below), so that the 1.5-hr. conversions, which are plotted in Figure 1, represent the initial rates of polymerization.

The curves obtained with three different amounts of CHP go through maxima in the neighborhood of 0.036 part ferric nitrate nonahydrate; evidently the initial rates of conversion depend on the *absolute amounts* of ferric iron and of CHP and not on the ratio between these amounts. The decrease in initial rates of conversion with large amounts of ferric iron cannot be explained at present. From the practical standpoint it is of importance that the amount of ferric iron can be varied over a fourfold range in the neighborhood of the maximum rate (0.018–0.072 part $Fe(NO_3)_3 \cdot 9H_2O$) with very little change in the rate of conversion.

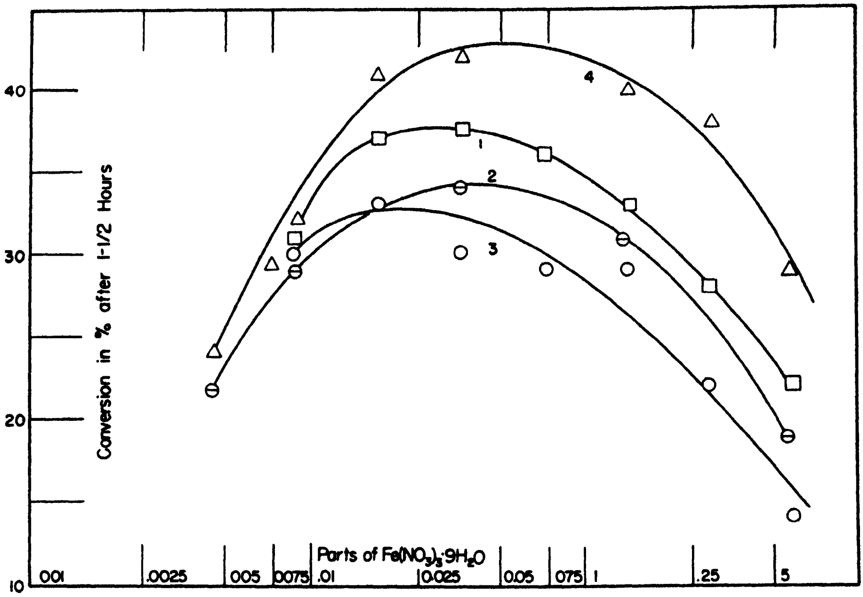

Fig. 1. Conversions after 1.5 hrs. of polymerization with 1 part of glucose.

(1) 0.0242 part of CHP; (2) 0.0483 part of CHP; (3) 0.0967 part of CHP; ferric iron variable in all three; (4) ferrous iron, with 0.0483 part of CHP in excess over ferrous iron (based on 1:1 molar reaction ratio). Amounts of ferrous iron expressed as equimolar amounts of ferric iron.

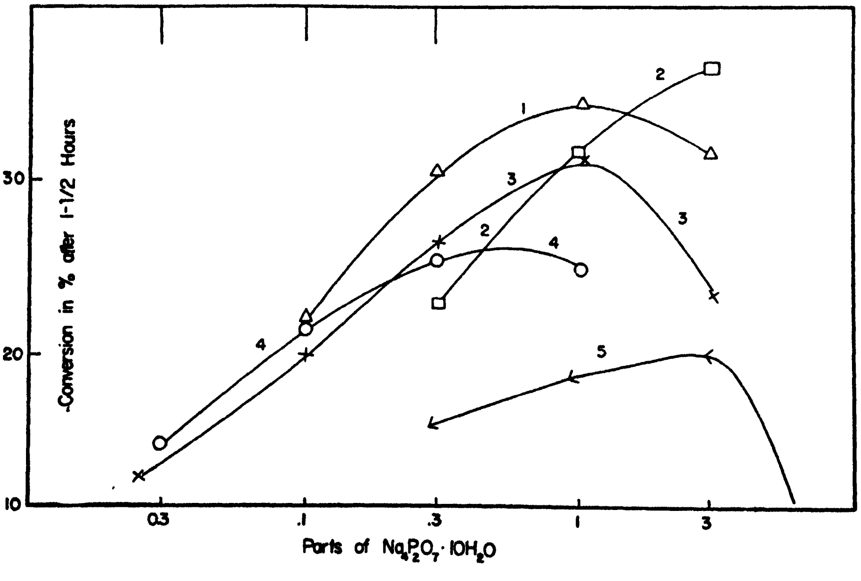

Fig. 2. Conversions after 1.5 hrs. of polymerization with 1 part of glucose and 0.0483 part of CHP.

(1) 0.036 part of $Fe(NO_3)_3 \cdot 9H_2O$; (2) 0.145 part of $Fe(NO_3)_3 \cdot 9H_2O$; (3) 0.009 part of $Fe(NO_3)_3 \cdot 9H_2O$; (4) 0.0045 part of $Fe(NO_3)_4 \cdot 9H_2O$; (5) 0.58 part of $Fe(NO_3)_3 \cdot 9H_2O$.

Variation of the Amount of Pyrophosphate

The effect of variation in amount of pyrophosphate, with constant amounts of iron, CHP, and glucose, is shown in Figure 2, which is plotted with a logarithmic abscissa. With a concentration of ferric nitrate nonahydrate of 0.036 part or less, the optimum amount of pyrophosphate is 1 part; while with larger amounts of iron, the optimum amount of pyrophosphate is greater than 1 part. The rates of conversion with the smaller amounts of iron (0.009 and 0.0045 part of $Fe(NO_3)_3 \cdot 9H_2O$) are all less than with 0.036 part of $Fe(NO_3)_3 \cdot 9H_2O$ and 1 part of pyrophosphate. While a slightly higher rate of conversion can be obtained by increasing the amounts of both iron and pyrophosphate above 0.036 and 1 part, respectively, this does not appear advisable from a practical standpoint. With 1 part of pyrophosphate and 0.036 part of ferric salt, the molar ratio of pyrophosphate to iron taken is 25.2.

Variation of the Amount of CHP

Conversion-time curves obtained with varying amounts of CHP are shown in Figure 3; conversions obtained after 1.5 hours of polymerization are plotted against the amount of CHP taken, in Figure 4. Curve 1 of Figure 3 is a typical polymerization curve obtained with the fundamental recipe with optimum concentrations of ingredients. The rate of conversion

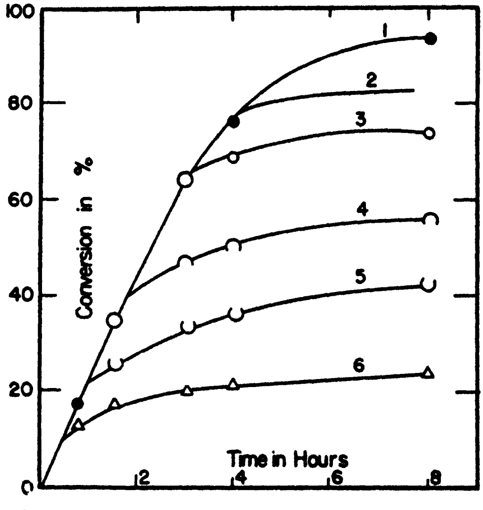

Fig. 3. Conversion-time curves with 1 part of glucose and 0.036 part of ferric nitrate nonahydrate.

(1) 0.0483 part of CHP; (2) 0.0242 part of CHP; (3) 0.0193 part of CHP; (4) 0.0145 part of CHP; (5) 0.00967 part of CHP; (6) 0.00483 part of CHP.

is practically constant from the beginning of polymerization up to about 70–80% conversion, after which it decreases continuously. Provided sufficient CHP was taken, curves of this shape have been obtained with all amounts of iron and pyrophosphate which have been studied. The virtual linearity of the conversion–time curve over such a wide range makes this recipe particularly attractive from a practical standpoint.

It is seen from Figure 3 that the initial rates of conversion obtained with varying amounts of CHP are nearly the same, but that the rate of conversion drops off sharply at conversions which are lower as less CHP is taken in the charge. Up to conversions at which this sharp drop takes place, an increase in the amount of CHP taken causes a slight decrease in the initial rate of conversion, as shown in Figure 4.

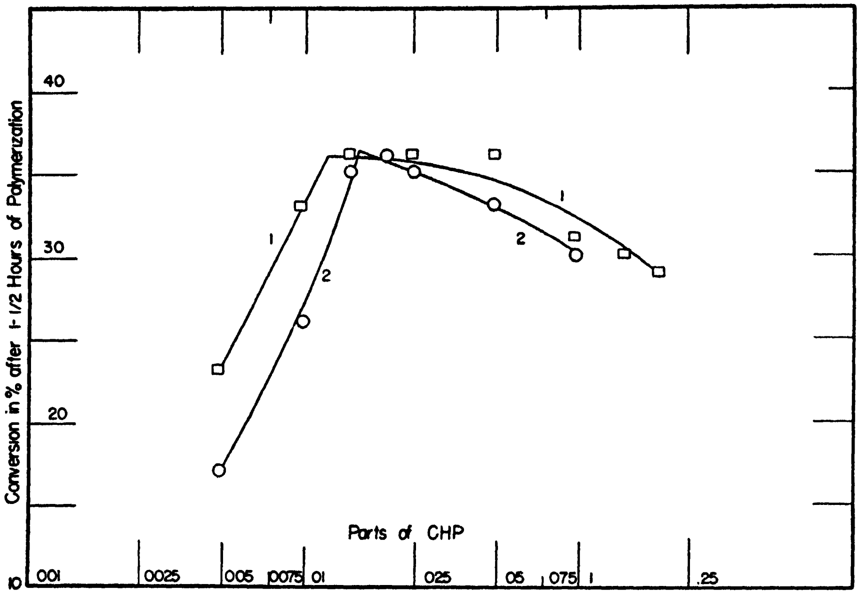

Fig. 4. Conversions after 1.5 hrs. of polymerization with 1 part of glucose. (1) 0.145 part of $Fe(NO_3)_3 \cdot 9H_2O$; (2) 0.036 part of $Fe(NO_3)_3 \cdot 9H_2O$.

With the exception of the charge prepared with the highest amount of CHP, very little conversion was found to take place in the charges of Figure 3 between 4 and 8 hours of polymerization, so that the conversions obtained at 8 hours may be tentatively regarded as the limiting conversions reached after complete exhaustion of the CHP; a more exact interpretation is given below. A plot of these 8-hour conversions *vs.* concentration of CHP (Fig. 5, curve 2) shows that the conversions reached with the four smallest amounts of CHP fall on a straight line, with a slope of 34% conversion per 0.01 part of cumene hydroperoxide (per 100 parts of monomer). The fact that the points obtained with larger amounts of CHP do not fall on the straight line is a result of the normal falling-off of the rate of conversion with any polymerization recipe at very high conversions.

Separate experiments have shown that injection of a small amount of CHP to a latex in which polymerization has practically ceased, such as Nos. 2–6 of Figure 3, brings about renewed rapid polymerization. While analyses have not been carried out of the very small amounts of CHP present in such latices, it is reasonable to suppose that the CHP is very nearly exhausted when the conversion–time curve starts to drop off sharply, *i.e.*, that nearly all the CHP taken is consumed over the linear portion of the conversion–time curve. Since the conversion–CHP curve is also linear over this range, this means that the rate of consumption of CHP is practically constant over the linear portion of the conversion–time curve.

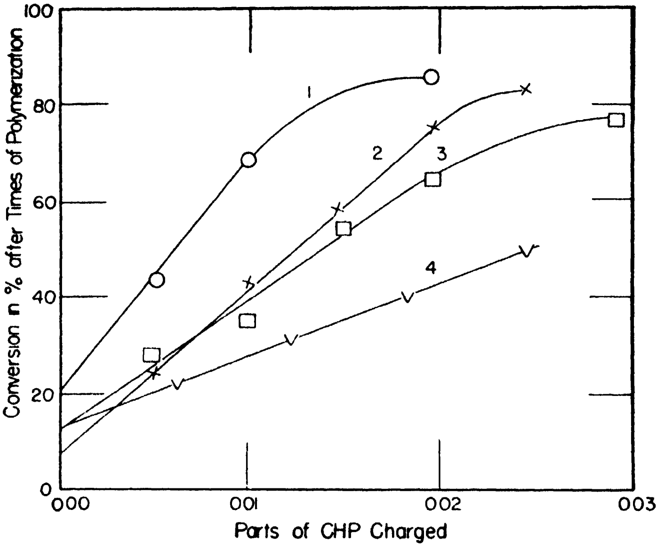

Fig. 5. Conversions after given times of polymerization with 0.036 part of $Fe(NO_3)_3 \cdot 9H_2O$.

(1) 0.3 part of glucose, 9 hrs. of polymerization; (2) 1.0 part of glucose, 8 hrs. of polymerization; (3) 3.0 parts of glucose, 9 hrs. of polymerization; (4) 10 parts of glucose, 3 hrs. of polymerization.

Data such as those of Figure 5 can be used to derive the rate of consumption of CHP, as shown in the following section.

From the practical standpoint, the above results indicate that in order to obtain a given conversion in the shortest time of polymerization, the amount of CHP taken should be the minimum required to keep the conversion–time curve linear up to this conversion. In large-scale industrial polymerizations, where close control of variables cannot be achieved, it would be preferable to take somewhat more than this optimum amount of CHP.

The practice is sometimes followed of determining the effect of variables upon a recipe by comparing the conversions of a series of charges after only a single time of polymerization. Particularly misleading results may be obtained in this way with redox recipes, where exhaustion of one of the redox components may cause a dead-stop; *cf.* Figures 3 and 4. With the present technique of sampling,[7] this operation requires relatively little time, so that complete determination of a conversion–time curve for each charge prepared, which is always desirable, is readily accomplished.

RELATION BETWEEN RATE OF CONVERSION AND RATE OF CONSUMPTION OF CHP

Determination of Rate of Consumption of CHP

The linear relationship between the amount of CHP charged and the conversion reached after longer times of polymerization, discussed above,

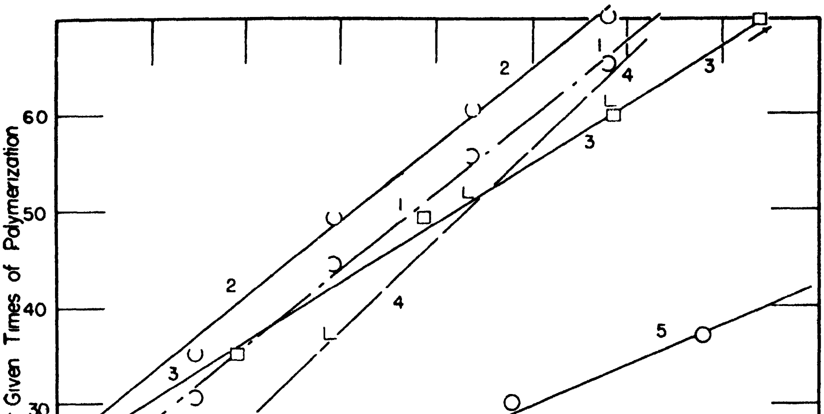

Fig. 6. Conversions obtained after given times of polymerization with 0.036 part $Fe(NO_3)_3 \cdot 9H_2O$ and varying amounts of potassium myristate, fructose, and cumene hydroperoxide.

(1) 10 parts K myristate, 0.3 part fructose, 1.5 hrs.; (2) 10 parts K myristate, 0.3 part fructose, 2.5 hrs.; (3) 10 parts K myristate, 1.0 part fructose, 3 hrs.; (4) 2.5 parts K myristate, 0.3 part fructose, 5.5 hrs.; (5) 2.5 parts K myristate, 1.0 part fructose, 2.5 hrs.

has been found with a number of recipes which give conversion–time curves similar to those of Figure 3. As an approximation it may be considered that in each of these recipes the initial rate of conversion is constant, independent of the amount of CHP charged or remaining, until no CHP is left, and that thereafter no conversion takes place. Although this approximation is not exact, a fairly accurate estimation of the rate of disappearance of CHP can nevertheless be obtained as follows. Charges are prepared containing different amounts of CHP, and the conversions obtained after a given time of polymerization are plotted against the amount of CHP taken in the charge. If the time chosen is such that all the CHP has been exhausted in each of the charges within this time, then the points (below about 75% conversion) are found to lie on a straight line, the slope of which is the percentage conversion resulting from the charging (or consumption) of a given amount of CHP; the slope is therefore the inverse of the conversion-rate of disappearance of cumene hydroperoxide. Thus the quotient of the rate of conversion by the slope of the conversion–CHP line is the rate of consumption of cumene hydroperoxide.

A large number of polymerizations has been carried out with varying amounts of soap and sugar (glucose or fructose), the amounts of CHP taken in each recipe being varied so as to permit determination of the rate of consumption of CHP, as above. Some of the data obtained are shown in Figures 5 and 6. The effects upon the rate of conversion of the amounts of soap and of sugar are best understood in terms of the relationship between the rate of conversion and the rate of consumption of CHP, which is accordingly discussed immediately below.

Theoretical

As indicated above, the mechanism of polymerization in the fundamental recipe is assumed to be as follows. The ferric iron, which is present in the aqueous phase as the pyrophosphate complex, is reduced by the sugar; the ferrous iron thus formed reacts with CHP, probably in the aqueous phase (see below), with the formation of the phenyldimethylmethoxy radical, $C_6H_5C\dot{O}(CH_3)_2$. This radical must soon enter the organic phase (taken here to include the soap micelles, in which monomer is solubilized, and the monomer-swollen polymer particles, in addition to the emulsion droplets and bulk organic phase), where it will react with monomer to form a growing polymer chain. Formation of a growing chain may also occur in the aqueous phase by reaction of the phenyldimethylmethoxy radical with dissolved monomer, but the growing chain will, in general, enter the organic phase early in its life. Conditions affecting this transfer are discussed in a following section.

By virtue of the extremely large interfacial area of the micelles and polymer particles compared with that of the emulsion droplets and of the bulk organic phase, transfer will be almost entirely to the micelles and swollen polymer particles, which together form the locus of polymerization.[8,10a–b] A general treatment of emulsion polymerization under such conditions, where the radicals are formed in the aqueous phase and are then transferred to the locus, has been given[8] and has been shown to be in agreement with results obtained for the persulfate-initiated emulsion polymerization of styrene.[9] On the other hand, the behavior of a persulfate-initiated butadiene-styrene copolymeratizion system cannot readily be interpreted according to this general theory, as will be shown in a subsequent publication from this laboratory.

Smith and Ewart[8] distinguish three limiting cases: *Case 1*, in which radicals can transfer rapidly out of the particles (locus), so that the average concentration of radicals per particle is much less than one; *Case 2*, in which radicals cannot leave the locus, but where termination is very rapid (or the particles are very small), so that half the particles have one radical, and the other half have no radical; and *Case 3*, in which each particle contains several radicals. In the absence of a chain-transfer agent like mercaptan, Case 2 or 3 would appear likely; but in the polymerizations being considered here, where chain transfer takes place through mercaptan, there exists the possibility of transfer of the RS· radicals out of the particles, so that Case 1 is also possible.

The equations by Smith and Ewart for the rate of conversion according to their three cases may be represented as follows:

Case 1 (with termination in the particles): $dM/dt =$

$$k_1(M)N^{1/2}v^{1/6}\rho^{1/2} \qquad (1)$$

Case 2: $$dM/dt = k_2(M)N \qquad (2)$$

Case 3: $$dM/dt = k_3(M)N^{1/2}v^{1/2}(\rho')^{1/2} \qquad (3)$$

where dM/dt is the rate of formation of polymer, and N is the number of particles, both per cubic centimeter of water; (M) is the concentration of monomer in the particle; v is the average volume of each particle; ρ and ρ' are the rates of formation of radicals and of their entry into the N particles, respectively; and the k values include kinetic and numerical constants.

In Table I are given values of dM/dt and of ρ (based on 100 parts of monomers rather than on 1 cc. of water). Clearly in order to decide which of the above equations (if any) fits these data, information is required concerning (M), v, and particularly N. The value of (M) decreases gradually after about 50% conversion, but apparently not earlier, in a persulfate-butadiene-styrene recipe studied in this laboratory.[11] The average volume of a particle should be proportional to the conversion, at least until (M) starts to decrease.

It is known that in emulsion polymerization recipes in general the number of particles in a charge remains nearly constant after about 10–20% conversion. Smith and Ewart predict that when Case 2 is followed, the value of N should be such that:

$$dM/dt = k_4(M)\rho^{2/5}\,(dv/dt)^{-2/5}(a_sS)^{3/5} \qquad (4)$$

where a_s is the area per gram of adsorbed soap, and S is the amount of soap (g./cc. of water). Analysis of Case 1 by the authors, following the procedure of Smith and Ewart, and assuming that ρ is constant and that all new chains are started in micelles (as long as any micelles remain) gives the equation:

$$N = k_5(a_sS)^{3/5}\rho \tag{5}$$

from which:

$$dM/dt = k_6(M)(a_sS)^{3/10}v^{1/6}\rho \tag{6}$$

Calculation of N for Case 3 is not required, since, as shown below, this case predicts conversion–time curves of a different shape from those actually found.

Results and Discussion

In the present work we have determined the rate of conversion and the rate of consumption of CHP; experimental difficulties have prevented accurate determination of the number of particles in these recipes. The experimental results are summarized in Table I and Figure 7.

Examination of Figure 7, which is plotted logarithmically, shows that a straight line with a slope of 0.5 can be drawn through the eight points, A, B, C, F, G, P, Q, and R, while the other points lie below this line. The eight points on this line include all those determined with 10 parts of soap, and also those with 5 parts of soap for which the rate of consumption of CHP is relatively small. Thus it is seen that when sufficient soap is used, the rate of conversion is proportional to the square root of the rate of consumption of CHP; that is,

$$dM/dt = k_7\rho^{1/2} \tag{7}$$

The same proportionality constant is found for different amounts of fructose or glucose, and for different amounts of soap. Of the five equations given above, only equation (1) is in apparent close agreement with this experimental equation. However, agreement between equations (1) and (7) would require that the number of particles, N, be independent of both the soap and sugar concentrations. Intuitive rejection of this condition is supported by the theoretical equation (5); although we have not succeeded in establishing this point experimentally, it is safe to say that Case 1 cannot be regarded as holding for this system.

Case 3 predicts that the rate of conversion would increase throughout the polymerization of a given charge, as the volume of the particles increases. Thus, the rate of conversion at 40% conversion should be 40% greater than at 20% conversion. Actually the conversion–time curves found over a wide range of conditions are virtually straight lines up to high conversions, with a slight decrease (rather than increase) discernible at moderate conversions. It does not seem likely that decrease in monomer concentra-

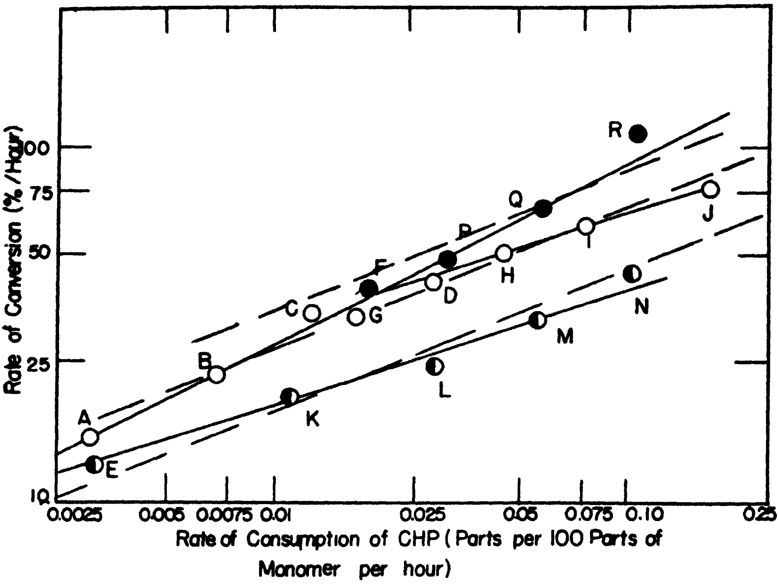

Fig. 7. Rate of conversion as a function of the rate of consumption of CHP in the fundamental recipe with 0.036 part of $Fe(NO_3)_3 \cdot 9H_2O$. Refer to Table I for description of points. Solid lines: best fit. Broken lines: slope of 2/5.

TABLE I

RATE OF CONVERSION AND RATE OF CONSUMPTION OF CUMENE HYDROPEROXIDE WITH VARYING AMOUNTS OF SOAP (POTASSIUM MYRISTATE) AND SUGAR, IN THE FUNDAMENTAL RECIPE WITH 0.036 PART OF FERRIC NITRATE NONAHYDRATE

Ingredients, pts./100 pts. monomers			Rate of conversion, %/hr.	Slope of conversion–CHP lines	Rate of consumption of CHP, pts./hr, ρ	Point of Fig 7
Soap	Glucose	Fructose				
5.0	0.3	—	15	50	0.0030	A
5.0	1	—	23	34	0.0068	B
5.0	3	—	34	27	0.0126	C
5.0	10	—	42	15	0.0276	D
2.5	1	—	13	42.5	0.0031	E
10.0	1	—	40	22.5	0.0178	F
5.0	—	0.3	34	20.4	0.0167	G
5.0	—	1	50	11.6	0.043	H
5.0	—	3	60	7.4	0.076	I
5.0	—	10	75	4.5	0.167	J
2.5	—	0.3	20	18.7	0.0107	K
2.5	—	1.0	24	8.7	0.0276	L
2.5	—	3.0	33	6.0	0.055	M
2.5	—	10.0	44	4.4	0.10	N
10.0	—	0.3	48	15.8	0.030	P
10.0	—	1.0	68	12.3	0.055	Q
10.0	—	3.0	110	10.5	0.105	R

tions, or activity, (M), would exactly compensate the increase in volume of the particles.

In Figure 7, straight lines with slopes of 2/5 (as predicted by equation (4), representing Case 2) are drawn through the points representing the experimental data obtained with different amounts of soap. Fair agreement is obtained with the data with 2.5 and 5 parts of soap; while with 10 parts of soap, agreement is poor. With a given rate of consumption of peroxide, the ratio of the rates of conversion with 5 and 2.5 parts of soap is 1.50, as compared with the value of 1.52 predicted according to equation (4). However, the best line (with slope of 2/5) through the points with 10 parts of soap, when compared with that through the points with 5 parts of soap, gives a ratio of only 1.24. Thus the equation for Case 2 appears to hold reasonably well with 5 or 2.5 parts of soap, but not with 10 parts of soap.

As shown above, a completely satisfactory interpretation of the effect of the concentration of soap upon the rate of conversion, with a given rate of consumption of CHP, cannot yet be given. Experimentally, it appears that with larger amounts of soap, or with small rates of consumption of CHP, the square root relationship (7) holds. The most significant effect of the amount of soap should be upon the number of particles, which, however, is difficult to measure accurately in these butadiene–styrene recipes of high rate of conversion.

The above equations (1–3) for the rate of conversion were derived on the assumption that all radicals are produced in the aqueous phase, but that all termination takes place in the locus. Radicals produced under such conditions may be said to have an efficiency of 100%, since all enter the locus and have the opportunity of initiating polymerization. With relatively few particles (resulting from use of relatively little soap), or with a relatively high rate of radical formation, the concentration of radicals in the aqueous phase may become sufficiently great so that considerable termination of the radicals may occur in the aqueous phase. Since the concentration of dissolved monomer in the aqueous phase (not considering micelles or polymer particles) is very low, radicals which do not leave this phase before termination cannot give rise to formation of such polymer. Radicals formed under these conditions have a low efficiency. Decomposition of CHP by reaction with radicals in the aqueous phase may also lead to an increased rate of consumption of CHP without a corresponding increase in rate of conversion.

The experimental data of Figure 7 may be interpreted according to the above concept. With 5 parts of soap, the rate of conversion is proportional to the square root of the rate of consumption of CHP (expression 7) when the latter rate is small; but the rate of conversion falls below the value expected on the basis of this relation when the rate of consumption of CHP is large. With 10 parts of soap, equation (7) is followed with all the concentrations of sugar studied; while with 2.5 parts of soap, it is not followed with any of the recipes studied.

Effect of Sugar

The kind and amount of sugar taken in the fundamental recipe determine the rate of reduction of ferric iron, and hence the rate of consumption of CHP. The rates of consumption of CHP found with varying amounts of glucose or fructose (Table I) are plotted as functions of the concentration of sugar in Figure 8. With a given amount of soap, it is seen that the rate of consumption of CHP is proportional to the two-thirds power of the concentration of sugar. The proportionality constant for fructose is six times as great as that for glucose, with 5 parts of potassium myristate. The significance of the two-thirds power is not understood at present, and

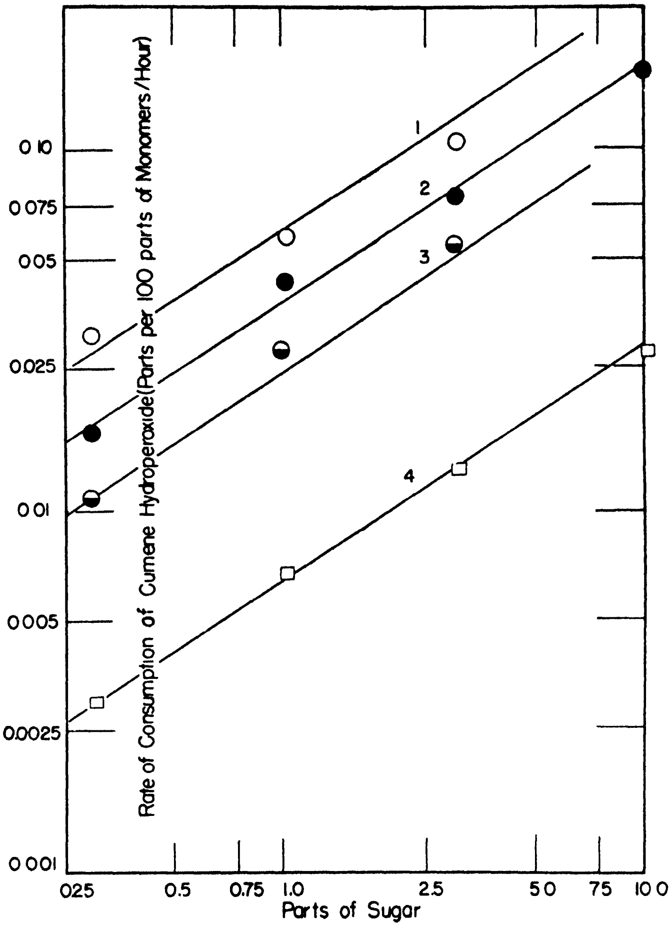

Fig. 8. Rates of consumption of CHP with 0.036 part of $Fe(NO_3)_3 \cdot 9H_2O$ and varying amounts of sugar and soap.

(1) 10 parts K myristate, fructose variable; (2) 5 parts K myristate, fructose variable; (3) 2.5 parts K myristate, fructose variable; (4) 5 parts K myristate, glucose variable.

this relationship may in fact be merely coincidental. If the amount of soap used is sufficient so that relation (7) holds, then the rate of conversion will be proportional to the one-third power of the concentration of sugar.

CRITICAL CONCENTRATIONS OF SOAP

It has been shown by Harkins[10a] and by McBain[10b] that the initial locus of polymerization in emulsion recipes is in the soap micelles. If the amount of soap present is below the critical concentration, so that no micelles are present, then the rate of polymerization should be negligible. If the amount of soap is above the critical, polymerization will proceed initially in the micelles, and will continue in the polymer particles, with a rate dependent upon the amount of soap. We have determined conversion–time curves of charges prepared according to the fundamental recipe with various amounts of potassium myristate, laurate, or caprate. It is seen from Figure 9 that the rates of conversion obtained with each amount of laurate are nearly constant over a wide range of conversions. The dependence upon soap concentration of the rate of conversion of this redox recipe is thus markedly different from that of the mutual recipe; the results obtained in the mutual recipe with varying amounts of soap will be reported in the near future.

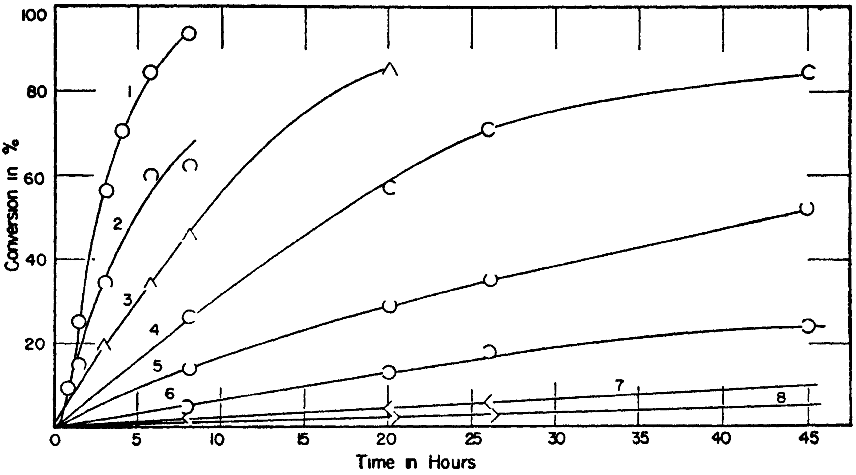

Fig. 9. Conversion-time curves with varying amounts of K laurate, in place of K myristate, and with 1 part of glucose, 0.036 part of $Fe(NO_3)_3 \cdot 9H_2O$, and 0.0967 part of CHP.

(1) 5.0 parts K laurate; (2) 2.5 parts K laurate; (3) 1.25 parts K laurate; (4) 0.70 part K laurate; (5) 0.60 part K laurate; (6) 0.575 part K laurate; (7) 0.55 part K laurate; (8) 0.50 part K laurate.

In Figure 10 the conversions obtained after given times of polymerization are plotted as functions of laurate concentration. The curves of Figure 10 have sharp "breaks," which occur at a concentration of 0.573 ± 0.005

part of potassium laurate. Below this concentration practically no polymerization takes place, while with larger amounts of soap the rate of conversion increases very rapidly with increasing amounts of soap.¶This concentration may be taken as the critical concentration of potassium laurate in this recipe. Values of the critical concentrations determined in this way with other soaps are given in Table II, together with values esti-

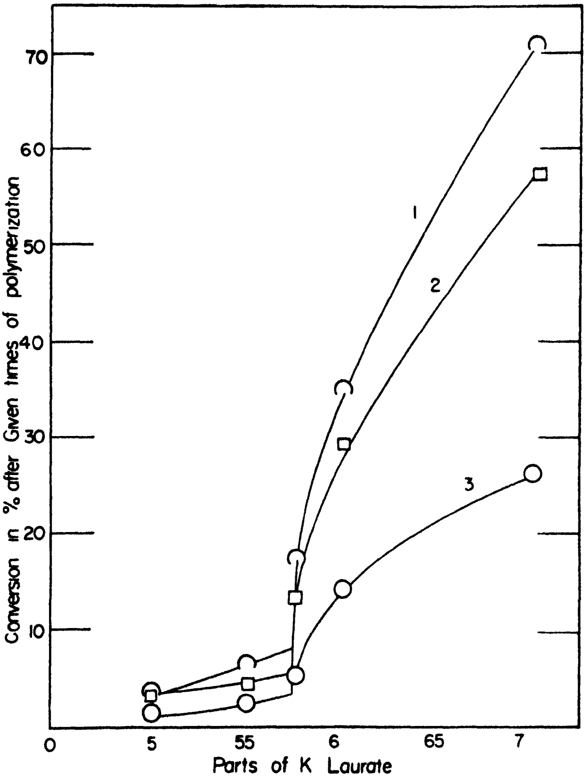

Fig. 10. Conversions after given times of polymerization (data of Fig. 9).
(1) 26 hrs.; (2) 20 hrs.; (3) 8 hrs.

TABLE II

CRITICAL CONCENTRATIONS OF SOAPS IN THE FUNDAMENTAL RECIPE

All Charges Contained 0.036 Part of $Fe(NO_3)_3 \cdot 9H_2O$

	Ingredients		Critical concn. in latex		Critical concn. (*M*) from dye solubilization measurements
Soap	Sugar (Parts)	CHP	Parts	Molarity	
Caprate	Fructose (3)	0.10	3.4	0.090	0.092
Laurate	Glucose (1)	0.0967	0.573	0.0134	0.017
Myristate	Glucose (1)	0.0967	0.44	0.0090	0.0053

mated from dye solubilization measurements[12] in solutions of approximately the same salt concentrations (0.05 N) as the aqueous phases of the latices.

The agreement between the critical concentrations obtained from polymerization data and from dye solubilization measurements is probably as good as can be expected. This appears to be the first recipe investigated in which critical concentrations can be established in this manner. A comparison between the over-all rates of conversion found with different soaps is given further below.

RECIPE WITH FERROUS IRON

As shown in Figure 11, somewhat more rapid polymerization, particularly in the early stages, is found if ferrous iron is used in place of ferric iron in the fundamental recipe. The maximum initial rate of conversion occurs with an amount of ferrous iron (0.025 part of ferrous sulfate heptahydrate) equivalent to the optimum amount of ferric iron (Fig. 1). In the recipe with ferrous iron, a certain amount of CHP is rapidly consumed by reaction with the ferrous iron charged. It is of both practical and theoretical importance to determine the reaction ratio of CHP to ferrous iron in this recipe. This ratio may be designated as a "critical ratio," since in order to achieve continuing polymerization up to high conversions it is necessary that the ratio of the amounts of CHP and ferrous iron charged be greater than the critical ratio.

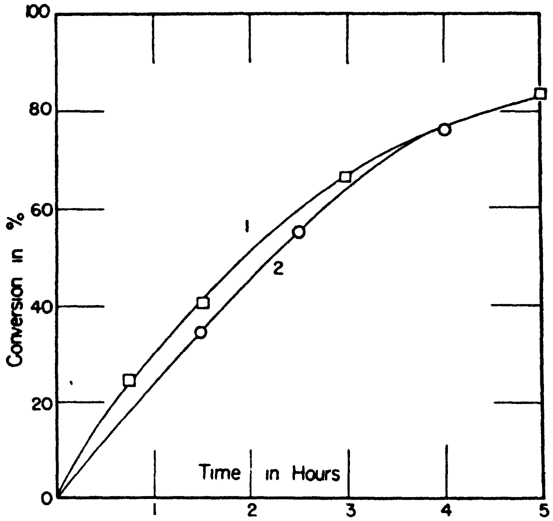

Fig. 11. Conversion–time curves with 1 part of glucose and ferrous or ferric iron.

(1) 0.10 part $FeSO_4 \cdot 7H_2O$ and 0.145 part cumene hydroperoxide; (2) 0.145 part $Fe(NO_3)_3 \cdot 9H_2O$ and 0.0483 part cumene hydroperoxide.

Determination of the Critical Ratio

Experimentally the principal difficulty in the determination of the critical ratio is the necessity for complete removal of oxygen from the charge. It is well known that the ferrous pyrophosphate complex is readily air-oxidized. Some titrations have been carried out to determine the extent of this air-oxidation in solutions of the concentrations used in the fundamental recipe with 0.1 part of $FeSO_4 \cdot 7H_2O$ and 1 part of $Na_4P_2O_7 \cdot 10H_2O$ per 180 parts of water. 10-ml. volumes of the pyrophosphate and ferrous

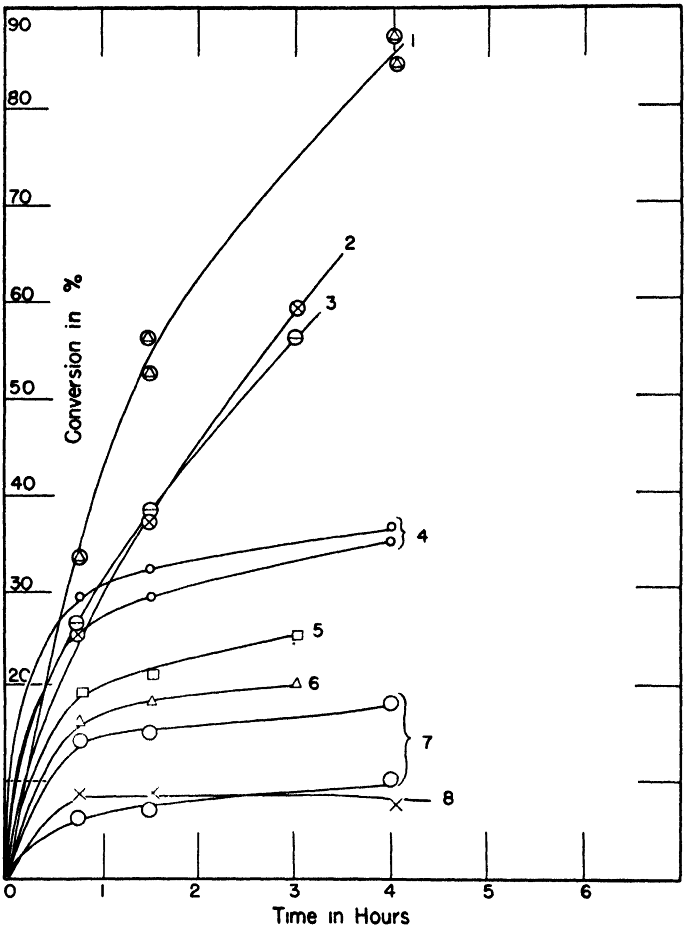

Fig. 12. Conversion–time curves with 1 part of glucose and 0.10 part of $FeSO_4 \cdot 7H_2O$; charges prepared in nitrogen.
(1) 0.145 part of CHP; mole ratio, 1.50; (2) 0.116 part of CHP; mole ratio, 1.20; (3) 0.106 part of CHP; mole ratio, 1.10; (4)[a] 0.0967 part of CHP; mole ratio, 1.00; (5)[a] 0.0967 part of CHP; mole ratio, 1.00; (6) 0.0870 part of CHP; mole ratio, 0.90; (7) 0.0725 part of CHP; mole ratio, 0.75; (8) 0.0484 part of CHP; mole ratio, 0.50. ([a] Charges run on different days with different solution.)

solutions were mixed in a 125-ml. Erlenmeyer flask and allowed to stand with or without air bubbling at room temperature. The solutions were then acidified and titrated with ceric sulfate. With no air bubbling, it was found that the ferrous iron was 40% air-oxidized in less than 15 sec., 70% in 10 min., and 85% in 30 min. With air bubbling, oxidation was 99.5% complete in 10 min.

If charges are prepared in such a way that some air-oxidation of the ferrous iron may occur, then the apparent critical ratio will be in error. We have found that with charges prepared in three different ways, but with the ferrous iron and pyrophosphate solutions mixed in the presence of air,

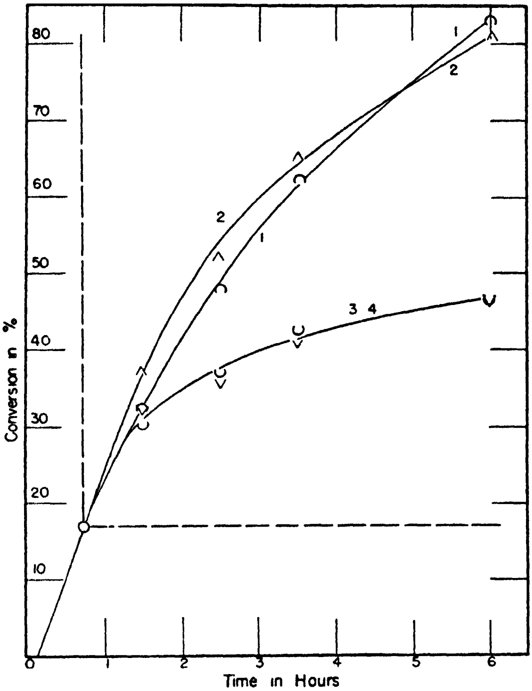

Fig. 13a. Conversion–time curves with 1 part of glucose and 0.036 part Fe(NO_3)$_3$·$9H_2O$, with ferrous iron injected after 45 min. of polymerization.

Curve	CHP taken	$FeSO_4 \cdot 7H_2O$ injected	Mole ratio
1	0.232	0.204	1.18
2	0.213	0.206	1.07
3	0.193	0.204	0.98
4	0 174	0.196	0.92

polymerization continues up to high conversions when the molar ratio of CHP to ferrous iron nominally taken is 0.75; whereas, as shown below, charging in such a manner as to prevent air-oxidation of ferrous iron results in very low conversions with this mole ratio of ingredients. With the method of charging described in the beginning of this paper, in which the ferrous iron is injected to the charge after addition of all other ingredients, air is removed from the gas phase by flushing with butadiene. To determine the critical ratio with greatest accuracy, it is also necessary to remove dissolved oxygen from the solutions. Experiments were carried out with charges prepared with all solution flushed for at least 30 min. with purified nitrogen, with the exception of the soap solution, which was prepared by adding the solid potassium myristate to the nitrogen-flushed water. The data are shown in Figure 12. It is seen that the rate of conversion in charges with a molar ratio of CHP to ferrous iron of approximately 1.0 or less drops off very sharply, coming to almost a dead stop at conversions which are in general higher as more CHP is taken. With ratios of 1.10 or 1.20, polymerization continues up to at least 55% conversion, with no indication of a dead-stop.

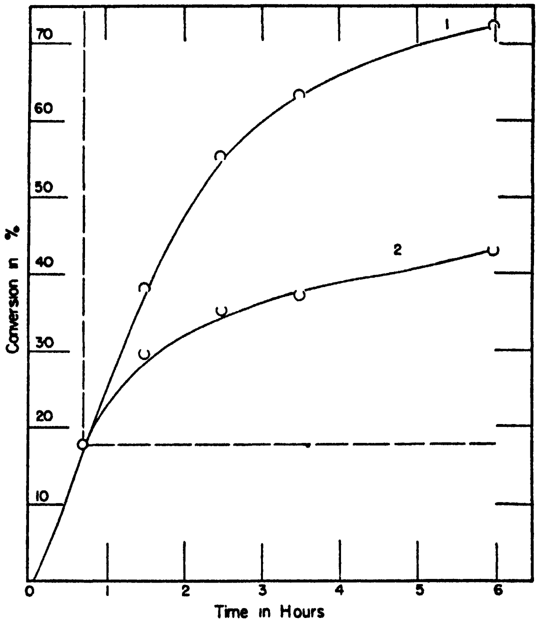

Fig. 13b. Conversion–time curves with 1 part of glucose and 0.036 part Fe(NO$_3$)$_3$·9H$_2$O, with ferrous iron injected after 45 min. of polymerization.

Curve	CHP taken	FeSO$_4$·7H$_2$O injected	Mole ratio
1	0.116	0.104	1.15
2	0.0871	0.102	0.88

Further experiments were carried out in which the solutions were not flushed with nitrogen, but in which dissolved oxygen was removed from the charge by allowing polymerization to proceed for a short time, with ferric iron as catalyst, before injecting ferrous iron. It is known[13] that growing polymer chains react rapidly with oxygen. The data obtained are shown in Figure 13, in which the dotted axes set off the curves obtained after addition of ferrous iron. As in the previous experiments, the conversions attained after longer times of polymerization are much higher with a molar ratio of slightly greater than 1.0 than with a slightly smaller molar ratio. Results similar to those of Figure 13 have been found with a sample of purified (95% pure) CHP. In contrast to the sudden rise in final conversion with a small increase in molar ratio in the neighborhood of 1.0, comparable or even larger increases in this ratio in the region below 1.0 give relatively small increases in final conversion (Figs. 12 and 13). Thus, with 0.2 part of ferrous sulfate heptahydrate, an increase of only 9% in the amount of CHP taken, in the neighborhood of a ratio of 1.0, almost doubles the conversion taking place between the time of injection of ferrous iron and the time at which the rate of conversion drops off sharply (Fig. 13a); with 0.1 part of iron, a similar increase in conversion results from a 30% increase in the amount of CHP taken, in the vicinity of this ratio (Fig. 13b); and with 0.05 part of iron, a 20% increase in CHP gives a similar increase in conversion (Fig. 13c). It may be concluded that an amount of CHP equimolar to that of ferrous iron is consumed rapidly by direct reaction with the ferrous iron charged (or injected) as such, while

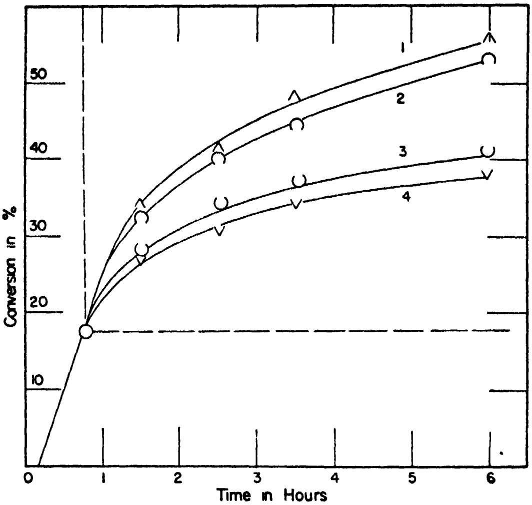

Fig. 13c. Conversion-time curves with 1 part of glucose and 0.036 part $Fe(NO_3)_3 \cdot 9H_2O$, with ferrous iron injected after 45 min. of polymerization.

Curve	CHP taken	$FeSO_4 \cdot 7H_2O$ injected	Mole ratio
1	0.0580	0.051	1.18
2	0.0628	0.052	1.25
3	0.0508	0 052	1.01
4	0.0459	0 052	0.91

any CHP charged in excess of this amount is consumed much more slowly by reaction with ferrous iron formed in the sugar–ferric iron reaction, as in recipes in which the iron is charged in the ferric state (discussed above). Thus, the critical ratio in the experiments of Figures 12 and 13 is 1.0.

Interpretation of these results presents some difficulty. By extension of the work of Baxendale, Evans, and Park[14] it would be expected that the reaction between ferrous iron and CHP would form free radicals which would initiate polymerization, and that consumption of radicals in this way would lead to a 1:1 molar reaction ratio. The experimentally determined critical ratio and the fact that considerable polymerization (up to 20%) takes place in charges with less than the critical amount of CHP (Fig. 12) are in apparent accord with this interpretation, if it is assumed that initiation by the direct reaction between CHP and the ferrous iron charged continues until the dead-stop is reached. However, separate experiments have shown that the initial rate of conversion in these charges is the same as in charges with a larger amount of CHP, and only slightly higher than in charges with ferric rather than ferrous iron. On the other hand, we have established[15] by analytical determinations that when ferrous iron and CHP are mixed to form an emulsion containing benzene, water, soap, and pyrophosphate, the reaction is 90% complete within 5 min. Furthermore, as shown in a subsequent section (Fig. 14), the rate of conversion in charges with no sugar, with either ferrous or ferric iron, is very small. Thus it appears that the sugar plays some direct role in promoting polymerization in charges such as those of Figures 12 and 13, with less than one mole of iron.

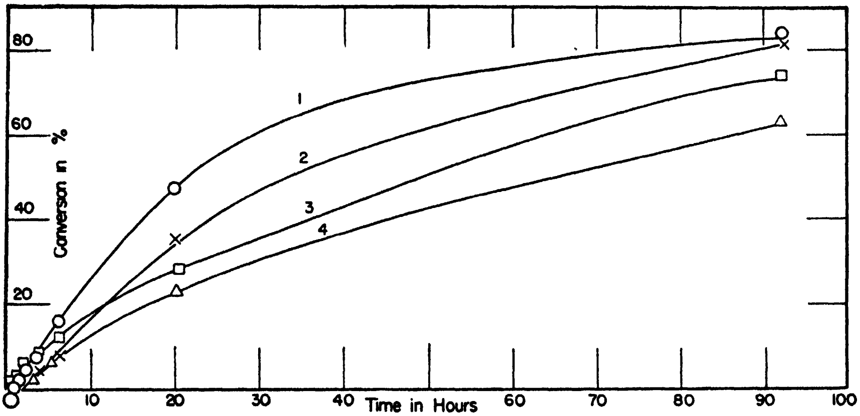

Fig. 14. Conversion–time curves in the absence of sugar.
(1) 0.025 part $FeSO_4 \cdot 7H_2O$, 0.0727 part of CHP; (2) 0.036 part $Fe(NO_3)_3 \cdot 9H_2O$, 0.0484 part of CHP; (3) 0.20 part $FeSO_4 \cdot 7H_2O$, 0.2422 part of CHP; (4) 0.29 part $Fe(NO_3)_3 \cdot 9H_2O$, 0.0484 part of CHP.

In a discussion of the Fenton reaction[1] we have shown that free radicals or other active intermediates, formed by interaction of ferrous iron with hydrogen peroxide or an organic hydroperoxide such as CHP, react with several organic compounds, including alcohols and sugars, with the formation of organic free radicals, ultimately leading to formation of stable oxidation products of the organic compounds. The radicals formed from sugars may themselves be able to initiate polymerization, but may be more stable than those formed by interaction of ferrous iron and CHP. It appears that CHP and reducing sugars can react directly with formation of free radicals which initiate polymerization; thus, in iron-free alkaline recipes containing CHP and sugar (Fig. 15), polymerization occurs which is considerably faster than that obtained in the absence of sugar (Fig. 14). However, it cannot be stated whether initiation in such recipes is brought about by radicals derived from the sugar, or from the CHP; or whether, indeed, minute traces of heavy metals present as impurities may not play an important role.

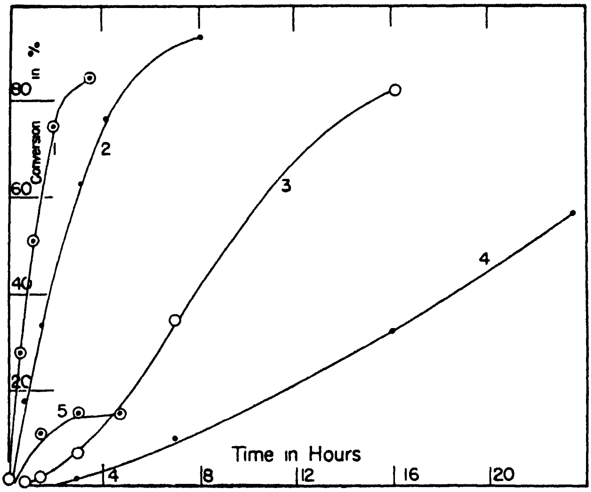

Fig. 15. Conversion–time curves in the presence or absence of iron, with 1 part of sugar.

(1) fructose, 0.036 part of $Fe(NO_3)_3 \cdot 9H_2O$, 0.0726 part of CHP; (2) glucose, 0.036 part of $Fe(NO_3)_3 \cdot 9H_2O$, 0.0483 part of CHP; (3) fructose, no iron, 0.08 part of CHP; (4) glucose, no iron, 0.08 part of CHP; (5) glucose, no iron, 0.121 part of CHP, 5.4 parts of KOH in place of pyrophosphate.

When ferrous iron and CHP react in aqueous solution, in the absence of monomers or other organic compounds, the molar reaction ratio is in the neighborhood of 1.0, as a result of induced decomposition of the CHP.[15,16] It is possible that in charges prepared with ferrous iron, the reaction of CHP with the ferrous iron charged actually initiates very little polymerization, owing to a very low efficiency of the radicals formed in the aqueous phase (see above); but that the reaction ratio nevertheless is in the neighborhood of 1.0, owing to induced decomposition of CHP, as above.

Radicals formed in a complex system such as the aqueous phase of a charge prepared according to the fundamental recipe can undergo a number of competing reactions with ferrous or ferric iron, dissolved monomers or CHP, free soap, or the sugar or its oxidation products, in addition to entering the micelles or polymer particles. Further studies are in progress to get a better understanding of the role of the sugar in the redox recipe under consideration.

Increment Addition of CHP and Ferrous Iron

If the reaction between ferrous iron and CHP initiates polymerization, it would be expected that addition of small amounts of these ingredients to a charge at frequent intervals would bring about rapid polymerization. Experiments have been carried out in which these ingredients were added at short intervals to charges containing sugar and other ingredients of the fundamental recipe. In a typical experiment, a charge was prepared according to the fundamental recipe with 1 part of glucose, 0.0967 part of CHP, and 0.010 part of $FeSO_4 \cdot 7H_2O$; at 10-min. intervals, 0.010 part of $FeSO_4 \cdot 7H_2O$ (dissolved in 0.2 ml. of water) was injected, until a total of 0.090 part of $FeSO_4 \cdot 7H_2O$ had been added (including that initially charged). The conversions obtained during the first 80 min. were approximately the same as those of the fundamental recipe without increment addition; the rate of conversion dropped off sharply at about 50% conversion, due to exhaustion of the CHP. In other experiments it appeared that some increase in conversion took place after each addition of ingredients; however, the results were not conclusive.

EFFECTS OF CHANGING KIND OF ACTIVATOR, EMULSIFIER, AND OTHER INGREDIENTS

In the preceding pages we have shown the effects of variation in the amounts of each of the ingredients of the fundamental recipe, with the exception of the monomers and water. The effects of omission of various ingredients or their replacement with similar compounds are presented below.

Omission of Sugar

Results of polymerizations with the fundamental myristate recipe in the absence of sugar are shown in Figure 14. With small amounts of iron, a rate of about 2% per hour is found. The rates obtained with the smaller amounts of iron are higher than those obtained with the larger amounts of iron. Ferrous iron eliminates the induction period found with ferric iron, which is probably caused by dissolved oxygen. However, it appears that in the absence of sugar the reaction between ferrous iron and CHP is too rapid to bring about significant polymerization; the recipes are in effect ferric iron recipes, whether ferrous or ferric iron is charged.

Sugar-free recipes have been developed with soap peroxides as oxidizing agent and complex ferric salts as "activators"; in these recipes we have found that the mercaptan is the active reducing agent. This work will be described later in detail. The mechanism of initiation in the ferric iron recipes of Figure 14 appears to be similar to that of the soap peroxide recipes.

In a rosin recipe (see below) with ferrous iron and DDM, a rate of conversion of 2% per hour was found in the absence of sugar.

In contrast to the poor rates of conversion found with the CHP–iron system in the absence of reducing agents, large rates have been found[17] with benzoyl peroxide and ferrous iron in the absence of other reducing agents. It is clear that with benzoyl peroxide, which is highly insoluble in water, the rate of reaction between benzoyl peroxide and ferrous iron under the conditions of the polymerization is sufficiently small so that this initiation reaction continues for a reasonable period of time; while with easily water-soluble CHP,[15,16] the reaction is so rapid as to give exhaustion of the CHP or ferrous iron in a short time. For this reason the use of reducing agents that react at a suitable rate with ferric iron is essential in the CHP recipe with soluble iron salts; the rate of conversion is then determined by the over-all rate of reduction of ferric iron. Redox recipes with various reducing agents other than sugars are being studied at present in this laboratory.

A suitably slow reaction between ferrous iron and CHP can also be accomplished in a sugar-free recipe in which the ferrous iron is introduced as a suspension of a very slightly soluble ferrous salt. In this manner, the concentration of dissolved ferrous iron is kept extremely small and the rate of production of free radicals is determined by the rate of solution of the ferrous suspension under the experimental conditions. Attractive rates of conversion have been obtained, even at 0°C., in a sugar-free recipe with CHP and a suspension of ferrous sulfide, as will be described in a subsequent paper. Undoubtedly, other slightly soluble ferrous iron compounds will be found suitable for this purpose. Recipes of this type demonstrate unequivocally that the reaction between ferrous iron and CHP can initiate copolymerization of butadiene and styrene.

If ferrous iron is added to a charge in the absence of pyrophosphate or other complexing agent, a precipitate of ferrous myristate is formed which dissolves to only a very limited extent in the organic phase, as shown in separate experiments which will be described at a later date. The behavior of ferrous myristate is thus comparable to that of ferrous sulfide, with the exception that solution of the former probably takes place into the organic phase, and of the latter, probably into the aqueous phase; although the extent to which both dissolve under the experimental conditions is very slight. In a charge containing only monomers and water, soap, sulfole mercaptan, ferrous sulfate heptahydrate (0.25 part), and CHP (0.394 part), without sugar or pyrophosphate, a conversion of 10% was obtained after one hour at 30°; thereafter, a rate of roughly 1% per hour was obtained up to 23 hours.

Omission of Iron in the Presence and Absence of Pyrophosphate

Omission of iron in the fundamental recipe, in the presence of pyrophosphate, leads to S-shaped conversion–time curves of much smaller rate of conversion than obtained in the presence of iron (Fig. 15, curves 1–4). The charges of Figure 15 were prepared with water which had been distilled in an all-glass system. It seems that direct reaction between the CHP and the reducing sugar takes place and that this reaction initiates polymerization with a relatively small rate in this recipe.

In recipes of high alkalinity (see below) the rate of conversion in the absence of iron is very great, but a large amount of CHP is consumed. Thus in curve 5 of Figure 15 a final conversion of 15% was attained (with 0.121 part of CHP), while in a similar charge with 0.0242 part of CHP a final conversion of only 7% was reached.

Aluminum gives no catalysis of polymerization in recipes with either pyrophosphate or potassium hydroxide (see below), whether the aluminum is used in place of or in addition to the iron.

We have obtained data in a rosin recipe (see below) in the absence of iron and pyrophosphate, at a temperature of 50°. Here also, the curve is S-shaped and the rate is much less than in the presence of iron. Similar data have been reported by Vandenberg and Hulse[3]; however, these authors emphasized the effect of the iron "to eliminate initial periods of very slow polymerization" and suggested that "the iron activator does not exert a controlling influence on the polymerization rate." This view does not seem tenable for the recipes under consideration in light of the low rates of conversion found *throughout* the polymerizations in the absence of iron.

Use of Various Complexing Agents

Complexing agents other than pyrophosphate have been studied in the fundamental recipe (with myristate). As seen from Figure 16, the rates of conversion obtained with the five complexing agents studied are of the same order of magnitude; it is possible that systematic study of the optimum conditions of polymerization with any of these compounds might yield recipes of equal or greater rate of conversion than that of the pyrophosphate recipe at 30°.

Complexes in which ferric iron and the reducing sugar are chemically bound together may be of interest in redox recipes. Traube and co-workers[18,19] have investigated the complex salts of ferric iron and various polyhydric alcohols, sugars, and sugar acids which are formed in alkaline solution.

Following their procedure, a solution of the soluble sodium salt of the ferric iron–glucose complex was prepared by pouring 24 ml. of a solution of glucose (2.97%) and ferric nitrate nonahydrate (0.431%) into an equal volume of 0.5 *N* potassium hydroxide. A clear orange solution was formed; the absence of a precipitate indicates the stability of the glucose–iron complex. This solution was tried as an activator in the fundamental recipe in place of the glucose, iron, and pyrophosphate; thus, the recipe contained 1 part of glucose, 0.145 part of ferric nitrate nonahydrate, and 0.9 part of KOH, with no pyrophosphate. The conversions obtained with this recipe are given in Figure 17. The rate of conversion is roughly 18% per hour. Approximately the same rate of conversion was obtained with a charge prepared in a similar manner, with 1 part of tripotassium phos-

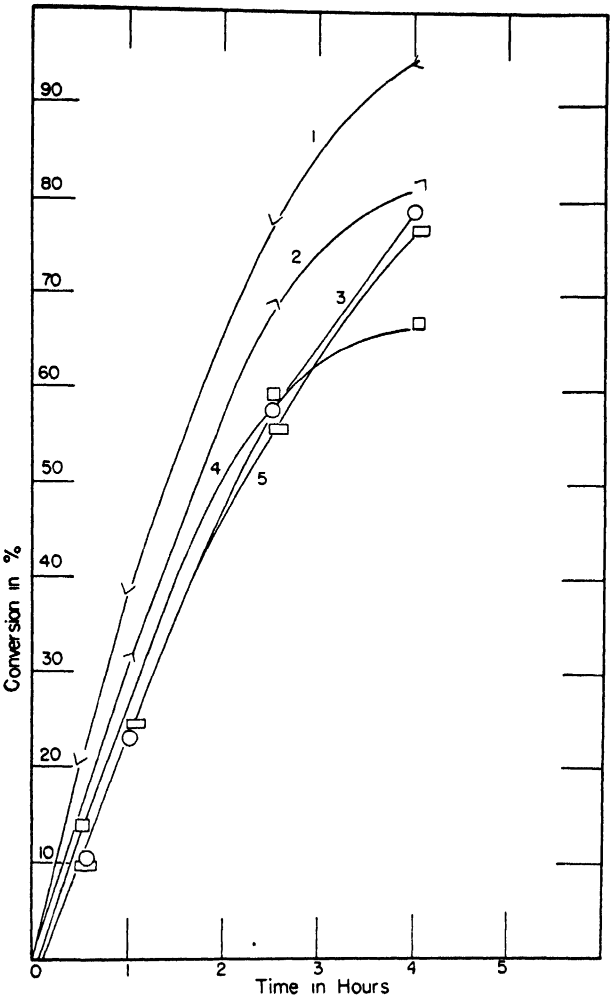

Fig. 16. Conversion–time curves with 0.036 part of Fe$(NO_3)_3 \cdot 9H_2O$, 1 part of fructose, and 0.0967 part of CHP, and complexing agents other than pyrophosphate.

Complexing agent (all 1 part): (1) sodium pyrophosphate decahydrate; (2) potassium oxalate monohydrate; (3) potassium tartrate hemihydrate; (4) potassium fluoride; (5) potassium citrate monohydrate.

phate in place of sodium hydroxide. The rate in the recipe with KOH depends upon the amount of alkali taken (Fig. 17); with 5.4 parts of KOH, the initial rate is higher than that of the fundamental recipe (with pyrophosphate), but the polymerization comes to a dead-stop (compare with curve 5 in Fig. 15, carried out in the absence of iron). In a similar recipe with 1 part of fructose and 5.4 parts of KOH, a conversion of 41% was found in 1 hour, but polymerization soon came to a dead-stop at 55% conversion. With 1 part of fructose and 1 part of tripotassium phosphate, a rate of 32% per hour was found, and polymerization continued up to high

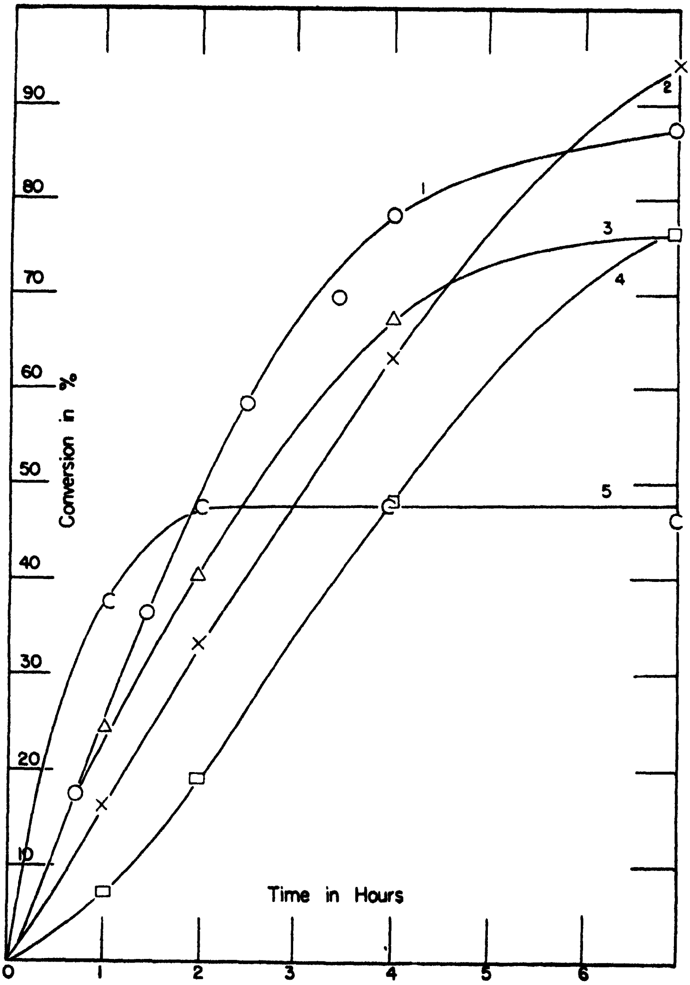

Fig. 17. Conversion-time curves with ferriglucose complexes. (1) 0.145 ferric nitrate, 0.0242 CHP (fundamental recipe); (2) 0.145 ferric nitrate, 0.145 CHP, 1.0 K_3PO_4; (3) 0.145 ferric nitrate, 0.145 CHP, 0.9 KOH; (4) 0.145 ferric nitrate, 0.145 CHP, 0.15 KOH; (5) 0.145 ferric nitrate, 0.145 CHP, 5.4 KOH.

conversions. The rate of consumption of CHP is unusually high in these recipes. From experiments carried out in the absence of iron (Fig. 15) it may be concluded that a large proportion of the CHP is consumed by direct reaction with the sugar in strongly alkaline media, without at the same time leading to much polymerization.

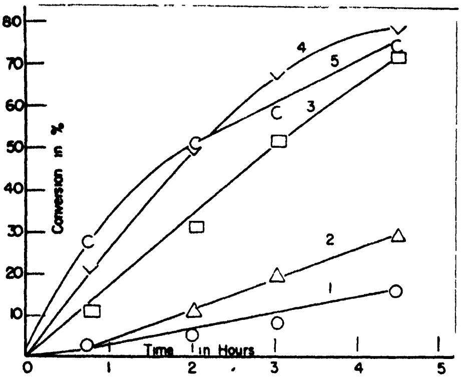

Fig. 18. Conversion–time curves with 0.5 part of K_2SO_4 in place of pyrophosphate.

(1) no $Fe(NO_3)_3 \cdot 9H_2O$; (2) 0.0022 part of $Fe(NO_3)_3 \cdot 9H_2O$; (3) 0.009 part of $Fe(NO_3)_3 \cdot 9H_2O$; (4) 0.036 part of $Fe(NO_3)_3 \cdot 9H_2O$; (5) 0.144 part of $Fe(NO_3)_3 \cdot 9H_2O$.

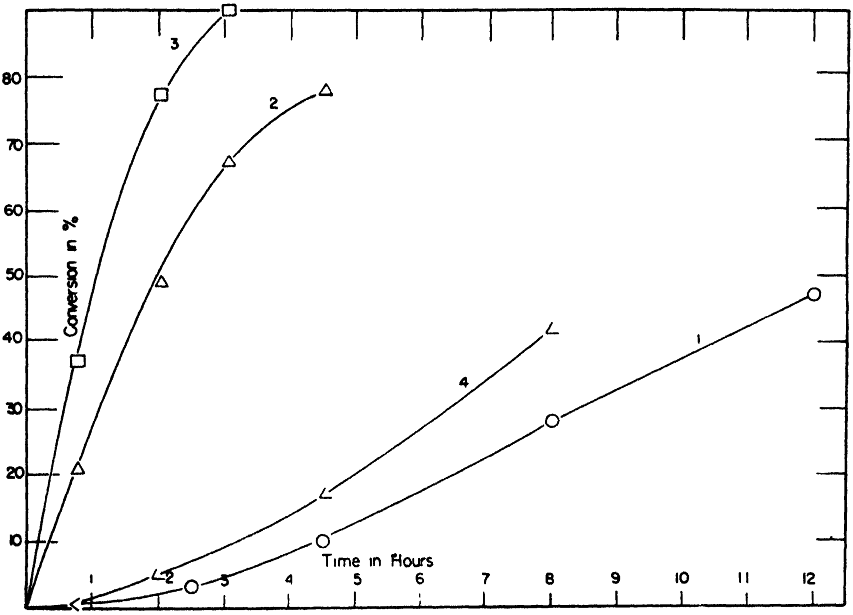

Fig. 19. Conversion–time curves with various salts in the presence and absence of iron.

(1) no iron, no salt; (2) 0.036 part of $Fe(NO_3)_3 \cdot 9H_2O$, 0.5 part of K_2SO_4; (3) 0.036 part of $Fe(NO_3)_3 \cdot 9H_2O$, 0.5 part of $Na_4P_2O_7 \cdot 10H_2O$; (4) no iron, 1 part of $Na_4P_2O_7 \cdot 10H_2O$.

Experiments have been carried out to determine whether iron can exert its normal catalytic function in the fundamental recipe in the absence of complexing agent. Data obtained with potassium sulfate (added to maintain latex fluidity) in place of pyrophosphate are shown in Figs. 18 and 19. Small amounts of iron are seen to give a very pronounced increase in the rate of conversion in the absence of pyrophosphate. As in the presence of pyrophosphate, the optimum amount of $Fe(NO_3)_3 \cdot 9H_2O$ is 0.036 part. The rate of conversion with this amount of iron is about 2/3 as great in the absence as in the presence of pyrophosphate. Similar results were found with potassium chloride, potassium carbonate, or potassium sulfate, or with no added salt; also, identical conversions were obtained

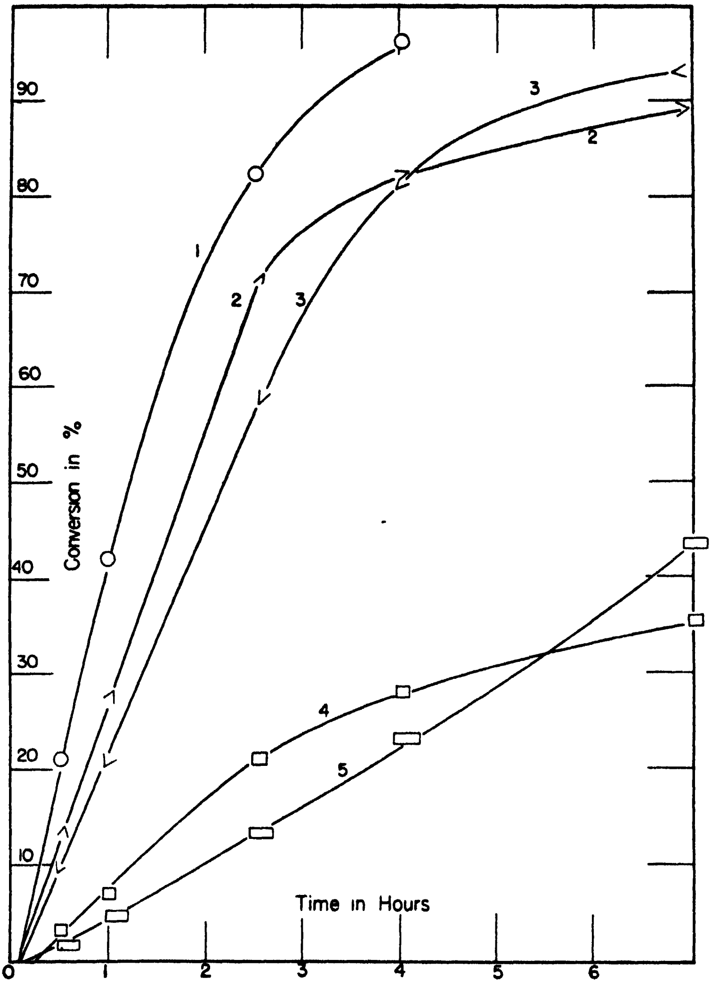

Fig. 20. Conversion–time curves with various peroxides (myristate recipe, 1 part of fructose).
(1) cumene hydroperoxide (0.0967 part); (2) Uniperox 90 (0.05 part); (3) Uniperox 90 (0.20 part); (4) *tert*-butyl hydroperoxide (0.05 part); (5) *tert*-butyl hydroperoxide (0.20 part).

with charges to which the iron had been injected after mixing all the other ingredients, and with charges to which the iron had been added after adding the soap and potassium sulfate solutions but before adding the fructose.

The rate of conversion in these recipes without pyrophosphate is less than in the recipes in which the ferric iron-fructose complex is formed according to the procedure of Traube (above). It is not certain whether, in the recipes of Figure 18, an appreciable amount of the iron may be kept in solution as the complex with fructose, or whether virtually all the iron may be present as the iron soap.

Use of Various Peroxides

Redox recipes employing benzoyl peroxide have been described by Marvel and co-workers.[17] Since the behavior of these recipes differs fundamentally in many respects from that of the CHP recipes, presentation of results which we have obtained with such recipes will be deferred to a later date. Recipes developed in this laboratory, employing soap peroxides in both the presence and absence of reducing agents, will also be described subsequently; in general, the behavior of soap peroxide recipes is very similar to that of CHP recipes. Use of various other peroxides in place of CHP in the fundamental recipe is described below.

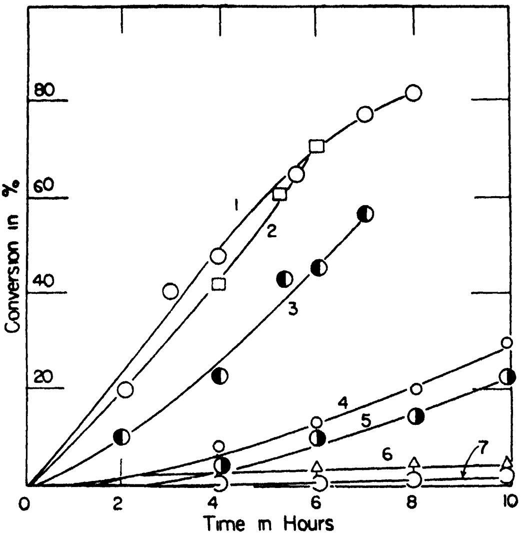

Fig. 21. Conversion–time curves with rosin soap, using 1 part of glucose and 0.1 part of $FeSO_4 \cdot 7H_2O$.

(1) CHP (0.17 part); (2) Uniperox (0.15 part); (3) Uniperox (0.30 part); (4) *tert*-butyl hydroperoxide (0.15 part); (5) *tert*-butyl hydroperoxide (0.30 part); (6) *tert*-butyl hydroperoxide (0.05 part); (7) Uniperox (0.05 part).

The following two peroxides have been investigated in the fundamental recipe with myristate at 30°: Uniperox 90, a mixture of hydroperoxides of structure similar to that of CHP, supplied by Union Oil Company of California; and *tert*-butyl hydroperoxide (Union Bay State Co.). It is seen from Figure 20 that Uniperox gives somewhat less rapid polymerization than does CHP, while *tert*-butyl hydroperoxide is much less effective.

Similar results have been found with the rosin recipe (see below); here, however, the rate of conversion obtained with the optimum amount (0.15 part) of Uniperox 90 is only very slightly less than that with CHP (Fig. 21).

Use of Various Emulsifiers

Conversion–time curves obtained with various soaps are shown in Figure 22. Similar rates of conversion are found with 5 parts of laurate or myristate, while with 5 parts of caprate a much lower rate is obtained, due in part to the fact that less than half the caprate charged is micellized (see above). The rate with a commercial sodium soap (Procter & Gamble RRC Standard SF flakes) is about 18% per hour, compared with 23% for myristate in the same recipe. Emulsifiers other than fatty acid soaps have also been used in this recipe. With SA-178 (technical sodium di-*sec*-butylnaphthalene sulfonate) and with Aerosol OT (dioctylsodium sulfosuccinate) very small rates of conversion were found. In the case of Aerosol OT, the small rate of conversion appears to be due to nearly complete transfer of the detergent into the organic phase. With 5 parts of

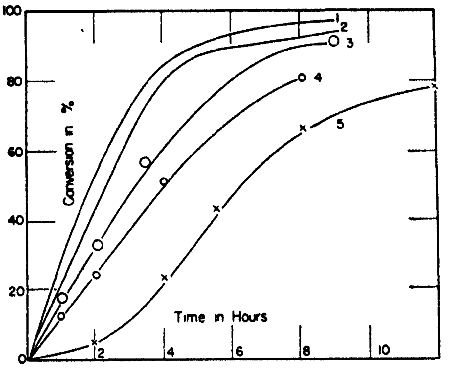

Fig. 22. Conversion–time curves with 0.025 part of $FeSO_4 \cdot 7H_2O$, 0.0725 part of CHP, and various soaps.

(1) K myristate (5 parts), glucose (1 part); (2) K laurate (5 parts), glucose (1 part); (3) SF (Procter & Gamble) (5 parts), glucose (1 part); (4) Aerosol AY (10 parts), fructose (1 part); (5) K caprate (5 parts), glucose (1 part).

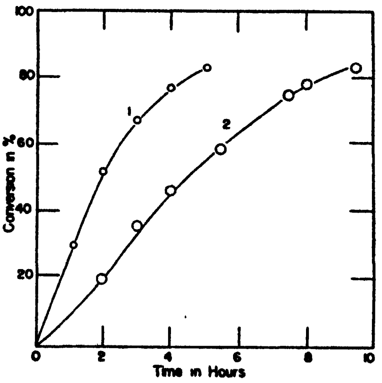

Fig. 23. Comparison of myristate and rosin recipes.

(1) fundamental recipe with myristate; 1 part of glucose, 0.10 part of $FeSO_4 \cdot 7H_2O$, and 0.145 part of CHP; (2) fundamental recipe with rosin 731 soap (5 parts); 1 part of glucose, 0.10 part of $FeSO_4 \cdot 7H_2O$, and 0.17 part of CHP.

Aerosol AY (the corresponding amyl ester), small and poorly reproducible rates were obtained. This is because the amount of Aerosol AY charged was in the neighborhood of the critical concentration of this detergent.[12]

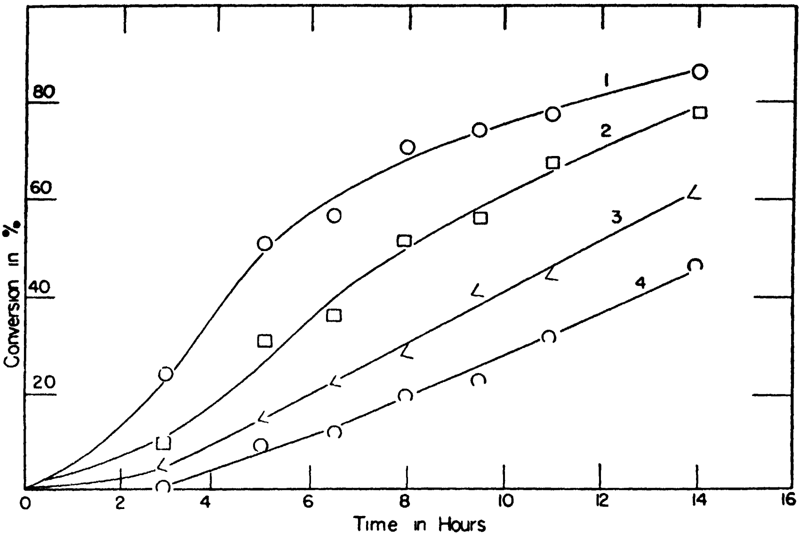

Fig. 24. Conversion–time curves with rosin soap, using 1 part of glucose, 0.17 part CHP, and various amounts of $FeSO_4 \cdot 7H_2O$.
(1) 0.1 part of $FeSO_4 \cdot 7H_2O$; (2) 0.05 part of $FeSO_4 \cdot 7H_2O$; (3) 0.02 part of $FeSO_4 \cdot 7H_2O$; (4) 0.01 part of $FeSO_4 \cdot 7H_2O$.

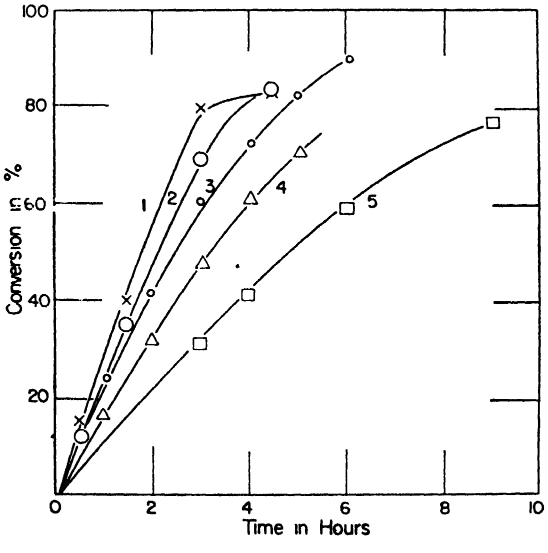

Fig. 25. Conversion–time curves with rosin soap, using various sugars. (1) L-sorbose (1 part); (2) fructose (1 part); (3) invert sugar (1 part); (4) glucose (3 parts); (5) glucose (1 part).

With 10 parts of Aerosol AY, a somewhat higher rate results (Fig. 22), but the rate is still much less than that obtained with myristate.

As mentioned in the beginning of this paper, the early study of this recipe was carried out with dehydrogenated rosin soap (sodium soap of Hercules rosin #731). As shown in Figure 23, the rate of conversion obtained with this emulsifier in the fundamental recipe with 0.1 part of ferrous sulfate is approximately half as great as in the recipe with myristate. In contrast to the myristate recipe, decrease of the amount of ferrous sulfate in the rosin recipe below 0.1 part lowered the rate of conversion quite sharply (Fig. 24). Variation of the amount of CHP gave results which were qualitatively similar to those found in the myristate recipe, but the investigation was not extensive. Increase of the amount of glucose or replacement of glucose with L-sorbose, fructose, or invert sugar gives an increased rate of conversion (Fig. 25). Some of these recipes, particularly that with invert sugar, are of practical importance. The effects of omission and replacement of other ingredients in both the myristate and the rosin recipes have been considered together above.

Omission of Mercaptan. Use of Primary *vs.* Tertiary Mercaptan Retardation by Ammonium Ion

In butadiene-styrene recipes with persulfate as "catalyst," mercaptan is essential to obtain high rates of conversion.[20] In redox recipes, on the other hand, high rates of conversion are obtained in the absence as well as

TABLE III

EFFECT OF MERCAPTAN AND AMMONIUM SULFATE

All Charges Contained 1 Part of Glucose

Soap	Mercaptan (part)	$(NH_4)_2SO_4$ (part)	Conversion after 3 hrs., %
Myristate............	—	—	55
	—	0.002	48
	—	0.01	31
	—	0.10	15
	Sulfole (0.35)	—	67
	Sulfole (0.05)	—	70
	Sulfole (0.35)	0.002	69
	" "	0.01	65
	" "	0.10	47
	Sulfole (0.05)	0.10	40
	DDM (0.5)	—	68
	" (0.075)	—	69
	" (0.5)	0.10	57
	" (0.075)	0.10	50
Rosin................	Sulfole (0.35)	—	33
	" "	0.0125	28
	" "	0.125	16
	" "	0.125[a]	34

[a] Charge contained 0.1 part of sodium hydroxide.

the presence of mercaptan.[2,4,17] The principal role of mercaptan in such recipes is as a modifier or chain-length regulator of the polymer.

The ammonium ion has been found to be a retarder in other polymerization recipes and its effect upon the fundamental recipe was therefore studied. Both in the recipe with rosin soap and in the recipe with myristate, the ammonium ion acts as a retarder in the absence of mercaptan, the retardation being more pronounced with rosin than with myristate. Addition of mercaptan tends to overcome this retardation; a primary mercaptan of the average composition of *n*-dodecyl mercaptan is more effective in this respect than a tertiary mercaptan (sulfole). Data illustrating this are given in Table III. Special precautions were taken in cleaning the Buna-N gaskets used with the mercaptan-free charges; some controls were run with aluminum gaskets. All water used was made ammonia-free by distillation from dilute sulfuric acid.

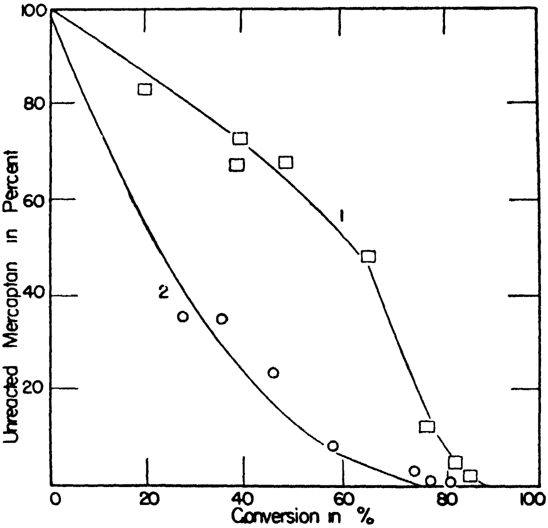

Fig. 26. Disappearance curves of DDM and sulfole mercaptan in the rosin recipe: (1) DDM; (2) sulfole.

In the myristate recipe with 0.35 part of *tert*-dodecyl mercaptan (sulfole), as much as 0.01 part of ammonium sulfate causes no appreciable retardation. This amount of ammonium sulfate is equivalent to 15 mg. of ammonium ion per liter of water in the charge. Ordinarily it should not be necessary to remove ammonia from water used in preparing charges according to the myristate recipe with sufficient mercaptan; however, in this recipe in the absence of mercaptan, or in the rosin recipe in the presence of mercaptan, purification of the water is advisable. Addition of alkali in the rosin recipe counteracts the retardation caused by ammonium ion.

In the rosin recipe without added ammonium ion, nearly identical rates of conversion were found with sulfole or DDM; however, normal modification was obtained with sulfole, whereas DDM gave poor modification. This is illustrated in Figure 26, giving the disappearance curves of *tert*-(sulfole) and *n*-dodecyl(DDM) mercaptans, respectively.

The authors wish to acknowledge the advice and interest of Prof. E. J. Meehan of this University, particularly on the work with rosin soap. Most of the experimental work described in this paper was carried out by Miss Rebecca Held, for whose careful technique the authors have great appreciation.

References

1. A. I. Medalia and I. M. Kolthoff, *J. Polymer Sci.*, **4,** 377 (1949).
2. See report by E. R. Weidlein, Jr., *Chem. Eng. News*, **24,** 771 (1946).
3. E. J. Vandenberg and G. E. Hulse, *Ind. Eng. Chem.*, **40,** 932 (1948).
4. H. Hock and S. Lang, *Ber.*, **B77,** 257 (1944).
5. A. B. Lamb and A. G. Jacques, *J. Am. Chem. Soc.*, **60,** 1215 (1938).
6. S. A. Harrison and E. R. Meincke, *Anal. Chem.*, **20,** 47 (1948).
7. D. E. Williams and W. F. Johnson, *J. Polymer Sci.*, **2,** 346 (1947).
8. W. V. Smith and R. H. Ewart, *J. Chem. Phys.*, **16,** 592 (1948).
9. W. V. Smith, *J. Am. Chem. Soc.*, **70,** 3695 (1948).
10a. W. D. Harkins *et al.*, Report to Office of Rubber Director, March 20, 1943; *J. Chem. Phys.*, **13,** 381 (1945).
10b. J. W. McBain, Report to Office of Rubber Director, March 23, 1943.
11. E. J. Meehan, *J. Am. Chem. Soc.*, **71,** 628 (1949).
12. I. M. Kolthoff and W. Stricks, *J. Phys. Chem.*, **52,** 915 (1948).
13. I. M. Kolthoff and F. A. Bovey, *Chem. Revs.*, **42,** 491 (1948).
14. J. H. Baxendale, M. G. Evans, and G. S. Park, *Trans. Faraday Soc.*, **42,** 155 (1946).
15. A. I. Medalia, Ph.D. thesis, University of Minnesota, June 1948.
16. I. M. Kolthoff and A. I. Medalia, *J. Am. Chem. Soc.*, **71,** 3789 (1949).
17. C. S. Marvel, R. Deanin, C. G. Overberger, and B. M. Kuhn, *J. Polymer Sci.*, **3,** 128 (1948).
18. W. Traube and F. Kuhbier, *Ber.*, **65,** 187, 190 (1932).
19. W. Traube, F. Kuhbier, and H. Harting, *ibid.*, **66,** 1545 (1933).
20. I. M. Kolthoff and W. E. Harris, *J. Polymer Sci.*, **2,** 41 (1947).

English Synopsis, see Summaries, page S21, Vol. V, 1950.

Resumé

Une recette redox de copolymérisation du butadiène et du styrène à 30° est décrite. Les composants de ce système sont: l'hydroperoxyde de cumène (CHP), un complexe soluble pyrophosphate de fer, et un sucre réducteur; l'émulsifiant est le myristate de potassium pur, et le *tert*-dodécyl mercaptan est additionné comme modificateur. Les concentrations optimales de fer ferrique, du pyrophosphate et du CHP ont été établis expérimentalement. S'il y a très peu de CHP, la polymérisation s'arrète brusquement à des conversions, qui sont en rapport linéaire avec la quantité de CHP utilisé. De cette relation, et étant donné une vitesse de conversion sensiblement constante, on a pu calculer la vitesse de consommation du CHP. Cette vitesse est proportionnelle à la puissance $^2/_3$ de la quantité de sucre, la constante de proportionalité étant six fois plus élevées avec le fructose qu'avec le glucose. Quand on utilise suffisament de savon, la vitesse de conversion est proportionnelle à la racine carrée de la vitesse de consommation du CHP; avec trop peu de savon, cette relation fait défaut; apparemment, la réaction CHP–fer ferreux, qui produit les radicaux, se passe en phase aqueuse; si il y a suffisa-

ment de savon présent, ces radicaux pénètrent la phase organique, où la polymérisation a lieu. Au contraire, avec peu de savon, beaucoup de radicaux sont terminés en phase aqueuse par réaction réciproque, sans donner lieu à polymérisation. Alternativement, les résultats avec 2.5 et 5 (non avec 10) parties de savon sont en accord avec les relations, prédites par Smith et Ewart, dans le cas 2 envisagé par ces auteurs, au cours duquel la vitesse de conversion est proportionnelle à la puissance $^2/_5$ de la vitesse de production de radicaux et à la puissance $^3/_4$ de la concentration en savon.

Avec des concentrations de savon inférieures à la valeur critique, il n'y a pas de polymérisation; par contre, un léger accroissement de la quantité du savon au voisinage de la concentration critique donne lieu à un accroissement considérable de la vitesse de conversion. Quand on utilise un sel ferreux, celui-ci réagit rapidement avec le CHP dans un rapport moléculaire apprximatif de 1/1. Les effets de différentes modifications dans les ingrédients de la formule proposée sont renseignés.

Zusammenfassung

Es wird eine Redox-Vorschrift für die Copolymerisation von Butadien und Styrol bei 30° beschrieben. Die Komponenten des Redox-Systems sind Cumolhydroperoxyd (CHP), ein löslicher Pyrophosphat–Eisen Komplex und ein reduzierender Zucker; das Emulsionsmittel ist reines Kaliummyristat, und tertiäres Dodecylmerkaptan wird als Modifikationsmittel beigefügt. Optimale Konzentrationen für 3-wertiges Eisen, Pyrophosphat und CHP wurden experimentell bestimmt. In Gegenwart von sehr kleinen Mengen von CHP kommt die Polymerisation plötzlich vollständig zum Stehen, bei Umsatzgraden, die in linearer Beziehung zu der angewendeten Menge CHP stehen. Aus dieser Beziehung, zusammen mit der nahezu konstanten Umsatzgeschwindigkeit, kann die Verbrauchsgeschwindigkeit von CHP berechnet werden. Diese Verbrauchsgeschwindigkeit ist der $^2/_3$ Potenz der Zuckermenge proportionell, wobei die Proportionalitätskonstante für Fruktose 6 mal so gross wie die für Glukose ist. In Gegenwart von genügend Seife ist die Umsatzgeschwindigkeit der Quadratwurzel der Verbrauchsgeschwindigkeit von CHP proportionell; aber mit wenig Seife stimmt diese Beziehung nicht. Offenbar findet die Reaktion zwischen CHP und 2-wertigem Eisen, welche freie Radikale hervorbringt, in der wässrigen Phase statt; wenn genügend Seife vorhanden ist treten die Radikale in die organische Phase über, wo Polymerisation stattfindet; mit wenig Seife dagegen enden viele Radikale in der wässrigen Phase, indem sie unter einander reagieren, ohne dass Polymerisation eintritt. Möglicherweise kann man annehmen, dass Daten mit 2.5 und 5 (aber nicht mit 10) Teilen Seife der von Smith und Ewart vorausgesagten Beziehung für den Fall 2 dieser Autoren folgen, wobei die Umsatzgeschwindigkeit der $^2/_5$ Potenz der Produktionsgeschwindigkeit der Radikale und der $^3/_5$ Potenz der Seifenkonzentration proportionell ist.

Bei Seifenkonzentrationen unterhalb der kritischen Konzentration tritt praktisch keine Polymerisation ein; dagegen bewirkt eine kleine Zunahme der Seifenmenge in der Gegend der kritischen Konzentration einen scharfen Anstieg der Umsatzgeschwindigkeit. Bei Benutzung von 2-wertigem Eisen reagiert dieses schnell mit CHP im ungefähren Molverhältnis 1:1. Die Wirkung verschiedener Änderungen der Bestandteile der Vorschrift wird gegeben.

Received June 18, 1949

JOURNAL OF POLYMER SCIENCE VOL. V, NO. 4, PAGES 429–442

Untersuchung einer katalysierten Leinölstandölkochung unter Heranziehung der Ultraviolettspektrographie (Vergleich mit nichtkatalysierten Prozessen)

A. MASCHKA und A. MENDL, *Institut fur Physikalische Chemie der Technischen Hochschule, Wien*

EINLEITUNG

Über die Vorgänge, die sich beim Kochen von Leinöl abspielen und die zur Bildung eines Standöles führen, gibt es verschiedene Ansichten. Auf Grund der Ergebnisse neuerer Arbeiten erscheint nachstehende Reaktions folge als die wahrscheinlichste:

Die isolierten Doppelbindungen der Leinölfettsäuren lagern sich beim Erhitzen zu konjugierten um.[1,2] Die Systeme mit konjugierten Doppelbindungen gehen dann Ringschlussreaktionen im Sinne einer Diensynthese nach Diels-Alder ein.[2] Dies kann eintreten—bei Vorliegen einer dreifachen Konjugation—innerhalb einer Fettsäurekette, zwischen zwei Fettsäureketten, die demselben Glyceridmolekül angehören, und schliesslich zwischen solchen verschiedener Glyceridmoleküle. Im ersten Falle spricht man von Intrafettsäure, "polymerisation," im zweiten von intramolekularer "Polymerisation" und im letzten von intermolekularer Polymerisation. Nur die letzte ist eine wirkliche Polymerisation, die zu einer Molekülvergrösserung führt.

Nach diesem Schema müsste es während des Kochprozesses zunächst zu einer Anreicherung der Systeme mit konjugierten Doppelbindungen und im weiteren Verlauf wieder zu einer Abnahme kommen, was nach den Untersuchungen von Pestemer und Tschinkel,[3] sowie Bradley und Richardson[4] auch zutrifft. Die erstgenannten Autoren sprechen die Vermutung aus, dass die intramolekulare Polymerisation zunächst abläuft und erst im Anschluss daran die intermolekulare stattfindet. Damit finden sie auch den experimentellen Befund in Übereinstimmung, dass der steile Anstieg der Viskosität erst zu einem Zeitpunkt eintritt, wenn pro Glyzeridmolekül zwei Doppelbindungen aufgespalten sind, was einer intramolekularen Polymerisation pro Molekül im Sinne einer Diels-Alder Diensynthese entspricht. (Wegen näherer Einzelheiten sei auf die Originalarbeit hingewiesen.) In einer Arbeit von E. Schauenstein[5] wird gezeigt, dass die Zunahme der Viskosität von einer angenähert proportionalen Mokekulargewichtszunahme begleitet ist, womit die Vermutung von Pestemer und

Tschinkel nach Ansicht des Autors eine weitere Bestätigung erfährt.

In der vorliegenden Arbeit werden Leinölstandölkochungen mit und ohne Katalysator untersucht um festzustellen, ob beim katalysierten Prozess ähnliche Verhältnisse auftreten wie sie oben beschrieben wurden. Weiters wird auch der Kochprozess eines mit 0.2 Gew. % Bleiglätte siccativisierten Firnisses sowie der eines Leinölstandölfirnisses untersucht.

EXPERIMENTELLES

Zur Verwendung gelangte ein handelsübliches Lackleinöl, das aus Kanada stammte und das in der Fabrik mit Schwefelsäure raffiniert und mit Lauge entsäuert worden war. Seine Daten sind: Jodzahl (nach Wijs, Einwirkungsdauer 30 Minuten): 181.5 g. Jod/100 g. Leinöl; Verseifungszahl: 183 mg. KOH/Gramm Leinöl; Säurezahl: 1.56 mg. KOH/Gramm Leinöl; Brechungsindex: $n_D^{20°} = 1.4785$; spezifisches Gewicht: 0.9312 g./cm.^{3}; Viskosität: 0.4785 Poisen bei 20°C.

Prozess I: 750 cm.^{3} dieses Leinöls wurden in einem 1 Liter Jenaer-Weithalsrundkolben bei 285 ± 1°C. im Luftbad 28 Stunden gekocht. Dabei wurde Kohlensäure durch das Öl geleitet (11.2 Liter pro Stunde), um eine inerte Atmosphäre zu schaffen und das Öl durchzumischen. Die Kohlensäure wurde einer Bombe entnommen und durch Pyrogallollösung und konz. Schwefelsäure geleitet. In Abständen von 4 Stunden wurden mittels einer vorgewärmten Pipette 75 cm.^{3} als Probe zur Untersuchung entnommen und zwecks Stoppung des Reaktionsablaufes mit Leitungswasser gekühlt. Die Pipette wurde durch eine für diesen Zweck vorgesehene, verschliessbare Öffnung des Korkstopfens eingeführt.

Prozess II: wie oben, jedoch wurden dem Leinöl 0.5 Gew.% Nickelformiat und 0.5 Gew.% Asbestfasern zugegeben.[6] Bei dieser Methode wird das katalysierende Nickel unmittelbar im Medium hergestellt, weil sich während der Anheizperiode bei etwa 230°C. das Nickelformiat zersetzt, wobei sich das feinverteilte metallische Nickel in aktivster Form auf den Asbestfasern niederschlägt. In diesem Falle wurde die Kohlensäure bloss über das Leinöl geleitet und die Durchmischung von einem mit 95 Umdrehungen pro Minute rotierenden Glasrührer besorgt. Intervall zwischen aufeinanderfolgenden Probenahmen 30 Minuten, Kochdauer fünf Stunden.

Prozesse III und IV: 250 cm.^{3} Leinöl bzw. 50 cm.^{3} Standöl entsprechend der Probe D (siehe später), jeweils mit 0.2 Gew.% Bleiglätte versetzt, wurden ohne Kohlensäure bei 230°C. zwei Stunden gekocht.

An den einzelnen Proben wurden folgende Bestimmungen vorgenommen: Jodzahl (nach Wijs, Einwirkdauer 30 Minuten), Viskosität, spezifisches Gewicht, Brechungsindex (aus den letzten beiden wurde die spezifische Refraktion berechnet), Säurezahl und Ultraviolettabsorption.

Die Messung der Viskosität erfolgte mit einem Ubbelohde-Viskosimeter mit hängendem Kugelniveau bei 20°C. unmittelbar an der entnommenen Probe. Die so erhaltene kinematische Zähigkeit wurde in die absolute umgerechnet.

Die spektroskopischen Untersuchungen wurden mit dem Universalspektrographen von Zeiss (9 × 12) unter Verwendung des 21 teiligen Küvettensatzes nach Scheibe durchgeführt. Als Lösungsmittel diente *n*-Heptan oder ein bis zur optischen Leere gereinigtes Leichtbenzin. Als Lichtquelle wurde ein Funke zwischen Wolframelektroden verwendet.

VERSUCHSERGEBNISSE

Die Werte der Kennzahlen der Prozesse I und II sind in den Tabellen I und II und die graphische Darstellung in den Abbildungen 1 und 2 wiedergegeben, wobei der Zeitmasstab in Abbildung 2 fünfmal so gross gewählt wurde. Um einen Vergleich zu ermöglichen, sind in Abbildung 3 die von Pestemer und Tschinkel[3] mitgeteilten Ergebnisse einer technischen Leinölstandölkochung bei 285°C. unter vermindertem Druck (5-10 mm. Hg) dargestellt.

TABELLE I

PROZESS I

Koch-dauer in Std	Probe	Wijs'sche Jodzahl g J/100 g	Viscosität $\eta_{20°}$	Dichte $\rho_{20°}$	Refraktion $n_D^{20°}$	Spez Refraktion	S Z mg. KOH /g.
0	O	181 5	0 4785	0 9312	1 4761	0 30395	1 56
4	A	167 6	0 693	0 9315	1 4778	0 30378	2 95
8	B	144 8	3 33	0 9449	1 4811	0 30117	3 38
12	C	114.4	12 85	0 9547	1 4838	0 30053	3 39
16	D	96 6	78 23	0 9605	1 4863	0 29907	3 40
20	E	85 2	225 00	0 9646	1 4869	0 29811	3 42
24	F	75 9	—	0 9650	1 4878	0 29745	3 44
28	G	71 1	—	0 9652	1 4881	0 29712	3 45

TABELLE II

PROZESS II

Koch-dauer in Std.	Probe	Wijs'sche Jodzahl g. J/100 g.	Viscosität $\eta_{20°}$	Dichte $\rho_{20°}$	Refraktion $n_D^{20°}$	Spez Refraktion $\frac{(n^2-1)}{(n^2+2)} \cdot \frac{1}{\rho}$	S Z mg KOH/g.
0	0	181 5	0 4785	0 9312	1.4785	0 3040	1.56
0 5	I	174 9	0 6323	0 9316	1 4783	0 3039	3 82
1	II	153 4	1 19	0 9325	1 4771	0 3030	4 39
1 5	III	127 2	1.96	0 9356	1 4761	0 3016	4 57
2	IV	107 8	2 92	0 9410	1 4771	0 3002	4 68
2 5	V	95 1	4.07	0 9452	1 4785	0 2995	4 72
3	VI	86 8	5 18	0 9464	1.4747	0 2990	4 74
3.5	VII	81 2	7 55	0 9488	1 4746	0 2986	4.76
4	VIII	76 5	12 5	0.9502	1 4790	0.2983	4 81
4.5	IX	73.1	30.1	0 9519	1 4800	0 2981	4 81
5	X	70 1	83 5	0.9525	1 4801	0 2979	4.83

Die Absorptionskurven des Leinöls und der beim Prozess I entnommenen Proben sind in der Abbildung 4 dargestellt. Die entsprechenden Kurven von Prozess II zeigen die Abbildungen 5 und 6.

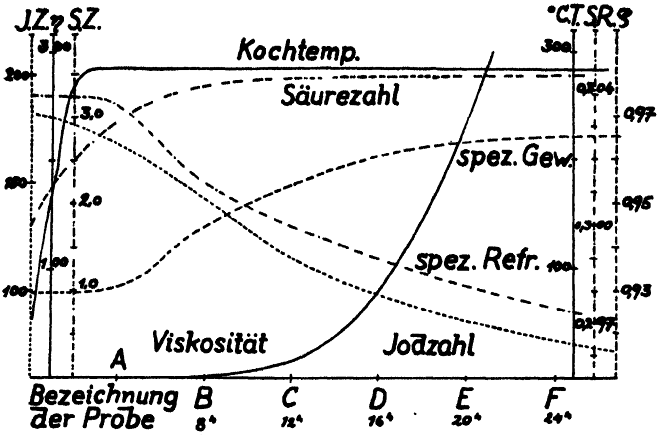

Abb. 1. Kennzahlenänderung des Prozesses I.

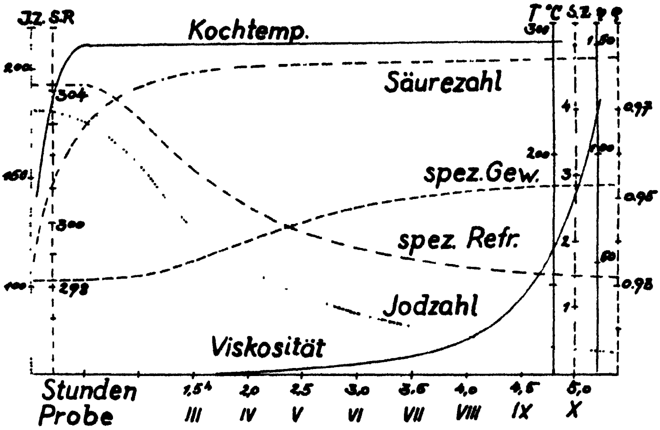

Abb. 2. Kennzahlenänderung des Prozesses II.

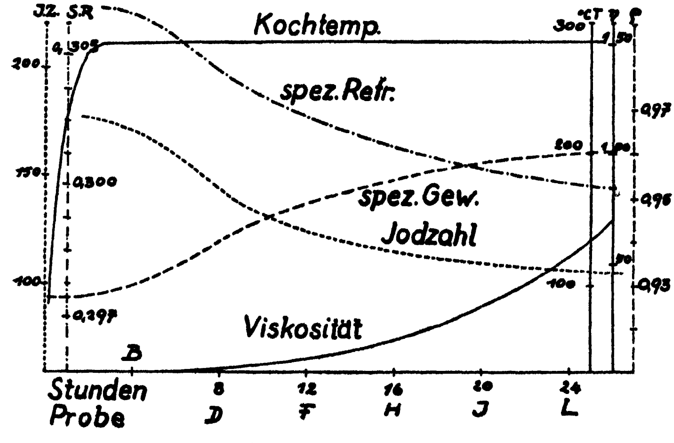

Abb. 3. Kennzahlenänderung des technischen Prozesses.

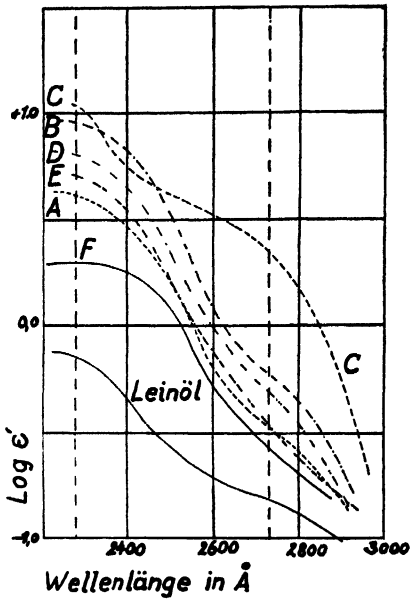

Abb. 4. Absorption-Kurven der Proben des Prozesses I.

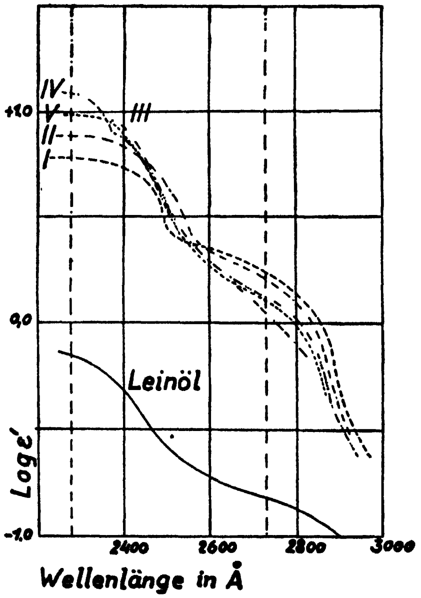

Abb. 5. Absorption-Kurven des Prozesses II.

Man erkennt, dass die Absorptionskurve des Leinöls zwei deutlich abgesetzte Maxima (bei 2288 A. und 2725 A.) aufweist, die auch bei den einzelnen im Laufe der Prozesse entnommenen Proben erhalten bleiben. Die Absorption des Leinöls im langwelligen Ultraviolett wird praktisch nur von Fettsäuren mit konjugierten Doppelbindungen hervorgerufen und zwar

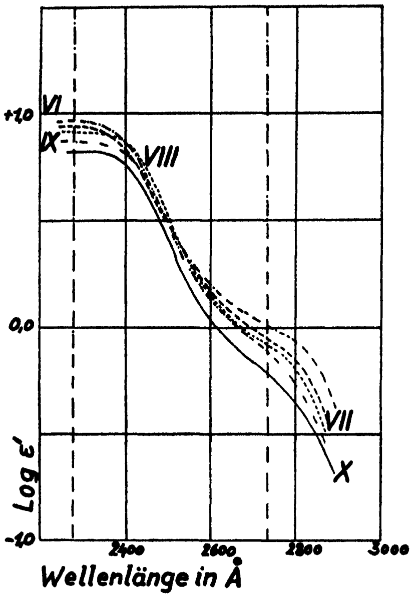

Abb. 6. Absorption-Kurven der Proben des Prozesses II.

wird nach M. Pestemer[7] das Maximum bei 2288 A. durch Fettsäuren mit zwei konjugierten Doppelbindungen (im vorliegenden Falle 9,11-Linolsäure) und das bei 2725 A. durch Fettsäuren mit drei konjugierten Doppelbindungen (Elaeostearinsäure oder hier eine isomere Linolensäure) hervorgerufen. Diesen: Maximalwerten entsprechen die molaren Extinktionskoeffizienten (nach Pestemer[7]): 9,11-Linolsäure ϵ = 40,700 und Elaeostearinsäure ϵ = 52,500. Daraus kann man den speziellen Extinktionskoeffizienten für den Tri-9,11-Linolsäureglycerinester ϵ' = 140 und den für das entsprechende Glycerid der Elaeostearinsäure ϵ' = 180 berechnen

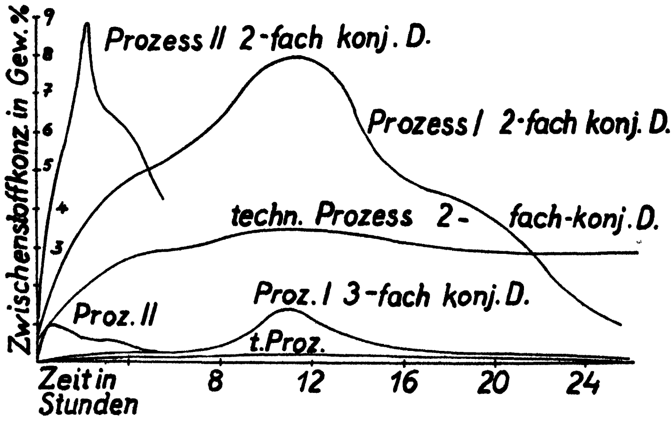

Abb. 7. Zwischenstoffkonzentration der zwei- und dreifach konjugierten Doppelbindungen, enthalten in Fettsäuren in Gew.% in Abhängigkeit von der Zeit in Stunden.

($\epsilon' = 3\epsilon$ dividiert durch Molekulargewicht des Glycerides). ϵ' ist gleich der Extinktion E bei der Schichtdicke $d = 1$ cm. und der Konzentration $c' = 1$ g. Glycerinester pro Liter Lösung.

Den Anteil in Gew. % an Fettsäureglyceriden mit zwei, bzw. drei konjugierten Doppelbindungen in den einzelnen Proben berechnet man aus der Extinktion E bei dem entsprechenden Maximum auf folgende Weise:

$$E = \epsilon_g' c' d \qquad 100\% : x\% = \epsilon' : \epsilon_g'$$

In den Abbildungen 4 bis 6 ist jeweils log ϵ' gegen die Wellenlänge in Angström Einheiten (A.) aufgetragen.

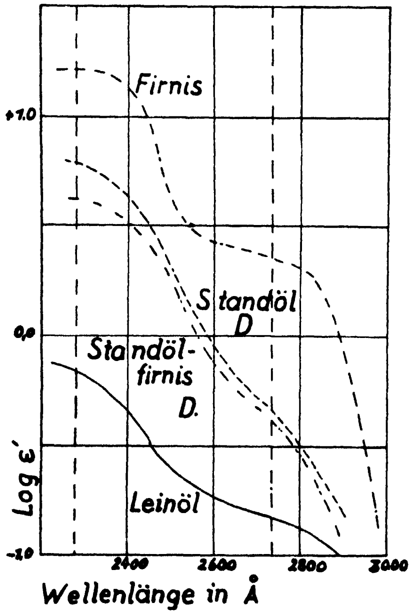

Abb. 8. Absorptionskurven von Firnissen.

TABELLE III

Prozess I

Probe	Log ϵ' 2725 A.	Log ϵ' 2288 A.	ϵ_g' 2725 A.	ϵ_g' 2288 A.	Gew % Fetts mit —C=C—C=C—C=C—	Gew % Fetts mit —C=C—C=C—
0	−0.828	−0 155	0.149	0 787	0 070	0.565
A	−0 480	+0 625	0.332	6 69	0 185	4.82
B	−0.237	+0.950	0 580	8 92	0 326	6.425
C	+0.350	+1.037	2.24	10 93	1 244	7.92
D	−0.308	+0.812	0 493	6.50	0 271	4.67
E	−0.450	+0 712	0 355	5.16	0.171	3.71
F	−0 575	+0.280	0.267	1 908	0 148	1.37

Errechnet man in der oben angegebenen Weise die Anteile an Fettsäureglyceriden mit zwei und drei konjugierten Doppelbindungen für die einzelnen Proben der Prozesse I und II (siehe die Tabellen III und IV) und trägt deren Werte gegen die Zeit auf, dann erhält man Abbildung 7. Ausserdem sind noch die entsprechenden Kurven der schon angeführten technischen Standölkochung eingezeichnet.

Abb. 8 schliesslich zeigt die Absorptionskurven von Leinöl-und Standölfirnis (Prozesse III und IV).

TABELLE IV

PROZESS II

Probe	Log ϵ' 2725 A.	Log ϵ' 2288 A.	ϵ_g' 2725 A.	ϵ_g'' 2288 A.	Gew.% Fetts. mit —C=C—C=C—C=C—	Gew.% Fetts. mit —C=C—C=C—
0	−0.828	−0.155	0.149	0.787	0.070	0.565
I	+0.241	+0.772	1.747	5.94	0.971	4.26
II	+0.208	+0.878	1.619	7.56	0.899	5.43
III	+0.132	+0.981	1.358	9.58	0.754	6.88
IV	+0.109	+1.083	1.288	12.13	0.716	8.72
V	+0.061	+0.983	1.151	9.625	0.639	6.92
VI	+0.015	+0.961	1.037	9.18	0.576	6.59
VII	−0.048	+0.940	0.896	8.74	0.498	6.27
VIII	−0.079	+0.913	0.836	8.20	0.465	5.88
IX	−0.105	+0.870	0.786	7.43	0.436	5.33
X	−0.204	+0.811	0.627	6.48	0.348	4.66

DISKUSSION DER VERSUCHSERGEBNISSE

Beim Vergleich der Abbildungen 1 bis 3 erkennt man, dass der Verlauf der Kennzahlenänderung mit der Zeit bei allen drei Prozessen qualitativ derselbe ist. Die mit Nickel katalysierte Kochung verläuft jedoch etwa fünfmal so rasch. Auch die von uns durchgeführte Standölkochung unter Durchleiten von Kohlensäure bei Atmosphärendruck verläuft schneller als der technische Prozess.

Sehr deutlich kommen diese Verhältnisse zum Ausdruck, wenn man die Zeiten vergleicht, die zur Erreichung einer bestimmten Viskosität erforderlich sind. Auch Jodzahl und spezifisches Gewicht sind bei gleicher Viskosität recht unterschiedlich (Tabelle V).

TABELLE V

	Viskosität 30 Poisen (100 Poisen) Kochzeit (Studen)	Jodzahl	Spezifisches Gewicht (20°C.)
Techn. Kochung	20 (28)	109 (103)	0.9582 (0.9630)
Prozess I	13.5 (17)	106 (94)	0.9565 (0.9615)
Prozess II	4.5 (5.5)	74 (70)	0.9520 (0.9530)

In Abbildung 9 sind die spezifischen Refraktionen und die Viskositäten in Abhängigkeit von der Jodzahl dargestellt. Man kann zwei Tatsachen erkennen: (*1*) Die spezifische Refraktion ändert sich während der ganzen Kochung angenähert linear mit der Jodzahl; (*2*) Die starke Zunahme der

Viskosität erfolgt erst dann, wenn die Jodzahl (und wie aus *1* folgt auch die spezifische Refraktion) nur noch wenig abnimmt.

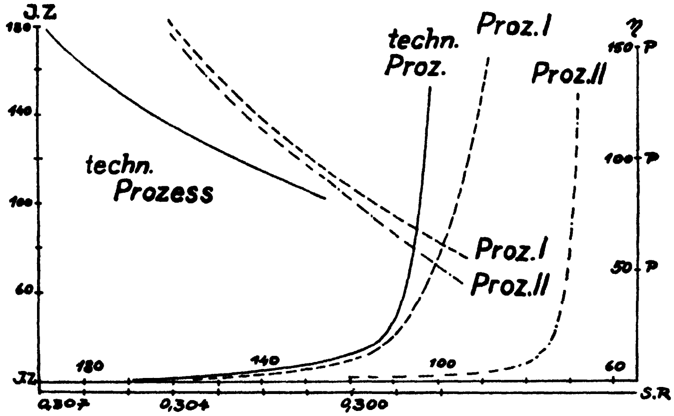

Abb. 9. **Änderung der Viskosität mit Jodzahl und Änderung der Jodzahl mit der spezifischen Refraktion.**

Wenn man voraussetzt, dass die Jodzahlsenkung durch das Verschwinden von Doppelbindungen infolge von Diensynthesen nach Diels-Alder bedingt* und das Molekulargewicht bei "beendeter" Kochung doppelt so gross als zu Beginn ist,† dann spricht dieser letztere Befund gegen die Annahme, dass die starke Zunahme der Viskosität (bzw. des Molekulargewichtes) durch intermolekulare Polymerisation (nach Diels-Alder) bewirkt wird. Denn bei den intermolekularen Polymerisationen müssten ebensoviele Doppelbindungen verschwinden wie bei den intramolekularen. Dies würde vielmehr dafür sprechen, dass der starke Viskositäts (Molekulargewichts) anstieg durch einen Vorgang bedingt ist, der keine Doppelbindungen verbraucht. Als solcher kommt wohl in erster Linie die Umesterung in Frage. Man hätte also anzunehmen, dass in Ansehung der Viskositätszunahme zunächst (solange die Jodzahl abnimmt) die intermolekulare Polymerisation und Umesterung nebeneinander verlaufen, wobei über den Beitrag, den jeder dieser Vorgänge zur Viskositätserhöhung liefert, nichts ausgesagt wird. Es ist zu bedenken, dass in diesem Stadium eine Umesterungsreaktion zwischen zwei Glyceriden zu einem Dimeren führen kann und die inverse Umesterung daraus wieder zwei Monomere liefert. Das heisst also, dass die Umesterung in diesem Falle sowohl viskositätserhöhend wie auch erniedrigend wirken kann. Anders ist es jedoch, wenn die Möglichkeiten zu Diensynthesen weitgehend erschöpft sind, wenn also eine bedeutende Jodzahlabnahme nicht mehr stattfindet. Dann kann die Umesterung jedenfalls nicht mehr viskositätserniedrigend wirken. Wenn man annimmt, dass die Umesterung während der gesamten Kochung mit einer angenähert gleichbleibenden Geschwindigkeit verläuft, dann würde sie in der ersten Periode (solange noch keine Cyclohexenringe gebildet sind- Periode der Konjugation der isolierten Doppelbindungen) naturgemäss auch keine Viskositätserhöhung bewirken können. In der zweiten Periode (die Jodzahlsenkung zeigt Polymerisation—etwa im Sinne der intramolekularen Cyclohexenbildung an) liefert sie positive und negative Beiträge zur Viskosität, wobei die positiven wegen der grösseren Zahl der Möglichkeiten überwiegen dürften. Im nächsten Stadium des Kochprozesses, wenn die intermolekulare Polymerisation (Dimerisierung) an Bedeutung gewinnt, kommt auch noch der Beitrag dieses Vorganges zur Viskositätserhöhung dazu. Schliesslich wird der oben angedeutete Zustand erreicht (praktisch keine weiteren Möglichkeiten zu Diensynthesen), in dem die überwiegende Zahl der möglichen Umesterungen zu grösseren Molekülen führt. Dies ist die Phase des starken Anstieges der Viskosität.

---

* Diese Voraussetzung ist nur in erster Näherung richtig, da die konjugierten Doppelbindungen mittels der Wijs'schen Jodzahl nicht quantitativ erfasst werden; daher besteht auch keine streng lineare Proportionalität zwischen den Abnahmen der Jodzahl und der spezifischen Refraktion. (Vgl. die zitierte Arbeit von Schauenstein.)

† Bei den Prozessen I und II wurden Molekulargewichtsbestimmungen allerdings nicht durchgeführt.

Sehr deutlich kommen diese Verhältnisse zum Ausdruck, wenn man in Abbildung 9 die Jodzahlverminderung im Bereiche des steilen Viskositätsanstieges mit derjenigen vergleicht, die bis zum Beginn des Viskositätsanstieges auftritt. Bei Umrechnung der Jodzahlensenkungen auf die pro Molekül Trilinolsäureglycerinester aufgespaltenen Doppelbindungen findet man folgende Zahlen (Tabelle VI).

TABELLE VI

	Verminderung der Doppelbindungen pro Molekül Trilinolsäureglycerinester	
	bis zum steilen Anstieg der Viskosität	im Bereich des steilen Anstieges
Techn. Prozess	2.36	0.28
Prozess I	2.36	0.80
Prozess II	3.64	0.24

Hieraus ersieht man, dass schon vor dem Viskositätsanstieg mehr Doppelbindungen pro Molekül verbraucht wurden, als einer intramolekularen Polymerisation entspricht, woraus folgt, dass offenbar auch die intermolekulare schon vorher stattfindet. Liegt das Standöl, wie Schauenstein[5] festgestellt hat, am Ende der Kochung dimer vor, dann müsste, wenn der Viskositätsanstieg durch intermolekulare Polymerisiation erfolgt, während dieser Periode pro Molekül eine weitere Doppelbindung verschwinden, was aber nicht zutrifft. Entspräche das Molekulargewicht am Ende der normalen Kochung nicht gerade dem Dimeren wie es der Fall ist, dann könnte man noch denken, dass die geringe intermolekulare Polymerisation (die durch die minimale Jodzahlsenkung angezeigt wird) keinen sehr grossen Beitrag zur Viskosität liefert, und auf die Heranziehung der Umesterung zur Erklärung weitgehend verzichten. Ein gleicher Befund ergibt sich, wenn man anstelle der Jodzahlen die Molekularrefraktionen heranzieht, weil diese Grössen einander fast direkt proportional sind (Abb. 9).

Eine Voraussetzung für die Richtigkeit der vorstehend entwickelten Anschauungen über die Viskositätszunahme wäre eine weitere Erhöhung der Viskosität bei fortgesetztem Kochen des Standöls. Das Zutreffen dieser Forderung könnte jedoch nicht als sicherer Beweis für die Richtigkeit betrachtet werden, weil die Proportionalität zwischen Viskosität und Molekulargewicht[5] nicht bestehen bleiben muss.

Aus Abbildung 7 geht hervor, dass die zeitliche Anderung der Anteile mit zwei konjugierten Doppelbindungen bei den drei Prozessen ähnlich ist. Entsprechend der grossen Geschwindigkeit beim katalytischen Vorgang ist das Maximum der Zwischenstoffkonzentration viel früher erreicht als bei den anderen beiden Prozessen, bei denen die Maxima zeitlich praktisch zusammenfallen. Auffallend ist jedoch, dass es im ersten Falle einen wesentlich höheren Wert erreicht als beim technischen Prozess und ebenso auffallend ist, dass das Maximum unserer nicht katalysierten Kochung nahezu ebenso hoch liegt.

Ahnliche Verhältnisse liegen auch für die zeitliche Veränderung der Systeme mit drei konjugierten Doppelbindungen vor, die nur in untergeordneter Menge auftreten. Jedoch sind hier zwei Umstände bemerkenswert: (*1*) Das Maximum beim Prozess I ist wesentlich höher als das bei der technischen Kochung, beide fallen aber zeitlich praktisch zusammen und treten gleichzeitig mit dem Maximum der zweifach konjugierten Systeme auf; (*2*) das Maximum beim katalysierten Prozess II hat angenähert den gleichen Wert wie in Prozess I (ähnlich wie für die zweifach konjugierten Systeme), wird aber zeitlich viel früher erreicht.

Die deutliche Unterschiedlichkeit des Prozesses II gegenüber den beiden anderen kann nicht überraschen, wohl aber die beträchtliche Verschiedenheit zwischen unserer und der technischen Standölkochung. Die Ursache dafür kann nicht mit Sicherheit angegeben werden. Es kommt aber vor allem offenbar der Umstand in Frage, dass unser Versuch bei einer Atmosphäre Druck und der technische Prozess im Vakuum verlief. Da die Polymerisation mit einer Dichtezunahme einhergeht, kann demnach der Druck einen Einfluss, ausüben. Es ist aber auch denkbar, dass die Kohlensäure in irgendeiner Weise dabei eine Rolle spielt. Dafür spricht aber zunächst kein anderer Grund als der, dass sich ein Vorgang bei Anwesenheit und der zweite bei Abwesenheit von Kohlensäure abspielte.

Wenn die Zwischenstoffkonzentrationskurven einer quantitativen Auswertung auch nicht zugänglich sind, so kann man aus dem Anstieg der Kurven doch erkènnen, dass der Ubergang der isolierten in konjugierte Doppelbindungen bei Prozess II weitaus am schnellsten und bei der technischen Kochung am langsamsten erfolgt. Dass dieser Vorgang auch beim Prozess I viel rascher vor sich geht als beim technischen Kochen lässt sich vielleicht auch auf den Einfluss des Druckes zurückführen. Versuche zur Feststellung ob und welchen Einfluss der Druck tatsächlich ausübt, sind beabsichtigt.

Da die Kurven für Prozess II qualitativ mit den anderen übereinstimmen, kann man schliessen, dass der Katalysator alle Teilreaktionen ziemlich gleichmässig beschleunigt. Das rasche Erreichen des Maximums für dreifach konjugierte Systeme im katalysierten Prozess könnte so erklärt werden: Der Katalysator beschleunight die Isomerisierung der Doppelbindung; sobald in einer Fettsäurekette ein System von zwei konjugierten Doppelbindungen vorliegt, wirkt dieses auf die dritte—noch isolierte—Doppelbindung dieser Fettsäure ebenfalls aktivierend, sodass diese unter der gleichsinnigen Wirkung beider Einflüsse besonders rasch auch in Konjugation übergeht.

Es ist auffallend, dass beim katalysierten Vorgang bei allen Viskositäten die Jodzahl wesentlich niedriger ist als bei den anderen Prozessen. Dies kann als Folge des Katalysators aufgefasst werden, der die Doppelbindungen aktiviert und so rascher zum Abreagieren bringt. Es kann dies jedoch auch eine andere Folge des Katalysators sein*: Das Nickel könnte in den vorhandenen Cyclohexenringen dehydrierend wirken; der entstehende Wasserstoff lagert sich an Doppelbindungen, wodurch die Jodzahl sinkt.

Sehr interessant erscheint uns der Umstand, dass bei allen drei Zwischenstoffkonzentrationskurven für zwei konjugierte Doppelbindungen sowohl im ansteigenden als auch im absteigenden Ast ein zweites Maximum auftritt. Die vorliegenden Resultate sind für eine genaue kinetische Betrachtung nicht geeignet. Hiefür müsste man vor allem durch entsprechende experimentelle Bedingungen günstigere Voraussetzungen schaffen. Das im vorliegenden Falle angewandte Leinöl enthält offenbar Glyceride von Fettsäuren mit einer, zwei und drei Doppelbindungen. Letztere sind zum Teil anfangs schon konjugiert. Systeme mit drei Doppelbindungen, von denen aber vorerst nur zwei konjugiert sind, täuschen einen gar nicht vorhandenen Anteil an Fettsäuren mit bloss zwei konjugierten Doppelbindungen vor. Die Zahl aller Zwischenformen und -Reaktionen, die möglich sind, um zu einem dimeren Glycerid ohne konjugierte Doppelbindungen als Endprodukt zu gelangen, ist ausserordentlich gross. Bei Vorliegen eines derart komplexen Substrates wie es technisches Leinöl darstellt, ist die exakte kinetische Behandlung unmöglich. Selbst wenn man diese Untersuchungen an einem Modellkörper—etwa dem reinen Trilinolsäureglycerinester—anstellt, wird die exakte Lösung wegen mathematischer Schwierigkeiten vielleicht unmöglich sein, sind doch auch in diesem Falle noch mehr als ein Dutzend verschiedener Zwischenstoffe mit und ohne konjugierte Doppelbindungen denkbar, die in einer noch grösseren Zahl von mono- und bimolekularen Reaktionen† zu einem dimeren Endprodukt ohne konjugierte Doppelbindungen führen können.

Die Ergebnisse der Firniskochungen (Abbildung 8) zeigen, dass bei Prozess III (Leinöl mit 0.2 Gew.% Bleiglätte zwei Stunden bei 230°C. unter

---

* Diesen Hinweis verdanken wir einer privaten Mitteilung von Herrn Prof. Dr. Waldmann.

† Dabei sind zur Vereinfachung nur Diels-Alder'sche Diensynthesen als konjugierte Doppelbindungen verbrauchende Reaktionen angenommen.

Atmosphärendruck gekocht) die Anteile der Fettsäuren mit zwei konjugierten Doppelbindungen von 0.56 Gew.% auf 11.6 Gew. % und bei drei konjugierten Doppelbindungen von 0.08 Gew.% auf 0.35 Gew.% zunehmen. Die Jodzahl sinkt dabei von 181 auf 141. Für Prozess IV (Standölfirniskochung: Standölprobe D mit 0.2 Gew.% Bleiglätte zwei Stunden bei 230°C. unter Atmosphärendruck gekocht) lauten die Zahlen: Anteil der konjugierten Doppelbindungen nimmt von 4.7 Gew.% auf 3.3 Gew.% ab, der von dreifach konjugierten von 0.27 Gew.% auf 0.21 Gew.%. Die Jodzahl bleibt praktisch unverändert auf 96. Die Viskosität bei 20°C. steigt von 78.2 Poisen auf 96.3 an. Nach den Ergebnissen von Prozess III, der qualitativ mit II übereinstimmt, könnte man der zugesetzten Bleiglätte ähnliche aktivierende Wirkung zuschreiben wie dem Nickelkatalysator. IV liefert keine charakteristischen Resultate. Dieser Vorgang könnte als beschleunigte Weiterführung der Standölkochung aufgefasst werden.

Literaturverzeichnis

1. J. Scheiber, *Farbe u. Lack*, **1929**, 585–587.
2. C. P. A. Kappelmeier, *Farben-Ztg.*, **38**, 1018–1020, 1077–1079 (1933).
3. M. Pestemer und J. Tschinkel, *Fette u. Seifen*, **50**, 153–158 (1943).
4. T. F. Bradley und D. Richardson, *Ind. Eng. Chem., Ind. Ed.*, **32**, 963–969 (1940).
5. E. Schauenstein, *Oesterr. Chem. Ztg.*, **50**, 2–5 (1949).
6. Verfahren zur Katalysierung nach D.R.P. 606,869 (Ölwerke Noury und Van der Lande).
7. M. Pestemer, *Fette u. Seifen*, **48**, 179 (1941).

English Synopsis, see Summaries, page S9, Vol. V, 1950.

Zusammenfassung

(*1*) Laboratoriumsmässige Leinölstandölkochungen mit und ohne Katalysator in Kohlensäureatmosphäre, sowie eine Leinölfirnis- und eine Leinölstandölfirniskochung werden untersucht. (*2*) Neben den üblichen Kennzahlen werden auch die Ultraviolettabsorptionsspektren der einzelnen Proben ermittelt und daraus die Mengen der intermediär auftretenden Systeme mit zweifach und dreifach konjugierten Doppelbindungen berechnet. (*3*) Diese Zwischenstoffkonzentrationskurven und die übrigen Kennzahlen stimmen für die beiden Standölkochungen und einen in der Literatur beschriebenen technischen Prozess qualitativ überein. Naturgemäss verläuft der katalysierte Vorgang viel rascher. (*4*) Aus den Ergebnissen wird der Schluss gezogen, dass die in der Literatur als wahrscheinlich hingestellte Reaktionsfolge (Konjugation der isolierten Doppelbindungen—intra—bzw. intermolekulare Polymerisation im Sinne einer Diensynthese nach Diels–Alder) auch beim katalysierten Prozess auftritt. Der Katalysator beschleunigt alle Teilreaktionen. (*5*) Es wird der Versuch gemacht, aus der Zunahme der Viskosität und der Jodzahlsenkung die Bedeutung der Umesterung für die Viskositäts (Molekulargewichts) zunahme abzuleiten.

Résumé

(*1*) Les produits de cuisson de standolie d'huile de lin, des vernis d'huile de lin et les vernis de standolie d'huile de lin obtenus au laboratoire avec et sans catalyseur dans une atmosphère d'acide carbonique, ont été examinés. (2) Outre les indices habituels les spectres d'absorption ultra-violets des échantillons ont été déterminés, de là, on a cal-

culé les quantités des systèmes intermédiaires caractérisés par 2 ou 3 doubles soudures conjuguées. (*3*) Ces courbes de concentration en produit intermédiaire confirment qualitativement les autres indices pour les deux produits de standolie de même qu'un procédé technique décrit dans la littérature. Evidement le phénomène est beaucoup plus rapide en présence de catalyseur. (*4*) Des résultats on conclut, que la suite de réactions habituellement renseignée dans la littérature comme probable, se passe également dans le procédé catalytique (conjugaison des doubles soudures isolées-polymérisation intra -et intermoléculaire par synthèse diénique de Diels-Alder). Le catalyseur accélère toutes les réactions partielles. (5) De l'augmentation de la viscosité et de la diminution d'indice d'iode les auteurs essaient de déduire la signification de l'estérification pour la viscosité.

Received May 19, 1949

JOURNAL OF POLYMER SCIENCE VOL. V, NO. 4, PAGES 443–463

Aging of Solutions of Cellulose Nitrate

H. CAMPBELL* and P. JOHNSON, *The Royal Institution, London, England*

During the course of work on cellulose nitrates[1–3] some properties of their dilute solutions were observed to change with time and, consequently, were difficult to interpret in terms of the molecular structures present in the solutions. An attempt has been made to determine the mechanisms responsible for this "aging," and although incomplete, the information obtained is sufficient to support certain mechanisms and to exclude others.

The decrease in viscosity of a solution of cellulose nitrate with time has been observed on many occasions and the literature on the aging of such solutions has been recently reviewed.[4] In the majority of these cases, the concentrations of the solutions were greater than 1 gm. of cellulose nitrate in 100 cc. of solution, but in a few experiments more dilute solutions were used, similar in strength to those considered in the present paper. The general conclusions were: (*1*) Cellulose nitrate solutions, on standing in the dark, show a decrease in viscosity. (*2*) The decrease in viscosity is accelerated by standing in strong light. (*3*) The decrease in relative viscosity is more marked the more concentrated the solution. (*4*) The decrease in viscosity is more marked in the early than in the late stages of the aging process. (*5*) The decrease in viscosity has been observed with solutions in acetone and in many other solvents.

The causes suggested by the various workers have been either the breakdown of structure in the solutions or a change in the solvation of the solute molecules. Morozov and Pamfilov[4,5] have attempted to show that the aging was entirely due to a decrease in structural viscosity. Their experiments are, however, not convincing, as incomplete experimental data are given and no attempt is made to determine whether the shear dependence of the viscosity coefficient is reversible or not. Pascal and Grevy[6] have suggested that the change in viscosity is influenced by alkali from the glass of the storage flasks.

Lawton and Nason[7] have shown that ultraviolet light increases the rate of decrease of viscosity of solutions of cellulose nitrate, especially in the presence of oxygen. In the normal storage of solutions, ultraviolet light is completely absent, so that this cannot be considered as a mechanism for the aging of solutions to be discussed below.

---

* Present address: Messrs. May & Baker Ltd., Dagenham, Essex.

Wehr[8] has examined the degradation of solutions of cellulose nitrate in acetone at 20°C. and at 60°C. and has interpreted the results in terms of a shortening of the average chain length. In the reaction at 20°C. the degradation appeared, after a time, to stop, but it continued indefinitely at 60°C. The decrease in viscosity was irreversible. Degradation was accelerated by acids, bases, and organic peroxides and was inhibited by antioxidants. Spurlin[9] has obtained similar results.

The effect of electrolytes on the viscosity of solutions of cellulose derivatives may be very marked and has been discussed recently by Campbell and Johnson.[2]

EXPERIMENTAL METHODS AND MATERIALS

In order to determine whether aging is a property of the cellulose nitrate molecule or represents the slow establishment of equilibrium in a concentrated solution in which there is considerable interaction between the cellulose nitrate chains, it is necessary to eliminate these interactions as far as possible by working in dilute solution. In the present experiments, solutions in acetone of about 0.1 g. in 100 cc. of solution have been used. This concentration is similar to those used in the molecular characterization of cellulose nitrate.

The industrial cellulose nitrates used were derived from various wood and cotton celluloses by nitration with a mixture of nitric acid, sulfuric acid, and water and were stabilized by a series of acid and alkaline boils. Cellulose nitrates were also prepared in the laboratory from celluloses of different natural sources and chemical treatment. The preparation of the celluloses together with the nature of their departure from the ideal cellulose structure is described with the experimental results obtained with them. These celluloses were air dried at 50°C. for 24 hours before nitration with one of two general types of nitrating mixture:

(*i*) Nitric acid–sulfuric acid–water mixture of composition chosen to give the desired nitrogen content (Miles and Milbourn[10]). This method causes considerable degradation of the cellulose.

(*ii*) Nitric acid–phosphoric acid–phosphorus pentoxide mixture which gives a cellulose nitrate of high nitrogen content ($> 13.5\%$) with minimum degradation of the cellulose.[11]

In both methods, nitration was carried out at 0°C. using 30 cc. of nitrating mixture to 1 g. of cellulose. After 2.5 hours nitration for method (*i*) and 30 minutes for (*ii*), as much as possible of the excess acid was pressed out of the cellulose nitrate which was then drowned in distilled water at 0°C. The cellulose nitrate was repeatedly washed with distilled water until, on standing in contact with the cellulose nitrate for 15 minutes, the wash water was neutral to universal indicator. In the majority of cases, stabilization was carried out by dehydrating the cellulose nitrate with ethyl alcohol for 12 hours and then refluxing for three periods of 3 hours, each with fresh alcohol. In a few cases, stabilization was carried out by a series of water boils similar to those used for the industrial cellulose nitrate. Adhering liquids were removed from the cellulose nitrate by pumping off in a vacuum and collecting in a trap cooled in liquid air. The nitrogen content of the cellulose nitrates was estimated by a semi-micro Devarda method.[12]

The aging of the solutions was generally followed by viscosity measurements in an Ostwald viscometer. In this paper, a plot of the decrease in viscosity with time will be referred to as the aging curve of the given cellulose nitrate. In addition, where desirable, viscosities have been measured in a Couette viscometer and in a few cases the change in sedimentation constant has been determined to assist in the interpretation of viscosity measurements.

Two of the more obvious experimental errors are due to evaporation of acetone from the solution and to the absorption of water. Both would tend to increase the viscosity of the solutions, whereas the present experiments are concerned only with decreasing viscosity.

In the next main section various physical and chemical factors which might influence the aging process are considered.

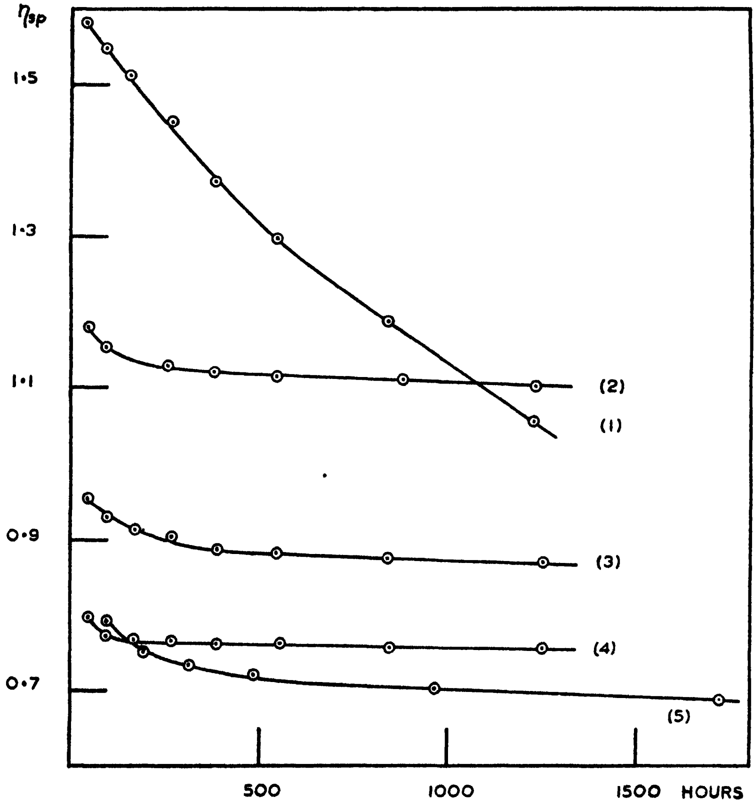

Fig. 1. Typical aging curves of different samples of cellulose nitrate. Solutions of 0.2 ± 0.001 g./100 cc. in acetone at 20°C.

EXPERIMENTAL RESULTS

Typical aging curves of different cellulose nitrates in acetone are given in Figure 1. The majority have characteristics similar to those summarized at the beginning of this paper, but an occasional sample shows a very much more marked aging, as sample 1 in Figure 1. At present there is no explanation for this and it has been found only in two very high molecular weight samples. Inspection of the more usual curves of Figure 1 suggests (more evidence is presented later) that there may be two processes which will be referred to as the "initial rapid" and the "later slow" process.

The decrease in viscosity is irreversible. If the cellulose nitrate is recovered from a solution by pumping off the acetone at 20°C. in a vacuum and then all the cellulose nitrate recovered is dissolved to give a solution of the same strength as before, the viscosity after recovery is never greater than the least and latest measured viscosity of the original solution. By dissolving all the cellulose nitrate recovered, the possibility of a change of viscosity due to fractionation is eliminated. Some results are given in Table I. All cellulose nitrates recovered from solutions (both with and without nonsolvent) dissolved in acetone very much more rapidly (a few minutes rather than several hours) than the original cellulose nitrate. Solution occurred without the formation of a thick gel which was invariably the first stage in the solution of cellulose nitrate that had not been recovered from solution. This ease of dispersion in acetone of recovered cellulose nitrate may be of importance in deciding upon the mechanism of aging and is discussed later (under *Discussion*).

TABLE I

Measurement	Cellulose nitrate *11* Conc. g /100 cc.	Cellulose nitrate *11* η_{sp}	Cellulose nitrate *17* Conc. g./100 cc.	Cellulose nitrate *17* η_{sp}
After initial dissolution	0.251	0.820	0.253	1.517
Before recovery	—	0.774	—	0.980
After dissolving recovered cellulose nitrate	0.251	0.776	0.253	0.812

No confirmation has been obtained of the theory, referred to above, of Morozov and Pamfilov,[4,5] in which the decrease in viscosity during aging is ascribed to a reduction in the structural viscosity of the solution. The dependence of viscosity upon rate of shear due to structural viscosity will occur at low rates of shear and must be distinguished from a dependence at high rates of shear due to orientation of the molecules. In both cases the viscosity decreases with increasing rate of shear. The viscosities of solutions of cellulose nitrate *11* were measured in a Couette viscometer within 30 minutes of the completion of dissolution. At this time the solutions are in the initial more rapid part of the aging curve. The results are given in Figure 2. The results for the different solutions are represented by straight lines which, within the experimental error, pass through the origin, so that there is no structural viscosity at low rates of shear. Similar results were obtained for solutions which had been aged for a long time. To test whether there was any effect on viscosity at high rates of shear other than a reversible one which would not explain the irreversible aging, solutions were squirted under pressure through a very fine capillary. The viscosities before and after were identical. With these samples of cellulose nitrate, it is clear that the decrease in viscosity of their solutions on standing cannot be explained by a reduction of the structural viscosity. It is difficult to explain this disagreement with the results of Morozov and Pamfilov[4] but it is of interest to note that Glikman[13] found that solutions of cellulose esters sometimes showed anomalous viscosities which could be removed by repeated filtration through sintered discs. They ascribed these results to microscopic and macroscopic aggregation due to incomplete dissolution of the cellulose nitrate.

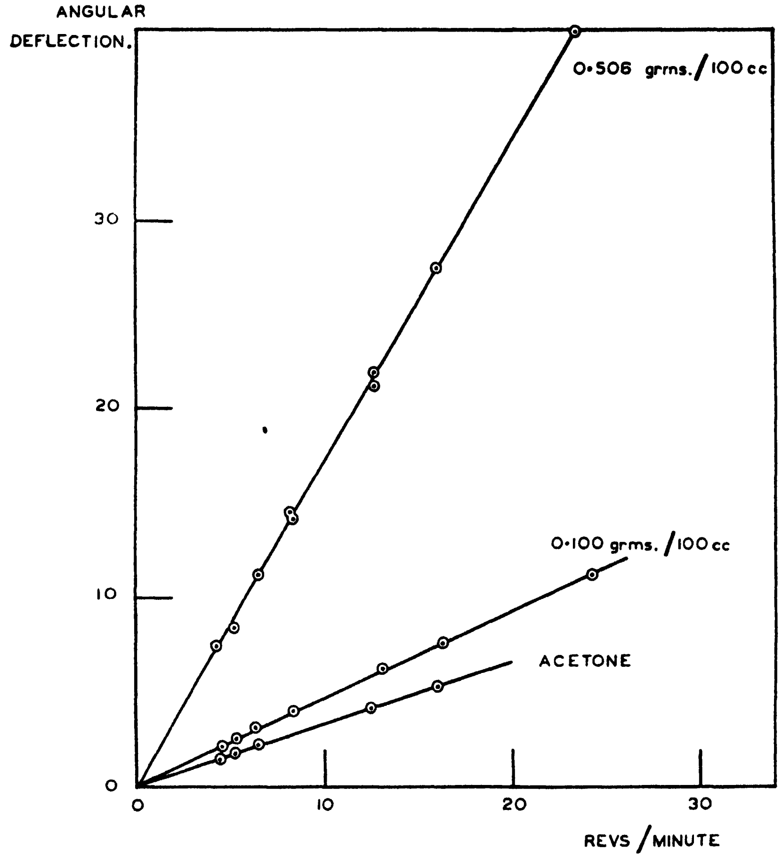

Fig. 2. The dependence upon rate of shear of the viscosity of solutions of cellulose nitrate which are showing the initial rapid aging. Solutions in acetone at 20°C. of cellulose nitrate 11 (12.2% nitrogen).

The effect of concentration on the aging of a cellulose nitrate solution was determined. A stock solution of about 0.2 g. of cellulose nitrate *11* (12.2%

nitrogen) was prepared and, as soon as solution was complete, less concentrated solutions were prepared by dilution so that, at this time, all the solutions contained similar molecules. The viscosities of these solutions were measured at intervals and the results are given in Figure 3. Within the limits of experimental error, the plot of η_{sp}/c *vs.* c for each time interval is linear. It has been found, with samples of different cellulose nitrates, that η_{sp}/c *vs.* c is always linear during the initial rapid aging process but that, at longer times, during the slow aging process, the plot shows a greater scatter than that shown in Figure 3 for 285 hours. This scatter appears to be random and increases with time. It cannot be explained by any simple dependence of the rate of aging upon concentration but is more likely to be due to trace impurities (possibly from the glass of the storage flasks) which act as catalysts in the slow aging process. From these data, it seems that the rate of aging in both the rapid and the slow processes is independent of the cellulose nitrate concentration and that the initial rapid process is not nearly so readily catalyzed, if it is catalyzed at all, as the later slow process.

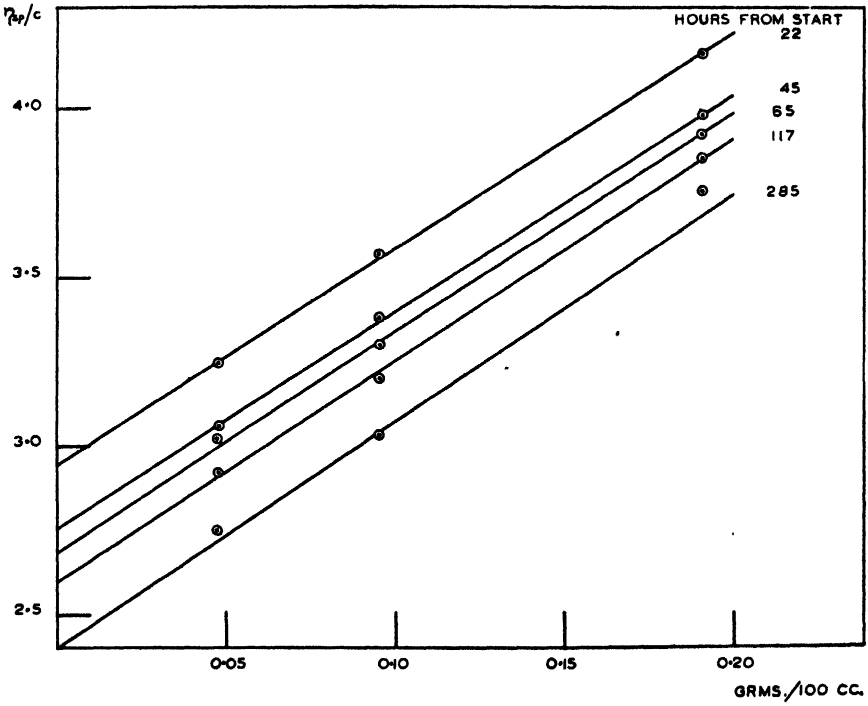

Fig. 3. Effect of solution concentration on the aging of solutions of cellulose nitrate *11* (12.2% nitrogen).

Effect of Variations in the Original Cellulose

Variations in the nature of the cellulose which might conceivably effect the aging of solutions of the derived cellulose nitrates are: (*a*) average molecular weight; (*b*) distribution of molecular weights; (*c*) crystalline–amorphous ratio in the fiber; and (*d*) presence of defective and modified glucose units in the cellulose due to oxidation.

The effect of the molecular weight of the cellulose nitrate is discussed later. Cellulose nitrates have been prepared from wood cellulose, cotton linters, and ramie fiber, all of which differ in the crystalline–amorphous ratio of their fibers, and no marked differences were observed between their aging curves. Therefore, it appears that the crystalline–amorphous ratio has certainly not got a dominant effect on the aging.

The accidental oxidation occurring during technical purification of a cellulose should be small and consists of reactions in which aldehydic or carboxylic groups are formed from the hydroxyl groups with or without fission of the glucose ring. Davidson[14,15] has shown that at low degrees of oxidation, aqueous sodium periodate oxidizes the two secondary hydroxyl groups with breakage of the glucose ring between them. This oxidized glucose unit was shown to be sensitive to dilute alkali but was not destroyed by nitration. Yackel and Kenyon[16] prepared a cellulose in which the primary hydroxyl groups were oxidized to carboxyl groups by gaseous nitrogen tetroxide. Of the many methods of preparing oxidized celluloses, these two reactions have probably the fewest complications, and yield materials whose structures are most exactly known. Therefore, celluloses prepared by these methods have been used. Provided only small degrees of oxidation are used, cellulose nitrates can be prepared from them which are soluble in acetone. It was found that oxidation with nitrogen tetroxide to give more than about 2% by weight of carboxyl groups, yielded a cellulose nitrate (12.3% nitrogen content) which, although apparently possessing normal acetone adsorption,[3] was insoluble in this solvent It is suggested that this may be due to the formation of cross-linkages between different cellulose nitrate molecules, either of an ester or anhydride type.

A series of cellulose nitrates was prepared from the same nitrating mixture of sulfuric acid, nitric acid, and water and was stabilized with alcohol. The celluloses used, derived from cotton waste, were as follows: (*6*) untreated*; (*7*) treated with 0.1 *N* sodium hydroxide for 24 hours and then washed with distilled water; (*8*) oxidized with 0.01 *M* sodium periodate for 3 hours and then washed with distilled water; (*9*) cellulose *8* treated with 0.1 *N* sodium hydroxide for 24 hours and then washed with distilled water; (*10*) oxidized for 1 hour with excess gaseous nitrogen tetroxide and then washed with distilled water.

With the exception of the cellulose nitrate from *10*, which contained 12.3% nitrogen, all these cellulose nitrates had a nitrogen content of 12.8%. The aging curves of these cellulose nitrates in acetone solution (0.1 g./100 cc.) are given in Figure 4.

---

* The cellulose nitrates referred to in this paper, and the corresponding celluloses from which they are derived, are numbered serially. Samples *1–5* are those of Figure 1.

The decrease in viscosity between cellulose nitrates *8* and *9* indicates that there are alkali sensitive linkages in the cellulose nitrates prepared from the cellulose oxidized with periodate. The small difference between curves (6) and (7) is probably due to small variations in the nitrating conditions, although the presence of a few alkali sensitive linkages in the original cotton waste cannot be ruled out. The curves (6), (7), (8), and (9) are approximately parallel, indicating that alkali sensitive linkages of the type postulated by Davidson[14] have no effect on the aging curves of solutions of cellulose nitrate.

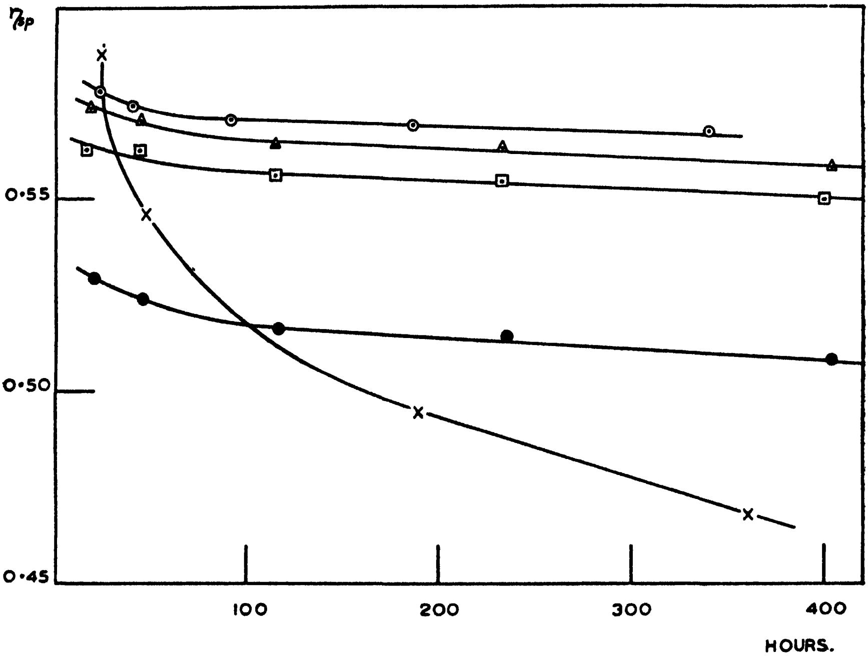

Fig. 4. Effect of oxidation of cellulose on the aging of the derived cellulose nitrate: (*6*) cotton waste, ⊙; (*7*) cotton waste + 0.1 *N* NaOH, △; (*8*) cotton waste + 0.1 *M* $NaIO_4$, ⊡; (*9*) cellulose *8* + 0.01 *N* NaOH, ●; (*10*) cotton waste + gaseous N_2O_4, ×.

Cellulose nitrate *10*, in which some of the primary alcoholic groups are oxidized to carboxylic groups, ages in a manner which is similar to the exceptionally rapid aging (curve 1 of Fig. 1) referred to above. Wehr[8] and others have shown that acids greatly accelerate the aging of cellulose nitrate solutions and it is always possible that such a marked aging may be due to inadequate removal of acid during stabilization. Further samples similar to cellulose nitrate *10* were prepared and gave similar aging even after extra stabilization so that it seems unlikely that the aging is acid-catalyzed in this case. Although it cannot be completely ruled out, it is also unlikely that the carboxyl groups produce the catalysis. It was observed in solutions of cellulose nitrate *10*, which contained about 1 carboxyl group per 150 glucose residues, that insoluble particles developed on standing. In a similar cellulose nitrate (*ca.* 12% nitrogen), which contained about 1 carboxyl group per 15 glucose residues, a considerable portion of the sample, although swollen by the acetone, was never in solution. It is therefore suggested that this insolubility is due to the formation of a network structure through ester or, possibly, anhydride linkages, and that the unusual aging in this case is due to cross-linking of molecules to form aggregates which have a smaller axial ratio (and hence smaller viscosity) than the original molecules, and which may ultimately be insoluble. It is also a possibility that the decrease does not depend upon a special structure in the aggregates but is due entirely to a decrease in concentration following the removal of solute particles from solution. Although the aging observed in cellulose nitrate *10* may or may not be the same as the exceptionally rapid aging of sample *1*, it is very different from that normally found in a cellulose nitrate.

Effect of Degree and Method of Nitration

If the nitrogen content is increased to about 13.5% or more, there are some cellulose nitrates whose solutions show either no change in viscosity on standing or a very much smaller change. Most of these cellulose nitrates were prepared by the Berl[11] method and were stabilized by alcohol. Figure 5 shows the change in viscosity with time of three samples from the same specimen of cellulose: (*11*) 12.2% nitrogen, prepared by factory nitration; (*12*) 13.5% nitrogen, prepared from cellulose nitrate *11* by the Berl method; (*13*) 13.4% nitrogen, prepared from the original paper cellulose by the Berl method.

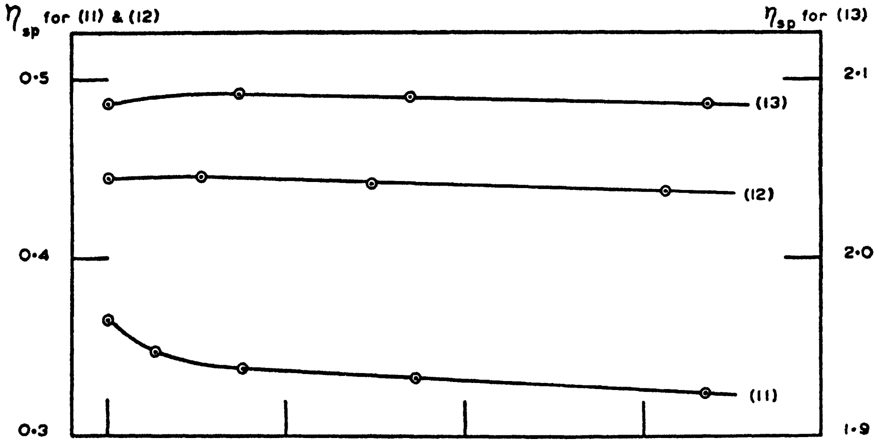

Fig. 5. Aging curves of cellulose nitrates of high nitrogen content: (*11*) 12.2% nitrogen; factory nitration; (*12*) 13.5% nitrogen; from *11*, in laboratory; (*13*) 13.4% nitrogen; from original cellulose, in laboratory. All solutions in acetone at 20°C., 0.1 ± 0.001 g./100 cc.

These results show that a cellulose nitrate that shows only slight aging can be prepared from either cellulose or another cellulose nitrate that does show aging. In Figure 6, aging curves for the following cellulose nitrates of high nitrogen content are given: (*14*) 13.74% nitrogen, prepared from low viscosity cotton linters by the sulfuric acid method, alcohol stabilization; (*15*) 13.81% nitrogen, prepared from high viscosity cotton linters by the sulfuric acid method, alcohol stabilization; (*16*) 13.4% nitrogen, commercial sample of unknown preparation.

In these six different cellulose nitrates there are at least four main sets of variables that might conceivably affect aging: (*a*) type of nitration mixture (phosphoric or sulfuric acid); (*b*) extent of nitration and hence the number of free hydroxyl groups; (*c*) calcium content of the cellulose nitrate; and (*d*) mean chain length.

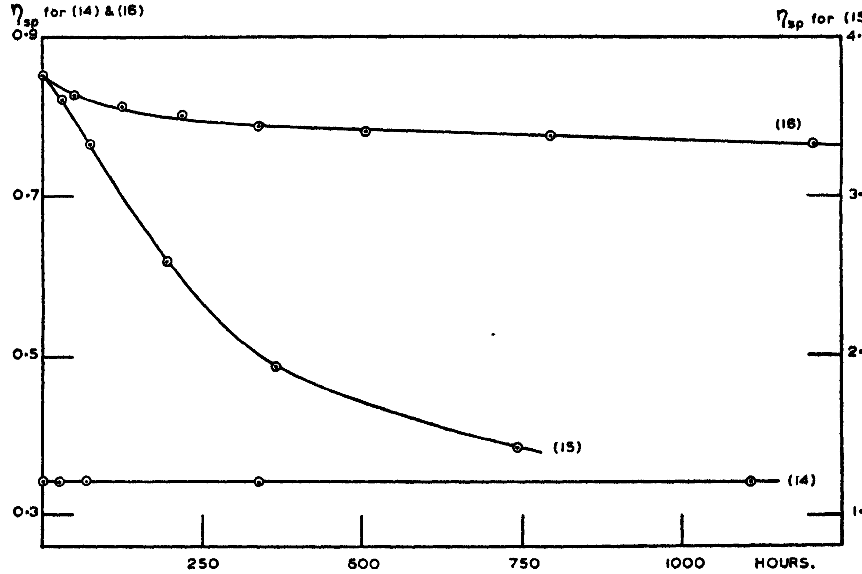

Fig. 6. Aging curves of cellulose nitrates of high nitrogen content: (*14*) 13.74% nitrogen; from low viscosity linters; (*15*) 13.81% nitrogen; from high viscosity linters; (*16*) 13.4% nitrogen; unknown preparation. All solutions in acetone at 20°C.: (*14*) and (*15*) 0.1 ± 0.001 g./100 cc.; (*16*) 0.2 ± 0.001 g./100 cc.

Cellulose nitrates *13* and *14*, similar in nitrogen content and mean chain length (as indicated by viscosity), both show little aging. It appears, therefore, that the presence of phosphoric or sulfuric acids in the nitrating mixtures does not, of itself, introduce aging. Although the type of stabilization may be of importance, other factors must be involved, since the alcoholic stabilization of a 12.2% nitrogen, calcium-free cellulose nitrate did not remove aging, whereas cellulose nitrate *13*, of higher nitrogen content similarly treated did not age. The smaller aging effect for higher nitrogen contents is also evident between *11* and *12*, and it does seem that in some cases at least when the content of free hydroxyl groups is reduced the tendency to age is greatly reduced.

With regard to the calcium content of the cellulose nitrate, most of the materials in which aging has been observed were commercial samples that usually contain some calcium, derived from the stabilization process. However, a factory cellulose nitrate (12.2% nitrogen) was obtained immediately after the nitrating acid had been removed and this was stabilized in the complete absence of calcium by repeated boiling with distilled water and then with alcohol. Solutions of this sample aged in a way similar to those which were stabilized in the presence of calcium carbonate. Thus the introduction of the latter into cellulose nitrate during stabilization is not the cause of aging in acetone solutions. Some of the effects of calcium salts on the viscosity of solutions of cellulose nitrate have been described in another paper.[2]

No completely general rule for the effect of molecular weight on aging has been found, but there seems to be a greater tendency for aging to occur in cellulose nitrates of high rather than low molecular weight as is shown by the pronounced aging of cellulose nitrate *15*, which is of high nitrogen content and, except for chain length, of characteristics similar to *14*.

Effect of Nonsolvents and Precipitants

The effect of nonsolvents on the aging of solutions of cellulose nitrate has been examined. Figure 7 gives the decrease with time of specific viscosity for solutions of cellulose nitrate *11* that contain various concentrations of water. These solutions were stored at 20 °C. The solution containing 15 cc. of water in 100 cc. was in a state of incipient precipitation and after about 450 hours a long thread of cellulose nitrate had precipitated out. Water cannot be regarded as a completely inert solvent, as there is

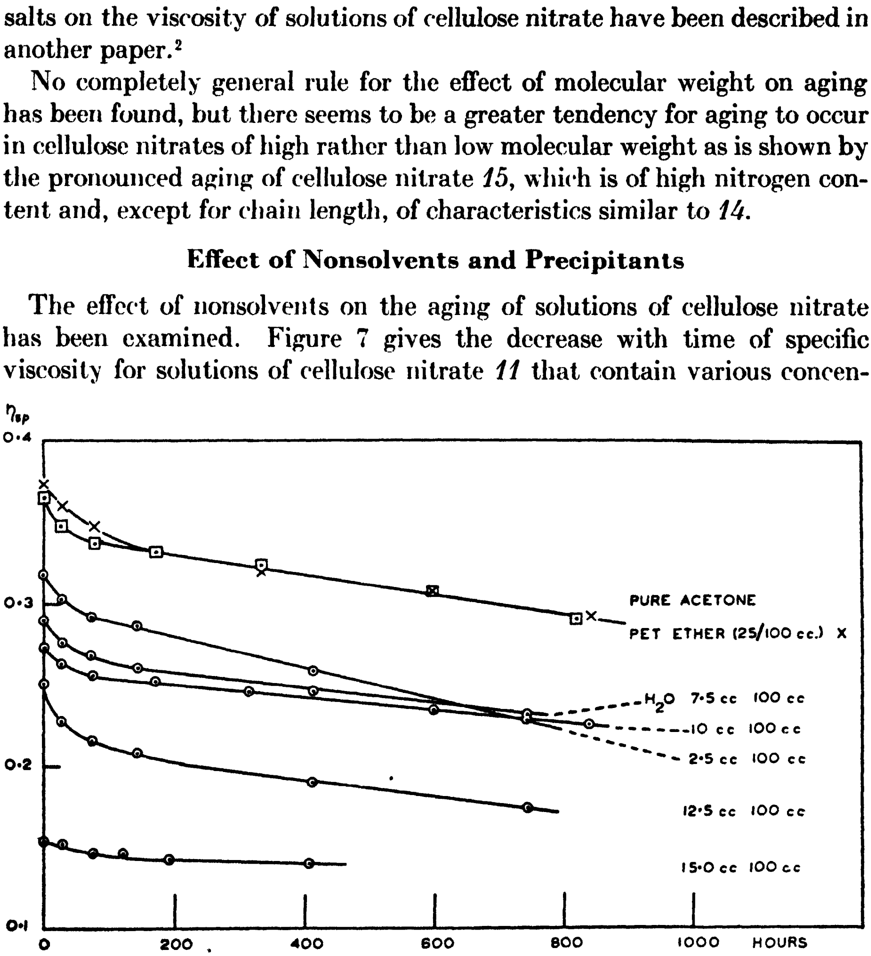

Fig. 7. The effect of water and petroleum ether on the aging of cellulose nitrate solutions (12.2% nitrogen) at 20°C. All solutions 0.1 ± 0.001 g./100 cc.

some evidence that it is slightly solvated on the cellulose nitrate. Therefore, for comparison, Figure 7 gives the effect of another nonsolvent, petroleum ether, which has an extremely small interaction with cellulose nitrate as indicated by adsorption and thermochemical experiments.[17] Whereas petroleum ether has no effect on the specific viscosities or aging curves outside the experimental error, increase in the water concentration produces an immediate large decrease in viscosity but does not eliminate the aging of the solution. The differences in the rates of the slow aging process show no trend with increasing water concentration and may possibly be due to catalysis by trace impurities as suggested above. After correcting for the altered viscosity and buoyancy of the solvent, there was no large change in the sedimentation constant of the cellulose nitrate solute particle as water up to 12.5 cc. per 100 cc. of solution was added. Only a small decrease in the constant was observed with this increasing water content, but it should be noted that sedimentation constants are not a sensitive method of detecting small changes in the molecular weight of linear molecules, and the decrease observed cannot be said to be in conflict with the observed viscosity changes.

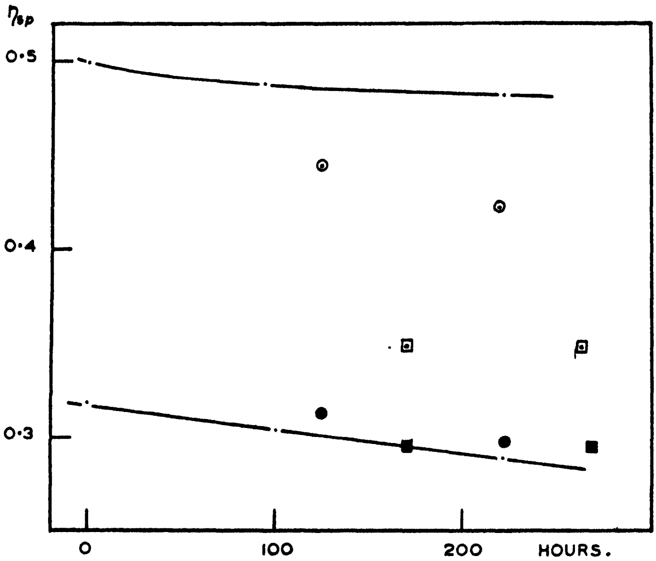

Fig. 8. The aging of cellulose nitrate *II* recovered from acetone and aqueous acetone solutions. All solutions 0.13 ± 0.001 g./100 cc. Upper curve: original solution in acetone; Lower curve: original solution in aqueous acetone (10 cc. water/100 cc. solution. Cellulose nitrate recovered from acetone solution in acetone, ⊙; in aqueous acetone, ●. Cellulose nitrate recovered from aqueous acetone in acetone, ⊡; in aqueous acetone, ■.

To determine whether the viscosity decrease produced by water was reversible or not, solutions containing 0.1 g. in 100 cc. of solution dissolved in acetone, and in acetone containing 10 cc. of water per 100 cc. of solution, were made and their aging curves determined. Samples of cellulose nitrate from these solutions were recovered by pumping off the solvents at 20°C. in a vacuum. Each of these samples was dissolved to give two solutions (*a*) in acetone and (*b*) in acetone containing 10 cc. of water in 100 cc. of solution. The viscosities of these four solutions were measured and the results are given in Figure 8. Acetone solutions of cellulose nitrate recovered from aqueous acetone have a lower viscosity than those recovered from pure acetone, while both of these viscosities are lower than that of the original cellulose nitrate. In aqueous acetone the viscosity is not appreciably altered by any of these recovery processes. Solutions of recovered cellulose nitrate still show aging. It appears, therefore, that treatment of the cellulose nitrate with a given concentration of water in acetone irreversibly lowers the viscosity from the value in pure acetone by some means which is not repeated on further treatment with the same concentration of water in acetone.

The effect of water on cellulose nitrate of higher nitrogen content, which in acetone solution showed only slight aging, was also examined. Results for samples *12* and *14* are given in Tables II and III. For cellulose nitrate *14*, in which aging is completely absent in pure and in aqueous acetone, it is also to be noted that the percentage decrease in specific viscosity on adding water is at least three times as small as for cellulose nitrate *11* (Figs. 7 and 8). For cellulose nitrate *12*, although aging has merely been diminished, the effect of adding water on the viscosity in acetone is considerably less than for cellulose nitrate *11*. It appears, therefore, that the mechanism of the aging process may also be involved in the viscosity decrease on adding

TABLE II

AGING OF SAMPLE *12* CELLULOSE NITRATE

Age of soln., hours	η_{sp} in acetone, 0.0988 g./100 cc.	η_{sp} in aqueous acetone (10 cc. water/100 cc. total soln.), 0.0972 g /100 cc.
0	0.441	0.379
142	—	0.363
147	0.441	—
312	0.437	—

TABLE III

AGING OF SAMPLE 14 CELLULOSE NITRATE

Age of soln., hours	η_{sp} in acetone, 0.0997 g /100 cc.	η_{sp} in aqueous acetone (7.2 cc. water/100 cc. total soln.), 0.0980 g./100 cc.
0	0.443	0.406
57	—	0.405
1100	0.443	

water. A sample of cellulose nitrate *14* recovered from aqueous acetone has the viscosities given in Table IV. As both recovery processes might be expected to affect the viscosity in the same way, it is possible that the low value after the first recovery is due to an incorrect concentration. It is clear that the permanent decrease in viscosity produced by water is considerably less than that in cellulose nitrate *11* and it would appear that, simultaneously with the disappearance of aging in cellulose nitrate *14*, sensitivity to water in acetone solution is also removed.

TABLE IV

EFFECT OF RECOVERY FROM AQUEOUS ACETONE ON VISCOSITY OF CELLULOSE NITRATE *14* IN ACETONE SOLUTION

Age of soln., hours	Conc. of cellulose nitrate, g./100 cc.	η_{sp}
0	0.0997	0.443
1106	—	0.443
RECOVER FROM AQUEOUS ACETONE SOLUTION		
1180	0.0997	0.419
1246	—	0.419
RECOVER FROM AQUEOUS ACETONE SOLUTION		
1387	0.1000	0.445

Effect of Temperature

The effect on the aging of increasing the temperature has been examined Solutions were sealed into glass tubes and stored in the absence of light in suitable thermostats. At intervals, samples were removed and their viscosities at 20 °C. were measured. A typical series of curves for acetone solutions of cellulose nitrate *11* (12.2% nitrogen) are given in Figure 9. In the experiments at 1, 18, and 55 °C. there was no discoloration of the solutions over the period of the observations, but at 98 °C. the solution was colored brown within two hours of the start and this color rapidly deepened. It appears that in the 98 °C. reaction some new mechanism becomes important and this may be the internal oxidation of the cellulose nitrate molecule which is generally suggested as the process for the discoloration of cellulose nitrate solutions. Both the initial more rapid and the later slow aging processes are markedly temperature dependent. At present no attempt has been made to determine energies of activation for the two processes from these curves since their interpretation is obscure. It appears that both the rate and the apparent extent of the initial rapid process change with temperature. Thus at 18 °C. the slow linear portion of the curve extrapolated to zero time gives a value of $\eta_{sp} = 0.77$, whereas at 55 °C. the similar value is $\eta_{sp} = 0.68$. It has been shown above that at 18 °C. the initial rapid process is irreversible but there is evidence that part, at least, of the extra initial rapid decrease at 55 °C. is reversible. Thus a solution of cellulose nitrate *11* in acetone was heated at 60 °C. for 22 hours,

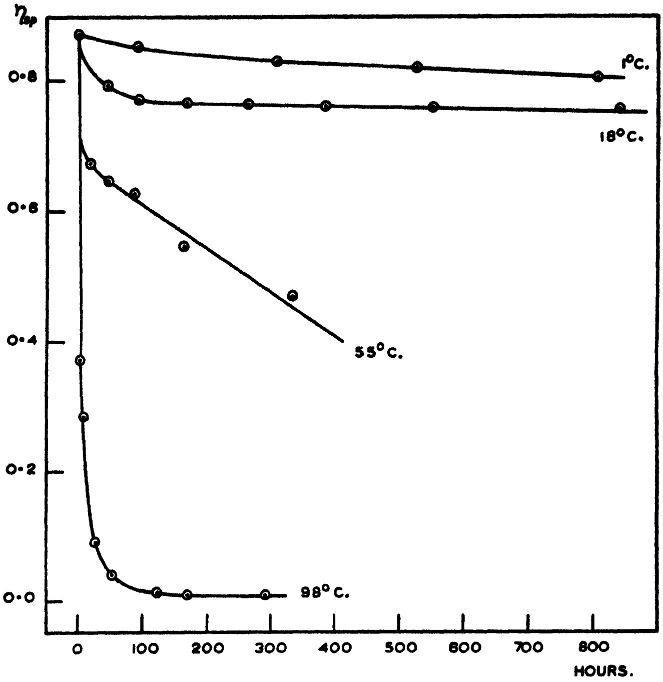

Fig. 9. The effect of temperature on the aging of acetone solutions of cellulose nitrate *11*. All solutions 0.2 g./100 cc.

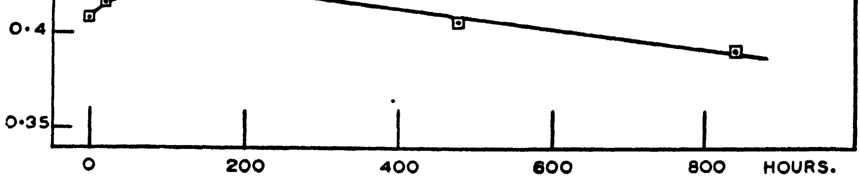

Fig. 10. The change in viscosity on storing at 20°C. cellulose nitrate *11* solution which has been heated to 60°C. ⊙, stored at 20°C.; ⊡, heated at 60°C. before storing at 20°C.

and then stored at 20 °C. The change in viscosity with time of this and of the original unheated solution are given in Figure 10. There is an initial increase in viscosity of the heated solution before the slow aging becomes dominant and similar in rate to the aging of the unheated solution. No similar increase in viscosity has been observed with solutions prepared at 20 °C. and then stored at 1 °C., but this may be due to the fact that all solutions were heated again to 20 °C. when their viscosities were measured. An attempt was made to determine the energy of activation of the slow process by using cellulose nitrate of high nitrogen content which showed no initial rapid aging and aged only extremely slowly. With these it was found that an initial rapid decrease still did not occur at 60 °C. The changes in the rate of the slow process due to temperature changes were smaller than those due to unknown causes which are believed to include catalysis by trace impurities. The energy of activation of the uncatalyzed slow process cannot, therefore, be determined with any degree of accuracy.

Effect of Impurities and Antioxidants

The most likely impurities which might be expected to catalyze the aging of cellulose nitrate solutions are (*a*) residual acid absorbed on the cellulose nitrate fibers and not completely removed during stabilization, and (*b*) substances, possibly alkaline, dissolved from the glass of the storage flasks. In agreement with Wehr[8] and Spurlin,[9] it was found that both acids (*e.g.*, acetic acid) and bases (*e.g.*, triethylamine) increased the rate of the slow aging process. There was some indication that the rate of the initial rapid process was not altered by a change in the *p*H of the solution, but this could by no means be regarded as definitely proved.

In order to determine whether any of the aging was due to the chemical degradation postulated by Wehr,[8] the effect of various antioxidants on solutions of cellulose nitrate *11* (12.2% nitrogen) was examined. At 20 °C., the addition of ethyl gallate and β-naphthol to the solution had no effect on the aging. At 60 °C., the experimental results for ethyl gallate show a much bigger scatter than usual but they are sufficiently good to suggest that ethyl gallate has no effect on the aging. Hydroquinone, however, accelerates the aging, a result which is quite different from that found by Wehr.[8]

DISCUSSION

While it must be admitted that the observations presented above are insufficient basis for a theory to explain completely the apparently very complex mechanism of the aging of cellulose nitrate solutions, some conclusions can be drawn about possible mechanisms. In this discussion the only type of aging to be considered is that referred to above as normal (*i.e.*, curves of type 1 of Figure 1 are not considered). As was suggested above from a consideration of the shape of such aging curves in acetone, there are probably at least two mechanisms responsible for this lowering in viscosity. This view is supported by: (*a*) the variation in rate of the slow process caused by catalysts which have no effect on the rapid process; and (*b*) the possibility of eliminating the rapid reaction by increasing the nitrogen content or by treatment with water, without affecting the slow process.

It is possible that even more than two mechanisms may be involved and alteration of the experimental conditions (*e.g.*, the addition of acids and bases, the addition of water, or the increase of temperature) may involve new possibilities or change the relative importance of mechanisms already present to a minor degree in the normal aging at 20 °C. in acetone solution. A detailed kinetic treatment of aging would involve the interpretation of specific viscosities in terms of average molecular weights. This problem is in itself very difficult, since the specific viscosity depends not only on molecular weight but also on molecular shape, a factor which may be changing during aging. Therefore, it seems that until mechanisms have been ascribed to the aging processes little is to be gained from a kinetic treatment.

In explaining aging, the following would appear to be possible mechanisms: (*a*) the dispersion of individual molecules may be a slow process, retardation being due, possibly, to residual macroscopic fiber structure; (*b*) a change in the solvation of the molecule; (*c*) aggregation of the molecules; (*d*) rupture of main valency linkages in the cellulose nitrate chains; (*e*) chemical change without rupture of main chain linkages; and (*f*) the formation or destruction of complexes between calcium and cellulose nitrate.

Of these mechanisms the first three are essentially physical changes, whereas the last three are largely chemical. From evidence given above, it appears that, although calcium compounds may under certain circumstances have an effect on the aging of acetone solutions of cellulose nitrate,[2,18] a mechanism such as (*f*) cannot be regarded as the cause of the aging studied here.

Consideration of the time factor in aging is of use in attempting to decide between the different possible aging mechanisms. Figure 1 shows that the most rapid part of the aging at 20 °C. is nearly completed in about 300 hours, while the slow aging seems to continue indefinitely. Therefore, mechanisms that are essentially physical changes of the cellulose nitrate might reasonably be considered to be involved in the initial rapid aging, but it is very unlikely that they play any part in the slow change, chemical changes being more probable. This does not exclude chemical change as an explanation of the rapid process.

The interaction of cellulose nitrate and acetone has been discussed elsewhere[3] and it is unlikely that once the solution is visually homogeneously dispersed solvation undergoes any marked change, except when conditions are altered, *e.g.*, on the addition of a nonsolvent such as water or on a change of temperature. With increasing temperature, the degree of solvation decreases but the change from a less to a more solvated molecule is probably too fast a process to explain the slow increase in viscosity of a solution stored at 20 °C. after having been heated to 60 °C. (Fig. 10).

When cellulose nitrate chains are fully solvated by acetone, they are almost completely inert toward one another. Thus the heats of dilution of cellulose nitrate solutions in acetone, under conditions where the solution process is complete, are very small. Tendency to aggregation must, therefore, be small and, although interactions between different chains must occur simply because of the asymmetric nature of the molecules, they will not lead to any permanent association. Further, if aggregation due to attraction between cellulose nitrate chains tended to occur, it could not lead to a regular symmetrical type of association, but would result in a ramifying network occupying the whole bulk of the solution. Such a structure ought to be detectable either by its tendency to gel if the attractive forces were strong, or by the presence of structural viscosity. For pure cellulose nitrate in acetone there are no such indications of structure, so that it appears that aggregation is not the cause of aging.

From the data reported above, the slow continuous aging process appears to be characteristic of all types and physical conditions of cellulose nitrate. Therefore it seems very probable that it is due to the hydrolysis of the glucosidic linkages. It is difficult to eliminate completely the possibility of degradation of the chain molecules by internal oxidation and reduction of the nitrated glucose units, a reaction similar to that found in the alkaline hydrolysis of many organic nitrates, since the loss of nitrogen which might be expected to account for the observed decrease in viscosity is too small to be measured. It is probable that a reaction of this type sets in at higher temperatures and it is accompanied by a marked discoloration of the solution which is not observed with the aging at room temperatures. The strongest argument against this reaction is that it would be expected that increase in nitrogen content would result in an increase in the rate and that it has frequently been observed that increasing the nitrogen content, if anything, lowers the rate of the slow aging. Hydrolysis of a limited number of specially sensitive linkages similar to those postulated by Davidson[14] is not a likely mechanism owing to the apparently unlimited extent of the slow aging and also to the observation that the deliberate introduction of the Davidson type linkages has no effect on the rate of aging. At room temperatures and in pure acetone, therefore, it seems that rupture of the main chain glucosidic linkages must be the chief reaction involved in slow aging, but at high temperatures and under special conditions this hydrolysis may be accompanied by other chemical changes.

In contrast to the slow reaction, the initial fast reaction appears to be limited in extent. This decrease in viscosity could be due to a reaction of a limited number of weak linkages in the cellulose nitrate molecule, but since the deliberate introduction of one type of weak linkage produced no effect, this mechanism seems unlikely. A more likely mechanism is that complete dispersion of the individual molecular chains is a slow process. The observation (see under *Experimental Results*) that cellulose nitrate recovered from acetone solution simply by removal of the solvent or by precipitation by water followed by drying dissolves much more rapidly than the original fiber cellulose nitrate may be of significance. It would appear that during solution in acetone and recovery, a factor causing slow dispersion of the cellulose nitrate-acetone gel is removed. This view is supported by the work of Demougin[19] and Kraus,[20] who have shown that fiber cellulose nitrate appears to be less soluble than precipitated or amorphous material. If the forces retarding dispersion were the general physical forces of cohesion between molecules in the solid state, it would be expected that undispersed aggregates of ultramicroscopic dimensions should occur in the early stages of dissolving and especially just after the bulk of the gelled cellulose nitrate has disappeared. An examination of cellulose nitrate solutions in acetone immediately after becoming visually homogeneous, when rapid aging is occurring, failed to show the presence of ultramicroscopic particles. The refractive index increment of cellulose nitrate in acetone is not small ($dn/dc = 120 \times 10^{-5}$), so that aggregates should have been seen if they really occurred. The absence of rapid aging in solutions of reprecipitated cellulose nitrate confirms that the existence of general physical forces of cohesion in the solid cannot be the explanation of rapid aging. Indeed, since cellulose nitrate is strongly solvated by acetone with a large evolution of heat (Kargin and Papkov[21]; Calvet[22]), it would appear that such solvation might offset any such resistance to dispersion. Therefore, in order to explain rapid aging there must exist in fiber cellulose nitrate, but not in reprecipitated, relatively strong cohesion between the molecules at a certain number of localized positions so that in the early stages of solution there may exist groups of a small number of cellulose nitrate chains which are not visible in the ultramicroscope and which are sufficiently strongly held together not to break down on shearing the solution. The slow dispersion of these aggregates would result in the rapid aging process. It is impossible on the present evidence to do more than speculate on the nature of the localized cohesion. It may be due to a few cross linkages of a primary valency nature between different cellulose nitrate chains, possibly the ester bridges suggested by Staudinger.[23] Some form of intensified physical interaction due to the orderly arrangement of the cellulose nitrate chains in the crystalline portions of the fiber may be the cause. The absence of rapid aging in cellulose nitrates containing few free hydroxyl groups suggests that rapid aging might involve the breaking of hydrogen bonds between the free hydroxyl groups in the crystalline portion of the fiber. Such hydrogen bonding in cellulose has been postulated by Mark[24] and by Pierce[25] in order to explain its crystal structure and by Ellis and Bath[26] in order to explain its infrared spectrum. The absence of this type of aging in reprecipitated cellulose nitrate is explained on this last hypothesis by the greater randomness of the chains and hence the smaller probability of the formation of interchain hydrogen bonding in recovered solid material.

There remains to be explained the effect of water and of increased temperatures. Both would be expected to destroy side chain hydrogen bonding but both appear to produce a change which is larger than that due to rapid aging at room temperatures in acetone. This may or may not represent a new mechanism. A small part, at least, of the change in viscosity on heating is reversible and this may represent a shift in some equilibrium, possibly of the ester linkages postulated by Staudinger.[23]

Whatever the explanation of the changes described above, certain suggestions for the examination of a cellulose nitrate in solution can be made:

(*1*) All cellulose nitrates should be carefully stabilized by boiling with alcohol immediately before use in order to reduce the slow aging process as much as possible.

(*2*) Wherever possible, an anhydrous solvent should be used.

(*3*) Any property (*e.g.*, viscosity, osmotic pressure) should be measured at various times after dissolving the solution and not just at one time. Values of the property during the slow aging are probably much more characteristic of the sample of cellulose nitrate than values obtained during the rapid aging, since these latter values depend very much more on the exact time from the beginning of the solution and on variable factors such as the physical state and history of the sample.

(*4*) In fractionating cellulose nitrate, the effect of the nonsolvent should be determined. If water is used, some irreversible change in the molecules is produced, but the absence of any further change on additional treatment with water has been proved.

We wish to thank Professor E. K. Rideal for his encouragement during the course of this work, which was carried out in the Department of Colloid Science, Cambridge University. This paper is published by permission of the Chief Scientist, Ministry of Supply.

References

1. H. Campbell and P. Johnson, *Trans. Faraday Soc.*, **40**, 221 (1944).
2. H. Campbell and P. Johnson, *J. Polymer Sci.*, **3**, 735 (1948).
3. H. Campbell and P. Johnson, *J. Polymer Sci.*, **4**, 247 (1949).
4. A. A. Morozov and A. V. Pamfilov, *J. Gen. Chem. U. S. S. R.*, **9**, 759 (1939).
5. A. A. Morozov and A. V. Pamfilov, *J. Gen. Chem. U. S. S. R.*, **8**, 175 (1938).
6. P. Pascal and J. Grévy, *Compt. rend.*, **195**, 726, 896 (1932).
7. T. S. Lawton and H. K. Nason, *Ind. Eng. Chem.*, **36**, 1128 (1944).
8. W. Wehr, *Kolloid-Z.*, **88**, 185, 290 (1939).
9. H. M. Spurlin, in E. Ott, ed., *Cellulose and Cellulose Derivatives.* Interscience, New York, 1943, p. 860.
10. F. D. Miles and M. Milbourn, *J. Phys. Chem.*, **34**, 2598 (1930).
11. E. Berl, *Ind. Eng. Chem., Anal. Ed.*, **13**, 322 (1941).
12. H. Campbell and P. Johnson, unpublished work.
13. S. A. Glikman, *J. Chem. Phys.*, **31**, 458 (1934).
14. G. F. Davidson, *J. Textile Inst.*, **29**, 195T (1938).
15. G. F. Davidson, *J. Textile Inst.*, **31**, 81T (1940).
16. E. C. Yackel and W. C. Kenyon, *J. Am. Chem. Soc.*, **64**, 121 (1942).
17. J. W. McBain and coworkers, *Trans. Faraday Soc.*, **29**, 1086 (1933).
18. J. S. Gourlay, *J. Soc. Chem. Ind.*, **63**, 123 (1944).
19. P. Demougin, *Compt. rend.*, **196**, 408 (1933).
20. A. Kraus, *Nitrocellulose*, **12**, 63 (1941).
21. V. Kargin and S. Papkov, *J. Phys. Chem. U. S. S. R.*, **7**, 483 (1936).
22. E. Calvet, *Compt. rend.*, **212**, 542 (1941).
23. H. Staudinger, *Die hochmolekularen organischen Verbindungen.* Springer, Berlin, 1932.
24. H. Mark, *Chem. Revs.*, **26**, 169 (1940).
25. F. T. Pierce, *Nature*, **153**, 586 (1944).
26. J. W. Ellis and J. Bath, *J. Am. Chem. Soc.*, **62**, 2859 (1940).

English Synopsis, see Summaries, page S10, Vol. V, 1950.

Résumé

Les courbes viscosité-temps (vieillisement) pour les solutions de nitrate de cellulose dans l'acétone et d'autres solvants sont, généralement, caractérisés par une diminution initiale rapide de viscosité, suivie d'une décroissance lente et contenue. Des agrégats ultramicroscopiques n'ont pas été observés, et une viscosité de structure était également absente durant des deux procédés de vieillissement. Le vieillissement initial rapide ne se manifeste pas ou est très faible pour les nitrates de cellulose à forte teneur en azote (c. à. d. peu d'hydroxyles libres), ainsi que dans ceux qui ont été récupérés au départ des solutions ou traités avec des faibles quantités d'eau en solution. Un vieillissement lent se manifeste à un degré plus ou moins fort pour tous les nitrates de cellulose, indépendamment de l'origine ou du traitement chimique de la cellulose, du degré ou de la méthode de nitration, de la méthode de stabilisation, de la concentration de la solution ou de la présence de précipitants. La vitesse du vieillissement lent s'accroît par une augmentation de température, mais est due, peut-être, à la présence d'impuretés catalytiques éventuelles; des variations considérables de vitesse pour une même température déterminée ont été observées en effet. On suppose que le vieillisement rapide est dû à une rupture lente d'un nombre peu élevé de liaisons relativement faibles, existant entre les chînes, probablement dues à des liaisons hydrogènes. Le vieillissement lent semble dû à la rupture des liaisons présentes dans les chaînês glucosidiques principales.

Zusammenfassung

Viskositäts-Zeit (Alterungs-) Kurven für Cellulosenitratlösungen in Azeton und anderen Lösungsmitteln sind im allgemeinen charakterisiert durch eine anfänglich schnelle Abnahme der Viskosität, die von einer langsamen kontinuierlichen Abnahme ge folgt wird. Ultramikroskopische Aggregate wurden nicht beobachtet und Strukturviskosität war während beider Alterungsprozesse nicht vorhanden. Das anfänglich schnelle Altern war nicht vorhanden oder es war klein in Cellulosenitraten mit hohem Stickstoffgehalt (mit wenig freien Hydroxylgruppen) und in solchen Cellulosenitraten, die aus Lösung zurückgewonnen worden waren oder in Lösung mit einer kleinen Menge Wasser behandelt worden waren. Das langsame Altern trat mehr oder weniger stark in allen Cellulosenitraten auf, unabhängig von der Herkunft oder der chemischen Behandlung der Cellulose, vom Grad oder der Methode der Nitration, von der Stabilisierungsmethode, von der Konzentration der Lösung oder von der Gegenwart des Fällungsmittels. Die Geschwindigkeit des langsamen Alterungsprozesses wird durch Temperaturzunahme erhöht, es wurden aber, möglicherweise durch die Gegenwart zufällig vorhandener katalytischer Verunreinigungen, erhebliche Variationen der Geschwindigkeit bei einer gegebenen Temperatur beobachtet. Der schnelle Alterungsprozess ist wahrscheinlich auf eine langsame Spaltung einer kleinen Anzahl relativ schwacher Bindungen zwischen den Ketten zurückzuführen, möglicherweise vom Typus der Wasserstoffbindung. Das langsame Altern stellt wahrscheinlich die Spaltung von glukosidischen Bindungen in der Hauptkette dar.

Received June 14, 1949

JOURNAL OF POLYMER SCIENCE VOL. V, NO. 4, PAGES 465–471

Some Polymeric Derivatives of Phosphonitrile Chloride

C. J. BROWN,* *Research Department, Imperial Chemical Industries Limited (Nobel Division), Stevenston, Scotland*

The ability of phosphonitrile chloride to polymerize was demonstrated by Schenck and Römer[1] who, on heating the crystalline material at 250–300° in a sealed tube, obtained a colorless, elastic substance whose analysis was roughly the same as that of the starting material, and whose properties resembled those of natural rubber. For this reason, the new polymer was termed "inorganic rubber." In the stretched condition the polymer exists in chains of —P=N— groups as shown by the x-ray evidence of Rénaud,[2] and of Meyer, Lotmar, and Pankow.[3] Another type of "inorganic rubber" was obtained by Schmitz-Dumont and others,[4] who, by treating phosphonitrile chloride with lead, silver, or zinc fluoride, prepared liquids consisting of mixed chlorofluorides of the tetraphosphonitrile radical; these liquids polymerized on heating to form rubberlike materials. The kinetics of polymerization of these phosphonitrile compounds have been worked out by Schmitz-Dumont.[5] A further example of phosphonitrile polymers is provided by Lipkin,[6] who condensed phosphonitrile chloride with butylamine, thereby obtaining a resinous product.

It was suggested by Rosset[7] that the phosphonitrile radical (—P=N—) behaves in a similar manner to the cyanogen (—C=N—) radical. There is, however, very little evidence in support of this idea. Certainly, cyanuric chloride $(CNCl)_3$ is analogous to phosphonitrile chloride $(PNCl_2)_3$, but the analogy appears to stop there, as no other similar monomers are known, and there is no polymeric C=N chain series comparable with the P=N chains. Wétroff[8] considered phosphonitrile as a radical like CN, PO, and SiN, and in support of this theory prepared a magnesium phosphonitrile amide of empirical formula (Mg_2PN_3) analogous to magnesium cyanamide $(MgCN_2)$. It is thus evident that whatever similarity does exist between phosphonitrile and these other radicals, it is restricted to one or two compounds only, and no general series of comparable derivatives is known. In particular, phosphonitrile is the only one which gives rise to chain polymers.

In the course of an investigation into the properties and reactions of phosphonitrile chloride, the experiments described by Lipkin[9] were repeated. An aqueous solution of sodium phenate was refluxed for some hours with dry phosphonitrile chloride, resulting in the formation of a colorless, oily product. All the evidence indicates this substance to be phosphonitrile phenate, probably contaminated with excess phosphonitrile chloride, the reaction taking place according to the equation:

---

* Present address: Imperial Chemical Industries Ltd. (Dyestuffs Division), Blackley, Manchester 9.

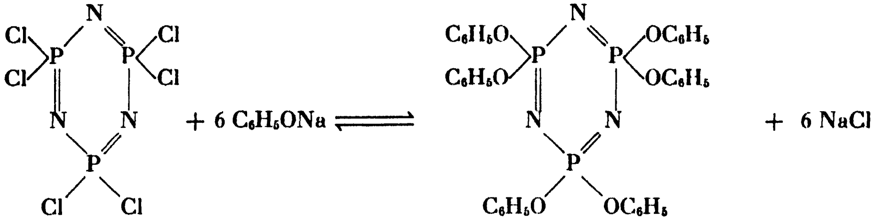

Attempts at purification of the product were unsuccessful; it did not boil below 320° at a few millimeters pressure, and it is possible that the phosphonitrile phenate remains inseparably associated with a small proportion of unchanged chloride. Extended heating at 320° resulted, however, in a change of the physical properties of the oily substance; its viscosity increased, its color gradually darkened, its solubility in aromatic solvents decreased, and, on cooling, the material set solid. The analytical figures throughout the process remained substantially the same, so it was apparent that a form of self-polymerization was occurring. It is probable that this takes place through the medium of ring breakage with the formation of chains, *e.g.*:

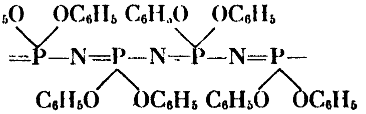

in a manner analogous to the polymerization of the chloride to form "inorganic rubber."

Similar experiments were carried out using as reactants phosphonitrile chloride and *p*-cresol, *o*-nitrophenol, *m*-nitrophenol, and *p*-nitrophenol. In each case an oily product was formed which polymerized on continued heating at elevated temperature to a viscous mass which set on cooling to a hard thermoplastic resin, ductile over a certain range of temperature, but brittle when cold. Polymerization with the nitro compounds occurred more readily than with the unsubstituted phenols, but a certain amount of decomposition took place simultaneously. Other phenols were tried, including catechol, resorcinol, quinol, phloroglucinol, salicylic acid, and benzoic acid, but under similar conditions to those given above, no reaction was observed. The difficulty in getting the condensation to occur readily would seem to be the heterogeneity of the reaction mixture. In general, sodium derivatives of phenols are not soluble in the same type of solvent as phosphonitrile chloride, and no suitable mutual solvent being available, the reaction has to be carried out in a heterogeneous medium which renders it slow and inefficient. There is the further point, too, that the chlorine in phosphonitrile chloride is covalently bound and not very readily replaceable by ions.

A further set of reactions investigated were those between phosphonitrile chloride and amines. It has[1,10] previously been reported that phosphonitrile chloride reacts with aniline, toluidine, and piperidine, in each case by elimination of hydrochloric acid from the chlorine and an amine hydrogen atom. Reactions were found to occur between phosphonitrile chloride and diphenylamine, ethylaniline, diethylamine, triethylamine, dimethylaniline, phthalimide, methylene urea, urea, semicarbazide, quinoline, benzylaniline, and a number of other substituted amines, but no definite compounds were isolated. It was found,[11] however, that the reaction between phosphonitrile chloride and certain substituted anilides, *e.g.*, acetanilide and diphenylurea, gave rise to products which could readily be identified. Thence an attempt was made to explain the course of the reaction.

When phosphonitrile chloride and acetanilide are heated together at 150–200° the mixture turns red and evolves gases. The red material solidifies on cooling, but remains as a transparent, thermoplastic, resinous substance. Extended heating renders it darker in color, eventually becoming black, infusible, and insoluble. In the earlier stages of the polymerization process, the material is soluble in water, alcohol, and organic solvents. Both qualitative and quantitative experiments were conducted on a micro scale in order to investigate the reaction completely. The gaseous products evolved from the reaction mixture were found to be hydrochloric acid and acetyl chloride, as shown by the equation:

$$P_3N_3Cl_6 + 3\ C_6H_5NHCOCH_3 \rightleftharpoons P_3N_3(NC_6H_5)_3 + 3\ CH_3COCl + 3\ HCl$$

In one quantitative experiment, 87% of the theoretical amount of hydrochloric acid was collected by absorption in sodium hydroxide solution, but only half the total amount of acetyl chloride required by the equation was collected. The main product of the reaction, $P_3N_3(NC_6H_5)_3$, polymerizes in a similar way to the other compounds already mentioned, giving a chain structure:

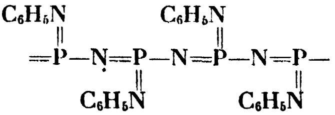

$$=\overset{\begin{array}{c}C_6H_5N\\ \|\end{array}}{P}-N=\underset{\begin{array}{c}\|\\ C_6H_5N\end{array}}{P}-N=\overset{\begin{array}{c}C_6H_5N\\ \|\end{array}}{P}-N=\underset{\begin{array}{c}\|\\ C_6H_5N\end{array}}{P}-$$

The reaction also takes place in boiling nitrobenzene solution (b.p. 209°), from which the product is eventually precipitated, rather more slowly in *o*-dichlorobenzene (b.p. 180°), perceptibly in *sym*-tetrachloroethane (b.p. 147°), and scarcely at all in chlorobenzene (b.p. 132°). The sodium derivative of acetanilide gives an identical product, with elimination of sodium chloride instead of hydrochloric acid. When propionanilide is used as starting material, an identical product is also obtained, but propionyl chloride and hydrochloric acid are evolved as gaseous products. Structurally homologous compounds were obtained from phosphonitrile chloride and *α*-acetonaphthylamide, and from phosphonitrile chloride and *p*-

nitroacetanilide, but the nitro compound showed a tendency to char and decompose.

The reaction between phosphonitrile chloride and diphenylurea took place in a manner similar in most respects to that between phosphonitrile chloride and acetanilide. The resinous condensation product was, however, yellowish-green instead of red, and was insoluble in water in the early stages of the polymerization. Qualitative microinvestigation of the products of the reaction showed that hydrochloric acid and phenylisocyanate were evolved, the equation being:

$$P_3N_3Cl_6 + 3\ C_6H_5NHCONHC_6H_5 \rightleftharpoons P_3N_3(NC_6H_5)_3 + 3\ C_6H_5NCO + 6\ HCl$$

Phenylurea gives a similar product to diphenylurea on heating with phosphonitrile chloride, probably because it is converted into diphenylurea on heating. Similar reactions were found to occur, giving rise to the same polymer and homologous volatile products, when dimethyldiphenylurea and diethyldiphenylurea were heated with phosphonitrile chloride. The resinous condensation products are ductile when warm, and may be drawn into filaments. This fact tends to confirm the opinion that polymerization gives rise to chains consisting of alternating phosphorus and nitrogen atoms, the side chains being attached to the phosphorus atoms.

EXPERIMENTAL

Preparation of Phosphonitrile Chloride. The method used was essentially the same as that described by Schenck and Römer,[1] but with slight modifications to improve the yield. 140 grams of ammonium chloride, previously dried, were added to a solution of 450 grams of phosphorus pentachloride in 1200 ml. of dried *sym*-tetrachloroethane, and the mixture refluxed on an oil bath. Heating was continued until hydrogen chloride ceased, or almost ceased, to be evolved; this operation usually took about 12 hours. A calcium chloride tube was attached to the open end of the condenser. The mixture was cooled and the unchanged ammonium chloride filtered off. The solvent was distilled off at 50° under water-pump vacuum, and the residual butterylike mass transferred to an open dish and allowed to cool. The oil and traces of excess solvent were removed by suction on a sintered-glass funnel, and the product washed with a little aqueous ethanol. The powder, which consisted almost entirely of triphosphonitrile chloride was recrystallized several times from benzene. *Yield:* 120 grams (*i.e.*, 48% theoretical). About 30 batches have been made by this method. Analytical figures for a typical batch are: *found:* P 26.1, N 12.2, Cl 62.6; *calculated* for $PNCl_2$: P 26.76, N 12.08, Cl 61.16%. Low yields are thought to be due to the use of excess ammonium chloride which reacts with the phosphonitrile chloride formed to give phospham or phosphonitrile amide, and also to the use of too high a reaction temperature: it appears that 120–130° is the most suitable.

Polyphosphonitrile Chloride. 5 grams of phosphonitrile chloride were heated to 300° in a sealed tube for several hours. The elastic polymeric material obtained was identical with Schenck and Römer's "inorganic rubber."

ANALYSIS: *Found:* P 23.5; Cl 57.2. *Calculated* for $PNCl_2$: P 26.76, Cl 61.16%. Heating of this material at 350° followed by sudden chilling deposited crystals of triphosphonitrile chloride on the walls of the tube.

Phosphonitrile Chloride and Phenol. 40.5 grams of phenol were dissolved in a solution of 20 grams of sodium hydroxide in 135 ml. of water. This was refluxed with 25 grams of phosphonitrile chloride for 28 hours. The oily product was colorless, and was washed with benzene which was removed under reduced pressure. Attempts to distil the product for purification were unsuccessful as it did not boil below 320° at a few millimeters pressure. Analysis showed that it was probably contaminated with excess phosphonitrile chloride. *Found:* P 16.6, N 8.3, C 52.8, H 4.6; $P_3N_3(OC_6H_5)_6$ requires P 13.4, N 6.1, C 62.3, H 4.3%. No ready means of purifying this compound were found. Further heating causes polymerization.

Phosphonitrile Chloride and *p*-Cresol. 35 grams of *p*-cresol were treated with 8 grams metallic sodium with benzene as diluent, and the mixture refluxed with 20 grams phosphonitrile chloride for 10 hours. The benzene was removed by distillation, and the brown oil dissolved in ether, dried, and concentrated. It would not distil below 360° at 3 mm. pressure. *Found:* P 14.8, N 7.7, C 59.6, H 6.7; $P_3N_3(OC_7H_7)_6$ requires P 12.0, N 5.1, C 64.9, H 5.6%. No method of purification was available; it was apparent that excess of phosphonitrile chloride was present, either dissolved in the oil, or in combination with it. Continued heating caused polymerization to a thermoplastic resin.

Phosphonitrile Chloride and Nitrophenols. Condensation reactions were carried out with phosphonitrile chloride and *o*-, *m*-, and *p*-nitrophenols separately. 14 grams of the nitrophenol were dissolved in 80 ml. toluene, and 2.5 grams sodium added. The mixture was then refluxed with 11 grams of phosphonitrile chloride for 5–15 hours. The toluene solution yielded a red condensation product similar in properties to that obtained from *p*-cresol, but subject to more ready decomposition. No analyses were made.

Phosphonitrile Chloride and Acetanilide. 11.5 grams of phosphonitrile chloride and 12 grams of acetanilide were intimately mixed and warmed in a distillation apparatus to a temperature not exceeding 200° for a few minutes until evolution of gases appeared complete. In the receiver 4 grams of acetyl chloride were collected, and in a sodium hydroxide absorption apparatus attached to the side-arm of the receiver 3.1 grams of hydrochloric acid were absorbed. This corresponds to roughly 50% of the theoretical acetyl chloride and 87% of the theoretical hydrochloric acid. The red solid polymer left in the distillation flask was ground under benzene when cold, and washed several times with benzene to remove unchanged phosphonitrile chloride and acetanilide. The reaction was also carried out by refluxing the mixture for several hours in boiling nitrobenzene and in boiling *o*-dichlorobenzene.

Phosphonitrile Chloride and Other Anilides. The reaction was carried out as above, but using the appropriate amount of propionanilide in place of acetanilide; the solid product of the reaction was identical, but the gaseous products evolved were propionyl chloride and hydrochloric acid. Benzanilide reacted similarly, giving off benzoyl chloride and hydrochloric acid, and producing the same red resinous condensation product. By using phosphonitrile chloride with α-acetonaphthylamide, and phosphonitrile chloride and *p*-nitroacetanilide, structurally homologous compounds were obtained, although the nitro compound charred before the reaction was complete.

Phosphonitrile Chloride and Diphenylurea. 11.5 grams of phosphonitrile chloride and 21 grams of *sym*-diphenylurea were intimately mixed and treated in the same apparatus as described above at 240° for four minutes. The products evolved from the reaction were identified as hydrochloric acid and phenyl isocyanate. The reaction mixture in the flask became yellowish-green in color, and, on completion of evolution of volatile products, was purified in a manner similar to that described above.

Phosphonitrile Chloride and Diphenylguanidine. This reaction was carried out as described above for diphenylurea, but the resinous product was darker green in color, and the volatile products other than hydrochloric acid were not identified.

Phosphonitrile Chloride and Other Substituted Ureas. Phosphonitrile chloride and phenylurea, on condensation and polymerization, gave a product apparently identical with that obtained from diphenylurea, probably because phenylurea is converted into diphenylurea on heating. Similar reactions were also observed to occur when phosphonitrile chloride was heated with dimethyldiphenylurea and with diethyldiphenylurea. The resinous products were hard when cold, tending to become brittle after continued heating, but softening sufficiently for the drawing of filaments to be carried out on warming.

Methods of Analysis. Carbon and hydrogen were determined by the ordinary Pregl method; for phosphorus, the polymeric materials were incinerated with nitric acid followed by the usual phosphomolybdate precipitation; nitrogen was determined by the ordinary Kjeldahl method.

The author wishes to record his thanks to Dr. A. A. Houghton for carrying out the analyses.

References

1. R. Schenck and G. Römer, *Ber.*, **B57**, 1343 (1924); **B60**, 160 (1927).
2. P. Rénaud, *Compt. rend.*, **194**, 2054 (1932); *Ann. Chem.*, **11**, 443 (1935).
3. K. H. Meyer, W. Lotmar, and G. W. Pankow, *Helv. Chim. Acta*, **19**, 930 (1936); *Trans. Faraday Soc.*, **32**, 148 (1936).
4. O. Schmitz-Dumont *et al.*, *Z. anorg. Chem.*, **238**, 189 (1938); **243**, 113 (1939).
5. O. Schmitz-Dumont, *Z. Elektrochem.*, **45**, 651 (1939); *Angew. Chem.*, **52**, 498 (1939).
6. D. Lipkin, U. S. Patent 2,214,769.
7. H. Rosset, *Compt. rend.*, **180**, 750 (1925).

8. G. Wétroff, *Compt. rend.*, **208**, 580 (1939); **210**, 436 (1940).
9. D. Lipkin, U. S. Patent 2,192,921.
10. A. W. Hofmann, *Ber.*, **17**, 1909 (1884); *Bull. Soc. Chim.*, **44**, 374 (1885).
11. C. J. Brown, U. S. Patent 2,374,646, British Patent 568,594.

English Synopsis, see Summaries, page S17, Vol. V, 1950.

Résumé

Les réactions du chlorure de phosphonitrile avec les phénols et les amides substituées ont été étudiées. Certaines de ces substances polymérisent facilement en formant des huiles à point d'ébullition élevée ou des résines thermoplastiques. Une nouvelle réaction a été trouvée entre le chlorure de phosphonitrile et certaines anilides substituées, telles l'acétanilide et la diphénylurée. Les équations de ces réactions sont suggérées. Il est évident que le radical phosphonitrilique se comporte comme une unité de stabilité élevée, présentant des possibilités chromophores, et donnant facilement formation à des polymères en chaîne.

Zusammenfassung

Die Reaktionen von Phosphonitrilchlorid mit Phenolen und substituierten Amiden wurden untersucht. Einige der erhaltenen Substanzen polymerisieren leicht und geben hoch siedende Öle oder thermoplastische Harze. Eine neue Reaktion zwischen Phosphonitrilchlorid und einigen substituierten Aniliden, wie Acetanilid und Harnstoff, wurde gefunden. Gleichungen für diese Reaktionen werden vorgeschlagen. Das Phosphonitrilradikal wirkt offensichtlich wie eine hochbeständige Einheit mit chromophoren Eigenschaften, die leicht Kettenpolymere bildet.

Received February 21, 1949

JOURNAL OF POLYMER SCIENCE VOL. V, NO. 4, PAGES 473–482

Viscosity and Sedimentation of Linear Macromolecules Exhibiting Partial Solvent Immobilization

ANTON PETERLIN, *Institute of Physics, University, Ljubljana, Yugoslavia*

I. DISCUSSION OF VARIOUS FORMULAS

The unbranched linear macromolecule in solution resembles a loosely coiled chain. The flow of solvent through the coil is impeded much more near the center than near the periphery because of much greater density of chain elements near the center. The solvent is said to be partly immobilized in the central part of the coil. This situation is reflected in the dependence of the intrinsic viscosity and sedimentation constant on the molecular weight. Thus a freely draining random coil behaves in accordance with Staudinger's law and has a sedimentation constant that is independent of molecular weight. On the other hand, if the flow is totally hampered, the intrinsic viscosity and sedimentation constant increase in proportion to the square root of the molecular weight, M, or the polymerization degree, Z, provided the mean distance of the two chain elements and the effective length, R, of the molecule show the same square root dependency upon the number of links involved. (In regard to this latter requirement the recent calculation[10] of the influence of the space-filling property of the polymer chain, that is the volume effect, and the polymer–solvent interaction on the average dimensions of the polymer molecule is of importance.) The majority of linear polymer molecules are found to exhibit a behavior intermediate between these two extremes. Therefore it is of interest to work out a more exact description of the transition from the free-draining coil to the impenetrable coil.

The two limiting values and the relations in the intermediate region have often been investigated. H. and W. Kuhn[7] infer an interpolation formula from the limiting laws and model tests.[6] By considering the hydrodynamic interaction the same relations had been found by J. J. Hermans[4] for sedimentation and by Peterlin[9] for the viscosity. The calculations of Hermans do not allow an immediate translation into viscosity, as only the interaction of the extremities of the molecule is taken in consideration. With Peterlin's treatment both the viscosity and the sedimentation can be obtained. By equal consideration of all parts of the thread molecule he finds—in case of a purely statistical coil the effective distance R of the extremities being $A_0N^{1/2}$—the results*:

$$[\eta] = \left[\left(\frac{\eta}{\eta_0} - 1\right)\Big/c\right]_{c\to 0} = \frac{\pi}{4}\frac{a_0A_0^2}{M_0}\frac{N}{1 + 1.2(6/\pi)^{1/2}(a_0/A_0)N^{1/2}} \tag{1}$$

$$[s] = \frac{s\eta}{1 - \bar{v}\rho} = \frac{1}{6\pi}\frac{M_0}{a_0}\left[1 + \frac{8}{3}\left(\frac{6}{\pi}\right)^{1/2}\frac{a_0}{A_0}N^{1/2}\right] \tag{1a}$$

where A_0 is the effective length, a_0 the hydrodynamic radius, and M_0 the molecular weight of the statistical element. Such an element is chosen so that its orientation is independent of the neighboring segments of the molecule. It is composed of ζ fundamental units. The number of such segments is $N = Z/\zeta$.

Because of the approximations made in averaging over all possible molecular configurations, the numerical factor 1.2 in Eq. (1) is not quite correct and should be replaced by another value. In any case it is clear that it must be smaller than $^8/_3$, since in sedimentation all elements work in the same sense as they move in the same direction (exterior diffusion), while in viscous flow, where the two extremities of the molecule move toward one another (interior diffusion), the influence of one half of the chain elements is opposed on the average to the other half.

It further appears that the term unity occurring in the sum in both equations is influenced by the hydrodynamic interaction. It should be replaced by two new constants, a_1 and a_2, which we shall not consider more closely because they prove to be of no importance for the effective length R which alone is of interest. With these new constants we obtain:

$$[\eta] = [\eta]_0' N/(a_1 + b_1N^{1/2}) = [\eta]_0''N/(1 + c_1N^{1/2}) \tag{2}$$

with:

$$[\eta]_0'' = [\eta]_0'/a_1 \qquad c_1 = b_1/a_1$$

and:

$$[s] = [s]_0'(a_2 + b_2N^{1/2}) = [s]_0''(1 + c_2N^{1/2}) \tag{2a}$$

with:

$$[s]_0'' = [s]_0'a_2 \qquad c_2 = b_2/a_2$$

The values of the constants a and b depend essentially upon the way in which the interaction of the individual segments is taken in consideration, as well as upon the hydrodynamic resistance of the elements Inasmuch as the latter cannot be well determined, both Eqs. (1) and (2) shall be considered essentially as interpolation formulas.

---

* The intrinsic viscosity here and in all later formulas refers to the mixed weight concentration, *i.e.*, g./cc. This is better applicable in practice because it is not necessary always to multiply by the specific volume $\bar{v}$ of the solute. For the same reason in $[s]$ the factor $\bar{v}$ in the numerator is omitted.

The results of Kirkwood and Riseman,[5] Brinkman,[1] and Debye and Bueche[2] show the same uncertainty. The two first authors regard the hydrodynamic interaction of all segments and average over all statistically permitted configurations of the molecule very precisely. They obtain by solution of an integral equation a tabulated function for viscosity and a formula similar to Eq. (1a) for the sedimentation constant. Brinkman and Debye and Bueche replace the thread molecule by a sphere of constant density into which the solvent can penetrate only partially, and solve exactly the resulting hydrodynamic problem. The solutions are given in form of tabular functions. Debye and Bueche further showed that their formula for viscosity is identical with the results of Kirkwood and Riseman, except for an uncertainty in the numerical constants.

One can go on still further and compare the results of all the calculations made earlier. All have two essential constants:†

$$[\eta] = B'y^2F(y) \qquad (3)^5$$

$$= B''\sigma^2\Phi(\sigma) \qquad (3a)^{1,2}$$

$$= Bx^2/(1 + x) \qquad (3b)^{10}$$

and:

$$[s] = [s]_0(1 + 8y/3) \qquad (4)^5$$

$$= 2[s]_0\sigma^2/9\Psi(\sigma) \qquad (4a)^{1,2}$$

$$= [s]_0\,(1 + x^*) \qquad (4b)^{10}$$

with:

$$y = (6/\pi)^{1/2}(a_0'/b')(M/M_0')^{1/2} \qquad (5)$$

$$\sigma^2 = (g/1.054)(a_0'/b')(M/M_0')^{1/2} \qquad (5a)$$

$$x = 1.2(6/\pi)^{1/2}(a_0/A_0)(M/M_0)^{1/2} = M^{1/2}/A \qquad (5b)$$

$$x^* = (8/3)(6/\pi)^{1/2}(a_0/A_0)(M/M_0)^{1/2} = M^{1/2}/A^* \qquad (5b)$$

In Eqs. (5) and (5a) the symbols a_0', b' and M_0' denote the hydrodynamic radius, the effective length, and the molecular weight of the fundamental unit (monomeric unit) of the macromolecule. Evidently it is:

$$a_0'/(b'M_0'^{1/2}) = a_0/(A_0M_0^{1/2}) \quad .$$

i.e., the effective length and the resistance of the molecule must not depend on the way in which the flexibility of the molecule is taken into account. One can either include the valency angles and the rotational hindrance in the calculation or take these into account by introducing the number ζ

---

† Eqs. (3b) and (4b) are derived from (1) and (1a). If one proceeded from Eqs. (2) and (2a), the factors in x and x^* (Eqs. (5b) and (5b)*) should be still divided by a_1 and a_2. For the length R (Eq. (6) ff.) to be calculated later the factors a_1 and a_2 are really of no importance.

specifying how many fundamental units are to be joined in order to form segments that are statistically independent of one another.

The general behavior of the above functions can be compared independently of the special value of the essential constants A and B if log $[\eta]$ and log $[s]$ are plotted against the logarithm of the independent variables y, σ, and x or x^*, which all are proportional to $M^{1/2}$ and the resulting curves are brought into coincidence by shifting the scale.

As may be seen from Figures 1 and 2 all three functions in the case of viscosity as well as at the sedimentation can be made to coincide although the shifting of the scale is not the same for the two cases. The full curves correspond to Eqs. (3b) and (4b), the crosses to the values of Kirkwood and Riseman,[5] and the circles to those of Brinkman[1] and Debye and Bueche.[2]

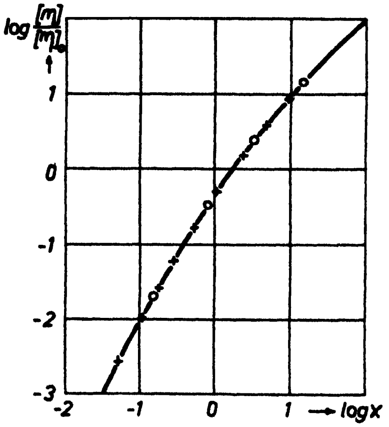

Fig. 1. Viscosity according to Kirkwood and Riseman[5] (crosses), Brinkman[1], and Debye and Bueche[2] (circles) and Peterlin[10] (solid line).

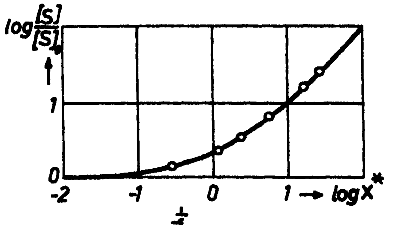

Fig. 2. Relative sedimentation constant $[s]/[s]_0$ according to Debye and Bueche[2] (circles), Peterlin[10], and Kirkwood and Riseman[5] (solid line).

The crosses and the circles lie so well on the curves that the differences no doubt lie within the errors of observation. All three pairs of formulas are consequently equally good for interpolation. It is, therefore, hardly possible to establish by experiment which function better reproduces the measurements. If measurements yield a different result for the dependence of the sedimentation constant or the intrinsic viscosity on the molecular weight than that represented in Figures 1 and 2, something must be altered in the fundamental suppositions. It may be, for instance, that the mean distance R of the extremities of the molecule increases more or less rapidly than the square root of the polymerization degree.[10]

By shifting the curve 3b toward 3 one can determine a better value for the uncertain factor 1.2. We get the value 0.52 so that Eq. (5b) should be altered to:

$$x = 0.52(6/\pi)^{1/2}(a_0/A_0)(M/M_0)^{1/2} \tag{5c}$$

This shifting is now neither very exact nor has it a deeper sense. It would be preferable to determine an empirical value for this factor at a known length of the molecule.

For interpolation purposes the simplest possible formula is desired. We shall therefore try to interpret the measurements of the intrinsic viscosity and sedimentation for a polymer series by Eqs. (3b) and (4b) because they are the simplest. We proceed by plotting the experimental values $M/[\eta]$ and $[s]$ against $M^{1/2}$. For large M, where the above suppositions are valid, a straight line should result if the molecules behave like a random coil with partial solvent immobilization.

II. EFFECTIVE RADIUS *R* OF THE MOLECULE

From the slope of the plot of $M/[\eta]$ and $[s]$ against $M^{1/2}$ as abscissa:

$$\tan \alpha = A/B$$

$$\tan \alpha^* = [s]_0/A^*$$

we obtain the effective length R from viscosity data:

$$R_\eta = (3^{1/6}2^{5/6}/\pi^{1/2})(1.2 \cot \alpha/N_A)^{1/3}M^{1/2} = 1.52 \times 10^{-8}(\cot \alpha)^{1/3}M^{1/2} \tag{6}$$

and from sedimentation data:

$$R_s = (2^{5/2}/3^{3/2}\pi^{3/2})(\cot \alpha^*/N_A)M^{1/2} = 3.25 \times 10^{-25} \cot \alpha^* M^{1/2} \tag{6a}$$

with the above mentioned uncertainty in the factor 1.2. N_A represents Avogadro's number.

The difference between Eqs. (1) and (2) does not influence the value of R because it affects only the position and not the slope of the straight lines. It is further significant that the special choice of the size of the statistically independent elements, that is of the number ζ, does not appear in expressions (6) and (6a) and, therefore, does not influence the calculation of the length R from experimental data.

The frictional constant, f, is given by the following expression:

$$f = M/(N_A[s]) = (1/a_0)(3\pi A_0/8)^2 \cdot x^{*2}/(1 + x^*) = C \cdot x^{*2}/(1 + x^*) \tag{7}$$

Since the intrinsic viscosity and the frictional constant are often represented by Mark's interpolation formulas:

$$[\eta] = K_1 M^a \tag{8}$$

$$f = K_2 M^b \tag{8a}$$

the exponent

$$a = (1 + x/2)/(1 + x)$$

is plotted in Figure 3 as it follows from Eqs. (3b) and (8). The same curve represents the exponent b, if x is replaced by x^*.

From the experimentally determined value of a or b we obtain the effective length R:

$$R_\eta = (2/\pi)^{1/2}3^{1/6}(1.2/N_A)^{1/3}([\eta]M/(1-a))^{1/3} = 1.21 \times 10^{-8}\cdot([\eta]M/(1-a))^{1/3} \quad (9)$$

$$R_s = (2/3\pi)^{3/2}\cdot f/(1-b) = 0.098f/(1-b) \quad (9a)$$

or:

$$R_s = (2/3\pi)^{3/2}M/(N_A[s](1-b)) = 1.62 \times 10^{-25}M/([s](1-b)) \quad (9b)$$

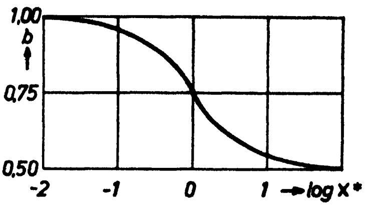

Fig. 3. The exponent b (or a) as a function of the parameter $x^* = M^{1/2}/A^*$ (or $x = M^{1/2}/A$).

The simplicity of the correct interpolation formulas Eqs. (3b) and (4b) makes the use of them preferable to the exponential representation by Eqs. (8) and (8a).

III. COMPARISON WITH EXPERIMENTS

If we want to apply our formulas on macromolecular solutions we find that the viscosity and the sedimentation has been measured on the same preparations in only a few cases. As far as I know, there are only the nitrocellulose fractions in butyl acetate and acetone for which Fivian[3] had measured the viscosity and Mosiman[8] the sedimentation and the cellulose

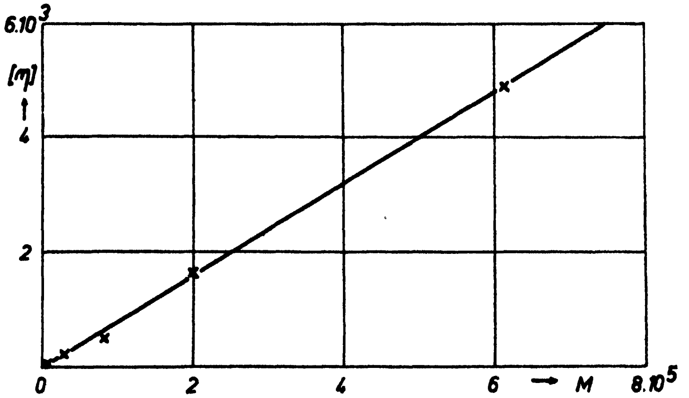

Fig. 4. Intrinsic viscosity of nitrocellulose in butyl acetate (Fivian[3]).

acetate fractions in acetone in which Sookne and Harris[16] measured the viscosity and Singer[14] the sedimentation.

For the nitrocellulose the measurements yielded the following results. The viscosity (Fig. 4) can in the entire measured range, *i.e.*, from $M = 6200$ to $M = 613{,}000$ be represented by the straight line:

$$[\eta]_v = -24.3 + 8.05 \times 10^{-3} M$$

where $[\eta]_v$ is intrinsic viscosity of nitrocellulose in butyl acetate and subscript v refers to volume concentration (cc./cc.). These solutions can be cited as models for the linear Staudinger law. Hence it would follow that

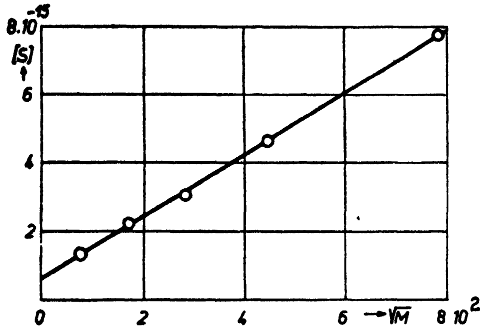

Fig. 5. Sedimentation constant of nitrocellulose in acetone (Mosiman[8]).

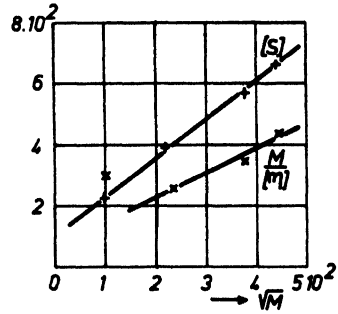

Fig. 6. $M/[\eta]$ and $[s]$ in arbitrary units over $M^{1/2}$ for cellulose acetate in acetone.

these molecules are free-draining coils. The values for sedimentation velocity (Fig. 5), however, lie on a straight line, if plotted against $M^{1/2}$, which would point to a statistical coil with a fair immobilization of the solvent. In order to solve this contradiction one will be forced to make essential alterations of the random coil model, and treat more accurately the transition from the nearly stiff molecule to the statistically coiled molecule, as was already pointed out by Sadron.[12] More precise results referring hereto will be reported shortly.

The experimental data for cellulose acetate in acetone fit somewhat better into the frame of the present theory, but an ideal consistency is lacking. Plotting $M/[\eta]$ and $[s]$ against $M^{1/2}$, one obtains (Fig. 6) straight lines in both cases, if the viscosity value for the lowest fraction is neglected. Making use of the formulas (6) and (6a) we obtain for the effective length:

$$R_\eta = 1.44 \times 10^{-8} M^{1/2}$$

$$R_s = 1.85 \times 10^{-8} M^{1/2}$$

If this difference were to be due only to an error in the factor 1.2 in the viscosity formula, it should be replaced by 2.56. This is very unlikely, for then the hydrodynamic interaction of the segments in viscous flow would be almost as large as in the sedimentation; this cannot happen. If, however, we compare the lengths R_1 with the length L of the stretched molecule, we see from the Table I that in the lowest fractions the molecule is quite extended. The suppositions of the random coil with partial solvent immobilization are surely not realized. This has been already stated for these preparations by Singer and Mark,[15] who found a similar discrepancy in R when applying the theory of Debye and Bueche.

TABLE I

M	R_η, Å.	R_1, Å.	L, Å.	$L/$
10,350	148	190	190	1.0
51,000	325	419	930	2.2
143,000	545	701	2600	3.7
194,000	634	817	3500	4.3

Considering, on the other hand, the viscosity measurements of Ewart and Gingey on polystyrenes known to me only from the above quoted paper of Kirkwood and Riseman,[5] we have:

$$R_\eta = 1.18 \times 10^{-8} M^{1/2}$$

which for molecular weight of 1,000,000 yields $R = 1180$ Å. From light scattering measurements this length has been determined as 1080 Å. In the viscosity formula Eq. (1), therefore, the uncertain factor 1.2 is to be replaced by 0.91 in order to obtain agreement in the viscometric and optical determination of effective length in polystyrene molecules. After this correction Eqs. (6) and (9) become:

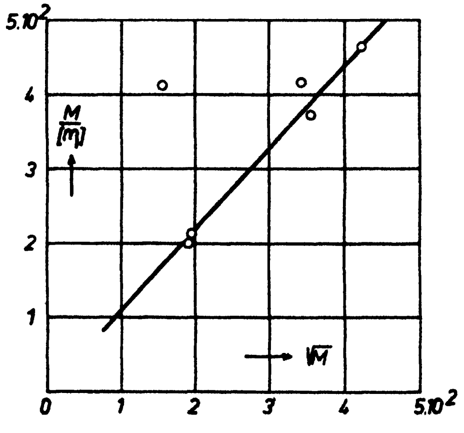

Fig. 7. $M/[\eta]$ *vs.* $M^{1/2}$ for amylose triacetate in chloroform.

$$R_\eta = 1.39 \times 10^{-8}(\cot\alpha)^{1/3}M^{1/2} \tag{10}$$

and:

$$R_\eta = 1.10 \times 10^{-8}([\eta]M/(1 - a))^{1/3} \tag{10a}$$

With values thus corrected we obtain, for instance for amylose triacetate in chloroform (Fig. 7) which had been viscometrically investigated by Samec and Knop,[13] the effective length:

$$R_\eta = 1.34 \times 10^{-8} M^{1/2}$$

The molecular lengths calculated in this manner are all considerably smaller than the extended molecule. For instance, taking $M = 178{,}000$ we have $R = 565$ Å., while the extended molecular chain measures 2863 Å. or 2414 Å. if we consider the valency angle of the oxygen atom linking the glucose residues into a chain. If these residues can rotate freely around the oxygen links, the valency angle of 115° yields an effective length of 191 Å. for the randomly coiled molecule. The above measured length is 3.0 times larger; this indicates a hindered rotation. It can be explained either by a steric hindrance with a permitted angle of 131° or by a potential barrage of the height $W_0 = 5.4kT$.[11]

IV. CONCLUSIONS

The actual results of viscosity and sedimentation measurements show that an entirely satisfactory description of the linear macromolecule in dilute solution, particularly of the comparatively stiff molecules of various celluloses, does not yet exist. It seems, as Sadron[12] has intimated, that with cellulose the conception of the random coil can be adopted only at an extraordinarily high degree of polymerization, while with a smaller molecular weight we have to deal with a transition from the state of an almost rigid small rod to a more and more inflected thread. In conformity with the theoretical expectations the sedimentation velocity shows also in this intermediate region an almost linear dependence of $M^{1/2}$, while in the case of viscosity there can be ascertained a steady transition from the almost quadratic function with the smallest molecules over the linear Staudinger rule up to the square root region at extreme molecular weights.

In the case of the polystyrenes and amylose, the theory of a coil with partial solvent immobilization is expected to be valid. The values $M/[\eta]$ plotted against $M^{1/2}$ lie well on a straight line and the resulting molecular lengths R are all so much smaller than the extended length L that the coiling and the hydrodynamic interaction must be very considerable. One must wait to see whether measurements of sedimentation will lead to the same value of R as the viscosity. If this will be so, then we shall be able to say that the model of the statistic coil with hydrodynamic interaction is realized at least with the comparatively soft flexible chain molecules and that with stiffer molecules with increasing molecular weight a slow approach to this state is realized.

References

1. H. C. Brinkman, *Physica*, **13**, 447 (1947).
2. P. Debye and A. M. Bueche, *J. Chem. Phys.*, **16**, 573 (1948).
3. W. Fivian, *Dissertation*, Bern, 1939.

4. J. J. Hermans, *Rec. trav. chim.*, **63**, 219 (1944).
5. J. C. Kirkwood and J. Riseman, *J. Chem. Phys.*, **16**, 565 (1948).
6. H. Kuhn, *Habilitationsschrift*, Basel, 1946.
7. H. Kuhn and W. Kuhn, *Helv. Chim. Acta*, **26**, 1324 (1943).
8. H. Mosiman, *Helv. Chim. Acta*, **26**, 61 (1943).
9. A. Peterlin, *Proc. Acad. Ljubljana, Math. Phys. Sec., in press.*
10. A. Peterlin, paper read at the Conference on Macromolecular Physics, Paris, Nov. 1948.
11. A. Peterlin, *Proc. Acad. Ljubljana, Chem. Sec., in press.*
12. C. Sadron, paper read at the Rheology Congress, Scheveningen, 1948.
13. M. Samec and L. Knop, *Proc. Acad. Ljubljana, Chem. Sec., in press.*
14. S. J. Singer, *J. Chem. Phys.*, **15**, 341 (1947).
15. S. J. Singer and H. Mark, *J. Applied Phys.*, **19**, 97 (1948).
16. A. Sookne and M. Harris, *Ind. Eng. Chem.*, **37**, 475 (1945).

English Synopsis, see Summaries, page S6, Vol. V, 1950.

Résumé

On a comparé les divers formules pour la viscosité et la sedimentation des grosses molécules linéaires qui se rendent compte de l'interaction hydrodynamique, et on a trouvé un accord étendu entre elles. Pour l'usage pratique la plus simple formule rendra le meilleur service. Si l'on porte les valeurs expérimentales de $[s]$ et de $M/[\eta]$ sur la racine carrée de la masse moléculaire, on reçoit des lignes droites. La pente donne la longueur effective des molécules. On a donné les formules relatives et on les a appliquées aux divers polymers.

Zusammenfassung

Es werden verschiedene Formeln für die Viskosität und Sedimentation von linearen Hochpolymeren, die unter Berücksichtigung der hydrodynamischen Wechselwirkung aufgestellt worden sind, miteinander verglichen und ihre weitgehende Übereinstimmung festgestellt. Für die Praxis wird die einfachste Formel die besten Dienste leisten. Durch Auftragen der Messwerte $[s]$ und $M/[\eta]$ gegen die Quadratwurzel aus dem Molekulargewicht erhält man Gerade, aus deren Neigung die effektive Länge der Moleküle abgelesen werden kann. Diesbezügliche Formeln werden angegeben und auf verschiedene Hochpolymere angewandt.

Received April 19, 1949

JOURNAL OF POLYMER SCIENCE VOL. V, NO. 4, PAGES 483–486

Polymerization of *m*- and *p*-Formylstyrenes*

RICHARD H. WILEY** and PATRICK H. HOBSON,† *Venable Chemical Laboratory, University of North Carolina*

The purpose of this investigation was to provide some information concerning the polymerization of *m*- and *p*-formylstyrenes, which as substituted styrenes having electrophilic substituents in the nucleus[1] might show variations in polymerization tendency such as have been observed with *m*- and *p*-nitrostyrenes.[2]

p-Formylstyrene prepared by the decarboxylation of *p*-formylcinnamic acid[3] was readily polymerized by benzoyl peroxide in bulk to a hard, clear plug, and by potassium persulfate in emulsion. The polymer did not precipitate from the monomer during bulk polymerization. The resulting polymer was characterized by its insolubility in a wide variety of organic solvents. 0.02 g. failed to dissolve after refluxing and stirring for approximately 24 hours in 25-cc. portions of benzene, toluene, xylene, methyl ethyl ketone, methyl isobutyl ketone, cyclohexanone, benzaldehyde, acetophenone, chloroform, tetrachloroethylene, dichloroethyl ether, diphenyl ether, Cellosolve, dioxane, nitrobenzene, nitromethane, dimethylformamide, butyl acetate, phenol, and tricresyl phosphate. No appreciable degree of swelling was observed in any of these solvents. No satisfactory solvent for the polymer was found. This is difficult to reconcile with the observed solubility of the polymer in monomer during bulk polymerization. The polymer softened at 140–150°C. and was pressed into a pliable, transparent film. This indicates that extensive cross linking is not the cause of insolubility.

p-Formylstyrene was copolymerized with butadiene in aqueous emulsion. The polymerization was carried out in $1^3/_4$-ounce screw-cap bottles rotated end over end 34 r.p.m. at 48 ± 0.5°C. A standard 75–25 emulsion recipe[4] was used. Conversions of 65 and 90%, respectively, were obtained at the end of 10 and 21 hours. The copolymer was a firm, light-colored, rubberlike material. It swelled greatly in benzene and was only slightly soluble in this solvent. 0.2 g. of the copolymer isolated at 65% conversion was allowed to stand in 50 cc. of dry benzene at room temperature. Removal of the benzene from a gel-free aliquot portion indicated that 0.12 g. of the copolymer had dissolved. This gel-free, undiluted solution had an intrinsic viscosity of 0.96 as calculated from the equation used by Marvel *et al.*[5]

---

* Contribution from the Venable Chemical Laboratory of the University of North Carolina.

** Present address: University of Louisville, Louisville 8, Kentucky.

† Du Pont Company Postgraduate Fellow, 1948–1949.

m-Formylstyrene was prepared by condensing isophthalaldehyde with 1 mole of malonic acid, decarboxylating the resulting mixture of *m*-formylcinnamic acid and *m*-phenylenediacrylic acid by a technique previously described,[3] and separating the *m*-formylstyrene from the *m*-divinylbenzene thus obtained by fractional distillation under reduced pressure. No satisfactory method for the separation of *m*-formylcinnamic acid from *m*-phenylenediacrylic acid was found and the separation of the two vinyl compounds by fractional distillation was not clean-cut. *m*-Formylstyrene was readily polymerized by benzoyl peroxide in bulk, to a hard, clear plug, and by potassium persulfate in emulsion. The resulting polymers were similar to those formed from the *para* isomer with regard to appearance, insolubility, and moldability. The ease with which these monomers polymerize indicates that an electrophilic group does not *per se* introduce complications in the polymerization of substituted styrenes.

Data from our studies are now available for a comparison of the properties and polymerization of three styrenes with electrophilic substituents in the *meta* position. These data are summarized in Table I. *m*-Nitrostyrene is the slowest of these to polymerize, and polymerizes, under comparable conditions, to the lowest molecular weight polymer. The other two resemble styrene itself on bulk polymerization. This indicates that the retardation is peculiar to the nitro group and is not general for electrophilic groups in the *meta* position. The Hammett sigma values suggest no such peculiarity in the *m*-nitro group. The values for formyl, cyano, and nitro groups in the *m*- and *p*-positions vary from +0.381 to 1.27 with *m*-nitro, +0.710, very close to *m*-cyano, +0.678. This then raises the question as to whether or not determination of the relative reactivity of the *m*-nitrostyrene radical toward the unsubstituted styrene radical from copolymerization data[6] will show the *m*-nitro substituent as abnormal.

TABLE I

Substituent in *meta* position	B p. of monomer	Polymerization[a]			Softening point of polymer	Viscosity[b]
		Bulk	Emulsion	Cationic		
NO_2	96°/3·5 mm.	x	x	x	130°	1.05
CN	83°/3·5 mm.	x	—	—	100°	1.270
CHO	102°/11 mm.	x	x	—	135°	Insol.

[a] x indicates successful;—indicates not tired.
Relative viscosity for 0.4 g. in 100 ml. CH_3NO_2.

EXPERIMENTAL

Condensation of Isophthalaldehyde with Malonic Acid

45 g. (0.34 mole) of isophthalaldehyde was dissolved in 70 cc. of ethanol and 6 cc. of pyridine was added. To the stirred solution heated on a steam

bath a solution of 33 g. (0.32 mole) of malonic acid in 110 cc. of ethanol was added dropwise over a period of about five hours. The solution was heated for 1$^1/_2$ hours after the addition of malonic acid and 100 cc. of alcohol was removed by distillation. After cooling the solid was filtered off and washed with 30 cc. ethanol and 150 cc. of cold chloroform to remove unreacted isophthalaldehyde. There remained 41 g. of a mixture of *m*-formylcinnamic acid and *m*-phenylenediacrylic acid, neutral equivalent 163, calculated neutral equivalent of formylcinnamic acid 176.

Preparation of *m*-Formylstyrene

37 g. of the above mixed acids was decarboxylated with quinoline and copper using the technique previously described.[3] From the quinoline distillate there was obtained 8 g. of a mixture of *m*-formylstyrene and *m*-divinylbenzene. This mixture was distilled and the following fractions collected: 85–100° (11 mm.), 1.4 g.; 100–102° (11 mm.), 3.6 g.; 102–103° (11 mm.), 1.5 g. The third fraction n_D^{25} 1.5811, d_4^{25} 1.035 was analyzed.

ANALYSIS. *Calcd.* for C_9H_8O: C, 81.79; H, 6.10. *Found*: C, 82.20; H, 6.15.

The phenylhydrazone was prepared[9] and recrystallized twice from ethanol, m.p. 129–130°.

ANALYSIS. *Calcd.* for $C_{15}H_{14}N_2$: N, 12.61. *Found*: N, 13.14.

1 g. (0.0076 mole) *m*-formylstyrene was oxidized to *m*-carboxystyrene with silver oxide.[8] Yield 0.48 g. (43%), m.p. 95–96° (after recrystallization from 20% ethanol). Reported[9] m.p. 95°. *Polymerizations* were carried out by standard procedures as described above.

References

1. R. H. Wiley and N. R. Smith, *J. Am. Chem. Soc.*, **70,** 1560 (1948).
2. R. H. Wiley and N. R. Smith, *J. Polymer Sci.*, **3,** 444 (1948).
3. R. H. Wiley and P. H. Hobson, *J. Am. Chem. Soc.*, *in press.*
4. F. T. Wall and L. F. Beste, *ibid.*, **69,** 1761 (1947).
5. C. S. Marvel, *et al.*, *Ind. Eng. Chem.*, **40,** 2371 (1947); **39,** 1488 (1946).
6. Walling, Briggs, Wolfstirn, and Mayo, *J. Am. Chem. Soc.*, **70,** 1537 (1948).
7. Shriner and Fuson, *The Systematic Identification of Organic Compounds*, Wiley, New York, 1940, p. 64.
8. M. Délépine and P. Bonnet, *Compt. rend.*, **149,** 39 (1909).
9. G. Komppa, *Ber.*, **26,** reg. 677 (1893).

English Synopsis, see Summaries, page S10, Vol. V, 1950.

Résumé

Les polymères et copolymères du *m*- et *p*-formylstyrène, obtenus par polymérisation en bloc et en émulsion, sont fusibles et insolubles dans un grand nombre de solvants. La présence du groupe formyle électrophile ne semble pas altérer la polymèrisabilité de ces composés. Le *m*-formylstyrène a été obtenu par décarboxylation de l'acide *m*-formylcinnamique, et ses constantes sont indiqueés.

Zusammenfassung

Es wurde gefunden, dass Polymere und Copolymere von *m*- und *p*-Formylstyrol, hergestellt durch Block- und Emulsionstechnik, schmelzbar und unlöslich in einer grossen Anzahl von organischen Lösungsmitteln sind. Die Gegenwart der elektrophilen Formylgruppen scheint die Polymerisationsfähigkeit dieser Bestandteile nicht zu äandern. *m*-Formylstyrol wurde durch Dekarboxylieren von *m*-Formylzimtsäure hergestellt und charakterisiert.

Received June 29, 1949

JOURNAL OF POLYMER SCIENCE VOL. V, NO. 4, PAGES 487-504

Mechanism of Emulsion Polymerizations. IV. Kinetics of Polymerization of Styrene in Water and Detergent Solutions*

F. A. BOVEY† and I. M. KOLTHOFF, *School of Chemistry, University of Minnesota*

In order to gain further insight into the mechanism of the emulsion polymerization of styrene, it was believed to be of interest to investigate its rate of polymerization in pure water solution and in aqueous solutions of detergents, no excess of styrene being present as a separate phase. Under such conditions, the rate of polymerization can be measured as a function of the concentration of styrene, as well as of the concentration of persulfate and of detergent. Measurements of the polymerization rate in water alone may throw light on the role of the "true water phase" (the aqueous solution exclusive of the micelles and polymer particles) in normal emulsion polymerization, in which a large excess of monomer is initially present as a separate phase. Present theories[1,2] postulate the soap micelles as the locus of reaction during the early stages of emulsion polymerization, and the polymer particles as the locus during the later stages of conversion, after the soap has been adsorbed on the surfaces of the particles. Measurements of the rate of polymerization of styrene solubilized in detergent solutions provide a means of investigating the kinetics of the reaction under conditions corresponding to those existing in the very early stage of the emulsion polymerization process, before the polymer particles have assumed a role of importance. Such measurements thus focus attention on the part played by the detergent micelles. Particular attention has also been given to the determination of the rate of production of monomer radicals (rate of activation) in the presence and absence of micelles.

Very few studies of the rates of polymerization of vinyl monomers in water and in aqueous solutions of detergents have been described in the literature. Bacon[3] has studied the polymerization of acrylonitrile in water solution at 30° with persulfate as initiator in combination with sodium sulfite, sodium hydrosulfite, and hydroquinone. These reducing agents all greatly increase the rate of polymerization. The conversion curves ob-

---

* Contribution from the School of Chemistry of the University of Minnesota. This Work was carried out under the sponsorship of the Office of Rubber Reserve, Reconstruction Finance Corporation, in connection with the Synthetic Rubber Program of the United States Government.

† Present address: Minnesota Mining and Manufacturing Co., St. Paul, Minn.

tained are S-shaped. No theoretical treatment of the results was offered.

Baxendale and coworkers[4,5] have studied the polymerization of methyl methacrylate in aqueous solution, using the ferrous iron–hydrogen peroxide system as initiator. They found the rate of polymerization to be proportional to the monomer concentration up to about 40% conversion, after which the rate became slower than corresponded to first-order kinetics. This retardation was attributed to the coagulation of the polymer formed. When cetylpyridinium bromide was added to the system, the rates became very much faster and did not "die out" until much higher conversions were reached. It was stated that the emulsifier had no effect on the ferrous iron–hydrogen peroxide initiating system, but it was found that amounts of cetylpyridinium bromide as small as 0.0003% (presumably far below the critical concentration for micelle formation) had a very marked accelerating effect on the rate. The accelerating effect was attributed to a stabilization of the polymer particles formed. This explanation hardly seems adequate to account for the marked effect even on the initial rate.

Morgan[6] has studied the polymerization of acrylonitrile in aqueous solution, using ammonium persulfate as initiator. He found that the rate was approximately proportional to the $^3/_2$ power of the monomer concentration, and to the square root of the persulfate concentration. Deviations were observed, however, particularly above 50% conversion of the monomer.

Frilette and Hohenstein[7] have investigated the polymerization of styrene in 2.0% aqueous potassium oleate solutions at various temperatures from 75 to 118°. It does not appear certain, however, that the polymerization was actually thermally initiated, as intended. Because of the readiness with which oleic acid forms peroxides, it seems possible that the polymerization may have been initiated by unknown quantities of these substances.

The authors cited, with the exception of the last, have used relatively large concentrations of monomers, of the order of 0.1 M, and have employed monomers whose solubilities in pure water are much greater than that of styrene. However, the corresponding polymers are not water-soluble, and the coagulation and precipitation of the polymers complicate the interpretation of the results considerably. To avoid this complication as far as possible, we have used relatively low concentrations of styrene (less than 0.02 M) even when employing solutions in which the solubility is higher than this.

EXPERIMENTAL TECHNIQUE

Materials

Dodecylamine hydrochloride, potassium persulfate, styrene, and *water* are as previously described.[8]

Potassium palmitate was prepared by I. K. Miller in this laboratory by neutralization of a solution of Eastman Kodak White Label palmitic acid in alcohol with carbonate-free alcoholic potassium hydroxide. The potassium palmitate was separated by crystallization at 0°.

Potassium laurate was prepared by dissolving the calculated amount of Eastman Kodak White Label lauric acid in aqueous potassium hydroxide of known concentration, carbon dioxide being excluded by flushing with nitrogen.

S. F. Flakes soap was not employed as emulsifier because it absorbs bromine and thus interferes with the styrene titration.

Apparatus and Analytical Methods

To carry out the kinetic investigations described in this paper, the apparatus shown in Figure 1 was employed. This consisted of a thick-walled vessel A of 500-ml. capacity, fitted with tubes B and C and stopcock D by means of which a stream of nitrogen could be passed through either the liquid or gas phases. The reaction mixture was stirred by a Pyrex-coated magnetic stirrer E actuated by a rotating magnet F. Samples

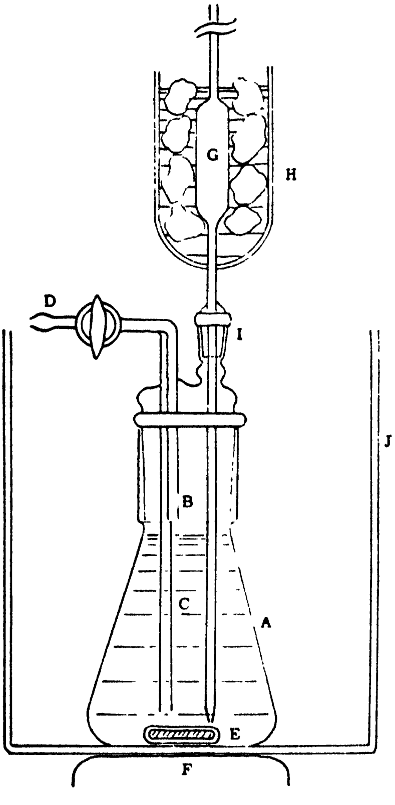

Fig. 1. Apparatus for measuring rate of reaction of styrene in aqueous solution.

could be withdrawn by applying nitrogen pressure through tube B, thus forcing a sample into the 25-ml. pipet G. The withdrawn sample was cooled by an ice–water mixture in jacket H if styrene was to be determined. The cooling served to minimize volatilization of the styrene. The pipet was attached to the vessel by the ground-glass joint I. The reaction mixture was maintained at the desired temperature by the thermostated water bath J.

To carry out a reaction, 500 ml. of conductivity water was pipetted into the vessel. To remove oxygen, a brisk stream of nitrogen was passed through C for 30 minutes if no detergent was present. If detergent was present, foaming prevented oxygen removal by this means, and, instead, the reaction vessel was alternately connected to a water aspirator and refilled with nitrogen. This cycle was repeated at least ten times. After flushing, styrene and persulfate solution were added from burets. Styrene was determined by amperometric titration with potassium bromate in the manner previously described.[9] For concentrations of 0.005 *M* or over, 0.01817 *M* potassium bromate was employed, and for concentrations less than this, 0.001817 *M* potassium bromate was employed. There was a slight absorption of bromine by the fatty acid soaps, for which correction was made. The dodecylamine hydrochloride absorbed no bromine.

EXPERIMENTAL RESULTS AND DISCUSSION

Solubility of Styrene in Water and Detergent Solutions

The solubility of styrene in water at 25, 40, and 50° was determined by stirring 300 ml. of water in the reaction vessel with 2 ml. of styrene until equilibrium was reached (about one hour). Samples were then removed and titrated. The results obtained are shown in Table I.

TABLE I

SOLUBILITY OF STYRENE IN WATER

Temp., °C.	Mole/liter	Per cent
25.0	0.00261	0.0271
40.0	0.00308	0.0320
50.0	0.00368	0.0382

Lane[10] has determined the solubility of styrene in water by a colorimetric method employing a formaldehyde–sulfuric acid reagent, and also by a cloud-point method. His values are 10–15% higher than those shown above; our values are believed to be more reliable and to be accurate within 2%.

The solubility of styrene in 0.093 *M* DDA·HCl and 0.093 *M* potassium palmitate solutions at 40 and 50° was determined by visual inspection of a series of small flat-sided bottles containing 50 ml. portions of emulsifier solution and varying quantities of styrene, added from a microburet. These mixtures were allowed one hour to reach solubility equilibrium, and the solubility was taken as equal to the quantity of styrene in the bottle showing the first faint turbidity. The presence of oxygen prevented polymerization. The results obtained are presented in Table II.

TABLE II

SOLUBILITY OF STYRENE IN 0.093 *M* SOLUTIONS OF DODECYLAMINE HYDROCHLORIDE AND POTASSIUM PALMITATE

Solvent	Temp., °C.	Solubility Mole/liter	Solubility Per cent
Dodecylamine hydrochloride	40	0.062	0.65
	50	0.091	0.95
Potassium palmitate...............	40	0 096	1.00
	50	0.139	1.45

Rate of Polymerization of Styrene in Water Solution

Rates of polymerization of styrene in water solution were measured at 50° as a function of the persulfate concentration. The initial concentration of styrene was approximately 0.0019 *M*, or 51.5% of saturation. The concentration of persulfate was made 0.00620 *M* (corresponding to a 1X-persulfate recipe, based on the aqueous phase), 0.00154 *M* ($^1/_4$X), and 0.000383 *M* ($^1/_{16}$X). The reaction curves are shown in Figure 2. In Figure 3, the quantity $x/a(a - x)$, where a is the initial concentration of

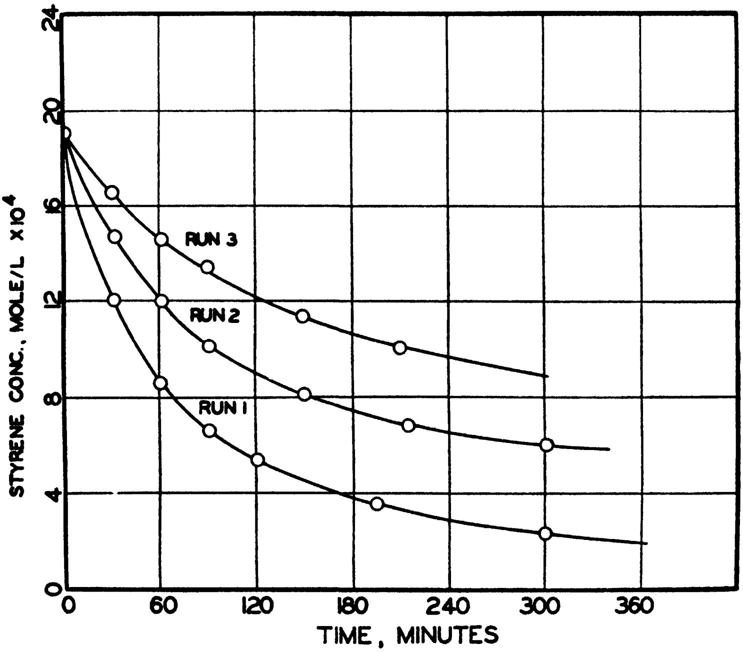

Fig. 2. Rates of polymerization of styrene in water solution at 50° with persulfate. Run 1, 1X $K_2S_2O_8$ = 0.00620 *M*. Run 2, $^1/_4$X $K_2S_2O_8$ = 0.00154 *M*. Run 3, $^1/_{16}$X $K_2S_2O_8$ = 0.000385 *M*.

styrene and $a - x$ is the concentration at time t (minutes), is plotted against t for these three runs. It will be observed that the rates are approximately bimolecular in styrene, but that deviations occur at higher conversions. These deviations are probably to be attributed to the effect of the polymer particles formed in the system. In these reactions, a distinct turbidity appears within 15 minutes from the start of the reaction.

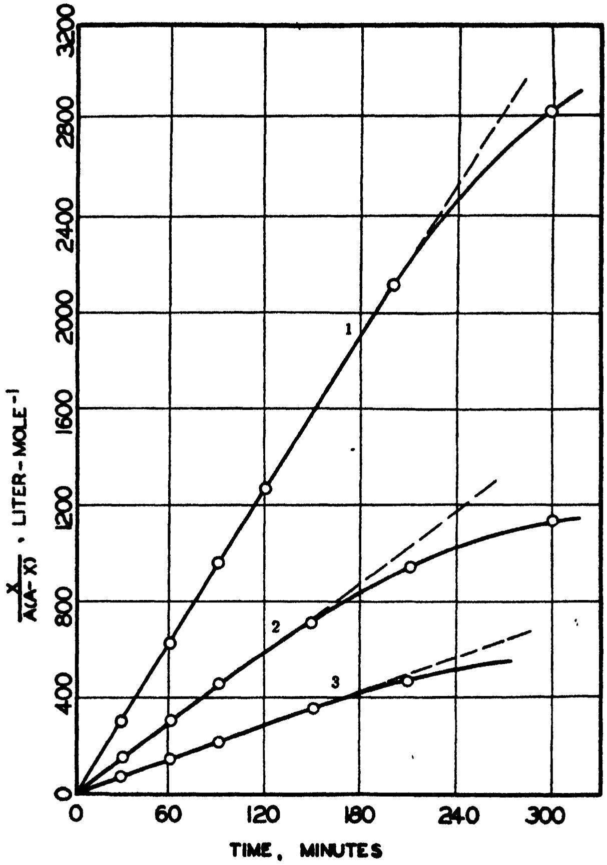

Fig. 3. Polymerization of styrene in aqueous solution at 50°, plotted as a second-order reaction. 1, 1× $K_2S_2O_8$. 2, $^1/_4$× $K_2S_2O_8$. 3, $^1/_{16}$× $K_2S_2O_8$.

In Table III, the bimolecular rate constants and extrapolated rates of polymerization in a saturated styrene solution at 50° (0.00368 *M*), calculated from the rate constants, are presented.

From these data, it is found that the rate of polymerization of styrene in water solution at 50° with persulfate as activator is given by the expression:

$$-d(\mathrm{M})/dt = k_2(\mathrm{M})^2(\mathrm{C})^{1/2}$$

where (M) is the styrene concentration and (C) the persulfate concentration.

TABLE III

Run	Persulfate concentration, mole/liter	Second-order rate constant, liter/mole/min.	Extrapolated rates of polymerization, mole/liter/min., at satn. (0.00368 *M*)
1	0.00620	10.9	0.0001480
2	0.00154	5.12	0.0000695
3	0.000385	2.56	0.0000347

It appears that in emulsion polymerization with an excess of styrene the rate is much greater than corresponds to that found in a saturated solution of styrene in water in the absence of detergents. From the data in Table III it is calculated that in a saturated solution of styrene in water made 0.00620 *M* (1×) in potassium persulfate, the rate of polymerization would

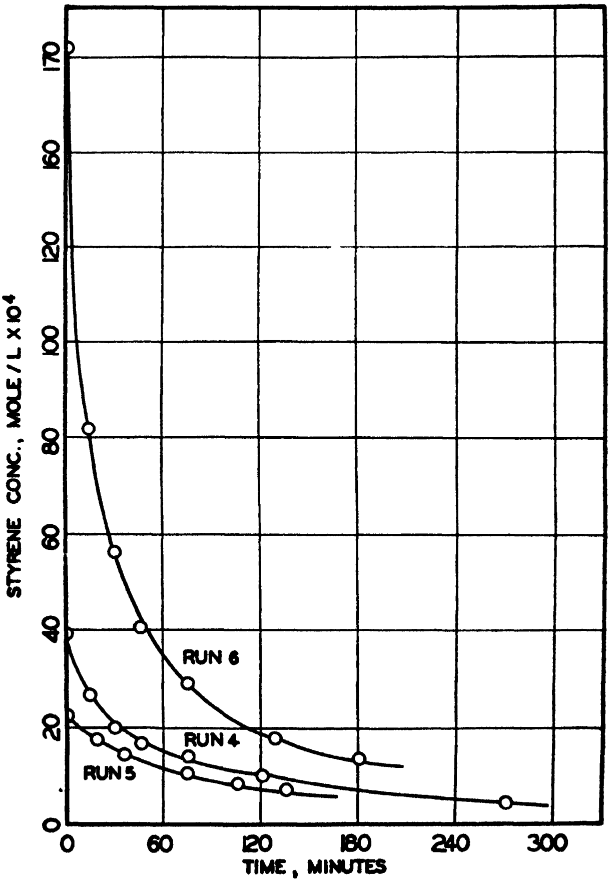

Fig. 4. Polymerization of styrene in 0.093 *M* aqueous dodecylamine hydrochloride solution at 50°. Runs 4 and 5: 0.0062 *M* $K_2S_2O_8$, 1×. Run 6: 0.0015 *M* $K_2S_2O_8$, $^1/_4$×. See page 494.

be 0.0001480 × 60 = 0.0089 mole/liter/hour, whereas in the presence of 1× DDA·HCl, the rate is 3.54 moles/liter/hour. Thus, the detergent must increase the rate of activation of the styrene (*v.i.*) or the micelles of the detergent play a direct part in the propagation reaction, or both. It appears unlikely that the micelles merely function as reservoirs to maintain the "true" water phase saturated with monomer.

Rate of Polymerization of Styrene in Solutions of Dodecylamine Hydrochloride

Rates at 50° in 0.093 *M* DDA·HCl solution rates were measured employing the initial styrene concentrations and persulfate concentrations indicated in Table IV. In Figure 4, the rate curves are presented. In Figure 5, $x/a(a - x)$ is plotted against t.

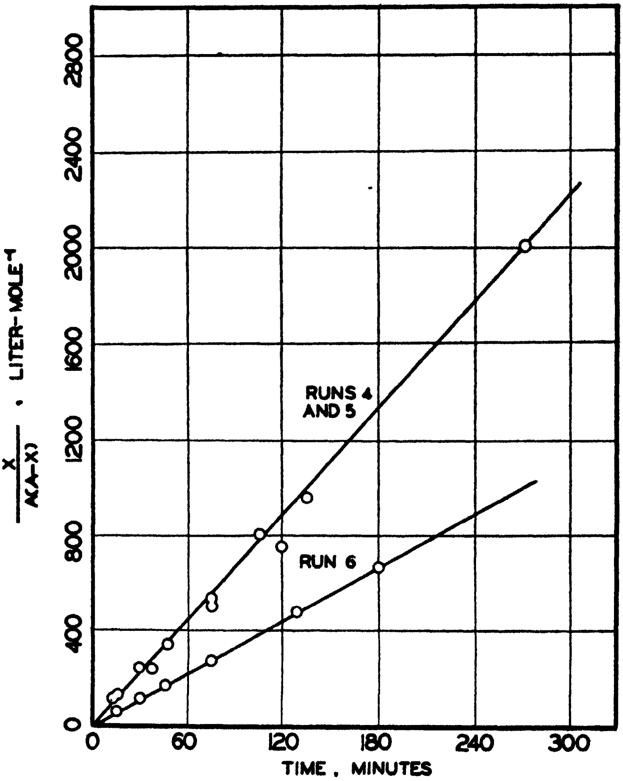

Fig. 5. Polymerization of styrene in 0.093 *M* aqueous dodecylamine hydrochloride solution; 50°. Test of second-order reaction.

Rates have also been measured at 40°, using concentrations of styrene and persulfate indicated in Table V. The rate curves are presented in Figure 6, and in Figure 7 $x/a(a - x)$ is plotted against t.

TABLE IV

RATE CONSTANTS FOUND IN 0.093 *M* DDA·HCl AT 50°

Run	Persulfate concn., mole/liter	Styrene concn., mole/liter	Second-order rate constant, liter/mole/min.
4	0.00620	0.00223	7.40
5	0.00620	0.00392	7.40
6	0.00154	0.01620	3.83

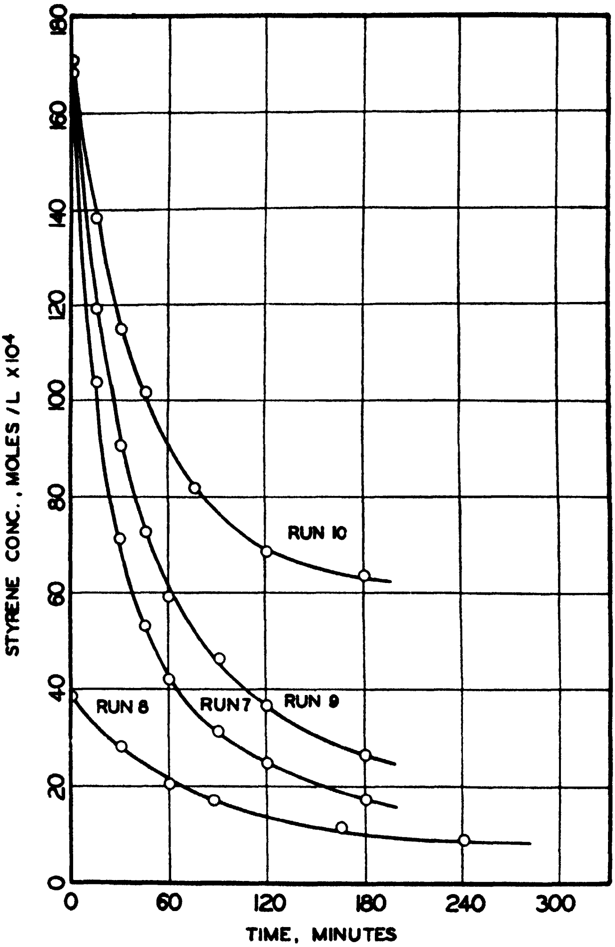

Fig..6. Polymerization of styrene in 0.093 *M* dodecylamine hydrochloride at 40°. Runs 7, 8: 1× $K_2S_2O_8$. Run 9: $^1/_4$× $K_2S_2O_8$. Run 10: $^1/_{16}$× $K_2S_2O_8$.

It will be observed that the rates of polymerization in the DDA·HCl solution are, as in water alone, proportional to the square of the monomer concentration and to the square root of the persulfate concentration. By comparison of the rate constants in Table IV to those in Table III, it

TABLE V

RATE CONSTANTS FOUND IN 0.093 *M* DDA·HCl AT 40°

Run	Persulfate concn., mole/liter	Styrene concn., mole/liter	Second-order rate constant, liter/mole/min.
7	0.00620	0.0166	2.92
8	0.00620	0.00386	3.48
9	0.00154	0.0168	1.75
10	0.000385	0.0171	0.845

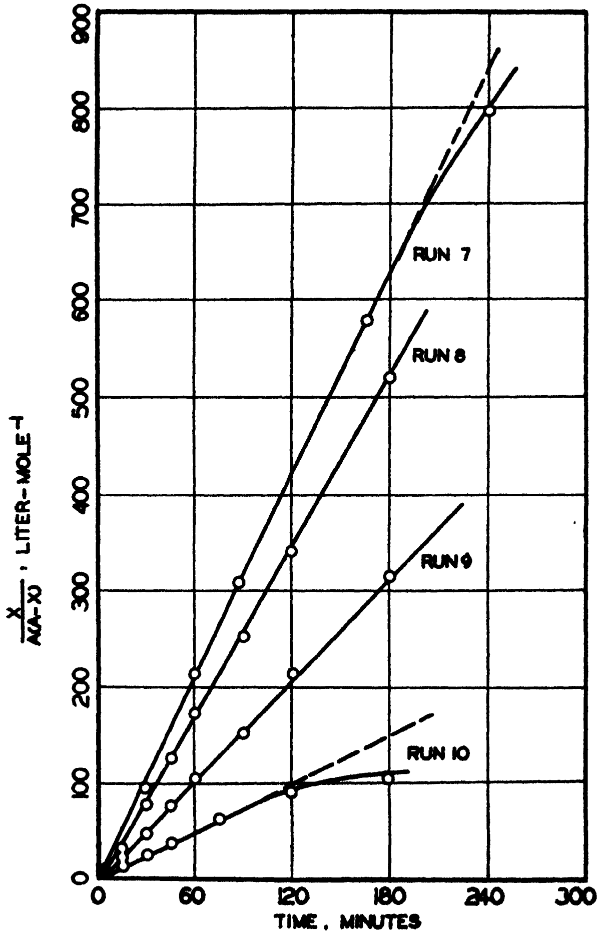

Fig. 7. Rates of polymerization of styrene in 0.093 *M* dodecylamine hydrochloride at 40°. Test of second-order reaction. Runs 7, 8: 1× $K_2S_2O_8$. Run 9: $^1/_4$× $K_2S_2O_8$. Run 10: $^1/_{16}$× $K_2S_2O_8$.

will be observed that the rate constants in DDA·HCl solution are about 68% of those in water solution.

In the emulsion polymerization of styrene at 50° with 0.093 *M* DDA·

HCl and 1× persulfate, the initial rate should be given by an extrapolation of the rates found in Runs 4 and 5 (Table IV) to a styrene concentration of 0.091 *M* (corresponding to the saturation of the emulsifier solution with styrene). We thus expect the emulsion rate to be:

$$7.4 \times (0.091)^2 \times 60 = 3.68 \text{ moles/liter/hour}$$

which is in good agreement with the observed rate at 50° of 3.54 moles/liter/hour.

This suggests, as seems reasonable, that the polymerization mechanism is *initially* the same in emulsion polymerization with excess of styrene as when all the styrene is dissolved in the emulsifier solution. The polymerization of styrene in DDA·HCl solution seems to be second-order over at least a 100-fold range of styrene concentration.

Rate of Polymerization of Styrene in Solutions of Fatty Acid Emulsifiers

An investigation has also been made of the rates of polymerization of styrene in solutions of fatty acid soaps. It has been found that the rates

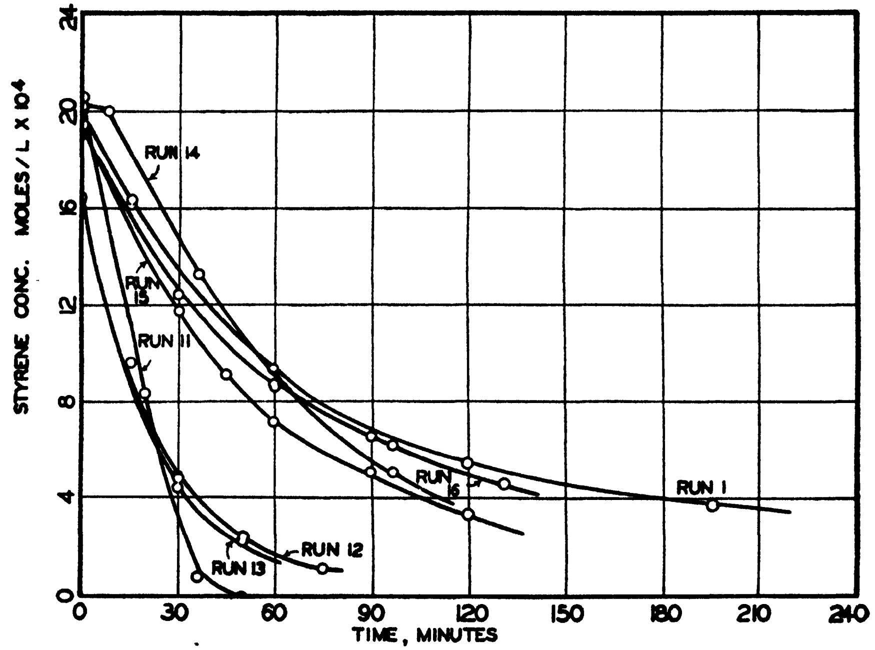

Fig. 8. Polymerization of styrene in solutions of fatty acid soap emulsifiers at 50° with 0.0062 *M* (1×) $K_2S_2O_8$. Run 1: No emulsifier. Run 11: 0.093 *M* K palmitate. Run 12: 0.0187 *M* K palmitate. Run 13: 0.0187 *M* K laurate. Run 14: 0.0047 *M* K laurate. Run 15: 0.093 *M* Na acetate. Run 16: 0.031 *M* Na_2HPO_4.

are considerably faster than in the presence of DDA·HCl under otherwise equivalent conditions. At 50°, the initial rates are too great for accurate measurement, but some approximate data have been obtained using potassium palmitate and potassium laurate. The rate curves are shown in Figure 8, in which the curve for Run 1 (water alone) is reproduced for comparison. It will be observed that whereas the presence of 0.093 *M* DDA·HCl somewhat retards the polymerization, compared to water alone, the presence of 0.093 *M* potassium palmitate increases the rate very markedly, while even 0.0187 *M* potassium palmitate and 0.0187 *M* potassium laurate produce increases of 2 to 3 fold. The rate of disappearance of styrene in Runs 12 and 13 is not second-order with respect to styrene, but is approximately first-order with a rate constant of 0.037 min.$^{-1}$ For Run 11, a first-order rate constant of 0.05 min.$^{-1}$ is found.

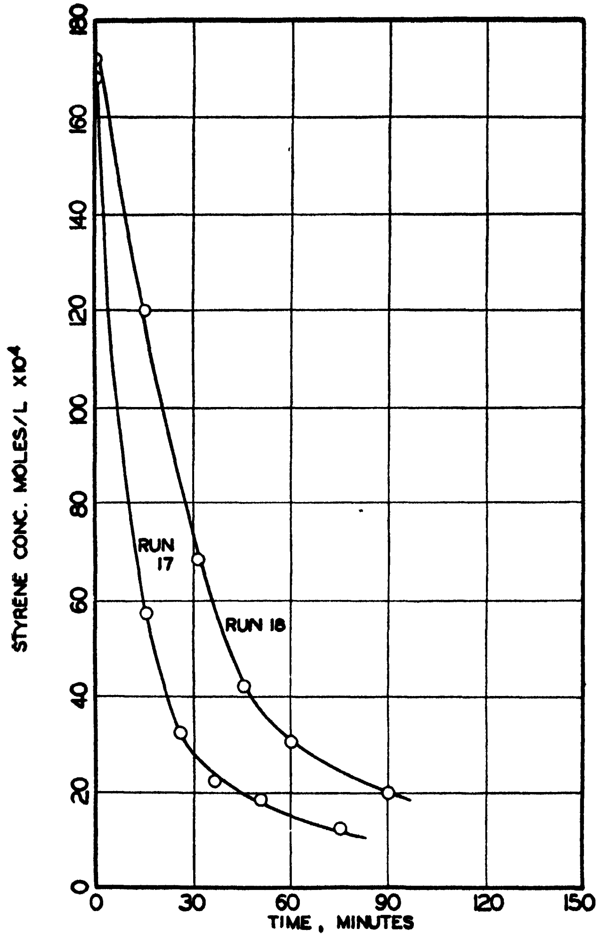

Fig. 9. Polymerization of styrene in 0.093 *M* K palmitate at 40°. Run 17: 1× $K_2S_2O_8$. Run 18: $^1/_4$× $K_2S_2O_8$.

Because not only the rate but the order of the reaction is changed by addition of the fatty acid soaps, it appears that these substances increase the rate of production of free radicals by a chemical interation with the persulfate. Independent evidence demonstrating such interactions has been obtained in this laboratory.[11] Such an effect may also occur in DDA·HCl solutions, but to a smaller degree. Run 15 shows that 0.093 *M* sodium acetate (*p*H 8.8) has only a small accelerating effect, while Run 16 shows that in 0.031 *M* disodium phosphate (*p*H 9.5; ionic strength is 0.093 *M*, the same as in 0.093 *M* sodium acetate), which is not conceivably subject to chemical attack by persulfate, the rate is essentially the same as in pure water. The interaction of persulfate with the carboxylate group in sodium acetate evidently has at most a small effect on the polymerization.

The presence of 0.0047 *M* potassium laurate (critical concentration: 0.02 *M*) has only a small effect on the rate. It is of particular interest that at a concentration of 0.0187 *M*, potassium laurate and potassium palmitate accelerate the rate to the same degree, in spite of the fact that the potassium palmitate solution (critical concentration about 0.001 *M*) is almost entirely micellized, whereas the potassium laurate is almost entirely unmicellized. The micelles as such apparently do not play an important role in this effect.

The rates of polymerization of styrene in 0.093 *M* potassium palmitate at 40° have also been measured. The rate curves are shown in Figure 9. The form of the curves in general resembles that of those observed in the presence of 0.093 *M* DDA·HCl, but the rates are more than twice as great. Exact comparison is difficult, however, because the curves of Figure 9 obey no simple kinetic law, being neither first nor second order, although more nearly the former. Observed qualitatively, the difference between the reaction curves in DDA·HCl and in potassium palmitate appears to be that in the latter case the period of rapid polymerization extends to higher conversions before the reaction begins to "die out."

Effect of Persulfate Concentration on Molecular Weight of Polymer Formed in DDA·HCl Solution and Water

The effect of the persulfate concentration on the molecular weight of the polymer formed in DDA·HCl was measured. Polymers formed in Runs 6, 7, 9, and 10 were isolated by liberating the free dodecylamine by addition of potassium hydroxide, dissolving the amine by addition of alcohol, and filtering the polymer on a sintered glass crucible. The intrinsic viscosities were determined in benzene at 25.0°, and are tabulated in Table VI. The intrinsic viscosity – molecular weight relationship is

TABLE VI

MOLECULAR WEIGHT OF POLYSTYRENE FORMED IN 0.093 *M* DDA·HCl

Run	Temp., °C.	Persulfate concn.	$[\eta]_{25}$	$\bar{P}_n$
6	50	0.00155 *M*, $^1/_4\times$	0.64	625
7	40	0.0062 *M*, $1\times$	0.55	505
9	40	0.00155 *M*, $^1/_4\times$	1.33	1540
10	40	0.000385 *M*, $^1/_{16}\times$	1.84	2280

that of Ewart *et al.*[12] $\bar{P}_n$ is the number-average degree of polymerization, taken as one-half the degree of polymerization indicated by the Ewart data.

It is seen that the molecular weights are approximately in the inverse ratio of the square roots of the persulfate concentrations, although $\bar{P}_n$ increases somewhat more rapidly than does $(C)^{1/2}$.

The polymer formed in water solution was also isolated by reacting ten liters of a solution initially 0.0024 *M* in styrene and 0.0019 *M* in potassium persulfate at 50°C. When polymerization was complete, the excess persulfate was destroyed with hydroxylamine hydrochloride and the polymer isolated by evaporation, followed by purification by dissolving in toluene and precipitation in a large volume of methanol. The intrinsic viscosity (in benzene at 25°) was found to be 0.49, corresponding to $\bar{P}_n = 456$.

Estimation of Rates of Activation of Styrene in Water and Detergent Solutions

From the data of Table III, it is easily calculated that the initial rate of polymerization (essentially equal to the rate of propagation) under the conditions of the experiment described immediately above, in which the polymer was isolated, *i.e.*, 0.0024 *M* initial styrene concentration, 0.0019 *M* potassium persulfate, and 50° reaction temperature, without detergent, is 21.0×10^{-4} mole per liter per hour. Since it was only possible, because of experimental limitations, to measure the molecular weight of the polymer produced over the entire reaction period, it is necessary to employ the average rate of polymerization over this period. From this, the *average rate of initiation* over this period can be obtained (assuming disporportionation of recombining radicals) as the average rate of propagation divided by the average degree of polymerization of the polymer. Since the rate varies as $(M)^2$, we have:

$$\left(\frac{\overline{d(\mathrm{R})}}{dt}\right) = k_2 \frac{\int_{(\mathrm{M})_0}^{(\mathrm{M})_t} (\mathrm{M})^2 d(\mathrm{M})}{\bar{P}_n \int_{(\mathrm{M})_0}^{(\mathrm{M})_t} d(\mathrm{M})} = \frac{k_2}{3\bar{P}_n} \frac{(\mathrm{M}_0)^3 - (\mathrm{M}_t)^3}{(\mathrm{M}_0) - (\mathrm{M}_t)} \tag{1}$$

which in the case of a reaction carried to completion becomes:

$$\left(\frac{\overline{d(\mathrm{R})}}{dt}\right) = \frac{1}{3}\left(\frac{d(\mathrm{M})}{dt}\right)_0 \Big/ \bar{P}_n \tag{2}$$

where $(\overline{d(\mathrm{R})}/dt)$ is the average rate of initiation and $(d(M)/dt)_0$ is the initial rate of polymerization. Substituting the experimental data we find:

$$\left(\frac{\overline{d(\mathrm{R})}}{dt}\right) = \frac{1}{3}\,\frac{21.0 \times 10^{-4}}{4.56 \times 10^{2}} = 0.15 \times 10^{-5} \text{ mole/liter/hour}$$

When the persulfate concentration is 1 × (0.0062 *M*), the rate of radical production will be approximately:

$$0.5 \times 10^{-5} \text{ mole/liter/hour at } 50°$$

It is not known at present how this rate depends upon the styrene concentration. Because we are satisfied at the present time to obtain only the order of magnitude of this rate, we shall employ the above average figure as the rate of activation of styrene in water in the presence of 1× persulfate. In this calculation, chain transfer with monomer has not been considered.

Confirmation of the order of magnitude of this figure is obtained from induction period experiments with *p*-benzoquinone as inhibitor. In principle, measurement of induction periods produced by *p*-benzoquinone in the absence of emulsifier should give an estimate of the rate of activation under these conditions.[8] In practice, however, the rate of polymerization in the absence of emulsifier is too small for the end of the induction period to be distinctly observed. Therefore, the expedient has been employed of injecting $^1/_2$× dodecylamine hydrochloride (DDA·HCl) in the form of a concentrated solution in water after various times to each of a series of bottles containing initially $^1/_2$× persulfate and 0.01 millimole *p*-benzoquinone per 100 g. of monomer. It is found that at 50°, after 12.5 hours reaction time in the absence of emulsifier, the induction period produced by the unreacted quinone, after injection of DDA·HCl, is only 0.18 hour, which is 9% of the value 2.0 hours observed when the emulsifier is present from the start. Accordingly, 91% of the original quantity of *p*-benzoquinone must have reacted in 12.5 hours. This corresponds to a rate of activation (remembering that the volume of the aqueous phase is 180 ml.) of:

$$0.01 \times 10^{-3} \times 0.91 \times 1/12.5 \times 1000/180 = 0.8 \times 10^{-5} \text{ mole/liter/hour}$$

in the presence of $^1/_2$× persulfate, or 1.6×10^{-5} mole/liter/hour in the presence of 1× persulfate. If the quinone disappears also by some competing reactions during this period, this estimate will be higher than the true rate of activation.

Previously, it has been deduced[8] from the length of the induction period produced by *p*-benzoquinone that in a 1× dodecylamine hydrochloride, 1× persulfate recipe at 50°, the rate of initiation is approximately 11.5×10^{-5} mole/hour/liter of aqueous phase. It appears that the rate of activation is much increased by the presence of dodecylamine hydrochloride as emulsifier.

The average rates of initiation in 0.093 *M* DDA·HCl at 40 and 50° with $^1/_4$× persulfate can also be approximately calculated from the molecular weights of Table VI and the initial rates of polymerization from the data in Tables IV and V, using the last expression in equation (1) above. From Run 9, we find:

$$\left(\frac{d(\mathrm{R})}{dt}\right)_{40^\circ} \begin{aligned} &= 0.77 \times 10^{-5} \text{ mole/liter/hour at } {}^1/_4\times \text{ persulfate} \\ &= \text{or } 3.08 \times 10^{-5} \text{ mole/liter/hour at } 1\times \text{ persulfate} \end{aligned}$$

From Run 6, we find:

$$\left(\frac{d(\mathrm{R})}{dt}\right)_{50^\circ} \begin{aligned} &= 3.52 \times 10^{-5} \text{ mole/liter/hour at } {}^1/_4\times \text{ persulfate} \\ &= \text{or } 14.1 \times 10^{-5} \text{ mole/liter/hour at } 1\times \text{ persulfate} \end{aligned}$$

This last value is of the same order of magnitude as that deduced from induction period experiments for emulsion polymerization at 50° with 1× persulfate. It appears from this that the rate of initiation in DDA·HCl solution cannot be proportional to the concentration of dissolved styrene, for in emulsion the concentration of styrene in the aqueous layer (including the micelles) is almost 0.1 *M* at 50°, whereas in the present experiments it is only about $^1/_6$ of this value. In this connection the fact reported elsewhere,[8] that the induction period produced by quinone in emulsion polymerization is insensitive to the DDA·HCl concentration and therefore to the concentration of solubilized styrene, substantiates the above conclusion.

Unfortunately, it has not been possible to make a direct comparison of the rates of activation with and without detergent under otherwise identical conditions because of the difficulty of isolating a very small quantity of polymer in the presence of much emulsifier.

From the rate constants for the polymerization of styrene in 0.093 *M* DDA·HCl at 40 and 50° we find an apparent over-all activation energy of 15,750 cal. per mole. From the above rates of initiation, we find an activation energy for the initiation step of 30,600 cal. per mole. This is in reasonable agreement with the value of 30,600 cal. per mole deduced from quinone induction periods.[8]

DISCUSSION

It is not known at present whether the second-order form of the polymerization of styrene in DDA·HCl solutions and in water is of fundamental significance, or the result of secondary factors, such as the formation of polymer particles in the system as the reaction proceeds. However, it does not seem likely that the formation of polymer particles is a major factor under the conditions of the present experiments, because the rate constants are practically the same (compare Runs 4 and 5 or 7 and 8) over as much as a 5-fold range of initial styrene concentrations. Thus, the initial rate of Run 8 is very nearly the same as the rate of Run 7 when the styrene concentration in Run 7 has become equal to the initial concentration in Run 8, despite the accumulation of polymer in Run 7 at this point. This seems to us to indicate very strongly that the reaction may be properly treated as a homogeneous one. In this connection, it is of interest that whereas in water alone or in the presence of sodium acetate or disodium phosphate the reaction mixture becomes very turbid as conversion proceeds, in DDA·HCl solution no perceptible turbidity appears even when five times as much polymer is present per unit volume as in the reactions in the absence of emulsifiers. The particles formed in solutions of emulsifiers under these conditions are evidently very small and considerably smaller than those formed in water without emulsifier.

The fact that the rates of polymerization in water and DDA·HCl solutions are accurately proportional to the square root of the persulfate concentration and that the molecular weights of the polymers formed are inversely proportional to the square root of the persulfate concentration furnishes good evidence of "normal" bimolecular radical termination.

The elucidation of the exact nature of the initiation step and of the role (probably both chemical and physical) played by the detergent must await further investigation.

References

1. W. D. Harkins, *J. Am. Chem. Soc.*, **69,** 1370 (1947).
2. R. E. Ewart and W. V. Smith, *J. Chem. Phys.*, **16,** 592 (1948).
3. R. G. R. Bacon, *Trans. Faraday Soc.*, **42,** 140 (1946).
4. J. H. Baxendale, M. G. Evans, and G. S. Park, *ibid.*, **42,** 155 (1946).
5. J. H. Baxendale, M. G. Evans, and J. K. Kilham, *ibid.*, **42,** 688 (1946).
6. L. B. Morgan, *ibid.*, **42,** 169 (1946).
7. V. J. Frilette and W. P. Hohenstein, *J. Polymer Sci.*, **3,** 22 (1948).
8. F. A. Bovey and I. M. Kolthoff, "Studies of Retarders and Inhibitors in the Emulsion Polymerization of Styrene. II. Inhibitors," *ibid.*, **5,** in press (1950).
9. I. M. Kolthoff and F. A. Bovey, *Ind. Eng. Chem., Anal. Ed.*, **19,** 498 (1947).
10. H. E. Morris, R. B. Stiles, and W. H. Lane, *ibid.*, **18,** 294 (1946). W. H. Lane, *ibid.*, **18,** 295 (1946).
11. I. K. Miller, *unpublished observations.*
12. R. Ewart, C. Roe, H. Tingey, and M. Wales, *private communication;* referred to by W. V. Smith, *J. Am. Chem. Soc.*, **68,** 2063 (1946); **71,** 4077 (1949); see F. A. Bovey and I. M. Kolthoff, "Studies of Retarders and Inhibitors in the Emulsion Polymerization of Styrene. II. Inhibitors," *J. Polymer Sci.*, **5,** in press (1950), reference 11.

English Synopsis, see Summaries, page S22, Vol. V, 1950.

Résumé

Les vitesses de polymérisation du styrène en solution dans l'eau, et en solution en présence de chlorhydrate de dodécylamine, de palmitate potassique et de laurate de potassium ont été mesurées. En solution dans l'eau et en présence de chlorhydrate de dodécylamine la vitesse de polymérisation est donnée par l'équation

$$-d(\mathrm{M})/dt = K(\mathrm{M})^2(\mathrm{C})^{1/2}$$

où M est la concentration en styrène et C la concentration en persulfate potassique. Cette expression est valide pour une concentration variant de 0.001 à 0.1 *M* dans la solution de chlorhydrate de dodécylamine.

La valeur de *K* en solution de ce chlorhydrate de dodécylamine est légèrement inférieure à celle dans l'eau pure. Les vitesses de polymérisations et les poids moléculaires des polymères obtenus ont été mesurés à 40° et 50° en présence de 0.0062 *M* de persulfate potassique et de 0.093 *M* de chlorhydrate de dodécylamine; les vitesses d'activation ont ainsi été mesurées à 40° et 50°.
Leurs naleurs sont égales à

$$[d(\mathrm{R})/dt]_{40^\circ} = 3.08 \times 10^{-5} \text{ mole/litre/heure}$$

$$[d(\mathrm{R})/dt]_{50^\circ} = 14.1 \times 10^{-6} \text{ mole/litre/heure}$$

La vitesse d'activation est essentiellement indépendante de la concentration en styrène dissous, et est du même ordre de grandeur dans les expériences que dans la polymérisation en émulsion habituelle avec une phase styrènique distincte. La concentration de chlorhydrate de dodécylamine n'a que peu d'effet sur la vitesse d'activation, mais en absence complète d'émulsifiant la vitesse d'activation devient plus faible. Le poids

moléculaire du polymère formé varie inversement proportionnellement à la racine carrée de la concentration en persulfate. En solution en présence de savons d'acides gras, les vitesses de polymérisation du styrène sont plus élevées qu'en solution en présence de chlorhydrate de dodécylamine, et elles ne suivent pas de loi cinétique simple en ce qui concerne la concentration en styrène; elles procèdent toutefois plutôt du 1r que du 2d ordre.

Zusammenfassung

Die Polymerisationsgeschwindigkeiten von Styrol in wässriger Lösung, und in Lösungen von Dodecylaminhydrochlorid, Kaliumpalmitat und Kaliumlaurat wurden gemessen. In wässriger Lösung und in Dodecylamin-hydrochlorid-Lösung ist die Polymerisationsgeschwindigkeit durch:

$$-d(\mathrm{M})/dt = K(\mathrm{M})^2(\mathrm{C})^{1/2}$$

gegeben, worin (M) die Konzentration von Styrol und (C) die Konzentration von Kaliumpersulfat ist. Diese Formel ist für das Konzentrationsbereich 0.001 bis 0.1 *M* in Dodecylamin-hydrochlorid-Lösung gültig. Es wurde gefunden, dass der Wert von *K* in Dodecylamin-hydrochlorid-Lösung etwas geringer ist als in Wasser allein. Durch Messen der Polymerisationsgeschwindigkeit und der Molekulargewichte der Polymeren bei 40° und 50° in Gegenwart von 0.0062 *M* Persulfat und 0.093 *M* Dodecylamin-hydrochlorid wurden die Aktivierungsgeschwindigkeiten bei 40° und 50° gemessen. Diese Geschwindigkeiten sind:

$$[d(\mathrm{R})/dt]_{40°} = 3.08 \times 10^{-5} \text{ Mole/Liter/Stunde}$$

$$[d(\mathrm{R})/dt]_{50°} = 14.1 \times 10^{-5} \text{ Mole/Liter/Stunde}$$

Es wurde gefunden, dass die Aktivierungsgeschwindigkeit im wesentlichen unabhängig von der Konzentration von in Lösung gegangenem Styrol ist. Sie ist von der gleichen Grössenordnung in diesen Versuchen wie in einer normalen Emulsionspolymerisation mit einer getrennten Styrolphase. Die Konzentration von Dodecylamin-hydrochlorid hat kaum eine Wirkung auf die Aktivierungsgeschwindigkeit, aber in vollständiger Abwesenheit von Emulsionsmittel wird die Aktivierungsgeschwindigkeit viel geringer. Es wird gefunden, dass das Molekulargewicht des erhaltenen Polymers im umgekehrten Verhältnis zu der Quadratwurzel der Persulfatkonzentration steht. In Lösungen von Fettsäureseifen sind die Polymerisationsgeschwindigkeiten von Styrol grösser als in Lösungen von Dodecylamin-hydrochlorid, und sie folgen keinem einfachen Kinetik-Gesetz in Bezug auf Styrol, sie sind jedoch der ersten Ordnung näher als der zweiten.

Received July 5, 1949

JOURNAL OF POLYMER SCIENCE VOL. V, NO. 4, PAGES 505–514

Viscosities of Binary Polymeric Mixtures

WILLIAM R. KRIGBAUM and FREDERICK T. WALL, *Noyes Chemical Laboratory, University of Illinois, Urbana, Illinois*

INTRODUCTION

Numerous attempts have been made to relate the viscosity of a binary polymeric mixture to the viscosities of the components.[1–7] Considerable difficulty has been encountered in expressing the viscosity of a single component as a function of its concentration for all but the lowest concentrations. To overcome this difficulty a modification of the power law originally due to Baker[8] was proposed by Hess and Philippoff,[9] *viz.*:

$$\eta_r = \left(1 + \frac{[\eta]}{8} c_g\right)^8 \tag{1}$$

where c_g is the concentration in weight per cent. The constants therein were chosen to give the best fit for data covering a wide concentration range. Philippoff[10] successfully applied equation (1) to mixtures by use of the further relation:

$$[\eta]_m = \sum_i [\eta]_i x_i \tag{2}$$

where x_i is the weight fraction of the *i*th component. He found the agreement with available experimental data was as good or better than that obtained by any of the mixture laws previously proposed.

A relation similar to (1) and (2), but employing volume fractions and concentration in volume per cent, had been suggested by Atsuki and Ishiwara[11] and was found by Shimoda and Uehara[12] to reproduce their measurements on acetylcellulose–nitrocellulose and acetylcellulose–benzylcellulose if the exponent was given the values 7 and 9. Kauppi and Bass[13] rearranged the Philippoff-Hess relation to obtain:

$$(\eta)^{1/8} = K' + Kc_g \tag{3}$$

Results of their investigation of ethylcellulose mixtures of different molecular weights were reported by plotting $(\eta)^{1/8}$ *vs.* c_g. The curves were nonlinear in region of low concentration and showed a sharp break at $c_g = 5\%$, above which all became linear. It was further stated that the same relation held within experimental error for mixtures of ethylcellulose–nitrocellulose. From this result and those of Shimoda and Uehara, Philippoff[14] concluded that the only forces operating in polymer solutions are hydrodynamic in nature, and that no specific forces exist between polymer molecules.

The conclusion that only hydrodynamic forces exist between macromolecules in solution rests upon experimental measurements of mixtures in which the components differ in molecular weight, or at most have only slight dissimilarities in chemical structure. Since specific interactions would not be evident in such solutions, we have undertaken an investigation of polymer mixtures in which the components are widely divergent in chemical nature with the belief that these mixtures might exhibit positive or negative deviations from a reasonably defined ideal behavior. The three mixtures studied are rubber–polystyrene, rubber–ethylcellulose, and ethylcellulose–polyethylene glycol. By restricting measurements to solutions of low concentrations, the viscosity of one component can be represented adequately by:

$$\eta_{sp} = [\eta]c + bc^2 \tag{4}$$

where:

$$[\eta] = \lim_{c\to 0} \eta_{sp}/c \tag{5}$$

It is apparent that $[\eta]$, the value of the reduced viscosity at infinite dilution, is a measure of the polymer–solvent interaction, and that the term involving b arises from polymer–polymer interactions at finite concentrations. In a mixture of polymer types 1 and 2 the total polymer–polymer interactions are given by $c_1(c_1b_{11} + c_2b_{12})$ for type 1 and $c_2(c_1b_{12} + c_2b_{22})$ for type 2. Corresponding to (4) for a single component, there is obtained:

$$\eta_{spm} = [\eta]_1c_1 + [\eta]_2c_2 + b_{11}c_1^2 + 2b_{12}c_1c_2 + b_{22}c_2^2 \tag{6}$$

If this is compared to the analog of (4) for the mixture,

$$\eta_{spm} = [\eta]_m(c_1 + c_2) + b_m(c_1 + c_2)^2 \tag{7}$$

it is found that the Philippoff relation (2) between the intrinsic viscosity of the mixture and those of the components holds; and a further expression is obtained relating the polymer–polymer interaction for the mixture to those of the components, namely:

$$b_m = x_1^2b_{11} + 2x_1x_2b_{12} + x_2^2b_{22} \tag{8}$$

We shall now define an ideal mixture as one for which $b_{12} = (b_{11}b_{22})^{1/2}$, since that renders the various equations simple in form.

It is of interest to compare (4) and (6) with the corresponding expressions obtained by expanding the power law of Philippoff and Hess and retaining only the first three terms for dilute solutions:

$$\eta_{sp}/c = [\eta] + 0.43[\eta]^2c + \ldots \tag{9}$$

A series of this form has been suggested by Huggins[15] and employed by Mark and coworkers[16] in the form:

$$\eta_{sp}/c = [\eta] + k'[\eta]^2c \tag{10}$$

For many linear polymers in good solvents k' takes the value 0.38, although this is by no means always the case. A similar expansion of the Philippoff-Hess power law for a mixture of two components results in:

$$\eta_{spm} = [\eta]_1c_1 + [\eta]_2c_2 + 0.43\{[\eta]_1^2c_1^2 + 2[\eta]_1[\eta]_2c_1c_2 + [\eta]_2^2c_2^2\} \qquad (11)$$

Assuming $0.43[\eta]^2 = b$ requires that $b_{12} = (b_{11}b_{22})^{1/2}$ for every mixture, a result consistent with our definition of ideality.

EXPERIMENTAL

Throughout this work concentration is expressed in grams of solute per 100 ml. solution and kinematic viscosities (designated by ν) are reported.

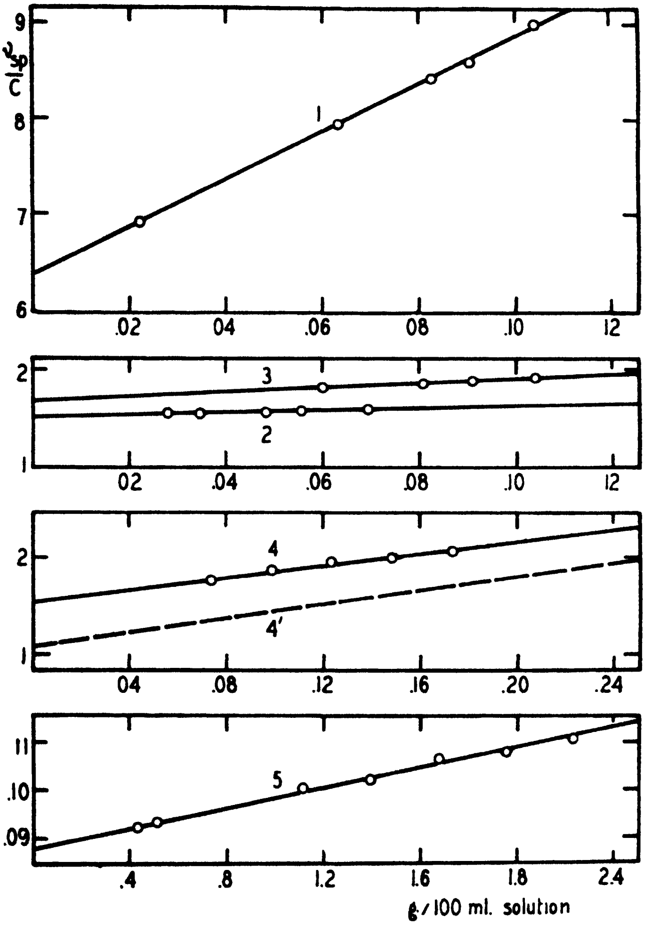

Fig. 1. Reduced kinematic viscosity *vs.* concentration for the polymers: (1) rubber, (2) polystyrene, (3) ethylcellulose A, (4) ethylcellulose B, (5) polyethylene glycol.

These were determined using a Ubbelohde viscometer calibrated against water and benzene. The values for these standard viscosities were taken from *International Critical Tables.* A kinetic energy correction was applied using the formula:

$$\nu = At - B/t \tag{12}$$

in which t is the flow time and the constants A and B were determined by the calibration previously mentioned. The constant temperature bath was maintained at 25° ± 0.003°C. by means of a thyratron relay and a mercury regulator. Several values for each flow time were taken using a free-running stopwatch. After each sample was run, the viscometer was allowed to stand in hot chromate cleaning solution, rinsed thoroughly in distilled water, and dried in an oven.

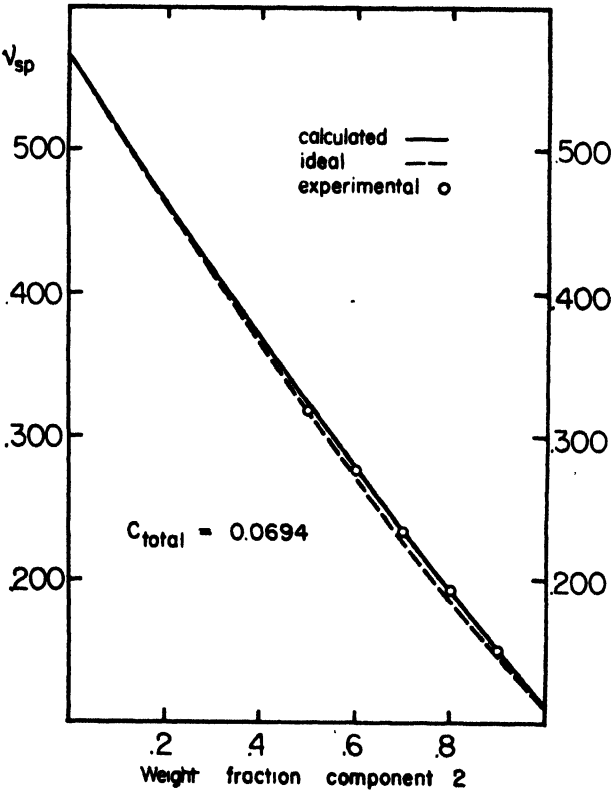

Fig. 2. Specific kinematic viscosity of rubber–polystyrene *vs.* weight fraction polystyrene.

The range of weight fractions investigated was chosen so that each component would make approximately an equal contribution to the specific viscosity of the mixture. For this reason it was impractical to maintain the total polymer concentration constant in the third mixture. Thiophene-free benzene was used as the solvent throughout; the solutions were filtered through a fine screen to remove gel and finally through sintered glass. Concentrations were determined by evaporating duplicate aliquots in aluminum dishes, followed by drying at 60°C. *in vacuo* for twenty hours. Dried ethylcellulose was found to be somewhat hygroscopic; since the viscosity of ethylcellulose in benzene is a function of the amount of water present, it was necessary in the second and third mixtures to determine the viscosity constants for this component from the same solutions used in the mixtures. This effect appears in still another form in the third mixture and will be discussed in detail in the next section.

RESULTS

The reduced kinematic viscosities of the component polymers are given in Table I. These values, plotted against concentration, appear in Figure 1, from which it can be seen that the linear relationship expressed by (4) holds throughout the concentration range investigated. The slopes and intercepts obtained by the method of least squares are given in Table II along with the average per cent error in the specific kinematic viscosities for each component calculated therefrom. Table III contains the meas-

TABLE I

REDUCED KINEMATIC VISCOSITIES OF COMPONENT POLYMERS

Polymer	c	t	ν	ν_{sp}	ν_{sp}/c
Rubber...................	0.10390	372.71	1.3354	0.93839	9.0317
(1)	.09050	342.43	1.2253	.77859	8.6032
	.08245	326.70	1.1681	.69549	8.4353
	.06330	290.45	1.0359	.50369	7.9546
	.02420	227.26	0.80416	.16786	6.9362
Polystyrene.................	0.06955	216.57	0.76523	0.11076	1.5926
(2)	.05564	212.24	.74927	.087602	1.5745
	.04846	210.10	.74138	.076150	1.5642
	.03477	205.94	.72603	.053872	1.5492
	.02782	203.91	.71854	.042993	1.5455
Ethylcellulose A............	0.10388	233.20	0.82638	0.19954	1.9208
(3)	.09080	227.88	.80684	.17116	1.8851
	.08050	223.86	.79206	.14971	1.8598
	.06010	216.29	.76419	.10926	1.8181
Ethylcellulose B............	0.24730	302.67	1.0805	0.56840	2.2984
(4)	.17311	262.82	.93496	.35717	2.0632
	.14838	251.75	.89443	.29830	2.0104
	.12365	240.71	.85395	.23955	1.9373
	.09892	230.48	.81639	.18503	1.8705
	.07419	220.48	.77962	.13166	1.7746
Polyethylene glycol.........	2.2296	242.49	0.86048	0.24903	0.1117
(5)	1.9509	235.19	.83369	.21015	.1077
	1.6722	229.15	.81151	.17794	.1064
	1.3935	222.45	.78687	.14218	.1020
	1.1148	216.85	.76626	.11226	.1007
	0.50994	204.82	.72181	.04774	.0936
	.43709	203.45	.71674	.04039	.0924

TABLE II

EXPERIMENTAL VISCOSITY CONSTANTS FOR COMPONENTS

Component	$[\nu]$	b	Av. % dev. in calcd. ν_{sp}
Rubber (1)	6.306	25.89	0.232
Polystyrene (2)	1.511	1.152	.113
Ethylcellulose A(3)	1 675	2.333	.149
Ethylcellulose B (4)	1.567	2.947	.439
Polyethylene glycol (5)	0.0882	0 0104	.538

TABLE III

SPECIFIC KINEMATIC VISCOSITIES OF MIXTURES

Mixture	No. or c_t	$x\dagger^a$	t	ν	ν_{sp}
Rubber–polystyrene	No. 1	0 5001	255 45	0 9080	0 3180
(1–2†)	2	6001	247 62	8793	.2763
c_t = 0 06954	3	.7001	239 50	.8495	.2331
	4	.8001	231 83	.8214	.1922
	5	9000	224 11	.7930	.1510
Rubber–ethylcellulose A	No. 1	.4870	249 50	.8862	.2863
(1–3†)	2	.5874	242 72	8613	.2503
c_t = 0 0607	3	.6889	235 25	8339	2105
	4	7919	228 71	.8099	.1756
	5	8952	222 26	.7862	.1412
Rubber–ethylcellulose A	No. 1′	.5880	265 01	.9430	3688
(1–3†)	2′	.6894	254 45	.9043	.3127
c_t = 0.0807	3′	.7919	244 29	.8671	.2586
	4′	.8954	234 92	.8327	.2086
Ethylcellulose B–polyethylene glycol	0.5013	5560	280 58	.9999	4514
(4-5†)	.8823	.7898	275 13	.9800	.4225
	.8712	8712	271 77	.9677	.4046
	.9185	.9185	267.90	.9535	.3841
	.9495	.9495	264 38	.9407	.3654
	.9713	.9713	260 52	.9265	.3449

[a] Weight fraction given for component designated by †.

TABLE IV

VALUES OF MIXTURE INTERACTION CONSTANTS

No.	b_{12}	b_{13}	b_{45}
1	5.62	4.36	0.212
2	6.86	5.74	.248
3	6.92	4.21	.272
4	7.71	4.77	.302
5	7.91	4.02	.314
6	—	—	.265
1′	—	3.88	
2′	—	4 44	
3′	—	4.02	
4′	—	4.34	
Average b_{ij}	7.00 ± 0.96	4.41 ± 0.37	0.269 ± 0.027
Ideal $(b_{ii}b_{jj})^{1/2}$	5.46	7 77	0.175

ured specific kinematic viscosities of the mixtures. The values for the first two mixtures are plotted against the weight fraction of one of the components in Figures 2 and 3. A direct plot of the points for ethylcellulose-polyethylene glycol is not possible since the total polymer concentration was not held constant; however, by assigning an arbitrary total concentration and employing each b_{45} at its original weight fraction, the points of Figure 4 were obtained. Substitution of the viscosity constants for the components from Table II and the experimental specific kinematic viscosities of the mixtures from Table III into equation (6) permits calculation of the mixture interaction constant, b_{ij}. Values obtained in this way for the first two mixtures appear in Table IV.

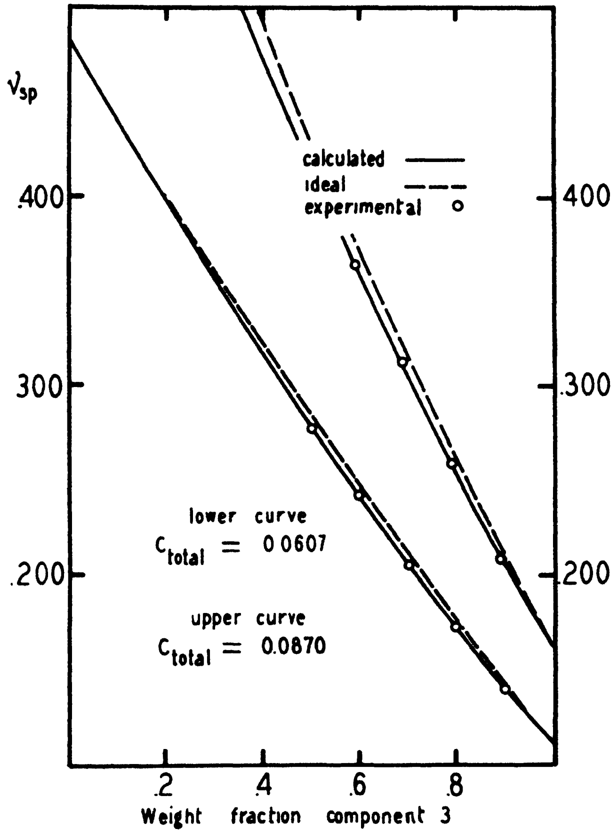

Fig. 3. Specific kinematic viscosity of rubber-ethylcellulose A *vs.* weight fraction ethylcellulose A for two total polymer concentrations.

The interaction constant so obtained for the mixture ethylcellulose-polyethylene glycol is not constant, but decreases and becomes negative as the weight fraction of ethylcellulose is increased. This apparently anomalous behavior is related to the ability of ethylcellulose to coordinate in benzene solution. As pointed out by Suida,[17] the presence of traces of moisture decreases the viscosity of ethylcellulose in benzene. Staudinger and Reinecke[18] repeated the experiments of Suida and concluded that ethylcellulose does not dissolve as macromolecules; instead, they believe that benzene exerts solvent action only on the organic residue of the cellulose molecule, leaving the unethylated carboxyl groups free to coordinate.

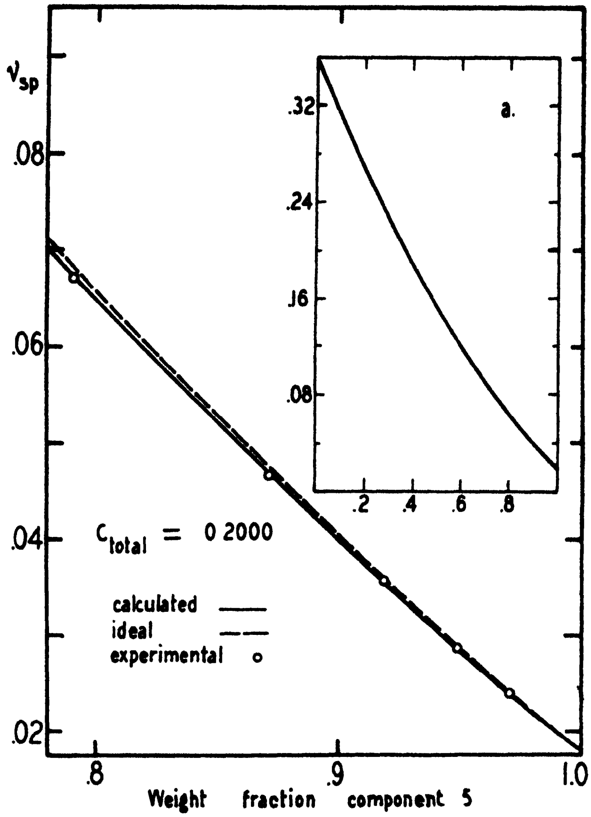

Fig. 4. Specific kinematic viscosity of ethylcellulose B – polyethylene glycol *vs.* weight fraction polyethylene glycol over the experimental range. Inset (4a): calculated mixture curve for the same total concentration over the entire weight fraction range.

They checked this assumption by acetylating the remaining carboxyl groups and found that addition of water up to the saturation value had no effect on the viscosity of ethylacetylcellulose in benzene. Okamura[19] reported viscosities of ethylcellulose two to three times higher in benzene than in *m*-cresol or chloroform solutions. He also found that an increase in temperature resulted in a more rapid decrease in viscosity when benzene was the solvent. Then, in brief, benzene exerts solvent action on the organic residue of the cellulose molecule, allowing some of the unethylated hydroxyls to coordinate; however, the resulting high viscosity is reduced upon addition of a polar compound which breaks the coordinate links. This is precisely what is accomplished by addition of polyethylene glycol.

If it is assumed that $[\nu]_4$ and b_{44} for ethylcellulose decrease linearly with x_5, the weight fraction of polyethylene glycol,

$$[\nu]_4' = [\nu]_4 - \rho_4 x_5 \qquad (13)$$

$$b_{44}' = b_{44} - \omega_4 x_5 \qquad (14)$$

then equation (6) may be rewritten as:

$$\nu_{pm} - [\nu]_4 c_4 - [\nu]_5 c_5 - b_{44}c_4^2 - b_{55}c_5^2 = 2b_{45}c_4c_5 - x_5(\rho_4 c_4 + \omega_4 c_4^2) \qquad (15)$$

The value of ρ_4 and ω_4 obtained from the mixture viscosities by the method of least squares were $\rho_4 = 0.788$ and $\omega_4 = 0.151$, corresponding to $[\nu]_4' = 1.567 - 0.788x_5$ and $b_{44}' = 2.947 - 0.151x_5$. Substitution of these values into (15) gave the values of the interaction constant for the third mixture which appear in Table IV. The calculated and ideal curves of Figures 2, 3, and 4 were obtained by use of the average b_{ij} for each mixture, or the ideal value, $(b_{ii}b_{jj})^{1/2}$.

DISCUSSION

It has been possible by means of the measurements described to obtain values of the interaction constant b_{ij} for the three mixtures investigated. These constants, appearing in Table IV, are to be compared with the ideal value $(b_{ii}b_{jj})$,$^{1/2}$ keeping in mind that b_{ij} represents the interaction between i and j type polymer molecules. Although b_{12} for rubber–polystyrene appears to increase as the weight fraction of polystyrene is increased, the other mixtures show no such trend. It is evident from the values of b_{13} for two sets of rubber–ethylcellulose mixtures that the interaction constant is independent of the total polymer concentration. The average error is given in Table IV, the probable error being approximately 0.7 times this value.

The interaction constant b_{12} for rubber–polystyrene is somewhat larger than ideal. The reason for this deviation is not immediately apparent. On the other hand, rubber–ethylcellulose exhibits a considerable negative deviation, which is to be expected from the extreme differences in their chemical natures and in their physical behaviors in various solvents.[20] Ethylcellulose–polyethylene glycol shows a large positive deviation. Apparently polyethylene glycol and ethylcellulose attract each other probably through hydrogen bonding, which results in an increased mixture interaction.

For polymer mixtures differing only in molecular weight the interaction constant would presumably take the ideal value. The applicability of the Philippoff relation to the data previously available is thereby explained, since the interaction constant is tacitly assumed to have the ideal value. This effectively gives a first approximation to the viscosity of the mixture, an approximation which is very good when the polymers are similar and becomes poorer as the dissimilarities in the components become more marked. For the first two mixtures the average error in ν_{sp_m} as calculated by the Philippoff relation was 2.9%; whereas the error using (6) was but 0.3%, or about the accuracy with which the specific viscosity of the component polymers could be calculated by use of the least square viscosity constants appearing in Table II.

References

1. H. G. Bungenberg de Jong and W. A. L. Dekker, *Biochem. Z.*, **212**, 318 (1929).
2. H. G. Bungenberg de Jong and O. S. Gwan, *ibid.*, **221**, 166 (1930).
3. H. G. Bungenberg de Jong and W. A. L. Dekker, *Kolloid-Beihefte*, **43**, 143 (1935).
4. H. Finkentscher and H. Mark, *Kolloid-Z.*, **49**, 135 (1929).
5. J. Duclaux, and E. Wollmann, *Bull. soc. chem. France*, **27**, 414 (1920).
6. W. Kumichel, *Kolloid-Beihefte*, **26**, 161 (1928).
7. H. J. Rocha, *ibid.*, **30**, 230 (1930).
8. F. Baker, *J. Chem. Soc., London*, **103**, 1653 (1913).
9. K. Hess, and W. Philippoff, *Ber.*, **70**, 639 (1937).
10. W. Philippoff, *ibid.*, **70**, 827 (1937).
11. K. Atsuki and M. Ishiwara, *J. Soc. Chem. Ind. Japan*, **33**, 508B (1930).
12. I. Shimoda and S. Uehara, *Cellulose Ind.* (*Tokyo*), **13**, 75 (1937).
13. T. A. Kauppi and S. L Bass, *Ind. Eng. Chem.*, **29**, 800 (1937).
14. W. Philippoff, *Viscosität der Kolloide.* Steinkopff, Dresden, 1942, p. 334.
15. M. L. Huggins, *J. Am. Chem. Soc.*, **64**, 2716 (1942).
16. T. Alfrey, A. Bartovics, and H. Mark, *ibid.*, **65**, 2319 (1942).
17. H. Suida, *Cellulosechemie*, **12**, 310 (1931).
18. H. Staudinger and F. Reinecke, *Ann.*, **535**, 71 (1938).
19. I. Okamura, *Cellulosechemie*, **14**, 135 (1933).
20. T. Alfrey, *J. Colloid Sci.*, **2**, 99 (1947).

English Synopsis, see Summaries, page S11, Vol. V, 1950.

Résumé

Les viscosités spécifiques cinématiques, en solutions diluées, sont données pour trois mélanges, et pour les composants purs correspondant. Les résultats sont rapportés à l'équation

$$\nu_{sp_m} = [\nu]_1 c_1 + [\nu]_2 c_2 + b_{11} c^2 + 2 b_{12} c_1 c_2 + b_{22} c_2^2$$

et les valeurs résultants de la constante d'interaction b_{12} est comparée à la valeur idéale $(b_{11} b_{12})^{1/2}$. Les mélanges de polymères non-semblables manifestant des déviations de l'idéalité positives ou négatives; on essaie de relier ces déviations aux propriétés physiques et aux structures chimiques des composants. La loi des mélanges de Philippoff suppose de façon tacite, un mélange idéal, et, de ce fait ne donne qu'une première approximation de la viscosité du mélange, lorsque les composants sont dissemblables.

Zusammenfassung

Spezifische kinematische Viskositäten in verdünnten Lösungen werden für drei Mischungen und die entsprechenden reinen Komponenten angegeben. Die Daten wurden in die Folgende Gleichung eingesetzt

$$\nu_{sp_m} = [\nu]_1 c_1 + [\nu]_2 c_2 + b_{11} c_1^2 + 2 b_{12} c_1 c_2 + b_{22} c_2^2$$

und die erhaltenen Werte der Interaktionskonstante b_{12} wurden mit dem Idealwert $(b_{11} b_{22})^{1/2}$ verglichen. Es wird gezeigt, dass Mischungen von unähnlichen Polymeren positive oder negative Abweichungen vom Idealwert aufweisen, und es wird der Versuch gemacht, diese Abweichungen mit den physikalischen Eigenschaften und der chemischen Struktur der Komponenten in Verbindung zu bringen. Es wird gezeigt, dass das Philippoff-Mischungs-Gesetz schweigend ein ideales Mischen voraussetzt und deshalb nur eine erste Annäherung an die Mischungsviskosität gibt, wenn die Komponenten ungleichartig sind.

Received July 5, 1949

LETTERS TO THE EDITORS

Degradation of High Polymers

In two recent communications under the above title,[1,2] expressions are presented for the dependence on time of the number-average polymerization degree P_n of a randomly degrading system. The integrated form of these equations can be written as:

$$\frac{P_n - 1}{P_n} = \frac{P_0 - 1}{P_0} e^{-kt}$$

where P_0, is the initial DP and k the first-order rate constant for breakage of links.

It may be worth while to point out that this result has already been given some time ago.[3] As has been indicated,[4] and as it should, it follows also from the general kinetic and statistical theories of depolymerization.

References

1. E. F. Casassa, *J. Polymer Sci.*, **4**, 405 (1949).
2. H. H. G. Jellinek, *ibid.*, **5**, 264 (1950).
3. M. L. Wolfrom, J. C. Sowden, and E. N. Lassettre, *J. Am. Chem. Soc.*, **61**, 1072 (1939).
4. R. Simha, *J. Applied Phys.*, **12**, 569 (1941); see equations (3′), (4a), and following. M_n should be replaced by M_n/M_0 in (4a).

ROBERT SIMHA

National Bureau of Standards
Washington, D. C.

Received May 1, 1950

Catalysis of the Dechlorination by Zinc

Flory,[1] Wall,[2,3] Marvel,[4,5] and Merz[6] have made theoretical and experimental studies of the removal of substituents from vinyl polymers and copolymers. During a study of reactions of this type,[7] specifically those between zinc and dilute dioxane solutions of polyvinyl chloride and vinyl chloride-vinyl acetate copolymers, it has been observed that dechlorination often proceeds slowly or not at all. All conversion curves obtained by following the formation of zinc chloride show induction periods. The addition of small amounts of zinc chloride at the start of the reactions has resulted in disappearance of the induction periods and considerable increases in rate. Whether or not this is a true case of autocatalysis has not been determined.

Immediate application to simpler organic reactions was undertaken. No reaction takes place between zinc and dioxane solutions of 1,3-dichloropropane and 1,2-dichloroethane[8] at 100°C. However, in the presence of an initial amount of zinc chloride, dechlorination proceeds at a measurable rate. Recently, Cohen, Wolosinski, and Scheuer[9] observed that the reaction between zinc and α,β-dichloro-α,β,β-trifluoroethylbenzene is greatly facilitated in the presence of a small amount of zinc chloride and yields α,β,β-trifluorostyrene.

Thus, the Freund and Frankland reactions, which ordinarily involve the removal of 1,2- or more widely separated bromine atoms by means of zinc, may be extended to dichlorides by the use of zinc chloride. This immediately suggests alternative methods for the preparation of olefins, cyclic compounds, and unsaturated polymeric materials.

References

1. P. J. Flory, *J. Am. Chem. Soc.*, **61**, 1518 (1939).
2. F. T. Wall, *ibid.*, **62**, 803 (1940).
3. F. T. Wall, *ibid.*, **63**, 821 (1941).
4. C. S. Marvel, J. H. Sample, and M. F. Roy, *ibid.*, **61**, 3241 (1939).
5. C. S. Marvel, G. D. Jones, T. W. Mastin, and G. T. Schertz, *ibid.*, **64**, 2356 (1942).
6. E. Merz, T. Alfrey, and G. Goldfinger, *J. Polymer Sci.*, **1**, 75 (1946).
7. Ph.D. Thesis, unpublished results, Polytechnic Institute of Brooklyn, 1949.
8. C. Lewis, private communication.
9. S. G. Cohen, H. T. Wolosinski, and P. J. Scheuer, *J. Am. Chem. Soc.*, **71**, 3439 (1949).

HOWARD C. HAAS*

Institute of Polymer Research
Polytechnic Institute of Brooklyn
Brooklyn, New York

Received June 19, 1950

* Present address: Polaroid Corporation, Cambridge, Massachusetts.

REVIEWS

Proceedings of the Second Rubber Technology Conference, 1948. T. R. DAWSON, C. M. BLOW, and G. GEE, eds., Heffer, Cambridge (Rubber Age, New York), 1949, 523 pp., $13.00.

The Second Rubber Technology Conference held under the auspices of the Institution of the Rubber Industry in London, England, on June 23–25, 1948, was patterned after a similar meeting in London in 1938. The proceedings of the second conference, issued in the same format as those of the first conference, represent an important contribution to the literature on rubber. Of the 43 papers presented, 19 originated in the United Kingdom, 11 in the United States, 6 in the Netherlands, 2 in the Netherlands East Indies, 2 in Germany, and 1 each in France, Canada, and Malaya.

The opening session consisted of six papers, each dealing with a different type of synthetic rubber. These included butadiene-styrene copolymers, nitrile rubbers, silicone rubber, condensation rubbers, butyl rubber, and neoprene.

The session devoted to the chemistry of rubber included work on the nature of sulfur linkages in rubber-sulfur vulcanizates, a novel method for hydrochlorinating rubber in the latex form, an analytical study of rubber halides, and three papers relating to the oxidation of rubber.

Papers relating to the physics of rubber described work on refractive index as a function of wavelength, osmometry, crystallization, free retraction and permanent set, and included as well two papers dealing with the application of physical theories and physical factors to engineering practice.

The theory of reinforcement by fillers, and the particular properties of carbon black were discussed in several papers in other sessions. Still other sessions were devoted to latices, testing and analysis, and factory processes.

Those more concerned with general polymer science than with rubber technology will find a half dozen papers of particular importance. Details regarding the polymerization of nitrile rubbers (Buna N type) including the use of mercaptans as modifiers were given in a paper by J. F. Nelson and B. M. Vanderbilt. A paper by H. W. Walker and W. E. Mochel shows the effect of polymerization temperature on the properties of neoprene. The lower the temperature of polymerization the more rapid is the crystallization of the resulting polymer.

In kinetic studies of the oxidation of rubber LeBras and Salvetti generate oxygen by electrolysis. The pressure is maintained essentially constant by an arrangement which interrupts the current when the pressure rises slightly. The refractive index of rubber and its change with wavelength are essentially the same as those found for hydrocarbons of similar structure but low molecular weight, according to Wood and Tilton. Experimental methods used in the osmometry of dilute polymer solutions are described by H. W. Melville and G. R. Masson. The degree of crystallization found in natural rubber by the x-ray studies of J. M. Goppel does not exceed 30%.

The proceedings of the conference will be a very valuable source of information in this field for years to come.

L. A. Wood

Encyclopedia of Chemical Technology. Vol. 3, Raymond E. Kirk and Donald F. Othmer, eds., Interscience, New York, 1949, 971 pp., $20.00 per volume.

The third volume, of the proposed ten, of this encyclopedia continues the series of well-written authoritative articles on the materials, methods, and phenomena of chemical technology.

It opens with a continuation of the articles on *Carbon*. A highly informative article on *Carbon Black* (W. R. Smith), covers the channel and furnace production processes, and the physical properties, chemical composition, and methods of analysis of the blacks. Applications in rubber, etc., are discussed less completely and will probably be taken up in subsequent articles dealing with the end products. There are detailed articles on *Baked and Graphitized Carbon* (H. W. Abbott), *Natural Graphite* (S. B. Seeley and E. Emendorfer) and *Carbonization* (W. O. Keeling and F. W. Jung) and shorter articles on *Lampblack* and *Structural Carbon*. The interesting article on *Diamond* (C. V. R.) is concise and comprehensive.

Cellulosic materials are covered in a series of articles. Information on the structure and properties of cellulose is summarized and the processes of manufacturing wood pulp and chemical cotton are described in one article (J. Barsha and P. VanWyck), and the manufacture and properties of cellophane are covered in another (L. L. Leach). In a third (E. D. Klug), a general discussion of cellulose derivatives is followed by detailed methods of production and properties of nitrocellulose, cellulose acetate, ethyl cellulose, methyl cellulose, hydroxyethyl cellulose, cellulose acetate-butyrate and cellulose acetate-propionate. An article on *Cellulose Derivative Plastics* (W. O. Bracken) describes typical formulations, methods and materials of compounding, and fabrication techniques These articles, supplemented by pertinent literature references, furnish valuable information both to those who may wish to prepare and those who use cellulosic materials.

A large section of this volume is devoted to comprehensive technological articles on *Cement Products* and *Ceramics*, complex materials, the polymeric structures of which have not been completely elucidated.

The remainder of this volume includes comprehensive articles on *Electric Cells* (W. J. Hamer), *Cereals* (W. F. Geddes and F. L. Dunlap), *Chocolate and Cocoa* (W. T. Clarke); an interesting survey of the *Theory and Techniques of Catalysis* (V. I. Komarewsky and J. R. Coley); articles on *Casein, Castor Oil and Its Derivatives, Carcinogens, Cardiovascular Agents, Cathartics, Centrifugal Separation, Cerium, Chlorophyll, Choline, Chromatography,* and *Chromium;* and a number of articles on individual carbon compounds and inorganic and organic chlorine containing compounds.

Saul G. Cohen

ERRATA: Quantitative Investigation of X-Ray Diffraction by "Amorphous" Polymers and Some Other Noncrystalline Substances

(*J. Polymer Sci.*, 5, 269–281, 1950)

by P. H. HERMANS and A. WEIDINGER

Institute for Cellulose Research, AKU and Affiliated Companies, Utrecht, Netherlands

On page 273, line 13 from bottom: the word "coherent" should read 'incoherent.'

JOURNAL OF POLYMER SCIENCE VOL. V, NO. 5, PAGES 519-541

Effects of Hampered Draining of Solvent on the Translatory and Rotatory Motion of Statistically Coiled Long-Chain Molecules in Solution. Part I. Translation Resistance; Rate of Diffusion and Sedimentation*

HANS KUHN and WERNER KUHN, *Institute of Physical Chemistry, University of Basel, Switzerland*

I. INTRODUCTION AND DEFINITION OF λ_{trans}

Certain of the solution properties of long-chain polymer molecules, *e.g.*, viscosity, streaming birefringence, dielectric relaxation, and rates of diffusion and sedimentation, are related to movements of the entire chain molecule, or parts of it, relative to the surrounding solvent.

An exact calculation of the forces that are necessary to maintain such relative motions between a statistically coiled molecule, or portion of a molecule, and the surrounding solvent is difficult. To appreciate this we need only reflect on the hydrodynamic problems which arise when, for example, a certain part of the molecule comes into spatial juxtaposition with other portions of the same chain during the motion of the molecule.

In view of such difficulties, attempts have been made to obtain approximate solutions both by theoretical consideration of limiting cases, and [1,4,7] more generally, by means of experiments with large-scale models.[2] Our main purpose in this paper will be to discuss the validity of some of these approximations, and to present the more general results achieved by experiments with such models.

One of the earliest pictures made to obtain an approximate description of the hydrodynamic properties of statistically coiled chain molecules in solution was published by W. Kuhn[1] in 1934. We are here referring to the idea of totally hampered flow which was developed simultaneously with the introduction and quantitative postulation of the concept of the statistical coil. According to this *totally hampered flow model* the statistically coiled molecule forms a closely matted structure in which the solvent molecules lie completely immobilized between the intertwining coils of the polymer. The behavior in solution is then the same as if the entire coiled-up molecule were contained in a closed skin which separates the molecule and the solvent included between its coils, from the rest of the solution. If the velocity gradient in the solution is not too high, the entire material included in this skin will then behave as though it were a rigid body.

---

* Translated by Alexander Silberberg.

With the help of this model the viscous behavior of macromolecular solutions could be discussed in the paper[1] just mentioned, while in a subsequent paper[3] also the streaming birefringence, the rate of sedimentation, and the dielectric constant of solutions of Zwitter ions could be treated. According to the former of these papers[1] the viscosity of a solution of long-chain molecules (characterized by total immobilization of solvent between portions of the chain) will show an increase in η_{sp}/c in proportion to the square root of the degree of polymerization Z. It was moreover shown that this will still further depend on how the effect of the space requirements of the solute molecules is taken into account, so that the increase will really be proportional to $Z^{0.5+\epsilon}$, where ϵ will vary between 0 and 0.3 or 0.4 according to space requirements.

The other limiting case, that of the freely draining, coiled-chain molecule was first discussed by Huggins in 1938.[4] Using methods which were developed by W. Kuhn to describe the shape of the statistical coil and to account for the hydrodynamic behavior of a rodlike or threadlike structure in solution ("pearl necklace model"),[5] Huggins could show that, assuming unhampered draining of solvent through the solute molecules, η_{sp}/c must be directly proportional to the degree of polymerization, Z.[6] A theoretical basis for the empirical Staudinger viscosity law was thus found.

In a paper by W. Kuhn and H. Kuhn[7] the hydrodynamic behavior of a freely draining, randomly coiled, long-chain molecule in a streaming solution was treated with regard to the partial opening up of the coils of the molecule when the velocity gradient is very high. Parallel with discussing the viscosity, the streaming birefringence was treated, and relationships between these quantities could be established.[8] In later papers[9] these treatments were improved in particular by taking into account the shape resistance (rigidity of the chain) due to restricted rotation.

Already in the 1943 paper[7] it was pointed out that neither the assumption of free draining nor the assumption of complete immobilization of solvent in the coils of the molecule could represent the actual behavior. Both models are merely limiting cases, with the actual conditions somewhere between. Further it was there pointed out that a coiled molecule of low degree of polymerization is near the limiting case of the freely draining coil, while an increase of the degree of polymerization in a polymer homologous series must bring about a gradual transition to the totally hampered flow model.

It was also shown in this paper[10] that the freely draining coil of molecular weight M must be characterized by a rate of sedimentation which is independent of M, while the completely hampered flow coil will possess a rate of sedimentation which increases in proportion to $(M)^{1/2}$. Thus in the case of polymer homologous nitrocellulose solutions in acetone, for example, the sedimentation constant s could be represented by the following formula:

$$s = a[1 + 1.4 \times 10^{-2}(M)^{1/2}] \tag{1}$$

where a is a constant and M is the molecular weight. This is a formula which well illustrates the theoretical requirements made above. It is evident that s will be practically independent of M when M is small, but will increase in proportion to $(M)^{1/2}$ as we make the transition to high molecular weight homologs. In a series of papers, J. J. Hermans[11] and recently also P. Debye[12], Brinkman,[13] and Kirkwood and Riseman[14] have adopted the partially hampered flow model for coiled-up chain molecules, and have added further examples and theoretical discussion.

On the other hand the partial immobilization of solvent by the coils was neglected both by Debye in his 1946 paper[6] and by Kramers.[15]

In the equations of W. and H. Kuhn the partial immobilization of solvent in the statistically shaped chain molecules was allowed for by the inclusion of a form factor λ which characterized the degree of immobilization. In view of the fact that the conditions of percolation of solvent are rather different in the two cases of translational and rotational motion of the coiled molecule it was moreover necessary to make a distinction between λ_{trans} and λ_{rot}.

The form factor λ_{trans} will be defined by the following expression for the force F which is necessary to propel a chain molecule of hydrodynamic length L with velocity $\bar{u}$ through a fluid of viscosity η:

$$F = \eta L \bar{u} \lambda_{trans} \tag{2}$$

It is seen that the form factor λ_{trans} is dimensionless and will essentially depend on the degree to which draining is possible through the coiled chain. The hydrodynamic length L used in equation (2) is defined as the length of the molecule when it is extended to a linear zigzag chain without deformation of interatomic distances and valency angles. The quantity $\bar{u}$ in equation (2) denotes the mean velocity of a chain molecule on which a force F is acting. It is a mean taken over all the shapes through which the molecule passes due to its spontaneous constellation changes. The actual velocity u of the coil at any instant will of course depend upon the shape of the molecule at that time and its orientation to the direction of motion. In analogy to equation (2) we may therefore define an instantaneous resistance factor $\lambda_{i,trans}$ as follows:

$$F = \eta L u \lambda_{i,trans} \tag{2a}$$

$\lambda_{i,trans}$ therefore, corresponds to u, and will also depend upon the configuration of the molecule and the direction of motion relative to it.

The corresponding definition of the values of λ_{rot} and $\lambda_{i,rot}$ in the case of a rotation of the chain molecules is quite analogous, and will be given in Part II.

A rough estimate of the main form factors λ_{trans} and λ_{rot} has been made by W. Kuhn[16] in the case of a freely draining chain. His results were:

$$\lambda_{trans} \simeq \lambda_{rot} \simeq 3\pi/2 \tag{3}$$

In the following sections we shall be able to improve upon this estimate and determine better values of λ_{trans} in the two limiting cases of free draining and of completely hampered flow in the coiled chain molecule. Thereafter we shall discuss the experiments on large-scale models by means of which the gap between these extremes can be bridged and a gradual transition demonstrated experimentally. Following on from there we shall deal with those phenomena which depend essentially on λ_{trans}, namely the sedimentation constant and the diffusion constant of the chain molecule.

In Part II we shall discuss the resistance to rotation, that is, λ_{rot}, and correspondingly deal with quantities dependent thereon, namely the viscosity and streaming birefringence.

II. TRANSLATORY MOTION OF CHAIN MOLECULES IN SOLUTION

a. External Dimensions of Statistically Formed Chain Molecules

In order to describe the external shape of the statistically formed chain molecule we replace it by a chain made up of N_m preferential statistical chain elements of hydrodynamic length A_m. It is assumed that each statistical chain element has complete freedom of orientation, that is, the orientation of a given element will be uninfluenced and independent of the orientations of neighboring elements. In order that this model may have the same mean square end-to-end distance h and the same hydrodynamic length L as the molecule (preferential values), the relationship:

$$L = N_m A_m \tag{4}$$

must be fulfilled besides the following, now well-known, equation:[1]

$$\overline{h^2} = N_m A_m^2 = L A_m \tag{5}$$

The distance h between the end points of the chain is at best equal to, but in most cases appreciably smaller than, the distance H_1 representing the distance between the two points in the chain furthest apart in space. Let us demonstrate this by placing the chain molecule into a coordinate system such that one end point is in the origin and the other in the z axis at the point $z = h$. It is then easily seen that there will be portions of the chain belonging in particular to that half whose end is in the origin, which will possess negative z coordinates, so that these points at any rate will be at a distance from the other end which is larger than h. The problem of determining the mean value of H_1 (or more generally its distribution function) as well as the problem of finding the mean lateral extension H_2 of the coil has been treated some time ago[17] with the following result:

$$\bar{H}_1 = 1.5\bar{h} = 1.4(\overline{h^2})^{1/2} = 1.4\,(N_m)^{1/2}A_m \tag{6}$$

$$\bar{H}_2 = 0.5\bar{H}_1 = 0.75\bar{h} = 0.7(\overline{h^2})^{1/2} = 0.7(N_m)^{1/2}A_m \tag{7}$$

where $\bar{H}_2$ is the mean lateral extension, that is, the simultaneous mean maximum extension of the chain molecule in a direction perpendicular to H_1. In addition it was shown that the mean external dimension of the chain in a freely selected direction, *e.g.*, the x direction (whereby the direction of the vector h is to be considered statistically random) can be expressed as follows:[17,18]

$$\bar{X} = \bar{h} = 0.92(\bar{h}^2)^{1/2} = 0.92(N_m)^{1/2}A_m \tag{8}$$

Using the result of equation (8) we can, in rough approximation, compare the external shape of the loosely coiled chain molecule with that of a *sphere* of radius r such that:

$$r = \bar{X}/2 = 0.46(N_m)^{1/2}A_m \tag{9}$$

Its volume then is:

$$V = {}^4/_3\ \pi r^3 = {}^4/_3\ \pi\ (0.46)^3 N_m^{3/2} A_m^3 = 0.41 N_m^{3/2} A_m^3 \tag{10}$$

In better approximation we can account for the shape of the coil by means of a prolate *ellipsoid of revolution* whose large semiaxis is given by

$$c = \bar{H}_1/2 = 0.7(N_m)^{1/2}A_m \tag{11}$$

and whose small semiaxis is:

$$a = \bar{H}_2/2 = 0.35(N_m)^{1/2}A_m \tag{12}$$

The axial ratio of this body is consequently given by:

$$p = c/a = 2.0 \tag{12a}$$

while the eccentricity ϵ of the ellipse, defined by

$$\epsilon^2 = \frac{c^2 - a^2}{c^2} \tag{13}$$

in this case will be:

$$\epsilon^2 = 0.75 \tag{14}$$

In an earlier paper of W. Kuhn[1] the coil was described as a general ellipsoid with three axes of different length whose proportions were given by $h_1:h_2:h_3 = 6:2.3:1$.

b. Hydrodynamic Resistance of Nondraining Coil to Translatory Motion in a Fluid

According to Stokes' law the force necessary to transport a rigid (nondraining) sphere of radius r with velocity $u = \bar{u}$ through a fluid of viscosity η is given by:

$$F = 6\pi\eta r\bar{u} \tag{15}$$

Consequently, if, as rough approximation, we replace the coiled chain molecule by a nondraining sphere of radius r (given by equation 9) we can write:

$$F = 6\pi\eta[0.46(N_m)^{1/2}A_m]\bar{u} = 8.7\eta(N_m)^{1/2}A_m\bar{u} \tag{16}$$

Equating this with expression (2) and introducing equation (4) we obtain:

$$\eta N_m A_m \bar{u} \lambda_{trans} = 8.7\eta(N_m)^{1/2}A_m\bar{u}$$

which transforms to:

$$\lambda_{trans} = 8.7/(N_m)^{1/2} \tag{17}$$

(statistically coiled nondraining chain molecule)

We see, therefore, that the hydrodynamic behavior of a statistically coiled, nondraining chain molecule which undergoes translatory motion through a fluid can be described by expression (2) provided a form factor λ_{trans} calculated from equation (17) is introduced. In this case, when solvent is completely immobilized between the coils of the molecule, λ_{trans} is proportional to $(N_m)^{-1/2}$, while in the case of unhampered draining we have seen from equation (3) that it is constant, and therefore independent of the degree of polymerization.

Instead of regarding the coiled chain as a sphere of radius r (equation 9), we can improve the approximation by assuming that it is an ellipsoid of revolution with semiaxes c and a according to equations (11) and (12). We shall see, however, that λ_{trans} is then given by an expression which is practically identical with equation (17).

If a prolate ellipsoid of revolution with semiaxes c and a is propelled by a force $F_{\|}$ parallel to its longest axis (parallel to c) through a fluid of viscosity η its velocity $u_{\|}$ can, according to Gans,[19] be expressed by:

$$u_{\|} = F_{\|}\frac{\dfrac{1+\epsilon^2}{\epsilon^3}\ln\dfrac{1+\epsilon}{1-\epsilon} - \dfrac{2}{\epsilon^2}}{16\pi\eta c} \tag{18}$$

If the motion takes place perpendicular to the c axis the corresponding velocity $u_{\perp}$ is given by

$$u_{\perp} = F_{\perp}\frac{\dfrac{1}{\epsilon^2} - \dfrac{1-3\epsilon^2}{2\epsilon^3}\ln\dfrac{1+\epsilon}{1-\epsilon}}{16\pi\eta c} \tag{18a}$$

As a result of Brownian motion the ellipsoid will alter its orientation relative to the direction of motion, so that during the course of a measurement we can say that the motion will only be parallel to the c axis for one-third of the time and be perpendicular to it for the remaining two-thirds. The mean velocity $\bar{u}$ attained when a force F is applied will then, using equations (18) and (18a), be given by:

$$\bar{u} = \frac{u_{\|} + 2u_{\perp}}{3} = F\frac{\dfrac{1}{\epsilon}\ln\dfrac{1+\epsilon}{1-\epsilon}}{12\pi\eta c} \tag{18b}$$

Transforming:

$$F = \frac{12\pi\eta c\epsilon}{\ln \frac{1+\epsilon}{1-\epsilon}}\bar{u} \tag{18c}$$

and introducing for ϵ and c their values from equations (14) and (11), respectively, we finally obtain:

$$F = 8.7\eta(N_m)^{1/2}A_m\bar{u} \tag{18d}$$

This is identical with equation (16) so that (compare equation 17) we again obtain:

$$\lambda_{trans} = 8.7/(N_m)^{1/2} \tag{17a}$$

(nondraining coil, the coil regarded as ellipsoid)

We can conclude, therefore, that whether we regard the coil as a nondraining sphere of mean radius $\bar{X}/2$ (equation 9) or as a nondraining ellipsoid with semiaxes c and a (equations 11 and 12) the result obtained for the hydrodynamic resistance will, for practical purposes, be identical. Consequently the rate of sedimentation and the diffusion constant to be expected in these cases will also be the same.

c. Hydrodynamic Resistance of a Freely Draining Coil to Translatory Motion in a Fluid

To express the frictional resistance of a freely draining coil we could introduce into equation (2) the form factor:

$$\lambda_{trans} = 3\pi/2 \qquad \text{(completely drained coil)} \tag{19}$$

from equation (3). This, as has been pointed out before, is, however, only an estimate which was made[16] by comparing the hydrodynamic resistance of the "pearl necklace model" with the mean hydrodynamic resistance to translation of elongated ellipsoids of revolution in the fluid.

A certain refinement of this treatment can now be attempted in the following manner.

We assume that each preferential statistical chain element possesses besides length A_m also a thickness d_h (the hydrodynamical thickness) such that in its motion through the fluid it will behave as though it were a very long stretched ellipsoid of revolution with semiaxes $^1/_2A_m$ and $^1/_2d_h$. We further assume that a statistical chain element will be left uninfluenced in its hydrodynamic behavior by the remaining elements, and in particular by those two elements which are at either side of it. The force F which is necessary to move the entire chain through a fluid of viscosity η with a certain velocity $\bar{u}$ will then simply be N_m times larger than the mean force required to propel the individual statistical chain element with the same velocity $\bar{u}$. Taking means over the various orientations which the statistical chain elements can adopt with the direction of motion, that is, by a suitable application of the result of equation (18c), we find that the force F on the total chain is given by:

$$F = N_m \frac{12\pi\eta \frac{A_m}{2}\left(\frac{A_m^2 - d_h^2}{A_m^2}\right)^{1/2}}{\ln \frac{1 + [1 - (d_h/A_m)^2]^{1/2}}{1 - [1 - (d_h/A_m)^2]^{1/2}}} \tag{20}$$

When A_m is much greater than d_h this transforms to:

$$F = N_m \frac{3\pi\eta A_m}{\ln (2A_m/d_h)} \bar{u} \tag{21}$$

Equating now with expression (2) and introducing the result of equation (4) we finally obtain:

$$\lambda_{trans} = \frac{3\pi}{\ln (2A_m/d_h)} \tag{22}$$

(completely drained coil, more exact estimate)

According to the above, λ_{trans} is basically determined by the ratio of length to thickness of the statistical chain element, although in a somewhat insensitive manner, namely only by the logarithm of this ratio. When $A_m/d_h = 3.7$, equation (22) would reduce to equation (19).

But even the replacement of the approximation (19) by the more exact expression (22) does not really stand the test of critical investigation. This is due to the fact that the hydrodynamic behavior of the individual chain element is in reality not left uninfluenced by the presence of other chain elements in the vicinity and in particular by its two immediate neighbors. Consequently, all further refinements of the theory are really attempts to estimate the extent of this mutual interaction.

In view of the difficulty of estimating theoretically the extent of the departure from the behavior of the freely draining coil, an *experimental method* was devised to obtain the value of the parameter λ_{trans}. This method, as will now be fully discussed, makes use of the hydrodynamic behavior of large-scale models of the molecule.

d. Determination of the Hydrodynamic Resistance of Partially Draining Chain Molecules by Means of a Theorem of Hydrodynamic Similarity

1. Formulation of the Theorem

Let us consider the motion through a fluid of a body of any given shape. We shall assume that the walls of the container are so far removed from the site of the experiment that these distances are always large compared with the linear dimensions of the body. Furthermore we assume that the linear velocity u of the body is so small that forces resulting from an acceleration of the fluid particles can be neglected.

Under these conditions the parts of the fluid in immediate contact with the surface of the body acquire the velocity u while those at the (infinitely distant) walls of the container remain at rest. In this manner a velocity gradient q is set up in the fluid. If η now is the viscosity of the fluid the mechanical energy transformed into heat as a result of internal friction can be expressed by the well-known relationship, $dW/dt = q^2\eta$ ergs/cc./sec. The total quantity of work transformed into heat per second is then obtained by integrating over the entire volume, V, of the fluid in which the body is moving.

Thus:

$$dW/dt = \int_V q^2\eta \, dv \tag{23}$$

The given expression is only then strictly applicable when in the region considered the velocity vector of the moving fluid has the same direction in every point. However, as was shown in reference 2, the results that follow from equation (23) are of unaltered validity when applied under any other conditions of viscous flow.

If F is the force required to act on the body in order to maintain the velocity u, it is obvious that:

$$Fu = \int_V q^2\eta \, dv \tag{24}$$

We now imagine that all linear dimensions of the test body are changed by a factor α, *e.g.*, magnified. We do the same with the velocity u and the dimensions of the container in which the fluid of viscosity η is placed. In this way we can allocate to each point of our original system a corresponding point in our expanded system. This applies equally to the test body as also to points in the fluid. It will now become apparent that due to the simultaneous magnification of all linear dimensions and the velocity by the same factor the mean velocity gradient between test body and wall remains the same. As similarity has been achieved at all points of the system we can in general conclude that *the absolute value of the velocity gradient remains the same at corresponding points, but that the magnitude of corresponding volume elements has been increased by* α^3. If we label the quantities belonging to the new expanded system with an apostrophe we have the following relationships:

$$q' = q \qquad \eta' = \eta \qquad dv' = \alpha^3 \, dv \qquad u' = u\alpha$$

Instead of equation (24) we must now write:

$$F'u\alpha = \int_{V'} q'^2\eta' \, dv' = \int_V q^2\eta\alpha^3 \, dv \tag{25}$$

Introducing equation (24):

$$F'u\alpha = \alpha^3 \int_V q^2\eta \, dv = \alpha^3 Fu$$

So that consequently:

$$F' = \alpha^2 F$$

Further by dividing this equation by $u' = u\alpha$:

$$\frac{F'}{u'} = \frac{F'}{u\alpha} = \frac{\alpha^2 F}{u\alpha} = \alpha\,\frac{F}{u} \tag{26}$$

According to the definition (2a) the following equation applies in the case of a statistically shaped chain molecule:

$$F/u = \eta L\lambda_{t,trans} \tag{27}$$

If, therefore, we have a chain molecule expanded by a factor α such that it forms a geometrically similar structure of length $L' = \alpha L$, we can, using equation (26), now write:

$$F'/u' = \alpha(F/u) = \eta\alpha L\lambda_{t,trans} = \eta L'\lambda_{t,trans} \tag{27a}$$

Therefore, if we are able to determine the force F' necessary to drive the expanded model with a velocity u' through the fluid we can calculate from this the proportionality factor $\lambda_{t,trans}$ (equation (2a)), that is, we can determine the degree of free draining. Furthermore, now that $\lambda_{t,trans}$ is known we can find the force F which is necessary to propel an actual molecule with any chosen velocity u. We have in this case:

$$F = \eta Lu\lambda_{t,trans} \tag{27b}$$

We conclude that the factor $\lambda_{t,trans}$ which measures the extent of free draining of fluid through the coils of the submicroscopic chain molecules can be determined by means of experiments with large-scale models in view of the fact that the value of $\lambda_{t,trans}$ remains the same for geometrically similar shapes.

2. *Experimental Determination of λ_{trans} of Statistically Shaped Chain Molecules*

In order to determine the shape factor λ_{trans} for a chain molecule consisting of N_m statistical chain elements of length A_m and of hydrodynamic thickness d_h we can proceed as follows. We prepare a large-scale model of the statistically shaped chain molecule such that it consists of N_m elements of length $A = \alpha A_m$ and thickness $d = \alpha d_h$ using a material which has a density ρ. Placing this model into a fluid of density ρ_0 we can measure the velocity u' with which it sinks. The volume of the macroscopic model is obviously equal to $^1/_4 d^2\pi N_m A$ and the force which causes it to sink with velocity u' is given by:

$$F' = g\,\frac{d^2\pi}{4}\,N_m A(\rho - \rho_0) \tag{28}$$

where g is the acceleration due to gravity. Remembering that $L' = N_m A$ we can introduce equation (28) in equation (27a) at the same time substituting for u' the observed velocity of sinking. We thus obtain the dimensionless resistance factor $\lambda_{t,trans}$. From experiments on a number of models we can obtain values for $\lambda_{t,trans}$ corresponding to different chance configurations of the molecule and their orientation to the direction of motion. By averaging over these, the mean shape factor λ_{trans}, which is seen to be a function of N_m and $A/d = A_m/d_h$ is found.

Preparation of the Large-Scale Models. Particular care was taken in preparing the large-scale models that were to be used in the experiments. As these must have a statistical shape, any selection or aesthetic feeling on the part of the experimenter had to be eliminated. To do this a sphere was taken, and a dot marked on its surface. The line from the center to the dot on the surface then forms a vector whose direction will be truly statistical if the sphere is rolled along a random path on a level surface and suddenly arrested. We can then obtain a statistical coil if we proceed to make the model consisting of N_m elements in such a way that we place the first element in the direction observed after the first "rolling" of the sphere and, retaining this orientation, place the second element in the direction indicated by the second "rolling." Keeping this direction fixed we then roll the sphere for the orientation of the third element, so that proceeding in this manner N_m times in all we shall have completed the model.

Models made in this way which agree in the values of N_m, A, and d will naturally possess the different external shapes that result from the statistical method adopted in their preparation. Consequently, for each group of N_m, A, and d values as large a number of models as possible must be made, in the manner indicated above, in order that a good average can be obtained. Furthermore an average has to be taken over the possible orientations in which each model can sink.

Experimental Results. The results of experiments in which the ratio A_m/d_h was equal to 1.9 are recorded in Figure 1, which shows the dependence of $\lambda_{t,trans}$ on the value of N_m. (Actually, $1/\lambda_{t,trans}$, *i.e.*, the reciprocal of the shape factor $\lambda_{t,trans}$, determined from the velocity of sinking u', is plotted against the square root of the number of statistical chain elements in the molecule, *i.e.*, against $(N_m)^{1/2}$.)

The large-scale models were made of pieces of aluminum wire, 1 mm. in diameter and 1 to 25 cm. in length. The viscous fluid in which the models were allowed to sink was a concentrated invert sugar solution which had a viscosity of 63 poise at 20°C. It was contained in a glass vessel 30 cm. in diameter and 60 cm. tall which was placed in a room where the temperature was thermostatically controlled to 20°C.

For each value of N_m recorded in Figure 1, 6 to 10 models were constructed. A mean value of $1/\lambda_{t,trans}$, found for each individual model by averaging over the various orientations in which it was allowed to sink, is entered as one point in Figure 1. The reciprocal λ_{trans} values which result as mean when the average is taken for each set of results for a given value of N_m are recorded as small circles.

One sees from Figure 1 that models composed of the same number of statistical chain elements are represented by points which are scattered over relatively large interval, *i.e.*, the values of $1/\lambda_{t,trans}$ for the various chance configurations, having the same N_m value, differ widely among one another. The scatter is as much as 10 to 15% from the mean value. Thus, these mean values calculated from such individual results cannot, in turn, be very good. Nevertheless the points of Figure 1 show a distinct linear relationship between $1/\lambda_{trans}$ and $(N_m)^{1/2}$.

In all the models to which Figure 1 refers the ratio of length to thickness of the statistical chain element, A_m/d_h, was equal to 1.9. Corresponding tests were also performed with models where the ratio A_m/d_h was equal to 3.8, 7.6, and 15.2, respectively. It was shown that the resistance factor λ_{trans} becomes markedly smaller as d_h is decreased at constant A_m and N_m.

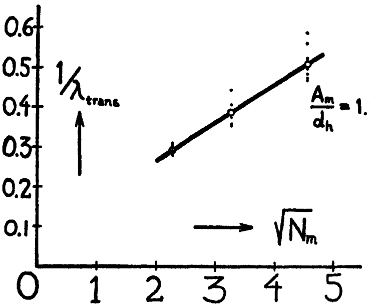

Fig. 1. Plot of $1/\lambda_{trans}$ against $(N_m)^{1/2}$ in a case where $A_m/d_h = 1.9$. λ_{trans} is the shape factor defined by equation (2) and determined by the rate of sinking of large-scale models of molecules. N_m is the number of statical chain elements in the model. *Dots:* reciprocals of the $\lambda_{i,trans}$ values of the various models. Each point refers to one individual model and already represents a mean taken over the various orientations. *Circles:* reciprocals of the λ_{trans} values which are found when averaging over the values yielded by all models with common N_m value. The positions of the mean values indicate that within the experimental error a linear relationship exists between $1/\lambda_{trans}$ and $(N_m)^{1/2}$.

This result, namely that the resistance to flow of a coiled chain molecule whose shape and total length are specified will under all circumstances become smaller when the thickness of the chain is decreased, is of course only what one would expect.

The linear relationship between $1/\lambda_{trans}$ and $(N_m)^{1/2}$ and the increase of $1/\lambda_{trans}$ with A_m/d_h can, with the accuracy obtainable at present, be represented by the following formula:

$$1/\lambda_{trans} = 0.16 \log (A_m/d_h) + 0.02 + 0.1(N_m)^{1/2} \qquad (29)$$

3. Discussion of Equation (29)

It is easily seen that the above empirical formula gives a satisfactory account of the manner in which $1/\lambda_{trans}$ depends on the quantities A_m, d_h, and N_m, *i.e.*, there is evident agreement with our earlier conclusions. In the two limiting cases, when the number of chain elements, N_m, is either very large or very small, we can, moreover, make direct comparisons between the new results and the theoretical values calculated earlier and, as will now be shown, semiquantitative agreement can be demonstrated.

The Limiting Case of Very Small Values of N_m. In the event that $N_m = 1$, *i.e.*, when only a single statistical chain element is being considered, equation (29) can be written in the form:

$$1/\lambda_{trans} = 0.16 \log (A_m/d_h) + 0.12 \qquad (30)$$

Such a molecule may be compared with an ellipsoid with axes in the ratio A_m/d_h and with resistance factor λ_{trans} given by expression (22). We need, therefore only transform this latter equation to obtain:

$$1/\lambda_{trans} = 0.24 \log (A_m/d_h) + 0.07 \qquad (30a)$$

(from equation 22, in the case $N_m = 1$, the individual statistical chain element regarded as ellipsoid).

$1/\lambda_{trans}$ as derived from equation (30) is *somewhat* smaller than the value obtained from equation (30a), *i.e.*, the resistance factor λ_{trans} is somewhat larger when calculated from equation (30) than when obtained from equation (22). The small discrepancy between equation (30) and (30a) is not surprising, since an extrapolation of equation (29) to its value at $N_m = 1$ is not really justified. As, therefore, when $N_m = 1$ no great precision can be expected from equation (29), we may conclude that satisfactory agreement with equation (22) has been established in this region.

If s_m is the number of monomers in each statistical chain element we may still further discuss the case when the degree of polymerization Z is *so small* that $Z \lesseqgtr s_m$, *i.e.*, when $N_m = Z/s_m \lesseqgtr 1$. We thus have a case when the chain molecule contains less than one statistical chain element. In this case the chain molecule is not a statistical coil, but may be compared to a straight rod, or ellipsoid, of length Zb, where b is the hydrodynamic length of the monomer. The hydrodynamic thickness will continue to be d_h, and we can represent $1/\lambda_{trans}$ by substituting in equation (22). We obtain:

$$1/\lambda_{trans} = \frac{2.303}{3\pi} \log \frac{2bZ}{d_h} \qquad (30b)$$

(from equation 22 when $N_m < 1$, $Zb \gg d_h$)

The Limiting Case of Very Large Values of N_m. In the limit when N_m is very large we can, in comparison to the term containing N_m, always neglect the first two terms on the right-hand side of equation (29). The expression thus becomes:

$$1/\lambda_{trans} = 0.1(N_m)^{1/2} \qquad (31)$$

(from equation 29 in the case when N_m is large)

We have seen in section 1 that a coiled chain molecule can be regarded as nondraining when N_m is very large, and we have found that λ_{trans} in this case can be represented, in fair approximation, by equation (17a). Writing this expression in the same form as equation (31) we obtain in satisfactory agreement with the above:

$$1/\lambda_{trans} = \frac{1}{8.7}(N_m)^{1/2} \tag{31a}$$

(from equation 17a in the case when N_m is large)

Therefore expression (29) reproduces just that which in the limit of large values of N_m one would expect on the basis of other facts and theoretical considerations. We may consequently conclude that also, in general, this formula will substantially represent the actual conditions. This applies even if further experiments may bring about changes in the numerical values of the coefficients or otherwise alter the present form of the expression.

III. DIFFUSION CONSTANT

Once the resistance factor λ_{trans} is known we can immediately formulate an expression for the diffusion constant of the freely, partially, or nondraining chain molecule.

By means of equation (2) we can express the mobility μ of a particle. It is defined as the velocity acquired by the particle when a force of 1 dyne is applied. Therefore

$$\mu = \frac{1}{\eta L \lambda_{trans}} \tag{32}$$

As is well known the diffusion constant D and the mobility μ are connected by the relation:

$$D = \mu kT \tag{33}$$

so that using equation (32) we immediately obtain:

$$D = \frac{kT}{\eta L \lambda_{trans}} \tag{33a}$$

If we now substitute for λ_{trans} from equation (29) and introduce equation (4), the result will be:

$$D = \frac{kT}{\eta N_m A_m}\left[0.02 + 0.16 \log \frac{A_m}{d_h} + 0.1(N_m)^{1/2}\right] \tag{34}$$

As:

$$N_m A_m = L = Zb \tag{34a}$$

where Z is the degree of polymerization and b is the hydrodynamic length of the monomer, we can rewrite equation (34) and obtain:

$$D = \frac{kT}{\eta b}\frac{1}{Z}\left[0.02 + 0.16 \log \frac{A_m}{d_h} + 0.1\left(\frac{b}{A_m}\right)^{1/2}(Z)^{1/2}\right] \tag{34b}$$

Moreover:

$$Z = M/M_0 \tag{34c}$$

where M is the molecular weight of the whole chain molecule, and M_0 is the molecular weight of the monomer, so that we can also write the above expression for D in the following manner:

$$D = \frac{kT}{\eta b} M_0 \frac{1}{M}\left[0.02 + 0.16 \log \frac{A_m}{d_h} + 0.1 \left(\frac{b}{A_m M_0}\right)^{1/2} (M)^{1/2}\right] \qquad (34d)$$

In a polymer homologous series all the quantities occurring in equation (34b), with the exception of Z, are constants, so that instead of (34b) we may write more simply:[2]

$$D = \frac{1}{Z}\left[a_D + b_D(Z)^{1/2}\right] \qquad (35)$$

where we then have to put:

$$a_D = \frac{kT}{\eta b}\left(0.02 + 0.16 \log \frac{A_m}{d_h}\right) \qquad (35a)$$

$$b_D = 0.1 \frac{kT}{\eta}\left(\frac{1}{A_m b}\right)^{1/2} \qquad (35b)$$

We see from expression (35), that when the degree of polymerization is low (freely draining coil), the diffusion constant will be proportional to $1/Z$, while, when the degree of polymerization is high, it will vary as $1/Z^{1/2}$ (nondraining coil).

If the degree of polymerization is so small that $Z < s_m$ we can combine the results of equations (30b) and (33a) and obtain:

$$D = \frac{2.303}{3\pi} \frac{kT}{\eta b} \frac{\log (2bZ/d_h)}{Z} \qquad (36)$$

(in the case where $Z < s_m$, $bZ \gg d_h$)

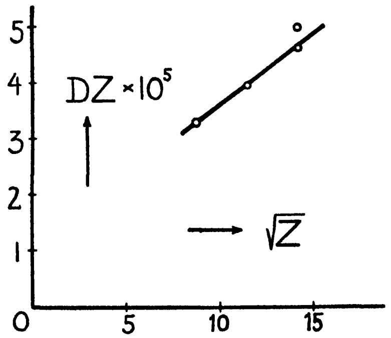

Fig. 2. Plot of DZ against $(Z)^{1/2}$ from measurements by Polson in the case of methylcellulose in water.

D is the diffusion constant and Z is the degree of polymerization. The points lie almost on a straight line as was expected from equation (35).

Comparison with Experimental Findings

To test the above formula against some experimental results we can use rate of diffusion measurements by Polson[20] on methylcellulose in water. From his data we have plotted the quantity DZ against $(Z)^{1/2}$ and it can be seen that the experimental points lie very nearly on a straight line in agreement with equation (35). From Figure 2 we find that:

$$DZ = [1.1 + 0.26\,(Z)^{1/2}] \times 10^{-5}$$

For the case of methylcellulose in water we can consequently write that:

$$a_D = 1.1 \times 10^{-5} \qquad b_D = 0.26 \times 10^{-5}$$

If we now put the viscosity of the solvent equal to $\eta = 1.0 \times 10^{-2}$ and the hydrodynamic length b of a methylcellulose monomer equal to 5.15×10^{-8} cm., we find from equation (35b) that $A_m = 5 \times 10^{-7}$ cm. Similarly from equation (35a) we find that $d_h = 8 \times 10^{-8}$ cm. This is obviously of the correct magnitude. For a detailed discussion see Section IV.

IV. SEDIMENTATION CONSTANT

The sedimentation constant of chain molecules is directly dependent on their mobility μ (see equation 32) and their diffusion constant D (see equation 33) and is therefore, fully determined once λ_{trans} is known.

If M is the molecular weight of a chain molecule we see that the force acting on the individual particle in a gravitational field of acceleration g will be gM/N_A dyne, where N_A is Avogadro's number. At the same time the volume occupied by a single chain molecule is given by $Mv_{part.}/N_A$, where $v_{part.}$ is the partial specific solution volume of the solute. Let ρ_0 again be the density of the solvent. Then, taking the buoyancy of the solvent into account, we can give the following accurate expression for the net force acting on the individual particle:

$$F = \frac{M}{N_A}(1 - v_{part.}\,\rho_0)g \tag{37}$$

Equating this with expression (2), and solving for the velocity of sedimentatión, we find:

$$u = \frac{1}{\eta L}\,\frac{M}{N_A}\,(1 - v_{part.}\rho_0)g\,\frac{1}{\lambda_{trans}}$$

In the above we may put $M = M_0 Z$ and $L = bZ$, where M_0 is the molecular weight of the monomer and b is its hydrodynamic length, and obtain:

$$u = \frac{M_0\,g}{N_A \eta b \lambda_{trans}}\,(1 - v_{part.}\,\rho_0) \tag{38}$$

In this equation we now introduce $1/\lambda_{trans}$ from equation (29), so that the rate of sedimentation of a chain molecule of degree of polymerization Z will be given by:

$$u = \frac{M_g}{N_A b} \frac{1 - v_{part.}\rho_0}{\eta} g \left[0.02 + 0.16 \log \frac{A_m}{d_h} + 0.1 \left(\frac{b}{A_m} \right)^{1/2} (Z)^{1/2} \right] \tag{39}$$

Seeing that $M = M_g Z$ we can also write this as:

$$u = \frac{M_g}{N_A b} \frac{1 - v_{part}\ \rho_0}{\eta} g \left[0.02 + 0.16 \log \frac{A_m}{d_h} + 0.1 \left(\frac{b}{A_m M_g} \right)^{1/2} (M)^{1/2} \right] \tag{39a}$$

Dividing equation (39) by the acceleration g and putting:

$$u/g = s_0 \tag{40}$$

where s_0 is then the sedimentation constant (the rate of sedimentation in a gravitational field of 1 cm. sec.$^{-2}$), we obtain as our final expression:

$$s_0 = a_s + b_s(Z)^{1/2} \tag{41}$$

where:

$$a_s = \frac{M_g}{N_A b} \frac{1 - v_{part}\ \rho_0}{\eta} \left[0.02 + 0.16 \log \frac{A_m}{d_h} \right] \tag{41a}$$

$$b_s = \frac{M_g}{N_A b} \frac{1 - v_{part.}\ \rho_0}{\eta} \left[0.1 \left(\frac{b}{A_m} \right)^{1/2} \right] \tag{41b}$$

From expression (39), or (41), we can deduce that the velocity of sedimentation, or the sedimentation constant, as the case may be, will be independent of the degree of polymerization Z as long as Z is small (freely draining coil), but will vary with the square root of Z once high degrees of polymerization have been reached (nondraining coil).

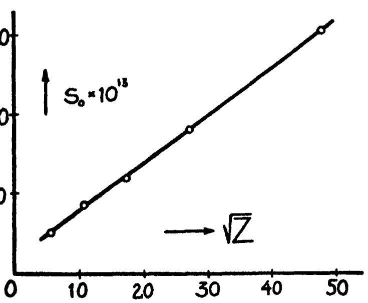

Fig. 3. Plot of the sedimentation constant s_0, against $(Z)^{1/2}$ from measurements of Mosimann on nitrocellulose in acetone.

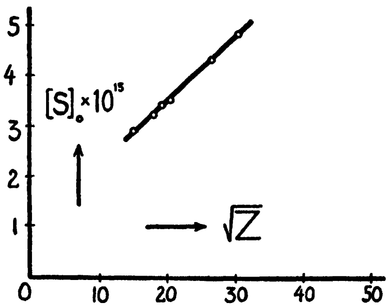

Fig. 4. Plot of the intrinsic sedimentation constant $[s]_0$ against the square root of the degree of polymerization (Z).$^{1/2}$ Taken from measurements by Kraemer and Nichols on cellulose acetate in acetone.

Comparison with Experimental Findings. Figures 3 and 4 illustrate the behavior of the sedimentation constant in some actual cases. As can be seen the straight line law expected from equation (41) is observed when the sedimentation constant s_0 is plotted as ordinate against the square root of the degree of polymerization, *i.e.*, against $(Z)^{1/2}$ as abscissa. Figure 3 illustrates the behavior of nitrocellulose in acetone, determined by Mosimann,[21] while Figure 4 represents the results obtained for cellulose acetate in acetone by Kraemer and Nichols.[22]

From Figure 3 we find that in the case of nitrocellulose in acetone:

$$a_s = 2.2 \times 10^{-13}$$

$$b_s = 0.58 \times 10^{-13}$$

The other relevant data in this case are as follows:

η = 0.0030 poise (the viscosity of acetone at the temperature of the experiment).
$b = 5.15 \times 10^{-8}$ cm. (the result of x-ray measurements of the hydrodynamic length of the nitrocellulose monomer.)
M_g = 268 (approximately) (molecular weight of a monomer of the nitrocellulose considered).
$v_{part.}$ = 0.51 (the value given by Mosimann for the partial specific volume of nitrocellulose in acetone).
ρ_0 = 0.79 (density of acetone).

Using these figures we obtain from equation (41b) that $A_m = 44 \times 10^{-8}$ cm. With this result we can now calculate the hydrodynamic thickness of the chain and find:

$$d_h = 9.2 \times 10^{-8} \text{ cm.}$$

In quite similar fashion we find from the results of Kraemer and Nichols that in the case of cellulose acetate (Fig. 4):

$$A_m = 108 \times 10^{-8} \text{ cm. and } d_h = 10.8 \times 10^{-8} \text{ cm.}$$

(Here the relevant data are as follows: $M_g = 240$; $b = 5.15 \times 10^{-8}$ cm.; and $v_{part.} = 0.68$.)

In the paper of Kraemer and Nichols, as well as in Figure 4, the intrinsic sedimentation constant $[s]_0$ has been used instead of the constant s_0 defined in equations (40) and (41). The intrinsic sedimentation constant $[s]_0$ is related to s_0 by the following equation:

$$[s]_0 = \frac{\eta v_{part.}}{1 - v_{part.}\,\rho_0}\, s_0$$

It is seen that the factor connecting $[s]_0$ with s_0 becomes a constant in the case considered here of a polymer homologous series tested in one solvent and at one temperature. The linear relationship (evidenced by Fig. 4) which exists between $[s]_0$ and $(Z)^{1/2}$ must therefore apply to s_0 and $(Z)^{1/2}$ as well.

In commenting on these results, we may mention that the value for A_m in the case of cellulose acetate is in very good agreement with the value calculated for this substance in an earlier paper[7] when using viscosity and streaming birefringence data.

The results found for d_h on the basis of equations (41a) and (35a), respectively, are all of the same order of magnitude, *i.e.*, about equal to the actual thickness, d_s, of the corresponding chain as determined from molecular structural data.*

There is considerable doubt about the exact value of d_s to be selected for comparison with d_h. This arises from the circumstance that the molecular chain does not possess a uniform cross-sectional aspect from which d_s could be uniquely determined. On the contrary some groups in the monomer are at much greater distances from the molecular axis than others, corresponding to fluctuations in diameter.

One method, by neglecting these fluctuations, leads to a lower limit for d_s. Here the volume $M_0 v_{part.}{}^{-1} N_A^{-1}$ occupied by each monomeric residue in the solution is regarded as being smoothed out to a cylinder of length b and thickness d_s. It then easily follows that:

$$d_s = \left(\frac{4M_0}{\pi N_A b v_{part.}}\right)^{1/2} \qquad \text{(lower limit)}$$

In the case of methylcellulose, b equals 5.15×10^{-8} cm., $v_{part.}$ equals 0.72, and M_0 equals 189; and therefore d_s equals 7.4×10^{-8} cm. In the cases of nitrocellulose and cellulose acetate considered above one finds similarly the values 7.5×10^{-8} and 8×10^{-8} cm., respectively.

Another reasonable approach takes account of the fact mentioned that it may not be the average, but the maximum cross-sectional dimension which is the determining factor for the hydrodynamic resistance. Thus, using available data for the bond and van der Waals radii of the atoms composing the molecule we can estimate the maximum distances from the chain axis. In the case of the substances considered above we obtain in this manner, by way of an upper limit, the values d_s equal to 13×10^{-8}, 14×10^{-8}, and 15×10^{-8} cm. for methylcellulose, nitrocellulose, and cellulose acetate, respectively.

A comparison of these values of d_s with the values of d_h reported above shows that the results found for d_h lie somewhere between these lower and upper limits for d_s:

	d_h in A.	d_s in A.
Methylcellulose	8	7.4 to 13
Nitrocellulose	9.2	7.5 to 14
Cellulose acetate	10.8	8 to 15

It must be mentioned, however, that in discussing the connection between d_h and d_s two further points require consideration:

(*1*) The possibility arises that the chain molecules may become solvated with molecules of the solvent. This would tend to increase the value of d_h with respect to that of d_s.

(*2*) It should be remembered that in thickness the chain molecules are of the same size as the molecules of the solvent. This, as has actually been demonstrated by W. Kuhn,[23] tends to decrease the value of d_h with respect to that of d_s. To show this, Kuhn compared the experimentally measured mobilities of approximately spherical molecules. He found, first that particles which are smaller, or equal in size to the molecules of the solvent have a somewhat greater mobility than would be expected from Stokes' law, and, second, that an asymptotic transition to Stokes' law mobility takes place with increasing diameter of the solute particle. Thus the diffusion constant of small molecules, such as N_2, O_2, CO_2 and urea in water, is about one and a half times the value expected from their known diameter by means of Stokes' law, while larger molecules such as glucose have a diffusion constant in agreement with hydrodynamics. In the case of chain molecules the fact that d_s and the diameter of the solvent molecules are of the same magnitude must be expected to produce a decrease of the hydrodynamic resistance, and thus of d_h, though to a very limited extent.

---

* The following section was somewhat expanded during the translation of this article.

We may conclude, therefore, that satisfactory agreement has been demonstrated between d_h and d_s. It would be futile to pursue the comparison without a great deal of further information.

Note Added in Proof

After this article was submitted for publication, papers by Kirkwood and Riseman[14] and Debye and Bueche[12] have appeared concerning the same subject.

Kirkwood and Riseman have found the same linear relationship, expressing s_0 and DZ as a function of $Z^{1/2}$, which we have reported above. Their result can, therefore, be expressed in equations which are similar to (35) and (41), *i.e.*, in terms of the length A_m of the preferential statistical chain element, and of a friction factor, ζ, of the monomer unit. ζ is a parameter which corresponds to our hydrodynamic thickness d_h. A comparison of Kirkwood and Riseman's equations with ours leads to the following relationships between their parameters (indicated by KR) and ours:

$$(A_m)_{KR} = 3.9A_m$$

$$(\zeta/\eta)_{KR} = \frac{b}{0.02 + 0.16 \log (A_m/d_h)}$$

From the first of these equations it follows that, given the same experimental diffusion and sedimentation data, the length of the preferential statistical chain element will, using Kirkwood and Riseman's treatment, turn out about four times larger than with ours.

Values of the friction factor ζ which are found by Kirkwood and Riseman and also by Newman, Riseman, and Eirich[24] are about ten times smaller than those expected on the basis of hydrodynamics. This result is therefore in some disagreement with ours, according to which rough agreement between d_h and d_s has been established, showing that hydrodynamics can be used to describe the behavior of these molecules. It has however been pointed out[25] that the experimental results of these authors[24] can be interpreted just as satisfactorily by using larger values of ζ which would be in agreement with hydrodynamics.

Debye and Bueche's treatment fails to account for the linear dependence of s_0 and DZ on $Z^{1/2}$ mentioned above. Nevertheless, there is a rough agreement between their results and ours. The best agreement is found in the limiting case of complete immobilization. In that case we find from Debye and Bueche's treatment that the translational resistance F equals $[9.94/(N_m)^{1/2}]\eta L\bar{u}$ in good agreement with the results $F = [10/(N_m)^{1/2}]\eta L\bar{u}$ which follows from equations (31) and (2). (A considerably different result is found from Kirkwood and Riseman's treatment, namely, $F = [5.1/(N_m)^{1/2}]\eta L\bar{u}$.)

References

1. W. Kuhn, *Kolloid-Z.*, **68,** 2 (1934).

2. For previous publications on this subject, see: H. Kuhn, *Habilitationsschrift*, Basel, 1946; *Schweiz. Chem.-Ztg.*, **1945,** 373; *Experientia*, **2,** 64 (1946); *Proceedings of the International Rheological Congress*, Holland, 1948.

For an application of the results to calculations of diffusion, sedimentation and viscosity constants in the case of solutions of branched chain molecules see: W. Kuhn and H. Kuhn, *Helv. Chim. Acta*, **30,** 1233 (1947).

3. W. Kuhn, *Z. angew. Chem.*, **49,** 858 (1936).

4. M. L. Huggins, *J. Phys. Chem.*, **42,** 911 (1938).

5. W. Kuhn, *Z. physik. Chem.*, **A161,** 1 (1932); *Kolloid-Z.*, **62,** 269 (1933).

6. The same model (free draining, "pearl necklace" structure) was also used by P. Debye. The same result was obtained. P. Debye; *J. Chem. Phys.*, **14,** 636 (1946).

7. W. Kuhn and H. Kuhn, *Helv. Chim. Acta*, **26,** 1394 (1943).

8. After the appearance of this paper,[7] the behavior of freely draining chain molecules in streaming solution was also treated by J. J. Hermans. The discussion was, however, limited to the case of a low-velocity gradient, and no solution of the differential equation determining the distribution function was given. J. J. Hermans, *Physica*, **10,** 777 (1943).

9. W. Kuhn and H. Kuhn, *Helv. Chim. Acta*, **28,** 98, 1533 (1945); **29,** 71, 609, 830 (1946); *J. Colloid Sci.*, **3,** 11 (1948).

10. *Loc. cit.*, ref. 7; see in particular pages 1397–98.

11. J. J. Hermans, *Rec. trav. chim.*, **63,** 219 (1944); *J. Polymer Sci.*, **1,** 233 (1946).

12. P. Debye, *Phys. Rev.*, **71,** 486 (1947). P. Debye and A. M. Bueche, **16,** 573 (1948).

13. H. C. Brinkman, *Applied Sci. Research*, **A1,** 27 (1947); *Koninkl. Nederland. Akad. Wetenschap. Proc.*, **50,** No. 6 (1947).

14. J. G. Kirkwood and J. J. Riseman, *J. Chem. Phys.*, **16,** 565 (1948); **17,** 442 (1949).

15. H. A. Kramers, *J. Chem. Phys.*, **14,** 415 (1946).

16. W. Kuhn, *Z. physik. Chem.*, **A161,** 1 (1932).

17. H. Kuhn, *Experientia*, **1,** 28 (1945); *Helv. Chim. Acta*, **31,** 1677 (1948).

18. H. E. Daniels, *Proc. Cambridge, Phil. Soc.*, **37,** 244 (1941). S. Chandrasekhar, *Rev. Modern Phys.*, **15,** 1 (1943). C. A. Hollingsworth, *J. Chem. Phys.*, **16,** 544 (1948).

19. R. Gans, *Ann. Physik*, **86,** 652 (1928).

20. A. Polson, *Kolloid-Z.*, **83,** 173 (1938).

21. H. Mosimann, *Helv. Chim. Acta*, **26,** 61 (1943).

22. E. O. Kraemer and J. B. Nichols in T. Svedberg and K. O. Pedersen, *The Ultracentrifuge.* Oxford Univ. Press, London. 1940.

23. W. Kuhn, *Exposé au Colloque; Cérémonies Langevin-Perrin, section des grosses molécules*, Paris, in press.

24. S. Newman, J. Riseman, and F. Eirich, *Proceedings of the International Colloquium on Macromolecules, Amsterdam 1949*, Centen's Uitgevers-Maatschappij N. V. Amsterdam, 1950.

25. Discussion remark of H. Kuhn to the paper in ref. 24, p. 388.

English Synopsis, see Summaries, page S21, Vol. V, 1950.

Résumé

La résistance aux mouvements de translation d'une pelote statistique est discutée en se basant sur des approximations differentes. La théorie est développée pour deux cas limites, savoir celui d'une pelote imperméable pour le solvent et celui d'une pelote complètement perméable. Dans le premier cas, la resistance de la pelote peut être obtenue approximativement en la comparant à une sphère (ou en meilleure approximation à un ellipsoide) de dimensions correspondantes. Par contre, la pelote complètement perméable est traitée en admettant que chaque élément statistique de la chaîne se comporte comme un ellipsoide de revolution allongé, et que la résistance hydrodynamique d'un élément consideré n'est pas influencée par les autres éléments de la chaîne.

Dans le cas général, où les molécules en chaîne ne sont que partiellement perméables pour solvant, la résistance hydrodynamique est déterminée expérimentalement en employant des modèles à grande échelle et par application d'un théorème de similitude hydrodynamique. Les modèles ont été construits en ployant des fils statistiquement.

Les formules empiriques, résultant de ces expériences, s'appliquent à tous les degrés de pelotage des macromolécules, depuis le cas limite de la pelote complètement perméable (degré de polymerisation petit) jusqu'au cas de la pelote imperméable (degré de polymerisation extrêmement grand). Dans ces cas limites, un bon accord est trouvé avec les résultats derivés théoriquement de la facon mentionée en haut.

Des expressions pour les constantes de sédimentation et de diffusion des molécules enroulées en pelotes statistiques sont également données. Elles sont en accord avec les données expérimentales. Ces résultats permettent de déduire les valeurs de la longueur A_m et de l'epaisseur hydrodynamique d_h d'un élément de la chaîne. Les valeurs de d_h ainsi obtenues sont en accord suffisant avec les valeurs de d_s, de l'épaisseur moyenne de la chaîne, déduite des données de la structure moléculaire. Ceci montre, que l'utilisation de modèles macroscopiques ainsi que l'application du principe de similitude hydrodynamique permettent une approche rationelle du comportement des macromolécules en solution, et la qualité des résultats ainsi obtenus prouve que l'application du principe de similitude à des particules d'aussi petites dimensions ne constitute pas une approximation irraisonable.

Zusammenfassung

Der Translationswiderstand eines statistisch geknäuelten Fadenmoleküls wird auf Grund verschiedener Näherungsverfahren ermittelt. Die beiden Grenzfälle des undurchspülten und des gleichmässig bespülten Knäuels werden theoretisch behandelt. Für die modellmässige Betrachtung wird angenommen, dass sich ein undurchspültes Knäuel hydrodynamisch so verhält wie eine Kugel (bzw. bei verfeinerter Betrachtung wie ein Ellipsoid) entsprechender äusseren Abmessungen. Der Translationswiderstand eines gleichmässig bespülten Fadens anderseits wird unter der Annahme berechnet, dass sich jedes der statistischen Vorzugselemente der Kette hydrodynamisch so verhält wie ein langgestrecktes Rotationsellipsoid und dass der hydrodynamische Widerstand eines herausgegriffenen Elementes von den Nachbarelementen nicht beeinflusst wird.

Der hydrodynamische Widerstand teilweise durchspülter Knäuel wird auf Grund von Translationsversuchen mit makroskopischen Molekülmodellen ermittelt unter Verwendung eines hydrodynamischen Aehnichkeitsprinzips. Die Modelle werden durch geeignetes Biegen von Draht nach einem statistischen Verfahren hergestellt.

Auf Grund dieser Versuche ergibt sich eine empirische Beziehung für den Translationswiderstand, welche auf den gesamten Bereich, ausgehend vom Grenzfall gleichmässiger Bespülung bis zum Grenzfall fehlender Durchspülung, anwendbar ist. Die Beziehung geht in diesen beiden Grenzfällen in Ausdrücke über, welche gut übereinstimmen mit den Relationen, welche theoretisch in der oben angedeuteten Weise erhalten wurden.

Auf Grund dieser für den hydrodynamischen Widerstand gültigen Beziehungen lassen sich Ausdrücke für die Sedimentations- und Diffusionskonstante statistisch geknäuelter Fadenmoleküle angeben. Sie werden an der Erfahrung bestätigt. Der Vergleich von Theorie und Experiment führt zur Ermittlung von Werten für die Länge A_m und die hydrodynamische Dicke d_h des Vorzugselementes. Die so erhaltenen Werte für die hydrodynamische Fadendicke d_h stimmen angenähert überein mit den aus molekularstrukturellen Daten sich ergebenden Werten für die wahre Fadendicke d_s. Aus dieser Uebereinstimmung geht hervor, dass die beschriebenen Modellversuche verbunden mit dem hydrodynamischen Aehnlichkeitsprinzip zu einer befriedigenden Deutung des Verhaltens von Fadenmolekülen in Lösung führen und dass eine Uebertragung des Aehnlichkeitsprinzips auf Teilchen dieser Dimension im Rahmen der beschriebenen Näherung zulässig ist.

Received December 1, 1947

JOURNAL OF POLYMER SCIENCE VOL. V, NO. 5, PAGES 543-549

Optische Anisotropie und Form von Fadenmolekülen. I. Depolarisationsgrad der Lichtzerstreuung von Lösungen mit Fadenmolekülen

H. A. STUART, *Hannover*, und A. PETERLIN, *Physikalisches Institut der Universitat, Ljubljana, Yugoslavia*

I. ALLGEMEINE VORAUSSETZUNGEN

Wir zerlegen wie üblich das aus P monomeren Resten bestehende Fadenmolekül in Z voneinander unabhängige statische Fadenelemente der mittleren Länge A, die wie durch Kugelgelenke miteinander verbunden unabhängig voneinander jede beliebige Richtung einnehmen können. Jedes Fadenelement enthält $s = P/Z$ monomere Reste. Wir ordnen ferner jedem Element die optischen und elektrischen Hauptpolarisierbarkeiten α_{01}, α_{02}, α_{03} bzw. $\bar{\alpha}_{01}$, $\bar{\alpha}_{02}$, $\bar{\alpha}_{03}$ sowie die mittlere Polarisierbarkeit:

$$\alpha_0 = (\alpha_{01} + \alpha_{02} + \alpha_{03})/3$$

zu. Ist α_{gr} die mittlere Polarisierbarkeit des monomeren Restes (Grundmoleküls), so ist $\alpha_0 = s\alpha_{gr}$. Die Hauptpolarisierbarkeit sowie die optische Anisotropie des Fadenelements, definiert durch:

$$\delta_0^2 = \frac{(\alpha_{01} - \alpha_{02})^2 + (\alpha_{02} - \alpha_{03})^2 + (\alpha_{03} - \alpha_{01})^2}{[\alpha_{01} + \alpha_{02} + \alpha_{03}]^2}$$

sind bei einem Fadenmolekül in Lösung oder in flüssigem Zustande wegen der Anisotropie des inneren elektrischen Feldes nicht gleich den entsprechenden Werten für das freie Molekül im Dampfzustande und grundsätzlich vom Lösungsmittel sowie der Ordnung und Dichte der Lösungsmittelmolekule um das Gelöste (orientierte Solvatation), d.h. auch von der Temperatur abhängig.*,†

---

* Der von den polarisierten irgendwie geordneten Lösungsmittelmolekülen herrührende Beitrag zum inneren Felde macht dieses anisotrop und bewirkt allgemein eine scheinbare Abnahme der Polarisierbarkeit in Richtung der Grössenausdehnung des Fadenelements und quer dazu eine Vergrösserung, d.h. meist eine Abnahme der Anisotropie. Vergl. dazu auch die folgende Arbeit, Anm. 2, sowie etwa H. A. Stuart, *Hand- und Jahrb. der chem. Physik*, Bd. 10, III, Leipzig, 1939; *Z. Elektrochem.*, **45**, 180 (1938). Dazu kommt, dass sowohl die Grösse, wie die mittlere Länge A des Fadenelements grundsätzlich vom Lösungsmittel abhängen und in einer Lösung im allgemeinen grösser als im Dampfe sind. Infolge der mehr oder weniger anliegenden Lösungsmittelmoleküle ist die Kette sperriger. Der statistische Charakter des Aufbaues bleibt erhalten.

† Der Inhalt dieser und der folgenden Arbeit wurden erstmals im Physikalischen Kolloquium der T. H. München im Juni 1944 vorgetragen (vergl. Ref. 2).

Aus diesem Grunde ist eine absolute Berechnung der optischen Anisotropie und des Depolarisationsgrades des molekular gestreuten Lichtes sowie jeder Art von Doppelbrechung aus dem Modell für Fadenmoleküle in Lösung ebensowenig möglich wie eine entsprechende molekular-theoretische Berechnung dieser Grössen bei niedermolekularen Flüssigkeiten. Wohl aber kann man die Abhängigkeit dieser Grössen mit dem Polymerisationsgrade angeben, da diese von der Struktur des inneren Feldes unabhängig ist.

Alle Ableitungen in dieser und der folgenden Arbeit gelten nur für den Fall, dass das Molekül klein gegen die Wellenlänge des erregenden Lichtes ist, genauer, dass für die grösste Molekülabmessung d gilt $d \ll \lambda$.

Bezüglich der Formen eines Fadenmoleküls wollen wir von vornherein folgende Stufen unterscheiden:

(*1*) *Kräftefreier Fall.* Sind die innermolekularen Kräfte von derselben Grösse wie die zwischenmolekularen, so haben wir ein rein statistisch, d.h. nach Wahrscheinlichkeitsgesetzen gebautes Knäuel. Bei kürzeren Ketten, wo jedes Fadenelement von Lösungsmittelmolekülen frei umgeben, bzw. solvatisiert ist, sprechen wir von der *losen Fadenform* (durchspülter Faden nach Kuhn). Mit wachsender Kettenlänge treten rückläufige Stücke, Verschlingungen auf und infolge der gegenseitigen räumlichen Behinderung eine zunächst geringfügige, meist vernachlässigbare Aufweitung des Gebildes auf. Die Abweichungen von der rein zufälligen Richtungsverteilung der Fadenelemente werden sich dabei herausmitteln.

(2) Bei längeren Ketten werden mehr und mehr Lösungsmittelmoleküle umschlossen, immobilisiert, wir erhalten ein schwammartiges Knäuel, das wir als *Schwammknäuel* bezeichnen wollen.

Auch hier bleibt die Zufallsstatistik erhalten (Kuhns undurchspülter Faden). Da sich dieses Gebilde in einem Strömungsfelde, aber nicht in einem Potentialfelde als Ganzes bewegt und einstellt, erhalten wir charakteristische Unterschiede bei der Viskosität, Strömungsdoppelbrechung und bei der Sedimentation. Dagegen werden die dielektrische Polarisation und wohl auch die dielektrischen Verluste nicht beeinflusst.

(*3*) *Knäuel mit innerer Anziehung.* Ueberwiegende innermolekulare Kräfte führen zu einer inneren Vernetzung durch Haftpunkte und damit einer stärkeren Ballung und Verdichtung.

Trotz der inneren Verfestigung ist der Fall denkbar, dass bei einem völlig versteiften starren Gebilde die Richtungsverteilung der Fadenelemente oder monomeren Reste im Mittel dieselbe ist wie bei einem kräftefreien Gebilde, die Richtungsstatistik also anwendbar bleibt. In diesem Falle wollen wir von einem *idealen starren Knäuel* sprechen. Das in sich verfestigte Knäuel wird sich wie das Schwammknäuel im Strömungsfelde als Ganzes einstellen, in einem Potentialfelde erst dann, wenn die Länge der Fadenelemente gross gegen die Abstände der Haftpunkte wird, d.h., wenn jede mikrobrownsche Bewegung aufhört, was an den Relaxationszeiten der DK und der elektrischen Doppelbrechung erkennbar wäre. In diesem Grenzfalle wird allerdings auch der Begriff des unabhängigen Fadenelementes sinnlos.

Bei allen Abweichungen von den Gesetzmässigkeiten für den losen Faden bzw. das ideale starre Knäuel sind jedenfalls der Einfluss einer Aufweitung bzw. Verdichtung und derjenige einer durch innermolekulare Kräfte modifizierten Richtungsverteilung der Fadenelemente getrennt zu diskutieren. Ausserdem ist zu prüfen, ob nicht bei guter Solvatation das Molekül so versteift wird, dass s gegenüber P so gross, Z also so klein wird, dass die üblichen statistischen Mittelwertsbildungen ihre Gültigkeit verlieren.[1]

II. DEPOLARISATIONSGRAD BEI DER MOLEKULAREN LICHTZERSTREUUNG

A. Theorie

Der Einfachheit halber nehmen wir für die Polarisierbarkeiten des Fadenelements Rotationssymmetrie an, also $\alpha_{02} = \alpha_{03}$. Die Allgemeingültigkeit unserer Ergebnisse wird dadurch nicht beeinflusst. α_{01} falle in die Richtung des Fadenelements, d.h. in die Verbindungslinie der Endpunkte. Das j-te Fadenelement bilde mit der z-Achse eines raumfesten Systems den Winkel Θ_j. Seine Projektion auf dessen x-y-Ebene den Winkel φ_j. Das in der positiven y-Richtung einfallende, linearpolarisierte Licht, dessen Vektor in der z-Richtung schwingen möge, $f = f_z$, induziert dann im Element j ein Moment p_j. Da wir das Molekül als klein gegen die Wellenlänge des erregenden Lichtes vorausgesetzt haben, können die Phasenunterschiede des elektrischen Feldes in den einzelnen Elementen vernachlässigt werden, so dass die im ganzen Molekül induzierten Momentkomponenten einfach die algebraische Summe der in den einzelnen Elementen erregte Momenten sind. Die Komponenten dieses Gesamtmomentes sind also durch die Gleichungen bestimmt:

$$\begin{aligned} p_y &= \sum p_{jy} = (\alpha_{01} - \alpha_{02}) f \sum \sin\theta_j \cos\theta_j \sin\varphi_j \\ p_z &= \sum p_{jz} = f \sum (\alpha_{01}\cos^2\theta_j + \alpha_{02}\sin^2\theta_j) = f \sum [\alpha_0 + \\ &\qquad (\alpha_{01} - \alpha_{02})(\cos^2\theta_j - {}^1/_3)] \end{aligned}$$

Die Intensitäten des in der y- und z-Richtung schwingenden Streulichtes erhalten wir durch Quadrieren und Mitteln über alle räumlichen Lagen der Fadenelemente,* also†

$$\begin{aligned} J_y &= \text{const. } J_0(\alpha_{01} - \alpha_{02})^2(Z/15) \\ J_z &= \text{const. } J_0[\alpha_0{}^2 Z^2 + (\alpha_{01} - \alpha_{02})^2(4Z/45)] \end{aligned} \tag{2}$$

---

* Die Mittelung über alle Orientierungen der Fadenelemente ist wegen der vorausgesetzten völligen Unabhängigkeit der Richtungen identisch mit der Mittelung über alle Konfigurationen des Moleküls und seine räumlichen Lagen.

† Man sieht leicht ein, dass bei der Mittelung für J_y die gemischten Glieder aus Symmetriegründen wegfallen, also lediglich Z Glieder der gleichen Form $\sin^2\theta_j \cos^2\theta_j \sin^2\varphi_j = {}^1/_{15}$ übrig bleiben. Bei J_z hat man es, je kleiner die Anisotropie $(\alpha_{01} - \alpha_{02})$ ist, umso ausschliesslicher mit der mittleren Polarisierbarkeit des ganzen Moleküls $\alpha = Z\alpha_0$ zu tun. Daher wird die Intensität vor allem durch das quadratische Glied bestimmt. Die weiteren in Z quadratischen Glieder heben sich weg.

wo J_0 die Intensität des einfallenden Lichtes bedeutet. Damit erhalten wir für den Depolarisationsgrad bei linearpolarisiertem erregenden Licht

$$\Delta' = \frac{J_y}{J_z} = \frac{(\alpha_{01} - \alpha_{02})^2}{15 Z \alpha_0{}^2 + {}^4/_3(\alpha_{01} - \alpha_{02})^2} \tag{3}$$

Da zwischen Δ' und der mittleren optischen Anisotropie des Moleküls $\overline{\delta^2}$ allgemein die Beziehung

$$\Delta' = \frac{3\overline{\delta^2}}{10 + 4\overline{\delta^2}} \tag{4}$$

besteht, erhält man für $\overline{\delta^2}$ den Wert[2]

$$\overline{\delta^2} = \frac{2(\alpha_{01} - \alpha_{02})^2}{Z(\alpha_{01} + 2\alpha_{02})^2} = \frac{\delta_0^2}{Z} \qquad \delta_0^2 = \frac{2(\alpha_{01} - \alpha_{02})^2}{(\alpha_{01} + 2\alpha_{02})^2} \tag{5}$$

Es ist also die mittlere optische Anisotropie des ganzen Moleküls gleich derjenigen des Fadenelements dividiert durch die Zahl der Elemente. Sie nimmt daher mit wachsendem Polymerisationsgrade ab. Das ist einfach die Folge davon, dass mit wachsender Zahl der Fadenelemente, deren Richtungsverteilung immer gleichmässiger, das Gebilde im Mittel damit optisch isotroper wird. Der Depolarisationsgrad Δ für unpolarisiertes Licht bestimmt sich im gleichen Geltungsbereich zu

$$\Delta = \frac{2J_y}{J_z + J_y} = \frac{2\Delta'}{1 + \Delta'} = \frac{6\overline{\delta^2}}{10 + 7\overline{\delta^2}} \tag{6}$$

Wegen der Kleinheit von Δ und Δ' kann man für (4) und (6) genähert schreiben

$$\Delta = {}^3/_5\overline{\delta^2}; \qquad \Delta' = {}^3/_{10}\overline{\delta^2} \tag{7}$$

Die mittlere optische Anisotropie des Gesamtmoleküls ist definiert durch

$$\overline{\delta^2} = \frac{\overline{(\alpha_1 - \alpha_2)^2 + (\alpha_2 - \alpha_3)^2 + (\alpha_3 - \alpha_1)^2}}{Z^2(\alpha_{01} + \alpha_{02} + \alpha_{03})^2}$$

α_1, α_2, α_3 die Polarisierbarkeiten in Richtung der optischen Hauptachsen der betreffenden Molekülform. Diese fallen im allgemeinen nicht mit den Polarisierbarkeiten $\parallel$ und $\perp$ zur Verbindungslinie der Endpunkte zusammen. Man erhält die Anisotropie $\overline{\delta^2}$ als Mittelwert über alle Molekülformen einer bestimmten Länge mit nachfolgender Mittelung über alle Längen. Diese Mittelung ergibt im Einklang mit der obigen Ableitung

$$\overline{\delta^2} = \frac{2(\alpha_{01} - \alpha_{02})^2}{Z(\alpha_{01} + 2\alpha_{02})^2}$$

oder

$$\overline{(\alpha_1 - \alpha_2)^2 + (\alpha_2 - \alpha_3)^2 + (\alpha_3 - \alpha_1)^2} = 2Z(\alpha_{01} - \alpha_{02})^2$$

Die hier auftretenden quadratischen Mittelwerte sind nicht mit dem linearen Mittelwert zu verwechseln, der nach Kuhn und Grün[3] in erster

Näherung durch $(\overline{\alpha_x} - \overline{\alpha_y}) = {}^3/_5(\alpha_{01} - \alpha_{02})$ gegeben, also unabhängig vom Polymerisationsgrade ist.

B. Gültigkeitsbereich der Theorie

Unsere Ableitung setzt voraus, dass die grösste Abmessung des Moleküls 500 A. nicht wesentlich überschreitet, was bei Molekulargewichten bis zu einigen Hunderttausend meist zutrifft. In diesem Falle ist auch die Gleichung $\Delta = 2\Delta'$ gültig. Ist diese also experimentell erfüllt, so kann man sicher sein, dass die Molekülabmessungen klein gegen die Wellenlänge des Lichtes sind. Gleichung (5) ist auch unabhängig davon, wie weit die Anisotropie des Fadenelements auf einer Formanisotropie beruht, bzw. durch die Eigenanisotropie der einzelnen Bindungen bedingt ist und schliesslich auch unabhängig vom Lösungsmittel. Dieses beeinflusst lediglich über die Grösse den Absolutwert des Depolarisationsgrades und zwar, wie eine Messung von Lotmar†,[4] an Nitrocellulose in Aceton und Methylalkohol zeigt, recht erheblich. Schliesslich gilt die Beziehung $\Delta \backsim 1/P$ für jedes Gebilde, dessen Fadenelemente nach Wahrscheinlichkeitsgesetzen über alle Richtungen verteilt sind, unabhängig von dessen innerer Starrheit, also sowohl für den losen Faden wie für das Schwammknäuel und ebenso für das in sich verfestigte ideale starre Knäuel. Sobald durch die innermolekularen Kräfte die Richtungsverteilung der Elemente modifiziert wird, z.B. wenn durch eine innermolekulare Faltung oder spiralförmigen Aufbau eine Richtung oder Ebene besonders ausgezeichnet oder durch Solvatation das Gebilde besonders stark gestreckt wird, können wir über den Zusammenhang von Δ und P von vornherein nichts aussagen. Bei starker Verdichtung oder erheblicher innerer Vernetzung verliert der Begriff des Fadenelementes mit einer charakteristischen Polarisierbarkeit und unabhängigen Einstellung und damit auch die Beziehung (5) ihren Sinn.

Infolge der grundsätzlichen Abhängigkeit sowohl der Form wie der Anisotropie des Fadenelements vom Lösungsmittel kann man aus der Grösse des Depolarisationsgrades in verschiedenen Lösungsmitteln allein keine Schlüsse auf die Formvariation ziehen.

Unsere ganze Betrachtung gilt natürlich auch nur für eine hinreichend verdünnte Lösung, wo die Fadenmoleküle völlig unabhängig voneinander das Licht streuen. Sobald die Fäden mit wachsender Konzentration sich gegenseitig mehr und mehr durchdringen, werden der Depolarisationsgrad ebenso wie die Intensität des Streulichtes vom Molekulargewicht immer unabhängiger und gehen gegen einen Grenzwert. Man kann im Sinne der Schwankungstheorie sagen, dass es schliesslich nur noch auf die Zahl und Orientierung der Fadenelemente bzw. monomeren Reste im Volumenele-

† Für ein Polystyrol mit $P = 5000$, $M = 520{,}000$ wird die Länge des gestreckten Moleküls 12,500 A. Der mittlere Abstand der Endpunkte h ist dagegen für ein statistisch geknicktes Gebilde mit $s = 10$ oder $Z = 500$, also $\bar{A} < 25$ A., gleich $h = \bar{A}\ (Z)^{1/2} < 550$ A.

ment ankommt, gleichgültig ob diese sehr vielen oder nur ganz wenigen Molekülen angehören.

C. Einfluss der Polydispersität[2]

Es seien die Zahlen pro ccm $N_1, N_2, \ldots N_n$ der Anteile mit den Polymerisationsgraden $P_1, P_2 \ldots P_n$ gegeben. Dann gilt für die mittlere Anisotropie

$$\overline{\delta^2} = \delta_0^2 s\left(\sum NP/\sum NP^2\right)$$

bzw. für den umgekehrt aus Δ bestimmten mittleren Polymeriationsgrad

$$\bar{P} = \left(\sum NP^2/\sum NP\right)$$

Ist die Verteilung der Molekülzahlen auf die einzelnen Polymeriationsgrade durch eine Gauss'sche Fehlerfunktion gegeben

$$N(P) = \frac{N}{B(\pi)^{1/2}} \exp\left(-\left(\frac{P - P_0}{B}\right)^2\right)$$

P_0 der häufigste Wert, B die Breite der Polydispersität, so gilt:*

* Innerhalb des Bereiches $P_0 - B$, $P_0 + B$ befinden sich 84% aller Moleküle.

$$\overline{\delta^2} = \delta_0^2 s \frac{1}{P_0(1 + B^2/2P_0)}$$

Ist die Verteilungsfunktion wieder eine Gauss'sche, jetzt aber in Volumenkonzentrationen ausgedrückt, also

$$c(P) = \frac{c}{B(\pi)^{1/2}} \exp\left(-\left(\frac{P - P_0}{B}\right)^2\right)$$

so gilt einfach

$$\overline{\delta^2} = \delta_0^2 s/P_0$$

D. Vergleich mit der Erfahrung

Für diesen Zweck stehen uns die Messungen von Lotmar an Methyl- und Nitrocellulosen zur Verfügung, die in Tabelle I zusammengestellt sind. Wie man sieht, sinkt der Depolarisationsgrad mit wachsendem Molekulargewicht ab. Zwar sind die Produkte $M\Delta$ und $M\Delta'$ nicht konstant. Doch kann man diese Abweichungen auf die Polydispersität der unter-

TABELLE I

DEPOLARISATIONSGRADE VON LÖSUNGEN MIT FADENMOLEKÜLEN

Stoff	100Δ	$100\Delta'$	M	$M\Delta$	$M\Delta'$
Methylzellulose in Wasser..........	1.5	0.27	18,500	278	50
	1.4	0.41	46,000	645	188
	0.53	0.14	98,000	518	137
Nitrozellulose in Methylalkohol.....	3.0	1.5	17,400	52.2	26.1
	3.0	1.1	24,200	72.6	26.6
	2.0	0.58	65,200	130	37.7

suchten Fraktionen und die besonders bei kleinen Depolarisationsgraden sehr erheblichen Fehler schieben. Wie gross die letzteren vor allem wohl infolge von Staubgehaltes sind, erkennt man schon daraus, dass die bei kleinen Molekülen (im Sinne der Bedingung $d < (\lambda/2\pi n)$ allgemein gültige Beziehung $\Delta = 2\Delta'$ fast nirgends erfüllt ist. Bei einem Vergleich mit der Erfahrung muss natürlich auch der Einfluss des Lösungsmittels auf die Streuung berücksichtigt werden. Da der Beitrag von Wasser, Methanol und Aceton sehr gering ist, kann in diesem Falle davon abgesehen werden.

References

1. Vgl. für das Folgende z.B. den Artikel "Lichtzerstreuung" von H. A. Stuart im *Hand- und Jahrb. der chem. Phys.*, Bd. 8, II, Leipzig, 1936.
2. Vgl. A. Peterlin, *Verh. Akad. Ljubljana, Math. Phys. Kl.*, 3, 79 (1947), eingereicht Mai 1944.
3. W. Kuhn und F. Grün, *Kolloid-Z.*, 101, 248 (1942).
4. W. Lotmar, *Helv. Chim. Acta*, **22**, 813 (1938).

English Synopsis, see Summaries, page S7, Vol. V, 1950.

Zusammenfassung

Es wird der Depolarisationsgrad bei der molekularen Lichtzerstreuung von statistisch geknickten Fadenmolekülen in Abhängigkeit vom Polymerisationsgrade berechnet und die Gültigkeitsgrenzen der Theorie näher diskutiert.

Résumé

Le degré de dépolarisation dans la diffusion moléculaire de la lumière des molécules filamenteuses enroulées statistiquement a été calculé en fonction du degré de polymérisation, et les limites de validité de la théorie sont discutées.

Received April 25, 1949

JOURNAL OF POLYMER SCIENCE VOL. V, NO. 5, PAGES 551-563

Optische Anisotropie und Form von Fadenmolekülen. II. Künstliche Doppelbrechung

H. A. STUART, *Hannover*, und A. PETERLIN, *Physikalisches Institut der Universität, Ljubljana, Yugoslavia*

I. ALLGEMEINE VORAUSSETZUNGEN

Das Molekül setzen wir in erster Näherung als starr voraus, d.h. wir vernachlässigen die Deformation des Moleküls als Ganzes. Das bedeutet bei der elektrischen und magnetischen Doppelbrechung, wo das homogene äussere Feld keine ziehenden, sondern nur drehende Kräfte ausübt, keine Einschränkung, wohl aber bei der Strömungsdoppelbrechung, siehe Abschn. C. Im übrigen gelten dieselben Voraussetzungen und Hinweise wie in der vorhergehenden Arbeit I.[1] Die Anisotropie des inneren Feldes lassen wir wieder ausser acht. Zwar kann diese die Polarisierbarkeiten des Fadenelementes so beeinflussen, dass beim Uebergang von einem Lösungsmittel zum anderen ein Vorzeichenwechsel in $\alpha_{01} - \alpha_{02}$ und somit auch im Betrag der Doppelbrechung auftritt.

Das innere Feld im Achsensystem des Fadenelementes sei durch die Gleichungen gegeben

$$F_1 = \frac{\epsilon + 2}{3}(1 - 2l)f_1 \qquad F_2 = F_3 = \frac{\epsilon + 2}{3}(1 + l)f_2$$

Dann wird, wenn α'_{01} und α'_{02} die Polarisierbarkeiten des Fadenelements im freien Molekül im Dampfzustande bedeuten,

$$\alpha_{01} = \alpha'_{01}(1 - 2l) \qquad \alpha_{02} = \alpha'_{02}(1 + l)$$

Vgl. A. Peterlin und H. A. Stuart.[2]

Auf die Abhängigkeit der Doppelbrechung vom Polymeriationsgrad hat das innere Feld aber keinen Einfluss.

II. THEORIE DER ELEKTRISCHEN UND MAGNETISCHEN DOPPELBRECHUNG

Die spezifische elektrische Doppelbrechung K_{sp} definieren wir im Anschluss an frühere Arbeiten[3] als

$$K_{sp} = \frac{\Delta n}{c_v n f_0^2} = \left(\frac{\epsilon + 2}{3}\right)^2 \left(\frac{n^2 + 2}{3n}\right)^2 \frac{2\pi}{V} \frac{\overline{\Delta\alpha}}{f^2} \tag{1}$$

wo c_v die Volumenkonzentration, V das Volumen des Fadenmoleküls und

$\overline{\Delta\alpha}$ die mittlere Differenz der optischen Polarisierbarkeiten $\alpha_{\|}$ und $\alpha_{\perp}$ des Einzelmoleküls parallel und senkrecht zur Feldrichtung f bedeutet, oder

$$\overline{\Delta\alpha} = \bar{\alpha}_{\|} - \alpha_{\perp} = \overline{(\Delta\alpha)_1} + \overline{(\Delta\alpha)_2} \tag{2}$$

wo $\overline{(\Delta\alpha)_1}$ den Verschiebungs- und $\overline{(\Delta\alpha)_2}$ den Dipolanteil bedeutet.

Setzen wir das innere Feld F als isotrop und als $(\epsilon + 2)/3 \cdot f$ an und nehmen wir für die Polarisierbarkeiten des Fadenelements der Einfachheit halber wiederum Rotationssymmetrie an, so ergibt die Durchrechnung[8a]

$$\begin{aligned} \overline{(\Delta\alpha)_1} &= \frac{f^2}{kT}\,\frac{(\alpha_{01} - \alpha_{02})(\bar{\alpha}_{01} - \bar{\alpha}_{02})}{15}\,Z \\ \overline{(\Delta\alpha)_2} &= \frac{f^2}{k^2T^2}\,\frac{(\alpha_{01} - \alpha_{02})}{15}\,\mu_0^2 Z \end{aligned} \tag{3}$$

μ_0 das elektrische Moment des Fadenelements. Wir erkennen daraus, dass die Beiträge zur Doppelbrechung pro Molekül linear mit dem Polymerisationsgrade ansteigen. Die spezifische Doppelbrechung wird dagegen von P unabhängig, nämlich

$$K_{sp} = \frac{\Delta n}{c_t n f^2} = \left(\frac{\epsilon + 2}{3}\right)^2 \left(\frac{n^2 + 2}{3n}\right)^2 \frac{3\pi}{V}\, Z(\theta_1 + \theta_2)_0 \tag{4}$$

oder mit $V = Z \cdot V_0$

$$K_{sp} = \left(\frac{\epsilon + 2}{3}\right)^2 \left(\frac{n^2 + 2}{3n}\right)^2 \frac{3\pi}{V_0}\, (\theta_1 + \theta_2)_0 \tag{5}$$

wo θ_{01} und θ_{02} die Doppelbrechungsfaktoren der einzelnen Fadenelemente bedeuten.

$$\theta_{01} = \frac{2(\alpha_{01} - \alpha_{02})(\bar{\alpha}_{01} - \bar{\alpha}_{02})}{45kT}; \quad \theta_{02} = \frac{2(\alpha_{01} - \alpha_{02})}{45k^2T^2}\,\mu_0^2 \tag{6}^*$$

Führen wir die Kerrkonstante $B = (\Delta n/\lambda f^2)$ ein, so erhalten wir mit

$$B = \frac{\pi}{n\lambda}\left(\frac{\epsilon + 2}{3}\right)^2 \left(\frac{n^2 + 2}{3}\right)^2 N_{ccm}\, Z(\theta_1 + \theta_2) \tag{7}$$

Bei konstanter Konzentration, $N_{ccm}\, Z = \text{const.}$ wird B und ebenso K_{sp} unabhängig vom Polymerisationsgrade und der Art der Polydispersität.

Entsprechende Formeln gelten für die magnetische Doppelbrechung, wobei nur die elektrostatischen Polarisierbarkeiten α_e durch die magnetischen α_m und das elektrische Moment μ_0 durch das magnetische μ_m zu ersetzen ist.

---

[*] Diese Ausdrücke entsprechen völlig denen der Doppelbrechung für kleine Moleküle. Ist das Fadenelement optisch und elektrisch nicht mehr rotationssymmetrisch, so sind die Ausdrücke θ_1 und θ_2 durch die allgemeineren, aus der Theorie des Kerr-Effekts für kleine Moleküle bekannten Beziehungen zu ersetzen.

Die obigen Beziehungen gelten in dieser einfachen Form nur solange, als das Lösungsmittel keinen wesentlichen Beitrag zur Doppelbrechung liefert. Sonst kommt noch ein entsprechend gebautes, von den Lösungsmittelmolekülen herrührendes Glied B hinzu.[3]

Da bei der Ableitung nur die ungeordnete Verteilung der Fadenelemente vorausgesetzt wird, gilt diese wie diejenige des Depolarisationsgrades für jedes Fadenmolekül, dessen Elemente nach Zufallsgesetzen orientiert sind, also sowohl für den losen Faden wie für ein Schwamm- und ein ideales starres Knäuel.

Die Unabhängigkeit der spezifischen Doppelbrechung vom Polymerisationsgrade kann man übrigens bereits ohne jede Rechnung einsehen. Da sich jedes Fadenelement unabhängig von andern im Felde einstellt und somit unabhängig seinen Beitrag zur Doppelbrechung des Mediums liefert, wird die Doppelbrechung der Gesamtzahl der Fadenelemente direkt proportional unabhängig davon, ob sich diese auf einige wenige ganz lange oder auf sehr viele kurze Moleküle verteilen. Dasselbe gilt auch für die Orientierungspolarisation $P_0 \sim N_{\text{ccm}} Z \mu_0^2$. Da ausserdem allgemein $P_0 \sim N_{\text{ccm}} \overline{\mu^2}$ ist, $\overline{\mu^2}$ der quadratische Mittelwert des Gesamtmomentes, folgt daraus sofort die bekannte Beziehung $\overline{\mu^2} = Z \mu_0{}^2$.

Wären die Fadenmoleküle starr und gestreckt, so würden sowohl das elektrische Moment, wie bei längeren Ketten—sobald nämlich die Formanisotropie ihren Grenzwert erreicht hat, vgl. Abschn. IV—die Differenz der Polarisierbarkeiten längs und quer zur Kette linear mit Z ansteigen. Es würde also in diesem Falle eines starren Stäbchens das Dipolglied der spezifischen Doppelbrechung quadratisch, das Anisotropieglied dagegen linear mit dem Polymerisationsgrade verlaufen.

Da zwischen der elektrischen Doppelbrechung und der optischen, Anisotropie der Moleküle allgemein die Beziehung $\Delta n \sim N_{\text{ccm}} \overline{\delta^2} \alpha^2$ besteht, folgt bei statistisch gebauten Molekülen aus der Konstanz von Δn bei festgehaltener Konzentration, $N_{\text{ccm}} Z = \text{const}$, unmittelbar die bei der Lichtzerstreuung in AI abgeleitete Abnahme der optischen Anisotropie mit dem Polymerisationsgrade, nämlich

$$\overline{\delta^2} = \frac{\text{const.}}{N_{\text{ccm}} \alpha^2} = \frac{\text{const.}}{N_{\text{ccm}} Z^2 \alpha_0^2} \sim \frac{1}{Z} \sim \frac{1}{P} \tag{8}$$

Für die gestreckte starre Form würde wegen des mit P linearen Anstieges des Anisotropiebeitrages zu Δn die optische Anisotropie $\overline{\delta^2} \sim P/N_{\text{ccm}}\, \alpha^2$, also konstant werden.

III. THEORIE DER STRÖMUNGSDOPPELBRECHUNG[3a]

Wir beschränken uns auf den zweidimensionalen Fall und weiterhin auf so kleine Geschwindigkeitsgefälle q, dass wir die Deformation des Moleküls durch die abwechselnd dehnend und stauchend wirkenden hydrodynamischen Kräfte vernachlässigen können. In diesem Sinne können wir das

Molekül als "starr"* behandeln, d.h. als ein Gebilde, das aus völlig ungeordnet aneinander gereihten Elementen aufgebaut, durch die Strömung nicht merklich deformiert wird.

Es sind also wesentlich dieselben Voraussetzungen, unter denen Huggins[4] die Staudingersche lineare Viskositätsbeziehung abgeleitet hat. Unsere Betrachtungsweise der Bewegung des "starren" Moleküls ist der seinerzeit von Huggins gewähl ten ähnlich.

Im linearen Strömungsfelde ist die Geschwindigkeit der Strömung gegeben durch

$$v_x = 0 \qquad v_y = qx \tag{9}$$

Auf das Element j wirkt die hydrodynamische Reibungskraft $K_j = \eta\lambda v_{j,\,rel}$ $v_{j,\,rel}$ die Relativgeschwindigkeit. Den Widerstandkoeffizienten λ des Elements betrachten wir zur Vermeidung zusätzlicher unsicherer Annahmen als Unbekannte. Die hydrodynamische Wechselwirkung vernachlässigen wir, was einigermassen zulässig ist. Es sind ja die Strömungen am Ort beider Molekülhälften entgegengesetzt, so dass sich z.B. ihre Wirkungen auf den Molekülmittelpunkt gerade aufheben. Das starre Molekül macht die Translation und Rotation der Strömung soweit wie möglich mit, sodass die Resultante aller Kräfte K_j und ihrer Momente M_j in jedem Augenblick verschwindet, also

$$\sum K_j = 0 \tag{10}$$

$$\sum M_j = \sum (x_j K_{jy} - y_j K_{jx}) = 0$$

beiden Bedingungen wird durch den Ansatz

$$v_{jx} = v_{0x} - \omega y_j; \quad v_{jy} = v_{0y} + \omega x_j \tag{11}$$

für die Geschwindigkeit v_j des j-ten Elements genügt, wo v_0 die Translation und ω die Rotation des starren Moleküls bedeuten. Da wir es mit einer reinen Drehung zu tun haben, muss (11) der Bedingung $\sum v_j = 0$ genügen. Damit erhalten wir für die Drehgeschwindigkeit

$$\omega = q\,\frac{\sum x_j^2 - (1/Z)(\Sigma x_j)^2}{[r^2]} = \frac{q[x^2]}{[r^2]} \tag{12}$$

mit den weiteren Abkürzungen

$$[r^2] = [x^2] + [y^2]; \quad [y^2] = \sum y_j^2 - (1/Z)(\sum y_j)^2$$

Wir führen nun ein molekülfestes System x', y', in dem der Anfang des Moleküls in den Koordinatenursprung, sein Endpunkt in die positive x'-Achse fällt. Die x'-Achse bilde mit der x-Achse den Winkel φ. Dann folgt für ω

$$\omega = \dot{\varphi} = (q/2)(1 + \beta_0 \cos 2\varphi + 2\gamma_0 \sin 2\varphi) \tag{13}$$

---

* Bereits durch die grosse Packungsdichte der umgebenden Moleküle wird die Diffusionsgeschwindigkeit der Fadenelemente und damit auch ihre Formänderungsgeschwindigkeit soweit herabgesetzt, dass das Molekül z.B. genüber kurzperiodigen Kräften sich wie ein starrer Körper verhält. Darauf beruht z.B. die Depolymerisation von Polystyrolen im Gebiet mässiger Geleigenschaften durch Ultraschall.

mit den für jedes einzelne Molekül konstanten Koeffizienten

$$\beta_0 = \frac{[x'^2] - [y'^2]}{[r^2]} = \frac{\beta}{[r^2]}$$

$$\gamma_0 = \frac{[x'y']}{[r^2]} = \frac{\gamma'}{[r^2]} \tag{14}$$

Der Orientierung in der Strömung, wie sie durch die ungleichmässige Drehung des Moleküls bedingt ist, wirkt nun die Brownsche Bewegung entgegen, als deren Mass die Rotationsdiffusionskonstante

$$D = \frac{RT}{W} = \frac{RT}{\lambda\eta[r^2]}$$

auftritt. W das Widerstandsmoment, $W = \sum M_j/\omega$. Die Verteilungsfunktion $F(\varphi)$ ergibt sich bekantlich aus der Forderung, dass die räumliche Verteilung stationär ist, zu

$$\dot{\varphi}F - D\frac{dF}{d\varphi} = \text{const.} = \frac{q}{4\pi} \tag{15}$$

Für überwiegende Brownsche Bewegung kann man F in eine Reihe nach steigenden Potenzen von q entwickeln

$$F(\varphi) = \frac{1}{2\pi}\Big[1 + S(\beta \sin 2\varphi + 2\gamma \cos 2\varphi) + S^2\Big\{[r^2](2\gamma \sin 2\varphi - \beta \cos 2\varphi) + \beta\gamma \sin 4\varphi - \frac{\beta^2 - 4\gamma^2}{4} \cos 4\varphi\Big\} + \ldots\Big] \tag{16}$$

mit der Abkürzung

$$S = \frac{q\eta\lambda}{4kT} \tag{17}$$

Es ist bezeichnend, dass die Rotationsdiffusionskonstante im linearen Gliede, das für den Anfangswert der Doppelbrechung massgebend ist, explizit nicht mehr auftritt.

Schliesst das Element j mit der Verbindungslinie der Molekülendpunkte den Winkel θ'_j ein, so erhält man in üblicher Weise für den Auslöschwinkel χ und die Dopperbrechung $\overline{\Delta\alpha}$.

$$\chi - \frac{\pi}{4} = \frac{S}{2} \times \tag{18}$$

$$\frac{\overline{(Z - 2\sum \cos^2 \theta'_j)\left(\frac{\beta}{2}[r^2] + \ldots\right)} + \overline{2\sum \sin \theta'_j \cos \theta'_j(\gamma[r^2] + \ldots)}}{\overline{(Z - 2\sum \cos^2 \theta'_j)\left(\frac{\beta}{2} + \ldots\right)} - \overline{2\sum \sin \theta'_j \cos \theta'_j(\gamma + \ldots)}}$$

$$\overline{\Delta\alpha} = (\alpha_{01} - \alpha_{02})S\left[\overline{(Z - 2\sum\cos^2\theta_j')\frac{\beta}{2}} - 2\,\overline{\sum\sin\theta_j'\cos\theta_j'\,\gamma}\right] + \ldots \tag{19}$$

Wir erkennen, dass für kleines q bezw. stark überwiegende Brownsche Bewegung der Auslöschwinkel 45° beträgt und dass die Doppelbrechung sowie die Abweichung vom 45°-Winkel q proportional sind. Bei der Berechnung der Mittelwerte ist zu beachten, dass das Mittel $\overline{\sum\sin\theta_j\cos\theta_v'}$ aus Symmetriegründen verschwindet,* während $\overline{(Z - 2\sum\cos^2\theta_j')}$ gleich $^1/_4$ ist. Ferner sind β sowie $[r^2]$ von der Grössenordnung $\sum r_j^2 = \overline{\sum r_j^2} = \sum jA^2 \approx {}^1/_2\,Z^2A^2$ Die spezifische Maxwellsche Konstante ist nach früheren Arbeiten[5] definiert als

$$M_{sp} = \lim_{c\to 0,\,q\to 0}\left(\frac{\Delta n}{cnq\eta}\right) = \left(\frac{n^2+2}{3n}\right)^2\frac{2\pi}{V}\frac{\overline{\Delta\alpha}}{q\eta} \tag{20}$$

V das Volumen des Moleküls. Wir erhalten daher

$$M_{sp} \approx \left(\frac{n^2+2}{3n}\right)^2\frac{\pi}{V}\frac{(\alpha_{01}-\alpha_{02})}{16kT}\lambda Z^2A^2 \tag{21}$$

oder wenn wir das Volumen des Fadenelements $V_0 = V/Z$ einführen

$$M_{sp} = C_2\left(\frac{n^2+2}{3n}\right)^2\frac{(\alpha_{01}-\alpha_{02})}{kT}\frac{\lambda}{V_0}\frac{A^2}{s}P = K_0P \tag{22}$$

Für den Auslöschwinkel bezw. die Orientierungszahl $\chi - \pi/4$ ergibt sich

$$\left(\frac{\chi - (\pi/4)}{q\eta}\right)_{q\to 0} \approx \frac{\lambda}{16kT}Z^2A^2 = C_3\frac{\lambda}{kT}\frac{A^2}{s^2}P^2 = K_\omega P^2 \tag{23}$$

Die Strömungsdoppelberechung ist also dem Polymerisationsgrade direkt und die Abweichung vom 45°-Winkel dem Quadrate von P proportional, wie das auch experimentell von Signer und Gross[6] sowie Wissler[7] bei polymerhomologen Reihen gefunden worden ist. Die Konstanten C sind allgemeiner Art und unabhängig von der Molekülart und vom Lösungsmittel solange nur die Molekülformen durch die Zufallsgesetze für grosse Zahlen bestimmt werden. In diesem Falle beeinflusst das Lösungsmittel nur die Steifheit der Kette, d.h. die Grössen A und s sowie vor allem die Anisotropie $(\alpha_{01} - \alpha_{02})$, wo es sogar zu einem Vorzeichenwechsel kommen kann.

IV. BEMERKUNGEN ZUR BESTIMMUNG DER FORM

Die Frage der *Makroform*, d.h. ob ein in allen drei Dimensionen grosses Molekül, ein sog. *Kornmolekül* oder ein Fadenmolekül, d.h. etwa ein globuläres oder fibrilläres Proteinmolekül vorliegt, lässt sich mit Hilfe von Messungen der künstlichen Doppelberechung entscheiden. Ferner gewinnt man, vor allem durch Kombination mit anderen Untersuchungen, insbesondere von solchen der spezifischen Viskosität, und Sedimentationsgeschwindigkeit Aussagen über die Verzweigung sowie über den Bau des statistischen Fadenelements, d.h. über die *Mikroform* des Moleküls.

---

* Jeder Molekülform entspricht eine spiegelbildlich gleiche, $\theta_i' = -\theta''$.

A. Makroform

Ist die spezifische elektrische Doppelberechung K_{sp} innerhalb einer homologen Reihe unabhängig vom Polymerisationsgrade, so liegt ein statistisch gebautes Fadenmolekül vor. Bei einer starren Stäbchenform erhalten wir bei unpolaren Molekülen einen linearen, bei polaren einen quadratischen Anstieg von K_{sp} mit P. Im Falle eines Kornmoleküls, dessen Form durch ein Ellipsoid approximiert werden kann, wird bei gleichbleibender Form, d.h. bei einem konstanten Achsenverhältnis p, K_{sp} proportional dem Volumen und damit auch P.[8]

Bei der Strömungsdoppelbrechung finden wir bei statistisch gebauten Fadenmolekülen für den Betrag der spezifischen Doppelbrechung einen linearen und für die Orientierungszahl $\chi - (\pi/4)$ einen quadratischen Anstieg mit P. Bei einem starren Stäbchen erhält man für beide Messgrössen genähert einen Anstieg mit der dritten Potenz. Kornmoleküle mit konstantem p würden in beiden Fällen eine lineare Zunahme ergeben.

Für die Stäbchenform übersteigen infolge des besonders starken Anstieges mit P schon bei Polymerisationsgraden von wenigen hundert die Werte für Δn die für eine statistische Fadenform gültigen bereits um 4–5 Grössenordnungen, so wird für ein Polystyrol von $P = 330$ die für die starre Stäbchenform abgeschätzte spezifische Doppelbrechung etwa 100,000 mal grösser als die beobachtete. Da extrem grosse Δn-Werte bisher nicht gefunden worden sind, ist der Grenzfall eines durch innermolekulare Kräfte höchst versteiften gestreckten Fadenmoleküls offenbar nie oder nur höchst selten verwirklicht.

Hat man in der angedeuteten Weise ein Kornmolekül festgestellt, so kann man, wie wir in früheren Arbeiten gezeigt haben,[8,9] durch geeignete Kombinationen von Messgrössen der künstlichen Doppelbrechung und der spezifischen Viskosität die Form des Moleküls sowie seine Eigen- und Formanisotropie getrennt bestimmen.

B. Verzweigungen

Sowohl die elektrische und magnetische, wie die Strömungsdoppelbrechung sind der optischen Anisotropie des Fadenelements δ_0^2 bzw. $(\alpha_{01} - \alpha_{02})$ proportional. Diese ist aber, wie der eine von uns in früheren Arbeiten gezeigt hat,[10] ein unmittelbares Abbild der geometrischen Form. Wie empfindlich die optische Anisotropie bzw. die elektrische Doppelbrechung gegen Formänderungen durch Verzweigungen ist, möge Tabelle 1 zeigen, in der die von dem einen von uns an synthetischen isomeren Oktanen gemessenen Werte zusammengestellt sind.* Wie man sieht, gehen die geometrische Form und die Kerr-Konstante, also auch die optische Symmetrie völlig parallel. Es gibt keine physikallische Konstante, die gegen Verzweigungen von unpolaren Molekülen so empfindlich ist, mit Ausnahme wohl der Strömungsdoppelbrechung, und der Viskosität, für die aber sehr wenige diesbezügliche Messungen vorliegen.

Sind im Molekül noch Doppelbindungen oder Benzolringe eingebaut, so muss bei Schlüssen auf die Form deren besonderer Beitrag zur Anisotropie (grosse Eigenanisotropie) berücksichtigt werden. Die Richtung grösster Polarisierbarkeit kann meist auf Grund der Beobachtung an kleinen Molekülen von vornherein angegeben werden Ausserdem ist die Abhängigkeit vom Lösungsmittel zu beachten.

TABELLE 1

KERR-EFFEKT DER ISOMEREN DES OKTANS C_8H_{18}.

n-Oktan	8 0
3-Methylheptan	6.5
3,4-Dimethylhexan	5.5
2,5-Dimethylhexan	5.4
2,3-Dimethylhexan	5.8
2,2,4-Trimethylpentan	5 6
2,2,3-Trimethylpentan	5.9
3-Methyl-3-Aethylpentan	4.7

Zur Untersuchung von Verzweigungen eignen sich praktisch nur Messgrössen, die vom Polymerisationsgrade und der meist unbekannten Polydispersität unabhängig sind, was für die elektrische Doppelbrechung unmittelbar zutrifft. Betrachten wir eine Kette mit so zahlreichen, statistisch oder regelmässig eingebauten Seitengruppen oder -ketten, dass jedes Fadenelement mindestens eine Verzweigung enthält, sich daher in seinem Aufbau und charakteristischen Konstanten vom Fadenelement der unverzweigten Kette unterscheidet. Der Einbau einer Verzweigung bedeutet bei konstantem P eine Verkürzung der Hauptkette und damit eine Verkleinerung von Z. Es gilt jetzt nicht mehr $Z = P/s$, sondern $Z < P/s$.) Dazu kommt die Vergrösserung von s als Folge der Versteifung durch die Seitengruppen, was eine zusätzliche Verkleinerung von Z ergibt Beide Effekte führen also zu einer erheblichen Verkleinerung von K_{sp}. Dazu kommt noch der Einfluss der Verzweigung auf die optische Anisotropie des Elements. Soweit nicht Doppelbindungen oder Benzolringe vorhanden sind, wird das verzweigtere Gebilde auch dasjenige mit der geringeren Anisotropie sein. In diesem Falle ist also das Produkt mit der kleineren el. Doppelbrechung eindeutig das verzweigtere—es ist von praktischer Bedeutung, dass dabei der Polymerisationsgrad nicht bekannt zu sein braucht. In anderen Fällen muss man zur Diskussion noch die Erfahrungen bei kleinen Molekülen heranziehen.

---

* Unveröffentlichte Messungen von H. A. Stuart und Mitarbeitern an synthetischen Paraffinen, die uns von der Bataafschen Petroleum M. A. Amsterdam zur Verfügung gestellt wurden. Aus Kriegsgründen konnten die Messungen nicht zu Ende geführt werden.

Zweckmässiger ist es, noch andere Messgrössen heran zu ziehen, wie z.B. eine Kombination der spez. Maxwellschen Konstanten und der Viskositätszahl. Für die letztere können wir nach der hydrodynamischen Theorie für statistisch geknickte Fadenmoleküle schreiben:[3a]

$$\eta_{sp}/c_v = C_1 \frac{\lambda}{V_0} \frac{A^2}{s} P \tag{24}$$

C_1 wiederum eine vom Lösungsmittel und der Molekülart unabhängige Konstante. Die für das Makromolekül charakteristischen Konstanten stecken in den zunächst unbekannten Kenngrössen des Fadenelements, wie s, A, $(\alpha_{01} - \alpha_{02})$ und λ, die alle vom Lösungsmittel und vom Verzweigungsgrade abhängen. Bilden wir nun das Verhältnis $M_{sp}/(\eta_{sp}/Z_v)$ so fallen alle Unbekannten bis auf $(\alpha_{01} - \alpha_{02})$ heraus, so dass wir beim Vergleich zweier Substanzen unmittelbar das Produkt mit der kleineren Anisotropie erkennen können. Zieht man noch die elektrische Doppelbrechung hinzu, so können wir weiterhin, da ja jetzt das Verhältnis der Anisotropieen bekannt ist, auch die Substanz mit der kleineren Z-Zahl bezw. dem grösseren s, die ja eindeutig die verzweigtere ist, bestimmen.

Während die obige Kombination vom Polymerisationsgrad und der Polydispersität unabhängig ist, sind andere Kombinationen, wie das Verhältnis $M_{sp}/[(\chi - \pi/4)/q\eta]$ praktisch nur dann brauchbar, wenn die Einheitlichkeit der Produkte genügend gewährleistet ist.

Ist P bekannt, so kann man aus dem Auslöschwinkel oder einfacher aus der spez. Viskosität einen Schluss auf die Verzweigung ziehen, Man geht dabei zweckmässig von folgenden Gleichungen aus:

$$\eta_{sp} = C_1 N_{ccm} \lambda_0 \overline{h_0^2} L_{max}, \qquad \frac{\chi - (\pi/4)}{q\eta} = C_3 \frac{\lambda_0 h_0^2}{kT} L_{max}{}^* \tag{25}$$

$\overline{h_0^2}$ das mittlere Längenquadrat, L_{max} die Länge der gestreckten Kette, λ_0 der Widerstandskoeffizient bezogen auf die Längeneinheit des monomeren Restes, b dessen Länge. Wird z.B. die Zahl der Hauptkettenglieder durch eine Verzweigung auf die Hälfte reduziert, so werden $\overline{h_0^2}$ und L_{max} je halb so gross, also η'_{sp} auf ein Viertel des ursprünglichen Wertes erniedrigt. Das ist allerdings die unterer Grenze der Verkleinerung, da durch die Seitenketten das Molekül versteift, also $\overline{h_0^2}$ vergrössert wird, ebenso wird auch λ_0 bezw. λ_{gr} zunehmen. Wir können daher sagen, dass die Abnahme der Hauptkettengliederzahl durch Verzweigung mindestens mit der Wurzel aus dem Verhältnis der spez. Viskositäten geht, bezw. der Orientierungszahlen, vorausgesetzt, dass auch die verzweigte Kette noch so viele statistische Elemente aufweist, dass die obigen Gleichungen gültig bleiben.

* Es ist $\overline{h_0^2} = ZA^2 = A^2P/s$, $\lambda_0 = \lambda_{gr}/b$; λ_{gr} = der Widerstandskoeffizient des monomeren Restes definiert durch $\lambda_{gr} = \lambda/s$.

C. Mikroform

Zu einer genaueren Untersuchung der Mikroform eines Fadenmoleküls, d.h. des Aufbaues des statistischen Fadenelementes in Abhängigkeit vom sterischen Bau, den innermolekularen Kräften und von Lösungsmittel reichen die obigen Beziehungen (22)–(24) nicht aus. Zwar liessen sich die Konstanten C_i durch erhöhten Rechenaufwand genauer bestimmen, doch treten ja die Unbekannten λ, s und A stets in derselben Kombination auf. Man ist also auf weitere Messgrössen angewiesen. In erster Linie kommt dabei die Sedimentationsgeschwindigkeit u in Frage, für die nach Hermans die allgemeine Beziehung $u = B + C(P)^{1/2}$ gilt. Dabei ist $B = \frac{K}{P}\frac{s}{\eta\lambda}$ und $C = \frac{K}{P}\frac{b(s)^{1/2}}{\eta\lambda}$ wo K die treibende Kraft pro Molekül und $b =$ const. (λ/A) eine vorläufig nur abschätzbare Konstante bedeutet.

Ohne zusätzliche Annahmen erhält man also aus Messungen von u in Abhängigkeit von P zunächst nur die Grössen s/λ und weiter den auf das Grundmolekül bezogenen Widerstandskoeffizienten $\lambda_{gr} = \lambda/s$. Aus der Gleichung für den Auslöschwinkel oder die Viskosität folgt dann die Grösse A^2/s, d.h. der auf das Grundmolekül reduzierte Mittelwert des Längenquadrates des Fadenelements, also ein Mass für die *Mikroknäuelung*. Mittels der Gleichung $\overline{h_0^2} = (P/s)A^2$ folgt dann weiter das mittlere Längenquadrat des ganzen Moleküls und schliesslich aus dem Betrag der Strömungsdoppelbrechung die optische Anisotropie des Fadenelements. Die Grösse $\overline{\delta^2}$ erhält man unmittelbar aus einer Messung der elektrischen Doppelbrechung. Unbekannt bleibt nur die Zahl der Glieder pro Fadenelement, die ohnehin nicht scharf zu definieren ist.

Systematische Messungen der genannten und anderer Erscheinungen in Abhängigkeit vom Lösungsmittel und für verschiedene Hochpolymere würden wertvolle Aufschlüsse über den Feinbau von Fadenmolekülen liefern. Ebenso wäre es nützlich durch Messungen an den Anfangsgliedern homologer Reihen den allmählichen Aufbau der Fadenelemente und den Uebergang zum statistischen Fadenmolekül zu verfolgen. Diesbezügliche Untersuchungen waren während des Krieges in Dresden vorbereitet, sie konnten nicht mehr durchgeführt werden.

Hermans[11] hat zuerst darauf hingewiesen, dass man bei der Berechnung der Sedimentationsgeschwindigkeit unbedingt die hydrodynamische Wechselwirkung berücksichtigen muss und unter bestimmten Modellannahmen auch die Konstanten B und C abgeschätzt. Wir wollen hier aber umgekehrt ohne zusätzliche hypothetische Annahmen unmittelbar aus den Beobachtungen die Konstanten des Fadenelements ableiten. Dazu gehen wir von der Gleichung aus: $u = (K_0/\eta\lambda)(1 + b\sqrt{P/s})$, who K_0 die treibende Kraft pro Fadenelement $K_0/\eta\lambda$ also die Geschwindigkeit des isolierten Elements wäre. $(K_0/\eta\lambda)b(Z)^{1/2}$ ist die durch die hydrodynamische Wechselwirkung der Z Fadenelemente hervorgerufene zusätzliche Geschwindigkeit. Ganz ohne Modellannahmen ist b nicht berechenbar. Hermans erhält $b = (6/\pi)^{1/2}(a/A)$ während wir durch eine genauere Durchführung der Statistik $b = (8/3)(6/\pi)^{1/2}(a/A)$ finden, dabei ist A die mittlere Länge des Fadenelements, und a der hydrodynamische Radius des Elements definiert durch $\lambda = 6\pi a$.

V. DIE FORM VON PARAFFINMOLEKÜLEN IM DAMPFZUSTANDE

Um einmal direkt experimentell und möglichst hypothesenfrei die Frage zu beantworten, sind Fadenmoleküle freie, z.B. gesättigte unverzweigte Kohlenwasserstoffketten im Dampfzustande gestreckt oder geknäuelt, haben wir die elektrische Doppelbrechung der normalen Paraffine im Dampfzustande bis zum Dodekan gemessen† und aus der Kerrkonstante $K = (n_p - n_s)/nE^2$ mittels der für dipollose Moleküle gültigen Beziehung

$$K = \frac{3\pi N_{\text{ccm}}\alpha^2(n_\infty - 1)}{5kT(n - 1)}\,\delta^2$$

die optische Anisotropie berechnet.

Die Messungen erfolgten mit der schon früher beschriebenen Versuchsanordung in einer starkwandigen Glasapparatur aus Duranglas mit angeschlossenem heizbaren Quarzspiralmanometer. Um eine grössere Doppelbrechung zu erhalten wurden die niederen Kohlenwasserstoffe bei Drucken bis zu 7 atm, die höheren bis zu Temperaturen von 275°C. gemessen.

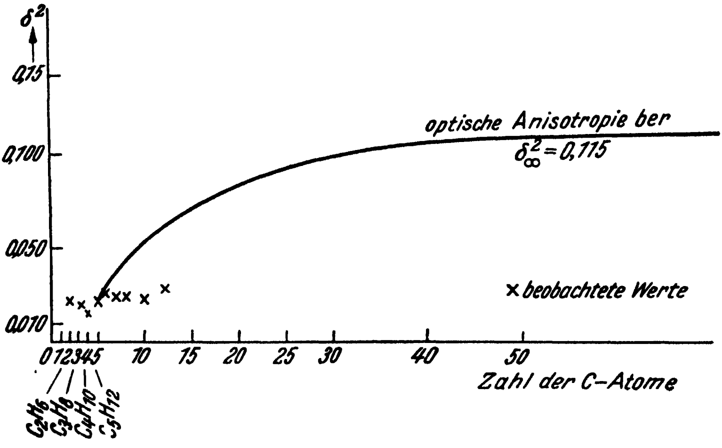

Abbildung 1

Diesen experimentell bestimmen Anisotropien haben wir die nach der Kontinuumstheorie* und zwar für die gestreckte Zickzackform berechneten Werte gegenübergestellt. Ersetzen wir die Form des gestreckten Moleküls durch ein Rotationsellipsoid, dessen Achsen gleich der Länge und Dicke der Kette und dessen Polarisierbarkeit gleich der des Moleküls ist, so erhalten wir für die Formanisotropie die in Abb. 1 dargestellte Kurve.[12] Man erkennt daraus, dass die Formanisotropie ihren Grenzwert von

---

† Messungen von Stuart, Schiesszl und Lehmann.

* Im Gegensatz zur Flüssigkeit bestehen im Dampfe, wo die umgebenden Moleküle soweit entfernt sind, dass wir als umgebendes Medium das Vakuum ansetzen können keine Bedenken gegen die Anwendung der Kontinuumstheorie.

$\delta^2 = 0.115$ erst etwa beim $C_{60}H_{102}$, d.h. bei einem Achsenverhältnis von etwa $p = 15$ erreicht. Unsere Werte sind aber schon vom Hexan ab konstant. Der geringe Anstieg beim Dodekan ist wohl auf die verhältnismässig hohe Messtemperatur von 275° zurückzuführen, da mit wachsender Temperatur die Moleküle merklich weniger geknäult sein dürften als bei tiefen Temperaturen, wo wegen der Anziehungsenergie benachbarter CH_2-Gruppen geballtere Formen bevorzugt sind.[13] Man sieht ferner, dass die beobachteten Anisotropien, $\delta^2 \sim 0.025$, durchweg viel kleiner als die berechneten sind.**

Diese beiden Tatsachen beweisen eindeutig, dass die normalen Paraffine im Dampfzustande nicht gestreckt sind. Sie können aber auch keine dichtgeballte kugelige Form besitzen, da sonst die Anisotropie viel kleiner, nämlich von der Grösse der beim Zyklohexan, $\delta^2 = 0.008$, oder beim 2,2,4-Trimethylpentan, $\delta^2 = 0.015$, gefundenen sein müsste. Berechnet man für Äthan die Formanisotropie mit dem sicher schon zu grossen Achsenverhältnis $p = 1.63$, so ergibt sich $\delta^2 = 0.01$, d.h. innerhalb der Unsicherheit der Rechnung eine viel geringere Anisotropie als die in $\delta^2 = 0.023$ beobachtete. Es heben sich also offenbar die Eigenanisotropieen der C—H— und C—C—Bindung nicht auf. Beachten wir diese sicher vorhandene, ihrer Grösse nach aber nur ungefähr bekannte Eigen-Anisotropie, so werden unsere obigen Folgerungen noch mehr erhärtet.

Über den Einfluss des Bindungstypus auf die Eigen-Anisotropie vergl. H. A. Stuart, und J. von Schiesszl, *Ann. d. Phys.*, **2**, 322 (1948), sowie H. A. Stuart und A. Fink unveroffentliche Messungen.

Der Beitrag der Eigen-Anisotropie zur Gesamtanisotropie, der bei einer gestreckten Molekülform konstant bleiben, bei zunehmender Knäulung abnehmen würde, beeinflusst den allgemeinen Verlauf der Kurve, insbesondere den Wert der Gliederzahl, für den praktisch Sättigung eintritt, nur wenig.

Schlussfolgerung

Das Lösungsmittel beeinflusst alle charakteristischen Konstanten des statistischen Fadenelements, wie die Zahl der monomeren Reste, die Mikroknäuelung, den hydrodynamischen Widerstandskoeffizienten, die optische Anisotropie und das elektriche Moment. Darüber hinaus kann durch die inner- und zwischenmolekularen Kräfte das Molekül im Innern so geordnet, z.B. geballt, vernetzt oder auch so gestreckt werden, dass es den Charakter eines statistisch ungeordneten Gebildes verliert. Diese Umstände, sowie die häufigen Unsicherheiten bezüglich der Polydispersität bezw. der Verzweigung zeigen, wie vorsichtig man bei allen Schlüssen auf die Form sein sollte, wenn man nur eine einzige Messgrösse, sei es in Abhängigkeit vom Polymerisationsgrade, sei es vom Lösungsmittel als Unterlage hat. Die

---

** Das Ellipsoid ergibt, besonders bei den höheren Gliedern, eine grössere Anisotropie als der entsprechende, die Raumerfüllung des Mokeküls besser darstellende Zylinder der Länge $2a_1$ und des Durchmessers $2a_2$. Wählen wir daher ein wesentlich geringeres und sicher zu kleines Achsenverhältnis, z.B. beim Dodekan $p = 3$ statt 4, $2a_1 = 17.4$ und $2a_2 = 2a_3 = 4.3$, so wird $\delta^2 = 0.043$, bleibt also immer noch viel grösser, als der beobachtete Wert.

Theorie hat uns jedoch so viele Methoden geliefert, dass es nur der nötigen Kritik bei ihrer Anwendung bedarf, um Erfolg zu haben.

References

1. H. A. Stuart und A. Peterlin, *J. Polymer Sci.*, **5,** 543 (1950).
2. A. Peterlin und H. A. Stuart, *Z. Physik,* **113,** 663 (1939).
3. Vgl. dazu den Artikel "Elektrischer Kerreffekt" von H. A. Stuart im *Hand- und Jahrb. der chem. Phys.*, Bd. 10, III, Leipzig, 1939.

3a. A. Peterlin, *Verh. Akad. Ljubljana, Math. Phys. Kl.*, **3,** 79 (1947), eingereicht Mai 1944.

4. M. Huggins, *J. Phys. Chem.*, **42,** 911 (1938); **43,** 439 (1939).
5. Für die weitere Ableitung vergl. man A. Peterlin und H. A. Stuart im *Hand- und Jahrb. der chem. Phys.*, Bd. 8 IB, Leipzig, 1943.
6. R. Signer und H. Gross, *Z. physik. Chem.*, **A165,** 161 (1933).
7. A. Wissler, Diss., Bern, 1941.
8. A. Peterlin und H. A. Stuart, *Z. Physik,* **112,** 129 (1939).
9. H. A. Stuart, *Kolloid-Z.*, **96,** 161 (1941).
10. Vgl. z.B. H. A. Stuart, *Molekülstruktur.* Berlin, 1934.
11. J. J. Hermans, *Rec. trav. chim.*, **63,** 219 (1944).
12. Vergl. dazu A. Peterlin und H. A. Stuart (ref. 8).
13. H. A. Stuart und H. Volkmann, *Physik Z.*, **35,** 564 (1934).

English Synopsis, see Summaries, page S7, Vol. V, 1950.

Zusammenfassung

Es werden die Beziehungen für die elektrische, magnetische und die Strömungsdoppelbrechung von Fadenmolekülen in Lösung in Abhängigkeit vom Polymerisationsgrade angegeben. Ferner werden einige Möglichkeiten die Makro- und die Mikroform eines hochpolymeren Moleküls zu bestimmen und Verzweigungen zu erkennen, besprochen. Schliesslich wird durch Messungen der elektrischen Doppelbrechung am Dampf nachgewiesen, dass Paraffinketten lose Knäuel bilden.

Résumé

Les auteurs indiquent les relations, existant entre la biréfringence électrique, magnétique et la biréfringence d'écoulement des solutions de macromolécules linéaires avec le degré de polymérisation. Quelques possibilités de déterminer la "macro- et micro-" -forme d'une molécule de haut polymére, et d'identifier les ramifications sont discutées. Finalement, les auteurs démontrent que les chaînes parafiniques constituent une pelote lâche, par des mesures de biréfringence électrique sur les vapeurs.

Received April 25, 1949

JOURNAL OF POLYMER SCIENCE VOL. V, NO. 5, PAGES 565-568

Crystallinity of Precipitated Cellulose

P. H. HERMANS and A. WEIDINGER,* *Institute for Cellulose Research, AKU and Affiliated Companies, Utrecht, Netherlands*

INTRODUCTION

Previously we have reported that intensity measurements on monochromatic x-ray exposures of cellulose fibers lead to the conclusion that in the majority of rayons (with either low or high orientation) the crystalline fraction seems to be constant within experimental error, amounting to about 40%.[1]

True, it has been emphasized that differences exist in the degree of lateral order according to the 101 or 002 planes in various rayons, the former showing marked variation. Hence the concept "crystallinity" as derived from measurements of total crystalline x-ray intensity should be handled critically.[2]

Later it has been shown that, upon acid hydrolysis at 100°C., the crystalline fraction in rayon is rapidly increased to about 50%, to remain constant at prolonged treatment with boiling acid.[3]

Recently the same conclusion was reached by Howsmon,[4] who also stressed the general parallelism that seems to exist between crystallinity and sorptive capacity for water vapor (also emphasized earlier by one of us.[5] This author correctly points out that, on a number of grounds, strict parallelism, however, cannot be expected.

The enhanced crystallinity upon acid hydrolysis can be explained by release of strain as a result of the cutting of chains in the amorphous regions, the strain being introduced previously at the process of random crystallization when the fiber is produced from the cellulose solution.

Since the process of coagulation as used in the production of various rayons is not too different in various products, the constancy of the crystalline fraction is perhaps comprehensible. Drastic changes in the conditions of coagulation, however, should then be expected to yield different results.

It was therefore decided to investigate the products obtained by precipitating very dilute viscose solutions by acid. The "precipitated celluloses" so obtained, when investigated with x-rays using the same technique previously applied, actually do exhibit a somewhat higher degree of crystallinity than the majority of rayons.

---

* Communication No. 63 from the Institute for Cellulose Research of the AKU and affiliated Companies, Utrecht, Netherlands.

EXPERIMENTS

Ordinary viscose containing 8% cellulose and 6% total alkali (ammonium chloride number 6.8) was diluted with water to 20 times its original volume. This solution was precipitated with acid under continuous stirring in four different ways:

A. 200 ml. of the solution was diluted to 1 liter and 25 ml. of 1 *N* acetic acid was added dropwise in 15 mm. Then a solution of 250 mg. sodium chloride was added and stirring continued for 5 min. A very finely disperse precipitate was formed and allowed to settle overnight. It was collected by repeated decantations and finally by centrifugation. Then it was sucked off on hard filter paper until a pasty consistency was reached. The paste (which proved to be free of chlorine ions) was spread out on a glass plate and allowed to dry in circulating air. It was then obtained in the form of flakes.

B. The same operation was followed except that the moist product was heated in water on the water bath for 10 min. before the last centrifugation.

C. 200 ml. of the 1.20 viscose dilution was mixed with 550 ml. water and precipitated at room temperature by adding 250 ml. 0.1 *N* hydrochloric acid in 15 min. Collection of precipitate as under A.

D. The same operation as under C, except that the solution was heated to 90°C. before precipitation with hydrochloric acid. Brief recapitulation is given in Table I. Upon x-ray examination the dried flakes showed preferred orientation of the 101 planes. In order to get isotropic samples, they were powdered and then pressed into tablets of about 1 mm. thickness, which now appeared to be isotropic.

TABLE I

MODE OF PREPARATION OF PRECIPITATES

Sample	Acid used	Precipitation temperature	Treatment before drying	Drying
A........	Acetic	Cold	None	Cold
B............	Acetic	Cold	Heated	Cold
C............	Hydrochloric	Cold	None	Cold
D............	Hydrochloric	Hot	None	Cold

The quantitative x-ray work was carried out as previously described[1] and the results expressed in terms of standard conditions of primary radiation and standard amount of irradiated cellulose (as determined by absorption measurements).

TABLE II

RESULTS OF X-RAY MEASUREMENTS

Sample	I_{tot}	I_{cr}	A_m	$100x$
A...............	4.50	1.27	0 51	45
B...............	4.25	1.36	0.47	48
C...............	4.40	1 30	0.51	45
D...............	4.40	1.51	0 46	53
Rayon...........	4.40	1.10	0.56	39

In Table II the total radiation diffracted I_{tot}, the radiation diffracted by the crystalline portion I_{cr}, and the height of the maximum of the diffuse background A_m are listed together with the crystallinity percentage

(100x), where x = crystalline fraction as derived therefrom. The average figures found for ordinary rayons are added for comparison.

The half width of the 002 lines of the precipitated samples was invariably 3.1 mm. as against 3.4 in the common rayons under identical conditions of exposure. That of the 101 lines was 1.5–1.6 mm., which lies on the sharp side of the variability range which various rayons show (1.5–2.4 mm.).

Moisture uptake was determined for samples A and B. Contrary to expectation the figures were within the normal range for regenerated cellulose, namely, 13.5% and 13.9% at 65% relative humidity (upon absorption). Various rayons and model filaments give 13.5–14.6% under identical conditions.

DISCUSSION

The x-ray results show that the crystallinity of the various objects increases in the order: rayon, cold precipitated, cold precipitated and heated before drying, hot precipitated cellulose.

The figures from Table II fit the straight line of our standard crystallinity nomogram[6] quite well, as shown in Figure 1. In this figure we have also indicated the observations for two specimens of particular rayons, Fortisan (Celanese Corp.) and Fiber G (Du Pont), which are distinguished by unusual high crystallinity. (In an earlier paper[6] we reported observations on Fortisan which lie rather off the line for reasons not yet clear. Repeated measurements on a newly obtained sample yielded the point plotted in Figure 1.)

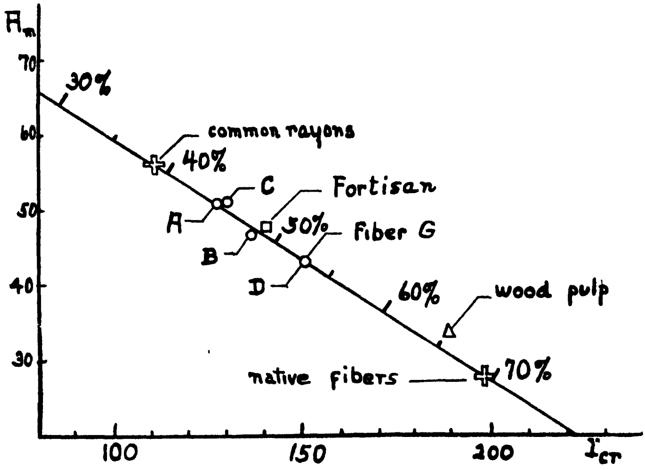

Fig. 1. Precipitated celluloses (A, B, C, and D) plotted in the crystallinity nomogram. Scale along oblique line indicates percentage crystallinity. Crosses: calibration points derived from measurements on rayons and native fibers, respectively.

If sorptive capacity were univocally associated with the amount of noncrystalline fraction, the sorption of samples A and B should have been markedly lower than that of ordinary rayon (as it actually is in Fortisan rayon and Fiber G, whose equilibrium moisture content upon absorption amounts to 11.5% and 12%). That this has not been observed is another illustration of the correctness of Howsmon's considerations[4] to which we may refer.

Nevertheless, the experiments show that the degree of crystallinity of regenerated cellulose as derived from x-ray measurements may show an increase upon drastic variations of the conditions of precipitation. As previously shown this cannot be reached by stretching of either swollen or dry fibers.[1,7]

It is a pleasure to acknowledge the assistance of Mr. H. J. H. Scheers in the experiments. The x-ray work was carried out by one of us (W.) in the Physical Laboratory of the Technical University, Delft.

References

1. P. H. Hermans and A. Weidinger, *J. Applied Phys.*, **19**, 491 (1948); *Bull. soc. chim. Belges*, **57**, 123 (1948).
2. P. H. Hermans, *J. Polymer Sci.*, **4**, 145 (1949).
3. P. H. Hermans and A. Weidinger, *J. Polymer Sci.*, **4**, 709 (1949).
4. J. A. Howsmon, *Textile Research J.*, **19**, 152 (1949).
5. P. H. Hermans, *Contribution to the Physics of Cellulose Fibres.* Elsevier, New York–Amsterdam, 1946.
6. P. H. Hermans and A. Weidinger, *J. Polymer Sci.*, **4**, 135 (1949).
7. O. Kratky and A. Sekora, *Kolloid-Z.*, **108**, 169 (1944).

English Synopsis, see Summaries, page S11, Vol. V, 1950.

Résumé

La cellulose précipitée d'une viscose très diluée par addition d'acide manifeste un degré de cristallinité croissante, par comparaison à une viscose rayonne ordinaire. L'effet est faible si la précipitation est effectuée à température de chambre, mais est considérable à la température d'ébullition. La teneur la plus élevée atteint 53%, contre 40% pour la rayonne.

Zusammenfassung

Cellulose, die aus einer sehr verdünnten Viskose durch Säuren ausgefällt wird, zeigt einen erhöhten Kristallisationsgrad in Vergleich zu gewöhnlicher Viskose-Kunstseide. Die Wirkung ist klein, wenn das Ausfällen bei Zimmertemperatur ausgeführt wird und erheblich bei Siedetemperatur. Die höchste Zahl, die erreicht wurde, war 53%, verglichen mit 40% bei Kunstseide.

Received July 5, 1949

JOURNAL OF POLYMER SCIENCE VOL. V, NO. 5, PAGES 569-586

Studies of Retarders and Inhibitors in the Emulsion Polymerization of Styrene. II. Inhibitors*

F. A. BOVEY† and I. M. KOLTHOFF, *School of Chemistry, University of Minnesota*

In a previous paper,[1] we have described the behavior of typical retarders, *m*-dinitrobenzene and 3,5-dinitrobenzoic acid, in the emulsion polymerization of styrene. A retarder is defined as a substance which does not cause an induction period in a polymerization reaction, but which gives rise to a retardation throughout the entire reaction. An ideal inhibitor is defined as a substance which gives a well-defined induction period during which no noticeable polymerization occurs and after which the rate is the same as in the absence of the inhibitor. An inhibitor is used up quantitatively during the induction period, whereas the consumption of a retarder during the polymerization is, as a rule, small, and the concentration may be considered to remain nearly constant.

The behavior of inhibitors and retarders in the bulk polymerization of styrene and a few other monomers has been studied by several investigators, and these studies have been summarized in a recent review[2] in which a general description of the action of inhibitors and retarders is given. It appears (see also the more recent work of Breitenbach *et al.*[3]) that the distinction between retarders and inhibitors, although important from a practical viewpoint, is probably in essence one of degree rather than kind. Inhibitors react very rapidly with monomer radicals to produce adduct radicals which have a very small reactivity or none toward the monomer. Retarders generally react less rapidly with the monomer radicals, producing adduct radicals which may or may not be capable of carrying on the chain at a reduced rate. The essential mechanism of the action of both is the same.

Oxygen appears to behave like a typical inhibitor in the emulsion polymerization of styrene, as it produces a well-defined induction period, during which the oxygen is entirely consumed. Close investigation,[4] however, reveals that the oxygen actually copolymerizes with the styrene to produce a polymeric styrene peroxide. Oxygen is thus not to be regarded as an ideal

---

* Contribution from the School of Chemistry of the University of Minnesota. This investigation was carried out under the sponsorship of the Office of Rubber Reserve, Reconstruction Finance Corporation, in connection with the Synthetic Rubber Program of the United States Government.

† Present address: Minnesota Mining and Manufacturing Co., St. Paul, Minn.

inhibitor. No other studies of inhibiting substances in emulsion polymerization appear to have been made. It is the object of this paper to present some studies of the reactions of certain quinones whose behavior in the emulsion polymerization of styrene approaches in varying degrees that of an ideal inhibitor.

EXPERIMENTAL TECHNIQUE

Materials

The *styrene, water, dodecylamine hydrochloride, and potassium persulfate* used have been described in a previous paper.[1]

p-Benzoquinone. A stockroom sample was purified by sublimation. The melting point of the sublimed product was 115° (Lit.: 115.7°).

Chloranil. Eastman White Label chloranil was employed.

Potassium 9,10-phenanthrenequinone-3-sulfonate. A sample of this material was kindly supplied by Dr. L. Michaelis of the Rockefeller Institute for Medical Research.

All reagents employed were of analytical reagent grade.

Polymerization Technique

The polymerizations were carried out in screw-cap bottles of 130 ml. capacity, sealed with pierced caps containing Buna-N self-sealing gaskets, and rotated end-over-end at about 35 r.p.m. in a thermostat. The bottles were sampled with hypodermic syringes, and monomer conversions were determined in the manner previously described.[1]

The polymerization recipe is that employed in the previous study,[1] and will be presented again here for convenience: styrene 35.6 g. (39.3 ml. at 25°), designated as 100 parts; water, 65.7 ml., or 185 parts; emulsifier, 1.78 g. or 5 parts, based on the styrene. This quantity of emulsifier is designated as 1×, and other quantities as fractions or multiples thereof. Potassium persulfate, 0.107 g. or 0.3 part, based on the styrene. This quantity of persulfate is designated as 1× and other quantities as fractions or multiples thereof. The potassium persulfate was added as a solution in water. For 1× persulfate, 15.7 ml. of a 0.68% solution was added to each bottle.

p-Benzoquinone and potassium 9,10-phenanthrenequinone-3-sulfonate were added to the charges as water solutions. Chloranil was added as a solution in styrene.

The same precautions against the presence of oxygen were taken as in the previous study. Since the exclusion of oxygen is not complete, short and well-defined induction periods due to traces of residual oxygen were observed. As will be mentioned below, corrections were made for these induction periods in determining the lengths of those caused by the quinones.

Analytical Methods

Quinones. The determination of quinones was carried out with a manual polarograph. Details are given in the next section.

Chlorine. Analysis of polymers for chlorine was carried out by fusion of an approximately 0.2 g. sample of the polymer with sodium peroxide, using a Parr bomb. Ignition was initiated by a small electrically heated iron fuse wire. In order to ignite the charges it is necessary to mix about 1 g. of a 50:50 mixture of sucrose and potassium nitrate into the charge, and to arrange the fuse wire so that it dips into a small quantity of this mixture on top of the charge.

After fusion, the contents of the bomb are dissolved in water with heating. The alkaline solution is boiled for a short time, with the addition of 1 ml. of a 0.01 *M* solution of osmium tetroxide to decompose the peroxide. The solution is then filtered to remove ferric hydroxide, made acid by cautious addition of nitric acid, and diluted to 250 or 500 ml. From this solution, aliquots are then removed and titrated for chloride amperometrically with 0.01 *M* silver nitrate in the presence of a small amount of gelatin, as described by Laitinen, Jennings, and Parks.[5]

EXPERIMENTAL RESULTS

Effect of p-Benzoquinone. In an effort to extend the results obtained with oxygen in the emulsion polymerization of styrene with fatty acid soaps,[3] the use of *p*-benzoquinone and hydroquinone as inhibitors was attempted. It was found, however, that in such alkaline recipes, amounts of these substances comparable on a molar basis to the amounts of oxygen used in the earlier work had no inhibitory effect but produced only retardation. It was observed that both quinone and hydroquinone rapidly produce a dark purplish-brown color in these recipes, and it was concluded that at this *p*H (about 9.5), they are decomposed to complex degradation products having no true inhibitory power. Hydroquinone is often used as an inhibitor or shortstop for polymerization latices with fatty acid soaps. It seems probable that its effectiveness is due to the retarding power of these degradation products, which produce practically complete cessation of the polymerization when sufficient hydroquinone is added (0.1–0.2% based on monomers).

It was believed that *p*-benzoquinone should act as a true inhibitor if a recipe were used in which it is stable. It was found that when dodecylamine hydrochloride (DDA·HCl) was employed as emulsifier, *p*-benzoquinone produced induction periods roughly proportional to the quantity of the quinone initially present. The development of a reddish tinge in the reaction mixtures, however, indicated that the quinone was reacting slowly with the small amount of free dodecylamine formed by hydrolysis, probably with the formation of amino quinones having lower reactivities toward free radicals. To prevent this reaction, hydrolysis of the DDA·HCl was suppressed by making the aqueous phase 0.1 *N* in hydrochloric acid. Under these conditions the results shown in Table I and Figure 1 were obtained.

TABLE I

INDUCTION PERIODS

Corrected for Residual Oxygen, Produced by *p*-Benzoquinone in 1× DDA·HCl, $^1/_2$× Persulfate Recipe at 50°. Aqueous Phase 0.1 *N* in HCl. Quinone Concentration expressed as Millimoles per 100 Grams Styrene

p-Benzoquinone concn.	I.P., hours	I.P./(quinone)
0.005	0.97	194
0.010	1.90	190
0.020	3 80	190

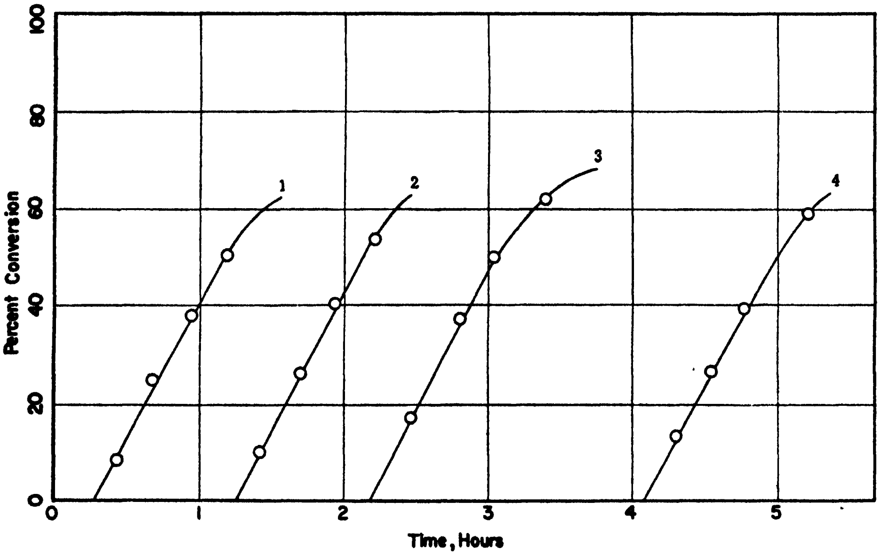

Fig. 1. Induction periods produced by *p*-benzoquinone in 1× dodecylamine hydrochloride, $^1/_2$× $K_2S_2O_8$ recipe at 50°; aqueous phase 0.1 *N* in HCl. 1, Blank, no quinone. 2, 0.005 millimole quinone per 100 g. styrene. 3, 0.010 millimole quinone per 100 g. styrene. 4, 0.020 millimole quinone per 100 g. styrene.

The induction periods observed were corrected for residual oxygen by subtracting from each the induction period observed in the absence of the quinone. It can be seen that the induction periods are proportional to the amount of the quinone initially present.

Table II and Figure 2 show that, as with oxygen, the induction period produced by a given amount of *p*-benzoquinone varies inversely as the persulfate concentration, while Figure 3 shows that the induction periods depend very little upon the concentration of emulsifier employed. From these data, it can be seen that the effects of *p*-benzoquinone on the emulsion polymerization of styrene appear to be qualitatively the same as those of oxygen. Quantitatively, however, there is a great difference. Kolthoff

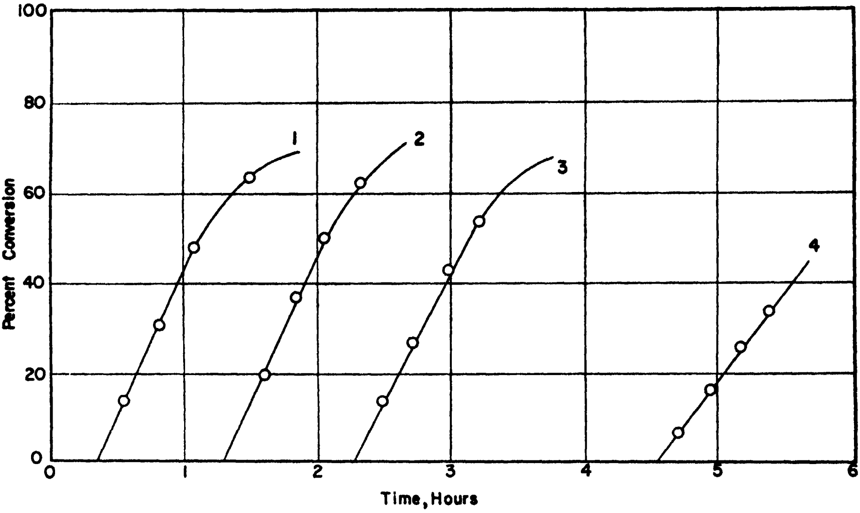

Fig. 2. Induction periods produced by 0.01 millimole *p*-benzoquinone (per 100 g. styrene) in 1× dodecylamine hydrochloride recipe as a function of persulfate concentration 50°. 1, Blank, no quinone, 1× $K_2S_2O_8$. 2, 0.01 millimole quinone, 1× $K_2S_2O_8$. 3, 0.01 millimole quinone, $^1/_2$× $K_2S_2O_8$. 4, 0.01 millimole quinone, $^1/_4$× $K_2S_2O_8$.

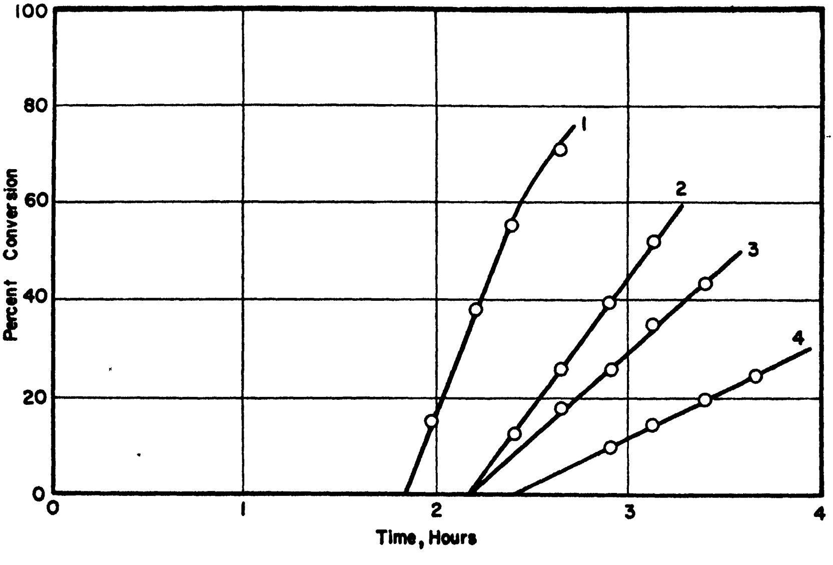

Fig. 3. Effect of dodecylamine hydrochloride concentration (in 0.1 *N* HCl) on induction period produced by 0.01 millimole *p*-benzoquinone; $^1/_2$× $K_2S_2O_8$; 50°. 1, 2× dodecylamine hydrochloride. 2, 1× dodecylamine hydrochloride. 3, $^1/_2$× dodecylamine hydrochloride. 4, $^1/_4$× dodecylamine hydrochloride.

and Dale[6] have found that an induction period of 1.8 hours is caused by 0.52 millimole oxygen, whereas from the present data it appears that an equal induction period is caused by only about 0.02 millimole of *p*-benzoquinone. On a molar basis, *p*-benzoquinone is thus about 25–26 times more effective as an inhibitor than oxygen.

TABLE II

INDUCTION PERIODS

Corrected for Residual Oxygen, Produced by 0.01 Millimole *p*-Benzoquinone per 100 Grams Styrene in 1× DDA·HCl Recipe as a Function of Persulfate Concentration (C) at 50°

(C)	I. P., hours	I.P. × (C)
1×	0 90	0.90
$^1/_2$×	1.70	0.85
$^1/_4$×	3.40	0.85

Effect of Chloranil. In Table III are shown the induction periods produced by chloranil in a 1× DDA·HCl recipe.

TABLE III

INDUCTION PERIODS

Corrected for Residual Oxygen, Produced by Chloranil in 1× DDA·HCl recipe at 50°

Chloranil concn.	I.P., hours	I.P./(chloranil)
	WITH $^1/_2$× $K_2S_2O_8$	
0 01	1.03	103
0.02	1.95	97.5
0.04	3.28	82
	WITH 1× $K_2S_2O_8$	
0.04	2.00	50
0.40	6.50	16.3

It will be observed that the induction period is not proportional to the quantity of chloranil employed. The discrepancy becomes very great when the amount of chloranil is increased to 0.40 millimole, in which case the induction period is only one-third as long as expected. With *p*-benzoquinone, on the other hand, the induction period produced by 0.02 millimole in a 1× persulfate recipe is 2.0 hours, while 0.20 millimole produces an induction period of 21.9 hours. It will also be observed that even at the lowest concentration, the induction period produced by chloranil is only about half that produced by an equimolar quantity of benzoquinone.

Potassium 9,10-phenanthrenequinone-3-sulfonate. In Figure 4 are shown time–conversion curves in the presence of potassium 9,10-phenanthrenequinone-3-sulfonate. This substance is clearly a nonideal inhibitor. As its concentration is diminished, the quinone is unable to react with all the monomer radicals produced, and some chain propagation occurs. The rate of polymerization thus increases as the quinone concentration falls.

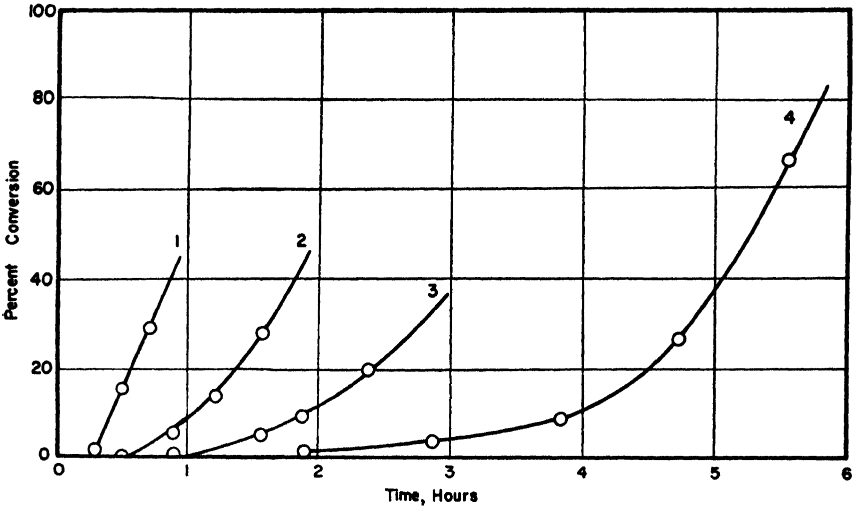

Fig. 4. Effect of K-phenanthrenequinone-3-sulfonate in 1× dodecylamine hydrochloride, 1× $K_2S_2O_8$ recipe; 50°; conc. quinone in millimoles per 100 g. styrene. 1, Control, no quinone. 2, 0.01. 3, 0.02. 4, 0.04.

Effect of Temperature on Induction Periods Produced by p-Benzoquinone. In Table IV, the induction periods produced by *p*-benzoquinone at 30, 40, and 50° in a 1× DDA·HCl (0.1 *N* HCl), 1× persulfate recipe are given.

TABLE IV

Induction Periods

Produced by *p*-Benzoquinone in 1× DDA·HCl (0.1 *N* HCl), 1× Persulfate Recipe at 30, 40, and 50°

Temp., °C	Quinone concn., millimole / 100 g. styrene	I P , hours	I P. corr. for O_2 I.P.	Polymerization rate after I.P.[a]
50	0.00	0.16	—	65
	0.01	1.00	0.84	65
	0.02	1.85	1.69	67
40	0.00	0.30	—	27
	0.01	4.75	4.45	30
	0.02	9.60	9.30	27
30	0.00	0.85	—	9
	0.01	21.90	21.05	9
	0.02	52.70	51.85	8

[a] In per cent conversion per hour.

Assuming tentatively (see below) that the rates of quinone disappearance, which are inversely proportional to the observed induction periods, are proportional to the rate of initiation of monomer free radicals in the emulsion, we may calculate the activation energy for the initiation process, E_1, from:

$$E_1 = R \frac{T_1 T_2}{T_2 - T_1} \ln \frac{(\text{I.P.})_1}{(\text{I.P.})_2}$$

where $(\text{I.P.})_1$ represents the observed induction period at temperature T_1, $(\text{I.P.})_2$ represents the induction period at temperature T_2, and R is the gas constant. E_1 is found to be 33,000 ± 400 cal. per mole. Foord[7] finds a value of 28,000 cal. per mole from the induction periods caused by *p*-benzoquinone in the bulk thermal polymerization of styrene.

Similar measurements carried out with oxygen by Kolthoff and Dale[8] have given a value of 19,600 cal. per mole for the "activation energy" of the induction periods caused by oxygen.

Reactivity of Oxygen toward Styrene Free Radicals Compared to That of Quinone and Hydroquinone. Experiments have been carried out with the purpose of comparing the relative reactivities of oxygen, quinone, and hydroquinone toward styrene-free radicals initiated by persulfate. To do this, rates of oxygen absorption in the presence of quinone and of hydroquinone were measured using the manometric apparatus, with fast-shaken reaction vessel, described earlier.[4] The reaction mixture contained 2×-persulfate, 1× DDA·HCl, and was made 0.1 *N* in hydrochloric acid. With hydroquinone, the acid was omitted to retard the oxidation of the hydroquinone by persulfate. It has been found that the rate of oxygen absorption under these conditions is independent of the *p*H of the emulsion between *p*H 1 and 5. In Table V and Figure 5 are shown the results obtained.

TABLE V

RATE OF OXYGEN UPTAKE

By a Styrene Emulsion in Presence of Quinone and Hydroquinone at 50°, with 2× Persulfate and 1× DDA·HCl

Inhibitor	Millimoles/100 g. styrene	Rate of O_2 uptake, mm. Hg/hour
	0	620
Quinone	0.04	620
Quinone	0.40	580
Hydroquinone	0.04	960
Hydroquinone	0.40	340

If *p*-benzoquinone were able to terminate the monomer radicals R· before they react with oxygen or the peroxide radicals RO_2·, its presence would retard the uptake of oxygen by cutting the chains of the oxygen-styrene copolymerization. Actually, *p*-benzoquinone has practically no effect even at a concentration (0.40 millimole) sufficient to stop normal polymerization for 20 hours under the conditions employed. It appears that *p*-benzoquinone is not only much less reactive toward R· than is oxygen, but that it must be much less reactive toward the peroxide free radical than is styrene. However, it is a powerful inhibitor for normal polymerizations, and must therefore, be much more reactive toward R· than is the monomer. These observations serve to illustrate the extraordinary affinity of oxygen for the monomer radicals.

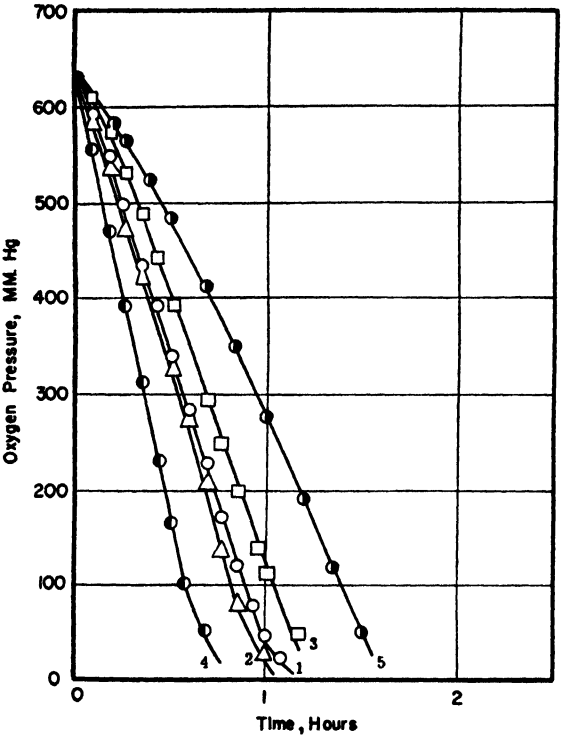

Fig. 5. Rate of oxygen uptake by styrene emulsion in presence of quinone and hydroquinone; 1× dodecylamine hydrochloride, 2× persulfate; 50°. 1, no quinone. 2, 0.04 millimole quinone. 3, 0.40 millimole quinone. 4, 0.04 millimole hydroquinone. 5, 0.40 millimole hydroquinone.

It is conceivable that the quinone may actually copolymerize with the styrene and the oxygen, and thus be consumed simultaneously with the oxygen rather than after it has all reacted. This hypothesis requires the assumption that the hypothetical quinone peroxide-free radicals, which we may designate QOO·, react at the same rate with monomer (or quinone) as the monomer peroxide radicals MOO· (where either Q or M may represent polymer chains). This does not seem plausible and we prefer at present the simpler interpretation given above.

Hydroquinone at a concentration of 0.04 millimole accelerates the rate of oxygen absorption, probably because it reacts with persulfate with the formation of free radicals,[9] thus effectively increasing the rate of activation by persulfate. The retarding effect of the large amount of hydroquinone (0.4 millimole) may be attributed, in part at least, to reaction of this reductant with $RO_2\cdot$ radicals. It is of interest to note that in the recipe under consideration hydroquinone is a very inefficient antioxidant for the monomer.

Summarizing, the following conclusions can be drawn from these data:

Reactivity with respect to R·

$$O_2 \gg \text{Quinone} \gg \text{Monomer}$$

Reactivity with respect to $RO_2\cdot$

$$\text{Monomer} \gg \text{Hydroquinone (?)} \gg \text{Quinone}$$

Nature of Interaction of Monomer Radicals with Quinones. *p-Benzoquinone.* An investigation was carried out to determine whether *p*-benzoquinone, on reacting with styrene radicals, forms a substituted quinone, as has been suggested,[10] or disappears by some other reaction. Four vessels of approximately 125 ml. capacity were employed. These vessels were fitted with stopcocks by means of which the contents could be flushed with nitrogen. Styrene was added to 110 ml. of water in the vessel by means of a microburet delivering 0.0137 ± 0.0002 g. (at 25°) of styrene. The aqueous phase was 0.00182 *M* in potassium persulfate, and 0.000910 *M* in *p*-benzoquinone. After flushing with nitrogen, the styrene was added, and the vessels were placed in an oil bath held at 50°. The solutions remained clear throughout the reaction period. At intervals, a vessel was removed, a 25 ml. sample was taken and to it was added 23.9 ml. of 1/7.5 *M* Na_2HPO_4, 1.25 ml. 1/7.7 *M* KH_2PO_4, and 0.5 ml. of 0.5% gelatin solution as a maximum suppressor. The *p*H of the final solution was 8.05. The polarographic wave of this solution was then determined. In Figure 6, the waves obtained at various reaction times are presented. The first wave is that of persulfate, and the second is that of the quinone. For comparison, the wave for the initial concentration of quinone (curve 4) in the absence of persulfate is also shown. It will be observed that as the *p*-benzoquinone wave decreases, no wave corresponding to a new quinone appears.

Chloranil. The reaction of chloranil with styrene in the presence of persulfate was studied. 200 ml. of a 0.648% (4×) aqueous solution of potassium persulfate, and 20 ml. of a 3.2% solution of chloranil in styrene (giving a nearly saturated solution at 50°) were placed in a bottle, and flushed with nitrogen. The bottle was then placed in a 50° thermostat, where it was rotated end-over-end. At the beginning of the experiment, the color of the styrene layer was intensely red. (It is of interest that a solution of chloranil in styrene is red, while in toluene or benzene it shows a yellow color.) As the chloranil was consumed, this color faded. After 28 hours, the mixture had become entirely white. A polarographic test for chloranil at this time indicated that 99.0% of the chloranil had disappeared.

Products were isolated after 16.5, 21.0, and 24.5 hours reaction time by drawing off the styrene layer into cold methanol to precipitate the polymer, which was washed, dried *in vacuo*, and analyzed for chlorine. The results obtained, together with the intrinsic viscosities in benzene, are shown in Table VI.

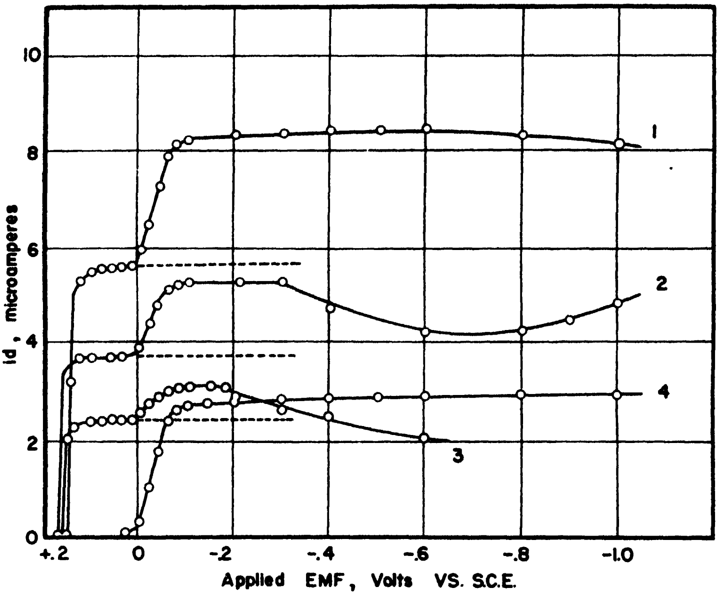

Fig. 6. Polarographic waves of $K_2S_2O_8$ (first wave) and *p*-benzoquinone (second wave) after reacting in aqueous solution in presence of styrene at 50°. 1, 0 hours. 2, 19.75 hours. 3, 43.5 hours. 4, Quinone at initial conc. in absence of $K_2S_2O_8$. Waves determined in phosphate buffer at *p*H 8.05.

TABLE VI

Reaction time, Hours	Per cent Cl	$[\eta]_{25}$
16.5	31.6	0.052
21.0	37.3	0.047
24.5	31.8	0.059

All three products were white powders that gave slightly yellow solutions in benzene. The intrinsic viscosities observed correspond to a number-average molecular weight of about 2000–3000 using the data of Ewart *et al.*[11] for polystyrene. This value is only an approximation, since the reaction product is quite different from polystyrene.

An attempt was made to measure the number-average molecular weight by osmotic pressure measurements, using the osmometers described by

Sands and Johnson,[12] but it was found that after an initial rise of solution in the capillary (the maximum rise corresponding to a molecular weight of 10,500), the solution level began to fall, indicating that the membrane was permeable to the solute. This result, therefore, only sets a maximum limit to the molecular weight.

The chlorine content of the 16.5-hour and 24.5-hour products (the reason for the higher chlorine content at 21.0 hours is unknown; this value was carefully rechecked) corresponds closely to a structure containing on the average one chloranil molecule to two styrene molecules (calculated chlorine content: 31.2%). If the number-average molecular weight is taken as approximately 2000, it appears that this substance is a copolymer of chloranil and styrene of average composition:

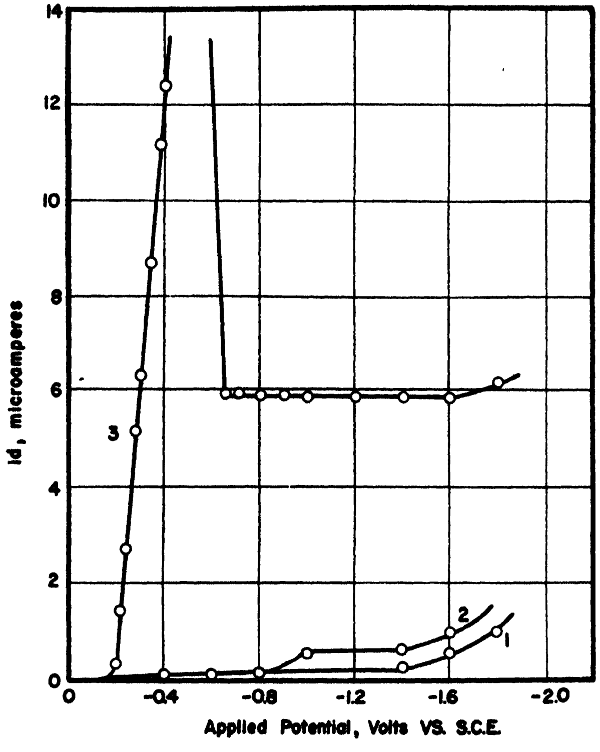

Fig. 7. Polarographic reduction waves in benzene-alcohol (5% water) 0.05 in tetraethyl ammonium bromide. 1, Blank. 2, Chloranil-styrene copolymer, 0.0494% solution. 3, chloranil, 0.0246% solution (0.001 *M*).

$$(\text{chloranil} \cdot 2\ \text{styrene})_{n \cong 4}$$

In Figure 7 is presented the polarographic wave of a 0.0494% solution of the polymer in a solvent composed of 5% water, 52.5% benzene, and 42.5%

ethanol, which was 0.05 *M* in tetraethyl ammonium bromide as supporting electrolyte. For comparison, the wave for 0.001 *M* chloranil (0.0246%) in the same solvent is also given. The polymer gives only a very small wave, which is evidently not due to residual chloranil, as it occurs at a potential more negative than that of the chloranil wave. The chloranil is bound into the polymer in such a way that the quinone structure is no longer present.

The same conclusion is indicated by the ultraviolet spectra of chloranil and the chloranil-styrene copolymer. In Figure 8, the specific extinctions of both substances from 248 to 310 millimicrons are presented, together with the curve for polystyrene. Chloroform was used as solvent, and the extinctions were measured with the Beckman Model DU Quartz Ultraviolet Spectrophotometer, using fused silica cells of 1 cm. path length. (The extinctions of the polymers are plotted on a scale five times larger than that for chloranil.) The chloranil-styrene copolymer absorption approaches a maximum in the neighborhood of 240 millimicrons, and shows no maximum at 260 millimicrons, as polystyrene does. It also shows a smaller peak with a maximum at 298 millimicrons, which is evidently not due to residual chloranil, since the chloranil maximum is at 292 millimicrons.

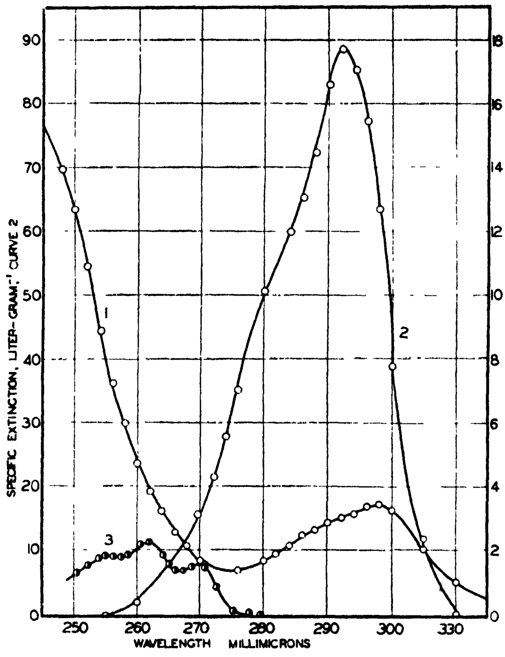

Fig. 8. Absorption spectra of: 1, chloranil-styrene copolymer; 2, chloranil; 3, polystyrene.

DISCUSSION

The experimental results indicate that when *p*-benzoquinone and chloranil react with monomer radicals in the emulsion polymerization of styrene, the product is not a quinone. The most reasonable hypothesis seems to be that, as Cohen[13] has suggested for the bulk polymerization of styrene, the monomer radical R· attacks the quinone molecule at the oxygen atom (M represents monomer):

(*1*) $K_2S_2O_8 + M \longrightarrow R\cdot$

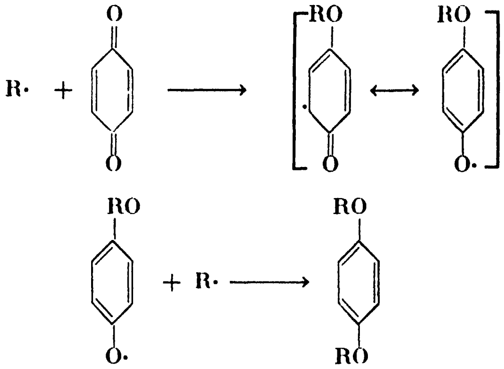
(2)

(*3*)

The product is thus an ether of hydroquinone.

We have represented the quinone-monomer adduct radical as capable of reacting only with R·, and not with M to continue the chain. If we accept this hypothesis, it is at once apparent that:

$$\frac{d(\mathrm{R}\cdot)}{dt} = -2\,\frac{d(\mathrm{Q})}{dt}$$

where Q represents *p*-benzoquinone. The data of Table I and Figure 1 show that the induction period produced by *p*-benzoquinone is proportional to the quantity initially present. The rate of disappearance of quinone is therefore of zero order with respect to (Q), and the induction periods should be inversely proportional to the rate of activation, $d(\mathrm{R}\cdot)/dt$. From the data of Tables I and II we thus find for the rate of activation of styrene at 50° in a 1× DDA·HCl, 1× $K_2S_2O_8$ recipe:

$$11.5 \times 10^{-5} \text{ moles/hour/liter of aqueous phase}$$

Table II shows that, as expected, the rate of activation is proportional to the persulfate concentration. If actually the ratio of *p*-benzoquinone reacting to radicals produced is greater than 1:2, the true rate of activation would be correspondingly smaller than this estimate. If, on the other hand, several molecules of styrene react for each molecule of quinone consumed, our conclusions as to the rate of activation are unaltered, provided only that the ratio of styrene radicals to quinone molecules reacting is approximately 2:1.

This estimate is confirmed by the following independent evidence.

(*a*) The number-average molecular weight of the polystyrene formed in a $1\times$ DDA·HCl, $1\times$ $K_2S_2O_8$ recipe at 50° and at 50% conversion (it varies only slightly with conversion) is about 2.75×10^6, estimated viscometrically from the relationship of Ewart *et al.*[11] Assuming disproportionation of recombining radicals, the rate of activation will then be given by:

$$\frac{d(\mathrm{R}\cdot)}{dt} = \frac{\text{rate of chain propagation, g./hour/liter}}{\bar{M}_n}$$

$$= \frac{370}{2.75 \times 10^6} = 13.4 \times 10^{\;5} \text{ mole/hour/liter of aqueous phase}$$

Recently, Mayo and Gregg[14] have presented evidence indicating that in the thermal polymerization of styrene the quinone-monomer adduct radical may be capable of continuing the chain, so that as many as 16 quinone molecules react for each R· produced. If copolymerization of the quinone with styrene occurs under the conditions of emulsion polymerization, we must assume that the true rate of initiation is actually smaller than that deduced from the quinone induction periods, and that the molecular weight of the polymer produced in the absence of the quinone is reduced by chain transfer (possible with monomer) to a degree just sufficient to counterbalance this effect. Only in this way can the correspondence of the apparent rates of initiation calculated from these independent measurements be accounted for if the hypothesis of the copolymerization of the quinone is retained. The experimental evidence does not allow us to exclude entirely the quinone polymerization–chain transfer interpretation, but we prefer at present the simpler interpretation which we have given above. Furthermore, Smith[15] has indicated that chain transfer with monomer is probably not an important factor in determining the molecular weight of polystyrene formed in emulsion.

(*b*) It will be shown in a subsequent paper that, when the styrene is entirely solubilized in the DDA·HCl solution, so that no excess is present, the rate of activation, estimated from the molecular weight of the product and the rate of polymerization, is of the same order of magnitude as above.

(*c*) From the sulfur content of the polymer, measured by means of a radioactive sulfur tracer in the persulfate, Smith[15] has estimated that the rate of activation at 50° in a 0.5% S.F. flakes, $1\times$ $K_2S_2O_8$ recipe is 3.7×10^{-5} mole/hour/liter, a value of the same order of magnitude as ours. The rate of polymerization under these conditions is about 170 g./hour/liter. It has been found in our laboratory that the rates of polymerization and molecular weights of polystyrene prepared in S.F. flakes and DDA·HCl under equivalent conditions are approximately the same.

Figure 3 shows that the rate of activation hardly depends on the emulsifier concentration. This appears to confirm the earlier conclusion[6] that the activation of the monomer occurs outside the soap micelles and in the "true" water phase of the reaction system. However, as will be shown and discussed in a subsequent paper, the rate of activation is much less (by a factor of at least ten) in the complete absence of the emulsifier.

We have shown that the apparent activation energy of the quinone induction period is 33,000 ± 400 cal. per mole. We believe that this value represents the energy of activation for the initiation of free radicals in this system. We have represented the activation process above as a bimolecular interaction of persulfate with the monomer. This appears to be a reasonable hypothesis, but the possibility that the rate-determining step in the activation process is a unimolecular decomposition of the persulfate cannot yet be definitely excluded. If the latter were true, the activation energy observed would represent that of the decomposition of the persulfate under these conditions. In water alone, the data of Green and Masson[16] indicate an activation energy of approximately 28,700 cal. per mole for the thermal decomposition of the persulfate ion to bisulfate ion and oxygen. The mechanism is unknown.

Estimates of the rates of persulfate activation of styrene dissolved in DDA·HCl solutions have been made by measuring rates of polymerization and molecular weights of the polymers. These experiments will be described in a subsequent paper. A value has been obtained in this way for the energy of activation of the activation process which is in agreement with the above value of 33,000 cal. per mole.

The experimental evidence indicates that chloranil, unlike *p*-benzoquinone, is a nonideal inhibitor. Although it produces sharply defined induction periods and therefore appears at first sight to be ideal, it copolymerizes with the styrene. Its rate of disappearance is thus more rapid than that of *p*-benzoquinone, even at very low concentrations. The following equations account for the reactions which occur in the presence of chloranil:

(1) $$K_2S_2O_8 + M \longrightarrow R\cdot$$

(2)

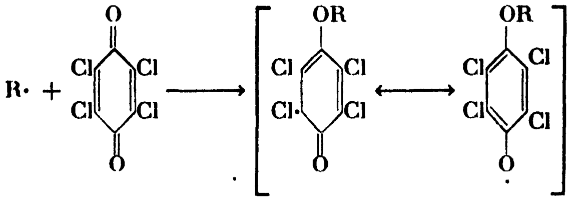

(I)

(3)

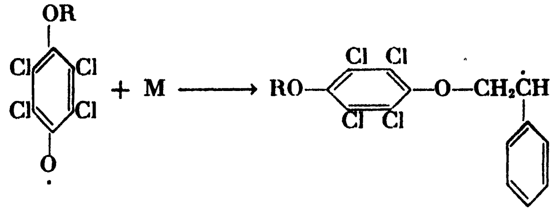

(II)

The radical (II) evidently does not react exclusively with chloranil—which would lead to a copolymer of strictly alternating structure—but may react with styrene also. The average composition and structure of the product obtained under our experimental conditions may be represented by:

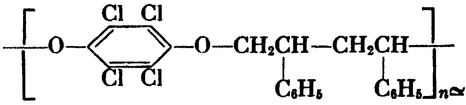

Previous investigations of the reactions of chloranil with styrene have been recently reviewed.[2] These studies are in general consistent with our proposed mechanism, although different structures have been assigned to the reaction products in some cases.

References

1. I. M. Kolthoff and F. A. Bovey, *J. Am. Chem. Soc.*, **70,** 791 (1948).
2. F. A. Bovey and I. M. Kolthoff, *Chem. Revs.*, **42,** 491 (1948).
3. J. W. Breitenbach and W. Schulz, *Monatsh.*, **80,** 463 (1949).
4. F. A. Bovey and I. M. Kolthoff, *J. Am. Chem. Soc.*, **69,** 2143 (1947).
5. H. A. Laitinen, W. P. Jennings, and T. D. Parks, *Ind. Eng. Chem.*, *Anal. Ed.*, **18,** 763 (1946).
6. I. M. Kolthoff and W. J. Dale, J. Am. Chem. Soc., **69,** 441 (1947).
7. S. G. Foord, *J. Chem. Soc.*, **1940,** 48.
8. I. M. Kolthoff and W. J. Dale, *unpublished observations.*
9. R. G. R. Bacon, *Trans. Faraday Soc.*, **42,** 140 (1946).
10. C. C. Price, *Advancing Fronts in Chemistry* (*High Polymers*, Vol. I). Reinhold, New York, 1945, p. 44.
11. R. Ewart, C. Roe, H. Tingey, and M. Wales. This relationship was presented at the 111th meeting of the American Chemical Society, and is given by Goldberg, Hohenstein, and Mark, *J. Polymer Sci.*, **2,** 503 (1947), and referred to by W. V. Smith, *J. Am. Chem. Soc.*, **68,** 2063 (1946). We have employed the original data, first reported as a Rubber Reserve research report, in which [η] is given as a function of the number-average molecular weight, determined by end-group analysis.
12. G. D. Sands and B. L. Johnson, *Ind. Eng. Chem.*, *Anal. Ed.*, **19,** 261 (1947).
13. S. Cohen, *J. Am. Chem. Soc.*, **69,** 1057 (1947).
14. F. R. Mayo and R. A. Gregg, *ibid.*, **70,** 1285 (1948).
15. W. V. Smith, *ibid.*, **71,** 4077 (1949).
16. L. Green and O Masson, *J. Chem. Soc.*, **1910,** 2083.

English Synopsis, see Summaries, page S22, Vol. V, 1950.

Résumé

Une étude expérimentale de la période d'induction causée par la *p*-benzoquinone, le 9,10-phenanthrène-quinone-3-sulfonate potassique et le chloranile a été faite dans le cas de la polymérisation en émulsion du styrène, en présence de chlorhydrate de dodécylamine comme émulsifiant et de persulfate potassique comme initiateur. Les périodes d'induction, dues à la *p*-benzoquinone sont proportionnelles à la quantité d'inhibiteur initiale, inversément proportionelles à la concentration en persulfate potassique, et environ indépendantes de la concentration en émulsifiant. Il est démontré que la vitesse de disparition de la *p*-benzoquinone est approximativement égale à la moitié de la vitesse de production de radicaux monomères libres produits dans le système. La vitesse de production des radicaux est proportionelle, au début de la polymérisation, à la concentration en persulfate, et sensiblement indépendant de la concentration en émulsifiant, depuis 0.625 g. à 500 g. de chlorhydrate de dodécylamine par 100 g. de monomère.

Le processus d'activation nécessite une énergie de 33,000 ± 400 cal. par mol. Le 9,10-phénanthrène-quinone-3-sulfonate potassique est un inhibiteur non-idéal. Le chloranile copolymérise avec le styrène. Le polymère résultant, formé au cours de nos conditions expérimentales, a été caractérisé, et a la composition suivante:

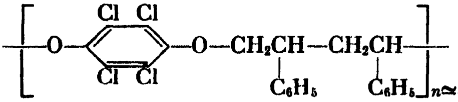

L'oxygène réagit plus rapidement avec les radicaux libres styrèniques que ne le font les quinones.

Zusammenfassung

Es wurde eine experimentelle Untersuchung der Induktionsperioden vorgenommen, die durch *p*-Benzochinon, Kalium-9,10-phenanthrenchinon-3-sulfonat und Chloranil in der Emulsionspolymerisation von Styrol unter Verwendung von Dodecylamin-hydrochlorid als Emulsionsmittel und Kaliumpersulfat als Initiator hervorgerufen wurden. Es wurde gefunden, dass die durch *p*-Benzochinon hervorgerufenen Induktionsperioden proportional der anfangs vorhandenen Menge des Initiators, umgekehrt proportional der Persulfatkonzentration und fast unabhängig von der Konzentration des Emulsionsmittels sind. Der Beweis wurde erbracht, dass die Abnahmegeschwindigkeit von *p*-Benzochinon annähernd gleich der Hälfte der Produktionsgeschwindigkeit von freien Monomer- Radikalen in dem System ist. Die Produktionsgeschwindigkeit von Radikalen zu Anfang der Polymerisation ist proportional der Persulfatkonzentration und fast unabhängig von der Konzentration des Emulsionsmittels zwischen 0.625 und 5.00 g. Dodecylamin-hydrochlorid pro 100 g. Monomer. Der Aktivierungvorgang zeigt eine Aktivierungsenergie von 33,000 ± 400 cal. pro Mol. Kalium-9,10-phenanthrenchinon-3-sulfonat ist ein nicht idealer Inhibitor. Es wurde gefunden, dass Chloranil mit Styrol copolymerisiert. Das Polymer, das unter unseren experimentalen Bedingungen erhalten wurde, wurde charakterisiert, und es wurde gefunden, dass es die folgende Zusammensetzung hat:

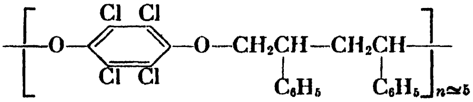

Sauerstoff reagiert hereitwilliger mit freien Styrol-Radikalen als Chinone.

Received July 5, 1949

JOURNAL OF POLYMER SCIENCE VOL. V, NO. 5, PAGES 587-590

Influence of Molecular Weight on the Properties of Polystyrene. II. Fractionation of the Polymer*

E. H. MERZ and R. W. RAETZ,† *Plastics Division, Research Laboratories, Monsanto Chemical Company, Springfield, Massachusetts*

I. INTRODUCTION

The dependence of the strength properties of cellulose acetate,[8,9] polyvinyl chloride,[5] cellulose nitrate,[10] and polyisobutylene[11] upon molecular weight has been established; it appeared of interest to carry out a similar investigation of polystyrene, since this polymer has a large molar cohesion, yet does not crystallize.[6] Part I of this series[7] described a method of casting and drying polystyrene films so that further stringent drying would not alter the values of the measured physical properties within the precision of their measurement. Part II describes the fractionation of a polystyrene on a scale large enough to yield fractions from which films could be cast and tested for strength properties.

II. PREPARATION OF POLYMER

Commercial monostyrene of 99.8% purity containing 10 p.p.m. of *p-tert*-catechol was polymerized in bulk at 93°C. under an oxygen-free atmosphere without the use of catalyst. After 12 hours, 15% conversion was reached, at which time the kettle charge was dumped onto Dry Ice and 0.1% hydroquinone was added. The polymer was isolated by running the solution as a fine thread into 10 volumes of stirred methanol. After filtration and washing with methanol, the polymer was dissolved in methyl ethyl ketone to make a 2% solution and precipitated in the form of a porous thread having a high surface/weight ratio.

III. FRACTIONATION OF THE POLYMER

Of the various known methods that are suitable for fractionating high polymers (see Cragg and Hammerschlag for an excellent review,[1]) the precipitation by nonsolvent addition to a solution of the polymer with temperature as equilibrant and final precipitation agent was most feasible in the available equipment. This method had been used successfully by Danes[2] on polystyrene as early as 1934.

---

* Contribution from the Monsanto Chemical Company, Plastics Division, Research Laboratories, Springfield, Mass.

† Present address: Armour Leather Co., Philadelphia, Pa.

The twice-precipitated dry polymer was dissolved in methyl ethyl ketone to make a 1.5% solution in a 200-gallon jacketed vessel. A calculated quantity of methanol was added to the stirred solution at 37.8°C. and then

TABLE I

SUMMARY OF FRACTIONATION DATA

Fraction No.[a]	Wt. % of original	Intrinsic viscosity	k'	$M_w \times 10^{-3}$ [b]	$M_w \times 10^{-3}$ [c]	μ
1	11.08	2.42	0.42	1550	1500	0.491
3	5.61	2.24	0.37	1350		
2	5.46	2.15	0.50	1250		
5[d]	5.14	2.07	0.36	1170		
4	4.76	2.03	0.43	1130	1190	0.489
7	5.46	1.92	0.27	1010		
6	3.54	1.82	0.44	920		
8	1.93	1.77	0.36	880		
9	2.41	1.75	0.38	860	880	0.489
11	2.85	1.67	0.38	790		
10	2.09	1.66	0.40	780		
12	1.88	1.66	0.36	780		
13	1.11	1.58	0.38	720		
14	3.82	1.56	0.35	700	660	0.489
16	2.38	1.51	0.32	660		
15	1.53	1.50	0.36	655		
17	2.36	1.41	0.36	590		
18	0.82	1.39	0.36	575		
19	2.92	1.37	0.35	560	554	0.494
20	1.88	1.34	0.33	540		
21	1.64	1.26	0.38	490		
22	2.46	1.23	0.35	470		
23	1.56	1.16	0.40	430		
24	2.33	1.14	0.34	420	470	0.484
25	2.23	1.08	0.37	385		
26	2.19	1.02	0.37	355		
27	2.32	0.96	0.37	320		
28	2.32	0.90	0.37	295		
29	2.16	0.84	0.38	270	266	0.483
30	2.27	0.77	0.39	240		
31	0.68	0.77	0.39	240		
32	1.05	0.71	0.39	215		
33	1.08	0.67	0.39	200		
34	1.55	0.59	0.45	170		
35	1.18	0.56	0.38	160		
36	2.34	0.42	0.52	120	128	0.480
37	0.38	0.42	0.45	120		
38	1.20	0.42	0.47	120		
39	0.03	0.19	0.44	60		
Original	100.00	1.59	0.36	725		

[a] Arranged in order of decreasing intrinsic viscosity; number in order of preparation.

[b] Read from smoothed curve of intrinsic viscosity versus measured $\bar{M}_w$.

[c] Measured.

[d] Distributed under the auspices of the Commission on Macromolecules of the Union Internationale de Chemie.

the temperature was raised to 58°C. to redissolve any precipitate. After cooling slowly and allowing the gel to settle overnight, the gel was withdrawn through a 2-in. gate valve at the bottom of the kettle, and dissolved in methyl ethyl ketone to make a 2% solution.

The fraction was then isolated by running the solution into 10 volumes of stirred methanol, filtering off the porous threads, washing with methanol, and drying to *ca.* 1% residual solvents on a Büchner funnel.

The quantity of methanol added to precipitate a given fraction was calculated from the results of a small (50 g.) pilot fractionation where turbidities could be observed by eye.

Repetition of this procedure yielded 39 fractions (the 40th was left in solution). Pertinent data are collected in Table I.

IV. CHARACTERIZATION OF THE FRACTIONS

The intrinsic viscosity of each fraction was determined in toluene solution at 28.5 ± 0.02°C. with an Ostwald-type viscometer modified so that dilutions could be made directly in the instrument. Values of k' were determined in the manner of Huggins.[4] Light scattering measurements on methyl ethyl ketone solutions of selected fractions yielded weight-average molecular weights and the Flory-Huggins solubility constant "μ" calculated from the slope of the curve.[3] The results of these measurements are given in Table I.

The relationship between the log of the intrinsic viscosity and the log of the molecular weight ($\bar{M}_w$) was plotted and because of scatter the weight-average molecular weights were read from the smoothed curve.

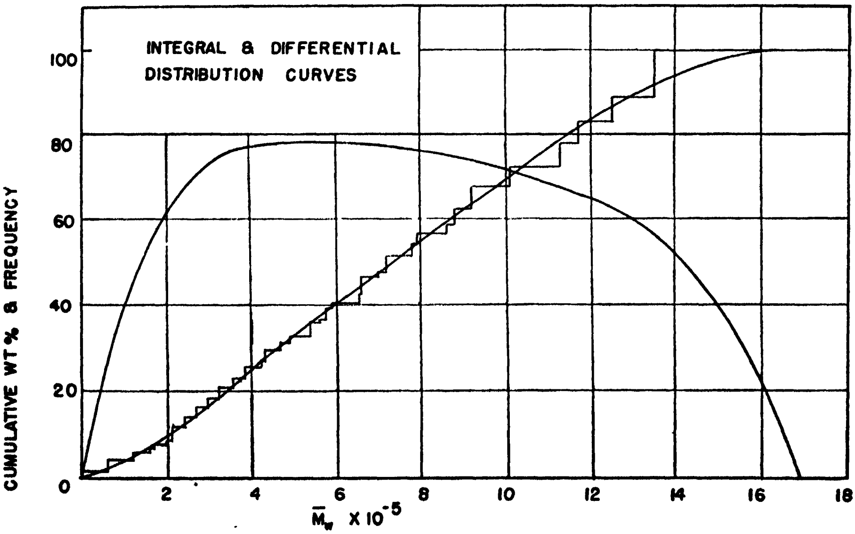

Figure 1

The Huggins k' values for the fractions were disappointingly nonuniform, but a Student's "t" test showed that the difference between the mean of the two sets of extreme values and the mean of the others was not significant at the 95% level.

V. DISTRIBUTION CURVES

The integral distribution curve was drawn through the midpoints of the $\Delta\bar{M}_w$ lines of the stepped boxes whose areas equaled $\Delta\bar{M}_{w_i}\Delta(\text{wt. }\%)_i$ and is given in Figure 1. The differential distribution curve given in Figure 1 was obtained by plotting the slope of the integral distribution curve at a given $\bar{M}_w$ versus that $\bar{M}_w$.

Of interest is the fact that the sum of the products "weight % of fraction times its intrinsic viscosity" equaled the intrinsic viscosity of the starting polymer which may be taken as evidence that the losses during fractionation were fairly uniformly distributed among the fractions.

The authors wish to thank Drs. N. N. T. Samaras and R. Buchdahl for their support and continued interest.

References

1. L. H. Cragg and H. Hammerschlag, *Chem. Revs.*, **39**, 79 (1946).
2. V. Z. Danes, *Kolloid-Z.*, **68**, 110 (1934).
3. P. M. Doty and H. Mark, *Ind. Eng. Chem.*, **38**, 682 (1946).
4. M. L. Huggins, *J. Am. Chem. Soc.*, **64**, 2716 (1942).
5. M. Jelling, QMC-36 Report of Research on Coated Fabrics and Thin Films, 271 (1946).
6. H. Mark, *Ind. Eng. Chem.*, **34**, 1343 (1942).
7. E. H. Merz, L. E. Nielsen, and R. Buchdahl, 1948 Annual Meeting Am. Phys. Soc., N. Y., *J. Polymer Sci.*, **3**, 605 (1949).
8. A. M. Sookne and M. Harris, *Ind. Eng. Chem.*, **37**, 475 (1945).
9. A. M. Sookne, M. Harris, and H. Mark, *J. Research Natl. Bur. Standards*, **29**, 123 (1942).
10. H. M. Spurlin, *Ind. Eng. Chem.*, **30**, 538 (1938).
11. R. L. Zapp, *ibid.*, **40**, 1508 (1948), and *private communication.*

English Synopsis, see Summaries, page S11, Vol. V, 1950.

Résumé

Un fonctionnement poussé d'un polystyrène isolé après une faible conversion, a été effectué par refroidissement progressif d'une solution dans un mélange méthanol-butanol. La viscosité intrinsèque est donnée pour toutes les 39 fractions, ainsi que les poids moléculaires de 8 fractions, déterminés par mesure de diffusion de la lumière. La courbe de distribution, qui présente un large maximum unique, est également indiqué.

Zusammenfassung

Eine Fraktionierung im Grossen von einem Polystyrolpolymeren niedriger Conversion wird beschrieben. Es wird dabei die Temperatur einer Butanon-Methanollösung schrittweise vermindert. Die Grenzviskosität wird für alle 39 Fraktionen angegeben und das Lichstreuungs-Molekulargewicht für 8 Fraktionen. Die Verteilungskurve, die eine einzige breite Spitze hat, wird ebenfalls gegeben.

Received July 10, 1949

JOURNAL OF POLYMER SCIENCE VOL. V, NO. 5, PAGES 591-608

Flow of Linear Amorphous Polymers

R. S. SPENCER, *The Dow Chemical Company, Midland, Michigan*

INTRODUCTION

A knowledge of the rheological properties of polymers is of greatest practical importance in two types of problems. The flow behavior of the material is a fundamental consideration in the customary fabrication techniques, molding, and extrusion. The creep characteristics at substantially lower temperatures are equally important in many applications. In the present paper we shall be concerned primarily with those properties which are pertinent to the first problem. That is to say, we shall be considering ranges of experimental conditions, such as temperature, shearing stress, etc., which are roughly equivalent to those encountered in fabrication.

The title of this paper implies a further restriction as to the types of polymers to be studied, although this is not as confining as might be expected. In the case of polymers that can crystallize at room temperature, such as rubber and polyethylene, fabrication temperatures are customarily above the melting point of the crystallites. For our purposes, then, we may regard such materials as amorphous polymers. The limitation to linear polymers merely means that we are avoiding such things as vulcanized rubber which have a three-dimensional network structure.

Before proceeding to the discussion, a few generalities about the rheological properties of polymers are perhaps in order. The deformation of a polymer under stress may be subdivided into contributions from three distinct mechanisms, which we shall consider very briefly. At temperatures well below the apparent second-order transition temperature most of the short-time deformation is due to *ordinary elasticity*. This is similar to the deformation of a crystalline material and is presumably due to stretching of valence bonds and/or bending of valence angles. The modulus is quite high and relatively insensitive to temperature variations; the response to applied stress is practically instantaneous and the deformation is completely recoverable. At temperatures near and above the apparent second-order transition temperature a considerable amount of strain may be contributed by *high elasticity*, frequently called *rubberlike elasticity*. This is attributed to the partial uncoiling of the threadlike polymer molecules under stress. The modulus is several orders of magnitude lower than that for ordinary elasticity; the question of its temperature dependence will be deferred for later discussion. Deformations by this mechanism are completely recoverable, but both the elastic response and recovery are delayed, *i.e.*, are time dependent. This behavior may be described by specifying a spectrum of relaxation times for the material. Major prerequisites for the existence of high elasticity in a polymer seem to be the presence of molecules that are "flexible" enough to coil up in the unstressed state and subsequently uncoil when stressed, together with points of linkage between molecules that are capable of transmitting stress. These linkage points may be strong chemical bonds (as in vulcanized rubber), chemical bonds capable of breaking under stress and subsequent reforming (as in polysulfide rubbers), or even points of strong secondary forces (as in polystyrene and other more or less linear polymers). The flexibility of the individual molecules is strongly influenced by temperature; thus it is found that the relaxation time spectrum shifts markedly when the temperature is changed. If the temperature is sufficiently greater than the apparent second-order transition temperature, it may even appear, in a given experiment, that rubberlike elastic response and recovery are practically instantaneous. The third deformation mechanism is that of *viscous flow*, which results in irrecoverable strains. At lower temperatures this is manifest as creep or stress relaxation. At higher temperatures it is the principal contributor to the relatively large deformations concommitant with fabrication. At low shearing stresses most polymers are substantially Newtonian, *i.e.*, the rate of shear is directly proportional to the shearing stress. There is no evidence for the existence of a yield point, at least in the fabrication range of temperature. The flow behavior may be characterized by a viscosity that, as might be expected, turns out to be dependent upon the temperature and polymer molecular weight. As the shearing stress is raised, however, the rate of shear increases much more rapidly than would be expected from Newton's law. This behavior, and its interpretation on a molecular basis, is one of the principal topics of the present paper.

In the discussion to follow, greatest emphasis will be given to the behavior of polymers in shear. This is natural when it is remembered that the primary concern is with flow under conditions roughly equivalent to those encountered in fabrication. If undue emphasis seems to be given at times to the properties of polystyrene, it is hoped that this may be forgiven on the grounds that the greater part of the author's personal experience has been with that material.

RELATIONSHIP BETWEEN RATE OF SHEAR AND SHEARING STRESS

It was pointed out in the introduction that high shearing stresses result in rates of shear which are much greater than would be expected from observations at low shearing stresses. Under conditions typical of extrusion or injection molding the rate of shear is very sensitive to the shearing stress. Practical considerations, then, in addition to the theoretical interest of the question, suggest this topic as a good starting point for discussion.

It is interesting to consider first what type of relationship between rate of shear and shearing stress might be expected, *a priori.* Eyring[1] has treated the problem from the viewpoint of the theory of absolute reaction rates and arrived at an expression, for the case of simple shear, which may be written in the form:

$$\phi_A = \phi_0 \frac{\sinh(\beta\tau)}{\beta\tau} \tag{1}$$

Here ϕ_A is the apparent fluidity, ϕ_0 is the fluidity in the limit of vanishing shearing stress, τ is the shearing stress, and β is a constant of the form:

$$\beta = \lambda A/2kT$$

where λA is the so-called "viscous volume," k is the Boltzmann constant, and T is the absolute temperature. The corresponding equation for flow through a capillary was developed by Tobolsky, Powell, and Eyring,[2] and may be written as:

$$\phi_A = \phi_0 \frac{4}{(\beta\tau)^3}\left[\left(\beta\tau + \frac{2}{\beta\tau}\right)\cosh(\beta\tau) - 2\sinh(\beta\tau) - \frac{2}{\beta\tau}\right] \tag{2}$$

where τ is the shearing stress at the capillary wall. This equation has been applied by its originators to data on the flow of rubber, and by Greenblatt and Fensom[3] to heterogeneous systems.

Several difficulties have arisen in more detailed attempts to apply the Eyring equations to experimental flow data. Tobolsky, Powell, and Eyring noted that the capillary flow equation did not fit data obtained with highly compounded rubber. Spencer and Dillon[4] pointed out that the observed behavior of polystyrene was not in agreement with the Eyring equation. The author has found that equation (1) will not give a satisfactory fit to the data of Treloar and Saunders[5] on the flow of masticated rubber. Another, less direct, bit of evidence may be found in the work of Ferry[6] on the flow of concentrated polystyrene solutions. Ferry observed that as the shearing stress is raised early deviations from Newton's law come about through a term which contains the first power of the shearing stress. Expansion of the hyperbolic sine of equation (1) into a power series shows that these early deviations should be due to a term containing the square of the shearing stress. It might be concluded, then, that the Eyring equations, as they stand, do not describe satisfactorily observed flow behavior of polymers, except, perhaps, in rare specific cases.

Somewhat better agreement between theory and experiment may be obtained if molecular orientation during flow is taken into account. The appearance of birefringence in a polymer solution which is being sheared is a well-known phenomenon. It is generally accepted that this is due to partial uncoiling and orientation of the polymer molecules (as in highly elastic deformation). It is also fairly widely recognized that a similar effect may be present in the flow of molten polymers. Kauzmann and Eyring[7] have pointed out that in the presence of appreciable flow orientation it is to be expected that the "constants" in the Eyring equation will depend upon the shearing stress. In the same vein, Kistler[8] reported that the viscous volume appears to decrease as the percent stretch of the polymer sample increases. Similarly, it was noted by Spencer and Dillon[4] that in the case of polystyrene the quantity β of equation (1) was approximately inversely proportional to the effective relative extension of the polymer during flow. This they attributed to a decrease in the viscous volume with increasing orientation.

Attractive as this approach may seem, only a qualitative improvement of the agreement between theory and experiment has resulted. It is difficult, although perhaps not impossible, to formulate a connection between viscous volume and flow orientation which will at the same time appear reasonable and lead to a satisfactory explanation of the experimental facts. To this difficulty must be added another, which has not been mentioned up to this point: the magnitude of the values computed for the viscous volume.[2,3,8,13] It invariably turns out that application of the Eyring equation leads to viscous volumes which are very much larger than one would have anticipated. This is usually taken as signifying that the flow unit must consist of a whole cluster of polymer molecules.[9] This picture is certainly at variance with that obtained by following Eyring's procedure[10] for calculating the size of the flow unit from the heat of activation for viscous flow. This latter method gives values of perhaps ten or twenty monomeric residues.

An alternative possibility is to look for the dependence of apparent fluidity upon shearing stress elsewhere than in the hyperbolic sine term of equation (1). That which follows should be taken as merely a suggestion of a possible direction of approach to the problem. More elegant and satisfactory treatments are certainly conceivable.

Let us assume that β is actually as small as might be expected from the heat of activation for viscous flow. In this case we can replace the hyperbolic sine of equation (1) by its argument. Eyring[10] has shown that in these circumstances the expression for fluidity becomes:

$$\phi = (V/hN) \exp\{-\Delta F^*/RT\} = (V/hN) \exp\{-\Delta H^*/RT\} \exp\{\Delta S^*/R\} \quad (3)$$

where V is the molar volume of a flow unit, h is Planck's constant, N is Avogadro's number, R is the gas constant, T the absolute temperature, ΔF^* the molar free energy of activation, ΔH^* the molar heat of activation, and ΔS^* the molar entropy of activation. Treloar and Saunders[5] have indicated that there is no significant dependence of the heat of activation upon shearing stress; this would seem also to rule out any influence of shearing stress upon V. It would appear, then, that the influence of shearing stress upon fluidity must enter through the entropy of activation. One way of bringing this about is to assume an asymmetrical flow unit, which is not too implausible, and which, further, is oriented in the direction of flow in the activated state. This concept is not completely foreign to the polymer field. Levi[11] has suggested that certain phenomena encountered in the diffusion of water vapor through polymers and in dielectric relaxation are best explained by assuming that the water molecule or the dipole is preferentially oriented in the activated state. If a similar situation were the case in viscous flow, the activated state would be characterized by a high degree of order. The degree of order in the normal state would depend upon the amount of flow orientation, and thus upon the shearing stress. That part of the entropy of activation which is associated with orientation would be negative in sign, and would become more positive (decrease in absolute magnitude) as the shearing stress increased. Referring to equation (3), we see that the fluidity would then increase with increasing shearing stress, as is observed experimentally.

Now let us divide the entropy of activation ΔS^* into a part associated with orientation, ΔS_0^* and a part independent of orientation (in the sense in which we are using the word), ΔS_1^*, so that:

$$\Delta S^* = \Delta S_0^* + \Delta S_1^* \tag{4}$$

We shall adopt Eyring's suggestion that $P\,\Delta V$ is negligible under usual experimental conditions, and so we may obtain ΔS_0^* from the work of deformation, ΔW^*, involved in going from the partially oriented normal state to the more highly oriented activated state by means of the equation:

$$\Delta W^* = -T\Delta S_0^* \tag{5}$$

It is perhaps well to mention here that in the theory of rubber elasticity it is pointed out that only an entropy change is associated with the uncoiling of a polymer molecule, the internal energy being independent of the molecular configuration. The work of deformation ΔW^* may be written as:

$$\Delta W^* = \Delta W_0^* - \Delta W_n^* \tag{6}$$

the difference between the work, ΔW_0^*, done in going from the unoriented state to the activated state and the work, ΔW_n^*, done in going from the unoriented state to the normal state corresponding to the given shearing stress. Substituting equations (4), (5), and (6) in equation (3), we obtain:

$$\phi = (V/hN)\exp\left\{-\Delta H^*/RT\right\}\exp\left\{(\Delta S_1^*/R) - (\Delta W_0^*/RT)\right\}\exp\left\{\Delta W_n^*/RT\right\} \tag{7}$$

The quantity ΔW_0^* will be constant for a given polymer at a given temperature, and ΔW_n^* will approach zero as the shearing stress approaches zero, so we may rewrite equation (7) as

$$\phi_A = \phi_0 \exp\left\{\Delta W_n^*/RT\right\} \tag{8}$$

In computing ΔW_n^*, we shall make use of the theory of rubber elasticity as formulated by James and Guth.[12] In so doing, the assumption will be made that the behavior on a molecular scale, when averaged over a large number of small units, is equivalent to the macroscopic behavior of a rubber network, insofar as the question of orientation and high elasticity is concerned. Our starting point will be the following relationship, for simple shear,

$$\tau = G\sigma \frac{\mathfrak{L}^{-1}[K(1+\sigma^2)^{1/2}]}{3K(1+\sigma^2)^{1/2}} \tag{9}$$

where τ is the shearing stress, σ is the shear strain, G is the modulus, K is the reciprocal of the maximum stretch, and $\mathfrak{L}^{-1}(x)$ is the inverse Langevin function. The work of deformation in going from the unstrained state to a state of strain, σ, is:

$$\text{work per cc.} = \int_0^\sigma \tau \, d\sigma \tag{10}$$

Substituting equation (9) in equation (10) and integrating,

$$\text{work per cc.} = (G/3K^2)[\Lambda[K(1+\sigma^2)^{1/2}] - \Lambda(K)] \tag{11}$$

where:

$$\Lambda(x) = \int_0^x \mathfrak{L}^{-1}(u)\,du = x\mathfrak{L}^{-1}(x) - \log\left\{\frac{\sinh[\mathfrak{L}^{-1}(x)]}{\mathfrak{L}^{-1}(x)}\right\}$$

It seems logical to assume that the orientation of a given flow unit necessitates a certain amount of cooperation on the part of nearby flow units of the same molecule. To obtain the work of deformation involved in orienting a mole of flow units we must, therefore, multiply equation (11) by nV, where V is the molar volume of flow units and n is the number of cooperating units. This gives finally,

$$\Delta W_n^*/RT = (nVG/3K^2RT)\,[\Lambda[K(1+\sigma^2)^{1/2}] - \Lambda(K)] \tag{12}$$

It should be noted that in the above equation R must be taken in units of ergs per mole per °C. if G is given in dynes per square centimeter.

The relationship between rate of shear and shearing stress, for simple shear, is now defined by:

$$\log \phi_A = \log \phi_0 + \frac{nVG}{RT} F\left(K, \frac{\tau}{G}\right) \tag{13}$$

where the new function in the last term is found by eliminating σ between the two equations

$$F\left(K, \frac{\tau}{G}\right) = \frac{1}{3K^2}(\Lambda[K(1+\sigma^2)^{1/2}] - \Lambda(K)) \tag{14}$$

and

$$\frac{\tau}{G} = \sigma \frac{\mathfrak{L}^{-1}[K(1+\sigma^2)^{1/2}]}{3K(1+\sigma^2)^{1/2}}$$

Various data on natural rubber suggest that $K = 1/8$, approximately, for this material. Figure 1 shows the corresponding function of equation (14) for this case.

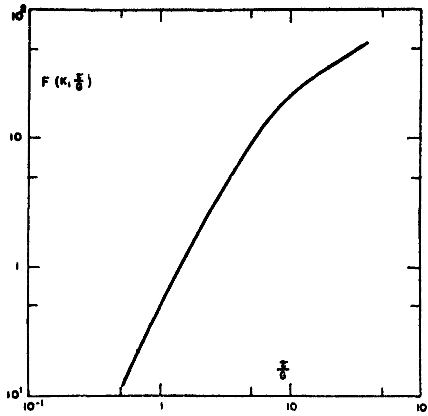

Fig. 1. Flow function of equation (14) for rubber.

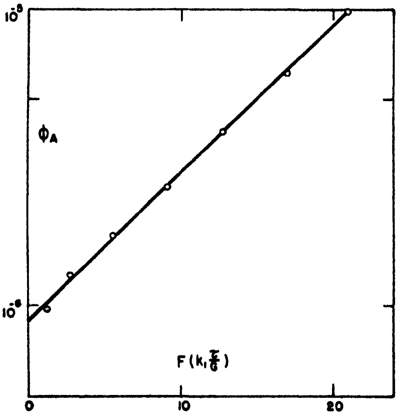

Fig. 2. Apparent fluidity of rubber at 140 °C. versus the flow function (Treloar and Saunders).

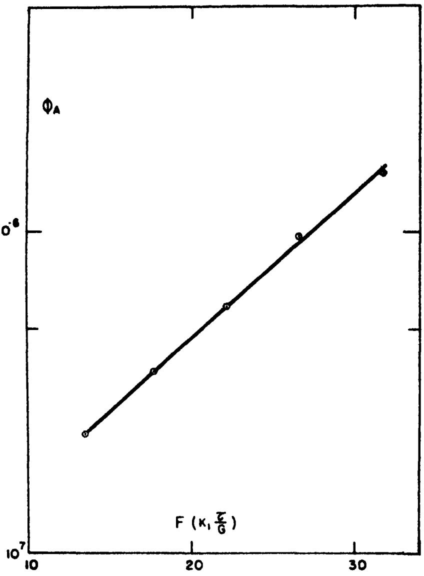

Fig. 3. Apparent fluidity of rubber at 50 °C. versus the flow function (Treloar and Saunders).

Let us now see how well this picture fits in with the experimental observations of Treloar and Saunders[5] on the flow of masticated rubber. The procedure followed was that of trial-and-error adjustment of the value of G to see if a linear relationship could be obtained between log ϕ_A and

$F(K,\tau/G)$. Figure 2 shows the result with the data obtained at 140°C., using a value $G = 10^5$ dynes/cm.^{2}. The data obtained at 50°C. are shown in Figure 3, using the same value for G. In both cases good straight lines were obtained of very nearly the same slope. The values of ϕ_0 indicated by these lines are slightly higher, by a factor of 1.5, than corresponding values obtained from the same data by the empirical method to be discussed later. From the slopes of the lines one can compute nV, arriving at a value of 39,400 cc./mole at 140°C. and 28,600 cc./mole at 50°. These are not to be taken too seriously as to absolute value, but the order of magnitude certainly suggests that a relatively large number of flow units cooperate in the orientation process.

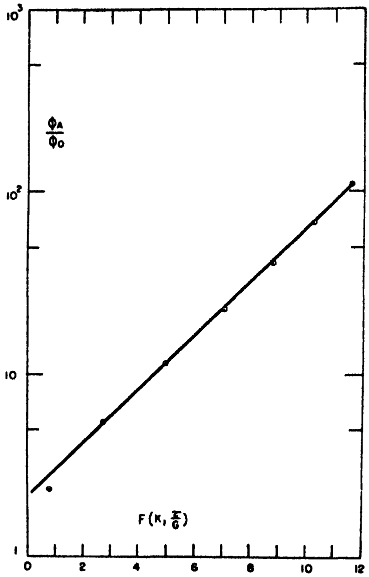

Fig. 4. Apparent fluidity of polystyrene versus the flow function.

Before leaving the subject some comment should be made on the applicability of these equations to polystyrene. In this case $K = 1/5$, roughly. Unfortunately very few data are available on the flow of polystyrene in simple shear. The work of Buchdahl[13] was carried out at shearing stresses too low for the results to provide a good example, but even here the data seem to fit in fairly well with the picture just set forth. A better example may be constructed by calculating the behavior in simple shear from the capillary flow data of Spencer and Dillon. An equivalent procedure is to use directly the empirical relationship set forth in equation (16). This leads to Figure 4, where we note that a fairly good straight line is again obtained, this time with $G = 1.5 \times 10^5$ dynes/cm.^{2} The intercept gives a value of ϕ_0 about twice that given by the empirical equation, and the slope suggests that perhaps about 70 flow units cooperate in the orientation process.

Let us now consider briefly the empirical approach of Spencer and Dillon[14] to this problem. Observations of the capillary flow of molten polystyrene under a variety of conditions led them to suggest the following relationship:

$$\phi_A = \phi_0 \left(1 + k\tau + \frac{k^2\tau^2}{2!} + \frac{k^3\tau^3}{3!} + \frac{k^4\tau^4}{4!}\right) \tag{15}$$

From this it may be shown that the corresponding relationship for simple shear is

$$\phi_A = \phi_0 \left(1 + \frac{5}{4}k\tau + \frac{6}{4}\frac{k^2\tau^2}{2!} + \frac{7}{4}\frac{k^3\tau^3}{3!} + \frac{8}{4}\frac{k^4\tau^4}{4!}\right) \tag{16}$$

In both of the above equations k is a constant expressing the extent of deviation from Newtonian behavior. At low shearing stresses the apparent fluidity increases linearly with the shearing stress; this type of behavior was also reported by Ferry[6] for concentrated polystyrene solutions. Up to moderately high shearing stresses equation (15) closely approximates an exponential function, as was observed experimentally by Spencer and Dillon.[4] At still higher shearing stresses the relationship approaches a power law, reminiscent of the Ostwald-de Waele equation.

The principal difficulty which has arisen in applying the above equations is the question of a satisfactory curve-fitting procedure. That is to say, what values of ϕ_0 and k give the best fit to a given set of flow data? The first method tried was to plot log ϕ_A against τ and fit a straight line to the points, the intercept giving ϕ_0 and the slope giving k. This works fairly well at moderately low shearing stresses, but was not of sufficiently wide applicability to be completely satisfactory. A second method was patterned after that used by Mayo and Lewis[15] in handling copolymerization data. Each experimental point was used to compute a whole set of corresponding values of ϕ_0 and k. These values were then plotted, log ϕ_0 versus k, to give one line for each experimental point. Ideally, the family of lines associated with a set of data should intersect at a single common point, giving the proper values of ϕ_0 and k for the data in question. Actually, of course, the intersections scattered over an area, from which appropriate values of ϕ_0 and k could be estimated. Two disadvantages detract greatly from the usefulness of this method. First of all, it is much too tedious a procedure to be used extensively in analyzing data. Perhaps even more important is the fact that, in locating the "best" values of ϕ_0 and k within the area of intersections, it is very difficult to see just what weight is being given to the various experimental points. That is to say, there is no clear indication of just how well the selected values of the constants fit the data, without replotting the empirical function. A third method was evolved to eliminate both of these difficulties. Equations (15) and (16) can be considered to be of the form

$$\phi_A = \phi_0 F(k\tau)$$

For each equation, then, log F was plotted against log ($k\tau$). From such a curve a Celluloid prototype was constructed on which was shown the curve, two axis guide lines, and a reference point located at $k\tau$, $F = 1$. In using this device, the first step is to plot the experimental points (on the same type of graph paper used in constructing the prototype) as log ϕ_A versus log τ. The Celluloid prototype is then laid over the graph paper and its curve fitted to the experimental points by translation along both axes. When this has been done the coordinates on the experimental graph of the prototype reference point are read off. The coordinate on the ϕ_A axis gives ϕ_0, and that on the τ axis gives $1/k$. This method is rapid and has proven to be entirely satisfactory.

Spencer and Dillon[14] have indicated that equation (15) gives a satisfactory representation of capillary flow data for polystyrene. We have also attempted to apply it to the capillary flow of several ethylcellulose formulations. For some of these materials it works quite well, for others it does not seem to fit the data. The behavior of masticated rubber in simple shear, as reported by Treloar and Saunders,[5] is in excellent agreement with equation (16). It is to be hoped that future rheological studies of other polymers will provide suitable additional data for assessing the usefulness of these relationships.

INFLUENCE OF TEMPERATURE, MOLECULAR WEIGHT, AND PLASTICIZER CONTENT

Continuing with the empirical approach, two constants have thus far appeared in our description of the flow properties of polymers, ϕ_0 and k. In the discussion to follow, ϕ_0 will be replaced by its reciprocal, η_0, which we shall call the Newtonian viscosity. Consideration will now be given to the influence of temperature, molecular weight, and plasticizer content upon these quantities.

TABLE I

INFLUENCE OF TEMPERATURE ON FLOW CONSTANTS OF POLYSTYRENE

Temp., °C.	η_0 poises	k, cm.²/dyne
250	4.72×10^4	0.335×10^{-5}
225	1.32×10^5	0.375
215	2.50×10^5	—
200	4.17×10^5	0.353
185	2.17×10^6	0.346, 0.366
175	3.76×10^6	—
165	1.17×10^7	—
150	8.45×10^7	—
148	1.07×10^8	—
125	1.40×10^9	—
110	9.40×10^9	—

Table I lists typical values of η_0 and k for a polystyrene sample at various temperatures.[14] Table II presents similar information for rubber.[5] From these and numerous similar data it appears that the constant k is relatively independent of temperature. The same conclusion was reached by Ferry[6] for the case of concentrated solutions of polystyrene in xylene. The Newtonian viscosity, however, turns out to be quite sensitive to temperature variations. This temperature-dependence is customarily characterized by the heat of activation for viscous flow, as in equation (3). Typical values for a number of polymers are listed in Table III. It is interesting to note that those polymers which have a tendency to crystallize also have the lowest heats of activation. This seems to be generally the case, and would be compatible with the concept of the activated state as one of a higher degree of order.

TABLE II

INFLUENCE OF TEMPERATURE ON FLOW CONSTANTS OF RUBBER

Temp., °C.	η_0 poises	k, cm.^{2}/dyne
140	1.67×10^6	0.247×10^{-5}
120	2.50×10^6	0.236
100	5.50×10^6	0.270
80	1.37×10^7	0.310
60	2.81×10^7	0.315
50	2.78×10^7	0.238

TABLE III

HEAT OF ACTIVATION FOR VISCOUS FLOW

Polymer	ΔH^*, kcal./mole	Reference
Cellulose acetate–butyrate	78	16
Vinylite VYHH	60	16
Ethylcellulose	40	
Vinylite VYNS	35	16
Polystyrene	23	14
Polyethylene	11	16
Polyisobutylene	10.3	17
Rubber	9.9	

The use of heats of activation implies that log η_0 is a linear function of the reciprocal of the absolute temperature, which may be true only over a limited range of temperature. Spencer and Dillon[14] have reported a change in the apparent heat of activation of polystyrene at about 200°C. The data of Fox and Flory[17] on polystyrene and polyisobutylene suggest that the apparent heat of activation may well vary continuously with the temperature. Whatever the final decision in this matter, the heat of activation will probably still be useful in comparing the relative temperature sensitivities of various materials.

It has been known for some time that polymer molecular weight is an important factor in determining the melt viscosity. Flory[18] originally proposed a linear relationship between log η_0 and the square root of the weight-average chain length on the basis of work with polyesters. This relationship has been used by a number of workers, but later developments have shown that it is not universally applicable. A better representation is given by a power law, with the viscosity proportional to the molecular weight raised to a power between three and four. Polymers that behave in this fashion include polystyrene,[14,17] polyisobutylene,[17] and the higher molecular weight polydimethylsiloxanes.[19]

It is generally assumed that polymer molecular weight does not seriously affect the heat of activation for viscous flow, but this cannot be considered as a well-established fact. It has been reported by Fox and Flory[17] that the form of the viscosity–temperature relationship is independent of molecular weight in the case of polystyrenes only if the molecular weight (number-average) is greater than 25,000. A similar constancy was found for polyisobutylenes of a wide range of molecular weights. These results suggest that ΔH^* is at least not markedly dependent upon molecular weight.

Spencer and Dillon[14] have reported that the constant *k* is independent of molecular weight as well as temperature. Reanalysis of their data, using the Celluloid prototype method, has shown that this is not true. Table IV lists values of *k* for polystyrenes of various molecular weights. It now appears that *k* is directly proportional to the molecular weight, in first approximation. The fluctuations evidenced in this table may be attributed, in part, to variations in the content of very low molecular weight materials. For example, the 170,000 molecular weight polymer is known to contain a relatively larger amount of volatile constituents than the others. This has a tendency to raise the value of *k*, as will be shown shortly.

It is well known that the addition of solvents or plasticizers to polymers

TABLE IV

DEPENDENCE OF *k* UPON MOLECULAR WEIGHT (POLYSTYRENE)

Wt.-av. mol. wt	*k*, cm.²/dyne	*k*/*M*
86,000	0.0571×10^{-5}	0.664×10^{-11}
170,000	0.250	1.47
196,000	0.189	0.964
213,000	0.153	0.718
228,000	0.260	1.14
242,000	0.351	1.45
280,000	0.367	1.31
294,000	0.356	1.21
378,000	0.455	1.20
490,000	0.476	0.971
508,000	0.526	1.04
510,000	0.625	1.23
527,000	0.435	0.825
560,000	0.645	1.15
710,000	0.634	0.893

lowers the melt viscosity. Flory[20] has suggested that the logarithm of the viscosity is a linear function of the square root of the weight fraction of polymer. This relationship holds fairly well in the intermediate concentration region, as illustrated by the work of Spencer and Williams.[21] At relatively lower polymer concentrations Martin's equation gives a better representation of the data. Behavior in the high polymer concentration region also deviates from Flory's equation, and Wiley[22] has observed that the limited data available suggest a linear relationship between log η_0 and the square root of the solvent weight fraction.

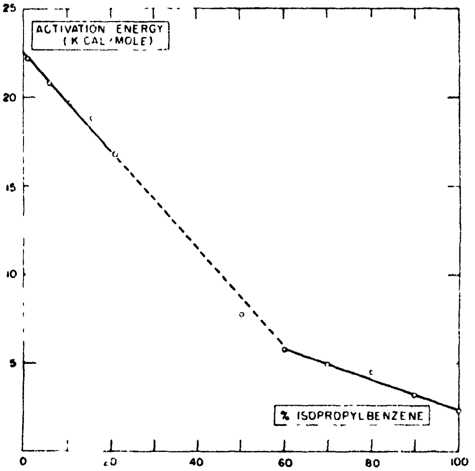

Fig. 5. Dependence of the heat of activation for viscous flow upon solvent content (Spencer and Dillon).

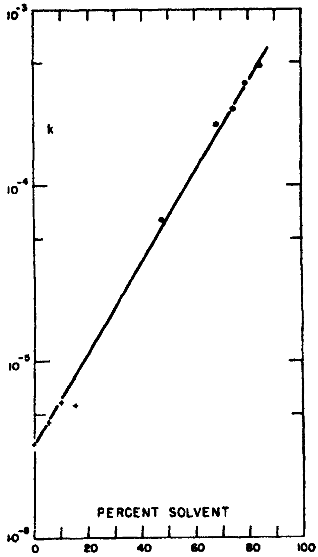

Fig. 6. Dependence of the constant *k* upon solvent content. The circled points are the data of Ferry[6] and the plusses are the data of Spencer and Dillon.[14]

Various workers have observed that the addition of solvent lowers the heat of activation for viscous flow. Little additional comment on this question is required at this point. Figure 5, taken from the paper by Spencer and Dillon,[14] illustrates this effect for the system polystyrene-isopropylbenzene.

It was reported by Spencer and Dillon[14] that the constant *k* increased with the addition of solvent. To this we may now add the observations of Ferry[6] in the more dilute region. In Figure 6 these data are combined to show the dependence of *k* upon solvent content. It is to be noted that the polystyrenes used by both investigators were of comparable molecular weight (about 360,000).

FLOW ORIENTATION PHENOMENA

It has been pointed out that when a hot polymer is sheared the molecules are partially uncoiled and oriented in the direction of flow, provided the molecules are sufficiently flexible. At fabrication temperatures it may frequently happen that the relaxation time is quite short as compared with cooling times. In such a case the molecules will have a tendency to coil back up again as soon as the stress is removed. This has been observed as elastic recovery in coaxial cylinder viscometers, as, for example, by Ferry[6] and Buchdahl.[13] In extrusion through a capillary it manifests as a swelling or "ballooning" of the filaments, as has been reported many times for rubber and for polystyrene.[4]

This ballooning of extruded filaments has been used by Spencer and Dillon[4] to calculate the modulus of high elasticity for polystyrene. They assumed that the average relative length, $\bar{\alpha}$, observed for the filament was the volume average of the microscopic relative lengths, α. That is to say, in capillary flow,

$$\bar{\alpha} = (1/Q) \int_0^R 2\pi r v \alpha \, dr \tag{17}$$

where Q is the volume rate of flow, R is the radius of the capillary, r is the radial distance from the center of the capillary, and v is the velocity of flow at r. It now seems more logical to assume, instead, that the average shear strain, $\bar{\sigma}$, calculated from the ballooning as

$$\bar{\sigma} = \bar{\alpha} - (1/\bar{\alpha})$$

is the volume average of the microscopic shear strains, σ. Thus

$$\bar{\sigma} = (1/Q) \int_0^R 2\pi r v \sigma \, dr \tag{18}$$

If we restrict ourselves to moderately low shearing stresses, we can assume Hookean behavior and write

$$\tau = G\sigma \tag{19}$$

Inserting this in equation (18), we obtain

$$G = P\bar{\rho}/2L\bar{\sigma} \tag{20}$$

where P is the pressure drop, L the length of the capillary, and $\bar{\rho}$ is a sort of effective radius, defined by

$$\bar{\rho} = \int_0^R r^2 v \, dr \Big/ \int_0^R r v \, dr \tag{21}$$

If we use the empirical flow equation (16) to calculate the velocity v, our final result is

$$G = \frac{\tau}{\bar{\sigma}} \frac{2}{3} \frac{\left(\frac{4}{5} + \frac{5}{6} k\tau + \frac{6}{7} \frac{k^2\tau^2}{2!} + \frac{7}{8} \frac{k^3\tau^3}{3!} + \frac{8}{9} \frac{k^4\tau^4}{4!}\right)}{\left(1 + k\tau + \frac{k^2\tau^2}{2!} + \frac{k^3\tau^3}{3!} + \frac{k^4\tau^4}{4!}\right)} \tag{22}$$

where τ is the shearing stress at the capillary wall. The rather involved expression on the right side of the above equation is actually relatively constant in value. It may be shown readily that

$$\lim_{k\tau \rightarrow 0} G = 0.533\tau/\bar{\sigma}$$

and

$$\lim_{k\tau \rightarrow \infty} G = 0.592\tau/\bar{\sigma}$$

Thus little error will be introduced if we were to assume

$$G = 0.56\tau/\bar{\sigma} \tag{23}$$

as a sort of average for the shearing stress range in which we are interested. The data of Spencer and Dillon[4] would then give a value of $G = 2.44 \times 10^5$ dynes/cm.^{2} for 360,000 molecular weight polystyrene.

It has been reported[4] that the modulus of high elasticity of polystyrene is relatively independent of temperature. Ferry[6] has reached a similar conclusion from observations of the elastic recoil of polystyrene solutions. This is at variance with the behavior of things like lightly vulcanized rubber, where both theory and experiment show the modulus to be directly proportional to the absolute temperature. A clue to the reasons for this difference may be found in a paper by Halsey and Eyring.[23] They showed that the presence of steric forces hindering free coiling could lead to a temperature-independent modulus. It is interesting to note in passing that their work indicated that the form of the stress–strain relationship is identical for a variety of partially rubberlike systems, the difference between systems appearing in the modulus.

Ferry[6] has reported a correspondence between the elastic shear strain σ and what amounts to $(5/4)k\tau$ in our nomenclature, for polystyrene solutions in simple shear. Thus $G = 4/5k$ in the moderate shearing stress region. It is interesting to see if this correspondence still holds for bulk polystyrene. If we apply this relationship to the 360,000 molecular weight polystyrene we obtain a value of $G = 2.25 \times 10^5$ dynes/cm.^{2}, which is in good agreement with the value just computed from elastic recovery data. This relationship between G and k fits in well with the behavior of k discussed in the last section. Both quantities are independent of the temperature. Addition of solvent raises k and is known to lower G. The quantity k is roughly proportional to the molecular weight, and it is not at all surprising that G should be inversely proportional to the molecular weight. More will be said on this point in a moment.

Elastic recovery is an important factor in determining the surface characteristics of extruded filaments. This was also pointed out by Mooney[24] for the case of calendered rubber. Spencer and Dillon[14] have observed that raising the shearing stress produces a roughening of the surface, and above a sharply defined value of stress the filaments take on a spiral form. They showed that the point at which spiralling begins corresponds to an isoelongated state in which $\bar{\alpha} = 3$. Application of equation (23) indicates that the microscopic relative extension at the surface of the filament under these conditions is $\alpha = 5$. This is approximately the maximum relative extension possible with polystyrene. The mechanism for spiral formation suggested by Spencer and Dillon was as follows:

> "The orientation in a filament is a maximum at the capillary wall and drops to zero at the center, along with the shearing stress. As the shearing stress is raised the surface eventually attains the maximum elongation possible for polystyrene, and further raising of the shearing stress only forms a thicker skin of polymer at maximum elongation. In this region we have a skin of maximum elongation and a core of constant average elongation, all of the core being oriented less than the skin. The only things that change with shearing stress are the thicknesses of the core and skin. When the filament emerges from the capillary it cannot cool fast enough to prevent recovery of the orientation, under our experimental conditions. The outside skin would like to contract axially more than the less oriented core and thus compresses it. The system is now unstable and the core buckles into a spiral. This may be demonstrated crudely by analogy, by stretching a thin walled rubber tube over a soft solder core and clamping it in the stretched condition. When the force is removed the system will form spirals, segments, etc., depending on the thickness of the rubber tubing and the amount of initial stretch. The similarity between the configurations exhibited by this model and those found in extruded filaments is rather striking."

If, then, spiralling begins at an isoelongated state in which $\bar{\alpha} = 3$ we can apply equation (23) and calculate the modulus from

$$G = 0.21\tau_s$$

where τ_s is the capillary wall shearing stress at spiral inception. Table V shows how the modulus obtained in this manner compares with the modulus calculated from the k value. The sharpness with which the spiral inception point can be defined experimentally suggests that this is a very good method of determining the modulus of high elasticity. The last column in this table reemphasizes the point that the modulus is inversely proportional to the molecular weight.

TABLE V

ELASTIC MODULUS FROM THE SPIRAL INCEPTION POINT

Mol. wt.	$G = {}^{4}/_{5}k$	$G = 0.21\tau_s$	$G \cdot M$ (spiral)
196,000	4.23×10^5	2.96×10^5	5.80×10^{10}
294,000	2.25	2.08	6.12
378,000	1.76	1.52	5.75
508,000	1.52	1.23	6.25
527,000	1.84	1.11	5.83

As might be expected, Spencer and Dillon observed, further, that the modulus calculated from the spiral inception point was independent of the temperature, and decreased with solvent addition.

References

1. H. Eyring, *J. Chem. Phys.*, **4,** 283 (1936).
2. A. V. Tobolsky, R. E. Powell, and H. Eyring, in R. E. Burk and O. Grummitt, *The Chemistry of Large Molecules* (*Frontiers in Chemistry,* Vol. *1*). Interscience, New York, 1943, pp. 125-190.
3. J. H. Greenblatt and D. Fensom, *Ind. Eng. Chem.*, **39,** 1037 (1947).
4. R. S. Spencer and R. E. Dillon, *J. Colloid Sci.*, **3,** 163 (1948).
5. L. R. G. Treloar and D. W. Saunders, *Trans. Inst. Rubber Ind.*, **24,** 92 (1948).
6. J. D. Ferry, *J. Am. Chem. Soc.*, **64,** 1330 (1942).
7. W. Kauzmann and H. Eyring, *J. Am. Chem. Soc.*, **62,** 3113 (1940).
8. S. S. Kistler, *J. Applied Phys.*, **11,** 769 (1940).
9. H. M. Smallwood, *J. Applied Phys.*, **8,** 505 (1937).
10. S. Glasstone, K. J. Laidler, and H. Eyring, *Theory of Rate Processes.* McGraw-Hill, New York, 1941.
11. D. L. Levi, *Trans. Faraday Soc.*, **A42,** 152 (1946).
12. H. M. James and E. Guth, *J Chem. Phys.*, **11,** 455 (1943).
13. R. Buchdahl, *J. Colloid Sci.*, **3,** 87 (1948).
14. R. S. Spencer and R. E. Dillon, *J. Colloid Sci.*, in press.
15. F. R. Mayo and F. M. Lewis, *J. Am. Chem. Soc.*, **66,** 1594 (1944).
16. G. J. Dienes, *J. Colloid Sci.*, **2,** 131 (1947).
17. T. G. Fox and P. J. Flory, *J. Am. Chem. Soc.*, **70,** 2384 (1948).
18. P. J. Flory, *J. Am. Chem. Soc.*, **62,** 1057 (1940).
19. A. J. Barry, *J. Applied Phys.*, **17,** 1020 (1946).
20. P. J. Flory, *J. Phys. Chem.*, **46,** 870 (1942).
21. R. S. Spencer and J. L. Williams, *J Colloid Sci.*, **2,** 117 (1947).
22. R. M. Wiley, The Dow Chemical Company, *private communication.*
23. G. Halsey and H. Eyring, *Textile Research J.*, **15,** (1945).
24. M. Mooney, *J. Colloid Sci.*, **2,** 69 (1947).

English Synopsis, see Summaries, page S11, Vol. V, 1950.

Résumé

Le but principal de cet article était de démontrer l'importance de l'orientation d'écoulement, comme facteur déterminant, sur le comportement des polymères au cisaillement. A la base de l'entière discussion, on fait la supposition implicite que les déviations à la loi de Newton sont attribuables, en ordre principal, à l'orientation d'écoulement, du moins pour les types de polymères étudiés ici. Sur cette base, une nouvelle relation entre la vitesse et la tension de cisaillement a été déduite, et trouvée en accord raisonnable avec les résultats expérimentaux. Utilisant une approximation plus empirique, on a montré que le comportement à l'écoulement d'un polymère est caractérisé par deux quantités, la viscosité Newtonienne (ou fluidité) et le module d'élasticité élevée. L'influence de la température, du poids moléculaire du polymère, de la teneur en émollient sur ces quantités a été montrée par des exemples. Des phénomènes tels que le gonflement et l'enroulement en spirales de filaments, ont été discutés sur cette base.

Zusammenfassung

Das Hauptziel dieser Veröffentlichung war es, die Bedeutung der Fliessungsorientierung als bestimmender Faktor für das Verhalten von Polymeren bei Scherbeanspruchung zu betonen. Die schweigende Voraussetzung für die ganze Diskussion war, dassAbweichungen von dem Newtonschen Gesetz in erster Linie der Fliessungsorientierung zuzuschreiben sind, zu mindestens für den Polymertyp, mit dem wir uns beschäftigen. Auf dieser Grundlage wurde eine neue Abhängigkeit zwischen Schergesch-

windigkeit und Scherdruck abgeleitet und es wurde gefunden, dass sie zufriedenstellend mit experimentellen Tatsachen übereinstimmt. Mehr von der empirischen Seite betrachtet, wurde gezeigt, dass das Fliessungsverhalten eines Polymeren durch zwei Grössen charakterisiert werden kann, die Newtonsche Viskosität (oder Fluidität) und der Hochelastizitätsmodul. Der Einfluss von Temperatur, Polymermolekulargewicht und Weichmachergehalt auf diese Grössen wurde gezeigt. Phänomene wie Aufblähen und Verdrehen von abgestossenen Fasern werden auf dieser Grundlage diskutiert.

Received July 10, 1949

JOURNAL OF POLYMER SCIENCE VOL. V, NO. 5, PAGES 609–614

Refractometric Determination of Second-Order Transition Temperatures in Polymers. V. Determination of the Refractive Indices of Elastomers at Temperatures from 25 to −120°C.*

RICHARD H. WILEY,† G. M. BRAUER, and A. R. BENNETT, *Venable Chemical Laboratory, University of North Carolina*

In previous papers a refractometric method was described for determining second-order transition temperatures of polymers whose transitions occur between 75 and −60°C.[1-4] In the present study, an Abbe refractometer has been insulated and used to determine the refractive indices of polymers down to −120°C. and the transition points of natural rubber and a number of synthetic rubbers.

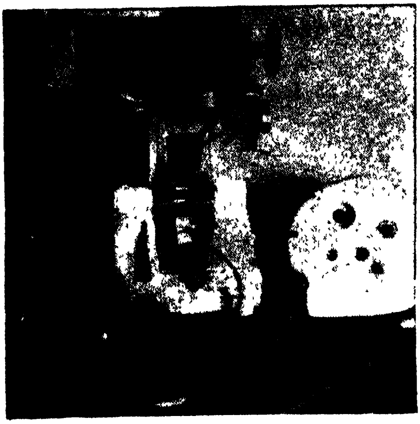

Figure 1

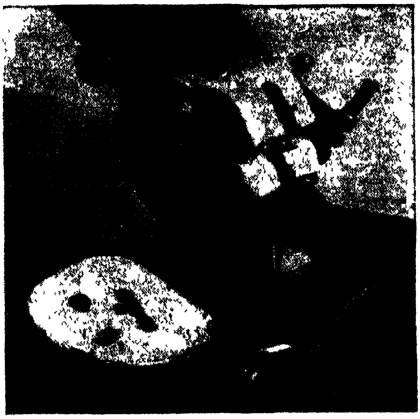

Figure 2

EXPERIMENTAL

Insulation of the Refractometer. The insulation of an Abbe refractometer requires separate coverings for the two prisms to allow opening and closing and a connecting piece to conduct the cooling medium from one jacket to the other when the prisms are closed. The description of the procedure used to insulate the refractometer for this work is described in three parts: (*1*) insulation of the prism jackets, (*2*) construction of the connecting piece, and (*3*) construction of the adapter for the liquid air tank. Figure 1 shows the refractometer with sample mounted prior to closing with the connecting piece unmounted. Figure 2 shows the prism jackets closed with the connecting piece ready to be attached. Figure 3 shows the three parts in position, and Figure 4 shows the entire assembly.

---

* Contribution from the Venable Chemical Laboratory, University of North Carolina.

† Present address: Department of Chemistry, University of Louisville, Louisville 8, Kentucky.

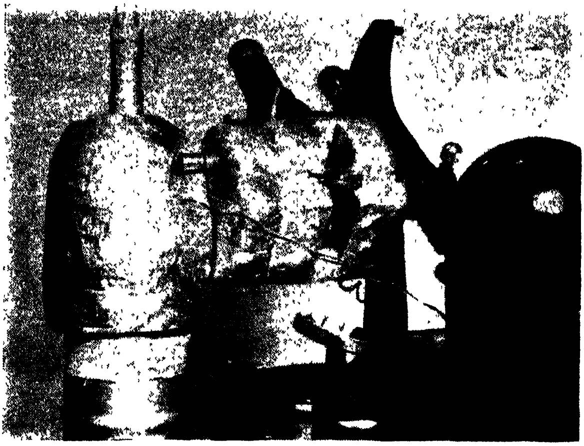

Figure 3

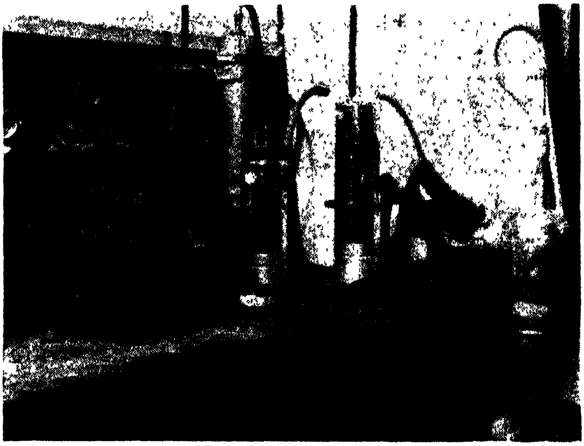

Figure 4

Insulation of the Prism Jackets. The four nipples used as inlet, inter-prism connectors, and outlet for the cooling medium path are removed, machined to accommodate bushings which will extend through the insulation, and replaced. The bushings to fit nipples a, b, and c, and the thermocouple well (e) as shown in Figure 5, are to be mounted in the connecting piece. The bushing for nipple d is put in place. A retainer screw is mounted in a hole drilled and tapped in the prism jacket. This screw reaches through the connecting piece and an attached nut serves to hold this piece in place. The swinging gate covering the upper prism opening is removed. Wooden blocks are cut to fit the necessary openings to the prism and a cardboard baffle placed between the closed prisms. These pieces extend $^3/_4$ inch beyond the surface of the prism jackets and will be removed to leave openings for the light path and to separate the prisms. The insulating material (Insulag) was applied over the entire surface of the prism jackets, except at the hinge, as shown in the figures. The windows were cut from microscope slides and mounted with Vaseline in slits in the insulation after placing a piece of anhydrous calcium chloride in the space to be enclosed.

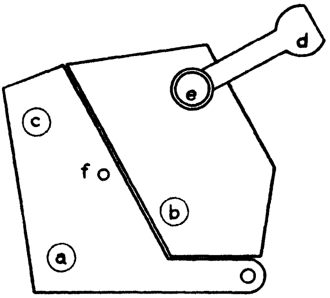

Fig. 5. Side view of prism jackets: (a, b) interprism connections; (c) inlet; (d) outlet; (e) T. C. well; (f) retainer screw.

Connecting Piece. This unit combined the inlet bushing (nipple c), a brass connector to unit nipples a and b, the thermocouple well bushing, and the attaching screw bushing. These units are installed on the refractometer (insulated as in the previous paragraph) while on its side and are held in place with a metal template which fits over the screw bushing and extends to each nipple. Wires were twisted around the bushings to anchor them in the insulation. The insulated face is greased with Vaseline and the units covered with insulation.

Adapter. The adapter is fitted to the top of a standard 15 liter liquid air container and serves to conduct the air stream (used as cooling medium) into the container and out to the refractometer at its inlet bushing. It is an insulated tube with its side opening to fit and turn freely in the refractometer inlet bushing and with its vertical shaft large enough to accommodate a tube which extends down into the liquid air and is connected to the air line.

The grazing incidence technique of Arnold and Wood[5] was used with this refractometer by replacing the lower prism with a brass block of the same shape as the prism except for a slit opening along its face for illumination.

Operation. The air for the cooling medium was taken from a 100-lb. pressure source and reduced and controlled with a diaphragm regulator. The air was passed through a calcium chloride drier and a Dry Ice precooler before introduction at the adapter. The tube extending into the

TABLE I

TRANSITION POINT DATA FOR ELASTOMERS

Polymer	T_m(°C.)[a]	T_m(°C)[b]	T_B(°C.)[c]	$n_D^{25°}$	Δn/°C.[d]	Δn/°C.[e]	Source of Sample[f]
Natural rubber[g].	−75	−73	−58	1.5188	3.6	1.0	RTA
Chloroprene[g]....	−50	—	−38.5	1.5578	3.5	1.0	N
Polybutadiene[g]..	−85	−88	−66	1.5190	4.0	1.8	RRC
GR-S X-387 (22% styrene)[g]......	−67	—	−58	1.5325	3.9	1.1	RRC
GR-S X-387 (extracted)[g,h]	−65	—	—	1.5337	3.8	1.4	RRC
GR-S (25.5% styrene)........	—	−61[i]	—	—	—	—	—
Polybutyl acrylate...........	−63[j]	—	−40	1.4634	3.7	1.1	Fi
GR.I. Y-25 (3% isoprene).....	−75	—	—	1.5081	3.0	0.8	EC
GR.I. Y-15 (2.5% isoprene).......	−79	—	—	1.5080	3.1	0.7	EC
GR.I. R-2 (2% isoprene)	−80	—	—	1.5078	3.1	0.8	EC
Vistanex........	−84	—	—	1.5078	2.8	1.1	EC
Polyisobutylene (M.W. 233,000)	−77	−65	50.2	1.5077	3.1	1.1	F
Polyisobutylene (M.W. 11,000).	−77	−65	50.2	1.5060	3.2	0.8	F
Polyisobutylene (M.W. 4900)..	—	−78	—	—	—	—	—
Polyisobutylene (M.W. 4300)..	−80.5	−78	−45	1.5018	3.0	0.9	F

[a] Refractometric method.

[b] Coefficient of thermal expansion. From the literature.

[c] Brittle point. From the literature.

[d] Above $T_m \times 1000 \pm 0.1$.

[e] Below $T_m \times 1000 \pm 0.1$.

[f] The authors wish to thank the various firms and individuals listed for generously providing the samples: RTA, Rubber Trade Association; N, E. I. du Pont de Nemours & Co.; RRC, Rubber Reserve Co.; Fi, Dr. C. H. Fisher (Eastern Regional Research Laboratory); EC, Enjay Company; F, Dr. P. J. Flory.

[g] Samples milled for 3 minutes.

[h] Extracted small strips of 0.3 g. of milled sample in three 30-ml. portions of 30% by volume solution of toluene in absolute alcohol (ethanol–toluene azeotrope) acidified with HCl at 80°C. Total extraction time 24 hours. Washed, extracted twice with acetone and dried for 12 hours at 100° C. and 2 mm. Pressed the sample (see reference 5).

[i] By heat capacity measurement.

[j] Value previously reported −70°C.[3] This difference in T_m is due to the fact that temperature readings were previously made by a thermocouple placed in the thermometer well of the Abbe refractometer.

liquid air container clogged up if the air was not completely dried but could be replaced quickly. By careful adjustment of the air flow, temperature control of ±0.5°C. from −10 to −120°C. was obtained for 10 to 20 minutes while readings of the refractive index were made. Substantially lower temperatures could be obtained by passing air through a cooling coil immersed in liquid air instead of through the liquid air container, but this method has the disadvantage of poor temperature control and excessive consumption of liquid air. At temperatures below −120°C. the dividing line often becomes indistinct, possibly through loss of contact between the polymer and prism by differential contraction. It is also possible to obtain refractive index values down to −120°C. using the Abbe refractometer without insulation, but again temperature control is difficult and liquid air consumption is increased. The refractive index and transition points agreed regardless of the method of cooling.

The temperatures were measured with a spot welded, flattened copper-constantan thermocouple (L and N, 1938 calibration) which was placed carefully, so as not to scratch the prisms, with the sample between the prisms. The thermocouple was calibrated down to −76°C. by the method of Scott.[6] Temperatures measured in the jacket thermocouple well were always lower than those between the prisms.

Refractive index readings were made most readily by the transmitted light technique, but the method of grazing incidence developed by Arnold and Wood[5] was also used. In the latter method the lower prism was replaced by the brass block previously described and a pressed sample of about 0.02-inch thickness with a sharp, clear-cut edge was placed on the upper prism with the edge cut away from the observer. Both methods gave values for n_D and T_m which agreed within the experimental error of ± 0.0002 in n_D and of ± 2°C. in T_m. The method of grazing incidence has the advantage of (*1*) giving more distinct boundary lines, (*2*) avoiding possible scratching of the prisms, (*3*) easier cleaning of the windows, and (*4*) no error in the n_D value due to finite thickness of sample. However, temperatures below −110°C. could not be reached by this method. The adjustment of light source to obtain a sharp dividing line is much simplified in the observation by transmitted light.

RESULTS AND DISCUSSION

The data for the polymers examined in this study are given in Table I. The second-order transition temperatures determined refractometrically agree with those obtained by the more tedious thermal expansion methods where the data are available for comparison. Several polymers not previously investigated are included in the table. The recorded brittle points are uniformly higher than the transition temperatures.

The data for the fractionated polyisobutylene show little change of transition temperature in the range of 4300 to 233,000 molecular weight. Previous data obtained by Überreiter[7] for polyisobutylene showed a drop from −65°C. for a polyisobutylene of molecular weight 200,000 to −78°C. at 4000 molecular weight. Previous comparisons[3] of fractionated and unfractionated polyethyl acrylates showed the transition temperatures of fractionated samples to be higher than those of unfractionated samples. This is not consistent with an assumption that Uberreiter's samples were unfractionated. In the absence of additional data on the history of Überreiter's samples it is difficult to clarify this discrepancy. Thermal expansion measurements with polyisobutylenes are known to involve difficulties.[8]

Values for the transition temperature of GR-S before and after extraction of antioxidants and other nonhydrocarbon organic impurities, such as soaps and fatty acids, are −67 and −65°C., respectively. These values are within the limits of accuracy and indicate that these ingredients in the commercial polymer do not significantly affect the transition point.

Emphasis in this work has been on relative and not absolute accuracy of n_D readings. No correction was made for the change in the refractive index of the prism itself due to the low temperature. The change of the refractive index of glass is known only in the range of 15 to 100°C. and amounts to 0.65×10^{-5} per degree.[9] It should be smaller at lower temperatures and hence the error introduced is probably only slightly larger than the experimental error. Experiments designed to establish the absolute accuracy of the refractive index values obtained in the Abbe refractometer over the wide temperature range used for the first time in this study are being conducted. This problem is complicated by the fact that there are no primary standards available for direct calibration experiments.

This work was completed under Contract N7onr-284, Task Order III between the University of North Carolina and the Office of Naval Research, Navy Department, as part of project NR 054 079. This support is gratefully acknowledged by the authors and the University.

References

1. R. H. Wiley, *J. Polymer Sci.*, **2**, 10 (1947).
2. R. H. Wiley and G. M. Brauer, *ibid.*, **3**, 455 (1948).
3. R. H. Wiley and G. M. Brauer, *ibid.*, **3**, 647 (1948).
4. R. H. Wiley and G. M. Brauer, *ibid.*, **3**, 704 (1948).
5. Arnold and Wood, *Natl. Bur. Standards, Tech. Repl.* (1949). We are indebted to Dr. Wood of the National Bureau of Standards for valuable suggestions for the use of the method of grazing incidence.
6. Scott, *J. Research Natl. Bur. Standards*, **25**, 459 (1940).
7. Uberreiter, *Kolloid-Z.*, **102**, 272 (1943).
8. Ferry and Parks, *J. Chem. Phys.*, **4**, 283 (1936).
9. A. V. Grosse, *J. Am. Chem. Soc.*, **59**, 2739 (1937).

English Synopsis, see Summaries, page S12, Vol. V, 1950.

Résumé

Les variations de l'indice de réfraction en fonction de la température, jusqu'à −120°C., sont données pour une série de polymères analogues au caoutchouc, qui présentent un point de transition de second ordre à des températures, inférieures à −60°C. Ces résultats indiquent une variation de tangente qui situe la température de transition. Une technique d'isolement du réfractomètre standard de Abbe et un système de refroidissement de celui-ci à l'air froid pour faciliter les opérations jusqu'à −120° sont décrites.

Zusammenfassung

Refraktionsindex-Temperaturdaten bis zu −120°C. herab werden für eine Reihe von kautschukähnlichen Polymeren Berichtet, welche Transitionen zweiter Ordnung bei einer Temperatur unter −60° haben. Diese Daten zeigen eine Änderung der Neigung, die die Transitionstemperatur festlegt. Eine Methode zur Wärme-Isolierung des Standard Abbé-Refraktometers und zur Kühlung mit gekühlter Luft, um das Arbeiten bis zu −120°C. herab zu ermöglichen, wird beschrieben.

Received July 11, 1949

JOURNAL OF POLYMER SCIENCE VOL. V, NO. 5, PAGES 615–632

Depolymerization as a Chain Reaction

ROBERT SIMHA and L. A. WALL, *National Bureau of Standards, Washington, D. C.*, and P. J. BLATZ, *The Catholic University of America, Washington, D. C.*

I. INTRODUCTION

Several experimental and theoretical investigations of the kinetics of depolymerization reactions are to be found in the literature. Older experimental work dealt mostly with the chemical attack of cellulose, starches, and other materials. These processes are step reactions and the various theoretical approaches were formulated accordingly.[1,2] In principle, the kinetics of the homogeneous, stepwise degradation appears solved for any dependence of the rate constants on chain length and position of susceptible bonds. The experiments mentioned indicate that the splitting occurs in the main at random with, at the most, a special position occupied by the terminal bonds. During the last few years earlier work on the thermal decomposition of polymers[3–5] has been extended in several laboratories. The change of molecular weight and the size distribution have been examined[6,7] and the volatile products analyzed.[8,9] The results vary widely with the chemical nature of the system. In general, they do not correspond to random splitting. The amount of monomer is larger and the decrease of molecular weight, where measured, smaller than would follow from such a mechanism. At first sight one might attribute this to preferential production of monomer from the chain ends in a stepwise fashion, a case which has been treated previously.[1] However, no quantitative agreement is obtained. Furthermore, on general grounds and considering the evidence presented by the decomposition of hydrocarbons of low molecular weight, one is led to assume that the cracking is a chain process, characterized by at least an initiation, propagation, and termination and, very likely, also transfer. Consequently, the equations previously derived are not immediately applicable. It will be shown later that they represent special cases of the general results for chain reactions.

In this paper a chain process is treated. The assumed reaction scheme may not completely cover all possibilities, since it has been somewhat simplified to facilitate the mechanics of solution of the rate equations. It should, nevertheless, provide an adequate basis for future treatments of depolymerization reactions of the chain type.

The final result can be stated as follows. If and as long as a steady state in respect to the depolymerizing radicals exists, the course of the chain reaction is approximately equivalent to that of a step reaction. The effective rate constants of this step process depend on the position of the bond to be broken.

In section II the reaction scheme is discussed and the corresponding rate equations are given. Section III contains the derivation of the radical distribution and the final rate equations. In the fourth section the solution is obtained and special cases are considered.

II. REACTION SCHEME

The steps of the free radical mechanism are presumably analogous to those in polymerization. Transfer should be relatively more important because of the high temperatures involved. We consider the following set of reactions:

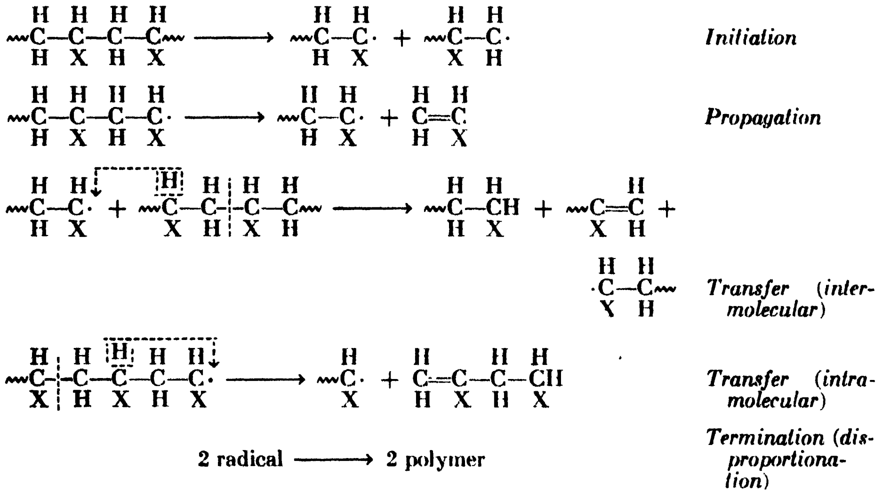
Initiation
Propagation
Transfer (intermolecular)
Transfer (intramolecular)
2 radical ⟶ 2 polymer
Termination (disproportionation)

Initiation is very likely due to several causes such as thermal effects, catalyst fragments, chemically incorporated oxygen, and weak bonds produced in the termination step of the polymerization reaction. Although the initiation is probably a composite of all the above factors, we have limited our treatment to the cases of random and terminal initiation, respectively. Any differences in reactivity between different types of radicals will be disregarded. Propagation is taken to be the reverse of growth, and radicals are envisioned to be the same as in polymerization.[10] A radical may be stabilized by transferring its activity to a stable molecule which decomposes into two fragments, one of them a radical, the other a stable chain. Transfer is presumed to consist in the abstraction of a hydrogen from another molecule. It is also likely that a radical can react with a hydrogen from its own chain, the most probable positions of attack being from the third to the seventh carbon atoms adjacent to the radical end.

Since this step is probably the distinguishing feature in the chain degradation of different systems, a discussion of the factors involved is desirable. Competition between the two types of transfer can widely alter the nature of the degradation process. In the intramolecular kind, local coiling plays a role. Hence, steric effects are important. This can be seen in the case of dienes, although here the unsaturation in the chain is a more favored locus of attack than a hydrogen atom. Copolymers of various dienes with styrene produce relatively more diene monomer and less dimer because of the isolation of the diene unit. This would indicate that a large fraction of the measured dimer is derived from adjacent units. It is also found that the relative amounts of the monomer of butadiene, isoprene, 2,3-dimethylbutadiene, and 2-methyl-1,3-pentadiene increase in this order on pyrolysis of the simple polymers.[9] It will be noted that the extent of steric hindrance which opposes coiling follows the same sequence and reduces the probability of forming larger than monomeric species.

Similarly in vinyl polymers intramolecular transfer may produce dimer and trimer unless steric factors interfere. In the mathematical analysis intramolecular transfer will be regarded as a special case of propagation. The term *transfer* will be restricted to the reaction between radicals and other polymer molecules.

Transfer and termination both increase the number of molecule ends present. These favor the ultimate production of nonmonomeric volatile material. Thus, the monomer yield obtained should be a measure of the kinetic chain length. In addition there appears to be a qualitative correlation between the monomer yields and the probability of transfer as deduced from the structure of the polymer. At least two factors need to be considered, the reactivity of the radicals and the presence of susceptible hydrogen atoms along the polymer chain. Hydrogens attached to a substituted carbon, such as the tertiary one on the phenyl-substituted carbon in polystyrene, are known to be readily attacked. If these hydrogens are replaced by methyl groups we find polymers which degrade rather cleanly into original monomer, *e.g.*, polymethyl methacrylate, and polyisobutene.[9] The methyl group presumably also renders the radical less active. The phenyl group apparently stabilizes the styrene radical to such an extent that a good monomer yield is obtained although reactive hydrogens are present. This group may also sterically impede the transfer process. Transfer should, however, be less prevalent in polymethyl methacrylate than in polystyrene. Where transfer appears probable because of the reasons cited, such as in polymethylacrylate and polyethylene,[9] very low yields of original monomer are obtained. Polytetrafluoroethylene, where the tightly held fluorine atoms make transfer unlikely, decomposes almost totally into monomer.[11]

In order to facilitate the mathematical treatment, disproportionation has been assumed to be the only termination step.

Based on the general reaction scheme just described, it is possible to formulate the following mathematical representation. In what follows, P_n denotes the number of stable polymer molecules with n carbon atoms, as well as the general type molecule of that weight. P_N is the original polymer, $P_N(0)$ its concentration at time zero. Since we are here considering units of two carbon atoms, P_2 is the monomer. Correspondingly, radical sizes and concentration are denoted by R_n. The four general steps of the reaction scheme are then:

$$\left.\begin{array}{ll}
\textit{Initiation:} & \\
\qquad P_n \xrightarrow{k_1} R_i + R_{n-i} \text{ or } P_n \xrightarrow{k_1} R_{n-2} + R_2 & \\
 & 2 \leqq i \leqq n-2 \\
\textit{Propagation:} & \\
\qquad R_n \xrightarrow{k_2} R_{n-2} + P_2 & \\
\textit{Transfer:} & \\
\qquad R_i + P_n \xrightarrow{k_3} P_i + R_j + P_{n-j} & 2 \leqq j \leqq n-2 \\
 & 4 \leqq n \leqq N \\
\textit{Termination:} & \\
\qquad R_i + R_n \xrightarrow{k_4} P_i + P_n &
\end{array}\right\} \qquad (1)$$

No distinction has been made between radicals created by initiation and transfer. There are three types of stable molecules that can participate in the transfer process, namely, those having either double bonds or saturated carbon atoms at both ends or one of each at either end. There are three different numbers of possible transferable hydrogens, *viz.*, $n-4$, $n-3$, and $n-2$, respectively, for the molecule with two double bonds, one double bond with the other end saturated, and finally two saturated carbons. An average value, $n-3$, will be used. Equation (1) leads to the following rate equations:

$$dR_{N-2}/dt = (2k_1 + k_3R)P_N - \left[k_2 + k_4R + k_3 \sum_4^N (i-3)P_i\right]R_{N-2}$$

$$dR_{N-3}/dt = (2k_1 + k_3R) \sum_{N-1}^N P_i - \left[k_2 + k_4R + k_3 \sum_4^N (i-3)P_i\right]R_{N-3}$$

$$dR_n/dt = (2k_1 + k_3R) \sum_{n+2}^N P_i + k_2R_{n+2} -$$

$$\left[k_2 + k_4R + k_3 \sum_4^N (i-3)P_i\right] R_n \qquad 4 \leqq n \leqq N-4$$

$$dR_3/dt = (2k_1 + k_3R) \sum_5^N P_i + k_2R_5 - \left[k_4R + k_3 \sum_4^N (i-3)P_i\right]R_3$$

$$dR_2/dt = (2k_1 + k_3R) \sum_4^N P_i + k_2R_4 - \left[k_4R + k_3 \sum_4^N (i-3)\, P_i\right]R_2$$

(1a)

$$
\begin{aligned}
dP_N/dt &= -(N-3)(k_1+k_3R)P_N \\
dP_{N-1}/dt &= -(N-4)(k_1+k_3R)P_{N-1} \\
dP_n/dt &= -(n-3)(k_1+k_3R)P_n + k_4RR_n + k_3\sum^{N}(i-3)P_i\cdot R_n + \\
&\qquad k_3R\sum_{n+2}P_i \qquad 3 \leqq n \leqq N-2 \\
dP_2/dt &= k_2\sum_{4}^{N-2}R_i + \left[k_4R + k_3\sum_{4}^{N}(i-3)P_i\right]R_2 + k_3R\sum_{4}^{N}P_i
\end{aligned}
$$

R denotes the total number of radicals. In the alternative assumption for the initiation step the sums in the k_1 expressions reduce to their first term. Summation of the radical equations leads to the auxiliary relation:

$$dR/dt = 2k_1\sum_{i=4}^{N}(i-3)P_i - k_4R^2 \tag{2}$$

Equation (1a) represents a nonlinear set in the P_i's and R_i's for which no analytic solution can be given. We shall confine ourselves to a situation in which a steady state concentration of radicals is maintained. This is not realized at the very start of the reaction and on approaching completion. The "induction" period, *i.e.*, the time necessary to reach initially a steady state may be estimated by integrating equation (2). Here the first term may be considered to be nearly constant, since N is large, and equal to $2k_1NP_N(0)$. Hence:

$$R(t) \doteq \left[\frac{2k_1}{k_4}NP_N(0)\right]^{1/2}\frac{e^{t/\lambda}-1}{e^{t/\lambda}+1}$$

with

$$2\lambda = [2k_1k_4NP_N(0)]^{-1/2} = 1/k_4R$$

where R now indicates the steady state value:

$$R = \left[\frac{2k_1}{k_4}NP_N(0)\right]^{1/2} \tag{3}$$

Since the duration of the over-all reaction is inversely proportional to the initial constant k_1, the familiar condition for the maintenance of a steady state results, *viz.*

$$k_1/k_4R \ll 1$$

III. THE RATE EQUATIONS

The approximation introduced transforms the differential equations for the radical species into difference equations:

$$dR_n/dt = dR/dt = 0$$

In view of equations (2) and (3) we define the quantities:

$$\alpha = k_2 + k_4R + (k_3k_4/2k_1)R^2 \qquad (4)$$

$$f(n) = (2k_1 + k_3R) \sum_n^N P_i$$

and obtain the following set of relations from equation (1a):

$$\begin{aligned} \alpha R_{N-2} &= f(N) \\ \alpha R_{N-3} &= f(N-1) \\ \alpha R_n - k_2R_{n+2} &= f(n+2) \qquad 4 \leqq n \leqq N-4 \qquad (5) \\ (\alpha - k_2)R_3 - k_2R_5 &= f(5) \\ (\alpha - k_2)R_2 - k_2R_4 &= f(4) \end{aligned}$$

Assuming N to be odd, the solution is:

$$\begin{aligned} R_n &= \frac{1}{\alpha} \sum_{i=0}^{(N-n-3)/2} \left(\frac{k_2}{\alpha}\right)^i f(n+2i+2) \qquad n \text{ even}; \quad 4 \leqq n \leqq N-3 \\ R_n &= \frac{1}{\alpha} \sum_{i=0}^{(N-n-2)/2} \left(\frac{k_2}{\alpha}\right)^i f(n+2i+2) \qquad n \text{ odd}; \quad 5 \leqq n \leqq N-2 \\ R_2 &= \frac{1}{(\alpha - k_2)} \sum_{i=0}^{(N-5)/2} \left(\frac{k_2}{\alpha}\right)^i f(4+2i) \qquad (6) \\ R_3 &= \frac{1}{(\alpha - k_2)} \sum_{i=0}^{(N-5)/2} \left(\frac{k_2}{\alpha}\right)^i f(5+2i) \end{aligned}$$

The physical significance of this result is apparent. k_2/α is the probability of reducing the size of a radical by one monomer unit. Each term in the sum measures the probability of producing a specified radical from an aggregate containing molecules of a given minimum size.

In order to avoid in the final result the distinction between even and odd species, we combine two radicals of successive size, n and $(n + 1)$. Doing the same for the stable polymer, we define

$$Q_n = P_n + P_{n+1} \qquad (7)$$

and set

$$P_n \doteq Q_n/2$$

This introduces an appreciable error only when n is close to N. Next the radical distribution is expressed in terms of stable polymer by means of equations (4) and (7). If n now signifies an even number, one finds by straightforward evaluation of the sums:

$$R_n + R_{n+1} = \frac{(2k_1 + k_3R)}{(\alpha - k_2)} \cdot 2 \sum_{i=0}^{(N-n-3)/2} \left[1 - \frac{\alpha + 3k_2}{4\alpha}\left(\frac{k_2}{\alpha}\right)^i\right] Q_{n+2i+2}$$

$$R_2 + R_3 = \frac{\alpha(2k_1 + k_3R)}{(\alpha - k_2)} \cdot 2 \sum_{i=0}^{(N-5)/2)} \left[1 - \frac{\alpha + 3k_2}{4\alpha}\left(\frac{k_2}{\alpha}\right)^i\right] Q_{4+2i} \tag{6a}$$

It will be noted that the factor in each bracket is approximately equal to:

$$\left(1 - \frac{k_2}{\alpha}\right)\left[1 + \frac{k_2}{\alpha} + \left(\frac{k_2}{\alpha}\right)^2 + \ldots \left(\frac{k_2}{\alpha}\right)^{i-1}\right] \text{if } k_2 \doteq \alpha$$

This in turn is proportional to the total number of ways in which a combination $R_n + R_{n+1}$ can be produced by initiating a species Q_{n+2i+2} and then degrading it to a size n. The differential equations (1a) can now be rewritten by means of equation (6a). Replacing $(n - 3)P_n + (n - 2)P_{n+1}$ by $(n - 3)Q_n$ one finds the final rate equations:

$$\frac{dQ_{N-1}}{dt} = -A_{N-1}Q_{N-1}$$

$$\frac{dQ_n}{dt} = -A_nQ_n + 2\left(K_0 - \frac{k_3R}{4}\right)Q_{n+2} + 2\sum_{i=1}^{(N-n-3)/2} K_iQ_{n+2i+2} \qquad 4 \leqq n \leqq N - 3 \tag{1b}$$

$$\frac{dQ_2}{dt} = k_2R + 2\left(\bar{K}_0 - \frac{k_3R}{4}\right)Q_4 + 2\sum_{i=1}^{(N-5)/2} \bar{K}_iQ_{4+2i}$$

with:

$$A_n = (k_1 + k_3R)(n - 3)$$

$$K_i = (2k_1 + k_3R)\left[1 - \frac{\alpha + 3k_2}{4\alpha}\left(\frac{k_2}{\alpha}\right)^i\right] + k_3R$$

$$\bar{K}_i = -\frac{\alpha(2k_1 - \alpha)}{(\alpha - k_2)^2} \cdot (2k_1 + k_3R)\left[1 - \frac{\alpha + 3k_2}{4\alpha}\left(\frac{k_2}{\alpha}\right)^i\right] + k_3R$$

Here n assumes only even values. Equation (1b) represents approximately a step reaction of the general type treated previously.[1]* The deg-

---

* There is no strict equivalence, as can be seen by inspection of the general rate equations for steplike degradation, eq. (1), of reference 1. If the rate constants are independent of chain length, a certain relationship must obviously exist between the coefficients of the negative and positive terms. It expresses the fact that molecules decompose in the same fashion in which they are produced from their parents. If eq. (1b) were to conform to this pattern, the following relation would be required to hold:

$$A_n = K_0 - (k_3R/4) + \sum_{i=1}^{(n-5)/2} K_i$$

This is fulfilled apart from terms which are negligible for large n, if k_2/α is small. Otherwise a given species is produced by initiation and subsequent propagation, termination, and/or transfer from its parents, while it is annihilated by initiation and transfer.

radation constants K_i depend in a specific manner on the position of the link to be broken. Since by definition $k_2/\alpha < 1$, bonds in the interior of a given chain are split more readily than those nearer the end. This is, of course, not an effect due to changes in bond strength or other energetic factors. The actual constants of the chain reaction have been assumed here to be independent of chain length or position within the chain. The nonrandomness effectively occurring is a purely statistical effect, as discussed above in connection with equation (6a). This effect should be kept in mind when weak spots are postulated in order to interpret kinetic results.

It is r[illegible]ily shown that, if initiation of the molecule ends prevails, decomposit[illegible] near the ends will be more frequent.

.V. SOLUTION OF RATE EQUATIONS

The solution of the system (1b) has been previously given.[1] It has the form:

$$Q_n(t) = \sum_{l=n}^{N-1} h_l a_{nl} e^{-A_l t} \qquad 4 \leqq n \leqq N-1; \quad l \text{ even} \qquad (8)$$

The h_l are determined by the initial conditions. The constants a_{nl} vanish for $n > l$. For the remainder one has the following linear system:

$$(A_j - A_l)a_{jl} = 2K_{(l-j-2)/2}\, a_{ll} + 2\left(K_0 - \frac{k_3R}{4}\right) a_{j+2,l} + 2\sum_{i=0}^{(l-j-6)/2} K_{i+1} a_{j+4+2i,l} \qquad (9)$$

Equations (8) and (9) represent the complete solution of the system (1b). From (9) one obtains all a_{jl}, $j < l$, in terms of a_{ll}. For large values of l and $j \ll l$, one may consider the corresponding integral equation of the infinite set. For our purposes, however, a different analysis is preferable. The important parameter is the number average kinetic chain length,

$$1/\epsilon = \alpha/(\alpha - k_2)$$

If $1/\epsilon$ is small in comparison with the degree of polymerization, the chain length of the degraded molecule will be largely determined by the position of the initial point of attack. This condition should be approached when transfer is an important factor. Although the actual process may still be quite different, it will tend toward the limiting case of random degradation. A relatively broad size distribution results. The randomizing effect of transfer is also apparent from the definition of the K_i's, equation (1b), where it is represented by a term k_3R independent of i. On the other hand, the average kinetic chain length may be large. Then small molecules and monomer will be preferentially formed and the measurable molecular weight will not be very much affected. Equation ([illegible] generally valid and successive approximations along either of the tw[illegible] [illegible]en[illegible]med can be obtained. The zero approximation correspon[illegible] ti[illegible] to random breaking has been discussed in previous work. In the specific cases of interest here it is apparently not realized except possibly in polyethylene.[12] The detailed analysis for random initiation will be limited to the case $\epsilon N/2 < 1$. In the absence of transfer this leads to an extreme distribution, consisting mostly of original material and very small species. The transfer reaction will modify this pattern and cause the appearance of intermediate sizes, mainly through the polymer initially present because of the large kinetic chain length.

The solution of the set of equations (9) can be expanded in a power series:

$$\frac{a_{jl}}{a_{ll}} = \epsilon\zeta_1^{(l)}(j) + \epsilon^2\zeta_2^{(l)}(j) + \ldots \tag{10}$$

The K_i's can be similarly expanded and a recurrence relation between $\zeta_1^{(l)}, \zeta_2^{(l)} \ldots$ etc. established. One finds, if $k_3 = 0$:

$$\begin{aligned} -(l-j)[\zeta_1^{(l)}(j) + \epsilon\zeta_2^{(l)}(j) + \ldots] &= 2(l-j) - 1 - \\ &\epsilon\frac{(l-j-2)}{2}(l-j-1) + \ldots + \\ &\epsilon\sum_{i=0}^{(l-j-4)/2}[4i+3-\epsilon i(2i+1)+\ldots]\cdot[\zeta_1^{(l)}(j+2+2i) + \\ &\epsilon\zeta_2^{(l)}(j+2+2i) + \ldots] \end{aligned} \tag{9a}$$

Neglecting terms of higher than second order in ϵ, the result is:

$$(l-j)\zeta_1^{(l)}(j) = -[2(l-j)-1]; \quad (l-j)\zeta_2^{(l)}(j) =$$

$$\frac{(l-j-2)(l-j-1)}{2} + \sum_{i=0}^{(l-j-4)/2}(4i+3)\frac{2(l-j-2)-4i-1}{(l-j-2-2i)}$$

The sum can be immediately evaluated in terms of the ψ function

$$\psi(n) + C = \sum_{i=1}^{n} 1/i$$

where C, the Euler-Mascheroni constant, has the value 0.57722. For large values of the argument the following expansion is valid:

$$\psi(n) = \ln n + \frac{1}{2n} + O\left(\frac{1}{n^2}\right)$$

This leads to:

$$\zeta_1^{(l)}(j) = -\left(2 - \frac{1}{l-j}\right); \quad \zeta_2^{(l)}(j) = \frac{l-j-2}{2}\left(3 - \frac{1}{l-j}\right) -$$

$$\left[1 - \frac{1}{2(l-j)}\right]\left[C + \psi\left(\frac{(l-j-2)}{2}\right)\right] \tag{11}$$

By means of relations [illegible] and (11) all $h_l a_{jl}$, $j \neq l$, can be expressed in terms of $h_l a_{ll}$ [illegible] condition it will be assumed that $Q_n(l = 0) =$

0, $n \neq N - 1$, $Q_{N-1}(t = 0) = Q_{N-1}(0)$. The introduction of an initial molecular weight distribution complicates the formulas without producing anything fundamentally new. If an appreciable amount of low molecular weight material is present to start with, it will tend to keep the average molecular weight constant, since it is more likely to be completely degraded than the larger molecules in the distribution. From equation (8) one has:

$$Q_n(0) = 0 = \sum_{l=n}^{N-1} h_l a_{nl}; \quad h_{N-1}a_{N-1,N-1} = Q_{N-1}(0)$$

By means of equation (11) one obtains, neglecting cubic and higher terms in ϵ:

$$\begin{aligned} h_n a_{nn} &= \left(2 - \frac{1}{N-n-1}\right) \epsilon Q_{N-1}(0) + \epsilon^2 g(n) Q_{N-1}(0) \\ h_l a_{nl} &= -\left(2 - \frac{1}{l-n}\right)\left(2 - \frac{1}{N-l-1}\right) \epsilon^2 Q_{N-1}(0) \end{aligned} \qquad (12)$$

$$g(n) = \sum_{l=n+2}^{N-3} \left(2 - \frac{1}{l-n}\right)\left(2 - \frac{1}{N-l-1}\right) - \frac{1}{2}\left(1 - \frac{2}{N-n-1}\right) \times [3(N-n-1) - 1] + \left[1 - \frac{1}{2(N-n-1)}\right] \times \left[C + \psi\left(\frac{N-n-3}{2}\right)\right]$$

The expression for $g(n)$ can be simplified, since N is a large number. For $n \approx N$ or $l \approx N$ each factor in the sum approaches the value 3/2, while for $n \ll N$, it is 2 or 3/2, depending on the value of l. Neglecting ln $(N - n)$ in comparison with $(N - n)/2$, that is for $(N - n) > 100$, the factor may be replaced by 4. Similar approximations are made in the other terms. The final result for the molecular weight distribution as a function of the reduced time $\tau = k_1 t$ is:

$$\frac{Q_n(\tau)}{Q_{N-1}(0)} = \epsilon e^{3\tau}\left(2 - \frac{1}{N-n-1}\right)[e^{-n\tau} - e^{-(N-1)\tau}] - \epsilon^2 e^{3\tau}\left\{\left[\frac{4e^{-2\tau}}{1-e^{-2\tau}} - \frac{N-n-3}{2}\right] e^{-n\tau} - \left[\frac{4}{1-e^{-2\tau}} + \frac{3}{2}(N-n-3)\right] e^{-(N-1)\tau}\right\}; \quad 4 \leq n \leq N-3 \qquad (8a)$$

$$\frac{Q_{N-1}(\tau)}{Q_{N-1}(0)} = e^{3\tau} e^{-(N-1)\tau}$$

and, neglecting the radicals present:

$$2Q_2(\tau) = (N-1)Q_{N-1}(0) - \sum_{4}^{N-1} nQ_n(\tau)$$

For the relative number average molecular weight excluding monomer we obtain up to linear terms in ϵ:

$$\frac{\bar{M}_n(\tau)}{\bar{M}(0)} = \frac{1 + 2\epsilon\left[\frac{e^{(N-1)\tau}}{(N-1)} \sum_4^{N-3} ne^{-n\tau} - \frac{(N+1)(N-5)}{4(N-1)}\right]}{1 + 2\epsilon\left[e^{(N-1)\tau} \sum_4^{N-3} e^{-n\tau} - \frac{(N-5)}{2}\right]} \tag{13}$$

with:

$$\sum_4^{N-3} e^{-n\tau} = \frac{e^{-4\tau}}{1 - e^{-2\tau}} [1 - e^{-(N-5)\tau}];$$

$$\sum_4^{N-3} ne^{-n\tau} = \frac{2e^{-4\tau}(2 - e^{-2\tau}) - e^{-(N-1)\tau}[(N-1) - (N-3)e^{-2\tau}]}{(1 - e^{-2\tau})^2}$$

To a given value of τ there corresponds a degree of conversion:

$$1 - \sum_4^{N-1} \frac{nQ_n(\tau)}{(N-1)Q_{N-1}(0)} = 1 - e^{-(N-1)\tau} e^{3\tau} \times \left\{1 + 2\epsilon\left[\frac{e^{(N-1)\tau}}{(N-1)} \sum_4^{N-3} ne^{-n\tau} - \frac{(N+1)(N-5)}{4(N-1)}\right]\right\} \tag{14}$$

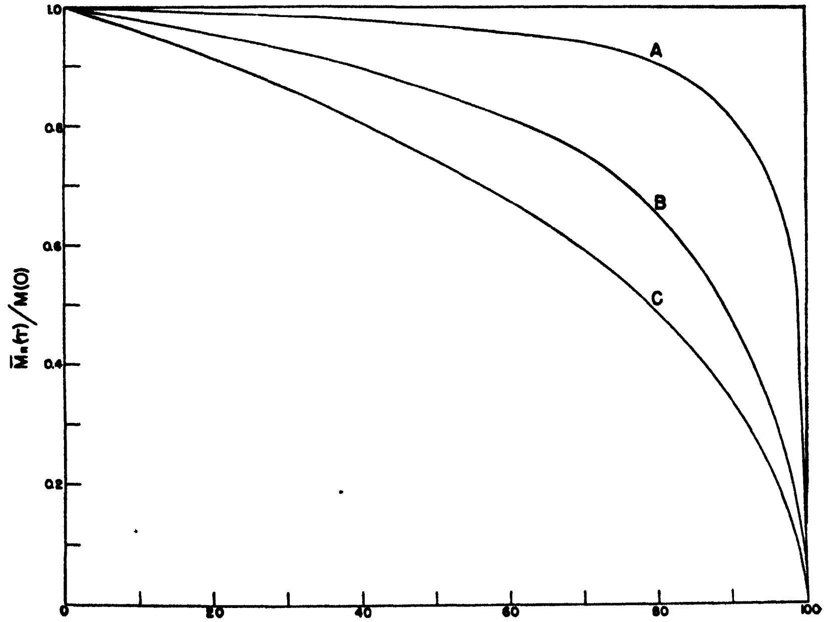

Fig. 1. Change of molecular weight ratio with extent of reaction, equations (13) and (14), for various values of the kinetic chain length $1/\epsilon$: (A) $N = 1000$, $\epsilon = 10^{-4}$; (B) $N = 1000$, $\epsilon = 5 \times 10^{-4}$; (C) $N = 1000$, $\epsilon = 10^{-3}$. The plot for $N = 500$, $\epsilon = 10^{-3}$, practically coincides with curve B.

Figure 1 shows plots of the change in molecular weight for various values of the ratio between initial degree of polymerization and kinetic chain length. For the largest value of ϵ used, the linear approximation, equation (13), is no longer sufficient, and the curve has been included only in order to show the trend. As is to be expected, the molecular weight of the residue remains practically constant to higher degrees of conversion for larger values of the kinetic chain length. In the summation (13) all species upward from four carbon atoms have been included. Had a higher limit been chosen in correspondence with the actual experimental possibilities, the molecular weight of the residue would have remained unchanged over even longer degrees of conversion.

These results permit a rough estimate of the orders of magnitude of the rate constants when the kinetic chain length is large. For the values of ϵ assumed, the reaction is complete at $\tau = 10^{-2}$ according to equation (14). In most experiments this corresponds to about one hour. Hence, $k_1 = 10^{-5}$ sec.$^{-1}$. An induction period of one minute gives $k_4R = 10^{-2}$ sec.$^{-1}$, and k_2 of the order of 10 sec. $^{-1}$. Lower values of the induction period lead to higher estimates of the propagation constant.

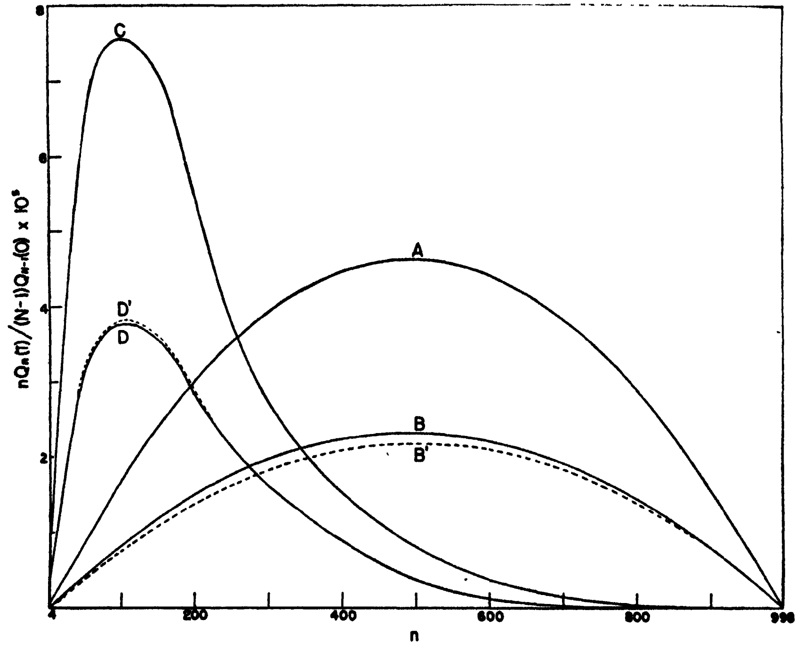

Fig. 2. Molecular weight distribution, equation (8a), at early and late stages of the reaction: (A) $N = 1000$, $\epsilon = 10^{-4}$, 9% conversion; (B) $N = 1000$, $\epsilon = 5 \times 10^{-4}$, 9% conversion, first approximation in respect to ϵ; (B′) same as in B, second approximation in respect to ϵ; (C) $N = 1000$, $\epsilon = 10^{-4}$, 99.9% conversion; (D) $N = 1000$, $\epsilon = 5 \times 10^{-4}$, 99.5% conversion, first approximation in respect to ϵ; (D′) same as in D, second approximation in respect to ϵ. Ordinate scale for curves A and C should be divided by ten.

In Figure 2 the molecular weight distribution of the reaction products is plotted for various degrees of conversion. It is seen that the second approximation, *i.e.*, larger values of ϵ, favors smaller chain lengths at the later stages of the reaction. Equation (8a) indicates that in the first approximation all small molecules are produced from the original material Q_{N-1} only. When the kinetic chain length is reduced intermediate products also give shorter species.

Finally we indicate briefly the results for the case in which initiation occurs at the chain ends only. The concentration of radicals then depends on the total number of polymer molecules as is seen by the modification of equation (2). Consequently, we would expect the steady state approximation to be less satisfactory than previously. Proceeding as before, one has the following system of rate equations when chain transfer is unimportant:

$$\frac{dQ_{N-1}}{dt} = -\, 2k_1 Q_{N-1}$$

$$\frac{dQ_n}{dt} = -2k_1 Q_n + 2k_1\epsilon \sum_{i=0}^{(N-n-3)/2} \left(\frac{k_2}{\alpha}\right)^i Q_{n+2i+2} \qquad 4 \leqq n \leqq N-3 \quad (1b')$$

$$\frac{dQ_2}{dt} = k_2 R - 2k_1 \frac{(2k_2 - \alpha)}{(\alpha - k_2)} \sum_{i=0}^{(N-5)/2} \left(\frac{k_2}{\alpha}\right)^i Q_{4+2i}$$

Thus, as indicated previously, bonds near the chain ends are preferentially broken. The solution of this system no longer consists of a sum of exponentials, but has the form:

$$Q_n(\tau) = Q_{N-1}(0)e^{-\tau} \left(\frac{k_2}{\alpha}\right)^{(N-n-3)/2} \sum_{i=0}^{(N-n-3)/2} \binom{\frac{N-n-3}{2}}{i} \left(\frac{k_2}{\alpha}\right)^{-i} \frac{(\epsilon\tau)^{i+1}}{(i+1)!} \qquad (8')$$

with $\tau = 2k_1 t$. For small values of ϵ this reduces to:

$$\frac{Q_n(\tau)}{Q_{N-1}(0)} = \epsilon\tau e^{-\tau} - \epsilon^2 \frac{(N-n-3)}{2}\left(\tau - \frac{\tau^2}{2}\right) e^{-\tau};$$

$$\frac{Q_{N-1}(\tau)}{Q_{N-1}(0)} = e^{-\tau} \qquad (8a')$$

The relative number average molecular weight of the mixture excluding monomer is given by the equation:

$$\frac{\bar{M}_n(\tau)}{M(0)} = \frac{1 + \epsilon\tau \dfrac{(N+1)(N-5)}{4(N-1)} - \epsilon^2\left(\tau - \dfrac{\tau^2}{2}\right)\dfrac{(N-7)(N-5)(N+3)}{24(N-1)}}{1 + \epsilon\tau \dfrac{N-5}{2} - \epsilon^2\left(\tau - \dfrac{\tau^2}{2}\right)\dfrac{(N-5)(N-7)}{8}} \qquad (13')$$

The degree of conversion is obtained by multiplying the numerator of equation (13′) by $e^{-\tau}$ and subtracting from unity. If the critical factor ϵN is very small, the molecular weight distribution, equation (8a′), is independent of n, all sizes between the original one and the monomer being equally frequent. Hence, for large times, when the concentration of initial polymer is negligible, the average molecular weight tends toward half the original value. In a second approximation, and for values of $\tau < 2$, large chains are slightly preponderant. Toward the end of the reaction, however, the situation is reversed. This occurs at about 80 percent conversion for the values of N and ϵ used here. Equation (13′) contains the first terms of an expansion in τ and hence is not valid in the limit $\tau \rightarrow \infty$.

The pertinent constants are readily evaluated from equation (13′). The reduced time τ_c necessary to produce a measurable decrease δ in the molecular weight ratio obeys the equation:

$$\tau_c = 4\delta/(1 - 2\delta)$$

in a first approximation. In practice one has $\delta \geq 0.1$. The data on a sample of methyl methacrylate with $M = 94{,}000$, $N = 1880^7$ indicate a decrease of 10 per cent in molecular weight at a conversion of about 40 percent. Equation (13′) then yields $\epsilon \approx 4 \times 10^{-4}$.

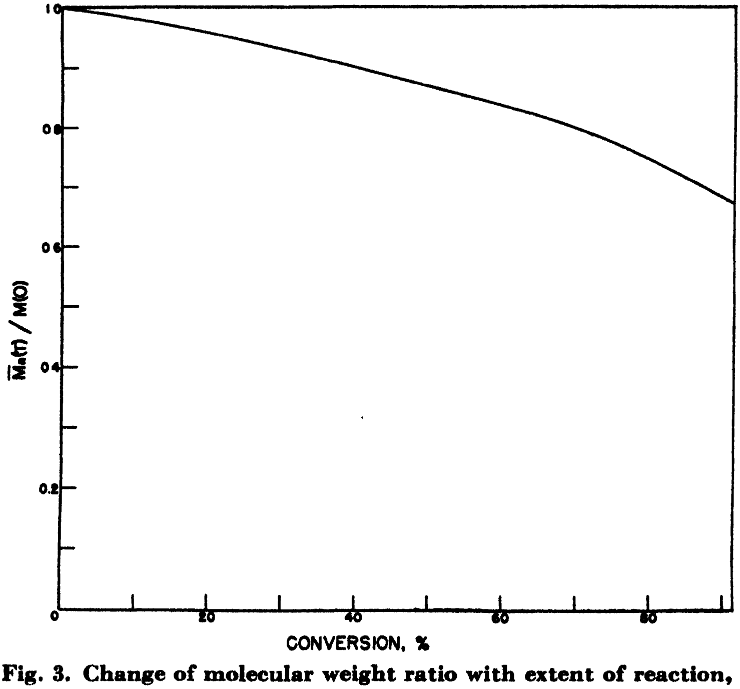

Fig. 3. Change of molecular weight ratio with extent of reaction, equation (13′): $N = 1000$, $\epsilon = 5 \times 10^{-4}$.

Figure 3 shows a plot of equation (13′). The trend of the curve is the same as in Figure 1. In the opposite limit of small kinetic chain length,

$1/\epsilon \ll N$, equation (8′) is to be expanded in powers of k_2/α. It has already been remarked that the zero-order approximation is equivalent to a practically random step reaction, if the points of initial attack are distributed along the whole chain. If they are situated only at the chain ends, the reaction corresponds to a stepwise splitting of terminal bonds. Actually, in the limit of small k_2/α, (8′) reduces to:

$$\frac{Q_n(\tau)}{Q_{N-1}(0)} = e^{-\tau}\,\frac{\tau^{(N-n-1)/2}}{\left(\dfrac{N-n-1}{2}\right)!} \times$$

$$\left\{1 + \frac{k_2}{\alpha}\,\frac{1}{\tau}\,\frac{N-n-1}{2}\left(\frac{N-n-3}{2} - \tau\right) + \right.$$

$$\left(\frac{k_2}{\alpha}\right)^2 \frac{1}{\tau^2}\,\frac{(N-n-1)(N-n-3)}{8}\left[\frac{(N-n-3)(N-n-5)}{4} - \right.$$

$$\left.\left.(N-n-3)\,\tau + \tau^2\right] + \ldots\right\} \qquad (8'')$$

The first term of this series has been derived previously in the treatment of stepwise degradation and expressions for the molecular weight have been presented.[1]

The over-all rate, r, of the reaction is found by differentiation of equation (14) and the corresponding expression following from equation (13′), respectively. The limiting values are:

$$\lim_{\tau\to 0}\frac{r}{k_1} = \begin{cases} N(1 - \epsilon N/6) & \text{initiation random} \\ \;\;1 - \epsilon N/4 & \text{'' \quad at ends} \end{cases} \qquad (15)$$

The first term in each equation represents the production of monomer from the initial material, the second is due to the presence of intermediate species.

V. DISCUSSION

The kinetic chain lengths are best derived from molecular weight data, as shown above in the case of methyl methacrylate. The analysis of cases intermediate between the extremes of very short and very large kinetic chain length including transfer requires a further examination of equations (8′) and (9). In the absence of intramolecular transfer, the molar ratio between monomer and all other degraded material after the completion of the reaction is determined by the relative probabilities of propagation and intermolecular transfer, that is according to (4) by:

$$p = k_2\left(\frac{k_3k_4R^2}{2k_1}\right)^{-1}$$

By definition:

$$1/\epsilon = 1 + p\left(1 + \frac{k_4}{k_2}\,p\right)^{-1}$$

This gives an inverse correlation between monomer yield and molecular weight drop, since a small value of p corresponds to a small value of the kinetic chain length $1/\epsilon$, unless k_4/k_2 is very large. Furthermore, if transfer is frequent, the ratio between monomer and other volatile products should decrease as the total number of molecules capable of transfer tends towards a maximum with increasing conversion.

The available analyses show the following results for the monomer ratios:[8,9,12] ethylene 0.005, styrene 1.87, isobutene 2.04, methyl methacrylate greater than 100. Actually, here p ought to be of the order of 2.5×10^3 according to our previous estimate of ϵ. Consequently the upper estimates for the kinetic chain lengths assuming $p(k_4/k_2) \ll 1$ would be 1.005, 2.9, 3.0 for the first three substances. Thus ethylene should degrade by a practically random process and exhibit the sharp initial drop in molecular weight characteristic for such reactions, while the relative decrease of molecular weight at a given conversion should be less for styrene and isobutene. No data sufficient to decide this point have come to our attention. In respect to the variations of the nature of the volatiles with conversion, the results so far obtained do not seem conclusive.

Intramolecular transfer due to local convolutions will have two tendencies, namely, to reduce the rate of decrease of D. P. and to keep the nature of the volatile products more nearly constant, as compared with the effect of intermolecular transfer. In sufficiently large chains, long range coiling can also lead to transfer which would tend to reduce the molecular weight but maintain the constancy of the products.

In applying the preceding results to experimental data certain limitations are encountered. The reaction has been assumed to be homogeneous. It may occur, however, at the surface of the material or at the part in contact with the furnace. Also in comparing the relative yields of monomer for different materials, differences in vapor pressure ought to be kept in mind. If the reacting unit is small and has a small cohesive energy density, the volatile products will contain fragments of larger degree of polymerization than in the opposite case.

The numerical calculations were carried out by Mrs. Helen H. Jeppson.

References

1. See, for instance, R. Simha, *J. Applied Phys.*, **12**, 569 (1941), where also references to the prior literature are given.

2. L. G. Sillén, *Svensk Kem. Tid.*, **55**, 221 (1943). R. F. Tuckett, *Trans. Faraday Soc.*, **41**, 351 (1945).

3. T. Midgley and A. L. Henne, *J. Am. Chem. Soc.*, **51**, 1215 (1929). See also F. O. Rice and K. K. Rice, *The Aliphatic Free Radicals*, Johns Hopkins Press, Baltimore, 1935.

4. H. Staudinger and A. Steinhofer, *Ann.*, **517**, 35 (1935).

5. G. S. Whitby, *Trans. Faraday Soc.*, **32**, 315 (1936).

6. H. H. G. Jellinek, *J. Polymer Sci.*, **3**, 850 (1948); **4**, 1, 13 (1949).

7. N. Grassie and H. W. Melville, Discussions of the Faraday Society, "The Labile Molecule," 1947, p. 378.

8. S. L. Madorsky and S. Straus, *J. Research Natl. Bur. Standards*, **40**, 417 (1948). S. L. Madorsky, S. Straus, D. Thompson, and L. Williamson, *ibid.*, **42**, 499 (1949).

9. L. A. Wall, *J. Research Natl. Bur. Standards*, **41**, 315 (1948).
10. H. S. Taylor and A. V. Tobolsky, *J. Am. Chem. Soc.*, **61**, 2063 (1945).
11. E. E. Lewis and M. A. Naylor, *J. Am. Chem. Soc.*, **69**, 1968 (1947).
12. S. L. Madorsky, *Science*, in press.

English Synopsis, see Summaries, page S12, Vol. V, 1950.

Résumé

La cinétique des réactions de dépolymérisation par mécanisme en chaîne est développée en supposant une initiation, suivie de réactions de propagation, de transfert et de terminaison des radicaux. La propagation produit des radicaux plus petits et des molécules de monomères. Le transfert stabilise un radical déterminé et en produit un nouveau qui, à son tour, se décompose en un radical plus petit et une chaîne stable. On suppose que la terminaison se passe exclusivement par disproportionnement. Un tel schéma entraine le résultat suivant: Dans le cas où, et aussi longtemps qu'il existe en état stationaire des radicaux, l'allure de la réaction, c'est à dire la production d'espèces moléculaires plus petites et stables aux dépens du matériel de départ, est approximativment égale à celle prévue pour une réaction par étapes successives du type traité antérieurement. Les constantes des vitesses effectives de cette réaction équivalente sont fonction des constantes d'initiation et de transfert, de la concentration des radicaux et de la longueur de chaîne cinétique. De plus, elles dépendent de la position de la liaison qui devra être rompue, bien que, à priori, on ne suppose pas de dépendance des processus élémentaires en fonction de la position au sein de la molécule (liaisons labiles) ou en fonction de la grandeur de la molécule. L'effet est purement statistique. Si le radical peut être initié tout le long de la molécule de polymère, les liaisons à l'intérieur de l'édifice sont effectivement brisées plus facilement que celles aux extrémités. Si l'initiation peut se passer uniquement aux liaisons terminales, la situation est renversée. Cette tendance sélective est contrariée par la réaction de transfert, qui exerce une influence statistique à côté d'une augmentation réelle de la probabilité d'initiation pour chaque molécule. La solution générale est donnée, et discutée en fonction de la longueur de la chaîne cinétique. Si celle-ci est très petite en comparaison du degré de polymérisation initial, l'allure de la réaction est déterminée par l'initiation et le transfert. Un tel cas peut être réalisé approximativement si le transfert est important. Si l'initiation se passe n'importe où, la conséquence sera une dégradation purement statistique. Le cas de l'initiation aux extrémités ramène le cas à une scission graduelle d'unités monomériques terminales. D'autre part, lorsque la longueur de chaîne est plus grande que le degré de polymérisation, les molécules petites sont produits de préférence. La distribution des grandeurs moléculaires et le poids moléculaire moyen sont indiqués en fonction du degré de conversion. Les valeurs de la longueur de chaîne cinétique et de la constante d'initiation sont évaluées.

Zusammenfassung

Die Kinetik von Depolymerisationsreaktionen vom Kettentypus wird entwickelt, indem eine Aktivierung von Radikalen vorausgesetzt wird, die von Fortpflanzung, Übertragung und Abbruch gefolgt, wird. Die Fortpflanzung erzeugt kleinere Radikale und Monomer-Moleküle. Die Übertragung stabilisiert ein gegebenes Radikal und erzeugt ein anderes, das sich weiterhin in ein kleineres Radikal und eine stabile Kette zersetzt. Es wird vorausgesetzt, dass Termination ausschliesslich durch Disproportionierung eintritt. Dieses Schema führt zu folgendem Resultat: Wenn und so lange als eine stationäre Konzentration von Radikalen beibehalten wird, ist der Reaktionsverlauf, das heisst die Erzeugung von kleineren stabilen Arten aus dem ursprünglichen Material ungefähr gleich dem, der bei einer Stufenreaktion von dem früher behandelten Typus vorausgesagt wurde. Die effektiven Geschwindigkeitskonstanten dieser equivalenten Reaktion sind eine Funktion der Initiation und Übertragungskonstanten, der

Radikalkonzentration und der kinetischen Kettenlänge. Sie sind weiterhin abhängig von der Lage der zu spaltenden Bindung, trotzdem a priori keine Abhängigkeit der wirklichen Geschwindigkeitsprozesse von der Lage im Molekül (schwache Bindungen) oder der Grösse des Moleküls angenommen wird. Der Effekt ist rein statistisch. Wenn ein Radikal überall in einem Polymermolekül initiiert werden kann, werden Bindungen im Inneren erheblich bereitwilliger gespalten als solche nahe den Enden. Wenn die Aktivierung nur an den endständigen Bindungen eintreten kann, ist die Situation umgekehrt. Dieser selektiven Tendenz setzt sich eine Übertragungsreaktion entgegen, welche abgesehen davon, dass sie die Wahrscheinlichkeit der Initiation für ein gegebenes Molekül erheblich erhöht, eine regellose Wirkung ausübt. Die allgemeine Lösung wird gegeben und diskutiert in Beziehung zu der kinetischen Kettenlänge. Wenn diese im Vergleich zum anfänglichen Polymerisationsgrad sehr klein ist, wird der Reaktionslauf durch die Initiation und die Übertragung bestimmt. Eine Annäherung an diesen Fall mag bestehen, wenn letztere sehr stark ist. Wenn Initiation regellos entlang der Kette auftritt, führt das Resultat im Grenzfalle zu einer stufenweisen Abspaltung der End-Monomeren. Wenn anderseits die Kettenlänge grösser ist als der Polymerisationsgrad, werden vorzugsweise kleine Moleküle erzeugt. Die molekulare Grössenverteilung und das mittlere Molekulargewicht werden als eine Funktion des Umsatzgrades dargestellt. Schätzungen der Werte der kinetischen Kettenlänge und der Initiationskonstanten werden gegeben.

Received July 15, 1949

JOURNAL OF POLYMER SCIENCE VOL. V, NO. 5, PAGES 633–638

LETTERS TO THE EDITORS

Intrinsic Viscosity of Macromolecules

Peterlin,[1] in a recent paper, proposed the following formula, to describe the intrinsic viscosity of a linear macromolecule:

$$[\eta] = \frac{\pi a_0 A_0^2}{4M_0} N \left(\frac{1}{1 + 1.2(6/\pi)^{1/2} a_0/A_0 N^{1/2}} \right) \tag{1}$$

where A_0, a_0, and M_0 are the effective length, hydrodynamical radius, and molecular weight of the statistical element, such that the number of statistical elements N and the degree of polymerization Z, are related through $N = Z/\zeta$. Furthermore, he pointed out that the above form gives results which are in essential agreement with those of Debye and Bueche,[2] and Kirkwood and Riseman.[3]

We would like, in this note, to indicate the relationship between Peterlin's formula,[1] equation (1), and that of Kirkwood and Riseman.[3]

$$[\eta] = \frac{N\zeta b^2}{3600\eta_0 M_0} Z F(\lambda_0 Z^{1/2})$$

$$F(\lambda_0 Z^{1/2}) = \frac{6}{\pi^2} \sum_{k=1}^{\infty} \frac{1}{k^2(1 + (\lambda_0 Z^{1/2})k^{-1/2})} \tag{2}$$

$$\lambda_0 = \frac{\zeta}{(6\pi^3)^{1/2}\eta_0 b}$$

If the sum defining $F(\lambda_0 Z^{1/2})$ is replaced by its first term, equation (2) becomes in this approximation:

$$[\eta] = \frac{N\zeta b^2}{3600\eta_0 M_0} Z \frac{6}{\pi^2} \left\{ \frac{1}{1 + (\zeta/\pi(6\pi)^{1/2}\eta_0 b)Z^{1/2}} \right\} \tag{2a}$$

identical in form with Peterlin's equation (1). If, furthermore, the above analysis were carried out in terms of statistical elements such that we could identify b with A_0 and let $\zeta = 6\pi\eta_0 a_0$ we would obtain, in Peterlin's notation:

$$[\eta] = \frac{1}{\pi} \frac{A_0^2 a_0}{M_0} N \left[\frac{1}{1 + (6/\pi)^{1/2}(a_0/A_0)N^{1/2}} \right] \tag{2b}$$

where the quantity in brackets differs from that of Peterlin by a factor of 1 compared to 1.2, and the coefficients of this quantity differ by a factor of $1/\pi$ compared to $\pi/4$. Peterlin has indicated that a numerical coefficient 0.52 is preferred to the 1.2.

In this connection, it is interesting to note that Wilson[4] has proposed an empirical equation of form similar to that of Peterlin, namely:

$$[\eta] = \frac{K_1 Z}{1 + K_2 Z^{1/2}} \tag{3}$$

where K_1 and K_2 are constants. He also points out that $F(\lambda_0 Z^{1/2})$ can be reasonably well approximated by the term $(1 + 0.76\lambda_0 Z^{1/2})^{-1}$.

If the Peterlin, Wilson and the Kirkwood-Riseman expressions are compared the following can be noted.

(*a*) Wilson's expression is an empirical summation of the infinite sum appearing in $F(\lambda_0 Z^{1/2})$ and approximates that quantity fairly well. The exponent α of the curve $[\eta] = KZ^{\alpha}$, tangent to the log-log plot of $[\eta]$ *vs.* Z at a particular value Z likewise compares reasonably well with the full Kirkwood-Riseman expression.

(*b*) Peterlin's expression, with the factor 1.2 almost amounts to using only the first term in the Kirkwood-Riseman theory. Comparison of Peterlin's results with the full $F(\lambda_0 Z^{1/2})$ as well as with the approximate expression using only the first term of the sum, denoted by $F_0(\lambda_0 Z^{1/2})$, and normalized so that $F_0(0) = 1$ is shown in Table I. It should be noted that the Peterlin expression can again almost be regarded as an approximate summation of the infinite sum in $F(\lambda_0 Z^{1/2})$, the summation with the factors 1.2 or 0.52 not comparing as well with the Kirkwood-Riseman expression as does that of Wilson.

(*c*) Both the Peterlin and Wilson expressions can consequently be regarded as approximate forms of the Kirkwood-Riseman expression, eq. (2).

TABLE I

x	$F(x)$	$F_0(x)$ (normalized)	$\frac{1}{1 + 1.2x}$	$\frac{1}{1 + 0.52x}$
0	1.0	1.0	1.0	1.0
0.1	0.925	0.906	0.893	0.05
0.2	0.861	0.833	0.806	0.905
0.5	0.717	0.667	0.625	0.793
1.0	0.564	0.500	0.454	0.658
1.5	0.467	0.400	0.357	0.562
2.0	0.400	0.332	0.294	0.491
3.0	0.312	0.250	0.218	0.391
4.0	0.256	0.199	0.172	0.325
5.0	0.218	0.166	0.145	0.278
10	0.216	0.083	0.077	0.161
20	0.07	0.048	0.040	0.087

References

1. A. Peterlin, *J. Polymer Sci.*, **5,** 473 (1950).
2. P. Debye and A. M. Bueche, *J. Chem. Phys.*, **16,** 573 (1948).
3. J. G. Kirkwood and J. Riseman, *J. Chem. Phys.*, **16,** 565 (1948).
4. J. N. Wilson, *J. Chem. Phys.*, **17,** 217 (1949).

International Resistance Company
Philadelphia, Pennsylvania

JACOB RISEMAN

Institute of Polymer Research
Polytechnic Institute of Brooklyn
Brooklyn, New York

FREDERICK R. EIRICH

Received May 10, 1950

Degradation of Ethyl Cellulose in Solution

In a recent letter, Jellinek[1] has given the relation:

$$-\ln\left(1 - \frac{1}{P_n}\right) = kt - \ln\left(1 - \frac{1}{P_0}\right)$$

to relate the degree of polymerization (P_n) to the time (t) in a chain degradation process. In the case in which P_n is large, the equation may be further approximated to the form:

$$\frac{1}{P_n} - \frac{1}{P_0} = kt$$

This relation should apply approximately to any polymer in which long chain molecules are being broken up by a continuous process of random fracture. At present it would seem that there are not too many systems in which this process may be experimentally investigated. I therefore thought it might be a good idea to publish certain results which I obtained some years ago on the acid-catalyzed degradation of Hercules "N" type ethyl dissolved in aqueous ethanol, (10% water, hydrochloric acid). It was then found that a plot of the reciprocal of an inherent viscosity (g./100 cc. basis)[2] was accurately linear with time, as would be expected if this viscosity was proportional to the molecular weight. At the time, this work was not published as it was decided not to put forward any such rela-

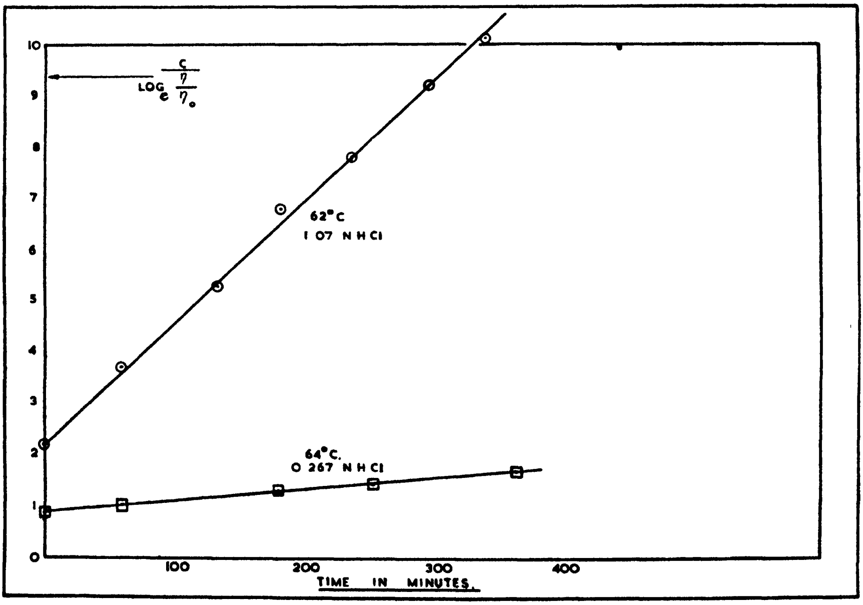

Figure 1

tion on a purely viscosity basis. However, in view of Jellinek's letter, I think the results, which are shown in Figure 1, might prove interesting. At any rate, they may serve to call the attention of workers in the field to a system which appears to be rather well fitted for experimental work on degradation processes.

The experiments were carried out by the writer at Colmore Adhesives Ltd., Team Valley Trading Estate, Gateshead-on-Tyne 11, as part of their research program. I am indebted to the directors of this company for permission to publish.

References

1. H. H. G. Jellinek, *J. Polymer Sci.*, **5**, 264 (1950).
2. L. Cragg, *J. Colloid Sci.*, **1**, 261 (1946).

R. N. Haward

Research Laboratories, Petrocarbon Ltd.
Twining Road, Trafford Park
Manchester 17, England

Received July 15, 1950

REVIEWS

Elastomers and Plastomers—Their Chemistry, Physics, and Technology. R. Houwink, ed., Vol. I, General Theory. Elsevier, New York-Amsterdam, 1950, 509 pp., $7.00.

This volume is a very welcome addition to the literature on high polymers. It is to be hoped that the two remaining volumes of the series will come up to the high standard set by the first.

In the first chapter H. A. Frank surveys the economic aspects of plastics, giving production and consumption data for various types. These are necessarily restricted largely to the United States, since but few figures were available for other countries at the time of writing. C. Koningsberger, in Chapter 2, gives the chemical composition of the more common natural and synthetic macromolecular substances and discusses the organic chemistry of the reactions by which the latter are formed. Wechsler, Hohenstein, and Mark next give an excellent and thorough treatment (108 pages) of reaction kinetics and the mechanism of polyreactions. G. H. van Amerongen contributes four chapters, on "Molecular Constitution," "Mechanical Properties," "Physics and Structure," and "Polymer-Liquid Interaction." The last-named is especially noteworthy, dealing with polymer solution theory and its application to solubility, swelling, osmotic pressure, light scattering, and viscosity data. The dielectric properties of high polymeric materials are ably discussed by L. Hartshorn. Mechanical operations in the plastics industry are treated by H. Gibello. In the final chapter R. S. Colborne presents a useful discussion of the theory and technology of plasticizers.

M. L. Huggins

Outlines of Biochemistry. R. A. Gortner, 3rd edition edited by R. A. Gortner, Jr., and W. A. Gortner, Wiley, New York, 1949, 1078 pp., $7.50.

The revision of this well-known text was carried out by a group composed mainly of the late Professor Gortner's former colleagues and students under the editorial leadership of his sons.

This edition, like the previous editions, places emphasis on the view that "much of the 'vital energy' can in the last analysis be traced back to energies characteristic of surface films and interfaces." The viewpoint is also taken that a thorough understanding of the materials of biochemistry is essential to the study of this field. Consequently, the emphasis is on bio*chemistry*. The physiological integration of the systems discussed is largely left to other texts. In the area set off by these considerations the book is unique and strikingly successful.

About one-quarter of the text is devoted to colloids, one-quarter to proteins, another to carbohydrates and the remainder to lipids, plant pigments, and biochemical regulators.

The section on colloids, revised by H. B. Bull and D. R. Briggs, provides an excellent introduction to this field. Discussions of hydrogen ion concentration and oxidation-reduction systems are included in this section.

W. M. Sandstrom and R. A. Gortner, Jr., revised the section on proteins and a new chapter on protein denaturation was contributed by H. B. Bull. The material in this section provides a good description of the behavior of these natural polymers. In the reviewer's opinion, however, the point is not sufficiently emphasized that certain well-characterized proteins behave as pure substances whose properties can be studied at the molecular level. It now seems clear that Sorensen's hypothesis of reversible-dissociable-components applies to complex naturally occurring mixtures, but not to single proteins. Further, too little emphasis is given the fact that the greater part of the titration curves of proteins can be correlated stoichiometrically with chemical composition.

The chapters on the chemistry of the carbohydrates were revised and expanded by W. F. Geddes. P. D. Boyer, J. J. Willaman, and S. I. Aronovsky contributed chapters on carbohydrate metabolism, pectic substances, and the tannins, respectively. The entire section is admirably executed.

The discussion of the chemistry of the lipids has been expanded and revised by W. A. Gortner. G. O. Burr revised the section on plant pigments, and W. A. Gortner, R. A. Gortner, Jr., and W. M. Sandstrom revised the chapters on vitamins, hormones, and enzymes, respectively.

The editorial difficulties of revising a book with a large group of collaborators have resulted in the inclusion of few references subsequent to 1946. The style, to the editors' great credit, is as fresh as was that of earlier editions. Since no other single volume contains such a wide variety of information on the organic and physical chemistry of naturally occurring substances, this book will be widely used by students in these fields.

George W. Schwert

Electron Microscopy—Technique and Applications. Ralph W. G. Wyckoff, Interscience, New York, 1949, 258 pp., $5.00.

The author states that this book was written "with the frank and limited purpose of pointing out and arousing interest in the possibilities of using the electron microscope to learn more about the hitherto unseen world it penetrates." In accomplishing this, he necessarily reviews the history and different types of electron microscopes. One of the ten chapters was devoted to the critical adjustment of the instrumentwhich is obviously required for high quality work. Specimen preparation has been stressed and detailed descriptions of different methods of preparing specimens were discussed.

No attempt was made to list all the applications of the electron microscope, and attention was concentrated on those which, at one time or another, had been of actual concern to the author. These many applications are illustrated with electron micrographs that have been made by him or his laboratory staff. The 202 illustrations are of the highest quality and have been reproduced remarkably well, which should serve as a guide for others. With each illustration is a complete caption which notes pertinent information and points of interest. However, most of the pictures are of a biological nature. The incompleteness of this book is supplemented by an extensive bibliography at the end of each chapter. These references are an excellent source of more complete information to the student and research worker.

The practical information in this publication makes it an ideal reference book for active workers in the field. In addition. it will serve as an excellent text to introduce a technician to the field of electron microscopy.

E. B. Bradford
R. F. Boyer

Les Dérivés Chimiques du Caoutchouc Naturel. F. Le Bras and A. Delalande, Dunod, Paris, 1949, 510 pp., 1,880 frs.

The seven chapters of the book give a comprehensive survey of the chemistry and technology of the chemical derivatives of natural rubber:

I. Generalities on the origin, the structure, and chemical properties of rubber (30 pp.).
II. Halogenated derivatives (116 pp.).
III. Hydrohalogenated derivatives (67 pp.).
IV. Hydrogenated rubber. Decomposition products of rubber and hydrogenated rubber (23 pp.).
V. Oxidized derivatives (69 pp.).
VI. Cyclized derivatives (94 pp.).
VII. Various derivatives and modified rubber (50 pp.).
Conclusions (1 p.).
Addresses of companies manufacturing chemical derivatives of rubber (in) England, the United States (and) France (1 p.).
Index (33 pp.).

It is an unusually complete work and a valuable source of information on an important subject. With the exception of Chapter One essentially the same pattern is followed throughout the book: The chemistry of the subject, manufacture (if such is done), properties and uses, the latter being replaced by "possible uses" in certain cases. The chemistry is discussed historically and thus the evolution of the ideas on the reactions of rubber with various agents appear. Regrettably the authors refrain from any editorial criticism and thus create the undoubtedly false impression that they do not have any opinion on the subject. Also, little attempt is made to speculate editorially or otherwise on the reasons why structural alterations of the molecule manifest themselves in changes of physical properties, although frequent mention is made and numerous references are given on structure examination (for example, six entries on x-ray studies).

The technological discussions are thorough and adequate, well illustrated by photographs and schematic drawings of machinery. The reference list is enormous, over 1400 entries were counted. Similarly the authors leave little to the imagination about the uses of the products discussed. On page 190, for example, a most appetizing looking bunch of celery (incidentally wrapped in Pliofilm) is shown.

George Goldfinger

JOURNAL OF POLYMER SCIENCE VOL. V, NO. 6, PAGES 639–652

Chlorination of Natural Rubber. I. Preparation and Properties of Chlorinated Rubber*

G. J. VAN AMERONGEN, C. KONINGSBERGER, and G. SALOMON,
Rubber Foundation, Delft, The Netherlands

INTRODUCTION

The chlorination of rubber has been the subject of extensive investigations,[1-5] the rubber being commonly treated in solution with gaseous chlorine at a given temperature and pressure. The properties of the products of rubber thus treated vary in close dependence upon the chlorine content, which may be as much as 70%. The drawback to a low chlorine content is that, as a rule, the chlorine is loosely bound, with the result that, when exposed to heat or light, it splits off as HCl with the formation of discolored and cyclized products and serious deterioration of the mechanical properties. But the higher the chlorine content, the more stable are these chlorinated rubbers. The stability of chlorinated products of natural rubber containing approximately 65% of chlorine is such that they are used commercially as a component of anticorrosive paint.

The instability of chlorinated rubber of low chlorine content is closely connected with its chemical constitution and the mechanism of reaction. The current opinion ten years ago[1] was that chlorine first adds on to the double bond of the rubber and that this primary product, while splitting off HCl, enters into further reaction with chlorine; but reexamination of this reaction in the laboratory of our affiliated English organization[3,4] and independently in our own laboratory has led to very different views. It was realized that rubber dichloride (the addition product of chlorine and rubber) is far too stable to act as an unstable intermediate product during the chlorinating reaction. Bloomfield[3] argued that during the primary reaction the chlorine is attached by substitution to an α-methylenic carbon atom of the rubber molecule and that there is a considerable amount of cyclization.

It was not our sole concern to study the mechanism of reaction; we were also bent on following the chlorination of rubber under the most diverse conditions, starting from dry rubber, rubber in solution, and rubber in latex, the sources of chlorine being highly diversified, such as from liquid chlorine, gaseous chlorine, hypochlorites, and sulfuryl chloride.

The normal course of reaction, involving the formation of unstable intermediate products, is discussed in Part I of this series; methods of producing comparatively stable rubber chlorides by adding chlorine onto the double bond will be considered in Part II.

---

* Communication No. 114 from the Rubber Foundation.

THE ANILINE TEST

The reaction of halides with organic bases has been used in this laboratory for the kinetic identification of halide groups in polymers.[6] It is sufficient for the purpose of this and the subsequent papers to state that allylic chlorides and tertiary chlorides react with aniline at 100°C. in a very short time, while dichlorides with vicinal chlorine and polychlorides of the chlorinated rubber type split off only part of the chlorine and at a much lower rate. Certain polychlorides with the $>CCl_2$ group are, however, unstable at 100°C. in aniline and this can interfere with the kinetic separation. The reactivity of typical mono- and dichlorides is summarized in the left-hand part of Figure 1, while the analogous reaction of some polymers with a polychloride structure is given in the right-hand half.

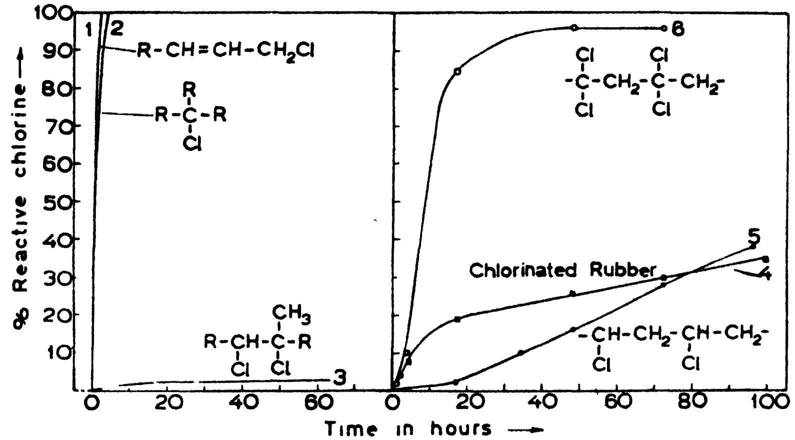

Fig. 1. Reactivity of chlorides with aniline at 100°C. *Model Compounds:* 1, allylic chlorides; 2, tertiary chlorides; 3, vicinal dichlorides. *Polymers:* 4, chlorinated rubber with about 64% chlorine; 5, polyvinyl chloride; 6, polyvinylidene chloride.

A polymer or a mixture of polymers consisting of allylic and/or tertiary groups will react very fast until all the reactive chlorine has been split off. This, in fact, is observed in the chlorination products of rubber (see Fig. 2).

Polymers with 30–55% total chlorine content split off part of their chlorine very fast, while the "slow" fraction reacts frequently with a rate found for chlorinated rubber with 64% Cl (curve 4, Fig. 1). The exact amount of reactive chlorine can be determined by an extrapolation to time zero. Above a total chlorine content of 55% this reactivity with aniline becomes less significant for two reasons: (*1*) the bend in the reaction time curve becomes less pronounced and extrapolation to time zero therefore becomes uncertain; and (2) —CCl_2 groups may be present and can interfere with the determination of the allylic fraction.

The reactivity with aniline by itself does not prove that the reactive fraction is allylic. Additional kinetic experiments[7] would be necessary to distinguish between allylic and tertiary chlorine in cases where it is not obvious from the type of reaction (chlorination or hydrochlorination, respectively).

Experiments were performed by heating 0.1–0.2 g. polymer with 4 cc. of purified aniline in a sealed tube. The contents of the tube were rinsed in a beaker with dilute (1:1) nitric acid and silver nitrate added. The dyestuffs formed from aniline were removed with charcoal and the filtered solution titrated according to Volhard.

As a matter of convenience we have usually determined the amount of reaction of chlorinated rubber with aniline after a heating time of 17 hours at 100°C. It is clear from Figure 2 that this value may be 4 to 7% higher than the extrapolated value, an inaccuracy which does not influence our conclusions.

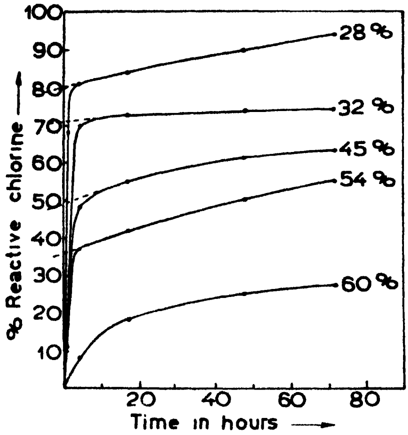

Fig. 2. Reaction of chlorinated rubber with aniline at 100°C. The figures on the curves refer to the total chlorine content of the polymer.

CHLORINE GAS WITH RUBBER IN SOLUTION

With the object of discovering the optimum conditions for the production of chlorinated rubbers of greater stability than usual, a large number of experiments were carried out in which rubber in solution was made to react with gaseous chlorine. These experiments, which are recorded in Tables I and II, were carried out quite simply by introducing gaseous chlorine into roughly 100 cc. of a rubber solution stirred vigorously. In some cases a solution of gaseous chlorine in carbon tetrachloride was added dropwise instead of introducing gaseous chlorine as such. The natural rubber used was masticated standard sheet or crepe; the deproteinized rubber a commercial crepe grade; the gutta-percha specially purified by recrystallization of first quality commercial gutta-percha. The reaction product was reprecipitated for analysis by dissolving it in benzene or chloroform and precipitating with alcohol. The Carius method was employed to determine the chlorine content. Generally, these determinations were accurate within 0.5%.

TABLE I

CHLORINATION OF NATURAL RUBBER AND GUTTA-PERCHA IN 5% SOLUTION WITH CHLORINE GAS

Polymer	Solvent	Catalyst	Time, hours	Temp., °C.	% Cl in product	% reactive Cl of total
Natural rubber	$CHCl_3$	—	17	−70	41.5	55
Deproteinized rubber	CCl_4	—	1	5	43.5	70
		—	2	5	49.5	65
		—	4	5	62.0	30
		—	7	5	64.0	15
		O_2	2	5	50.5	58
		O_2	7	5	50.5	57
Natural rubber	CCl_4	—	1	20	36.5	79
		2% Bz_2O_2	1	20	27.0	80
		—	2	20	48.0	57
		—	7	20	62.5	17
Gutta-percha	CCl_4	—	0.5	20	22.5	75
		5% Bz_2O_2	0.5	20	22.0	74
		—	1.5	20	58.5	19
Natural rubber	CCl_4	—	1	77	49.0	37
		5% Bz_2O_2	1	77	35.0	63
		—	4	77	60.5	13
		—	8	77	65.5	14
		—	16	77	68.0	21

TABLE II

INFLUENCE OF LIGHT ON CHLORINATION WITH GASEOUS CHLORINE OF NATURAL RUBBER IN 5% CCl_4 SOLUTION (REACTION TIME, 7 HOURS)

	Dark		100-watt electric bulb		U.V. light quartz	
Temp., °C.	% Cl in product	% reactive Cl	% Cl in product	% reactive Cl	% Cl in product	% reactive Cl
0	59.0	40	62.0	17		
20	62.5	19	64.0	17		
50	60.5	30	64.0	17	66.5	18
77	65.0	16	65.0	18	70.0	57

The nature of the reaction products is characterized by the percentage of reactive chlorine, *i.e.*, the portion of combined chlorine which is reactive in the aniline test (17 hours 100°C.). It is found that the stability of the products toward aniline is quite independent of the experimental conditions. Although the percentages of reactive chlorine vary strongly, the responsible factor has been found on careful investigation to be the total chlorine content of the reaction product. This chlorine content of chlorinated rubbers is governed by the duration and intensity of chlorination. A somewhat larger chlorine content is usually obtained at higher temperatures—*e.g.*, 50 to 70°C.—than at 0 to 20°C. The addition of benzoyl peroxide (Bz_2O_2) as a catalyst does not affect the nature of the chlorine and certainly does not help to increase the chlorine content. Experiments with purified gutta-percha have proved that exhaustive purification of the polyisoprene hydrocarbon also has no visible effect. Oxygen has a slight inhibiting effect during continued chlorination. Exposure to the light of an ordinary tungsten lamp hardly influences the rate of reaction, but ultraviolet light has a considerable influence, as is evident from Table II.

SOME EXPERIMENTS ON FRACTIONATION

Products of about 30% chlorine content, when fractionated, are found to be nonhomogeneous. A more regular reaction appears to result from the dropwise introduction of chlorine dissolved in carbon tetrachloride instead of in the gaseous form, but it is clear from the following experiments that even then the products are nonhomogeneous.

1. At −10°C., 10 g. chlorine, dissolved in 86 cc. CCl_4 were added drop by drop to 20 g. masticated crepe dissolved in 400 cc. CCl_4, the material being stirred constantly. The resulting product contained 18.5% of chlorine. This product was fractionated by solution in $CHCl_3$ (3% solution) and precipitating with progressive amounts of isoamyl alcohol. The following were obtained:

42% of a fraction with 41.3% Cl
7% " " " " 35.0% Cl
38% " " " " 1.5% Cl
13% " " " " 0.5% Cl

2. Another chlorinated rubber, treated in the same way, contained 18.0% of chlorine. This was fractionated by dissolving in benzene and precipitating in fractions with acetone and then with ethyl alcohol. The following were obtained:

37% of a fraction with 1.1% Cl
27% " " " " 22.5% Cl
36% " " " " 30.5% Cl

The chlorine in the two latter fractions was found to be reactive in the aniline test to the extent of 90 to 95%, which means that they contain approximately that amount of allylic chlorine.

A few experiments were also performed in a film reactor, but with the same result, *viz.*, the formation of nonhomogeneous products. We shall see in Part II of this series that it is possible to obtain homogeneous products by chlorinating with SO_2Cl_2.

The extremely rapid reaction between rubber and chlorine is in all probability responsible for this nonhomogeneity. This reaction, betrayed by the evolution of HCl, is seen to occur as soon as gaseous chlorine or a chlorine solution is mixed with the rubber solution and it is a tenable conjecture that the conversion takes place in a matter of a fraction of a second. Then, the viscosity of the solution stands in the way of rapid intensive mixing, with the result that, even with intensive stirring, there are likely to be local high concentrations of chlorine, in the vicinity of which the rubber reacts with greater ease than elsewhere in the solution.

CHLORINATION UNDER PRESSURE

There was good reason to believe that if the pressure of the chlorine gas was raised, the reaction of chlorine with rubber would be accelerated and the chlorine content of the chlorinated rubber increased. A special device was made by which rubber in solution can be chlorinated under pressure—see Figure 3.

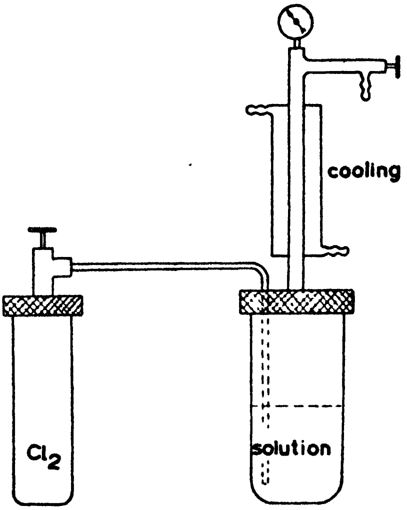

Fig. 3. Apparatus for chlorinating rubber solutions under pressure.

The apparatus comprises a couple of bronze autoclaves. A glass jacket in an autoclave of 200 cc. capacity contains about 100 cc. of a rubber solution. It is necessary to have chlorine gas flowing continuously through the solution to keep the latter sufficiently saturated and homogeneous, and also to evacuate the HCl formed during the reaction. An exhaust is accordingly provided for the surplus gas via a condenser through a regulated pressure valve. The required chlorine is in the liquid state in the other autoclave connected by pressure pipe with the reaction autoclave. The autoclaves can be heated to any temperature required. By keeping the temperature of the chlorine autoclave 10 to 20°C. below that of the reaction autoclave a constant stream of chlorine gas can be made to bubble through the solution via a silver inlet tube.

It was found expedient to chlorinate the rubber solution in the ordinary way for some time before applying pressure. The impression received from a comparison of Table III with Table I is that the application of pressure certainly does produce a higher chlorine content in less time. An added advantage is that the material can thus be chlorinated at temperatures far above the boiling point of the solvent. On the evidence of the recorded intrinsic viscosities, the solubility of the resulting products is satisfactory. Without exposure to light it is exceedingly difficult to obtain chlorine contents above 65% at ordinary pressure, so large-scale production of chlorinated rubber of a high chlorine content would without doubt benefit by the application of pressure.

TABLE III

INFLUENCE OF PRESSURE ON CHLORINATION OF NATURAL RUBBER IN 3% CCl_4 SOLUTION

First phase: chlorination at atmospheric pressure for 4 hours at 45 °C.

Pressure, atm.	Second phase Temp., °C.	Time, hours	Per cent Cl in product	$[\eta]^a$
7	70	5	65.5	0.48
11	70	2	67.5	0.18
12	120	2	66.5	0.14
13	90	2	68.5	0.09

[a] Intrinsic viscosity of the polymer solution in $CHCl_3$, determined at 25 °C. in an Ostwald viscometer.

CHLORINATION WITH LIQUID CHLORINE

The next point on our program was to discover how rubber responds to chlorination with liquid, instead of gaseous chlorine. We can see from Table IV what happens when liquid chlorine reacts at relatively low temperature with rubber in solution. In these experiments 10 cc. liquid chlorine was mixed with 10 cc. solution at −70°C. and, if necessary, was then warmed up in a closed tube to the desired reaction temperature. Apparently, the reaction, in the main, occurs at −70°C. The chlorine content does not differ appreciably from that resulting from chlorination with gaseous chlorine, which proves that the chlorine concentration does not have a great influence on the course of the reaction. A higher temperature would be needed to obtain larger chlorine content.

TABLE IV

CHLORINATION OF NATURAL RUBBER IN SOLUTION WITH LIQUID CHLORINE

Solvent	% rubber in solution	Temp., °C.	% Cl in product 1 hour	17 hours
$CHCl_3$	5	−70	51.0	54.5
	20		50.0	54.0
CCl_4	5	+20	52.5	58.5
	20		51.0	56.0

It was tempting to allow liquid chlorine to react direct with solid rubber, thus obviating the tedious and costly process of solution involved in the production of chlorinated rubber.[8–10] The technique in these experiments was to add about half a gram of rubber to roughly 10 cc. of liquid chlorine at −70°C. in a small autoclave and then to warm it up gradually to the desired temperature. It was found incidentally, that liquid chlorine is an excellent swelling agent for rubber. When the reaction has ceased, the chlorine is evaporated and the resulting chlorinated rubber purified by dissolving it in $CHCl_3$ and precipitating with alcohol.

TABLE V

CHLORINATION OF SOLID NATURAL RUBBER WITH LIQUID CHLORINE

Temp., °C.	Time, hours	% Cl in product	% reactive Cl
−70	17	38–43	50–40
−40	17	49–57	50–20
20	3–60	50–60	40–20
50	5	60	20
70	3–6	63–64	14–25
100	3–6	68–70	30–41
120	1–3	68–69	35

It will be seen from the data of Table V that the reaction proceeds with greater velocity at higher temperatures, when the normal chlorine contents for commercial chlorinated rubber are obtained and surpassed. There is, however, one serious drawback to this method: if the rubber and liquid chlorine are warmed too quickly, the reaction is liable to be too violent and cause charring. There may even be signs of kindling when finely divided pieces of rubber or gutta-percha are introduced into liquid chlorine at −50°C. It is therefore necessary to be on guard against any reaction of chlorine with rubber in anything like large quantities and one should, in any case, beware of letting liquid chlorine react at the more elevated temperatures with major amounts of rubber all at once, as the reaction is likely to become uncontrollable.[11] The products are generally insoluble, only those containing a very large percentage of chlorine (65–70%) being soluble. Apparently, cross-linking reactions are apt to occur during chlorination as a secondary reaction, this being a much rarer occurrence with chlorination in dilute solution because the solvent molecules keep the rubber molecules further apart. The solubility of products of large chlorine content is due to chlorinolysis. Under the severe conditions employed, the chlorine disrupts C—C bonds of the chlorinated rubber molecules with the formation of smaller fragments.

CHARACTER OF THE CHLORINE-RUBBER BOND

Some experiments were performed to discover how much chlorine is combined by substitution. This can be deduced fairly easily from the quantity of hydrochloric acid generated, since one molecule of HCl is liberated for every chlorine atom combined by substitution.

In these experiments, the results of which are given in Figure 4, a solution of chlorine gas in carbon tetrachloride of known concentration was dripped into a given amount of rubber solution in carbon tetrachloride at 60°C. It would seem that it is especially in the initial stages of chlorination (below 30% of combined chlorine) that the reaction proceeds almost entirely by substitution. In the case of products with 50–55% of combined chlorine, the chlorine is bound additively to the extent of 40%. This is consistent with the view that an addition of chlorine on the double bond follows substitution of one chlorine atom per isoprene unit. The possibility remains, however, that there may be a certain amount of splitting-off of HCl from the chlorinated rubber during the reaction. The aniline test indicates that the primarily bound substitution chlorine possesses a reactivity which, according to experiments with model substances, fits in with a linkage at the allylic position.

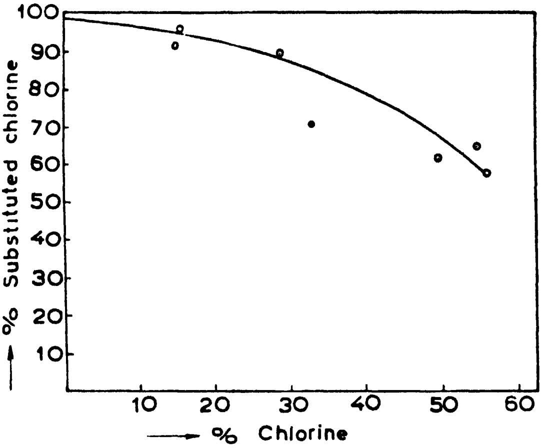

Fig. 4. The quantity of substituted chlorine as a function of the chlorine content.

It will be seen from Figure 5 that the quantity of reactive chlorine split off in the aniline test decreases with increasing chlorine content. Products containing about 30% of chlorine show that roughly 80% of this chlorine is reactive in the aniline test. This reactivity drops to approximately 15% in chlorinated rubbers with 60–66%, but begins to increase again above 67% of chlorine.

The remarkable point about this is that the results recorded in Figure 5 are those obtained with chlorinated rubbers produced under the most divergent reaction conditions with variation of temperature, pressure, source of chlorine (gaseous or liquid), rubber (solid or in solution), exposure to light, and catalysts. It is evident, therefore, that however much we varied these conditions we were unable to combine chlorine with rubber in any fundamentally different way. The minor variations found in Figure 5 may be due in part to lack of homogeneity of the chlorinated rubber. In Part II we shall discuss methods that do make it possible to combine chlorine with rubber in a different way and to which the relation found in Figure 5 does not apply.

The results of the aniline test tend to show that in all instances the chlorine is first mainly bound by substitution at an allylic position. With 50% of chlorine, chlorinated rubber contains, on an average, two chlorine atoms per isoprene unit. We have to assume that roughly half the isoprene units contain only one loosely bound allylic chlorine atom, whereas the other half of the isoprene units contain three atoms far more firmly attached. This is compatible with an average reactivity of the total chlorine in a chlorinated rubber of this kind with aniline of approximately 45%. The increase in reactivity with aniline of chlorinated rubber with more than 67% of chlorine may be due to the formation of —CCl_2 groups, which are very reactive with aniline, as has been shown in Figure 1 for polyvinylidene chloride.

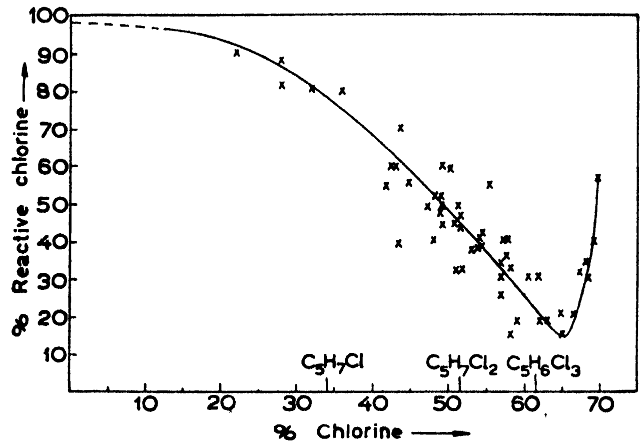

Fig. 5. Percentage of reactive chlorine in the aniline test as a function of chlorine content.

It has been stated[12] that a substitution of chlorine at the allylic position is liable to occur at very low temperatures (0 to −60°C.) with great rate of reaction in the chlorination of branched olefins, such as isobutene and trimethyl ethylene, in the liquid phase. The following two chlorides are formed from trimethyl ethylene:

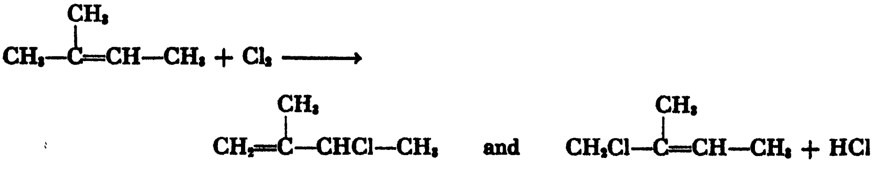

$$CH_3-\overset{\overset{\displaystyle CH_3}{|}}{C}=CH-CH_3 + Cl_2 \longrightarrow$$

$$CH_2=\overset{\overset{\displaystyle CH_3}{|}}{C}-CHCl-CH_3 \quad \text{and} \quad CH_2Cl-\overset{\overset{\displaystyle CH_3}{|}}{C}=CH-CH_3 + HCl$$

when at the same time allylic rearrangement between the two products takes place. This substitutive chlorination of isobutylene and trimethyl ethylene illustrates a fairly general rule formulated by Kondakoff[13] in 1891 to the effect that olefins which combine readily with mineral acids yield monochloro olefins, whereas those which do not, yield the normal addition products on treatment with chlorine. Natural rubber and gutta-percha possess a structure very similar to that of trimethylethylene and these polymers combine readily with a mineral acid such as HCl. Thus the primary substitutive reaction of these polymers is in line with the behavior of olefins in general.

Although the chlorination of hydrocarbons generally constitutes a free radical type of reaction, it is nevertheless a tenable conjecture that, with olefins, the primary reaction in chlorination is of an ionic nature.[14] It has been found that the normal primary chlorination of rubber and like olefins with chlorine cannot be accelerated by normal free-radical chain-initiating agents. Nor can the chlorination be arrested by the known chain reaction inhibitors. Arguments can be advanced[15] to show that the rate-determining step is addition of a positive chlorine ion to the double bond to form a carbonium ion and a negative chlorine ion.

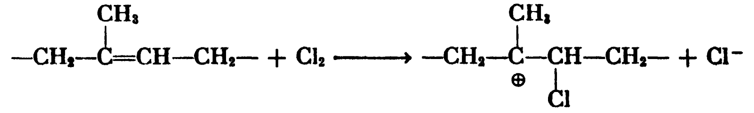

$$-CH_2-\overset{\displaystyle CH_3}{\overset{|}{C}}=CH-CH_2- + Cl_2 \longrightarrow -CH_2-\overset{\displaystyle CH_3}{\overset{|}{\underset{\oplus}{C}}}-\underset{\displaystyle Cl}{\underset{|}{CH}}-CH_2- + Cl^-$$

The intermediate carbonium ion follows several distinct reaction courses. It may be that a proton splits off. The double bond resulting from the elimination of the proton will be formed preferentially between the carbon bearing the positive charge and that adjacent carbon atom which is the most richly endowed with electrons, and it is from this carbon atom that the proton splits off.[15] We may then obtain the following chlorinated rubber structures:

(a)

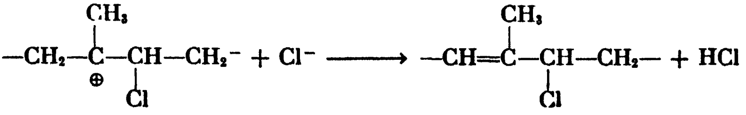

$$-CH_2-\overset{\displaystyle CH_3}{\overset{|}{\underset{\oplus}{C}}}-\underset{\displaystyle Cl}{\underset{|}{CH}}-CH_2^- + Cl^- \longrightarrow -CH=\overset{\displaystyle CH_3}{\overset{|}{C}}-\underset{\displaystyle Cl}{\underset{|}{CH}}-CH_2- + HCl$$

(b) and

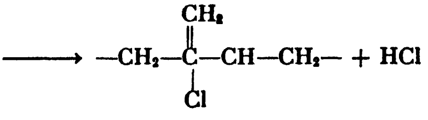

$$\longrightarrow -CH_2-\overset{\displaystyle CH_2}{\overset{\|}{\underset{\displaystyle Cl}{\underset{|}{C}}}}-CH-CH_2- + HCl$$

Apart from this, we have to allow for the possibility of the carbonium ion's reacting with a Cl⁻ ion with the formation of a normal chlorine addition product, as follows:

(c)

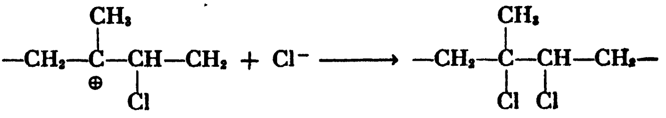

$$-CH_2-\overset{\displaystyle CH_3}{\overset{|}{\underset{\oplus}{C}}}-\underset{\displaystyle Cl}{\underset{|}{CH}}-CH_2 + Cl^- \longrightarrow -CH_2-\overset{\displaystyle CH_3}{\overset{|}{\underset{\displaystyle Cl}{\underset{|}{C}}}}-\underset{\displaystyle Cl}{\underset{|}{CH}}-CH_2-$$

On the evidence of the quantity of HCl split off and the results of the aniline test, however, it is quite certain that only infinitesimal amounts of this rubber dichloride are formed, if at all.

Bloomfield[8] argues from iodine number determinations that the following cyclization reaction is likely to take place:

(d) 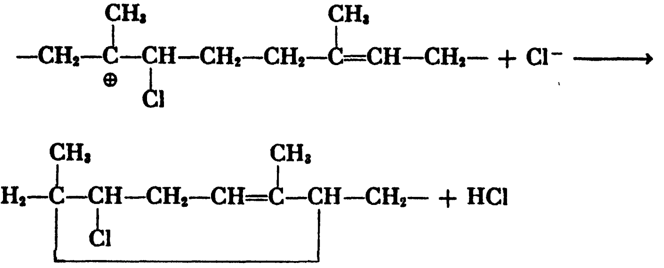

$$-CH_2-\overset{\overset{\displaystyle CH_3}{|}}{\underset{\oplus}{C}}-\underset{\underset{\displaystyle Cl}{|}}{CH}-CH_2-CH_2-\overset{\overset{\displaystyle CH_3}{|}}{C}=CH-CH_2- + Cl^- \longrightarrow$$

$$-CH_2-\overset{\overset{\displaystyle CH_3}{|}}{\underset{|}{C}}-\underset{\underset{\displaystyle Cl}{|}}{CH}-CH_2-CH=\overset{\overset{\displaystyle CH_3}{|}}{C}-\underset{|}{CH}-CH_2- + HCl$$

In view of the fact that chlorinated rubbers in solution are of relatively low viscosity compared to their molecular weight, Staudinger and Staudinger[16] likewise come to the conclusion that considerable cyclization must have taken place during the chlorination. These authors assign a different structure to cyclized chlorinated rubber from that suggested by Bloomfield. They presume that the methyl group reacts with the main chain during cyclization, and that other, unknown cyclization reactions also occur. It is certainly not difficult to see that there are alternatives to the structure assigned by Bloomfield to cyclized chlorinated rubber. The fact alone that the reaction products of liquid chlorine with solid rubber are usually insoluble shows that not only intramolecular, but also intermolecular cross-linking reactions are probably involved. It is especially at the more elevated temperatures that cyclization reactions are likely to predominate over the chlorination reactions (a) and (b).

It is interesting to note that, except when there is addition, the combination of chlorine is invariably accompanied by a shifting of the double bonds. Such displacement, with the formation of an $R_1R_2C{=}CH_2$ group is borne out by the evidence of infrared investigations.[17]

Where chlorination is slow, we must be prepared to find that the HCl evolved may be added on to the original polyisoprene double bond. This side reaction, which leads to rubber hydrochloride structures, can be avoided by chlorinating quickly, or by immediately evacuating the HCl generated by means of an inert gas.

The further chlorination of the primary products of chlorination may be supposed to proceed anew via a carbonium ion. The smaller quantity of HCl evolved at this stage would seem to indicate that considerable addition now takes place, even though, side by side, substitution may likewise occur with displacement of the double bond or cyclization. This greatly increases the number of conceivable chlorinated rubber structures with large chlorine contents, and the manner in which the chlorine is combined in these structures is very complicated.

The authors wish to express their thanks to W. H. Manger and J. V. van Ulden for their valuable assistance, and to the Rubber Foundation for permission to publish the results of the investigation.

References

1. A. Nielsen, *Chlorkautschuk.* Hirzel, Leipzig, 1937.
2. J. P. Baxter and J. G. Moore, *J. Soc. Chem. Ind.*, **57**, 327 (1938); *Rubber Chem. Tech.*, **12**, 82 (1939).
3. G. F. Bloomfield, *J. Chem. Soc.*, **1943**, 289.
4. G. F. Bloomfield, *J. Chem. Soc.*, **1944**, 114.
5. J. D. D'Ianni, F. J. Naples, J. W. Marsh, and J. L. Zarney, *Ind. Eng. Chem.*, **38**, 1171 (1946).
6. G. Salomon, C. Koningsberger, and A. J. Ultée, in *Proceedings of the Second Rubber Technology Conference*, London, 1948, p. 109.
7. G. Salomon and A. J. Ultée, *Rec. trav. chim.*, **69**, 95 (1950).
8. C. Ellis and N. Boehmer, U. S. Pat. 1,544,531 (1925).
9. C. Ellis, U. S. Pat. 1,544,533 (1925).
10. S. D. Kaganoff, Brit. Pat. 606,400 (1948).
11. R. L. Murray, *Chem. Eng. News*, **26**, 3369 (1948).
12. J. Burgin, W. Engs, H. P. A. Groll, and G. Hearne, *Ind. Eng. Chem.*, **31**, 1413 (1939).
13. J. Kondakoff, *Ber.*, **24**, 929 (1891).
14. A. E. Remick, *Electronic Interpretations of Organic Chemistry*, Wiley, New York, 1945, p. 222.
15. R. W. Taft, *J. Am. Chem. Soc.*, **70**, 3364 (1948).
16. H. Staudinger and Hj. Staudinger, *J. prakt. Chem.*, **162**, 148 (1943).
17. N. Sheppard and G. B. B. M. Sutherland, *Discussions, Faraday Soc.*, **2**, 374 (1947).

English Synopsis, see Summaries, page S13, Vol. V, 1950.

Résumé

En vue d'étudier les réactions entre le chlore et le caoutchouc, le caoutchous a été traité, à l'état solide et en solution, avec du chlore gazeux et liquide. Des quantités d'acide chlorhydrique, qui se forment au cours de la réaction, ainsi que de la réactivité du chlore combiné à l'égard de l'aniline, on conclut que la réaction primaire consiste principalement dans und réaction de substitution du chlore en position allylique. Cette substitution par le chlore est considérée du type ionique avec formation intermédiaire d'un ion carbonium. Par continuation de la chloruration, le chlore s'additionne à la double liaison. Il n'y a pas d'exception à ce cours normal de la réaction dans n'importe quelle des conditions envisagées. Des caoutchoucs chlorés contenant 65 à 70% de chlore ont été obtenus en un temps très court en traitant les solutions de caoutchouc avec le chlore gazeux sous une pression de 10 à 12 atmosphères à une température d'environ 100 °C. Les caoutchoucs chlorés d'une teneur similaire en chlore ont également été obtenus par réaction du chlore liquide sur du caoutchouc solide à une température voisine de 100 °C. Il y avait toutefois des signes de carbonisation au cours de cette dernière réaction, lorsque de grandes quantités de matériel sont soumises à la réaction en même temps.

Zusammenfassung

Um die Reaktion zwischen Kautschuk und Chlor zu untersuchen, wurde Kautschuk in Lösung und fester Kautschuk unter sehr verschiedenen Bedingungen mit gasförmigem und flüssigem Chlor in Reaktion gebracht. Aus der Menge HCl, die während der Reaktion entwickelt wird, und aus der Reaktionsfähigkeit von gebundenem Chlor gegenüber

Anilin kann geschlossen werden, dass die primäre Reaktion durch Substitution von Chlor in der Allylstellung vor sich geht. Diese Chlorsubstitution wird als eine Ionenreaktion angesehen, unter Bildung eines intermediären Carboniumions. Bei weiterer Chlorierung wird Chlor an die Doppelbindung angelagert. Unter keiner der angewandten Bedingungen trat eine deutliche Abweichung von diesem Reaktionsverlauf auf. Chlorierter Kautschuk mit 65 bis 70% Chlorgehalt wurde in kurzer Zeit bei Behandlung von Kautschuklösungen mit gasförmigem Chlor unter 10 bis 12 Atmosphären Druck bei Temperaturen von ungefähr 100°C. erhalten. Chlorierter Kautschuk mit ähnlichem Chlorgehalt wurde auf ähnliche Weise aus festem Kautschuk durch Reaktion von flüssigem Chlor bei Temperaturen in der Nähe von 100°C. hergestellt aber wenn grössere Mengen von Material zur gleichen Zeit in Reaktion gebracht wurden, traten bei dieser Reaktion Zeichen von Carbonisierung auf.

Received August 24, 1949

JOURNAL OF POLYMER SCIENCE VOL. V, NO. 6, PAGES 653-666

Chlorination of Natural Rubber. II. Preparation and Properties of Rubber Dichloride*

G. J. VAN AMERONGEN and C. KONINGSBERGER, *Rubber Foundation, Delft, The Netherlands*

INTRODUCTION

As we have seen in Part I, the chlorination of rubber with chlorine under the most varied conditions leads to products in which the chlorine is initially attached fairly loosely to an allylic carbon atom.[1] Consequently, chlorinated rubbers of low chlorine content have rather poor properties.

We shall now proceed to describe two methods by means of which, with saturation of the double bond, chlorine is introduced into rubber and the formation of products with allylic chlorine is avoided. In this way chlorinated rubbers of comparatively low chlorine content can be obtained, these being considerably more stable than the products of the same chlorine content resulting from the direct chlorination of rubber. One of these methods depends upon a catalytic additive chlorination of rubber with sulfuryl chloride; the principle of the other is the addition of HCl onto rubber followed by normal chlorination.

The aniline test described in Part I (in which the chlorinated rubber is heated with aniline for 17 hours to 100°C.) was again employed to establish the nature of the chlorine bond in chlorinated rubber. Under the conditions of this test, allylic and tertiary combined chlorine reacts quantitatively. Chlorine attached by addition to the double bond of the rubber reacts to the extent of only about 4%. We are therefore in a position to mark off clearly allylic and tertiary chlorine from addition chlorine. This reactive tertiary chlorine is introduced into rubber by the addition of HCl, with the formation of rubber hydrochloride. In the chlorination of rubber we are mainly concerned with allylic and addition chlorine, between which the aniline test distinguishes unmistakably. Moreover, the splitting off of the chlorine from chlorinated rubber with aniline gives us a good idea of its chemical stability.

REACTION OF SO_2Cl_2 WITH ORGANIC SUBSTANCES

SO_2Cl_2 is an interesting reagent because there are different ways in which it reacts with organic substances.[2,3]

It is a source of chlorine molecules at the more elevated temperatures or in presence of halogen carriers, such as iodine. Under these conditions the same chlorinating reaction can be induced as with gaseous chlorine, with the advantage that the reaction is far more orderly with SO_2Cl_2. This form of reaction has already been applied to natural rubber.[4-7]

---

* Communication No. 115 from the Rubber Foundation.

The second kind of reaction results in the introduction of a sulfonyl chloride group into organic molecules and takes place at 40–60°C. under exposure to light and in the presence of a catalyst, *e.g.*, pyridine.[2,8,9]

There is yet another technique—effecting a chain reaction catalyzed with peroxide, the study of which has been the special concern of Kharasch *et al.* The reactions can be divided roughly into two classes, *i.e.*, those with saturated and those with unsaturated organic compounds. Various substitutions can be effected with saturated compounds[10] the results being more or less the same as those obtained by chlorination with chlorine gas under exposure to light. There is reason to believe that this reaction proceeds via chlorine atoms. It has been applied to polyethylene.[11]

The chain reaction of SO_2Cl_2 with ethylenic compounds is of particular interest to those concerned with rubber.[12,13] Substances such as cyclohexene, allyl chloride, and the like react with SO_2Cl_2 when the corresponding dichlorides are formed; hence the double bond becomes saturated as chlorine is added on. Catalysts such as ascaridole or benzoyl peroxide are used. Kharasch and Brown[13] drew up the following scheme for a chain reaction of this kind:

$$\text{Peroxide} \longrightarrow R^*$$

$$R^* + SO_2Cl_2 \longrightarrow RCl + {}^*SO_2Cl$$

$${}^*SO_2Cl \longrightarrow SO_2 + Cl^*$$

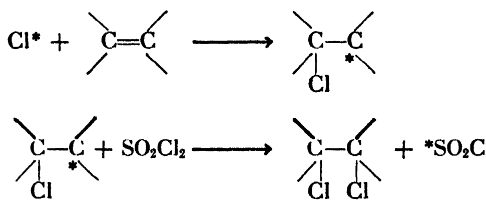

REACTION OF SO_2Cl_2 WITH GUTTA-PERCHA

Bloomfield[14] has applied the free-radical chain reaction of SO_2Cl_2 to rubber. He found that peroxides such as benzoyl peroxide catalyze the additive chlorination of very carefully purified natural rubber. With ordinary crepe rubber, on the other hand, the reaction was for the most part substitutive. It would seem that the contaminations of nonpurified rubber interfere with the free-radical chain reaction.

For a reliable study of the reaction between SO_2Cl_2 and natural rubber, therefore, a necessary condition is that the rubber used should have previously been dependably freed from all nonrubber constituents. Exhaustive purification of natural rubber, however, is a very difficult and tedious process. Here, Nature comes to our aid, for gutta-percha is a natural *trans* isomer of polyisoprene possessing chemical properties very similar to those of natural rubber and is very easily purified. There is good reason to believe that those reaction conditions that are found to apply to gutta-percha will be valid for natural rubber.

Prime quality commercial gutta-percha is purified by dissolving it in petrol ether at raised temperature and then crystallizing the gutta-percha by cooling the solution down to 0°C., when the crystal mass can be filtered off and dried. The melting point of purified gutta-percha is at approximately 65°C.

TABLE I

REACTION OF SO_2Cl_2 WITH GUTTA-PERCHA IN A 3% CCl_4 SOLUTION

Conditions	Time, min.	Temp., °C.	% Cl in product	% reactive Cl
As such	30	20	24.0	7
As such	10	5	32 5	6
+ ultraviolet light	30	20	34.5	5
+ 5% tetralin hydroperoxide	30	20	30.5	6
+ 5% benzoyl peroxide	2	10	32.5	6
+ 5% benzoyl peroxide	10	20	28.5	7
+ 5% benzoyl peroxide	30	77	37.5	7

The results of some reactions of SO_2Cl_2 with gutta-percha solutions in carbon tetrachloride of a 3% concentration by weight are listed in Table I. In these and subsequent experiments the quantity of solution was generally 60 cc., to which SO_2Cl_2 was added in the amount calculated to produce a chlorine content of 25 to 35%. The recorded times of reaction can generally be considerably shortened if peroxides are present, in which case the whole reaction is completed within a very short period—in about five minutes—with the evolution of a great deal of heat. Table I shows that chlorine combines during the reaction of purified gutta-percha with SO_2Cl_2, the combined chlorine having very little reactivity in the aniline test. The addition of peroxides, or radiation with ultraviolet light, produces virtually the same results. The slight reactivity of the chlorine in the aniline test goes to show that there has been addition of chlorine, a fact which was moreover proved by measurements made of the quantity of HCl which would have been evolved during a substitutive reaction. Very little HCl, or none at all, was formed during the experiments recorded in Table I. The additive chlorination reaction of SO_2Cl_2 with gutta-percha is entirely comparable to the additive reactions found by Kharasch and Brown[13] with olefins under the catalytic influence of peroxides. The very fact that an additive reaction is found with gutta-percha in itself points to the presence of gutta peroxides.

The particulars given in Table II corroborate the supposition that the reaction with gutta-percha is actuated by a chain mechanism. It is evident

TABLE II

REACTION OF SO_2Cl_2 WITH GUTTA-PERCHA IN A 3% CCl_4 SOLUTION IN THE PRESENCE OF INHIBITORS

Inhibitor	Time, min.	Temp., °C.	% Cl in product	% reactive Cl
5% hydroquinone	60	20	8.5	64
5% hydroquinone	90	20	10.0	77
5% di-*tert*-amylhydroquinone	90	15	6.5	91
5% β-naphthol	90	20	4.5	73
5% β-naphthol	60	70	21.0	72

from Table II that certain antioxidants serve as inhibitors in the additive chlorination reaction with gutta-percha. Insofar as there can be said to be any reaction at all, this, on the evidence of the percentage of reactive chlorine, takes place mainly by substitution. The substitutive reaction is fostered by letting the reaction take place at higher temperature, because this facilitates the decomposition of SO_2Cl_2 and the formation of chlorine molecules[15] which react in the ordinary way, that is to say, substitutively. The more soluble the agents are, so much more effectively do they inhibit the reaction. Hydroquinone dissolves badly and is therefore less useful than di-*tert*-amyl hydroquinone or β-naphthol. The very fact that substances exist which completely inhibit the additive reaction proves that there is a chain reaction. This chain reaction is obviously initiated by peroxides; hence the inhibitive effect of the antioxidants mentioned consists either in neutralizing the peroxides or reacting with whatever radicals are liberated from those peroxides.

TABLE III

REACTION OF SO_2Cl_2 WITH GUTTA-PERCHA IN A 3% CCl_4 SOLUTION IN THE PRESENCE OF CATALYSTS

Catalyst	Time, min.	Temp., °C.	% Cl in product	% reactive Cl
5% aldol α-naphthylamine	60	20	27.0	79
5% phenyl β-naphthylamine	60	20	27.0	81
5% pyridine	60	20	22.5	82
5% diazoaminobenzene	12	20	23.5	81
5% diazoaminobenzene	60	20	28.5	81
Some NO gas	60	20	30.5	80
5% cetylpyridinium bromide	60	20	28.5	74
5% tetraphenyl hydrazine	15	30	23.0	80
5% isoamyl nitrite	30	20	30.0	79

An entirely different state of affairs is revealed by Table III, from which it is clear that numerous substances, including several antioxidants, not only inhibit the additive reaction, but so change the course of things that, judging by the percentage of reactive chlorine, a considerable substitution of chlorine takes place. A fact common to all the catalysts listed in Table

III is that they contain nitrogen in the form of amino or nitroso groups. The substances probably owe their effect to their ability to liberate molecular chlorine from SO_2Cl_2, or to act as chlorine transmitters, when the chlorine reacts exactly as does ordinary chlorine gas, that is to say, substitutively. The quantity of HCl evolved was a further attestation to the presumed substitution of chlorine. The fact that only 80% of the combined chlorine is reactive would seem to show that some of the chlorine is not held at the allylic position, or that certain changes of structure have taken place during chlorination, possibly owing to cyclization and displacement of the double bond.

REACTION OF SO_2Cl_2 WITH NATURAL RUBBER

The reaction of SO_2Cl_2 with rubber in solution was initially studied for the main purpose of producing homogeneous products containing from 20 to 50% of chlorine. We saw in Part I that it is a fairly simple matter to obtain products of this chlorine content by introducing chlorine gas into a rubber solution, but that, upon fractionation, these products vary enormously in chlorine content. SO_2Cl_2, however, provides a means of obtaining products that are homogeneous.[7] The required quantity of SO_2Cl_2 was mixed with the rubber solution at a low enough temperature, *e.g.*, 0°C., to ensure homogeneous mixing before the reaction started. The reaction can be set in motion after the materials have been mixed, either by waiting for some time, or by raising the temperature slightly.

TABLE IV

REACTION OF SO_2Cl_2 WITH NATURAL RUBBER IN A 3% CCl_4 SOLUTION

Rubber	Time, min.	Temp., °C.	% Cl in product	% reactive Cl
Standard sheet	20	0	29.5	96
	60	20	20.0	86
	60	20	38.0	75
	60	77	28.5	88
	60	77	47.5	49
Deproteinized crepe	60	25	24.0	87
	60	77	29.0	82
Deproteinized purified rubber	30	25	31.0	19
	30	25	28.5	31

Table IV shows that the reaction with sheet or deproteinized crepe is substitutive, which is comprehensible, since sheet contains roughly 7% of nonrubber components consisting partly of amino acids and amines. These nitrogen-containing substances have the same catalytic effect upon the reaction as the agents listed in Table III. The deproteinized crepe is a commercial product which still contains 1 to 2% of nonrubber components, which apparently is quite enough to deflect the reaction toward substitution. The results are improved by careful purification of the rubber by treating latex with caustic soda and then extracting the rubber, but this is a very tedious process. Fractionating tests proved that the reaction products are, on the whole, highly homogeneous.

TABLE V

REACTION OF SO_2Cl_2 WITH NATURAL RUBBER IN A 3% CCl_4 SOLUTION IN THE PRESENCE OF CHAIN INITIATING AGENTS

Rubber	Catalyst	Time, min.	Temp., °C.	% Cl in product	% reactive Cl
Sheet..........	2% benzoyl peroxide	60	20	25.0	86
	5% benzoyl peroxide	60	77	27.5	82
Crepe..........	5% urea peroxide	40	20	6.5	81
	5% di-*tert*-butyl peroxide	40	20	11.5	75
	3% *tert*-butyl perbenzoate	40	20	13.5	76
Deproteinized crepe........	5% ascaridole	60	25	29.5	17
	5% ascaridole	60	77	26.0	68
	5% benzoyl peroxide	60	20	19.0	77
	Ultraviolet light	60	4	17.0	21
	" "	30	20	28.0	8
	" "	30	77	27.5	43
Crepe..........	Ultraviolet light	60	0	20.5	28
	" "	60	15	27.5	17
	" "	60	20	22.5	49
	" "	60	40	25.5	70
	" "	60	77	26.5	83

We see by Table V that ultraviolet irradiation of the reaction mixture in a quartz tube favors additive reaction. The low percentage of reactive chlorine testifies to the fact that ordinary and deproteinized rubber yield an addition product in the main, especially at low temperature. The other auxiliaries used, with the exception of ascaridole, have no appreciable effect. The startling point about this is the virtual inertia of benzoyl peroxide, which used to be a favorite promoter of the additive reaction. The probable explanation is that the quantity of radicals formed out of benzoyl peroxide is too small to suppress the substitutive reaction accelerated by the natural amines present.

It is evident from Table VI that organic hydroperoxides are exceedingly active chain initiators of the additive chlorination of rubber. These substances are apparently able to defeat the substitutive catalysis of the nonrubber components. The procedure is to add the hydroperoxide and subsequently the SO_2Cl_2 to the rubber solution. After a short induction time, the reaction starts violently with the evolution of a great deal of heat. As a rule, the reaction is completed within three minutes, though the mixture is generally allowed to continue to react a little longer, as in the majority of the experiments to which Table VI refers. It is advisable to

TABLE VI

REACTION OF SO_2Cl_2 WITH NATURAL RUBBER IN A 3% SOLUTION IN THE PRESENCE OF HYDROPEROXIDE CHAIN INITIATORS

Rubber	Solvent	Catalyst[a]	Time, min.	Temp., °C.	% Cl in product	% reactive Cl
Sheet..........	CCl_4	5% ethyl HP	60	25	26.0	13
	CCl_4	" " "	30	77	17.5	60
Deproteinized crepe........	CCl_4	" " "	60	77	16.5	33
Crepe.........	CCl_4	5% tetralin HP	10	25	23.5	6
	CCl_4	" " "	60	25	35.0	5
	$CHCl_3$	" " "	30	20	24.5	36
	Benzene	" " "	30	20	26.0	11
	CCl_4	1% *tert*-isobutyl HP	30	20	10.5	23
	"	3% " "	30	20	27.5	5
	"	4% " "	30	30	47.0	7
	"	4% " "	30	40	43.5	14
	"	5% " "	30	20	28.0	5
	"	5% 1-hydroxy-cyclohexyl HP	30	15	20.0	7

[a] HP = hydroperoxide.

mix at low temperature (*e.g.*, 0°C.) so that the reaction shall not begin before the SO_2Cl_2 has properly mixed with the material. At the higher temperatures (*e.g.*, 77°C.) the reaction is less favorable for addition, possibly because the peroxide then decomposes too soon and because SO_2Cl_2 dissociates more readily at high temperature into chlorine molecules[15] which react substitutively. It has been found that more than 3% of hydroperoxide relative to the rubber is required if the additive reaction is to proceed satisfactorily. The chlorine content of the end products depends upon the quantity of SO_2Cl_2 used. Generally speaking, a yield of 80 to 90% of the SO_2Cl_2 may be depended upon for additive reactions in presence of hydroperoxide. As a rule, the products also contain 1 to 2% of combined sulfur, which may be present in the form of SO_2Cl groups or as added on SO_2 evolved in the course of the reaction. The theoretical chlorine content of 51% is never attained. Then, some degree of substitution sometimes occurs and the chain reaction can come to a standstill if the reaction proceeds too slowly. The best reactions with the best yields are those which are obtained in the shortest time.

ANALYSIS OF SOME OF THE REACTIONS

(*1*) 5.02 g. SO_2Cl_2 were added to 100 g. of 3.06% solution of crepe in carbon tetrachloride and these reacted first for 45 minutes at 25°C., then for 45 minutes at 75°C. The escaping reaction gases—which may consist of SO_2, HCl, and some unconsumed SO_2Cl_2—were collected in a NaOH solution, in which chloride content was determined by titration, the SO_2 content by iodometry, and the SO_4 content (derived from SO_2Cl_2) by gravimetry. According to the SO_2 collected, 4.2 g. of SO_2Cl_2 had reacted. The amount of HCl collected was 1.232 g., 0.270 g. of which was derived from distilled SO_2-

Cl_2. From this we are able to calculate that 3.56 g. of SO_2Cl_2 had reacted substitutively and, therefore, 0.64 g. additively. Hence the chlorine content of the chlorinated rubber should be 29.4%, 74% of which was substituted. Actually the product contains 28.9% of chlorine, 83% of which is found to be reactive according to the aniline test.

(2) 153 mg. (5%) tetralin hydroperoxide and 4.24 g. SO_2Cl_2 were added to 100 g. of a 3.06% solution of crepe in carbon tetrachloride, these reacting for 30 minutes at 25 °C., and then for 30 minutes at 75 °C. On the evidence of the SO_2 collected, 2.62 g. SO_2Cl_2 had reacted with the rubber. 0.16 g. HCl was collected, this being derived entirely from distilled SO_2Cl_2. From these data the calculated chlorine content of the chlorinated rubber is 31.5%, added on to the extent of 100%. In fact, the product contains 29.7% chlorine, 8% of which is reactive according to the aniline test. The product also contains 1.3% sulfur.

Both these experiments, which could be supplemented by others, demonstrate the reliability of the aniline test as a standard for the degree of substitution and addition, since the results of this test accord with the quantity of HCl collected and the amount of SO_2Cl_2 which had reacted.

GELATION OF ADDITIVE CHLORINATED SOLUTIONS

One danger attending the preparation of additive chlorinated rubber with SO_2Cl_2 is that after the reaction the solution may show a strong tendency to jellify. Some experiments were performed with the special intention of discovering the conditions which encourage this gelation and how it is to be avoided. The line mainly followed was to observe the changing viscosity, determining this by approximation by measuring the time of efflux from a pipet. The following conclusions were drawn.

(*1*) The rate of gelation depends upon the reaction temperature. A higher temperature, though the contrary of conductive to additive chlorination, causes less gelation in the solution of the reaction product.

(*2*) The rate of gelation increases with the gelation temperature. A given reaction mixture jellifies at 65°C. within two hours of the reaction, within five hours at 20°C., and within 72 hours at 0°C. During the reaction itself, which is often accompanied by elevation of temperature, considerable increase in viscosity takes place as compared to that of the initial solution.

(*3*) Light appreciably fosters gelation.

(*4*) Traces of water (*e.g.*, 1% relative to the solution) considerably accelerate gelation, even in the dark. Antioxidants, such as benzidine or di-*tert*-amylhydroquinone, have no effect at all.

(*5*) The gases NO or N_2O_3 introduced in small amounts into the reaction mixture arrest gelation both in the dark and in light.

(*6*) The addition of a small amount of HI solution to the reaction mixture not only prevents any increase in viscosity, but even reduces it substantially in the long run. In a given instance the viscosity was reduced by half after three hours at 0°C. and after 72 hours at 20°C. to as much as one tenth, thus dropping to the viscosity of the initial rubber solution. Iodine too, which is always present in HI, similarly decreases the viscosity. The smallest amount still producing perceptible effect was 0.6% HI +

0.1% I_2 (relative to the chlorinated rubber) in a 10% solution in H_2O. The reducing effect upon the viscosity increases with the amount of HI used.

(*7*) A small amount of chlorine gas first increases the viscosity, this being followed by rapid and effective decrease upon exposure to diffuse daylight. HCl has no effect.

(*8*) The addition of approximately 5% of a hydroperoxide (relative to the chlorinated rubber) to the solution after the reaction stops gelation and greatly reduces the viscosity.

We thus see that there are various means by which gelation can be counteracted. The cause of gelation is not yet properly understood, but it may be suggested that the free radicals still present after the reaction initiate cross-linking reactions between the chlorinated rubber molecules. If this is so, the effect of HI, for example, would be due to destruction of the free radicals present. Similarly, the breaking up of the polymer network would be responsible for the activity of a hydroperoxide or chlorine and light.

Some connection might be suggested with the gelation which occurs during the reaction of SO_2 with rubber under the influence of a peroxide, with the formation of rubber sulfones,[16,17] as SO_2 in large quantities is also liberated in the reaction of SO_2Cl_2 with rubber in the presence of the same peroxides as those employed for the SO_2–rubber reaction.

CHLORINATION OF RUBBER HYDROCHLORIDE

The chlorination of rubber in solution leads to partially cyclized chlorinated rubber derivatives, the chlorine being distributed rather at random in the molecule. Rubber hydrochloride, in which the double bonds are saturated by the addition of HCl, seemed a suitable starting material for the production of more precisely defined chlorinated rubber derivatives. It is probable, moreover, that owing to the absence of double bonds only linear, noncyclized molecules of chlorinated rubber are formed.

The chlorine content of the rubber hydrochloride used was 30.1% and it was prepared by dissolving commercial Pliofilm in chloroform and pre-

TABLE VII

CHLORINATION OF RUBBER HYDROCHLORIDE IN A 2.5% CCl_4 SOLUTION WITH CHLORINE GAS

Conditions of light	Time, hrs.	Temp., °C.	% Cl in product
Dark	3	25	35.5
Dark	3	77	44.0
Daylight	3	25	60.0
Daylight	3	77	59.0
Electric 100-watt light	3	20	62.0
Ultraviolet light	3	20	71.5
Ultraviolet light	3	77	69.5

cipitating with alcohol. As a rule 60 cc. of carbon tetrachloride solution in a concentration of 2.5% by weight were used for an experiment. Table VII shows that radiation with light—especially with ultraviolet light—greatly accelerates the reaction,[18] which tends to result in chlorinated rubbers of exceptionally high chlorine contents, comparable with those obtained by direct chlorination of rubber.[1] There were several substances which had an inhibiting effect upon the chlorination at room temperature in daylight, *viz.*, diazoaminobenzene, phenyl β-naphthylamine and tetralin peroxide, in particular. Some degree of inhibition was experienced with oxygen too, which is consistent with its well-known inhibitive effect upon the chlorination of paraffins.[19] Iodine, on the other hand, in amounts as much as 5% relative to the rubber hydrochloride acted catalytically even in the dark, thus promoting chlorination.

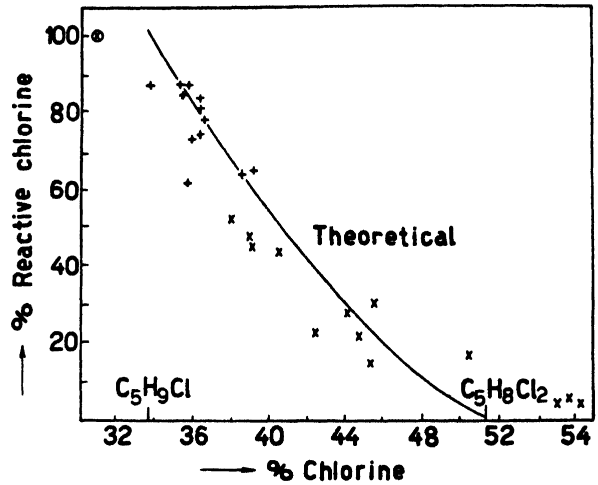

Fig. 1. Relation between chlorine content and percentage of reactive chlorine of chlorinated rubber hydrochloride.

As is evident from Figure 1, the percentage of reactive chlorine, as determined by the aniline test, was found to stand in a striking relation to the chlorine content in chlorination experiments carried out at room temperature. The introduction of a new chlorine atom into rubber hydrochloride stabilizes the chlorine atom already produced by the hydrochlorination. The total amount of the chlorine in rubber hydrochloride is reactive in the aniline test proving that this chlorine is attached to the tertiary carbon atom. By the introduction of a second chlorine atom—which is fully accomplished with a Cl content of 51%—a product is obtained in which both chlorine atoms are stable according to the aniline test. Figure 1 shows the theoretical line calculated on the assumption that every chlorine atom introduced stabilizes a chlorine atom already present. The experimental evidence proves to approximate this line very closely.

In monochloro paraffins the substitution of a second chlorine atom is often directly adjacent to the first.[20] It is also a general rule that secondary carbon atoms are chlorinated more quickly than primary ones.[21] If this is assumed also to hold good for the chlorination of rubber hydrochloride, the structure of a chlorinated rubber hydrochloride with 51% Cl should be mainly as follows:

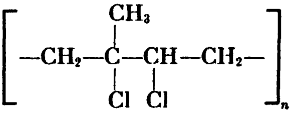

$$\left[-CH_2-\overset{CH_3}{\underset{Cl}{C}}-\underset{Cl}{CH}-CH_2- \right]_n$$

This is the same structure as that of the product obtained from the reaction of SO_2Cl_2 with rubber under the influence of a peroxide. The two products do, in fact, exhibit the same stability toward aniline, whereas the product derived from the direct chlorination of rubber containing 51% of chlorine is reactive to the extent of 45%.

Quite probably, however, the second chlorine atom is not always substituted on the same side to the first one, in which case the structure might be less regular than suggested. There will undoubtedly be some substitution of chlorine at the primary carbon atom (in the methyl group). The substitution of chlorine at the following secondary carbon atom (in the 1,3 position) cannot be ruled out completely, but it is unlikely because the tertiary chlorine atom would then be more reactive in the aniline test than it has in fact been found to be.

STABILITY AND MECHANICAL PROPERTIES

The chemical stability of various products of chlorination is apparent from Table VIII. The evidence of this stability is furnished by the splitting off of the chlorine, not only in the aniline test, but also in the H_2O test. In the latter test 1 g. chlorinated rubber is moistened with 1 cc. alcohol, after which 25 cc. H_2O are added and the whole is heated in a sealed tube to 100°C. for 17 hours. The amount of hydrochloric acid split off is titrated. The recorded percentages of split off chlorine are relative to the total amount of chlorine originally present. It is clear from Table VIII that the aniline and H_2O tests produce correlating figures. The stability of the products of the addition of Cl_2 to rubber with SO_2Cl_2 and peroxide, and that of chlorinated rubber hydrochloride is considerably greater than the stability of the others.

The mechanical properties of products chlorinated by addition depend very much upon the chlorine content. A product of additive chlorination containing 23.5% chlorine (prepared with SO_2Cl_2) was vulcanized for 10 minutes at 110° C., the composition being 100 parts of rubber, 1 part of zinc oxide, 2 parts of sulfur, 1 part of zinc diethyldithiocarbamate, 5 parts of triethylamine, 2 parts of the antioxidant Nonox. The tensile strength of this vulcanizate was 120 kg./cm.^{2}, the elongation at break being 705%. Its swelling in hexane amounted to 150%. After vulcanization, a rubber of

TABLE VIII

Chemical Stability of Various Chlorination Products

Polymer	% Cl in product	% reactive Cl Aniline test	 H_2O test
Chlorinated rubber			
With SO_2Cl_2 + peroxide	47.0	4	0.8
	38.0	5	1.2
	27.0	10	0.3
With SO_2Cl_2 + amine	44.0	71	2.5
With SO_2Cl_2 + amine	29.5	90	7.3
With Cl_2 gas	50.5	58	1.6
Rubber hydrochloride	30.0	100	27
Chlorinated rubber hydrochloride	53.0	6	0.2

this kind with 27.0% of chlorine exhibited 181 kg./cm.^{2} tensile strength, 365% elongation at break, and 45% swelling in hexane. Hence, chlorinated rubber vulcanizates of at least 27% chlorine content may be said to belong to the category of nonswelling rubbers. The recovery after elongation of these rubbers, however, is very slow and they are difficult to vulcanize. Their insufficient stability is an obstacle to their vulcanization at temperatures in the neighborhood of 145°C.

Products of higher chlorine content come into the thermoplastic class of materials. A product containing 38.0% chlorine and compounded in the proportion of 100 parts of chlorinated rubber to three parts of magnesium oxide was pressed at 110°C. to a small sheet having 480 kg./cm.^{2} tensile strength, 850 kg./cm.^{2} flexural strength, and 29 cm. kg./cm.^{2} impact resistance.

One drawback to chlorinated rubber of a chlorine content below 50% for use as a plastic is the comparatively low softening point, which is at about 90°C. Chlorinated rubber hydrochloride with 42 to 52% chlorine is known to possess good film-forming properties.[18,22]

The authors wish to express their thanks to W. H. Manger and J. V. van Ulden for their valuable assistance, to Dr. G. Salomon for his interest and suggestions, and to the Rubber Foundation for permission to publish the results of the investigation.

References

1. G. J. van Amerongen, C. Koningsberger, and G. Salomon, *J. Polymer Sci.*, **5**, 639 (1950).
2. H. J. Schumacher and J. Stauff, *Die Chemie*, **55**, 342 (1942).
3. H. C. Brown, *Ind. Eng. Chem.*, **36**, 785 (1944).
4. J. Peachey, British Patent 121,194 (1918).
5. H. Staudinger and Hj. Staudinger, *J. prakt. Chem.*, **162**, 148 (1943).
6. B. J. Habgood and L. B. Morgan, U. S. Patent 2,170,947 (1939).
7. C. Koningsberger, U. S. Patent, 2,448,809 (1948).
8. M. S. Kharasch and A. T. Read, *J. Am. Chem. Soc.*, **61**, 3089 (1939).
9. J. H. Helberger, *Die Chemie*, **55**, 172 (1942).
10. M. S. Kharasch and H. C. Brown, *J. Am. Chem. Soc.*, **61**, 2142 (1939).
11. A. McAlevy, U. S. Patent 2,405,971 (1946).
12. Badische Anilin und Soda-Fabrik, German Patent 251,100 (1911).

13. M. S. Kharasch and H. C. Brown, *J. Am. Chem. Soc.*, **61,** 3432 (1939).
14. G. F. Bloomfield, *J. Chem. Soc.*, **1944,** 114.
15. M. Trautz, *Z. Elektrochem.*, **35,** 534 (1908).
16. W. L. J. de Nie, U. S. Patent 2,265,722 (1941).
17. W. L. J. de Nie and G. E. Rumscheidt, Netherlands Patent 59,731 (1947).
18. W. M. Kutz, British Patent 544,387 (1942).
19. H. P. A. Groll, G. Hearne, F. F. Rust, and W. E. Vaughan, *Ind. Eng. Chem.*, **31,** 1239 (1939).
20. J. Egloff, R. E. Schaad, and C. D. Lowry, *Chem. Revs.*, **8,** 1 (1931).
21. H. B. Hass, E. T. McBee, and P. Weber, *Ind. Eng. Chem.*, **27,** 1190 (1935); **28,** 333 (1946).
22. J. W. Raynolds and W. M. Kutz, British Patent 542,269 (1942).

English Synopsis, see Summaries, page S13, Vol. V, 1950.

Résumé

Deux méthodes sont discutées pour l'obtention de caoutchoucs chlorés relativement stables, dont la teneur en chlore est comparable à celle du néoprène et du chlorure de polyvinyle. Une de ces méthodes est basée sur la chloruration, par addition, du caoutchouc à l'aide du chlorure de sulfuryle. Des expériences avec du guttapercha, utilisé comme substance-modéle pour le caoutchouc naturel, démontrent que la présence de substances organiques azotées, telles que des amines, induisent une chloruration par substitution. D'autre part, les peroxydes donnent des réactions en chaînes, qui amènent finalement à la formation d'un produit d'addition. Certains anti-oxydants, tels la di-*t*-amylhydroquinone ou le β-naphthol, agissent comme inhibiteurs de chaînes efficaces. De nombreux hydroperoxydes, tels l'hydroperoxyde de la tétraline et l'hydroperoxyde *t*-butyle, sont des catalyseurs utiles pour la chloruration par addition du caoutchouc naturel au moyen de chlorure de sulfuryle. Ces catalyseurs l'emportent apparemment sur les contaminations naturelles du caoutchouc naturel, qui favorisent la substitution. Les dérivés du caoutchouc, qui contiennent jusqu'à 47% de chlore, surtout par addition, ont été produits au départ de caoutchouc ordinaire non-purifié. L'autre méthode d'obtention de caoutchoucs chlorés consiste dans la chloruration du chlorhydrate de caoutchouc. Cette chloruration est accélérée par exposition à la lumière, spéciallement à la lumière ultra-violette. On a obtenu ainsi des produits contenent jusqu'á 70% de chlore. L'analyse cinétique montre que le chlorhydrate du caoutchouc chloré, contenant approximativement 50% de chlore, possède probablement une structure peu différente des produits d'addition du chlore au caoutchouc au moyen de chlorure de sulfuryle. Les propriétés mécaniques des divers produits ont été discutées brièvement. Les dichlorures de caoutchouc non-saturé, contenant environ 25% de chlore sont caoutchouteux, et se prètent à la vulcanisation en donnant des produits, gonflant faiblement dans les hydrocarbures. Les dichlorures contenant environ 50% de chlore sont thermoplastiques.

Zusammenfassung

Zwei Methoden zur Herstellung von verhältnismässig haltbarem chlorierten Kautschuk mit einem Chlorgehalt, der mit dem von Neopren und Polyvinylchlorid verglichen werden kann, werden diskutiert. Einer dieser Methoden liegt die Chlorierung (Addition) von Kautschuk mit Hilfe von Sulfurylchlorid zu Grunde. Experimente mit gereinigtem Gutta-percha, das als Modelsubstanz für natürlichen Kautschuk dient, zeigte dass die Gegenwart von stickstoffhaltigen organischen Substanzen wie Amine eine substituierende Chlorierung hervorruft. Peroxyde dagegen bewirken eine Kettenreaktion, welche letzten Endes zu einem Additionsprodukt führt. Einige Antioxydationsmittel wie di-*t*-Amylhydrochinon oder β-Naphtol wirken als wirksame Ketteninhibitoren. Mehrere Hydroperoxyde, *z.B.* Tetralinhydroperoxyd und *t*-Butylhydroperoxyd, sind nützliche Katalisatoren für die additive Chlorierung von natürlichem Kautschuk mit SO_2Cl_2. Diese Katalisatoren haben offenbar die Oberhand über die natür-

lichen Verunreinigungen von natürlichem Kautschuk, welche die Substitution begünstigen. Kautschukderivate, die bis 47% Chlor, meist additiv, enthalten, wurden aus gewöhnlichem, ungereinigten Kautschuk hergestellt. Die andere Herstellungsmethode für chlorierten Kautschuk besteht in der Chlorierung von Kautschukhydrochlorid. Diese Chlorierung wird durch Einfluss von Licht, besonders von ultraviolettem Licht, beschleunigt. Produkte mit bis zu 70% Chlorgehalt wurden erhalten. Begründet auf der kinetischen Chloranalyse wird angenommen, dass chloriertes Kautschukhydrochlorid mit ungefähr 50% Chlorgehalt wahrscheinlich eine Struktur besitzt, die nicht sehr verschieden von der Struktur von Produkten der Chloraddition an Kautschuk mittels SO_2Cl_2 ist. Die mechanischen Eigenschaften verschiedener Produkte werden kurz diskutiert. Ungesättigte Kautschukdichloride mit ungefähr 25% Chlorgehalt sind kautschukartig und eignen sich zur Vulkanisation, wobei sie Produkte mit wenig Quellungstendenz in Kohlenwasserstoffen geben. Kautschukdichloride mit ungefähr 50% Chlorgehalt sind thermoplastisch.

Received August 24, 1949

JOURNAL OF POLYMER SCIENCE VOL. V, NO. 6, PAGES 667–672

Potassium Ferricyanide–Diazothio Ether–Mercaptan Recipe for Emulsion Polymerization of Butadiene and Styrene. III. Determination of *p*-Methoxyphenyl Diazothio-(2-naphthyl)-ether*

I. M. KOLTHOFF, W. J. DALE, and I. K. MILLER, *School of Chemistry, University of Minnesota, Minneapolis, Minnesota*

Suitable diazothio ether recipes have been given for polymerizations at 40° and at ice temperatures,[1] and the effect of several chemical variables in the recipe has been reported.[2] In the present paper, a method is described for the determination of MDN in solution and in latex. Originally, it was planned to use this method for the determination of the rate of disappearance of *p*-methoxyphenyl diazothio-(2-naphthyl)-ether (MDN) during the polymerization. However, since further work on the recipe was discontinued, we did not apply the method to a study of dissipation of MDN during the polymerization.

OUTLINE OF THE METHODS

The methods for the quantitative determination of MDN are based on the following series of reactions:

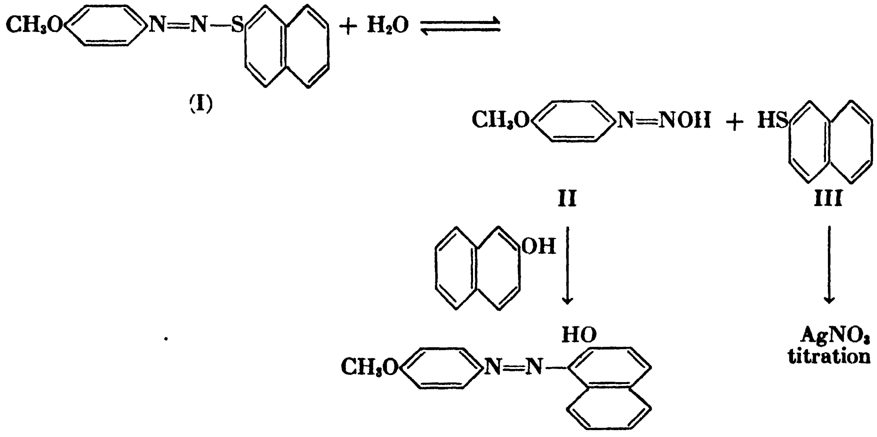

IV (red dye)

---

* This investigation was carried out under the sponsorship of the Office of Rubber Reserve, Reconstruction Finance Corporation, in connection with the U. S. Government Synthetic Rubber Research Program.

The hydrolysis of I to give II and III is facile and reversible, and since thio-beta-naphthol is a relatively strong acid, the equilibrium is displaced toward the right by addition of base. Thus, MDN reacts with silver nitrate just as do mercaptans; it can be titrated in ammoniacal solution by the amperometric method, using a platinum microwire electrode.[8] If a mercaptan is also present, the titration gives the sum of amounts of MDN and mercaptan. The colorimetric method (see below) then gives the amount of MDN and, by difference, the quantity of mercaptan present can be calculated.

In the colorimetric method, the diazonium fragment II is irreversibly coupled with beta-naphthol in basic solution to give the dye IV. The amount of MDN present is then determined with the aid of a spectrophotometer at the isobestic point, 469 mμ. An empirical factor corrects for the MDN decomposed during the dye formation. The precision of the colorimetric method is about 1% in benzene and only about 2% in latex.

TITRATION OF MDN WITH SILVER NITRATE

Discussion. MDN is unstable to heat and light and readily decomposes in polar solvents such as alcohols. When solutions of MDN in ethanol were titrated amperometrically with silver nitrate, it was found that the titer decreased with time of standing. It was concluded that the thio-beta-naphthol formed by solvolysis in protic solvents is further oxidized by oxygen from the air to dinaphthyl disulfide, the oxidation being faster in ammoniacal solutions than in neutral solutions. In the absence of air, this decrease in titer was greatly reduced.

The above conclusion was substantiated by titration of alcoholic solutions of thio-beta-naphthol, aqueous ammonium hydroxide being added just before the end point. The neutral alcoholic solutions of thio-beta-naphthol showed a significant decrease in titer when titrated at 15 minute intervals.

The presence of ferrous iron in the ammoniacal solution retarded the oxidation, but more satisfactory results were obtained using a back-titration procedure. A sample of thio-beta-naphthol was added to ethanol containing an excess of silver nitrate, and the excess silver was titrated in ammoniacal medium with a standard solution of *n*-dodecyl mercaptan. After addition of the excess silver, the rate of air oxidation of the thio-beta-naphthol became very small.

Since thio-beta-naphthol is a hydrolysis product of MDN, it was to be expected that MDN can be titrated in the same way. This was confirmed experimentally.

Procedure. The following solutions were used:

Silver nitrate in water. (0.841 g./liter). In this concentration, 1 ml. is equivalent to 1 mg. *n*-dodecyl mercaptan.

n-Dodecyl mercaptan in ethanol. The solution used contained 0.746 g./liter.

MDN in benzene. A 1–1.5 g. sample was contained in one liter of benzene solution; freshly prepared solutions were used.

5 ml. MDN solution was added to 100 ml. ethanol containing 10 ml. standard silver nitrate solution. To this, 2 ml. concentrated ammonia was added and the solution was titrated with standard mercaptan solution. The weight of MDN present was then calculated from the silver nitrate used. The following data, obtained with a sample of MDN several weeks old, show the precision of the method:

MDN added, g./liter	MDN found, g./liter	Recovery, %
1.461	1.431	98.0
	1.425	97.6
1.461	1.431	98.0
	1 427	97.7

Although MDN decomposes slowly even in benzene solution, a very carefully purified sample of MDN analyzed 99.6% pure when titrated by this procedure.

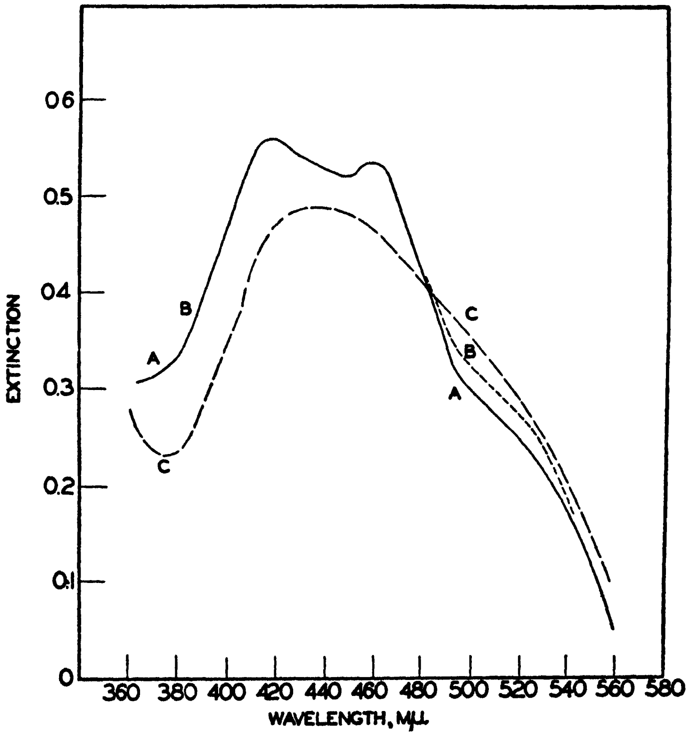

Fig. 1. Extinction of dye, IV, in ethanol-butanol (1:1). A, neutral; B, 0.05 N H_2SO_4; C, 0.01 N NaOH.

COLORIMETRIC DETERMINATION

Discussion. A pure sample of the dye IV, 1-(*p*-methoxyphenylazo)-2-naphthol, was prepared and its absorption spectrum was measured in ethanol-butanol solutions, using a Beckman spectrophotometer. As Figure 1 shows, the extinction of the dye is the same in acid and neutral solutions up to 480 mμ; it is unaffected by long standing in solutions of various *p*H. The extinction is also unchanged by presence of soap (which is present in latex), but water was found to affect the absorption at all wave lengths except at 469 mμ. The graphic determination of the isobestic point is illustrated in Figure 2.

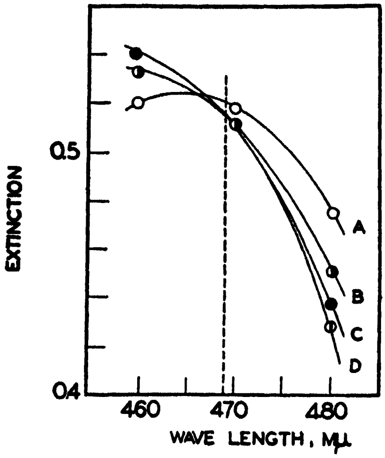

Fig. 2. Effect of water on extinction of dye, IV, near isobestic point. A, 25% H_2O; B, 6% H_2O; C, 2% H_2O; D, 0% H_2O.

The specific extinction was determined at the isobestic point with ethanol–butanol mixtures as solvent. The solution contained 2% water and was 0.05 *N* in acetic acid. The slit width was 0.2 mm. (The ratio of ethanol to butanol does not affect the extinction; such a mixture results from the coagulation of latex in butanol and dilution of subsequent filtrates with ethanol to volume.) Beer's law was found to hold at 469 mμ; the specific extinction was found to be 51.0 ± 0.1.

Although dye formation is carried out in diffuse light, not all of the MDN is converted to the stable dye due to the occurrence of side reactions. The following procedure gave consistently 91% (±1%) formation of the theoretical amount of dye, and this figure is used as an empirical factor in the calculation. The extinction divided by the extinction coefficient gives the weight of dye per liter.

MDN and its thermal decomposition products absorb only in the ultraviolet and hence do not interfere in the determination.

Procedures. The following reagents were used:

Ethanol
Butanol

Glacial acetic acid
Solution of beta-naphthol in butanol; a fresh solution containing 4.5 g. in 50 ml.
Solution of 1 *N* sodium hydroxide
Solution of sodium sulfite in water containing 1 g. in 100 ml.
Solution of zinc chloride containing 1 g. in 100 ml. and enough hydrochloric acid was added to clear the solution.

DETERMINATION OF MDN DISSOLVED IN BENZENE

A solution of MDN in thiophene-free benzene, containing about 0.15 g. in 250 ml., was prepared. To a mixture of 100 ml. butanol, 5 ml. water, 5 ml. sodium hydroxide, and 2 ml. beta-naphthol solution, was added a known volume (5–10 ml.) MDN solution. The mixture was stirred for one minute and allowed to stand for two hours in diffuse light. A blank was run at the same time. At the end of the two hour period, 3 ml. glacial acetic acid was added, together with 40 ml. ethanol. The acidified solution was diluted to volume with ethanol and the extinction was measured against the blank at the isobestic point, 469 mμ. The calculation is illustrated in Table I.

TABLE I

Colorimetric Analysis of Benzene Solutions of MDN
(Extinction Coefficient = 51.0)

Analysis	A	A	B	B	C	C
Extinction	0.610	0.608	0.609	0.603	0.128	0.132
Dye, g./liter	0.0120	0.0119	0.0119	0.0118	0.00251	0.00259
Volume, liters	0.5	0.5	0.25	0.25	0.25	0.25
MDN found, g.	0.00695	0.00690	0.00345	0.00342	0.000727	0.000752
MDN taken, g.	0.00692	0.00692	0.00346	0.00346	0.000692	0.000692
Error, %	+0.4	−0.3	−0.3	−1.2	+5.3[a]	+8.5[a]

[a] Actually, at this low extinction, the precision of the reading is only 4% instead of 1% at extinctions between 0.4–0.9.

DETERMINATION OF MDN IN LATEX NOT CONTAINING OXIDATIVE ACTIVATOR OR HYDROXYAROMATICS (SHORT-STOPS)

A 5–10 g. sample of latex was introduced dropwise into a vigorously stirred solution of 5 ml. water in 100 ml. butanol. The fine coagulum was stirred for 2 minutes, when 3 ml. beta-naphthol solution was added, followed by 5 ml. hydroxide solution. Stirring was continued for 2 minutes. The mixture was allowed to stand for 2 hours, and, after acidification as above, the rubber was removed by filtration through a cotton plug into a volumetric flask. The filtrate was diluted to volume with ethanol and the extinction was measured at the isobestic point.

A known amount of a benzene solution of MDN was added to a known weight of latex of 80% conversion. (No activator was present; the latex was prepared with peroxide-containing soap.) The mixture was shaken vigorously and analyzed for MDN according to the above procedure. About 94% of the MDN was consistently found back in a set of five experiments involving different amounts of MDN. Since the MDN was decomposed in part on shaking with the latex and since coprecipitation with the coagulum is probable, the figure of 93–94% is considered satisfactory for practical purposes.

When ferricyanide is present, the procedure is similar to the above, except that the ferricyanide is reduced by sulfite, and the ferrocyanide is precipitated as the zinc salt. After coagulation of the latex, 5 ml. sodium sulfite solution is added, and 1 ml. zinc chloride. After 2–3 minutes, the beta-naphthol and base are added and the mixtures are treated as above, except filtration of the dye–rubber mixtures is accomplished with filter paper to remove the flocculent zinc salt. Analyses of MDN in benzene solutions with ferricyanide added to the ethanol accounted for 100% of the added amount of MDN. In latex only about 94% of the MDN was found.

References

1. I. M. Kolthoff and W. J. Dale, *J. Polymer Sci.*, **3**, 400 (1948).
2. I. M. Kolthoff and W. J. Dale, *ibid.*, **5**, 301 (1950).
3. I. M. Kolthoff and W. E. Harris, *Ind. Eng. Chem.*, *Anal. Ed.*, **18**, 161 (1946).

English Synopsis, see Summaries, page S14, Vol. V, 1950.

Résumé

Les méthodes de détermination de l'éther *p*-méthoxyphenyl-diazothio-(2-naphtyl-) (MDN) en solution benzènique ou dans un latex sont décrites par titrage ampérométrique au nitrate d'argent, ou au moyen d'un spectrophotomètre après transformation en un colorant stable.

Zusammenfassung

Es werden Methoden angegeben zur Bestimmung von *p*-Methoxyphenyl-diazothio-(2-naphtyl)-Äther (MDN) in Benzollösung und in Latex durch amperemetrische Titration mit Silbernitrat oder mit Hilfe eines Spektrophotometers nach Umwandlung in einen haltbaren Farbstoff.

Received September 2, 1949

JOURNAL OF POLYMER SCIENCE VOL. V, NO. 6, PAGES 673-686

Heterogeneous System for Polymerization of Vinyl Chloride

J. B. O'HARA* and C. F. PRUTTON,† *Case Institute of Technology, Cleveland, Ohio*

INTRODUCTION

In the search for new methods of polymerization, a process has been developed by W. Heuer[1] to the extent that it was patentable. In this process various monomers such as vinyl chloride, vinyl methyl ether, ethylene oxide, or butadiene "were bubbled in the form of a gas in a fine state of subdivision through a liquid essentially incapable of dissolving the monomer, with a polymerization catalyst being contained in the liquid." It was claimed that a polymer of good characteristics was obtained. In spite of the claims made for the process and its products, no case of its industrial use is known.

Because this process represents a novel way of preparing polymeric materials and no quantitative data have been published relative to the exact nature of the polymer formed, the yields to be expected, or the effects of the variables such as monomer rate, catalyst concentration, temperature, and pressure on the yield or nature of the resulting polymer, it appeared to be of definite interest to investigate the process both from an academic point of view and to answer the questions which arose as to its possible commercial applications. From the nature of the process it was evident that it would lend itself readily to continuous operation with a minimum of complicating factors which would offer a distinct economic advantage over a batch process.

HISTORICAL

The bulk of the limited information pertaining to this type of process has appeared in the patent literature.

I. G. Farbenindustrie obtained patents in the United States,[1] Holland,[2] and France[3] in which this process was described. The author of the American patent claimed that an extraordinarily stable emulsion of polyvinyl chloride was obtained, which when coagulated, washed, and dried, showed good solubility properties and had the properties of a relatively highly polymerized polyvinyl chloride.

In spite of the fact that I. G. held the patents on the process, recent reports on the production of plastics in Germany[4] make no mention of its use for the production of polyvinyl chloride. A recent review on polymerization also completely ignores the existence of this method for the preparation of polymers.[5]

---

* Present address: Missouri School of Mines and Metallurgy, Rolla, Missouri.

† Present address: Mathieson Chemical Corporation, Baltimore, Md.

A recent patent[6] describes a process which has a great deal in common with the aforementioned method except that it covers the polymerization of ethylene and operates at elevated temperatures and pressures.

DESCRIPTION OF APPARATUS

The polymerization reaction took place in a jacketed glass tube 62 inches in length and 40 mm. in diameter, equipped with a stopcock at the bottom (Fig. 1). The heating jacket was a glass tube concentric with the reaction tube and was $57^1/_2$ inches long and 65 mm. in diameter. These two concentric tubes were fastened at top and bottom by means of ring seals.

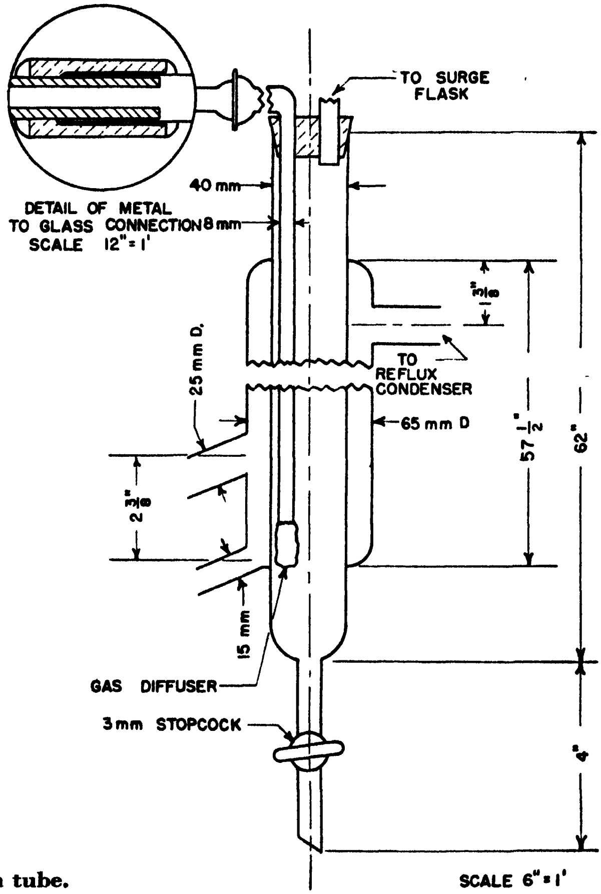

Fig. 1. Detail of reaction tube.

The source of heat to the reaction tube consisted of condensing vapors, the vapors being generated in a three-necked one-liter flask which was connected to the heating jacket by means of two side-arms located in the lower portion of the heating jacket. The upper side-arm served as a vapor line and the lower one served as a condensate return line. The condensate return line terminated at a point below the surface of the liquid in the reboiler flask, providing a liquid seal which prevented any vapor from rising through this line. The connections from the reboiler flask to the side-arms were made by means of ground-glass joints, both standard taper and ball and socket joints being used for this purpose, the ball and socket joints being inserted in the lines to provide flexibility and ease in assembling and disassembling.

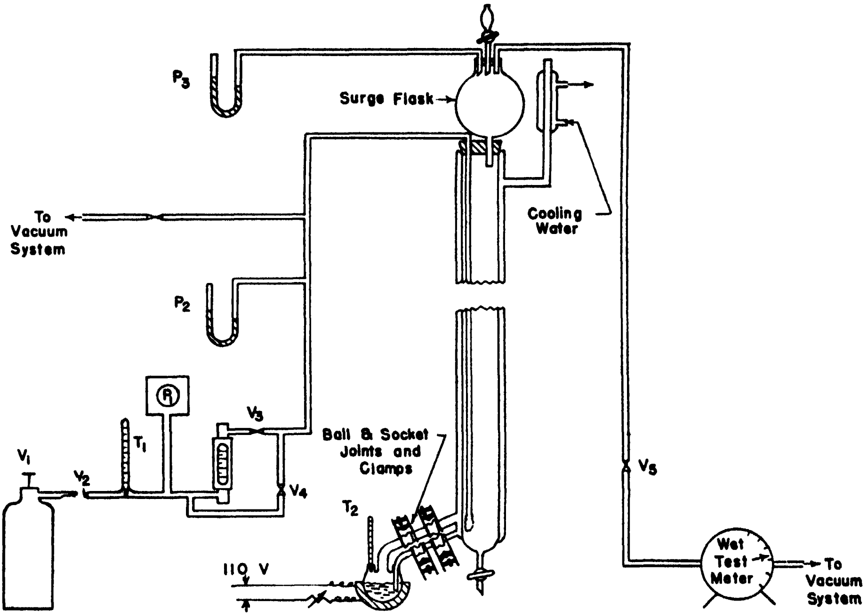

Fig. 2. Sketch of apparatus.

A third side-arm was located $1^3/_8$ inches from the top ring seal in the heating jacket. A water-cooled condenser was placed in a ground glass joint at the top of this side-arm, serving as a reflux condenser for the heating medium.

The auxiliary equipment is shown schematically in Figure 2 and pictorially in Figure 3. The vinyl chloride was contained in a stainless steel cylinder which was connected to a $^1/_4$ inch stainless steel line. All valves were $^1/_4$ inch stainless steel needle valves. A vent line was placed between valve V_3 and the reaction tube, the line being vented to a system at a vacuum of approximately 5.5 inches of water.

The connection from the stainless steel pipe to a glass line terminating in a sintered glass diffuser at the base of the reaction tube was made by means of a ball and socket joint. The details of the connection are shown in Figure 1. The male portion of the joint was slipped over the pipe and then a piece of pressure tubing forced over it, with the ends of the pressure tubing being sealed to the glass and pipe by means of Saureisen cement.

The female portion of the ball and socket joint was sealed to a line of 8 mm. glass tubing 66 inches long, at the end of which was a sintered glass diffuser, extra coarse grade. The diffuser served to break the gas into fine bubbles as it entered the reaction zone. This line containing the diffuser was placed directly in the reaction tube and terminated at a point 2 inches above the drainage stopcock at the bottom.

A surge flask, made by sealing a 16 mm tube $7^1/_2$ inches long to the bottom of a three-liter round-bottom flask, was placed in the rubber stopper used to seal the reaction flask. This was used so that if foaming occurred, the foam would rise in the surge flask. By this means the full capacity of the reaction tube could be used, rather than allowing space for foaming action in the reaction tube itself. In addition to the gas outlet line and a line to the reaction-pressure manometer, a 250 ml. separatory funnel was inserted in the top of the surge flask so that catalyst solution could be added while the monomer was flowing without leakage.

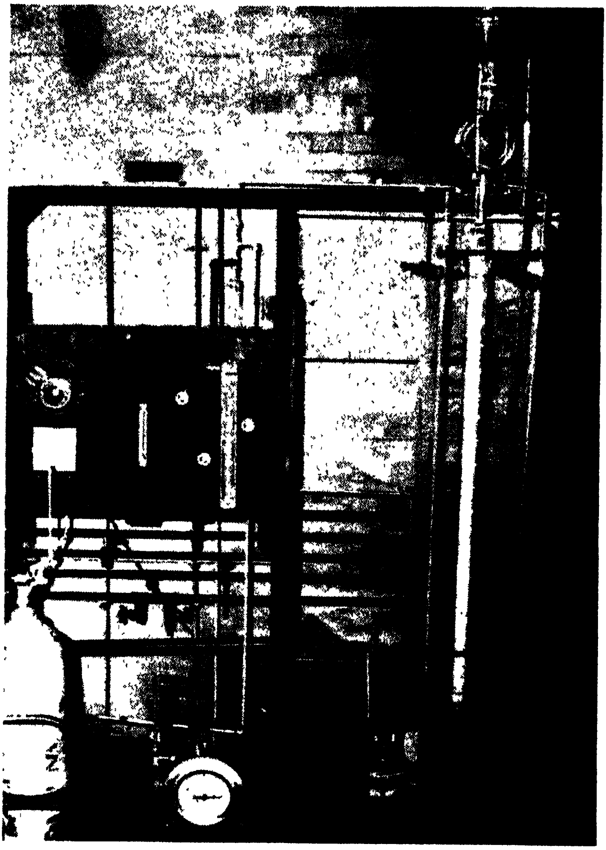

Fig. 3. Picture of apparatus.

PROCEDURE

The Flowrator was calibrated by means of a wet test meter maintaining the gas pressure at 10 p.s.i.g.

In each run the catalyst solution consisted of 1850 grams of doubly distilled water plus sufficient potassium persulfate to yield a solution of the desired concentration.

In making a run, 1400 grams of water were charged to the reaction tube. The heat was then turned on the reboiler which contained a heat transfer medium possessing the desired boiling point. The required amount of potassium persulfate (CP grade) was then weighed into a one-liter flask. To this was added 350 grams of the doubly distilled water, the flask stoppered and shaken to dissolve the catalyst. A third quantity of water, 100 grams, was weighed into another flask. The three portions of water totaled the desired 1850 grams.

When the heat transfer medium was condensing in the reflux condenser, the flow of vinyl chloride was started. The impurities present in the vinyl chloride were reported by Glenn L. Martin Co., the supplier, to be: aldehydes, nil; HCl, 0.01%; C_2H_2, 0.001%; H_2O, 0.5%; and nonvolatiles, 0.01%. The cylinder containing 60 pounds of vinyl chloride also contained 35 grams of phenol as an inhibitor. The phenol was assumed to remain in the cylinder when the flash vaporization of vinyl chloride from the cylinder took place.

When the rate of flow of vinyl chloride had been regulated to the desired value, the solution of potassium persulfate, which had been heated to approximately the reaction temperature, was added to the reaction tube through the separatory funnel. After adding the catalyst solution, the additional 100 grams of water, which had also been heated to approximately the reaction temperature, was used in two 50 cc. portions to wash out the flask used in preparation of the catalyst solution to be sure that all of the catalyst found its way into the reaction tube.

At periodic intervals samples were withdrawn from the reaction tube by draining some of the reaction mass through the stopcock located at the bottom of the reaction tube. To take a sample a 5–10 cc. portion of the material was first drained to ensure that a stagnant portion of the reaction mass was not obtained and then a 10–15 cc. sample was removed in a glass-stoppered sample bottle. This sample was then analyzed according to the procedure described in the following section

In the run at elevated pressure the procedure was the same as just described except that the pressure above the reaction mass was maintained at 5 inches of Hg gage by manipulation of valve V_5 and the catalyst solution had to be forced in with air pressure.

The heat transfer mediums and their boiling points as read by T_2 are given in Table I.

TABLE I

HEAT TRANSFER MEDIUMS USED AND THEIR BOILING POINTS

Heat transfer medium	Boiling point, °C.
Methylene chloride	40.0
Tertiary butyl chloride	46.0
Carbon disulfide	50.5
Acetone	56.0
Methyl alcohol	65.0

METHOD OF ANALYSIS

To determine the rate of reaction and the nature of the polymer formed, the percent solids of the samples and the specific viscosities of 0.4% solutions of polymer in nitrobenzene at 35 ± 0.02°C. were determined.

To determine the per cent solids, samples of the latex were dried in a natural circulation drying oven equipped with a thermoregulator which maintained the temperature at 39–41°C. This low temperature for drying was found necessary due to discoloration of the polymer at higher temperatures. Each sample was allowed to dry at least four days. All weighings were made on an analytical balance.

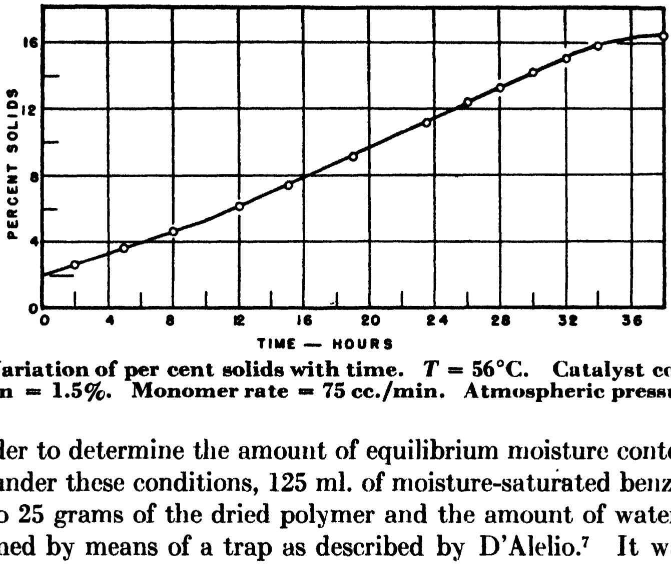

Fig. 4. Variation of per cent solids with time. $T = 56°C$. Catalyst concentration = 1.5%. Monomer rate = 75 cc./min. Atmospheric pressure.

In order to determine the amount of equilibrium moisture content when drying under these conditions, 125 ml. of moisture-saturated benzene were added to 25 grams of the dried polymer and the amount of water present determined by means of a trap as described by D'Alelio.[7] It was found that the equilibrium moisture content was 1.2%.

To determine specific viscosities, a 0.4% solution of washed, dried polymer was prepared, and allowed to stand overnight to ensure complete solution. The viscosities were run at 35.0 ± 0.02°C. using an Ostwald-Fenske type viscometer, the efflux time being of the order of 75–85 seconds. Check readings of 0.2 second were obtained in each case.

DATA AND RESULTS

Exploratory investigations of the process indicated that a reasonable rate of polymerization could be obtained when vinyl chloride was bubbled through an aqueous solution of potassium persulfate at 50–60°C. and that the process would lend itself readily to an investigation of the effects of the variables temperature, monomer rate, catalyst concentration, and pressure on rate of polymerization and nature of the polymer formed.

To determine the manner in which the rate of polymerization varied with time, a run was made using $1^1/_2$% potassium persulfate solution at 56°C., monomer rate of 75 cc./min., and atmospheric pressure. The variation of per cent solids of the catalyst solution with time is presented in Figure 4. In this and all subsequent data, the rate of monomer flow is expressed in cubic centimeters per minute at standard conditions of 0 °C. and 760 mm. Hg. From the results of this run it was found that the amount of polymer formed varied linearly with time over a considerable time interval. On the basis of this information it was decided to make the succeeding runs of approximately twelve hours duration.

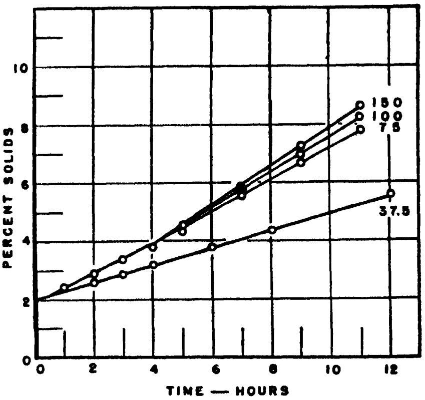

Fig. 5. Variation of per cent solids with time with monomer rate (in cc./min.) as the parameter. T = 56°C. Catalyst concentration = 2%. Atmospheric pressure.

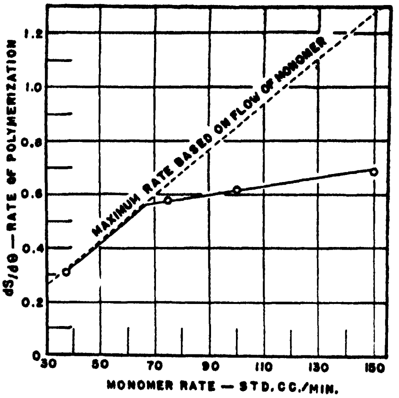

Fig. 6. Rate of polymerization as a function of monomer rate. T = 56°C. Catalyst concentration = 2%. Atmospheric pressure.

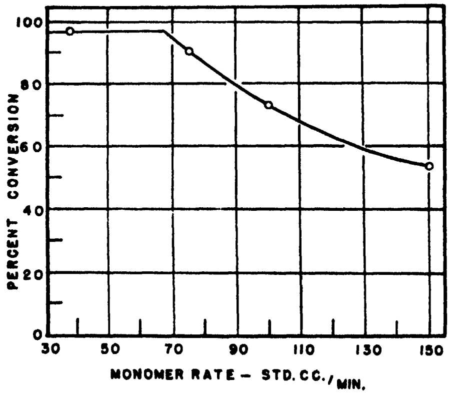

Fig. 7. Per cent conversion of vinyl chloride as a function of monomer rate. T = 56°C. Catalyst concentration = 2%. Atmospheric pressure.

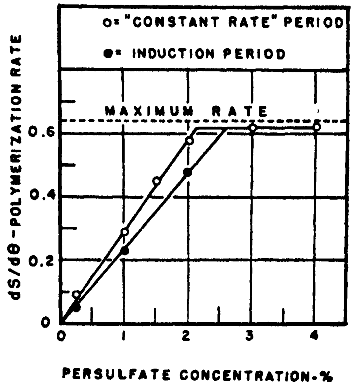

Fig. 8. Rate of polymerization as a function of catalyst concentration. T = 56°C. Monomer rate = 75 cc./min. Atmospheric pressure.

To study the effect of monomer rate on the rate of polymerization the catalyst concentration, temperature, and pressure were maintained constant while the monomer addition was varied. The results of varying the monomer rate fourfold are shown graphically in Figures 5 and 6. From the slope of the lines in Figure 5, $ds/d\theta$ was evaluated for each run, where

s is the per cent solids and θ is the time in hours. These values of $ds/d\theta$ are shown in Figure 6. The effect of monomer rate (R) on the per cent conversion is given in Figure 7, in which the per cent conversion was calculated as:

$$\frac{(ds/d\theta)_{actual}}{(ds/d\theta)_{max.}} \times 100$$

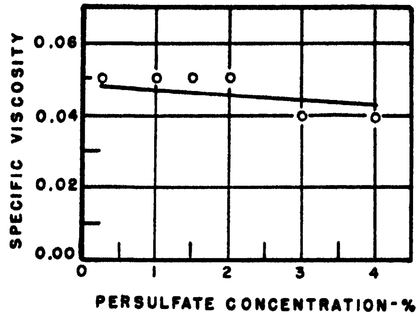

Fig. 9. Specific viscosity as a function of catalyst concentration. Reaction $T = 56°C$. Monomer rate = 75 cc./min. Atmospheric pressure.

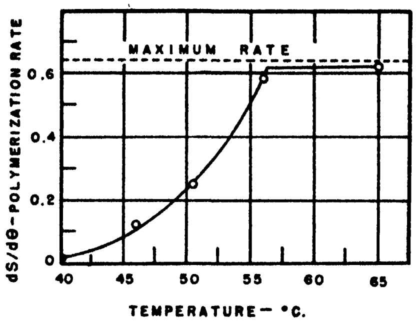

Fig. 10. Rate of polymerization as a function of temperature. Catalyst concentration = 2%. Monomer rate = 75 cc./min. Atmospheric pressure.

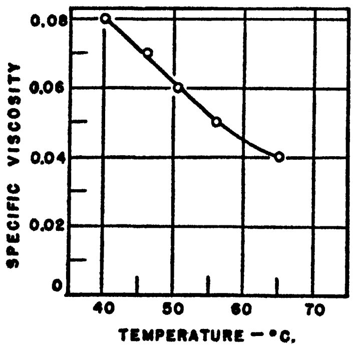

Fig. 11. Specific viscosity as a function of reaction temperature. Catalyst concentration = 2%. Monomer rate = 75 cc. per min. Atmospheric pressure.

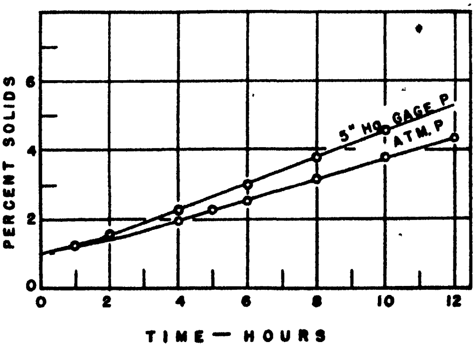

Fig. 12. Effect of pressure on reaction. $T = 56°C$. Catalyst concentration = 1%. Monomer rate = 75 cc./min.

and $(ds/d\theta)_{max.}$ was calculated from the rate of monomer addition based on the fact that if all of the monomer added polymerized, a maximum value of $ds/d\theta$ would be obtained.

Similarly, the effects of temperature (T), catalyst concentration (c) and pressure (P) were investigated by keeping all variables with the exception of the one being studied constant. In all cases the graphs of per cent solids *vs.* time consisted of two intersecting straight lines, with the point of intersection corresponding to the termination of the induction period.

The results are shown graphically in Figures 8–12. The investigation of the effect of pressure on the reaction was limited by the fact that the equipment was constructed of glass so that the investigation over a wide pressure range was not practical.

TABLE II

SUMMARY OF EFFECT OF REACTION VARIABLES ON SPECIFIC VISCOSITIES OF 0.4% SOLUTIONS OF POLYMER IN NITROBENZENE AT 35.0 ± 0.02°C., RATES OF REACTION AND PER CENT CONVERSION OF VINYL CHLORIDE

Catalyst concn., %	Temp., °C.	Monomer rate, std. cc./min.	Reaction pressure, in. Hg gage	Specific viscosity	Rate of reaction $ds/d\theta$	Per cent conversion of vinyl chloride
0.25	56	75	0	0.05	0.09	14.1
1.0	56	75	0	0.05	0.29	45.3
1.5	56	75	0	0.05	0.45	70.4
2.0	56	75	0	0.05	0.58	90.6
3.0	56	75	0	0.04	0.62	96.9
4.0	56	75	0	0.04	0.62	96.9
2.0	40	75	0	0.08	0.016	2.5
2.0	46	75	0	0.07	0.12	18.8
2.0	50.5	75	0	0.06	0.25	39.1
2.0	56	75	0	0.05	0.58	90.6
2.0	65	75	0	0.04	0.62	96.8
2.0	56	37.5	0	0.05	0.31	97.0
2.0	56	75	0	0.05	0.58	90.5
2.0	56	100	0	0.05	0.62	73.0
2.0	56	150	0	0.05	0.69	53.8
1.0	56	75	0	0.05	0.29	45.3
1.0	56	75	5	0.05	0.39	60.9

A summary of the effects of the variables on rate of reaction, conversion of vinyl chloride to polymer, and specific viscosity of the polymer is presented in Table II.

DISCUSSION

General

The inhibition period, if any, was short. In general, five to fifteen minutes after the start of a run the catalyst solution began to become turbid. With 2% persulfate solution the turbidity had increased within a half hour to the point where the solution had the appearance of milk. The time required to reach this point depended primarily on the catalyst concentration and temperature, decreasing with increasing values of these variables.

No mechanical agitation was required, for as the gas rose rapidly in the tube in the form of small bubbles it provided an efficient means of agitation.

To check the homogeneity of the emulsion and the accuracy of the method of sampling the following procedure was used. At the end of the run a sample was withdrawn in the usual manner from the stopcock at the bottom of the reaction tube. The tube was immediately drained and a second sample withdrawn when approximately half of the emulsion had been removed. The samples were then analyzed for the solids content. In two of the three cases where this procedure was used the checks were exact, while in the third the difference amounted to 0.01%. This indicates that the samples withdrawn in the manner previously described were representative of the latex.

An interesting sidelight is the stability of the emulsions obtained. An emulsion prepared in this way using a 2% persulfate solution as the catalyst has maintained its stability for a full year. The *p*H values of these emulsions, in general, lie in the range 1.5–2.0. They have withstood freezing and heating without breaking down and are stable a considerable period of time after adding salt.

A comparison of the specific viscosities of the polymers obtained in this study with commercial polyvinyl chlorides indicates that the molecular weights obtained are far below the values normally used for general plastic work such as molding and fiber formation. Marvinol (Glenn L. Martin Co.) and Geon (B. F. Goodrich Co.) showed specific viscosities of about 0.55 while the polymer prepared by the method described here yielded specific viscosities of 0.04–0.08 under the same conditions. However, low molecular polyvinyl chlorides have been used for protective coatings[8,9] and impregnating materials,[8] so the process is not without promise.

Variation of Reaction Rate with Time

An examination of Figure 4 provides some interesting information about the course of the reaction. The presence of an apparent inhibition period of 5–15 minutes duration at the start of the reaction has already been mentioned. After the reaction begins, a period of constant rate of reaction occurs which, in the case represented by Figure 4, lasted for about three hours. This may be called an induction period, for at the end of this time the rate of reaction increases, probably due to the fact that at that time the concentration of activating agents has reached a value such that it is capable of maintaining the higher rate of reaction. In this discussion the end of the induction period will be considered as the point of intersection of the two straight lines, one line representing the induction period and the other to be termed the "constant-rate" period, although it is recognized that the rate during the induction period is also constant within the limits of accuracy of the experimental methods used. At the end of approximately 24 hours the rate of polymerization begins to drop off, probably due to a decrease in the concentration of the activating agents because of the amount of catalyst decomposed.

Effect of Monomer Rate

The effect of varying the rate of addition of monomer while maintaining the catalyst concentration, temperature, and pressure constant is shown in Figures 5 and 6. For monomer rates of 75, 100, and 150 cc./min., it is seen that the rate of reaction during the induction period is independent of the monomer rate, and also that the length of the induction period is the same in the three cases. However, the rates of reaction $ds/d\theta$ are different during the constant-rate period, being greater for the higher flow rates. The apparent large discrepancy between the rate of reaction at the flow rate of 37.5 cc./min. and the rates at higher flows, plus the fact that no induction period was observed at 37.5 cc./min. may be explained after an examination of Figure 6, in which the rates of reaction as obtained from the slopes of the lines in Figure 5 are plotted. In Figure 6 the broken line represents the maximum rate of reaction based on the flow of vinyl chloride. It is seen that at a monomer rate of 37.5 cc./min. essentially complete reaction is obtained. On the basis of this information the absence of an induction period at a flow rate of 37.5 cc./min. may be explained as being due to the fact that the concentration of activating agents is sufficient, even in the early stages of the reaction, to cause complete polymerization of the vinyl chloride. Also, from Figure 6, it is seen that below a certain rate of flow, which under the conditions of catalyst concentration, temperature, and pressure used here is approximately 67 cc./min., essentially complete reaction takes place. Above this critical flow rate the rate of reaction is a function of the monomer rate, the relation being essentially linear. The factor controlling this critical flow rate is probably the rate at which the monomer can be activated in the reaction mass.

The per cent conversion for the constant-rate period is shown in Figure 7. As has been noted, at a flow rate of 37.5 cc./min., the reaction is, to all intents and purposes, complete. The per cent conversion remains high (95–100%) as long as the monomer rate is below the value of 67 cc./min. As the monomer rate is further increased the conversion drops off very rapidly, until at 150 cc./min. it is about 54%. Thus, while at high monomer rates the rate of polymer formation is high, the high rate of reaction is accomplished only by sacrificing economy in the utilization of vinyl chloride, with increased rate probably being due to increased agitation.

No change in specific viscosity of the product with monomer rate was observed (see Table II), so that it is concluded that the average chain length of the polymer formed is independent of the rate of monomer addition.

Effect of Catalyst Concentration

An examination of Figure 8 shows that, as the catalyst concentration is increased—the other variables being held constant—the rate of reaction also increases up to a certain catalyst concentration and then levels off sharply. This critical catalyst concentration at a given temperature, pressure, and monomer rate represents the catalyst concentration which is capable of furnishing a sufficient number of active molecules to cause complete reaction of the added vinyl chloride. Below this critical concentration, which in the case being considered is about 2.2%, the rate of reaction is proportional to the catalyst concentration. Further increase of catalyst concentration serves no useful purpose; in fact, the specific viscosity of the polymer formed decreases with increasing catalyst concentration, as shown by Figure 9.

From Figure 8 it is seen that the rate of reaction during the induction period is also a linear function of the catalyst concentration, the rate being about 80% of that during the constant-rate period. Also, the rate of reaction increases rapidly with increasing catalyst concentration, as does the conversion of monomer to polymer. On the other hand, specific viscosity of product changes only slightly with the catalyst concentration (Fig. 9), decreasing only 20% with a 16-fold increase in catalyst concentration. The conclusions to be drawn from this are that the conversion of vinyl chloride may be increased a great deal by increasing the catalyst concentration (up to the critical concentration) without appreciably affecting the average chain length of the polymer obtained, a fact which is probably due to the low concentration of the monomer.

Effect of Temperature

Figure 10 shows that as the reaction temperature is increased the rate of reaction increases exponentially up to a certain temperature (in this case 56°C.) at which point the persulfate is decomposing at a rate such that the concentration of active agents is sufficient to cause essentially complete reaction. Increasing the temperature above this point will not increase the rate of reaction. To determine if the data were consistent, the log of the rate of reaction was plotted against the reciprocal of the absolute temperature (Arrhenius equation). The result was a satisfactory straight line between the points corresponding to 46°, 50.5° and 56°C. The discrepancies existing at 40° and 65° may be explained as follows. The rate of reaction at 40° is essentially zero. This is in agreement with published data on the rate of decomposition of potassium persulfate in aqueous media in which it was stated that no decomposition was noted below 41°C.[10] Thus we may say that at 40° it is a "dead" reaction and would not be expected to give results consistent with the other cases. At 65°C. the case is quite different. Under these conditions complete conversion of vinyl chloride is being accomplished, since no gas was leaving the surface of the catalyst solution. The inference here is that under the reaction conditions more monomer would react if it were present, so this rate would not be expected to yield results comparable to those in which an excess of monomer were present.

The specific viscosity of the polymer formed is seen from Figure 11 to decrease with increasing temperature, which is consistent with accepted theories on polymer formation.

It should be noted that a very narrow temperature range is indicated by the results. For the lower limit, about 40°C., the limiting factor is the stability of the catalyst. On the other hand, the use of excessively high temperatures is impractical due to the poor stability of the polymer formed as indicated by the fact that the polymer formed at 65° showed discoloration when dried at 40°.

Effect of Pressure

As indicated previously, the pressure range investigated was limited by the fact that the reaction tube was made of glass. Since Heuer[1] mentioned the use of pressure, it was decided to investigate the effect of running the reaction under a slight pressure to indicate a qualitative effect as to the trend of results to be expected with varying pressure. The results as shown in Figure 12 indicate that with increasing pressure the rate of reaction increases. No effect on the specific viscosity was found, indicating the same average chain length was obtained at both pressures.

Locus of the Reaction

The bulk of the evidence available points to a solution-type polymerization in which the solution, although very dilute, is maintained saturated, or nearly so, by the absorption of vinyl chloride from the vapor phase. This is not in agreement with Heuer, who described the system as a process for the polymerization in the gaseous state.

The mechanism for the polymerization, assuming it to be solution-type, would be that, as the dissolved monomer reacted, the vinyl chloride removed by the polymerization would have to be replaced by absorption from the vapor phase. The variation of rate of reaction with monomer rate may then be ascribed to the fact that higher rates of flow of a gas past an absorbing medium results in thinner liquid films, which in turn increases the rate of absorption.[11] Thus, the higher rates of monomer flow will cause the gas to be more readily absorbed by the aqueous catalyst solution and will rapidly replenish the monomer that reacts and is thereby removed from solution. At lower rates of flow the rate of absorption will be lower and the vinyl chloride may not be absorbed as rapidly as it reacts, resulting in a lower monomer concentration which will in turn result in a lower rate of polymerization. On the basis of this discussion we may differentiate between two cases; in the first of these the controlling factor is the rate of reaction and in the second the controlling factor is the rate of absorption.

Another factor which indicates that the polymerization reaction takes place in solution is that an increase in pressure increases the rate of reaction. Since an increase in pressure also increases the concentration of the dissolved monomer (Henry's law), the result should be an increase in the rate of reaction. This was observed and is in agreement with the mechanism proposed.

Still another fact that supports this mechanism is that the catalyst is soluble in the water phase and no ready means of the catalyst passing into the vapor phase is apparent. The most probable manner in which the monomer in the vapor phase could be activated would consist of the original activation taking place in solution with the activated growing chain diffusing to the gas–liquid interface where it could come in contact with gaseous monomer. This explanation is not consistent with our present ideas on suspension polymerization[12] and lacks supporting evidence.

The vapor–liquid interface presents a possible seat of the reaction. Since some wetting action of the catalyst solution has been observed, it is not impossible that at least part of the reaction does take place there. However one fact that indicates that the major part of the reaction doesn't take place at the interface is the short chain length of the polymer. The highest concentration of monomer should exist at the interface, and under these conditions a much longer chain length would be expected than was actually observed.

In view of the foregoing discussion it is the authors' opinion that the most probable seat of the reaction is in solution, with some possibility of it occurring at the gas–liquid interface. It is apparent that more work is necessary to definitely establish the seat of the reaction.

The authors wish to thank The Glenn L. Martin Co. for making this investigation possible.

References

1. Werner Heuer (to I. G. Farbenindustrie), U.S. Pat. 2,179,040, Nov. 7, 1939.
2. Holl. Pat. 46,851 (to I. G. Farbenindustrie).
3. Fr. Pat. 820,749 (to I. G. Farbenindustrie).
4. De Bell, Goggins, and Gloor, *German Plastics Practice.* De Bell and Richardson, Springfield, Mass., 1946, p. 40.
5. R. D. Dunlop and F. E. Reese, *Ind. Eng. Chem.*, **40**, 654 (1948).
6. A. T. Larson (to E. I. du Pont de Nemours), U.S. Pat. 2,414,311, Jan. 14, 1947.
7. G. F. D'alelio, *A Laboratory Manual of Plastics and Synthetic Resins.* Wiley, New York, 1943, p. 180.
8. F. Krczil, *Kurzes Handbuch der Polymerizationstechnik*, Vol. I. Akadem. Verlagsgesellschaft, Leipzig, 1940, p. 363.
9. J. H. McGill (to Imperial Chemical Industries), U.S. Pat. 2,439,051, Apr. 6, 1948.
10. H. G. Levi and E. Migliorina, *Gazz. chim. ital.*, **36**, 599 (1906); *C.A.*, **1**, 1945 (1907).
11. Badger and McCabe, *Elements of Chemical Engineering.* 2nd ed., McGraw-Hill, New York, 1936, pp. 376–412.
12. W. P. Hohenstein, F. Vingiello, and H. Mark, *India Rubber World*, **110**, 291 (1944).

English Synopsis, see Summaries, page S14, Vol. V, 1950.

Résumé

Un procédé de polymérisation du chlorure de vinyle est décrit; au cours de celui-ci, le chlorure de vinyle gazeux est barbotté à travers une solution de persulfate de potassium, à une température relativement peu élevée, et à pression atmosphérique. La dépendance de la quantité de polymère formé en fonction du temps est indiquée. L'influence des divers facteurs—vitesse de passage du monomère, concentration en monomère, température et pression—sur la vitesse de la réaction et la viscosité spécifique du polymère formé a été envisagée. Le lieu, oú se passe la réaction est discuté.

Zusammenfassung

Es wird eine Methode zur Polymerisation von Vinylchlorid beschrieben, in welcher gasförmiges Vinylchlorid bei leicht erhöhten Temperaturen und bei im wesentlichen atmosphärischem Druck durch eine Kaliumpersulfatlösung geleitet wird. Die Art, in der sich die Menge des gebildeten Polymers im Verhältnis zur Zeit ändert, wird beschrieben. Der Einfluss der veränderlichen Grössen—Monomer-Geschwindigkeit, Konzentration des Katalysators, Temperatur und Druck—auf die Reaktionsgeschwindigkeit und die spezifische Viskosität des gebildeten Polymers wird gegeben. Der Reaktionsverlauf wird diskutiert.

Received September 8, 1949

JOURNAL OF POLYMER SCIENCE VOL. V, NO. 6, PAGES 687-708

Experiments on the Sonic, Thermal, and Enzymic Depolymerization of Desoxyribosenucleic Acid*

GILBERT GOLDSTEIN and KURT G. STERN, *Department of Chemistry, Polytechnic Institute of Brooklyn, Brooklyn, New York*

Increasing attention has been paid in recent years to the degree of poly merization of nucleic acids, isolated by different methods from a variety of natural sources, following Hammarsten's demonstration[1] of the macromolecular nature of the tetrasodium salt of desoxyribosenucleic acid as prepared under mild conditions from calf thymus tissue. The high molecular weight (500,000 to 1,000,000) and the extreme degree of asymmetry (axial ratio, 170 to 400:1) of the individual particles find their expression in the low osmotic pressure, high anomalous viscosity, and marked streaming birefringence of dilute aqueous solutions of the material (*cf.* ref. 2). The polynucleotide chains composing the molecules may reach a length of as much as 5000 A. (*cf.* ref. 3), corresponding to about one thousand tetranucleotide units in linear array. They are highly susceptible to depolymerization by a variety of physical and chemical agents, *e.g.*, x-rays,[4] ultraviolet radiation,[5] and a specific enzyme in animal tissues, designated as desoxyribonuclease or depolymerase.[6,7]

The object of the present experiments was to study, in a comparative and quantitative manner, the effect of intense vibrations of sonic frequency, of different, elevated temperatures, and of purified desoxyribonuclease on high-polymer sodium desoxyribosenucleinate preparations of the same type. It was hoped that information on the mechanism of depolymerization by these agents would contribute to our knowledge of the forces holding these linear molecules together.

EXPERIMENTAL

Materials and Methods

Preparation of Sodium Desoxyribosenucleinate

The material used for the majority of the present experiments was prepared as follows.

---

* The data presented in this paper are taken from a thesis to be submitted by Gilbert Goldstein to the Graduate Faculty of Polytechnic Institute of Brooklyn in partial fulfillment of the requirements for the degree of Ph.D. in Chemistry. A brief report on this work was presented before the Division of Biochemistry at the 114th meeting of the American Chemical Society, Washington, D.C., Sept. 2, 1948. The preparation of the material for publication was made possible by a grant from the National Cancer Institute, U. S. Public Health Service.

One pound of fresh calf thymus tissue, after freeing it from adhering fat and connective tissue, was subdivided into pieces of suitable size and then homogenized in the Waring Blendor in aliquots of a solution containing 0.14 *M* NaCl and 0.002 *M* sodium arsenate, using a total volume of one liter. The pink, creamy suspension thus obtained was collected in a flask immersed in an ice bath and stirred mechanically for four hours at 0 °C. The resultant, milky suspension was spun in 100 ml. Lusteroid tubes in a Servall superspeed angle centrifuge, using a magnesium alloy rotor of 800 ml. capacity, for about 10 minutes at approximately 3 to 4000 r.p.m. The pink-colored, opalescent supernatant fluid was decanted from the tightly packed sediment and discarded. The sediment was resuspended in 500 ml. of fresh NaCl-arsenate solution and stirred overnight in the refrigerator at 5 °C. The suspension was then centrifuged as described above, the supernatant was again discarded and the residue was extracted for the third time with 500 ml. 0.14 *M* NaCl solution omitting the arsenate. After mechanical stirring in the refrigerator for 30 minutes, the suspension was centrifuged as before, the supernatant decanted and discarded, and the residue was treated once more with 500 ml. 0.14 *M* NaCl solution as just described. The extraction of the tissue with physiological saline served to remove as much as possible of cytoplasmic proteins. The residue, consisting chiefly of a gelatinous mass of nuclear material, designated as "resting chromosomes" by Mirsky and Ris,[8] was next suspended in 300 ml. 1 *M* NaCl solution in order to dissolve the nuclear desoxyribosenucleoprotein. The viscous suspension was stirred for three hours in the refrigerator and then centrifuged in the superspeed angle centrifuge at 10,800 r.p.m. for 15 minutes. The highly viscous, opalescent supernatant fluid was carefully decanted and saved. The gelatinous residue was resuspended in about 200 ml. 1 *M* NaCl solution and stirred overnight in the refrigerator. The suspension was centrifuged at high speed (10,800 r.p.m.) for 15 minutes and the supernatant solution was combined with the first lot. This preparation, termed "chromosin" by Mirsky and Pollister,[9] has been shown to consist essentially of a mixture of sodium desoxyribosenucleinate and histone chloride.[10] In order to precipitate the basic protein, the solution was saturated with NaCl by adding an excess of solid salt to it and stirring for four hours in the refrigerator. The resultant, gel-like, milky suspension which could be clarified neither by centrifuging nor by filtration was stored overnight in the refrigerator. An aliquot, corresponding to one-fourth of the volume of the suspension, was diluted five times with saturated sodium chloride solution. A part of this diluted suspension was filtered by suction through Whatman No. 1 filter paper, yielding a slightly opalescent filtrate. The remainder of the suspension was centrifuged 15 minutes at 11,000 r.p.m. in the angle centrifuge and the resultant, slightly opalescent supernatant solution was combined with the filtrate yielding about 600 ml. total volume. The sediment, consisting chiefly of histone, was discarded. The solution, containing the sodium salt of desoxyribosenucleic acid was stored overnight in the refrigerator. It was added slowly to 1.5 volumes of 95%

ethanol while stirring mechanically with a wooden rod. The stringy sodium desoxyribosenucleinate precipitate wound itself onto the rod and was lifted out of the water-alcohol mixture. The spool of nucleinate was dried by pressing between layers of filter paper. It was resuspended in 500 ml. distilled water and brought largely into solution by stirring for 40 hours in the refrigerator. The solution was freed of undissolved particles by centrifuging and the alcohol precipitation was repeated. The precipitate was redissolved in 400 ml. water by stirring for several hours in the refrigerator. After centrifuging the sodium desoxyribosenucleinate was once more precipitated by alcohol after adding five ml. 1 *M* NaCl. The spool of material thus obtained was pressed between filter paper and further dried by means of 95% ethanol, alcohol-ether in equal parts, and, finally, ether. The ether was allowed to evaporate and the air-dried material was stored in a tightly stoppered bottle. The final yield was 1.58 g. corresponding to 115 g. of fresh thymus tissue. The sodium desoxyribosenucleinate thus obtained (Preparation STN-6) represented a white, dense, fibrous material of asbestoslike appearance. The preparation was readily water soluble and yielded, even at low concentration, solutions of high relative viscosity (a 0.1% solution in distilled water at atmospheric pressure had a relative viscosity of 7.2 at 26°) which exhibited marked streaming birefringence when examined between crossed Polaroid disks. It was free of protein as indicated by a negative biuret test, and of arginine as shown by a negative Sakaguchi reaction. The intensity of the orcinol reaction indicated a maximum content of 1.2% of pentose nucleic acid. The Dische reaction with diphenylamine was, of course, strongly positive. The microanalysis, kindly performed by Dr. Max M. Friedman, of the Queens General Hospital, N. Y., disclosed the presence of 16.5% nitrogen (micro-Kjeldahl) and 8.3% phosphorus (Fiske-Subbarow method) on a dry basis. The material contained 22.6% moisture before drying it for the analysis. The nitrogen/phosphorus ratio was 1.99, *i.e.*, somewhat higher than demanded by the theory (1.70). In the ultracentrifuge, a 0.2% solution of the material in phosphate buffer, *p*H 7.4, showed a single, hypersharp boundary, sedimenting at a rate of $s_{20} = 6.18 \times 10^{-13}$. In its properties, the material resembled closely the type of preparation obtained previously by Hammarsten[1] by a somewhat different procedure. It represents the tetrasodium salt of desoxyribosenucleic acid in highly polymerized form as shown by the high viscosity of its dilute solutions, its intense flow birefringence, and its behavior in the analytical ultracentrifuge. The absorption spectrum showed a maximum at 259 mμ (D = 1.282 in 0.008% solution) and a minimum at 231 mμ.

Viscometry

A simple viscometer of the Ostwald type was used in all viscosity determinations performed in the course of this work. The length of the capillary tube was approximately 105 mm., the volume of the upper bulb situated between the two marks was 2 ml., while the working volume of solution was

5 ml. The viscometer was suspended in a constant temperature bath which was usually regulated at 30° within ±0.1° or better. At that temperature the water constant of the instrument was 85.3 sec. The time required by the solutions to pass between the two marks was determined in the usual way with a stop watch. The relative viscosity was determined as usual with water or buffer as reference solvents. The determinations were made at atmospheric pressure although it is appreciated that different hydrostatic pressures would have yielded a more complete description of the systems under investigation, especially of those exhibiting non-Newtonian flow, *i.e.*, anomalous viscosity. The enzymic experiments were as a rule performed directly in the viscometer as the reaction vessel; the necessity of making viscosity determinations at frequent intervals throughout the course of the reaction would have rendered the variation of external pressure heads impractical.

Sonic Oscillator

An oscillator of the magnetostriction type was employed in our experiments. The nominal frequency of this instrument (Type R-22-1) which was built by the Submarine Signal Division of Raytheon Mfg. Co., Waltham, Mass., was 9 kilocycles. However, since the current delivered to the magnetostriction coil is tuned during operation to the frequency of mechanical resonance of the laminated nickel rod and diaphragm system using a decibel meter, the actual operating frequency may be as low as 8700 or as high as 9500 cycles per second. For a given instrument the tuned frequency is probably reproducible within 1%. The power delivered from the driver to the magnetostriction coil is about 50 watts at approximately 140 volts. The solution under study is placed in a metal

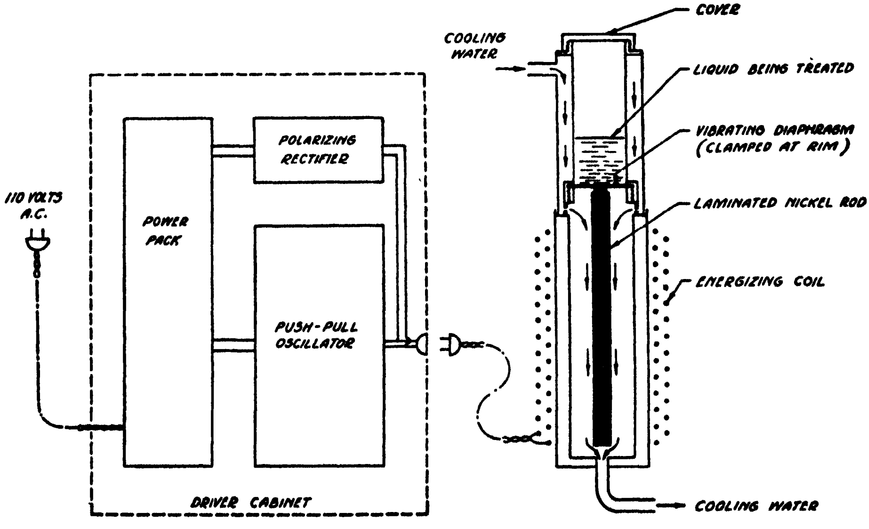

Fig. 1. Diagrammatic representation of sonic oscillator (courtesy of Raytheon Mfg. Co., Waltham, Mass.).

test cup the bottom of which is formed by the diaphragm attached to the nickel rod of the oscillator unit. This arrangement results in a good transfer of energy into the liquid. An appreciable rise in temperature during irradiation is prevented by a jacket surrounding the test cup through which cold water circulates during the experiment. The capacity of the cup is about 30 ml. of solution. A schematic diagram of the entire arrangement is shown in Figure 1.

Spectrophotometer

A Beckman quartz spectrophotometer, Model DU, was used for the measurement of the ultraviolet absorption spectra of the STN solutions. Matched, fused silica cells of 10 mm. layer of thickness of solution were employed.

Ultracentrifuge

An air-driven analytical ultracentrifuge of the turret type, designed according to Pickels and equipped with a schlieren optical system of the diagonal diaphragm-cylinder lens type, was used for the sedimentation experiments. The arrangement has been briefly described elsewhere.[11]

Desoxyribonuclease Preparation

The enzyme preparation employed in the present experiments was kindly placed at our disposal by Dr. M. McCarty of Rockefeller Institute for Medical Research. It was derived from pancreas tissue and purified as described by him.[6] In addition to high desoxyribonuclease activity, the purified material showed also a trace of proteolytic activity which was, however, negligible at the high dilutions employed. It was readily soluble in water and was usually stored in a diluent containing 0.1% gelatin as a stabilizing agent and 0.03 *M* $MgCl_2$ as an activator.

EXPERIMENTS AND RESULTS

Effect of Sonic Irradiation

Arrangement of Experiments

Solutions of sodium desoxyribosenucleinate (STN) of 0.1 to 0.2% concentration were prepared freshly for each experiment. Their relative viscosity was measured and 30 ml. of the solution were placed in the test cup of the sonic oscillator described above. The solution under study was irradiated for various time intervals at about 9000 cycles per second. After each interval, a 5 ml. aliquot was withdrawn and pipetted into the Ostwald viscometer where the relative viscosity was determined in a constant temperature bath. The contents of the viscometer were then returned to the oscillator cup and the sonic irradiation was continued. During the sonic treatment the test cup was cooled with running water and it was closed by a metal screw cap.

Viscometric Observations

In a preliminary experiment, a 0.125% solution of STN in distilled water was irradiated for a total time of 50 minutes. The temperature of the solution during irradiation was not determined. The relative viscosity was measured at 25.6° in 1-minute intervals of irradiation and, after the first 10 minutes, in 10-minute intervals. The relative viscosity decreased from 3.93 to 1.09 during the course of this experiment. The desoxyribose content, as determined colorimetrically with the Dische reaction, was found to be unchanged before and after the experiment. It was also ascertained that the mere contact of the STN solution with the metal of the oscillator cup for a period of 120 minutes produced no change in the relative viscosity of the system. In two subsequent experiments, the decrease in relative viscosity of 0.1 and 0.2% STN solutions through sonic irradiation was studied under more closely controlled conditions. In these experiments, constancy of the hydrogen ion concentration was insured by using veronal-HCl buffer of 0.1 ionic strength and pH 7.4 as the solvent. Measurements performed with the glass electrode (Macbeth pH meter) at the start and at the conclusion of the sonic treatment showed no change in pH. The cooling water was passed through a copper coil immersed in an ice bath prior to entering the jacket surrounding the oscillator cup. The temperature of the solutions was measured in the test cup before and after each period of irradiation. The determination of relative viscosity in these experiments was carried out at 30°.

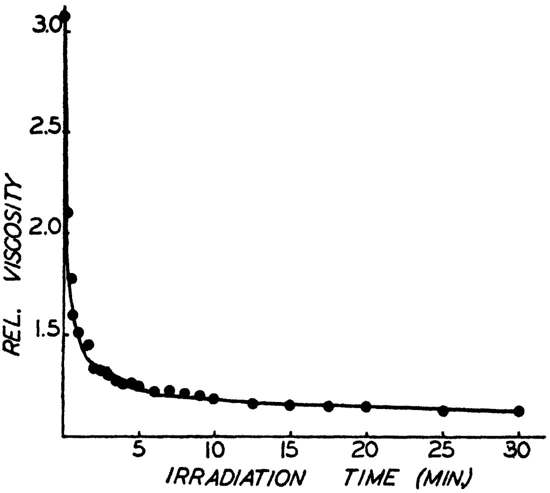

Fig. 2. Effect of sonic irradiation on the relative viscosity of STN solution.

0.1% STN-6 in veronal-HCl buffer, pH 7.4, irradiated in magnetostriction oscillator at 9000 c.p.s. Viscosity measured at 30° with 5 ml. aliquots. pH remained unchanged.

In all instances the relative viscosity of the STN solutions fell precipitously during the first few minutes of sonic treatment after which the decrease in viscosity with continued irradiation became more gradual until it levelled off at a value somewhat above that of the solvent alone. Taken in conjunction with the other observations reported later in this paper this fact appears to be significant. The results of the experiment performed on the 0.2% STN solution are recorded in Table I, while those of the experiment with the 0.1% solution are graphically presented in Figure 2.

TABLE I

EFFECT OF SONIC IRRADIATION ON VISCOSITY OF SODIUM DESOXYRIBOSENUCLEINATE[a]

Sonic irradiation, min.	Temperature in oscillator cup Initial	Final	Relative viscosity	*p*H
0	—	—	12.34	7.4
0.08	24	24	11.21	
0.17	25	25	11.40	
0.25	25	25	10.69	
0.5	25	26	9.21	
0.75	25	26	6.93	7.4
1.25	25	27	4.08	
1.75	25	27	2.91	
2.5	25	28	2.29	
5.0	25	28	1.72	
10.0	24	29	1.45	
15.0	24	38	1.35	
20.0	27	40	1.28	
25.0	28	41	1.26	7.4

[a] 30 ml. 0.2% STN-6 solution in veronal-HCl buffer, *p*H 7.4, irradiated at 9000 cycles per second. Viscosity measured at 30° with 5-ml. aliquots.

It will be noted from Table I that the temperature in this experiment rose to 41° during the last 5-minute interval of the irradiation. However, it is believed that this temperature rise did not affect the results significantly, since the greatest part of the viscosity drop had already occurred before that time when the temperature was below 30° and, furthermore, since independent experiments on the thermal depolymerization of STN (see later, under "Thermal Depolymerization") showed that even at 60° the relative viscosity is only slightly reduced after 7 minutes of heating. During the irradiation experiment depicted in Figure 2, the temperature of the solution in the test cup of the oscillator did not rise above 23° at any time.

Ultracentrifuge Experiments

With a view toward obtaining some insight into the nature of the changes produced in the sodium desoxyribosenucleinate molecules by sonic vibrations, irradiated solutions of STN were examined in the analytical ultracentrifuge and the sedimentation diagrams thus obtained were compared with those of the original, high-polymer material. These experiments were performed with the kind assistance of J. Wagman of this laboratory. The original STN preparation (No. 6), the chemical properties of which have been described above, exhibited in the ultracentrifuge a single, hypersharp boundary when examined in 0.2% solution in veronal-HCl buffer of *p*H 7.4 (see Fig. 3). The relative viscosity of the solution used was 12.3.

From the diagram, a sedimentation constant, s_{20}, of 5.5 svedberg units was computed. Another experiment yielded a value for s_{20} of 6.2. The latter agrees satisfactorily with the value found previously for another STN preparation by Tennent and Vilbrandt[12] who assigned a molecular weight of the order of 500,000 to this material. It should be noted that the *apparent* sedimentation constants, as found at finite concentrations of STN, would have to be extrapolated to zero concentration to yield the true sedimentation rate, free from molecular interaction.

A 0.2% solution of STN-6 in veronal-HCl buffer, *p*H 7.4, was sonically treated for 25 minutes in 5 minute intervals and at a temperature from 20 to 25°. The relative viscosity of the solution decreased from 10.67 to 1.22 as a result of the irradiation. The final solution, upon examination in the ultracentrifuge, exhibited a single, well-defined boundary lacking the hypersharpness of the original material (see Fig. 4). The appearance of the sedimenting boundary indicates that the irradiation has produced a paucidisperse product of still considerable particle size. The sedimentation constant, as calculated from the diagram shown in Figure 4, amounts to 5.9 svedberg units, a value of the same order as that found for the original material. Inasmuch as the relative viscosity and the particle interaction had been drastically reduced by the sonic treatment, the unchanged sedimentation rate indicates that the decrease in asymmetry was approximately balanced by a reduction in particle size. In the course of the irradiation experiment forming the basis of Table I, samples of the STN solution were removed after 45 seconds and 25 minutes of sonic treatment. Their examination in the ultracentrifuge showed that after 45 seconds of irradiation the appearance of the sedimenting boundary as well as the sedimentation rate (s_{20} = 6.5) remain essentially the same as those of the original material. However, a certain amount of heavy, polydisperse material was

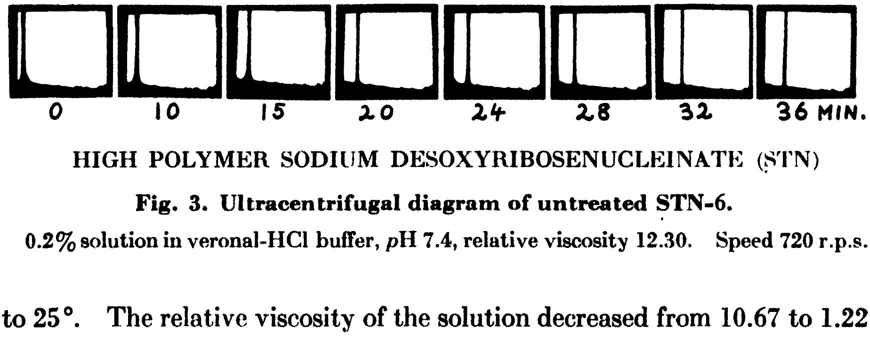

HIGH POLYMER SODIUM DESOXYRIBOSENUCLEINATE (STN)

Fig. 3. Ultracentrifugal diagram of untreated STN-6.

0.2% solution in veronal-HCl buffer, *p*H 7.4, relative viscosity 12.30. Speed 720 r.p.s.

observed during this run (O-274) in addition to the main component. The diagram, obtained in the ultracentrifuge with the material which had been irradiated for 25 minutes (O-275), as well as the sedimentation constant derived from it ($s_{20} = 6.2$) agreed substantially with the results of the experiment depicted in Figure 4.

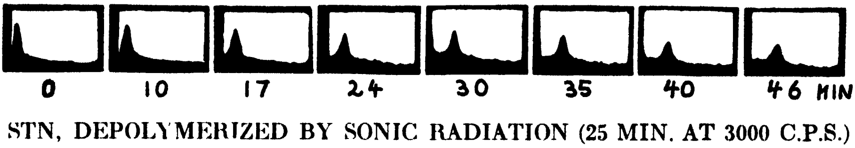

Fig. 4. Ultracentrifugal diagram of sonically irradiated STN-6.

0.2% solution in veronal-HCl buffer, pH 7.4, sonically treated 25 min. at 9000 c.p.s. Speed 700 r.p.s.

Other Observations

In order to determine whether the decrease in viscosity upon sonic irradiation is due to simple depolymerization or to a destruction of the purine or pyrimidine bases of the component nucleotides, the *ultraviolet absorption spectrum* of a sonically treated STN solution was compared with that of the original untreated material. It is known that the intense absorption of nucleic acids at about 260 mμ is due to their content in purine and pyrimidine bases and that the spectrum of ribosenucleic acid is only slightly modified by enzymic depolymerization.[13] The same is true for desoxyribosenucleic acid as will be shown later in this paper.

A 0.048% solution of sodium desoxyribosenucleinate (STN-6) in distilled water was sonically treated in the oscillator for a total period of 30 minutes in 5-minute intervals. Owing to efficient cooling the temperature rose during each irradiation period only from 14.5 to 18.5°. The relative viscosity of the solution decreased from 3.11 to 1.09 (measured at 30°). 1 ml. of the irradiated solution was diluted with 5 ml. water and the light absorption of the diluted solution was measured in a 10 mm. layer in the Beckman spectrophotometer, in the region from 220 to 340 mμ against distilled water as reference solution. Figure 5 shows that the resulting spectrum was practically identical with that of the original STN solution diluted in the same manner.

Tests for the liberation of *inorganic phosphate* as a consequence of sonic irradiation, carried out by the standard Fiske-Subbarow colorimetric method, were negative. Dr. Max M. Friedman determined the formation of *acid-soluble* phosphorus at three different temperatures from a sonically treated STN preparation and compared it with the corresponding behavior of untreated STN. The results, as shown in Table II, indicate that sonic irradiation does not produce low-molecular, mono- or oligonucleotides which would be soluble in trichloroacetic acid at low temperature.

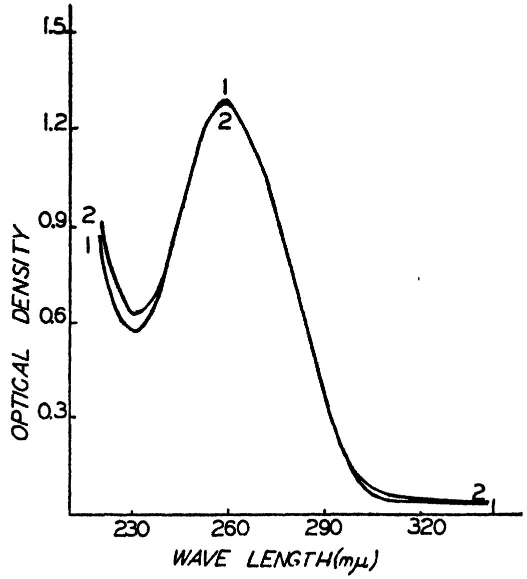

Fig. 5. Ultraviolet absorption spectra of STN-6 solutions: (1) untreated; (2) sonically treated.

TABLE II

Distribution of Acid-Soluble Phosphorus in Treated and Untreated STN Preparations[a]

STN Preparation	Temperature, °C.	Acid-soluble P, expressed as mg. DNA/ml.
Untreated	30	0.02
	60	0.05
	90	1.18
Sonically treated	30	0.02
	60	0.05
	90	1.05
Enzymatically treated	30	0.78
	60	0.09
	90	0.01
Thermally treated	30	0.00
	60	0.01
	90	1.12

[a] Aliquots of each preparation were extracted with 5% trichloroacetic acid for 15 minutes at 30°, 60°, and 90°, respectively, and the acid-soluble phosphorus determined in each case. Results are expressed in equivalent amounts of desoxyribosenucleic acid (DNA).

Experiments with Desoxyribonuclease

Arrangement of Experiments

The total volume of the test system was 5 ml. It was made up of 4.5 ml. substrate solution (0.05 to 0.2% sodium desoxyribosenucleinate (STN-

IV or STN-VI)) in distilled water or in veronal-HCl buffer, *p*H 7.4, plus 0.5 ml. enzyme solution, containing from 0.5 to 10 μg. of purified pancreas desoxyribonuclease per milliliter in a 0.1% gelatin-0.03*M* $MgCl_2$ solvent. In experiments employing specific inhibitors, these were added to the enzyme solution prior to its addition to the test systems. As a rule, the reaction was allowed to proceed in the lower bulb of the viscometer (see above, under "Viscometry") while it was immersed in a constant temperature bath held at 30°. In confirmation of previous observations[6] it was found that the presence of magnesium ions (or manganese ions) was indispensable for the activity of the enzyme.

Viscometric Observations

At a final enzyme concentration of 0.05 to 0.2 μg. per milliliter test system, a rapid fall in the viscosity of the STN solution was observed which, at 30° and within 10 to 60 minutes, depending on the amount of enzyme present, reduced the relative viscosity of the system to a value close to that of the solvent. By way of example, the changes in relative viscosity, as recorded in the course of a typical experiment, are reproduced in Table III. In this instance, determinations of viscosity were performed 1 minute after adding the enzyme and from then on in 5-minute intervals for an observation period of 30 minutes. A final determination was made after 60 minutes. The corrections, which are made necessary by the fact that the time required for measuring viscosity is appreciable when compared with the reaction time, are indicated in the Table III. In general, the viscometric observations made in this work agreed satisfactorily with those described by McCarty.[6]

TABLE III

EFFECT OF PANCREAS DESOXYRIBONUCLEASE ON VISCOSITY OF SODIUM DESOXYRIBOSENUCLEINATE (STN)[a]

Time elapsed after adding enzyme to substrate soln., min[b]	Time corrected for period required for viscosity detn., min.	Time required for system to pass marks of viscometer, sec.	Relative viscosity at 30°
1	2.5	189.6	2.22
5	6.5	172.0	2.02
10	11	153.2	1.80
15	16	140.3	1.64
20	21	126.8	1.49
25	26	119.7	1.40
30	31	112.6	1.32
60	61	95.3	1.12

[a] 4.5 ml. STN-4 (0.06%) in veronal-HCl buffer, *p*H 7.4, plus 0.5 ml. enzyme solution (0.5 μg. purified desoxyribonuclease per ml.) at 30°.

[b] The time listed in the first column was that which elapsed between the addition of the enzyme solution to the substrate in the viscometer and the start of the viscosity determination. The time listed in the second column was computed by adding one half of the time listed in the third column (rounded off to the nearest half minute) to that listed in the first column.

Inhibitor Experiments

The inhibitors studied by us were selected on the basis of previous reports containing references to their action on desoxyribonuclease. Thus, Fischer *et al.*[14] has reported that sodium arsenate and arsanilic acid in 0.001 *M* concentration will inhibit the liquefaction of Mg α-nucleinate gels, while McCarty[6] states that both fluoride and citrate inhibit the depolymerizing action of pancreas desoxyribonuclease on STN as well as on the *Pneumococcus* transforming principle.[15] The present experiments were undertaken to compare quantitatively the activity of the different inhibitors, in connection with work in our laboratory[16] on the isolation of native desoxyribosenucleoprotein from thymus tissue (Genoprotein T).

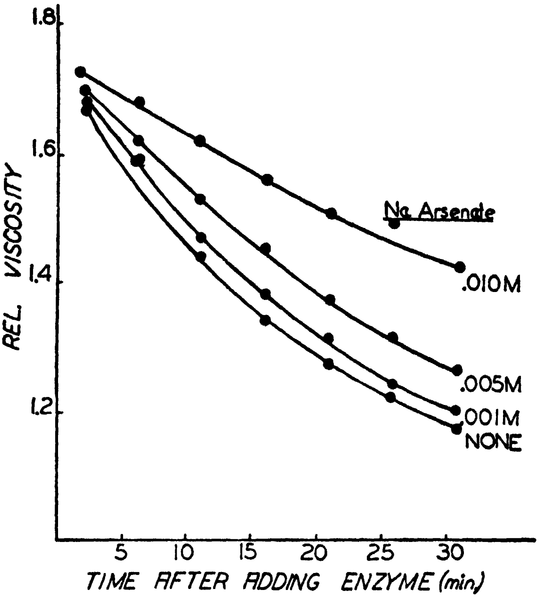

Fig. 6. Inhibition of desoxyribonuclease by sodium arsenate.

Viscosity measured at 30°. Volume of test system, 5 ml. (4.5 ml. 0.05% STN-IV in veronal-HCl buffer, *p*H 7.4. + 0.5 ml. enzyme-arsenate solution, containing 0.5 μg. enzyme per ml.).

Preliminary experiments with *sodium arsenate* at low concentration (0.001 *M*) and relatively large amounts of enzyme (2 μg./ml.) failed to show an inhibition when using viscosimetry as a criterion. Upon raising the arsenate concentration to 0.01 *M* and lowering the enzyme concentration to 0.2 μg. per milliliter and less, a definite inhibitory effect was observed. A series of viscosity curves recorded in experiments employing concentrations of arsenate ranging from 0.001 to 0.01 *M* and an enzyme concentration of 0.05 μg. per milliliter of the test system are reproduced in Figure 6. They show the increasing degree of inhibition produced by increasing arsenate concentrations. The apparent discrepancy between these findings and those of Fischer *et al.*[14] with regard to the effectiveness of arsenate as an inhibitor, might well be due to the difference in the test system and substrate employed. Experiments employing *arsanilic acid* over the same range of concentrations yielded results similar to those obtained with arsenate (see Fig. 7) except that the inhibition produced by 0.001 *M* arsanilic acid appeared more pronounced than that caused by 0.001 *M* arsenate under the same experimental conditions while the reverse was found to be the case at 0.01 *M* inhibitor concentration.

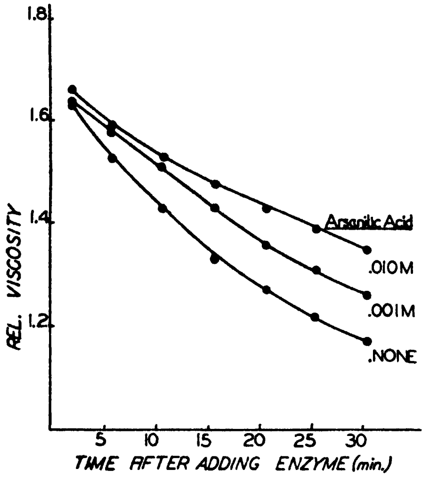

Fig. 7. Inhibition of desoxyribonuclease by arsanilic acid.

Viscosity measured at 30°. Volume of test system, 5 ml. (4.5 ml. 0.05% STN-4 in veronal-HCl buffer, *p*H 7.4 + 0.5 ml. enzyme-arsanilic acid solution, containing 0.5 μg. enzyme per ml.).

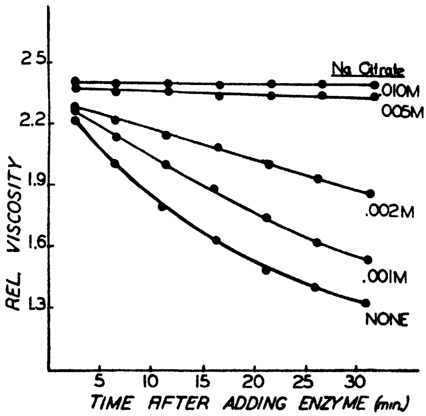

Fig. 8. Inhibition of desoxyribonuclease by sodium citrate.

Viscosity measured at 30°. Volume of test system, 5 ml. (4.5 ml. 0.05% STN-4 in veronal-HCl buffer, *p*H 7.4 + 0.5 ml. enzyme-citrate solution, containing 0.5 μg. enzyme per ml.).

Contrary to expectations, *sodium citrate* proved to be a more potent inhibitor of desoxyribonuclease action than arsenate, as may be seen from the experiments presented in Figure 8. It will be seen that 0.01 *M* citrate produces a complete inhibition in the presence of 0.05 μg. of enzyme per milliliter of the test system while 0.001 *M* citrate causes a distinct inhibition.

Sodium fluoride, when tested under similar conditions, was shown to possess an inhibitory effect on desoxyribonuclease of the same order as that exhibited by sodium arsenate (see Fig. 9).

In a single experiment, 8-*hydroxyquinoline,* which is known for its ability to form metal complexes at 0.001 *M* concentration was found to be ineffective as an inhibitor of the enzyme which was used at a concentration of

0.05 μg. per ml. The percentage inhibition of desoxyribonuclease by arsenate, fluoride, and citrate, as calculated from the linear portion of the various viscosity curves, is shown in Figure 10. In computing the percentage inhibitions, the formula:

$$\%\ \text{inhibition} = \frac{(a - b) - (c - d)}{(a - b)} \times 100$$

was used, where a represents the time in seconds required for the original STN solution to pass the viscometer marks, b represents the corresponding interval for the enzyme-substrate system in the absence of an inhibitor, c represents the same interval for the substrate-inhibitor mixture, and d represents the interval for the enzyme-substrate-inhibitor system t minutes after adding the enzyme. From the graph, Figure 10, the following values for the concentration at which 50% inhibition occurs are obtained: citrate, 1.4×10^{-3} M; fluoride, 6.4×10^{-3} M; and arsenate, 7.9×10^{-3} M. These values represent only a rough approximation but they are of practical use in selecting the most effective inhibitor for a given set of experimental conditions.

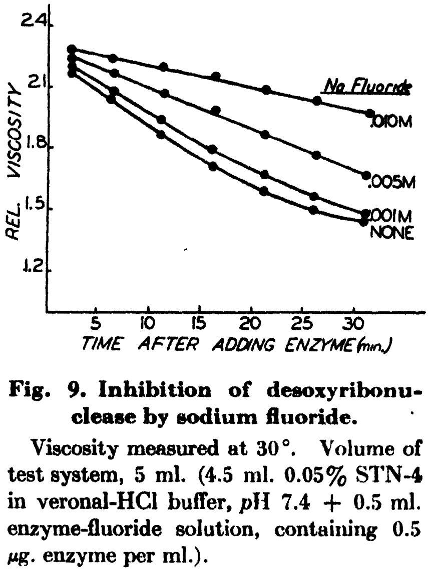

Fig. 9. Inhibition of desoxyribonuclease by sodium fluoride.

Viscosity measured at 30°. Volume of test system, 5 ml. (4.5 ml. 0.05% STN-4 in veronal-HCl buffer, pH 7.4 + 0.5 ml. enzyme-fluoride solution, containing 0.5 μg. enzyme per ml.).

Effect on Absorption Spectrum

In preliminary experiments, the desoxyribonuclease was allowed to act on STN in *unbuffered* solution at 30° for a length of time sufficient to cause a marked depolymerization, as measured viscometrically. Upon measuring the optical density of the solutions in the Beckman quartz spectrophotometer at various wave lengths ranging from 225 to 300 mμ, at an appropriate STN concentration, a distinct increase in extinction was observed as compared with the original STN solution. For example, the optical density of a 0.008% STN solution rose from 1.07 to 1.29 at 259 mμ upon incubation with desoxyribonuclease (final enzyme concentration, 1 μg. per ml.) for 30 minutes at 30°. When, however, the reaction was allowed to proceed in *buffered* solution (veronal-HCl buffer, *p*H 7.4) under otherwise similar conditions the extinction of the reaction system did not change appreciably. Thus, the optical density of a STN solution of the same concentration changed only from 1.03 to 1.05 upon incubation with the enzyme (0.1 μg. per ml.) for 30 minutes at 30°, although viscometric determinations showed that a far-reaching depolymerization had occurred.

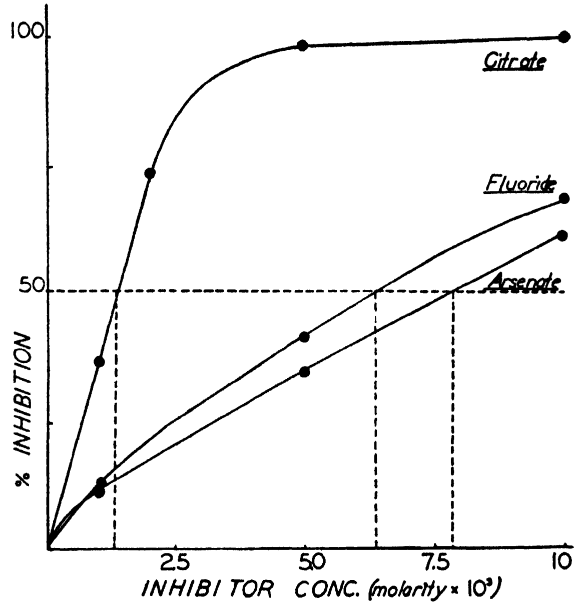

Fig. 10. Percentage inhibition of desoxyribonuclease.

The assumption that a shift in hydrogen ion concentration rather than the depolymerization itself was responsible for the spectral changes observed in the unbuffered system is further supported by the observation that the addition of alkali (*e.g.*, 0.03 *N* NaOH final concentration) or of acid (0.014 *N* HCl final concentration) will produce a change in extinction of STN of an order comparable to that produced by the enzyme in unbuffered solutions.* It might be mentioned that the enzyme itself shows an absorption maximum at about 280 mμ.

* *Note added in proof*: M. Kunitz (*J. Gen. Physiol.*, 33, 349 (1949–50)) reports an increase in the U. V. absorption of STN solutions after addition of *crystalline* desoxyribonuclease. A reinvestigation showed that the above concentrations of an enzyme of lower specific activity, while causing a rapid decrease in the viscosity of the test system, were insufficient to produce the gradual and relatively less pronounced changes in optical density observed by Kunitz.

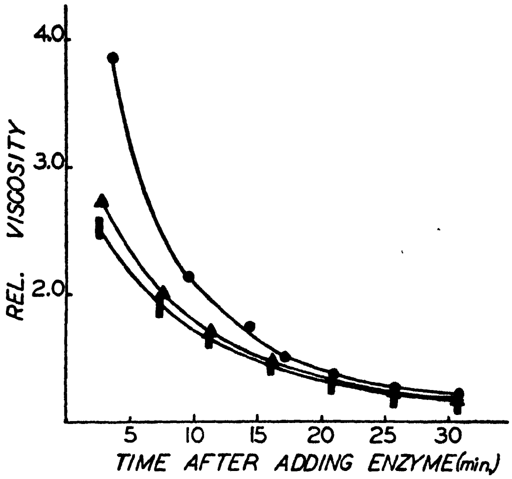

Fig. 11. Effect of combined sonic and enzymic treatment of STN.

Viscosity measured at 30°. Volume of test system, 5 ml. (4.0 ml. STN-6 in veronal-HCl buffer, pH 7.4 + 0.5 ml. 0.03 M $MgCl_2$ + 0.5 ml. enzyme solution, 10 μg. per ml. in distilled water). Circles: 0.2% STN-6, relative viscosity 10.67; triangles: 0.2% STN-6 partially depolymerized in sonic oscillator to a relative viscosity of 5.31; rectangles: 0.2% STN-6 diluted with water to a relative viscosity of 4.87.

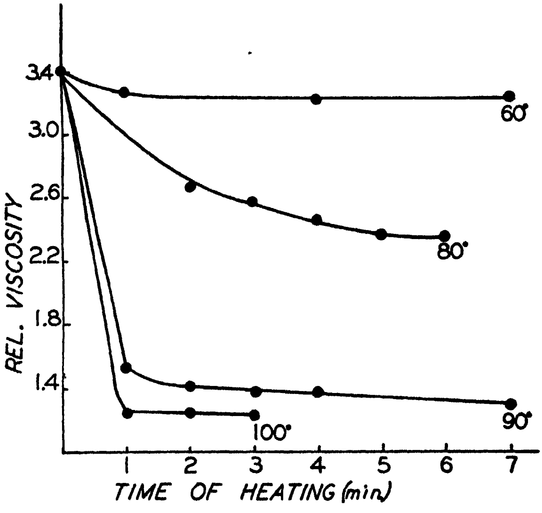

Fig. 12. Thermal depolymerization of STN.

0.1% STN-6 in veronal-HCl buffer, pH 7.2. Viscosity measured at 30° with 5 ml. aliquots.

Effect on Molecular Sedimentation

4 ml. of 0.2% STN-6 solution in veronal-HCl buffer, *p*H 7.4, were mixed with 0.5 ml. 0.03 *M* $MgCl_2$ and 0.5 ml. enzyme solution (final enzyme concentration, 1 μg. per ml.). The mixture was placed in the viscometer and allowed to react for 120 minutes at 30°. After that time, during which the relative viscosity of the system had fallen from 10.67 to 1.03, the solution was examined in the analytical ultracentrifuge. The sedimentation diagram recorded in this experiment (O-283) showed that the material had become extremely polydisperse and inhomogeneous: much heavy material sedimented at a very low speed, an indication of considerable aggregation of the split products, while some of the depolymerization products remained in solution and could not be sedimented even at high speed, indicative of their low molecular weight. (Additional evidence for aggregation of the split products is the readily visible white precipitate which invariably settles in the bend of the viscometer several hours after enzymic treatment of STN.) No well-defined boundary was recorded in this experiment.

Analytical Observations

Phosphorus determinations by the Fiske-Subbarow method failed to reveal the liberation of inorganic phosphate as a result of the enzymic depolymerization of the STN. However, the assay of acid-soluble phosphorus at different temperatures by Dr. Max M. Friedman (see Table II) showed that the bulk of the acid-soluble phosphorus is present in the fraction soluble in 5% trichloroacetic acid at 30°, which is indicative of the low molecular weight of the split products formed from STN by desoxyribonuclease.

Effect of Combined Sonic and Enzymatic Treatment

It was thought of interest to study the effect of the enzyme on sodium desoxyribosenucleinate following partial depolymerization by sonic irradiation. 30 ml. of 0.2% STN-VI solution (relative viscosity 10.67) were sonically treated for 20 seconds. The relative viscosity of the system decreased to 5.31 during that time. The partially depolymerized STN was now treated with the enzyme (1 μg. per milliliter final concentration) for 30 minutes at 30°. At the end of that period the viscosity had further decreased to 1.21 (see Fig. 11). It will be seen from the figure that the course of the viscosity change is practically the same as that of a STN solution which has been diluted to a viscosity level similar to that of the sonically treated material prior to the addition of the enzyme. It follows that a brief sonic treatment of STN does not impair the ability of the material to serve as a substrate for the enzyme. The sedimentation diagram, obtained with STN after 45 seconds of sonic irradiation, indicates that the molecular shape of STN has been only slightly affected by this treatment (see above under "Ultracentrifuge Experiments").

It might be mentioned in passing that the activity of the enzyme itself is not affected by sonic irradiation at 9000 cycles per second of up to 5 minutes duration.

Thermal Depolymerization

Preliminary tests showed that a highly viscous aqueous solution of sodium desoxyribosenucleinate loses its viscosity when it is heated almost to the boiling point and then permitted to cool to room temperature. Upon adding the solution to 1.5 volumes of ethyl alcohol a flocculent precipitate is formed instead of the fibrous material yielded by "native" nucleic acid preparations. This phenomenon of thermal "denaturation" was subsequently studied in some detail. When dilute STN solutions in veronal-HCl buffer of *p*H 7.1 are heated for periods of from 1 to 7 minutes in a water bath at temperatures ranging from 60 to 100° and are then rapidly cooled in an ice bath, the relative viscosity as measured at 30° changes as shown graphically in Figure 12. It will be seen that heating of a 0.1% STN solution for 7 minutes at 60° affects the relative viscosity only slightly. At 80°, however, and even more so at 90° and 100° a rapid fall in the relative viscosity of the solution occurs. At 100° the change to a viscosity close to that of the solvent is complete after one minute. It is evident from the curves shown in Figure 12 that the temperature coefficient of the thermal depolymerization of STN increases steeply between 80° and 100°. Thus, a point corresponding to a relative viscosity of 2.36 is reached at 80° within 6 minutes while the same value is attained at 90° in less than 1 minute, corresponding to a sixfold increase in rate over a temperature range of 10°. This is in contrast to the two- and three-fold increase in reaction rate over the same temperature interval usually observed in chemical reactions.

The examination in the Beckman spectrophotometer of a 0.048% STN solution in distilled water (after dilution to 0.008%) which had been heated for 15 minutes at 100° showed no change in the position of the maximum at 259 mμ or of the minimum at 231 mμ, although the relative viscosity had fallen from 3.11 to 1.35 as a result of this treatment. The rise in optical density from 1.28 to 1.46 at 259 mμ which was observed in this experiment may possibly be due to the fact that it was performed in the absence of a buffer system (see above, under "Effect on Absorption Spectrum").

No inorganic phosphate was liberated in the course of thermal depolymerization. The analysis for acid-soluble phosphorus (see Table II) showed that the bulk of that fraction was only solubilized at 90°, which is indicative of a relatively high molecular weight of the thermal split products.

When a STN solution (0.2%) was examined in the analytical ultracentrifuge (Expt. 0-284) after heating it for 15 minutes at 100° in buffered solution, at *p*H 7.4, no sedimenting boundary was observed at the speed employed (*ca.* 700 r.p.s.). The relative viscosity of the solution examined was 1.29.

Repolymerization Experiments

Vilbrandt and Tennent[17] have studied the reversibility of the depolymerization by acid and alkali of sodium desoxyribosenucleinate. It was thought to be of interest to examine the extent of *spontaneous* repolymerization of STN following depolymerization by sonic, enzymic, or thermal treatment.

A 0.16% STN solution in veronal-HCl buffer of *p*H 7.4 and of a relative viscosity of 8.19 was sonically irradiated for 25 minutes at a temperature not exceeding 12°. The relative viscosity decreased to 1.13 in the course of the sonic treatment. The final product was allowed to stand for a total of 21 hours at 30°. The relative viscosity was determined at various intervals during that period and it was found to remain unchanged. After standing for an additional 24 hours at room temperature, again no change in viscosity could be detected. It would appear, therefore, that there is no tendency on the part of the fragments to repolymerize under these conditions. In the instance of a STN solution which had been sonically treated for only 30 seconds, a slight increase in relative viscosity from 3.92 to 4.21 occurred on standing for 22 hours at 30°.

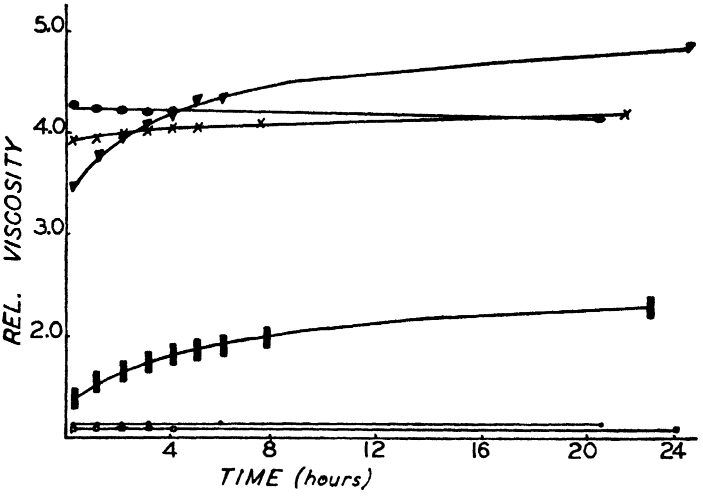

Fig. 13. Repolymerization curves of STN-6 at 30°.

Open circles: sonically treated 25 min. at 9000 c.p.s.; crosses: sonically treated 0.5 min. at 9000 c.p.s.; filled rectangles: thermally treated 20 min. at 100°; filled triangles: thermally treated 0.5 min. at 100°; open squares: enzymically treated 18 hours at 30°; filled circles: enzymically treated 50 min. at 30°.

A 0.14% STN solution was depolymerized by desoxyribonuclease in the presence of magnesium as activator. After 18 hours at 30°, the relative viscosity had reached a value of 1.05, whereas the 0.18% STN stock solution used in the experiment showed a relative viscosity of 9.64. At the conclusion of the enzymic treatment, citrate (final concentration, 0.03 *M*) was added in order to stop further enzyme action. No rise in relative viscosity of the solution was observed upon standing for 24 hours at the same temperature. Similar results were obtained when the enzymic depolymerization was interrupted by the addition of the inhibitor after 50 minutes, at which time the relative viscosity had fallen to 4.22.

A behavior differing from that of the enzymically or sonically treated STN solutions was exhibited by the material which had been thermally depolymerized: When a 0.16% STN solution (relative viscosity 8.10) was heated for 20 minutes at 100°, the relative viscosity fell to 1.36. On standing for 23 hours at 30° the viscosity of the solution rose to 2.31. Similarly, the relative viscosity of a STN solution of the same concentration, which had been reduced to 3.46 through heating for 30 seconds at 100°, increased to 4.86 upon standing for 24.5 hours at 30°. These viscosity changes are definitely outside the limit of experimental error or variation and they are, therefore, to be considered as indicative of a certain degree of repolymerization of the split products resulting from thermal treatment of the STN.

The observations made in these repolymerization experiments are summarized in Figure 13.

DISCUSSION

An attempt to explain the effect of the various physical and chemical agents on desoxyribosenucleic acid must take into account the following facts: (*1*) all three agents (sonic radiation, thermal, and enzymic treatment) lead to a depolymerization as judged by the marked decrease in relative viscosity; (*2*) they do not appear to cause fission of the heterocyclic structures of the purine and pyrimidine bases of the component nucleotides as evidenced by the absence of drastic alteration of the ultraviolet spectrum; and (*3*) they produce fragments of different type as indicated by their behavior in the ultracentrifuge, the results of the chemical fractionation of their acid-soluble phosphorus as a function of temperature, and their dissimilar tendency to repolymerize spontaneously.

If it is assumed that sodium desoxyribosenucleinate in the solvents employed exists in the form of more or less extended linear polynucleotide chains having a backbone formed of desoxyribose-phosphate-desoxyribose linkages, then it follows that depolymerization must involve the rupture of some of these main valency bonds of the low-energy phosphate ester type. A mere reduction in asymmetry of the particles without a change in mass could result from a folding or coiling of the long threads into more compact structures. There is no evidence that the changes here observed are due to such a reversible transformation.

There can be no doubt that the action of pancreas desoxyribonuclease on STN involves the fragmentation of the polynucleotide chain into numerous oligonucleotides of varying size and relatively low viscosity (*cf.* refs. 18 and 19). The present data are in agreement with that view. As far as the mechanism of the depolymerization of STN by sonic irradiation is concerned, the recent experiments by Oster[20] on the effect of this treatment on tobacco mosaic virus preparations are of special interest. On the basis of electron microscopic studies they lead to the view that the individual virus particles of 280 mμ length are broken first into halves and then into quarters through the cavitation effect resulting from the sonic vibrations. The sedimentation of sonically treated sodium desoxyribosenucleinate solutions in the analytical ultracentrifuge (Fig. 4) indicates that a similar mechanism operates in the present instance. A replotting of the viscosity data obtained by Oster on tobacco mosaic virus solutions after sonic irradiation[20] (Fig. 1) in a manner similar to that used in presenting the viscosity measurements on irradiated STN (see Fig. 2) discloses a comparable time course in both cases, in spite of the great disparity in the actual viscosity values. That main valency bonds may be broken through the application of purely mechanical forces to fiber structures is demonstrated by the recent experiments of Lundgren[21] on the splitting of disulfide cross-links in protein fibers on stretching. The depolymerization of desoxyribosenucleic acid by thermal treatment is of special interest in view of the high temperature coefficient and, hence, large energy of activation, observed in the range between 60 and 100° (see Fig. 12). While this phenomenon is similar to the heat inactivation and denaturation of proteins (*cf.* ref. 22), there exist important differences. Thus, the nucleic acid molecules appear to be split into many small fragments on heating while the thermal denaturation of proteins, as a rule, does not lead to a significant alteration of their molecular weight, although in some instances aggregation will occur under these conditions (*cf.* ref. 22). This would seem to indicate that the bond strength of the sugar–phosphate links in the polynucleotide chain is smaller than that of the peptide bonds in proteins. The increase in viscosity on standing in thermally depolymerized STN solutions (Fig. 13) indicates a certain affinity of the thermal split products for each other.

References

1. E. Hammarsten, *Biochem. Z.*, **144,** 383 (1924).
2. J. P. Greenstein, *Advances in Protein Chemistry*, **1,** 209 (1944).
3. A. Wissler, Ph.D. Thesis, Bern (1940).
4. B. Taylor, J. P. Greenstein, and A. Hollaender, *Cold Spring Harbor Symposia Quant. Biol.*, **XII,** 237 (1947).
5. A. Hollaender, J. P. Greenstein, and W. V. Jenrette, *J. Natl. Cancer Inst.*, **2,** 23 (1941).
6. M. McCarty, *J. Gen. Physiol.*, **29,** 123 (1946).
7. M. Kunitz, *Science*, **108,** 19 (1948).
8. A. E. Mirsky and H. Ris, *J. Gen. Physiol.*, **31,** 1 (1947).
9. A. E. Mirsky and A. W. Pollister, *J. Gen. Physiol.*, **30,** 101 (1946).
10. K. G. Stern and S. Davis, *Federation Proc.*, **5,** 156 (1946); S. Davis, M.S. Thesis, Polytechnic Institute of Brooklyn (1946).
11. K. G. Stern, S. Singer, and S. Davis, *Polymer Bull.*, **1,** 31 (1945).
12. H. G. Tennent and C. F. Vilbrandt, *J. Am. Chem. Soc.*, **65,** 424 (1943).

13. M. Kunitz, *J. Biol. Chem.*, **164**, 563 (1946).

14. F. G. Fischer, I. Boettger, and H. Lehmann-Echternacht, *Z. physiol. Chem.*, **271**, 246 (1941).

15. O. T. Avery, C. M. MacLeod, and M. McCarty, *J. Exptl. Med.*, **79**, 137 (1944).

16. K. G. Stern, G. Goldstein, J. Wagman, and J. Schryver, *Federation Proc.*, **6**, No. 1 (1947).

17. C. F. Vilbrandt and H. G. Tennent, *J. Am. Chem. Soc.*, **65**, 1806 (1943).

18. M. Laskowski and M. K. Seidel, *Arch. Biochem.*, **7**, 465 (1945).

19. M. Laskowski, *Arch. Biochem.*, **11**, 41 (1946).

20. G. Oster, *J. Gen. Physiol.*, **31**, 89 (1947).

21. H. P. Lundgren and A. M. Stein, Abstract of paper presented at 114th Meeting of Am. Chem. Soc., Portland, Oregon, Sept., 1948, Program No. 50-0.

22. H. Neurath, J. P. Greenstein, F. W. Putman, and J. O. Erickson, *Chem. Rev.*, **34**, 157 (1944).

English Synopsis, see Summaries, page S18, Vol. V, 1950.

Résumé

Les effets de vibrations intenses du domaine des fréquences acoustiques, des températures élevées, et de la desoxyribonucléase du pancréas sur le desoxyribosenucléinate sodique hautement polymérisé ont été étudiées de façon comparative et quantitative. Ces trois agents produisent une dépolymérisation du nucléinate, entrainant une diminution rapide de la viscosité des solutions aqueuses diluées. Le spectre d'absorption ultraviolet du nucléinate n'est pas modifié considérablement par ces traitements. A l'ultracentrifuge, on voit que le mécanisme de la dépolymérisation varie avec le type de l'agent utilisé. Contrairement à la substance dépolymérisée enzymatiquement et aux ondes acoustiques, le STN, traité thermiquement, a tendance à repolymériser spontanément. Le nucléinate sodique, partiellment dépolymérisé au traitement sonique, peut être dégradé ultérieurement à la désoxyribonucléase.

Zusammenfassung

Die Wirkung von starken Vibrationen im Hörbereich, von hohen Temperaturen und von gereinigter Pankreasdesoxyribonuklease auf hochpolymerisiertes Natriumdesoxyribonukleat wurde quantitativ und vergleichend untersucht. Alle drei Mittel rufen eine Depolymerisation des Nukleates hervor, die in einer schnellen Abnahme der Viskosität verdünnter wässriger Lösungen resultiert. Das Ultraviolett-Absorptionsspektrum des Nukleats wird durch diese Mittel nicht erheblich beeinflusst. Experimente in der Ultrazentrifuge zeigen, dass der Mechanismus der Depolymerisation je nach dem verwendeten Mittel verschieden ist. Im Gegensatz zu den enzymatisch und mit Schall depolymerisierten Substanzen zeigt das mit Hitze behandelte Natriumdesoxyribonukleat eine Neigung, spontan nach Stehenlassen zu repolymerisieren. Natriumnukleat, welches durch Schallbehandlung teilweise depolymerisiert wurde, kann durch Desoxyribonuklease weiter abgebaut werden.

Received October 20, 1949

JOURNAL OF POLYMER SCIENCE VOL. V, NO. 6, PAGES 709-718

Tetramethylthiuram Disulfide Vulcanization of Extracted Rubber. I. Introduction and Compounding

DAVID CRAIG, A. E. JUVE, and W. L. DAVIDSON, *The B. F. Goodrich Company Research Center, Brecksville, Ohio*

The scope of the present series of papers embraces a limited portion of the field of soft rubber vulcanization, namely, vulcanization with tetramethylthiuram disulfide (TMTD) in the absence of added sulfur. However, for perspective, it has seemed desirable to include a minimum of work on simple sulfur vulcanization in the presence of accelerators. Our reason for investigating the thiuram disulfide type of cure stems from the relatively simple structure and behavior of the TMTD molecule as compared to the eight-membered-ring sulfur molecule. Thus, the reaction products, including those of macromolecular weight which occur in TMTD vulcanizates might be fewer in number and simpler in structure than those occurring in accelerated sulfur vulcanizates.

The techniques which we have applied include short path distillation and radiosulfur tracer chemistry. Certain applications of these will be described in the succeeding papers. The small-scale compounding methods described by Garvey[8] and modified to suit our purposes were used. Certain of the compounding features of our study were chosen to be reported in this introductory paper.

Materials

One of the main purposes of the study was to isolate and identify the vulcanization products. Therefore, more than usual care was taken in selecting and characterizing those starting materials which sometimes are of uncertain composition.

Rubber. Preliminary experiments were conducted with crepe because of its recognized quality. Acetone-extracted crepe was chosen for later experiments mainly because of its low fatty acid content. The stability in air of this material was believed sufficient.

Sulfur. This element, according to Nier[20] contains 95% S^{32}, 0.74% S^{33}, 4.2% S^{34}, and 0.016% S^{36}. The radioactive sulfur, S^*, used contained S^{35} as a tracer. The half life of this isotope is 87 ± 1 days. It was obtained on allocation from the Isotope Division, U. S. Atomic Energy Commission at Oak Ridge, Tennessee. P^{32} was removed from the sample by oxidation to phosphoric acid with concentrated HNO_3. The sulfur was ground in a mortar, boiled with dilute Na_2CO_3, and recrystallized from styrene.

ANALYSIS. *Calcd. for* S_8: S, 100.00. *Found:* S, 100.07, 100.15.

Fatty Acid. Palmitic acid was chosen because of its occurrence as a major component in the fatty acid used in compounding. The sample selected for this study was Eastman Kodak White Label, m.p. 63°.

Zinc Oxide. A reagent grade French Process sample was used for chemical reactions while pigment grade French Process material was used for compounding.

Zinc Sulfide. This material was reagent grade.

ANALYSIS. *Calcd. for* ZnS: Zn, 67.1; S, 32.9. *Found:* Zn, 67.3, 67.3; S, 32.25, 32.20.

Zinc Palmitate. This salt was prepared as described in part IV of the present series.

Tetramethylthiuram Disulfide or TMTD. For most of the compounding studies a commercial grade containing about 3% hydrocarbon oil was used. It melted at about 155°. By recrystallization from alcohol in the presence of a little sulfur or from benzene, the melting point was raised to 159–160° with decomposition. The preparation of radioactive TMTD is set forth in part II of this series.

Tetramethylthiuram Monosulfide or TMTM. The commercial material melting at about 107° was used for compounding. A sample after recrystallization from alcohol melted at 109–110°. It was bright yellow in color.

Zinc Dimethyl Dithiocarbamate or ZnDMDC. The commercial salt melting at 243–245° was used.

The abbreviation PHR is used for "parts per hundred of rubber," TMTU for tetramethylthiourea, DMADC for dimethylammonium dimethyldithiocarbamate, and PBNA for phenyl-beta-naphthylamine.

Literature

Usually the assumption due to Bruni,[3,14] but studied also by Bedford and co-workers,[1,2,6,10,18,21] is made that one of the four sulfur atoms of TMTD is available for effecting vulcanization. This assumption finds support in the fact that TMTM does not vulcanize rubber in the absence of added sulfur although Cummings and Simmons[6] reported that 4.333 PHR TMTM + 0.667 PHR sulfur is equivalent to 5.00 PHR of TMTD for the vulcanization of rubber containing 5.00 PHR of zinc oxide. These investigators opined that this behavior supported the contention of Bedford and Gray[1] that TMTD is active as the result of the formation of ZnDMDC. Clark, LeTourneau, and Ball[4] detected this salt *in situ* in vulcanizates. Jarrijon[12] effectively used a somewhat obscure ultraviolet absorption technique for the quantitative analysis of acetone extracts. He found that 70–76% of the TMTD (3 PHR) added to a zinc oxide (2 PHR) stock could be accounted for as ZnDMDC. The spectrographic results were verified by a gravimetric procedure. Jarrijon found that either acetone extracted or deproteinized rubber vulcanized satisfactorily with TMTD provided zinc oxide was present. He considered that fatty acids were not necessary and that vulcanization occurred only when ZnDMDC was formed. Shephard,[22] previous to the above work, demonstrated by color reactions that the zinc salt was formed during vulcanization and this was confirmed by Shimada.[23] Morrison and Shephard[19] quote Cotton and Westhead[5] (erroneously) to the effect that fatty acids are required with TMTD and suggest that lack of H_2S formation with extracted rubber would prevent vulcanization. Hydrogen sulfide in small amounts was considered necessary by Bedford and Gray in that it effected the formation of ZnDMDC. They considered H_2S to be an inhibitor of vulcanization if present in excess of the amount required to convert the TMTD to ZnDMDC. The products of the latter reaction were reported to be zinc sulfide, CS_2, and dimethylammonium dimethyldithiocarbamate.

Most investigators[5,9,10,12,13,15–18,25,27] consider that zinc oxide is either necessary or desirable for the development of the best physical properties. The minimum quantity mentioned by Morrison and Shephard is 1 PHR but they prefer 5 PHR. However, Bedford and Sebrell[2] state that the accelerating activity of TMTD is not dependent on the presence of zinc oxide. Jarrijon suggested the addition of the TMTD molecule as dithiocarbamate radicals to the double bonds of rubber with the simultaneous formation of water and ZnDMDC. He proposed no exact mechanism but only a "statistical" reaction. He also commented with respect to the TMTD not converted to ZnDMDC, "the last one-third of the TMTD must either combine with the rubber or be decomposed, but in any event does not form TMTM." The main vulcanization reaction was postulated as a simultaneous polymerization and dehydrogenation. Both Farmer[7] and Gee[9] consider TMTD vulcanization to involve the formation of C to C linkages. Stiehler and Wakelin[24] believe that "vulcanization is not solely a cross linking of rubber with sulfur or other primary valence bonds, but rather that both the Tuads (*i.e.*, TMTD) and metallic ion become a part of the structure of the rubber molecules."

One object of the present study was to determine what unrecognized products are formed in the vulcanizate. A survey of the literature cited seemed to indicate that new compounding data were needed in order to avoid unnecessary isolations and analyses on unimportant stocks. The following account of our compounding studies also includes some work suggested by the use of our various techniques to be described in the later papers of the series.

RESULTS

Role of Fatty Acid in TMTD Cures. With respect to the effect of fatty acids on TMTD cures, our results (Table I) agree with those of Jarrijon.[12]

These data were obtained on compounds having the base formula A of extracted pale crepe 100, zinc oxide 5, TMTD 4, and PBNA 1.0. Recipe B had 1.5 parts of palmitic acid added.

TABLE I

	Recipe A				Recipe B			
Cure time at 310°F., min.	Mod. 500%	Mod. 600%	Tensile	Elongation	Mod. 500%	Mod. 600%	Tensile	Elongation
1.5	200	350	950	675	300	550	2400	867
2.5	300	525	1800	833	375	700	3175	853
5	450	875	3400	907	550	1200	3975	803
8	550	1250	3425	800	650	1600	3550	707
11	550	1350	3850	800	600	1600	3825	717
15	625	1550	3875	740	600	1750	3800	712
23	600	1475	3250	740	575	1300	3550	705

Except for a somewhat faster curing rate for the fatty acid containing stock B and a slightly higher modulus, the properties of the two stocks are similar.

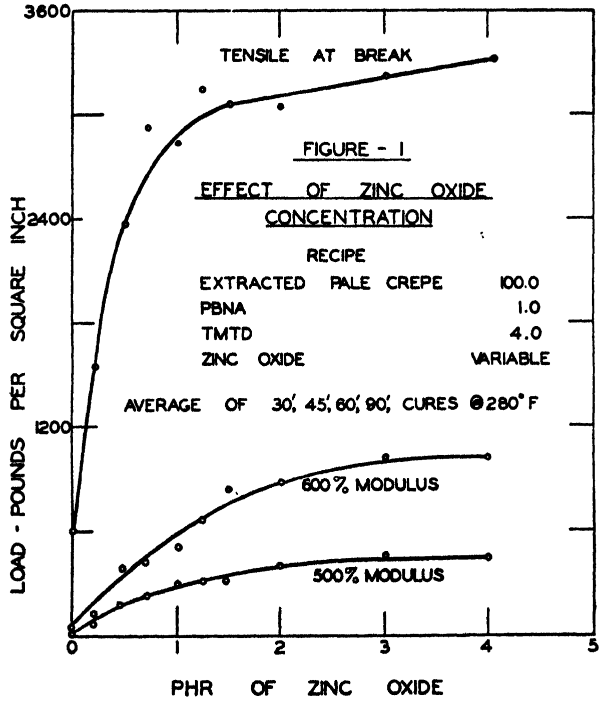

Effect of Variations in Concentration of Zinc Oxide. A series of compounds based on formula A and containing from 0 to 4 PHR of zinc oxide were prepared, cured, and tested. The results are illustrated in Figure 1. From these data it appears that for this concentration of TMTD about 1.5 PHR of zinc oxide are required to develop the maximum tensile strength while between 2.0 and 3.0 PHR are required to develop maximum modulus. These data are similar to those reported by Hull, Olsen, and France[11] for mercaptobenzothiazole stocks in which the ZnO concentration was similarly varied.

The above data show that with 4 parts of TMTD on 100 parts of extracted rubber and no zinc oxide a very poor cure results. However, a vulcanizate prepared from 10 parts of TMTD and 100 of rubber was found to have the following properties which show that it was well cured:

Cure	Mod. 600%	Tensile	Elongation
20 min. at 280°F.	250	3825	925

The vulcanizate was clear, had a strong objectionable odor, and was somewhat brittle when torn. This result definitely shows the nonessential nature of a metallic oxide for vulcanization, a fact that compounders have been aware of for a long time, although it must be admitted that certain physical properties are attributable to the presence of certain zinc compounds in the vulcanizing mixture. We have found that zinc palmitate when added in amounts up to at least 16 PHR results in increased activation. The palmitate is more active on a molar basis than the oxide.

Zinc Sulfide vs. Zinc Oxide as an Activator of TMTD Cures. Bedford and Sebrell reported ZnS as one of the products formed during vulcanization. (See, however, parts IV and V.) Therefore, it was decided to determine the effect of substituting ZnS for ZnO. The results in Table II were obtained using the recipe, extracted pale crepe 100, TMTD 4, and 5 PHR of the zinc compound.

TABLE II

EFFECTS OF ZINC OXIDE AND ZINC SULFIDE

EXTRACTED CREPE 100.00—TMTD 4.00

	Zinc oxide 5.00				Zinc sulfide 5.00			
Cure at 280°F., min.	Mod. 500%	Mod. 600%	Tensile	Elongation	Mod. 500%	Mod. 600%	Tensile	Elongation
5	—	—	—	—	50	100	700	1027
10	175	300	1900	945	175	275	2350	965
20	300	450	2750	875	250	500	3600	940
30	525	1025	3075	780	250	450	3200	925
45	575	1225	3350	733	250	350	2975	907
60	550	1225	4000	745	225	450	3200	925
90	775	1425	3450	710	200	275	2650	960
AFTER AGING 24 HOURS AT 212°F.								
45	575	1200	3100	733	200	375	2975	893
60	575	1250	2350	700	175	350	2900	875

These results demonstrate that a good cure is obtained using ZnS instead of ZnO but that a lower modulus and higher elongation is developed, indicating a less "tight" cure. Evidence that the ZnS is not inactive is shown

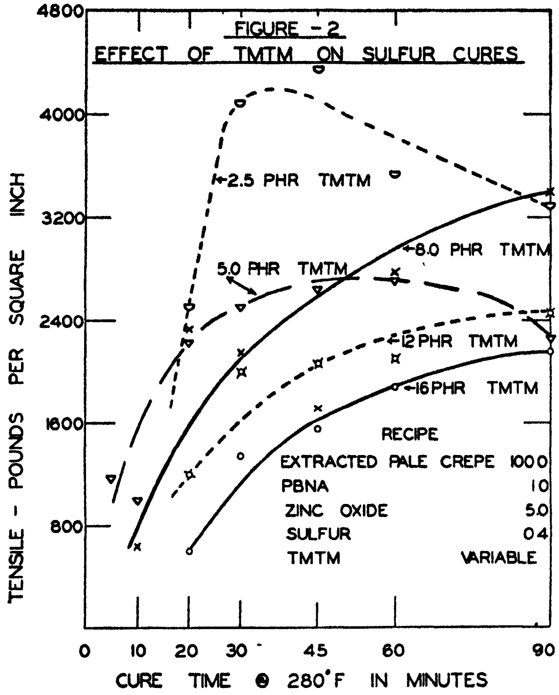
FIGURE - 2
EFFECT OF TMTM ON SULFUR CURES
2.5 PHR TMTM
5.0 PHR TMTM
8.0 PHR TMTM
12 PHR TMTM
16 PHR TMTM
RECIPE
EXTRACTED PALE CREPE 100.0
PBNA 1.0
ZINC OXIDE 5.0
SULFUR 0.4
TMTM VARIABLE
TENSILE - POUNDS PER SQUARE INCH
4800
4000
3200
2400
1600
800
0
10
20
30
45
60
90
CURE TIME @ 280°F IN MINUTES

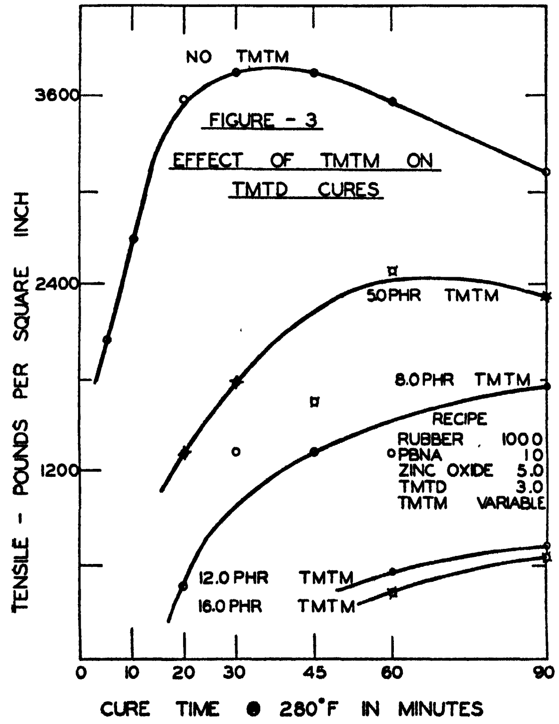
FIGURE - 3
EFFECT OF TMTM ON TMTD CURES
NO TMTM
5.0 PHR TMTM
8.0 PHR TMTM
12.0 PHR TMTM
16.0 PHR TMTM
RECIPE
RUBBER 100.0
PBNA 1.0
ZINC OXIDE 5.0
TMTD 3.0
TMTM VARIABLE
TENSILE - POUNDS PER SQUARE INCH
3600
2400
1200
0
10
20
30
45
60
90
CURE TIME @ 280°F IN MINUTES

by comparing these results with those shown in Figure 1 for the stock containing no ZnO.

Effect of Large Dosages of TMTM on Vulcanization. Since TMTD can be prepared by heating sulfur with TMTM (compare part II) it would be reasonable to expect that, even in the presence of rubber, sulfur and TMTM would form TMTD. It may be supposed also that if excessive ratios of TMTM were used they should have a retarding or inhibiting effect on the cure provided TMTD is incapable of vulcanization when thus stabilized.

To confirm this supposition the following two series of compounds were prepared: (*1*) extracted pale crepe 100, zinc oxide 5, sulfur 0.4, and TMTM 2.6, 5, 8, 12, and 16 PHR; and (*2*) extracted pale crepe 100, zinc oxide 5, TMTD 3.00, and TMTM 0, 5, 8, 12, and 16 PHR.

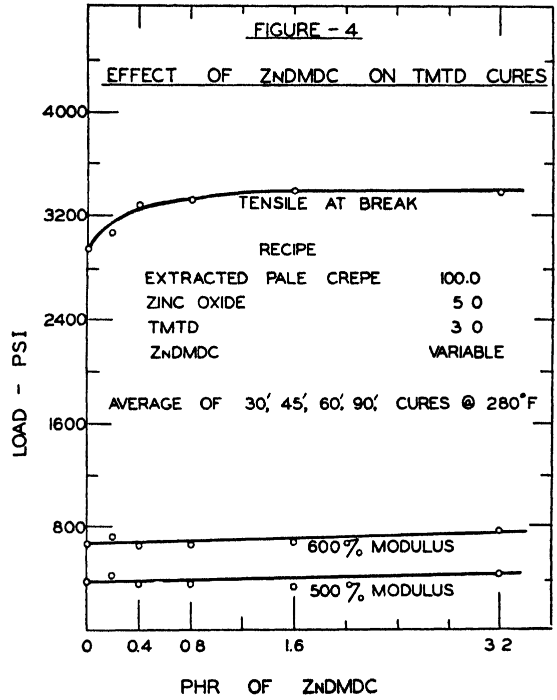

The stress–strain data obtained on these vulcanizates are illustrated in Figures 2 and 3. The marked inhibition observed is evidence that the above suppositions are correct. A similar effect was noted for sulfur vulcanization where ZnDMDC was used as the accelerator. A possibly related "retarding" effect of Captax and Altax on Tuads has been reported [*Vanderbilt News*, 1, 31 (1931)]. We have also found *n*-dodecyl mercaptan to strongly inhibit TMTD vulcanization, a result which recalls Bedford and Gray's experience with H_2S.

Effect of the Addition of ZnDMDC to a TMTD Stock. Since ZnDMDC is one of the principal products formed during vulcanization with TMTD and ZnO, it was of interest to determine the effect of the addition of increasing proportions of ZnDMDC to such a composition. To a base stock containing extracted pale crepe 100.0, TMTD 3.00, and ZnO 5.00, the following proportions of ZnDMDC were added: 0.20, 0.40, 0.80, 1.60, and 3.20. Stress-strain data on the vulcanizates are illustrated in Figure 4. The data show that additions of the dithiocarbamate enhance the state of cure only slightly if at all. When the dithiocarbamate was tested as an activator in the absence of ZnO it was found to be about 50% as effective as ZnO with respect to the maximum properties attainable, but with respect to the rate of reaction to be about the same as the oxide.

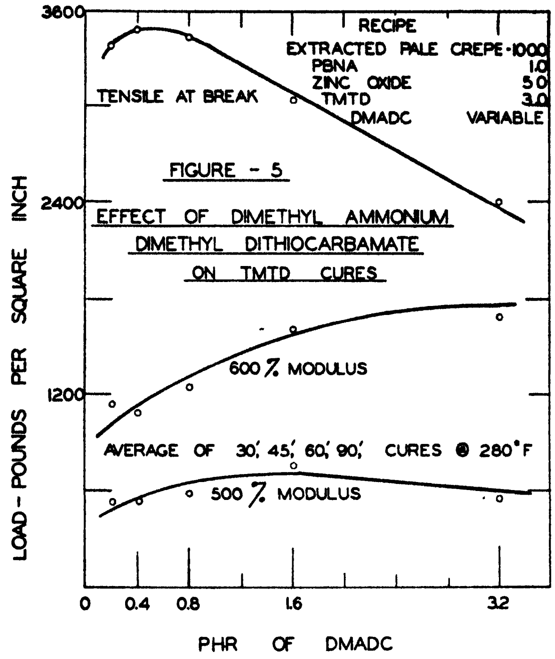

Effect of Addition of Dimethylammonium Dimethyldithiocarbamate to a TMTD Stock. Increasing proportions of dimethylammonium dimethyldithiocarbamate[26] were added to the base stock of the preceding paragraph. The stress-strain data for the vulcanizates of the resulting mixtures are illustrated in Figure 5. While the data indicate that high ratios of the ammonium salt have an adverse effect on the tensile strength, visual examination of the vulcanizates show an increased spottiness with increasing ratios. This nonhomogeneity was undoubtedly responsible for the short breaks and low tensile strength. It is concluded that the addition of this salt does not affect the cure of the TMTD stock.

SUMMARY OF COMPOUNDING STUDIES

(*1*) Large dosages of TMTM inhibit TMTD vulcanization or vulcanization with sulfur.

(*2*) That the presence of up to about 1.5 PHR zinc oxide is desirable for TMTD vulcanization was confirmed. If an unusually large amount of TMTD (10 PHR) is used, a well-vulcanized stock may be obtained without zinc activation.

(*3*) Palmitic acid displayed only a mild activating effect on TMTD vulcanization.

(*4*) Zinc dimethyldithiocarbamate, a main product of TMTD vulcanization, is not an activator for a TMTD-zinc oxide recipe.

(*5*) Dimethylammonium dimethyldithiocarbamate does not activate TMTD-zinc oxide formulations.

(*6*) Zinc sulfide was found to be an effective activator for TMTD vulcanization.

References

1. Bedford and Gray, *Ind. Eng. Chem.*, **15**, 720 (1923).
2. Bedford and Sebrell, *Ind. Eng. Chem.*, **14**, 25 (1922).
3. Bruni and Romani, *Giorn. chim. ind. applicata*, **3**, 197, 351 (1921); *India Rubber J.*, **64**, 937 (1922); *ibid.*, **62**, 63 (1921).
4. Clark, LeTourneau, and Ball, *Ind. Eng. Chem.*, **35**, 198 (1943); *Rubber Chem. and Technol.*, **16**, 621 (1943).
5. Cotton and Westhead, *Trans. Inst. Rubber Ind.*, **13**, 230 (1937); *Rubber Chem. and Technol.*, **11**, 331 (1938).
6. Cummings and Simmons, *Ind. Eng. Chem.*, **20**, 1173 (1928); *Rubber Chem. and Technol.*, **2**, 59 (1929).
7. Farmer. (a) *J. Polymer Science*, **1**, 293 (1946). (b) *J. Chem. Soc.*, **1947**, 1525. (c) *Trans. Faraday Soc.*, **42**, 228 (1946). (d) *Trans. Inst. Rubber Ind.*, **21**, 122 (1946). (e) *J. Soc. Chem. Ind.*, **66**, 86 (1947). (f) H. Mark and G. S. Whitby, eds., *Advances in Colloid Science*, Vol. II, Interscience, New York, 1946, p. 316. (g) *J. Soc. Chem. Ind.*, **66**, 86 (1947).
8. Garvey, *Ind. Eng. Chem.*, **34**, 1320 (1942); *Rubber Chem. and Technol.*, **16**, 679 (1943).
9. Gee, *J. Polymer Sci.*, **2**, 454 (1947).
10. Grenness, *Accelerated Vulcanization of Rubber*, Williams and Norgate, London, 1937, p. 41.
11. Hull, Olsen, and France, *Rubber Chem. and Technol.*, **20**, 649 (1941); *Ind. Eng. Chem.*, **38**, 1282 (1946).
12. Jarrijon, *Rev. gén. caoutchouc*, **20**, 155, 177 (1943); *Rubber Chem. and Technol.*, **19**, 1061 (1946); *Rubber Chem. and Technol.*, **17**, 941 (1944). Compare Dufraisse and Jarrijon, *Compt. rend.*, **215**, 181 (1942), and Dufraisse and Houpillart, *Rev. optique*, **16**, 321 (1943).
13. Jones and Depew, *Ind. Eng. Chem.*, **23**, 1467 (1931).
14. Langenbeck and Rhiem, *Kautschuk*, **12**, 156 (1936); *Rubber Chem. and Technol.*, **10**, 158 (1937).
15. Leduc, *Rev. gén. caoutchouc*, **6**, 20 (1929).
16. Martin and Davey, *J. Soc. Chem. Ind.*, **45**, 174T (1926).
17. Maximov, *Caoutchouc & gutta-percha*, **18**, No. 10, 944, 986 (1921); *Chem. Abstracts*, **15**, 3412 (1921).
18. Dunbrook and Morris, eds., English translation of Memmler, *Science of Rubber*, Reinhold, New York, 1934, page 320.
19. Morrison and Shepard, *Trans. Inst. Rubber Ind.*, *Rubber Chem. and Technol.*, **20**, 803 (1947).

20. Nier, *Phys. Rev.*, **53,** 282 (1938).

21. Scott and Sebrell, in Davis and Blake, *Chemistry and Technology of Rubber*, Reinhold, New York, 1937, p. 311.

22. Shephard, *Ind. Eng. Chem.*, **26,** 1200 (1934).

23. Shimada, *J. Soc. Rubber Ind. Japan, Chem. Abstracts*, **32,** 5253 (1938).

24. Stiehler and Wakelin, *Ind. Eng. Chem.*, **39,** 1647 (1947).

25. Twiss, Brazier, and Thomas, *J. Soc. Chem. Ind.*, **41,** 81T (1922).

26. Whitby and Simmons, in *Proceedings of the Rubber Technology Conference, 1938, London*, Heffer, Cambridge, 1938, page 316. Compare *J. Soc. Chem. Ind.*, **42,** 333T (1923).

27. Whitby and Evans, *J. Soc. Chem. Ind.*, 47, 122T (1928).

English Synopsis, see Summaries, page S14, Vol. V, 1950.

Résumé

La série d'articles, dont celui-ci est le premier, se rapporte à la vulcanisation lente du caoutchouc au moyen de disulfur e de tétraméthylthiurame en absence de soufre. L'étude des caractéristiques de cett e préparation montre que: (1) de grandes quantités de monosulfure inhibent la la vucanisation aussi bien avec que le TMTD qu'avec le soufre; (2) la présence de 1.5% d'oxyde de zinc est désirable; (3) l'acide palmitique exerce seulement un rôle activateur lent; (4) ni le diméthyldithiocarbamate de zinc ni le diméthyldithiocarbamate de diméthylammonium n'activent les procédés TMTD-oxyde de zinc; (5) le sulfure de zinc est un activateur efficace.

Zusammenfassung

Eine Reihe von Veröffentlichungen, von denen die vorliegende die erste ist, behandelt weiche Kautschuk-Vulkanisierungen unter Benutzung von Tetramethylthiuramdisulfid (TMTD) ohne Zugabe von Schwefel. Eine Untersuchung der Mischungscharakteristika in diesem System zeigt folgendes: (1) Grosse Mengen Monosulfid inhibieren die Vulkanisierung mit sowohl TMTD als auch Schwefel; (2) Die Gegenwart von 1.5% Zinkoxyd ist erwünscht; (3) Palmitinsäure hat nur eine leicht aktivierende Wirkung; (4) Weder Zinkdimethyldithiocarbamat noch Dimethylammoniumdimethyldithiocarbamat aktivieren TMTD-Zinkoxyd-Formulierungen; und (5) Zinksulfid ist ein wirksamer Aktivator.

Received September, 12, 1949

Experimental Study of Copolymerization. IV*

TURNER ALFREY, JR.,** JOHN BOHRER, HOWARD HAAS,† and CHARLES LEWIS, *Institute of Polymer Research, Polytechnic Institute of Brooklyn, New York*

We have investigated the copolymerization behavior of fourteen monomer pairs. The systems investigated and the reactivity ratios (r_1 and r_2) obtained are given in Table I.

TABLE I

System	M_1	M_2	r_1	r_2
I	Vinylidene chloride	Indene	0.40	0.33
II	*o*-Chlorostyrene	Indene	3.50	0 0
III	Vinylidene chloride	Coumarin	[a]	0.0
IV	Vinylidene chloride	Methacrylic acid	0 15	3 0
V	*o*-Chlorostyrene	Methacrylic acid	0 12	0.70
VI	Methyl methacrylate	2-Vinylpyridine	0.33	0.70
VII	Vinyl acetate	2-Vinylpyridine	0.0	30
VIII	Methyl methacrylate	Methyl α-chloroacrylate	0.30	1.2
IX	Acrylonitrile	Methyl α-chloroacrylate	0.15	2.0
X	Vinyl chloride	*tert*-Butylethylene	5.	0.0
XI	Vinyl acetate	1,1-Dichloro-2,2-difluoroethylene	0.6	0.0
XII	Vinyl acetate	Acrylonitrile	0.07	6.0
XIII	Vinyl chloride	Diethyl maleate	0.9	0.0
XIV	Styrene	Hexachlorobutadiene	[a]	0.0

[a] Very large.

Note: Estimated errors in above values are ±15% of reported values.

EXPERIMENTAL

The preparation of most of the monomers used has already been described.[1] The others are described below.

Coumarin (m.p. 71°C.) was purchased from Eimer & Amend, and used as received.

Indene (m.p. −2.0°C.) was obtained from Barrett Division, Allied Chemical & Dye Corp. The sample had been purified by recrystallization and was used as received.

1,1-Dichloro-2,2-Difluoroethylene was obtained from E. I. du Pont de Nemours & Co., Inc. The brass cylinder in which it was shipped was con-

---

[*] The work described in this paper was carried out under a research contract with the Office of Naval Research.

[**] Present address: Physical Research Division, The Dow Chemical Co., Midland, Mich.

[†] Present address: Polaroid Corporation, Cambridge, Mass.

nected to a Dry Ice trap, and the contents allowed to distil over at room temperature. Subsequent handling was similar to that used for vinyl chloride.[1]

Methyl α-chloroacrylate was prepared from methyl α,β-dichloropropionate, which was purchased from Eastman Kodak Co. The method described in *Experimental Plastics and Synthetic Resins* was used.[2]

A sample of 40% *methacrylic acid* in aqueous solution containing 0.1% hydroquinone was supplied by Rohm & Haas Co. 100 ml. of this material was shaken with 25 g. of sodium chloride in a 500 ml. separatory funnel. Two layers formed. The lower layer, consisting essentially of sodium chloride and water, was discarded. 5 g. of sodium chloride were added to the material in the funnel and shaken. A sludge of sodium chloride and water formed and was discarded. The crude methacrylic acid thus obtained was dried over calcium chloride for 15 hours and distilled at 4 mm. Practically all of the material came over in the range 44–46°C. The purity of the product was determined by titration. *Found*: 52.7% COOH; *theoretical* 52.3%.

Diethyl maleate (Eastman Kodak) was purified by vacuum distillation (b.p. 104–6°C. at 14 mm.).

o-Chlorostyrene (Dow) was purified by vacuum distillation.

tert-Butylethylene was obtained from Professor Newell C. Cook of Pennsylvania State College. It was distilled over sodium immediately before use.

2-Vinylpyridine (Reilly Coal Tar Products) was purified by vacuum distillation.

Hexachlorobutadiene (Eastman Kodak) was purified by vacuum distillation.

All copolymerizations were carried out in sealed Pyrex test tubes at 70°C.

SYSTEM I

(M_1) VINYLIDENE CHLORIDE–(M_2) INDENE

Tube	M_2	% Cl	m_2	% conversion	Time, days
1	0.096	60.31	0.151	16.5	82
2	0.213	47.21	0.314	10.4	82
3	0.341	Sample lost			
4	0.458	38.92	0.423	5.41	82
5	0.623	30.27	0.542	1.56	82
6	0.798	21.60	0.666	0.587	82
7	0.843	14.77	0.767	0.350	22

The M_2 values for samples 1, 2, and 4 have been corrected for high conversion according to the approximate formula:

$$M_2\ (\text{av.}) = M_2 + {}^1/_2\,(M_2 - m_2)\ (\text{conversion})$$

Samples 1 through 6 contained 0.1% benzoyl peroxide. Sample 7 contained no catalyst. Polymers 1–6 were precipitated three times with methanol using methyl ethyl ketone as solvent. Sample 7 was precipitated twice.

All M_2 values have been corrected for high conversion. The copolymers were purified by precipitating three times with methanol, using benzene as solvent.

SYSTEM II

(M_1) *o*-Chlorostyrene–(M_2) Indene

Tube	M_2	% Cl	m_2	% conversion	Time, hrs.
1	0.160	24.20	0.064	21.20	27
2	0.315	22.48	0.141	12.68	27
3	0.452	22.42	0.144	10.08	27
4	0.598	20.25	0.239	6.67	27
5	0.730	19.42	0.275	3.79	27
6	0.854	16.87	0.381	1.66	33

SYSTEM III

(M_1) Vinylidene Chloride–(M_2) Coumarin

Tube	M_2	% Cl	% conversion[a]	Time
2	0.101	70.6	2.40	0 hrs. 50 min.
4	0.305	67.9	4.47	2 15
3	0.332	70.8	3.37	1 50
5	0.391	71.0	4.94	2 15
1	0.611	70.0	11.20	7 0

[a] Based on vinylidene chloride monomer.

All tubes contained 0.1% benzoyl peroxide by weight. The polymers precipitated from the monomer mixtures in the form of fine white powders. No solvent could be found, and all were purified by prolonged extraction with boiling acetone. A mixture was also prepared containing 90.0 mole per cent coumarin. After 50 hours in the thermostat, the material had turned red. No residue remained upon extraction with hot water.

SYSTEM IV

(M_1) Vinylidene Chloride–(M_2) Methacrylic Acid

Tube	M_2	% Cl	m_2	% conversion	Time
1	0.130	43.94	0.428	1.24	5 hrs. 10 min.
2	0.269	30.66	0.609	0.56	7 25
3	0.412	21.12	0.735	1.06	8 25
4	0.546	15.24	0.811	5.85	8 10
5	0.690	9.76	0.880	5.39	7 10
6	0.845	4.01	0.951	3.48	4 45

0.1% benzoyl peroxide was used in each case. The copolymers precipitated from the monomer mixtures in the form of fine white powders. No suitable solvent could be found, and all were purified by prolonged extraction with hexane.

SYSTEM V. (M_1) *o*-CHLOROSTYRENE–(M_2) METHACRYLIC ACID

Tube	M_2	% Cl	m_2	% conversion	Time	
1	0.147	17.98	0.405	5.13	3 hrs.	10 min.
2	0.274	15.95	0.493	4.11	3	10
3	0.380	14.85	0.538	8.43	2	30
4	0.551	13.09	0.606	4.74	2	30
5	0.688	10.30	0.705	4.04	3	10
6	0.890	3.74	0.904	4.99	4	35

0.2% benzoyl peroxide was used in each case. The copolymers were purified by precipitating three times with hexane, using methyl ethyl ketone as solvent.

SYSTEM VI. (M_1) METHYL METHACRYLATE–(M_2) 2-VINYLPYRIDINE

Tube	M_2	% N	m_2	% conversion	Time, min.
1	0.909	11.76	0.877	4.7	5
2	0.722	10.10	0.748	3.7	5
3	0.556	8.69	0.640	6.5	10
4	0.348	6.00	0.438	5.9	15
5	0.249	4.94	0.360	6.3	20
6	0.132	3.28	0.237	7.8	25

0.2% benzoyl peroxide was used in each case. The copolymers were purified by precipitating three times with hexane, using methyl ethyl ketone as solvent.

SYSTEM VII. (M_1) VINYL ACETATE–(M_2) 2-VINYLPYRIDINE

Tube	M_2	% N	m_2	% conversion	Time
1	0.90	12 84	0.97	12	1 hr.
2	0.69	12.85	0.97	11	2 hrs.
3	0.49	12.48	0.93	6	2 hrs.
4	0.30	12.34	0.92	2	6 days
5	0.15	11.81	0.87	2	6 days

The copolymers were purified by precipitating three times with petroleum ether, using methyl ethyl ketone as solvent.

SYSTEM VIII. (M_1) METHYL METHACRYLATE–(M_2) METHYL α-CHLOROACRYLATE

Tube	M_2	% Cl	m_2	% conversion	Time	
1	0.142	9.51	0.284	4.39	25 hrs.	25 min.
2	0.282	12.84	0.392	7.85	23	20
3	0.418	18.03	0.568	6.06	23	20
4	0.555	21.64	0.698	5.43	10	10
5	0.717	24.26	0.796	3.40	3	25
6	0.859	26.00	0.863	3.58	3	25

No catalyst was used in preparing these polymers. They were purified by precipitating three times with heptane, using dioxane as solvent.

SYSTEM IX

(M_1) ACRYLONITRILE–(M_2) METHYL α-CHLOROACRYLATE

Tube	M_2	% Cl	m_2	% conversion	Time
1	0.098	15.16	0.319	2.00	22 hrs. 30 min.
2	0.195	19.93	0.480	2.50	3 20
3	0.311	22.72	0.599	4.57	2 10
4	0.458	24.99	0.713	2.36	45
5	0.615	26.13	0.778	2.18	45
6	0.783	27.53	0.865	1.49	3 35

0.1% benzoyl peroxide was used in tubes 1–5. No catalyst was used in 6. The copolymers were purified by precipitating twice with hexane, using acetone as the solvent.

SYSTEM X

(M_1) VINYL CHLORIDE–(M_2) *tert*-BUTYLETHYLENE

Tube	M_2	% Cl	m_2	% conversion	Time, hrs.
1	0.560	44.5	0.17	7.1	158
2	0.300	53.2	0.05	5.1	11
3	0.733	No polymerization after one month			
4	0.155	54.5	0.03	4.0	3

0.2% benzoyl peroxide was used in each tube. The copolymers were purified by precipitating three times with methanol, using acetone as solvent.

SYSTEM XI

(M_1) VINYL ACETATE–(M_2) 1,1-DICHLORO-2,2-DIFLUOROETHYLENE

Tube	M_2	% Cl	m_2	% conversion	Time
1	0.835	30.00	0.454	1.11	6 hrs. 5 min.
2	0.646	28.11	0.419	9.52	1 hr. 35
3	0.387	21.21	0.299	12.9	1 35
4	0.055	10.39	0.135	18.6	1 35

0.1% benzoyl peroxide was used in tubes 2, 3, and 4. No catalyst was added to 1. The copolymers were purified by precipitating three times with hexane, using benzene as solvent. All M_2 values have been corrected for high conversion.

SYSTEM XII

(M_1) Vinyl Acetate–(M_2) Acrylonitrile

Tube	M_2	% N	m_2	% conversion	Time, min.
1	0.104	10.37	0.512	2.8	105
2	0.213	15.45	0.696	1.8	50
3	0.406	18.12	0.782	2.7	50
4	0.491	20.62	0.855	4.6	50
5	0.676	22.20	0.896	6.0	50
6	0.881	26.30	0.981	2.3	70

0.3% benzoyl peroxide was used in each case. The copolymers were purified by precipitating three times with methanol, using dimethylformamide as solvent.

SYSTEM XIII

(M_1) Vinyl Chloride–(M_2) Diethyl Maleate

Tube	M_2	% Cl	m_2	% conversion	Time
1	0.088	44.8	0.088	8.8	3 hrs. 30 min.
2	0.182	35.7	0.176	11.3	3 30
3	0.315	29.9	0.247	5.7	4 30
4	0.548	21.5	0.372	4.5	7 15
5	0.732	15.9	0.481	2.2	14 15

0.25% benzoyl peroxide was used in each tube. Samples 1 through 3 were purified by precipitation with methanol, using methyl ethyl ketone as solvent. Samples 4 and 5 were purified by precipitation with 80% methanol, 20% water, using methyl ethyl ketone as solvent.

SYSTEM XIV

(M_1) Styrene–(M_2) Hexachlorobutadiene

Tube	M_2	% Cl	m_2	% conversion	Time
1	0.10	2.4	0.08	2.1	1 hr.
2	0.31	Trace	0.00	2.4	1 30 min.
3	0.52	Trace	0.00	1.9	1 30
4	0.70	Trace	0.00	2.7	5 hrs.
5	0.89	Trace	0.00	3.5	26

0.2% benzoyl peroxide was used in each case. The copolymers were purified by precipitating three times with methanol, using methyl ethyl ketone as solvent.

DISCUSSION

The copolymerization of indene with vinylidene chloride indicates that indene can add to its own free radical at an appreciable rate. This was not altogether unexpected, as the thermal polymerization of indene has been reported at 120, 170, and 188°C.[3] We have verified the polymerization of indene at 70°C. A small amount of polymer formed after 18 days in the 70° thermostat. It precipitated as a fine powder upon pouring into methanol.

Coumarin, on the other hand, behaves as an inert diluent with vinylidene chloride. The chlorine analyses indicate that if coumarin enters the polymer at all, it does so to an exceedingly small extent.

Methacrylic acid was copolymerized with vinylidene chloride and with *o*-chlorostyrene with the aim of comparing it with methyl methacrylate. The relative reactivities of these two monomers with the vinylidene chloride and *o*-chlorostyrene free radicals are indicated in Table II. It is seen that methacrylic acid is about 50% more reactive than methyl methacrylate toward the vinylidene chloride radical, and is over 4 times as reactive toward the *o*-chlorostyrene radical. This would indicate that the carboxyl group leads to a somewhat greater reactivity, and a somewhat more positive polarity of the double bond than the carbomethoxyl group.

TABLE II

	Monomer	
Radical	**Methyl methacrylate**	**Methacrylic acid**
Vinylidene chloride	4.1	6.7
o-Chlorostyrene	2	8.3

The data on the copolymerization of 2-vinylpyridine with methyl methacrylate and with vinyl acetate indicate that it is quite similar to styrene in reactivity.

Methyl α-chloroacrylate was copolymerized with methyl methacrylate and with acrylonitrile in order to compare its behavior with that of methyl methacrylate. The relative reactivities are in Table III. We see that methyl α-chloroacrylate is more reactive than methacrylate toward the methyl methacrylate free radical, and that they are about equally reactive toward the acrylonitrile and methyl α-chloroacrylate free radicals. This would imply that the double bond of methyl α-chloroacrylate is somewhat more reactive and more positive than that of methyl methacrylate.

TABLE III

	Monomer	
Radical	**Methyl methacrylate**	**Methyl α-chloroacrylate**
Acrylonitrile	7	7
Methyl methacrylate	1	3
Methyl α-chloroacrylate	0.8	1

The system vinyl chloride/*tert*-butylethylene was investigated because of the possibility that *tert*-butylethylene would show a behavior significantly different from that of other olefins because of the absence of α-methylenic hydrogen atoms. However, it was observed that this monomer copolymerized with vinyl chloride in a fashion very similar to that previously reported for 1-pentene.[1] Thus it did not polymerize by itself at 70°C. in the presence of benzoyl peroxide, and inhibited the polymerization of vinyl chloride.

The behavior of 1,1-dichloro-2,2-difluoroethylene indicates that it does not add to itself at a significant rate in the vinyl acetate copolymer. This nonreactivity may be attributed to steric hindrance of the halogen atoms. Similar results are reported in a recent paper.[4] However, these authors were able to polymerize this compound by using acetyl peroxide as catalyst at a temperature of 135°C.

As would be expected, acrylonitrile is much more reactive than vinyl acetate in copolymerization. Diethyl maleate is about as reactive as vinyl chloride toward the vinyl chloride free radical, but does not add to itself, probably because of steric hindrance. Hexachlorobutadiene is extremely unreactive. Again, we attribute this behavior to steric effects.

References

1. P. Agron, T. Alfrey, J. Bohrer, H. Haas, and H. Wechsler, *J. Polymer Sci.*, **3**, 157 (1948).
2. G. F. D'Alelio, *Experimental Plastics and Synthetic Resins.* Wiley, New York, 1946, p. 81.
3. H. Dostal and R. Raff, *Z. physik. Chem.*, **B32**, 417 (1936).
4. E. T. McBee, H. M. Hill, and G. B. Bachman, *Ind. Eng. Chem.*, **41**, 70 (1949).

English Synopsis, see Summaries, page S13, Vol. V, 1950.

Résumé

Les résultats expérimentaux obtenus pour quatorze copolymérisations sont indiquées. L'addition de l'indène à un radical indènique est confirmée. Ce monomère inhibe intensément la polymérisation du chlorure de vinylidène. La coumarine se comporte comme un diluant inerte à l'égard de la polymérisation du chlorure de vinylidène. L'effet des groupes suivants sur la réactivité de la double soudure est examinée: carboxyle, 2-pyridyle, tertiaire-butyle.

Zusammenfassung

Es werden experimentelle Resultat für 14 copolymere Systeme angegeben. Die Selbstaddition von Indol wurde untersucht. Dieses Monomere inhibiert Vinyliden stark. Cumarin benimmt sich bei der Polymerisation von Vinylidenchlorid als inertes Verdünnungsmittel. Der Effekt der folgenden Gruppen: Carboxyl, 2-Pyridyl, *tert*-Butyl wird auf die Reaktionsfähigkeit der Doppelbindung geprüft.

Received August 15, 1949

JOURNAL OF POLYMER SCIENCE VOL. V, NO. 6, PAGES 727-732

Titration Potentiométrique de la Viscose. III

P. HERRENT et G. JNOFF, *Centre de Recherches de la Fabelta, Union des Fabriques Belges de Textiles Artificiels, Tubize, Belgique*

Dans deux articles précédents,[1] nous avions pu mettre en évidence quelques faits nouveaux dans l'interprétation de l'évolution subie par les éléments constitutifs de la viscose au cours de son mûrissement.

En résumé, nous étions arrivés à conclure que:

1. les composés sulfurés (à l'exception du Na_2S), de même que le carbonate sodicocellulosique présents dans la viscose, devaient se trouver sous la forme "ortho" et non sous la forme "méta."
2. l'évolution du composé cellulosique de la viscose au cours de son mûrissement ne pouvait pas consister en une saponification pure et simple du groupe xanthique, comme on l'avait toujours cru jusqu'à présent. Pour expliquer les faits expérimentaux, nous avons émis l'hypothèse que le mûrissement devait plutôt être une évolution de différents équilibres. Ce ne serait que tout au bout d'une suite de réactions que l'on retrouve la régéneration classique, par saponification d'un groupe d'ou le soufre aurait disparu, des groupes hydroxyles de la cellulose initiale.
3. en vertu de l'essence même de ces différents équilibres, la teneur en sels: sulfure, mono-, di-, trithiocarbonates et carbonate de sodium, devait constamment changer à mesure que le mûrissement se prolongeait.

Il restait à faire, quantitativement, la séparation exacte entre l'évolution individuelle du composé cellulosique d'une part et d'autre part, celle de chacun des sels prenant naissance au cours du mûrissement. En d'autres termes et en abrégé: il fallait tracer les courbes individuelles de la variation de la teneur de chaque élement de la viscose en fonction de la durée du mûrissement.

Ce sera l'objet de l'article ci-dessous:

Avant de pouvoir aborder ce problème, nous avons dû nous livrer à une besogne fort longue et fort ingrate de mise au point de nos méthodes analytiques. Finalement, en combinant des méthodes connues de gazométrie, de titration ordinaire et d'iodométrie à notre méthode de titration potentiométrique, nous avons réussi à doser tous les élements en présence, avec une exactitude suffisante et dans une mesure parfaitement reproductible.

I. ANALYSE DE LA VISCOSE AVANT L'ISOLEMENT DU XANTHATE

La gazométrie nous permet de déterminer les quantités globales de CS_2, CO_2 et H_2S qui se dégageront en traitant la viscose par un acide. D'après nos travaux antérieurs, nous pouvons, par titration potentiométrique, déterminer les teneurs respectives en sulfure et en trithiocarbonate de sodium.

Nous pourrons ainsi, pour chaque moment du mûrissement, faire la discrimination complète de l'origine des gaz dégagés par un traitement acide de la viscose. Le tableau I contient les résultats.

TABLEAU I. ANALYSE DE LA VISCOSE COMPLETE

							Soufre		
Jours mûrissement A	CO_2 B	H_2S C	CS_2 D	Xanthate dans viscose en % E	Na_2S F	Na_4CS_3O G	Gazométrique H	Iodométrique I	Soufre xanthique dans viscose J
1	18.6	14.0	62.0	11.7	9.5	5.5	1.97	2.05	1.36
2	22.5	25.9	54.4	11.0	8.0	24.5	1.92	2.02	1.10
3	25.5	30.8	52.4	11.0	7.5	26.5	1.93	2.12	1.126
4	26.2	32.1	51.7	10.7	7.0	32.5	1.93	2.04	0.969
5	27.0	33.7	51.7	10.5	4.5	37.5	1.95	—	—
8	27.7	35.8	51.0	10.5	2.0	41.0	1 96	—	0.60

Les colonnes B, C et D indiquent respectivement le nombre de centimètres cubes de CO_2, H_2S et CS_2 dégagés par 10 gr. de viscose. Les colonnes F et G donnent le nombre de centimètres cubes de la solution d'$AgNO_3$, 01 *N* nécessaires pour précipiter le sulfure et le trithiocarbonate de sodium contenus dans 10 gr. de viscose. Les colonnes H et I montrent le pourcentage de soufre total de la viscose, obtenu par deux méthodes totalement différentes; l'une (colonne H) par gazométrie, donne la somme de CS_2 et H_2S dégagés, l'autre (colonne I) par iodométrie, est la méthode ordinaire au zincate. La colonne J donne le pourcentage de soufre xanthique dans la viscose, obtenu par la méthode habituelle (précipitation par NaCl et titration iodométrique au zincate).

II. ISOLEMENT DU XANTHATE

Pour faciliter l'exposé, nous continuerons à appeler "xanthate" le composé cellulosique de la viscose, bien que nous sachions que la nature et la constitution de ce composé évoluent constamment et ne correspondent exactement à la formule du xanthate de xanthate de cellulose que tout au début du mûrissement.

Nous nous sommes inspirés de la méthode de Lieser[2] dont nous avons encore soigné les détails. On pèse une certaine quantité de viscose. On fait couler, en un mince filet, cette viscose dans un grand bécher rempli de méthanol, en agitant constamment. On pèse ce qui reste de viscose. Après avoir lavé 4 fois le xanthate coagulé avec du méthanol frais, puis avec de l'éther sec, on achève le séchage sous vide à une température de 35° et on pèse. Nous avons eu soin de tenir compte de la faible quantité de xanthate dissoute dans le méthanol.

L'analyse gazométrique du xanthate isolé, nous donne les quantités de CS_2 et de CO_2 qu'il dégagera sous l'action d'un acide. Un calcul simple nous permettra de remonter à la viscose puisque nous connaissons sa teneur en xanthate.

Les résultats sont rassemblés dans le tableau II.

Les colonnes B et C donnent respectivement le nombre de centimètres cubes de CO_2 et de CS_2 dégagés par 1 gr. de xanthate. La colonne D indique le pourcentage de soufre xanthique obtenu par gazométrie du xanthate isolé et la colonne E donne le même pourcentage obtenu par iodométrie (méthode au zincate).

TABLEAU II. ANALYSE DU XANTHATE ISOLE

Jours mûrissement	CO_2	CS_2	Soufre xanthique	
			gazom.	iodom.
A	B	C	D	E
1	4.05	26.1	0.98	1.08
2	2.46	25 5	0.80	0.90
3	2.06	25.0	0.78	0 87
4	2.75	23.1	0.71	0 78
5	2 40	19 8	0.59	0.69
8	2.60	16.1	0.48	0.63

Les colonnes B, C et D de tableau III contiennent respectivement le nombre de centimètres cubes de CO_2, H_2S et CS_2, dégagés par 10 gr. d'une viscose privée de son xanthate. Ces chiffres ont été obtenus par simple différence des résultats mentionnés dans les deux tableaux précédents.

Les colonnes suivantes donnent le nombre de centimètres cubes de CS_2 ou de CO_2 ou d'H_2S dégagés par les sels sulfurés et par le carbonate de sodium contenus dans 10 gr. de viscose.

TABLEAU III. ANALYSE DE LA VISCOSE SANS XANTHATE

Jours mûrissement	CO_2	H_2S	CS_2	Na_2S	Na_4CS_3O	$Na_4CS_2O_2$	Na_4CSO_3	Na_4CO_4
A	B	C	D	E	F	G	H	I
1	13 9	14	24 2	10 64	3 08	21 12	0.28	13.62
2	19.8	25 03	22.87	8 96	13.72	9.15	3 25	16.55
3	23 22	30.85	21.96	8 4	14 84	9.12	7.65	14.61
4	23 25	32 06	24.36	7 84	18 2	6.16	6.02	17.23
5	24.48	33.7	27.48	5.04	21 0	6.48	7 66	16.82
8	24.93	35.8	28.95	2.24	22.96	5.99	10.6	14 33

III. DISCUSSION DES RESULTATS

Dans la viscose, les teneurs en CS_2 et en H_2S varient en sens inverse et tendent vers une valeur constante à mesure que le mûrissement se prolonge. La variation du CO_2 à la même allure que celle de la teneur en H_2S. L'évolution du soufre xanthique est connue.

La teneur en Na_2S baisse d'une façon continue presque en ligne droite. Celle du trithiocarbonate augmente. On remarquera que cette augmentation est plus rapide au début que vers la fin, où la courbe montre une nette tendance à l'applatissement.

Quant à ce que l'on est convenu d'appeler le "soufre xanthique" on verra que nous l'avons dosé par trois méthodes différentes. La gazométrie et l'iodométrie pratiquées sur le xanthate isolé de la viscose par le procédé au méthanol sont, à notre avis, les méthodes les plus sûres. Bien que l'iodométrie donne des résultats légèrement supérieurs, la concordance entre les deux séries de chiffres nous paraît suffisante, dans l'ensemble, pour ce genre d'analyses. La troisième méthode est la plus couramment employée en fabrication (précipitation du magma cellulosique par NaCl et dosage du soufre, avant et après, par iodométrie en présence d'un sel de zinc). Cette méthode nous a toujours donné des résultats de 30 à 40% supérieurs à ceux des deux premières méthodes. Le soufre libre que l'on dose par différence, est donc toujours nettement trop faible dans ce cas. Ceci n'a rien d'étonnant. Quelles que soient les précautions que l'on prenne, le magma cellulosique qui coagule sous l'action de NaCl, entraînera toujours avec lui—et ce, d'une façon tout-à-fait irrégulière—des quantités plus ou moins importantes de sels sulfurés. Les résultats de cette méthode, s'ils sont suffisants pour la pratique courante de la fabrication, ne peuvent entrer en ligne de compte pour une étude scientifique de la question.

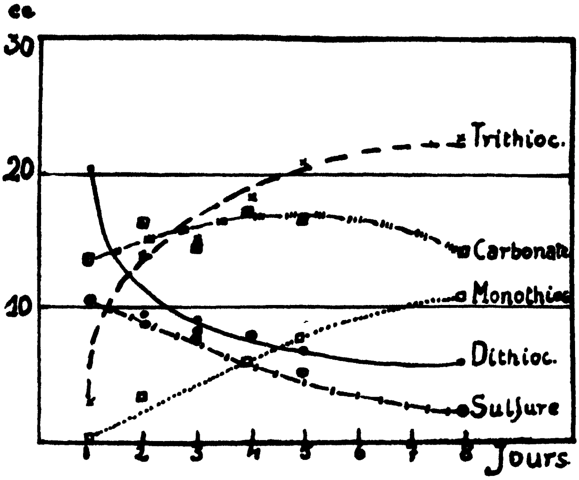

Figure 1

IV. CONCLUSIONS

Pour faciliter notre exposé, nous avons mis en courbe dans le graphique 1, la variation de la teneur des différents sels au cours du mûrissement. Ces teneurs ont été calculées en se basant sur les résultats reproduits dans le tableau III.

Pour la première fois—à notre connaissance, du moins—on a pu prouver l'existence, doser exactement et suivre l'évolution de leur teneur, au cours du mûrissement, du soufre xanthique vrai et des sels minéraux présents dans la viscose.

On constate que, pour une viscose jeune, tout au début de son mûrissement:

1. La quantité de dithiocarbonate est forte. Ceci résulte de l'action du CS_2 en excès, restant occlus dans le xanthate, sur la soude libre. Nous avons démontré, en effet, que si l'on fait réagir du CS_2 sur une solution de NaOH 2 *N*, le premier stade de la réaction est une simple réaction d'addition donnant naissance à l'orthodithiocarbonate de sodium.

2. La quantité de sulfure de sodium est également importante. Ceci résulte d'abord de la facile hydrolyse initiale du xanthate au début du mûrissement (voir nos travaux antérieurs cités plus haut). En second lieu, le dithiocarbonate formé en abondance au début de la dissolution (voir au 1) est instable, comme nous savons. Il perd facilement une molécule de Na_2S pour donner naissance au métamonothiocarbonate, lequel en milieu alcalin, se transformera immédiatement en orthomonothiocarbonate de sodium.

3. Le monothiocarbonate est pratiquement inexistant au début. En vertu de ce que nous venons de dire, ceci s'explique aisément, car nous qualifierions volontiers le monothiocarbonate de "corps secondaire," en ce sens qu'il résulte de réactions entre "corps primaires."

4. La quantité de trithiocarbonate est faible. Ceci n'a rien d'étonnant car, lui aussi doit être rangé dans la catégorie des corps secondaires. En effet, nous avons démontré que si l'on fait réagir des quantités croissantes de CS_2 sur une solution de NaOH 2 *N*, il faut attendre qu'il y ait suffisamment de Na_2S formé, pour voir apparaître le trithiocarbonate. Sa présence serait due à la réaction:

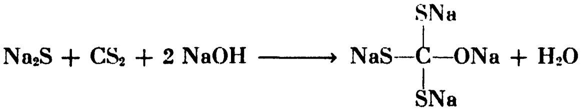

$$Na_2S + CS_2 + 2\,NaOH \longrightarrow NaS-\underset{SNa}{\overset{SNa}{C}}-ONa + H_2O$$

5. La quantité de carbonate de sodium est importante dès le début et l'allure de la variation de sa teneur est difficile à expliquer. Il serait, d'ailleurs, à tout le moins téméraire de vouloir le faire étant donné qu'indépendemment du CO_2 résultant de la variation des différents équilibres réactionnels en cause, il faut tenir compte des quantités de CO_2 éminemment variables et totalement étrangères au mécanisme du mûrissement, apportées ici par la carbonatation de l'alcali cellulose et de la lessive sodique de dissolution.

A mesure que le mûrissement se prolonge, on constate que:

1. La teneur en dithiocarbonate et en sulfure diminue assez rapidement et que cette diminution est presque parallèle. En se basant sur nos travaux antérieurs et sur ce que nous avons dit plus haut, il est aisé de trouver l'explication de cette diminution et de ce parallélisme.

2. La formation de trithiocarbonate rapide au début, diminue graduellement de vitesse. Etant un corps secondaire, sa teneur sera évidemment fonction de la teneur des corps primaires nécessaires à sa formation. Cette dernière diminuant, il est normal de prévoir et de constater que la formation de trithiocarbonate ira, elle aussi, en diminuant.

3. La formation du monothiocarbonate, pour les mêmes causes que ci-dessus, est nettement moins rapide.

Enfin, on trouvera dans le graphique 2 la variation de la teneur en xanthate dans la viscose, en fonction de la durée du mûrissement.

La diminution en poids du composé cellulosique de la viscose est absolument nette. Elle est de 10% en 8 jours. C'est la première fois, croyonsnous, qu'une courbe de ce genre est publiée. On remarquera l'excellente concordance de cette diminution de poids, observée par pesée directe et celle que l'on pourrait calculer à partir des chiffres gamma ou des pourcentages de soufre xanthique au début et à la fin du mûrissement.

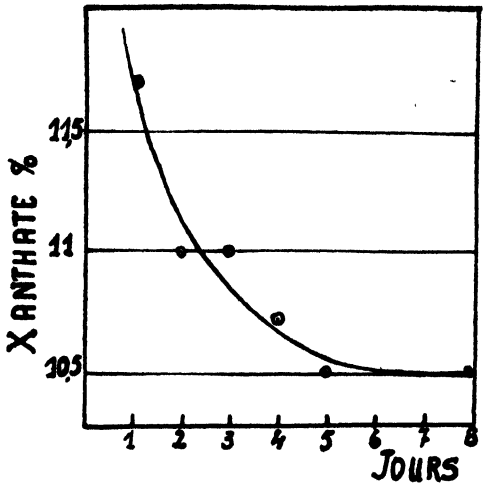

Figure 2

L'allure particulière de cette courbe, de même que celle de l'évolution du soufre xanthique, nous amènent à formuler l'opinion suivante: le coagulation totale ou plus exactement la régénération totale et définitive des groupes hydroxyles de la cellulose initiale, est un phénomène sur la durée duquel personne, à l'heure actuelle, ne peut avoir une idée, même approximative.

Bibliographie

1. P. Herrent et G. Jnoff, *J. Polymer Sci.*, 3, 487, 834 (1948).
2. Lieser, *Ann.*, 464, 43 (1928).

English Synopsis, see Summaries, page S12, Vol. V, 1950.

Résumé

En combinant différentes méthodes d'analyse courantes à notre méthode de titration potentiométrique, nous avons pu tracer la courbe individuelle de la variation de la teneur de chacun des éléments constitutifs d'une viscose en fonction de la durée du mûrissement de la viscose.

Zusammenfassung

Durch Kombinierung von verschiedenen bekannten Analysenmethoden mit der vorliegenden Methode für potentiometrische Titration war es möglich, die individuelle Kurve zu zeichnen, die die Änderung in der Zusammensetzung jedes Viskosebestandteils als eine Funktion des Reifens ausdrückt.

Received July 27, 1949

JOURNAL OF POLYMER SCIENCE VOL. V, NO. 6, PAGES 733-747

LETTERS TO THE EDITORS

New Method for Deriving the Intrinsic Viscosity of Polyelectrolytes

In a previous Letter to the Editors in this journal[1] we discussed some $\eta_{sp.}/C$ *vs.* C curves for sodium pectinate in aq. sodium chloride solutions. C is the pectinate concentration in grams per 100 ml. These curves show a maximum in the neighborhood of a C value at which the equivalent concentration of the polymer is about equal to that of the sodium chloride.

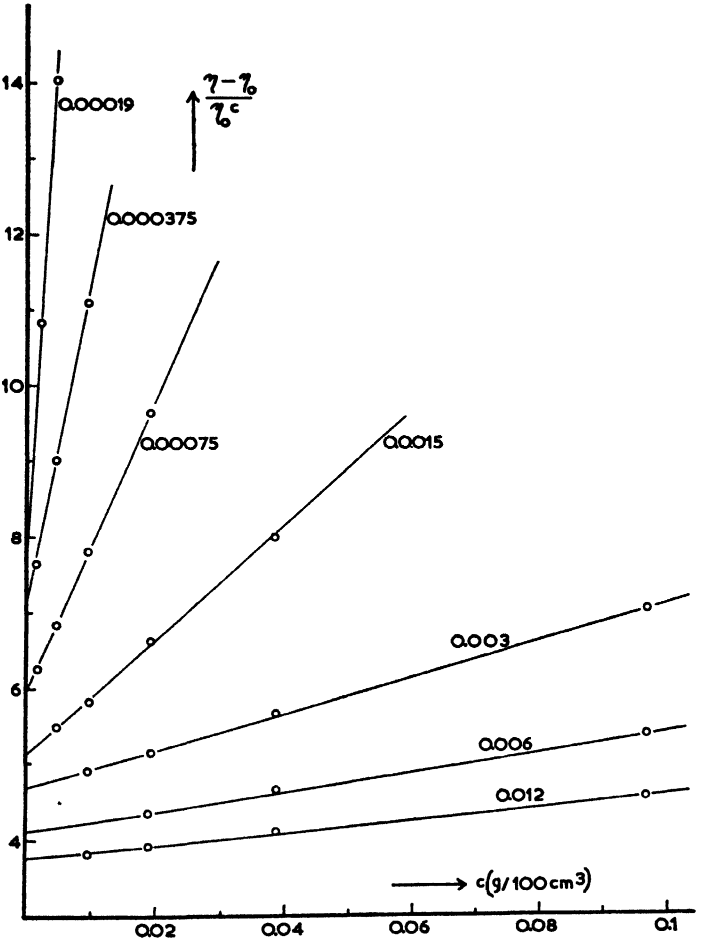

Fig. 1. $\eta_{sp.}/C$ *vs.* C **for sodium pectinate in solutions of NaCl. The value of** x_0 **denotes the NaCl concentration in millimoles per liter at the limit** $C = 0$.

It was suggested by us at that time that it might be possible to avoid the maximum by measuring the viscosity at various polymer concentrations in a series of electrolyte solutions in such a manner that the total ionic strength of the solution is kept constant.

It was found experimentally that this idea is correct. In our former work, all the points along a given $\eta_{sp.}/C$ curve refer to solutions of equal NaCl content, the polymer concentration being the only quantity that was changed. The straight lines in Figure 1, however, were obtained by gradually replacing the polyelectrolyte by an "equivalent" amount of NaCl. It was found that, for all these lines, 1.5 millimoles of NaCl must be considered as "equivalent" to 1 milliequivalent of the polyelectrolyte. In other words, if x denotes the concentration of NaCl in millimoles per liter and γ the polyelectrolyte content in milliequivalents per liter, we have $x = x_0 - 1.5\gamma$ along each of the lines. When the polymer is replaced by either less or more sodium chloride than this, the $\eta_{sp.}/C$ lines becomes slightly curved. A detailed discussion of these data, in conjunction with similar results obtained in solutions of carboxymethylcellulose, will be published later.

The phenomenon is not in itself very surprising except for the fact that the polymer-to-NaCl ratio has a constant value of 1.5 for all the lines in the whole range of C values investigated. The method may be used to obtain intrinsic viscosities with a higher degree of reliability, and is presumably applicable also to light scattering, osmotic measurements, and other data.

The pectinate used has been described in our previous note.[1] Its number-average molecular weight was measured in a Fuoss and Mead type of osmometer and was found to be 4.7×10^4.

Reference

1. D. T. F. Pals and J. J. Hermans, *J. Polymer Sci.*, 3, 897 (1948).

D. T. F. Pals
J. J. Hermans

Laboratory for Inorganic and Physical Chemistry
University of Groningen
The Netherlands

Received August 31, 1950

---

*Note on Density Determination of Cellulose Fibers by the Flotation Method in Carbon Tetrachloride**

In a recently published monograph,[1] as well as in a paper in this journal,[2] we have proposed a method for the determination of the density of cellulose fibers in an absolutely dry condition and with exclusion of air.

* Communication No. 29A from the Laboratory for Cellulose Research.

Since we know that several other workers have taken up this method we wish to draw attention to a source of error that was discovered later and eliminated.

It was found that the fiber pellets used for the flotation method in carbon tetrachloride frequently exhibited a slightly acid reaction after the density determination. Sometimes irreproducible results were obtained if this acid reaction was considerable. After a long search it was established that the acid contamination had its origin in the presence of phosphorous pentoxide in the bulb from which the carbon tetrachloride is distilled, though this oxide is not volatile under the conditions of the experiment. However, commercial pentoxide is usually contaminated with a small amount of phosphorous trioxide. The trioxide is readily volatile with the vapors of boiling carbon tetrachloride.

It is therefore recommended that the pentoxide used be tested for the presence of trioxide. To that end, the oxide is dissolved in water and neutralized with sodium hydroxide, using phenolphthalein. Then silver nitrate is added to precipitate the yellow silver phosphate. If trioxide is present, the latter turns brown or black upon boiling.

To purify contaminated pentoxide we have sublimed it at a temperature of 300–310°C. in a current of dry oxygen. Most of the trioxide can be oxidized in this way, though it appears to be difficult to destroy the last traces of it.

It is recommended that the fiber pellets be tested for the presence of phosphoric acid after termination of the density determination. The very sensitive test given in F. Feigl, *Qualitative Analyse mit Hilfe von Tüpfelreaktionen*, Leipzig, 1938, 3 Aufl., p. 334, can be used. The test should be negative or only faintly positive.

References

1. *Contribution to the Physics of Cellulose Fibres.* Elsevier, Amsterdam-N. Y., 1946.
2. P. H. Hermans, J. J. Hermans, and D. Vermaas, *J. Polymer Sci.*, **1**, 162 (1946).

P. H. Hermans
D. Vermaas

Laboratory for Cellulose Research
of the A.K.U. and Affiliated Companies
Utrecht, Netherlands

Received August 22, 1950

Molecular Weight of Nylon by End-Group Titration

Several authors[1] have described techniques for the end-group titration of dissolved polyamides. A certain difficulty is encountered because of the insolubility of certain nylons in normal organic solvents. Palit[2] has shown that weak bases can be easily titrated in organic solvents with a solution of perchloric acid in glycolic mixtures, such as glycol-isopropyl alcohol or propylene glycol-chloroform. Taking advantage of this fact nylon was dissolved in phenol containing a small amount of glycol and titrated electrometrically with $N/10$, $N/50$, and $N/100$ perchloric acid in 1:1 glycol:isopropyl alcohol. A typical titration curve is shown in Figure 1. The molecular weight was calculated from the equivalence point obtained from the inflexion point of the graph of apparent pH against volume (cc.) of acid added, assuming the existence of one free primary amino group at the end of each chain. The molecular weights obtained by this method were checked against those obtained by point depression of phenol (Table I).

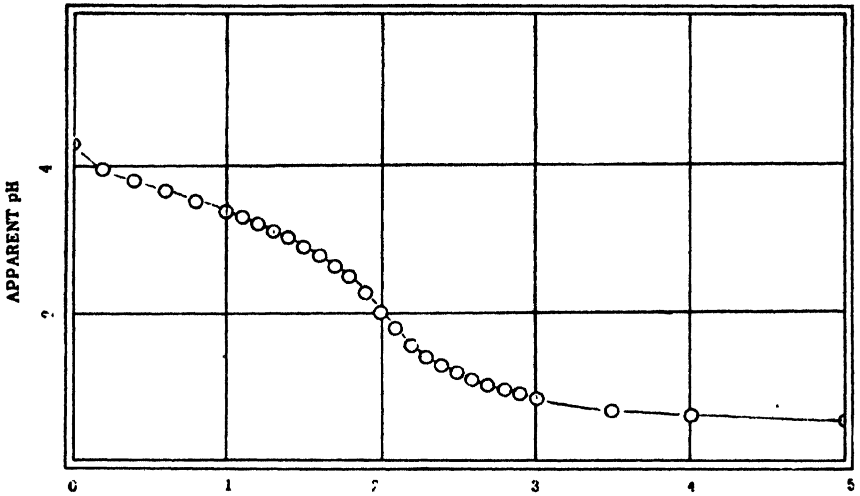

Fig. 1. Titration of nylon.

TABLE I

Titration with perchloric acid	Molecular weight
$N/10$	11,110
$N/50$	11,100
$N/100$	11,010

Depression of freezing point

8.5% solution in phenol gave $\Delta t = 0.070$....10,000

Thanks are due to Prof. Santi R. Palit for his keen interest and helpful suggestions.

References

1. W. H. Carothers and G. J. Berchet, *J. Am. Chem. Soc.*, **52**, 5289 (1930). H. Staudinger and W. Jorder, *J. prakt. Chem.*, **160**, 176 (1942). A. Matthes, *J. prakt. Chem.*, **162**, 245 (1943). G. B. Taylor, *J. Am. Chem. Soc.*, **69**, 635, 638 (1947).
2. S. R. Palit, *Ind. Eng. Chem., Anal. Ed.*, **18**, 246 (1946).

Sadhan Basu

Indian Association for the Cultivation of Science
Calcutta 12, India

Received May 20, 1950

New Observations on the Small-Angle X-Ray Diffraction of Synthetic Fibers

It has been reported by several workers[1-4] that synthetic polyester and polyamide fibers diffract x-rays at small angles to give diffuse interferences representing a definite periodicity along the fiber axis. Similar results have been reported by Fankuchen to Firth[5] for polythene. In all cases the interferences have been described as streaks across the meridian and have been interpreted as showing one-dimensional order in the fibers.

We have now observed that certain nylon (Fig. 1) and polythene (Fig. 2) fibers give small-angle maxima that are discrete interferences not lying on either the meridian or the equator. These results indicate that the units of fiber structure responsible for diffraction effects at small angles apparently are arranged with considerable regularity in two or three dimensions rather than in one direction only. For polythene fibers, both first- and second-order interferences have been observed.

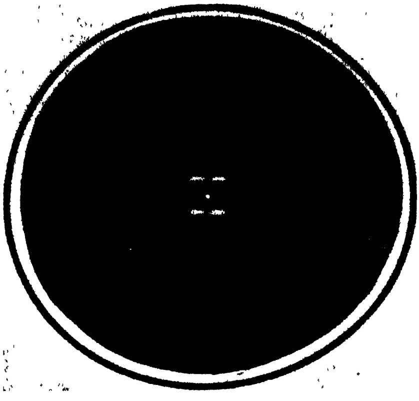

Fig. 1. Small-angle x-ray diffraction of nylon 610 filament. Specimen-to-plate distance 15.0 cm. Fiber axis vertical. CuKα radiation.

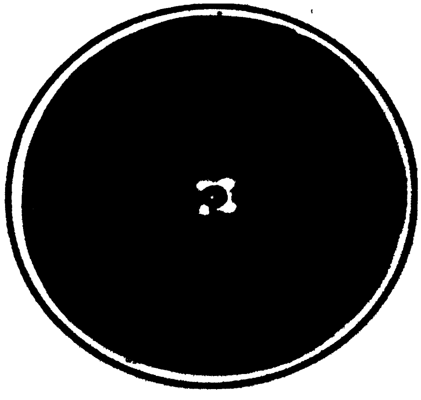

Fig. 2. Small-angle x-ray diffraction of polythene fiber. Specimen-to-plate distance 22.6 cm. Fiber axis vertical. CuKα radiation.

These observations were first noted with a fiber of a copolymer of polyhexamethylene adipamide and polyhexamethylene sebacamide containing the two ingredients in a proportion of 95:5 by weight. The fiber had been drawn to six times its original length at 212°C. The interferences observed corresponded to a layer line spacing of 98 A. and the angle of displacement of the spots from the meridian, δ, was 30°. It was subsequently found that a sample of polyhexamethylene sebacamide (nylon 610) drawn to four times its original length and relaxed in boiling water gave similar interferences with an identity period along the fiber axis of 87 A. The spots were displaced 33° from the meridian. Fibers of this polyamide which had been drawn only or had been drawn and subjected to drastic setting treatments by exposing them to hot aqueous phenol[6] after drawing gave only streaks across the meridian.

Oriented polythene fibers and films have given nonmeridional interferences which vary considerably according to the history of the sample. Typical observations on polythene are given in Table I.

TABLE I

SMALL-ANGLE X-RAY INTERFERENCES FOR POLYTHENE FIBERS

Sample	Identity period along fiber axis, A.	δ[a]
(a) Unit length of fiber drawn to length of 7.6	155	45°
(b) (a) relaxed 26% to length of 5.6	180	42°
(c) (b) redrawn 2/1 to length of 11.2	175	51°
(d) (a) relaxed 42% to length of 4.4	200 105 (second order)	35°
(e) (a) relaxed 57% to 3.3	200	14°

[a] Angle between meridian and radius from central spot to interference.

On the basis of reciprocal lattice theory, Hess and Kiessig[1] have proposed that the length of the interference along the layer line is an inverse measure of the width of the diffracting structure. Broad interferences are interpreted to mean that the diffracting plane is very small, approaching a point in size. Shortening of the interferences is taken to mean that the planes and accordingly also the diffracting structures have become wider. The observations reported here indicate that at least in the cases studied another explanation is necessary since it is not apparent how any combination of one-dimensional order and size of diffracting structure alone could cause the appearance of nonmeridional interferences on the layer line in all orders of diffraction.

Further evidence that the type of order found in these polymers is multidimensional is given by the observations that the long spacings of polythene do not change with the angle of tilt as would be expected from a material ordered essentially in one dimension, as has actually been observed in the case of collagen by Bear and Bolduan.[7] Samples of polythene tilted into the beam show shifts in the lateral position, and the spots merge on tilting, but the Bragg spacing remains constant.

References

1. Hess and Kiessig, *Z. physik. Chem.*, **193,** 196–217 (1944).
2. Fankuchen and Mark, *J. Applied Phys.*, **15,** 364–70 (1944).
3. Bergmann, Fankuchen, and Mark, *Textile Research J.*, **18,** 1 (1948).
4. Wallner, *Monats*, **79,** 279–95 (1948).
5. Firth, *Rubber Age* (*N. Y.*), **57,** 561 (1945).
6. Baker and Fuller, *J. Am. Chem. Soc.*, **65,** 1120 (1943).
7. Bolduan and Bear, *J. Polymer Sci.*, **5,** 159 (1950).

L. M. ARNETT
E. P. H. MEIBOHM
A. F. SMITH

Chemical Department, Experimental Station
E. I. du Pont de Nemours & Company, Inc.
Wilmington, Delaware

Received August 3, 1950

Transport of Uncharged Polymer Molecules by an Inhomogeneous Electric Field

Recently, Karagounis[1] has described some experiments in which nitrobenzene and *p*-nitroaniline in benzene solution tended to migrate into the region of highest field strength in an inhomogeneous electric field, giving measurable concentration changes. It is obvious that this effect will be larger in polymer solutions because of the large volume of the polymer molecules, provided, of course, that the total polarizabilities of the solvent and solute differ appreciably.

Therefore, it is of interest to derive the equilibrium condition between electrical forces and diffusion and to predict the order of magnitude of the concentration gradient obtainable with Karagounis' apparatus[1] for a typical case. The approach used is essentially the same as that of Debye[2] in his consideration of the salting-out effect. In his case, the local concentration of neutral molecules as a function of distance from an ion was desired. For the macroscopic case, the equilibrium condition may be written as:

$$(\partial\mu_2/\partial c_2)\,dc_2 + (\partial\mu_2/\partial P)\,dP + (\partial W_2/\partial x)\,dx = 0 \qquad (1)$$

where c_2 is the solute concentration, μ_2 is the chemical potential of solute, W_2 is the electrical potential energy of solute, P is the pressure, and x is the distance from some reference.

We immediately encounter the difficulty that W_2 may depend on the electrical interaction between solvent and solute, in contrast to the gravitational case where the potential energy is independent of the interaction. In general,[3] and in a binary system:

$$\epsilon - 1/4\pi = \{V_1\alpha_1 + V_2\alpha_2\}\beta \qquad (2)$$

Here ϵ is the dielectric constant of the solution, V_1 and V_2 are volume fractions, α_1 and α_2 are specific polarizabilities (including orientation polarization), and β is the ratio of the local field to the average field. According to Onsager,[3] $\beta = 3\epsilon/(2\epsilon + 1)$. As stated above, α_1 and α_2 may be concentration dependent. The energy per unit volume of dielectric is:

$$W = \frac{E^2(\epsilon - 1)}{8\pi} = \left\{\frac{V_1\alpha_1\beta E^2}{2} + \frac{V_2\alpha_2\beta E^2}{2}\right\} \qquad (3)$$

The average field strength is E.

Assuming that W_2 is given to a first approximation by the second term in equation (3) with constant α_2 and β, for dilute incompressible solutions, we have,

$$\frac{dc_2}{dx} = \bar{V}_2 E\,\frac{dE}{dx}\left\{\alpha_2\beta - \frac{\epsilon - 1}{4\pi}\right\}\Big/\frac{\partial\mu_2}{\partial c_2} \qquad (4)$$

The partial volume of the solute, on a consistent basis is denoted by $\bar{V}_2$.

It has also been assumed that saturation effects can be neglected (*i.e.*, the orientation part of α_2 can be approximated using the first term of the

Langevin function). According to some calculations by Debye,[3] it is believed that this assumption is justified. The change in dielectric constant caused by the orientation of nonpolar anisotropic particles has also been neglected. Equation (4) may be simplified for order of magnitude calculations by writing $\alpha_2\beta$ in terms of an "equivalent dielectric constant," ϵ_2. Then, to a very good approximation, using Karagounis' apparatus consisting of a thin insulated wire coaxial with a cylindrical metal shell, we may write,

$$\frac{dc_2}{dx} = \frac{-c_0AM}{x^3}\, e^{AM/2x^2} \tag{5}$$

$$c_2 = c_0e^{AM/2x^2} \tag{6}$$

Here x is measured from the center of the central wire. A monodisperse ideal solute of molecular weight M has been assumed. The concentration, c_0, is the initial value.

$$A = \frac{\Phi^2\bar{V}_2(\epsilon_2 - \epsilon)}{4\pi RT\epsilon^2\left\{\frac{\epsilon}{\epsilon_G}\ln\frac{a}{a_0} + \ln\frac{b}{a}\right\}^2} \tag{7}$$

Here Φ is the potential difference, ϵ_G is the dielectric constant of the insulation on the central wire, a_0 is the radius of the central wire, a is the radius of the central insulator, and b is the radius of the outer shell. For polyvinyl chloride[5,6] in dioxane, $M = 10^5$, $\epsilon_2 = 12.8$, $\epsilon = 2.3$, $\bar{V}_2 = 0.6$ cc./g., $c_0 = 0.5$ g./100 cc., we obtain c_a (at center insulator surface) $= 1.243\ c_0$. The concentration gradient in all cases is confined to the immediate neighborhood of the central wire, as illustrated below. ($A = 1.089 \times 10^{-10}$, $\Phi = 10^4$ volts.)

THEORETICAL CONCENTRATION GRADIENT AS FUNCTION OF DISTANCE FOR POLYVINYL CHLORIDE IN DIOXANE

dc/dx, g./100 cc./cm.	x, cm.
54.14	0.005
5.59	0.010
1.62	0.015
0.68	0.020
0.35	0.025
0.20	0.030
0.13	0.035
0.08	0.040
0.06	0.045

The values for $x = 0.020$ to $x = 0.040$ are of the order of magnitude usually encountered in sedimentation equilibrium experiments. It would be difficult, but probably not impossible, to devise an optical system to measure this very steep type of gradient. Furthermore, electrical end effects would have to be eliminated, either by the use of thin transparent diaphragms at the ends of the solution cell, the ends being further filled with a suitable liquid, or by the use of transparent solid endpieces of nearly the same dielectric constant as the solution. Knowing $\partial\mu_2/\partial c_2$, the method could be used to measure $\alpha_2\beta$ directly, or *vice versa*. One difficulty is that of finding polar polymers which will dissolve in nonpolar solvents. This difficulty might be met by the use of solvents which have polar groups, but which also have low dielectric constants. Dioxane, of course, is such a solvent. In this case α_2 would now probably be concentration dependent.

This work was supported by the Office of Naval Research, Contract N8onr-76300.

References

1. G. Karagounis, *Nature*, **161**, 855 (1948).
2. P. Debye, *Z. physik. Chem.*, **130**, 56 (1927).
3. P. Debye, *Polar Molecules*, Dover, New York, 1929.
4. L. Onsager, *J. Am. Chem. Soc.*, **58**, 1486 (1936).
5. R. M. Fuoss, *ibid.*, **63**, 378 (1941).
6. P. Doty, H. Wagner, and S. Singer, *J. Phys. & Colloid Chem.*, **51**, 32 (1947).

M. Wales

Department of Chemistry
University of Wisconsin
Madison, Wisconsin

Received September 14, 1950

Mechanism of the Heat Bodying of Linseed Oil

The conclusion of Maschka and Mendl,[6] from their study of heat bodying of linseed oil, that their results are explained by the assumption of the formation of an intrapolymer has previously been suggested[1,8]; unfortunately, the authors had very little new evidence in support of this hypothesis.

Some confusion exists in the literature in the use of the word "intrapolymer," the term being used to describe the product formed on cyclizing a fatty ester group in a glyceride structure. Some investigators[3] have even suggested intrapolymeric methyl esters. Since there is no evidence that the cyclic group adds to other glycerides, there is no justification for the use of the term "polymer" for such materials. The material formed by combination of two fatty ester groups in the same glyceride is considered here as the intrapolymer, and the designation can be defended because polymerization occurs by ester interchange with other glyceride molecules.

It should be pointed out that the formation of such an intrapolymer has not been generally accepted for a number of reasons, partly on account of steric considerations[8] and because the intrapolymer has not been regarded as necessary[4] to account for the rapid increase in viscosity with a small decrease in iodine number. The first objection does not seem to be tenable, since x-ray examination of crystalline glycerides has indicated a "tuning fork" arrangement of the glycerides which should be favorable to intrapolymer formation.

Maschka and Mendl[6] state that the formation of stand oil is not amenable to kinetic study, for quantitative data on many of the reactions involved are not available. However, the heat bodying of oils may be compared to polyester formation from a mixture of mono-, di-, and tri-basic acids, with possibly a small amount of acids of even higher functionality. Paschke and Wheeler[7] have shown that dimeric esters are formed early in the reaction, and trimeric esters are formed as the polymerization proceeds.

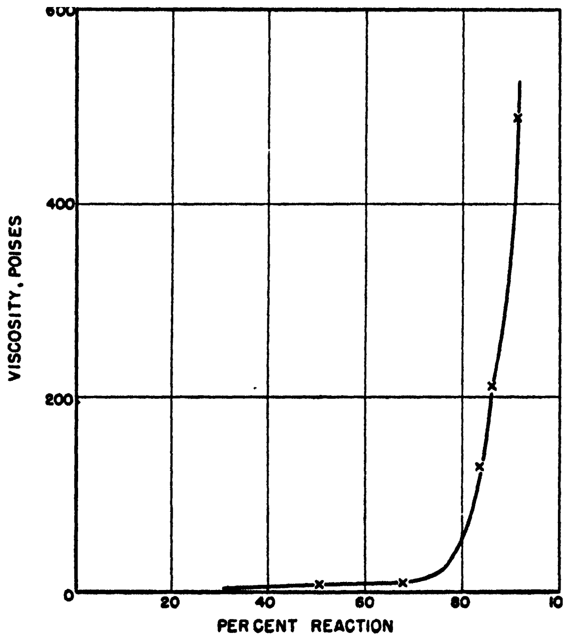

Fig. 1. Glycol dilinoleate.

In such polyester systems, particularly as functionality increases, a very rapid increase in viscosity can occur without any great amount of reaction.

The increase in viscosity of glycol linoleate[7] as esterification proceeds is probably a good model for heat bodying, since dilinoleic acid is typical of the dimeric acids formed in the heat bodying. It will be seen (Fig. 1) that a large increase in viscosity occurs between 85 and 90% reaction. If glycerol were used in place of glycol, the upsweep would be even more prominent.

While the viscosity-iodine value relationship does not provide conclusive proof of the formation of an intrapolymer, the change of physical properties affords somewhat better evidence. Density, specific refraction, hydrogen absorption, and heat of combustion all follow a pattern that indicates the formation of an intrapolymer.[1,2] The results indicate that about half of the groups polymerizing are in the intrapolymer.

Further confirmation of intrapolymer formation should result from isolation of the intrapolymer by heat polymerization of a dilinolein in dilute solution.[8] A sample of linseed oil polymerized in solution[2] was found to have much lower viscosity but to have the same iodine value as linseed oil polymerized in bulk under the same conditions.

References

1. H. E. Adams and P. O. Powers, *Ind. Eng. Chem.*, **36**, 1124 (1944).
2. H. E. Adams and P. O. Powers, *J. Applied Phys.*, **17**, 325 (1946).
3. I. M. Bernstein, *J. Polymer Sci.*, **1**, 495 (1946).
4. T. F. Bradley, *Ind. Eng. Chem.*, **30**, 689 (1938).
5. J. C. Cowan and D. H. Wheeler, *J. Am. Chem. Soc.*, **66**, 84 (1944).
6. A. Maschka and A. Mendl, *J. Polymer Sci.*, **5**, 429 (1950).
7. R. F. Paschke and D. H. Wheeler, "Thermal Polymerization of Drying Oils," PVP Division, ACS, Atlantic City, 1949.
8. A. Schwaeman, *Oil & Soap*, **21**, 204 (1944).

P. O. Powers

Battelle Memorial Institute
Columbus, Ohio

Received September 22, 1950

---

*Peroxide-Catalyzed Polymerization of Isopropenyl Acetate**

Hart and Smets[1] have recently reported on the bulk polymerization of isopropenyl acetate in the presence of benzoyl peroxide. Similar work had been carried out in our laboratories, prior to their publication, and tends to confirm the observations regarding the similarity of the polymerization of this monomer with the polymerization of allyl acetate.

Polymerizations carried out at 80°C. with 2.01 and 4.95% by weight of benzoyl peroxide indicate that, as in the case of allyl acetate,[2] the decomposition of peroxide is first order but the rate increases with increasing initial catalyst concentration. The linear relationship observed in a plot of the disappearance of monomer as a function of the disappearance of peroxide in a given polymerization, *i.e.*, dM/dP = constant, characteristic of "degradative chain transfer,"[2] is also dependent upon initial catalyst concentration. This concentration dependence can be attributed to induced decomposition of benzoyl peroxide.[3] The similarity of the polymerization of isopropenyl acetate to that of allyl acetate is seen in Table I, wherein the constants obtained in our work with both monomers are summarized.

---

* Taken from the dissertation submitted by N. G. Gaylord in partial fulfillment of the requirements for the degree of Doctor of Philosophy, Polytechnic Institute of Brooklyn, June, 1950.

TABLE I

SUMMARY OF CONSTANTS IN POLYMERIZATION OF ALLYL ACETATE AND ISOPROPENYL ACETATE BY BENZOYL PEROXIDE AT 80 ± 0.1 °C.

	Allyl acetate		Isopropenyl acetate	
Initial weight per cent peroxide...	2.05	4.94	2.01	4.95
Peroxide, moles/kg..............	0.0845	0.204	0.0830	0.205
k_1, hr.$^{-1}$ (dec. of Bz_2O_2)..........	0.193	0.203	0.200	0.235
$\overline{DP}$..........................	12.2	12.6	12.6	12.4
Per cent conversion (48 hrs.)......	26.1	46.1	27.1	48.9
dM/dP........................	25.5	20.8	25.1	18.6

The monomer concentration in allyl acetate was determined by bromination of the allyl alcohol resulting from alkaline saponification of the residual ester,[4] while in isopropenyl acetate the monomer concentration was determined by difference, after removal of residual monomer at room temperature, under vacuum, to constant weight. The peroxide concentration in allyl acetate was determined by iodometric titration in acid solution after addition of potassium iodide,[2] while peroxide in isopropenyl acetate was determined by the procedure of Siggia[5] involving back titration of arsenious oxide with iodine. Molecular weights were determined cryoscopically. Although the comparability of the results may be open to question, it is felt that the smallness of the possible error makes comparison feasible.

The implications of these results will be discussed in a forthcoming publication.

References

1. R. Hart and G. Smets, *J. Polymer Sci.*, 5, 55 (1950).
2. P. D. Bartlett and R. Altschul, *J. Am. Chem. Soc.*, 67, 816 (1945).
3. K. Nozaki and P. D. Bartlett, *ibid.*, 68, 1686 (1946).
4. P. D. Bartlett and R. Altschul, *ibid.*, 67, 812 (1945).
5. S. Siggia, *Quantitative Organic Analysis via Functional Groups*, Wiley, New York, 1949, p. 102.

N. G. GAYLORD†
F. R. EIRICH

Polytechnic Institute of Brooklyn
Brooklyn, New York

Received September 22, 1950

† Present address: E. I. du Pont de Nemours & Co., Inc., Yerkes Research Laboratory, Buffalo 7, N. Y.

*Molecular Configuration and Thermodynamic Parameters from Intrinsic Viscosities**

In previous publications[1,2] we pointed out that the intrinsic viscosity of a polymer in solution should be proportional to the ratio of the volume occupied by the molecule to the molecular weight M throughout the molecular weight range ordinarily of interest. As a convenient measure of the volume of a polymer molecule one may take the cube of the root-mean-square distance $(\overline{r^2})^{1/2}$ from beginning to end of the chain. In the absence of interactions of the segments with their environment, this distance, then designated as $(\overline{r_0^2})^{1/2}$, is proportional to the square root of the chain length, from which it follows that the intrinsic viscosity $[\eta]$ under such conditions should be proportional to $M^{1/2}$. In general, as the combined result of long range interactions between segments (the "volume filling" effect) and of segment–solvent interaction, the molecular dimensions will be increased appreciably.[1,3] Consequently, it is appropriate to write:

$$[\eta] = KM^{1/2}\alpha^3 \tag{1}$$

where $\alpha = (\overline{r^2}/\overline{r_0^2})^{1/2}$ represents the linear expansion factor arising from the above-mentioned interactions,[1,3] and:

$$K = \Phi(\overline{r_0^2}/M)^{3/2} \tag{2}$$

where Φ is a constant which should be *the same for all polymers irrespective of the solvent.*[3] According to the theory of Kirkwood and Riseman,[4] $\Phi \cong 3.6 \times 10^{21}$.[3]

The interaction of the chain segments with their environment may be treated as a mixing problem which leads to:[3]

$$\alpha^5 - \alpha^3 = 2\psi_1 C_M(1 - \Theta/T)M^{1/2} \tag{3}$$

where ψ_1 is an entropy of dilution factor[3,5] (equal to $^1/_2$ according to the simple lattice treatment[6,7]), Θ represents the temperature at which the second virial coefficient vanishes for the given solvent–polymer pair,[2,3,5,7] and:

$$\begin{aligned} C_M &= (27/2^{5/2}\pi^{3/2}\mathrm{N})(\bar{v}^2/\mathrm{v}_1)(M/\overline{r_0^2})^{3/2} \\ &= 1.4 \times 10^{-24}(\bar{\bar{v}}^2/\mathrm{v}_1)(\Phi/K) \end{aligned} \qquad (4)^{8}$$

where N is Avogadro's number and $\bar{v}$ and v_1 are the partial specific volume of the polymer and the molar volume of the solvent, respectively. The heat of dilution parameter $\kappa_1 = BV_1/RT$ does not appear in (3) but is given by $\kappa_1 = \Theta\psi_1/T$.

Intrinsic viscosities of polyisobutylenes covering a wide molecular weight range[2] and measured with unusual precision as functions of temperature in a wide variety of solvents[8] are in quantitative agreement with equations

---

* This investigation was carried out at Cornell University in connection with the Government Research Program on Synthetic Rubber under contract with the Office of Rubber Reserve, Reconstruction Finance Corporation.

(1) and (3). The value of K was found to be independent of the solvent and of molecular weight as required by theory. Preliminary measurements on polystyrene,[9] supplemented with other data published recently,[10–12] also confirm the above relationships. In fact, no deviations from the theory which exceed experimental error have yet been observed in any instance, except at quite low molecular weights. We wish to call attention to the apparent general validity of the above relations and to indicate preferred procedures for their use.

Ordinarily it is advantageous to begin with the determination of the intrinsic viscosity in a poor solvent at the absolute temperature $T = \Theta$. Θ is conveniently established by plotting the critical miscibility temperatures for several fractions against $1/M^{1/2}$ and finding the intercept, which equals Θ.[3,7] At $T = \Theta$, $\alpha = 1$ according to equation (3), and K is readily calculated from $[\eta]$ if M is known. If similar determinations are carried out in other poor solvents having suitably different Θ values, K may be obtained as a function of T. If this procedure is adopted the molecular weight of only one fraction is required; those of all other samples may, in principle at least, be calculated from their intrinsic viscosities at $T = \Theta$ and the value of K. If intrinsic viscosity measurements in a poor solvent at $T = \Theta$ are impractical, as may be true if the melting point of the polymer is high, K may be ascertained from the intercept of a plot of $[\eta]^{2/3}/M^{1/3}$ against $M/[\eta]$ using measurements made in a given solvent at a fixed temperature.[3] High accuracy over a wide molecular weight range is required for the successful application of this method. Having established K, the value of α may be calculated from the intrinsic viscosity in any solvent. The slopes and intercepts of linear plots of $(K_T/K_0)(\alpha^5 - \alpha^3)/M^{1/2}$ against $1/T$ lead to $\psi_1 C_M$ and Θ for the polymer in each solvent. The ratio (K_T/K_0) of K at temperature T to its value at a reference temperature T_0 is introduced in view of the slight temperature dependence of C_M, which, according to equation (4), is inversely related to the temperature coefficient of K.

Eliminating K from equations (1) and (2) and recalling that $\overline{r^2} = \alpha^2 \overline{r_0^2}$:

$$\Phi = M[\eta]/(\overline{r^2})^{3/2} \tag{5}$$

which suggests at once a means for establishing the value of the universal intrinsic viscosity constant Φ. Thus, the values of $\overline{r^2}$ deduced from measurements of the angular dissymmetry of light scattering by Zimm and coworkers[10] for polystyrenes of various molecular weights in several solvents, in conjunction with intrinsic viscosities in the same solvents, yield $\Phi \cong 2.1 \times 10^{21}$.[9] A similar value is indicated[8] by results of Kunst[11] on polyisobutylene solutions. Accurate assignment of the proper value for Φ is of the utmost importance, for it then becomes possible to calculate $\overline{r^2}$ from $[\eta]$ and M. Knowledge of Φ permits also the calculation of the important ratio $\overline{r_0^2}/M$ from K; the influence of hindrance to free rotation on chain dimensions is readily computed from $\overline{r_0^2}/M$.[3] In Table I are given values of K for several polymers obtained from recent investigations. For both polyisobutylene[8] and polystyrene,[9] K, and therefore $\overline{r_0^2}/M$ as well, appears to decrease gradually with increase in temperature (see Table I) indicating that barriers to free rotation are preferentially overcome in the direction of less extended configurations as the temperature is raised.

TABLE I

VALUES OF K AND CALCULATED DIMENSIONS OF THE RANDOMLY COILED POLYMER CHAINS UNPERTURBED BY THERMODYNAMIC INTERACTIONS

Polymer	T, °C.	$K \times 10^4$	$(\overline{r_0^2}/M) \times 10^{17}$	$\sqrt{\overline{r_0^2}/\overline{r_0^2}\text{ (free rot.)}}$[a]
Polyisobutylene[8]	25	10.6	6.32	1.93
	100	9.3	5.80	1.85
Polystyrene[9]	34	8.0	5.25	2.40
	70	7.3	4.24	2.32
Polymethyl methacrylate[b]	31.5	6.5	4.6	2.20

[a] $\overline{r_0^2}$ (free rotation) = $\overline{r_0^2}$ calculated assuming free rotation from the bond length (1.54 A.) and the fixed bond angle (109.5°).

[b] This value of K was obtained by a measurement of $[\eta]$ for a polymethyl methacrylate fraction of $M = 8.7 \times 10^5$ in di-*n*-propyl ketone at $T = \Theta = 31.5$°C.

Assuming tentatively that the theoretical expression (4) is exact, C_M may be computed from $\overline{r_0^2}/M$ obtained in the above manner. ψ_1 and κ_1 may then be computed from $\psi_1 C_M$ and Θ. Values of ψ_1 thus obtained are less than $^1/_2$ in all cases investigated thus far and are variable from one solvent to another over a tenfold range. These parameters should be independently determined from thermodynamic measurements in the future.

We believe that the procedures outlined above afford a simple and effective means for the investigation of both polymer chain configuration and the thermodynamics of polymer-solvent interaction. With respect to the former, the intrinsic viscosity procedure offers the advantage of greater sensitivity than other methods since it depends on the volume occupied by the polymer chain rather than on its linear dimension.

References

1. P. J. Flory, *J. Chem. Phys.*, **17,** 303 (1949).
2. T. G. Fox, Jr., and P. J. Flory, *J. Phys. & Colloid Chem.*, **53,** 197 (1949).
3. P. J. Flory and T. G. Fox, Jr., *to be published.*
4. J. G. Kirkwood and J. Riseman, *J. Chem. Phys.*, **16,** 560 (1948).
5. P. J. Flory and W. R. Krigbaum, *ibid.*, **18,** 1086 (1950).
6. M. L. Huggins, *J. Phys. Chem.*, **46,** 151 (1942); *Ann. N. Y. Acad. Sci.*, **43,** 1 (1942).
7. P. J. Flory, *J. Chem. Phys.*, **10,** 51 (1942).
8. T. G. Fox, Jr., and P. J. Flory, *to be published.*
9. T. G. Fox, Jr., and P. J. Flory, *to be published.*
10. P. Outer, C. I. Carr, and B. H. Zimm, *J. Chem. Phys.*, **18,** 830 (1950).
11. E. D. Kunst, *Rec. trav. chim.*, **69,** 125 (1950).
12. L. H. Cragg and J. E. Simkins, *Can. J. Research*, **B27,** 961 (1949).

PAUL J. FLORY
THOMAS G FOX, JR.†

Department of Chemistry
Cornell University
Ithaca, New York

Received September 25, 1950

† Present address: Rohm and Haas Company, Inc., Philadelphia, Pa.

REVIEW

The Terpenes. Vol. II. The Dicyclic Terpenes and Their Derivatives. J. L. SIMONSEN. Second Edition, revised by Sir JOHN SIMONSEN and L. N. OWEN, Cambridge Univ. Press, New York, 1949. 631 pp., $8.50.

Seventeen years have passed since the appearance of the first edition of this volume. In this interim the rapid growth of the literature of the dicyclic terpenes has influenced the authors to limit the new edition by relegating the sesquiterpenes to a third volume yet to appear. The third volume is also to include the chemistry of the diterpenes. Published work on the dicyclic terpenes is covered to the end of 1947 with some references to papers appearing in 1948.

The contents are divided into six chapters, each of which is appropriated to one of the parent hydrocarbons, thujane, carane, pinane, santene, camphane and isocamphane, fenchane and isobornylane. Each chapter is subdivided into sections dealing first with the parent hydrocarbon and its olefinic derivatives and then with the related alcohols, aldehydes and ketones. These sections include a detailed discussion of properties, both chemical and physical, reactions, degradative studies, and syntheses. Considerable space has been allotted to structural proofs inasmuch as the arguments involved are frequently complicated and manifold. Each section is liberally supplied with structural and reaction flow diagrams. An author and subject index completes the volume.

There are few fields in organic chemistry which have received the attention of as much talent and expenditure of effort as has terpene chemistry. The authors have done this work full justice by basing the development of structural elucidation upon the classical researches of Semmler, Wallach, and their contemporaries and by completely documenting all papers relevant to the subject. Indeed, the major value of the volume lies in its comprehensive treatment of the dicyclic terpenes and in its references to the original literature. The reader may confidently use the new edition as a guide to the literature prior to 1948.

There is a welcome, though small, extension of the paragraphs on terpenic rearrangements under the pinane heading. Since facile rearrangement is one of the most important characteristics of the dicyclic terpenes, this aspect would seem to merit a more detailed discussion than it has received. One error in structural representation has come to the reviewer's attention. On page 208, stereochemical forms Ia and Ib intended for pinocampheol and neopinocampheol, respectively, should be interchanged—*cf.* Schmidt, *Ber.*, 77, 544 (1944).

This new edition is recommended to the polymer chemist on the same grounds as it would be recommended to other chemists. It is a sound, accurate work containing an immense variety of interesting and stimulating chemistry. Although the subject matter pertains to dicyclic terpenes, the many reactions encountered will be of use in other fields as well.

Harold H. Zeiss

Errata: Mechanism of Emulsion Polymerizations. IV. Kinetics of Polymerization of Styrene in Water and Detergent Solutions

(*J. Polymer Sci.*, 5, S22–23, 487–504, 1950)

by F. A. BOVEY and I. M. KOLTHOFF, School of Chemistry, University of Minnesota

Page S23, lines 8–9 should read: $d(\bar{R})/dt\ (40°) = 3.08 \times 10^{-5}$ mole/liter/hour
$d(\bar{R})/dt\ (50°) = 14.1 \times 10^{-5}$ mole/liter/hour

Page 502, last sentence before "Discussion" should read:

> "This is in reasonable agreement with the value of 33,000 cal. per mole deduced from quinone induction periods."

JOURNAL OF POLYMER SCIENCE VOL. V, NO. 6, PAGES 749–751

AUTHOR INDEX

Alfrey, T., Jr.: Review. The physics of rubber elasticity, 387

——, Bohrer, J., Haas, H., and Lewis, C.: Experimental study of copolymerization. IV, 719

Amerongen, G. J. van: Influence of structure of elastomers on their permeability to gases, 307

——, and Koningsberger, C.: Chlorination of natural rubber. II. Preparation and properties of rubber dichloride, 453

——, ——, and Salomon, G.: Chlorination of natural rubber. I. Preparation and properties of chlorinated rubber, 639

Arnett, L. M., Meibohm, E. P. H., and Smith, A. F.: Letter to the Editors. New observations on the small-angle x-ray diffraction of synthetic fibers, 737

Atherton, E.: Letter to the Editors. Pyrolysis of polystyrene, 378

Basu, S.: Letter to the Editors. Molecular weight of nylon by end-group titration, 735

Bear, R. S.: see Bolduan, O. E. A.

Beau, D. S. le: Review. The colloid chemistry of the silicate minerals, 143

Bennett, A. R.: see Wiley, R. H.

Billmeyer, F. W., Jr., and Stockmayer, W. H.: Method of measuring molecular weight distribution, 121

Blatz, P. J.: see Simha, R.

Bohrer, J.: see Alfrey, T., Jr.

Bolduan, O. E. A., and Bear, R. S.: Unidirectional nature of the large periodic structure of collagen fibrils, 159

Bovey, F. A., and Kolthoff, I. M.: Mechanism of emulsion polymerizations. IV. Kinetics of polymerization of styrene in water and detergent solutions, 487; *errata*, 748

——, and ——: Studies of retarders and inhibitors in the emulsion polymerization of styrene. II. Inhibitors, 569

Boyer, R. F., and Spencer, R. S.: Letter to the Editors. Critical concentration effects in dilute high polymer solutions, 375

——: Letter to the Editors. Concentration dependence of diffusion of chloroform in polystyrene, 139

——: see Bradford, E. B.

Bradford, E. B., and Boyer, R. F.: Review. Electron microscopy—Technique and applications, 637

Brauer, G. M.: see Wiley, R. H.

Brown, C. J.: Some polymeric derivatives of phosphonitrile chloride, 465

Campbell, H., and Johnson, P.: Aging of solutions of cellulose nitrate, 443

Carr, C. W., Kolthoff, I. M., Meehan, E. J., and Stenberg, R. J.: Studies on the rate of the emulsion polymerization of butadiene-styrene (75:25) as a function of the amount and kind of emulsifier used. I. Polymerizations with commercial and pure soaps, 191

——, ——, ——, and Williams, D. E.: Studies on the rate of the emulsion polymerization of butadiene-styrene (75:25) as a function of the amount and kind of emulsifier used. II. Polymerizations with fatty acid soaps, rosin soaps, and various synthetic emulsifiers, 201

Cohen, S. G.: Review. Encyclopedia of chemical technology, Vol. 3, 518

Conn, W. R., and Neher, H. T.: Inhibiting effect of acrylonitrile on polymerization of vinyl acetate, 355

Corrin, M. L.: see Herzfeld, S. H.

Craig, D., Juve, A. E., and Davidson, W. L.: Tetramethylthiuram disulfide vulcanization of extracted rubber. I. Introduction and compounding, 709

Crank, J., and Park, G. S.: Letter to the Editors, 140

Dale, W. J.: see Kolthoff, I. M.

Davidson, W. L.: see Craig, D.

Dole, M.: Review. The adsorption of gases on solids, 266

Doty, P. M., and Steiner, R. F.: Letter to the Editors. Note on the distribution of polymer molecules in dilute solution, 383

——: Review. High-polymer physics—A symposium, 387

Eirich, F. R.: see Gaylord, N. G.

——: see Riseman, J.

Fineman, M., and Ross, S. D.: Letter to the Editors. Linear method for determining monomer reactivity ratios in copolymerization, 259

Finkelstein, P., and McLaren, A. D.: Photochemistry of proteins. VI. *p*H dependence of quantum yield and ultraviolet absorption spectrum of chymotrypsin; *errata*, 267

Flory, P. J., and Fox, T. G., Jr.: Letter to the Editors. Molecular configuration and thermodynamic parameters from intrinsic viscosities, 745

——, and Leutner, F. S.: Occurrence of head-to-head arrangements of structural units in polyvinyl alcohol; *errata*, 267

Foster, F. C.: Friedel-Crafts copolymerization of chloroprene–styrene, 369

Fox, T. G., Jr.: see Flory, P. J.

Fuller, C. S.: Review. Fundamentals of synthetic polymer technology, 388

Gaylord, N. G., and Eirich, F. R.: Letter to the Editors. Peroxide-catalyzed polymerization of isopropenyl acetate, 743

Goldfinger, G.: Review. Les dérivés chimiques du caoutchouc naturel, 638
Goldstein, G., and Stern, K. G.: Experiments on the sonic, thermal, and enzymic depolymerization of desoxyribosenucleic acid, 687
Haas, H. C.: Letter to the Editors. Catalysis of the dechlorination by zinc, 515
——: see Alfrey, T., Jr.
Harkins, W. D.: General theory of mechanism of emulsion polymerization. II, 217
——: see Herzfeld, S. H.
Hart, R., et Smets, G.: Vitesse de polymérisation et de copolymérisation de l'acétate d'isopropényle, 55
Haward, R. N.: Letter to the Editors. Degradation of ethyl cellulose in solution, 635
Hermans, J. J.: see Pals, D. T. F.
Hermans, P. H., and Vermaas, D.: Letter to the Editors. Note on density determination of cellulose fibers by the flotation method in carbon tetrachloride, 731
——, and Weidinger, A.: Crystallinity of precipitated cellulose, 565
——, and ——: Quantitative investigation of x-ray diffraction by "amorphous" polymers and some other noncrystalline substances, 269; *errata*, 518
Herrent, P., and Jnoff, G.: Titration Potentiométrique de la viscose. III, 727
Herzfeld, S. H., Roginsky, A., Corrin, M. L., and Harkins, W. D.: Monomer-polymer ratio in emulsion polymerization of styrene, 207
Hobson, P. H.: see Wiley, R. H.
Huggins, M. L.: Review. Elastomers and plastomers—their chemistry, physics, and technology. Vol. I, 636
Jellinek, H. H. G.: Letter to the Editors. Degradation of high polymers, 264
Jirgensons, B.: Denaturation of plant proteins. III. Optical rotation, viscosity, and reducing capacity of denatured proteins, 179
Jnoff, G.: see Herrent, P.
Johnson, D. H.: see Siegel, B. M.
Johnson, P.: see Campbell, H.
——: see Sheppard, E.
Juve, A. E.: see Craig, D.
Katchalsky, A., Künzle, O., and Kuhn, W.: Behavior of polyvalent polymeric ions in solution, 283
Kolthoff, I. M., and Dale, W. J.: Potassium ferricyanide–diazothio ether–mercaptan recipe for emulsion polymerization of butadiene and styrene. II. Effect of some chemical variables, 301
——, ——, and Miller, I. K.: Potassium ferricyanide–diazothio ether–mercaptan recipe for emulsion polymerization of butadiene and styrene. III. Determination of *p*-methoxyphenyl diazothio-(2-naphthyl)-ether, 667
——, and Medalia, A. I.: Redox recipes. II. Redox recipes in alkaline medium initiated by the system cumene hydroperoxide–iron–sugar at 30°, 391
——: see Bovey, F. A.
——: see Carr, C. W.
Koningsberger, C.: see Amerongen, G. J. van
Krigbaum, W. R., and Wall, F. T.: Viscosities of binary polymeric mixtures, 505
Kuhn, H., and Kuhn, W.: Effects of hampered draining of solvent on the translatory and rotatory motion of statistically coiled long-chain molecules in solution. Part I. Translation resistance; rate of diffusion and sedimentation, 519
Kuhn, W.: see Katchalsky, A.
——: see Kuhn, H.
Künzle, O.: see Katchalsky, A.
Leutner, F. S.: see Flory, P. J.
Lewis, C.: see Alfrey, T., Jr.
——: see McLaren, A. D.
McLaren, A. D., and Lewis, C.: Letter to the Editors. Concerning the inactivation-denaturation of pepsin, 379
——: see Finkelstein, P.
——: see Sheppard, E.
Mark, H.: see Siegel, B. M.
Maschka, A., und Mendl, A.: Untersuchung einer katalysierten Leinölstandölkochung unter Heranziehung der Ultraviolettspektrographie (Vergleich mit nichtkatalysierten Prozessen), 429
Medalia, A. I.: see Kolthoff, I. M.
Meehan, E. J.: see Carr, C. W.
Meibohm, E. P. H.: see Arnett, L. M.
Mendl, A.: see Maschka, A.
Merz, E. H., and Raetz, R. W.: Influence of molecular weight on the properties of polystyrene. II. Fractionation of the polymer, 587
Miller, I. K.: see Kolthoff, I. M.
Moore, W. R.: Nitrocellulose–solvent interaction, 91
Münster, A.: Die Löslichkeit hochpolymerer Fadenmoleküle, 333
Neher, H. T.: see Conn, W. R.
Nolle, A. W.: Dynamic mechanical properties of rubberlike materials, 1
O'Hara, J. B., and Prutton, C. F.: Heterogeneous system for polymerization of vinyl chloride, 673
Pals, D. T. F., and Hermans, J. J.: Letter to the Editors. New method for deriving the intrinsic viscosity of polyelectrolytes, 733
Park, G. S.: see Crank, J.
Peterlin, A.: Viscosity and sedimentation of linear macromolecules exhibiting partial solvent immobilization, 473
——: see Stuart, H. A.
Powers, P. O.: Letter to the Editors. "Bound" water in phenol-formaldehyde condensates, 262
——: Letter to the Editors. Mechanism of the heat bodying of linseed oil, 741
Prutton, C. F.: see O'Hara, J. B.
Raetz, R. W.: see Merz, E. H.
Riseman, J., and Eirich, F. R.: Letter to the Editors. Intrinsic viscosity of macromolecules, 633

Roginsky, A.: see Herzfeld, S. H.
Ross, S. D.: see Fineman, M.
Rothman, S., Simha, R., and Weissberg, S. G.: Letter to the Editors. Viscosities of very dilute polymer solutions, 141
Salomon, G.: see Amerongen, G. J. van
Schauenstein, E., and Treiber, E.: Ultraviolet absorption spectra of actomyosin. 1, 145
Schwert, G. W.: Review. Outlines of biochemistry, 637
Sheppard, E., McLaren, A. D., and Johnson, P.: Letter to the Editors. Ultracentrifuge studies on the crystalline compound of trypsin and soybean trypsin, 375
Siegel, B. M., Johnson, D. H., and Mark, H.: Molecular weight investigations of high polymers with the electron microscope, 111
Simha, R.: Letter to the Editors. Degradation of high polymers, 515
——, Wall, L. A., and Blatz, P. J.: Depolymerization as a chain reaction, 615
——: see Rothman, S.
Sips, R.: Mechanical behavior of viscoelastic substances, 69
Smets, G.: see Hart, R.
——: see Wilde, M. C. de
Smith, A. F.: see Arnett, L. M.
Smith, E. F., and Wangsgard, A. P.: Photoelastic strain analyzer, 169
Spencer, R. S.: Flow of linear amorphous polymers, 591
——: Review. Industrial rheology and rheological structures, 389
——: see Boyer, R. F.
Steiner, R. F.: see Doty, P. M.
Stenberg, R. J.: see Carr, C. W.
Stern, K. G.: see Goldstein, G.
Stockmayer, W. H.: see Billmeyer, F. W., Jr.
Stuart, H. A., und Peterlin, A.: Optische Anisotropie und Form von Fadenmolekülen. I. Depolarisationsgrad der Lichtzerstreuung von Lösungen mit Fadenmolekülen, 543
——, and ——: Optische Anisotropie und Form von Fadenmolekülen. II. Künstliche Doppelbrechung, 551
Treiber, E.: see Schauenstein, E.
Vermaas, D.: see Hermans, P. H.
Wales, M.: Letter to the Editors. Transport of uncharged polymer molecules by an inhomogeneous electric field, 739
Wall, F. T.: see Krigbaum, W. R.
Wall, L. A.: see Simha, R.
Wangsgard, A. P.: see Smith, E. F.
Weidinger, A.: see Hermans, P. H.
Weissberg, S. G.: see Rothman, S.
Wilde, M. C. de, et Smets, G.: Copolymérisation de l'anhydride maléique avec différents monomères vinyliques, 253
Wiley, R. H., Brauer, G. M., and Bennett, A. R.: Refractometric determination of second-order transition temperatures in polymers. V. Determination of the refractive indices of elastomers at temperatures from 25 to −120°C., 609
——, and Hobson, P. H.: Polymerization of *m*- and *p*-formylstyrenes, 483
Williams, D. E.: see Carr, C. W.
Wood, L. A. Review. Proceedings of the second rubber technology conference, 1948, 517
Zeiss, H. H.: Review. The Terpenes, Vol. II. The dicyclic terpenes and their derivatives, 748

SUBJECT INDEX

Analytical Techniques, Chemical

Catalysis of the dichlorination by zinc. *Letter to the Editors*, H. C. Haas, 515

Potassium ferricyanide–diazothio ether–mercaptan recipe for emulsion polymerization of butadiene and styrene. III. Determination of *p*-methoxyphenyl diazothio-(2-naphthyl)-ether, I. M. Kolthoff, W. J. Dale, and I. K. Miller, 667

Analytical Techniques, Physical

Molecular weight investigations of high polymers with the electron microscope, B. M. Siegel, D. H. Johnson, and H. Mark, 111

Photoelastic strain analyzer, E. F. Smith and A. P. Wangsgard, 169

Untersuchung einer katalysierten Leinölstandölkochung unter Heranziehung der Ultraviolettspektrographie (Vergleich mit nichtkatalysierten Prozessen), A. Maschka und A. Mendl, 429

Viscosities of very dilute polymer solutions. *Letter to the Editors*, S. Rothman, R. Simha, and S. G. Weissberg, 141

Cellulose and Cellulose Derivatives

Aging of solutions of cellulose nitrate, H. Campbell and P. Johnson, 443

Crystallinity of precipitated cellulose, P. H. Hermans and A. Weidinger, 565

Degradation of ethyl cellulose in solution. *Letter to the Editors*, R. N. Haward, 635

Nitrocellulose–solvent interaction, W. R. Moore, 91

Note on the density determination of cellulose fibers by the flotation method in carbon tetrachloride. *Letter to the Editors*, P. H. Hermans and D. Vermaas, 734

Titration potentiométrique de la viscose. III, P. Herrent and G. Jnoff, 727

Chemical Reactions of Polymers

Catalysis of the dechlorination by zinc. *Letter to the Editors*, H. C. Haas, 515

Chlorination of natural rubber. I. Preparation and properties of chlorinated rubber, G. J. van Amerongen, C. Koningsberger, and G. Salomon, 639

Chlorination of natural rubber. II. Preparation and properties of rubber dichloride, G. J. van Amerongen and C. Koningsberger, 653

Tetramethylthiuram disulfide vulcanization of extracted rubber. I. Introduction and compounding, D. Craig, A. E. Juve, and W. L. Davidson, 709

Copolymerization

Copolymerisation de l'anhydride maléique avec différents monomères vinyliques, M. C. de Wilde et G. Smets, 253

Experimental study of copolymerization. IV, T. Alfrey, Jr., J. Bohrer, H. Haas, and C. Lewis, 719

Friedel-Crafts copolymerization of chloroprene–styrene, F. C. Foster, 369

Linear method for determining monomer reactivity ratios in copolymerization. *Letter to the Editors*, M. Fineman and S. D. Ross, 259

Monomer–polymer ratio in emulsion polymerization of styrene, S. H. Herzfeld, A. Roginsky, M. L. Corrin, and W. D. Harkins, 207

Potassium ferricyanide–diazothio ether–mercaptan recipe for emulsion polymerization of butadiene and styrene. II. Effect of some chemical variables, I. M. Kolthoff and W. J. Dale, 301

Studies on the rate of the emulsion polymerization of butadiene-styrene (75:25) as a function of the amount and kind of emulsifier used. I. Polymerizations with commercial and pure soaps, C. W. Carr, I. M. Kolthoff, E. J. Meehan, and R. J. Stenberg, 191

Studies on the rate of the emulsion polymerization of butadiene-styrene (75:25) as a function of the amount and kind of emulsifier used. II. Polymerizations with fatty acid soaps,

rosin soaps, and various synthetic emulsifiers, C. W. Carr, I. M. Kolthoff, E. J. Meehan, and D. E. Williams, 201
Vitesse de polymérisation et de copolymérisation de l'acétate d'isopropényle, R. Hart et G. Smets, 55

Degradation

Degradation of ethyl cellulose in solution. *Letter to the Editors*, R. N. Haward, 635
Degradation of high polymers. *Letter to the Editors*, H. H. G. Jellinek, 264
Degradation of high polymers. *Letter to the Editors*, R. Simha, 515
Depolymerization as a chain reaction, R. Simha, L. A. Wall, and P. J. Blatz, 615
Pyrolysis of polystyrene. *Letter to the Editors*, E. Atherton, 378

Fibers

New observations on the small-angle x-ray diffraction of synthetic fibers. *Letter to the Editors*, L. M. Arnett, E. P. H. Meibohm, and A. F. Smith, 737
Unidirectional nature of the large periodic structure of collagen fibrils, O. E. A. Bolduan and R. S. Bear, 159

Mechanical Properties and the Solid State

Dynamic mechanical properties of rubberlike materials, A. W. Nolle, 1
Flow of linear amorphous polymers, R. S. Spencer, 591
Influence of molecular weight on the properties of polystyrene. II. Fractionation of the polymer, E. H. Merz and R. W. Raetz, 587
Mechanical behavior of viscoelastic substances, R. Sips, 69
Photoelastic strain analyzer, E. F. Smith and A. P. Wangsgard, 169

Molecular Structure and Shape

"Bound" water in phenol-formaldehyde condensates. *Letter to the Editors*, P. O. Powers, 262
Concentration dependence of diffusion of chloroform in polystyrene. *Letter to the Editors*, R. F. Boyer, 139
Critical concentration effects in dilute high polymer solutions. *Letter to the Editors*, R. F. Boyer and R. S. Spencer, 375
Effects of hampered draining of solvent on the translatory and rotatory motion of statistically coiled long-chain molecules in solution. Part I. Translation resistance; rate of diffusion and sedimentation, H. Kuhn and W. Kuhn, 519
Experiments on the sonic, thermal, and enzymic depolymerization of desoxyribosenucleic acid, G. Goldstein and K. G. Stern, 687
Influence of structure of elastomers on their permeability to gases, G. J. van Amerongen, 307
Letter to the Editors, J. Crank and G. S. Park, 140
Molecular configuration and thermodynamic parameters from intrinsic viscosities. *Letter to the Editors*, P. J. Flory and T. G. Fox, Jr., 743
Molecular weight investigations of high polymers with the electron microscope, B. M. Siegel, D. H. Johnson, and H. Mark, 111
Note on the distribution of polymer molecules in dilute solution, *Letter to the Editors*, P. M. Doty and R. F. Steiner, 383
Occurrence of head-to-head arrangements of structural units in polyvinyl alcohol, P. J. Flory and F. S. Leutner (*Errata*, article in *J. Polymer Sci.*, **3**, 880, 1948), 267
Optische Anisotropie und Form von Fadenmolekulen. I. Depolarisationsgrad der Lichtzerstreuung von Losungen mit Fadenmolekulen, H. A. Stuart und A. Peterlin, 543
Optische Anisotropie und Form von Fadenmolekülen. II. Kunstliche Doppelbrechung, H. A. Stuart und A. Peterlin, 551
Viscosity and sedimentation of linear macromolecules exhibiting partial solvent immobilization, A. Peterlin, 473

Molecular Weight and Molecular Weight Distribution

Influence of molecular weight on the properties of polystyrene. II. Fractionation of the polymer, E. H. Merz and R. W. Raetz, 587

Method of measuring molecular weight distribution, F. W. Billmeyer, Jr., and W. H. Stockmayer, 121
Molecular weight investigations of high polymers with the electron microscope, B. M. Siegel, D. H. Johnson, and H. Mark, 111
Molecular weight of nylon by end-group titration. *Letter to the Editors*, S. Basu, 735

Physical Properties

Concentration dependence of diffusion of chloroform in polystyrene. *Letter to the Editors*, R. F. Boyer, 139
Dynamic mechanical properties of rubberlike materials, A. W. Nolle, 1
Effects of hampered draining of solvent on the translatory and rotatory motion of statistically coiled long-chain molecules in solution. Part I. Translation resistance; rate of diffusion and sedimentation, H. Kuhn and W. Kuhn, 519
Influence of structure of elastomers on their permeability to gases, G. J. van Amerongen, 307
Letter to the Editors, J. Crank and G. S. Park, 140
Mechanical behavior of viscoelastic substances, R. Sips, 69
Mechanism of the heat bodying of linseed oil. *Letter to the Editors*, P. O. Powers, 741
Nitrocellulose–solvent interaction, W. R. Moore, 91
Note on the density determination of cellulose fibers by the flotation method in carbon tetrachloride. *Letter to the Editors*, P. H. Hermans and D. Vermaas, 734
Optische Anisotropie und Form von Fadenmolekulen. I. Depolarisationsgrad der Lichtzerstreuung von Lösungen mit Fadenmolekulen, H. A. Stuart und A. Peterlin, 543
Optische Anisotropie und Form von Fadenmolekulen. II. Künstliche Doppelbrechung, H. A. Stuart und A. Peterlin, 551
Quantitative investigation of x-ray diffraction by "amorphous" polymers and some other noncrystalline substances, P. H. Hermans and A. Weidinger, 269
Refractometric determination of second-order transition temperatures in polymers. V. Determination of the refractive indices of elastomers at temperatures from 25 to −120°C., R. H. Wiley, G. M. Brauer, and A. R. Bennett, 609
Ultraviolet absorption spectra of actomyosin. I, E. Schauenstein and E. Treiber, 145
Unidirectional nature of the large periodic structure of collagen fibrils, O. E. A. Bolduan and R. S. Bear, 159
Viscosity and sedimentation of linear macromolecules exhibiting partial solvent immobilization, A. Peterlin, 473

Polyelectrolytes

Behavior of polyvalent polymeric ions in solution, A. Katchalsky, O. Künzle, and W. Kuhn, 283
Experiments on the sonic, thermal, and enzymic depolymerization of desoxyribosenucleic acid, G. Goldstein and K. G. Stern, 687
New method for deriving the intrinsic viscosity of polyelectrolytes. *Letter to the Editors*, D. T. F. Pals and J. J. Hermans, 733
Titration potentiométrique de la viscose. III, P. Herrent and G. Jnoff, 727

Polymerization, Addition

General theory of mechanism of emulsion polymerization. II, W. D. Harkins, 217
Heterogeneous system for polymerization of vinyl chloride, J. B. O'Hara and C. F. Prutton, 673
Monomer–polymer ratio in emulsion polymerization of styrene, S. H. Herzfeld, A. Roginsky, M. L. Corrin, and W. D. Harkins, 207
Polymerization of *m*- and *p*-formylstyrenes, R. H. Wiley and P. H. Hobson, 483
Potassium ferricyanide–diazothio ether–mercaptan recipe for emulsion polymerization of butadiene and styrene. II. Effect of some chemical variables, I. M. Kolthoff and W. J. Dale, 301
Studies on the rate of the emulsion polymerization of butadiene-styrene (75:25) as a function of the amount

and kind of emulsifier used. I. Polymerizations with commercial and pure soaps, C. W. Carr, I. M. Kolthoff, E. J. Meehan, and R. J. Stenberg, 191
Studies of the rate of the emulsion polymerization of butadiene-styrene (75:25) as a function of the amount and kind of emulsifier used. II. Polymerizations with fatty acid soaps, rosin soaps, and various synthetic emulsifiers, C. W. Carr, I. M. Kolthoff, E. J. Meehan, and D. E. Williams, 201
Untersuchung einer katalysierten Leinölstandölkochung unter Heranziehung der Ultraviolettspektrographie (Vergleich mit nichtkatalysierten Prozessen), A. Maschka und A. Mendl, 429

Polymerization, Catalysts and Mechanisms

Copolymérisation de l'anhydride maléique avec différents monomères vinyliques, M. C. de Wilde et G. Smets, 253
General theory of mechanism of emulsion polymerization. II, W. D. Harkins, 217
Inhibiting effect of acrylonitrile on polymerization of vinyl acetate, W. R. Conn and H. T. Neher, 355
Mechanism of emulsion polymerizations. IV. Kinetics of polymerization of styrene in water and detergent solutions, F. A. Bovey and I. M. Kolthoff, 487; *errata*, 748
Peroxide-catalyzed polymerization of isopropenyl acetate. *Letter to the Editors*, N. G. Gaylord and F. R. Eirich, 743
Redox recipes. II. Redox recipes in alkaline medium initiated by the system cumene hydroperoxide–iron–sugar at 30°, I. M. Kolthoff and A. I. Medalia, 391
Studies on retarders and inhibitors in the emulsion polymerization of styrene. II. Inhibitors, F. A. Bovey and I. M. Kolthoff, 569
Studies on the rate of the emulsion polymerization of butadiene-styrene (75:25) as a function of the amount and kind of emulsifier used. I. Polymerizations with commercial and pure soaps, C. W. Carr, I. M. Kolthoff, E. J. Meehan, and R. J. Stenberg, 191
Studies on the rate of the emulsion polymerization of butadiene-styrene (75:25) as a function of the amount and kind of emulsifier used. II. Polymerizations with fatty acid soaps, rosin soaps, and various synthetic emulsifiers, C. W. Carr, I. M. Kolthoff, E. J. Meehan, and D. E. Williams, 201
Vitesse de polymérisation et de copolymérisation de l'acétate d'isopropényle, R. Hart et G. Smets, 55

Polymerization, Condensation

Some polymeric derivatives of phosphonitrile chloride, C. J. Brown, 465

Polymer News

Seventh Annual Series of Summer Laboratory Courses, Institute of Polymer Research, Polytechnic Institute of Brooklyn, 390
Symposium on Polymer Chemistry as Applied to Plastics, Society of Chemical Industry, Plastics and Polymer Group, Beveridge Hall, the University, London, 390

Proteins

Concerning the inactivation-denaturation of pepsin. *Letter to the Editors*, A. D. McLaren and C. Lewis, 379
Denaturation of plant proteins. III. Optical rotation, viscosity, and reducing capacity of denatured proteins, B. Jirgensons, 179
Photochemistry of proteins. VI. *p*H dependence of quantum yield and ultraviolet absorption spectrum of chymotrypsin, P. Finkelstein and A. D. McLaren (*Errata*, article in *J. Polymer Sci.*, 4, 573–582, 1949), 267
Ultracentrifuge studies on the crystalline compound of trypsin and soybean trypsin inhibitor. *Letter to the Editors*, E. Sheppard, A. D. McLaren, and P. Johnson, 375
Ultraviolet absorption spectra of actomyosin. I, E. Schauenstein and E. Treiber, 145
Unidirectional nature of the large periodic structure of collagen fibrils, O. E. A. Bolduan and R. S. Bear, 159

Reviews

Elastomers and plastomers—Their chemistry, physics, and technology, Vol. I, M. L. Huggins, 636
Electron microscopy—Technique and applications, E. B. Bradford and R. F. Boyer, 637
Encyclopedia of chemical technology, Vol. 3, S. G. Cohen, 518
Fundamentals of synthetic polymer technology, C. S. Fuller, 388
High-polymer physics—A symposium, P. M. Doty, 387
Les dérivés chimiques du caoutchouc naturel, G. Goldfinger, 638
Industrial rheology and rheological structures, R. S. Spencer, 389
Outlines of biochemistry, G. W. Schwert, 637
Proceedings of the second rubber technology conference, 1948, L. A. Wood, 517
The adsorption of gases on solids, M. Dole, 266
The colloid chemistry of the silicate minerals, D. S. le Beau, 143
The physics of rubber elasticity, T. Alfrey. Jr., 387
The Terpenes. Vol. II. The dicyclic terpenes and their derivatives, J. L. Simonsen, 748

Rubbers

Dynamic mechanical properties of rubberlike materials, A. W. Nolle, 1
Mechanical behavior of viscoelastic substances, R. Sips, 69
Studies on the rate of the emulsion polymerization of butadiene-styrene (75:25) as a function of the amount and kind of emulsifier used. I. Polymerizations with commercial and pure soaps, C. W. Carr, I. M. Kolthoff, E. J. Meehan, and R. J. Stenberg, 191
Studies on the rate of the emulsion polymerization of butadiene-styrene (75:25) as a function of the amount and kind of emulsifier used. II. Polymerizations with fatty acid soaps, rosin soaps, and various synthetic emulsifiers, C. W. Carr, I. M. Kolthoff, E. J. Meehan, and D. E. Williams, 201

Solutions and Solution Properties

Aging of solutions of cellulose nitrate, H. Campbell and P. Johnson, 443
Behavior of polyvalent polymeric ions in solution, A. Katchalsky, O. Künzle, and W. Kuhn, 283
Critical concentration effects in dilute high polymer solutions. *Letter to the Editors*, R. F. Boyer and R. S. Spencer, 375
Concentration dependence of diffusion of chloroform in polystyrene. *Letter to the Editors*, R. F. Boyer, 139
Die Löslichkeit hochpolymerer Fadenmoleküle, A. Münster, 333
Effects of hampered draining of solvent on the translatory and rotatory motion of statistically coiled long-chain molecules in solution. Part I. Translation resistance; rate of diffusion and sedimentation, H. Kuhn and W. Kuhn, 519
Experiments on the sonic, thermal, and enzymic depolymerization of desoxyribosenucleic acid, G. Goldstein and K. G. Stern, 687
Letter to the Editors, J. Crank and G. S. Park, 140
Nitrocellulose–solvent interaction, W. R. Moore, 91
Note on the distribution of polymer molecules in dilute solutions. *Letter to the Editors*, P. M. Doty and R. F. Steiner, 383
Optische Anisotropie und Form von Fadenmolekülen. I. Depolarisationsgrad der Lichtzerstreuung von Lösungen mit Fadenmolekülen, H. A. Stuart und A. Peterlin, 543
Optische Anisotropie und Form von Fadenmolekülen. II. Künstliche Doppelbrechung, H. A. Stuart and A. Peterlin, 551
Titration potentiométrique de la viscose. III, P. Herrent and G. Jnoff, 727
Transport of uncharged polymer molecules by an inhomogeneous electric field. *Letter to the Editors*, M. Wales, 739
Ultracentrifuge studies on the crystalline compound of trypsin and soybean trypsin inhibitor. *Letter to the Editors*, E. Sheppard, A. D. McLaren, and P. Johnson, 375

Viscosities of binary polymeric mixtures, W. R. Krigbaum and F. T. Wall, 505
Viscosities of very dilute polymer solutions. *Letter to the Editors*, S. Rothman, R. Simha, and S. G. Weissberg, 141
Viscosity and sedimentation of linear macromolecules exhibiting partial solvent immobilization, A. Peterlin, 473

Thermodynamics and Statistics

Behavior of polyvalent polymeric ions in solution, A. Katchalsky, O. Künzle, and W. Kuhn, 283
Critical concentration effects in dilute high polymer solutions. *Letter to the Editors*, R. F. Boyer and R. S. Spencer, 375
Die Löslichkeit hochpolymerer Fadenmoleküle, A. Münster, 333
Effects of hampered draining of solvent on the translatory and rotatory motion of statistically coiled long-chain molecules in solution. Part I. Translation resistance; rate of diffusion and sedimentation, H. Kuhn and W. Kuhn, 519
Note on the distribution of polymer molecules in dilute solution. *Letter to the Editors*, P. M. Doty and R. F. Steiner, 383
Optische Anisotropie und Form von Fadenmolekülen. I. Depolarisationsgrad der Lichtzerstreuung von Lösungen mit Fadenmolekülen, H. A. Stuart und A. Peterlin, 543
Optische Anisotropie und Form von Fadenmolekülen. II. Künstliche Doppelbrechung, H. A. Stuart und A. Peterlin, 551
Viscosity and sedimentation of linear macromolecules exhibiting partial solvent immobilization, A. Peterlin, 473

Viscosity

Degradation of ethyl cellulose in solution. *Letter to the Editors*, R. N. Haward, 635
Denaturation of plant proteins. III. Optical rotation, viscosity, and reducing capacity of denatured proteins, B. Jirgensons, 179
Flow of linear amorphous polymers, R. S. Spencer, 591
Intrinsic viscosity of macromolecules. *Letter to the Editors*, J. Riseman and F. R. Eirich, 633
Mechanical behavior of viscoelastic substances, R. Sips, 69
Method of measuring molecular weight distribution, F. W. Billmeyer, Jr., and W. H. Stockmayer, 121
Molecular configuration and thermodynamic parameters from intrinsic viscosities. *Letter to the Editors*, P. J. Flory and T. G Fox, Jr., 745
New method for deriving the intrinsic viscosity of polyelectrolytes. *Letter to the Editors*, D. T. F. Pals and J. J. Hermans, 733
Nitrocellulose–solvent interaction, W. R. Moore, 91
Viscosities of very dilute high polymer solutions. *Letter to the Editors*, S. Rothman, R. Simha, and S. G. Weissberg, 141
Viscosity of binary polymeric mixtures, W. R. Krigbaum and F. T. Wall, 505
Viscosity and sedimentation of linear macromolecules exhibiting partial solvent immobilization, A. Peterlin, 473

Vulcanization and Cross-Linking

"Bound" water in phenol-formaldehyde condensates. *Letter to the Editors*, P. O. Powers, 262
Tetramethylthiuram disulfide vulcanization of extracted rubber. I. Introduction and compounding, D. Craig, A. E. Juve, and W. L. Davidson, 709

X-Ray Investigations

Crystallinity of precipitated cellulose, P. H. Hermans and A. Weidinger, 565
New observations on the small-angle x-ray diffraction of synthetic fibers. *Letter to the Editors*, L. M. Arnett, E. P. H. Meibohm, and A. F. Smith, 737
Quantitative investigation of x-ray diffraction by "amorphous" polymers and some other noncrystalline substances, P. H. Hermans and A. Weidinger, 269
Unidirectional nature of the large periodic structure of collagen fibrils, O. E. A. Bolduan and R. S. Bear, 159

SUMMARIES OF ARTICLES RECEIVED

The following summaries are the English synopses of the papers accepted for publication. They include the articles appearing in this issue (Vol. V, No. 1), as well as articles scheduled for subsequent issues. This section is separately paginated as S1, S2, etc., and so printed that it can be bound with all the "Summaries" sections at the end of the year.

Dynamic Mechanical Properties of Rubberlike Materials. By A. W. Nolle.

Experimental results are presented for the complex dynamic Young's modulus of rubberlike materials in the frequency range 10^{-1} to 10^6 cycles per second and in a temperature range whose widest limits are −60° and +100°C. The real part of the modulus varies significantly with frequency over at least six decades, and increases with increasing frequency or with decreasing temperature. The imaginary part of the modulus is large in those parts of the temperature–frequency plane where the real part has a large gradient, and in some compounds reaches values larger than the real part. The behavior of the reciprocal modulus, or compliance, with respect to temperature and frequency is qualitatively the same as that of the dielectric constant of polar dielectrics having a wide range of dispersion. The most extensive measurements supporting these conclusions are performed on buna-N vulcanizates.

At very low frequencies the real part of the dynamic modulus is proportional to the absolute temperature as required by the kinetic theory of rubberlike elasticity. At a higher frequency, representing the onset of dispersion, the reverse temperature effect sets in. The frequency of the transition is of the order of 100 cps. for natural rubber and 1 cps. for butyl rubber.

The stiffening of rubber with decreasing temperature, sometimes regarded as evidence of a second-order transition, becomes progressively less abrupt with increasing frequency. It therefore appears that the "second-order" transition as observed at the higher frequencies is actually a relaxation rate effect. At very low frequencies there exists a temperature transition of the modulus whose form is almost independent of frequency and which is not necessarily a continuation of the relaxation stiffening found at higher frequencies.

The Cole arc in the complex plane is found to be an approximate representation of dynamic compliance data. Static deformation of the sample up to 50% elongation influences the dynamic modulus by a factor smaller than two in most cases, but the effect is seldom negligible. The presence or absence of vulcanization does not affect the high-frequency dynamic modulus critically; thus the increase of the real modulus with increasing frequency must be due in part to intermolecular relaxation hindrances which at sufficiently high frequency are equivalent to vulcanization bonds.

Data for buna-N, butyl, GR-S, neoprene, and natural rubber are compared. In the audiofrequency range, natural rubber has the smallest loss angle, while buna-N and butyl rubbers have the largest loss angles. As an alternate expression of the results, an approximate method is used to find a relaxation spectrum for a buna-N vulcanizate. The spectrum extends over at least six decades, but its extremes cannot be delineated with present data.

Activation energies for the molecular flow processes figuring in dynamic deformation are calculated by an approximate method from data for buna-N and natural rubbers. Values of approximately 30 and 10 kcal./mole, respectively, are found. These large activation energies suggest that the important relaxation effects in the frequency range of the present work arise from hindrances opposing motion of molecular segments composed of several monomer units rather than from hindered rotation about C—C bonds. *Received March 1, 1948.*

Molecular Weight Investigations of High Polymers with the Electron Microscope. By B. M. Siegel, D. H. Johnson, and H. Mark.

The electron microscope has been used to estimate the molecular weights of four polystyrene fractions which had molecular weights of 4.8×10^5, 1.1×10^6, 1.8×10^6, and 2.5×10^6 as determined by osmotic pressure and viscosity. Dilute solutions (~1 p.p.m.) of them in cyclohexane were deposited onto collodion substrates in minute droplets of approximately 2 microns radius. Shadow-casting with 3 Å. of uranium gave the necessary contrast for observing the dispersion of the single spheroidal particles obtained by this method of deposition. Assuming that the particles were single molecules and that their density could be taken for a first approximation as the density of bulk polystyrene, the molecular weights obtained were 6.0×10^5, 9.9×10^5, 1.9×10^6, and 2.5×10^6, which agrees within the limits of error with the osmotic pressure and viscosity values. The electron microscope should thus provide a useful method for characterizing macromolecules whose weight is greater than one million. *Received December 1, 1948.*

Copolymérisation de l'Anhydride Maléique avec Différents Monomères Vinyliques. By M. C. de Wilde and G. Smets.

The copolymerization of maleic anhydride with various vinyl compounds, namely, methyl methacrylate, methyl acrylate, vinyl chloride, vinyl acetate and isopropenyl acetate, was studied. The rate constants ratios r_1 and r_2 were determined in each case. The copolymerization with monomers, containing an electron-rich double bond, are characterized by high selectivity. In these cases the results are not completely interpreted by the scheme of Alfrey and Price. *Received January 3, 1949.*

Ultraviolet Absorption Spectra of Actomysin. I. By E. Schauenstein and E. Treiber.

The method of ultraviolet absorption spectrography is applied to high-molecular fibrous proteins. Measured under various conditions (swelling, change of *p*H, stretching, etc.), the spectrogram permits—apart from a quantitative analysis of the aromatic amino acids—new conclusions regarding the structure and the physicochemical and biological properties of the protein. *Received January 4, 1949.*

Denaturation of Plant Proteins. III. Optical Rotation, Viscosity, and Reducing Capacity of Denatured Proteins. By B. Jirgensons.

The optical rotation of native legumin and legumin denatured by heat, acetic acid, alkali, propyl alcohol, sodium salicylate, and sodium dodecylbenzenesulfonate has been investigated. It has been found that all the mentioned agents, except heating, cause a rise of rotatory power of legumin. The rotation angle of native legumin is constant in a *p*H range of 5.2–8.0 but increases in acid and alkaline solutions. Under the influence of a higher concentration of alkali, legumin is strongly denatured, and, after neutralizing and dialysis, becomes insoluble in 10% NaCl. The changes in rotatory power of legumin have been compared with the corresponding changes in reducing capacity, as estimated by titration with iodine, and with the viscosity. There is no change of reducing capacity on heating almost neutral solutions up to 90°, or upon treatment with propyl alcohol, or 40–50% acetic acid. However, the viscosity in all of the mentioned cases of legumin treated in this manner is somewhat higher than the viscosity of native legumin. Heating of dry legumin for three hours at 100–105° causes only a slight denaturation, but after heating for three hours at 115°, legumin becomes insoluble in 10% NaCl. The solutions of legumin in propyl alcohol–water–salt mixtures show only a transitory increase of rotation; after several hours the rotation angle decreases to the normal value of native protein. The rotation angle of legumin in solutions containing 40 volume per cent acetic acid and a salt with polyvalent cation increases with time; just after admixing of the salt the viscosity of these solutions decreases, but, gradually, gelatination occurs and the viscosity increases far above the initial value. The dependence of optical rotation on *p*H for legumin and tuberin, which have been denatured by sodium dodecylbenzenesulfonate or sodium salicylate, was investigated. It was found that in acid solutions the negative rotation angle decreases with growing hydrogen ion concentration; in alkaline solutions the rotation angle increases but little with a rising *p*H. Mildly deaminated legumin has almost the same rotatory power and the same dependence of specific rotation on *p*H as legumin itself. Deaminated legumin dissolves in detergent solution and the specific rotation of these solutions has a somewhat different dependence on *p*H than the corresponding solutions of legumin. *Received January 4, 1949.*

Mechanical Behavior of Viscoelastic Substances. By R. Sips.

Making use of a generalized Maxwell model or, alternatively, of Boltzmann's principle of linear superposition, we derive a general relation between force and deformation for a linear sample of a viscoelastic substance. This relation contains, as only experimental data, the relaxation function. Using this relation, we show how to predict all the usual properties, and particularly creep and recovery. The relation between the creep and relaxation functions can be expressed as a linear integral equation of the Volterra type. We give several methods of solution of this equation and we apply one of them to an experimental case, that of polyisobutylene. The calculated and observed values of the creep function agree remarkably well *Received January 7, 1949.*

Vitesse de Polymérisation et de Copolymérisation de l'Acétate d'Isopropényle. By R. Hart and G. Smets.

In the presence of benzoyl peroxide, isopropenyl acetate polymerizes like allyl acetate. Its behavior during the copolymerization with vinyl acetate, vinyl chloride, and methyl methacrylate indicates that this monomer has about the same general reactivity as vinyl acetate; the negative character of the double bond is more pronounced (−0.8). An

important chain transfer, due to the presence of isopropenyl acetate, occurs during these copolymerizations. Toward styrene, isopropenyl acetate acts as a solvent; there is no copolymerization, and also no chain transfer. *Received February 20, 1949.*

Nitrocellulose–Solvent Interaction. By W. R. MOORE.

The interaction of fibrous nitrocellulose and solvents has been studied by means of absorption of solvent from solvent–hexane mixtures, by swelling and solution in such mixtures, by precipitation from solution by hexane, and by viscosity measurements. Absorption and swelling results suggest that size of solvent molecules is important in determining entry into amorphous or crystalline regions of the fiber. Swelling, viscosity, and precipitation results indicate a relationship between interaction and cohesive energy density of solvent. It is suggested that current theories of polymer–solvent interaction, applicable where heat is absorbed in mixing, may also apply to the interaction of solvated nitrocellulose and solvent. *Received February 21, 1949.*

Studies on the Rate of the Emulsion Polymerisation of Butadiene-Styrene (75:25) as a Function of the Amount and Kind of Emulsifier Used. I. Polymerizations with Commercial and Pure Soaps. By C. W. CARR, I. M. KOLTHOFF, E. J. MEEHAN, and R. J. STENBERG.

The alkali soaps of the fatty acids, stearic, palmitic, and oleic, all produce the same rate of conversion when used as emulsifiers in the GR-S recipe. Linoleate in the soap causes serious retardation. All commercial soaps free of linoleate gave the same rate of conversion as the pure soaps. Tocopherol and lecithin in amounts likely to be found in commercial soaps have no effect on the rate of polymerization. In larger concentrations, tocopherol acts as an inhibitor, causing a typical induction period. Conversion data are given with the use of polymer soaps instead of fatty acid soaps. *Received March 28, 1949.*

Studies on the Rate of the Emulsion Polymerization of Butadiene-Styrene (75:25) as a Function of the Amount and Kind of Emulsifier Used. II. Polymerizations with Fatty Acid Soaps, Rosin Soaps and Various Synthetic Emulsifiers. By C. W. CARR, I. M. KOLTHOFF, E. J. MEEHAN, and D. E. WILLIAMS.

Fatty acid soaps containing 16 or 18 carbon atoms produce the same rate of conversion when used as emulsifiers in the GR-S recipe. With myristate, laurate, and caprate the initial rate of conversion becomes progressively lower. After about 20% conversion the further rate approaches that with the C_{16} and C_{18} soaps. Conversion data are given with the use of various commercial emulsifiers, disproportionated rosin soaps, and pure components of rosin soaps including sodium tetrahydroabietate, sodium dehydroabietate and sodium dihydroabietate. *Received March 28, 1949.*

Monomer–Polymer Ratio in Emulsion Polymerization of Styrene. By S. H. HERZFELD, A. ROGINSKY, M. L. CORRIN, and W. D. HARKINS.

Values are presented for the monomer–polymer ratio in the emulsion polymerization

of styrene at 35 and 40.7 °C. and for varying soap concentrations. Two experimental methods were employed; the experimental techniques are described in detail. The monomer–polymer ratios reported are presumably not equilibrium values but represent an attempt to obtain dynamic values of the ratio as occurring during polymerization. Whether these values as reported are in reasonable approximation to the dynamic values is uncertain. In agreement with the theory of emulsion polymerization presented by Harkins it is found that a large amount of monomer is dissolved in the monomer–polymer particles. It is further shown that the monomer–polymer ratio decreases with increasing yield. The data presented do not allow a correlation between the variation of the monomer–polymer ratio with yield and the soap concentration. *Recd. March 31, 1949.*

General Theory of Mechanism of Emulsion Polymerization. II. By W. D. HARKINS.

In emulsion polymerization the system begins with the monomer present as droplets surrounded by a monolayer of soap. The monomer diffuses through the water into the internal hydrocarbon part of soap micelles, which usually contain 40 to 100 soap molecules. If the catalyst or chain initiator is in the water, small free radicals are formed. Many of these enter micelles, where they grow before termination in about a thousandth of a second. Much of this growth occurs by extension of the free radicals into the water. This process continues until all micellar soap disappears by adsorption of soap on the monomer–polymer particles, which are formed by diffusion of monomer into the polymer particles thus formed. Almost all of the polymer is produced by polymerization of the monomer in these particles. *Received March 31, 1949.*

Method of Measuring Molecular Weight Distribution. By F. W. BILLMEYER, JR., and W. H. STOCKMAYER.

Based upon the suggestion of Spencer, a method for estimating the breadth of the molecular weight distribution of a high polymer has been devised: a polymer solution is divided into aliquots and part of the polymer in each aliquot is precipitated with nonsolvent so that the range from complete solution to complete precipitation is covered. The mass and weight-average molecular weight of each precipitate is measured. From these data the distribution breadth is estimated in terms of a parameter *H* representing the departure of the distribution from that of a single molecular species. In the theoretical section, *H* is related to other parameters of distribution breadth, such as M_w/M_n, for some well-known analytical distribution functions. A number of experiments with polymethyl methacrylates are described and the results are discussed with reference to polymerization kinetics. Determinations of osmotic pressure and light scattering have been made to evaluate directly M_w/M_n. The values compare favorably with M_w/M_n estimated from *H*. Errors in both the theoretical and experimental treatments are discussed. *Received April 1, 1949*

Quantitative Investigations of X-Ray Diffraction by "Amorphous" Polymers and Some Other Noncrystalline Substances. By P. H. HERMANS and A. WEIDINGER.

Radial intensity distribution curves of isotropic monochromatic x-ray exposures of various noncrystalline and partly crystalline polymers are quantitatively evaluated, corrected for incoherent radiation, and reduced to standard conditions of intensity and irradiated mass. It is shown that the intensity distribution curves thus reduced actually show constant integrated intensity within experimental error, irrespective of the atomic composition of the polymer. Amorphous cellulose is indicated to exhibit by far the largest degree of disordering of all polymers investigated. It is suggested that, in polymers consisting of no other elements than C, H, O, and N, the occurrence of a coherent background intensity in the range of diffraction angles of 35° and upward is indicative of hydrogen bonding in the noncrystalline portion. The coherent background in this region is of zero intensity in polymers where no hydrogen bonding is possible. Water, being a substance rich in hydrogen bonds, shows considerable intensity in the relevant region. In halogen-containing polymers, detection of hydrogen bonding in this way is impossible, owing to intermolecular interferences between halogen atoms of adjacent molecules which give rise to a background intensity in the same angular region. *Received April 7, 1949.*

Potassium Ferricyanide–Diazothio Ether–Mercaptan Recipe for Emulsion Polymerization of Butadiene and Styrene. II. Effect of Some Chemical Variables. By I. M. KOLTHOFF and W. J. DALE.

MDN added to latices of various conversions prepared by a ferricyanide–*n*-DDM recipe greatly increases the further rate of polymerization. The effect of different amounts of fatty acid soap in the MDN–ferricyanide-*tert*-dodecyl mercaptan recipe in the time–conversion curve is reported. The rate of conversion found with the MDN–ferricyanide recipe decreases greatly with decreasing amounts of mercaptan. Use of Aerosol AY and di-*tert*-butylnaphthalene sulfonate, respectively, instead of fatty acid soap in the recipe results in satisfactory rates of conversions. Several diazothio ethers as substitutes for MDN in the recipe have been investigated. *p*-Methylphenyldiazothio (2-naphthyl) ether gives an attractive time–conversion curve. *Received April 8, 1949.*

Unidirectional Nature of the Large Periodic Structure of Collagen Fibrils. By O. E. A. BOLDUAN and R. S. BEAR.

Small-angle x-ray diffraction patterns of collagen specimens (kangaroo tail tendon) were obtained with pinhole and slit cameras capable of resolving very large spacings (800 to 1400 Å.). The diffraction effects were examined with respect to layer-line shapes (lengths) and relative to the displacement of line positions and the persistence of diffraction intensities when the fibers were tilted from the usual normal incidence of the beam. In these respects dry specimens showed the diffraction behavior characterizing systems with less than three-dimensional periodic structure. Since only a single set of meridional diffractions could be observed, the dry collagen fibrils were concluded to possess only unidirectional (longitudinal) periodic structure and to lack regular order transversely. The same was found true of moist fibrils, except that these diffract coherently over a significantly larger cross-sectional area. Several peculiar observations indicated qualitatively that the dry fibrils do not diffract coherently over the same effective portions of their cross sections to all diffraction layer lines. *Received April 18, 1949.*

Viscosity and Sedimentation of Linear Macromolecules with Partial Solvent Immobilization. By ANTON PETERLIN.

Various formulas set up for viscosity and sedimentation of linear macromolecules that take into account the hydrodynamical interaction are compared and their extensive agreement is stated. In practice the simplest formulas will be of greatest service. By plotting the observed $[s]$ and $M/[\eta]$ values against the square root of the molecular weight, straight lines are obtained. The slope yields the effective length of the molecule. The respective formulas are given and applied to various polymers. *Received April 19, 1949.*

Influence of Structure of Elastomers on Their Permeability to Gases. By G. J. van Amerongen.

The subject of this study was the effect of the structure of rubberlike polymers upon the permeability, diffusivity, and solubility with a series of gases. It was found that butadiene-acrylonitrile copolymers lose much of their diffusivity and permeability with increasing nitrile content. The presence of methyl groups in the polymer molecules likewise usually reduces diffusivity and permeability. The knowledge gained enabled us to synthesize an isoprene-acrylonitrile copolymer which, besides possessing rubberlike properties, allows very little gas to permeate. The relationship between rate of diffusion and temperature gave the energy of activation E for diffusion. Greater energy of activation for a given gas in a series of rubbers always produces a lower rate of diffusion. The energy of activation E is shown to be greater in proportion to greater cohesive forces between the rubber molecules and to the larger size of the gas molecules. Measurements taken within a wide range of temperature (−18 to 100 °C.) make it clear that the activation energy is a function of the temperature, and an experimental equation is presented to describe this. The dependence of E upon the temperature is demonstrably compatible with Barrer's zone theory as also with Eyring's transition state theory for diffusion. The μ constant for several systems of gas and rubber is derived by calculation from the solubility of the gas. The heat of solution is derived from the dependence of the solubility of the gas in rubber upon the temperature. This heat of solution consists mainly of heat of mixing in the case of gases which condense with difficulty; compared with this the heat of condensation of the gas to the liquid phase is slight. *Received April 25, 1949.*

Optische Anisotropie und Form von Fadenmolekülen. I. Depolarisationsgrad der Lichtzerstreuung von Lösungen mit Fadenmolekülen. By A. Peterlin and H. A. Stuart.

The degree of depolarization in molecular light scattering experiments in the case of statistical coiled linear molecules is calculated as a function of the degree of polymerization, and the limits of the validity of the theory are discussed. *Received April 25, 1949.*

Optische Anisotropie und Form von Fadenmolekülen. II. Künstliche Doppelbrechung. By A. Peterlin and H. A. Stuart.

The relations existing between the electric, magnetic, and streaming birefringence of linear molecular solutions are given as functions of the degree of polymerization. Some possibilities are discussed for the determination of the "macro-" and "micro-" form of a high polymeric molecule, and for the identification of branching. Finally, it is shown, by electric birefringence on vapors, that paraffin chains are loosely coiled molecules. *Received April 25, 1949.*

Photoelastic Strain Analyzer. By E. F. Smith and A. P. Wangsgard.

The theory and instrumentation for photoelectrically determining "frozen in" strain levels is described when the thickness and strain optical constants are of such magnitude that the optical retardation is restricted to the less than π radians. The method is suited for use in an industrial laboratory and has been applied to control of planishing cycles in the production of transparent "Vinylite" plastic sheets. *Received May 3, 1949.*

Behavior of Polyvalent Polymeric Ions in Solution. By A. Katchalsky, O. Künzle, and W. Kuhn.

The addition of alkali to a dilute solution of polymethacrylic acid produces a strong increase of the intrinsic viscosity, *e.g.*, by a factor 130, if 50% of the COOH groups (of a particular sample) are neutralized. This phenomenon, as well as related effects in streaming birefringence, can be interpreted as a partial or complete uncoiling of the filament, produced by the electrostatic action if we pass from the neutral molecule to the polyvalent ion. A first and a second approximation are considered for the electrostatic energy of a filament as a function of the end-to-end distance h and the degree of ionization α. In this second approximation the assumption is made of a uniform distribution of the electric charges over the polyvalent ion. An additional consideration shows that this assumption is somewhat inexact because of a certain concentration of the charges near the ends of the filament; however, it is shown that this effect leaves the result obtained in the second approximation, concerning the energy of the system, practically unchanged. By use of this determination of the electrostatic energy as a function of h and α and by use of the Maxwell-Boltzmann principle, the distribution function with respect to h and thereby the partial uncoiling of the filament is determined as a function of the degree of ionization α. By introducing the mean value of h, thus accessible, into the formulas which give the intrinsic viscosity as a function of h, expressions for the viscosity as a function of α are obtained. A rough but comparatively simple approximation for this function can be developed. The dependence of the intrinsic viscosity on α thus obtained is found to agree satisfactorily with experimental values of the viscosities of polymethacrylic acid neutralized by addition of increasing quantities of alkali. *Received May 3, 1949.*

Friedel-Crafts Copolymerization of Chloroprene-Styrene. By F. C. Foster.

Relative reactivity ratios have been determined for the copolymerization of chloroprene–styrene at −18°C., catalyzed by boron trifluoride–etherate. Similar to the earlier findings of Alfrey, on a different copolymer system, it was found that there was a complete reversal of the relative reactivity of the two monomers on changing the system from a free radical type catalyst to a Friedel-Crafts type catalyst. This reversal of monomer reactivities enables the production of "constant composition" copolymers of any desired composition by a suitable choice of catalyst type. Indications are that the cationically catalyzed copolymers produced in the present work are low molecular copolymers. *Received May 9, 1949.*

Die Löslichkeit hochpolymerer Fadenmoleküle. By Arnold Münster.

The theory of solubility of high polymer fiber molecules is developed on the basis of thermodynamic and of the static theory of polydisperse solutions. The discussion of the distribution equilibrium between two nonmiscible solvents for monodisperse solutions results in the formula given by G. V. Schulz as a limit at infinite dilution, while at a definite concentration the relation between distribution ratio and degree of polymerization is more complicated. The examination of polydisperse solutions shows surprisingly that in this case the relation suggested by G. V. Schulz is valuable also for definite concentrations.

For the separation of a binary solution it has been shown that the critical concentration is located at very low concentrations of the fiber molecules and that the critical temperature increases only slightly with the degree of polymerization. Assuming that the sol phase is practically free of fiber molecules, the separation curve is calculated and a formula for the degree of swelling in dependence of the temperature is given. The theory explains the general solubility properties of high polymer substances and especially shows that nonsolvents, also, always have a swelling action. Such a limited swelling is therefore not due to a net structure. For high polymer products the composition of the gel phase—in particular, the degree of swelling- is independent of the degree of polymerization. The comparison of the theoretical curve of separation to the experimental results shows good agreement in all essential points. The extension of the experiment to polydisperse solutions shows that the separation curve is practically independent of the distribution of the degree of polymerization. The separation of ternary systems is first treated under the assumption that the sol phase does not contain fiber molecules. For a special case an entire separation diagram is calculated, which agrees very well with experimental results of Brönsted and Volqvartz and which shows especially the enrichment of precipitant in the sol phase. These results, as well as the preceding, are valid for polydisperse solutions independently of the distribution of the degree of polymerization. Starting from the condition of equilibrium for dissolved fiber molecules, a formula for the weight distribution function of a precipitate is derived. This function contains a parameter δ, which may be positive as well as negative. In the case of $\delta < 0$ the formula describes the usual fractionation. In the case of $\delta > 0$, reverse order precipitation occurs, discovered by Morey and Tamblyn, for which the low molecular constituents precipitate first. The properties of the reverse-order precipitation are developed from the theory in agreement with the experimental results. It is shown that in such cases the fractions are highly polydisperse and overlap each other. Therefore, systems with reverse-order precipitation cannot be used to produce uniform fractions and to examine the distribution of the degree of polymerization in the initial product. A new case of reverse-order precipitation in the system cellulose triacetate-tetrachloroethane-petroleum ether is reported *Received May 15, 1949.*

Untersuchung einer katalysierten Leinölstandölkochung unter Heranziehung der Ultraviolettspektrographie (vergleich mit nichtkatalysierten Prozessen). By A. Maschka and A. Mendl.

(*1*) Laboratory style boilings of linseed oil stand oil with and without catalyst in an atmosphere of carbon dioxide, as well as a boiling of linseed oil varnish and linseed oil stand oil varnish, are investigated. (*2*) Besides the usual characteristics the ultraviolet absorption spectra of each sample are determined and from this the amount of the intermediate systems with double and triple conjugated double bonds are calculated. (*3*) The concentration curves of these intermediate products and the other characteristics are qualitatively in agreement for both stand oil boilings with a technical process described in the literature. Of course, the catalyzed process takes a much quicker course. (*4*) From these results it is concluded that the succession of reactions described as probable in the literature (conjugation of isolated double bonds—intra- and intermolecular polymerization, respectively, as in a diene Diels-Alder synthesis) also occurs in the catalyzed process. The catalyst accelerates all of the partial reactions. (5) The attempt is made to derive the importance of transesterification for the increase of the viscosity (molecular weight) from the increase of the viscosity and the decrease of the iodine value. *Received May 19, 1949.*

Aging of Solutions of Cellulose Nitrate. By H. CAMPBELL and P. JOHNSON.

Viscosity–time (aging) curves for cellulose nitrate solutions in acetone and other solvents are, generally, characterized by an initial rapid decrease in viscosity followed by a slow continuous decrease. Ultramicroscopic aggregates were not observed and structural viscosity was absent throughout both aging processes. Initial rapid aging was absent or small in cellulose nitrates of high nitrogen content (few free hydroxyl groups), and in those which had been recovered from solution or treated with a small proportion of water in solution. Slow aging appeared to a greater or lesser degree in all cellulose nitrates, independently of origin or chemical treatment of the cellulose, degree or method of nitration, method of stabilization, concentration of solution or presence of precipitants. The rate of the slow aging process was increased by a rise in temperature but, owing possibly to the presence of adventitious catalytic impurities, considerable variation in rate at a given temperature was observed. It is suggested that the rapid aging process is due to the slow breakdown of a small number of relatively weak interchain linkages, probably of the hydrogen bond type. The slow aging probably represents the breakdown of the main chain glucosidic linkages. *Received June 14, 1949.*

Inhibiting Effect of Small Amounts of Acrylonitrile on Polymerization of Vinyl Acetate. By W. R. CONN and H. T. NEHER.

Small amounts of acrylonitrile inhibit the emulsion polymerization of vinyl acetate. Larger amounts merely retard the reaction and the retarding effect is inversely proportional to the amount of nitrile present, so that at around 40% nitrile content, the mixture polymerizes at about the same rate as vinyl acetate alone. In solution polymerization, the retarding effect of small amounts of acrylonitrile is directly proportional to the amount present. With mixtures of the two monomers in emulsion, the polymerization of both the acrylonitrile and the vinyl acetate becomes faster with increasing nitrile content; in solution the polymerization of both monomers becomes slower with increasing nitrile content. Methacrylonitrile, methacrylamide, and styrene strongly inhibit the polymerization of vinyl acetate. Ethyl methacrylate and acrylamide are mild inhibitors. *Received June 21, 1949.*

Polymerization of *m*- and *p*-Formylstyrenes. By R. H. WILEY and P. H. HOBSON.

Polymers and copolymers of *m*- and *p*-formylstyrene prepared by bulk and emulsion techniques have been found to be fusible and to be insoluble in a wide variety of organic solvents. The presence of the electrophilic formyl group does not appear to alter the polymerizability of these compounds. *m*-Formylstyrene has been prepared by decarboxylation of *m*-formylcinnamic acid and characterized. *Received June 29, 1949.*

Crystallinity of Precipitated Cellulose. By P. H. Hermans and A. Weidinger.

Cellulose precipitated from very dilute viscose by acids shows enhanced degree of crystallinity as compared to ordinary viscose rayon. The effect is small when precipitation is carried out at room temperature and considerable at boiling temperature. The highest figure reached was 53% as compared to 40% for rayon. *Received July 5, 1949.*

Viscosities of Binary Polymeric Mixtures. By W. R. Krigbaum and F. T. Wall.

Specific kinematic viscosities in dilute solutions are reported for three mixtures and for the corresponding pure components. The data are fitted to the equation

$$\nu_{sp,m} = [\nu]_1 c_1 + [\nu]_2 c_2 + b_{11}c_1^2 + 2b_{12}c_1c_2 + b_{22}c_2^2$$

and the resulting values of the interaction constant b_{12} compared with the ideal value, $(b_{11}b_{22})^{1/2}$. Mixtures of dissimilar polymers are shown to exhibit positive or negative deviations from ideality, and an attempt is made to correlate these deviations with the physical properties and chemical structures of the components. It is pointed out that the Philippoff mixture law tacitly assumes ideal mixing and therefore gives only a first approximation to the mixture viscosity when the components are dissimilar. *Received July 5, 1949.*

Flow of Linear Amorphous Polymers. By R. S. Spencer.

The principal aim of this paper was to emphasize the importance of flow orientation as a determining factor in the behavior of polymers in shear. The tacit assumption underlying the entire discussion has been that deviations from Newton's law are attributable primarily to flow orientation, at least for the type of polymers with which we have been concerned. On this basis a new relationship between rate of shear and shearing stress was derived and found to agree reasonably well with experimental fact. Taking a more empirical approach, it was shown that the flow behavior of a polymer may be characterized by two quantities, the Newtonian viscosity (or fluidity) and the modulus of high elasticity. The influence of temperature, polymer molecular weight, and plasticizer content on these quantities was illustrated. Such phenomena as ballooning and spiralling of extruded filaments were discussed on this basis. *Received July 10, 1949.*

Properties of Polystyrene. II. Fractionation of the Polymer. By E. H. Merz and R. W. Raetz.

A large-scale fractionation of a low conversion polystyrene polymer by stepwise reduction of the temperature of a butanone-methanol solution is described. The intrinsic viscosity is reported for all 39 fractions and the light-scattering molecular weight for 8 fractions. The distribution curve, having a single broad peak, is also presented. *Received July 10, 1949.*

Refractometric Determination of Second-Order Transition Temperatures in Polymers. V. Determination of the Refractive Indices of Elastomers at Temperatures from 25° to − 120°C. By R. H. Wiley, G. M. Brauer, and A. R. Bennett.

Refractive index–temperature data down to −120°C. are reported for a series of rubberlike polymers which have second-order transitions at temperatures below −60°C. These data show a change of slope which locates the transition temperature. A method for insulating the standard Abbe refractometer and refrigerating it with cooled air to facilitate operation down to −120°C. is described. *Received July 11, 1949.*

Depolymerization as a Chain Reaction. By R. Simha, L. A. Wall, and P. J. Blatz.

The kinetics of depolymerization reactions of the chain type is developed by postulating an initiation, followed by propagation, transfer, and termination of radicals. The propagation produces smaller radicals and monomer molecules. Transfer stabilizes a given radical and produces another which in turn decomposes into a smaller radical and a stable chain. Termination is assumed to occur exclusively by disproportionation. Such a scheme leads to the following result: If and as long as a steady state concentration of radicals is maintained, the course of the reaction, *i.e.*, the production of smaller stable species from the original material, is approximately equivalent to that predicted by a step reaction of the type treated previously. The effective rate constants of this equivalent reaction are a function of the initiation and transfer constants, the radical concentration, and the kinetic chain length. They furthermore depend upon the location of the bond to be broken, although no *a priori* dependence of the actual rate processes on the position within a molecule (weak links) or the size of a molecule is assumed. The effect is a purely statistical one. If a radical can be initiated all along a polymer molecule, bonds in the interior are effectively broken more readily than those near the ends. If initiation can occur only at the terminal bonds, the situation is reversed. This selective tendency is opposed by the transfer reaction, which exerts a randomizing influence besides effectively increasing the initiation probability for a given molecule. The general solution is given and discussed in terms of the kinetic chain length. If it is very small in comparison with the initial degree of polymerization, the course of the reaction is determined by initiation and transfer. Such a case may be approached when transfer is important. If initiation occurs at random, the result tends in the limit toward practically random degradation. The case of initiation at the ends reduces in the limit to a stepwise splitting of terminal monomer units. On the other hand, when the chain length is larger than the degree of polymerization, small molecules are preferentially produced. The distribution of molecular sizes and the average molecular weight are presented as a function of the degree of conversion. Estimates of the values of the kinetic chain length and of the initiation constant are given. *Received July 15, 1949.*

Titration Potentiometrique de la Viscose. III. By P. Herrent and G. Jnoff.

By combining various current methods of analysis with the present method of potentiometric titration, it was possible to plot the individual curve of the variation of composition of each of the constituents of viscose as a function of ripening. *Received July 27, 1949.*

Experimental Study of Copolymerization. IV. By T. Alfrey, Jr., J. Bohrer, H. Haas, and C. Lewis.

Experimental results for fourteen copolymer systems are reported. The self-addition of indene has been verified. This monomer strongly inhibits vinylidene chloride. Coumarin behaves as an inert diluent in the polymerization of vinylidene chloride. The effect of the following groups on the reactivity of the double bond is examined: carboxyl, 2-pyridyl, *tert*-butyl. *Received August 15, 1949.*

Chlorination of Natural Rubber. I. Preparation and Properties of Chlorinated Rubber. By G. J. van Amerongen, C. Koningsberger, and G. Salomon.

In order that the reaction between chlorine and rubber might be studied, rubber in solution and solid rubber were made to react under greatly varied conditions with gaseous and liquid chlorine. It may be inferred from the quantity of HCl evolved during the reaction and from the reactivity of the combined chlorine toward aniline that the primary reaction proceeds by substitution of chlorine at the allylic position. This substitution of chlorine is considered to be an ionic type of reaction involving the formation of an intermediate carbonium ion. With continued chlorination, chlorine is added on to the double bond. There was no distinct variation from this course of reaction under any of the conditions applied. Chlorinated rubbers of 65 to 70% chlorine content were obtained in a short time by treating rubber solutions with chlorine gas under a pressure of 10 to 12 atm. at temperatures of about 100°C. Chlorinated rubbers of similar chlorine content were likewise produced from solid rubber by reaction with liquid chlorine at temperatures in the neighborhood of 100°C., but there were signs of carbonization in this reaction when large amounts of the material were brought into reaction at a time. *Received August 24, 1949.*

Chlorination of Natural Rubber. II. Preparation and Properties of Rubber Dichloride. By G. J. van Amerongen and C. Koningsberger.

Two methods are discussed for the production of relatively stable chlorinated rubbers of a chlorine content comparable to that of neoprene and polyvinyl chloride. One of those methods is based on the chlorination, by addition, of rubber with the aid of sulfuryl chloride. Experiments with purified gutta-percha, serving as a model substance for natural rubber, provided evidence that the presence of nitrogenous organic substances such as amines induces a substitutive chlorination. Peroxides, on the other hand, set a chain reaction in motion, which ultimately leads to an addition product. Some antioxidants, such as di-*tert*-amyl hydroquinone or β-naphthol, act as effective chain inhibitors. Several hydroperoxides, *e.g.*, tetralin hydroperoxide and *tert*-butyl hydroperoxide, are useful catalysts for the additive chlorination of natural rubber with SO_2Cl_2. These catalysts apparently prevail over the natural contaminations of natural rubber which favor substitution. Rubber derivatives containing up to 47% of chlorine, mainly additive, were produced from ordinary, unpurified rubber. By the other method for the production of chlorinated rubbers, rubber hydrochloride was chlorinated. This chlorination is accelerated by exposure to light, especially to ultraviolet light. Products were obtained containing up to as much as 70% of chlorine. On the evidence of kinetic chlorine analysis it is believed that chlorinated rubber hydrochloride with approximately 50% of chlorine probably possesses a structure not very different from that of the products of the addition of chlorine to rubber with SO_2Cl_2. The mechanical properties of various products are briefly discussed. Unsaturated rubber dichlorides containing about 25% of chlorine are rubbery and lend themselves to vulcanization giving products with little tendency to swell in hydrocarbons. Rubber dichlorides containing roughly 50% of chlorine are thermoplastic. *Received August 24, 1949.*

Potassium Ferricyanide–Diazothio Ether–Mercaptan Recipe for Emulsion Polymerization of Butadiene and Styrene. III. Determination of *p*-Methoxyphenyl Diazothio-(2-naphthyl) ether. By I. M. Kolthoff, W. J. Dale, and I. K. Miller.

Procedures are described for the determination of *p*-methoxyphenyl diazothio-(2-naphthyl) ether (MDN) in benzene solution and in latex by amperometric titration with silver nitrate, or with the aid of a spectrophotometer after conversion to a stable dye. *Received September 2, 1949.*

Heterogeneous System for Polymerization of Vinyl Chloride. By J. B. O'Hara and C. F. Prutton.

A process for the polymerization of vinyl chloride is described in which gaseous vinyl chloride is bubbled through a solution of potassium persulfate at slightly elevated temperatures and essentially atmospheric pressure. The manner in which the amount of polymer formed varies with time is described. The effects of the variables—monomer rate, catalyst concentration, temperature, and pressure—on the rate of reaction and specific viscosity of the polymer formed is presented. The locus of the reaction is discussed. *Received September 8, 1949.*

Measurement of the Molecular Weight of Polyethylene by the Menzies-Wright Boiling Point Elevation Method. By H. Morawetz.

The Menzies-Wright ebullioscopic method was used to evaluate unfractionated polyethylene resin, DYNH (Blend 1004). This material was found to have a number average molecular weight in the range 9000–9200. Results of good reproducibility were obtained with concentrations not exceeding 2.1 g. per 100 ml. tetrachlorethylene solvent. From the curvature of the boiling point elevation *vs.* concentration plot, the solvent–solute interaction constant μ was calculated and found to be slightly higher than the value predicted by Huggins for solvents with zero heat of mixing. *Received November 3, 1949.*

Redox Recipes. III. Use of Various Sugars at 0° and 30°C. in a Cumene Hydroperoxide–Iron–Sugar Recipe. By I. M. Kolthoff, A. I. Medalia, and M. Youse.

The cumene hydroperoxide–iron–sugar recipe which gave attractive rates of conversion at 30°C. has been studied with several variations at 0°, using several sugars or sugarlike products. Dihydroxyacetone appears to be the most suitable reducing agent at 0°. *Received September 8, 1949.*

Tetramethylthiuram Disulfide Vulcanization of Extracted Rubber. I. Introduction and Compounding. By D. Craig, A. E. Juve, and W. L. Davidson.

The series of papers, of which this is the first, report on soft rubber vulcanizations using tetramethylthiuram disulfide (TMTD) in the absence of added sulfur. A study of the characteristics of compounding in this system demonstrated that: (*1*) large amounts of the monosulfide inhibit vulcanization with both TMTD and sulfur; (*2*) the presence of 1.5% zinc oxide is desirable; (*3*) palmitic acid displayed only a mild activating effect; (*4*) neither zinc dimethyldithiocarbamate nor dimethylammonium dimethyldithiocarbamate activates TMTD–zinc oxide formulations; and (*5*) zinc sulfide is an effective activator. *Received September 12, 1949.*

Tetramethylthiuram Disulfide Vulcanization of Extracted Rubber. II. Structure of Radioactive Tetramethylthiuram Disulfide. By D. Craig, W. L. Davidson, A. E. Juve, and I. G. Geib.

(*1*) A study of the four sulfur atoms in tetramethylthiuram disulfide (TMTD) by radiosulfur techniques disclosed that these sulfur atoms are equivalent chemically. (*2*). The synthesis and reactions of radio-TMTD were studied. (*3*) New reactions which were found for TMTD included those with the following substances: dimethylamine, *n*-dodecyl mercaptan, ZnS, ZnO, zinc dust, S^{8*}, and acetic acid. (*4*) Radiosulfur and the sulfur atoms in ZnDMDC do not undergo interchange, at least up to 150°. *Received September 12, 1949.*

Tetramethylthiuram Disulfide Vulcanization of Extracted Rubber. III. Short-Path Distillation of TMTD and Its Reaction Products from Rubber. By D. Craig, A. E. Juve, and W. L. Davidson.

(*1*) A technique has been described for the short-path distillation of substances from rubber. It has been found that sulfur, TMTM, TMTD, ZnDMDC, phenyl-beta-naphthylamine, and palmitic acid are recoverable by this procedure. (*2*) The conversion of zinc compounds such as zinc oxide and zinc palmitate to ZnDMDC in rubber by treatment first with CS_2 and then with dimethylamine has been studied. (*3*) The volatilization of zinc from vulcanizates after conversion to ZnDMDC has been shown to occur without devulcanization. *Received September 12, 1949.*

Tetramethylthiuram Disulfide Vulcanization of Extracted Rubber. IV. Behavior of Rubber as an Acid. By D. Craig, A. E. Juve, and W. L. Davidson.

(*1*) The reaction of rubber with zinc palmitate was found to liberate palmitic acid at low pressures, thus revealing that rubber is acidic. (*2*) The reaction of zinc oxide with palmitic acid in toluene solution was enhanced by the presence of water. (*3*) The small increase in the nitrogen content of rubber caused by its reaction with TMTD was equivalent to the palmitic acid liberated by the zinc palmitate reaction. (*4*) The use of TMTD as a reagent for organic acids has been studied and found to convert carboxyl groups into dimethylamide groups. This result suggests that the acidic nature of rubber is due to carboxyl groups in the rubber molecule, a suggestion which is compatible with the nearly complete removal of zinc from the TMTD vulcanizate by the zinc removal technique. *Received September 12, 1949.*

Tetramethylthiuram Disulfide Vulcanization of Extracted Rubber. V. Low Molecular Weight Products and the Mechanism of Zinc Oxide Activation. By D. Craig, W. L. Davidson, and A. E. Juve.

(*1*) The mechanism of zinc activation has been studied by the use of radiosulfur and short-path distillation techniques. (*2*) The activating effect of zinc compounds of TMTD vulcanization is ascribed to a buffering action on the concentration of H_2S dimethyldithiocarbamic acids, and other acids which may be present in the vulcanizing rubber compound. (*3*) Zinc compounds appear to prolong the life of TMTM in the vulcanizate by limiting the concentration of H_2S and thus make possible an efficient use of the available sulfur for cross-linking of the rubber molecules by a process which seems to be of the radical type. (*4*) The reaction of DMADC with CS_2 has been found to yield dimethylthioformamide and sulfur in the absence but not in the presence of rubber. (5) The application of the results obtained to the theory of vulcanization is discussed briefly. *Received September 12, 1949.*

Hydroperoxides as Initiators of Emulsion Polymerizations at Low Temperatures. By J. E. Wicklatz, T. J. Kennedy, and W. B. Reynolds.

The results of emulsion polymerizations in which twenty-eight different organic hydroperoxides were used as oxidizing agents in a standard redox recipe at 5 °C. have been presented. Each hydroperoxide was tested at several different concentration levels. The hydroperoxides of chlorodiisopropylbenzene, di-*t*-butylisopropylbenzene, cyclohexylbenzene, 1,2,3,4,4a,9,10,10a-octahydrophenanthrene, and *t*-butylisopropylbenzene were found to be the most effective of the compounds tested. Oxidation mixtures, concentrates of oxidation mixtures, and purified samples of hydroperoxides served as sources of hydroperoxide for the polymerization experiments reported. Similar results were obtained with oxidation mixtures and concentrates, but purification of the hydroperoxide usually resulted in improved polymerization rates. The amount of hydroperoxide which gives the optimum results in a given polymerization recipe varies for structurally different hydroperoxides and appears to be related to the molecular weight. *Received September 17, 1949.*

Propagation Phenomena in Elastic-Viscous Media. By R. Sips.

Using results from a former paper, the equation is given for the propagation of one-dimensional disturbances in an elastic-viscous medium defined by its relaxation function. The integro-differential equation so obtained is integrated in two important cases: the steady periodic motion and the propagation of an initially localized disturbance in an initially unstressed medium. *Received September 18, 1949.*

JOURNAL OF POLYMER SCIENCE VOL. V, NO. 2, PAGES S17–S20

SUMMARIES OF ARTICLES RECEIVED

Some Polymeric Derivatives of Phosphonitrile Chloride. By C. J. Brown.

The reactions of phosphonitrile chloride with phenols and substituted amides have been investigated. Some of the substances formed polymerize readily to give high-boiling oils or thermoplastic resins. A new reaction has been found between phosphonitrile chloride and certain substituted anilides, such as acetanilide and diphenylurea. Equations for these reactions are suggested. It is evident that the phosphonitrile radical behaves as a unit of high stability, with chromophoric potentialities, readily giving rise to chain polymers. *Received February 21, 1949.*

New Oxidants for Initiation of Emulsion Polymerization in Antifreeze Recipes at —10°C. By C. F. Fryling and A. E. Follett.

The introduction of the Dioxes as oxidants in emulsion polymerizations at subfreezing temperatures has opened up new horizons especially in the direction of the utilization of commercially available rosin acid soaps in formulations containing low iron concentrations. It is now possible to copolymerize butadiene and styrene to 60% conversion in 16 hours in an emulsion recipe containing only 0.3 millimole of iron per 100 g. of monomers with Diox* D, Dresinate 214, and potassium soap flakes; formerly it had been impossible to reach such a conversion within 24 hours. By the use of mixed potassium laurate-myristate emulsifier and Diox 7, a conversion of 60% with a fluid latex was achieved in 19 hours at −10°C. In order to attain these high rates of conversion, it is necessary that the redox components of the polymerization recipe be properly "balanced" with respect to the mole ratio of oxidant to iron, and that the potassium chloride concentration in the activator and the *p*H of the emulsifier solution be adjusted to their optimum values. *Received September 17, 1949.*

Studies on the Rate of the Emulsion Polymerization of Butadiene-Styrene (75:25) as a Function of the Amount and Kind of Emulsifier Used. III. Effect of the Amount of Soap on the Rate of Polymerization. By I. M. Kolthoff, E. J. Meehan, and C. W. Carr.

The rate of emulsion copolymerization of butadiene-styrene (75:25) has been studied at 50°C. as a function of the amount of soap. The following soaps were investigated: potassium myristate, potassium laurate, sodium caprate, sodium salt of disproportionated rosin acids, and a commercial soap (largely sodium palmitate, oleate, and stearate). The initial rate of polymerization is decreased as the amount of soap is decreased, but the rate after about 25% conversion becomes almost independent of the amount of soap. If the concentration of soap in the aqueous phase is less than the critical concentration for micelle formation the initial rate is extremely small and becomes about equal to the rate in the absence of emulsifier. The initial rate with varying amounts of different detergents is approximately proportional to the amount of solubilization by the soap or other detergent solution. The data confirm Harkins' theory that solubilization by soap micelles is a major factor in the initial stages of emulsion polymerization. *Received September 24, 1949.*

Copolymerization of Phenylacetylene with Vinylpyridine. By C. C. PRICE and C. E. GREENE.

Experiments on the copolymerization of phenylacetylene with 2-vinylpyridine gave values for the copolymerization ratios, $r_1 = 4.0 \pm 0.7$ and $r_2 = 0.20 \pm 0.05$. Estimates of the copolymerization constants, $Q = 0.3$ and $e = -0.6$, from these experiments agree with those estimated from values of copolymerization constants recently reported by Doak from studies of copolymerization of phenylacetylene with methyl acrylate and acrylonitrile. The experiments reported herein support the report by Doak that phenylacetylene acts as a marked retarder, as well as a commoner. *Received October 5, 1949.*

Ionic Polymerization of Mono-olefinic Hydrocarbons at Low Temperatures. Characterization of the System Alpha Methylstyrene–Sulfuric Acid. By R. G. HEILIGMANN.

The asymmetrical aryl-olefin alpha methylstyrene has been polymerized to products of high molecular weight in the presence of sulfuric acid at temperatures of 0 °C. and below. The polymerization characteristics are similar to those exhibited by systems activated by electrophilic metal halides. The amount of water that can be tolerated in the sulfuric acid catalyzed system without material diminution in rate and molecular weight corresponds to the monohydrate. A carbonium ion mechanism is postulated for the system, consisting of an extension of the Whitmore theory to low temperatures with attendant decrease in the magnitude of the intramolecular rearrangements. *Received October 10, 1949.*

Experiments on the Sonic, Thermal, and Enzymic Depolymerization of Desoxyribosenucleic Acid. By G. GOLDSTEIN and K. G. STERN.

The effect of intense vibrations in the sonic frequency range, of elevated temperatures, and of purified pancreas desoxyribonuclease on highly polymerized sodium desoxyribosenucleinate has been studied in a quantitative and comparative manner. All three agents produce a depolymerization of the nucleinate resulting in a rapid decrease of the viscosity of dilute aqueous solutions. The ultraviolet absorption spectrum of the nucleinate is not appreciably affected by these agents. Studies in the ultracentrifuge reveal that the mechanism of depolymerization varies with the type of agent employed. In contrast to the enzymically and sonically depolymerized materials, the thermally treated STN shows a tendency to repolymerize spontaneously on standing. Na nucleinate, which has been partially depolymerized by sonic treatment, may be further degraded by desoxyribonuclease. *Received October 20, 1949.*

Calculation of the Distribution of Molecular Weight of GR-S from Viscosity and Mercaptan Consumption Data. By E. J. MEEHAN.

The distribution of molecular weights of GR-S polymers can be represented approximately by a logarithmic distribution function involving two constants which can be evaluated from viscosity-average molecular weight and number-average molecular weight. The latter may be calculated from mercaptan disappearance data. The calculated distributions are in good agreement with experimental values. *Received October 27, 1949.*

Osmotic, Viscometric, and Turbidity Studies of Polystyrene in Mixed Solvents. By S. R. Palit, G. Colombo, and H. Mark.

Polystyrene is found to be completely insoluble in acetone and in methylcyclohexane but dissolves completely in their mixture containing from 13 to 77% acetone by volume. Viscometric studies show that the $[\eta]$ is maximum and Huggins k' value minimum at about 40:60 acetone–m.c.H. mixture. Osmotic studies show that the slope of the π/c curve is maximum near this composition. Light scattering studies show that the scattering is at a minimum and the dissymmetry of scattering is at a maximum near this composition. The above observations are considered to indicate that the composition showing the maximum solvent power is a true optimum composition and the dissolved unit is laterally more extended in this optimum composition than at any other composition of the two solvents. *Received November 2, 1949.*

Modified Osmotic Balance. By C. R. Masson and H. W. Melville.

The construction of a modified form of osmotic balance has been described. By suspending a cell from each arm, the instrument has been made insensitive to temperature changes. In place of weighings, measurements are recorded by altering the buoyancy of one of the cells. By the use of an optical lever in conjunction with a divided photocell, a considerable increase in sensitivity has been obtained, the movements of the balance pointer being magnified about 300 times. A new method of matching the levels of solvent and solution has been described. Difficulties due to evaporation of solvent are discussed. *Received November 10, 1949.*

Elastoviscous Properties of Polyisobutylene. II. Relaxation of Stress in Whole Polymers of Different Molecular Weights at Low Temperatures. By G. M. Brown and A. V. Tobolsky.

The relaxation of stress in polyisobutylene whole polymers of different average molecular weights and in a butyl gum vulcanizate has been studied over a temperature range from 0° to −70°C. As the polyisobutylenes take on a glassy character with decreasing temperature, their relaxation behavior shows marked dissimilarities from that observed at elevated temperatures. At −70° the magnitude of the initial stress value is greater by a factor of more than two powers of ten than at 30°, the major part of the increase appearing at the lowest temperatures. The apparent activation energy for relaxation increases from a value of about 16 kcal. in the range 30–100° to more than 40 kcal. at −65° for a polyisobutylene of molecular weight 1,240,000. At the lowest temperatures the rate of relaxation of polyisobutylene tends to lose its sensitivity to molecular weight, and identical curves were obtained for samples of molecular weights 720,000 and 1,240,000. Here also, relaxation curves for the polyisobutylenes and for the butyl gum rubber become very similar. Below −55°, relaxation for periods of about 10 hours in polyisobutylene of molecular weight 1,240,000 occurs without any permanent deformation of the sample resulting. Apparently the relaxation observed at low temperatures during the time interval of an experiment proceeds by a mechanism distinctly different from that of the relaxation observed at elevated temperatures, in that many more short-range changes of molecular configuration are involved. *Received November 23, 1949.*

Copolymerization of Butadiene-Styrene by Means of an Oxygen, Dodecyl Mercaptan, Iron and Cobalt Pyrophosphates System. By C. S. Marvel and O. Keplinger.

Copolymerization of butadiene-styrene in soap emulsion can be initiated by the interaction of oxygen and mercaptans catalyzed by traces of ferrous pyrophosphate and cobalt salts. A recipe is described which effects conversions of 53% within 36 hours at −1°. The resulting rubber is very soluble in benzene and has an intrinsic viscosity in the range of 3.5–4.36. *Received November 28, 1949.*

Effect of Dielectric Solvent Medium on Copolymerization. By C. C. PRICE and J. G. WALSH.

The lack of influence of the dielectric constant of the solvent medium on the Alfrey-Price electrical factor in copolymerization has been confirmed for the systems styrene–methyl methacrylate and alpha-methylstyrene–maleic anhydride. Examination of the transition state structure in the light of the influence of solvent dielectric on charge interactions within a molecule indicates that little or no influence of solvent dielectric on simple coulombic interactions would be expected in the active radical–monomer transition complex. *Received December 6, 1949.*

Redox Recipes. IV. Dihydroxyacetone Recipes at 0°C. By I. M. KOLTHOFF and A. I. MEDALIA.

A recipe for the emulsion copolymerization of butadiene and styrene, in which the initiating system consists of cumene hydroperoxide, ferric iron (as the pyrophosphate complex), and dihydroxyacetone, gives a conversion of 60% in 11.5–12 hours at 0°C., with as little as 0.07 part of dihydroxyacetone. Owing to the high cost of pure dihydroxyacetone, the preparation of crude products has been studied by means of the Fenton reaction. A procedure is described according to which glycerol, glucose, or sucrose may be oxidized with hydrogen peroxide and ferrous iron to give crude solutions whose activity in the polymerization recipe is equal to that of dihydroxyacetone. *Received December 8, 1949.*

Polyalkylene Sulfides with Rubberlike Properties. By C. S. MARVEL and H. E. BAUMGARTEN.

The reaction of hexamethylenedithiol with diolefins to form polyalkylene sulfides has been extended to the diolefins, 2,6-diallylphenol and diallylcarbinol. Polyalkylene sulfides with rubberlike properties have been obtained from the reaction of mixtures of diallyl, dimethallyl, and 2,6-diallylphenol with hexamethylenedithiol in the emulsion system utilizing MP-189-EF as emulsifier, ammonium persulfate as catalyst, and sodium bisulfite and cupric sulfate as catalyst activators. The polymers have been vulcanized (cross-linked) by heating with an excess of hexamethylenetetramine to give benzene-insoluble, rubbery solids. A polymer prepared from dimethallyl (90 mole per cent), diallylcarbinol (10 mole per cent), and hexamethylenedithiol has been vulcanized by heating the polymer in chlorobenzene solution with hexamethylene diisocyanate to give a rubbery solid. *Received December 8, 1949.*

Redox Recipes. V. The Redox System, Ferrous Sulfide–Cumene Hydroperoxide. By I. M. KOLTHOFF and A. I. MEDALIA.

A redox recipe is described in which freshly precipitated ferrous sulfide is the reducing agent and cumene hydroperoxide is the oxidizing agent. Attractive rates of conversion are obtained both at 30° and at 0°C., in the emulsion copolymerization of butadiene and styrene. Addition of reducing sugars, or of glycerol, increases the rate of conversion. *Received December 13, 1949.*

JOURNAL OF POLYMER SCIENCE VOL. V, NO. 3, PAGES S21-S26

SUMMARIES OF ARTICLES RECEIVED

Effects of Hampered Draining of Solvent on the Translatory and Rotatory Motion of Statistically Coiled Long-Chain Molecules in Solution. Part I. Translation Resistance; Rate of Diffusion and Sedimentation. By H. KUHN and W. KUHN.

The resistance to the translational motion of a randomly coiled molecule is discussed on the basis of several approximations. Theoretical treatments are given for the two limiting cases of the nondraining and the freely draining coil. The resistance of the nondraining coil of certain external dimensions is obtained by regarding it as a sphere and then as an ellipsoid of corresponding dimensions. The freely draining coil is treated by assuming that each of the preferential statistical chain elements into which the chain is divided behaves as though it were a long stretched ellipsoid of revolution and that its hydrodynamic resistance will remain uninfluenced by the other chain elements.

In the general case when the chain molecules are partially draining, the hydrodynamic resistance is determined from experiments on large-scale models in view of a theorem of hydrodynamic similarity applicable here. The models were constructed by bending pieces of wire in a statistical manner.

The empirical formula which results from these experiments applies to the whole range, *i.e.*, at all degrees of draining from the limiting case of the nondraining coil to the limiting case of free draining. In these limiting cases, good agreement is found with the results derived theoretically in the manner indicated above.

Expressions for the sedimentation and diffusion constants of randomly coiled molecules are given. They are found to be in agreement with experimental data. From a comparison with these data, values can be deduced for the length, A_m, and the hydrodynamic thickness, d_h, of the chain element. The values of d_h thus obtained are in rough agreement with the values of d_s, the average thickness of the chain deduced from molecular structural data. This serves to show that the use of large-scale model experiments in conjunction with the principle of hydrodynamic similarity represents a rational approach to the solution behavior of macromolecules and that the extension of the similarity principle down to such particle dimensions is not an unreasonable approximation.

Received December 1, 1947.

Redox Recipes. II. Redox Recipes in Alkaline Medium Initiated by the System Cumene Hydroperoxide–Iron–Sugar at 30°. By I. M. KOLTHOFF and A. I. MEDALIA.

A redox recipe for the copolymerization of butadiene and styrene at 30° is described. The components of the redox system are cumene hydroperoxide (CHP), a soluble pyrophosphate–iron complex, and a reducing sugar; the emulsifier is pure potassium myristate; and *tert*-dodecyl mercaptan is added as a modifier. Optimum concentrations have been found experimentally for ferric iron, pyrophosphate, and CHP. If very small amounts of CHP are taken, polymerization comes to a sudden dead stop at conversions which are in a linear relationship with the amount of CHP taken. From this relationship, together with the nearly constant rate of conversion, the rate of consumption of CHP can be calculated. This rate of consumption is proportional to the $^2/_3$ power of the amount of sugar, the proportionality constant for fructose being six times as great as that for glucose. When sufficient soap is taken, the rate of conversion is proportional to the square root of the rate of consumption of CHP; but with little soap, this relationship fails. Apparently the CHP–ferrous iron reaction which produces free radicals, takes place in the aqueous phase; if sufficient soap is present, the radicals enter the organic phase, where polymerization takes place; while with little soap, many radicals are terminated in the aqueous phase by reaction with one another without giving rise to polymerization. Alternatively, the data with 2.5 and 5 (but not with 10) parts of soap may be regarded as following the relationship predicted by Smith and Ewart for these authors' Case 2, in which the rate of conversion is proportional to the $^2/_5$ power of the rate of production of radicals and the $^3/_5$ power of the soap concentration.

With concentrations of soap below the critical, virtually no polymerization takes place; while a small increase in the amount of soap in the neighborhood of the critical concentration gives a sharp rise in the rate of conversion. When ferrous iron is used, this reacts rapidly with CHP in approximately a 1:1 mole ratio. The effects of various modifications in the ingredients of the recipe are presented. *Received June 18, 1949.*

Studies of Retarders and Inhibitors in the Emulsion Polymerization of Styrene. II. Inhibitors. By F. A. Bovey and I. M. Kolthoff.

An experimental study has been made of the induction periods produced by *p*-benzoquinone, potassium 9,10-phenanthrenequinone-3-sulfonate, and chloranil in the emulsion polymerization of styrene using dodecylamine hydrochloride as emulsifier and potassium persulfate as initiator. It has been found that the induction periods produced by *p*-benzoquinone are proportional to the amount of the inhibitor initially present, inversely proportional to the persulfate concentration, and nearly independent of the emulsifier concentration. Evidence has been adduced indicating that the rate of disappearance of *p*-benzoquinone is approximately equal to one-half the rate of production of monomer-free radicals in the system. The rate of production of radicals at the beginning of the polymerization is proportional to the persulfate concentration and nearly independent of the emulsifier concentration between 0.625 and 5.00 g. dodecylamine hydrochloride per 100 g. monomer. The activation processes exhibits an energy of activation of 33,000 ± 400 cal. per mole. Potassium 9,10-phenanthrenequinone-3-sulfonate is a nonideal inhibitor. Chloranil is found to copolymerize with styrene. The polymer resulting under our experimental conditions has been characterized, and found to have the composition:

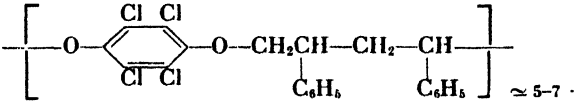

Oxygen reacts more readily with styrene-free radicals than do quinones. *Received July 5, 1949.*

Mechanism of Emulsion Polymerizations. IV. Kinetics of Polymerization of Styrene in Water and Detergent Solutions. By F. A. Bovey and I. M. Kolthoff.

The rates of polymerization of styrene in water solution, and in solutions of dodecylamine hydrochloride, potassium palmitate, and potassium laurate have been measured. In water solution and in dodecylamine hydrochloride solution, the rate of polymerization is given by:

$$-d(\mathrm{M})/dt = K(\mathrm{M})^2(C)^{1/2}$$

where (M) is the concentration of styrene and (*C*) the concentration of potassium persulfate. This expression holds over the concentration range 0.001 to 0.1 *M* in dodecylamine hydrochloride solution. The value of *K* in dodecylamine hydrochloride solution is found to be somewhat less than in water alone. By measurement of the rates of polymerization and molecular weights of the polymers at 40° and 50° in the presence of 0.0062 *M* persulfate and 0.093 *M* dodecylamine hydrochloride, the rates of activation at 40° and 50° were calculated. These rates are:

$$d(R)/dt\ (40^\circ) = 3.4 \times 10^{-6} \text{ moles/liter/hour}$$
$$d(R)/dt\ (50^\circ) = 16\ 3 \times 10^{-6} \text{ moles/liter/hour}$$

It is found that the rate of activation is essentially independent of the concentration of solubilized styrene, and is of the same order of magnitude in these experiments as in normal emulsion polymerization with a separate phase of styrene. The concentration of dodecylamine hydrochloride has hardly any effect on the rate of activation, but in the complete absence of emulsifier the rate of activation becomes much smaller. It is found that the molecular weight of the polymer formed varies inversely as the square root of the persulfate concentration. In solutions of fatty acid soaps, the rates of polymerization of styrene are greater than in solutions of dodecylamine hydrochloride, and follow no simple kinetic law with respect to styrene, being, however, nearer to first than second order. *Received July 5, 1949.*

Molecular Weight of Polyacrylic and Polymethacrylic Acids. By A. KATCHALSKY and H. EISENBERG.

(*1*) The molecular weight of polyacrylic and polymethacrylic acids may be determined by their transformation into the corresponding esters by diazomethane. Neither the chemical structure nor the chain length change during esterification. Hydrolysis of the polyesters to polyacids in acetic acid solution does not change the degree of polymerization.

(2) Measurements of the turbidity of dilute aqueous solutions on addition of HCl also give the true molecular weights. The molecular weights of 7 fractions of polymethacrylic acid ranging from 88,000 to 765,000 were determined by both methods and shown to be in good agreement.

(*3*) Comparison of the viscometric data in aqueous solutions, with the molecular weights obtained, shows that the molecules are highly coiled in acid solution ($[\eta] \sim M^{0.5}$), that they open by addition of small amounts of alkali ($[\eta] \sim M$), and that they become highly stretched at increasing degrees of neutralization ($[\eta] \sim M^2$). Excess of electrolyte reduces the intrinsic viscosity of the ionized polyacid to that of a randomly coiled chain. *Received December 9, 1949.*

Preparation of Cyclized Rubber from Natural Rubber Latex. By G. J. VAN VEERSEN.

In this paper a new method for the preparation of cyclized rubber from natural rubber latex is described. In this method, which follows logically from the new way of preparing rubber hydrochloride from natural rubber latex, latex stabilized with nonionic or cationic emulsifying agents is mixed with sulfuric acid. If a sufficient amount of sulfuric acid is added, cyclized rubber is formed after some heating. The influence of sulfuric acid concentration and the temperature on the rate of reaction have been investigated. Other cyclizing agents proved to be hydrogen fluoride and boron trifluoride. The advantage of the method described is that cyclized rubber can be obtained in the form of a latex. *Received December 13, 1949.*

Sedimentation Analysis of an Extract of the Prekeratinous Layers of Skin.

By E. H. MERCER and B. OLOFSSON.

(1) Sedimentation velocity analysis of a solution of the prekeratinous regions of skin in strong urea solution reveals the presence of several components with sedimentation constants ranging from 1–7. (2) Reduced solutions contain only a single component suggesting that the molecules with larger sedimentation constants are complexes, which are broken down by reduction. The average molecular weight of the principal constituent is of the order 60,000. The frictional ratio 3.5 implies a very asymmetric molecule. *(3)* In broad features this component resembles a fiber-forming derivative of wool keratin produced by reduction at moderate *p*H values. This type of molecule may play an important role in keratin synthesis. In molecular weight and shape it also resembles tropomyosin, a protein suspected of being an intermediate in myosin synthesis. *(4)* It is suggested that the synthesis of the fibrous and hardened keratin is effected by the aggregation of molecules in an ascending series of molecular weight, each aggregate being consolidated by disulfide cross-linking. *Received December 16, 1949.*

Treatment of Wood with Ultrasonic Waves.

By N. GRALÉN and S. BERG.

The treatment of wood with ultrasonic waves causes a disintegrating of the biostructure of wood and splits the bonds between lignin and cellulose or other carbohydrates. It is possible that the bonds of the cellulose molecule are split at the same time, but certainly to a lesser degree or at a slower rate. After treatment with ultrasound, about 50% of the wood can be dissolved in cuprammonium. The dissolved material (carbohydrates) consists of two main components with different sedimentation constants. The two components are approximately classified as the cellulose and the hemicellulose of the wood. *Received December 16, 1949.*

Polyelectrolytes. VI. Viscosities of 4-Polyvinylpyridine Hydrochloride in Methanol at 25°.

By R. M. FUOSS and W. N. MACLAY.

Viscosities of solutions in methanol of poly-4-vinylpyridine, to which varying amounts of hydrochloric acid were added, have been measured. Starting from zero acid at a given polymer concentration, the reduced viscosity $z = \eta_{sp}/C$, increases rapidly on initial addition of acid, reaching a maximum of the order of ten times the intrinsic viscosity of the parent polymer. The maximum in z appears before one equivalent of acid has been added to the polymer. Beyond the maximum, the reduced viscosity decreases slowly, and appears to approach an asymptotic value dependent on total polymer concentration. In the region of excess acid, the polyvinylpyridine hydrochloride behaves like a normal chain polyelectrolyte, in that z follows our empirical equation in the square root of polyelectrolyte concentration. The maximum in z is explained on the hypothesis that quaternization of the neutral polymer causes an initial rise in viscosity due to intramolecular electrostatic repulsion, and then association of the polycation with gegenions, with attendant neutralization of net charge, produces the decrease in z at excess acid. *Received December 19, 1949.*

Solubility of Crystallized Polymers. By G. J. VAN AMERONGEN.

The behavior in solution of three crystallized polymers, namely, gutta-percha, rubber hydrochloride, and nylon, was investigated. In all three cases it was found that, at a low enough temperature, these materials exhibit a separation of phases in the solution owing to the formation of crystallites. The melting point of these crystallites is lower in the better solvents and also in solutions of a higher dilution. *Received November 22, 1949.*

Cross-Linking Reaction in Butadiene Polymerization. By M. MORTON and P. P. SALATIELLO.

A study has been carried out on the emulsion polymerization of butadiene in an attempt to evaluate the relative rate of the cross-linking reaction and its variation with temperature.

Using a modified form of Flory's equation, the following values were obtained for the relative cross-linking rate constant (*i.e.*, ratio or the velocity constants of the cross-linking and propagation reactions):

Temperature, °C.	$K = k_x/k_p$
40	$1\ 02 \pm 0\ 03 \times 10^{-4}$
50	$1\ 36 \pm 0\ 05$
60	$1\ 98 \pm 0\ 06$

The data lead to a calculated value for the difference in the activation energy between the cross-linking reaction and the propagation reaction ($E_x - E_p$) of 7.5 ± 0.6 kcal.

On the basis of the assumptions made, it is then possible to calculate the weight average degree of polymerization ($\bar{y}_w$) at the gel point for any given temperature. Thus it can be shown that, whereas gelation occurs at 50° when the value of $\bar{y}_w$ reaches 3.1×10^3, it only occurs at 0° when $\bar{y}_w$ reaches a value of 2.6×10^4. Hence it should be possible to achieve a tenfold increase in weight average chain length without gelation by decreasing the temperature of polymerization from 50° to 0°. A change of this magnitude can be considered as a very significant factor in the improvement in physical properties observed in elastomers prepared at reduced temperatures. *Received December 18, 1949.*

Oriented Overgrowth on Cold-Drawn Polymers. By R. B. RICHARDS.

Oriented overgrowth of paraffin wax crystals, grown from solution, has been observed on the surface of cold-drawn strips of polyethylene and of polyethylene sebecate, but not on oriented gutta-percha, rubber, polyethylene terephthalate, or nylon. The distribution of the angles at which the platelike paraffin crystals lie on polyethylene has been measured. This is found to be narrower than the angular distribution of the crystalline regions in the polymer as a whole, as calculated from the x-ray diffraction pattern, suggesting that the crystallites in the polymer surface are more perfectly oriented than in the interior. *Received January 3, 1950.*

Stoichiometry of Vulcanization with Sulfur. By R. L. ZAPP, R. H. DECKER, M. S. DYROFF, and H. A. RAYNER.

The vulcanization with sulfur using a polymer of low unsaturation such as butyl rubber has been studied over a temperature range of 250° to 400°F. The extent of cross-linking by sulfur was followed by volume swelling measurements which were converted to molecular network dimensions with the aid of the Flory-Rehner model of a cross-linked system. Butyl networks were calibrated and an interaction coefficient between the polymer and the swelling solvent (cyclohexane) was given the value of 0.35.

The extent of vulcanization was also followed by combined sulfur measurements at appropriate points along the reaction curve. These combined sulfur values were differentiated between sulfur organically combined to the polymer chain and sulfur combined with zinc in the form of zinc sulfide.

From the molecular characterization of the vulcanized network the number of cross links per average molecule, and subsequently the amount of sulfur per cross link were calculated. Before the point of reversion set in, the amount of sulfur per cross link was of the order of two atoms regardless of the time or temperature at which the reaction took place. At the point of reversion this value began to increase. This stoichiometric aspect of vulcanization is discussed in the light of recent publications, and contradicts some reports on the inconsistency of combined sulfur and the physical properties imparted to the network. *Received January 8, 1950.*

General Nature of the Extension of Structure Transverse to Collagen Fibril Axes. By O. E. A. Bolduan and R. S. Bear.

The cylindrical collagen fibril (*e.g.*, of kangaroo tail tendon) scatters x-rays to its small-angle diffraction pattern in a manner indicating that its effective radius of coherent scatter, R_k (measured transverse to the ordered longitudinal axis), is often a function of layer-line index, k. Application of three methods for experimentally estimating R_k values discloses the following circumstances. For moist samples, R_k is large ($\gtrsim$ 1000 A.) and essentially independent of k, indicating that the entire fibril is then well organized and diffracts over much of its cross section to all layer lines. Drying, however, introduces a primary trend expressed by $R_k = 1000k$ A., upon which is superimposed minor secondary variation. It is suggested that the fibril is actually compounded of thin, parallel filaments which the drying distorts and displaces in statistical fashion to reduce the effective fibrillar cross sections for coherent scatter. An introductory model for a compound fibril is examined with respect to the types of refinement required to adapt it to the experimental facts more closely. *Received January 20, 1950.*

New Monomers of the Quinoid Type and Their Polymers. By M. Szwarc.

It was found that diradicals, stable in the gas phase and with structures analogous to that of the CH_2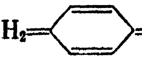CH_2 molecule, were formed by the pyrolysis of each of the following compounds: 2-fluoro-*p*-xylene, 2-chloro-*p*-xylene, 2,5-lutidine, 2,5-dimethylpyrazine, 1,4-dimethylnaphthalene, 5,8-dimethylquinoline. On condensation, the diradicals formed from these compounds polymerize, producing polymeric films which are insoluble in organic solvents. The properties of these "monomers" and of their polymers are described. *Received January 27, 1950.*

JOURNAL OF POLYMER SCIENCE VOL. V, NO. 5, PAGES S27–S34

SUMMARIES OF ARTICLES RECEIVED

Cationic Polymerization of Butadiene and Copolymerization of Butadiene and Styrene. By C. S. Marvel, R. Gilkey, C. R. Morgan, J. F. Noth, R. D. Rands, Jr., and C. H. Young.

(*1*) The cationic polymerization of butadiene with several Friedel-Crafts catalysts has been described. Aluminum chloride and chlorosulfonic acid are active catalysts at −75°. The rate of polymerization at −75° is much faster than at the higher temperatures. Except for boron trifluoride etherate, which catalyzes the polymerization at −30°, the other catalysts (sulfuric acid, fuming sulfuric acid, stannic chloride, and boron trifluoride hydrate) produce appreciable amounts of polymer only at 0° or higher.

(*2*) The effect of variables, such as catalyst concentration, catalyst solvent, dilution, reaction time, etc., differs with each individual catalyst. In some cases, results were not conclusive due to lack of reproducibility. It was found that the presence of moisture is mainly responsible for this lack of reproducibility. Traces of water promote the polymerization with stannic chloride or boron trifluoride etherate, but inhibit the polymerization when an ethyl bromide solution of aluminum chloride is used as catalyst.

(*3*) Rubberlike polybutadienes can be obtained with all catalysts except sulfuric and fuming sulfuric acids. However, the physical properties of these polymers show that the molecular weight is very low and that the polymer is not suitable as a rubber. Polymers ranging from viscous liquids to hard, brittle solids have also been obtained. In general, the solubility of the polymers is low. Approximately 60% of the butadiene enters the polymer chain by 1,4 addition.

(*4*) The copolymerization of butadiene and styrene at −75° with an ethyl bromide solution of aluminum chloride has also been studied. At conversions between 20 and 30% a soluble, rubberlike copolymer having a low molecular weight is formed. An insoluble, brittle polymer is obtained at higher conversions.

(*5*) The soluble, cationic copolymer has a characteristic ultraviolet absorption curve which is different from that of GR-S. It has a styrene content of approximately 50% by weight which demonstrates that the styrene is more active in cationic copolymerization than is butadiene *Received January 4, 1950.*

Denaturation of Plant Proteins. IV. Increase in Reducing Capacity, Viscosity, and Optical Rotation upon Denaturation with Guanidine Hydrochloride. By B. Jirgensons.

Legumin of vetch and tuberin of potato have been denatured by guanidine hydrochloride. It was found that the reducing capacity (as estimated by titration with iodine in slightly acid solutions), the optical rotation, and the viscosity thereby increase. The specific rotation of legumin is increased from −12° for native legumin up to −90° for denatured legumin. The optical rotation and reducing capacity decrease with decreasing *p*H. According to the titration data, only about 12% of the sulfide can be detected by iodine; upon denaturation, the amount of detectable SH groups increases up to 40–80%. *Received January 11, 1950.*

Heat of Crystallization of Cellulose. By E. Calvet and P. H. Hermans.

The measurement of the heats of dissolution of cellulose of diverse percentages of crystallization has permitted us to find the heat of crystallization of the cellulose. We have found 4100 cal./mole. This number is about 25% less than the heat of crystallization of the beta-glucose and it is very near that which had been found by one of the authors by means of the heats of wetting. The knowledge of the heats of crystallization of the cellulose and the determination of the heats of dissolution make possible the determination of the percentage of crystallization of a sample of cellulose when the composition of the sample in reference is known. *Received January 20, 1950.*

Free Energies of Formation of Hydrocarbon Free Radicals. I. Application to the Mechanism of Polythene Synthesis. By W. M. D. BRYANT.

Free energies of formation of twelve primary normal alkyl and seven other hydrocarbon free radicals at 298.2°K. were calculated from appropriate bond dissociation energies and from molecular entropies derived for the purpose. The new free energy data were used to show the relative thermodynamic importance of some free radical reactions assumed to occur in the synthesis of polythene by the usual vinyl mechanism of polymerization.

The entropies of the gaseous methyl, ethyl, *n*-propyl, isopropyl, *tert*-butyl, vinyl, and phenyl radicals at 298.2°K. were calculated from molecular data. A planar arrangement of substituent groups around the trivalent carbon was assumed. Entropies of the higher *n*-alkyl free radicals were estimated semiempirically. Heats of formation derived from bond dissociation data were used along with the entropies to obtain the free energies of formation.

Calculation of the free energies for intermediate steps of the polythene synthesis has shown that the initiation and propagation steps are favored, that chain transfer mechanisms vary from favorable to unfavorable, that chain branching is a moderately likely process. Termination reactions are thermodynamically very favorable. *Received February 1, 1950.*

Synthesis of Mixed Cellulose Esters Containing Phosphorus. By C. S. MARVEL and B. R. BLUESTEIN.

Mixed cellulose acetates chloroacetates were prepared from a partially acetylated cellulose with only slight degradation. These cellulose acetate chloroacetates were reacted with triethyl phosphite in the Arbuzov reaction to yield phosphorus-containing cellulose derivatives which were flame resistant. A mixed cellulose acetate diethyl phosphate was also prepared and it was found to be flame resistant. *Received February 7, 1950.*

Structure and Thermodynamics of Elastomeric Microgel. By A. I. MEDALIA.

Microgel consists of branched molecules of colloidal dimensions, formed by gelation occurring within the confines of a latex particle. It is shown that microgel should be (thermodynamically) soluble but, because of the large size of each molecule, it settles out of solution. The proportion of subchains which are connected to centers of crosslinkage at one end rather than both ends is calculated for gelled molecules of various values of the branching coefficient. *Received February 14, 1950.*

Determination of Microgel in GR-S Rubber. By A. I. MEDALIA and I. M. KOLTHOFF.

Microgel consists of branched molecules of colloidal dimensions, formed by gelation occurring within the confines of a latex particle. Thermodynamically, microgel is expected to be soluble in a "good" solvent, such as benzene. Experimentally, it is found that carefully dried microgel-containing polymers are completely soluble in benzene. Detection of microgel by solubility measurements requires the conversion of microgel to macrogel (gel of macroscopic dimensions) prior to the solubility measurement. This can be accomplished by heating under a variety of conditions. Milling of the polymer before heating aids in this conversion.

A Standard Procedure is recommended for the determination of microgel in standard GR-S rubber: the polymer (preferably coagulated in ethanol) is milled for about 10 passes, with the addition of 2% of phenyl-beta-naphthylamine; the milled polymer is heated for 12 hours in a vacuum oven at 80°, then placed inside a box of wire screen and immersed in benzene for 40 hours to extract the sol portion.

Solutions of microgel in benzene can be fractionally precipitated by addition of ethanol or nitroethane. The fractionation is primarily according to molecular weight rather than degree of cross-linkage. Viscosity and light-scattering measurements of the fractions show that the polymers are of high molecular weight and are cross-linked. *Received February 14, 1950.*

Rheology of Thermoplastics. II. Recoverable and Nonrecoverable Deformations of Polystyrene between 90 and 240°C. as a Function of Molecular Weight. By R. BUCHDAHL, L. E. NIELSEN, and E H. MERZ.

The rheological properties of polystyrene have been studied between 90 and 240°C. as a function of molecular weight. Three different methods have been used to obtain the data: rotational viscometer, extrusion-type capillary viscometer, and tensile creep measurements. It has been shown that the nonrecoverable (viscous) deformation is a function of molecular weight whereas the recoverable deformations are, within the investigated molecular weight range, practically independent of chain length. An explanation of this observation is suggested, based on the assumption of a labile network structure, which explains also the effect of "previous history" on the recoverable deformations. The temperature dependence of the recoverable and nonrecoverable deformations is shown to be very similar. Experimental evidence is presented to show that the dependence of the viscosity on shear stress (or rate of shear) is not a simple power relationship but is of the sigmoidal type. It is shown that the creep or compliance function a few degrees below the second-order transition point does not depend on the weight- or number average molecular weight. *Received February 28, 1950.*

Rate of Sorption of Organic Vapors by Films of Cellulose Acetate. By L. MANDELKERN and F. A. LONG.

A detailed study has been made of the rate of take-up of vapors of methylene chloride and acetone by thin films of cellulose acetate (37.9% acetyl) as a function of vapor pressure, film thickness, and temperature. It was found that the method of film preparation and conditioning greatly influenced the kinetics of the take-up. Films, which were not completely dry, exhibit a much faster rate of take-up than dry films. Dry films could be obtained by either long treatment in a vacuum oven, or by water leaching followed by vacuum drying for five days. In either case, identical kinetic results are obtained. The mercury cast films used in this work give reproducible results and show a much slower rate of take-up than a comparable glass cast film.

It was found that there was no fundamental difference in the rate of take-up for the vapors of methylene chloride and acetone, although in the liquid state the former is a limited swelling agent, while the latter is a solvent. For both these vapors there is a characteristic pressure above which several anomalies appear, which make a complete quantitative explanation of the data rather difficult. The most important of these anomalies is that, if one plots the amount of vapor taken up as a function of time, an inversion of slope is observed. This inversion is very marked and is a function of film thickness. Another anomaly that appears is that the absolute amount of vapor sorbed for thinner films is greater than that for thicker films for an appreciable time interval. The effect of temperature is complex. Above the pressures where the inversion of a slope occurs, the rate is lower at higher temperatures for a considerable range of the sorption. These effects cannot be explained on the basis of a generalized diffusion equation with the boundary conditions which have been considered so far, *i.e.*, assuming that the outer film surface is always in equilibrium with the vapor. *Received March 14, 1950.*

Polyelectrolytes. VII. Viscosities of Derivatives of Poly-2-vinylpyridine. By W. N. MACLAY and R. M. FUOSS.

Polyelectrolytes were prepared by partial quaternization of poly-2-vinylpyridine ($M = 45{,}000$) with methyl bromide and butyl bromide. Viscosities of the former salt were measured in water and methanol; of the latter in water, methanol, ethanol and nitrobenzene. A new method of calibrating viscometers is described. Shear constants of the salts in aqueous solution were determined. The viscosity data conform to the equation:

$$z = A/(1 + B\sqrt{C}) + D$$

Correlations between both structure of salt and dielectric constant of solvent, and the constants of the equation were found. Quaternary derivatives of poly-2-vinylpyridine are more rodlike than corresponding derivatives of poly-4-vinylpyridine. *Received March 14, 1950.*

Crystallinity of Celluloses after Treatment with Sodium Hydroxide (Mercerization). By P. H. HERMANS and A. WEIDINGER.

The crystallinity of rayons measured with a standardized x-ray method increases from 40 to 50% after previous treatment with 18% sodium hydroxide followed by removal of the alkali with boiling water. If the washing-out of the alkali is carried out at room temperature, or if 4% sodium hydroxide is employed, the increase in crystallinity is smaller. Neither exclusion of oxygen during mercerization nor addition of hydrogen peroxide to the soaking lye has an influence on the final crystallinity. Native celluloses (ramie and wood pulp), after soaking in 18% sodium hydroxide and washing at the boil, yield the same figure of 50% crystallinity. A crystallinity figure of 50% is also obtained upon heterogeneous acid hydrolysis of rayon fibers at 100°C. and in cellulose precipitated from dilute viscose solution at 100°. *Received March 20, 1950.*

Sulfonation of Natural Rubber. By G. J. VAN AMERONGEN.

The sulfonation reaction of rubber with SO_2 is discussed. It proves to be a chain reaction which can be catalyzed by various compounds. Diazoamino compounds, hydroperoxides, some metal nitrates and nitrites, NO, and NO_2 are found to be catalytically active. The activity of these substances varies considerably; the hydroperoxides NO and NO_2 inducing immediate reaction; the diazoamino compounds within a few minutes; and the metal nitrates, such as $LiNO_3$, in several hours.

The reaction has a ceiling temperature at about 35 to 40°C., above which no reaction takes place. The properties of the reaction products are governed by the amount of SO_2 bound and vary from rubbery to horny, and ultimately brittle and resinlike. Products of moderate SO_2 content swell in organic solvents; products of high SO_2 content dissolve only in concentrated H_2SO_4 of HNO_3. The workability of the products is rather poor. *Received March 25, 1950.*

Adhesion of Polyethylene and Polystyrene to Steel. By G. KRAUS and J. E. MANSON.

A conservative estimate of the molecular forces involved in the adhesion of polymers to conducting surfaces leads to bond tensile strengths considerably above those realizable in practice. This is explained by the occurrence of flaws, thermal stresses, and deformation under load. In order to minimize these factors, very thin films of polystyrene and polyethylene were molded between steel cylinders and experimental conditions were carefully controlled with the result that joint strengths in excess of bulk tensile strengths were obtained. Curves of joint failure stress *versus* film thickness at various temperatures are given, and extrapolated to zero thickness. The extrapolated adhesion values represent a lower limit of the specific adhesion. At 25°C. they are 183 kg./cm.^{2} for polyethylene, and 412 kg./cm.^{2} for polystyrene. *Received April 3, 1950.*

Azo-bis Nitriles. II. Use of 2,2′-Azo-bis-isobutyronitrile as a Catalyst for the Polymerization of Styrene. By C. G. Overberger, P. Fram, and T. Alfrey, Jr.

(*1*) The rate of polymerization catalyzed by 2,2′-azo-bis-isobutyronitrile was found to be proportional to the square root of the catalyst concentration at 47.8° and 67.8° at a monomer concentration of 4 moles/liter. A square root dependence was also observed at 80.3° with 1-azo-bis-cyclohexanecarbonitrile in pure monomer. At these temperatures, the number average degree of polymerization, assuming combination for the termination step, was inversely proportional to the square root of the catalyst concentration. These facts are additional evidence to support the unimolecular first-order decomposition of the azo-bis compound into radicals.

(*2*) The monomer dependence on the over-all rate was found to be 1.2, again at 68.2° this result is consistent with first-order initiation and bimolecular termination.

(*3*) The decomposition of 2,2′-azo-bis-isobutyronitrile in pure styrene or in toluene and styrene is a unimolecular first-order decomposition with a rate constant similar to that observed in pure toluene. *Received April 10, 1950.*

Influence of Molecular Weight Distribution on the Intrinsic Viscosity–Molecular Weight Relationship. By H. P. Frank and J. W. Breitenbach.

Polystyrene made by polymerization at 140° (polymer yield 18.9%) was fractionated successively into a number of fractions of increasing homogeneity. Intrinsic viscosity and osmotic molecular weight of the unfractionated polymer and of the fractions were determined. In the relation between them the constant K was found to decrease from $K_0 = 14.2 \times 10^{-7}$ for the unfractionated polymer to $K_\infty = 6.8 \times 10^{-7}$ for the most homogeneous fractions. The distribution function of G. V. Schulz for the polymer and a Gaussian function for the most homogeneous fractions are discussed. From the ratio $K_0/K_\infty = 2.09$ (±0.15) we draw conclusion on the mechanism of polymerization under assumption of the validity of $[\eta] = K\overline{M}^{\alpha}$ instead of the simple Staudinger equation. A possible explanation for the deviation of the experimental value 2.09 from the theoretical 1.877 is given. *Received April 15, 1950.*

Determination of Molecular Weight of High Polymers by Measurement of Osmotic Pressures at Low Concentrations. By G. A. Gilbert, C. Graff-Baker, and C. T. Greenwood.

An equilibrium osmometer for the measurement of very low osmotic pressures has been designed. It is constructed of metal and employs a large horizontal membrane. A rapid approach to equilibrium is obtained by the use of a fine capillary and a bacterial cellulose membrane (Masson and Melville) in conjunction with complete thermostatting. To avoid displacement, the membrane is stretched in a frame and held over a grooved domed support of the Carter-Record type. Details of procedure, including concentration estimation and the preparation of membranes, are given.

Measurements of the osmotic pressure of a fractionated sample of polystyrene, of molecular weight approximately one million, have served to determine the precision of the osmometer. At a pressure of 0.026 cm. of chloroform, the standard deviation was found to be 0.002 cm. The importance of correcting for the density of the solution, when measuring high molecular weights, is discussed. *Received May 1, 1950.*

Some Aspects of Depolymerization Kinetics. By R. SIMHA and L. A. WALL.

A brief discussion of the importance of the transfer step and its effect in the pyrolysis of polyethylene is given. In this case the removal, by molecular distillation, of smaller species from the reacting mixture modifies the kinetics. The molecular weight decreases less rapidly and tends to a limiting value depending on the maximum size of the evaporating molecules. The number distribution of the latter is, in a first approximation, independent of their size. The pertinent expressions are presented and the general solution of the rate equations which can be used to obtain higher approximations is given. *Received May 10, 1950.*

Role of the Semipermeable Membrane in the Osmotic Molecular Weight Determination of Cellulose Acetate. By H. J. PHILIPP and C. F. BJORK.

Osmotic pressure measurements are reported for solutions of unfractionated and fractionated cellulose acetate in acetone, using denitrated collodion, gel-cellophane, and caustic-treated cellophane as semipermeable membranes. Although techniques are employed that are presumably correct for the effect of diffusion, different osmotic pressures and hence apparent molecular weights are obtained with the three types of membranes. No correlation is found between osmotic pressure and either the permeability constant or the average pore diameter of the membranes. Measurements with a very low molecular weight cellulose acetate, the molecular weight of which is known from independent measurements, show that the rate of diffusion of small solute molecules through various membranes is not related to the rate of transfer of solvent molecules.

It appears that the observed differences between membranes are caused by rapid diffusion of low molecular weight material at the beginning of the osmotic measurement, before even the first readings by a dynamic method can be taken. From measurements with the very low molecular weight cellulose acetate it is concluded that, in the case of cellulose acetate in acetone, correct osmotic molecular weights are obtained only with undried gel-cellophane membranes, and that molecular weights determined with either the faster denitrated collodion or the slower caustic-treated cellophane membranes are appreciably too high. *Received May 15, 1950.*

New Dynamic Method for Osmotic Pressure Measurements. By H. J. PHILIPP.

A new dynamic method of measuring osmotic pressures of high polymer solutions is described, which greatly reduces the time for each measurement. Accuracy and precision of this method are similar to those of other osmotic techniques. Close temperature control is essential for reliable results, especially with slow membranes. Convenient apparatus to control the temperature within 0.001°C. is described. Examples are given for the determination of the "zero-correction" of a membrane with solvent on both sides, and for a complete molecular weight determination of a commercial cellulose acetate in acetone. *Received May 15, 1950.*

Viscosity–Molecular Weight Relationship for Cellulose Acetate in Acetone. By H. J. PHILIPP and C. F. BJORK.

Careful viscosity and osmotic pressure measurements with a membrane of known reliability are reported for 14 fractions of cellulose acetate prepared by repeated refractionation. For molecular weights up to 115,000 the following relation is obtained between intrinsic viscosity and absolute molecular weight:

$$[\eta](25\,°\text{C., acetone}) = 8.97 \times 10^{-5} \times M^{0.90}$$

the units of $[\eta]$ being 100 ml./g. An explanation is offered for the difference between this equation and other equations in the literature as well as for the discrepancies among the various literature equations. *Received May 15, 1950.*

Electrolytic Initiation of Polymerization. By I. M. Kolthoff and L. L. Ferstandig.

Two new principles are discussed by which polymerization may be initiated electrolytically. One of these methods, the continuous electrolytic formation of the activator in a redox activation polymerization system, under various conditions, has been used successfully in the polymerization of acrylonitrile, but not of isoprene or styrene. The second method, based on the formation of free radicals in the electrolytic reduction of perdioxy compounds, has been tested under a limited number of conditions without significant success. Emulsion systems also have been employed in this research and the results are discussed. *Received May 20, 1950.*

Swelling of Polyvinyl Alcohol in Water. By W. J. Priest.

Swelling and solubility characteristics of polyvinyl alcohol and polyvinyl alcohol-acetate copolymers in liquid water have been examined. For a given species, swellings are found to be variable in a continuum of metastable states depending on the previous history of the polymer. Changes in swelling are induced in a predictable manner by treatments such as humidification. Changes are interpreted in terms of cumulative secondary bond cross-linkages arising from the development of microcrystalline regions within the gel. *Received June 6, 1950.*

Polyelectrolytes. VIII. Quaternized Polyesters of Succinic Anhydride and Methyldiethanolamine. By R. M. Fuoss and D. Edelson.

Linear polyelectrolytes have been prepared by quaternizing with methyl bromide the polyester obtained by condensation between succinic anhydride and methyldiethanolamine. Molecular weights, determined by end group titration, were in the range 2000–43,000. The polysalts hydrolyze in water but are stable in absolute methanol. Viscosities in methanol of the polysalt of highest molecular weight conform to the empirical equation:

$$\eta_{sp}/C = A/(1 + BC^{1/2})$$

Conductance curves are sharply concave upward on a $\Lambda - c^{1/2}$ scale, indicating a high degree of association of counter ions with the polycation at finite concentrations. Estimates of limiting mobility suggest a curved rodlike structure for the polycation at infinite dilution. *Received June 13, 1950.*

Propriétés de Dilatation Thermique des Polyamides. By F. Ecochard.

A description is given for a simple method of measuring the expansion coefficient of plastic material, and other quantities, derived thereof (density of the liquid sample). A practical application is given in the case of some polyamides. This study makes it possible to show the presence of a maximum in the expansion curve; that maximum is probably related with the appearance, under thermal agitation, of a new degree of freedom of the molecules. *Received June 20, 1950.*

Polymerization of Allyl Compounds. V. Inhibition by Nitro Compounds. By G. S. Hammond and P. D. Bartlett.

The effect of various nitro compounds on the peroxide-induced short-chain polymerization of allyl acetate has been investigated. Of the compounds studied, *sym*-trinitrobenzene is the most active as a retarder. Nitromethane and dinitrodurene were found to be less effective than aromatic nitro compounds which have replaceable nuclear hydrogen atoms but both exerted a measurable retarding influence on the polymerization reaction. It is found that trinitrobenzene reacts with a minimum of 5.9 radicals per molecule. This and other data are discussed in connection with the hypothesis that radicals react by an alkylation mechanism. An alternative mechanism involving attack on the nitro group itself is suggested. *Received July 15, 1950.*

Some Improvements on the Osmotic Balance. By B. ENOKSSON.

An osmotic balance is described, whose principle is the same as that of an earlier one, but with the readings simplified by use of a chainomatic balance. A new cell has been constructed. Due to thin walls in the tube of the cell, this cell makes it possible to measure osmotic pressure without determining the reference point, the position at which the meniscus in the cell is at the same level as that in the container. A determination of osmotic pressure can be made in half the time by this new arrangement, compared with the older method. An example of the use of the balance has been given for a sample of cellulose nitrate and a fraction of polystyrene. *Received July 17, 1950.*

I.A.R.I. 75

INDIAN AGRICULTURAL RESEARCH
INSTITUTE LIBRARY, NEW DELHI.

Date of Issue	Date of Issue	Date of Issue
5/11/54 wbm 58n.		

GIPNLK—H-40 I.A.R I.—29-4-55—15,000